

INDUSTRIAL BURNERS

H A N D B O O K

INDUSTRIAL COMBUSTION SERIES

Edited by Charles E. Baukal, Jr.

PUBLISHED TITLES

Computational Fluid Dynamics in Industrial Combustion

Charles E. Baukal, Jr., Vladimir Y. Gershtein, and Xianming Li

Heat Transfer in Industrial Combustion

Charles E. Baukal, Jr.

The Industrial Combustion Handbook

Charles E. Baukal, Jr.

The John Zink Combustion Handbook

Charles E. Baukal, Jr.

Oxygen-Enhanced Combustion

Charles E. Baukal, Jr.

INDUSTRIAL BURNERS

H A N D B O O K

EDITED BY

CHARLES E. BAUKAL, JR.



CRC PRESS

Boca Raton London New York Washington, D.C.

Library of Congress Cataloging-in-Publication Data

Industrial burners handbook / edited by Charles E. Baukal, Jr.

p. cm.

Includes bibliographical references and index.

ISBN 0-8493-1386-4 (alk. paper)

1. Heating—Equipment and supplies—Handbooks, manuals, etc. 2. Combustion engineering—Handbook, manuals, etc. I. Baukal, Charles E.

TJ254.5.I517 2003

621.402'3—dc21

2003051466

This book contains information obtained from authentic and highly regarded sources. Reprinted material is quoted with permission, and sources are indicated. A wide variety of references are listed. Reasonable efforts have been made to publish reliable data and information, but the author and the publisher cannot assume responsibility for the validity of all materials or for the consequences of their use.

Neither this book nor any part may be reproduced or transmitted in any form or by any means, electronic or mechanical, including photocopying, microfilming, and recording, or by any information storage or retrieval system, without prior permission in writing from the publisher.

All rights reserved. Authorization to photocopy items for internal or personal use, or the personal or internal use of specific clients, may be granted by CRC Press LLC, provided that \$1.50 per page photocopied is paid directly to Copyright Clearance Center, 222 Rosewood Drive, Danvers, MA 01923 USA. The fee code for users of the Transactional Reporting Service is ISBN 0-8493-1386-4/04/\$0.00+\$1.50. The fee is subject to change without notice. For organizations that have been granted a photocopy license by the CCC, a separate system of payment has been arranged.

The consent of CRC Press LLC does not extend to copying for general distribution, for promotion, for creating new works, or for resale. Specific permission must be obtained in writing from CRC Press LLC for such copying.

Direct all inquiries to CRC Press LLC, 2000 N.W. Corporate Blvd., Boca Raton, Florida 33431.

Trademark Notice: Product or corporate names may be trademarks or registered trademarks, and are used only for identification and explanation, without intent to infringe.

Visit the CRC Press Web site at www.crcpress.com

© 2004 by CRC Press LLC

No claim to original U.S. Government works

International Standard Book Number 0-8493-1386-4

Library of Congress Card Number 2003051466

Printed in the United States of America 1 2 3 4 5 6 7 8 9 0

Printed on acid-free paper

Preface

This book focuses specifically on industrial burners. This book should be of interest to anyone working in or with the field of industrial combustion. This includes burner designers, researchers, end users, furnace designers, government regulators, and funding agencies. It can also serve as a reference work for those teaching and studying combustion. The book covers a wide range of burner designs used in a broad array of applications in the metals, minerals, incineration, hydrocarbon/petrochemical, and power generation industries. The authors represent a number of prominent burner suppliers and have hundreds of years of combined experience with industrial burners.

The book is organized in three sections. Section I deals with the basics of combustion in industrial applications. It includes five general chapters on heat transfer, fluid flow, combustion, and computer modeling. These chapters are written from the narrow scope of how they apply to burners. Section II concerns burner fundamentals. It includes five chapters on the topics of burner heat transfer, burner noise, burner controls, burner testing, and burner physical modeling. Section III deals with 11 specific burner designs, including chapters on high-velocity burners, regenerative burners, thermal radiation burners, radiant tube burners, radiant wall burners, natural-draft burners, boiler burners for single-burner applications, boiler burners for multi-burner applications, duct burners, air-oxy/fuel burners, and oxy/fuel burners.

There are very few books that consider burners used in industrial applications. Combustion textbooks contain little if anything on practical combustion equipment such as burners. There are several books that consider industrial burners in differing levels of detail. The *North American Combustion Handbook* (two volumes: Vol. 1, 3rd edition, 1986; Vol. 2, 3rd edition, 1997; published by North American Manufacturing Co.) has been the industry standard since the 1950s and discusses many aspects of practical combustion systems, including burners. However, it does not go into much detail on burners, nor does it cover the range of burner types that are considered here. Another book that is longer in print, but considers industrial burners, is entitled *Combustion Engineering and Gas Utilization* (3rd edition, E&FN Spon, 1992, edited by J.R. Conforth, and sponsored by British Gas in the U.K.). It has two detailed and generously illustrated chapters on burners, but specifically focuses on natural gas applications. The Industrial Heating Equipment Association (IHEA) is comprised of most of the U.S. industrial burner manufacturers. The IHEA publishes a book entitled *Combustion Technology Manual* (5th edition, IHEA, 1994), which contains several brief chapters on industrial burners.

As with any book of this type, there are some topics that are not covered and some that are not treated extensively. Because the vast majority of industrial applications use gaseous fuels, that is the focus of this book, with limited discussion of liquid fuels and no discussion of solid fuels. This book concerns atmospheric-pressure combustion, which is the predominant type used in industry. There are some burner designs that are not considered, particularly those intended for narrow and limited applications.

As with any book of this type, there are sure to be author preferences and biases, but the coverage is fairly extensive and comprehensive. There are also generous discussions of many common industrial applications to help the reader better understand the requirements for different burner designs. Particularly because of the increasing emphasis on the environment, the design of most industrial burners continues to change and improve to reduce pollutant emissions. While industrial burner design and development is a dynamic area of continuing research, the principles considered here are expected to be applicable well into the foreseeable future.

About the Editor

Charles E. Baukal, Jr., Ph.D., P.E., is the Director of the R&D Test Center, the John Zink Institute, and Burner and Flare R&D for the John Zink Co., LLC (Tulsa, OK) which is a leading supplier of industrial combustion equipment in the chemical, petrochemical, and power generation industries. He previously worked for 13 years at Air Products and Chemicals, Inc. (Allentown, PA) in the areas of oxygen-enhanced combustion and rapid gas quenching in the ferrous and nonferrous metals, minerals, and waste incineration industries. He has also worked for Marsden, Inc. (Pennsauken, NJ) in the paper, printing, and textile industries and Selas Corp. (Dresher, PA) in the metals industry, both in the area of industrial combustion equipment. He has more than 20 years of experience in the fields of industrial combustion, pollution, and heat transfer and has authored more than 70 publications in those areas. He is the editor of the books *Oxygen-Enhanced Combustion*, *Computational Fluid Dynamics in Industrial Combustion*, and *The John Zink Combustion Handbook*, the author of the book *Heat Transfer in Industrial Combustion*, and the general editor of the *Industrial Combustion* series, all with CRC Press (Boca Raton, FL).

He has a Ph.D. in mechanical engineering from the University of Pennsylvania (Philadelphia), a B.S. and M.S. in mechanical engineering from Drexel University (Philadelphia), an M.A. in Biblical Studies from Dallas Theological Studies (Dallas, TX), and is working on an M.B.A. from the University of Tulsa (Tulsa, OK). He is a licensed Professional Engineer in the state of Pennsylvania, a certified Diplomate Environmental Engineer (DEE), and a Qualified Environmental Professional (QEP). He has been an adjunct instructor at several colleges, is an expert witness in the field of combustion, has nine U.S. patents, and is a member of several *Who's Who* compilations. He is a member of the American Society of Mechanical Engineers, the Air and Waste Management Association, the Combustion Institute, the American Society of Safety Engineers, and several honor societies.

Acknowledgments

Chuck Baukal would like to thank his wife Beth and his daughters Christine, Caitlyn, and Courtney for their patience and help during the writing of this book. He would also like to thank the good Lord above, without whom this would not have been possible.

Joe Colannino dedicates his work to Jesus the Christ, his wife Judy, and their three children, F. Christian, Nathanael J., and Jamie D.

Tom Eldredge would like to express thanks to his wife Nancy, who always encourages him to be the best he can be. Additionally, he is thankful to his Lord and Savior, Jesus Christ, for every good gift, and for his vocation as a mechanical engineer.

Abraham Lincoln once said “Everything I am,... I owe to my angel mother.” Joseph Smith would like to gratefully acknowledge his family, friends, and associates for the part they have had in shaping his life. He expresses his thanks to Dr. Chuck Baukal for his encouragement and example in taking time to contribute to the scientific literature, and to the publisher for supporting this effort. Lastly, he expresses deepest gratitude to his wife, Eileen, and his children. They have made life worth living!

Rémi Tsiava thanks Olivier Charon, his former manager who was the first contact for this work. Special thanks to Bernard Labegorre who is the major pusher to perform this work. Also thanks to Bernard Zamuner and Bertrand Leroux for data collection.

Lev Tsirulnikov would like to dedicate his work to the memory of his teachers in low-NO_x combustion and boiler fields — J.B. Zeldovich, V.V. Pomerantsev, N.V. Koznetsov, and A.D. Garbanenko.

Timothy Webster would like to thank his wife Sharon for all her love, support, and encouragement.

Contributors

Bruce B. Abe is a Combustion and Process Control Specialist at The North American Manufacturing Company, Ltd., Cleveland, OH, where he has worked with combustion controls for 30 years in an engineering and sales/marketing capacity. He is a frequent lecturer on combustion controls at North American Combustion and Controls Seminars and at the Industrial Heating Equipment Association's annual Safety Standards Seminar for Industrial Furnaces and Ovens.

Wes Bussman, Ph.D., is a Senior Development Engineer at the John Zink Company, LLC (Tulsa, OK). He has more than 10 years of experience as a research and product development engineer for the company, and has a Ph.D. in mechanical engineering from the University of Tulsa. He holds five U.S. patents, and has authored several publications. He has taught undergraduate courses in mechanical engineering at the University of Tulsa. Honors include Kappa Mu Epsilon Mathematical Society and Sigma Xi Research Society.

Michael G. Claxton is a Senior Principal Engineer in the Burner Process Engineering Group of the John Zink Company, LLC (Tulsa, OK). He has a B.S. in Mechanical Engineering from the University of Tulsa and has worked for the John Zink Co. in the field of industrial burners and combustion equipment since 1974. He has co-authored a number papers and presentations covering combustion, combustion equipment, and combustion-generated emissions, and is co-holder of several combustion-related patents.

Joseph Colannino, P.E., is the Director of Engineering and Design at the John Zink Company, LLC (Tulsa, OK) and a chemical engineer. He has more than 15 years of experience in the combustion arts and over 20 publications to his credit. He is listed in *Who's Who in Science and Engineering* and *Who's Who in California*. Joseph is a member of the American Chemical Society (ACS) and the American Statistical Association (ASA).

Tom Eldredge, Ph.D., currently works as a combustion and modeling engineer at the John Zink Company, and is involved in both computational and physical fluid flow modeling of burners and boiler components. He previously worked for more than 5 years at the Lehigh University Energy Research Center. He has worked on optimizing combustion on coal and natural gas fired boilers over the past 9 years. He worked on a project team as a primary developer of software for combustion optimization of coal-fired boilers. He is well experienced in computational fluids modeling as well as physical fluids modeling. He has a number of publications related to modeling of power plant components, power plant emissions reductions, and performance improvements. He holds a Ph.D. in mechanical engineering from the University of Tennessee, and is a member of the American Society of Mechanical Engineers and The Combustion Institute.

Mahmoud Fleifil, Ph.D., is the Acoustics Engineer of John Zink Company, LLC (Tulsa, OK). He has a Ph.D. in mechanical engineering from a co-supervisory program between Ain Shams University and MIT. His areas of expertise are fluid dynamics, combustion instability, and noise control. He has more than 20 publications on Active Control of Combustion Instability in *IEEE*, *Combustion Science and Technology*, and *Combustion and Flame* journals. He is listed in *Who's Who in America*, *Who's Who in Science and Engineering*, *Lexington Who's Who*, and *The National Aviation and Space Exploration Wall of Honor*. He is a member of the ASME and AIAA.

Joe Gifford is a Senior Engineer, Instrumentation and Control Systems, at the John Zink Company, LLC (Tulsa, OK). He has worked in the field of control and facilities design for 40 years and has a B.S. in physics. For many years he has conducted company training classes for control engineers and technicians. He has received numerous awards for innovative control system designs throughout his career, including the General Electric Nuclear Energy Division's Outstanding Engineering Award. Technical society memberships have included the Pacific Association of General

Electric Scientists and Engineers (PAGESE), the Instrument Society of America (ISA), the American Society of Mechanical Engineers (ASME), and the National Fire Protection Association (NFPA).

John P. Guarco is the Combustion Specialist for the TODD Combustion Group of John Zink Company. He joined John Zink in September of 1993 as a utility project engineer. In 1995, he added the role of R&D Engineer to his portfolio. In 1998, he assumed the responsibility of heading up TODD's physical modeling effort, focusing on streamlining the modeling process, while generating new opportunities for business and product development. John has authored papers on several combustion topics, including field results of low-NO_x combustion in several utility boilers, ultra-low emission burners, field results of gas-coal co-firing, physical modeling, and other NO_x reduction techniques for boilers. He is also one of the contributing authors of *The John Zink Combustion Handbook*. John received both a bachelor's and master's degree in mechanical engineering from the University of Connecticut, as well as an MBA from the University of New Haven.

R. Robert Hayes is a combustion engineer at the John Zink Company LLC (Tulsa, OK). He holds a Master's degree in mechanical engineering from Brigham Young University and has worked in the fields of combustion and thermal sciences for 7 years. He is the author or co-author of more than ten publications in the fields of combustion and heat transfer and two patents pending.

Eric M. Hixson joined the CD adapco group in January 2003 as an engineer of CDa-access, a wholly owned subsidiary of adapco. Before joining CD adapco, Hixson worked as a CFD engineer for the John Zink Company (Tulsa, OK).

Jaiwant D. Jayakaran (Jay Karan) is a director in the Technology & Commercial Development Group at the John Zink Company LLC (Tulsa, OK). He has worked in the fields of combustion, petrochemicals, and power for 17 years, with responsibilities in R&D, plant operations, and engineering. Jay has an M.S. in mechanical engineering from Texas Tech University. He has authored several technical articles and papers, and has several patents pending.

Hisashi (Sho) Kobayashi, Ph.D., is a Corporate Fellow at Praxair, Inc. (Danbury, CT). He has developed oxygen combustion systems and processes for glass, steel, aluminum, petrochemical, power plant, and other industries for 27 years, and has authored or co-authored more than 40 U.S. patents and over 50 technical papers. He has a B.S. in aeronautical engineering from the University of Tokyo and M.S. and Ph.D. degrees in mechanical engineering from the Massachusetts Institute of Technology.

Zachary Kodesh, P.E., is a controls engineer at John Zink Company (Tulsa, OK). He has more than 12 years of experience as a process design and controls engineer. He has a Master's degree in mechanical engineering from Oklahoma State University.

Russ Lang is a project manager at The North American Manufacturing Company, Ltd., Cleveland, OH. He has an associate's degree in mechanical technology from Cuyahoga Community College. At North American since 1978, he has worked in project and systems engineering and management, with regenerative burner systems as a specialty. He is co-holder of several combustion-related patents.

Jeff Lewallen, P.E., is an account manager at the John Zink Company LLC (Tulsa, OK). He has worked in the field of combustion for 11 years. He graduated from the University of Tulsa in 1992 and holds a B.S. in mechanical engineering.

Michael Lorra, Ph.D., started working for John Zink Co. LLC as a CFD engineer in 1999 after finishing his Ph.D. (Dr.-Ing.) at Ruhr-Universitaet (Bochum, Germany). He worked at Gaswaerme-Institut (Essen, Germany), a well-known and established research facility, for 9 years. He gained experience in NO_x reduction techniques, especially reburning technology. During his time at Gaswaerme Institut, he developed his own CFD code for the calculation of turbulent reacting flows including chemistry with the laminar flamelet-libraries. Parts of his research have been presented at international conferences and are published in *Gaswaerme-International*.

Clive Lucas is a product manager at The North American Manufacturing Company, Ltd., Cleveland, OH. He has a B.S. in mechanical engineering from Cleveland State University and has worked for North American in the field of industrial burners and combustion systems since 1994,

with specific responsibility for the company's direct-fired regenerative burner line. He is co-holder of a patent for a diaphragm-actuated cycle valve.

Todd A. Miller is a research and design engineer at The North American Manufacturing Company, Ltd., Cleveland, OH. He has a B.S. in mechanical engineering technology from Cleveland State University and has worked for North American on burner product design and development since 1983. He is co-holder of several combustion-related patents.

John Newby is Vice President for The North American Manufacturing Company, Ltd., Cleveland, OH. His career spans over 35 years in the industrial combustion field, where he has worked in all major industrial areas of the world. Formerly the managing director of Hotwork Development Ltd. in England, he operated reGen Systems Inc. in the U.S. until 1986 when he joined North American. He has authored and co-authored numerous papers and presentations on combustion equipment, systems, and applications, and is co-holder of several combustion-related patents.

Dennis E. Quinn is manager of market development at The North American Manufacturing Company, Ltd., Cleveland, OH. For over 20 years he has worked in various development, engineering, and design capacities with lead responsibilities for custom burner designs and their applications. He has co-authored papers and presentations for the Industrial Heating Equipment Association and is co-holder of several combustion-related patents. He is a graduate of Cleveland State University's Fenn College of Engineering and has a B.S. in mechanical engineering and combustion application.

Tom Robertson is manager of research and development at The North American Manufacturing Company, Ltd., Cleveland, OH, where he has, for over 18 years, worked in the field of fundamental and applied combustion. He has co-authored papers and taught classes in applied combustion technology at North American Manufacturing and the Center for Professional Advancement. He is a graduate of Case Western Reserve University and has a B.S. and an M.S. in fluid and thermal science, and is co-holder of several combustion-related patents.

Joseph D. Smith joined the CD adapco group in January 2003 as president of CDa-acces, a wholly owned subsidiary of adapco. CDa-acces' main goal is to establish StarCD, adapco's CFD-based engineering software, as the premier tool to help solve problems with turbulent reacting flow systems unique to the hydrocarbon and chemical process industries. Joseph's expertise includes CFD, waste incineration, pulverized-coal combustion/gasification, fumed metal-oxides production, and gas flaring, all with a special emphasis on reaction engineering. Before joining CD adapco, Joseph worked as director of flare technology and computational fluid dynamics for the John Zink Company. He has taught at Tennessee Technological University, the University of Michigan, and the University of Illinois-Urbana/Champaign. He currently serves as an adjunct professor and teaches at Oklahoma State University and the University of Tulsa. Joseph has also consulted for The Dow Chemical Company, Destec Energy Systems, Southern Company Services, and several others. He holds six patents, and has authored more than 30 published articles and more than 40 conference papers. He is an active member of AIChE and has served as chair of both the Tulsa and Mid-Michigan Sections of AIChE. He has also served as national chair of the Student Chapters Committee. He is also a member of Sigma-Xi and Tau Beta Pi. He received B.S., M.S., and Ph.D. degrees in chemical engineering from Brigham Young University.

Thomas M. Smith is the President and CEO of Marsden, Inc., a leading manufacturer of high-efficiency, zero-pollution gas thermal radiation emitters. He studied mechanical/industrial engineering at the Drexel Institute of Technology (Philadelphia, PA) and business management at Rutgers University (Camden, NJ). He worked at TRW, Philco-Ford, and HRB Singer as an industrial engineer and senior industrial engineer over a 10-year period before joining a manufacturers representative firm as a sales engineer. He first became a business owner when he purchased the manufacturers' representative firm in 1972. In 1976, he applied for the first of over 50 granted U.S.A. and foreign Letters Patent on various embodiments of gas thermal radiation emitters. He formed Marsden, Inc. in 1976 to manufacture and market worldwide the unique Marsden Infrared equipment. Mr. Smith has taught national TAPPI courses and has had articles published in various technical journals and magazines.

Stephen L. Somers is a senior process engineer at the John Zink Company, LLC (Tulsa, OK). He has over 30 years of experience in combustion and process design, with the past 15 years in the application and design of duct burners for HRSG supplementary firing. He has an M.S. in chemical engineering from the University of Oklahoma and a B.S. in chemical engineering from the University of Tulsa.

Rémi Tsiava, Ph.D., is an engineer at Air Liquide (France) in the R&D Combustion Division and is responsible for burner conception, design, and development. He has expertise in combustion and industrial processes. He previously worked as an engineer in the Burner Division of the Stein Heurtey Company. He has a Ph.D. from Université Paul Sabatier (Toulouse, France), and has published papers on the use of oxy/fuel combustion in the glass and metals industries.

Lev Tsirolnikov, Ph.D., is a senior research engineer for the John Zink Company, LLC/Todd Combustion Group (Shelton, CT). He has developed low-emission combustion technologies, low-NO_x burners, and other equipment for gas/oil fired utility and industrial boilers. He holds 49 patents in the combustion/boiler field, and has published more than 100 technical papers, including four books. He is also a contributing author to *The John Zink Combustion Handbook*.

Demetris Venizelos, Ph.D., has been actively involved in the combustion field for the last sixteen years, including working for two burner companies, John Zink Company, LLC and Zeeco, Inc. He received his Ph.D. in mechanical engineering from Louisiana State University. Dr. Venizelos has conducted basic scientific research work, industrial technology research and development, and combustion design engineering. He has experience in premixed and lean-premixed combustion, industrial combustion systems, and laser and optical combustion diagnostics, as well as numerical modeling. He has authored several peer-reviewed technical papers, government technical reports, technical articles, and patent applications.

Richard T. Waibel, Ph.D., is a Senior Principal Engineer in the Burner Process Engineering Group at the John Zink Company, LLC (Tulsa, OK). He works in the field of burner design and development and has a doctorate in fuel science from the Pennsylvania State University. He has published over 70 technical papers, publications, and presentations. Dr. Waibel has been the Chairman of the American Flame Research Committee since 1995.

Timothy Webster is the director of power systems at the John Zink Company, LLC. He has worked in the field of industrial combustion for 10 years and is a licensed professional mechanical engineer in California. He holds a B.S. degree in mechanical engineering from San Jose State University and a Master of Engineering degree from the University of Wisconsin. He has authored more than 20 publications on combustion and emissions reduction.

Table of Contents

Section I

Industrial Combustion Basics

Chapter 1 Introduction

Charles E. Baukal, Jr., Ph.D., P.E.

Chapter 2 Heat Transfer

Charles E. Baukal, Jr., Ph.D., P.E.

Chapter 3 Fluid Flow

*Wes Bussman, Ph.D., Demetris Venizelos, Ph.D.,
and R. Robert Hayes*

Chapter 4 Combustion Basics

Joseph Colannino, P.E.

Chapter 5 CFD in Burner Development

*Joseph D. Smith, Michael Lorra, Ph.D., Eric M. Hixson,
and Tom Eldredge, Ph.D.*

Section II

Burner Fundamentals

Chapter 6 Heat Transfer from Burners

Charles E. Baukal, Jr., Ph.D., P.E.

Chapter 7 Burner Noise

*Mahmoud Fleifil, Ph.D., Jay Karan,
and Wes Bussman, Ph.D.*

Chapter 8 Combustion Controls

Joe Gifford and Zachary Kodesh, P.E.

Chapter 9 Burner Testing

Jeffrey Lewallen, P.E. and Charles E. Baukal, Jr., Ph.D., P.E.

Chapter 10 Burner Physical Modeling

John P. Guarco and Tom Eldredge, Ph.D.

Section III Burner Designs

Chapter 11 High-Velocity Burners

Tom Robertson, Todd A. Miller, and John Newby

Chapter 12 Regenerative Burners

Russ Lang, Bruce B. Abe, Clive Lucas, and John Newby

Chapter 13 Thermal Radiation Burners

Thomas M. Smith and Charles E. Baukal, Jr., Ph.D., P.E.

Chapter 14 Radiant Tube Burners

Dennis E. Quinn and John Newby

Chapter 15 Radiant Wall Burners

Demetris Venizelos, Ph.D., R. Robert Hayes, and Wes Bussman, Ph.D.

Chapter 16 Natural-Draft Burners

Charles E. Baukal, Jr., Ph.D., P.E.

Chapter 17 Burners for Industrial Boilers

Lev Tsirulnikov, Ph.D., John Guarco, and Timothy Webster

Chapter 18 Multi-Burner Boiler Applications

Lev Tsirulnikov, Ph.D., John Guarco, and Timothy Webster

Chapter 19 Duct Burners

Stephen L. Somers

Chapter 20 Air-Oxy/Fuel Burners

Charles E. Baukal, Jr., Ph.D., P.E.

Chapter 21 Oxy-Fuel Burners

Hisashi Kobayashi, Ph.D. and Rémi Tsiava, Ph.D.

Section IV
Appendices

Appendix A Common Conversions

Appendix B Design Data

Appendix C Material Properties

Section I

Industrial Combustion Basics

1 Introduction

Charles E. Baukal, Jr., Ph.D., P.E.

CONTENTS

- 1.1 Industrial Combustion
 - 1.2 Industrial Combustion Applications
 - 1.2.1 Metals Production
 - 1.2.2 Minerals Production
 - 1.2.3 Chemicals Production
 - 1.2.4 Waste Incineration
 - 1.2.5 Industrial Boilers and Power Generation
 - 1.2.6 Drying
 - 1.3 Combustion System Components
 - 1.4 Burner Design Factors
 - 1.4.1 Fuel
 - 1.4.2 Oxidizer
 - 1.4.3 Gas Recirculation
 - 1.5 General Burner Classifications
 - 1.5.1 Mixing Type
 - 1.5.2 Fuel Type
 - 1.5.3 Oxidizer Type
 - 1.5.4 Draft Type
 - 1.5.5 Heating Type
 - 1.5.6 Burner Geometry
 - 1.6 Burner Components
 - 1.7 Combustors
 - 1.7.1 Design Considerations
 - 1.7.1.1 Load Handling
 - 1.7.1.2 Temperature
 - 1.7.1.3 Heat Recovery
 - 1.7.2 General Classifications
 - 1.7.2.1 Load Processing Method
 - 1.7.2.2 Heating Type
 - 1.7.2.3 Geometry
 - 1.7.2.4 Heat Recuperation
 - 1.8 Heat Load
 - 1.8.1 Opaque Materials
 - 1.8.2 Transparent Materials
 - 1.9 Heat Recovery Devices
 - 1.9.1 Recuperators
 - 1.9.2 Regenerators
 - 1.10 Conclusions
 - References
-

1.1 INDUSTRIAL COMBUSTION

The field of industrial combustion is very broad and touches, directly or indirectly, nearly all aspects of our lives. The electronic devices we use are generally powered by fossil-fuel-fired power plants. The cars we drive use internal combustion engines. The planes we fly in use jet-fuel-powered turbine engines. Most of the materials we use have been made through some type of heating process. While this book is concerned specifically with industrial combustion, all of the above combustion processes share many features in common.

Industrial combustion is complicated by many factors. First, the science of combustion is still developing and has a long way to go until we have a complete understanding of it so it can be better applied and controlled. While fire has been with us since the beginning of time, much remains to be learned about it. The science of combustion combines heat transfer, thermodynamics, chemical kinetics, and multi-phase turbulent fluid flow, to name a few areas of physics. Therefore, the study of industrial combustion is interdisciplinary by necessity.

Combustion has been the foundation of worldwide industrial development for the past 200 years.¹ Industry relies heavily on the combustion process as shown in Table 1.1. The major uses for combustion in industry are shown in Table 1.2. Hewitt et al. (1994) have listed some of the common heating applications used in industry, as shown in Table 1.3.² Typical industrial combustion applications can also be characterized by their temperature ranges as shown in Figure 1.1. As can be seen in Figure 1.2, the demand for energy is expected to continue to rapidly increase. Most of the energy (88%) is produced by the combustion of fossil fuels such as oil, natural gas, and coal. According to the U.S. Dept. of Energy, the demand in the industrial sector is projected to increase by 0.8% per year to the year 2020.³

As shown in Figure 1.3, three elements are required to sustain combustion processes: fuel, oxidizer, and an ignition source (usually in the form of heat). Industrial combustion is defined here as the rapid oxidation of hydrocarbon fuels to generate large quantities of energy for use in industrial heating and melting processes. Industrial fuels can be solids (e.g., coal), liquids (e.g., oil), or gases (e.g., natural gas). The fuels are commonly oxidized by atmospheric air (which is approximately 21% O₂ by volume) although it is possible in certain applications to have an oxidizer (sometimes referred to as an “oxidant” or “comburent”) containing less than 21% O₂ (e.g., turbine exhaust gas⁴) or more than 21% O₂ (e.g., oxy/fuel combustion⁵). The fuel and oxidizer are typically mixed in a device referred to as a burner, which is discussed in more detail below and is the subject of this book. An industrial heating process can have one or many burners, depending on the specific application and heating requirements.

Many theoretical books have been written on the subject of combustion, but they have little if any discussion of industrial combustion processes.^{6–11} Edwards (1974) has written a brief chapter on applications, including both stationary (boilers and incinerators primarily) and mobile sources

TABLE 1.1
The Importance of Combustion in Industry

Industry	% Total Energy From (at the point of use)		
	Steam	Heat	Combustion
Petroleum refining	29.6	62.6	92.2
Forest products	84.4	6.0	90.4
Steel	22.6	67.0	89.6
Chemicals	49.9	32.7	82.6
Glass	4.8	75.2	80.0
Metal casting	2.4	67.2	69.6
Aluminum	1.3	17.6	18.9

Source: U.S. Dept. of Energy.¹

TABLE 1.2
Major Process Heating Operations

Metal Melting
Steel making
Iron and steel melting
Nonferrous melting
Metal Heating
Steel soaking, reheat, ladle preheating
Forging
Nonferrous heating
Metal Heat Treating
Annealing
Stress relief
Tempering
Solution heat treating
Aging
Precipitation hardening
Curing and Forming
Glass annealing, tempering, forming
Plastics fabrication
Gypsum production
Fluid Heating
Oil and natural gas production
Chemical/petroleum feedstock preheating
Distillation, visbreaking, hydrotreating, hydrocracking, delayed coking
Bonding
Sintering, brazing
Drying
Surface film drying
Rubber, plastic, wood, glass products drying
Coal drying
Food processing
Animal food processing
Calcining
Cement, lime, soda ash
Alumina, gypsum
Clay Firing
Structural products
Refractories
Agglomeration
Iron, lead, zinc
Smelting
Iron, copper, lead
Nonmetallic Materials Melting
Glass
Other Heating
Ore roasting
Textile manufacturing
Food production
Aluminum anode baking

Source: U.S. Dept. of Energy.¹

TABLE 1.3
Examples of Processes in the Process Industries Requiring Industrial Combustion

Process Industry	Examples of Processes Using Heat
Steel making	Smelting of ores, melting, annealing
Chemicals	Chemical reactions, pyrolysis, drying
Nonmetallic minerals (bricks, glass, cement and other refractories)	Firing, kilning, drying, calcining, melting, forming
Metal manufacture (iron and steel, and nonferrous metals)	Blast furnaces and cupolas, soaking and heat treatment, melting, sintering, annealing
Paper and printing	Drying

Adapted from Reference 3.

(primarily internal combustion engines).¹² Barnard and Bradley (1985) have a brief chapter on industrial applications.¹³ A book by Turns (1996), which is designed for undergraduate and graduate combustion courses, contains more discussions of practical combustion equipment than most similar books.¹⁴

There have also been many books written on the more practical aspects of combustion. Griswold's (1946) book has a substantial treatment of the theory of combustion, but is also very practically oriented and includes chapters on gas burners, oil burners, stokers and pulverized-coal burners, heat transfer, furnace refractories, tube heaters, process furnaces, and kilns.¹⁵ Stambuleanu's (1976) book on industrial combustion has information on actual furnaces and on aerospace applications, particularly rockets.¹⁶ There is much data in the book on flame lengths, flame shapes, velocity profiles, species concentrations, liquid and solid fuel combustion, with a limited amount of information on heat transfer. A book on industrial combustion has significant discussions on flame chemistry, but little on pollution from flames.¹⁷ Keating's (1993) book on applied combustion is aimed at engines and has no treatment of industrial combustion processes.¹⁸ A book by Borman and Ragland (1998) attempts to bridge the gap between the theoretical and practical books on combustion.¹⁹ However, the book has little discussion of the types of industrial applications considered here. Even handbooks on combustion applications have little if anything on industrial combustion systems.^{20–24}

1.2 INDUSTRIAL COMBUSTION APPLICATIONS

Burners are a key component in industrial combustion applications. An understanding of these applications is necessary when selecting the proper burner design. Some of the more common burner designs are considered in this book. The uses of each burner type in specific applications are discussed in relevant chapters. Some of the most common industrial applications are briefly discussed next. Note that not every type of industrial burner is considered in this book as there are numerous special designs for specific applications.

1.2.1 METALS PRODUCTION

Metals are used in nearly all aspects of our lives and play a very important role in society. The use of metals has been around for thousands of years. There are two predominant classifications of metals: ferrous (iron-bearing) and nonferrous (e.g., aluminum, copper, and lead). Ferrous metal production is often high temperature because of higher metal melting points compared to nonferrous metals. Many metal production processes are done in batch, compared to most other industrial combustion processes considered here which are typically continuous. Another fairly unique aspect of metal production is the very high use of recycled materials. This often lends itself

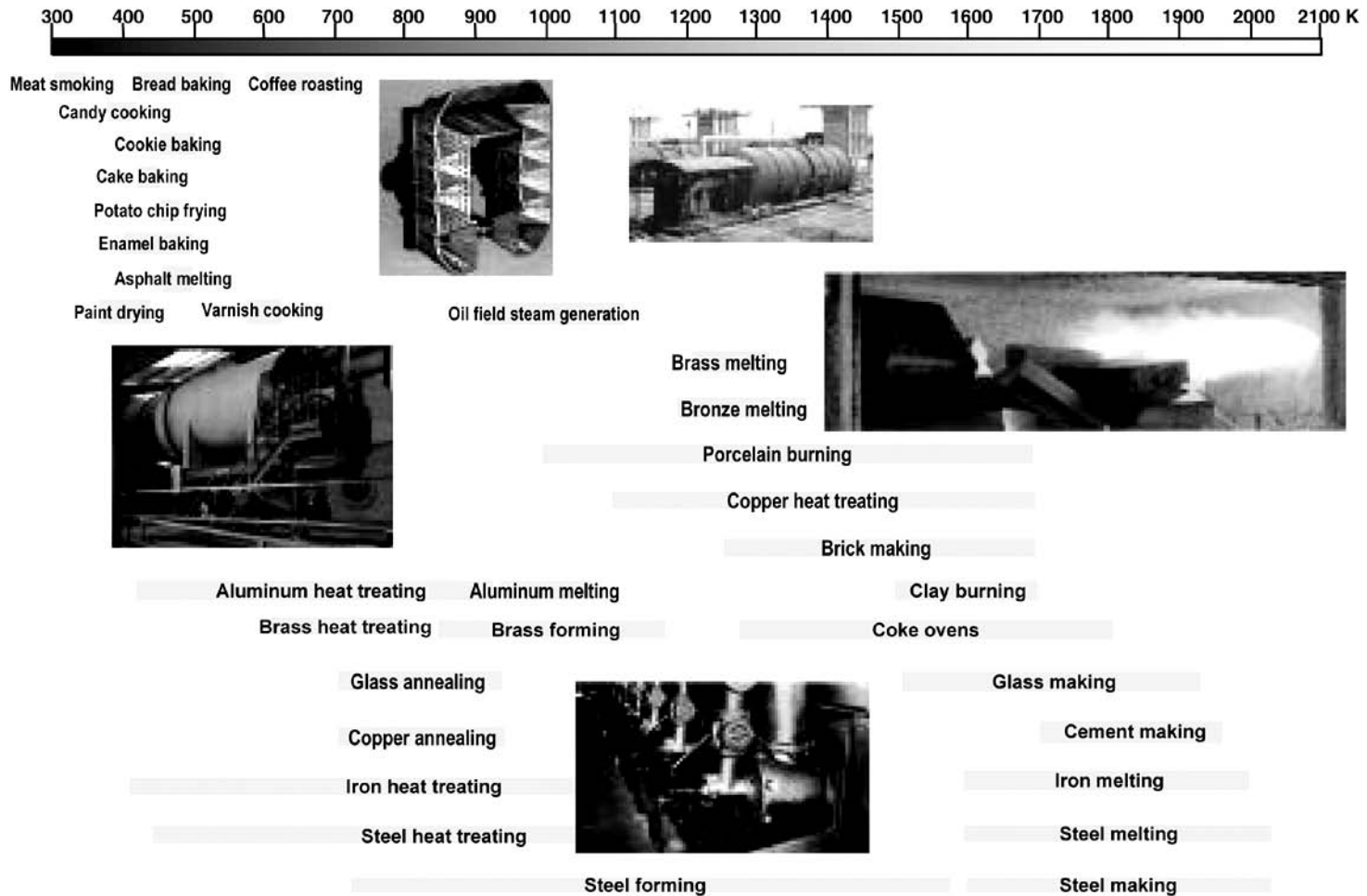


FIGURE 1.1 Temperature ranges of common industrial combustion applications. (Courtesy of Werner Dahm, 1998.)

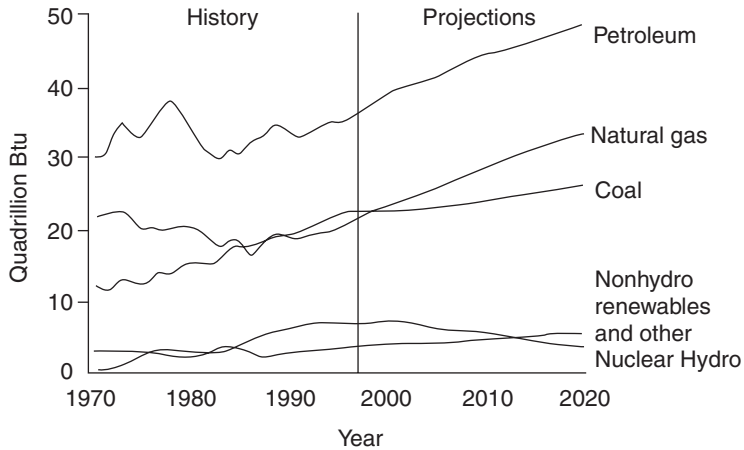


FIGURE 1.2 Historical and projected world energy consumption. (Source: U.S. Dept. of Energy.³)

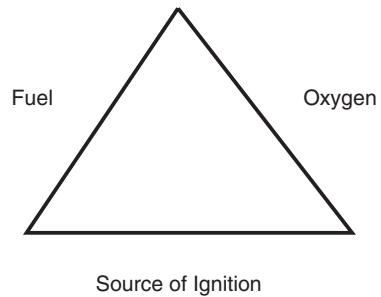


FIGURE 1.3 Combustion triangle.⁵

to batch production because of the somewhat unknown composition of the incoming scrap materials that may contain trace impurities that could be very detrimental to the final product if not removed. The metals are typically melted in some type of vessel and then sampled to determine the chemistry so that the appropriate chemicals can be either added or removed to achieve the desired grade of material. Another unique aspect of the metals industry is that transfer vessels are preheated prior to the introduction of molten metals into the vessel to minimize the thermal shock to the refractory. Figure 1.4 shows an example of preheating a transfer ladle.

Because metals melt at higher temperatures, higher intensity burners are often used in these applications. This includes, for example, oxygen-enhanced combustion^{25,26} and air preheating to increase the flame temperatures and metal melting capability. These higher intensity burners have the potential to produce high pollutant emissions, so burner design is important to minimize these emissions.

Another somewhat unique aspect of metals production is that supplemental heating may be required to reheat the metals for further processing. For example, ingots might be produced in one location and then transported to another location to be made into the desired shape (e.g., wheel castings are often made from remelting aluminum ingots or sows). While this process can be economically efficient, it is energy and pollutant inefficient due to the additional heating. Burners are used in the original melting process as well as in the reheating process. This is something that has begun to attract more attention in recent years, where the entire life cycle of a product is considered rather than just its unit cost and initial energy requirements. For example, aluminum has a low life-cycle cost compared to many other metals because of its high recycle

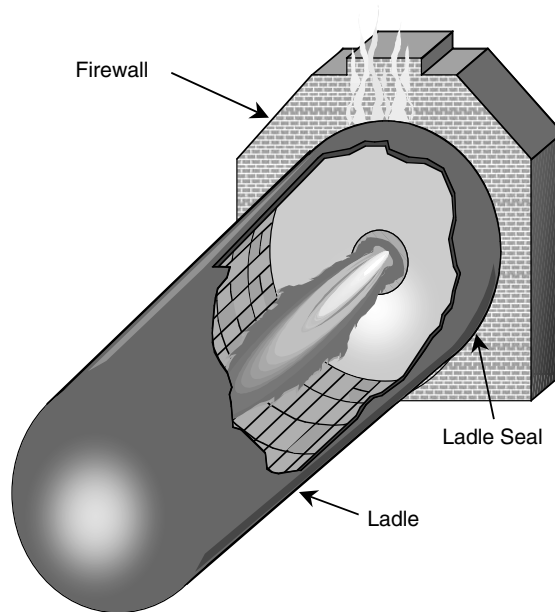


FIGURE 1.4 Ladle preheater.

ratio. While the energy consumption to make aluminum from raw ore is fairly high, remelting scrap aluminum takes only a fraction of that energy, which also means less overall pollution. Burners commonly used in the metals industry include high-velocity burners (Chapter 11), regenerative burners (Chapter 12), radiant tube burners (Chapter 14), air-oxy/fuel burners (Chapter 20), and oxy/fuel burners (Chapter 21).

1.2.2 MINERALS PRODUCTION

Some common minerals processes include the production of glass, cement, bricks, refractories, and ceramics. These are typically high-temperature heating and melting applications that require a significant amount of energy per unit of production. They also tend to have fairly high pollutant emissions as a result of the high temperatures and unit energy requirements. Most mineral applications are continuous processes, but there is a wide range of combustors. Large glass furnaces are typically of rectangular shape and have multiple burners. On the other hand, cement kilns are long refractory-lined rotating cylinders that are slightly inclined so that the materials flow gradually downhill (see [Figure 1.5](#)). A typical cement plant is shown in [Figure 1.6](#).

Many minerals applications employ some type of heat recovery in the form of air preheating to improve energy efficiency. However, the heat recovery typically significantly increases NO_x emissions. While recycling of used glass (referred to as cullet) is practiced in some applications, there is generally much less recycling in the minerals industry compared to the metals industry. Some burners used in minerals applications include regenerative burners (Chapter 12), air-oxy/fuel burners (Chapter 20), and oxy/fuel burners (Chapter 21).

1.2.3 CHEMICALS PRODUCTION

This is a very broad classification that encompasses many different types of production processes that have been loosely sub-categorized into chemicals (organic and inorganic) and petrochemicals (organic) applications. A typical refinery is shown in [Figure 1.7](#). There is some overlap in terms

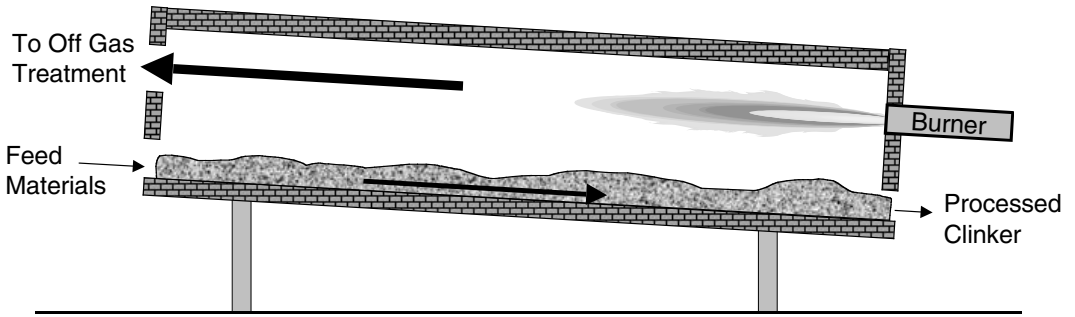


FIGURE 1.5 Counter-current rotary cement kiln schematic.



FIGURE 1.6 Cement plant.



FIGURE 1.7 Refinery.

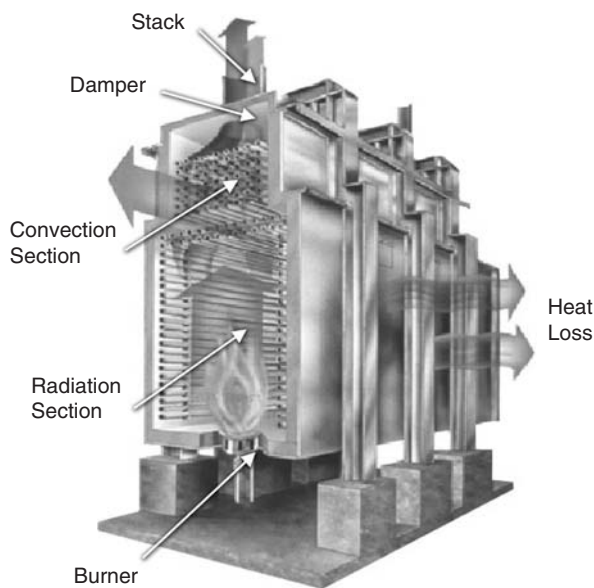


FIGURE 1.8 Process refinery heater. (Courtesy of John Zink Co., LLC.³⁶)

of the types of heating equipment used where many of the incoming feed materials are in liquid form (e.g., crude oil) that are processed in heaters with tubes running inside them. These are generally lower temperature applications ($<2300^{\circ}\text{F}$ or $<1300^{\circ}\text{C}$) that incorporate heat recovery to preheat the incoming feed materials. Nearly all chemicals heating applications employ multiple burners, but in a much more diverse configuration compared to many other industries. Burners may be fired horizontally, vertically up, vertically down, or at some angle in between, depending on the specific process. There are numerous configurations for fired process heaters (see [Figure 1.8](#)).

There are some aspects that make this industry unique compared to others. The first and one of the most important is the wide range of fuel compositions used to fire the heaters. These are mostly gaseous fuels that are by-products of the production process. These gaseous fuels often contain significant quantities of hydrogen, methane, and propane, and may include large quantities of inert gases such as nitrogen and carbon dioxide. A given heater might need to be able to fire on multiple fuels that may be present during various times in the production process. Another unique aspect of this industry is that many of the heaters are fired with natural-draft burners (see Chapter 16) where no blower is used to supply the combustion air. These burners are designed differently than conventional forced-draft burners and are more susceptible to variations in ambient conditions such as air temperature, humidity, and wind speed. A specific type of burner used in petrochemical applications is the radiant wall burner (see Chapter 15).

1.2.4 WASTE INCINERATION

The objective of waste incineration processes is to reduce or eliminate waste products, which involves combusting those materials. Not only is the incinerator (see [Figure 1.9](#)) fired with burners, but the waste material itself is often part of the fuel that generates heat in the process. However, the waste usually has a very low heating value, and hence the need for supplemental fuel. Compared to most other industrial combustion processes, by the very nature of the variability of the feed material, incineration is a more complicated and dynamic process. [Figure 1.10](#) shows a schematic



FIGURE 1.9 Municipal waste incinerator.

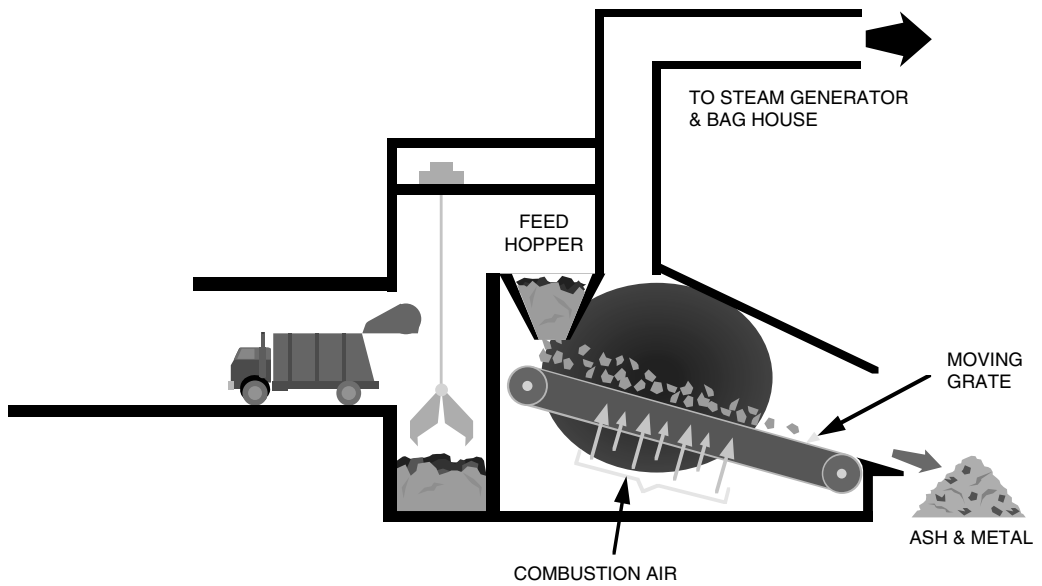


FIGURE 1.10 Schematic of municipal solid waste incinerator.

of a municipal solid waste incinerator. The waste may be very wet after a rain storm, which may put a huge extra heat load on the incinerator. In some locations where waste materials are separated for recycling, the waste actually fed into the incinerator may have a much higher heating value compared to other incinerators where there is no separation of the waste.

A complicating factor with incinerators is that the end product (e.g., the noncombustible waste) must also be disposed of, which means that one of the goals of most incineration processes is to produce minimal waste output. Because of waste material variability, other pollutants can be generated that are not normally associated with industrial combustion processes. An example is the burning of plastics, which can produce dioxins and furans. The types of incinerators can vary greatly, depending on a variety of factors. In some cases, waste materials to be destroyed can be fed through the burners. This is particularly true of waste hydrocarbon liquids. Some of the burners used in incineration include air-oxy/fuel (Chapter 20) and oxy/fuel (Chapter 21).

1.2.5 INDUSTRIAL BOILERS AND POWER GENERATION

Boilers are used for a variety of purposes in an assortment of applications. Common uses include producing hot water or steam for heating, producing steam for use within a plant such as atomizing oil for oil-fired burners, and producing steam to generate power in large power plants. Applications range from small single-burner uses in hospitals, schools, and small businesses, up to large multi-burner boilers in power plants. The burners used in boilers are typically regulated because of their proliferation and widespread use in applications involving the general public. The burners are normally required to have a full complement of safety controls to ensure safe operation. These burners are often highly regulated to minimize pollutant emissions, particularly in large power plants because of the size of the source. The types of burners used in smaller single-burner boiler applications are considered in Chapter 17. Boiler burners used in larger applications requiring multiple burners are considered in Chapter 18.

A special category of burners sometimes used in large power generating plants with gas turbines are called duct burners (see [Figure 1.11](#)). A schematic of the typical location of duct burners downstream of the turbine is shown in [Figure 1.12](#). These burners are unique because they use the combustion products from a turbine as their combustion “air.” The turbine exhaust gas (TEG) is at an elevated temperature and contains significant quantities of carbon dioxide and water, which are the products of the upstream combustion process. The TEG is also at a depleted oxygen level, so duct burners are designed to operate under these conditions. They are treated in detail in Chapter 19.

1.2.6 DRYING

Burners are used in a wide variety of lower-temperature drying applications to remove water from products that was added during the manufacturing process. These are lower-temperature applications that include paper manufacturing, printing and publishing, textile manufacturing, and food processing. Drying is defined as “a process in which a wet solid is heated or contacted with a hot gas stream, causing some or all of the liquid wetting the solid to evaporate.”²⁷ Kudra and Mujumdar (2002) have written a new book²⁸ on advanced drying technologies that covers a wide range of industries. One example is the drying of paper produced from a wet slurry. A typical paper mill is shown in [Figure 1.13](#).

In many drying processes, moisture is removed from webs that may be traveling at high speeds. Radiant heating is often used to supplement steam-heated cylinders or high-velocity hot air dryers.²⁹ The radiant heaters are either electric or fired with a fuel gas such as natural gas. Thermal radiation burners used in many of these applications are discussed in Chapter 13.

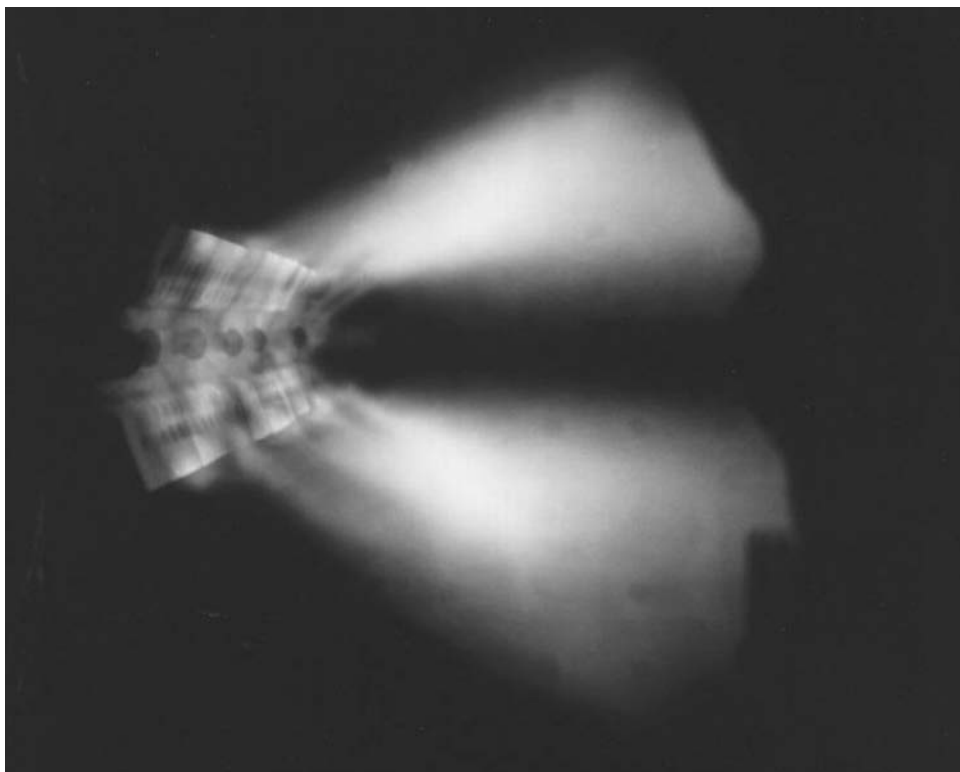


FIGURE 1.11 Duct burner flame. (Courtesy of John Zink Co., LLC.³⁶)

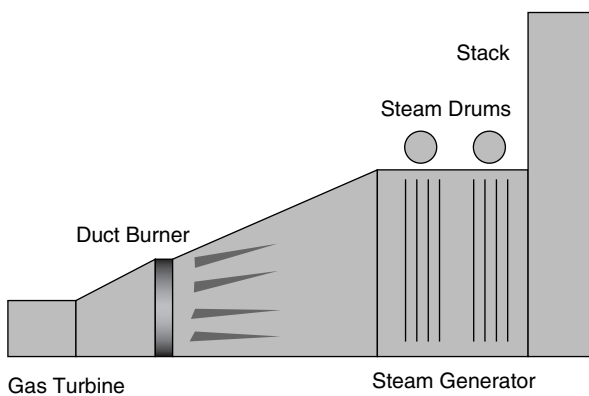


FIGURE 1.12 Duct burner process schematic. (Courtesy of John Zink Co., LLC.³⁶)

1.3 COMBUSTION SYSTEM COMPONENTS

There are six components that may be important in industrial combustion processes (see [Figure 1.14](#)). One component is the burner, which combusts the fuel with an oxidizer to release heat. Another component is the load itself, which can greatly affect how the heat is transferred from the flame. In most cases, the flame and the load are located inside a combustor, which may be a furnace, heater, or dryer and constitutes the third component in the system. In some cases, there may be some type



FIGURE 1.13 Paper mill.

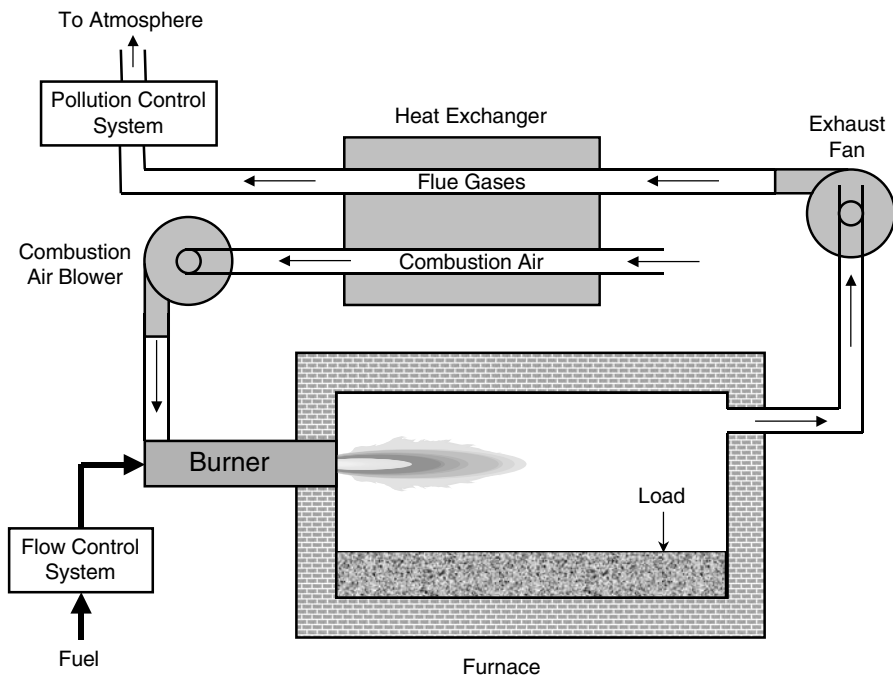


FIGURE 1.14 Schematic of an industrial combustion process.

of heat recovery device to increase the thermal efficiency of the overall combustion system, which is the fourth component of the system. The fifth component is the flow control system used to meter the fuel and the oxidant to the burners. The sixth and final component is the air pollution control system used to minimize the pollutants emitted from the exhaust stack into the atmosphere. Various aspects of these components are discussed in more detail in other sections of the book.

1.4 BURNER DESIGN FACTORS

The burner is the device used to combust the fuel with an oxidizer to convert the chemical energy in the fuel to thermal energy. A given combustion system may have a single burner or many burners, depending on the size and type of the application. For example, in a rotary kiln, a single burner is located in the center of the wall on one end of a cylindrically shaped furnace (see [Figure 1.15](#)). The heat from the burner radiates in all directions and is efficiently absorbed by the load. However, the cylindrical geometry has some limitations concerning size and load type, which make its use limited to certain applications such as melting scrap aluminum or producing cement clinker. A more common combustion system has multiple burners in a rectangular geometry (see [Figure 1.16](#)). This type of system is generally more difficult to analyze because of the multiplicity of heat sources and because of the interactions between the flames and their associated products of combustion.

There are many factors that go into the design of a burner. This section briefly considers some of the important factors that are taken into account for a particular type of burner. These factors affect things such as heat transfer and pollutant emissions. There have been many changes in the traditional designs used in burners, primarily because of the recent interest in reducing pollutant emissions. In the past, the burner designer was primarily concerned with efficiently combusting the fuel and transferring the energy to a heat load. New and increasingly more stringent environmental regulations have added the requirement to consider the pollutant emissions produced by the burner. In many cases, reducing pollutant emissions and maximizing combustion efficiency are at odds with each other. For example, a well-accepted technique for reducing NO_x emissions is known as staging, where the primary flame zone is deficient in either fuel or oxidizer.³⁰ The balance of fuel or oxidizer can be injected into the burner in a secondary flame zone or, in a more extreme

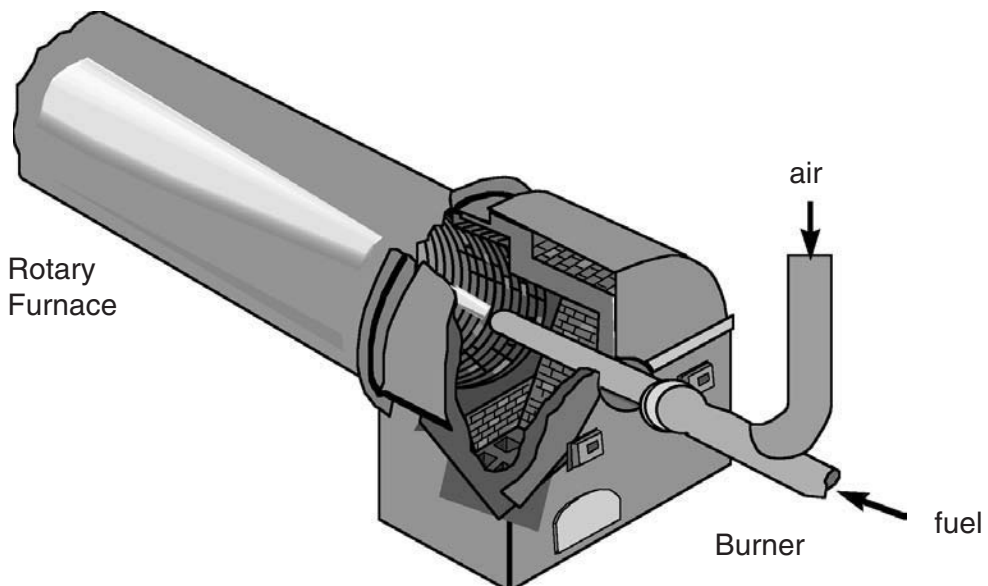


FIGURE 1.15 Rotary kiln with single burner.²⁹

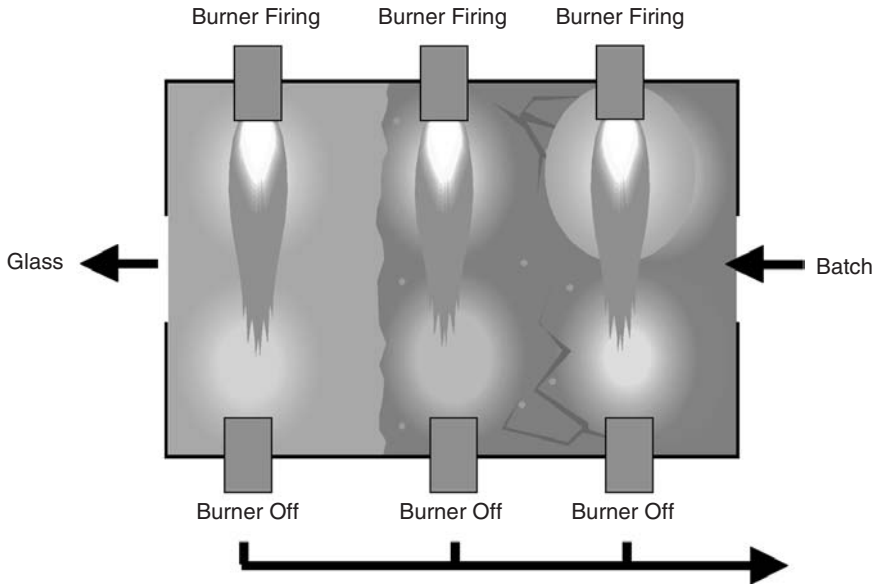


FIGURE 1.16 Plan view of multiple burners in a glass furnace.²⁹

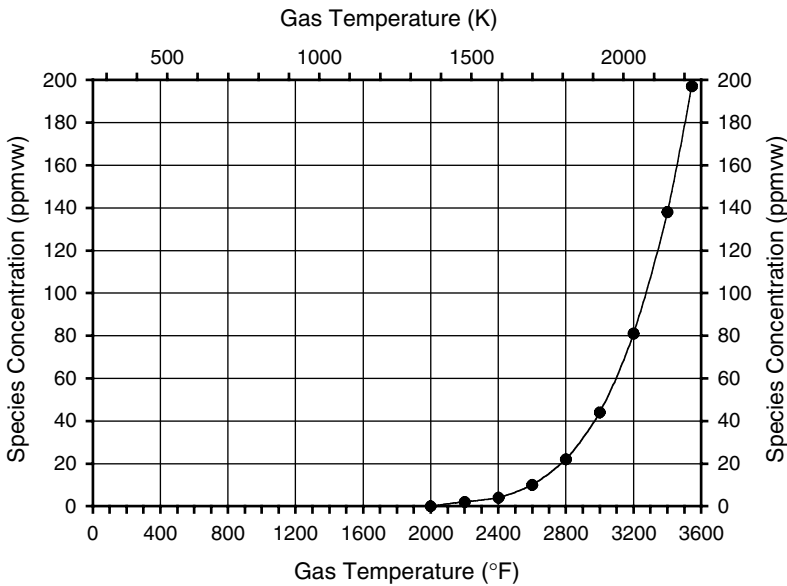


FIGURE 1.17 NO_x as a function of gas temperature.²⁹

case, can be injected somewhere else in the combustion chamber. Staging reduces the peak temperatures in the primary flame zone and also alters the chemistry in a way that reduces NO_x emissions because fuel-rich or fuel-lean zones are less conducive to NO_x formation than near-stoichiometric zones. Figure 1.17 shows how the NO_x emissions are affected by the exhaust product temperature. Because thermal NO_x is exponentially dependent on the gas temperature, even small reductions in the peak flame temperature can dramatically reduce NO_x emissions. However, lower flame temperatures often reduce the radiant heat transfer from the flame because radiation is

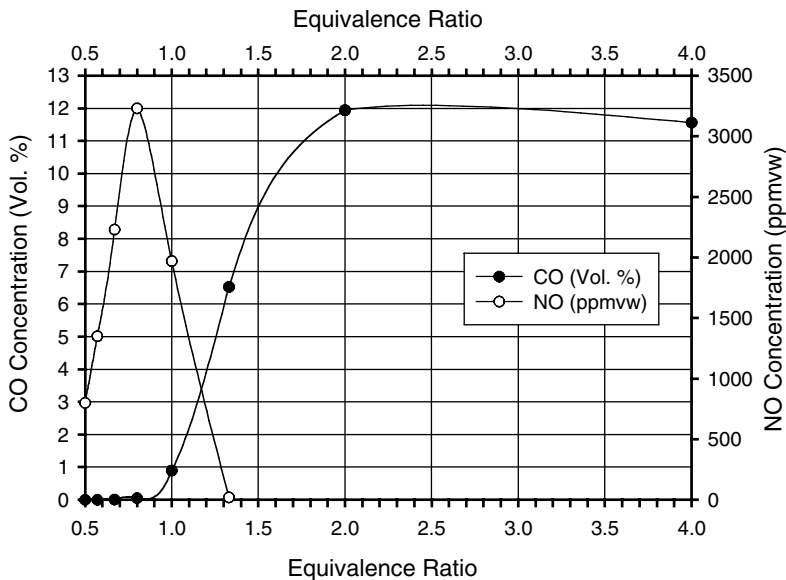


FIGURE 1.18 NOx and CO as a function of stoichiometry.²⁹

dependent on the fourth power of the absolute temperature of the gases. Another potential problem with staging is that it may increase CO emissions, which is an indication of incomplete combustion and reduced combustion efficiency. However, it is also possible that staged combustion can produce soot in the flame, which can increase flame radiation. The actual impact of staging on the heat transfer from the flame is highly dependent on the actual burner design.

In the past, the challenge for the burner designer was often to maximize the mixing between the fuel and the oxidizer to ensure complete combustion, especially if the fuel was difficult to burn, as in the case of low heating value fuels such as waste liquid fuels or process gases from chemicals production. Now, the burner designer must balance the mixing of the fuel and the oxidizer to maximize combustion efficiency while simultaneously minimizing all types of pollutant emissions. This is no easy task as, for example, NOx and CO emissions often go in opposite directions, as shown in Figure 1.18. When CO is low, NOx may be high and vice versa. Modern burners must be environmentally friendly, while simultaneously efficiently transferring heat to the load.

Many types of burner designs exist due to the wide variety of fuels, oxidizers, combustion chamber geometries, environmental regulations, thermal input sizes, and heat transfer requirements (including flame temperature, flame momentum, and heat distribution). Some of these design factors are briefly considered here. Other important design factors, such as heat transfer (Chapter 6), noise (Chapter 7), and controls (Chapter 8), are discussed elsewhere in the book. Some of the tools used to optimize burner design include computational fluid dynamic modeling (Chapter 5), testing (Chapter 9), and physical modeling (Chapter 10).

1.4.1 FUEL

Depending on many factors, certain types of fuels may be preferred for certain geographic locations due to cost and availability considerations. Gaseous fuels, particularly natural gas, are commonly used in most industrial heating applications in the United States. In Europe, natural gas is also commonly used along with light fuel oil. In Asia and South America, heavy fuel oils are generally preferred although the use of gaseous fuels is on the rise. Fuels also vary depending on the application. For example, in incineration processes, waste fuels are commonly used either by themselves or with other

fuels such as natural gas. In the petrochemical industry, fuel gases often consist of a blend of several fuels, including gases such as hydrogen, methane, propane, butane, and propylene.

The fuel choice has an important influence on the heat transfer from a flame. In general, solid fuels (e.g., coal) and liquid fuels (e.g., oil) produce very luminous flames that contain soot particles that radiate like blackbodies to the heat load. Gaseous fuels such as natural gas often produce nonluminous flames because they burn so cleanly and completely without producing soot particles. A fuel such as hydrogen is completely nonluminous as there is no carbon available to produce any soot. In cases where highly radiant flames are required, a luminous flame is preferred. In cases where convection heat transfer is preferred, a nonluminous flame may be preferred in an effort to minimize the possibility of contaminating the heat load with soot particles from a luminous flame. Where natural gas is the preferred fuel and highly radiant flames are desired, new technologies are being developed to produce more luminous flames. These include pyrolyzing the fuel in a partial oxidation process,³¹ using a plasma to produce soot in the fuel,³² and generally controlling the mixing of the fuel and oxidizer to produce fuel-rich flame zones that generate soot particles.³³ Therefore, the fuel itself has a significant impact on the heat transfer mechanisms between the flame and the load. In most cases, the fuel choice is dictated by the customer as part of the specifications for the system and is not chosen by the burner designer. The designer must make the best of whatever fuel has been selected. In most cases, the burner design is optimized based on the choice for the fuel.

The fuel also has a large impact on pollutant emissions. For example, gaseous fuels generally contain little or no sulfur so SO_x emissions are usually small. However, heavy oils often contain significant quantities of sulfur and therefore SO_x emissions are of concern and need to be controlled. Another example is particulate emissions. Gaseous fuels generally burn very cleanly and produce negligible particulates. However, heavy liquid oil fuels can generate high levels of particulate emissions. Therefore, burner design is important in minimizing pollutant emissions, depending on the fuel.

In some cases, the burner may have more than one type of fuel. An example is shown in Figure 1.19.³⁴ Dual-fuel burners are typically designed to operate on either gaseous or liquid fuels. These burners are used where the customer may need to switch between a gaseous fuel (e.g., natural gas) and a liquid fuel (e.g., oil), usually for economic reasons. These burners normally operate on one fuel or the other, and occasionally on both fuels simultaneously. Another application in which

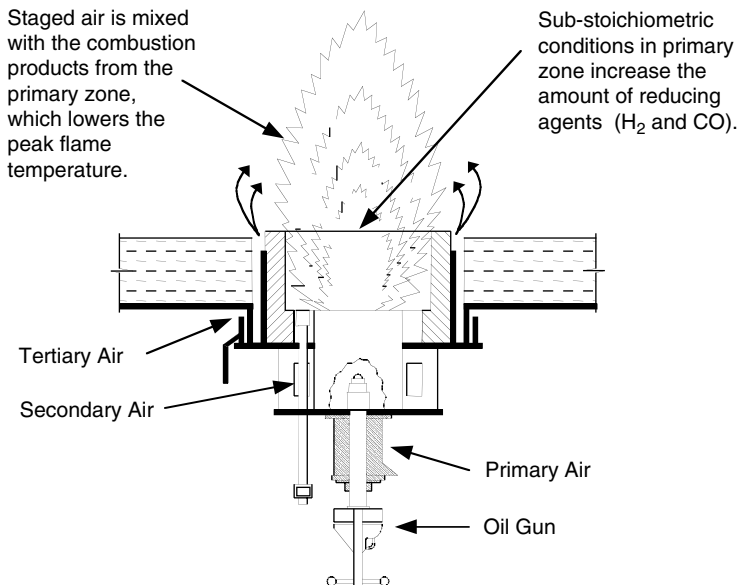
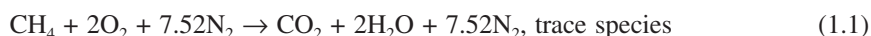


FIGURE 1.19 Dual fuel burner. (Courtesy of John Zink Co., LLC.³⁶)

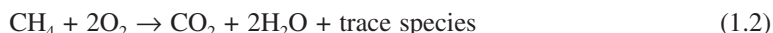
multiple fuels might be used is in waste incineration. One method of disposing of waste liquids contaminated with hydrocarbons is to combust them by direct injection through a burner. The waste liquids are fed through the burner, which is powered by a traditional fuel such as natural gas or oil. The waste liquids often have very low heating values and are difficult to combust without auxiliary fuel. This further complicates the burner design, where the waste liquid must be vaporized and combusted concurrently with the normal fuel used in the burner.

1.4.2 OXIDIZER

The predominant oxidizer used in most industrial heating processes is atmospheric air. This can present challenges in some applications where highly accurate control is required due to the daily variations in the barometric pressure and humidity of ambient air. The combustion air is sometimes preheated and sometimes blended with some of the combustion products, which is usually referred to as flue gas recirculation (FIGR). In certain cases, preheated air is used to increase the overall thermal efficiency of a process. FIGR is often used to both increase thermal efficiency and to reduce NO_x emissions. The thermal efficiency is increased by capturing some of the energy in the exhaust gases that are used to preheat the incoming combustion oxidizer. NO_x emissions may also be reduced because the peak flame temperatures are reduced, which can reduce the NO_x emissions, which are highly temperature dependent. There are also many high-temperature combustion processes that use an oxidizer containing a higher proportion of oxygen than the 21% (by volume) found in normal atmospheric air. This is referred to as oxygen-enhanced combustion (OEC) and has many benefits, including increased productivity and thermal efficiency while reducing the exhaust gas volume and pollutant emissions.⁵ A simplified global chemical reaction for the stoichiometric combustion of methane with air is given as follows:



This compares to the same reaction where the oxidizer is pure O₂ instead of air:



The volume of exhaust gases is significantly reduced by the elimination of N₂. In general, a stoichiometric oxygen-enhanced methane combustion process can be represented by:



where $0 \leq x \leq 7.52$, depending on the oxidizer. The N₂ contained in air acts as a ballast that may inhibit the combustion process and have negative consequences. The benefits of using oxygen-enhanced combustion must be weighed against the added cost of the oxidizer, which in the case of air is essentially free except for the minor cost of the air handling equipment and power for the blower. The use of a higher-purity oxidizer has many consequences with regard to heat transfer from the flame and pollutant emissions generated. These are considered elsewhere in the book. Oxygen-enhanced combustion is considered in more detail in Chapters 20 and 21.

1.4.3 GAS RECIRCULATION

A common technique used in combustion systems is to design the burner to induce furnace gases to be drawn into the burner to dilute the flame, usually referred to as furnace gas recirculation (FuGR). Although the furnace gases are hot, they are still much cooler than the flame itself. This dilution may accomplish several purposes. One is to minimize NO_x emissions by reducing the peak temperatures in the flame, as in FIGR (see [Figure 1.20](#)). However, furnace gas recirculation may be preferred to FIGR because no external high-temperature ductwork or

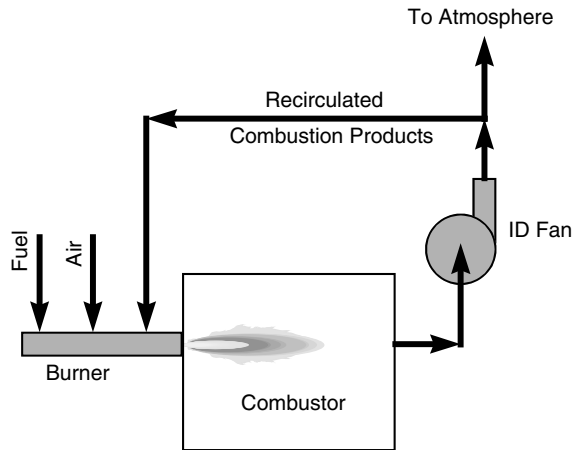


FIGURE 1.20 Schematic of flue gas recirculation.²⁹

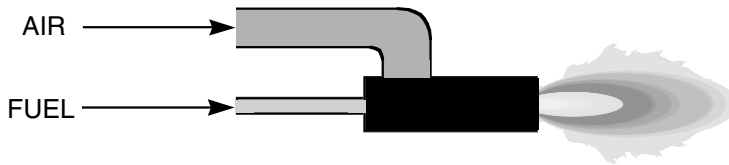


FIGURE 1.21 Diagram of a premixed burner.²⁹

fans are needed to bring the product gases into the flame zone. Another reason to use furnace gas recirculation may be to increase the convective heating from the flame because of the added gas volume and momentum. An example of flue gas recirculation into the burner is given in Figure 1.20.³⁵ A specific type of burner incorporating furnace gas recirculation is called a regenerative burner (see Chapter 12).

1.5 GENERAL BURNER CLASSIFICATIONS

There are numerous ways to classify burners. Some common ones are discussed below, with a brief consideration as to how burner performance is impacted.

1.5.1 MIXING TYPE

One common method for classifying burners is according to how the fuel and the oxidizer are mixed. In premixed burners, shown in the diagram in Figure 1.21 and schematically in Figure 1.22, the fuel and the oxidizer are completely mixed before combustion begins. Thermal radiation burners (Chapter 13) and radiant wall burners (Chapter 15) usually are of the premixed type. Premixed burners often produce shorter and more intense flames, as compared to diffusion flames. This can produce high-temperature regions in the flame, leading to nonuniform heating of the load and higher NO_x emissions, although this is very dependent on the specific design. However, in flame impingement heating, premixed burners are useful because the higher temperatures and shorter flames can enhance the heating rates.

In diffusion-mixed burners, shown schematically in Figure 1.23, the fuel and the oxidizer remain separated and unmixed prior to combustion, which begins where the oxidizer/fuel mixture is within the flammability range (assuming the temperature is high enough for ignition). Oxygen/fuel burners (see Chapter 21) are usually diffusion burners, primarily for safety reasons, to prevent flashback

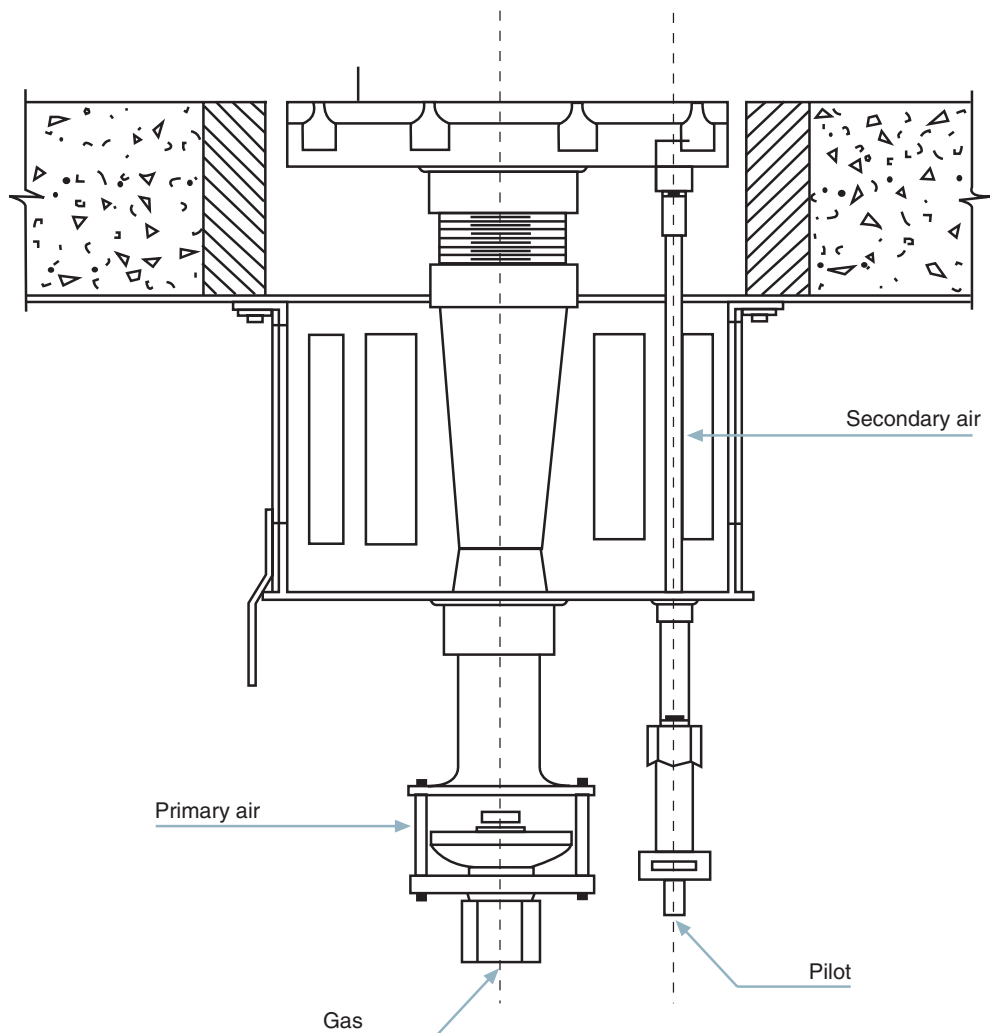


FIGURE 1.22 Schematic of a premixed burner. (Courtesy of John Zink Co., LLC.³⁶)

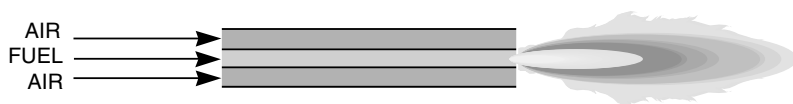


FIGURE 1.23 Schematic of a diffusion-mixed burner.²⁹

and explosion in a potentially dangerous system. Diffusion gas burners are sometimes referred to as “raw gas” burners, as the fuel gas exits the burner essentially intact with no oxidant mixed with it. Diffusion burners typically have longer flames than premixed burners, do not have as high temperature a hot spot, and usually have a more uniform temperature and heat flux distribution. They may also have lower NO_x emissions although, again, this is design dependent.

It is also possible to have partially premixed burners, shown schematically in [Figure 1.24](#) and [Figure 1.25](#), where a portion of the fuel is mixed with the oxidizer prior to exiting the burner. This is often done for stability and safety reasons, wherein the partial premixing helps anchor the flame, while

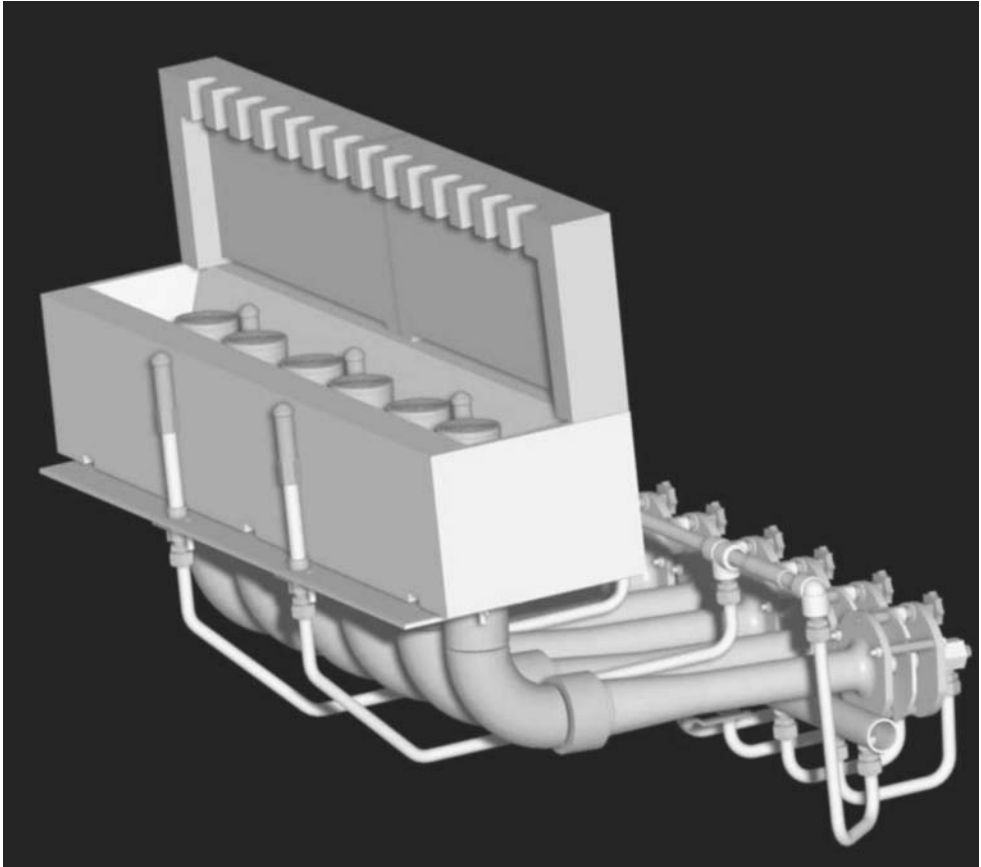


FIGURE 1.24 Partially premixed burner (Courtesy of John Zink Co., LLC).

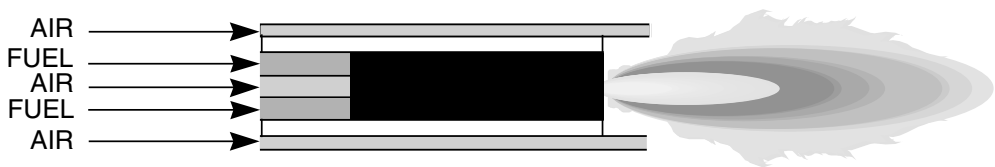


FIGURE 1.25 Schematic of a partially premixed burner.²⁹

not fully premixing lessens the chance for flashback. This type of burner often has a flame length and temperature and heat flux distribution that is between the fully premixed and diffusion flames.

Another burner classification based on mixing is known as staging: staged air and staged fuel. A staged air burner is shown in the diagram in [Figure 1.26](#) and schematically in [Figure 1.27](#). A staged fuel burner is shown in the diagram in [Figure 1.28](#) and schematically in [Figure 1.29](#). Secondary and sometimes tertiary injectors in the burner are used to inject a portion of the fuel and/or the oxidizer into the flame, downstream of the root of the flame. Staging is often done to control heat transfer, produce longer flames, and reduce pollutant emissions such as NO_x. These longer flames typically have a lower peak flame temperature and more uniform heat flux distribution than nonstaged flames. However, an additional challenge is that multiple longer flames might interact with each other and produce unpredictable consequences compared to single shorter flames.

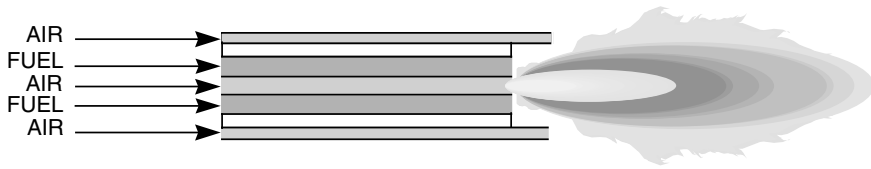


FIGURE 1.26 Diagram of a staged-air burner.²⁹

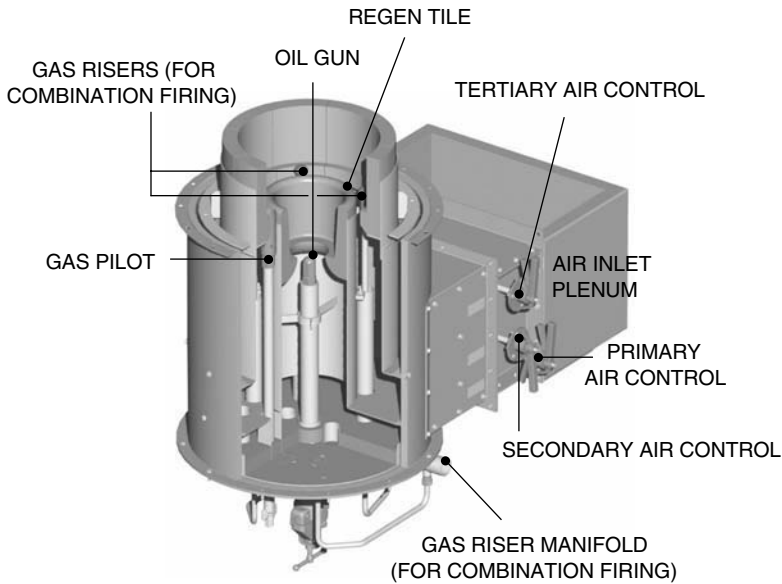


FIGURE 1.27 Schematic of a staged-air process. (Courtesy of John Zink Co., LLC.³⁶)

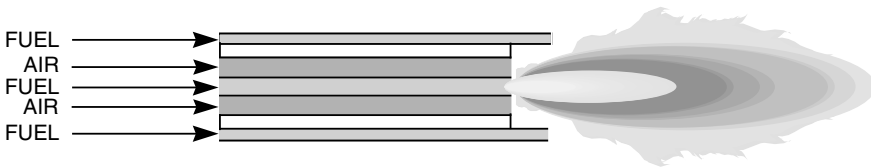


FIGURE 1.28 Diagram of a staged fuel burner.²⁹

1.5.2 FUEL TYPE

Burners can also be classified according to fuel type. Gaseous fuel burners are the predominant type used in most of the applications considered here. In general, natural gas is the predominant gaseous fuel used because of its low cost and availability. However, a wide range of gaseous fuels are used in, for example, the chemicals industry.³⁶ These fuels contain multiple components such as methane, hydrogen, propane, nitrogen, and carbon dioxide and are sometimes referred to as refinery fuel gases. Figure 1.30 shows an example of a typical nonluminous gaseous flame from a burner used in the petrochemical industry. Gaseous fuels are among the easiest to control because no vaporization is required, as is the case for liquid and solid fuels. They are also often simpler to control to minimize pollution emissions because they are more easily staged compared to liquid and solid fuels. Table 1.4 shows typical data for the combustion of common hydrocarbons.

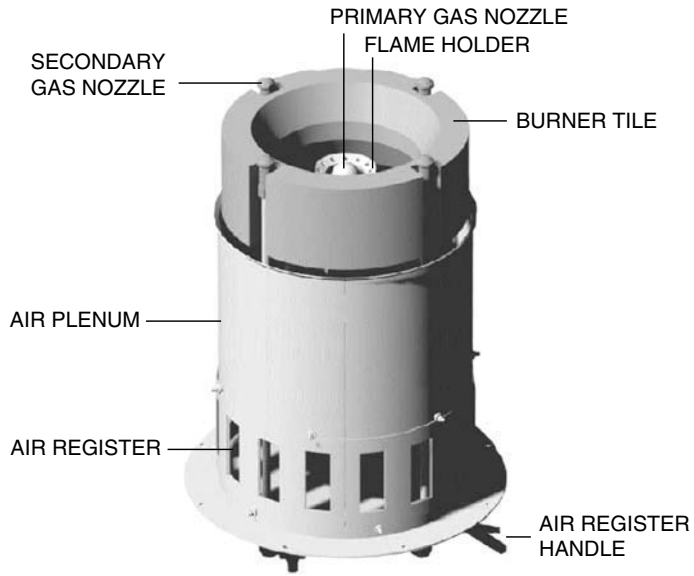


FIGURE 1.29 Schematic of a staged fuel burner.²⁹



FIGURE 1.30 Typical nonluminous flame. (Courtesy of John Zink Co., LLC.³⁶)

TABLE 1.4
Combustion Data for Common Hydrocarbons²

Hydrocarbon	Formula	Higher Heating Value, Vapor (Btu/lb _m)	Theor. Air/Fuel Ratio, by mass	Max. Flame Speed (ft/s)	Adiabatic Flame Temp., in Air (°F)	Ignition Temp., in Air (°F)	Flash Point (°F)	Flammability Limits, in Air (% by volume)	
Paraffins or Alkanes									
Methane	CH ₄	23875	17.195	1.1	3484	1301	(gas)	5.0	15.0
Ethane	C ₂ H ₆	22323	15.899	1.3	3540	968–1166	(gas)	3.0	12.5
Propane	C ₃ H ₈	21669	15.246	1.3	3573	871	(gas)	2.1	10.1
<i>n</i> -Butane	C ₄ H ₁₀	21321	14.984	1.2	3583	761	-76	1.86	8.41
<i>Iso</i> -Butane	C ₄ H ₁₀	21271	14.984	1.2	3583	864	-117	1.80	8.44
<i>n</i> -Pentane	C ₅ H ₁₂	21095	15.323	1.3	4050	588	<-40	1.40	7.80
<i>iso</i> -Pentane	C ₅ H ₁₂	21047	15.323	1.2	4055	788	<-60	1.32	9.16
Neopentane	C ₅ H ₁₂	20978	15.323	1.1	4060	842	(gas)	1.38	7.22
<i>n</i> -Hexane	C ₆ H ₁₄	20966	15.238	1.3	4030	478	-7	1.25	7.0
Neohexane	C ₆ H ₁₄	20931	15.238	1.2	4055	797	-54	1.19	7.58
<i>n</i> -Heptane	C ₇ H ₁₆	20854	15.141	1.3	3985	433	25	1.00	6.00
Triptane	C ₇ H ₁₆	20824	15.141	1.2	4035	849	—	1.08	6.69
<i>n</i> -Octane	C ₈ H ₁₈	20796	15.093	—	—	428	56	0.95	6.20
<i>iso</i> -Octane	C ₈ H ₁₈	20770	15.093	1.1	—	837	10	0.79	5.94
Olefins or Alkenes									
Ethylene	C ₂ H ₄	21636	14.807	2.2	4250	914	(gas)	2.75	28.6
Propylene	C ₃ H ₆	21048	14.807	1.4	4090	856	(gas)	2.00	11.1
Butylene	C ₄ H ₈	20854	14.807	1.4	4030	829	(gas)	1.98	9.65
<i>iso</i> -Butene	C ₄ H ₈	20737	14.807	1.2	—	869	(gas)	1.8	9.0
<i>n</i> -Pentene	C ₅ H ₁₀	20720	14.807	1.4	4165	569	—	1.65	7.70
Aromatics									
Benzene	C ₆ H ₆	18184	13.297	1.3	4110	1044	12	1.35	6.65
Toluene	C ₇ H ₈	18501	13.503	1.2	4050	997	40	1.27	6.75
<i>p</i> -Xylene	C ₈ H ₁₀	18663	13.663	—	4010	867	63	1.00	6.00
Other Hydrocarbons									
Acetylene	C ₂ H ₂	21502	13.297	4.6	4770	763–824	(gas)	2.50	81
Naphthalene	C ₁₀ H ₈	17303	12.932	—	4100	959	174	0.90	5.9

Liquid fuel burners are used in some limited applications, but are more prevalent in certain areas of the world such as South America. No. 2 and no. 6 oil are the most commonly used liquid fuels. Waste liquid fuels are also used in incineration processes. One of the specific challenges of using oils is vaporizing the liquid into small enough droplets to burn completely. Improper atomization produces high unburned hydrocarbon emissions and reduces fuel efficiency. Steam and compressed air are commonly used to atomize liquid fuels. The atomization requirements often reduce the options for modifying the burner design to reduce pollutant emissions. Another challenge is that liquid fuel oils often contain impurities such as nitrogen and sulfur that produce pollution emissions. In the case of fuel-bound nitrogen, so-called fuel NO_x emissions increase. In the case of sulfur, essentially all of the sulfur in a liquid fuel converts to SO_x emissions.

Solid fuels are not commonly used in most industrial combustion applications. The most common solid fuels are coal and coke. Coal is used in power generation and coke is used in some primary metals production processes. However, neither is considered a traditional industrial combustion process and therefore is not considered here. Another type of pseudo solid fuel is sludge that is processed in incinerators. Solid fuels also often contain impurities such as nitrogen and sulfur that can significantly increase pollutant emissions. Some solid fuels may also contain hazardous chemicals that can produce carcinogenic pollution emissions. Because solid fuels are not used frequently in the applications considered, they are only discussed in those specific cases.

There are some applications that require the burner to be able to fire on a gaseous fuel such as natural gas, a liquid fuel such as fuel oil, or both simultaneously. This is generally due to the economics of the fuel costs. In some locations, a more favorable fuel cost rate can be obtained, for example, on natural gas, if the supply can be interrupted with sufficient notice. The backup fuel is typically fuel oil. These dual-fuel burners have special challenges because of significant differences in the design of gaseous and liquid burners.

1.5.3 OXIDIZER TYPE

Burners and flames are often classified according to the type of oxidizer that is used. The majority of industrial burners use air for combustion. In many of the higher-temperature heating and melting applications, such as glass production, the oxidizer is pure oxygen. These burner types are discussed in Chapter 21. In other applications, the oxidizer is a combination of air and oxygen, often referred to as oxygen-enriched air combustion. These burner types are discussed in Chapter 20.

Figure 1.31 shows a schematic of an air/fuel burner, which is the most commonly used type in industrial combustion applications. In most cases, the combustion is supplied by a fan or blower, although there are many applications in the petrochemical industry where natural-draft burners are commonly used (see Chapter 16). There are numerous variations of air/fuel burners and these are discussed throughout this book.

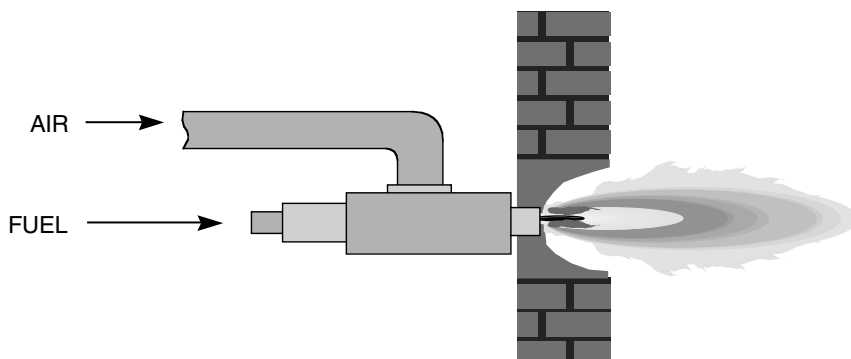


FIGURE 1.31 Schematic of an air/fuel burner.²⁹

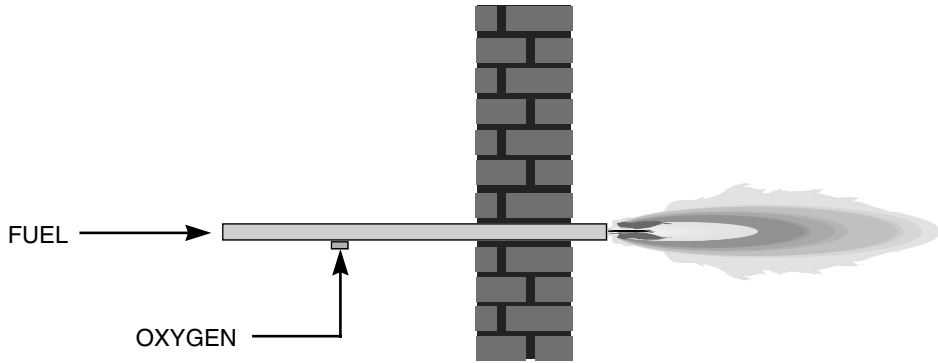


FIGURE 1.32 Schematic of an oxy/fuel burner.⁵

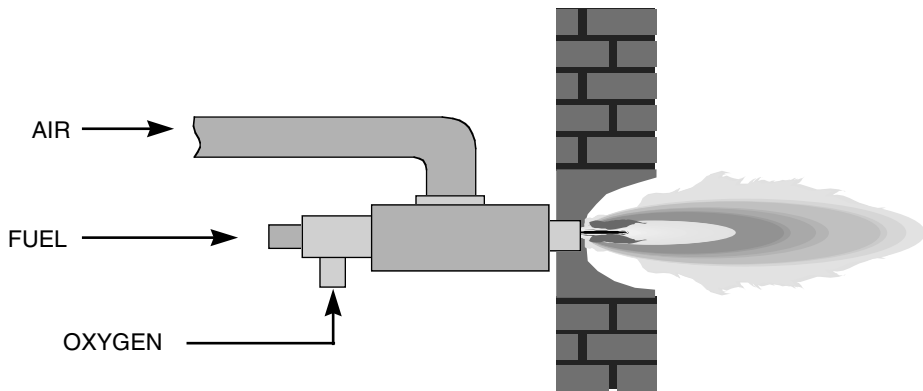


FIGURE 1.33 Schematic of an air-oxy/fuel burner.⁵

Figure 1.32 shows a method of using OEC and commonly referred to as an oxy/fuel burner. In nearly all cases, the fuel and the oxygen remain separated inside the burner. They do not mix until reaching the outlet of the burner. This is commonly referred to as a nozzle-mix burner, which produces a diffusion flame. For safety reasons, there is no premixing of the gases. Because of the extremely high reactivity of pure O_2 , there is the potential for an explosion if the gases are premixed. In this method, high-purity O_2 (>90% O_2 by volume) is used to combust the fuel. As discussed later, there are several ways of generating the O_2 . In an oxy/fuel system, the actual purity of the oxidizer will depend on which method has been chosen to generate the O_2 . As shown later, oxy/fuel combustion has the greatest potential for improving a process, but it also may have the highest operating cost.

Figure 1.33 shows an air/fuel process in which the air is enriched with O_2 . This can be referred to as low-level O_2 enrichment, or premix enrichment. Many conventional air/fuel burners can be adapted for this technology.³⁷ The O_2 is injected into the incoming combustion air supply, usually through a diffuser to ensure adequate mixing. This is usually an inexpensive retrofit that can provide substantial benefits. Typically, the added O_2 will shorten and intensify the flame. However, there may be some concern if too much O_2 is added to a burner designed for air/fuel. The flame shape may become unacceptably short. The higher flame temperature may damage the burner or burner block. The air piping may need to be modified for safety reasons to handle higher levels of O_2 .

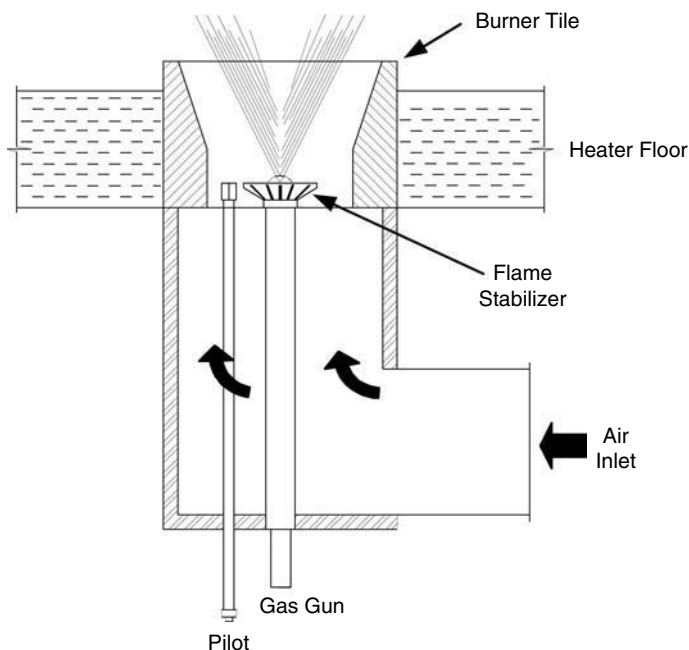


FIGURE 1.34 Schematic of a natural-draft burner. (Courtesy of John Zink Co., LLC.³⁶)

1.5.4 DRAFT TYPE

Most industrial burners are known as forced-draft burners. This means that the oxidizer is supplied to the burner under pressure. For example, in a forced-draft air burner, the air used for combustion is supplied to the burner by a blower. In natural-draft burners (see Chapter 16), the air used for combustion is induced into the burner by the negative draft produced in the combustor and by the motive force of the incoming fuel, which may be at a significant pressure. A schematic is shown in Figure 1.34 and an example is shown in Figure 1.35. In this type of burner, the pressure drop and combustor stack height are critical in producing enough suction to induce sufficient combustion air into the burners. This type of burner is commonly used in the chemical and petrochemical industries in fluid heaters. The main consequence of the draft type on burner performance is that the natural-draft flames are usually longer than the forced-draft flames so that the heat flux from the flame is distributed over a longer distance and the peak temperature in the flame is often lower.

1.5.5 HEATING TYPE

Burners are often classified as to whether they are of the direct (see Figure 1.36) or indirect heating type (see Figure 1.37). In direct heating, there is no intermediate heat exchange surface between the flame and the load. In indirect heating, such as radiant tube burners (see Chapter 8), there is an intermediate surface between the flame and the load. This is usually done because the combustion products cannot come in contact with the load because of possible contamination.

Radiation heat transfer (see Chapter 2) from the flame to the product is the primary mode used in many industrial combustion systems (see Chapter 6). There are a variety of burner designs that rely primarily on this mechanism. Thermal radiation burners are discussed in Chapter 13. Radiant tube burners are discussed in Chapter 14. Radiant wall burners are discussed in Chapter 15. Other burner designs discussed throughout this book also use thermal radiation as the primary heat transfer mechanism.

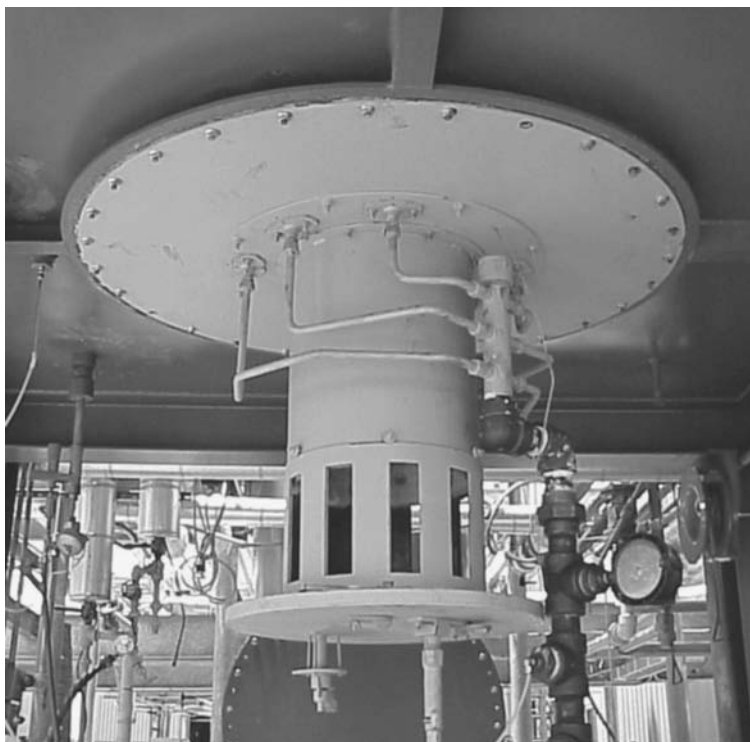


FIGURE 1.35 Photo of a natural-draft burner. (Courtesy of John Zink Co., LLC.²⁹)

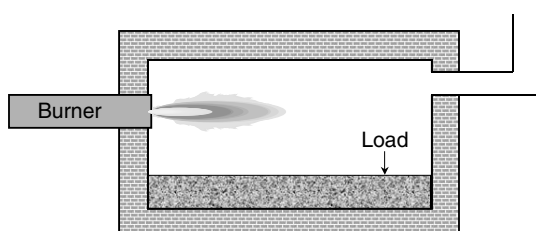


FIGURE 1.36 Direct fired process.

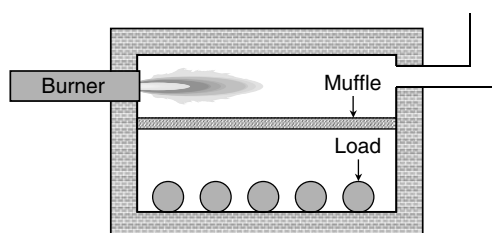


FIGURE 1.37 Indirect fired process.

Forced convection (see Chapter 2) is the other predominant mechanism for transferring heat from flames to a load. For example, high-velocity burners are considered in Chapter 11. These are particularly useful in applications where primarily radiant heating may overheat the surface with much less energy getting inside the load. An example would be heating a pile of scrap metal. Highly radiant heating could melt the outside of the pile and cause excessive oxidation, leading to

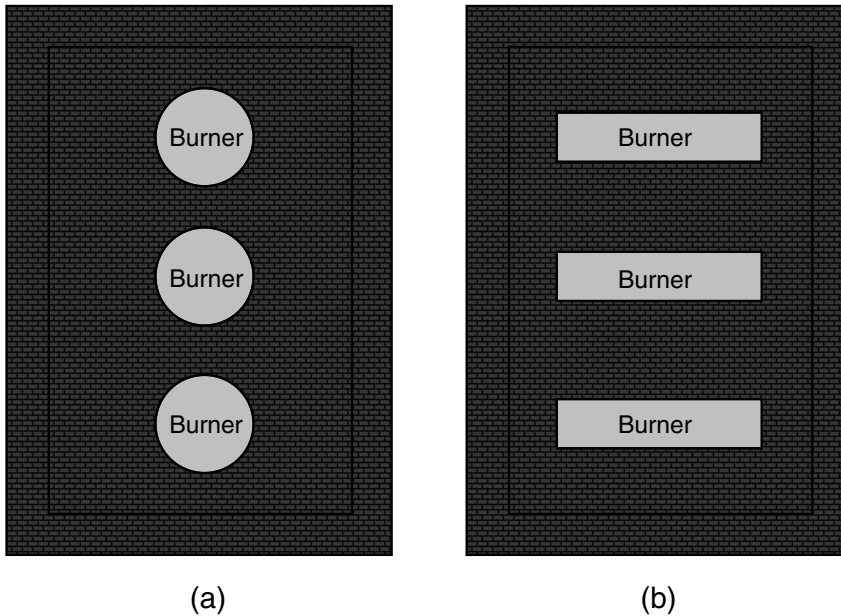


FIGURE 1.38 Round (a) and rectangular (b) burner shapes in identical combustors.

high metal yield losses. Convective heating can penetrate inside the load to cause more uniform heating. In certain applications, high-velocity burners may not be preferred because the materials being heated may contain fine particles that can easily become airborne. An example is glass manufacturing, where the incoming batch materials contain fine powders.

1.5.6 BURNER GEOMETRY

There are two primary shapes for the outlet nozzle of industrial burners: round or rectangular. [Figure 1.38](#) shows identical heaters with the same number of burners but with different burner shapes: round flame and flat flame. These are briefly considered next.

Round flames are the predominant shape used in industry. Most of the burners discussed in this book are predominantly round. This is often due to the lower cost of making round shapes compared to making rectangular shapes. It is also often due to the burner tile; round shapes generally require less maintenance compared to rectangular tiles, which have corners that are more susceptible to cracking. Another reason may be due to more preferred flow patterns inside round burner plenums compared to rectangular shapes.

Rectangular shapes are sometimes preferred in certain applications, depending on the geometry of the combustor and the load. Burners with a fairly high aspect ratio (length to width) are sometimes referred to as “flat” flame burners because the flame shape appears to be flat. One example is in ethylene cracking furnaces where flat-shaped burners fire up along a refractory wall to heat the wall to radiate to tubes opposite that wall. Another example is in glass furnaces where flat-shaped flames fire over the molten glass; these flat shapes often give better flame coverage, more uniform heating, and better thermal efficiency.

1.6 BURNER COMPONENTS

There are several important components briefly considered here that impact the burner design.

The *ignition system* is an important component in the burner system to ensure safe and reliable operation. The ignition system is often built into the burner, but in some cases it may be separate

from the burner. The system may be fully automatic or completely manual. Different types of ignitors are available. In many cases, a pilot is used to ignite the main flame. This may be continuous or interruptible, depending on the system design. The pilot may be permanent or removable, and may be ignited by something like a spark-ignitor or by an external torch. Pilots require a separate fuel supply and are typically premixed.

Plenums are used to homogenize the incoming gas flows to evenly distribute them to the outlet of the burner. This is important to ensure proper operation of the burner over the entire range of operating conditions, especially at turndown. These gases may include combustion air, premixed fuel and air, or partially premixed fuel and air. If the plenum is too large, then the flows may be unevenly distributed across the burner nozzle outlet. If the plenum is too small, then the pressure drop through the plenum may be excessive.

The *burner tile*, sometimes referred to as a *block* or *quarl*, is an important component because it helps shape the flame and protects the internal parts from overheating. In the majority of designs, the burner tile is made of some type of ceramic that often contains alumina and silica, depending on the temperature requirements. The burner tile can also play an important role in the ignition and fluid dynamics of the combustion process. The tile may have bluff body components that enhance flame stability. There may be holes through the tile to enhance mixing of furnace gases with the gases fed into the burner. Advances in ceramics and manufacturing processes have led to increasingly more complicated burner tiles.

Controls refer not to the control equipment for the flows coming to the burner, but to controls that may be on the burner. For example, there is often a damper built into natural-draft burners (see Chapter 16) to control the incoming air flow and the furnace draft. Other controls on a burner may be for adjusting the distribution of fuels or air throughout the burner. For example, if a burner has multiple fuel injectors, particularly for fuel staging, controls on the burner can be used to control how much fuel goes to each injector. Chapter 8 has a detailed discussion of the controls leading up to the burner.

The *flame safety system* is critical to the safe operation of the combustion system. This may include some type of flame scanner or flame rod to ensure that either the burner or the pilot is operating. These are connected to the fuel supply system so that the fuel flow will be stopped if the flame goes out to prevent a possible explosion for unignited fuel gases contacting a hot surface somewhere in the combustor. This is also discussed in Chapter 8.

1.7 COMBUSTORS

This section briefly introduces the combustors that are commonly used in industrial heating and melting applications.

1.7.1 DESIGN CONSIDERATIONS

There are many important factors that must be considered when designing a combustor. This section only briefly considers a few of those factors and how they might influence the heat transfer in the system.

1.7.1.1 Load Handling

A primary consideration for any combustor is the type of material that will be processed. The various types of loads are considered later in this chapter. One obvious factor of importance in handling the load and transporting it through the combustor is its physical state — whether it is a solid, liquid, or gas. Another factor is the transport properties of the load. For example, the solid may be granular or it might be in the form of a sheet (web). Related to that is how the solid will be fed into the combustor. A granular solid could be fed continuously into a combustor with a

screw conveyor or it could be fed in with discrete charges from a front-end loader. The shape of the furnace will vary according to how the material will be transported through it. For example, limestone is fed continuously into a rotating and slightly downward-inclined cylinder.

1.7.1.2 Temperature

Industrial heating applications can be divided into two categories: higher and lower temperatures. The division between the two is somewhat arbitrary but mainly concerns the different types of applications used in each. For example, most metal and glass melting applications fall into the higher-temperature categories as the furnace temperatures are often well over 2000°F (1400K). They use technologies such as air preheating and oxygen enrichment (see Chapters 20 and 21) to achieve those higher temperatures. Lower-temperature applications include dryers, process heaters, and heat treating and are typically below about 2000°F (1400K). Although many of these processes use air preheating, it is primarily employed to improve the thermal efficiency and not to get higher flame temperatures. Those processes rarely use oxygen enrichment, which usually only works economically for higher-temperature processes. Both the combustors and the burners are designed differently for higher- and lower-temperature processes. The heat transfer and pollutant generation mechanisms are often different as well. In higher-temperature processes, the primary mode is often radiation, while in lower-temperature applications, convection often plays a significant role. NO_x emissions, for example, are much more significant at higher temperatures compared to lower temperatures.

1.7.1.3 Heat Recovery

When heat recovery is used in an industrial combustion process, it is an integral part of the system. The two most popular methods are regenerative and recuperative. The heat recovery system is important in the design of the combustor as it determines the thermal efficiency of the process and the flame temperatures in the system. It also influences the heat transfer modes, as it can increase both the radiation and convection because of higher flame temperatures. Another type of heat recovery used in some processes is furnace or flue gas recirculation, where the exhaust products are recirculated back through the flame. This also influences the heat transfer and furnace design because it can moderate the flame temperature but increase the volume flow of gases through the combustion chamber.

1.7.2 GENERAL CLASSIFICATIONS

There are several ways that a combustor can be classified and these are briefly discussed in this section. Each type has an impact on the heat transfer mechanisms in the furnace.

1.7.2.1 Load Processing Method

Furnaces are often classified as to whether they are *batch* or *continuous*. In a batch furnace, the load is charged into the furnace at discrete intervals where it is heated. There may be multiple load charges, depending on the application. Normally, the firing rate of the burners is reduced or turned off during the charging cycle. On some furnaces, a door may also need to be opened during charging. This significantly impacts the heat transfer in the system as the heat losses during the charge cycle are very large. The radiation losses through open doors are high and the reduced firing rate may not be enough to maintain the desired furnace temperature. In some cases, the temperature on the inside of the refractory wall, closest to the load, may actually be lower than the temperature of the refractory at some distance from the inside, due to the heat losses during charging. The heating process and heat transfer are dynamic and constantly changing as a result of the cyclical nature of the load charging. The burners may cycle on and off or between high-fire

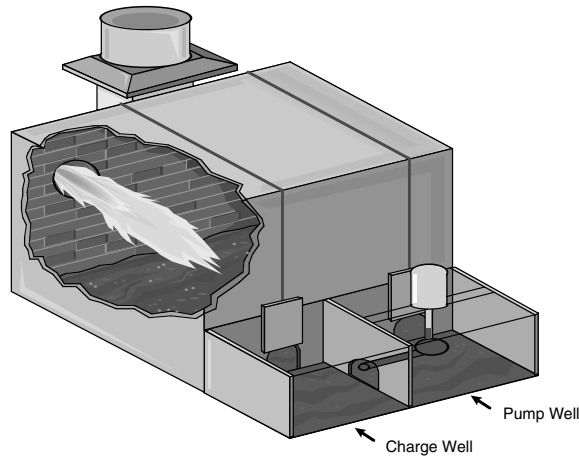


FIGURE 1.39 Aluminum reverberatory furnace.²⁹

and low-fire. This makes analysis of these systems more complicated because of the need to include time in the computations.

In a continuous furnace, the load is constantly fed into and out of the combustor. The feed rate can change, sometimes due to conditions upstream or downstream of the combustor or to the production needs of the plant, but the process is nearly steady-state. This makes continuous processes simpler to analyze, because there is no need to include time in the computations. It is often easier to make meaningful measurements in continuous processes due to their steady-state nature.

There are some furnaces that are semicontinuous, wherein the load can be charged in nearly continuous fashion, but the finished product can be removed from the furnace at discrete intervals. An example is an aluminum reverberatory furnace that is charged using an automatic side-well feed mechanism (see [Figure 1.39](#)). In that process, shredded scrap is continuously added to a circulating bath of molten aluminum. When the correct alloy composition has been reached and the furnace has a full load, some or all of that load is then tapped out of the furnace. The effect on heat transfer is somewhere between that for batch and continuous furnaces.

1.7.2.2 Heating Type

As described above for burners, combustors are often classified as *direct* (see [Figure 1.36](#)) or *indirect* (see [Figure 1.37](#)) heating. In indirect heating, there is some type of intermediate heat transfer medium between the flames and the load that keeps the combustion products separate from the load. One example is a muffle furnace where there is a high-temperature ceramic muffle between the flames and the load. The flames transfer their heat to the muffle, which then radiates to the load, which is usually some type of metal. The limitation of indirect heating processes is the temperature limit of the intermediate material. Although ceramic materials have fairly high temperature limits, other issues such as structural integrity over long distance spans and thermal cycling can still reduce the recommended operating temperatures. Another example of indirect heating is in process heaters, where fluids are transported through metal tubes that are heated by flames. Indirect heating processes often have fairly uniform heat flux distributions because the heat exchange medium tends to homogenize the energy distribution from the flames to the load. The heat transfer from the heat exchange surface to the load is often fairly simple and straightforward to compute because of the absence of chemical reactions in between. However, the heat transfer from the flames to the heat exchange surface and the subsequent thermal conduction through that surface are as complicated as if the flame was radiating directly to the load. Indirect heating may

also have the advantage of reducing pollutant emissions when contact of the high-temperature exhaust gases with the load could possibly generate pollutants.

As a result of the temperature limits of the heat exchange materials, most higher-temperature processes are of the direct heating type where the flames can directly radiate heat to the load.

1.7.2.3 Geometry

Another common way of classifying combustors is according to their geometry, which includes their shape and orientation. The two most common shapes are rectangular and cylindrical. The two most common orientations are horizontal and vertical, although inclined furnaces are commonly used in certain applications such as rotary cement furnaces. An example using the shape and orientation of the furnace as a means of classification would be a vertical cylindrical heater (sometimes referred to as a VC) used to heat fluids in the petrochemical industry. Both the furnace shape and orientation have important effects on heat transfer in the system. They also determine the type of analysis that will be used. For example, in a VC heater, it is often possible to model only a slice of the heater due to its angular symmetry, in which case cylindrical coordinates would be used. On the other hand, it is usually not reasonable to model a horizontal rectangular furnace using cylindrical coordinates, especially if buoyancy effects are important.

Some furnaces are classified on the basis of what they look like. An example is a shaft furnace used to make iron. The raw materials are loaded into the top of a tall, thin, vertically oriented cylinder. Hot combustion gases generated at the bottom, via combustion of coke, flow up through the raw materials, which get heated. The melted final product is tapped out of the bottom. The furnace looks and acts almost like a shaft because of the way the raw materials are fed in through the top and exit at the bottom. A transfer chamber used to move molten metal around in a steel mill is often referred to as a ladle because of its function and appearance. These ladles are preheated using burners before the molten metal is poured into them; this is done to prevent the refractory-lined vessels from thermally shocking.

Another aspect of the geometry that is important in some applications is whether or not the furnace is moving. For example, in a rotary furnace for melting scrap aluminum, the furnace rotates to enhance mixing and heat transfer distribution. This again affects the type of analysis that would be appropriate for that system and can add some complexity to the computations.

The burner orientation with respect to the combustor is also sometimes used to classify the combustor. For example, a wall-fired furnace has burners located in and firing along the wall.

1.7.2.4 Heat Recuperation

In many heat processing systems, energy recuperation is an integral part of the combustion system. Often, the heat recuperation equipment is a separate component of the system and not part of the burners themselves. Depending on the method used to recover the energy, the combustors are commonly referred to as either *recuperative* or *regenerative* (see discussion later in this chapter). The heat transfer in these systems is a function of the energy recovery system. For example, the higher the combustion air preheat temperature, the hotter the flame and the more radiant heat that can be produced by that flame. The convective heat transfer might also be increased due to the higher gas temperature and to the higher thermal expansion of the gases, which increases the average gas velocity through the combustor.

1.8 HEAT LOAD

This section is a brief introduction to some of the important issues concerning the heat load in a furnace or combustor. In petrochemical production processes, process heaters are used to heat petroleum products up to operating temperatures. The fluids are transported through the process heaters in process tubes. These heaters often have a radiant section and a convection section.

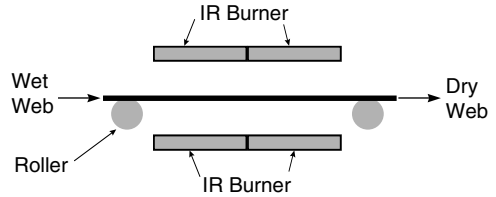


FIGURE 1.40 Elevation view of infrared burner heating a moving web.²⁹

In the radiant section, the radiation from burners heats the process tubes. In the convection section, the combustion products heat the tubes by flowing over the tubes. The design of the radiant section is especially important as flame impingement on the tubes can cause premature failure of the tubes or cause the hydrocarbon fluids to coke inside the tubes, which reduces the heat transfer to the fluids.

In some applications, heaters and burners are used to heat or dry moving substrates or webs. An example is shown in [Figure 1.40](#). One common application is the use of gas-fired infrared (IR) burners (see Chapter 13) to remove moisture from paper during the forming process.³⁸ These paper webs can travel at speeds over 300 m/s (1000 ft/s) and are normally dried by traveling over and contacting steam-heated cylinders. IR heaters are often used to selectively dry certain portions of the web that may be wetter than others. For example, if the target moisture content for the paper is 5%, then the entire width of the paper must have no more than 5% moisture. Streaks of higher moisture areas often occur in sections along the width of the paper. Without selectively drying such areas, the streaks would be dried to the target moisture level, which means that the rest of the sheet would be dried to even lower moisture levels. This creates at least two important problems. The first is lost revenue, because paper is usually sold on a weight basis. Any water unnecessarily removed from the paper decreases its weight and therefore results in lost income. Another problem is a reduction in the quality of the paper. If areas of the paper are too dry, they do not handle as well in devices such as copiers and printers, and are not nearly as desirable as paper of uniform moisture content. Therefore, selective drying of the paper only removes the minimum amount of water from the substrate. The challenge of this application is to measure the moisture content profile across the width of a sheet that may be several meters wide and moving at hundreds of meters per second. That information must then be fed to the control system for the IR heaters, which then must be able to react almost instantaneously. This is possible today because of advances in measurement and controls systems.

Another example of a moving substrate application is the use of IR burners to remove water during the production of fabrics in textile manufacturing.³⁹ Moving substrates present unique challenges for burners. Often, the material being heated can easily be set on fire if there is a line stoppage and the burners are not turned off quickly enough. This means that the burner control system must be interlocked with the web handling equipment so that the burners can be turned off immediately in the event of a line stoppage. If the burners have substantial thermal mass, then they may need to be retracted away from the substrate during a stoppage, or heat shields may need to be inserted between the burners and the substrate to prevent overheating.

Convection dryers are also used to heat and dry substrates. Typically, high-velocity heated air is blown at the substrate from both sides so that the substrate is elevated between the nozzles. In many cases, the heated air is used for both heat and mass transfer, to volatilize any liquids on or in the substrate such as water, and then carry the vapor away from the substrate.

An important aspect of heating webs is how the energy is transferred into the material. For example, dry paper is known to be a good insulator. When steam cylinders are used to heat and dry paper, they become less and less effective as the paper becomes drier because the heat from the cylinder cannot conduct through the paper as well as when it is moist (because the thermal conductivity of the paper increases with increasing moisture content). Infrared burners are effective for drying paper because the radiant energy transfers into the paper and is absorbed by the water. The radiant penetration into the paper actually increases as the paper becomes drier, unlike with

steam cylinders, which become less effective. Another important aspect related to burner design is the ability to cool down rapidly to prevent causing a fire, for example, when a paper web stops unexpectedly during processing due to some type of problem. An alternative is to shield the burner from the web in the event of a sudden line stoppage.

1.8.1 OPAQUE MATERIALS

This type of load encompasses a wide range of materials, including granular solids such as limestone and liquids such as molten metal. For this type of load, the heat transfers to the surface of the load and must conduct down into the material. This process can be enhanced by proper mixing of the materials so that new material is constantly exposed to the surface, as in rotary kilns or in aluminum reverberatory furnaces, which have molten metal pumps to continuously recirculate the metal through the heating zone. The potential problems with this method include overheating the surface materials or having lower thermal efficiencies by limiting the heat transfer to the surface to prevent overheating.

1.8.2 TRANSPARENT MATERIALS

The primary example of this type of load is glass, which has selective radiant transmission properties. In glass melting processes, the primary mode of heat transfer is radiation. As shown in Chapter 6, flames have specific types of radiant outputs that vary as a function of wavelength. If the flame is nonluminous, it usually has higher radiant outputs in the preferred wavelengths for water and carbon dioxide bands. If the flame is luminous, it has a broader, more graybody-type spectral radiant profile. Chapter 6 shows that luminous flames are preferred in melting glass because of the selective transmission properties of molten glass. This allows a significant portion of the radiation received at the surface of the glass to penetrate into the glass, which enhances heat transfer rates and reduces the chances of overheating the surface that would reduce product quality.

1.9 HEAT RECOVERY DEVICES

Heat recovery devices are often used to improve the efficiency of combustion systems. Some of these devices are incorporated into the burners, but more commonly they are another component in the combustion system, separate from the burners. These heat recovery devices incorporate some type of heat exchanger, depending on the application. The two most common types include *recuperators* and *regenerators*, which are briefly discussed next. Reed (1987) predicts an increasing importance for heat recovery devices in industrial combustion systems for increasing heat transfer and thermal efficiencies.⁴⁰

1.9.1 RECUPERATORS

A recuperator is a low- to medium-temperature (up to about 1300°F or 700°C), continuous heat exchanger that uses the sensible energy from hot combustion products to preheat the incoming combustion air. These heat exchangers are commonly counterflow, where the highest temperatures for both the combustion products and the combustion air are at one end of the exchanger and the coldest temperatures are at the other end. Lower-temperature recuperators are normally made of metal, while higher-temperature recuperators can be made of ceramics. Recuperators are typically used in lower-temperature applications because of the limitations of the metals used to construct these heat exchangers.

1.9.2 REGENERATORS

A regenerator is a higher-temperature, transient heat exchanger used to improve the energy efficiency of high-temperature heating and melting processes, particularly in high-temperature processing industries such as glass production. In a regenerator, energy from the hot combustion

products is temporarily stored in a unit constructed of refractory firebricks. This energy is then used to heat the incoming combustion air during a given part of the firing cycle up to temperatures in excess of 2000°F (1000°C).

Regenerators are normally operated in pairs. During one part of the cycle, the hot combustion gases are flowing through one of the regenerators and heating the refractory bricks, while the combustion air is flowing through and cooling the refractory bricks in the second regenerator. Both the exhaust gases and the combustion air directly contact the bricks in the regenerators, although not both at the same time because each is in a different regenerator at any given time. After a sufficient amount of time (usually from 5 to 30 min.), the cycle is reversed so that the cooler bricks in the second regenerator are then reheated while the hotter bricks in the first regenerator exchange their heat with the incoming combustion air. A reversing valve is used to change the flow from one gas to another in each regenerator. The burners used in these systems must be capable of not only handling the high-temperature preheated air, but also the constant thermal cycling.

1.10 CONCLUSIONS

Burners can be thought of as the engine for the industrial combustion system. They are responsible for taking the incoming fuel and oxidizer, mixing them in proper proportions, shaping the resulting flame, and transferring heat from the flame to the load, while simultaneously minimizing pollutant emissions. There are numerous burner designs that are tailored to specific operating conditions and applications. Some of the more common designs are considered in this book. There are many factors that influence burner design, including the fuel, oxidizer, heat release rate, flame shape, primary mode of heat transfer, load type, emission requirements, draft type, and geometry of the combustor, to name a few. As relevant, these factors are considered in more detail in the chapters that follow.

REFERENCES

1. U.S. Department of Energy (DOE), Industrial Combustion Vision: A Vision by and for the Industrial Combustion Community, U.S. DOE, Washington, D.C., 1998.
2. G. F. Hewitt, G. L. Shires, and T. R. Bott. *Process Heat Transfer*. CRC Press, Boca Raton, FL, 1994.
3. U.S. Dept. of Energy, Energy Information Administration. Annual Energy Outlook 1999, report DOE/EIA-0383(99), Washington, D.C.
4. P. Barry and S. Somers, Duct burners, in *The John Zink Combustion Handbook*, C.E. Baukal, Ed., CRC Press, Boca Raton, FL, 2001, 523–544.
5. C. E. Baukal, Ed., *Oxygen-Enhanced Combustion*, CRC Press, Boca Raton, FL, 1998.
6. R. A. Strehlow, *Fundamentals of Combustion*, Inter. Textbook Co., Scranton, PA, 1968.
7. F. A. Williams, *Combustion Theory*, Benjamin/Cummings Publishing, Menlo Park, CA, 1985.
8. B. Lewis and G. von Elbe, *Combustion, Flames and Explosions of Gases*, 3rd edition, Academic Press, New York, 1987.
9. W. Bartok and A. F. Sarofim, Eds., *Fossil Fuel Combustion*, Wiley, New York, 1991.
10. R. M. Fristrom, *Flame Structure and Processes*, Oxford University Press, New York, 1995.
11. I. Glassman, *Combustion*, 3rd edition, Academic Press, New York, 1996.
12. J. B. Edwards, *Combustion: The Formation and Emission of Trace Species*, Ann Arbor Science Publishers, Ann Arbor, MI, 1974.
13. J. A. Barnard and J. N. Bradley, *Flame and Combustion*, 2nd edition, Chapman & Hall, London, 1985.
14. S. R. Turns, *An Introduction to Combustion*, McGraw-Hill, New York, 1996.
15. J. Griswold, *Fuels, Combustion and Furnaces*, McGraw-Hill, New York, 1946.
16. A. Stambuleanu, *Flame Combustion Processes in Industry*, Abacus Press, Tunbridge Wells, U.K., 1976.
17. E. Perthuis, *La Combustion Industrielle*, Éditions Technip, Paris, 1983.
18. E. L. Keating, *Applied Combustion*, Marcel Dekker, New York, 1993.
19. G. Borman and K. Ragland, *Combustion Engineering*, McGraw-Hill, New York, 1998.

20. C. G. Segeler, Ed., *Gas Engineers Handbook*, Industrial Press, New York, 1965.
21. R. D. Reed, *Furnace Operations*, 3rd edition, Gulf Publishing, Houston, TX, 1981.
22. R. Pritchard, J. J. Guy, and N. E. Connor, *Handbook of Industrial Gas Utilization*, Van Nostrand Reinhold, New York, 1977.
23. R. J. Reed, *North American Combustion Handbook*, Vol. I, 3rd edition, North American Mfg. Co., Cleveland, OH, 1986.
24. IHEA, *Combustion Technology Manual*, 5th edition, Industrial Heating Equipment Assoc., Arlington, VA, 1994.
25. M. D. Kistler and J. S. Becker, Ferrous metals, in *Oxygen-Enhanced Combustion*, C. E. Baukal, Ed., CRC Press, Boca Raton, FL, 1998, chap. 5.
26. D. Saha and C. E. Baukal, Non-ferrous metals, in *Oxygen-Enhanced Combustion*, C. E. Baukal, Ed., CRC Press, Boca Raton, FL, 1998, chap. 6.
27. R. M. Fedler and R. W. Rousseau, *Elementary Principles of Chemical Process*, 3rd edition, John Wiley & Sons, New York, 2000.
28. T. Kudra and A. S. Mujumdar, *Advanced Drying Technologies*, Marcel Dekker, New York, 2002.
29. C. E. Baukal, *Heat Transfer in Industrial Combustion*, CRC Press, Boca Raton, FL, 2000.
30. J. L. Reese, G. L. Moilanen, R. Borkowicz, C. Baukal, D. Czerniak, and R. Batten, State-of-the-Art of NO_x Emission Control Technology, ASME paper 94-JPGC-EC-15, *Proc. Int. Joint Power Generation Conf.*, Phoenix, October 3–5, 1994.
31. M. L. Joshi, M. E. Tester, G. C. Neff, and S. K. Panahi, Flame particle seeding with oxygen enrichment for NO_x reduction and increased efficiency, *Glass*, Vol. 68(6), 212–213, 1990.
32. R. Ruiz and J. C. Hilliard, Luminosity enhancement of natural gas flames, *Proc. of 1989 Int. Gas Research Conf.*, T. L. Cramer, Ed., Government Institutes, Rockville, MD, 1990, 1345–1353.
33. A.G. Slavejkov, T. M. Gosling, and R. E. Knorr, Low-NO_x Staged Combustion Device for Controlled Radiative Heating in High Temperature Furnaces, U.S. Patent 5,611,682, March 18, 1997.
34. API Publication 535: Burner for Fired Heaters in General Refinery Services, 1st edition, American Petroleum Institute, Washington, D.C., July 1995.
35. K. J. Fioravanti, L. S. Zelson, and C. E. Baukal, Flame Stabilized Oxy-Fuel Recirculating Burner, U.S. Patent 4,954,076, issued September 4, 1990.
36. C. E. Baukal, Ed., *The John Zink Combustion Handbook*, CRC Press, Boca Raton, FL, 2001.
37. S. V. Joshi, J.S. Becker, and G. C. Lytle, Effects of oxygen enrichment on the performance of air-fuel burners, in *Industrial Combustion Technologies*, M.A. Lukaszewicz, Ed., American Society of Metals, Warren, PA, 1986, 165.
38. S. Longacre, Using infrared to dry paper and its coatings, *Process Heating*, 4(2), 45–49, 1997.
39. T. M. Smith and C. E. Baukal, Space-age refractory fibers improve gas-fired infrared generators for heat processing textile webs, *J. Coated Fabrics*, 12(3), 160–173, January 1983.
40. R. J. Reed, Future consequences of compact, highly effective heat recovery devices, in *Heat Transfer in Furnaces*, C. Presser and D. G. Lilley, Eds., ASME HTD-Vol. 74, pp. 23–28, New York, 1987.

2 Heat Transfer

Charles E. Baukal, Jr., Ph.D., P.E.

CONTENTS

- 2.1 Introduction
 - 2.2 Radiation
 - 2.2.1 Surface Radiation
 - 2.2.2 Nonluminous Gaseous Radiation
 - 2.2.2.1 Theory
 - 2.2.2.2 Combustion Studies
 - 2.2.3 Luminous Radiation
 - 2.2.3.1 Theory
 - 2.2.3.2 Combustion Studies
 - 2.3 Convection
 - 2.3.1 Forced Convection
 - 2.3.1.1 Forced Convection from Flames
 - 2.3.1.2 Forced Convection from Hot Gases to Tubes
 - 2.3.2 Natural Convection
 - 2.4 Conduction
 - 2.4.1 Steady-State Conduction
 - 2.4.2 Transient Conduction
- References

2.1 INTRODUCTION

Heat transfer plays a critical role in industrial combustion processes where the primary objective is to transfer heat from the hot combustion products to some type of load. In industrial processes, radiation is often the dominant mechanism and forced convection also plays an important function. The more efficient the heat transfer processes, the higher the overall system efficiency. This is important for many reasons. The operating costs in the form of fuel are inversely proportional to the efficiency — the higher the efficiency, the lower the fuel consumption. Pollution emissions are indirectly proportional to fuel efficiency. The higher the efficiency, the lower the fuel consumption and therefore the lower the emissions per unit of product, because less fuel is combusted and therefore less emissions are produced. More efficient processes usually mean that either the combustors can be smaller for a given production rate or, alternatively, more can be produced in a given size combustor. This means that capital costs may be reduced per unit of product. That also translates indirectly into more emissions reductions because less energy is needed to make the combustor and therefore less pollutants are generated. A smaller combustor per unit of product means that less space is required in the plant. Higher thermal efficiencies usually also mean that less energy is lost through the walls of the combustor, which benefits the workers in the vicinity who will be less likely to be overheated and burned. Improved thermal efficiencies are therefore dependent on maximizing the heat transfer from the combustion products to the load.

There are some nondimensional numbers that are commonly used in heat transfer analysis. The Reynolds number is the ratio of the inertial forces to the viscous forces in a flow:

$$\text{Re} = \frac{\rho v l}{\mu} = \frac{v l}{\nu} \quad (2.1)$$

where ρ is the fluid density, v is the fluid velocity, l is the characteristic length scale (e.g., diameter for a pipe for flow through a pipe), μ is the absolute viscosity, and ν is the kinematic viscosity. The Reynolds number is low for laminar flows and high for turbulent flows, with transition flow at values in between. The actual range for each type of flow depends on the flow geometry. The Prandtl number is the ratio of momentum diffusivity to thermal diffusivity and is defined as:

$$\text{Pr} = \frac{c_p \mu}{k} \quad (2.2)$$

where c_p is the fluid constant pressure specific heat and k is the fluid thermal conductivity. For many gases, $\text{Pr} \approx 0.7$. The Nusselt number is the ratio of the convective and conductive heat transfer rates:

$$\text{Nu} = \frac{h l}{k} \quad (2.3)$$

where h is the convective heat transfer coefficient. In forced convection flows, Nu is commonly a function of the Pr and Re , and is used to determine the convection coefficient.

The three primary modes of heat transfer include convection, radiation, and conduction. These are discussed next as they pertain to the heat transfer in industrial combustion processes, particularly from burners. There are other modes of heat transfer such as boiling and condensation. While these are important in some specific processes, they are not included due to their limited applicability. Much of the information in this chapter has been taken from Baukal et al. (2000, 2001).^{1,2}

2.2 RADIATION

Thermal radiation is one of the most important heat transfer mechanisms in industrial furnaces.³ Radiation is a unique method of heat transfer because no medium is required for energy transport — it can be transmitted through a vacuum or through a medium. Radiation is simply the transmission of energy by electromagnetic waves, which are characterized by their wavelength or frequency and are related as follows:

$$\lambda = \frac{c}{\nu} \quad (2.4)$$

where λ is the wavelength, c is the speed of light, and ν is the frequency. In the fields of heat transfer and combustion, wavelength is more commonly used. The classification of the various types of radiation is shown in [Figure 2.1](#). In industrial combustion heating, the most important type of radiation is infrared. The human optic nerves are sensitive to radiation in the wavelengths from 0.38 to 0.76 μm , which means that we can see radiation in that band. In practical terms, humans cannot see thermal radiation from bodies at temperatures below about 900°F (500°C).⁴

There are four possible things that can happen to radiation incident on a medium (solid, liquid, or gas). The radiation can be absorbed, reflected, transmitted, or some combination of these three, which is most often the case, as shown in [Figure 2.2](#). In general,

$$\alpha + \rho + \tau = 1 \quad (2.5)$$

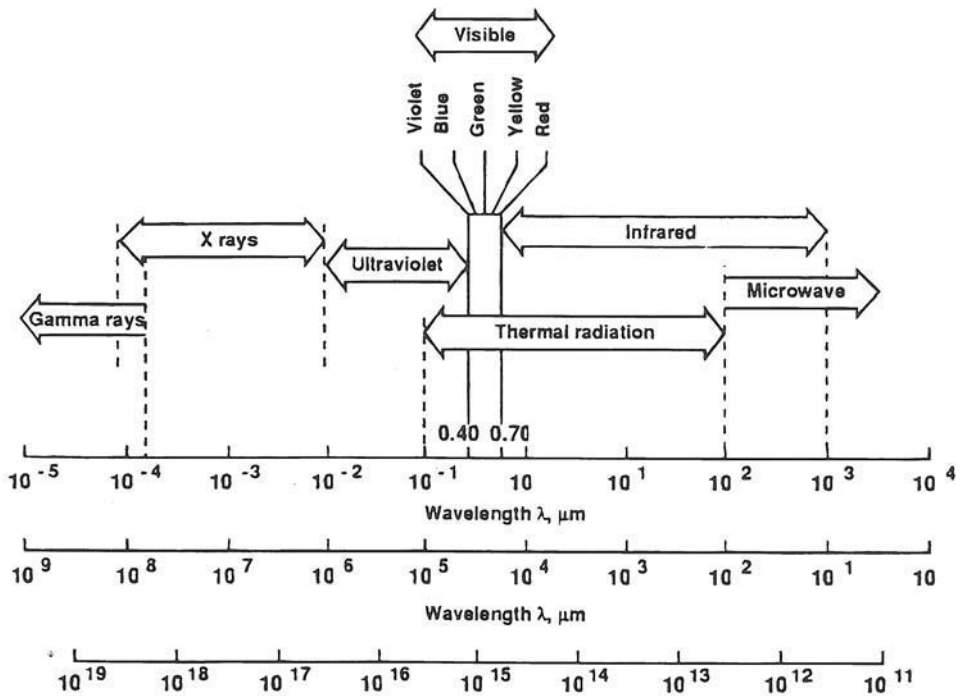


FIGURE 2.1 Electromagnetic spectrum.¹³⁵

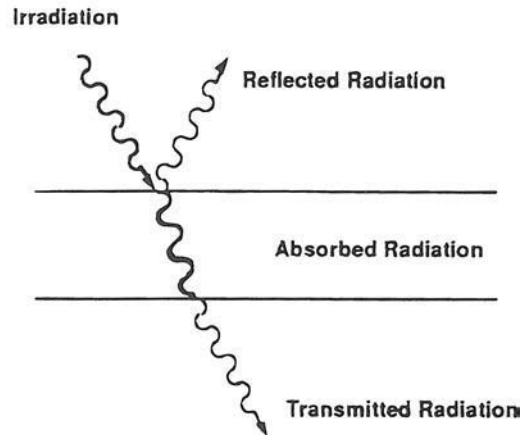


FIGURE 2.2 Radiant energy absorbed, reflected, and transmitted through a material.¹³⁵

where α is the absorptivity of the medium, ρ is the reflectivity, and τ is the transmissivity, which are defined as:

$$\alpha \equiv \frac{\text{absorbed part of incoming radiation}}{\text{total incoming radiation}}$$

$$\rho \equiv \frac{\text{reflected part of incoming radiation}}{\text{total incoming radiation}}$$

$$\tau \equiv \frac{\text{transmitted part of incoming radiation}}{\text{total incoming radiation}}$$

For most solid materials, the transmissivity is low except for things like glass and plastics. The reflectivity of most solids is low, unless they are highly polished (e.g., new stainless steel). For liquids, the transmissivity may be significant, especially for fluids with high water contents. For most gases, the transmissivity is generally very high with negligible absorptance and reflectance. These radiative properties are extremely important in determining how much radiation will be transferred to and from a medium. This is further complicated by the fact that these radiative properties may be functions of wavelength, angle of incidence, surface condition, and thickness. An example of wavelength dependence is solid glass, which transmits shorter wavelength UV radiation but absorbs longer wavelength IR radiation. At high angles of incidence, a surface may be more reflective, while at normal incident angles, a surface may be more absorptive. Highly oxidized metals have high absorptivities and low reflectivities, while highly polished metals have lower absorptivities and high reflectivities. A very thin layer of a solid material can have a significant transmissivity, while a thick layer of the same solid may have no transmissivity. The radiative properties can also change over time, such as when an initially reflective metal surface becomes less reflective as it oxidizes. Therefore, an important challenge in computing radiative heat transfer in combustion systems is determining radiative properties.

There are three common forms of radiation heat transfer in industrial heating applications: (1) radiation from a solid surface, (2) radiation from a gaseous medium (usually referred to as non-luminous radiation), and (3) radiation from particles in a gaseous medium (usually referred to as luminous radiation). The latter two types are of most interest for the heat transfer from burners. Each of these three types is considerably different and must be treated accordingly. Also, it is not uncommon for two or all three types to be important in industrial heating. In industrial furnaces, as much as 90% of the heat transfer to the load can be by radiation.⁵

The “Total Schmidt Method” has been used to determine the amount of radiation coming from the walls and that coming from the flame, which are received by the load.⁶ The flame radiation is measured by sighting the flame with a radiation pyrometer, where the background behind the flame is water-cooled. The radiation from the water-cooled wall is negligible compared to that from the flame and is ignored:

$$q_1 = \sigma A \epsilon_f T_f^4 \quad (2.6)$$

where σ is the Stefan-Boltzmann constant (see Equation 3.28), ϵ_f is the average flame emissivity, A is the area radiating, and T_f is the average absolute flame temperature. Then the radiation from the flame with a hot blackbody background (furnace wall) is measured:

$$q_2 = \sigma A \epsilon_f T_f^4 + \sigma A (1 - \alpha_f) T_w^4 \quad (2.7)$$

where α_f is the average flame absorptivity and T_w is the average wall temperature. Finally, the radiation from the hot blackbody background (furnace wall) is measured immediately after the flame is extinguished:

$$q_3 = \sigma A T_w^4 \quad (2.8)$$

The flame is assumed to be a graybody so that:

$$\alpha_f = \epsilon_f \quad (2.9)$$

Solving the above four equations for the flame emissivity ϵ_f :

$$\epsilon_f = 1 - \left(\frac{q_2 - q_1}{q_3} \right) \quad (2.10)$$

and then solving for flame temperature T_f :

$$T_f = \left(\frac{q_1}{\sigma A \epsilon_f} \right)^{1/4} \quad (2.11)$$

Lowes and Newall (1974) note that there are some errors that arise with this method:⁷

1. The absorptivity of the flame is not equal to the emissivity unless the blackbody source is at the flame temperature.
2. The emissivities obtained assume a graybody, which is normally not strictly true.
3. Soot particles in the flame can cause radiation scattering and may give high absorptivity values.

They showed that the error due to the blackbody not being at the flame temperature can be 42% if the blackbody temperature was 1000K and the flame temperature was 2000K. Leblanc et al. (1974) used a variation of this technique to distinguish between the radiation from the walls and from the flame, to the load.⁸ An ellipsoidal radiometer was used to measure the total radiation received by the load. Then the flame was turned off and the radiation was again measured, which was the contribution by the walls. The radiation from the flame was then the difference between that total and the wall:

$$q_{\text{rad,total}} = K q_{\text{rad,walls}} + q_{\text{rad,flame}} \quad (2.12)$$

where the flame radiation from the walls has been corrected by a nonabsorption factor K that is obtained experimentally. Lihou (1977) reviewed analytical techniques for calculating nonspectral radiation for use in furnace design.⁹ Many general books on radiation heat transfer are available.^{4,10-17}

2.2.1 SURFACE RADIATION

The spectral or monochromatic emissive power of a blackbody is dependent on the wavelength of the radiation and on the absolute temperature of the blackbody, and is calculated as follows:

$$E_{b\lambda} = \frac{C_1}{\lambda^5 (e^{C_2/\lambda T} - 1)} \quad (2.13)$$

where $E_{b\lambda}(T)$ is the monochromatic emissive power of a blackbody in Btu/hr-ft²-μm (W/m³), $C_1 = 1.1870 \times 10^8$ Btu/μm⁴-ft²-hr (3.7415×10^{-16} W-m²), $C_2 = 2.5896 \times 10^4$ μm-°R (1.4388×10^{-2} m-K), T is the absolute temperature of the body in °R (K), and λ is the wavelength in μm (m). [Figure 2.3a](#) and [b](#) show some graphs of this relation as a function of wavelength and temperature. As can be seen, the peak radiation shifts to shorter wavelengths as the body temperature increases. That wavelength can be computed from Wein's displacement law as follows:

$$\lambda_{\text{max}} = \frac{c}{T} \quad (2.14)$$

where $c = 5215.6$ μm-°R (2897.6 μm-K).

Example 2.1

Given: Blackbody temperature = 2000°F.

Find: Wavelength for peak radiation.

Solution: $\lambda_{\text{max}} = \frac{c}{T} = \frac{5215.6 \mu\text{-}^\circ\text{R}}{(2000 + 460)^\circ\text{R}} = 2.12 \mu\text{m}$

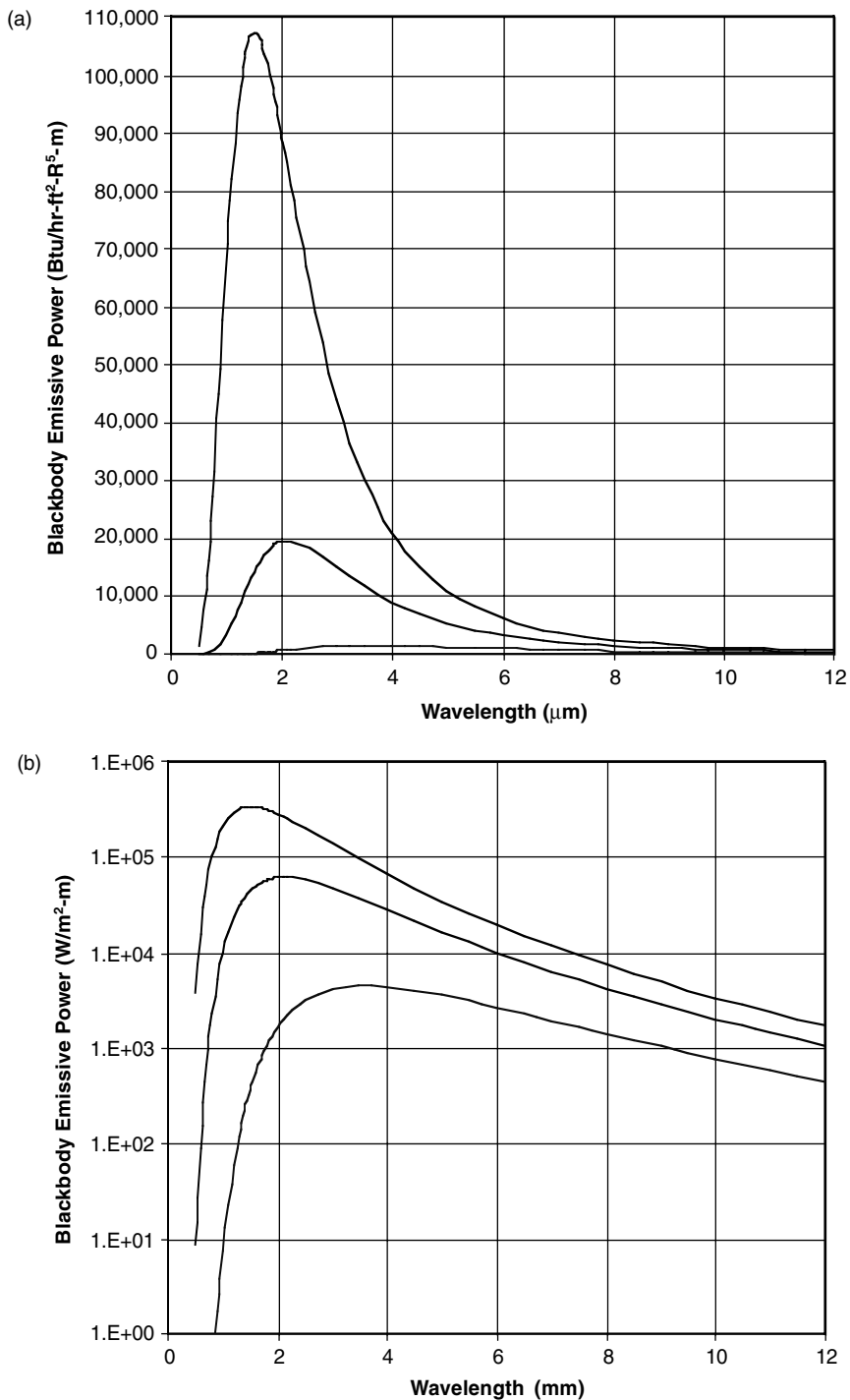


FIGURE 2.3 Blackbody emissive power: (a) English units, linear scale, and (b) metric units, logarithmic scale.¹

This wavelength may be important for certain types of heat loads that selectively absorb radiation at preferred wavelengths. In those cases, to maximize the radiant efficiency, the heat source temperature should be coupled to the preferred wavelength of the load. Note that this will not necessarily maximize the radiation to the load as higher temperatures produce more radiation and

more energy may be absorbed by the load, even if the spectral absorptivity is lower because of the higher radiant power density, as will be shown in a later example.

The integrated hemispherical emissive power of a blackbody, computed over all wavelengths, is a function only of its absolute temperature and is described by:

$$e_b = \sigma T^4 \quad (2.15a)$$

$$E_b = \sigma A T^4 \quad (2.15b)$$

where A is the area (ft^2 or m^2), T is the absolute temperature of the body ($^\circ\text{R}$ or K), and σ is the Stefan-Boltzmann constant, which has the value of:

$$\sigma = 0.1714 \times 10^{-8} \text{ Btu/hr-ft}^2\text{-}^\circ\text{R}^4 \quad (5.669 \times 10^{-8} \text{ W/m}^2\text{-K}^4) \quad (2.16)$$

Example 2.2

Given: Surface temperature = 2000°F .

Find: Blackbody emissive power.

Solution: $e_b = \sigma T^4 = (0.1714 \times 10^{-8} \text{ Btu/hr-ft}^2\text{-}^\circ\text{R}^4)(2000 + 460^\circ\text{R})^4 = 62,800 \text{ Btu/hr-ft}^2$

If all of the radiation received at a solid surface is absorbed by that surface, the body is referred to as a *blackbody* and has an absorptivity of unity ($\alpha = 1$). In addition, a blackbody not only absorbs all incident radiation, but it also emits the maximum amount of energy possible for the given temperature. The emissivity (ϵ) of a medium is the fraction of energy a body emits (E) for a given temperature, compared to the amount it could emit (E_b):

$$\epsilon = \frac{E}{E_b} \quad (2.17)$$

Then, for a blackbody $E = E_b$ and $\epsilon = 1$. Real bodies are typically not perfect blackbodies and do not absorb all the incident energy received on their surfaces or emit the maximum amount of energy possible. The radiant heat transfer absorbed by real surfaces is a function of the absorptivity of the surface, and the total radiant energy emitted by a body can be calculated from:

$$E = \epsilon \sigma A T^4 \quad (2.18)$$

Example 2.3

Given: Surface temperature = 2000°F , $\epsilon = 0.4$, $A = 10 \text{ ft}^2$.

Find: Total radiant energy emitted by the body.

Solution: $E_b = \epsilon \sigma A T^4 = (0.4)(0.1714 \times 10^{-8} \text{ Btu/hr-ft}^2\text{-}^\circ\text{R}^4)(10 \text{ ft}^2)(2000 + 460^\circ\text{R})^4 = 251,000 \text{ Btu/hr}$

Thus, a surface with an emissivity of 0.4 will emit 40% of the energy that a blackbody would emit at the same temperature.

The above equation for E_b assumes that the emissivity is a constant value. The absorptivity and emissivity of some surfaces is a function of the temperature and the wavelength of radiation. Kirchoff's law states that:

$$\epsilon(\lambda, T) = \alpha(\lambda, T) \quad (2.19)$$

so that, at equilibrium conditions, a surface absorbs and emits the same amount of radiation. This assumes that the surface condition remains the same. If the absorptivity and emissivity are independent of wavelength, the surface is said to be a *graybody*. In engineering calculations, most surfaces can be treated as graybodies. The spectral emissive power can be written as:

$$e_{\lambda} = \epsilon_{\lambda} \sigma T^4 \quad (2.20)$$

The following example shows a comparison of the radiation absorbed as a function of wavelength for a load whose emissivity varies with wavelength.

Example 2.4

Given: Surface emissivities: $\epsilon_{2\mu\text{m}} = 0.4$, $\epsilon_{3\mu\text{m}} = 0.8$.

Find: Radiant energy absorbed for heat sources matched to these wavelengths.

Solution: Find temperature whose blackbody curve peaks at the given wavelengths:

$$T_1 = \frac{5215.6 \mu\text{m}^{\circ}\text{R}}{2 \mu\text{m}} = 2608^{\circ}\text{R} \quad \text{and} \quad T_2 = \frac{5215.6 \mu\text{m}^{\circ}\text{R}}{3 \mu\text{m}} = 1739^{\circ}\text{R}$$

Then calculate the radiation that would be absorbed at those temperatures at the given wavelength:

$$e_{2\mu\text{m}} = \epsilon_{2\mu\text{m}} \sigma T_1^4 = (0.4)(0.1714 \times 10^{-8} \text{ Btu/hr-ft}^2\text{-}^{\circ}\text{R}^4)(2608^{\circ}\text{R})^4 = 31,700 \text{ Btu/hr-ft}^2$$

$$e_{3\mu\text{m}} = \epsilon_{3\mu\text{m}} \sigma T_2^4 = (0.8)(0.1714 \times 10^{-8} \text{ Btu/hr-ft}^2\text{-}^{\circ}\text{R}^4)(1739^{\circ}\text{R})^4 = 12,500 \text{ Btu/hr-ft}^2$$

As can be seen in this example, the spectral radiant efficiency is higher at 3 μm with a source temperature of 1739 $^{\circ}\text{R}$ because 80% of the radiant energy is absorbed ($\epsilon_{3\mu\text{m}} = 0.8$). However, much more energy is absorbed at the higher source temperature, although it is less efficient. Figure 2.4

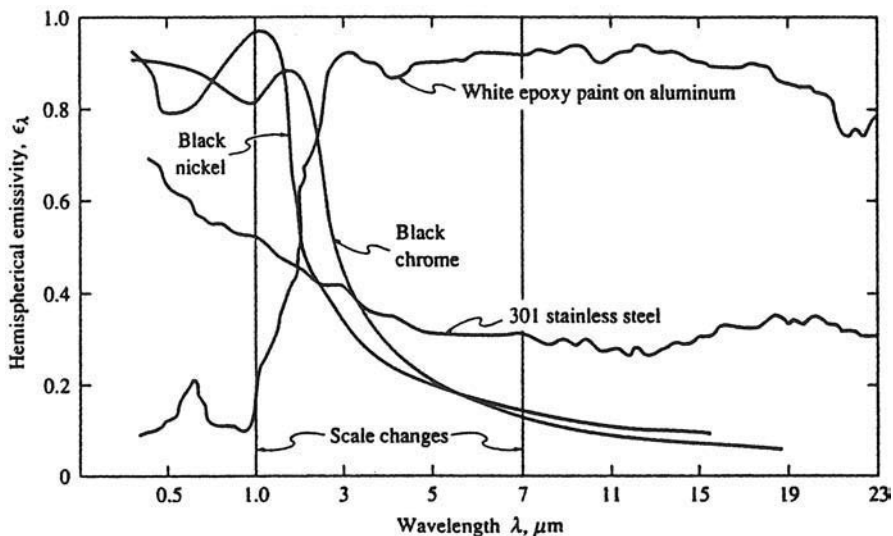


FIGURE 2.4 Spectral, hemispherical emissivities of several spectrally selective surfaces.¹³⁶

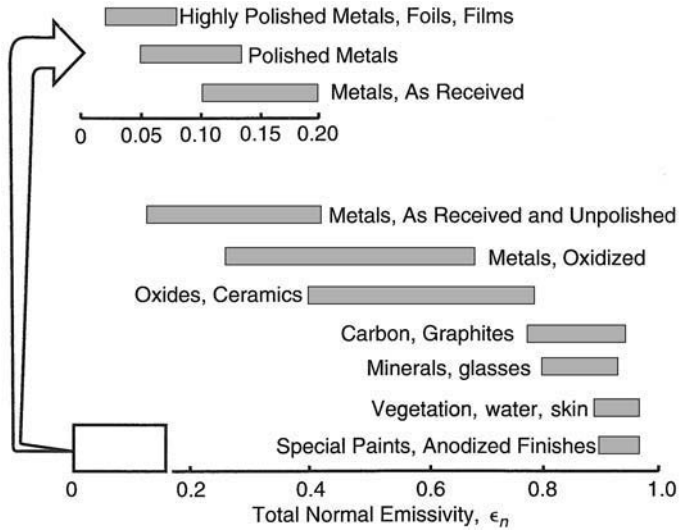


FIGURE 2.5 Total emissivity ranges for various materials.¹³⁷

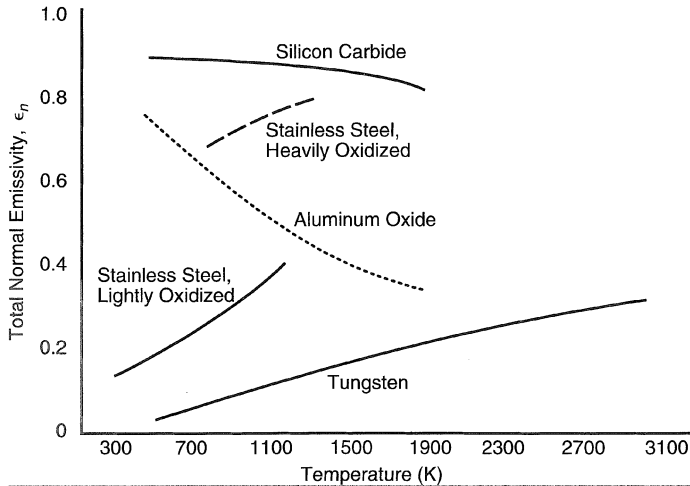


FIGURE 2.6 Total normal emissivity as a function of temperature for various materials.¹³⁷

shows an example of the spectral emissivity of some materials. Figure 2.5 shows that some materials may have a wide a range of total emissivities. Figure 2.6 shows how the total normal emissivity varies with temperature. Table 2.1 gives a list of normal total emissivities for various surfaces as a function of temperature. Table 2.2 shows total emissivities for refractory materials, commonly used in furnaces, as a function of temperature.¹⁸ Glinkov (1974) gave several examples of how the emissivity varies with temperature and wavelength for different solids, including refractories, copper, brass, steel and steel alloys, and open-hearth slags.¹⁹

The emissivity of the refractory used in a combustor is important in determining the surface radiation heat transfer between the walls, the load, and the flame. The heat transfer in many industrial combustion processes is dominated by radiation from the hot refractory walls. Docherty and Tucker (1986) numerically studied the influence of wall emissivity on furnace performance.²⁰ The predictions

TABLE 2.1
Normal Total Emissivities of Various Surfaces as a Function of Temperature¹³⁷

Surface	$t(^{\circ}\text{C})$	Emissivity
A. Metals and their Oxides		
Aluminum		
Polished	100	0.095
Commercial sheet	100	0.09
Heavily oxidized	95–505	0.20–0.31
Brass		
Highly polished		
73.2 Cu, 26.7 Zn	245–355	0.028–0.031
62.4 Cu, 36.8 Zn, 0.4 Pb, 0.3 Al	255–375	0.033–0.037
82.9 Cu, 17.0 Zn	275	0.030
Rolled plate, natural surface	20	0.06
Dull plate	50–350	0.22
Oxidized by heating at 600°C	200–600	0.61–0.59
Copper		
Carefully polished electrolytic copper	80	0.018
Commercial emered, polished, but pits remaining	20	0.030
Commercial, scraped shiny, but not mirrorlike	20	0.072
Plate, heated for a long time, covered with thick oxide layer	25	0.78
Molten copper	1075–1275	0.16–0.13
Gold		
Pure, highly polished	225–625	0.018–0.035
Iron and steel (not including stainless)		
Electrolytic iron, highly polished	175–225	0.052–0.064
Steel, polished	100	0.066
Iron, polished	425–1025	0.14–0.38
Cast iron, polished	200	0.21
Cast iron, newly turned	20	0.44
Cast iron, turned and heated	880–988	0.60–0.70
Mild steel, cleaned with organic solvents	25	0.12, 0.15
Oxidized surfaces		
Iron plate, pickled, then rusted red	20	0.61
Iron plate, completely rusted	20	0.69
Rolled sheet steel	20	0.66
Cast iron, oxidized at 600°C	200–600	0.64–0.78
Steel, oxidized at 600°C	200–600	0.79
Sheet steel		
With rough oxide layer	25	0.80
With shiny oxide layer	25	0.82
Steel plate, rough	40–370	0.94–0.97
Molten surfaces		
Cast iron	1300–1400	0.29
Mild steel	1600–1800	0.28
Lead		
Pure (99.96%) unoxidized	125–225	0.057–0.075
Oxidized at 150°C	200	0.63
Mercury	0–100	0.09–0.12
Nickel		
Electroplated, polished	25	0.045
Polished	100	0.072

(Continued)

TABLE 2.1
Normal Total Emissivities of Various Surfaces as a Function of Temperature (Continued)

Surface	$t(^{\circ}\text{C})$	Emissivity
Electroplated, not polished	20	0.11
Plate, oxidized by heating at 600°C	200–600	0.37–0.48
Nickel alloys		
Copper-nickel, polished	100	0.059
Nichrome wire, bright	50–1000	0.65–0.79
Platinum		
Pure polished plate	225–625	0.054–0.104
Silver		
Polished, pure	225–625	0.020–0.032
Stainless steels		
Type 304 (8 Cr; 18 Ni) Polished	100	0.074
Light silvery, rough, brown, after heating	215–490	0.44–0.36
After 42 h at 525°C	215–525	0.62–0.73
Thorium oxide	275–500	0.58–0.36
Thorium oxide	500–825	0.36–0.21
Tin		
Bright	50	0.06
Commercial tin-plated sheet iron	100	0.07,0.08
Zinc		
Commercial 99.1% pure, polished	225–325	0.045–0.053
Oxidized by heating at 400°C	400	0.11
Galvanized sheet iron, fairly bright	30	0.23
Galvanized sheet iron, gray oxidized	25	0.28
B. Refractories, Building Materials, Paints, and Miscellaneous Materials		
Alumina (99.5–85 Al ₂ O ₃ ; 0–12 SiO ₂ ; 0–1 Fe ₂ O ₃)		
Effect of mean grain size		
10 μm	1010–1565	0.30–0.18
50 μm		0.39–0.28
100 μm		0.50–0.40
Alumina-silica (showing effect of Fe)		
80–58 Al ₂ O ₃ ; 16–38 SiO ₂ ; 0.4 Fe ₂ O ₃	1010–1570	0.61–0.43
36–26 Al ₂ O ₃ ; 50–60 SiO ₂ ; 1.7 Fe ₂ O ₃		0.73–0.62
61 Al ₂ O ₃ ; 35 SiO; 2.9 Fe ₂ O ₃		0.78–0.68
Asbestos		
Board	25	0.96
Paper	40–370	0.93–0.94
Brick		
Red, rough but no gross irregularities	20	0.93
Building	1000	0.45
Fireclay	1000	0.75
Carbon		
Filament	1040–1405	0.526
Graphitized	100–320	0.76–0.75
Graphitized	320–500	0.75–0.71
Thin layer on iron plate	20	0.927
Thick coat	20	0.967
Glass		
Smooth	20	0.94
Magnesite refractory brick	1000	0.38

(Continued)

TABLE 2.1
Normal Total Emissivities of Various Surfaces as a Function of Temperature (Continued)

Surface	$t(^{\circ}\text{C})$	Emissivity
Paints, lacquers, varnishes		
Snow-white enamel varnish on rough iron plate	25	0.906
Black shiny lacquer, sprayed on iron	25	0.875
Radiator paint; white, cream, bleach	100	0.79, 0.77, 0.84
Plaster, rough line	10–90	0.91
Quartz		
Rough, fused	20	0.93
Glass, 1.98 mm thick	280–840	0.90–0.41
Glass, 6.88 mm thick	280–840	0.93–0.47
Silica (98 SiO ₂ ; Fe-free), effect of grain size		
10 μm	1010–1565	0.42–0.33
70–600 μm		0.62–0.46
Water	0–100	0.95–0.963

From data tabulated by Hottel and Sarofim (1967). With permission.

TABLE 2.2
Normal Total Emissivities of Refractories as a Function of Temperature¹⁸

Material	Temperature, $^{\circ}\text{F}$ ($^{\circ}\text{C}$)						
	200 (93)	400 (200)	800 (430)	1600 (870)	2000 (1090)	2400 (1320)	2800 (1540)
Fireclay brick	0.90	0.90	0.90	0.81	0.76	0.72	0.68
Silica brick	0.90	—	—	0.82–0.65	0.78–0.60	0.74–0.57	0.67–0.52
Chrome-magnesite brick	—	—	—	0.87	0.82	0.75	0.67
Chrome brick	0.90	—	—	0.97	0.98	—	—
High-alumina brick	0.90	0.85	0.79	0.50	0.44	—	—
Mullite brick	—	—	—	0.53	0.53	0.62	0.63
Silicon carbide brick	—	—	—	0.92	0.89	0.87	0.86

showed that fuel consumption decreases as furnace wall emissivity increases, although there is no effect when the furnace atmosphere is gray. Transient furnace operation or poor wall insulation reduces the beneficial effects of high wall emissivity. Elliston et al. (1987) analytically and numerically showed that wall surface emissivity has only a negligible impact on heat transfer to a load inside a furnace.²¹ In a study sponsored by the Gas Research Institute (Chicago, IL), it was determined that the total normal emittances of common, commercially available refractories, including dense insulating firebrick and porous ceramic fiber, ranged from 0.3 to 0.7 at 1800 $^{\circ}\text{F}$ (1300K).²² The emissivity of so-called high-emittance coatings was also measured, and it was found that few of the coatings actually had high emissivities. Those coatings could extend the range of refractory emittances from 0.3 to 0.9 at 1800 $^{\circ}\text{F}$ (1300K). Another part of that study investigated the effect of using high-emittance coatings in large industrial furnaces.²³ Testing was done on a 50-ton/hr (45 m-ton/hr) reheat furnace. Experimental results showed no significant change in furnace efficiency (at most, a 6% increase) using the highest available emissivity coatings on the refractory walls of the furnace. Another study showed that high-emissivity coatings applied to hundreds of furnaces in metallurgical, petrochemical, ceramic, mechanical, and other industries in the Peoples Republic

of China afforded energy savings of 5 to 10%, up to a maximum of 28%.²⁴ The reported emissivity of the coating ranged from 0.80 to 0.92, depending on the surface temperature and wavelength.

In some industrial combustion processes, the surface absorptivity can change over time, which affects the performance of the system. This is particularly true of coal-fired processes, where the ash may be deposited on tube surfaces. Wall et al. (1993) showed that the normal emittance of particulate ash is highly dependent on the particle size and surface temperature.²⁵ In a subsequent study, Wall et al. (1995) studied the effects of ash deposits on the heat transfer in a coal-fired furnace.²⁶ The heat transfer from the combustion products to the tubes is primarily by radiation, with a lesser amount by convection heating. The heat must conduct through the ash deposits and the tube wall, before heating the fluid inside the tubes primarily by convection. As the ash deposit melts to form a slag, the absorptance increases dramatically to values approaching 0.9. The thermal conductivity of the deposit is highly dependent on its physical state, especially its porosity. It is interesting to note that the heat flux through the deposits decreases during the initial phases of its growth and then actually increases before reaching a steady-state value when the deposits have reached maturity. The measured thermal conduction coefficient ranged from 0.3 to 0.5 kW/m²-K (53 to 88 Btu/ft²-hr-°F). The important conclusion of these studies is that the radiative and conductive properties of ash deposits depend on the physical and chemical character of the deposits.

An important analysis in combustion processes is often radiation heat transfer in an enclosure. The furnace walls are normally at a higher temperature than the heat load and radiate energy to that load. When the space inside an enclosure is either a vacuum or contains a gas such as air that is essentially transparent to radiation, then the medium in the combustion space is referred to as nonparticipating. This means that it does not absorb any of the radiation passing through it. If the combustion space contains a radiatively absorbing gas such as CO₂, H₂O, or CO, then the medium is referred to as *participating*, because it does absorb some of the radiation passing through it. In the combustion of fossil fuels, the products of combustion usually contain significant quantities of CO₂ and H₂O, so the combustion space contains participating media. An assumption that is often made for a first-order analysis is that the concentrations of participating gases are low enough due to dilution by N₂ that the combustion space can be treated as nonparticipating to simplify the analysis. The net radiant heat transfer from one surface to another can be calculated from:

$$q_{1\leftrightarrow 2} = \sigma A_1 F_{1\rightarrow 2} (T_1^4 - T_2^4) = \sigma A_2 F_{2\rightarrow 1} (T_1^4 - T_2^4) \quad (2.21)$$

where $q_{1\leftrightarrow 2}$ is the net energy transferred between surfaces 1 and 2; $F_{i\rightarrow j}$ is the view factor or radiation shape factor, which is the diffuse radiation leaving surface i and received at surface j ; and,

$$A_1 F_{1\rightarrow 2} = A_2 F_{2\rightarrow 1} \quad (2.22)$$

due to the reciprocity theory. Equations, charts, tables, and graphs of radiation view factors are available elsewhere.^{10,14} An example will be given to illustrate this type of analysis. The view factor between two identical, parallel, directly opposed rectangles (see [Figure 2.7](#)) is given by:

$$F_{1\rightarrow 2} = F_{2\rightarrow 1} = \frac{2}{\pi XY} \left\{ \begin{aligned} & \ln \sqrt{\frac{(1+X^2)(1+Y^2)}{1+X^2+Y^2}} + X\sqrt{1+Y^2} \tan^{-1} \frac{X}{\sqrt{1+Y^2}} \\ & + Y\sqrt{1+X^2} \tan^{-1} \frac{Y}{\sqrt{1+X^2}} - X \tan^{-1} X - Y \tan^{-1} Y \end{aligned} \right\} \quad (2.23)$$

where $X = a/c$, $Y = b/c$, a = length of the rectangles, b = width of the rectangles, and c = spacing between the rectangles. As can be seen, this is a fairly complicated relationship for a relatively simple geometric configuration. For more complicated and for general surface orientations, computer analysis becomes necessary.

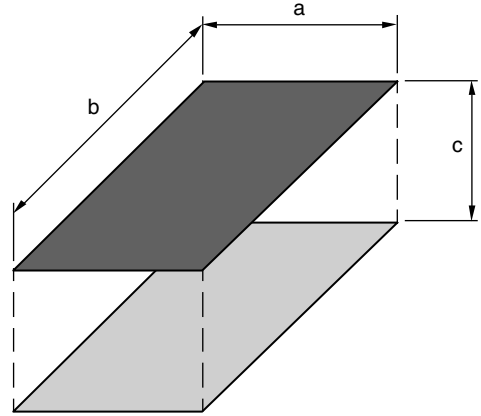


FIGURE 2.7 Geometry for radiation between parallel plates.¹

Example 2.5

Given: Furnace roof temperature of 2000°F, average load temperature = 300°F, combustion space length = 20 ft, width = 10 ft, height = 8 ft.

Find: Net radiant heat transfer from the roof to the floor assuming both are blackbodies.

Solution: Find view factor from floor to ceiling:

$$a = 20 \text{ ft}, b = 10 \text{ ft}, c = 8 \text{ ft}, X = a/c = 20/8 = 2.5, Y = b/c = 10/8 = 1.25$$

Using the formula above for the view factor between parallel rectangles,

$$F_{1 \rightarrow 2} = 0.356$$

$$T_1 = 2000^\circ\text{F} = 2460^\circ\text{R}, T_2 = 300^\circ\text{F} = 760^\circ\text{R}$$

$$q_{1 \rightarrow 2} = (0.1714 \times 10^{-8} \text{ Btu/hr-ft}^2\text{-R}^4)(0.356)(20' \times 10')[(2460^\circ\text{R})^4 - (760^\circ\text{R})^4] \\ = 4.43 \times 10^6 \text{ Btu/hr}$$

Beér studied flame impingement inside a furnace and experimentally determined that radiation was at least 10% of the total heat flux.⁹⁵ It was not specified how much of that radiation came from the hot walls and how much came from the flame. Vizioz¹¹¹ and Smith¹¹³ studied flame impingement on a flat plate in a hot furnace. It was determined that radiation and convection were of comparable magnitudes. Vizioz measured radiation to be 4 to 100% of the total heat flux. Smith calculated the surface radiant emission to the target using Hottel's zone method.¹⁰ It was 30 to 43% and 10 to 17% of the total heat transfer to water-cooled and air-cooled flat plates, respectively. Matsuo studied turbulent, preheated air/coke oven gas flames, impinging on a metal slab, inside a hot furnace.¹¹⁴ The top of the slab was exposed to the impinging flame. The remainder was exposed to the radiation from the furnace walls. Furnace radiation was the dominant mechanism: (1) for large L, (2) for high t_w , and (3) for large R. Ivernel calculated the radiation from hot furnace walls to a hemi-nosed cylinder.¹¹⁶ It was up to 42% of the total heat flux for impinging O_2 /natural gas flames. You measured the convective and total heat flux, using gages plated with gold and black foils, respectively.¹⁰⁷ By subtracting the convection from the total heat flux, radiation was calculated to be up to 35% of the convective flux. Van der Meer estimated that the radiation from the hot inner refractory wall of a tunnel burner was up to 15% of the total heat flux to the target.¹²²

2.2.2 NONLUMINOUS GASEOUS RADIATION

2.2.2.1 Theory

The equation of radiative transfer will not be considered here, as it is discussed in many radiation textbooks and is not commonly used as such to solve industrial combustion problems. The complete combustion of hydrocarbon fuels produces, among other things, CO_2 and H_2O . These gaseous

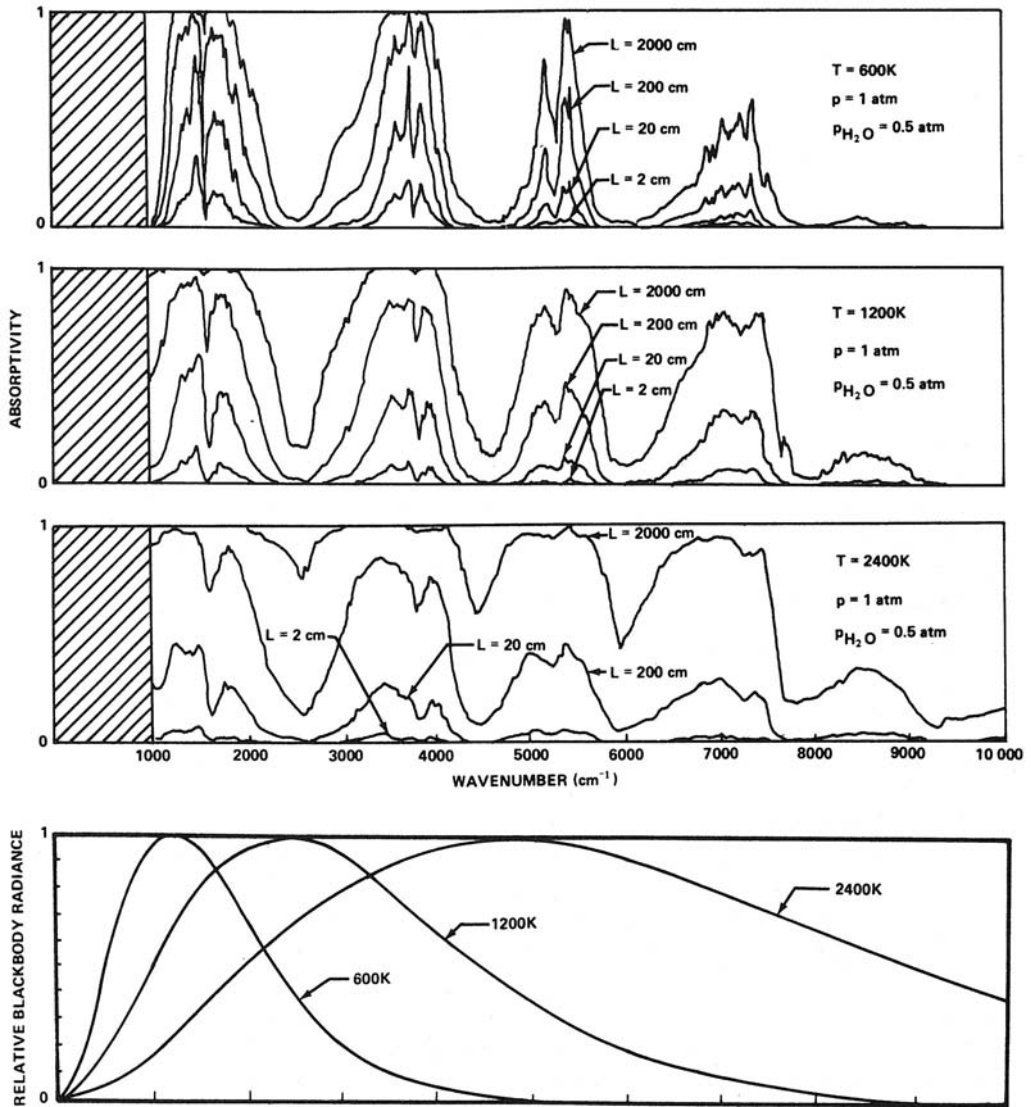


FIGURE 2.8 Calculated spectral emissivity of H_2O as a function of wavelength and path length. (From Ludwig et al., *Handbook of Infrared Radiation from Combustion Gases*, NASA, 1973.)

products generate nonluminous radiation, which has been extensively studied.¹¹ This heat transfer mode depends on the gas temperature level, the partial pressure and concentration of each species, and the molecular path length through the gas. Based on the study of CO flames, Garner (1965) concluded that most of the radiant energy from the flames was primarily chemiluminescence,²⁷ but this was later proven wrong.²⁸ Ludwig et al. (1973) gave a very detailed discussion of the theory of infrared radiation from combustion gases, including the terms and their definitions, calculation techniques for both homogeneous and inhomogeneous gases, models for specific molecules (both diatomic and polyatomic), actual computed radiation data, a discussion of the accuracy of the models, and some predictive techniques for calculating rocket exhausts.²⁹ Examples of the spectral emissivity of H_2O and O_2 as a function of wavelength and path length are shown in [Figure 2.8](#) and [Figure 2.9](#), respectively.

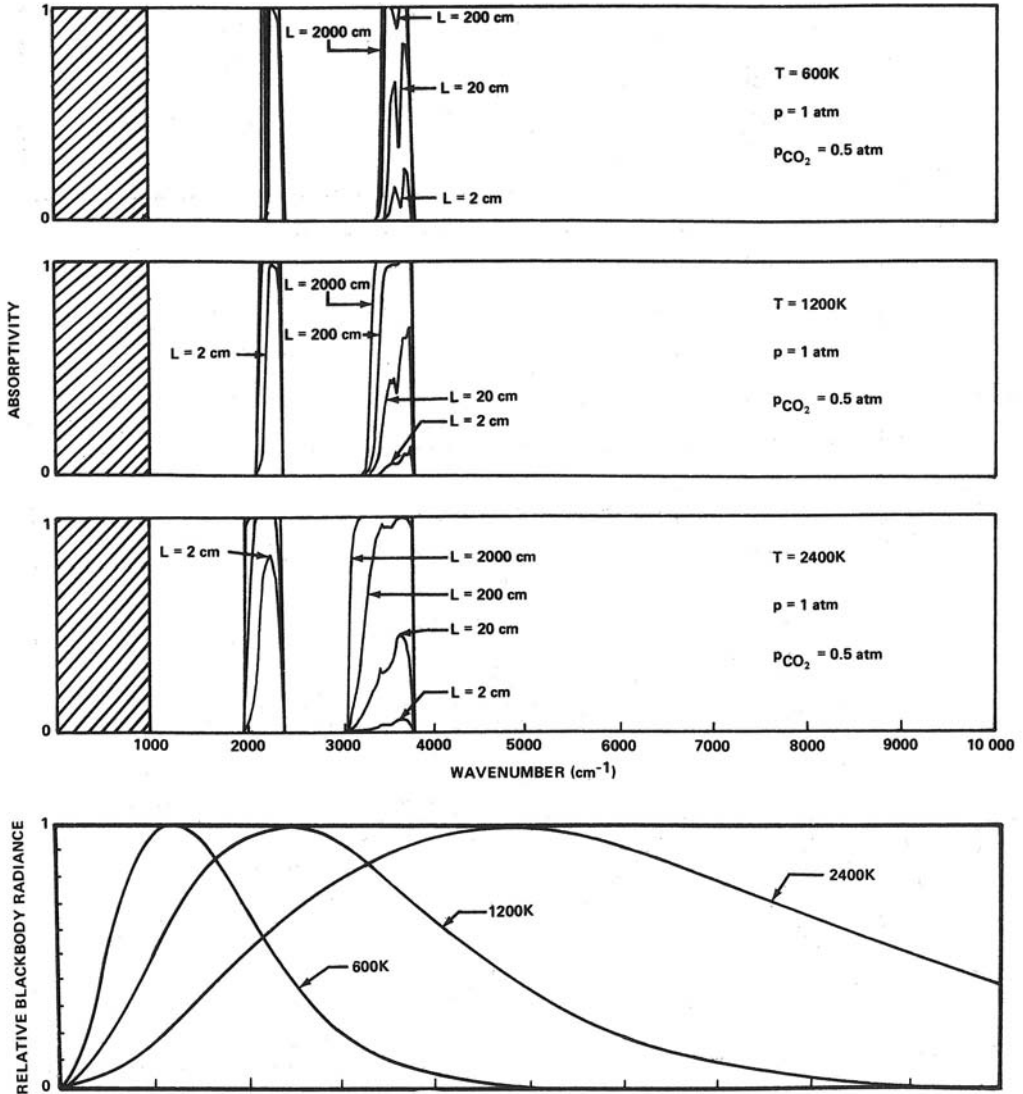


FIGURE 2.9 Calculated spectral emissivity of CO₂ as a function of wavelength and path length. (From Ludwig et al., *Handbook of Infrared Radiation from Combustion Gases*, NASA, 1973.)

The total emissivity can be calculated from Leckner (1972).³⁰ The individual emissivity of either CO₂ or H₂O is given by:

$$\epsilon_i(p_a L, p, T_g) = \epsilon_0(p_a L, T_g) \left(\frac{\epsilon}{\epsilon_0} \right) (p_a L, p, T_g) \quad (2.24)$$

where ϵ_i = emissivity of the individual gas, p_a = partial pressure of the gas, L = path length through the gas, T_g = absolute temperature of the gas, and ϵ_0 = emissivity of the individual gas at a reference

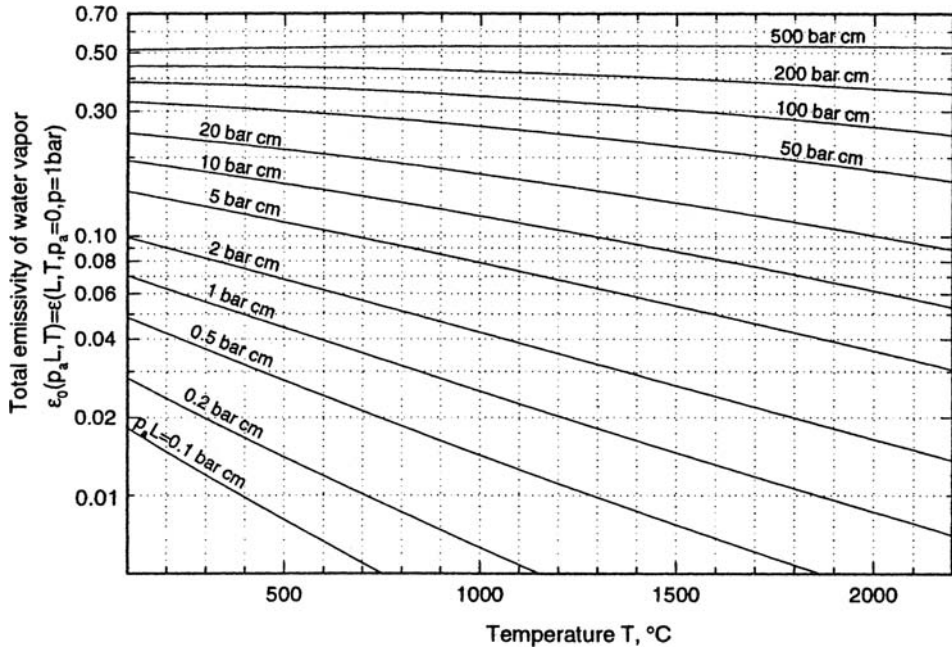


FIGURE 2.10 Total emissivity of water vapor at the reference state of a total gas pressure $p = 1$ bar and a partial pressure of H_2O $p_a \rightarrow 0$.¹³⁶

state (atmospheric pressure and $p_a \rightarrow 0$ but $p_a L > 0$). The first term in Equation 2.24 is calculated using:

$$\epsilon_0(p_a L, T_g) = \exp \left[\sum_{i=0}^M \sum_{j=0}^N c_{ij} \left(\frac{T_g}{T_0} \right)^j \left(\log_{10} \frac{p_a L}{(p_a L)_0} \right)^i \right] \quad (2.25)$$

where T_0 = absolute reference temperature of the gas (1000K) and c_{ij} are constants. The second term of the equation is calculated from:

$$\left(\frac{\epsilon}{\epsilon_0} \right) (p_a L, p, T_g) = \left\{ 1 - \frac{(a-1)(1-P_E)}{a+b-1+P_E} \exp \left[-c \left(\log_{10} \frac{(p_a L)_m}{p_a L} \right)^2 \right] \right\} \quad (2.26)$$

where a , b , c , P_E , and $(p_a L)_m/p_a L$ are given in Table 2.3. Graphical results for H_2O and CO_2 are shown in Figure 2.10 and Figure 2.11, respectively. The total emissivity is then calculated using:

$$\epsilon_{\text{CO}_2+\text{H}_2\text{O}} = \epsilon_{\text{CO}_2} + \epsilon_{\text{H}_2\text{O}} - \Delta\epsilon \quad (2.27)$$

where the $\Delta\epsilon$ accounts for the overlap between the H_2O and CO_2 bands and is calculated from:

$$\Delta\epsilon = \left(\frac{\xi}{10.7 + 101\xi} - 0.0089\xi^{10.4} \right) \left(\log_{10} \frac{(p_{\text{H}_2\text{O}} + p_{\text{CO}_2})L}{(p_a L)_0} \right)^{2.76} \quad (2.28)$$

TABLE 2.3
Correlation Constants for the Determination of the Total Emissivity for Water Vapor and Carbon Dioxide¹³⁶

Gas	Water Vapor				Carbon Dioxide			
M, N	2, 2				2, 3			
$c_{00} \dots c_{N1}$	-2.2118	-1.1987	0.035596	-3.9893	2.7669	-2.1081	0.39163	
$\vdots \dots \vdots$	0.85667	0.93048	-0.14391	1.2710	-1.1090	1.0195	-0.21897	
$c_{0M} \dots c_{NM}$	-0.10838	-0.17156	0.045915	-0.23678	0.19731	-0.19544	0.04464	
P_E	$(p + 2.5bp_a/\sqrt{t})/p_c$				$(p + 0.28p_a)/p_0$			
$(p_0L)_m/(p_aL)_0$	$13.2t^2$				$0.054/t^2, t < 0.7$			
					$0.225t^2, t > 0.7$			
a	2.144,		$t < 0.75$		$1 + 0.1/t^{1.45}$			
	1.88-2.053 $\log_{10} t,$		$t > 0.75$					
b	$1.10/t^{1.4}$				0.23			
c	0.5				1.47			

Note: $T_0 = 1000$ K, $p_0 = 1$ bar, $t = T/T_0$, $(p_a, L)_0 = 1$ bar cm.

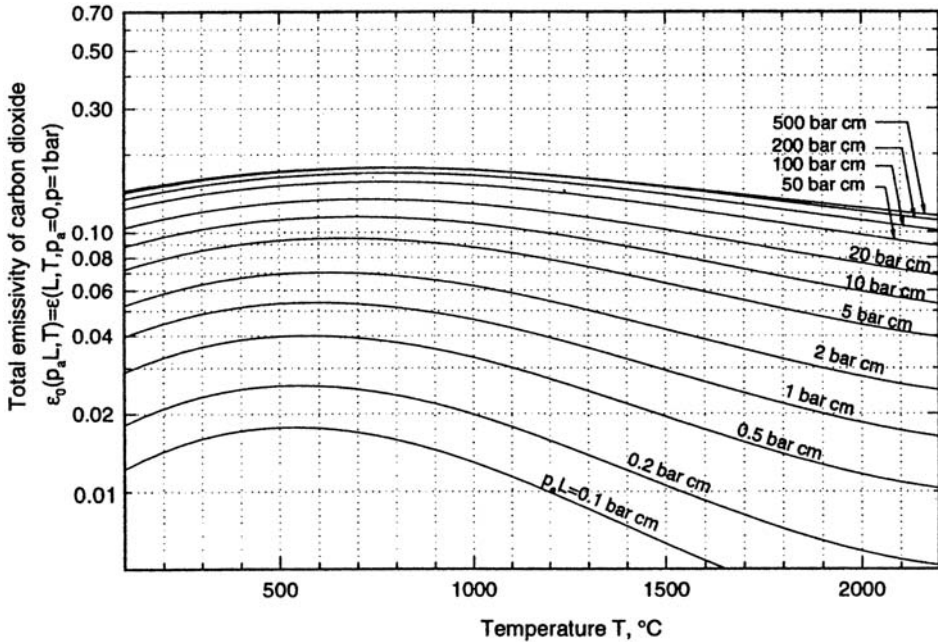


FIGURE 2.11 Total emissivity of carbon dioxide at the reference state of a total gas pressure $p = 1$ bar and a partial pressure of CO_2 $p_a \rightarrow 0$.¹³⁶

and

$$\xi = \frac{P_{\text{H}_2\text{O}}}{P_{\text{H}_2\text{O}} + P_{\text{CO}_2}} \quad (2.29)$$

Example 2.6

Given: Combustion products containing 9% CO₂, 18% H₂O, and the balance N₂, at a temperature of 1500°F, with a mean beam length of 10 ft, at atmospheric pressure.

Find: Gas emissivity.

Solution: Calculate $p_a L$ for CO₂ and H₂O to use graphs:

$$\text{CO}_2: p_a L = (0.09 \text{ bar})(305 \text{ cm}) = 27 \text{ bar-cm}$$

$$\text{H}_2\text{O}: p_a L = (0.18 \text{ bar})(305 \text{ cm}) = 55 \text{ bar-cm}$$

Look up on graphs the ϵ_0 for CO₂ and H₂O at a temperature of 820°C:

$$\text{CO}_2: \epsilon_0 \approx 0.12$$

$$\text{H}_2\text{O}: \epsilon_0 \approx 0.29$$

Calculate correction factors ϵ/ϵ_0 using Equation 2.26 and Table 2.3:

$$t = T/T_0 = (1090\text{K}/1000\text{K}) = 1.09$$

$$\text{CO}_2: P_E = (1.0 + 0.28(0.09))/1.0 = 1.03$$

$$\text{H}_2\text{O}: P_E = (1.0 + 2.56/\sqrt{1.09})/1.0 = 3.45$$

$$\text{CO}_2: \frac{(p_a L)_m}{p_a L} = 0.225t^2 = 0.225(1.09)^2 = 0.267$$

$$\text{H}_2\text{O}: \frac{(p_a L)_m}{p_a L} = 13.2t^2 = 13.2(1.09)^2 = 15.7$$

$$\text{CO}_2: a = 1 + 0.1/(1.09)^{1.45} = 1.09; b = 0.23; c = 1.47$$

$$\text{H}_2\text{O}: a = 1.88 - 2.053 \log_{10}(1.09) = 1.80; b = 1.10/(1.09)^{1.4} = 0.97; c = 0.5$$

$$\text{CO}_2: \left(\frac{\epsilon}{\epsilon_0} \right) = \left\{ 1 - \frac{(1.09 - 1)(1 - 1.03)}{1.09 + 0.23 - 1 + 1.03} \exp \left[-1.47 (\log_{10} 0.267)^2 \right] \right\} = 1.001$$

$$\text{H}_2\text{O}: \left(\frac{\epsilon}{\epsilon_0} \right) = \left\{ 1 - \frac{(1.80 - 1)(1 - 3.45)}{1.80 + 0.97 - 1 + 3.45} \exp \left[-0.5 (\log_{10} 15.7)^2 \right] \right\} = 1.184$$

$$\text{CO}_2: \epsilon = (\epsilon/\epsilon_0) \epsilon_0 = (1.001)(0.12) = 0.120$$

$$\text{H}_2\text{O}: \epsilon = (\epsilon/\epsilon_0) \epsilon_0 = (1.184)(0.29) = 0.343$$

$$\text{Calculate } \xi: \xi = \frac{0.18}{0.18 + 0.09} = 0.67$$

Calculate $\Delta\epsilon$:

$$\Delta\epsilon = \left(\frac{0.67}{10.7 + 101(0.67)} - 0.0089(0.67)^{10.4} \right) \left(\log_{10} \frac{(0.18 + 0.09)(305 \text{ cm})}{1 \text{ bar-cm}} \right)^{2.76}$$

$$\Delta\epsilon = 0.051$$

$$\epsilon = 0.120 + 0.343 - 0.051 = 0.412$$

The absorptivity of H₂O and CO₂ can be estimated using:

$$\alpha(p_a L, p, T_g, T_s) = \left(\frac{T_g}{T_s}\right)^{1/2} \epsilon\left(p_a L \frac{T_s}{T_g}, p, T_s\right) \quad (2.30)$$

where T_s is the surface temperature, such as a furnace wall. The correction for the band overlap between H₂O and CO₂ is calculated using:

$$\alpha_{\text{CO}_2+\text{H}_2\text{O}} = \alpha_{\text{CO}_2} + \alpha_{\text{H}_2\text{O}} - \Delta\epsilon \quad (2.31)$$

where $\Delta\epsilon$ is estimated with a pressure path length of $p_a L T_s / T_g$.

Example 2.7

Given: Using the data from the previous example and a wall temperature of 1000°F.

Find: Gas absorptivity.

Solution: Calculate $p_a L T_s / T_g$ for CO₂ and H₂O to use graphs:

$$\text{CO}_2: p_a L T_s / T_g = (0.09 \text{ bar})(305 \text{ cm})(1000 + 460)/(1500 + 460) = 20 \text{ bar-cm}$$

$$\text{H}_2\text{O}: p_a L T_s / T_g = (0.18 \text{ bar})(305 \text{ cm})(1000 + 460)/(1500 + 460) = 41 \text{ bar-cm}$$

Look up on graphs the ϵ_0 for CO₂ and H₂O at a temperature of 540°C (1000°F):

$$\text{CO}_2: \epsilon_0 \approx 0.12, \text{H}_2\text{O}: \epsilon_0 \approx 0.28$$

Calculate correction factors ϵ/ϵ_0 using Equation (2.26) and [Table 2.3](#):

$$t = (811\text{K}/1000 \text{ K}) = 0.811$$

$$\text{CO}_2: P_E = (1.0 + 0.28(0.09))/1.0 = 1.03$$

$$\text{H}_2\text{O}: P_E = (1.0 + 2.56/\sqrt{0.811})/1.0 = 3.84$$

$$\text{CO}_2: \frac{(p_a L)_m}{p_a L} = 0.225t^2 = 0.225(0.811)^2 = 0.148$$

$$\text{H}_2\text{O}: \frac{(p_a L)_m}{p_a L} = 13.2t^2 = 13.2(0.811)^2 = 8.68$$

$$\text{CO}_2: a = 1 + 0.1/(0.811)^{1.45} = 1.14; b = 0.23; c = 1.47$$

$$\text{H}_2\text{O}: a = 1.88 - 2.053 \log_{10}(0.811) = 2.07; b = 1.10/(0.811)1.4 = 1.47; c = 0.5$$

$$\text{CO}_2: \left(\frac{\epsilon}{\epsilon_0}\right) = \left\{1 - \frac{(1.14 - 1)(1 - 1.03)}{1.14 + 0.23 - 1 + 1.03} \exp\left[-1.47(\log_{10} 0.148)^2\right]\right\} = 1.001$$

$$\text{H}_2\text{O}: \left(\frac{\epsilon}{\epsilon_0}\right) = \left\{1 - \frac{(2.07 - 1)(1 - 3.84)}{2.07 + 1.47 - 1 + 3.84} \exp\left[-0.5(\log_{10} 8.68)^2\right]\right\} = 1.307$$

$$\text{CO}_2: \epsilon = (\epsilon/\epsilon_0) \epsilon_0 = (1.001)(0.12) = 0.120$$

$$\text{H}_2\text{O}: \epsilon = (\epsilon/\epsilon_0) \epsilon_0 = (1.307)(0.28) = 0.366$$

$$\text{CO}_2: \alpha = \sqrt{\frac{1500 + 460}{1000 + 460}} (0.120) = 0.139$$

$$\text{H}_2\text{O: } \alpha = \sqrt{\frac{1500 + 460}{1000 + 460}} \quad 0.366 = 0.424$$

$$\alpha = 0.139 + 0.424 - 0.051 = 0.512$$

Relatively simple but accurate calculations for isothermal gases, which are absorbing–emitting but not scattering, in an isothermal black-walled enclosure can be computed using:

$$q = \sigma \left\{ [1 - \alpha(L_m)] T_w^4 - \epsilon(L_m) T_g^4 \right\} \quad (2.32)$$

where L_m is the average mean beam length and T_w is the absolute temperature of the isothermal wall. The mean beam length is a function of the geometry of the enclosure and can be calculated using the formulae in Table 2.4. For geometries not listed in that table, the following formula can be used:

$$L_m = 3.6 V/A \quad (2.33)$$

where V is the volume of the enclosure and A is the surface area inside the enclosure. Gulic (1974) gave a modified form to calculate the mean beam length:³¹

$$L_m = 3.6 \frac{V}{A} \left(\frac{\tau e^{-\tau}}{\tau - 1 + e^{-\tau} + \tau e^{-\tau}} \right) \quad (2.34)$$

where τ is the optical density of the gas.

Cess (1974) gave a relatively simple procedure for calculating infrared gaseous radiation that uses an analytical approximate band model.³² The results showed good agreement with a numerical solution. Greif (1974) presented some experimental and theoretical results for infrared radiation from a turbulent flow of air, CO₂, and steam.³³ Kovotny (1974) showed the importance of pressure in calculating gaseous radiation heat transfer.³⁴ In a review article, Edwards (1976) cautioned about the use of gray-gas models and analysis to represent the truly spectrally dependent phenomena of gaseous radiation.³⁵ Trout (1977) gave some simple methods for estimating both nonluminous and luminous radiation from industrial flames³⁶ Tien and co-workers (1968, 1982) reviewed radiation from flames.^{37,38} They extensively reviewed the available models for both nonluminous and luminous gaseous radiation. Edwards and Balakrishnan (1973) presented some correlations for calculating the radiative properties of H₂O, CO₂, CO, NO, SO₂ and CH₄ for use in solving gas radiation problems.³⁹ Taylor and Foster (1974) presented empirical curve-fitted equations for the total emissivities of nonluminous and luminous flames, for CO₂–H₂O and CO₂–H₂O–soot mixtures arising in oil and gas combustion.⁴⁰ Coppalle and Vervisch (1983) calculated the total emissivities of high temperature (2000 to 3000K) gases (CO₂–H₂O mixtures).⁴¹ Edwards and Matavosian (1984) developed some scaling rules for calculating the total absorptivity and emissivity of gases and tabulated and graphed results for various combinations of gas composition, product of partial pressure times the path length, and gas temperature.⁴² Howell (1988) reviewed thermal radiation in participating media and gave numerous references for further information.⁴³ The P-N, two-flux, discrete ordinate, finite-element, zoning, and Monte Carlo methods of analysis were briefly discussed. Wieringa et al. (1990) modeled the spectral radiation produced by natural gas flames in a regenerative glass furnace.⁴⁴ The spectral radiation from H₂O and CO₂ were modeled using 15 spectral bands. The numerical results showed that the furnace wall emissivity had only a minimal impact on the furnace efficiency.

TABLE 2.4
Mean Beam Lengths for Radiation from a Gas Volume to a Surface on Its Boundary¹³⁶

Geometry of Gas Volume	Characterizing Dimension	Geometric Mean Beam Length	Average Mean Beam Length	L_m/L_0
	L	L_0/L	L_m/L	
Sphere radiating to its surface	Diameter, $L = D$	0.67	0.65	0.97
Infinite circular cylinder to bounding surface	Diameter, $L = D$	1.00	0.94	0.94
Semi-infinite circular cylinder to:	Diameter $L = D$			
Element at center of base		1.00	0.90	0.90
Entire base		0.81	0.65	0.80
Circular cylinder (height/diameter = 1) to:	Diameter, $L = D$			
Element at center of base		0.76	0.71	0.92
Entire surface		0.67	0.60	0.90
Circular cylinder (height/diameter = 2) to:	Diameter, $L = D$			
Plane base		0.73	0.60	0.82
Concave surface		0.82	0.76	0.93
Entire surface		0.80	0.73	0.91
Circular cylinder (height/diameter = 0.5) to:	Diameter, $L = D$			
Plane base		0.48	0.43	0.90
Concave surface		0.53	0.46	0.88
Entire surface		0.50	0.45	0.90
Infinite semicircular cylinder to center of plane rectangular face	Radius, $L = R$	—	1.26	—
Infinite slab to its surface	Slab thickness, L	2.00	1.76	0.88
Cube to a face	Edge L	0.67	0.6	0.90
Rectangular $1 \times 1 \times 4$ parallelepipeds:	Shortest edge, L			
To 1×4 face		0.90	0.82	0.91
To 1×1 face		0.86	0.71	0.83
To all faces		0.89	0.81	0.91

2.2.2.2 Combustion Studies

Two types of nonluminous radiation measurements have been made in previous combustion studies: total and spectral. The total radiation measurements were typically made with some type of detector that measured the overall radiation received, with no wavelength dependence. More recent measurements have been made which give the radiation as a function of the wavelength. These two methods of measurements applied to nonluminous radiation are discussed briefly here.

2.2.2.2.1 Total Radiation

In some previous combustion experimental studies, nonluminous gaseous radiation has been significant. Kilham (1949) tested nearly stoichiometric, laminar, air/CO flames, impinging normal to an uncooled refractory cylinder.⁹⁸ Flame radiation was 5 to 16% of the total heat flux. Jackson and Kilham (1956) also tested laminar flames, impinging normal to refractory cylinders.⁹⁷ A variety of fuels, oxidizers, and stoichiometries were tested. The measured flame radiation was up to 5% of the total heat flux. Dunham (1963) tested nearly stoichiometric, laminar, air/CO flames, impinging normal to the nose of a hemi-nosed cylinder.⁴⁵ The estimated nonluminous radiation was up to

13% of the total heat flux. Ivernel and Vernotte (1979) tested nearly stoichiometric, natural gas flames, impinging normal to the nose of a hemispherical cylinder.¹¹⁶ The calculated nonluminous flame radiation was up to 34% of the total heat flux.

In other combustion studies, nonluminous radiation was not significant. Giedt et al. (1960) measured and calculated nonluminous radiation at less than 2% of the total heat flux.⁴⁶ Woodruff and Giedt (1966) used the same configuration as Giedt, except that the flames were turbulent.¹⁰⁰ The measured nonluminous radiation was negligible compared to the total heat flux. Shorin and Pechurkin (1968) tested a wide variety of flames impinging normal to a flat plate.¹¹⁰ Radiation was experimentally determined to be negligible. Purvis (1974) studied O_2/CH_4 and O_2/C_3H_8 flames, impinging normal to a flat plate.⁴⁷ The calculated nonluminous flame radiation was negligible compared to the total heat flux. Although the C_3H_8 flames were very fuel rich, there was no discussion of luminous flame radiation. Hoogendoorn et al. (1978) tested stoichiometric, laminar, air/natural gas flames impinging normal to a water-cooled flat plate.¹⁰⁵ Flame radiation effects did not exceed 5% of the total heat flux. No radiation measurements or calculations were given. Davies (1979) tested natural gas flames impinging normal to a water-cooled cylinder.⁴⁸ A range of stoichiometries and oxidizers was tested. Using an estimated flame emissivity of 0.01, the calculated nonluminous radiation was only 2% of the total heat flux. Van der Meer (1987) tested stoichiometric, laminar, and turbulent air/natural gas flames impinging normal to a water-cooled plate.⁴⁹ The flame radiation was said to be negligible because of the very low emissivity of a thin hot gas layer. No supporting calculations were cited.

Baukal and Gebhart (1997) studied total flame radiation from oxygen-enhanced natural gas flames.⁵⁰ A total, narrow-angle radiometer was used to measure the flame radiation as a function of position from the burner as shown in Figure 2.12. Five parameters were investigated, including the burner firing rate (q_f), the oxidizer composition (Ω), the equivalence ratio (ϕ), the axial position along the flame (L_r), and the radial position from the flame (D_r). The parameters of primary interest were Ω , q_f , and L_r . Most of the tests were done at $\phi = 1.0$ and $D_r = 0.5$. The equivalence ratio was only varied through a narrow range for two reasons. The first is that the equivalence ratio operates in a narrow band around stoichiometric conditions in nearly all industrial heating and melting processes. The second reason is that only nonluminous radiation was studied here. If the burner had been operated at very fuel-rich conditions ($\phi \rightarrow \infty$), luminous radiation would have become important. Figure 2.13 shows the effects of both the firing rate and the axial distance along the flame length. The minimum L_r was 0.5. For $L_r < 0.5$, the radiometer would have viewed the flame and part of the burner itself. At low firing rates, the flame radiation decreased rapidly with the distance from the burner exit. At intermediate and higher firing rates, the flame radiation was

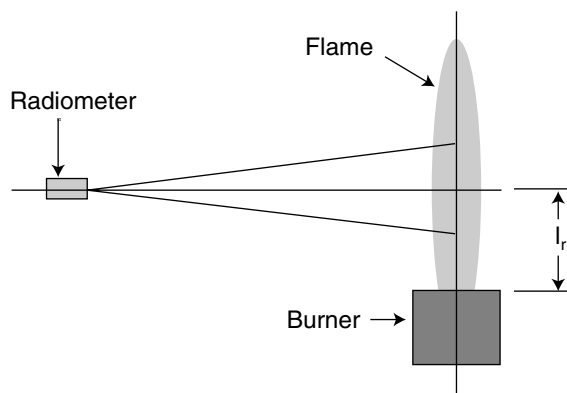


FIGURE 2.12 Experimental setup for measuring total nonluminous gaseous radiation from an open-flame diffusion burner as a function of the distance from the burner outlet.⁵⁰

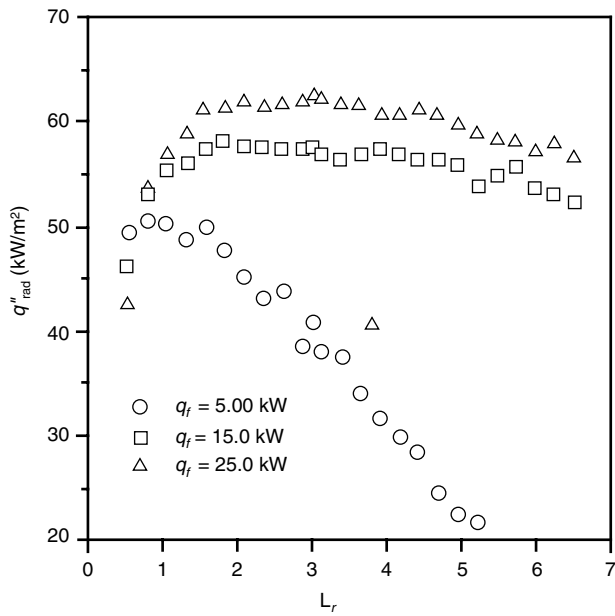


FIGURE 2.13 Total nonluminous gaseous radiation (q''_{rad}) as a function of distance from the burner (L_r) and firing rate ($q_f = 5.0, 15.0, 25.0$ kW) for $\Omega = 1.00$, $\phi = 1.00$, and $D_r = 0.5$.⁵⁰

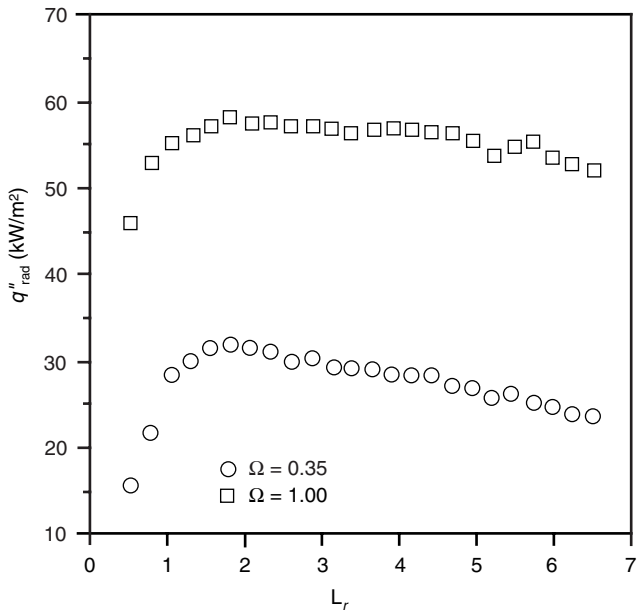


FIGURE 2.14 Total nonluminous gaseous radiation (q''_{rad}) as a function of distance from the burner outlet (L_r) and oxidizer composition ($\Omega = 0.35, 1.00$) for $q_f = 15.0$ kW, $\phi = 1.00$, and $L_r = 3.0$.⁵⁰

relatively constant for L_r from about 2 to 5. Figure 2.14 is a similar graph except that the oxidizer composition, instead of the firing rate, was varied. The flame radiation was relatively constant over a wide range of L_r , for $\Omega = 1.0$. At $\Omega = 0.35$, the peak flame radiation occurred at about $L_r = 1.5$ and then slowly decreased with L_r . Figure 2.15 shows how the radial location of the radiometer

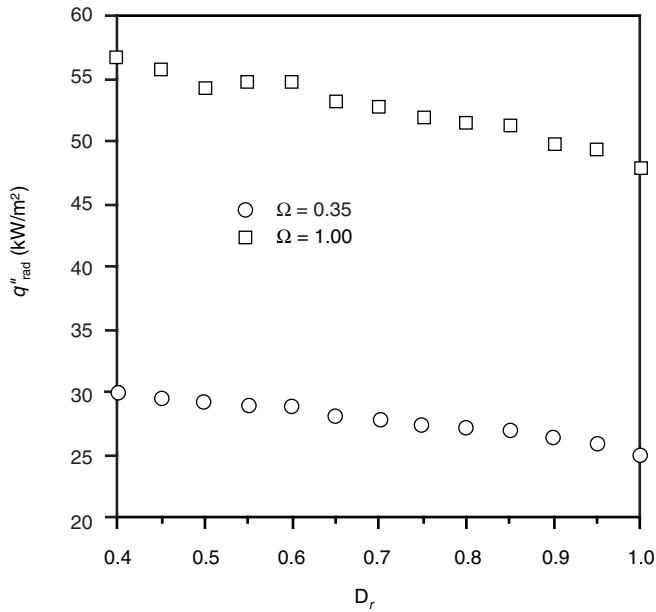


FIGURE 2.15 Total nonluminous gaseous radiation (q''_{rad}) as a function distance from the burner outlet (D_r) and oxidizer composition ($\Omega = 0.35, 1.00$) for $q_f = 15.0$ kW, $\phi = 1.00$, and $L_r = 3.0$.⁵⁰

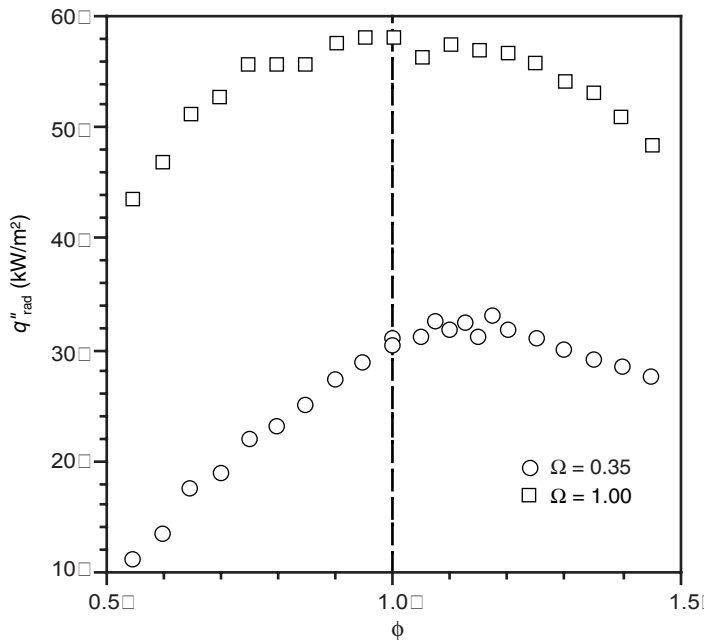


FIGURE 2.16 Total nonluminous gaseous radiation (q''_{rad}) as a function of the equivalence ratio (ϕ) and oxidizer composition ($\Omega = 0.35, 1.00$) for $q_f = 15.0$ kW, $L_r = 3.0$, and $D_r = 0.5$.⁵⁰

affected the measurements. At $D_r = 1.0$, the radiometer viewed the entire width of the flame. The effective path length decreased as D_r increased, because the flame had a circular cross section. This reduced the average flame radiation as shown in the plot. However, the reduction was relatively small. Figure 2.16 shows how the equivalence ratio and the oxidizer compositions affected the

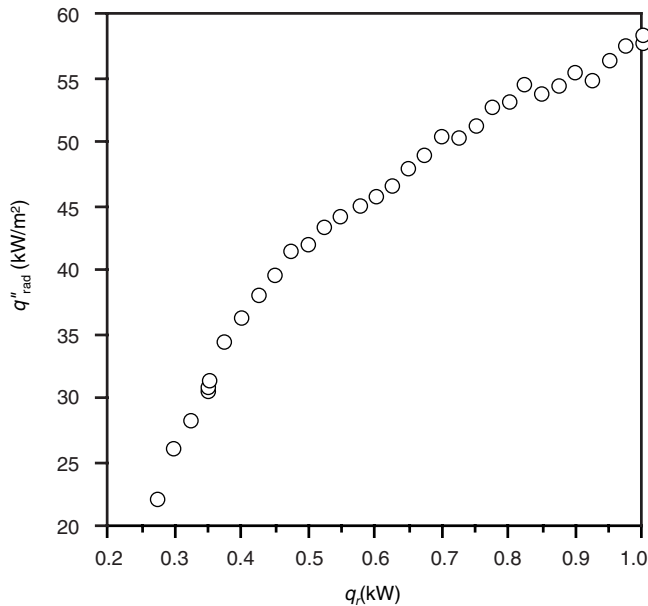


FIGURE 2.17 Total nonluminous gaseous radiation (q''_{rad}) as a function of the oxidizer composition (Ω) for $q_f = 15.0 \text{ kW}$, $\phi = 1.00$, $L_r = 3.0$, $D_r = 0.5$.⁵⁰

flame radiation. For the smaller Ω , the highest flame radiation occurred at slightly fuel-lean conditions. For a pure O_2 oxidizer, the highest flame radiation occurred in a band around stoichiometric conditions ($\phi = 1.0$). Figure 2.17 shows how the flame radiation varied as a function of the oxidizer composition for a fixed firing rate and equivalence ratio. The only thing that was varied was the amount of N_2 in the oxidizer. The fuel and O_2 flow rates were constant. Re_n decreased from 6800 to 2400 as Ω increased from 0.28 to 1.00. The plot shows that the flame radiation increased by more than 2.5 times by removing N_2 from the oxidizer. This is a result of higher flame temperatures and partial pressures of CO_2 and H_2O . Figure 2.18 shows how the flame radiation increased as the firing rate increased and as the equivalence ratio increased. Figure 2.19 is a plot of flame radiation as a function of the equivalence ratio and the firing rate for a constant Reynolds number of 4500. As N_2 was removed from the oxidizer (Ω increasing), the firing rate had to be increased to maintain a fixed Re_n . This shows that, for a given nozzle diameter, a higher heat release density can be achieved by increasing the O_2 concentration in the oxidizer. It also implies that Re_n by itself is not a sufficient parameter to indicate the performance of oxygen-enhanced flames. The oxidizer composition Ω must also be specified. Figure 2.20 shows the peak flame radiation measured for a given firing rate and oxidizer composition. For $\Omega = 1.00$, the peak radiation increased with the firing rate. For $\Omega = 0.35$, the peak radiation was relatively constant over a wide range of firing rates. Figure 2.21 shows the approximate axial location for the peak flame radiation. Initially, the peak flame locations were closer to the burner for $\Omega = 1.00$ compared to $\Omega = 0.35$. At higher firing rates, this trend reversed. For $\Omega = 1.00$, these locations were fairly well defined. For $\Omega = 0.35$, there was a range of positions along the flame length where the maximum flame radiation values were obtained. The locations given in the figure are approximately in the center of the range. Figure 2.22 is a plot of the location for the peak flame radiation that has been normalized to the visible length of the flame. This shows that for high Ω flames, the axial location of the peak flame radiation was at about 14% of the visible flame length. For the lower Ω flames, this location was between about 9 and 15% of the flame length.

The important conclusions of the study included: (1) thermal radiation increased dramatically by removing N_2 from the oxidizer; (2) the flame radiation increased with the firing rate with a more

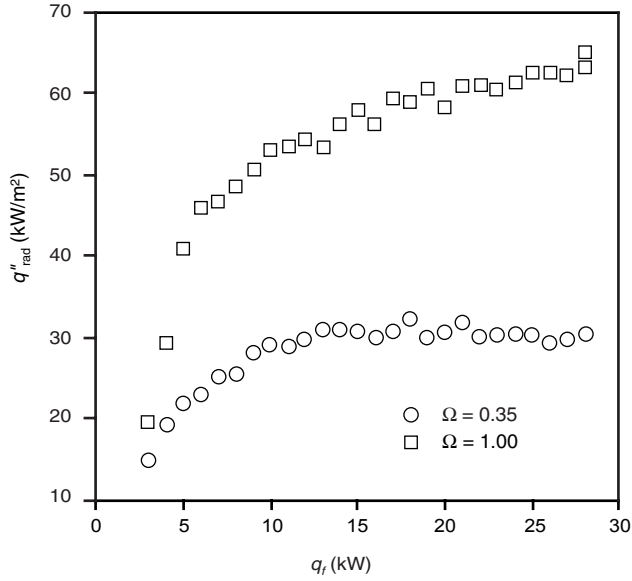


FIGURE 2.18 Total nonluminous gaseous radiation (q''_{rad}) as a function of the firing rate (q_f) and oxidizer composition ($\Omega = 0.35, 1.00$) for $\phi = 1.00$, $L_r = 3.0$, and $D_r = 0.5$.⁵⁰

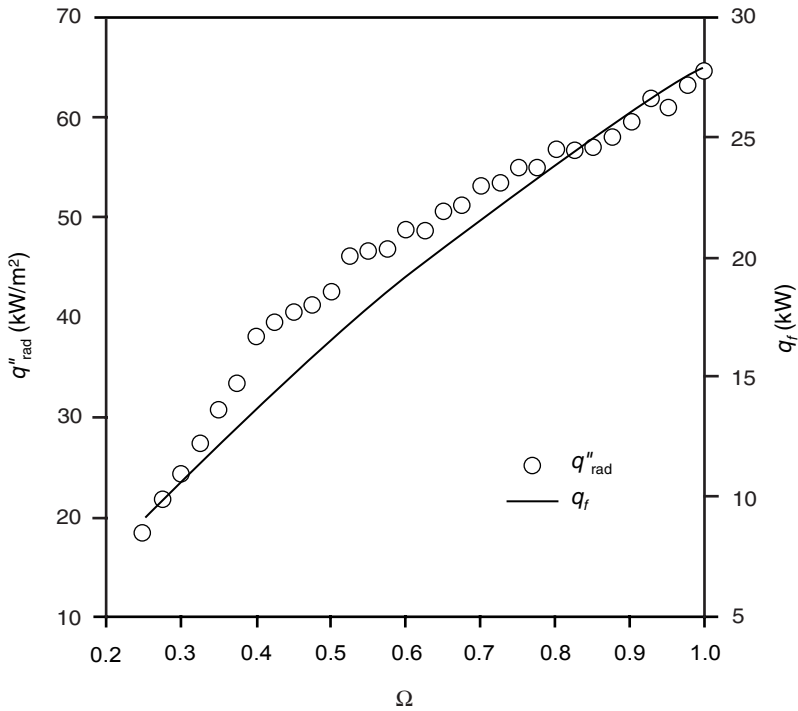


FIGURE 2.19 Total nonluminous gaseous radiation (q''_{rad}) as a function of the oxidizer composition (Ω) for $Re_n = 4500$, $\phi = 1.00$, $L_r = 3.0$, and $D_r = 0.5$.⁵⁰

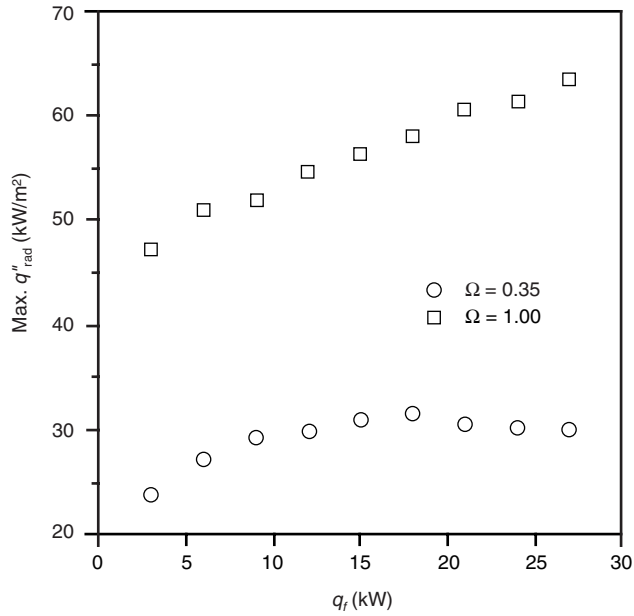


FIGURE 2.20 Maximum total nonluminous gaseous radiation (q''_{rad}) as a function of the firing rate (q_f) and oxidizer composition ($\Omega = 0.35, 1.00$) for $\phi = 1.00$ and $D_r = 0.5$ with L_r variable.⁵⁰

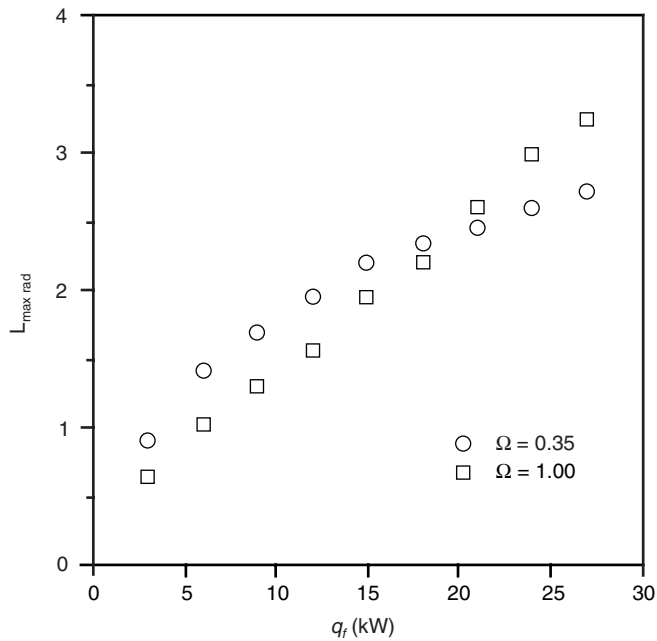


FIGURE 2.21 Axial distance of maximum radiation ($L_{max rad}$) as a function of the firing rate (q_f) and oxidizer composition ($\Omega = 0.35, 1.00$) for $\phi = 1.00$ and $D_r = 0.5$.⁵⁰

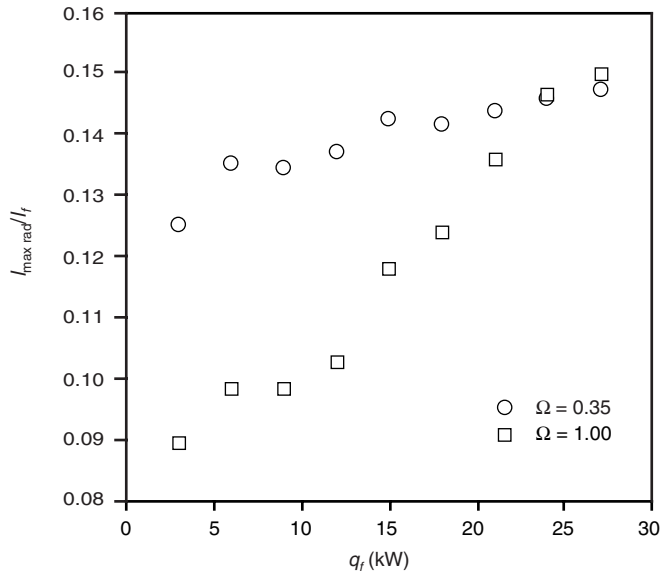


FIGURE 2.22 Normalized axial location of maximum radiation ($I_{\max \text{ rad}}/I_f$) as a function of firing rate (q_f) and oxidizer composition ($\Omega = 0.35, 1.00$) for $\phi = 1.00$ and $D_r = 0.5$.⁵⁰

dramatic increase at higher O_2 concentrations in the oxidizer; (3) higher flame radiation was measured at or near stoichiometric conditions where typical industrial heating processes operate; (4) for higher firing rates, the radiation was nearly constant over a wide range of axial locations in the flame; and (5) at lower firing rates, the flame radiation decreased with the axial distance from the burner outlet. For higher O_2 concentrations, the peak flame radiation increased with the firing rate. For lower O_2 concentrations, the peak flame radiation was nearly constant over a wide range of firing rates. The location of the peak flame radiation varied from 9 to 15% of the visible flame length. This location was more defined for the higher O_2 flames in terms of both its absolute position and the position normalized by the flame length.

2.2.2.2.2 Spectral Radiation

Ji and Baukal (1998) did the first systematic experimental study of the nonluminous and luminous spectral radiation from oxygen-enhanced flames.⁵¹ Two common quantities are measured in spectral radiometry: spectral radiance and spectral irradiance. Spectral radiance quantifies the energy flux in a unit wavelength interval that is emitting from a source surface per unit area and unit solid angle. The spectral irradiance is a measure of the energy flux in a unit wavelength interval that is incident on a target surface per unit area. For an optical source with a well-defined uniform emitting surface, spectral radiance can be measured accurately and converted into spectral irradiance. The lack of such well-defined and uniform radiating surfaces for flames renders the measurement of spectral radiance impractical. However, spectral irradiance is still a valid quantity to measure in flames and has more practical meaning in heat transfer to targets. For this reason, spectral irradiance was measured, despite the fact that spectral radiance has been used in some previous theoretical studies on flame radiation.³

A custom-built version of the commercial ICSM burner from Nordsea Gas Technology Ltd. (Cheshire, England) was used for the study as shown in Figure 2.23, where $d_n = 38.5$ mm. It was a round form of the rectangular burners⁵² used in industrial heating and melting processes. Details of this burner and its operating characteristics, as well as fuel and oxidizer flow specifications, are given elsewhere.⁵³ A key feature of the burner was the wide variety of oxidizers that can be used,

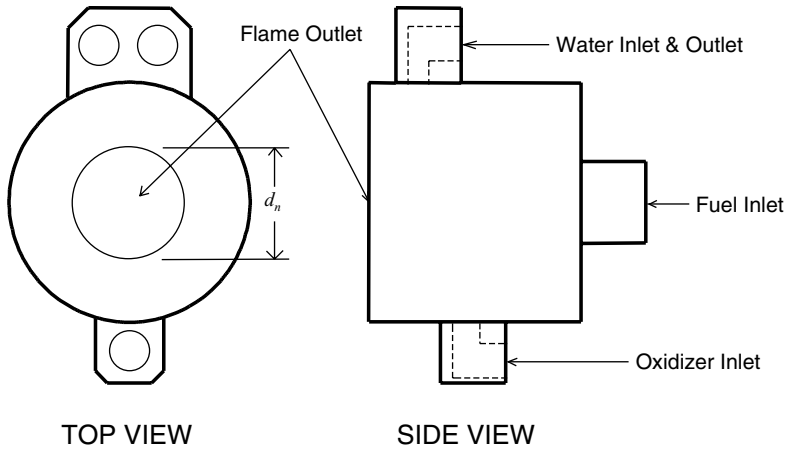


FIGURE 2.23 Burner used for flame radiation study using oxygen-enhanced burners.⁵³

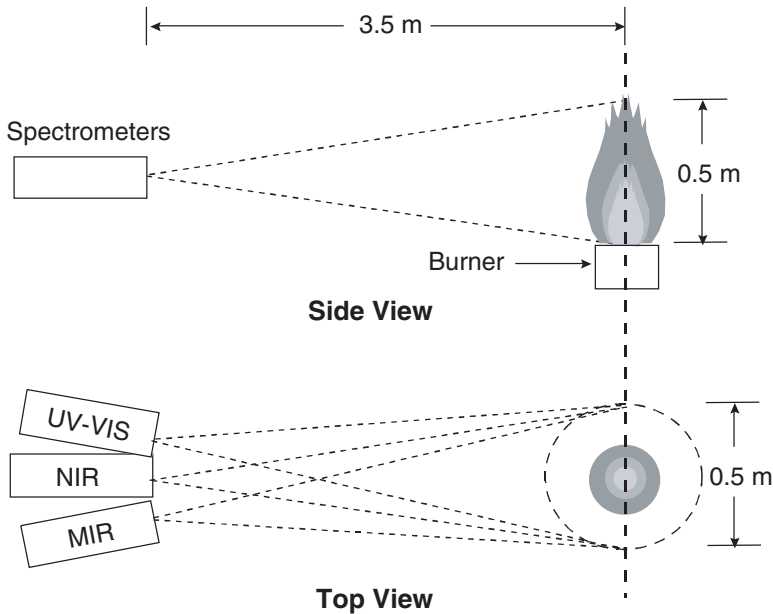


FIGURE 2.24 Experimental setup of the Monolith spectral radiometer (UV-VIS = UV and visible, NIR = near-IR, MIR = mid-IR).⁵¹

ranging from air to pure oxygen, for a range of firing rates. Another key feature was that the burner produced a uniform, nearly one-dimensional flame, so that the flame radiation was more uniform compared to diffusion flames. A firing rate of 17,000 Btu/hr (5.0 kW) was used for most of the measurements, so that there was no significant radiation at a height 1.6 ft (0.5 m) above the burner surface.

As shown in Figure 2.24, three spectral monochromators were set 11 ft (3.5 m) away from the burner centerline, and 0.82 ft (0.25 m) above the burner surface so that their field of view covered the entire radiation length of the flames. Because the flames were in open air, without any furnace enclosure and without impinging on any targets or nearby walls, ambient emission and reflection from the surroundings were negligible. Three parameters were varied to study their effects on the

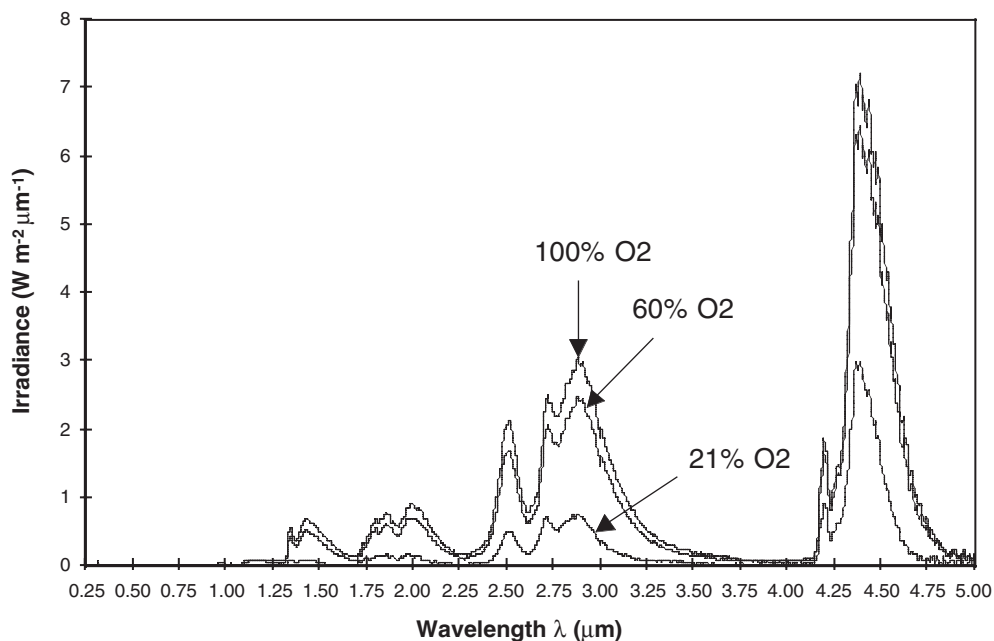


FIGURE 2.25 Overall spectra for flame radiation dependence on oxygen enrichment ratio Ω .⁵¹

spectral radiation from oxygen-enhanced/natural gas flames: (1) oxygen enrichment ratio (Ω), (2) fuel equivalence ratio (ϕ), and (3) firing rate or fuel input (q_f). The oxygen enrichment ratio ranged from $\Omega = 0.21$ (air) to $\Omega = 1.00$ (pure O_2). For the specific natural gas composition used, the stoichiometric ratio of oxygen to fuel was 2.08. Fuel-rich and fuel-lean flames had fuel equivalence ratios greater than 1.0 and less than 1.0, respectively.

As will be shown in the flame radiation spectra, most of the flame radiation fell within the infrared region. Ultraviolet (0.25 to 0.38 μm) radiation, while important in some flame diagnostics, contributed little to the total radiation intensity. Visible (0.38 to 0.78 μm) radiation also made only a small contribution to the total radiation intensity. However, as shown in [Chapter 4](#), the visible radiation is a direct indicator of the penetrating radiation that is most effective for glass heating and melting. For a relative comparison among the flames studied, the radiation spectra over the entire wavelength region (0.25 to 5.0 μm) was numerically integrated and then normalized to the integrated radiation intensity of the flame with $q_f = 5.0$ kW, $\Omega = 1.0$, and $\phi = 1.0$. This normalization eliminated possible errors due to the uncertainties in the spectral radiometer calibration. Normalization also helped reveal the general trends as the flame parameters changed. The results are summarized in [Figure 2.25](#), which shows three flame radiation spectra with $q_f = 5.0$ kW, $\phi = 1.0$, and $\Omega = 1.00, 0.60,$ and 0.21 , respectively. The integrated results are listed in [Table 2.5](#). The radiation intensity from the pure oxygen/natural gas flame ($\Omega = 1.00$) was about four times that from the air/natural gas flame ($\Omega = 0.21$), for the same fuel consumption. This is because nitrogen in the air absorbs energy from the combustion reaction but N_2 does not radiate. [Figure 2.26](#) is the UV portion of the spectra plotted on a logarithmic scale. Despite the relatively small contribution of UV radiation to the total intensity, the presence of UV emissions (predominantly from the electronically excited OH radicals) can be explored as a way to visualize nonluminous flames in hot and highly luminous furnaces. The UV radiation from a pure oxygen flame was about three orders of magnitude stronger than that from the air/fuel flame. Such a dramatic difference cannot be simply accounted for by thermodynamic equilibrium at different flame temperatures. Rather, this was an indication that significantly more nonequilibrium chemiluminescence of OH radicals exists in

TABLE 2.5
Flame Radiation Intensity Measurements⁵¹

Ω	ϕ	$I_{\text{nm}}(\text{total})$	$I_{\text{nm}}(\text{pen.})$	$I_{\text{nm}}(\text{BK7})$	γ
1.00	0.67	0.90 ± 0.06	0.89 ± 0.06	0.82 ± 0.06	0.15 ± 0.01
1.00	0.80	0.99 ± 0.07	0.98 ± 0.07	0.95 ± 0.07	0.13 ± 0.01
1.00	1.00	1.00 ^a	1.00 ^a	1.00 ^a	0.14 ± 0.01
1.00	1.33	0.93 ± 0.07	0.98 ± 0.07	0.99 ± 0.07	0.17 ± 0.01
1.00	1.50	0.91 ± 0.06	0.93 ± 0.07	0.87 ± 0.06	0.20 ± 0.01
1.00	1.60	0.84 ± 0.06	0.83 ± 0.06	0.88 ± 0.06	0.21 ± 0.01
1.00	1.79	0.80 ± 0.06	0.83 ± 0.06	0.83 ± 0.06	0.37 ± 0.03
1.00	1.89	0.75 ± 0.05	0.87 ± 0.06	0.96 ± 0.07	0.55 ± 0.04
1.00	2.00	0.80 ± 0.06	1.12 ± 0.08	1.10 ± 0.08	1.02 ± 0.07
0.60	1.00	0.73 ± 0.05	0.70 ± 0.05	0.75 ± 0.05	0.12 ± 0.01
0.21	1.00	0.26 ± 0.02	0.19 ± 0.01	0.19 ± 0.01	0.005 ± 0.001

The $\Omega = 1.0$, and $\phi = 1.0$ intensities were used as the reference in the normalization.

Courtesy of GRI Press.

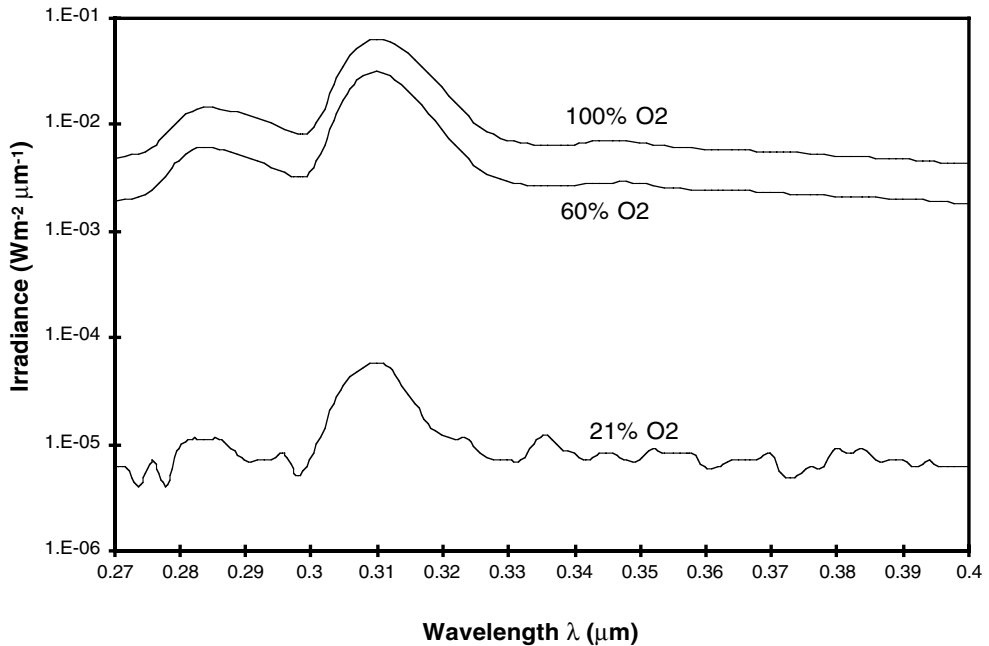


FIGURE 2.26 UV region of the spectra on a logarithmic scale for the flame radiation dependence on oxygen enrichment ratio Ω .⁵¹

oxygen-enhanced flames. It can be inferred that the OH emission-based band-reversal method, while successfully performed in $\text{CH}_4/\text{N}_2\text{O}$ flames,⁵⁴ will not yield the correct flame temperature in oxygen-enhanced flames. Figure 2.27 shows three flame radiation spectra with $q_f = 5.0$ kW, $\Omega = 1.0$, and $\phi = 0.67, 1.00$, and 2.00 , respectively. The normalized total radiation intensities for ϕ in the range of 0.67 to 2.00 are summarized in Table 2.7. The reduced radiation intensities in the fuel-lean cases ($\phi < 1.0$) are due to the fact that excessive oxygen carries away heat but does not radiate. Although the radiation intensities in the fuel-rich cases ($\phi > 1.0$) are apparently less than that in the stoichiometric case ($\phi = 1.00$), it should be noted that not all of the fuel was consumed, due

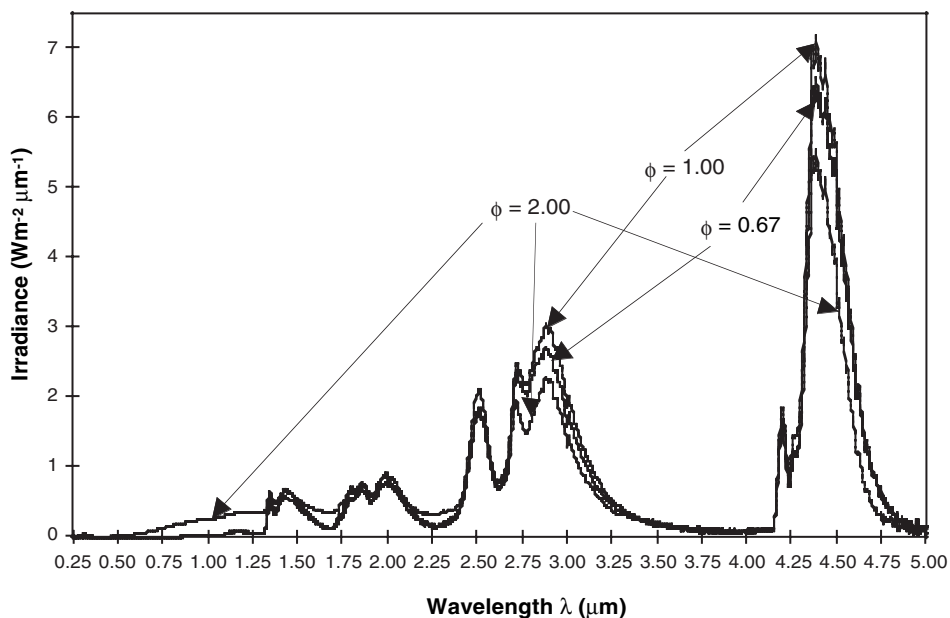


FIGURE 2.27 Flame radiation dependence on fuel equivalence ratio ϕ . Spectra were plotted with $q_f = 5.0$ kW, $\Omega = 1.0$, and $\phi = 0.67, 1.00$, and 2.00 , respectively.⁵¹

to lack of available oxygen. In a more realistic combustion system, oxygen would be introduced in a later stage to complete the combustion. With this in mind, the fuel-rich cases would actually provide more radiation for the same fuel consumption. Because the flames were in open air, actual equivalence ratios were different from the control settings due to air entrainment. Nevertheless, the general trends remain the same.

The integrated spectral radiation intensities were nearly the same for stoichiometric flames with $\Omega = 1.00$, $q_f = 5$ kW and $\Omega = 0.60$, $q_f = 7$ kW. For a given O_2 enrichment level, the radiation intensity increased more slowly than the increase in firing rate. Figure 2.28 shows radiation spectra from stoichiometric flames with different oxygen enrichment ratios and firing rates. The radiation intensity did not increase for air-fired flames ($\Omega = 0.21$) when the firing rate increased from 5 to 10 kW. These trends for the change in radiation as a function of the firing rate are consistent with the findings in another study.⁵³ While a quantitative comparison may depend on the specific burner design, the qualitative trend is generally true. Nitrogen in the air reduces radiation intensity. Because increasing the firing rate in air/natural gas flames is accompanied by increasing nitrogen flow, the increase in combustion heat cannot be as efficiently released by radiation as in the oxygen-enriched flames.

2.2.3 LUMINOUS RADIATION

2.2.3.1 Theory

Luminous flames are produced by the continuous radiant emission of particles in the flame, such as soot, that radiate approximately as blackbodies. Yagi and Iino (1961) studied both the luminous (q_{rs} = radiation from soot) and nonluminous (q_{rg} = gaseous radiation) from turbulent diffusion flames.⁵⁵ A comparison of the two types of radiation is shown in Figure 2.29, which shows that the soot radiation is greater than the gaseous radiation. Echigo et al. (1967) studied luminous radiation from flames.⁵⁶ They noted that a rigorous definition of luminous and nonluminous flames does not exist. It had long been assumed that soot remains in the solid phase during the combustion process and emits a continuous spectrum of visible and infrared radiation. Based on experiments,

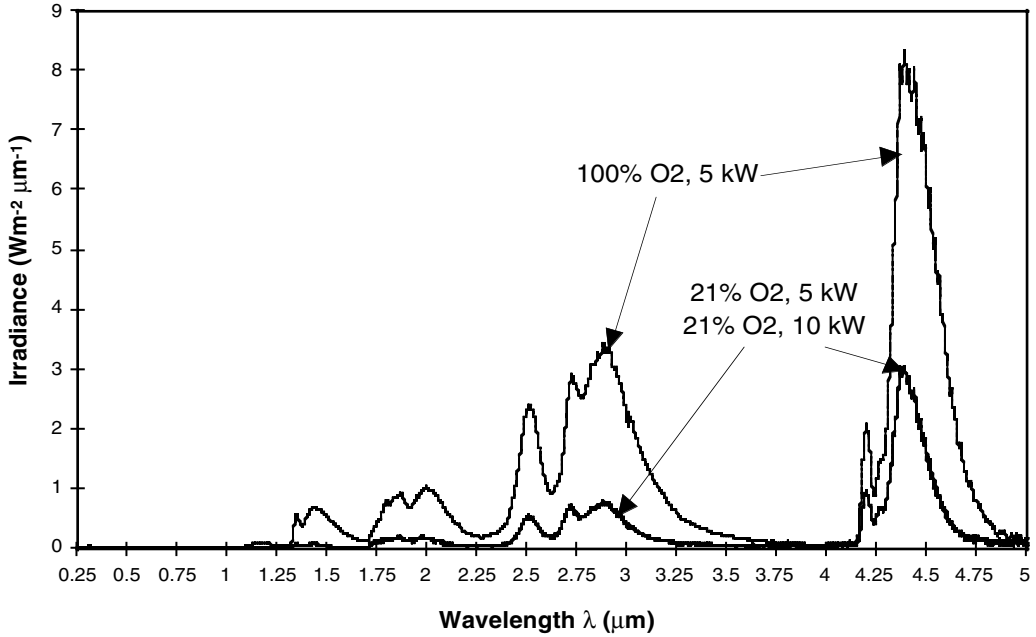


FIGURE 2.28 Flame radiation dependence on firing rate and oxygen enrichment ratio.⁵¹

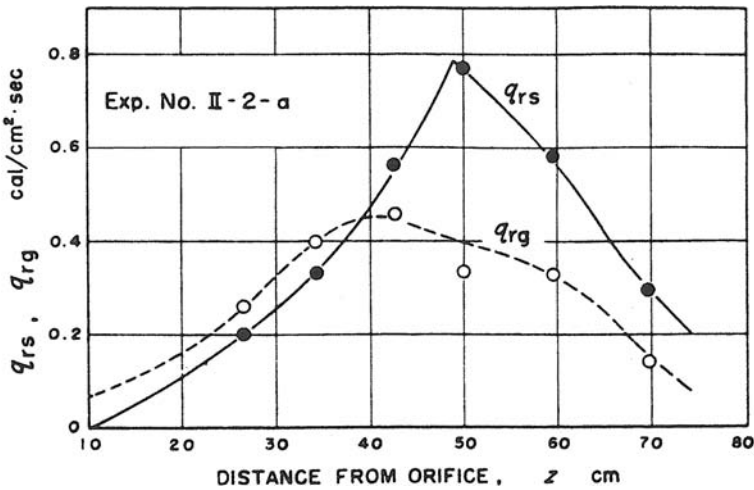


FIGURE 2.29 Soot (q_{rs}) and gaseous (q_{rg}) radiation from a turbulent diffusion flame with a fuel consisting of 11.9% CH_4 , 7.5% C_3H_8 , 22.5% C_3H_6 , 2.8% heavy hydrocarbons, 8.4% CO , 18.9% H_2 , 3.5% O_2 , 2.1% CO_2 , 22.4% N_2 , and a nozzle diameter of 7 mm. (Courtesy of The Combustion Institute.⁵⁵)

they hypothesized that the dehydrogenation and polymerization of hydrocarbon fuels occurs in the liquid phase, and that the decomposed and polymerized compound (“presoot substance”) emits banded spectra. Then the soot particles agglomerate after dehydrogenation and polymerization are complete. Gray et al. (1976) noted three size categories for particles: large, small, and intermediate.⁵⁷ Particles absorb, diffract, or attenuate radiation to varying degrees, depending on their size. The soot generated in a flame is highly dependent, among other things, on the fuel composition. Luminous radiation is usually important when liquid and solid fuels (e.g., oil and coal) are used.

TABLE 2.6
Sooting Tendency of Common Gaseous Fuels¹

Fuel	Formula	C	H	C/H Mass Ratio
Hydrogen	H ₂	0	2	0.00
Methane	CH ₄	1	4	2.97
Ethane	C ₂ H ₆	2	6	3.96
Propane	C ₃ H ₈	3	8	4.46
Butane	C ₄ H ₁₀	4	10	4.76
Propylene	C ₃ H ₆	3	6	5.95
Acetylene	C ₂ H ₂	2	2	11.89
Carbon monoxide	CO	1	0	∞

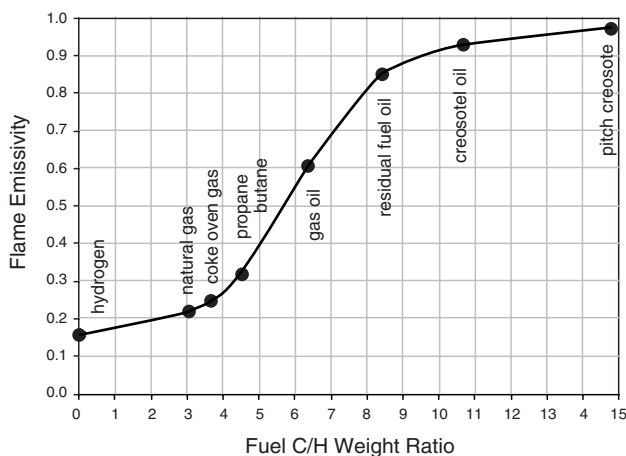


FIGURE 2.30 Emissivities of industrial-scale, turbulent diffusion flames of various fuels. (Courtesy of Gulf Publishing.⁶⁰)

It is usually not significant for gaseous fuels (e.g., natural gas). Fuels with higher carbon-to-hydrogen (C:H) weight ratios (see Table 2.6) tend to produce sootier flames. In a survey article, Wagner (1978) reviews soot formation in combustion.⁵⁸ It is noted that soot forms at temperatures ranging from 1000 to 2500°C (1800 to 4500°F). Soot consists primarily of carbon, formed into long chains. The total amount of soot formed is usually small in comparison to the amount of available carbon. Tien and Lee (1982) reviewed some of the various models available for calculating the emissivity of luminous flames, including the homogeneous nongray model, the homogeneous gray model, and the nonhomogeneous nongray model.³⁸ Glassman (1988) discussed the detailed chemistry of soot formation as it relates to fuel composition.⁵⁹ The graph in Figure 2.30 shows how the flame emissivity varies with fuel type.⁶⁰ For fuel gases with C:H weight ratios between 3.5 and 5.0, the data were correlated by either of two correlations:

$$\epsilon = 0.20 \sqrt{\frac{\text{LHV}}{900}} \quad (2.35)$$

where LHV is the lower heating value of the fuel in Btu/ft³, or

$$\varepsilon = 0.048\sqrt{MW_{\text{fuel}}} \quad (2.36)$$

where MW_{fuel} is the molecular weight of the fuel. For liquid fuels with C:H ratios between 5 and 15, the following correlation was determined:

$$\varepsilon = 1 - 68.2e^{-2.1\sqrt{C/H}} \quad (2.37)$$

where C/H is the weight ratio of carbon to hydrogen for the fuel. Haynes (1991) reviewed soot formation in flames, but did not specifically discuss the effects on heat transfer.⁶¹

The laminar smoke point for a fuel is another indicator of flame luminosity.⁶² Fuels with lower smoke point heights produce more luminous flames than high smoke point fuels. The laminar smoke point is determined by measuring the distance from the burner outlet where a vertical, laminar jet of burning pure fuel just begins to produce smoke. The lower the height where smoke starts to form, the higher tendency the fuel has to produce soot.

Lahaye and Prado (1983) have edited an extensive book on soot generated in combustion.⁶³ The focus of the book is on the chemistry of soot formation and destruction, with no real consideration of the heat transfer from luminous flames. Propane and acetylene have been two commonly used fuels to study soot. Longwell reports that soot in the form of polycyclic aromatic hydrocarbons (PAHs) can come from the fuel, fuel nonflame pyrolysis, or from quenching fuel-rich mixture regions in the flame.⁶⁴ Howard and Bittner (1983) note the formation of high-molecular-weight species prior to and during the appearance and growth of soot.⁶⁶ Bittner et al. (1983) note that soot formation is strongly related to fuel composition and that aromatic fuels have a much higher propensity to soot.⁶⁶ Prado et al. (1983) discuss soot inception and growth through nucleation and agglomeration.⁶⁷ Calcote (1983) notes the steps involved in soot formation:⁶⁸

1. Formation of precursors
2. Nucleation, which transforms molecules into particles
3. Soot particle growth, which increases the molecular weight
4. Coagulation of soot particles to form single, larger particles where the identity of the original colliding particles has been lost
5. Agglomeration of particles that adhere to each other to form a chain
6. Aggregation of colliding particles to form a cluster of individual particles that are still individually distinguishable
7. Oxidation of particles in any of the above steps to reduce the particle size and C:H ratio

Blokh (1988) has a lengthy treatment of luminous flame radiation produced by the burning of pulverized coal, oil, natural gas, and combinations of these.⁶⁹

Chemiluminescence is light emission produced when an atom or molecule is elevated to an electronically excited state in a chemical reaction. Stambuleanu (1976) notes that visible luminosity in flames is often actually chemiluminescence, and not luminosity at all.⁷⁰

Blokh (1974) discusses theoretical and experimental research on radiative properties of soot particles in luminous flames and coal particles in pulverized coal flames.⁷⁰ Kunitomo (1974) developed a method for calculating luminous flame radiation from a liquid fuel at pressures up to 20 atm (20 bar).⁷² Hammond and Beér (1974) made spectroradiometric measurements in sooty oil flames to determine spectral attenuation coefficients.⁷³ Ku and Shim (1990) developed models to predict the radiative properties of soot particles in flames.⁷⁴ To calculate luminous radiation from soot particles, the extinction coefficient, single-scattering albedo, and phase function are needed in the visible and near-infrared wavelengths. The formation processes and physical properties of soot,

light scattering and extinction by small particles, the effect of complex refractive index, the effects of particle size distribution, and the effect of agglomeration are all discussed. In addition to the discussions of models available and suggested refinements for soot particle properties, diagnostic techniques for making these measurements are also discussed. Bockhorn (1994) edited a book on soot formation in combustion, including several sections on modeling, although nothing specifically on industrial combustion.⁷⁵ Fridman et al. (1997) showed that flame luminosity can be enhanced by adding pyrene (C₁₆H₁₀).⁷⁶ Farias et al. (1998) computed the soot radiation properties of phase function, albedo, extinction coefficient, and emissivity using the integral equation formulation for scattering (IEFS).⁷⁷

The properties of a luminous gas can be expressed as:^{78,79}

$$\epsilon_\lambda = 1 - \exp(-\kappa_L L) \quad (2.38)$$

where ϵ_L is the monochromatic emittance of the luminous gas, κ_L is the absorption coefficient of the luminous gas, and L is the equivalent length of the radiating system. Hottel has recommended the following forms for the absorption coefficient:⁸⁰

$$\kappa_L = \frac{Ck_1}{\lambda^{0.95}} \quad (2.39a)$$

in the infrared region (0.8 to 10 μm), or

$$\kappa_L = \frac{Ck_2}{\lambda^{1.39}} \quad (2.39b)$$

in the visible region (0.3 to 0.8 μm), where C is the soot concentration and k_1 and k_2 are constants specific to the flame under investigation. The need for empirically determined constants is undesirable because each flame must be tested prior to analysis of a given system.¹⁰

2.2.3.2 Combustion Studies

This section provides a sampling of combustion studies concerning luminous radiation. Leblanc and Goracci (1973) note the inverse relationship between flame luminosity and flame temperatures.⁵ That is, if the flame is very luminous, it radiates its energy more efficiently and therefore has a lower temperature. If it is very nonluminous, then the flame temperature will generally be much higher because it does not release its energy as efficiently. Leblanc and Goracci reported flame emissivities ranging from 0.2 to 0.7. Example 2.8 shows a comparison of how much the flame temperature can change, depending on the emissivity (luminosity) of the flame.

Example 2.8

Given: Flame 1: $\epsilon_1 = 0.2$, $t_1 = 3000^\circ\text{F}$, flame 2: $\epsilon_2 = 0.7$, load: $t_L = 300^\circ\text{F}$.

Find: Find temperature of flame 2 (t_2), assuming same total radiant outputs.

Solution: Because total radiant outputs are the same,

$$\epsilon_1(T_1^4 - T_L^4) = \epsilon_2(T_2^4 - T_L^4)$$

or,

$$T_2 = \left[\frac{\epsilon_1}{\epsilon_2}(T_1^4 - T_L^4) + T_L^4 \right]^{1/4}$$

$T_2 = 2533^\circ\text{R}$, or $t_2 = 2073^\circ\text{F}$.

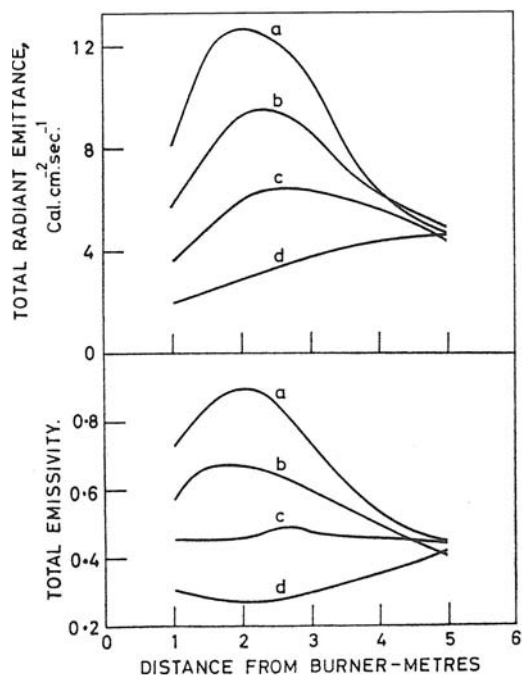


FIGURE 2.31 Effect of fuel composition and distance from an industrial burner for the following fuels: (a) 100% oil, (b) 40% oil/60% coke oven gas, (c) 20% oil/80% coke oven gas, and (d) 100% coke oven gas. (Courtesy of The Combustion Institute.)⁸¹

The flame temperature of the luminous flame is nearly 1000°F (560°C) lower than for the non-luminous flame. Although the assumptions made in the above example would not be strictly true for most flames, it shows how the flame emissivity affects the flame temperature.

2.2.3.2.1 Total Radiation

Beér and Howarth (1968) presented radiation measurements from industrial flames produced by fuels having a variable composition of oil and coke oven gas as shown in Figure 2.31.⁸¹ As expected, the more oil in the flames, the more radiation from the flame. Maesawa et al. (1968) reported radiation measurements from industrial residual oil flames in a vertical cylindrical furnace.⁸² As shown in Figure 2.32, the peak emissivity and radiant heat flux occurred at about 1 m (3 ft) from the burner in a 3-m (10-ft)-long furnace. Gill et al. (1968) measured and predicted the radiant heat transfer from pulverized coal flames in a 6-m (20-ft)-long × 1-m (3-ft)-wide rectangular, water-cooled furnace.⁸³ The peak heat flux occurred at approximately the midpoint of the furnace length. You (1985) measured the radiation from pure diffusion ($\phi = \infty$), natural gas flames.¹⁰⁷ Much of this radiation may have been luminous, because these are very fuel-rich flames. Radiation, to the stagnation point, was 13 to 26% of the total heat flux. Radiation was negligible at the edge of the plate ($R = 7.3$). Hustad calculated the radiant flux to be 7 to 14% and 20 to 40% of the total flux for CH_4 and C_3H_8 pure diffusion flames ($\phi = \infty$), respectively.¹²¹ Hustad assumed that these long flames were optically thick radiating cylinders. The convective flux was calculated using correlations for flow over a cylinder. This was subtracted from the measured total flux to determine a calculated radiant flux. This calculated radiation compared favorably with the measured radiation. The following empirical correlation was derived:

$$q''_{b,\text{rad}} = 5 + 3.9(l_j - x_{\text{liftoff}}) \quad (2.40)$$

where $q''_{b,\text{rad}}$ is in kW/m^2 and x_{liftoff} is the axial distance from the nozzle exit to the start of the flame. Luminous radiation was not considered in other studies, where the flames were very fuel rich (e.g., see Reference 112), although it may have been important.

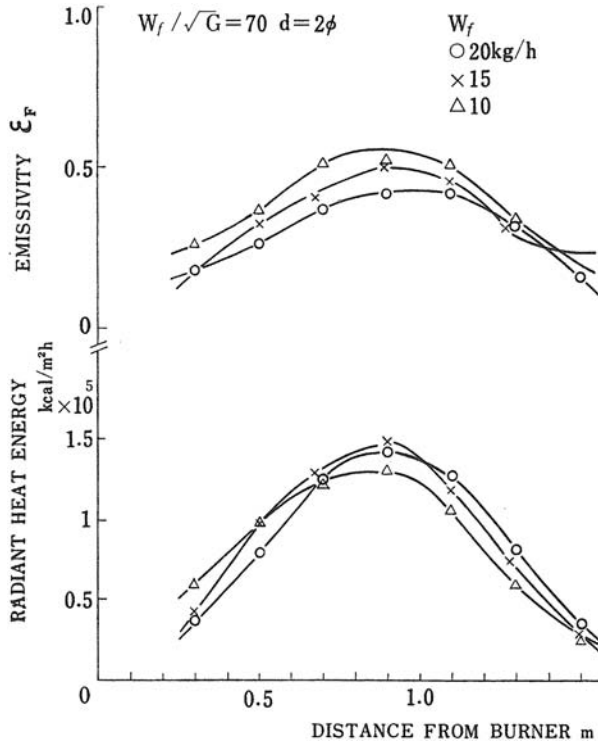


FIGURE 2.32 Measured radiant heat flux and calculated flame emissivity as a function of the distance from the burner for a residual oil flame in a vertical cylindrical furnace. (Courtesy of The Combustion Institute.⁸²)

2.2.3.2.2 Spectral Radiation

The Ji and Baukal (1998) study discussed above also investigated luminous flame radiation.⁵¹ The increased penetrating radiation in the extreme fuel-rich case ($\phi = 2.00$) reported above comes from the soot radiation. Incomplete combustion causes the fuel to crack, which forms soot particles at high temperatures. These hot soot particles emit blackbody-type radiation. The total radiation in this case is composed of discrete molecular band spectra (from hot combustion products) superimposed onto a blackbody continuum (from soot particles). The continuum radiation in the $\phi = 2.00$ flame spectra can be accounted for by a blackbody at 2318 K (3713°F), which has peak radiation at 1.25 μm . Figure 2.33 decomposes the $\phi = 2.00$ flame spectra into its soot blackbody continuum and its molecular band spectra components. The discrete band spectra are dominated by the hot combustion products: H_2O bands at 1.14, 1.38, 1.87, and 2.7 μm , and CO_2 bands at 2.7 and 4.3 μm . The CH_4 fuel molecules (2.3 and 3.3 μm bands) and combustion intermediate CO molecules (4.7 μm band) do not make a significant contribution to the flame radiation.

For quantitative characterization of the relative contributions from soot and molecular radiation, a soot radiation index γ was defined as:

$$\gamma = \frac{I_{(\text{soot at } 1.250 \mu\text{m})}}{I_{(\text{molecule at } 1.346 \mu\text{m})}} \quad (2.41)$$

Because the soot blackbody radiation peaks at 1.250 μm and there is little molecular radiation at this wavelength, it was therefore assumed that:

$$I_{(\text{soot at } 1.250 \mu\text{m})} = I_{(\text{total at } 1.250 \mu\text{m})} \quad (2.42)$$

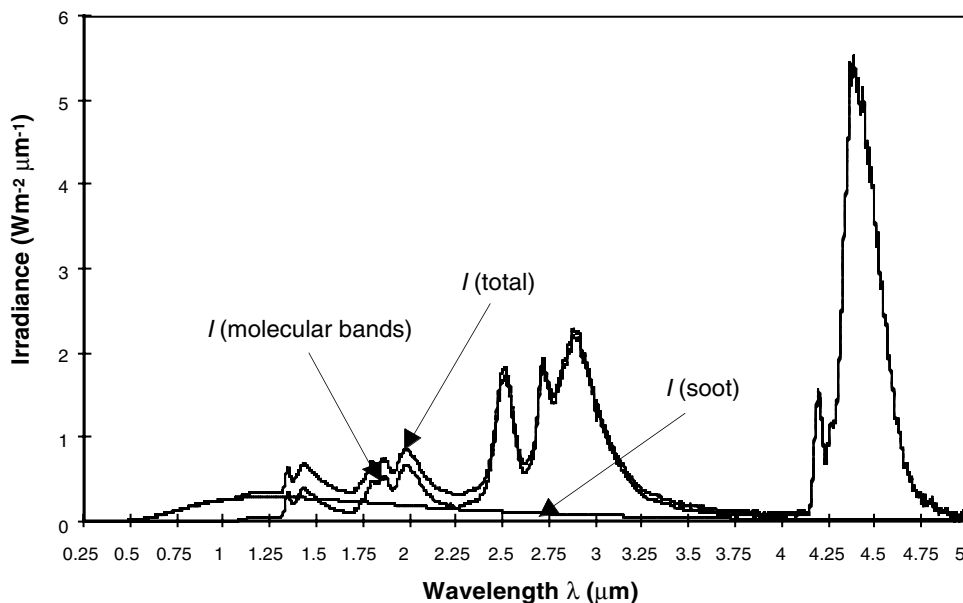


FIGURE 2.33 Soot radiation from a fuel-rich flame ($\phi = 2.00$). (Courtesy of The Combustion Institute.)⁵¹

The H_2O molecular radiation has a sharp rising (band head) peak at $1.346 \mu\text{m}$; therefore, it can be approximated that:

$$I_{(\text{molecule at } 1.346 \mu\text{m})} = I_{(\text{total at } 1.346 \mu\text{m})} - I_{(\text{soot at } 1.250 \mu\text{m})} \quad (2.43)$$

And, because the Monolight spectrometer had a nearly flat response sensitivity over the narrow wavelength range from 1.250 to $1.346 \mu\text{m}$, the value of soot radiation index γ reported here is independent of the spectrometer calibration. Table 2.5 lists the soot radiation index γ for $q_f = 5.0$ kW flames.

Figure 2.34 shows the normalized total radiation intensity $I_{\text{nr}(total)}$, the normalized penetrating radiation intensity $I_{\text{nr}(pen.)}$, and the soot radiation index γ as a function of the fuel equivalence ratio (ϕ) for $\Omega = 1.00$, $q_f = 5.0$ kW flames. As ϕ increased to fuel rich, both $I_{\text{nr}(total)}$ and $I_{\text{nr}(pen.)}$ decreased first due to incomplete combustion. At $\phi = 1.79$, $I_{\text{nr}(pen.)}$ started to increase due to increased soot radiation. This increase in $I_{\text{nr}(pen.)}$ corresponds to a rapid increase in the soot radiation index γ . Finally, at $\phi = 2.00$, $I_{\text{nr}(total)}$ also increased because the much-increased soot radiation became a significant part of the total radiation. The soot radiation index γ correlates closely to the soot concentration in the flame. A new, commercial, high-radiation burner⁸⁴ has a soot index close to 4 compared to the highest value in this study, which was slightly greater than 1 (see Table 2.5).

2.3 CONVECTION

Convection heat transfer is caused by fluid motion past a material, where the fluid is either at a higher or lower temperature than the material. In industrial combustion applications, the fluid is usually at a higher temperature than the medium it is heating. At least one person has argued that convection is not actually a separate mode of heat transfer, but that it is a subset of conduction, because the energy must still conduct from the fluid to the material.⁸⁵ While that may be true on a microscopic scale in the boundary layer next to the material, convection is a fundamentally different process than conduction and is treated here as such, which is the convention in standard heat transfer texts. Forced convection is often a very important mode of heat transfer in industrial combustion

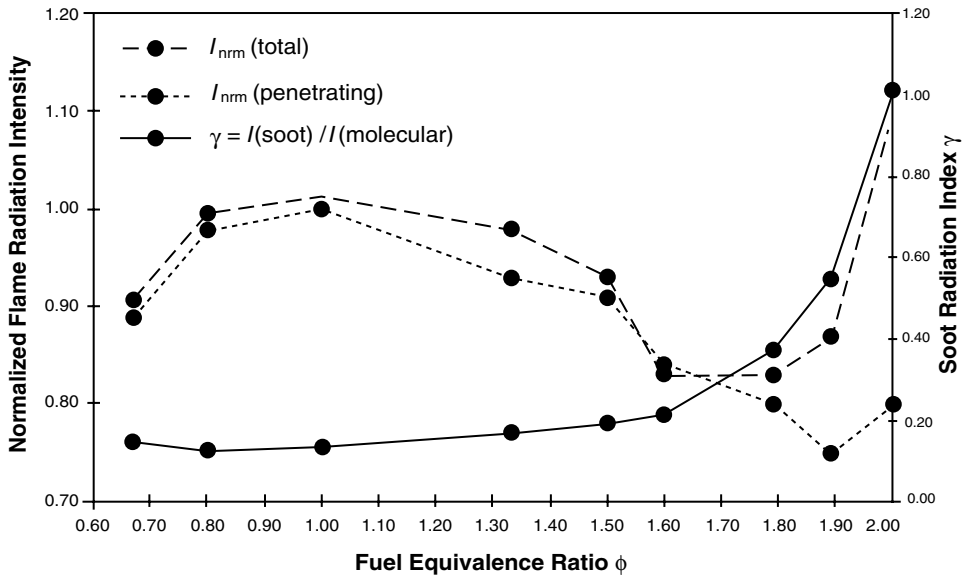


FIGURE 2.34 Normalized total radiation intensity $I_{nrm(\text{total})}$, normalized penetrating radiation intensity $I_{nrm(\text{pen.})}$, and soot radiation index γ as a function of fuel equivalence ratio ϕ for $\Omega = 1.00$ flames.⁵¹

systems. In some limited applications, natural convection may also be important because of the high temperature gradients that may exist. However, natural convection is not typically a significant mechanism in the majority of industrial combustion processes and is therefore not considered here. A number of books are available that specifically address convection heat transfer.⁸⁶⁻⁹⁴

2.3.1 FORCED CONVECTION

Forced convection heat transfer occurs when a fluid is forcefully directed at or over a medium (liquid or solid) and can be simply calculated using:

$$q = hA(t_f - t_m) \quad (2.44)$$

where q is the heat flux to the medium (Btu/hr or kW), h is the convective heat transfer coefficient (Btu/ft²-hr-°F or W/m²-K), A is the surface area of the medium in contact with the moving fluid, t_f is the fluid temperature (°F or K), and t_m is the temperature (°F or K) of the medium. A simple example is given below:

Example 2.9

Given: $h = 10$ Btu/ft²-hr-°F, $A = 10$ ft², $t_f = 300^\circ\text{F}$ and $t_m = 70^\circ\text{F}$.

Find: q .

Solution: $q = h A (t_m - t_p) = (10 \text{ Btu/ft}^2\text{-hr-}^\circ\text{F})(10 \text{ ft}^2)(300^\circ\text{F} - 70^\circ\text{F}) = 23,000 \text{ Btu/hr}$

This is an overly simplified example, because the convection heat transfer coefficient h has been given. In most problems, this value must be calculated from an appropriate correlation that may be fairly complicated, or worse, may not exist for the exact configuration under study. In the latter case, either experiments need to be done to determine this value or an approximate value must be used. The correlations for the convection coefficient are often complicated functions that normally depend on the flow geometry, the fluid velocity, and the fluid properties. In addition, for most real problems, the fluid and medium temperatures vary by location and are not constants over the entire medium surface.

Forced convection heat transfer from a flame to the load and inner combustor walls and from the outer combustor walls to the ambient are both potentially important mechanisms. Forced convection heat transfer in industrial combustion is often more difficult to analyze and calculate because of the large temperature difference between the combustion products and the surfaces (furnace walls and heat load) and because the gas properties vary widely as a function of both temperature and composition.

2.3.1.1 Forced Convection from Flames

In many conventional furnace heating processes, forced convection is only a small fraction of the total heat transfer to the product. Most of the heating comes from the radiation from the hot refractory walls. However, in flame impingement, with no furnace enclosure, forced convection can be 70 to 90% of the total heat flux.^{95,96} For flame temperatures up to about 2600°F (1700K), forced convection is the dominant mechanism in flame impingement heat transfer.⁹⁷

For low-temperature flames, as is common in air/fuel combustion systems, forced convection has generally been the only mechanism considered. In highly dissociated oxygen/fuel flames, a large fraction of the heat release is from exothermic reactions. However, even for those flames, forced convection is still an important contributor to the overall heat transfer to the target.

The turbulence level directly affects the importance of forced convection. The flow regime is determined by the Reynolds number, defined in Equation 2.1. For example, for flame jet impingement (see Figure 2.35), there are many possible choices for the length l . One is the burner outlet nozzle diameter, d_n ; another is the axial distance from the nozzle exit to the surface being heated, l_j ; and a third possibility is the width of the jet at the edge of the stagnation zone d_j . Yet another is some dimension of the material being heated. For a disk or cylinder, it might be the diameter d_b . For a plane surface, it might be the radial distance from the stagnation point r . In one case, the width of the water cooling channel in a target used in a flame impingement study was used.⁹⁷

Laminar flames have been used in many flame impingement studies.⁹⁷⁻¹⁰⁷ Sibulkin (1952) developed a semi-analytic solution for the heat transfer for laminar flow, normal to the stagnation point of an axisymmetric, blunt-nosed target:¹⁰⁸

$$q_s'' = 0.763(\beta_s \rho_e \mu_e)^{0.5} \text{Pr}_e^{-0.6} c_{p_e} (t_e - t_w) \quad (2.45)$$

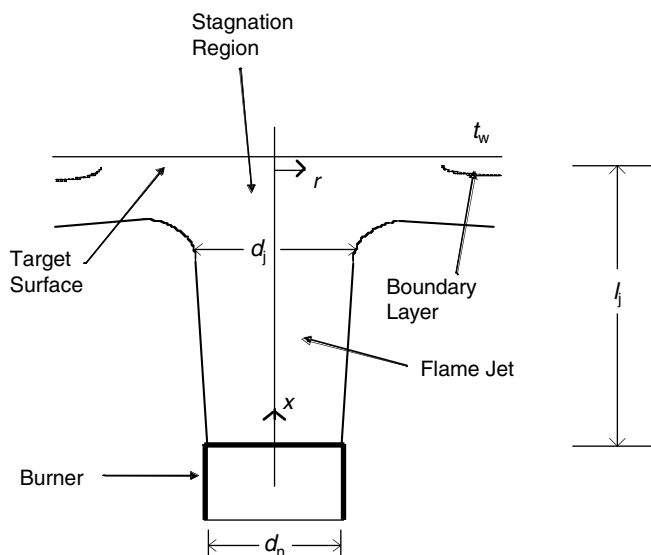


FIGURE 2.35 Flame jet impingement.¹³⁸

This result has been the basis for all other semi-analytical flame impingement heat transfer solutions.¹⁰⁹

Turbulent flames have also been commonly used.^{96,110-122} A typical example of an empirical equation, incorporating the turbulence intensity Tu , was given by Hustad and Sønju (1991)¹²¹ as:

$$q_s'' = \frac{k_e}{d_b} \left\{ 0.41 \text{Re}_{b,e}^{0.6} \text{Pr}_e^{0.35} Tu^{0.15} \left(\frac{\text{Pr}_e}{\text{Pr}_w} \right)^{0.25} \right\} (t_e - t_w) \quad (2.46)$$

This was developed for flames produced by jets of CH_4 and C_3H_8 , into ambient air. These are known as pure diffusion ($\phi = \infty$) flames. The flames impinged normal to uncooled steel pipes. These experiments were done to simulate fires caused by ruptured fuel pipes in the petrochemical industry.

Babiy (1974) presents a correlation for the convective heat transfer from combustion gases to carbon particles in pulverized coal combustion processes.¹²³ A commonly used equation for the convective heat transfer between a gas and a sphere is given by:

$$q_b'' = 31.2 \left(q_f / l_j^2 \right) \text{Ra}_e^{-1/6} \text{Pr}_e^{-3/5} \quad (2.47)$$

where d is the diameter of the sphere. For pulverized coal combustion, this equation is modified as follows:

$$q_b'' = 31.2 \left(q_f / l_j^2 \right) \text{Ra}_e^{-1/6} \text{Pr}_e^{-3/5} \quad (2.48)$$

where T_g is the absolute temperature (K) of the gas. The equation applies for $T_g = 1200$ to 1600K (1700 to 2400°F), $\text{O}_2 = 5$ – 21% , $d = 150$ to $1000 \mu\text{m}$, and $\text{Re}_d < 1$.

2.3.1.2 Forced Convection from Hot Gases to Tubes

In the convection section of a heater, Monrad (1932)¹²⁴ recommended the following empirical correlation for the convective heat transfer from hot exhaust products to a bank of staggered tubes:

$$q_b'' = 31.2 \left(q_f / l_j^2 \right) \text{Ra}_e^{-1/6} \text{Pr}_e^{-3/5} \quad (2.49)$$

where h_c = convection coefficient ($\text{Btu/hr-ft}^2\text{-}^\circ\text{F}$), G = gas mass velocity at minimum free cross-sectional area ($\text{lb/ft}^2\text{-s}$), T_g = absolute gas temperature ($^\circ\text{R}$), and d = tube diameter (in.).

2.3.2 NATURAL CONVECTION

Natural convection is sometimes referred to as buoyancy-induced flow.¹²⁵ Natural convection heat transfer from flames may be important in industrial combustion systems. This can occur when the gas velocities are very low.

One measure of the intensity of natural convection is the Rayleigh number:

$$\text{Ra} = g \tilde{\beta}_e q_f l_j^2 / \rho_e c_{p_e} \nu_e^3 \quad (2.50)$$

which is analogous to the Reynolds number for forced convection. Higher Rayleigh numbers indicate more natural convection. Another measure of intensity is the Grashoff number:

$$Gr = \frac{g\tilde{\beta}(t_w - t_\infty)\ell^3}{\nu^2} \quad (2.51)$$

where g is the gravity constant, $\tilde{\beta}$ is the volume coefficient of expansion ($=1/T$ for an ideal gas), and ν is the kinematic viscosity. The Richardson number Ri is one measure of the importance of buoyancy compared to forced convection. It is defined as:

$$Ri = \frac{Gr}{Re_n^2} \quad (2.52)$$

which is the ratio of the buoyant force to the inertial force. Conolly and Davies (1972) studied stoichiometric laminar flames impinging on a hemi-nosed cylinder.¹⁰³ The flame was parallel to the cylinder and impinging on the nose. A variety of fuels and oxidizers were used. Buoyancy effects were negligible. The criterion was that buoyancy could be neglected, compared to forced convection, for $Ri < 0.05$. Wang (1993) numerically modeled a nonreacting jet of ambient air impinging on an infinite flat plate.¹²⁶ It was concluded that natural convection is important only when Re_j is low, and that the temperature difference between the jet and the stagnation surface is large. The critical Ri value was estimated to be approximately 0.02. You (1985) determined the heat transfer from a buoyant flame to a flat plate, in terms of the Rayleigh number as:¹⁰⁷

$$q_b'' = 31.2(q_f/l_j^2)Ra_e^{-1/6}Pr_e^{-3/5} \quad (2.53)$$

The flames were produced by upward jets of pure natural gas ($\phi = \infty$) into ambient air. The jets impinged on a horizontal surface, to simulate a fire spreading over the ceiling of a room. Natural convection is more important in low-velocity flames. Both Beér (1968)⁹⁵ and Vizioz (1971)¹¹¹ stated that the effects of buoyancy were negligible in their studies, due to the high burner exit velocities.

2.4 CONDUCTION

Thermal conduction is often overlooked when considering heat transfer in combustion systems. Although it is not an important heat transfer mode in the combustion space, it is important in determining the heat loss through the refractory walls. Conduction is important in the design of furnaces because of the thermal expansion that occurs as the furnace heats up, especially considering the difference in expansion between refractories and the metal shell.¹²⁷

Thermal conduction has played an important role in many flame impingement heating applications. In some processes, high thermal conduction rates are desired. An example is a rapid reheat furnace. There, the goal is to raise the temperature of metal parts. Because metals generally have high thermal conductivities, heat may be quickly conducted through the part. This reduces the temperature gradient between the surface and the interior of the part. High gradients may cause the part to warp or deform. In other applications, low thermal conduction is desired. An example is thermal spallation. In this process, a high-intensity flame impinges directly on a solid having a low thermal conductivity. The heat transfers slowly into the solid, due to its low conductivity. The surface is very hot. Just below the surface, the solid is near ambient temperature. This results in very large internal temperature gradients that produce high thermal stresses. These stresses cause the solid to fracture. Thermal spallation has been shown to be a cost-effective method to “drill” through rocks.¹¹⁹

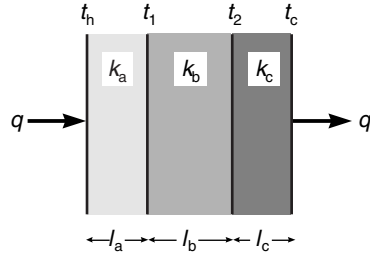


FIGURE 2.36 Thermal conduction through a composite wall.¹

In addition to transferring heat through the target, conduction has been used to measure the heat flux in flame impingement experimental studies. Both steady-state and transient methods have been used (see [Figure 7.4](#)). These are briefly discussed here. More detailed information on thermal conduction heat transfer is available in books specifically written on that subject.^{128–133}

2.4.1 STEADY-STATE CONDUCTION

Thermal conduction through refractory walls is important in determining the heat losses for a given process. The heat loss through a composite wall made of different refractory materials, shown in [Figure 2.36](#), can be calculated using:

$$q = \frac{t_h - t_c}{l_a/k_a A + l_b/k_b A + l_c/k_c A} \quad (2.54)$$

where t_h is the hotface temperature, t_c is the coldface temperature, l_i is the thickness of layer i , k_i is the thermal conductivity of layer i , and A is the cross-sectional area for conduction. Equation 2.54 assumes that the thermal conductivity of each layer does not change with temperature, which makes the analysis more complicated. It also assumes that there is no contact resistance between each layer. For example, if there is an air gap between each layer, this would give a large resistance to heat flow that should be included. The equation above is for a three-layer system, but any number of layers can be used by adding or subtracting the appropriate number of thermal conductances ($l_i/k_i A$). This equation can be used to solve for the hot or cold face temperatures, for the heat flux through the wall, or for a temperature inside the wall. It is assumed that the thicknesses (l_i), thermal conductivities (k_i), and cross-sectional area are known. Table 2.10 shows the thermal conductivity for various ceramics and other insulating materials.¹³⁴

Example 2.10

Given: Cold face temperature of 140°F, heat flux to the wall of 400 Btu/hr-ft², 8 in. of fireclay brick.

Find: Find the hot face temperature.

Solution: Assume that the conductivity through the steel shell is negligible. Note that the heat flux per unit area is given (q/A). Rearrange the equation above to solve for the hot face temperature:

$$t_h = t_c + \left(\frac{q}{A} \right) \left(\frac{l_{\text{firebrick}}}{k_{\text{firebrick}}} \right)$$

From [Table 2.7](#), $k_{\text{firebrick}} = 1.1 \text{ W/m-K} = 0.64 \text{ Btu/hr-ft-}^\circ\text{F}$,

$l_{\text{firebrick}} = 8/12 \text{ ft}$, $t_c = 140^\circ\text{F}$

solving for $t_h = 557^\circ\text{F}$

TABLE 2.7
Thermal Conductivity of Ceramics and Other Insulating Materials¹

Material	Dens. g/cm ³	t °C	Ther. cond, W/m K
Alumina (Al ₂ O ₃)	3.8	100	30
		400	13
		1300	6
		1800	7.4
Al ₂ O ₃ + MgO	3.5	100	17
		800	7.6
		1000	5.6
Asbestos	0.4	-100	0.07
		100	1
		0	0.09
Asbestos + 85% MgO	0.3	30	0.08
Asphalt	2.1	20	0.06
Beryllia (BeO)	2.8	100	210
		400	90
		1000	20
		1800	15
		1.85	50
Brick, dry	1.54	200	40
		600	23
		0	0.04
Brick, refractory:	alosite	1000	1.3
		400	1.2
		1000	1.3
	aluminous	100	0.2
		500	0.24
	diatomaceous	100	0.08
		500	0.1
	fireclay	400	1
		1000	1.2
	silicon carbide	200	2
600		2.4	
vermiculite	0.77	200	0.26
	600	0.31	
Calcium oxide		100	16
		400	9
		1000	7.5
Cement mortar	2	90	0.55
Charcoal	0.2	20	0.055
Coal	1.35	20	0.26
Concrete	1.6	0	0.8
Cork	0.05	0	0.03
		100	0.04
		0	0.06
Cotton wool	0.08	100	0.08
		30	0.04
		0	0.05
Diatomite	0.2	0	0.05

(Continued)

TABLE 2.7
Thermal Conductivity of Ceramics and Other Insulating Materials (Continued)

Material	Dens. g/cm ³	<i>t</i> °C	Ther.cond, W/m K
		400	0.09
	0.5	0	0.09
		400	0.16
Ebonite	1.2	0	0.16
Felt, flax	0.2	30	0.05
	0.3	30	0.04
Fuller's earth	0.53	30	0.1
Glass wool	0.2	-200 to 20	0.005
		50	0.04
		100	0.05
		300	0.08
Graphite			
100 mesh	0.48	40	0.18
20-40 mesh	0.7	40	1.29
Linoleum cork	0.54	20	0.08
Magnesia (MgO)		100	36
		400	18
		1200	5.8
		1700	9.2
MgO + SiO ₂		100	5.3
		400	3.5
		1500	2.3
Mica:			
muscovite		100	0.72
		300	0.65
		600	0.69
phlogopite		100	0.66
Canadian		300	0.19
		600	0.2
Micanite		30	0.3
Mineral wool	0.15	30	0.04
Perlite, expanded	0.1	-200 to 20	0.002
Plastics:			
bakelite	1.3	20	1.4
celluloid	1.4	30	0.02
polystyrene foam	0.05	-200 to 20	0.033
mylar foil	0.05	-200 to 20	0.0001
nylon		-253	0.10
		-193	0.23
		25	0.30
polytetrafluoroethylene		-253	0.13
		-193	0.16
		25	0.26
		230	2.5
urethane foam	0.07	20	0.06
Porcelain		90	1
Rock:			
basalt		20	2
chalk		20	0.92

(Continued)

TABLE 2.7
Thermal Conductivity of Ceramics and Other Insulating Materials (Continued)

Material	Dens. g/cm ³	<i>t</i> °C	Ther.cond, W/m K
granite	2.8	20	2.2
limestone	2	20	1
sandstone	2.2	20	1.3
slate		95	1.4
slate		95	2.5
Rubber:			
sponge	0.2	20	0.05
92 percent		25	0.16
Sand, dry	1.5	20	0.33
Sawdust	0.2	30	0.06
Shellac		20	0.23
Silica aerogel	0.1	-200 to 20	0.003
Snow	0.25	0	0.16
Steel wool	0.1	55	0.09
Thoria (ThO ₂)		100	10
		400	5.8
		1500	2.4
Titanium dioxide		100	6.5
		400	3.8
		1200	3.3
Uranium dioxide		100	9.8
		400	5.5
		1000	3.4
Wood:			
balsa,	0.11	30	0.04
fir,	0.54	20	0.14
fir,	0.54	20	0.35
oak		20	0.16
plywood		20	0.11
pine,	0.45	60	0.11
pine,	0.45	60	0.26
walnut,	0.65	20	0.14
Wool	0.09	30	0.04
Zinc oxide		200	17
		800	5.3
Zirconia (ZrO ₂)		100	2
		400	2
		1500	2.5
Zirconia + silica		200	5.6
		600	4.6
		1500	3.7

Thermal conductivity values for ceramics, refractory oxides, and miscellaneous insulating materials are given here. The thermal conductivity refers to samples with density indicated in the second column. Since most of these materials are highly variable, the values should only be considered as a rough guide.

REFERENCES

1. Powell, R.L. and Childs, G.E., in *American Institute of Physics Handbook, 3rd Edition*, Gray, D.E., Ed., McGraw-Hill, New York, 1972.
2. Perry, R. H. and Green, D., *Perry's Chemical Engineer's Handbook, Sixth Edition*, McGraw-Hill, New York, 1984.

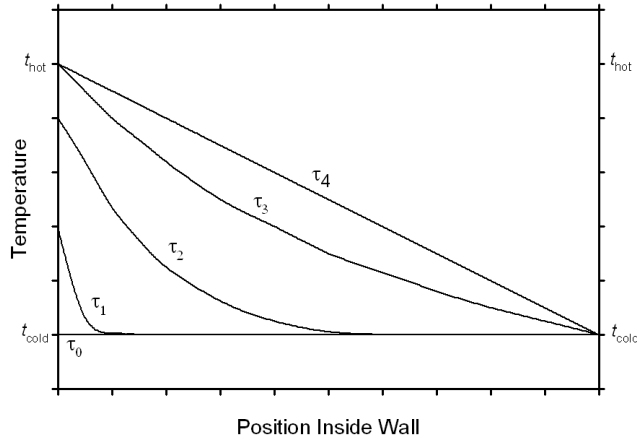


FIGURE 2.37 Transient thermal conduction through a wall.¹

Steady-state conduction has been important in flame impingement studies. Internally cooled targets have been used in many of the experimental studies.^{48,49,99,101,103,105,110–113,115,117,118,120} The flame impinges on the hot side of the target. The coolant flows past the cold side of the target. In other studies, the target has been an uncooled ceramic.^{95,97,98,102,111} In both the cooled metal and uncooled ceramic studies, the hot side and cold side temperatures were approximately constant, producing steady-state conduction through the target.

Steady-state conduction methods have been employed in the design of heat flux gages (see [Chapter 6](#)) used in flame impingement studies. These methods involve measuring the temperature gradient through a piece of metal in the gage. The gage is heated on one side by the flame. The other side is commonly maintained at a fixed temperature, using a coolant. Long, thin, solid rods;^{95,99,101,112,117,120} thin disks,¹¹⁰ and heat flux transducers^{107,113,122} have been used as gages.

2.4.2 TRANSIENT CONDUCTION

Transient conduction is an important aspect of heat transfer in industrial combustion that is often overlooked. It is significant during the start-up of a process where the heat distribution through the walls of a furnace has not reached steady-state. [Figure 2.37](#) shows how the temperature distribution through a refractory wall changes as a function of time. At t_0 , the temperature through the wall is uniform (t_{cold}), when heat is then applied to the left side of the wall. After some time (t_g), the wall temperature distribution reaches steady-state.

Another instance where transient conduction is important is during the heating of a load in a batch heating process. The load is initially cold after it is first charged into the furnace. As heat is applied to the surface, the surface temperature rises quickly, while the temperatures inside the load are still low until the heat has time to conduct through the load. The thermal conductivity of the load determines how fast the temperature profile equilibrates inside the load. For example, aluminum conducts very quickly compared to a refractory material such as bricks or ceramics. This can be an important consideration if the material conducts slowly because the surface can be overheated before the heat has a chance to conduct inside the load. This reduces the product quality and process yield.

Uncooled metal targets have been used in previous flame impingement experimental studies. The target materials have been steel,^{96,102,114,121} inconel,¹¹⁶ iron,⁴⁶ molybdenum,¹⁰⁰ brass,¹⁰⁴ and copper.¹¹⁹ These targets were exposed to the flame for only a short time. Kilham and Purvis (1971)¹⁰² and Nawaz (1973)¹⁰⁴ inserted the target into the flame for less than 1 second. Giedt and co-workers (1960, 1966) had test durations of between 20 and 50 seconds.^{46,100} The targets were instrumented

with an array of thermocouples. The heat flux to the surface was estimated, using an inverse transient heat conduction calculation. This method is discussed by Gebhart (1993).¹³²

Transient conduction has also been used in the design of slug calorimeter heat flux gages, as used in previous studies.^{102–104,116,118,120,121} Heat is received on a slug of metal inside the calorimeter. The slug is assumed to be internally isothermal at any instant in time. The heat flux is calculated from the rise in the thermal capacitance of the slug, as a function of time.

REFERENCES

1. C.E. Baukal, *Heat Transfer in Industrial Combustion*, CRC Press, Boca Raton, FL, 2000.
2. P. Singh, M. Henneke, J.D. Jaykaran, R. Hayes, and C.E. Baukal, *The John Zink Combustion Handbook*, edited by C.E. Baukal, CRC Press, Boca Raton, FL, 2001.
3. G.M. Faeth, J.P. Gore, S.G. Chuech, and S.-M. Jeng, Radiation from turbulent diffusion flames. *Annu. Rev. of Fluid Mech. & Heat Transfer*, 2, 1–38, 1989.
4. W.A. Gray and R. Müller, *Engineering Calculations in Radiative Heat Transfer*, Pergamon, Oxford, U.K., 1974.
5. B. Leblanc and E. Goracci, Example of applications in the field of heat transfer in hot wall furnaces, *La Rivista dei Combustibili*, 27(4-5), 155–164, 1973.
6. H. Schmidt, Prüfung der Strahlungsgesetze der Bunsenflamme, *Annln. Phys.*, 29, 971–1028, 1909.
7. T.M. Lowes and A.J. Newall, Problems associated with the characterisation (sic) of flame radiation in glass tanks, *Glass Tech.*, 12(2), 32–35, 1971.
8. B. Leblanc, A.B. Ivernel, and J. Chedaille, New concepts on heat transfer processes in high temperature furnaces, *Heat Transfer, Proceedings of International Heat Transfer Conference, 5th*, Vol. 1, 61–65, Japanese Soc. Mech. Eng., Tokyo, 1974.
9. D.A. Lihou, Review of furnace design methods, *Trans. Chem. E*, 55(4), 225–242, 1977.
10. J.A. Wiebelt, *Engineering Radiation Heat Transfer*, Holt, Rinehart and Winston, New York, 1966.
11. H.C. Hottel and A.F. Sarofim, *Radiative Transfer*, McGraw-Hill, New York, 1967.
12. T.J. Love, *Radiative Heat Transfer*, Merrill Pub., Columbus, OH, 1968.
13. E.M. Sparrow and R.D. Cess, *Radiation Heat Transfer*, Augmented Edition, Hemisphere, Washington, D.C., 1978.
14. D.K. Edwards, *Radiation Heat Transfer Notes*, Hemisphere, Washington, D.C., 1981.
15. R. Siegel and J.R. Howell, *Thermal Radiation Heat Transfer*, 2nd edition, Hemisphere, Washington, D.C., 1981.
16. M.Q. Brewster, *Thermal Radiative Transfer and Properties*, Wiley, New York, 1992.
17. M.F. Modest, *Radiative Heat Transfer*, McGraw-Hill, New York, 1993.
18. D.H. Hubble, Steel plant refractories, in *The Making, Shaping and Treating of Steel*, 11th edition, Steelmaking and Refining Volume, R.J. Fruehan, Ed., AISE Steel Foundation, Pittsburgh, PA, 1998, 159–290.
19. M.A. Glinkov, Flame as a problem of the general theory of furnaces, in *Heat Transfer in Flames*, N.H. Afgan and J.M. Beer, Eds., 1974, chap. 9, 159–177, Scripta Book Company, Washington, D.C., 1974.
20. P. Docherty and R.J. Tucker, The influence of wall emissivity on furnace performance, *J. Inst. Energy*, 59(438), 35–37, 1986.
21. D.G. Elliston, W.A. Gray, D.F. Hibberd, T.-Y. Ho, and A. Williams, The effect of surface emissivity on furnace performance, *J. Inst. Energy*, 60(445), 155–167, 1987.
22. C.L. DeBellis, Effect of refractory emittance in industrial furnaces, in *Fundamentals of Radiation Heat Transfer*, W.A. Fiveland, A.L. Crosbie, A.M. Smith, and T.F. Smith, Eds., ASME HTD-Vol. 160, 105–115, New York, 1991.
23. C.L. DeBellis, Evaluation of high-emittance coatings in a large industrial furnace, in *Heat Transfer in Fire and Combustion Systems — 1993*, B. Farouk, M.P. Menguc, R. Viskanta, C. Presser, and S. Chellaiah, Eds., ASME HTD-Vol. 250, pp. 190–198, New York, 1993.
24. X. Xin, G. Qingchang and J. Yi, High emissivity refractory coating improves furnace output in China, *Industrial Heating*, LXVI(6), 49–50, 1999.
25. T.F. Wall, S.P. Bhattacharya, D.K. Zhang, R.P. Gupta, and X. He, The properties and thermal effects of ash deposits in coal fired furnaces, *Prog. Energy Combust. Sci.*, 19, 487–504, 1993.

26. T.F. Wall, S.P. Bhattacharya, L.L. Baxter, Ge. Richards, and J.N. Harb, The character of ash deposits and the thermal performance of furnaces, *Fuel Processing Technology*, 44, 143–153, 1995.
27. W.E. Garner, Radiant energy from flames, *First Symposium (International) on Combustion*, The Combustion Institute, Pittsburgh, PA, 1965, 19–23.
28. A.F. Sarofim, Radiative Heat Transfer in Combustion: Friend or Foe, Hoyt C. Hottel Plenary Lecture, *Twenty-First Sym. (Int.) on Combustion*, The Combustion Institute, Pittsburgh, PA, 1986, 1–23.
29. C.B. Ludwig, W. Malkmus, J.E. Reardon, and J.A.L. Thomson, *Handbook of Infrared Radiation from Combustion Gases*, National Aeronautics and Space Administration report SP-3080, Washington, D.C., 1973.
30. B. Leckner, Spectral and total emissivity of water vapor and carbon dioxide, *Comb. Flame*, 19, 33–48, 1972.
31. M. Gulic, A new formula for determining the effective beam length of gas layer or flame, in *Heat Transfer in Flames*, N.H. Afgan and J.M. Beer, Eds., 1974, chap. 12, 201–208, Scripta Book Company, Washington, D.C., 1974.
32. R.D. Cess, Infrared GASEOUS RADIATION, in *Heat Transfer in Flames*, N.H. Afgan and J.M. Beer, Eds., Scripta Book Company, Washington, D.C., 1974, chap. 15, 231–248.
33. R. Grief, Experimental and theoretical results with infrared radiating gases, in *Heat Transfer in Flames*, N.H. Afgan and J.M. Beer, Eds., Scripta Book Company, Washington, D.C., 1974, chap. 16, 249–253.
34. J.L. Kovotny, The effect of pressure on heat transfer in radiating gases, in *Heat Transfer in Flames*, N.H. Afgan and J.M. Beer, Eds., Scripta Book Company, Washington, D.C., 1974, chap. 17, 255–269.
35. D.K. Edwards, Molecular gas band radiation, in *Advances in Heat Transfer*, Vol. 12, T.F. Irvine and J.P. Hartnett, Eds., Academic Press, New York, 1976, 115–193.
36. H.E. Trout, Heat transfer: Part IV. Radiation from gases and flames, *Industrial Heating*, Vol. XLIV(8), 28–33, 1977.
37. C.L. Tien, Thermal radiation properties of gases, *Advances in Heat Transfer*, T.F. Irvine and J.P. Hartnett, Eds., Academic Press, New York, Vol. 5, 253–324, 1968.
38. C.L. Tien and S.C. Lee, Flame radiation, *Prog. Energy Combust. Sci.*, 8, 41–59, 1982.
39. D.K. Edwards and A. Balakrishnan, Thermal radiation by combustion gases, *Int.J. Heat Mass Transfer*, 16, 25–40, 1973.
40. P.B. Taylor and P.J. Foster, The total emissivities of luminous and non-luminous flames, *Int. J. Heat Mass Transfer*, 17, 1591–1605, 1974.
41. A. Coppalle and P. Vervisch, The total emissivities of high-temperature flames, *Combust. Flame*, 49, 101–108, 1983.
42. D.K. Edwards and R. Matavosian, Scaling rules for total absorptivity and emissivity of gases, *J. Heat Transfer*, 106, 684–689, 1984.
43. J.R. Howell, Thermal Radiation in Participating Media: The Past, the Present, and Some Possible Futures, *J. Heat Transf.*, 110, 1220–1229, 1988.
44. J.A. Wieringa, J.J.Ph. Elich, and C.J. Hoogendoorn, Spectral effects of radiative heat-transfer in high-temperature furnaces burning natural gas, *J Inst. Energy*, 63(456), 101–108, 1990.
45. P.G. Dunham, Convective Heat Transfer from Carbon Monoxide Flames, Ph.D. thesis, The University of Leeds, Leeds, U.K., 1963.
46. W.H. Giedt, L.L. Cobb, and E.J. Russ, Effect of Hydrogen Recombination on Turbulent Flow Heat Transfer, ASME Paper 60-WA-256, New York, 1960.
47. M.R.I. Purvis, Heat Transfer from Normally Impinging Hydrocarbon Oxygen Flames to Surfaces at Elevated Temperatures, Ph.D. thesis, The University of Leeds, Leeds, U.K., 1974.
48. D.R. Davies, Heat Transfer from Working Flame Burners, B.S. thesis, Univ. of Salford, Salford, U.K., 1979.
49. T.H. van der Meer, Heat Transfer from Impinging Flame Jets, Ph.D. thesis, Technical University of Delft, The Netherlands, 1987.
50. C.E. Baukal and B. Gebhart, Oxygen-enhanced/natural gas flame radiation. *Int.J. Heat Mass Transfer*, 44(11), 2539–2547, 1997.
51. B. Ji and C.E. Baukal, Spectral radiation properties of oxygen-enhanced/natural gas flames, *Proc. 1998 International Gas Research Conference*, D. Dolenc, Ed., November 8–11, 1998, San Diego, CA, Vol. 5, 422–433, 1998.
52. D.R. Davies, D.R. and P.J. Young, Strip Edge Heating Burner, U.S. Patent 4,756,685, issued July 12, 1988.

53. C.E. Baukal, Heat Transfer from Flames Impinging Normal to a Plane Surface, Ph.D. Thesis, University of Pennsylvania, 1996.
54. W.R. Anderson, Measurement of the Line Reversal Temperature of OH in CH₄/N₂O Flames, *Technical Report ARBRL-TR-02280*, 1981.
55. S. Yagi and H. Iino, Radiation from soot particles in luminous flames, *Eighth Symposium (International) on Combustion*, The Combustion Institute, Pittsburgh, PA, 1961, 288–293, (reprinted 1991).
56. R. Echigo, N. Nishiwaki, and M. Hirata, A study on the radiation of luminous flames, *Eleventh Symposium (International) on Combustion*, The Combustion Institute, Pittsburgh, PA, 1967, 381–389.
57. W.A. Gray, J.K. Kilham, and R. Müller, *Heat Transfer from Flames*, Elek Science, London, 1976.
58. H.G. Wagner, Soot formation in combustion, *Seventeenth Symposium (International) on Combustion*, The Combustion Institute, Pittsburgh, PA, 1978, 3–19.
59. I. Glassman, Soot formation in combustion processes, *Twenty-Second Symposium (International) on Combustion*, The Combustion Institute, Pittsburgh, PA, 1988, 295–311.
60. E. Talmor, *Combustion Hot Spot Analysis for Fired Process Heaters*, Gulf Publishing, Houston, 1982.
61. B.S. Haynes, Soot and hydrocarbons in combustion, in *Fossil Fuel Combustion*, W. Bartok and A.F. Sarofim, Eds., Wiley, New York, 1991, chap. 5.
62. P.B. Sunderland, S. Mortazavi, G.M. Faeth, and D.L. Urban, Laminar smoke points of nonbuoyant jet diffusion flames, *Combust. Flame*, 96, 97–103, 1994.
63. J. Lahaye and G. Prado, Eds., *Soot in Combustion Systems and its Toxic Properties*, Plenum Press, New York, 1983.
64. J.P. Longwell, Polycyclic aromatic hydrocarbons and soot, in *Soot in Combustion Systems and its Toxic Properties*, J. Lahaye and G. Prado, Eds., Plenum Press, New York, 1983, 37–56.
65. J.B. Howard and J.D. Bittner, Structure of sooting flames, in *Soot in Combustion Systems and its Toxic Properties*, J. Lahaye and G. Prado, Eds., Plenum Press, New York, 1983, 57–93.
66. J.D. Bittner, J.B. Howard, and H.B. Palmer, Chemistry of intermediate species in the rich combustion of benzene, in *Soot in Combustion Systems and its Toxic Properties*, J. Lahaye and G. Prado, Eds., Plenum Press, New York, 1983, 95–125.
67. G. Prado, J. Lahaye, and B.S. Haynes, Soot particle nucleation and agglomeration, in *Soot in Combustion Systems and its Toxic Properties*, J. Lahaye and G. Prado, Eds., Plenum Press, New York, 1983, 145–161.
68. H.F. Calcote, Ionic mechanisms of soot formation, in *Soot in Combustion Systems and its Toxic Properties*, J. Lahaye and G. Prado, Eds., Plenum Press, New York, 1983, 197–215.
69. A.G. Blokh, *Heat Transfer in Steam Boiler Furnaces*, Hemisphere, Washington, D.C., 1988.
70. A. Stambuleanu, *Flame Combustion Processes in Industry*, Abacus Press, Tunbridge Wells, U.K., 1976.
71. A. Blokh, The problem of flame as a disperse system, in *Heat Transfer in Flames*, N.H. Afgan and J.M. Beer, Eds., Scripta Book Company, Washington, D.C., 1974, chap. 6, 111–114.
72. T. Kunitomo, Luminous flame emission under pressure up to 20 atm, in *Heat Transfer in Flames*, N.H. Afgan and J.M. Beer, Eds., Scripta Book Company, Washington, D.C., chap. 18, 271–281.
73. E.G. Hammond and J.M. Beér, Spatial distribution of spectral radiant energy in a pressure jet oil flame, in *Heat Transfer in Flames*, N.H. Afgan and J.M. Beer, Eds., Scripta Book Company, Washington, D.C., chap. 19, 283–291.
74. J.C. Ku and K.-H. Shim, The effects of refractive indices, size distribution, and agglomeration on the diagnostics and radiative properties of flame soot particles, in *Heat and Mass Transfer in Fires and Combustion Systems*, W.L. Grosshandler and H.G. Semerjian, Eds., ASME HTD-Vol. 148, pp. 105–115, New York, 1990.
75. H. Bockhorn, Ed., *Soot Formation in Combustion*, Springer-Verlag, Berlin, 1994.
76. A.A. Fridman, S.A. Nestor, and A.V. Saveliev, Effect of pyrene addition on the luminosity of methane flames, in *ASME Proc. 32nd National Heat Transfer Conf., Vol. 3: Fire and Combustion*, L. Gritz and J.-P. Delplanque, Eds., 1997, 7–12, ASME, New York.
77. T.L. Farias, M.G. Carvalho, and Ü.Ö. Köylü, Radiative heat transfer in soot-containing combustion systems with aggregation, *Int.J. Heat Mass Trans.*, 41(17), 2581–2587, 1998.
78. M. Jacob, *Heat Transfer*, Vol. 2, Wiley, New York, 1957.
79. W.H. McAdams, *Heat Transmission*, McGraw-Hill, New York, 1954.
80. H.C. Hottel and F.P. Broughton, Determination of true temperature and total radiation from luminous gas flames, *Ind. Eng. Chem.*, 4, 166–175, 1933.

81. J.M. Beér and C.R. Howarth, Radiation from flames in furnaces, *Twelfth Symposium (International) on Combustion*, The Combustion Institute, Pittsburgh, PA, 1968, 1205–1217.
82. M. Maesawa, Y. Tanaka, Y. Ogisu, and Y. Tsukamoto, Radiation from the luminous flames of liquid fuel jets in a combustion chamber, *Twelfth Symposium (International) on Combustion*, The Combustion Institute, Pittsburgh, PA, 1968, 1229–1237.
83. D.W. Gill, D.J. Loveridge, and G.G. Thurlow, A comparison of predicted and measured heat-transfer rates in a pulverized-coal-fired furnace, *Twelfth Symposium (International) on Combustion*, The Combustion Institute, Pittsburgh, PA, 1968, 1239–1246.
84. A.G. Slavejkov, T.M. Gosling, and R.E. Knorr, Method and Device for Low-NO_x High Efficiency Heating in High Temperature Furnace, U.S. Patent 5,575,637, 1996.
85. T.M. Smith, private communication, 1982.
86. V.S. Arpaci, *Convection Heat Transfer*, Prentice Hall, Englewood Cliffs, NJ, 1984.
87. C.S. Fang, *Convective Heat Transfer*, Gulf Publishing, Houston, 1985.
88. S. Kakac, R.K. Shah, and W. Aung, Eds., *Handbook of Single-Phase Convective Heat Transfer*, Wiley, New York, 1987.
89. L.C. Burmeister, *Convective Heat Transfer*, 2nd ed., Wiley, New York, 1993.
90. W.M. Kays and M.E. Crawford, *Convective Heat and Mass Transfer*, 3rd ed, McGraw-Hill, New York, 1993.
91. A. Bejan, *Convection Heat Transfer*, 2nd ed., Wiley, New York, 1994
92. M. Kaviany, *Principles of Convective Heat Transfer*, Springer-Verlag, New York, 1994.
93. S. Kakac and Y. Yener, *Convective Heat Transfer*, 2nd ed., CRC Press, Boca Raton, FL, 1995.
94. P.H. Oosthuizen, *An Introduction to Convective Heat Transfer*, McGraw-Hill, New York, 1999.
95. J.M. Beér and N.A. Chigier, Impinging jet flames, *Comb. Flame*, 12, 575–586, 1968.
96. A. Milson and N.A. Chigier, Studies of methane-air flames impinging on a cold plate, *Comb. Flame*, 21, 295–305, 1973.
97. E.G. Jackson and J.K. Kilham, Heat transfer from combustion products by forced convection, *Ind. Eng. Chem.*, 48(11), 2077–2079, 1956.
98. J.K. Kilham, Energy transfer from flame gases to solids, *Third Symposium on Combustion and Flame and Explosion Phenomena*, The Williams and Wilkins Co., Baltimore, MD, 1949, 733–740.
99. R.A. Cookson and J.K. Kilham, Energy transfer from hydrogen-air flames, *Ninth Symposium (International) on Combustion*, Academic Press, New York, 1963, 257–263.
100. L.W. Woodruff, and W.H. Giedt, 1966, Heat Transfer Measurements From a Partially Dissociated Gas With High Lewis Number, *J. Heat Trans.*, 88, 415–420, 1966.
101. J.K. Kilham and P.G. Dunham, Energy transfer from carbon monoxide flames, *Eleventh Symposium (International) on Combustion*, The Comb. Inst., Pittsburgh, PA, 1967, 899–905.
102. J.K. Kilham and M.R.I. Purvis, Heat transfer from hydrocarbon-oxygen flames, *Comb. Flame*, 16, 47–54, 1971.
103. R. Conolly and R.M. Davies, A study of convective heat transfer from flames, *Int.J. Heat Mass Trans.*, 15, 2155–2172, 1972.
104. S. Nawaz, Heat Transfer from Oxygen Enriched Methane Flames, Ph.D. thesis, The University of Leeds, Leeds, U.K., 1973.
105. C.J. Hoogendoorn, C.O. Popiel, and T.H. van der Meer, Turbulent heat transfer on a plane surface in impingement round premixed flame jets, *Proc. 6th Int. Heat Trans. Conf.*, Toronto, 4, 107–112, 1978.
106. J.K. Kilham and M.R.I. Purvis, Heat transfer from normally impinging flames, *Comb. Sci. Tech.*, 18, 81–90, 1978.
107. H.-Z. You, An investigation of fire-plume impingement on a horizontal ceiling. 2. Impingement and ceiling-jet regions, *Fire & Materials*, 9(1), 46–56, 1985.
108. M. Sibulkin, Heat transfer near the forward stagnation point of a body of revolution, *J. Aero. Sci.*, 19, 570–571, 1952.
109. C.E. Baukal and B. Gebhart, A review of semi-analytical solutions for flame impingement heat transfer, *Int.J. Heat Mass Trans.*, 39(14), 2989–3002, 1996.
110. S.N. Shorin and V.A. Pechurkin, Effectivnost' teploperenosa na poverkhnost' plity ot vysokotemperaturnoi strui produktov sgoraniya razlichnykh gazov, *Teoriya i Praktika Szhiganiya Gaza*, 4, 134–143, 1968.
111. J.-P. Vizioz and T.M. Lowes, Convective Heat Transfer from Impinging Flame Jets, Int. Flame Res. Found. Report F 35/a/6, IJmuiden, The Netherlands, 1971.

112. E. Buhr, G. Haupt, and H. Kremer, Heat transfer from impinging turbulent jet flames to plane surfaces, *Combustion Institute European Symposium 1973*, F.J. Weinberg, Ed., Academic Press, New York, 1973, 607–612.
113. R.B. Smith and T.M. Lowes, Convective Heat Transfer from Impinging Tunnel Burner Flames — A Short Report on the NG-4 Trials, Int. Flame Res. Found. Report F 35/a/9, IJmuiden, The Netherlands, 1974.
114. M. Matsuo, M. Hattori, T. Ohta, and S. Kishimoto, The Experimental Results of the Heat Transfer by Flame Impingement, Int. Flame Res. Found. Report F 29/1a/1, IJmuiden, The Netherlands, 1978.
115. J.B. Rajani, R. Payne, and S. Michelfelder, Convective heat transfer from impinging oxygen-natural gas flames — Experimental results from the NG5 Trials, Int. Flame Res. Found. Report F 35/a/12, IJmuiden, The Netherlands, 1978.
116. A. Ivernel and P. Vernotte, Etude expérimentale de l'amélioration des transferts convectifs dans les fours par suroxygénation du comburant, *Rev. Gén. Therm., Fr.*, Nos. 210–211, 375–391, 1979.
117. G.K. Hargrave and J.K. Kilham, The effect of turbulence intensity on convective heat transfer from premixed methane-air flames, *Inst. Chem. Eng. Symp. Ser.*, 2(86), 1025–1034, 1984.
118. M.E. Horsley, M.R.I. Purvis, and A.S. Tariq, Convective heat transfer from laminar and turbulent premixed flames, *Heat Transfer 1982*, U. Grigull, E. Hahne, K. Stephan, and J. Straub, Eds., Hemisphere, Washington, D.C., Vol. 3, 409–415, 1982.
119. Rauenzahn, R.M., Analysis of Rock Mechanics and Gas Dynamics of Flame-Jet Thermal Spallation Drilling, Ph.D. thesis, MIT, Cambridge, MA, 1986.
120. G.K. Hargrave, M. Fairweather, and J.K. Kilham, Forced convective heat transfer from premixed flames. 2. Impingement heat transfer, *Int.J. Heat Fluid Flow*, 8(2), 132–138, 1987.
121. J.E. Hustad and O.K. Sønju, Heat transfer to pipes submerged in turbulent jet diffusion flames, in *Heat Transfer in Radiating and Combusting Systems*, Springer-Verlag, Berlin, 1991, 474–490.
122. T.H. van der Meer, Stagnation point heat transfer from turbulent low reynolds number jets and flame jets, *Exper. Therm. Fluid Sci.*, 4, 115–126, 1991.
123. V.I. Babiy, Solid/gas phase heat exchange in combustion of powdered fuel, in *Heat Transfer in Flames*, N.H. Afgan and J.M. Beer, Ed., Scripta Book Company, Washington, D.C., 1974, chap. 7, 131–139.
124. C.C. Monrad, Heat transmission in convection sections of pipe stills, *Ind. Eng. Chem.*, 24, 505–509, 1932.
125. B. Gebhart, Y. Jaluria, R. Mahajan, and B. Sammakia, *Buoyancy-Induced Flows and Transport*, Hemisphere, New York, 1988.
126. Y.B. Wang, C. Chaussavoine, and F. Teyssandier, Two-dimensional modelling of a non-confined circular impinging jet reactor–fluid dynamics and heat transfer, *Int.J. Heat Mass Trans.*, 36(4), 857–873, 1993.
127. J.D. Gilchrist, *Fuels, Furnaces and Refractories*, Pergamon Press, Oxford, U.K., 1977.
128. V.S. Arpaci, *Conduction Heat Transfer*, Addison-Wesley, Reading, MA, 1966.
129. M.N. Özisik, *Boundary Value Problems of Heat Conduction*, Dover, New York, 1968.
130. U. Grigull and H. Sandner, *Heat Conduction*, Hemisphere, Washington, D.C., 1984.
131. G.E. Myers, *Analytical Methods in Conduction Heat Transfer*, Genium Publishing, Schenectady, NY, 1987.
132. B. Gebhart, *Heat Transfer and Mass Diffusion*, McGraw-Hill, New York, 1993.
133. D. Poulidakos, *Conduction Heat Transfer*, Prentice Hall, Englewood Cliffs, NJ, 1994.
134. D.R. Lide, Ed., *CRC Handbook of Chemistry and Physics*, 79th ed., CRC Press, Boca Raton, FL, 1998.
135. G.F. Hewitt, G.L. Shires, Y.V. Polezhaev, and Iu.V. Polezhaev (eds.), *International Encyclopedia of Heat & Mass Transfer*, CRC Press, Boca Raton, FL, 1997.
136. F. Kreith (ed.), *The CRC Handbook of Mechanical Engineering*, CRC Press, Boca Raton, FL, 1994.
137. G.F. Hewitt, G.L. Shires, and T.R. Bott (eds.), *Process Heat Transfer*, CRC Press, Boca Raton, FL, 1994.
138. C.E. Baukal and B. Gebhart, A review of empirical correlations for flame impingement heat transfer, *Int. J. Heat Fluid Flow*, 17, 4, 386–396, 1996.

3 Fluid Flow

*Wes Bussman, Ph.D., Demetris Venizelos, Ph.D.,
and R. Robert Hayes*

CONTENTS

- 3.1 Introduction
 - 3.2 Gas Properties
 - 3.2.1 Density
 - 3.2.1.1 Density at Actual and Standard Conditions
 - 3.2.1.2 Density of Mixtures
 - 3.2.2 Ratio of Specific Heat of Gas Mixtures
 - 3.2.3 Fuel Heating Value
 - 3.3 Fluid Dynamic Concepts Commonly Used in the Burner Industry
 - 3.3.1 Laminar and Turbulent Flow
 - 3.3.2 Free Jet Entrainment
 - 3.3.3 Eduction Processes
 - 3.3.4 Pressure
 - 3.3.4.1 Definition and Units of Pressure
 - 3.3.4.2 Atmospheric Pressure
 - 3.3.4.3 Gage and Absolute Pressure
 - 3.3.4.4 Furnace Draft
 - 3.3.4.5 Static, Velocity, and Total Pressure
 - 3.3.4.6 Pressure Loss
 - 3.4 Calculating the Heat Release from a Burner
 - 3.4.1 Definition of Heat Release
 - 3.4.2 Fuel Gas Orifice Calculations
 - 3.4.2.1 Discussion of Sonic and Subsonic Flow
 - 3.4.2.2 Equations for Calculating Fuel Flow Rate
 - 3.4.2.3 Discharge Coefficient
 - 3.4.3 Example Calculation: Heat Release from a Burner
 - 3.5 Combustion Air Flow Rate through Natural-Draft Burners
- References

3.1 INTRODUCTION

Fluid dynamics is one of the most important areas of engineering science. Over the past 100 years, research into the science of fluid dynamics has grown at an exponential rate. Today, there are hundreds of papers published and dozens of conferences and symposia held every year devoted to the subject. Fluid dynamics is a broad subject because it is an important tool used in many engineering fields, for example, turbulence, acoustics, and aerodynamics. There are many good textbooks on the subject; those by Panton,¹ White,² Fox and McDonald,³ Vennard and Street,⁴ Hinze,⁵ Schlichting,⁶ and Hughes and Brighton⁷ are a few examples.

When designing combustion equipment, engineers might perform several fluid dynamic calculations. For example, it is common for engineers to size the fuel ports using orifice calculations or determine the size of the burner using pressure drop equations. A good familiarity with fluid dynamics is essential to the burner engineer. The purpose of this chapter is to give the reader a fundamental understanding of some of the fluid dynamic concepts that are important in combustion systems and show how they are commonly applied to burner design.

3.2 GAS PROPERTIES

The properties of a gas describe its physical characteristics and are commonly used in burner design calculations. Table 3.1 contains a list of various pure-component gases with their corresponding properties. This section presents a brief description of these properties and describes how the properties of a mixture are calculated. For a list of additional gas properties, the reader is referred to Geerssen,⁸ Baukal,⁹ Turns,¹⁰ and Bartok and Sarofim.¹¹

TABLE 3.1
Properties of Various Gases

Gas Composition	Molecular Weight	Density (lb/scf)	Ratio of Specific Heat*	LHV** (BTU/scf)	HHV*** (BTU/scf)
Methane (CH ₄)	16.043	0.04238	1.31	909.40	1010.00
Ethane (C ₂ H ₆)	30.070	0.07943	1.19	1618.70	1769.60
Propane (C ₃ H ₈)	44.097	0.11648	1.13	2314.90	2516.10
n-Butane (C ₄ H ₁₀)	58.123	0.15352	1.10	3010.80	3262.30
Pentane (C ₅ H ₁₂)	72.150	0.19057	1.08	3706.90	4008.90
n-Hexane (C ₆ H ₁₄)	86.177	0.22762	1.06	4403.80	4755.90
Cyclopentane (C ₅ H ₁₀)	70.134	0.18525	1.12	3512.10	3763.70
Cyclohexane (C ₆ H ₁₂)	84.161	0.22230	1.09	4179.70	4481.70
Ethylene (C ₂ H ₄)	28.054	0.07410	1.25	1498.50	1599.80
Propene (C ₃ H ₆)	42.081	0.11115	1.15	2181.80	2332.70
Butene (C ₄ H ₈)	56.108	0.14820	1.11	2878.70	3079.90
Pentene (C ₅ H ₁₀)	70.134	0.18525	1.08	3575.00	3826.50
Butadiene (C ₄ H ₆)	54.092	0.14288	1.12	2789.00	2939.90
Carbon Dioxide (CO ₂)	44.010	0.11625	1.29	0.00	0.00
Water (H ₂ O)	18.015	0.04758	1.33	0.00	0.00
Oxygen (O ₂)	31.999	0.08452	1.40	0.00	0.00
Nitrogen (N ₂)	28.013	0.07399	1.40	0.00	0.00
Sulfur Dioxide (SO ₂)	64.060	0.16920	1.27	0.00	0.00
Hydrogen Sulfide (H ₂ S)	34.080	0.09002	1.32	586.80	637.10
Carbon Monoxide (CO)	28.010	0.07398	1.40	320.50	320.50
Ammonia (NH ₃)	17.031	0.04498	1.31	359.00	434.40
Hydrogen (H ₂)	2.016	0.00532	1.41	273.80	324.20
Argon (Ar)	39.944	0.10551	1.67	0.00	0.00
Acetylene (C ₂ H ₂)	26.038	0.06878	1.24	1423.20	1473.50
Benzene (C ₆ H ₆)	78.144	0.20633	1.12	3590.90	3741.80

*At 59°F (standard temperature)

**LHV (Lower Heating Value) at 59°F and 14.696 psia

***HHV (Higher Heating Value) at 59°F and 14.696 psia

3.2.1 DENSITY

3.2.1.1 Density at Actual and Standard Conditions

Atmospheric air is a mixture of many gases plus water vapor and other pollutants. Aside from pollutants, which may vary considerably from place to place, the composition of dry air is relatively constant; the composition varies slightly with time, location, and altitude.¹² The *ASHRAE Handbook of Fundamentals*¹³ provides the following approximate composition of dry air on a volume fraction basis:

Nitrogen	0.78084
Oxygen	0.20948
Argon	0.00934
Carbon dioxide	0.00031
Neon, helium, methane, sulfur dioxide, hydrogen, etc.	0.00003

In 1949, a standard composition of dry air was fixed by the International Joint Committee on Psychrometric Data,¹⁴ as shown below.

Constituent	Molecular Weight	Volume Fraction
Oxygen	32.000	0.2095
Nitrogen	28.016	0.7809
Argon	39.944	0.0093
Carbon dioxide	44.010	0.0003
	28.965	1.0000

Density is defined as the mass per unit volume of a fluid and is usually given the Greek symbol ρ (rho). The units of density, for example, can be written as lbm/ft^3 or kg/m^3 . Based on the composition of dry air given above, the density is 0.0765 lbm/ft^3 or 1.225 kg/m^3 . This is the density of air at standard temperature, standard pressure, and is usually denoted as STSP (59.0°F or 15°C , 14.696 lbf/in.^2 or 101.325 kPa).

The density of a gas can change with temperature and pressure. For example, the density of dry air at 59.0°F and at 14.696 psia is 0.0765 lbm/ft^3 STSP. If we compress the air and cool it down from standard conditions, its density will increase. We can calculate the density of a gas at any condition using the following equation:

$$\rho_{\text{actual}} = \rho_{\text{STSP}} \left(\frac{460 + 59}{460 + T(^{\circ}\text{F})} \right) \left(\frac{14.696 + P(\text{psig})}{14.696} \right) \quad (3.1)$$

Example 3.1

Determine the density of dry air at 5 psig and 40°F . Substituting the appropriate values into Equation 3.1 gives:

$$\rho_{\text{actual}} = 0.0765 \left(\frac{519}{460 + 40} \right) \left(\frac{14.696 + 5}{14.696} \right) = 0.1064 \text{ lbm/ft}^3 \text{ ATAP}$$

In this example, the density of the air has increased from 0.0765 at STSP to 0.1064 lbm/ft^3 . This is the density at actual conditions and is usually denoted as ATAP (actual temperature, actual pressure). Notice from Equation 3.1 that as the temperature of the gas increases, the density decreases;

but as the pressure increases, the density increases. The density of any gas at ATAP conditions can be calculated using Equation 3.1 if one knows the density of that gas at STSP conditions.

If only the molecular weight of a gas is known, one can calculate the density of that gas at ATAP conditions. First, the density of the gas at STSP is calculated using the following equation:

$$\rho_{\text{gas,STSP}} = \rho_{\text{air,STSP}} \left(\frac{MW_{\text{gas}}}{MW_{\text{air}}} \right) = 0.0765 \frac{\text{lbm}}{\text{ft}^3} \left(\frac{MW_{\text{gas}}}{28.965} \right) \quad (3.2)$$

where MW_{gas} is the molecular weight of gas, MW_{air} is the molecular weight of air, and $\rho_{\text{gas,STSP}}$ is the density of the gas at STSP conditions. After the density of the gas has been calculated at STSP conditions, the density at actual conditions can be determined using Equation 3.1.

Example 3.2

Find the density of methane at 100°F and 30 psig.

Step 1: Using Equation 3.2, calculate the density of methane at STSP conditions.

$$\rho_{\text{methane,STSP}} = \rho_{\text{air}} \left(\frac{MW_{\text{methane}}}{MW_{\text{air}}} \right) = 0.0765 \frac{\text{lbm}}{\text{ft}^3} \left(\frac{16.043}{28.965} \right) = 0.0424 \frac{\text{lbm}}{\text{ft}^3} \text{ STSP}$$

Step 2: Using Equation 3.2, calculate the density of methane at ATAP conditions.

$$\rho_{\text{methane,ATAP}} = \rho_{\text{methane,STSP}} \left(\frac{460 + 59}{460 + T(^{\circ}\text{F})} \right) \left(\frac{14.696 + P(\text{psig})}{14.696} \right)$$

$$\rho_{\text{methane,ATAP}} = 0.0424 \left(\frac{519}{460 + 100} \right) \left(\frac{14.696 + 30}{14.696} \right) = 0.1195 \frac{\text{lbm}}{\text{ft}^3} \text{ ATAP}$$

Notice that the density is higher than at STSP conditions. The reason is because we are calculating the density at a pressure higher than standard conditions, thus resulting in an increase in density.

3.2.1.2 Density of Mixtures

The molecular weight and density of a gas mixture can be determined by the following equations, respectively:

$$MW_{\text{mixture}} = MW_1 x_1 + MW_2 x_2 + \dots + MW_n x_n \quad (3.3)$$

$$\rho_{\text{mixture,STSP}} = \left(\frac{\rho_{\text{air,STSP}}}{MW_{\text{air}}} \right) [MW_1 x_1 + MW_2 x_2 + \dots + MW_n x_n], \quad (3.4)$$

where MW_n and x_n is the molecular weight and volume fraction of the n th component, respectively.

Example 3.3

Determine the molecular weight and density of a gas mixture containing 25% hydrogen and 75% methane (volume basis).

We know the following variables:

$$MW_1 = 2.0159$$

$$MW_2 = 16.043$$

$$x_1 = 0.25$$

$$x_2 = 0.75$$

$$\rho_{\text{air,STSP}} = 0.0765 \text{ lbm/ft}^3$$

$$MW_{\text{air}} = 28.965$$

Substituting these values into Equations 3.3 and 3.4 gives:

$$MW_{\text{mixture}} = MW_1x_1 + MW_2x_2 = 2.0159 \times 0.25 + 16.043 \times 0.75 = 12.536$$

$$\rho_{\text{mixture,STSP}} = \left(\frac{\rho_{\text{air,STSP}}}{MW_{\text{air}}} \right) [MW_1x_1 + MW_2x_2 + \dots + MW_nx_n]$$

$$\rho_{\text{mixture,STSP}} = \left(\frac{0.0765}{28.965} \right) [2.0159 \times 0.25 + 16.043 \times 0.75] = 0.0331 \frac{\text{lbm}}{\text{ft}^3} \text{ STSP}$$

3.2.2 RATIO OF SPECIFIC HEAT OF GAS MIXTURES

The *ratio of specific heat*, denoted by the letter k , is a fluid property used in many engineering calculations and is mathematically defined as:

$$k = \frac{c_p}{c_v} \quad (3.5)$$

where c_p and c_v is the specific heat at constant pressure and volume, respectively. For most hydrocarbons, the ratio of specific heat varies between a value of nearly 1.0 to 1.7 and exhibits a strong dependence on the gas temperature and composition. For example, methane at standard temperature (59°F) has a k value of approximately 1.31, while propane has a value of 1.13. However, at 200°F, the ratios of specific heat of methane and propane decrease to a value of approximately 1.27 and 1.10, respectively. Values of k for several pure-component gases at standard temperature (59°F) are listed in Table 3.1.

One can think of the ratio of specific heat as being a value that relates to the compressibility of a gas. How much a gas compresses when a pressure is applied to it is an important property that influences the flow rate of a gas through an orifice. Later in this chapter we show how the ratio of specific heat is utilized in orifice calculations.

For a mixture of gases, at a given temperature, the ratio of specific heat can be determined with the following equation:

$$k_T = \frac{\frac{k_1x_1}{(k_1-1)} + \frac{k_2x_2}{(k_2-1)} + \dots + \frac{k_nx_n}{(k_n-1)}}{\frac{x_1}{(k_1-1)} + \frac{x_2}{(k_2-1)} + \dots + \frac{x_n}{(k_n-1)}} \quad (3.6)$$

where k_n is the ratio of specific heat, x_n is the volume fraction, and MW_n is the molecular weight of n th component.

Example 3.4

Determine the ratio of specific heat of the following fuel mixture (percentage by volume) at a gas temperature of 59°F:

- 75% Hydrogen
- 14% Methane
- 11% Propane

The volume fraction x of each gas component is:

$$x_1 = 0.75 \text{ (hydrogen)}$$

$$x_2 = 0.14 \text{ (methane)}$$

$$x_3 = 0.11 \text{ (propane)}$$

The molecular weight and ratio of specific heat of each gas component can be obtained from Table 3.1.

$$MW_1 = 2.0159 \text{ (hydrogen)}$$

$$MW_2 = 16.043 \text{ (methane)}$$

$$MW_3 = 44.097 \text{ (propane)}$$

$$k_1 = 1.41 \text{ (hydrogen)}$$

$$k_2 = 1.31 \text{ (methane)}$$

$$k_3 = 1.13 \text{ (propane)}$$

Substituting the above values into Equation 3.5 and solving gives the ratio of specific heat of the fuel mixture at 59°F.

$$k_T = \frac{\frac{1.41 \times 0.75}{(1.41-1)} + \frac{1.31 \times 0.14}{(1.31-1)} + \frac{1.13 \times 0.11}{(1.13-1)}}{\frac{0.75}{(1.41-1)} + \frac{0.14}{(1.31-1)} + \frac{0.11}{(1.13-1)}} = 1.32$$

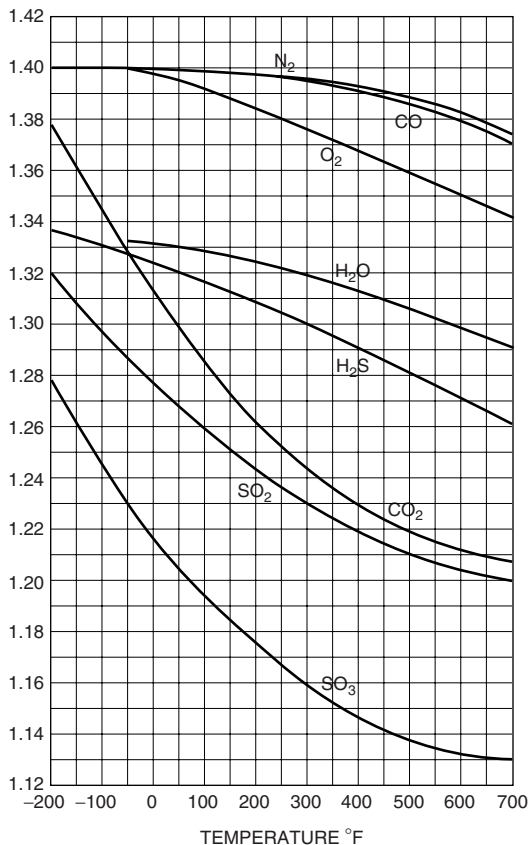
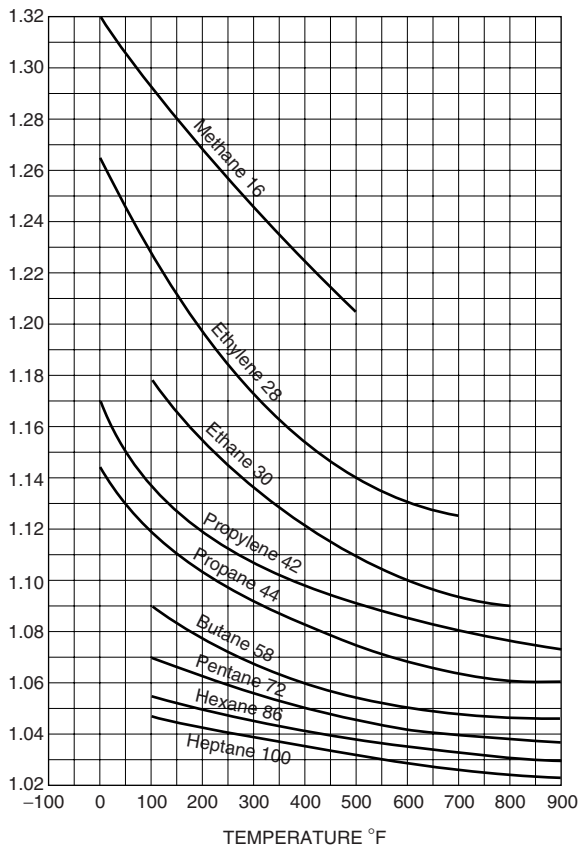
As mentioned, the ratio of specific heat also varies with the temperature of the gas. Typically, as the gas temperature increases, the ratio of specific heat decreases as shown in Table 3.2 for several pure gas components. To determine the ratio of specific heat of a fuel mixture at various temperatures, one must determine the ratios of specific heat for each gas component at that given temperature. Using these ratios of specific heat values, Equation 3.5 can be used to determine the ratio of specific heat of the mixture at the given temperature.

3.2.3 FUEL HEATING VALUE

The amount of energy released when a fuel is burned depends on its composition. For example, suppose we take 1 cubic foot each of hydrogen, methane, and propane. Which fuel will output the most energy when burned? The answer is propane. Propane has a heating value of 2590 BTU per cubic foot while methane and hydrogen have 1013 and 325 BTU per standard cubic foot, respectively. So, one can see that the heating value of a fuel depends on the components in the fuel blend. The heating values just mentioned are based on what is referred to as the *Higher Heating Value* (HHV) of the fuel. Fuels can also be related to their *Lower Heating Value* (LHV).

The HHV of a fuel is based on the energy released assuming that the water vapor in the combustion products condenses to liquid. When the water vapor condenses to liquid form, additional energy is released. This energy is referred to as the heat of condensation or latent heat of vaporization.

TABLE 3.2
Plots of Ratio of Specific Heat (k) for Various Pure-Component Gas at Different Temperatures



The HHV represents the total heat obtained by first burning a fuel and then cooling the products to standard temperature. If the water vapor in the products is not condensed, the total amount of energy released from the fuel is less than the HHV and is referred to as the LHV. So, for example, the LHV and HHV of propane are 2385 and 2590 BTU per standard cubic foot, respectively.

Heating values are also provided on a mass basis. For example, the LHV of propane, methane, and hydrogen are 19,944, 21,520, and 51,623 BTU per pound, respectively. Notice that hydrogen, on a pound basis, has a much higher energy output than propane and methane; however, on a volume basis, the energy output is much lower due to its low density. Typical hydrocarbons, such as a methane, ethane, butane, etc., have an LHV of approximately 20,000 BTU per pound.

To determine the heating value of a mixture of gases, it is necessary to know the heating value of each compound and the composition of the gases in terms of volume or mass fractions. The following equations are used to calculate heating value of a gas mixture:

$$HV_{\text{mixture,vol}} = HV_1x_1 + HV_2x_2 + \dots + HV_nx_n \quad (3.7)$$

$$HV_{\text{mixture,mass}} = HV_1y_1 + HV_2y_2 + \dots + HV_ny_n \quad (3.8)$$

where $HV_{\text{mixture,vol}}$ = heating value of mixture, volume basis; HV_n = heating value of n th component, volume basis; x_n = volume fraction of n th component; $HV_{\text{mixture,mass}}$ = heating value of mixture, mass basis; HV_n = heating value of n th component, mass basis; and y_n = mass fraction of n th component.

Example 3.5

Determine the LHV of the following mixture:

Mixture Content, by Volume	LHV (BTU/scf)
40% hydrogen	275
55% methane	913
5% propane	2385

Substituting the appropriate values into Equation 3.7 gives:

$$LHV_{\text{mixture,vol}} = LHV_1x_1 + LHV_2x_2 + LHV_3x_3$$

$$LHV_{\text{mixture,vol}} = (0.4)(275) + (0.55)(913) + (0.05)(2385) = 731.4 \text{ BTU/scf}$$

3.3 FLUID DYNAMIC CONCEPTS COMMONLY USED IN THE BURNER INDUSTRY

3.3.1 LAMINAR AND TURBULENT FLOW

If you have ever watched the smoke trailing from a cigarette or incense burner in a calm room, you probably noticed that the flow of the smoke is initially smooth and then quickly transitions into a chaotic motion. The smooth part of the flow is called *laminar flow*; that is, the flow of the smoke is laminated. The chaotic or random motion is called *turbulent flow*. Turbulent flow is very easy to find in nature; flow from a volcano, wind, flow of rivers, exhaust from a jet engine are a few examples. Laminar flow, however, is more difficult to find in nature.

Flames are typically classified as either *laminar* or *turbulent*. [Figure 3.1](#) contains photographs of a burning match and a forest fire. One can easily recognize the forest fire as being a turbulent flame and the burning match as a laminar flame. Notice that the flame front on the burning match

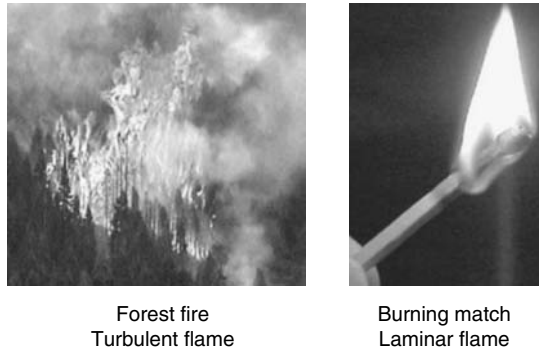


FIGURE 3.1 Photographs showing examples of turbulent (left) and laminar (right) flames.

is smooth while the forest fire is chaotic. For detailed discussions of laminar and turbulent flames, the reader is referred to Kuo¹⁵ and Lipatnikov and Chomiak.¹⁶

In the burner industry, one will see both types of flames. Sometimes, a burner engineer will design a burner that produces a flame that is laminar in order to prevent a phenomenon called flashback — an event that occurs in premix burners when the flame propagates back through the burner tip. Sometimes, burners are designed to create turbulence to enhance mixing of the fuel with combustion air and furnace flue gases. The rate at which these gases are mixed is critical to the design of a burner because it can affect the flame shape and size.

A common method used to determine if the flow of a fluid is laminar or turbulent is to relate several of the flow parameters to a nondimensional index called the Reynolds number. Mathematically, the Reynolds number (Re) is defined as:

$$Re = \frac{VD}{\nu} \quad (3.9)$$

where V is the velocity of the flowing fluid, D is a length variable in the flow field (e.g., pipe diameter), and ν is the kinematic viscosity. The flow of a fluid in a pipe is turbulent, for example, if the Reynolds number is greater than 4000; but if the Reynolds number is less than 2300, the flow is laminar. The Reynolds number is used in many fields of fluid dynamics. In the burner industry, the Reynolds number is used, for example, to scale orifice discharge coefficients, relate the pressure drop of a fluid flowing through an obstruction, and calculate heat transfer rates.

3.3.2 FREE JET ENTRAINMENT

When a fluid emerges from a nozzle, it will interact with the surrounding fluid. This is called a *free jet* and is common in combustion systems; for example, fuel gas exiting a burner nozzle. [Figure 3.2a](#) is a photograph showing a gas exiting a nozzle. The white streak-lines in the photograph are small particles that have been released in the vicinity of the jet. The photograph clearly shows that the particles are pulled toward the flow path of the free jet. These particles are pulled into the jet because, as the gas exits the nozzle, a low-pressure region is created downstream of the exit. This low-pressure region causes the surrounding gas to be pulled in. As the surrounding gas is pulled in, turbulence causes the free jet and surrounding gas to mix as shown in [Figure 3.2b](#). As the free jet captures the surrounding gas, the jet diameter increases.

The rate at which a free jet entrains and mixes with the surrounding gas is a critical parameter when designing burners. For example, sometimes an engineer designs a burner to mix large quantities of furnace flue gas with the fuel prior to combustion in order to reduce the flame

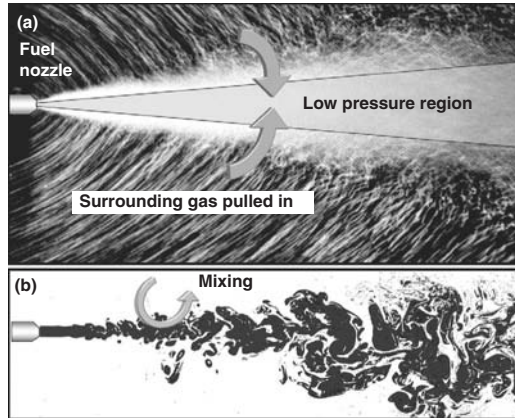


FIGURE 3.2 Photographs showing the mixing and entrainment of a free jet.

temperature and lower NO_x emissions. However, when designing a burner for low BTU gases that are difficult to burn, the engineer may want to delay the mixing of the fuel with the furnace flue gases and air in order to provide a stable flame.

The engineer controls the rate of mixing of fuel with combustion air and furnace flue gases by designing the fuel nozzle to utilize a certain amount of pressure. For example, suppose we have two nozzles passing the same mass flow-rate of fuel (same heat release); one of the nozzles is 0.0625 in. in diameter and the other nozzle is 0.25 in. in diameter. Obviously, the smaller diameter nozzle must operate at a higher pressure than the larger diameter nozzle in order to pass the same amount of fuel. If we measure the amount of surrounding gas entrained by each nozzle at any given location downstream of the nozzle exit, which one would have more surrounding gas mixed with the fuel? The smaller diameter nozzle would have more surrounding gas mixed with the fuel because it exits the nozzle with more energy. Because more work is required to compress the fuel to a higher pressure for the smaller nozzle than for the larger nozzle, one should expect more work from the fuel as it exits the nozzle; this additional energy results in better mixing.

The amount of surrounding gas entrained by a turbulent jet can be estimated¹⁷ from the following equation:

$$\frac{m_{\infty}}{m_f} = 0.32 \left(\frac{\rho_{\infty}}{\rho_f} \right)^{1/2} \left(\frac{x}{d} \right) \quad (3.10)$$

where m_{∞} is the mass of the surrounding gas, m_f is the mass of the fuel, ρ_{∞} is the density of the surrounding gas, ρ_f is the density of the fuel, x is the distance downstream of the nozzle exit, and d is the diameter of the port. It should be noted that this equation is valid for $x/d > 18$.

Example 3.6

Suppose two nozzles are discharging methane into ambient air. The temperature of both the methane and the air is 60°F. One nozzle has a port diameter equal to 0.0625 in. and the other nozzle has a port diameter equal to 0.25 in. Determine the mass ratio of air-to-fuel for each nozzle at a location 8 in. downstream of the exit.

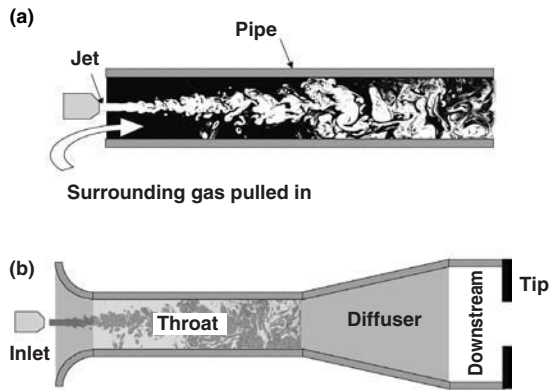


FIGURE 3.3 Eductor systems: (a) simple version, and (b) more complex version.

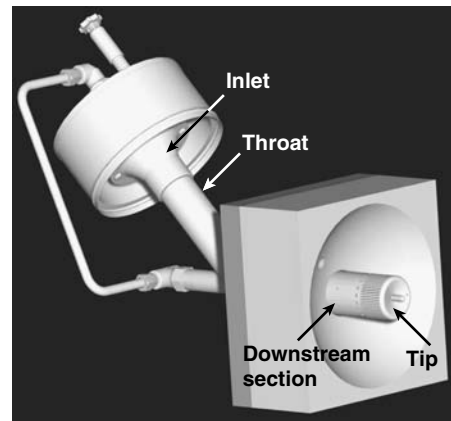


FIGURE 3.4 Radiant wall, eductor-style burner.

First, notice that the value of x/d is greater than 18 for both nozzles; therefore, Equation 3.10 is valid. The values of each variable in this example are: $\rho_{\infty} = 0.0765 \text{ lbm/ft}^3$, $\rho_f = 0.0422 \text{ lbm/ft}^3$, $x = 8 \text{ in.}$, $d = 0.0625 \text{ in.}$ and 0.25 in. Substituting these values into Equation 3.10, the mass ratio of air to fuel for the 0.0625-in. and 0.25-in. diameter nozzles are 55.1 and 13.8, respectively. Notice that the smaller port has entrained four times more ambient air than the larger port. Again, this illustrates that burner engineers can control the rate of mixing of fuel with the surrounding gas by drilling fuel nozzles to a particular diameter.

3.3.3 EDUCTION PROCESSES

If a pipe is placed just downstream of a free jet as illustrated in Figure 3.3, a low-pressure zone will be created inside the pipe, causing the surrounding gas to be pulled in through the inlet. This system is sometimes referred to as an *eductor* or *jet pump* and is commonly used throughout the combustion industry. These systems consist of two main parts: a primary nozzle and a pipe commonly referred to as a mixer or venturi. In the burner industry, it is common to see more complex venturi designs as illustrated in Figure 3.4. These more complex designs usually consist of five components: inlet, throat, diffuser, downstream section, and tip. Each component plays a major role in the entrainment performance of the eductor system.

The inlet typically consists of a well-rounded bell design. The purpose of a bell inlet is to reduce the pressure losses as the secondary gas enters into the eductor system. By reducing pressure

losses, the engineer can improve the entrainment performance; sometimes this is critical, especially when designing premixed burners. Located just downstream of the venturi inlet is the throat.

The design of the venturi throat is critical to the entrainment performance of an eductor system. Both the diameter of the throat and the ratio of the length to the diameter are the critical design parameters. Eductor systems can be designed with a specific throat diameter that will provide maximum entrainment performance. The throat diameter that provides the maximum entrainment performance depends on the momentum of the motive gas and the overall momentum losses as the gas flows through the eductor system. The length-to-diameter ratio (“L over D” ratio) is also a critical design parameter and has an optimum value that provides maximum entrainment performance. If the “L over D” ratio is too large, additional momentum will be consumed by friction losses as the gas flows along the throat wall. If the “L over D” ratio is too small, the motive gas jet will not impinge the wall of the venturi throat, thus resulting in a reduction in entrainment performance. Values of “L over D” ratios that provide optimized entrainment performance typically vary from 5 to 7. Located just downstream of the venturi throat is the diffuser section.

The diffuser is conical in shape and provides a transition from the venturi throat to the downstream section. Typically, diffusers are designed with small transition angles to provide smooth flow in order to reduce the pressure losses as gas flows from the throat to the downstream section.

The design of the downstream section can be as simple as a straight pipe or quite complex, consisting of a variety of fittings. Usually, in the burner industry the outlet of the downstream section consists of a tip. There are a variety of tips used in the burner industry, depending on the design application. The pressure loss associated with the flowing gas through the downstream section and tip can have a major influence on the design and performance of an eductor system.

Due to the large number of variables involved, it can be challenging for burner engineers to properly predict and optimize the performance of eductor systems. Burner designers usually rely on experiments or computer models to determine eductor performance. Some of the first theoretical and experimental studies on entrainment performance of an eductor system began in the early 1940s.¹⁸ Since that time, a lot of work has been devoted to understanding the mechanisms governing the performance of these systems.¹⁹ The trends shown in [Figure 3.5](#) are a typical representation of how the pressure of the primary jet influences the entrainment performance of an eductor system. It is convenient for engineers to analyze these trends plotted with the ratio of

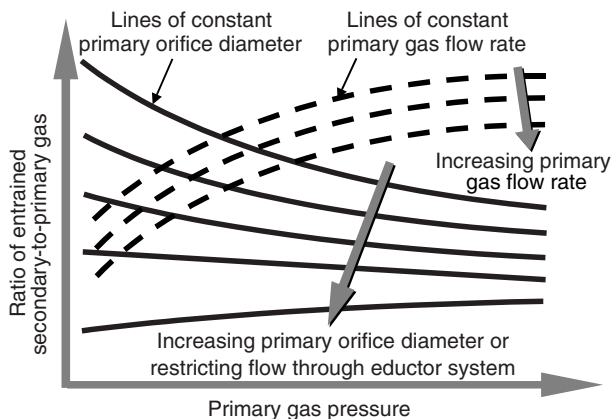


FIGURE 3.5 A typical representation of how the motive energy of the primary fuel jet affects the entrainment performance of an eductor system.

entrained secondary-to-primary gas. These general trends can provide valuable insight to engineers who design eductor systems and can be summarized as follows:

1. At a constant primary gas pressure, increasing the orifice diameter results in a decrease in the entrainment performance.
2. At a constant primary gas flow rate, increasing the primary gas pressure increases the entrainment performance.

3.3.4 PRESSURE

3.3.4.1 Definition and Units of Pressure

Pressure is created by the collision of molecules on a surface and is defined as the force exerted per unit area on that surface. Pressure is generally measured in units of Pascals ($\text{Pa} = \text{N}/\text{m}^2$); however, burner system designers will use a variety of pressure units because the choice of units will vary, depending on the customer. For example, customers in the United States will typically use units of psi (pounds per square inch) or inches of water column (inches of WC), whereas in Europe and Asia the units are usually Pa or millimeters of water column (mm of WC). The conversion of these pressure units are as follows: $1 \text{ lb}/\text{in.}^2 = 27.68 \text{ inches of water column} = 6895 \text{ Pa} = 703.072 \text{ mm of water column}$.

3.3.4.2 Atmospheric Pressure

Atmospheric pressure refers to the pressure created by a column of air that extends from the surface of the Earth to several miles above it. Initially, engineers developed a *Standard Atmospheric Pressure* so that the performance of aircraft and missiles could be evaluated at a standard condition. The idea of a standard atmospheric pressure was first introduced in the 1920s.²⁰ In 1976, a revised report was published that defined the U.S. standard atmosphere that is the currently accepted standard. This standard is an idealized representation of the mean conditions of the Earth's atmosphere in one year. The standard atmospheric pressure at sea level is equal to 14.696 psi (407 inches of WC or 101,325 N/m^2).

The atmospheric pressure varies with elevation. As one moves away from the surface of the Earth, the atmospheric pressure decreases because there is less atmosphere overhead to create pressure. For example, in Denver, Colorado, the elevation is about 1 mile above sea level. The atmospheric pressure at this elevation is approximately 12.1 psi. The atmospheric pressure in the troposphere, defined as the layer between sea level and 10,769 m, can be estimated using the following equation:²¹

$$p = 101,325 \left[\frac{T_o - 6.5 \times 10^{-3}(H)}{T_o} \right]^{5.259} \quad (3.11)$$

where p is the pressure in N/m^2 , T_o is the temperature at sea level in Kelvin, and H is the height above sea level in meters.

Example 3.7

If the temperature at sea level is 60°F, what is the atmospheric pressure at an elevation 1 mile above sea level?

First, let's determine the temperature at sea level in units of Kelvin (K).

$$T_o(\text{K}) = [T_o(^{\circ}\text{F}) - 32]/1.8 + 273.15 = [60 - 32]/1.8 + 273.15 = 288.71 \text{ K}$$

Next, let's convert the height above sea level (H) to units of meters.

$$H(\text{m}) = 1 \text{ mile} = 5280 \text{ ft} \times 1 \text{ m}/3.281 \text{ ft} = 1609.27 \text{ m}$$

Substituting these values into Equation 3.11 gives $p = 83,450.77 \text{ N/m}^2 = 12.10 \text{ psi}$.

3.3.4.3 Gage and Absolute Pressure

If the Earth was in a perfect vacuum, there would be no column of air above the surface; hence, the atmospheric pressure would be zero. The *absolute pressure* is measured relative to a perfect vacuum. Therefore, when a pressure measurement is taken at the surface of the Earth, the absolute pressure is equal to the atmospheric pressure. When writing the units for pressure, it is customary to designate absolute pressure with the letter “a” or “abs” after the units; for example, psia, psi (abs), or kPa (abs). The absolute pressure can never be less than zero; however, the gage pressure can.

The *gage pressure* is always measured relative to the atmospheric pressure. A gage pressure of less than zero can exist. For example, suppose there is a sealed container that holds a vacuum at 10 psia at sea level. The gage pressure, which is measured relative to the absolute pressure, would be $10 \text{ psia} - 14.7 \text{ psia} = -4.7 \text{ psig}$. The letter “g” after the pressure units represents gage pressure. Now suppose the container is pressurized to 20 psia. The gage pressure will then be $20 \text{ psia} - 14.7 \text{ psia} = 5.3 \text{ psig}$. Thus, the gage pressure can either be a positive or negative number and is just the difference in pressure between the atmospheric pressure and the pressure at interest.

3.3.4.4 Furnace Draft

The term “draft” is commonly used to describe the pressure inside a heater.²² Draft is defined as the pressure difference between the atmosphere and the interior of the heater *at a particular elevation*. Because both the atmospheric pressure and the pressure inside the heater vary with elevation, it is important to make these pressure measurements at the same elevation.

Draft is established in a heater because the hot flue gases in the stack have a lower density than the surrounding air. The difference in density of the flue gas and air creates a buoyant force, causing the flue gases to flow vertically upward as illustrated in Figure 3.6; this effect is similar to why a hot-air balloon rises. As this column of hot flue gases rises from the furnace, it creates a negative pressure inside the furnace, drawing combustion air in through the burners. In the burner industry, furnace draft can be as low as 0.0036 psi. This low pressure is usually measured using a sensitive pressure transmitter or an inclined manometer.

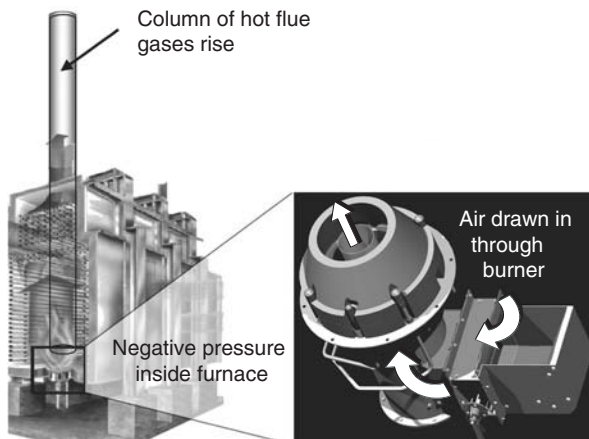


FIGURE 3.6 Description of furnace draft.

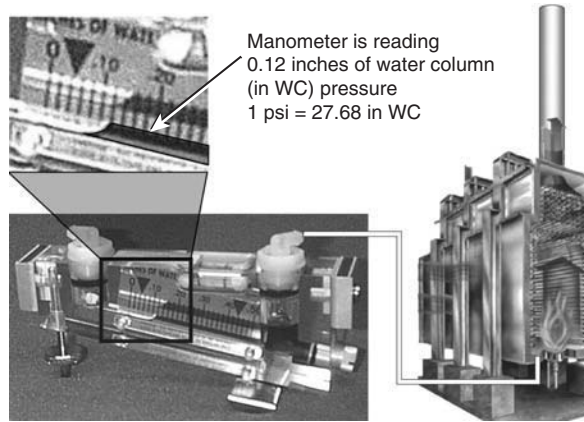


FIGURE 3.7 Inclined manometer.

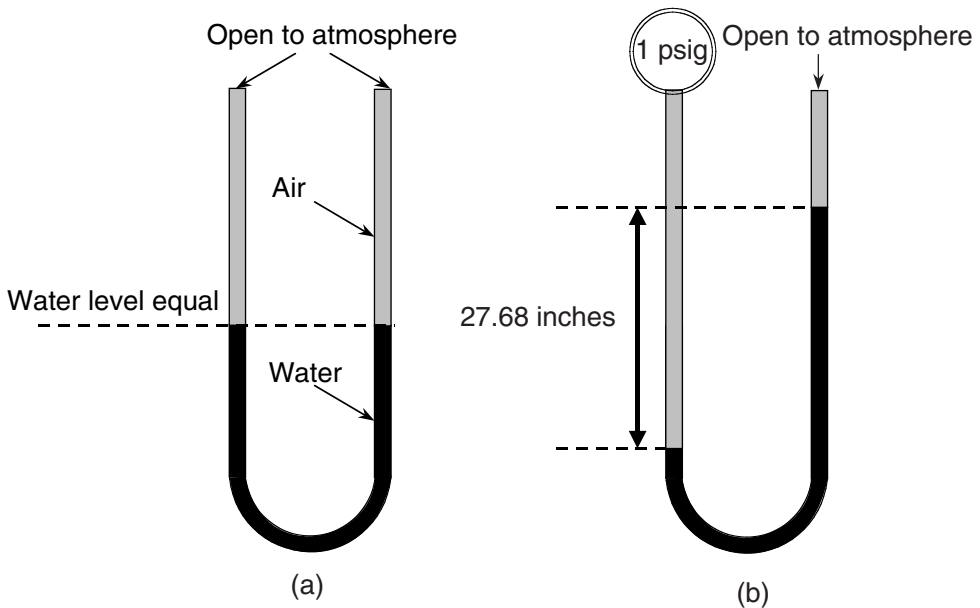


FIGURE 3.8 U-tube manometer illustrating the principle of water column pressure.

An inclined manometer consists of a clear tube positioned at a slight angle relative to the horizontal as shown in Figure 3.7. The tube is typically filled with a light, red oil with a specific gravity of 0.8. One end of the tube is connected to the furnace while the other end is left open to the atmosphere. The negative pressure inside the heater pulls the oil down the tube. A marked gage located parallel to the tube is calibrated to provide the pressure in a particular unit.

The unit of draft typically used in the burner industry is expressed in inches or millimeters of water column (in. WC or mm WC). The unit of pressure, *inches of WC*, can be described with a simple example. Suppose a tube, shaped in the form of a U, is partially filled with water, as illustrated in Figure 3.8a. If both ends of the tube are open to the atmosphere, the water will equalize to the same level on each side of the tube. If a pressure of 1 psi is applied to one end of the tube, the difference in water level will now be 27.68 in., as illustrated in Figure 3.8b. That is, a pressure

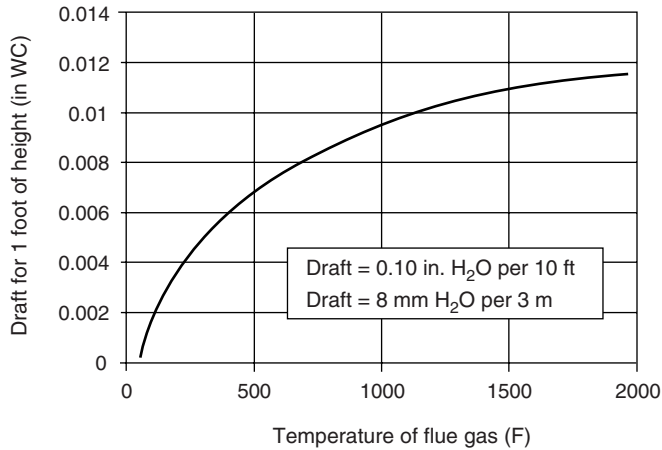


FIGURE 3.9 Plot of flue gas temperature versus draft per 1 foot of height.

of 1 psi will create a pressure head equal to 27.68 in. of water column. Typically in the burner industry, the furnace draft varies between 0.1 and 1 in. of water column. The draft can be estimated using the following equation:

$$P = \frac{27.68 \times H \times (\rho_{\text{flue}} - \rho_{\text{ambient}})}{144} \quad (3.12)$$

where P represents the furnace draft in inches of WC, H is the stack height in units of feet, and ρ_{flue} and ρ_{ambient} are the density of the flue gas and ambient air in lbm/ft^3 , respectively.

Example 3.8

A heater located at sea level has a stack that is 160 ft tall with an average flue gas temperature of 800°F (assuming a molecular weight of 28). If the ambient temperature is 60°F, estimate the draft that can be achieved by the stack at these conditions.

Using Equations 3.1 and 3.2, the density of the flue gas and ambient air can be calculated: $\rho_{\text{flue}} = 0.0305 \text{ lbm}/\text{ft}^3$ and $\rho_{\text{ambient}} = 0.0765 \text{ lbm}/\text{ft}^3$. Substituting these values into Equation 3.12 gives a draft level equal to 1.41 inches of WC. As a quick reference for determining the draft, refer to [Figure 3.9](#).

As mentioned, the draft does not remain constant throughout the furnace. For example, [Figure 3.10](#) is an illustration showing the draft in a heater at various elevations. First, notice that the atmospheric pressure represented by the dashed line decreases with elevation as discussed earlier. If this furnace were located at sea level, the atmospheric pressure would be 14.696 psi or 407 inches of WC. At the top of the stack, an elevation of 160 ft above sea level, the atmospheric pressure is approximately 404.7 inches of WC (calculated using Equation 3.11 at 60°F). The difference in the atmospheric pressure at grade and at an elevation of 160 ft is the maximum draft that can be achieved for this particular heater. That is, 2.3 inches WC (407 – 404.7) is the maximum achievable draft. This would be the draft if the density of the gas inside the heater was equal to zero and there were no pressure losses as the flue gases flow through the heater and stack. In reality, however, the density of the flue gases can never equal zero and there are always pressure losses associated with the flow of the flue gases through the furnace. Notice in [Figure 3.10](#) that the pressure inside the furnace continually varies with elevation. Again, the draft is defined as the pressure difference between the atmosphere and the interior of the heater *at a particular elevation*. In this particular example, the draft available for the burners is approximately 0.8 inches of WC

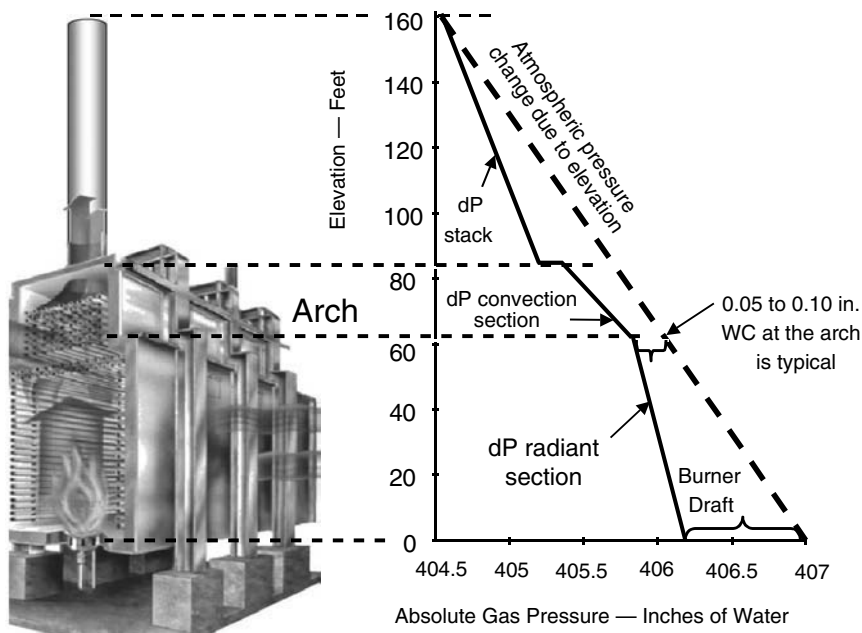


FIGURE 3.10 Furnace draft at various elevations.

(406.2 to 407). Also notice that minimum draft occurs just after the radiant section (arch). In most industrial furnaces, this is typically the location of minimum draft and is the most important location to measure and control draft (also called target draft). Typically, draft levels at this location are maintained at a pressure of 0.05 to 0.1 inches of WC. Maintaining a slight negative pressure at this location normally ensures a negative pressure throughout the heater, which is desirable.

3.3.4.5 Static, Velocity, and Total Pressure

The *total pressure* is defined as the velocity pressure plus the static pressure:

$$P_T = P_V + P_S \quad (3.13)$$

where P_T is the total pressure, P_V is the velocity pressure, and P_S is the static pressure. The *velocity pressure* is defined as the pressure created by a flowing gas impacting a surface. The *static pressure* is defined as the pressure created by gas molecules impacting a surface at a location where the velocity of the gas is equal to zero. For example, suppose a sealed vessel contains a gas at a pressure of 1 psig as illustrated in Figure 3.11. What is the static pressure inside the vessel? We know that the total pressure inside the vessel is equal to 1 psig. Because the velocity of the gas inside the vessel is zero, we can say that the pressure created by a flowing gas, or the velocity pressure, inside the vessel is equal to zero. Therefore, from Equation 3.13 we can conclude that the static pressure inside the vessel is equal to the total pressure of 1 psig.

Now suppose that we open a valve to a pipe located on the vessel. If we assume that there are no pressure losses as the gas flows from the vessel to a location in the pipe just downstream of the vessel, then we can say that the total pressure inside the pipe is still equal to 1 psig. Because the gas is moving, we now have a pressure created by flowing gas, or a velocity pressure. We can measure the total pressure at any traverse location in the pipe using an impact probe. The impact probe will measure the static pressure inside the pipe plus the impact pressure, or velocity pressure, of the flowing gas, as illustrated in Figure 3.11. Regardless of where we traverse the impact probe inside the pipe,

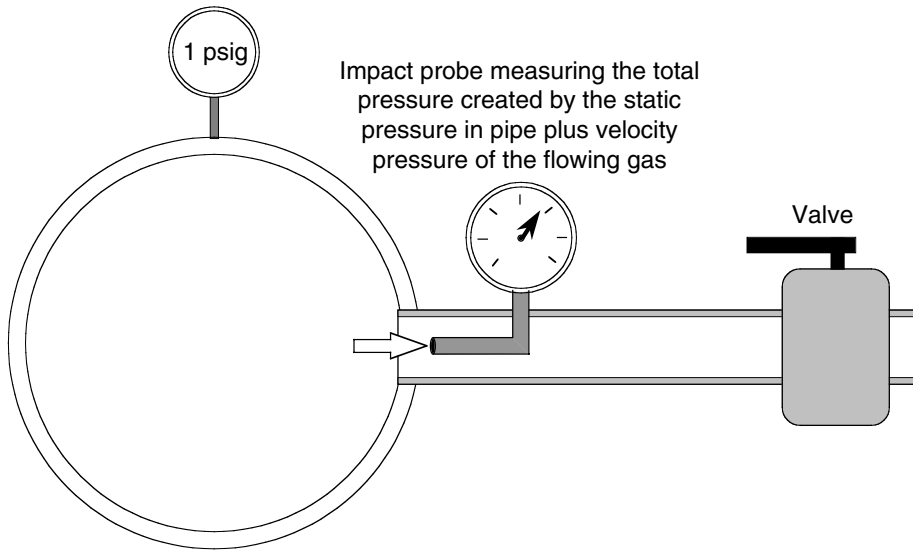


FIGURE 3.11 The difference between static, velocity, and total pressure.

we will get a total pressure reading of 1 psig. For example, if we place the impact probe directly on the pipe wall where the velocity is zero, we will read a total pressure of 1 psig. Because the velocity of the gas at the pipe wall is equal to zero, we can conclude that the static pressure at the wall is equal to 1 psig. If we locate the impact probe at the center of the pipe, we will still read a total pressure of 1 psig. At this location the static pressure will be lower because we now have a velocity pressure at this point. The velocity pressure can be calculated using the following equation:

$$P_v = \frac{\rho V^2}{2g_c} \quad (3.14)$$

where ρ is the density of the flowing gas, V is the velocity, and g_c is the gravitational constant.

Example 3.9

Suppose air is flowing inside a pipe with a velocity at the centerline equal to 200 feet per second and a density equal to 0.0765 lbm/ft³. What is the velocity pressure at the centerline of the pipe?

The value of $\rho = 0.0765$ lbm/ft³, $V = 200$ ft/s, $g_c = 32.2$ lbm-ft/lbf-s². Substituting these values into Equation 3.14 yields $P_v = 47.5$ lbf/ft² = 0.33 psig. Suppose at the centerline of the pipe an impact probe measures a total pressure of 1 psi; what is the static pressure at this location. From Equation 3.13 we can calculate the static pressure at the centerline of the pipe as $P_s = P_T - P_v = 1 - 0.33 = 0.67$ psig.

3.3.4.6 Pressure Loss

Obstructions within the flow stream of a pipe or duct can alter the flow direction and pattern of a fluid. An obstruction, for example, might consist of a fitting such as an inlet, elbow, tee, contraction, or expansion.

When a fluid flows through an obstruction, a reduction in the total pressure will occur. Pressure losses are the result of additional turbulence and/or flow separation created by sudden changes in the fluid momentum. This section discusses the general procedure for estimating the pressure drop through various fittings.

A complete theoretical analysis for calculating the flow through fittings has not yet been developed. Thus, the pressure drop is based on equations that rely heavily on experimental data. The most common method used to determine the pressure loss is to specify the *loss coefficient* K_L , defined as follows:

$$K_L = \frac{\Delta P}{\frac{1}{2}\rho V^2} \quad (3.15)$$

where ΔP is the pressure drop through the fitting, ρ is the approaching fluid density, and V is the approaching fluid velocity. Notice that the loss coefficient is dimensionless and is defined as the ratio of the pressure drop through a fitting to the approaching velocity pressure of the fluid stream. Solving Equation 3.15 for ΔP relates the pressure drop through a fitting:

$$\Delta P = K_L \frac{\rho V^2}{2g_c} \quad (3.16)$$

If the loss coefficient is equal to 1.0, then the pressure loss through that fitting will equal the velocity pressure of the approaching fluid stream, $\rho V^2/2$. The loss coefficient is strongly dependent on the geometry of the obstruction and the Reynolds number. The loss coefficient for turbulent flow through various fittings is given in Table 3.3. For more detailed information on loss coefficients through various fittings, refer to Idelchik²³ and Crane.²⁴

TABLE 3.3
Loss Coefficient for Various Fittings

Description	Sketch	Additional Data	K_L		
			$\Phi = 60^\circ$	$\Phi = 180^\circ$	
Contraction $\Delta P = K_L V^2 / (2 g_c)$		D_2/D_1			
			0.0	0.08	0.50
			0.20	0.08	0.49
			0.40	0.07	0.42
			0.60	0.06	0.32
			0.80	0.05	0.18
			0.90	0.04	0.10
Expansion $\Delta P = K_L V^2 / (2 g_c)$		D_1/D_2			
			0.0		1.00
			0.20	0.13	0.92
			0.40	0.11	0.72
			0.60	0.06	0.42
			0.80	0.03	0.16
Pipe Entrance $\Delta P = K_L V^2 / (2 g_c)$		R/D			
			0.0	$\Phi = 60^\circ$	
			0.10	0.50	0.12
			> 0.20	0.12	0.03

Example 3.10

Combustion air flows through the entrance of an eductor system. Compare the pressure drop through the entrance of a well-rounded inlet with a radius of 0.4 in. to a straight pipe inlet ($r = 0$). The diameter of the downstream pipe is 2 in. and the air velocity and density is 100 ft/s and 0.0765 lbm/ft³, respectively.

From Table 3.3, the loss coefficient for the well-rounded inlet ($R/D = 0.4/2 = 0.2$) is 0.03, and for the straight pipe inlet ($R/D = 0$) the loss coefficient is 0.5. Substituting the appropriate values into Equation 3.16, the pressure loss can be determined as:

$$\Delta P_{\text{bell}} = K_L \frac{\rho V^2}{2g_c} = 0.03 \frac{0.0765 \frac{\text{lbm}}{\text{ft}^3} \times (100)^2 \frac{\text{ft}^2}{\text{s}^2}}{2 \times 32.2 \frac{\text{lbm} \cdot \text{ft}}{\text{lbf} \cdot \text{s}^2}} = 0.356 \frac{\text{lbf}}{\text{ft}^2} = 0.069 \text{ in WC}$$

$$\Delta P_{\text{pipe}} = K_L \frac{\rho V^2}{2g_c} = 0.5 \frac{0.0765 \frac{\text{lbm}}{\text{ft}^3} \times (100)^2 \frac{\text{ft}^2}{\text{s}^2}}{2 \times 32.2 \frac{\text{lbm} \cdot \text{ft}}{\text{lbf} \cdot \text{s}^2}} = 5.94 \frac{\text{lbf}}{\text{ft}^2} = 1.143 \text{ in WC}$$

Notice that the straight pipe inlet has a pressure drop that is approximately 16.5 times greater than the well-rounded-bell inlet. Typically in the burner industry, one will see well-rounded inlets to burner appurtenances in order to reduce the pressure drop.

3.4 CALCULATING THE HEAT RELEASE FROM A BURNER

3.4.1 DEFINITION OF HEAT RELEASE

When shopping for a light bulb, one makes a selection depending on the lighting condition that is needed. For example, one might buy a 25-W bulb for a small reading lamp; but to light an entire room, one would use a bulb with more power output, such as a 100-W bulb. Power is a measure of how much energy is released in a given amount of time. In SI units, power is usually written as watts (W) or kilowatts (kW), and in English units as BTU/hr or MMBTU/hr (MM = millions of BTU/hr) (1 W = 3.41 BTU/hr). The amount of power output from a burner, referred to as *burner heat release*, depends on how much fuel the burner consumes and how much chemical energy the fuel has (heating value), which is referred to as the heating value of the fuel and can be written mathematically as:

$$HR = \dot{m} \times HV \quad (3.17)$$

where HR is the heat release of the burner, \dot{m} is the mass flow rate of the fuel, and HV is the heating value of the fuel.

The heat release of a burner is used throughout many areas of interest in combustion. For example, burner manufacturers will sometimes relate the length of a flame to the heat release of a burner. One might describe the length of a flame, for example, as 2 ft per MMBTU/hr. Burner manufacturers will often relate emissions from a burner to the heat release. Sometimes, one will refer to the emissions from a burner as the pounds of NO_x emitted per MMBTU/hr. Also, burner manufacturers will size the burner based on the heat release. For example, a 20-MMBTU/hr burner will have larger physical dimensions than a 4-MMBTU/hr burner operating under the same furnace conditions.

In the burner industry, the heat release typically varies between 1 and 20 MMBTU/hr. If one were to compare the power output from a burner to the power output of a light bulb, one would find that a burner operating at 20 MMBTU/hr has a power output equivalent to approximately 60,000 light bulbs at 100 W each.

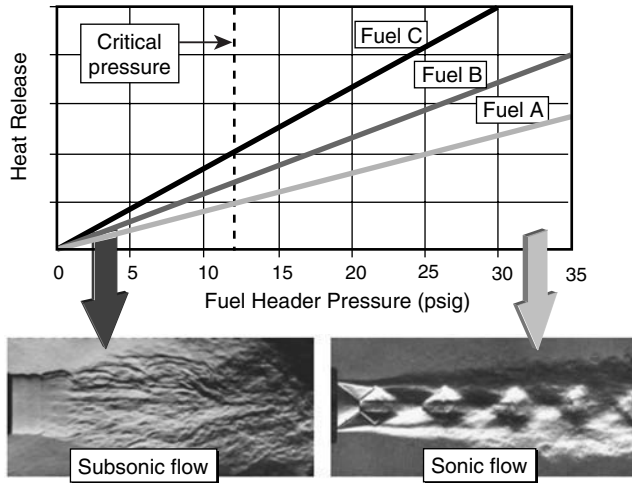


FIGURE 3.12 A typical fuel capacity curve for subsonic and sonic flow.

3.4.2 FUEL GAS ORIFICE CALCULATIONS

3.4.2.1 Discussion of Sonic and Subsonic Flow

Burner manufacturers typically provide customers with curves that show the heat release of a burner at various fuel pressures and compositions. For example, Figure 3.12 shows a typical capacity curve. The y-axis represents the heat release of the burner in MMBTU/hr and the x-axis represents the fuel pressure. Sometimes, several curves will be displayed, each representing a different fuel mixture with a different heating value.

Notice the shape of the capacity curve in Figure 3.12: for a fuel pressure ranging from zero to approximately 12 psig, the shape of the curve is bent; but above 12 psig, the shape becomes linear. The shape of the curve changes from a bent shape to a linear shape at a point called the *critical pressure*. The critical pressure usually varies from 12 to 15 psig, depending on the fuel composition and the temperature. Below the critical pressure, the burner heat release varies as the square root of the fuel pressure. Above the critical pressure, the burner heat release varies linearly with the fuel pressure. Why does this phenomena occur?

The region below the critical pressure is referred to as the *subsonic* region while the region above the critical pressure is referred to as the *sonic* region. In the subsonic region, the fuel exits the orifice at a velocity less than the speed of sound in the fuel gas. However, when the fuel pressure reaches the critical pressure, the fuel exits the orifice at a velocity equal to the speed of sound. The speed of sound in the fuel gas is the limiting velocity of the fuel at the orifice exit. That is, at fuel pressures above the critical pressure, the velocity of the fuel remains constant at the speed of sound (also called choked flow). If the velocity of the gas remains constant at fuel pressures above the critical pressure, then how does the burner heat release (or mass flow rate of fuel) increase as one increases the fuel pressure?

At a fuel pressure above the critical pressure, a marked change occurs in the structure of the fuel jet. At fuel pressures above the critical pressure, shock waves form at the orifice exit plane and downstream, as shown in Figure 3.12. The shock wave at the orifice exit plane consists of a thin layer of compressed fuel that acts as a barrier causing the fuel to compress upstream of the orifice exit. This, in turn, increases the density of the fuel at the orifice exit, allowing for an increase in the fuel mass flow rate.

3.4.2.2 Equations for Calculating Fuel Flow Rate

When designing a burner, burner engineers must determine the correct area of the fuel orifice. If they design the fuel orifice area too large, the burner will operate at a low fuel pressure. This could result in the fuel not properly mixing with the combustion air creating flames that produce soot or that could impinge on the process tubes. If the burner engineer designs the orifice area too small, the burner will not be able to achieve the required heat release at the customer's design pressure. How does a burner engineer determine the orifice size?

Burner engineers use equations based on the ideal gas law and assumptions of ideal flow to calculate the flow rate of fuel through an orifice. The first step in calculating the amount of fuel gas discharging through an orifice is to determine if it is operating above or below the critical pressure. This can be determined by calculating the critical pressure ratio defined as follows:

$$P_c = \left[\frac{2}{k+1} \right]^{k/(k-1)} \quad (3.18)$$

where P_c is the critical pressure ratio and k is the ratio of specific heats of the fuel.

If $P_c > P_b/P_t$, then the fuel exits the orifice at sonic conditions. If $P_c < P_b/P_t$, then the fuel exits the orifice at subsonic conditions. The P_b and P_t terms represent atmospheric pressure and fuel pressure in absolute, respectively.

The second step is to determine the mass flow rate of the fuel through the orifice. If the fuel exits the orifice at sonic conditions, Equation 3.19 is used to determine the mass flow rate:

$$\dot{m} = \frac{c_d P_t g_c A}{\sqrt{T_t \bar{R} g_c / MW}} k^{1/2} \left[\frac{2}{k+1} \right]^{k+1/2} \quad (3.19)$$

where c_d is the orifice discharge coefficient (to be discussed later in this chapter), A is the area of the orifice, T_t is the total temperature of the fuel gas, \bar{R} is the universal gas constant equal to 8314.34 J/kmol/K = 1545.32 (ft-lbf)/(lb-mole-R), MW is the molecular weight of the fuel, and g_c is the gravitational constant equal to 32.2 (lbm · ft)/(lbf · s²) = 1.0 (kg · m)/(N · s²).

If the fuel exits the orifice at subsonic conditions, Equation 3.20 can be used to determine the mass flow rate:

$$\dot{m} = c_d \rho_e A M_e c_e \quad (3.20)$$

where

$$M_e = \sqrt{\frac{2}{k-1} \left[\left(\frac{P_t}{P_b} \right)^{k-1} - 1 \right]} \quad (3.21)$$

$$T_e = \frac{T_t}{1 + \frac{k-1}{2} M_e^2} \quad (3.22)$$

$$c_e = \left[\frac{k T_e \bar{R}}{MW} \right]^{1/2} \quad (3.23)$$

$$\rho_e = \frac{P_b}{\frac{T_e \bar{R}}{MW}} \quad (3.24)$$

The subscript e denotes the orifice exit, M_e is the Mach number of the fuel, T_e is the temperature of the fuel, c_e is the speed of sound in the fuel, and ρ_e is the density of the fuel.

3.4.2.3 Discharge Coefficient

Many different fuel nozzle types are used in the burner industry, the type depending on the application. Figure 3.13 shows various types of nozzles commonly employed in the industry. Each of these nozzles is designed with a different internal shape. The internal shape of the nozzle can significantly affect the mass flow rate of the fuel. For example, Figure 3.14 is a schematic that



FIGURE 3.13 Various burner fuel nozzles.

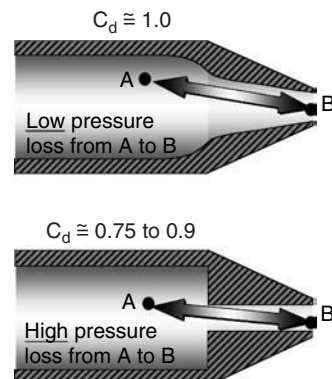
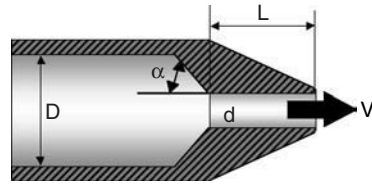


FIGURE 3.14 Orifice discharge coefficient explanation.



- Length-to-diameter ratio = L/d
- Reynolds number = $V \times d/\nu$
- Beta ratio = d/D
- Port angle = α

FIGURE 3.15 Variables affecting the orifice discharge coefficient.

shows the internals of two nozzles with the same port diameter. If these nozzles were operating under identical conditions, which one would flow more fuel? The upper one would, because it has less pressure drop as the fuel speeds toward the exit. The lower orifice design would create a small recirculation pattern just downstream from the entrance (called a vena contracta). This vena contracta creates a restriction in the flow, thus reducing the effective orifice area. To compensate for the results of the ideal equations and assumptions, a constant is introduced to account for the complexity of the flow that makes it nonideal. This constant is called the *orifice discharge coefficient*.

The discharge coefficient is defined as the ratio of the actual mass flow rate of a fluid through a nozzle to the ideal mass flow rate and is written as:

$$c_d = \frac{\dot{m}_{\text{actual}}}{\dot{m}_{\text{ideal}}} \quad (3.25)$$

The ideal mass flow rate is defined as the mass flow rate calculated using the ideal gas law and assumptions of ideal flow — no pressure losses due to the internals of the nozzle or tip. The value of the discharge coefficient, for a burner nozzle, is usually determined experimentally. Typically, in the burner industry, the discharge coefficient varies from about 0.75 to 0.95. Several factors that can affect the discharge coefficient include the (1) length-to-diameter ratio of the port, (2) Reynolds number of the fluid in the port, (3) beta ratio, (4) port angle, and (5) manufacturing tolerances.²⁵ See [Figure 3.15](#) for a description of these variables.

3.4.3 EXAMPLE CALCULATION: HEAT RELEASE FROM A BURNER

Example 3.11

A fuel is flowing through an orifice with the following values:

- LHV of fuel = 909 BTU/scf
- Orifice area = 0.5 in.²
- Molecular weight (MW) of fuel = 16
- Ratio of specific heat of fuel = 1.31
- Total fuel pressure = 35 psig
- Total fuel temperature = 60°F
- Atmospheric pressure = 14.7 psia.

Find the heat release of the burner.

Step 1: Determine if the flow is sonic or subsonic using Equation (3.18).

$$P_c = \left[\frac{2}{k+1} \right]^{k/(k-1)} = \left[\frac{2}{1.31+1} \right]^{1.31/(1.31-1)} = 0.544$$

$$\frac{P_b}{P_t} = \frac{14.7}{35+14.7} = 0.296$$

Because $P_c > P_b/P_t$, the fuel exits at sonic conditions.

Step 2: Determine the mass flow rate of fuel. Because the flow is choked, we will use Equation (3.19) to determine the mass flow rate:

$$\dot{m} = \frac{c_d P_t g_c A}{\sqrt{T_t R g_c / MW}} k^{1/2} \left[\frac{2}{k+1} \right]^{k+1/2}$$

$$\dot{m} = \frac{0.85 \times (35 + 14.7) \times 144 \times 32.2 \times 0.5}{\sqrt{\frac{(60 + 460) \times 1545.32 \times 32.2}{16}}} (1.31)^{1/2} \left[\frac{2}{1.31+1} \right]^{1.31+1/2}$$

$$\dot{m} = 0.35784 \frac{\text{lb}}{\text{s}} = 1288.2 \frac{\text{lb}}{\text{hr}}$$

Step 3: Determine the heat release of the burner. First determine the density of the fuel at standard conditions using Equation (3.2):

$$\rho = 0.0765 \frac{\text{lb}}{\text{ft}^3} \times \frac{16}{29} = 0.0422 \frac{\text{lb}}{\text{ft}^3}$$

$$HR = \dot{m} \left(\frac{\text{lb}}{\text{hr}} \right) \times \text{LHV} \left(\frac{\text{BTU}}{\text{lb}} \right) = \left(1288.2 \frac{\text{lb}}{\text{hr}} \right) \times \left(909 \frac{\text{BTU}}{\text{ft}^3} \times \frac{1}{0.0422 \text{ lb}} \frac{\text{ft}^3}{\text{lb}} \right) = 27.75 \frac{\text{MMBTU}}{\text{hr}}$$

Example 3.11 continued — If the fuel pressure is reduced to 10 psig, what is the burner heat release?

Step 1: Determine if the flow is sonic or subsonic.

$$P_c = \left[\frac{2}{k+1} \right]^{k/(k-1)} = \left[\frac{2}{1.31+1} \right]^{1.31/(1.31-1)} = 0.544$$

$$\frac{P_b}{P_t} = \frac{14.7}{10+14.7} = 0.595$$

Because $P_c < P_b/P_t$, the fuel exits at subsonic conditions.

Step 2: Determine the mass flow rate of fuel. Because the flow is not choked, we use Equation 3.20 to determine the mass flow rate.

$$M_e = \sqrt{\frac{2}{k-1} \left[\left(\frac{P_t}{P_b} \right)^{\frac{k-1}{k}} - 1 \right]} = \sqrt{\frac{2}{1.3-1} \left[\left(\frac{10+14.7}{14.7} \right)^{\frac{1.3-1}{1.3}} - 1 \right]} = 0.921$$

$$T_e = \frac{T_t}{1 + \frac{k-1}{2} M_e^2} = \frac{60 + 460}{1 + \left(\frac{1.3-1}{2} \right) (0.921)^2} = 461.31 \text{ R}$$

$$c_e = \left[\frac{k T_e \bar{R} g_c}{MW} \right]^{\frac{1}{2}} = \left[\frac{1.3 \times 461.31 \times 1545.32 \times 32.2}{16} \right]^{\frac{1}{2}} = 1365.67 \frac{\text{ft}}{\text{s}}$$

$$\rho_e = \frac{P_b}{T_e \bar{R}} = \frac{14.7 \times 144}{461.31 \times 1545.32} = 0.0475$$

$$\dot{m} = c_d \rho_e A M_e c_e = 0.85 \times 0.0475 \times \frac{0.5}{144} \times 0.921 \times 1365.67$$

$$\dot{m} = 0.1763 \frac{\text{lb}}{\text{s}} = 634.8 \frac{\text{lb}}{\text{hr}}$$

Step 3: Determine the heat release of the burner using Equation 3.17.

$$HR = \dot{m} \left(\frac{\text{lb}}{\text{hr}} \right) \times \text{LHV} \left(\frac{\text{BTU}}{\text{lb}} \right) = \left(634.8 \frac{\text{lb}}{\text{hr}} \right) \times \left(909 \frac{\text{BTU}}{\text{ft}^3} \times \frac{1}{0.0422} \frac{\text{ft}^3}{\text{lb}} \right) = 13.67 \frac{\text{MMBTU}}{\text{hr}}$$

3.5 COMBUSTION AIR FLOW RATE THROUGH NATURAL-DRAFT BURNERS

Figure 3.16 shows a plot of a typical capacity curve that many burner manufacturers use for sizing burners. Capacity curves describe the airside pressure drop through burners of various sizes at different heat releases. These curves are usually generated based on experimental data. The curves shown in this particular example are based on burners operating in the natural-draft mode with 15% excess air in the furnace at an atmospheric temperature and pressure of 59°F (15°C) and 14.696 psia (1 bar), respectively.

When burners operate at different ambient conditions and excess air levels, the value of the airside pressure drop obtained from the capacity curves must be corrected. The equation used to correct for the airside pressure drop can be derived as follows. The airside pressure drop through a burner is proportional to the velocity pressure of the air and can be written as:

$$\Delta P \propto \rho V^2 \tag{3.26}$$

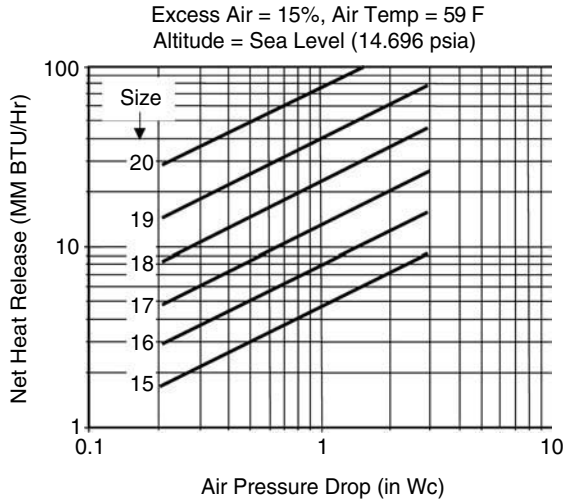


FIGURE 3.16 Capacity curves used by many burner manufacturers for sizing burners.

where dP is the pressure drop through the burner, ρ is the density of the combustion air, and V is the mean velocity of the air at a particular location in the burner. The density of the combustion air can be related to the combustion air temperature T and atmospheric pressure P using the ideal gas law:

$$\rho \propto \frac{P}{T} \quad (3.27)$$

The velocity V of the air through the burner is proportional to the mass flow of air going through the burner and the density. This can be written as:

$$V \propto \frac{\dot{m}}{\rho} \propto \frac{(100 + EA)}{\rho} \quad (3.28)$$

where \dot{m} represents the mass flow rate and EA represents the percent excess air in the furnace. Substituting Equations 3.27 and 3.28 into Equation 3.26 gives:

$$\Delta P \propto (100 + EA)^2 \times \frac{P}{T} \quad (3.29)$$

Equation 3.29 can be used to write the following equation to correct for the airside pressure drop at actual firing conditions:

$$\Delta P_{\text{Actual}} = \Delta P_{CC} \times \left(\frac{100 + EA_{\text{Actual}}}{100 + EA_{CC}} \right)^2 \times \left(\frac{T_{\text{Actual}}}{T_{CC}} \right) \times \left(\frac{P_{CC}}{P_{\text{Actual}}} \right) \quad (3.30)$$

where subscript *Actual* represents the actual firing conditions and the subscript *CC* represents the variables from the capacity curves (i.e., $T_{CC} = 460 + 59$, $P_{CC} = 14.696$ psia, $EA_{CC} = 15\%$). Notice that as the temperature of the combustion air increases, the airside pressure drop through the burner also increases. This occurs because increasing the temperature reduces the density of the combustion air. A reduction in the density of the combustion air requires a higher volumetric airflow rate, through the burner, which results in an increase in the pressure drop. Similarly, if

the atmospheric pressure is reduced, the combustion air density is reduced and, hence, the airside pressure drop is increased.

Example 3.12

Using Figure 3.16, determine the pressure drop through a size 15 burner with a heat release of 3 MMBTU/hr operating at 13% excess air. The combustion air temperature is 100°F and the atmospheric pressure is 14.0 psia.

From the capacity curves in Figure 3.16, for a heat release of 3 MMBTU/hr at standard conditions, the pressure drop will be approximately 0.5 inches of water column. This will be the pressure drop if the burner is operating at 15% excess air with the combustion air temperature at 59°F and an atmospheric pressure of 14.696 psia. To correct for the actual firing conditions, we can use Equation 3.30.

$$\Delta P_1 = 0.5 \times \left(\frac{100 + 13}{100 + 15} \right)^2 \times \left(\frac{460 + 100}{460 + 59} \right) \times \left(\frac{14.696}{14.0} \right) = 0.547 \text{ (in WC)}$$

Although the percent excess air is reduced from 15 to 13%, the pressure drop through the burner has increased because the density of the combustion air is lower at actual conditions than at standard conditions. This results in a higher volumetric flow rate of combustion air through the burner and, hence, a larger pressure loss.

REFERENCES

1. R.L. Panton, *Incompressible Flow*, John Wiley & Sons, New York, 1984.
2. F.M. White, *Viscous Fluid Flow*, McGraw-Hill, New York, 1991.
3. R.W. Fox and A.T. McDonald, *Introduction to Fluid Mechanics*, 2nd ed., John Wiley & Sons, New York, NY, 1978.
4. J.K. Vennard and R.L. Street, *Elementary Fluid Mechanics*, 5th ed., John Wiley & Sons, 1975.
5. J.O. Hinze, *Turbulence*, McGraw-Hill, New York, 1975.
6. H. Schlichting, *Boundary-Layer Theory*, McGraw-Hill, New York, 1979.
7. W.F. Hughes and J.A. Brighton, *Schaum's Outline of Theory and Problems of Fluid Dynamics*, McGraw-Hill, New York, 1967.
8. T.M. Geerssen, *Physical Properties of Natural Gases*, N.V. Nederlandse Gasunie, 1980.
9. C.E. Baukal, *The John Zink Combustion Handbook*, CRC Press, Boca Raton, FL, 2001.
10. S.R. Turns, *An Introduction to Combustion*, McGraw-Hill, Boston, 2000.
11. W. Bartok and A.F. Sarofim, *Fossil Fuel Combustion*, John Wiley & Sons, New York, 1991.
12. F.C. McQuiston and J.D. Parker, *Heating and Ventilating, and Air Conditioning*, John Wiley & Sons, New York, 1982.
13. *ASHRAE Handbook of Fundamentals*, American Society of Heating, Refrigerating and Air-Conditioning Engineers, New York, 1977.
14. J.A. Goff, Standardization of thermodynamic properties of moist air, *Trans. ASHVE*, 55, 1949.
15. K.K. Kuo, *Principles of Combustion*, John Wiley & Sons, New York, 1986.
16. A.N. Lipatnikov and J. Chomiak, Turbulent flame speed and thickness: phenomenology, evaluation, and application in multi-dimensional simulations, *Progress in Energy and Combustion Science*, 28, 2002.
17. J.M. Beer and N.A. Chigier, *Combustion Aerodynamics*, Krieger Publishing, Malabar, FL, 1983.
18. J.H. Keenan and E.P. Neumann, A simple air ejector, *J. Applied Mechanics*, 1942, p. A-75.
19. E. Kroll, The design of jet pumps, *Chemical Engineering Progress*, 1(2), 21, 1947.
20. R.R. Munson, D.F. Young, and T.H. Okiishi, *Fundamentals of Fluid Mechanics*, John Wiley & Sons, New York, 1990, 52.

21. J.A. Roberson and T. Crowe, *Engineering Fluid Mechanics*, Houghton Mifflin Company, Boston, 1965.
22. R.D. Reed, *Furnace Operations*, 3rd ed., Gulf Publishing, Houston, 1981.
23. I.E. Idelchik, *Handbook of Hydraulic Resistance*, Hemisphere, New York, 1986.
24. Engineering Division Crane, *Flow of Fluids through Valves, Fitting, and Pipe*, Crane Co., New York, 1969.
25. A.J. Ward-Smith, Critical flowmetering: the characteristics of cylindrical nozzles with sharp upstream edges, *Int. J. Heat and Fluid Flow*, Vol., No. 3.

4 Combustion Basics

Joseph Colannino, P.E.

CONTENTS

- 4.1 Introduction
 - 4.1.1 Conservation of Mass
- 4.2 Moles
- 4.3 Molecular Weight of Air
- 4.4 The Ideal Gas Law
- 4.5 Conservation of Energy
- 4.6 Lower and Higher Heating Values
- 4.7 Enthalpy and Latent Heat
- 4.8 Sensible Heat and Heat Capacity
- 4.9 Some Properties of Flames
 - 4.9.1 Flammability Limits
 - 4.9.2 Laminar Flame Speed
- 4.10 Liftoff and Flashback
- 4.11 Premix and Diffusion Flames
- 4.12 Turbulent Flame Speed and Flame Holders
- 4.13 Quenching
- 4.14 Natural- and Forced-Draft Burners
- 4.15 NO_x and CO
 - 4.15.1 NO_x Emissions
 - 4.15.2 Thermal NO_x
 - 4.15.3 Fuel-Bound NO_x
 - 4.15.4 Prompt NO_x

4.1 INTRODUCTION

This chapter gives a brief overview of some basic combustion tenets, including:

- Principles of mass and energy conservation
- Concept of moles and molecular weight
- Energy, heat, and temperature
- Important flame properties
- Flame liftoff and flashback
- Diffusion and premix burners
- Natural and forced draft, NO_x and CO emissions

Where appropriate, brief examples reinforce these concepts and provide worked solutions.

4.1.1 CONSERVATION OF MASS

In chemical reactions, including combustion, mass is conserved. That is to say, mass is neither created nor destroyed during the combustion reaction: 100 kg of fuel + 1000 kilograms of air will generate 100 + 1000 (=1100) kg of products. Notwithstanding, the species will change. For example, one can write a reaction for methane (CH₄) combustion with oxygen as follows:



The subscripted numbers refer to the number of elements in a given molecule. Oxygen molecules are diatomic (comprising two oxygen atoms). The antecedent numbers refer to the number of molecular entities. A molecular entity with no antecedent number is presumed to refer to a single molecule. Hence, Equation 4.1 shows that one molecule of methane (CH₄) reacts with two molecules of oxygen (2O₂) to produce one molecule of carbon dioxide (CO₂) and two molecules of water (2H₂O).

Equation 4.1 is a *balanced* equation, meaning that the left and right sides of the equation comprise identical amounts of each element, C, H, and O. However, the molecular species have changed. On the left side, CH₄ and O₂ are present; on the right side, CO₂ and H₂O.

4.2 MOLES

A single molecule like CH₄ has an infinitesimal weight, so engineers deal with a more tractable quantity known as the *mole* (abbreviated *mol*). A mole is 6.02×10^{23} molecules. Table* 4.1 gives the mass for moles of the corresponding elements. The mass of a mole of an element is known as the *atomic weight*. The mass of a mole of molecules is known as the *molecular weight*.

Example 4.1

Calculate the molecular weight of CH₄.

Solution:

To calculate the molecular weight (M), one combines the atomic weights, e.g., $M_{\text{CH}_4} = M_{\text{C}} + 4M_{\text{H}} = 12.01 + 4(1.01) = 16.05$ g. Therefore, one mole of CH₄ has a mass of 16.05 g, which is the molecular weight.

Combustion engineers often work with British units, such as the pound (lb_m), where the subscript “m” is used to denote a pound mass (as opposed to a pound of force, lb_f — a fundamentally different quantity). A pound-mole (lbmol) has the same numerical value as the mol but is related to the lb_m rather than the gram. With this definition, a lbmol of CH₄ comprises 16.02 lb_m. For this reason, most atomic weights are listed as pure numbers. It is up to the combustion engineer to decide which basis to use — the mol (sometimes called the g-mol) or the lbmol.

4.3 MOLECULAR WEIGHT OF AIR

Air is comprised of two species — nitrogen (N₂) and oxygen (O₂) — in the approximate respective proportion of 79% and 21% by volume.

Example 4.2

Calculate the “molecular weight” of air.

* Table 4.1 in *The John Zink Combustion Handbook*, CRC Press, Boca Raton, FL, 2001, 36.

TABLE 4.1
Alphabetical List of Atomic Weights for Common Elements¹

Name	Symbol	At. No.	Atomic Weight	Footnotes	Name	Symbol	At. No.	Atomic Weight	Footnotes
Actinium	Ac	89	[227]		Europium	Eu	63	151.964(1)	
Aluminum	Al	13	26.981538(2)		Fermium	Fm	100	[257]	
Americium	Am	95	[243]		Fluorine	F	9	18.9984032(5)	
Antimony	Sb	51	121.760(1)	g	Francium	Fr	87	[223]	
Argon	Ar	18	39.948(1)	g r	Gadolinium	Gd	64	157.25(3)	g
Arsenic	As	33	74.92160(2)		Gallium	Ga	31	69.723(1)	
Astatine	At	85	[210]		Germanium	Ge	32	72.61(2)	
Barium	Ba	56	137.32(7)		Gold	Au	79	196.96655(2)	
Berkelium	Bk	97	[247]		Hafnium	Hf	72	178.49(2)	
Beryllium	Be	4	9.012182(3)		Hassium	Hs	108	[269]	
Bismuth	Bi	83	208.98038(2)		Helium	He	2	4.002602(2)	g
Bohrium	Bh	107	[264]		Holmium	Ho	67	164.93032(2)	
Boron	B	5	10.811(7)	g m r	Hydrogen	H	1	1.00794(7)	g m r
Bromine	Br	35	79.904(1)		Indium	In	49	114.818(3)	
Cadmium	Cd	48	112.411(8)	g	Iodine	I	53	126.90447(3)	
Calcium	Ca	20	40.078(4)	g	Iridium	Ir	77	192.217(3)	
Californium	Cf	98	[251]		Iron	Fe	26	55.845(2)	
Carbon	C	6	12.0107(8)	g r	Krypton	Kr	36	83.80(1)	g m
Cerium	Ce	58	140.116(1)	g	Lanthanium	La	57	138.9055(2)	g
Cesium	Cs	55	132.90545(2)		Lawrencium	Lr	103	[262]	
Chlorine	Cl	17	35.4527(9)	m	Lead	Pb	82	207.2(1)	g
Chromium	Cr	24	51.9961(6)		Lithium	Li	3	6.941(2)	g m r
Cobalt	Co	27	58.933200(9)		Lutetium	Lu	71	174.967(1)	g
Copper	Cu	29	63.546(3)	r	Magnesium	Mg	12	24.3050(6)	
Curium	Cm	96	[247]		Manganese	Mn	25	54.938049(9)	
Dubnium	Db	105	[262]		Meitnerium	Mt	109	[268]	
Dysprosium	Dy	66	162.59(3)	g	Mendelevium	Md	101	[258]	
Einsteinium	Es	99	[252]		Mercury	Hg	80	200.59(2)	
Erbium	Er	68	167.26(3)	g	Molybdenum	Mo	42	95.94(1)	g

(Continued)

TABLE 4.1
Alphabetical List of Atomic Weights for Common Elements¹ (Continued)

Name	Symbol	At. no.	Atomic Weight	Footnotes	Name	Symbol	At. no.	Atomic Weight	Footnotes
Neodymium	Nd	60	144.24(3)	g	Ruthenium	Ru	44	101.07(2)	g
Neon	Ne	10	20.1797(6)	g m	Rutherfordium	Rf	104	[261]	
Neptunium	Np	93	[237]		Samarium	Sm	62	150.36(3)	g
Nickel	Ni	28	58.6934(2)		Scandium	Sc	21	44.955910(8)	
Niobium	Nb	41	92.90638(2)		Seaborgium	Sg	106	[266]	
Nitrogen	N	7	14.00674(7)	g r	Selenium	Se	34	78.96(3)	
Nobelium	No	102	[259]		Silicon	Si	14	28.0855(3)	r
Osmium	Os	76	190.23(3)	g	Silver	Ag	47	107.8682(2)	g
Oxygen	O	8	15.9994(3)	g r	Sodium	Na	11	22.989770(2)	
Palladium	Pd	46	106.42(1)	g	Strontium	Sr	38	87.62(1)	g r
Phosphorus	P	15	30.973761(2)		Sulfur	S	16	32.066(6)	g r
Platinum	Pt	78	195.078(2)		Tantalum	Ta	73	180.9479(1)	
Plutonium	Pu	94	[244]		Technetium	Tc	43	[98]	
Polonium	Po	84	[209]		Tellurium	Te	52	127.60(3)	g
Potassium	K	19	39.0983(1)	g	Terbium	Tb	65	158.92534(2)	
Praseodymium	Pr	59	140.90765(2)		Thallium	Tl	81	204.3833(2)	
Promethium	Pm	61	[145]		Thorium	Th	90	232.0381(1)	g
Protactinium	Pa	91	231.03588(2)		Thulium	Tm	69	168.93421(2)	
Radium	Ra	88	[226]		Tin	Sn	50	118.710(7)	g
Radon	Rn	86	[222]		Titanium	Ti	22	47.867(1)	
Rhenium	Re	75	186.207(1)		Tungsten	W	74	183.84(1)	
Rhodium	Rh	45	102.90550(2)		Uranium	U	92	238.0289(1)	g m
Rubidium	Rb	37	85.4678(3)	g	Vanadium	V	23	50.9415(1)	

Xenon	Xe	54	131.29(2)	g	m	Zinc	Zn	30	65.39(2)	
Ytterbium	Yb	70	173.04(3)	g		Zirconium	Zr	40	92.224(2)	g
Yttrium	Y	39	88.90585(2)							

g – geological specimens are known in which the element has an isotopic composition outside the limits for normal material. The difference between the atomic weight of the element in such specimens and that given in the table may exceed the stated uncertainty.

m – modified isotopic compositions may be found in commercially available material because it has been subjected to an undisclosed or inadvertent isotopic fractionation. Substantial deviations in atomic weight of the element from that given in the table can occur.

r – range in isotopic composition of normal terrestrial material prevents a more precise atomic weight being given; the tabulated atomic weight value should be applicable to any normal material.

This table of atomic weights is reprinted from the 1995 report of the IUPAC Commission on Atomic Weights and Isotopic Abundances. The Standard Atomic Weights apply to the elements as they exist naturally on Earth, and the uncertainties take into account the isotopic variation found in most laboratory samples. Further comments on the variability are given in the footnotes.

The number in parentheses following the atomic weight value gives the uncertainty in the last digit. An entry in brackets indicates that mass number of the longest-lived isotope of an element that has no stable isotopes and for which a Standard Atomic Weight cannot be defined because of wide variability in isotopic composition (or complete absence) in nature.

REFERENCE

IUPAC Commission on Atomic Weights and Isotopic Abundances, Atomic Weights of the Elements, 1995, *Pure Appl. Chem.*, 68, 2339, 1996.

Source: Courtesy of CRC Press.¹

TABLE 4.2
Mass and Mole Balance for Hydrogen Combustion with Air

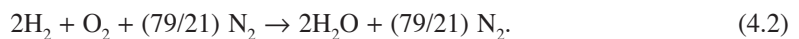
Species	IN		OUT	
	Moles In	Mass In	Moles Out	Mass Out
H ₂	200	404	0	0
O ₂	100	3,200	0	0
N ₂	376	10,536	376	10,536
H ₂ O	0	0	200	3,604
Totals	676	14,140	576	14,140

Note: Mass is conserved, but not moles.

Solution:

For convenience of calculation, combustion engineers often treat air as if it were a single entity having a “molecular weight” of 29. This weight is calculated from the molecular weights of nitrogen and oxygen as follows: $(0.79)(2)(14.01) + (0.21)(2)(16.00) = 29.0$.

Knowing the ratio of N₂ and O₂ in air, we can derive an equation for combustion of a fuel in air. For example, Equation 4.2 gives the balanced equation for hydrogen combustion with air.



Nitrogen is not significantly consumed in the reaction.

Example 4.3

Calculate the mass of fuel, air, and combustion products for hydrogen combustion of 100 lbmol of H₂.

Solution:

Equation 4.2 gives the molar proportions for hydrogen combustion. Table 4.2 derives the weights of each species in Equation 4.2. If there are 100 lbmol of O₂, then there must be $(79/21) 100$ lbmol N₂ = 376 lbmol N₂. Multiplying 376 lbmol N₂ by its molecular weight gives $(2)(14.01)(376) = 10,536$ lb_m. In a similar manner, Table 4.2 arrives at all quantities. The totals in Table 4.2 clearly show that mass is conserved, but moles are not.

4.4 THE IDEAL GAS LAW

One may have noticed that the volume percent and mole percent were presumed identical when calculating the molecular weight of air. This behavior is allowed for by the ideal gas law, which can be written as:

$$pV = nRT \quad (4.3)$$

where p is the pressure (psia), V is the volume (ft³), n is the number of lbmols, R is a universal constant, 10.73 psia-ft³/lbmol °R, and T is the absolute temperature (°R).

* Table 4.2, in *The John Zink Combustion Handbook*, CRC Press, Boca Raton, FL, 2001,164.

First, a word about some of the units. The ideal gas law requires temperature and pressure in absolute units. One such unit is the lb_f/in^2 absolute, or pounds per square inch, absolute, a.k.a. *psia*. One standard atmosphere of pressure exerts 14.7 psia. However, most pressure gages are calibrated to read “0” at atmospheric pressure (denoted as *psig*), where the “g” indicates that it is a gage pressure. So, a tire pressure gage reading 32 psig is equivalent to 46.7 psia ($32 + 14.7 = 46.7$).

Likewise, the ideal gas law references a temperature known as absolute zero. Once all the thermal energy is extracted from a substance, it can grow no colder. Absolute zero is approximately -460°F . To reference temperature above absolute zero, the Rankine temperature scale ($^\circ\text{R}$) was developed. To convert $^\circ\text{F}$ to $^\circ\text{R}$, add 460. Therefore, $70^\circ\text{F} \approx 530^\circ\text{R}$.

With this understanding, one can easily convert between mass, mols, and volume of gas. We have already shown that 100 lbmol O_2 has a mass of 3200 lbm. The volume can be calculated by rearranging Equation 4.3 and solving for V .

Example 4.4

Calculate the volume of 100 lbmol of any gas at standard atmospheric pressure and 32°F . How much volume would 1 lbmol of gas occupy under these conditions?

Solution:

$V = nRT/p = 100 \text{ [lbmol]} \cdot 10.73 \text{ [psia ft}^3/\text{lbmol R]} \cdot (32 + 460) \text{ [R]} / 14.7 \text{ [psia]} = 35,913 \text{ ft}^3$. Therefore, 1 lbmol of gas under the above conditions would occupy $\sim 359 \text{ ft}^3$.

From Equation 4.3 we can also see that n and V are proportional. Therefore, volume and mol percent are identical. The ideal gas law is quite accurate at all but very low temperatures and high pressures. Because industrial combustion is a high-temperature, low-pressure affair, the ideal gas law is perfectly suited to combustion calculations.

4.5 CONSERVATION OF ENERGY

Like mass, energy is also a conserved quantity for combustion reactions. Energy is stored in the chemical bonds that make up a molecular entity. Depicting Equation 4.2 graphically for the reacting species gives:



Molecular entities as depicted in Equation 4.4 are known as *structural formulas* because they reveal some elements of the structure of each molecule, where the single and double lines are known as *single* and *double* bonds, respectively. Hydrogen generally shares one bond, oxygen two, nitrogen three, and carbon four. If the products represent a lower energy state than the reactants, heat will be liberated and the reaction is known as an *exothermic reaction*. Fuels are, by definition, those entities that can produce heat (exothermic) upon reaction with oxygen. To calculate the heat of combustion, one can use a heat of combustion table. Table 4.3 gives the heats of combustion of several important fuels.

4.6 LOWER AND HIGHER HEATING VALUES

There are two possible ways to calculate a heating value. One way is to presume that the combustion exit gases are sufficiently hot that the water vapor from the combustion process does not condense. With this assumption, the heat released is known as the *net* or *lower heating value (LHV)*. In other cases — for example, a condensing turbine where the combustion products are cooled to the point of water condensation — one obtains the gross or *higher heating value (HHV)*.

TABLE 4.3
Physical Constants of Typical Gaseous Fuel Mixture Components

No.	Fuel Gas Component	Chemical Formula	Molecular Weight	Boiling Point 14.696 psia (°F)	Vapor Pressure 100°F (psia)	Specific Heat Capacity, C_p 60°F & 14.696 psia (Btu/lb _m /°F)	Latent Heat of Vaporization & Boiling Point (Btu/lb _m)	Heating Value				Unit Volume per Unit Volume of Combustible				Unit Mass per Unit Mass of Combustible				Flammability Limits (vol% in air mixture)												
								Gas Density Ideal Gas, 14.696 psia, 60°F			Btu/scf		Btu/lb _m		Required for Combustion		Flue Gas Products		Required for Combustion		Flue Gas Products		Theoretical Air Required (lb _m /10,000 Btu)	Lower	Upper	No.						
								Specific Gravity (Air = 1)	Gas Density (lb _m /ft ₃)	Specific Volume (ft ³ /lb _m)	LHV (Net)	HHV (Gross)	LHV (Net)	HHV (Gross)	O ₂	N ₂	Air	CO ₂	H ₂ O	N ₂	SO ₂	O ₂					N ₂	Air	CO ₂	H ₂ O	N ₂	SO ₂
Paraffin (alkane) Series (C_nH_{2n+2})																																
1.	Methane	CH ₄	16.04	-258.69	—	0.5266	219.22	0.554	0.042	23.651	912	1,013	21,495	23,845	2.0	7.547	9.547	1.0	2.0	7.547	—	3.989	13.246	17.235	2.743	2.246	13.246	—	7.219	5.0	15.0	1
2.	Ethane	C ₂ H ₆	30.07	-127.48	—	0.4097	210.41	1.038	0.079	12.618	1,639	1,792	20,418	22,323	3.5	13.206	16.706	2.0	3.0	13.206	—	3.724	12.367	16.092	2.927	1.797	12.367	—	7.209	2.9	13.0	2
3.	Propane	C ₃ H ₈	44.10	-43.67	190	0.3881	183.05	1.522	0.116	8.604	2,385	2,592	19,937	21,669	5.0	18.866	23.866	3.0	4.0	18.866	—	3.628	12.047	15.676	2.994	1.624	12.047	—	7.234	2.1	9.5	3
4.	n-Butane	C ₄ H ₁₀	58.12	31.10	51.6	0.3867	165.65	2.007	0.153	6.528	3,113	3,373	19,679	21,321	6.5	24.526	31.026	4.0	5.0	24.526	—	3.578	11.882	15.460	3.029	1.550	11.882	—	7.251	1.8	8.4	4
5.	Isobutane	C ₄ H ₁₀	58.12	10.90	72.2	0.3872	157.53	2.007	0.153	6.528	3,105	3,365	19,629	21,271	6.5	24.526	31.026	4.0	5.0	24.526	—	3.578	11.882	15.460	3.029	1.550	11.882	—	7.268	1.8	8.4	5
6.	n-Pentane	C ₅ H ₁₂	72.15	96.92	15.57	0.3883	153.59	2.491	0.190	5.259	3,714	4,017	19,507	21,095	8.0	30.186	38.186	5.0	6.0	30.186	—	3.548	11.781	15.329	3.050	1.498	11.781	—	7.267	1.4	8.3	6
7.	Isopentane	C ₅ H ₁₂	72.15	82.12	20.44	0.3827	147.13	2.491	0.190	5.259	3,705	4,017	19,459	21,047	8.0	30.186	38.186	5.0	6.0	30.186	—	3.548	11.781	15.329	3.050	1.498	11.781	—	7.283	1.4	8.3	7
8.	Neopentane	C ₅ H ₁₂	72.15	49.10	35.9	0.3666	135.58	2.491	0.190	5.259	3,692	3,994	19,390	20,978	8.0	30.186	38.183	5.0	6.0	30.186	—	3.548	11.781	15.329	3.050	1.498	11.781	—	7.307	1.4	8.3	8
9.	n-Hexane	C ₆ H ₁₄	86.18	155.72	4.956	0.3664	143.95	2.975	0.227	4.403	4,415	4,767	19,415	20,966	9.5	35.846	45.346	6.0	7.0	35.846	—	3.527	11.713	15.240	3.064	1.463	11.713	—	7.269	1.2	7.7	9
Naphthene (cycloalkane) Series (C_nH_n)																																
10.	Cyclopentane	C ₅ H ₁₀	70.13	120.60	9.917	0.2712	137.35	2.420	0.180	5.556	3,512	3,764	19,005	20,368	7.5	27.939	35.180	5.0	5.0	28.939	—	3.850	11.155	14.793	3.146	1.283	11.155	—	7.262	—	—	10
11.	Cyclohexane	C ₆ H ₁₂	84.16	177.40	3.267	0.2901	153.25	2.910	0.220	5.545	4,180	4,482	18,849	20,211	9.0	33.528	42.970	6.0	6.0	33.528	—	4.620	13.386	17.750	3.146	1.283	11.155	—	7.848	1.3	8.4	11
Olefin Series (C_nH_n)																																
12.	Ethene (Ethylene)	C ₂ H ₄	28.05	-154.62	—	0.3622	207.57	0.969	0.074	13.525	1,512	1,613	20,275	21,636	3.0	11.320	14.320	2.0	2.0	11.320	—	3.422	11.362	14.784	3.138	1.284	11.362	—	6.833	2.7	34.0	12
13.	Propene (Propylene)	C ₃ H ₆	42.08	-53.90	226.4	0.3541	188.18	1.453	0.111	9.017	2,185	2,336	19,687	21,048	4.5	16.980	21.480	3.0	3.0	16.980	—	3.422	11.362	14.784	3.138	1.284	11.362	—	7.024	2.0	10.0	13
14.	1-Butene (Butylene)	C ₄ H ₈	56.11	20.75	63.05	0.3548	167.94	1.937	0.148	6.762	2,885	3,086	19,493	20,854	6.0	22.640	28.640	4.0	4.0	22.640	—	3.422	11.362	14.784	3.138	1.284	11.362	—	7.089	1.6	9.3	14
15.	Isobutene	C ₄ H ₈	56.11	19.59	63.4	0.3701	169.48	1.937	0.148	6.762	2,868	3,069	19,376	20,737	6.0	22.640	28.640	4.0	4.0	22.640	—	3.422	11.362	14.784	3.138	1.284	11.362	—	7.129	1.6	—	15
16.	1-Pentene	C ₅ H ₁₀	70.13	85.93	19.115	0.3635	154.46	2.421	0.185	5.410	3,585	3,837	19,359	20,720	7.5	28.300	35.800	5.0	5.0	28.300	—	3.422	11.362	14.784	3.138	1.284	11.362	—	7.135	1.4	8.7	16
Aromatic Series (C_nH_{2n-6})																																
17.	Benzene	C ₆ H ₆	78.11	176.17	3.224	0.2429	169.31	2.697	0.206	4.857	3,595	3,746	17,421	18,184	7.5	28.300	35.800	6.0	3.0	28.300	—	3.072	10.201	13.274	3.380	0.692	10.201	—	7.300	1.38	7.98	17
18.	Toluene	C ₇ H ₈	92.14	231.13	1.032	0.2598	154.84	3.181	0.243	4.118	4,296	4,497	17,672	18,501	9.0	33.959	42.959	7.0	4.0	33.959	—	3.125	10.378	13.504	3.343	0.782	10.378	—	7.299	1.28	7.18	18
19.	o-Xylene	C ₈ H ₁₀	106.17	291.97	0.264	0.2914	149.1	3.665	0.280	3.574	4,970	5,222	17,734	18,633	10.5	39.619	50.119	8.0	5.0	39.619	—	3.164	10.508	13.673	3.316	0.848	10.508	—	7.338	1.18	6.48	19
20.	m-Xylene	C ₈ H ₁₀	106.17	282.41	0.326	0.2782	147.2	3.665	0.280	3.574	4,970	5,222	17,734	18,633	10.5	39.619	50.119	8.0	5.0	39.619	—	3.164	10.508	13.673	3.316	0.848	10.508	—	7.338	1.18	6.48	20
21.	p-Xylene	C ₈ H ₁₀	106.17	281.05	0.342	0.2769	144.52	3.665	0.280	3.574	4,970	5,222	17,734	18,633	10.5	39.619	50.119	8.0	5.0	39.619	—	3.164	10.508	13.673	3.316	0.848	10.508	—	7.338	1.18	6.48	21
Additional Fuel Gas Components																																
22.	Acetylene	C ₂ H ₂	26.04	-119	—	0.3966	—	0.899	0.069	14.572	1,448	1,499	20,769	21,502	2.5	9.433	11.933	2.0	1.0	9.433	—	3.072	10.201	13.274	3.380	0.692	10.201	—	7.300	2.5	8.0	22
23.	Methyl alcohol	CH ₃ OH	32.04	148.1	4.63	0.3231	473	1.106	0.084	11.841	767	868	9,066	10,258	1.5	5.660	7.160	1.0	2.0	5.660	—	4.498	4.974	6.482	1.373	1.124	4.974	—	6.309	6.72	36.5	23
24.	Ethyl alcohol	C ₂ H ₅ OH	46.07	172.92	2.3	0.3323	367	1.590	0.121	8.236	1,449	1,600	11,918	13,161	3.0	11.320	14.320	2.0	3.0	11.320	—	2.084	6.919	9.003	1.911	1.173	6.919	—	6.841	3.28	18.95	24
25.	Ammonia	NH ₃	17.03	-28.2	212	0.5002	587.2	0.588	0.045	22.279	364	441	7,966	9,567	0.75	2.830	3.582	—	1.5	3.330	—	1.409	4.679	6.008	—	1.587	5.502	—	6.298	15.50	27.00	25
26.	Hydrogen	H ₂	2.02	-423.0	—	3.4080	193.9	0.070	0.005	188.217	274.6	325.0	51,625	61,095	0.5	1.887	2.387	—	1.0	1.887	—	7.936	26.323	34.290	—	8.937	26.353	—	5.613	4.00	74.20	26
27.	Oxygen	O ₂	32.00	-297.4	—	0.2186	91.6	1.15	0.084	11.858	—	—	—	—	—	—	—	—	—	—	—	—	—	—	—	—	—	—	—	—	—	27
28.	Nitrogen	N ₂	29.16	-320.4	—	0.2482	87.8	0.972	0.074	13.472	—	—	—	—	—	—	—	—	—	—	—	—	—	—	—	—	—	—	—	—	—	28
29.	Carbon monoxide	CO	28.01	-313.6	—	0.2484	92.7	0.967	0.074	13.546	321.9	321.9	4,347	4,347	0.5	1.877	2.387	1.0	—	1.887	—	1.897	2.468	1.571	—	1.870	—	5.677	12.50	74.20	29	
30.	Carbon dioxide	CO ₂	44.01	-109.3	—	0.1991	238.2	1.519	0.116	8.621	—	—	—	—	—	—	—	—	—	—	—	—	—	—	—	—	—	—	—	—	—	30
31.	Hydrogen sulfide	H ₂ S	34.08	-76.6	394.0	0.2380	235.6	1.177	0.090	11.133	595	646	6,537	7,097	1.5	5.660	7.160	—	1.0	5.680	1.0	1.410	4.682	6.093	—	0.529	4.682	1.880	8.585	4.30	45.50	31
32.	Sulfur dioxide	SO ₂	64.06	14.0	88	0.1450	166.7	2.212	0.169	5.923	—	—	—	—	—	—	—	—	—	—	—	—	—	—	—	—	—	—	—	—	—	32
33.	Water vapor	H ₂ O	18.02	212.0	0.9492	0.4446	970.3	0.622	0.047	21.061	—	—	—	—	—	—	—	—	—	—	—	—	—	—	—	—	—	—	—	—	—	33
34.	Air	—	29.97	-317.6	—	0.2400	92	1.000	0.076	13.099	—	—	—	—	—	—	—	—	—	—	—	—	—	—	—	—	—	—	—	—	—	34

Example 4.5

Calculate the heat release rate (LHV) for 1000 ft³/hr of CH₄

Solution:

The LHV is given directly in Table 4.2 for CH₄ as 912 Btu/ft³. For 1000 ft³/hr of CH₄, the total heat release rate becomes:

$$1000 \text{ [ft}^3\text{/hr]} \times 912 \text{ [Btu/ft}^3\text{]} = 912,000 \text{ Btu/hr}$$

(or 0.91 million Btu/hr, often abbreviated as 0.91 MMBtuh).

In the hydrocarbon, petroleum, and chemical process industries, the usual convention is to use the LHV. In boilers, the usual convention is HHV, although most boilers do not condense the water in the combustion products. For these reasons, it is important to state the basis clearly and use it consistently throughout the calculation.

4.7 ENTHALPY AND LATENT HEAT

When energy is absorbed by a gas, the gas increases in temperature and expands. The contribution of the internal energy stored in the gas plus the energy required to expand the gas is termed *enthalpy*. Because combustion reactions are typically carried out at constant pressure, a change in temperature will always be accompanied by an expansion, according to the ideal gas law.

Remarkably, in some cases, adding heat to a substance does not change its temperature. For example, adding heat to water at the boiling point transforms it to steam at the same temperature. Combustion engineers refer to this heat as *latent* heat because it is stored in the gas as internal energy rather than expressed as a temperature increase. The latent heat of water vapor is ~970 Btu/lb_m. This means that for every lb_m of steam condensed at the boiling point, one will liberate 970 Btu.

4.8 SENSIBLE HEAT AND HEAT CAPACITY

Sensible heat is the energy stored as a temperature rise. It is termed “sensible heat” because the absorption of energy results in a temperature rise, a common-sensical phenomenon. The proportionality constant between the energy absorbed and the temperature rise is known as the *heat capacity*. It has units of energy per mass per degree. For example, the heat capacity of liquid water is approximately 1 Btu/lb_m °F. A basic formula used to relate the enthalpy to the heat capacity and temperature is:

$$\Delta H = C_p \Delta T \quad (4.5)$$

where ΔH is the difference in enthalpy between the two states (Btu/lb_m), C_p is the heat capacity at constant pressure (Btu/lb_m °F), and ΔT is the temperature difference (°F or °R).

Example 4.6

Find the energy required to heat liquid water from its freezing point (32°F) to its boiling point (212°F)

Solution:

From Equation 4.4, the energy necessary to heat liquid water from its freezing point at 32°F to its boiling point at 212°F is:

$$\Delta H = 1 \text{ [Btu/lb}_m \text{ °F]} (212 - 32) \text{ [°F]} = 180 \text{ Btu/lb}_m$$

Example 4.7

Find the energy required to change liquid water to steam at the boiling point.

Solution:

The latent heat to change phase from liquid water to steam is $\Delta H = 970 \text{ Btu/lb}_m$. Therefore, the required heat to convert liquid water at the freezing point to steam is the sum of the sensible and latent heats, or:

$$\Delta H = (970 + 180) [\text{Btu/lb}_m] = 1150 \text{ Btu/lb}_m$$

Note that most of the energy requirement to generate steam is the latent heat requirement. It cannot be neglected!

As enthalpy can be expressed in various units (e.g., Btu/lb_m , Btu/lbmol , Btu/ft^3), so heat capacity can also be expressed on a mass, molar, or volume basis. One can convert from one form to another by making use of molecular weights and the ideal gas law (in the case of gases). Enthalpy for liquids is not typically expressed volumetrically. However, if desired, one can easily convert between volumetric- and mass-based units for liquids if the liquid density [lb_m/ft^3] is known.

4.9 SOME PROPERTIES OF FLAMES

Combustion typically results in an intense luminous zone of fuel oxidation known as a *flame*. One important property related to a flame is the *ignition temperature*. Table* 4.4 lists the ignition temperatures and other important properties of some common fuels. Once ignition takes place, there is more than enough energy liberated from the fuel combustion to ignite other fuel molecules. Thus, combustion, once started, is self-sustaining. If the ignition temperature is not achieved, sufficient fuel molecules cannot combust to ignite others. By extracting sufficient energy from the flame, the reaction may be *quenched*, that is, extinguished.

4.9.1 FLAMMABILITY LIMITS

Another very important requirement for sustained combustion is that the fuel and air be within certain limits known as *flammability limits*. Table 4.4 also gives lower and upper flammability limits for various fuels. The *upper flammability limit (UFL)* is the maximum fuel volume concentration that will sustain a flame. As the fuel concentration increases, more air is required to combust the fuel. However, because the fuel and air must sum to 100%, the fuel concentration can only be increased at the expense of reducing the available air. As the air becomes limiting, not all of the fuel can combust completely. Ultimately, a limit is reached where sufficient fuel cannot react with air to sustain the reaction. This is the upper flammability limit.

The *lean or lower flammability limit (LFL)* represents the opposite case. When the LFL is reached, there is insufficient fuel to release sufficient energy to sustain combustion, and the flame goes out. The ideal fuel/air mixture is determined by constructing a balanced equation for the fuel/air mixture (e.g., Equation 4.2). However, because fuel and air cannot be perfectly mixed, *excess air* is required as a good combustion practice to ensure complete combustion. For many fuels, 3% excess air (1.03 times more air than theoretically necessary) is usually sufficient. However, the actual excess air requirement is dependent on some unique factors of the equipment and fuel, and is ultimately determined from experience.

* Table 4.4, in *The John Zink Combustion Handbook*, CRC Press, Boca Raton, FL, 2001, 45.

TABLE 4.4
Combustion Data for Hydrocarbons

Hydrocarbon	Formula	Higher Heating Value (vapor) (Btu lb _m ⁻¹)	Theor. Air/Fuel Ratio, by Mass	Max. Flame Speed, (ft s ⁻¹)	Adiabatic Flame Temp. (in air) (°F)	Ignition Temp. (in air) (°F)	Flash Point (°F)	Flammability Limits (in air) (% by volume)	
Paraffins or Alkanes									
Methane	CH ₄	23875	17.195	1.1	3484	1301	Gas	5.0	15.0
Ethane	C ₂ H ₆	22323	15.899	1.3	3540	968–1166	Gas	3.0	12.5
Propane	C ₃ H ₈	21669	15.246	1.3	3573	871	Gas	2.1	10.1
<i>n</i> -Butane	C ₄ H ₁₀	21321	14.984	1.2	3583	761	-76	1.86	8.41
<i>iso</i> -Butane	C ₄ H ₁₀	21271	14.984	1.2	3583	864	-117	1.80	8.44
<i>n</i> -Pentane	C ₅ H ₁₂	21095	15.323	1.3	4050	588	<-40	1.40	7.80
<i>iso</i> -Pentane	C ₅ H ₁₂	21047	15.323	1.2	4055	788	<-60	1.32	9.16
Neopentane	C ₅ H ₁₂	20978	15.323	1.1	4060	842	Gas	1.38	7.22
<i>n</i> -Hexane	C ₆ H ₁₄	20966	15.238	1.3	4030	478	-7	1.25	7.0
Neohexane	C ₆ H ₁₄	20931	15.238	1.2	4055	797	-54	1.19	7.58
<i>n</i> -Heptane	C ₇ H ₁₆	20854	15.141	1.3	3985	433	25	1.00	6.00
Triptane	C ₇ H ₁₆	20824	15.151	1.2	4035	849	—	1.08	6.69
<i>n</i> -Octane	C ₈ H ₁₈	20796	15.093	—	—	428	56	0.95	3.20
<i>iso</i> -Octane	C ₈ H ₁₈	20770	15.093	1.1	—	837	10	0.79	5.94
Olefins or Alkenes									
Ethylene	C ₂ H ₄	21636	14.807	2.2	4250	914	Gas	2.75	28.6
Propylene	C ₃ H ₆	21048	14.807	1.4	4090	856	Gas	2.00	11.1
Butylene	C ₄ H ₈	20854	14.807	1.4	4030	829	Gas	1.98	9.65
<i>iso</i> -Butene	C ₄ H ₈	20737	14.807	1.2	—	869	Gas	1.8	9.0
<i>n</i> -Pentene	C ₅ H ₁₀	20720	14.807	1.4	4165	569	—	1.65	7.70

(Continued)

TABLE 4.4
Combustion Data for Hydrocarbons (Continued)

Hydrocarbon	Formula	Higher Heating Value (vapor) (Btu lb _m ⁻¹)	Theor. Air/Fuel Ratio, by Mass	Max. Flame Speed, (ft s ⁻¹)	Adiabatic Flame Temp. (in air) (°F)	Ignition Temp. (in air) (°F)	Flash Point (°F)	Flammability Limits (in air) (% by volume)	
Aromatics									
Benzene	C ₆ H ₆	18184	13.297	1.3	4110	1044	12	1.35	6.65
Toluene	C ₇ H ₈	18501	13.503	1.2	4050	997	40	1.27	6.75
<i>p</i> -Xylene	C ₈ H ₁₀	18663	13.663	—	4010	867	63	1.00	6.00
Other Hydrocarbons									
Acetylene	C ₂ H ₂	21502	13.297	4.6	4770	763–824	Gas	2.50	81
Naphthalene	C ₁₀ H ₈	17303	12.932	—	4100	959	174	0.90	5.9

Note: Based largely on: "Gas Engineers' Handbook," American Gas Association, Inc., Industrial Press, 1967. For heating value in J kg⁻¹, multiply the value in Btu lb_m⁻¹ by 2324. For flame speed in ms⁻¹, multiply the value in fts⁻¹ by 0.3048.

REFERENCES

- American Institute of Physics Handbook*, 2nd ed., D.E. Gray, Ed., McGraw-Hill Book Company, 1963.
Chemical Engineers' Handbook, 4th ed., R.H. Perry, C.H. Chilton, and S.D. Kirkpatrick, Eds., McGraw-Hill Book Company, 1963.
Handbook of Chemistry and Physics, 53rd ed., R.C. Weast, Ed., The Chemical Rubber Company, 1972; gives the heat of combustion of 500 organic compounds.
Handbook of Laboratory Safety, 2nd ed., N.V. Steere, Ed., The Chemical Rubber Company, 1971.
Physical Measurements in Gas Dynamics and Combustion, Princeton University Press, 1954.

4.9.2 LAMINAR FLAME SPEED

An important property related to flame propagation is the flame speed (see Table 4.4). Consider a large open container of fuel and air, intimately mixed in ideal proportions. If the fuel is ignited at one end of the container, the flame will flash or propagate to the other end at a particular velocity. This is a measure of the kinetics of the flame — that is, how fast can the fuel and air react and pass its energy on to the adjacent but unreacted fuel/air mixture? The *laminar flame speed* is one such measure of the kinetics of the flame. Table 4.4 gives laminar flame speeds for several fuels. Most hydrocarbons have a similar flame speed. But hydrogen, owing to its high enthalpy per mole and its low viscosity and rapid diffusion, has a flame speed more than triple most hydrocarbon fuels.

4.10 LIFTOFF AND FLASHBACK

One can envision two scenarios for a propagating flame. In the first scenario, already discussed, the air and fuel are premixed and stationary. The flame then propagates within the quiescent mixture. In such a case, the mixture is stationary and the flame is moving. Another scenario is to move the fuel and air, and allow the flame to remain stationary. The typical industrial burner functions in this way, having moving reactants and a stationary flame. A stationary flame confined to the burner and certain portions of the furnace is critical. Otherwise, the high flame temperatures of wayward flames would be destructive to boilers and process tubes.

If the reactants are metered at a velocity exceeding the flame speed, the flame will begin to move in the direction of the reactant flow. This condition is known as *lift-off*. If the flame is carried to a region downstream of the burner, combustion products within the furnace may dilute the fuel/air mixture below the LFL. This would extinguish the flame and result in a very dangerous condition — uncombusted fuel may accumulate and later find an ignition source. This could result in an explosion.

If the reactants are metered at a velocity much lower than the flame speed, the flame moves opposite the direction of the reactant flow. In the case of premixed fuel and air, the flame can *flashback* or enter an area of the burner that cannot tolerate the high temperature, thus destroying the burner. The following section considers combustion with premixed reactants.

4.11 PREMIX AND DIFFUSION FLAMES

In certain industrial settings requiring rapid combustion and short flame lengths, it may be desirable to mix the fuel and air prior to combustion. The device is known as a *premix* burner. Figure 4.1 shows such a burner. It comprises a venturi section, whereby the fuel pressure aspirates combustion air and provides the mixing energy. The fuel is ignited outside the mixing chamber and anchors to the outside of the burner by a mechanism we explain shortly. If the flame were to flashback within the interior of the burner, the burner would be destroyed in short order.

A *diffusion burner* avoids this situation by metering the fuel and air in separate streams (Figure 4.2). Because neither pure air nor fuel alone is able to sustain combustion, the flame cannot propagate into the fuel line or air inlets. This eliminates the potential for flashback. However, the flame may still lift off or move to an area of insufficient fuel and air. Therefore, in both premixed and diffusion flames, some method is needed to anchor the flame.

4.12 TURBULENT FLAME SPEED AND FLAME HOLDERS

In practice, industrial burners cannot rely on an exact metering of the fuel and air to exactly match the flame speed for several reasons. First, small changes in hydrogen content (usual in refinery applications) would require real-time fuel analysis and some system of precision metering.

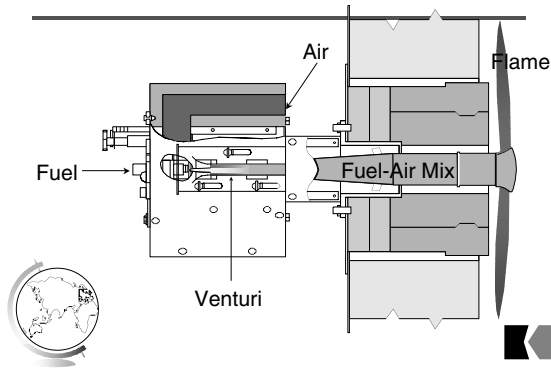


FIGURE 4.1 Premixed burner.

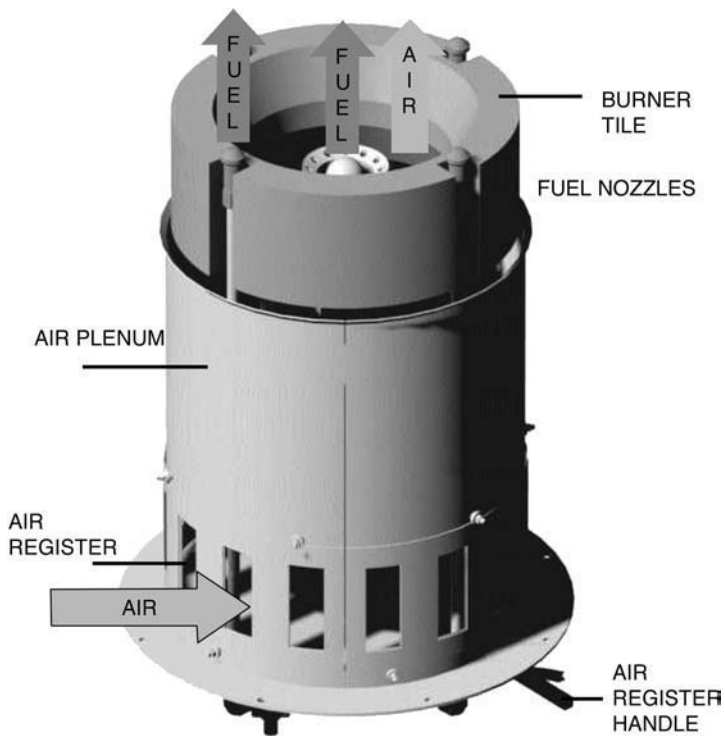


FIGURE 4.2 Staged diffusion burner. Note that fuel and air streams are not mixed prior to combustion.

In practice, neither exists. Second, the laminar flame speed is much too slow to anchor the flame. That is, in most industrial settings, the fuel and air are metered at velocities that well exceed the laminar flame speed. How then can the flame be anchored? One makes use of two phenomena: the turbulent flame speed and flame holders.

Unlike laminar flame speed, *turbulent flame speed* is not properly a function of the fuel alone, but also of the flow conditions. If the velocity is sufficiently high, the flow shifts from laminar flow to turbulent flow. Turbulent flow is characterized by macroscopic recirculation within the flame structure.

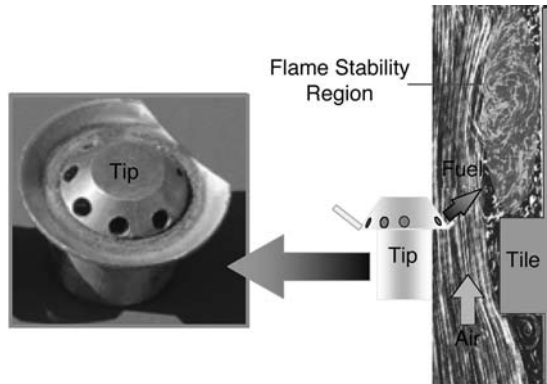


FIGURE 4.3 Burner ignition ledge: tile ledge/fuelport position and angle.

This recirculation mixes hot product gases with the reactants. The result is that the effective flame speed is much higher. It is not uncommon for fuel and air flows to be many times greater than the laminar flame speed in turbulent combustion.

However, because the turbulent flame speed depends on the flow conditions as well as the fuel composition, it is not practical to stabilize the flame front by fuel and air metering. Instead, combustion engineers make use of *flame holders*. As the name implies, a flame holder is a device that anchors the leading edge of the flame. This usually involves providing a region of low velocity in the flame path. For example, [Figure 4.3](#) shows one type of flame holder known as an *ignition ledge*. As the fuel and air flow by the ledge at high velocity, the ledge or step forces some gas to recirculate. Thus, the velocity at the ledge is virtually zero. This allows the flame to burn back to the ignition ledge. The recirculation ensures that the region is recharged with fresh fuel and air. Thus, the flame is anchored or held to the ignition ledge, despite much higher velocities in the adjacent flow field.

The ignition ledge is part of a class of flame holders known as *bluff bodies*. A bluff body is any nonstreamlined shape inserted into the flow field. The trailing edges of the body cause recirculation and anchor the flame. Because the bluff body or ignition ledge must tolerate direct flame impingement, it must be made of high-temperature alloy or refractory. Otherwise, the flame holder will degrade and compromise the flame stability of the burner.

4.13 QUENCHING

In premix burners (see [Figure 4.1](#)), some mechanism must be used to prevent the flame from propagating upstream and causing the premixed fuel and air to ignite inside the burner. There are several methods for doing this. The first is to design the burner so that the fuel/air mixture exceeds the turbulent flame speed. This will cause the flame to move downstream. To keep the flame from lifting off, the burner itself can be designed with slots having square-edged exits. Like the ignition ledge or bluff body, the bluff trailing edge causes recirculation and functions as a flame holder. Because the flame is anchored at this edge, the burner material at this edge must be made of high-temperature alloy.

The flowing fuel and air help cool the burner. However, the hot flame is anchored just outside the burner and just millimeters away from combustible gases. If the only mechanism keeping the flame from flashing back were fuel and air velocity, a momentary fuel reduction would allow the flame to propagate upstream to the interior of the burner. Because the velocity in the interior of the burner is lower than through the passage that the flame has propagated, there is no mechanism

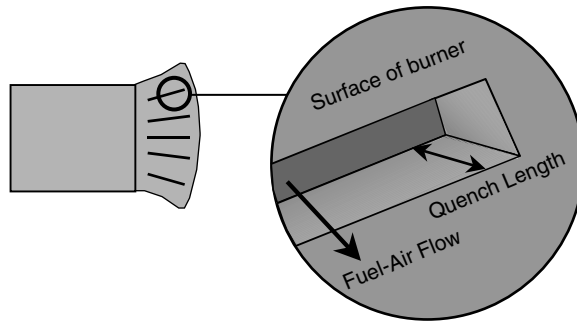


FIGURE 4.4 Detail of premix burner slot.

to force the flame back to the outside when the fuel and air flows resume their design flows. In such a case, the flame will remain internal to the venturi and destroy it in short order. Changes in fuel composition and flow rates occur often enough in refinery environments to mandate additional mechanisms to prevent flashback.

If sufficient enthalpy can be removed from the flame as it begins to flash back, the flame will extinguish. The key is to extinguish or quench only the portion of the flame that is beginning to flash back, while leaving the remainder of the flame to burn as intended. This is done using a *quench distance*. Consider [Figure 4.4](#), an enlarged section of the premix burner exit. The gas flows through long metal passageways before being ignited. The sidewalls of this passageway are relatively cool because of the flowing but unignited gases. Should the flame begin to flash back, the cool metal will extract heat and quench the flame, preventing it from entering the interior of the burner. However, the method is not foolproof. If the flow is reduced beyond the design limit for extended periods, the entire burner may reach a temperature insufficient to quench flame propagation. In short, burner design requires a thorough knowledge of fluid mechanics, heat transfer, combustion, and prior art.

4.14 NATURAL- AND FORCED-DRAFT BURNERS

Burners can receive their airflow in two ways. If the flame must be short and compact, one can provide air to the burner using a fan or blower. The resulting system is known as a *forced-draft* system, and the burners are forced-draft burners. Forced draft provides additional mixing that helps increase flame turbulence and shorten the flame. It also allows for smaller furnace volumes. Thus, it decreases the capital cost of the boiler or process heater. However, the capital cost is reduced at the expense of operating cost for the blower or fan. One way of compensating for this cost is to allow the air to be preheated by the exiting flue gases in a device known as an air preheater. The recovery of heat allows the process to operate more efficiently. Cooler flue gases exit the stack.

Natural-draft burners rely on the natural tendency of cold air to displace hot gases in the furnace, forcing them out the exit stack. Resorting to the ideal gas law and conservation of energy, we can model this phenomenon. The difference in weight between a hot and cool volume of gas (Δmgh) can be harnessed to perform work (pV). Normalizing the quantities by the mass (m) gives Equation 4.6:

$$\Delta p = \Delta \rho gh \tag{4.6}$$

where Δp is the stack draft, $\Delta \rho$ is the density difference between the cool and hot flue gases, g is the acceleration due to gravity (32.174 ft/s^2), and h is the height of the furnace. Making use of the

ideal gas law and the definition of molecular weight, we can recast the equation in terms of temperature difference:

$$\Delta p = \frac{PM}{R} \left(\frac{1}{T_2} - \frac{1}{T_1} \right) h \quad (4.7)$$

Example 4.8

Calculate the draft at the floor given by a 40-ft furnace with an average temperature of 1600°F. Assume a molecular weight of the flue gas of 28 lb_m/lbmol, and an outside temperature of 60°F. Further, assume that the exit of the furnace is at -0.1 inches of WC due to the influence of a warm stack.

Solution:

From Equation 4.7,

$$\Delta p = \frac{14.7[\text{psia}] \left[28 \left[\frac{\text{lb}_m}{\text{lbmol}} \right] \right]}{10.73 \left[\frac{\text{psia ft}^3}{\text{lbmol}^\circ\text{R}} \right]} \left(\frac{1}{1600 + 460} - \frac{1}{60 + 460} \right) \left[\frac{1}{^\circ\text{R}} \right] 32.2 \left[\frac{\text{ft}}{\text{s}^2} \right] 40[\text{ft}] = -71.03 \left[\frac{\text{lb}_m}{\text{ft s}^2} \right]$$

This is not a very useful unit of pressure. In general, draft is measured in inches of water column (in. WC). As the name denotes, in. WC represents the pressure necessary to raise a column of water 1 inch in elevation. For example, the pressure in one's mouth must be a few inches of WC below atmospheric to drink water through a straw. To convert lb_m/ft s² to in. WC, one divides by 167.6. Therefore, the resulting pressure is -0.42 in. WC. The negative sign means that the pressure in the furnace is lower than atmospheric. A general rule of thumb is that a furnace generates ~0.1 in. WC for each 10 ft in height. Adding back the -0.1 in. WC from the stack contribution, the draft available at the burner is -0.52 in. WC.

To convert inches of WC to psi, divide by 27.67.

Although this force appears to be quite feeble, it is capable of drafting an enormous amount of air in through the burner opening; 1 in. WC is capable of drafting air at velocities up to 66 ft/s at 60°F! Under these conditions, a single burner with a throat opening of 1 ft² (~8 in. diam.) can support up to 7 MMBtu/hr HHV of CH₄ combustion. Typical natural-draft burners for the petrochemical industry operate on ~0.5 in. WC draft and deliver 8 MMBtuh with 2 to 3 ft² of throat area. Some additional area is required to account for air friction through the throat and burner internals.

4.15 NO_x AND CO

An *emission* is any unwanted egress of a substance or quantity. CO, and NO_x are byproducts of the combustion process. With proper design, they can be reduced to acceptable levels, but never eliminated. CO emissions are generally an indicator of too little air, poor mixing, or insufficient furnace temperature. With proper burner design, excess oxygen concentrations of 2 to 5%, and greater than 1100°F furnace temperatures, CO is not typically a problem.

The combustion process also produces CO₂ and H₂O, which cannot be considered byproducts because proper combustion results in complete conversion of hydrocarbon fuels to CO₂ and H₂O. Both H₂O and CO₂ are chemical products of aerobic respiration and produced by plants, animals, and humans. However, CO₂ is coming under scrutiny as a so-called greenhouse gas — an active

infrared absorber and emitter that can potentially elevate terrestrial temperatures. Actually, H₂O is more active in this regard, but CO₂ is a greater political concern.

If and to what extent CO₂ is considered an emission will dictate some combustion practices in the future. There are only two ways to control CO₂ emissions: reduction of carbon in the fuel or post-combustion treatment; that is, capturing CO₂ after it is produced. Hydrogen combustion produces no CO₂ (see Equation 4.2). However, many are surprised to learn that hydrogen combustion with air produces more NO_x than hydrocarbon fuels such as natural gas and gasoline. This is due to hydrogen's very high flame temperature and the thermal-bound NO_x mechanism. We consider NO_x next.

4.15.1 NO_x EMISSIONS

NO_x is formed in very low quantities (parts per million on a volume basis) as a byproduct of combustion in several ways. NO_x contributes to ground-level ozone via a complex reaction with hydrocarbons and other reactive compounds. Ground-level ozone can be a severe problem for a certain distressed portion of the population (e.g., asthmatics and those with diminished lung capacity). For these and other reasons, NO_x emissions are regulated to very low levels (e.g., <30 ppm). Typical industrial combustion produces 100 to 200 ppm NO_x. However, low-NO_x burners can achieve remarkably low levels of NO_x emissions, on the order of 10 ppm (Figure 4.5).

4.15.2 THERMAL NO_x

The *thermal NO_x* mechanism comprises several steps, but can be reduced for discussion purposes, to two main ones:



Equations 4.8 and 4.9 give *elemental* steps and are shown by an equals sign (=). An elemental step represents the exact atomic and molecular entities involved in an actual product-forming collision. Therefore, according to Equation 4.8, in a favorable collision, a nitrogen atom collides with an oxygen molecule to form a nitric oxide molecule and an oxygen atom. In Equation 4.9, the oxygen atom collides with a nitrogen molecule to produce another molecule of nitric oxide

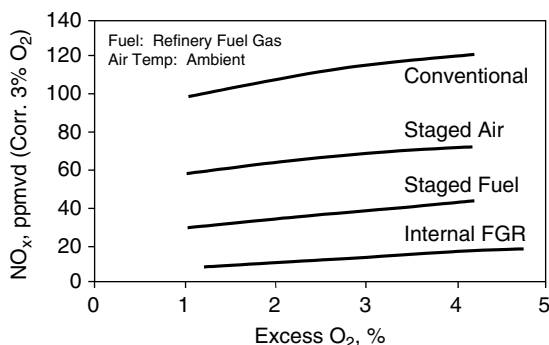


FIGURE 4.5 Effect of burner model on NO_x.

and a nitrogen atom, continuing the chain represented in Equation 4.8. The net result (Equation 4.10) is that nitrogen and oxygen generate nitric oxide (NO).

NOx in combustion generally refers to NO or NO₂ (nitrogen dioxide), although nitrogen can form other molecular species (e.g., N₂O, N₂O₃). However, only NO and NO₂ are regulated or formed in any quantities of concern.

High temperatures are required to generate the atomic species in Equations 4.8 and 4.9. Industrial flames can achieve such temperatures. Oxygen molecules comprise a double bond (O=O) and molecular nitrogen comprises a triple bond (N≡N). Therefore, the oxygen double bond is the easiest to rupture (Equation 4.8). Owing to the difficulty of rupturing the N≡N triple bond, Equation 4.9 is the *rate-limiting step* and paces the reaction. If we presume that atomic oxygen is in equilibrium with its molecular counterpart, we can write a rate law governing nitric oxygen production. Details of the derivation are given in other texts.¹

$$[\text{NO}] = A[\text{N}_2] \int e^{\frac{b}{T}} \sqrt{[\text{O}_2]} d\theta \quad (4.11)$$

where the square brackets [] denote volume concentrations of the enclosed species, A and b are constants, T is the absolute temperature, and θ is the time under those conditions.

Unfortunately, one cannot integrate Equation 4.11 because one does not have sufficient information regarding the oxygen-temperature history within the flame. However, Equation 4.11 is useful as a heuristic for pointing out the main features of thermal NOx formation.

First, temperature is an exponent indicating that NOx formation is very sensitive to temperature. Hot spots in the flame contribute significantly to NOx formation. Second, high oxygen concentration inflates NOx. The relation is square root proportional within the integral. However, upon integration, NOx would be related to oxygen concentration raised to a higher power. Studies² show that NOx is approximately proportional to oxygen concentration. Nitrogen varies little over the course of combustion and there is no convenient way to reduce nitrogen concentration. Therefore, it can be regarded as approximately constant. Hence, it is shown outside the integral.

Equation 4.11 suggests the following NOx reduction strategies:

1. Reduce peak flame temperatures.
2. Reduce oxygen concentration.
3. Reduce the time of high-temperature combustion in the vicinity of oxygen.

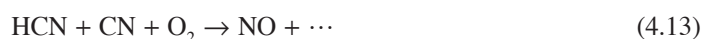
4.15.3 FUEL-BOUND NOx

When nitrogen is a part of the fuel molecule, it can form NOx. It is important to emphasize that the nitrogen must be part of the fuel molecule. Diluting natural or refinery gas with molecular nitrogen cannot contribute to the fuel-bound mechanism. Indeed, the addition of diluents such as nitrogen to the fuel stream will reduce NOx from both the thermal and fuel-bound mechanisms as it reduces the concentrations of the active species and the flame temperature.

The first step in forming NOx from the fuel-bound mechanism is a rapid pyrolysis of the parent molecule into cyano intermediates:



These intermediates are oxidized with oxygen to form nitric oxide:



We can write a rate law with the following assumptions:

1. The oxidation of the cyano intermediates is the rate-limiting step, involving, as it does, the rupture of a C≡N triple bond,
2. Cyano intermediates are proportional to the nitrogen concentration in the parent [N].

$$[\text{NO}] = k \int [\text{N}]^\alpha [\text{O}_2]^\beta d\theta \quad (4.14)$$

where k , α , and β are experimentally determined constants.

Equation 4.14 suggests that minimizing the oxygen concentration and reducing the nitrogen concentration in the fuel will reduce NO_x from the fuel-bound mechanism. In localities having strict NO_x limits, nitrogen is eliminated from the fuel supply, thereby eliminating all possibility of fuel-bound NO_x. Low-NO_x burners greatly reduce NO_x from the thermal mechanism. However, another mechanism contributes to NO_x production — the *prompt NO_x* mechanism.

4.15.4 PROMPT NO_x

Prompt NO_x is similar to fuel-bound NO_x, with the important exception that the nitrogen comes from the molecular nitrogen in the combustion air. Notwithstanding, cyano intermediates are still formed per Equation 4.15:



However, the cyano intermediates involve the rupture of a N≡N triple bond, as opposed to simple pyrolysis in the fuel-bound case. Therefore, the mechanism is not facile and is responsible for less than 20 ppm of NO_x in most cases. The cyano intermediates are oxidized per Equation 4.13.

Presuming that Equation 4.15 represents a rate-limiting sequence, a possible rate law is:

$$[\text{NO}] = k[\text{N}_2] \int [\text{CH}_x] d\theta \quad (4.16)$$

It is not practical to limit nitrogen concentration in combustion air for most applications. Glass melting furnaces are an exception. In some cases, it can be economically feasible to justify combustion with pure oxygen. However, this is not the general case for boilers or process heaters. Therefore, the only strategy for reducing prompt NO_x is to dilute the fuel species before combustion. This can be done in the burner itself by allowing the fuel jet to entrain combustion products in the furnace before reaching an ignition zone.

REFERENCE

1. I. Glassman, *Combustion*, Third Edition, Academic Press, 1996.

5 CFD in Burner Development

*Joseph D. Smith, Michael Lorra, Ph.D., Eric M. Hixson,
and Tom Eldredge, Ph.D.*

CONTENTS

- 5.1 Introduction
- 5.2 Solving Burner Problems with CFD
 - 5.2.1 Key Ingredients of CFD
 - 5.2.2 Main Goal of CFD Modeling
 - 5.2.3 Choosing the Domain
 - 5.2.4 Selecting Boundary Conditions
 - 5.2.5 Numerical Analysis and Computational Meshes
- 5.3 Building Blocks of CFD-Based Combustion Models
 - 5.3.1 Turbulent Fluid Mechanics
 - 5.3.1.1 Problem of Closure
 - 5.3.1.2 Favre and Reynolds Averaging
 - 5.3.1.3 Turbulence Models
 - 5.3.1.4 Other Turbulence Modeling Approaches
 - 5.3.2 Homogeneous Chemistry
 - 5.3.2.1 Mixture Fraction Approach for Equilibrium or Nonequilibrium Chemistry
 - 5.3.3 Wall Heat Transfer
 - 5.3.3.1 Thermal Radiation Heat Transfer
 - 5.3.3.2 Properties of Radiating Gases
 - 5.3.3.3 Radiative Boundary Conditions
- 5.4 Illustrative Examples
 - 5.4.1 Flame Shape Analysis Case Study
 - 5.4.1.1 Combustion Modeling and Boundary Conditions
 - 5.4.1.2 Predicted Flame Shapes and Modifications to Burner Geometry
 - 5.4.2 Thermal Oxidizer Burner/Reactor Case Study
- 5.5 Conclusions and Summary
- References

5.1 INTRODUCTION

Computational fluid dynamics (CFD) has become an accepted tool to help in the design and operation of aerodynamic equipment. More recently, CFD has also found tremendous application in the analysis of combustion equipment, such as industrial burners. Widespread acceptance is limited due to the nonlinear relationship between reaction chemistry and turbulent fluid mechanics. Smith et al.¹ list several related issues that tend to limit the application of CFD to industrial problems, which include the following:

- *Limited understanding of the physics involved in reactive flow systems.* This includes uncertainty in fundamental chemical reaction kinetics for complex fuels, the chaotic nature of turbulent mixing, the heterogeneous chemistry related to solids (e.g., soot formation, catalysis, etc.), thermophoretic transport of solids to walls and the associated deposition mechanisms, and the radiative properties of complex multiphase systems.
- *The large disparity in both spatial and temporal time scales in typical reacting flow systems.* To capture the flow characteristics responsible for momentum transfer, one needs to resolve the flow to the smallest characteristic size (i.e., Kolmogorov scale). To capture the associated reaction kinetics, it is believed that one must further resolve the spatial features to the Batchelor scale. Pitts² points out that traditionally it was argued that one should resolve spatial features on the order of size of the Batchelor scale (product of Kolmogorov scale and inverse square root of Schmidt number), typically a few hundred micrometers for most laboratory flows. More recently, however, it has been suggested that the required spatial resolution may be 12 to 25 times larger than the Batchelor scale. Unfortunately, recent experiments, including scalar dissipation measurements along a line in an axisymmetric jet of propane into air at the National Institute of Standards and Technology, have shown that the larger estimates for the required spatial resolution will result in partial averaging of the scalar dissipation. Taken together, the studies suggest that to fully capture scalar dissipation fluctuations, the spatial resolution must be no larger than two to three times the Batchelor scale. The computational difficulty of coupling the many important aspects of chemistry and physics in a way that is efficient enough to be achievable for computations simulating practical furnaces, which have such a wide disparity of spatial and temporal scales.
- *Full-scale verification of actual CFD codes in real furnaces is difficult and costly.* In addition, local, detailed data for model validation is also expensive and tedious to obtain. This dearth of “realistic” data for evaluation of predictions brings with it uncertainty about both the numerical error in the predictions and the experimental error in the data.
- *Typical computational combustion tools have not been designed to optimize combustion equipment such as industrial burners.*

This leaves an engineer uncertain as to how to effectively use CFD predictions to address constrained design or operational problems. However, current trends in environmental and operational costs are making it increasingly necessary to explore operating conditions that are beyond the current empirical database of industrial burners. Recent work by Smith et al.³ and Henneke et al.⁴ have demonstrated the basic fact that CFD-based tools hold great promise for economically exploring new burner designs.

This chapter begins with a brief discussion of how these commercial codes are used to analyze a typical industrial burner. Attention focuses on producing an “appropriate” computational mesh. It also discusses different issues related to computational meshes. Next, it discusses in some detail the multi-physics involved in combustion modeling. In particular, it describes the necessary physical sub-models inherent in a typical CFD-based combustion simulation package. Finally, it provides three examples of how these types of tools have been used recently to address various issues related to industrial burners. In conclusion, the chapter summarizes key issues related to using CFD in industrial burner design, evaluation, and optimization. It also provides recommendations for future work needed to advance this science.

5.2 SOLVING BURNER PROBLEMS WITH CFD

Computational fluid dynamics (CFD) has been successfully used for many years in a number of industries, beginning with aerospace and expanding into aeronautics, automotive, electronics, and electric power generation. More recently, CFD has found application in the chemical process and the hydrocarbon process industries (HPI/CPI) where it has gained a foothold as a tested, validated, and

now regularly accepted, problem-solving tool. Engineers involved in designing and building advanced combustion equipment for the HPI and CPI industries routinely use CFD to advance new burner technology.

The science and technology of CFD has matured to the point where performance predictions are made with a degree of confidence from models covering a wide range of complex furnace, burner, and reactor geometries. CFD allows the engineer to explore operational parameters previously considered impossible or prohibitively expensive using normal testing procedures. Combustion-based CFD has become an extremely valuable tool in providing direction to the timely execution of industrial experiments, which further reduces the impact that retrofits and other equipment changes may have on an organization's bottom line.

Although a proven tool in modeling equipment behavior and performance, CFD is not without limitations. Most notable are the current limitations with respect to modeling turbulent reacting flow. Commercial CFD codes utilize a standard approach to simulate chemical kinetics, which approximate the consumption and production of chemical species. This causes the engineer to use simplifying assumptions about the chemistry considered in the simulation. While this simplified chemistry includes adequate information to predict flow patterns and local heat transfer, these models lack sufficient information to accurately predict NO_x and CO production. Alternatively, the NO_x chemistry is decoupled from the main calculation and obtained using post-processing techniques. However, for species more closely related to the base fuel, such as CO, a similar, abridged treatment is not currently available.

Recent efforts to include more complex chemical kinetics, such as those used by StarCDTM with the ChemkinTM* suite of programs, are helping push CFD technology closer to more fundamentally based mechanistic solutions. However, correctly coupling detailed kinetics with turbulent fluid mechanics is very difficult and, with the enhancement of mesh generation techniques, stands as one of the biggest areas for potential growth in the next five years.

Computer simulations are also only as good as the data with which they are validated. In many cases, sufficient data are not available to accurately calibrate a CFD model. Physical or scaled-flow modeling has traditionally been used to generate baseline data to help validate flow predictions. In addition, well-controlled, full-scale burner tests have been used to verify predictions of burner performance. CFD coupled with cold-flow physical modeling and hot-flow burner tests provides a powerful analytical tool to develop accurate, timely, and cost-effective burner designs.

5.2.1 KEY INGREDIENTS OF CFD

At its roots, CFD relies on three worlds (see [Figure 5.1](#)).⁵ First, CFD requires a comprehensive understanding of the physical phenomena involved in any process. Second, the physics of the phenomena must be translated into mathematical relationships. Third, due to the complexity of nonlinear mathematics (see [Table 5.1](#)), the governing equations must be solved using numerical algorithms. Effective use of CFD relies equally on each of these worlds. Error in any one translates into erroneous predictions, and failing to understand the limitations of each can lead to incorrect conclusions and potentially catastrophic results. For optimal use, the engineer must understand the physics, mathematics, and numerics to determine when simulation results represent reality.

When used appropriately, CFD helps reduce burner development cycle time, improves burner efficiency, and extends burner lifetime. This is due to reduced computer costs, increased computer power, and better and more detailed physics in commercially available CFD codes. CFD also helps reduce operating costs, improves product yield, and increases product quality through system optimization. In some instances, CFD helps the engineer evaluate various design options that otherwise

* Chemkin is a software tool for incorporating complex chemical kinetics into simulations of reacting flow. This commercial tool is supplied by Reaction Design, currently located in San Diego, CA.

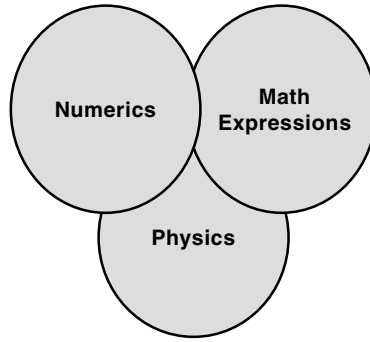


FIGURE 5.1 Three worlds of CFD.

TABLE 5.1
Cartesian Set of Differential Equations Solved in CFD

$$-\frac{\partial(\bar{\rho}\tilde{u}\phi)}{\partial x} + \frac{\partial(\bar{\rho}\tilde{v}\phi)}{\partial y} + \frac{\partial(\bar{\rho}\tilde{w}\phi)}{\partial z} - \frac{\partial}{\partial x}\left(\Gamma_\phi \frac{\partial(\phi)}{\partial x}\right) - \frac{\partial}{\partial y}\left(\Gamma_\phi \frac{\partial(\phi)}{\partial y}\right) - \frac{\partial}{\partial z}\left(\Gamma_\phi \frac{\partial(\phi)}{\partial z}\right) = S_\phi$$

Equation	ϕ	Γ_ϕ	S_ϕ
Continuity	1	0	0
X-momentum	\tilde{u}	μ_e	$-\frac{\partial p}{\partial x} + \frac{\partial}{\partial x}\left(\mu_e \frac{\partial \tilde{u}}{\partial x}\right) + \frac{\partial}{\partial y}\left(\mu_e \frac{\partial \tilde{v}}{\partial x}\right) + \frac{\partial}{\partial z}\left(\mu_e \frac{\partial \tilde{w}}{\partial x}\right) + \bar{\rho}g_x - \frac{2}{3}\bar{\rho}\tilde{k}$
Y-momentum	\tilde{v}	μ_e	$-\frac{\partial p}{\partial y} + \frac{\partial}{\partial x}\left(\mu_e \frac{\partial \tilde{u}}{\partial y}\right) + \frac{\partial}{\partial y}\left(\mu_e \frac{\partial \tilde{v}}{\partial y}\right) + \frac{\partial}{\partial z}\left(\mu_e \frac{\partial \tilde{w}}{\partial y}\right) + \bar{\rho}g_y - \frac{2}{3}\bar{\rho}\tilde{k}$
Z-momentum	\tilde{w}	μ_e	$-\frac{\partial p}{\partial z} + \frac{\partial}{\partial x}\left(\mu_e \frac{\partial \tilde{u}}{\partial z}\right) + \frac{\partial}{\partial y}\left(\mu_e \frac{\partial \tilde{v}}{\partial z}\right) + \frac{\partial}{\partial z}\left(\mu_e \frac{\partial \tilde{w}}{\partial z}\right) + \bar{\rho}g_z - \frac{2}{3}\bar{\rho}\tilde{k}$
Mixture fraction	\tilde{f}	$\frac{\mu_e}{\sigma_f}$	0
Mixture fraction variance	\tilde{g}	$\frac{\mu_e}{\sigma_g}$	$-\frac{C_{g1}\mu_e}{\sigma_g} + \left[\left(\frac{\partial \tilde{f}}{\partial x}\right)^2 + \left(\frac{\partial \tilde{f}}{\partial y}\right)^2 + \left(\frac{\partial \tilde{f}}{\partial z}\right)^2\right] - C_{g2}\bar{\rho}\tilde{g}\frac{\tilde{\epsilon}}{k}$
Turbulent energy	\tilde{k}	$\frac{\mu_e}{\sigma_k}$	$G - \bar{\rho}\tilde{\epsilon}$
Dissipation rate	$\tilde{\epsilon}$	$\frac{\mu_e}{\sigma_\epsilon}$	$\left(\frac{\tilde{\epsilon}}{k}\right)(c_1G - c_2\bar{\rho}\tilde{\epsilon})$

where:

$$G = \mu_e \left\{ 2 \left[\left(\frac{\partial \tilde{u}}{\partial x}\right)^2 + \left(\frac{\partial \tilde{v}}{\partial y}\right)^2 + \left(\frac{\partial \tilde{w}}{\partial z}\right)^2 \right] + \left(\frac{\partial \tilde{u}}{\partial y} + \frac{\partial \tilde{v}}{\partial x}\right)^2 + \left(\frac{\partial \tilde{u}}{\partial x} + \frac{\partial \tilde{w}}{\partial z}\right)^2 + \left(\frac{\partial \tilde{v}}{\partial x} + \frac{\partial \tilde{w}}{\partial y}\right)^2 \right\}$$

would not be possible to evaluate experimentally because of safety constraints. Thus, CFD has also led to improvements in safe operations.

Because a model is only as good as the data it represents, CFD is best conducted hand-in-hand with experiments. CFD can help identify the key experiments needed instead of performing all tests required in a complete factorial design. This allows the researcher to spend more time on the tests

that will lead him or her closer to a determination or solution. In this way, CFD helps expand traditional methods instead of replacing them. While many plants have been designed and built using rules-of-thumb, empirical correlations, and spreadsheets, CFD bridges the gap between theory and practice by increasing the practical use of fundamentals in process design, operation, and optimization.

Today, engineers use commercially available, advanced CFD-based combustion packages, including Fluent and Star-CD. Other software tools such as Chemkin™ are used to simulate the chemical kinetics responsible for NO_x and CO emissions. The rapid expansion of computer power has led to more comprehensive CFD simulations that require large numbers of calculations. A typical burner simulation may require in excess of 10⁶ computational cells or nodes points. Based on current computer power, these simulations require between 24 and 72 hours each. As CPU power increases, more and more complex physics are added to the simulation, which improves an engineer's ability to solve "real" problems with CFD-based tools.

Today's challenge continues to be simulating fully three-dimensional, turbulent, reacting compressible flows inside very complex burner/furnace geometries. With recent advances in parallel computing, however, highly parallel workstation clusters are now used to solve problems with more than 10⁷ nodes with transient behavior.

5.2.2 MAIN GOAL OF CFD MODELING

The main goal for performing CFD related to industrial burners is to reduce the cost of developing new technology. When a new industrial burner is designed to meet certain performance standards, including heat release, reduced emissions levels, flame shape, and operational stability, an iterative testing process is common. Past experience shows that this process may require upward of 2 years and a minimum of \$1 million. Once the final prototype design is determined and installed in the field, the burner may undergo several subsequent modifications. A good example of this is the John Zink PSMR burner. Developed in the early 1990s as a low NO_x round-flame burner, it has become the industrial standard of today. However, the basic design has undergone several iterations to get to where it is today. During this development period, CFD has also become a common tool used to evaluate and optimize burner design.

Today, CFD is routinely used to investigate potential burner designs in conjunction with experimental testing. Using CFD to expand and understand test results, as well as using CFD to direct future testing to focus on key issues, is the most productive way of shortening the design cycle. Taken together, testing and CFD modeling have helped shorten the development cycle by an estimated 20%. In addition, CFD modeling has helped reduce warranty work once a new burner is installed in the field. This helps reduce expensive rework at the customer's facility, which helps maintain good will with customers.

5.2.3 CHOOSING THE DOMAIN

One of the key issues in developing a CFD model for an industrial burner is to select the appropriate domain for the analysis. A full-process furnace used in the hydrocarbon refining industry may include hundreds of burners of various designs and configurations (see [Figure 5.2](#), Reference 6). To reduce the computational demand for analyzing such a system in sufficient detail (see below), the recommended approach utilizes symmetry planes to reduce the overall computational domain. An example would be to use the natural symmetry in the furnace shown and only analyze half of the complete volume (see [Figure 5.3⁶](#)).

A simplified burner model can be used to reduce the overall complexity of the CFD model. Here, experience has shown that a model must resolve each fuel jet to capture the governing physics that result in flame shape and spread inside a furnace. [Figure 5.4⁶](#) shows a typical burner model for

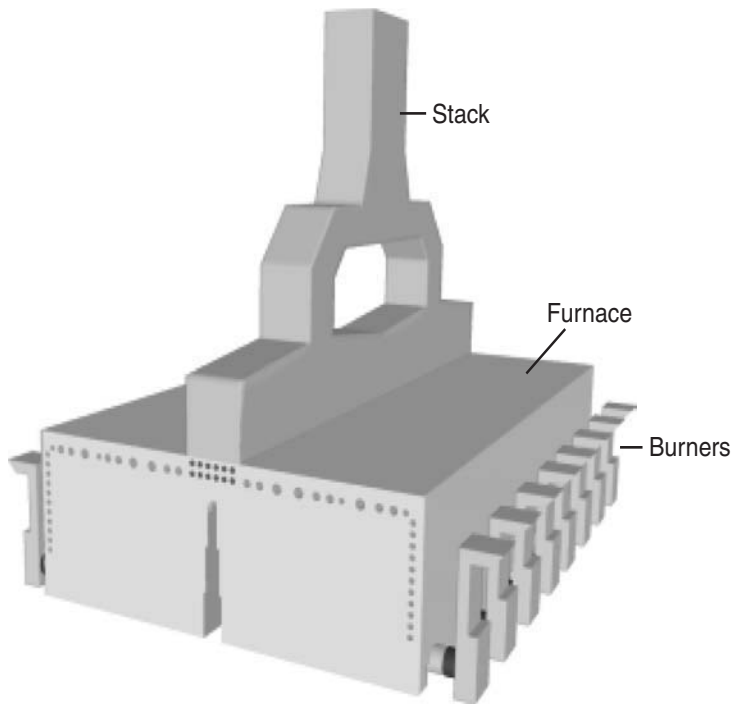


FIGURE 5.2 Outside view of a typical industrial furnace geometry with existing burners installed on furnace side with convection section and stack on top.

one of John Zink’s multi-fuel burners used in the furnace shown in Figures 5.3 and 5.4. Note that enough detail is included in each fuel tip to accurately approximate the respective flow dynamics around the refractory tile. In all cases, experience is required to understand what level of detail is required for a specific burner/furnace system. In some cases, one can avoid analyzing the full system geometry. On the other hand, one should include as much of the domain as is practically reasonable given available computer resources.

5.2.4 SELECTING BOUNDARY CONDITIONS

Before a CFD simulation is possible, the user must define the conditions around the entire boundary of the system. This means one must define what goes into and out of the system, as well as what conditions exist at the system walls. In general, these “boundary conditions” must provide adequate information to solve the governing second-order, elliptic partial differential equations describing the conservation of mass, momentum, and energy. This form of equation requires one boundary condition per order per equation. Thus, for the three momentum equations, one would need to specify two boundary conditions per equation. Typically, this would include inlet velocity and either the velocity at the wall or the centerline velocity (for axisymmetric geometries). The inlet velocity is a fixed or “Dirichlet”-type boundary condition. The wall condition would also be a fixed boundary condition while the centerline condition would be a flux or “Neumann”-type boundary condition. The same is true for the mass and energy equations. In general, the following boundary conditions are required to fully specify a system:

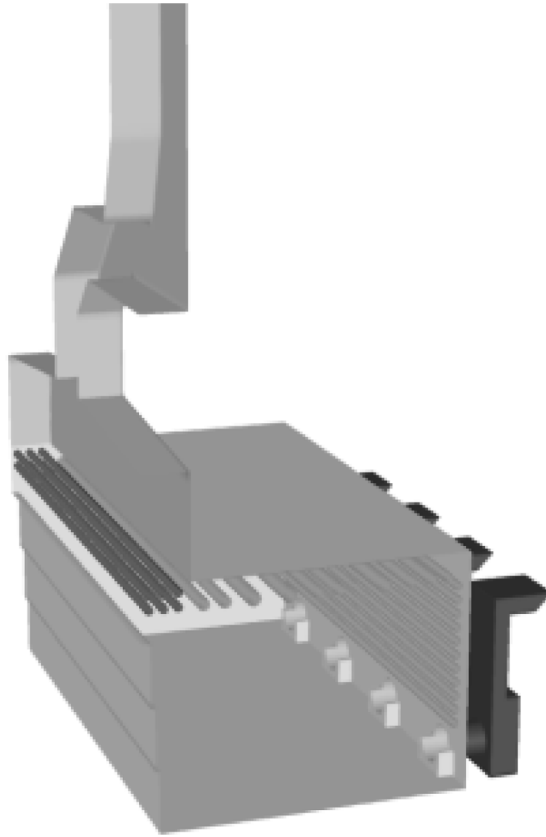


FIGURE 5.3 After applying natural symmetry planes, this view shows the actual section (1/4 entire furnace/ burner system) to be modeled.

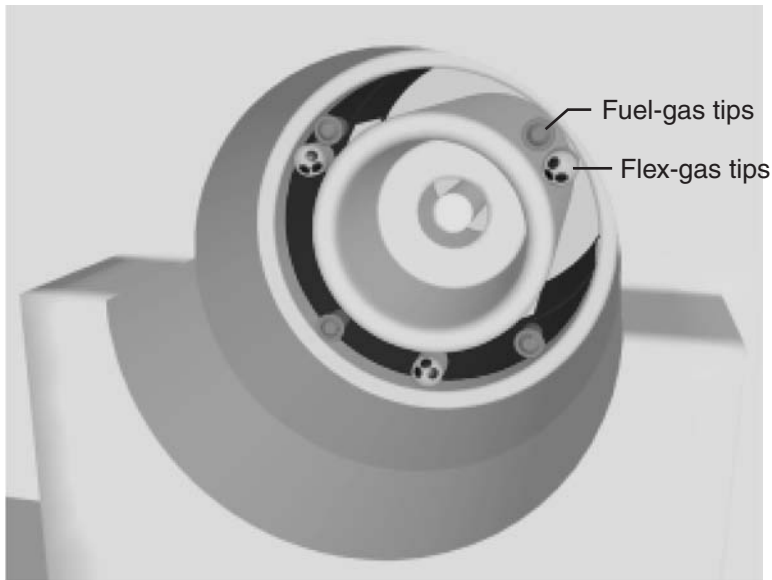


FIGURE 5.4 Detailed front view of one of John Zink's multi-fuel burners. Note the fuel-gas tips shown adjacent to the flex-gas tips. Note the local detail included in the fuel tips of this burner model.

1. All inlet streams must be characterized. Specific information should include mass flow rates, compositions, pressures, and temperatures. When a stream is composed of gas/liquid (as in atomization) or gas/solid (as in pulverized coal combustion), the relative percentage of each phase would also be required, as would information on droplet or particle size distribution.
2. Standard operating conditions for the reactor or furnace should be specified. This includes the system pressure, wall thermal properties such as thermal conductivity, construction materials (e.g., refractory, bare steel, water wall), refractory thickness, external wall temperatures, and internal wall radiative properties (e.g., surface emissivity and in some cases surface roughness).
3. Outlet conditions can also be set, including a flux condition for velocity (parallel exit flow, which means no velocity gradients at the exit). An exit pressure condition may be set as well.

5.2.5 NUMERICAL ANALYSIS AND COMPUTATIONAL MESHES

Closed-form mathematical relationships (either of a partial differential or integral form) that describe the general conservation equations are central to the simulation of engineering problems. These systems of nonlinear equations may have bifurcated solutions for a particular domain and set of boundary conditions. Simple analytical solutions to these theoretical relationships are most often intractable for anything other than very simple geometries and, therefore, offer very little practical value. To obtain a solution, the mathematical expressions must be reduced to simplified but analogous discrete algebraic equations that require solution at discrete points representing specific sub-volumes of the overall computational domain.⁷ This replacement of “continuum” equations with those utilizing discrete numbers is referred to as discretization. Hence, the simulation becomes possible with the associated computational load related to the number of discrete points where values of conserved scalars are calculated in the general domain. These discrete points are referred to as grid points and the collection of grid points represents a computational mesh. Once the calculation within the domain is broken down into these discrete points, the closed-form of the mathematical expressions can be expressed as a series of algebraic equations. This allows for numerical solution of the various flow-field variables at each of the grid points. For definition, if the partial differential equation form of the conservation relationships is used, the resulting methodology is known as a finite difference scheme. If the integral form of the equations is used, the resulting technique is known as the finite volume method. A third form of discretization, known as finite elements, also exists but is not part of this discussion.

The arrangement of the discrete points mentioned above is referred to as the computational mesh or grid and provides a segmented approximation of the system geometry to be analyzed or simulated by a CFD model. The density or number of grid points in any one portion of the computational domain should be sufficient to resolve the important geometric features, as well as capture the significant physics (e.g., boundary layer, shear layer, recirculation zone, reaction layer, etc.). The density of grid points typically varies from one region of the domain to another to help resolve these features. However, care must be taken to not take too large a jump in grid spacing from one section to another to maintain numerical stability. Typical expansion/contraction ratios for cells are in the range of 0.8 to 1.2. Too large a difference in neighboring grid spatial dimensions can lead to computational inaccuracy and numerical instability.

A couple of approaches are available to describe the geometry of a particular domain:⁸

1. Use regularly spaced or structured grid points with an orthogonal coordinate system.
2. Use an unstructured mesh with a boundary or body-fitted coordinate system.

Each approach handles the presence of curved surfaces differently. In the structured grid approach, the mesh is composed of hexahedral elements that simulate curved surfaces by allowing for a series of stair-steps to approximate the curve. Resolution of the curved surface depends on the

number of cells in this region. The three-dimensional elements retain their hexahedral shape but result in a curved, jagged surface. Increasing the refinement of the grid along these surfaces can reduce the impact this might have on the overall flow-field calculations; however, this will subsequently increase the computational load as cell refinements in one region of the grid are propagated into regions away from the curved surface. Another structured grid-based technique allows regularly shaped hexahedral cells to be “sliced” or “trimmed” at curved boundaries, resulting in element faces at the boundary that are irregularly shaped. Special algorithms then treat communication of flow-field information across these faces.

The use of body-fitted or unstructured grids allows for regularly shaped boundary surfaces to be more closely approximated by the grid elements that follow the curved surface using elliptic curvature. This approach reduces to a structured grid when all the domain elements are hexahedral and the edges of elements form continuous mesh lines. Unstructured grids allow the combined use of a wide variety of element shapes (e.g., tetrahedrons, pyramids, prisms, hexahedrons, and polyhedrons). This allows for the greatest amount of flexibility in approximating complex geometries.

Generally, it is acknowledged that greater grid densities (i.e., larger number of elements describing the domain) produce more accurate simulation results. However, in the particular case of unstructured grids, the quality of the mesh, which is directly related to the ability of a particular mesh to provide a reliable, robust solution, is also related to the shape of individual elements. Long, thin elements, as well as single faces with highly skewed angles or a high degree of curvature, can result in substantial errors in the calculation and cause the overall model to diverge in regions where these “bad” elements are used.

5.3 BUILDING BLOCKS OF CFD-BASED COMBUSTION MODELS

The mathematical simulation of turbulent combustion in industrial burners has been recognized as a difficult problem not only due to the numerical challenges associated with solving the differential equation set, but also the challenge of physically describing the important chemical and physical processes, such as chemistry–turbulence interactions, turbulent mixing, etc. Commercial CFD codes rely on available mathematical technology to combine knowledge of fluid mechanics with a reasonable approach to the reaction (combustion) processes. Care must be taken to maintain the scope of the simplifying approximations on an equivalent level.

CFD codes have been developed to address nonreacting flow systems, gaseous diffusion combustion, pulverized coal-fired systems, entrained flow gasification, droplet combustion, and slurry combustion or gasification. These codes typically utilize general coordinate systems to capture complex geometries common in industrial burner designs. Variation of properties can be included when deemed necessary. Symmetry planes can be used to simplify large-scale systems to reduce the computational demands required to simulate full furnaces. Models predict mean gas field properties for general three-dimensional, steady-state (and unsteady in special cases) turbulent flames (i.e., local velocity, temperature, density, and species composition). For special cases, multiphase combustion (e.g., gas/particle, gas/oil, etc.) is required. In these cases, particle/droplet properties are also computed, such as coal burnout, particle or droplet velocity, and temperature. [Figure 5.5](#) illustrates the various sub-models incorporated into a comprehensive CFD-based computer code used to simulate the relevant processes occurring inside industrial burners.

5.3.1 TURBULENT FLUID MECHANICS

5.3.1.1 Problem of Closure

The governing equations of fluid mechanics are derived from three physical laws: conservation of mass, conservation of momentum, and conservation of energy. If solving for additional species, such as required for a combustion model, conservation equations for the additional species are also required.

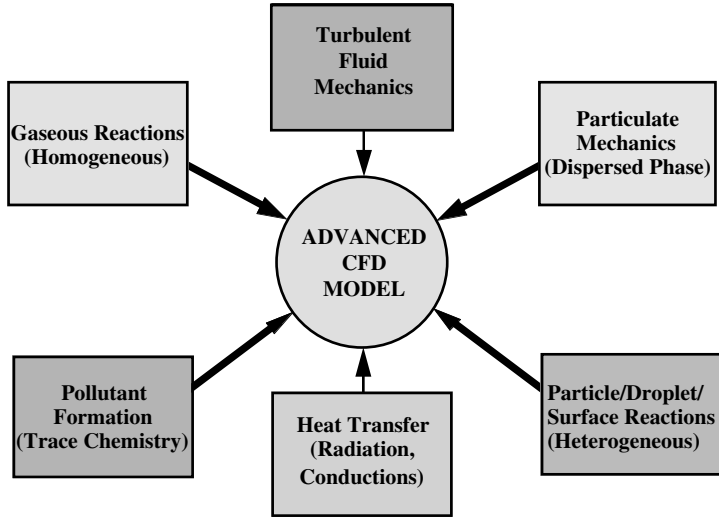


FIGURE 5.5 Typical sub-model components in comprehensive CFD code. Physical sub-models simulate specific physics involved in combustion processes that occur in industrial burners.

A conservation equation for each specie can be derived by performing a mass balance for that specie. Equations 5.1, 5.2a, 5.2b, and 5.3 show the continuity (conservation of mass), momentum equations, and species transport equations in Cartesian tensor form, respectively.

$$\frac{\partial(\rho u_i)}{\partial x_i} = 0 \quad (5.1)$$

$$\frac{\partial(\rho u_i u_j)}{\partial x_j} = -\frac{\partial P}{\partial x_i} + \frac{\partial \tau_{ij}}{\partial x_j} + \rho g \quad (5.2a)$$

$$\tau_{ij} = \mu \left(\frac{\partial u_i}{\partial x_j} + \frac{\partial u_j}{\partial x_i} \right) + \lambda \frac{\partial u_k}{\partial x_k} \delta_{ij} \quad (5.2b)$$

$$\frac{\partial(\rho \Phi u_j)}{\partial x_j} = \frac{\partial}{\partial x_j} \left(\Gamma_\Phi \frac{\partial \Phi}{\partial x_j} \right) + S_\Phi \quad (5.3)$$

where:

τ_{ij} = viscous stress tensor

δ_{ij} = Kronecker delta ($\delta_{ij} = 0$, when $i \neq j$)

μ = molecular viscosity of the fluid

λ = coefficient of bulk viscosity of the fluid

Φ = transported variable (chemical species, enthalpy, etc.)

Γ_Φ = molecular diffusion coefficient for Φ

S_Φ = source term for Φ

ρ = density of the fluid

P = static pressure

g = acceleration of gravity

White⁹ provides background information on the coefficient of bulk viscosity, and it remains a controversial quantity. Wilcox¹⁰ advises setting $\lambda = -\frac{2}{3}\mu$, which he says has been proven correct for monatomic gases, but White states that the kinetic theory actually assumes rather than proves this. Whatever the case, Wilcox states that the bulk viscosity of $\lambda = -\frac{2}{3}\mu$ is generally used in standard computational fluid dynamic (CFD) codes.

There are several characteristics that can be used to describe turbulence, as given by Tennekes and Lumley.¹¹ Turbulence flows are random and irregular, which makes deterministic methods very difficult. Turbulent diffusivity is almost always much larger than molecular diffusivity. This results in much higher rates of momentum, heat, and mass transfer for turbulent flows, as opposed to laminar flows. Turbulence is characterized by three-dimensional vorticity fluctuations. Turbulent vorticity fluctuations could not be maintained without vortex stretching, and vortex stretching does not occur in two-dimensional flows. Therefore, by nature, all turbulent flows are three-dimensional — turbulence is dissipative. Viscous shear stresses convert the turbulent kinetic energy of the fluid into internal energy. Therefore, turbulence needs a continuous supply of energy to replace the losses of viscous dissipation. Finally, turbulence occurs over a continuum and is governed by the continuum equations of fluid mechanics. The smallest turbulent scales are ordinarily much larger than molecular scales.

As mentioned, randomness and irregularity characterize turbulence. To characterize turbulence mathematically, quantities such as velocities, pressures, temperatures, etc. are expressed as having mean and fluctuating components. From a computational point of view, it is desirable to compute averaged quantities and, therefore, it is desirable to express the governing equations (Equations 5.1 through 5.3) in terms of average quantities. To do this, instantaneous values of quantities are put into the governing equations, and then the governing equations are averaged in some fashion. Because Equations 5.2 and 5.3 are nonlinear, averaging the equations results in unknown quantities ($\overline{u'_i u'_j}$ and $\overline{u'_i \Phi'}$). These unknown quantities must then be modeled. For most engineering applications, a semi-empirical turbulence model is used to compute the unknown quantities.

5.3.1.2 Favre and Reynolds Averaging

Turbulent transport occurs in the momentum, energy, and specie transport equations, and a turbulence closure model is required to correctly model the turbulent transport terms in each equation. At this point, the governing equations (Equations 5.1 through 5.3) plus any additional transport equations should be averaged in some fashion to determine the transport terms resulting from turbulence. It is assumed that the dependent variables in the governing equations are comprised of an average term plus a fluctuating term. There are two methods for averaging the equations: Reynolds averaging and Favre averaging. Wilcox² provides a good review of both methods. Favre averaging is applicable when compressibility is an important issue. Morkovin¹² hypothesized that the effects of density fluctuations on turbulence are insignificant, provided that the fluctuations are small relative to the mean density, $\frac{\rho'}{\bar{\rho}} \ll 1$. It is clear that for flows with combustion and/or significant heat transfer, the density fluctuations are not small relative to the mean density. Therefore, for modeling flows with combustion, Favre averaging is clearly preferable, as confirmed by Wilcox. Favre averaging of velocity is defined by Equation 5.4:

$$\tilde{u}_i = \frac{1}{\bar{\rho}} \lim_{T \rightarrow \infty} \int_0^{i+T} \rho u_i dt \quad (5.4)$$

Averaging of other transported variables, such as enthalpy or a chemical species, is done in a similar fashion to Equation 5.4. It should be noted for Favre averaging that the fluctuating velocities are denoted by double primes, $u_i = \tilde{u}_i + u_i''$; and, because products of velocity and density are

averaged, $\overline{u_i''} \neq 0$, but $\overline{\rho u_i''} = 0$. The Favre averaged mean continuity and momentum equations are given by Equations 5.5 and 5.6.

$$\frac{\partial(\overline{\rho \tilde{u}_i})}{\partial x_i} = 0 \quad (5.5)$$

$$\frac{\partial(\overline{\rho \tilde{u}_i \tilde{u}_j})}{\partial x_j} = -\frac{\partial \overline{P}}{\partial x_i} + \frac{\partial}{\partial x_j} \left(\overline{\tau_{ij}} - \overline{\rho u_j'' u_i''} \right) + \overline{\rho} g \quad (5.6)$$

The Favre-averaged Reynolds stress tensor is given by $\tau_{ij} = -\overline{\rho u_j'' u_i''}$.

5.3.1.3 Turbulence Models

There are generally four types of turbulence models commonly used in engineering practice:

1. Algebraic models
2. One-equation models
3. Two-equation models
4. Second-order closure models

Wilcox² and Rodi¹³ provide good reviews of various methods of turbulence modeling. Most of the models that fall into one of the first three categories have an underlying commonality; that is, the Boussinesq approximation. The Boussinesq approximation assumes that the Reynolds-stress tensor is proportional to the mean strain-rate tensor for every location in a turbulent flow. The constant of proportionality between the Reynolds-stress tensor and the mean strain-rate tensor is the eddy viscosity (μ_T).

5.3.1.3.1 Algebraic Models

Many algebraic models calculate an eddy viscosity from the Prandtl mixing-length hypothesis, given by Equation 5.7.

$$\mu_T = \rho (l_m^2) \left| \frac{\partial U}{\partial y} \right| \quad (5.7)$$

where:

- l_m = mixing length
- U = mean velocity

Algebraic models are not very general because the mixing length depends on the flow scenario (i.e., jet, boundary layer, pipe flow, etc.). Therefore, an expression for the mixing length must be obtained for each type of flow when using an algebraic model.

5.3.1.3.2 One- and Two-Equation Models

One-equation and two-equation models attempt to overcome the difficulties with the Prandtl mixing-length hypothesis by solving transport equations for quantities that are related to the type of flow. In the above-mentioned algebraic model, there is a direct link between the fluctuating velocity scale and the mean velocity gradients, as shown by Equation 5.7. In one-equation and two-equation models, the link between the fluctuating velocity scale and the mean velocity gradients is found by solving one or more transport equations. Wilcox² describes two, more recent one-equation turbulence models that appear to show promise. The Baldwin-Barth¹⁴ model employs a transport equation for the turbulent Reynolds number and the Spalart-Allmaras¹⁵ model employs a transport equation for the eddy viscosity.

Prandtl chose the turbulent kinetic energy as the basis for a turbulent velocity scale shown in Equation 5.8. The eddy viscosity can be computed using the Kolmogorov-Prandtl expression given by Equation 5.9.

$$k = \frac{1}{2} \overline{u'_i u'_i} = \frac{1}{2} (\overline{u'^2} + \overline{v'^2} + \overline{w'^2}) \quad (5.8)$$

$$\mu_T = C_1 \rho \sqrt{kl} \quad (5.9)$$

where:

- k = turbulent kinetic energy
- l = turbulence length scale
- C_1 = constant of proportionality

Wilcox² provides a derivation of the Reynolds-stress equation, obtained by taking moments of the Navier-Stokes equation. The Reynolds-stress equation is a tensor equation and, by taking the trace of it, a transport equation is obtained for turbulence kinetic energy. This transport equation for the turbulence kinetic energy forms the basis for a number of one- and two-equation turbulence models. The turbulence kinetic energy transport equation has various terms that have been given physical interpretations. Included in the terms is a dissipation term (ϵ), which represents the rate at which turbulence kinetic energy is converted to thermal internal energy. From the turbulence kinetic energy equation, ϵ is the product of the viscosity and the square of the fluctuating vorticity. Therefore, based on dimensional arguments, the dissipation (ϵ) should be related to the turbulence kinetic energy and length scale as shown in Equation 5.10:

$$\epsilon = \frac{C_2 k^{3/2}}{l} \quad (5.10)$$

where C_2 = constant of proportionality.

5.3.1.3.3 k - ϵ Turbulence Model

Perhaps the most commonly used turbulence model for practical flow problems is the k - ϵ model. The earliest developments related to the k - ϵ model were by Chou,¹⁶ Davidov,¹⁷ and Harlow and Nakayama.¹⁸ The most well-known paper on the k - ϵ model is that of Jones and Launder,¹⁹ which according to Wilcox² has almost reached the status of the Boussinesq and Reynolds papers within the turbulence modeling community. The k - ϵ model is based on the turbulence kinetic energy transport equation discussed above, and a second transport equation for the dissipation rate. The equation for the dissipation rate (ϵ) is derived by taking a moment of the Navier-Stokes equation using the fluctuating vorticity. The resulting equation is a relatively complicated equation, which Wilcox² states needs “drastic surgery” to make it practical. The Standard k - ϵ model is shown below by Equations 5.11 through 5.13:

$$\rho U_j \frac{\partial k}{\partial x_j} = \tau_{ij} \frac{\partial U_i}{\partial x_j} - \rho \epsilon + \frac{\partial}{\partial x_j} \left[\left(\mu + \frac{\mu_T}{\sigma_k} \right) \frac{\partial k}{\partial x_j} \right]: \text{ Turbulence Kinetic Energy} \quad (5.11)$$

$$\rho U_j \frac{\partial \epsilon}{\partial x_j} = C_{\epsilon 1} \frac{\epsilon}{k} \tau_{ij} \frac{\partial U_i}{\partial x_j} - C_{\epsilon 2} \rho \frac{\epsilon^2}{k} + \frac{\partial}{\partial x_j} \left[\left(\mu + \frac{\mu_T}{\sigma_k} \right) \frac{\partial \epsilon}{\partial x_j} \right]: \text{ Dissipation Rate} \quad (5.12)$$

$$\mu_T = \frac{C_\mu \rho k^2}{\epsilon}: \text{ Eddy Viscosity} \quad (5.13)$$

The eddy viscosity relationship (Equation 5.13) follows from combining Equations 5.9 and 5.10. The empirical closure coefficients given by Wilcox² are shown below:

$$C_{\varepsilon 1} = 1.44, \quad C_{\varepsilon 2} = 1.92, \quad C_{\mu} = 0.09, \quad \sigma_k = 1.0, \quad \sigma_{\varepsilon} = 1.3 \quad (5.14)$$

The optimal closure coefficients will vary somewhat, depending on the application and what investigators have found the coefficients should be to agree with experimental results. Therefore, the coefficients shown in Equation 5.14 are not universally optimal, and any CFD results obtained using the k - ε turbulence model should be closely scrutinized.

5.3.1.3.4 k - ε Turbulence Model Boundary Conditions

Establishing boundary conditions for the k - ε turbulence model results from an order of magnitude analysis of the boundary layer momentum equation in the log layer. The log layer is an overlap region between the viscous sublayer and the defect layer, where the law of the wall applies. An order of magnitude analysis of the boundary layer momentum equation suggests that convection, pressure gradient, and molecular diffusion terms can be neglected. Applying these simplifications to the transport equations for k and ε (Equations 5.13 and 5.14) results in relations for k and ε at the boundaries, which are referred to as wall functions. The standard wall functions are given by Equations 5.17 and 5.18:

$$k = \frac{u_{\tau}^2}{\sqrt{C_{\mu}}}: \quad \text{Standard Wall Functions for } k \quad (5.17)$$

$$\varepsilon = \frac{k^{3/2} C_{\mu}^{3/4}}{\kappa y}: \quad \text{Standard Wall Functions for } \varepsilon \quad (5.18)$$

where:

u_{τ} = friction velocity

$$u_{\tau} = \sqrt{\frac{\tau_w}{\rho}}$$

τ_w = wall shear stress

κ = Kármán constant ($\kappa \approx 0.4$)

y = distance measured normal from the wall

The wall functions (Equations 5.15 and 5.16) are applied to the node adjacent to the wall, which should lie within the log layer region. The law of the wall equation (Equation 5.19) is used to find the friction velocity (u_{τ}) at the node adjacent to the wall, and then the wall functions are used to specify k and ε :

$$U = u_{\tau} \left[\frac{1}{\kappa} \ln \left(\frac{u_{\tau} y}{\nu} \right) + B_1 \right] \quad (5.19)$$

where:

U = mean velocity

ν = kinematic viscosity

B_1 = constant

If the surface is smooth, Equation 5.19 should be used; however, if the surface is not smooth, an equation equivalent to Equation 5.19 is given by Equation 5.20, and was developed by Nikuradse.

Equations 5.19 and 5.20 are given in most engineering fluid mechanics texts, such as Roberson and Crowe.²⁰

$$U = u_{\tau} \left[\frac{1}{\kappa} \ln \left(\frac{y}{k_s} \right) + B_2 \right] \quad (5.20)$$

where:

k_s = surface roughness height

B_2 = constant

Wilcox² notes that numerical solutions are sensitive to the location of the node adjacent to the surface and recommends using near-wall grids. Another potential problem with using wall functions is that theoretically they do not apply for flows that separate from the wall. Finally, Wilcox points out that the standard k - ϵ model with standard wall functions does not perform well for boundary layers with adverse pressure gradients. Kim and Choudhury²¹ have proposed modifications to the standard k - ϵ wall functions to account for adverse pressure gradient.

5.3.1.4 Other Turbulence Modeling Approaches

The vorticity that characterizes turbulent flow has a large range of length and time scales that can exist in relatively close proximity to one another. When Reynolds-averaged Navier-Stokes (RANS) equations are utilized to simulate turbulent flow, all of the turbulent fluctuations are modeled using algebraic approximations rather than directly calculated, which results in a significant reduction in computational requirements. Various other approaches exist that are used to compute the turbulent relationships that exist in flowing systems. Two of the more popular methodologies are known as direct numerical simulation (DNS) and large-eddy simulation (LES).²²

DNS looks at solving the Navier-Stokes equations over the complete range of time and length scales present in a particular system. Perhaps the greatest issue with DNS is that the computational domain must be large enough to accommodate the largest length scales present, with a grid small enough to allow for resolution of the smallest scales where kinetic energy dissipation occurs. This criterion ensures that the number of grid points required to solve a problem of practical size will be quite large as compared to more conventional RANS-type calculations. By way of example, the number of grid points required in each direction of a three-dimensional calculation is proportional to $Re^{3/4}$, the Reynolds Number based upon the magnitude of the velocity fluctuations and the integral scale. Hence, for $Re = 10^6$ (which is not unusual for flows in typical engineering systems), the resulting grid requirement for a three-dimensional simulation would be on the order of 10^{15} . While the results of such calculations would contain very useful information, the current limits of available computer hardware make routine use of this approach to solve practical engineering problems prohibitive. In addition to the large grid requirements, the time scales required for this approach are constrained to very small time steps to capture the fluctuations at the very small end of the range, which further increases the computational load. Currently, DNS is used to solve small, low-Reynolds number flow circumstances based upon simple geometries.

Large-eddy simulation (LES) is positioned between DNS and the RANS approaches. This approach separates the range of length scales (eddies) into two groups. The first consists of relatively large eddies that can be numerically simulated and represent the majority of the turbulent energy. These are generally constrained more by boundary conditions and domain geometries. The second group is comprised of small eddies, which are more influenced by molecular viscous forces. The second group tends to be more isotropic and, therefore, it is easier to justify the use of numerical approximations to model them. Hence, the simulation rationale focuses on the direct resolution of the large eddies and filtering out eddies smaller than some lower limit or smaller than the local grid resolution and allowing them to be modeled. A significant issue related to the utilization of the LES

approach is the “communication” that must occur between the simulation of the two groups as large eddies degrade into smaller ones. The impact this has on grid requirements is that much coarser grids than are required by DNS can be used, although the grid requirements for LES are still much greater than for the Reynolds-/Favre-averaged approaches. Recent improvements in computer hardware performance have allowed this approach to be considered for engineering analysis.

5.3.2 HOMOGENEOUS CHEMISTRY

In general, the mathematical modeling of combustion processes includes the simulation of several physical and chemical processes in reacting flows. The modeling of any reacting or combustion process in a turbulent flow field can, at the very least, be called challenging. What can be observed as a flame is the result from interaction of convection and molecular diffusion with many chemical reactions and very small length and time scales. In general, a differentiation has to be made for types of flames as there are:

- Premixed flames
- Partially premixed flames
- Nonpremixed or diffusion flames

Depending on the Reynolds, Damkoehler, and Karlovitz numbers, a further separation has to be made in laminar, turbulent, wrinkled, corrugated flames, and homogeneous reaction zones.²³ Because almost every flow regime in a technical combustion application is highly turbulent, the laminar flame modeling will not be included in this discussion. Further information on laminar reaction systems can be found in Kee,^{24,25} Glarborg,²⁶ and Rogg.^{27–29}

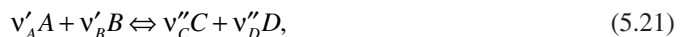
The type of turbulent flame determines the combustion sub-model to be used. For premixed flames, the models available include:

- Progress variable C
- Transport equation for the flame front G
- Eddy breakup (EBU), eddy dissipation combustion model (EDX), and the eddy dissipation concept (EDC)
- Partially premixed presumed pdf model with equilibrium chemistry

For nonpremixed combustion, the models available include:

- Presumed pdf with equilibrium chemistry (adiabatic and nonadiabatic)
- Presumed pdf with finite rate chemistry (flamelet model)
- Eddy dissipation and eddy dissipation combustion model

The general form for a reaction with educts A and B and the products C and D can be written as:



where v is the stoichiometric coefficient.

For example, in methane combustion, the global one-step formulation would be:



The reaction rate can formally be written as the product of the reaction rate coefficient and all participating species:

$$r_i = \left(\frac{dc_i}{dt} \right) = kc_1^{a_1} c_2^{a_2} c_3^{a_3} \dots c_N^{a_N} \quad (5.23)$$

with the reaction coefficient k , the reaction order a , and the species c_i , where the concentration of each species i is defined as:

$$c_i = \frac{\rho_i Y_i}{M}, \quad (5.24)$$

with M as the mean molar mass of the mixture. The rate coefficient k can be written in general form as:

$$k = AT^m e^{\left(-\frac{E_A}{RT}\right)}, \quad (5.25)$$

with R as the gas constant (8.3143 kJ/mole-K). The parameters here are the pre-exponential Arrhenius factor A , the temperature exponent m , and the activation energy E_A .

The final formulation for a concentration change of species i , over all elementary reactions k , can be formulated as:

$$\frac{\partial c_i}{\partial t} = \sum_{k=1}^M (v''_{i,k} - v'_{i,k}) (AT^a)_k \exp\left(-\frac{E_k}{RT}\right) \prod_{j=1}^N \left(\frac{\rho Y_j}{W_j}\right)^{v_{j,k}} \quad (5.26)$$

or written as reaction rate:

$$\frac{\partial c_i}{\partial t} W_i = \dot{Y}_i = W_i \sum_{k=1}^K v_{ik} r_k \quad (5.27)$$

And, finally, the additional source term for the equation for energy conservation. The total released energy can be written as the sum of the product of reaction enthalpy H and the concentration change of species i :

$$q_r = \sum_{k=1}^K q_k = \sum_{k=1}^K -\left(\frac{\Delta H_k}{v_{i,k}}\right) \cdot \left(\frac{dc_i}{dt}\right)_k = -\sum_{i=1}^N h_i \omega_i \quad (5.28)$$

The equation governing species transport is:

$$\frac{\partial}{\partial t} \rho Y_i + \nabla \cdot (\rho \bar{u} Y_i) = \nabla \cdot (\rho D_i \nabla Y_i) + \dot{Y}_i, \quad (5.29)$$

where \dot{Y}_i is the source term of the species i . The determination of that source term can be done according to aforementioned equations, or due to the complexity and number of involved species using approaches, which reduce the computational effort — as, for example, the EBU, EDX, and EDC models.

The eddy breakup model (EBU) was developed by Spalding³⁰ for the calculation of turbulent, premixed flame with irreversible one-step reaction. The assumption was that the rate of reaction is totally controlled by dissipation of eddies either containing unburned fuel or burned hot gases. The reaction rate of the unburned mixture \dot{Y}_F , as used in Equation 5.29, is determined by the decay rate of these eddies:

$$\dot{Y}_{F,\text{eddy}} = C(1 - \tau) \rho \left| \frac{du}{dy} \right|, \quad (5.30)$$

following the mixing length hypothesis.

To estimate the actual rate of fuel consumption, we have to take into account the kinetically controlled reaction rate as defined by:

$$\dot{Y}_{F,\text{kin}} = AY_F Y_{\text{O}_2} \exp(-E_A/RT), \quad (5.31)$$

where A is the pre-exponential factor, E_A is the activation energy, and R is the universal gas constant. The actual rate of fuel consumption can be determined by:

$$\dot{Y}_{F,\text{actual}} = \frac{1}{\tau \dot{Y}_{\text{kin}} + \dot{Y}_{\text{eddy}}} \quad (5.32)$$

The major drawback of this approach is the assumption of homogeneous distribution and perfect mixing of fuel and oxidant. The formulation would only be valid for a turbulent, premixed flame with homogeneous distribution of fuel/air and flue gas pockets.

A development of the EBU model is the eddy dissipation combustion model (EDX) formulated by Magnussen.³¹ He takes into account the unmixedness of fuel and oxidizer and postulates that the rate of combustion will be determined by the turbulent intermixing of fuel and oxygen eddies on a molecular scale; or, in other words, by dissipation of these eddies. The reaction rate can be written in general form as:

$$\dot{Y}_i = C \bar{Y}_i \frac{\epsilon}{k}, \quad (5.33)$$

where C is a constant depending on the structure of the flame, and \bar{Y}_i is the time-averaged concentration. This approach acknowledges the distribution and unmixedness of fuel oxidizer and hot products, and is therefore also valid for the calculation of nonpremixed flames. The actual reaction rate is determined by the minimum of the following criteria:

1. The reaction rate is determined by the concentration of fuel:

$$\dot{Y}_F = A \bar{Y}_F \frac{\epsilon}{k}, \quad (5.34)$$

where $A = 4.0$ and Y_F is the time-averaged fuel concentration.

2. The reaction rate is determined by the concentration of oxygen:

$$\dot{Y}_{\text{O}_2} = A \frac{\bar{Y}_{\text{O}_2}}{r_{\text{O}_2}} \frac{\epsilon}{k}, \quad (5.35)$$

with Y_{O_2} the local mean oxygen concentration and r_{O_2} the stoichiometric oxygen requirement.

3. The reaction rate is limited by the presence of hot products:

$$\dot{Y}_{\text{Pr}} = AB \frac{\bar{Y}_{\text{Pr}}}{1 + r_{\text{O}_2}} \frac{\epsilon}{k}, \quad (5.36)$$

with $A = 4.0$, $B = 0.5$, Y_{Pr} the local mean product concentration, and r_{O_2} the stoichiometric oxygen requirement.

The disadvantage of this approach is the fact that global reactions still have to be used. An extension of these models is the eddy dissipation concept (EDC).³² This model is still based on eddy dissipation along the turbulent energy cascade, but differentiates between areas of chemical reaction, the so-called fine structure region, and their surrounding nonreactive regions. These fine structures are situated at the end of the turbulent energy cascade. Their length scale is that of eddies in the Kolmogorov scale, where the species are mixed on a molecular level and react as the energy level meets their respective activation energy. The chemistry inside these fine structures can be treated as a perfectly stirred reactor.

This model takes into account that the dissipation is not homogeneously distributed in the computational domain, but takes place mainly in strained areas, the separating area from the reacting and nonreacting volumes. Magnussen proposes the following definition for the mass fraction contained in these fine structures:

$$\gamma = (u^*/u')^3, \quad (5.37)$$

where u^* is the characteristic velocity of the fine structure and u' is the turbulent velocity. Any mass transfer from surrounding nonreacting fluid into these fine structures follows the expression:

$$\dot{m} = 2 \frac{u^*}{L^*} \gamma^*, \quad (5.38)$$

where the characteristic velocity u^* and the characteristic length L^* can be expressed by:

$$u^* = 1.74(\nu\varepsilon)^{1/4} \quad (5.39)$$

and

$$L^* = 1.43\nu^{3/4}/\varepsilon^{1/4}, \quad (5.40)$$

where ν is the kinematic viscosity and ε is the rate of dissipation of turbulent energy. Assuming isotropic turbulence, the mass fraction of the fine structure and the mass transfer between the fine structure and the surrounding can be written as:

$$\gamma^* = 9.7 \left(\frac{\nu\varepsilon}{k^2} \right)^{3/4} \quad (5.41)$$

and for the mass transfer:

$$\dot{m} = 23.6 \left(\frac{\nu\varepsilon}{k^2} \right)^{1/4} \frac{\varepsilon}{k} \quad (5.42)$$

If we assume that the reactions inside the fine structures are infinitely fast, the mass transfer between the surrounding fluid and the fine structure itself limits the reaction rate. Thus, the rate of reaction can be written as depending on the mass transfer:

$$\dot{Y}_F = 23.6 \left(\frac{\nu\varepsilon}{k^2} \right)^{1/4} \frac{\varepsilon}{k} \bar{Y}_{\min}, \quad (5.43)$$

where Y_{\min} is the smallest concentration of Y_F or Y_{O_2} , limiting the reaction rate. It cannot be assumed that all fine structures are on the same temperature level, so the concentration of hot products must be taken into account. A correction factor:

$$\chi = \frac{\bar{Y}_{Pr}/(1+r_{O_2})}{\bar{Y}_{Pr}/(1+r_{O_2}) + Y_F} \quad (5.44)$$

is introduced and the final expression for the reaction rate becomes:

$$\dot{Y}_F = 23.6 \left(\frac{\nu \epsilon}{k^2} \right)^{1/4} \frac{\epsilon}{k} \chi \bar{Y}_{\min} \quad (5.45)$$

The main advantage of this approach is the possibility of including elementary reactions to describe the kinetics within the fine structures. Because any given set of reactions has only to be solved within these small regions, the computational time can be reduced significantly. Another method for the calculation of reacting flows is the mixture fraction approach.

5.3.2.1 Mixture Fraction Approach for Equilibrium or Nonequilibrium Chemistry

For nonpremixed or diffusion flames, one approach is using the presumed probability density function (ppdf) model, with or without equilibrium chemistry. Assuming that the chemistry is one-step, infinitely fast and irreversible (equilibrium chemistry), with equal diffusivities, this model can be interpreted as a zero-dimensional, perfectly stirred reactor with infinity residence time. The input for the PSR is given by the local value of the mixture fraction. Because the enthalpy is fixed by the mixture fraction, the temperature can be obtained using:

$$h_i = h_{f,i}^0 + \int_{T_0}^T cp_i(T) dT, \quad (5.46)$$

and

$$h = \sum Y_i h_i \quad (5.47)$$

with T_0 as reference temperature and $h_{f,i}^0$ the enthalpy of formation of species i . Values for $h_{f,i}^0$ can be found in [Table 5.2](#). The results of these calculations can be stored in look-up tables and used afterward from the CFD code to determine the concentration distribution within the computational domain. This approach is often applied to turbulent flames using a presumed pdf for the mixture fraction. The schematics for an adiabatic calculation are shown in [Figure 5.6](#).^{33,34}

The mixture fraction Z is defined as an element mass fraction of matter originating from the fuel stream. It is a so-called conserved scalar because elements are conserved during combustion and it is not directly influencing the underlying fluid mechanics. The element mass fraction of an element i in an N -species mixture is:

$$Z_i = \sum_{j=1}^N a_{ji} Y_j \frac{M_i^{\text{atom}}}{M_j}, \quad (5.48)$$

where a_{ji} is the number of atoms I in species j , M_j is the molecular weight of species j , and M_i^{atom} is the atomic mass of atom i . The mixture fraction Z is defined as linear combination of Z_i , where it is 0

TABLE 5.2
Standard State Values at $T = 298.15\text{K}$

Species	ΔH_f° (kJ/mol)	S° (J/K·mol)	ΔG_f° (kJ/mol)
Carbon			
C(s, graphite)	0	5.74	0
C(s, diamond)	1.895	2.377	2.9
C(g)	716.682	158.096	671.257
CH ₄ (g, methane)	-74.81	186.264	-50.72
C ₂ H ₂ (g, ethyne)	226.73	200.94	209.2
C ₂ H ₄ (g, ethene)	52.26	219.56	68.15
C ₂ H ₆ (g, ethane)	-84.68	229.6	-32.82
C ₃ H ₈ (g, propane)	-103.8	269.9	-23.49
C ₄ H ₁₀ (g, butane)	-888		
C ₆ H ₆ (l, benzene)	49.03	172.8	124.5
C ₆ H ₁₄ (l)	-198.782	296.018	-4.035
C ₈ H ₁₈ (l)	-249.952	361.205	6.707
CH ₃ OH(l, methanol)	-238.66	126.8	-166.27
CH ₃ OH(g, methanol)	-200.66	239.81	-161.96
C ₂ H ₅ OH(l, ethanol)	-277.69	160.7	-174.78
C ₂ H ₅ OH(g, ethanol)	-235.1	282.7	-168.49
CH ₃ COOH(l)	-276.981	160.666	-173.991
CO(NH ₂) ₂ (s, urea)	-333.5	104.6	-197.4
CO(g)	-110.525	197.674	-137.168
CO ₂ (g)	-393.509	213.74	-394.359
CS ₂ (g)	117.36	237.84	67.12
Hydrogen			
H ₂ (g)	0	130.684	0
H(g)	217.965	114.713	203.247
H ⁺ (g)	1536.202	—	—
H ₂ O(l)	-285.83	69.91	-237.129
H ₂ O(g)	-241.818	188.825	-228.572
H ₂ O ₂ (l)	-187.78	109.6	-120.35
Nitrogen			
N ₂ (g)	0	191.61	0
N(g)	472.704	153.298	455.563
NH ₃ (g)	-46.11	192.45	-16.45
N ₂ H ₄ (l)	50.63	121.21	149.34
NO(g)	90.25	210.76	86.55
NO ₂ (g)	33.18	240.06	51.31

(Continued)

TABLE 5.2
Standard State Values at $T = 298.15\text{K}$ (Continued)

Species	ΔH_f° (kJ/mol)	S° (J/K·mol)	ΔG_f° (kJ/mol)
Nitrogen			
$\text{N}_2\text{O}(\text{g})$	82.05	219.85	104.2
$\text{N}_2\text{O}_4(\text{g})$	9.16	304.29	97.89
$\text{HNO}_3(\text{l})$	-174.1	155.6	-80.71
$\text{HNO}_3(\text{g})$	-135.06	266.38	-74.72
$\text{HNO}_3(\text{aq})$	-207.36	146.4	-111.25
Oxygen			
$\text{O}_2(\text{g})$	0	205.138	0
$\text{O}(\text{g})$	249.17	161.055	231.731
$\text{O}_3(\text{g})$	142.7	238.93	163.2
Sulfur			
$\text{S}(\text{s, rhombic})$	0	31.8	0
$\text{S}(\text{g})$	278.805	167.821	238.25
$\text{S}_2\text{Cl}_2(\text{g})$	-18.4	331.5	-31.8
$\text{H}_2\text{S}(\text{g})$	-20.63	205.79	-33.56
$\text{SO}_2(\text{g})$	-296.83	248.22	-300.194
$\text{SO}_3(\text{g})$	-395.72	256.76	-371.06
$\text{H}_2\text{SO}_4(\text{l})$	-813.989	156.904	-690.003
$\text{H}_2\text{SO}_4(\text{aq})$	-909.27	20.1	-744.53

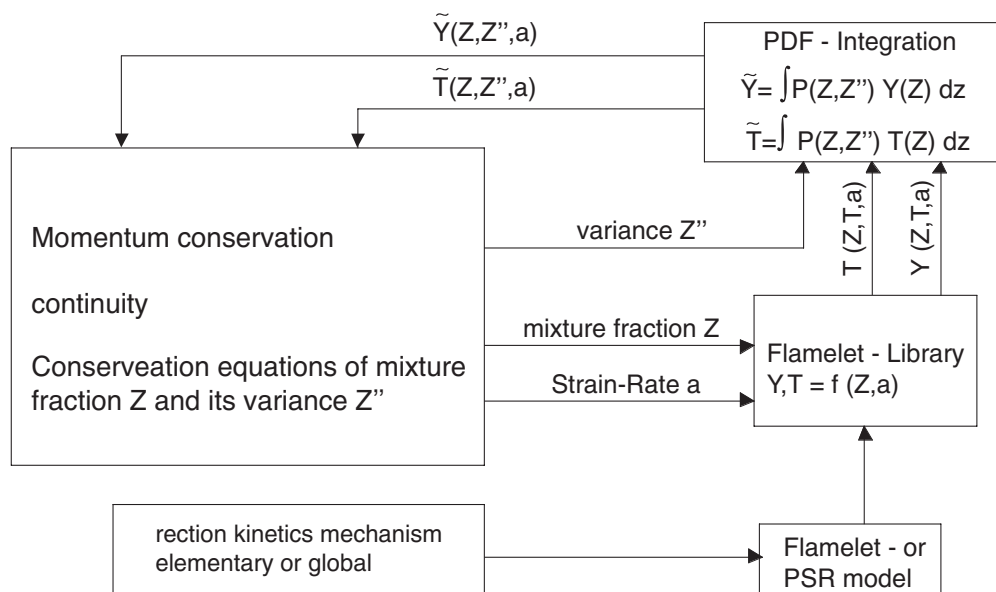


FIGURE 5.6 Application of a presumed pdf approach.

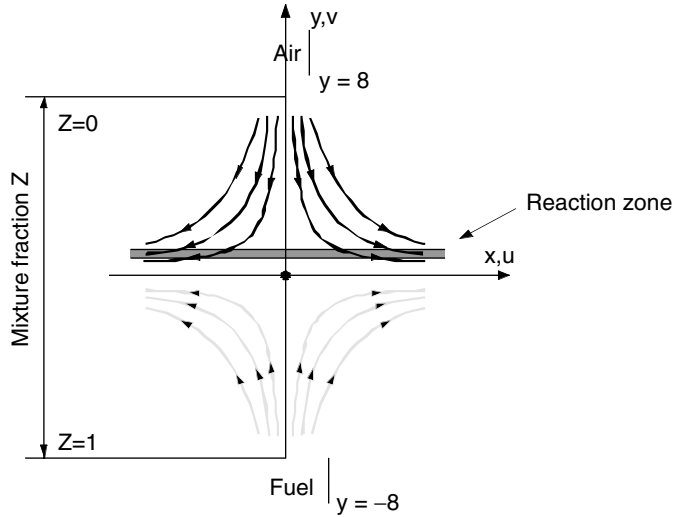


FIGURE 5.7 Illustration showing mixing process between fuel and oxidizer with resulting reaction zone.

in the oxidizer stream and 1 in the fuel stream (see [Figure 5.7](#)). In a two-feed system with a fuel stream mass flow \dot{m}_1 and an oxidizer stream mass flow \dot{m}_2 , the mixture fraction represents the mass fraction of the fuel stream locally in the unburned mixture:

$$Z = \frac{\dot{m}_1}{\dot{m}_1 + \dot{m}_2} = \frac{Z_F}{Y_{F,1}} = 1 - \frac{Z_O}{Y_{O_2,2}} \quad (5.49)$$

with $Y_{F,1}$ the mass fraction of fuel in the fuel stream and $Y_{O_2,2}$ the mass fraction of oxygen in the oxidizer stream. Z_F and Z_O are the fuel element mass fraction coming from the fuel and from the oxidizer stream, respectively. The fuel element mass fraction Z_F is equivalent to the sum of fuel atoms. In the case of hydrocarbon combustion, it is equal to:

$$Z_F = Z_C + Z_H \quad (5.50)$$

The mixture fraction in the presence of combustion can be written as:

$$Z = \frac{\nu Y_F - Y_{O_2} + Y_{O_2,2}}{\nu Y_{F,1} - Y_{O_2,2}} \quad (5.51)$$

For the case of a stoichiometric mixture with $\nu Y_F = Y_{O_2}$, the stoichiometric mixture fraction Z_{st} can be calculated from:

$$Z_{st} = \frac{Y_{O_2,2}}{\nu Y_{F,1} - Y_{O_2,2}} = \left[1 + \frac{\nu Y_{F,1}}{Y_{O_2,2}} \right]^{-1} \quad (5.52)$$

To include this approach in a CFD model, two additional equations must be solved. The first one is the conservation equation for the mixture fraction Z ; the second one is the conservation equation for the mixture fraction variance Z'' .

The transport equation for the mixture fraction Z as it is represented in a flow simulation

$$\frac{\partial(\rho u Z)}{\partial x} + \frac{\partial(\rho v Z)}{\partial y} + \frac{\partial(\rho w Z)}{\partial z} = \left(D_f + \frac{\mu_t}{Sc_f} \right) \left(\frac{\partial^2 Z}{\partial x^2} + \frac{\partial^2 Z}{\partial y^2} + \frac{\partial^2 Z}{\partial z^2} \right) \quad (5.53)$$

and the transport equation for the mixture fraction variance Z''

$$\begin{aligned} \frac{\partial(\rho u Z'')}{\partial x} + \frac{\partial(\rho v Z'')}{\partial y} + \frac{\partial(\rho w Z'')}{\partial z} - \left(D_g + \frac{\mu_t}{Sc_g} \right) \left(\frac{\partial^2 Z''}{\partial x^2} + \frac{\partial^2 Z''}{\partial y^2} + \frac{\partial^2 Z''}{\partial z^2} \right) \\ = 2 \frac{\mu_t}{Sc_g} \left(\frac{\partial Z}{\partial x} + \frac{\partial Z}{\partial y} + \frac{\partial Z}{\partial z} \right)^2 - 2\rho \frac{\epsilon}{k} g \end{aligned} \quad (5.54)$$

The pdf integration as shown in the preceding figure is commonly done using the β -pdf. The β -function is defined as:

$$\beta(\alpha, \chi) = \frac{\Gamma(\alpha)\Gamma(\chi)}{\Gamma(\alpha + \chi)}, \quad (5.55)$$

where;

$$\alpha = Z \left(\frac{Z(1-Z)}{Z''^2} - 1 \right) \quad (5.56)$$

and

$$\chi = (1-Z) \left(\frac{Z(1-Z)}{Z''^2} - 1 \right) \quad (5.57)$$

where:

$$\Gamma(\phi) = \int_0^{\infty} t^{\phi-1} e^{-t} dt \quad (5.58)$$

The shape of the β -function is shown in [Figure 5.8](#). This graph shows the distribution for a mixture fraction $Z = 0.6$ and several values for the mixture fraction variance Z'' .

The concentration and temperature distribution after integration over β -function can be determined from:

$$\tilde{Y}(Z, Z'') = \int Y(Z) P(Z, Z'') dz \quad (5.59)$$

and

$$\tilde{T}(Z, Z'') = \int T(Z) P(Z, Z'') dz \quad (5.60)$$

The result for Equation 5.60 is shown in [Figure 5.9](#). The graph shows the calculated temperatures of a methane/air flame for different variances Z'' .^{33,35}

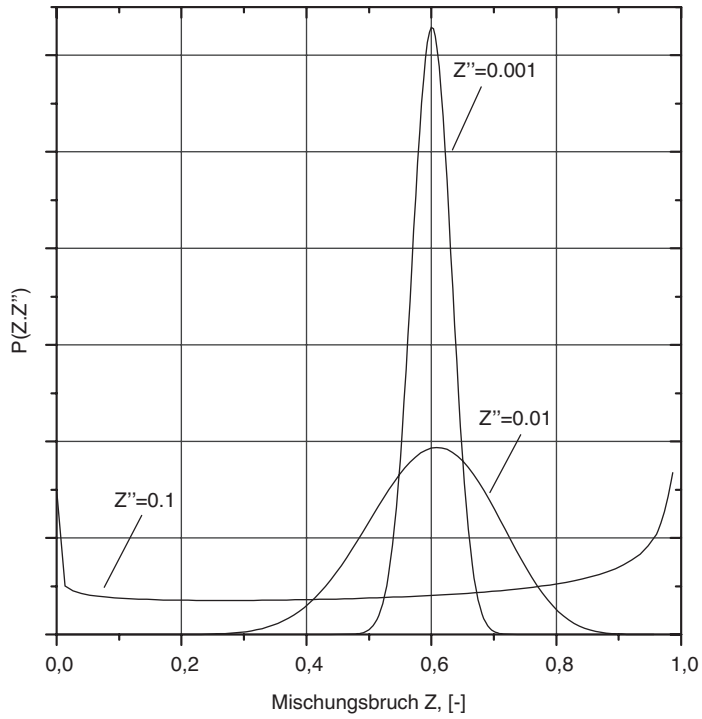


FIGURE 5.8 β -Function distribution for mixture fraction $Z = 0.6$ with several values for mixture fraction variance, Z'' .

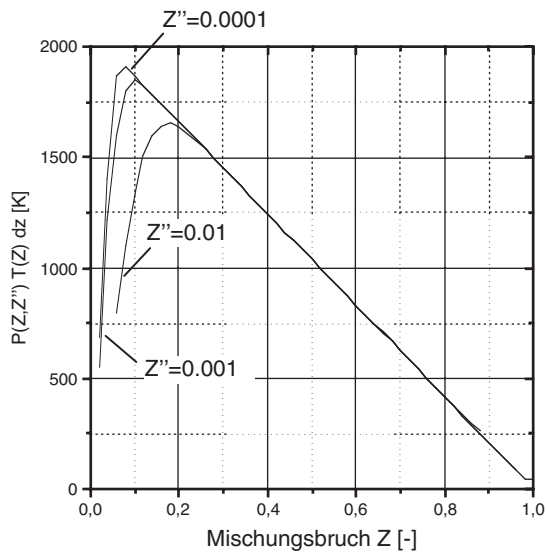


FIGURE 5.9 Temperature profile after integration over β -function for several values of mixture fraction variance Z'' .

5.3.3 WALL HEAT TRANSFER

Heat transfer between a burner flame and the furnace walls or tubes is a critical issue that must be resolved by a CFD simulation for the model to be useful for optimizing furnace efficiency. Thermal efficiency, defined as the total energy transferred to the furnace divided by the total available energy of the fuel, is largely dependent on radiative heat transfer within the industrial furnace and continues to be the focus of considerable research.

Radiative transfer theory deals with the propagation of intensity. Shuster³⁶ and Hamaker³⁷ were two of the first workers to describe the radiation process by writing equations for the rate of change of positive radiation fluxes in the positive and negative coordinate directions. Basic radiation transfer is governed by an integro-differential equation that accounts for the scattering and absorption of radiation by participating media:

$$(\mathbf{S} \cdot \nabla) I_v = -(K_{a_v} + K_{s_v}) I_v + K_{e_v} I_{b,v}(T) + \frac{K_{s_v}}{4\pi} \int_{\Omega'=4\pi} P_v(\vec{S} \rightarrow \vec{S}') I_v(S') d\Omega' \quad (5.61)$$

Figure 5.10 depicts the radiant energy balance in a specified direction. The term on the left-hand side of Equation 5.61 represents the net change in the intensity of radiation. The first term on right-hand side of the equation accounts for attenuation due to absorption and scattering while the second term on the right-hand side represents the addition due to emission. Finally, the integral term accounts for addition due to “in-scattering.” In-scattering is the radiation scattered by surrounding particles in the direction of travel of the radiation beam under consideration. This term, also known as the source term, is the most difficult to resolve given its integral nature of summing all incident radiation on a hemispherical section at a point. To simplify this equation, the source term is reduced to a differential form using various approaches.

5.3.3.1 Thermal Radiation Heat Transfer

Radiative heat transfer models for gas- or oil-fired^{38,39} and pulverized coal-fired furnaces⁴⁰ have been developed using the zoning method^{41,42} and the flux method.⁴³⁻⁴⁵ These approaches used simple empirical assumptions for flow characteristics, temperatures, heat release rates, and gas composition. However, they suffered from a lack of coupling between the individual directional fluxes. Other computational techniques developed to minimize this effect included the Monte Carlo method,⁴⁶ the diffusional method,⁴⁷ and, more recently, the discrete-ordinates method.⁴⁸

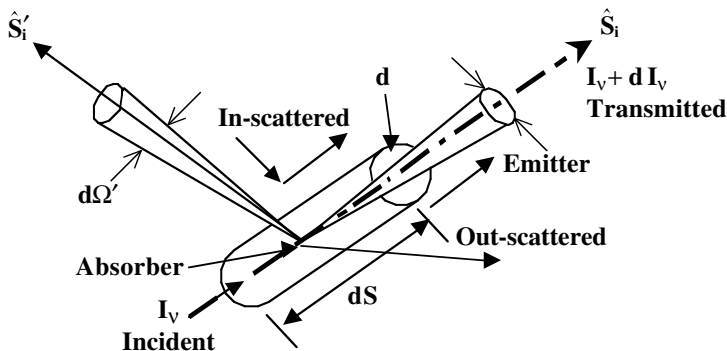


FIGURE 5.10 Radiant energy balance in a specified direction. (From Field, 1981.)

Zonal methods were first developed by Hottel and Cohen in 1958³¹ to simulate radiation exchange within a furnace chamber.³¹ Later, Hottel and Sarofim³⁷ refined the zone method to include non-ideality of the furnace and gases. This method is more rigorous on radiative transfer and combustion in industrial furnaces than the related flux methods.

Flux-based radiation models developed by Gosman and Lockwood³⁴ and by Varma³⁹ described geometrically simple systems that accounted for radiative transport via flux equations in two, four, or six flux directions. The derivation of the flux equations describing radiation transfer is relatively straightforward, and the computational demands for such an approach are far less than the comparative zonal approach. However, both the flux and zonal methods' inability to address coupling between directional fluxes makes them less popular today.

One method that captures the coupling between directional fluxes is the Monte Carlo method.³⁶ This method generates a "bundle" of intensities within a control volume and fires them in all directions and then traces the resulting rays throughout their lifetime as they undergo simulated absorption, emission, and scattering. This method provides a powerful and flexible solution to the nongray gas problem as well as the directional dependence of radiation. However, it suffers from poor economy in computer time. The discrete ordinates method attempts to address coupling between directional fluxes in a more efficient fashion.

Discrete ordinates (DO) solutions of the radiative transfer equation in multi-dimensional enclosures containing absorbing-emitting-scattering media have been developed for S_2 , S_4 , S_6 , and S_8 approximations (see Figure 5.11 for the S_2 and S_4 configurations). The S_4 approximation solves the radiative transport equation in 24 directions, the angular integral being discretized through the assumption of nonvariance of radiative intensities in prescribed solid angles surrounding representative directions. This discrete ordinates method has been tested in two-dimensional axisymmetric

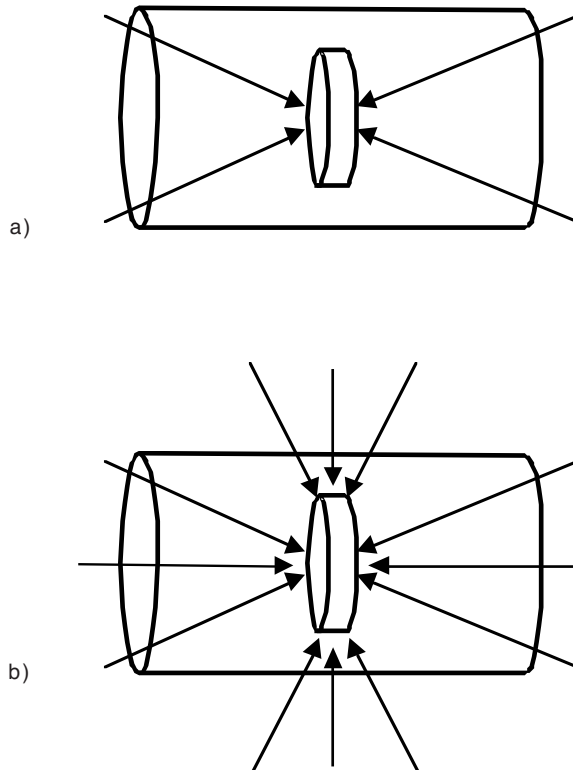


FIGURE 5.11 Directional intensities reaching a volume element: (a) S_2 and (b) S_4 .

geometries,⁴⁹ two-dimensional Cartesian geometries,⁵⁰ three-dimensional rectangular geometries,⁵¹ and three-dimensional geometries with generalized shapes.⁵² It has also been tested in nonscattering and scattering media. Comparison to exact solutions, the S_2 approximation is shown to have significant error while the S_4 approximation has been shown to be adequate. Today's CFD-based combustion models use this formulation of the DO method to approximate radiative transport in general furnaces and burners.

5.3.3.2 Properties of Radiating Gases

To carry out radiation calculations, information is needed on the absorption and scattering cross sections for particulates, as well as the scattering phase functions. These can be calculated using Mie theory⁵³ if the particle size, the wavelength of the radiation, and the complex refractive index of the particle are known.

Soot particles absorb but do not scatter radiation significantly due to their size. For this reason, soot radiation is typically ignored in most CFD codes.

Absorption coefficients for combustion gases are evaluated from gas emissivity data as:

$$k_{ag} = \left(\frac{1}{\ell}\right) [\ln(1 - \epsilon_g)] \quad (5.62)$$

where:

$$\epsilon_g = C_{\text{CO}_2} \epsilon_{\text{CO}_2} + C_{\text{H}_2\text{O}} \epsilon_{\text{H}_2\text{O}} - \Delta\epsilon \quad (5.63)$$

where ℓ is the mean beam length evaluated as:

$$\ell = 3.5(V_F/A_F) \quad (5.64)$$

and C_{CO_2} and $C_{\text{H}_2\text{O}}$ represent the pressure corrections to the gas emissivities, $\Delta\epsilon$ represents the spectral overlap correction, and V_F and A_F represent the averaged volume and cross-sectional area of the reactor. The gas emissivity data are taken from Hottel and Sarofim.⁴⁷

5.3.3.3 Radiative Boundary Conditions

In a well-controlled test furnace, the thermal boundary conditions along the wall, required by the radiation model, are well defined and can be supplied for the simulation. In most industrial furnaces, this is not the case. Instead, a wall heat transfer model is typically used that incorporates the local radiative fluxes (incident and emitted), local net convective heat flux, and a thermal resistance through the furnace wall (including any surface scaling or deposits). This model allows for specification of the boundary condition to be the local temperature outside the furnace wall. This requires specification of both a local temperature and the local thermal resistance of the wall.

Previous work has shown that the local radiation and temperature field is strongly dependent on this boundary condition. To improve accuracy, one can use measured external temperatures of the wall or ambient fluid or one can use the measured exit gas temperature to check this boundary condition. In the absence of local furnace data, a common assumption is that the wall resistance is uniform throughout the furnace. Although this is probably a weak assumption, the resistance is adjusted until the predicted and measured exit gas temperatures agree.

This definition of the boundary condition for the wall heat transfer also affects the reaction chemistry and the fluid dynamics. This assumption is believed to be the limiting assumption in the modeling of large industrial furnaces. Thus, more measurements and theoretical development

are needed to better resolve these boundary conditions for more thorough model definition and evaluation.

5.4 ILLUSTRATIVE EXAMPLES

5.4.1 FLAME SHAPE ANALYSIS CASE STUDY

CFD is commonly used to address customers' concerns directly related to thermal equipment performance in their individual applications. For example, our company used CFD to essentially duplicate conditions observed in an ethylene pyrolysis furnace, then devise a solution that was successfully implemented in the field.

Ethylene pyrolysis (“cracking”) furnaces are found in many olefin plants and produce ethylene and propylene from feedstock containing ethane, propane, butane, and hydrocarbons through naphtha. The physical phenomena involved in this process include radiant heat transfer, gaseous combustion, convective heating of the process fluid in the process tubes, and convective cooling of the furnace effluent gases in the convection section of the furnace. In summary, the process entails rapidly heating the feedstock for a short time (less than 1 second is typical) to a temperature of about 1600°F (870°C). The feed gases are then quickly cooled and subjected to a number of separation processes. These phenomena are represented by the respective mathematical equations. The numerics required to solve these equations involve algorithms that solve large systems of nonlinear equations. As pointed out, successful application of CFD requires that all key physics are included in the simulation, that these physics are correctly captured in comprehensive mathematical expressions, and that the numerics accurately provide a reproducible solution to this nonlinear system of equations. If weakness exists in any of these three worlds, inaccurate CFD results are likely to occur.

Figure 5.12 is a photograph of burners operating in a cracking furnace. These burners are wall-fired and produce a flat flame. In this study, the installed flat flame burners produced a flame that “rolled off” the wall of the furnace and into the process tubes. Because flame impingement on the tubes can cause premature coking and tube failure, the furnace operators were forced to operate the furnace at only 50% capacity to avoid damaging the tubes.

In single burner tests at the lab, the flame shape observed in the furnace could not be reproduced, which required a CFD study of the burners in the actual furnace geometry.

Figure 5.13 illustrates three views of the CFD model of the burner. This model includes all the critical geometric features. The multiple jets created by the drillings in the primary and staged tips must be modeled in enough detail to simulate the individual jets. This requires significant experience with meshing tools as well as some knowledge of the fluid dynamic processes and resolution requirements. As observed in practical systems, the direction and size of these jets are critical to burner performance, and must be modeled in the CFD simulation to capture the correct flame shape and resultant heat flux profile.

Figure 5.14 shows a plan view of the furnace layout. The CFD model used to study the flame rolover problem assumed symmetry about certain planes to reduce the computational demands of the calculations, which allowed for rapidly generated solutions to the various burner changes. Figure 5.14 illustrates the symmetry planes used as dashed lines. This assumption allowed for study of flame interaction from adjacent burners while only including a “half-burner” in the model. This assumption greatly reduces the cell count to facilitate making several calculations to optimize the system.

5.4.1.1 Combustion Modeling and Boundary Conditions

The per-burner airflow is 5886 lbm/hr of ambient temperature air. The per-burner fuel flow is 325.3 lbm/hr. The fuel composition is given in Table 5.3. The lower heating value (LHV) of the fuel is 973 Btu/scf and its molecular weight is 18.5. The heat release per burner is 6.4 MMBtu/hr based on LHV.

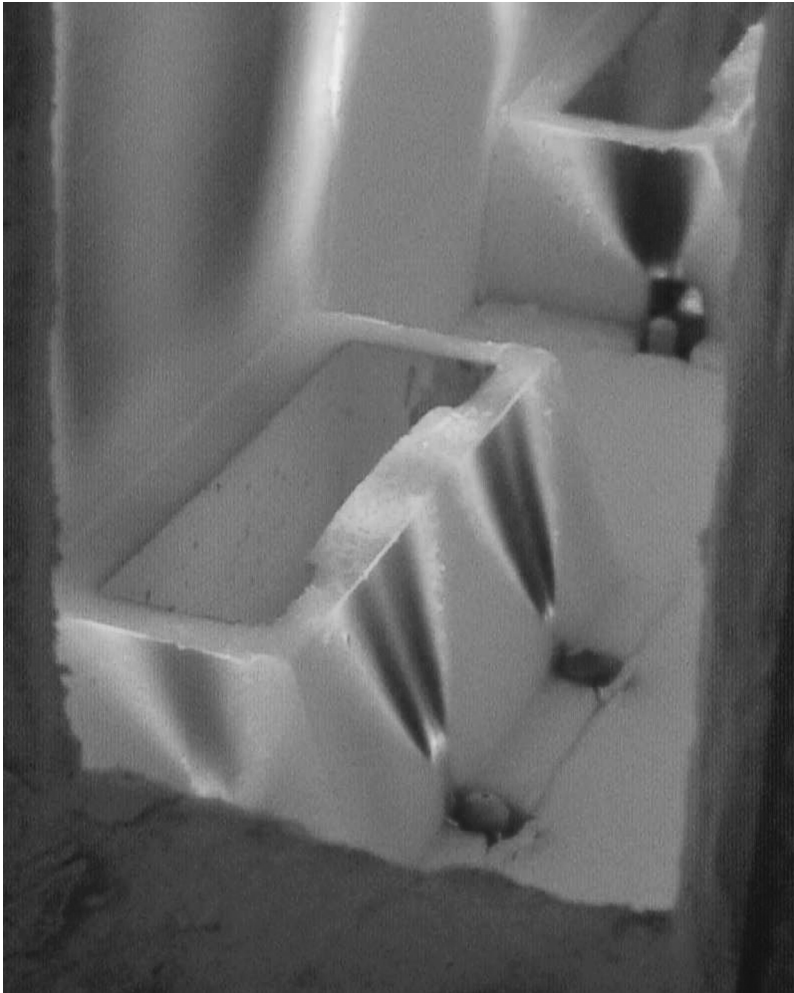


FIGURE 5.12 Closeup of burners firing in a cracking furnace.

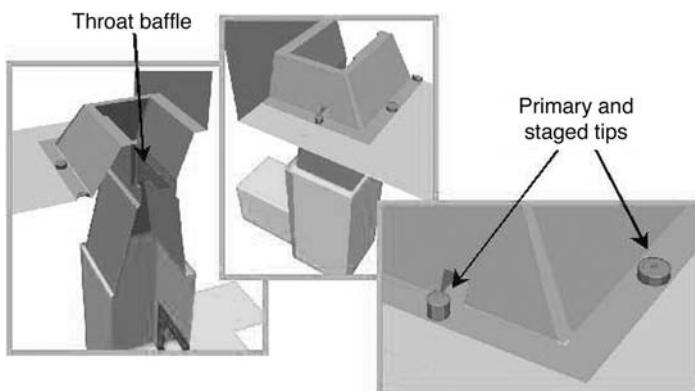


FIGURE 5.13 Closeup of CFD geometry for a flat-flame burner.

TABLE 5.3
Mole Fractions of Chemical Species
in Fuel and Combustion Air

Species	Fuel Fraction	Air Fraction
O ₂	0	0.206
N ₂	0.017	0.78
H ₂ O	0	0.014
CO ₂	0.0145	0.0003
CH ₄	0.861	0.0
C ₂ H ₆	0.0865	0.0
C ₃ H ₈	0.0166	0.0
C ₄ H ₁₀	0.0037	0.0

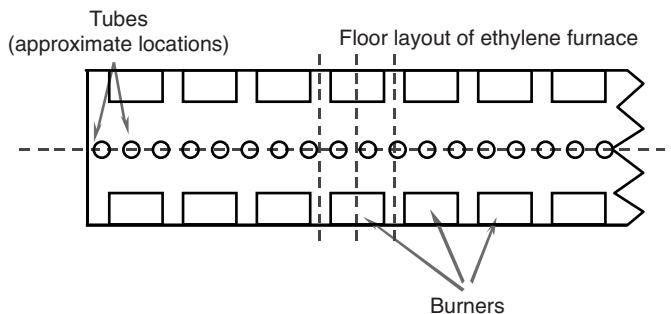


FIGURE 5.14 Plan view of furnace layout showing burner locations, tube locations, and symmetry planes used in CFD model (dashed lines).

Because these burners produce a nonpremixed flame, the presumed probability density function (PPDF) combustion model⁴ was used to simulate combustion. This model assumes that the combustion process is limited by fluid mixing rather than by chemical kinetics, a valid assumption for most hydrocarbon fuels in many combustion devices.

The CFD simulation used the realizable k - ϵ (RKE) turbulence model to simulate the effect of turbulence of the flow and mixing.^{54,55} Thermal radiation was simulated using the discrete ordinates model.⁵⁶ Thermal radiation is the most significant heat transfer mechanism in the radiant section of the furnace, and a significant fraction of the radiant flux to the tubes is directly from the gas, requiring a model capable of simulating optically thin gas radiation. The Weighted-Sum-of-Gray-Gases model⁵⁷ was used to compute the gas-phase absorption coefficients using an assumed surface emissivity of 0.85 on the tubes and 0.65 on refractory surfaces.

5.4.1.2 Predicted Flame Shapes and Modifications to Burner Geometry

Figure 5.15 shows the predicted flame shape (visualized by showing a constant mixture fraction isosurface) for the as-installed burners. The predicted flame shape is consistent with the observation that the flame rolls over into the tubes. The predicted flame shape also shows large “wings” of flame coming from the sides of the burner. These are consistent with the fuel placement in the burner, although the size of these wings is disconcerting. This burner was designed with an unusual constraint so that the burner could be easily operated when the furnace is in its “hot-standby” condition, which occurs regularly when the tubes undergo steam decoking.

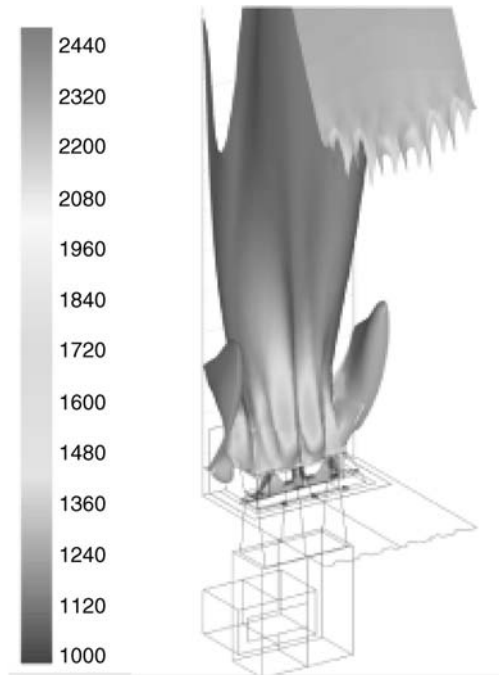


FIGURE 5.15 Flame shape ($\tilde{f} = 0.0575$ stoichiometric isosurface) predicted with initial burner geometry and tip drilling. The isosurface is colored by temperature ($^{\circ}\text{F}$).

After reviewing this predicted flame shape with burner engineers and furnace engineers, the conclusion was made that the combination of burner spacing in the furnace and the design constraint for hot-standby operation led to the flame rollover problem. This problem was not observed in single-burner tests or even in dual-burner tests, but the CFD model did reveal the problem. In a long row of burners as in the operating furnace, the combustion air will be “pinned” against the fired wall and unable to flow freely around the fuel. In a single- or dual-burner test, the air can flow around the flame and oxidize the fuel stream from both sides of the flame.

As a result of these discussions, seven additional CFD simulations were performed, each with a different fuel distribution around the tile. Figure 5.16 shows the flame selected as having the most optimal shape. This conclusion was reached by reviewing the predicted flame shapes for all seven tip-drilling changes with combustion engineers and furnace engineers.

Figure 5.17 shows the normalized heat flux profiles for the seven tip drillings considered. These are the heat fluxes to the process tube directly in front of the burner centerline.

Heat flux profiles are very important in ethylene pyrolysis furnaces because the tube metallurgy usually limits capacity. The furnaces are frequently operated with some portion of the tubes near the metallurgical temperature limit. For this reason, the more uniform the heat flux profile on the tubes, the higher the furnace capacity.

Upon completion of the CFD modeling study and test furnace evaluation of the selected tip drilling, new fuel tips were fabricated and delivered to the site. These tips were installed online. Upon installation, the flame impingement problem disappeared.

5.4.2 THERMAL OXIDIZER BURNER/REACTOR CASE STUDY

This case study considers the incineration of a dilute gas stream consisting of small amounts of sulfur-containing species (i.e., H_2S , COS , CS_2) and aromatic hydrocarbons. The thermal oxidizer had been operating for a period of time with a lower than desired destruction efficiency and this was developing into a regulatory compliance issue. It was suspected that mixing of the fuel, waste,

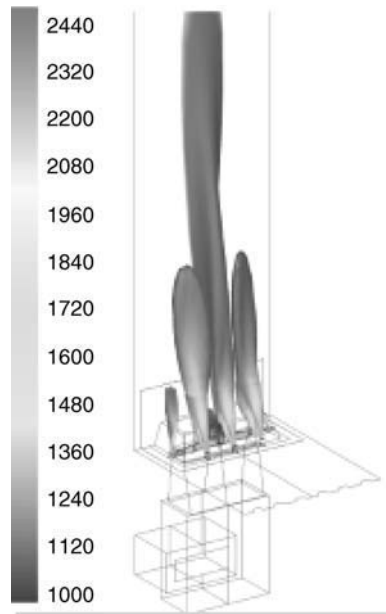


FIGURE 5.16 Flame shape ($\bar{f} = 0.0575$ stoichiometric isosurface) predicted with optimized burner geometry and tip drilling. The isosurface is colored by temperature ($^{\circ}\text{F}$).

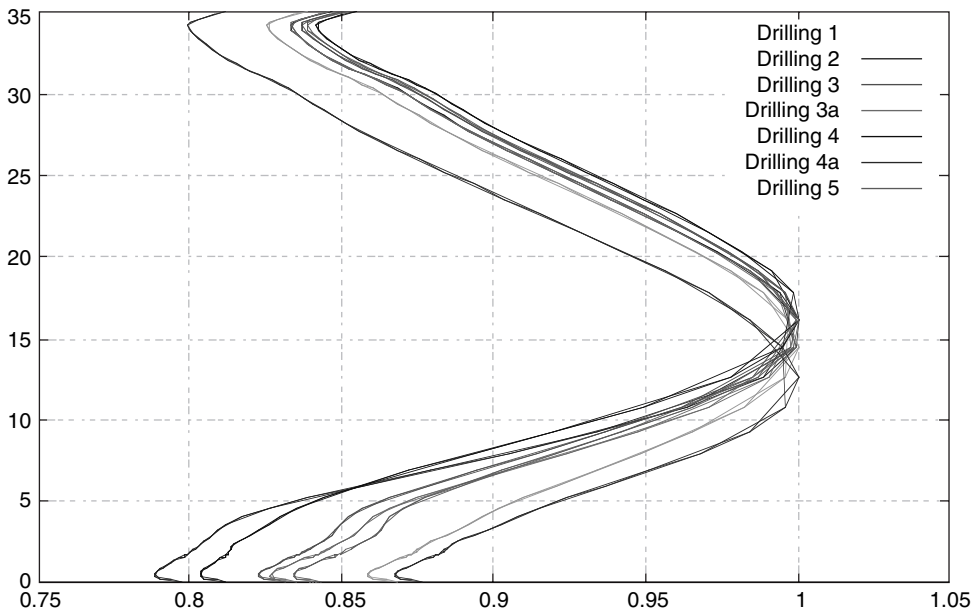


FIGURE 5.17 Normalized heat flux profiles for the various tip drillings studied.

and oxidant streams within the unit was less than optimal and a different style of burner was suggested to help improve this important parameter. Timing and the cost of renovation restricted the user to utilizing the existing reactor shell rather than make major modifications. The study was then designed to simulate the existing unit and then evaluate the effects related to the their replacement with the new, proposed burners.

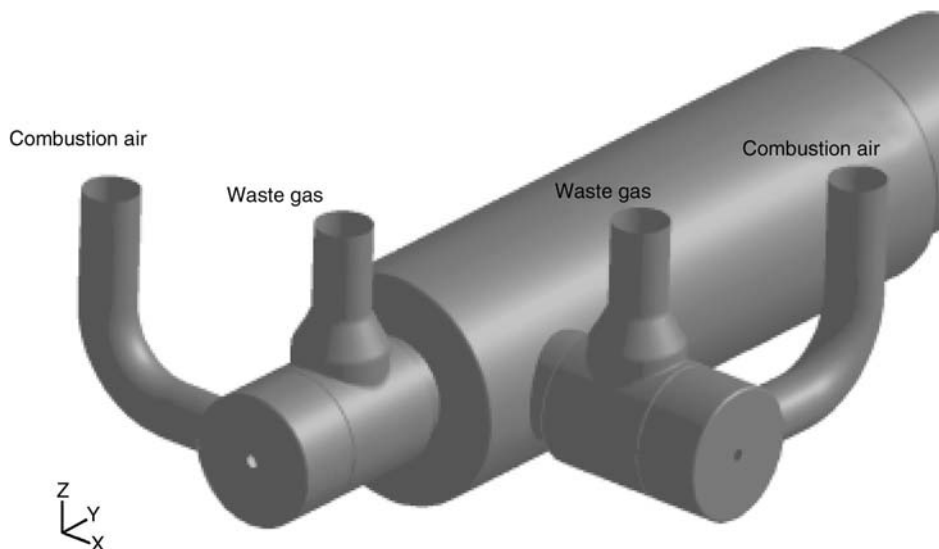


FIGURE 5.18 Overview of the modeled reactor.

The existing thermal oxidizer is a horizontal cylindrical furnace with two identical burners positioned at the head of the reactor perpendicular to one another on the reactor's horizontal mid-plane (see Figure 5.18). The original burners consisted of a single, center fuel gas riser, capped with a cone to help stabilize the flame. Air entered the burner by the gap around the center riser. Waste vent gas enters the burner assembly via a cylindrical gap concentric to the fuel gas riser's axis located outside of the burner tile. The fuel gas tip had drillings such that gas was allowed to enter in a conical pattern. The proposed burner modifications consisted of changing the fuel gas injection pattern by placing a number of individual tips around the interior burner periphery and providing drillings allowing for more tangential spin. Reducing the available concentric flow area slightly increased the pressure drop for the waste gas stream across the burner. A riser with a cone was added to allow for future fuel additions, but did not serve as an inlet to this particular burner simulation. The intent behind the new burner configuration was to increase local mixing sooner in the burner assembly, thereby helping to improve the potential for complete burnout of waste components. The two fuel gas tip arrangements are shown in Figure 5.19.

The fluid density was based on an ideal gas assumption, using a fixed value of system pressure. This approach is reasonable when large fractions of the pressure field fluctuations in the domain are expected to differ only slightly (<1%) from the user-input nominal system pressure. This approximation reduces the computational load per iteration. The RANS equations were used to account for momentum conservation and the "realizable $k-\epsilon$ " model was used to account for turbulent fluctuations. The combustion processes in these studies were modeled using the beta form of an assumed PDF (probability density function) of mixture fraction model. Heat loss from the reactor walls was assumed to be 1000 Btu/(hr-ft²).

The components that made up the fuel and waste gas streams are shown in Table 5.4. The air composition assumed to be at 94°F and 65% relative humidity.

Velocity profiles for the two different types of burners, shown along a plane perpendicular to the axis of the burner's centerline, are shown in Figure 5.20. The figures show the proximity of the plane to the burner's cone. The differences between the two are immediately obvious. The gas tip arrangement used in the older, existing burner was intended to provide a conical distribution of fuel gas with no swirl induced by the drilled pattern. The contours representing the calculation for the existing burner support this and show little to no rotation. The color map is shown to the left and

TABLE 5.4
Fuel and Waste Acid Gas Composition

Fuel Gas		Waste Acid Gas			
Specie	% Vol	Specie	% Vol	Specie	% Vol
CH ₄	82.5	CH ₄	0.16	H ₂ O	20.65
C ₂ H ₆	8.3	C ₆ H ₆	0.06	H ₂ S	0.5
C ₃ H ₈	3.9	CO	1.71	N ₂	41.61
N ₂	5.3	CO ₂	34.66	SO ₂	0.25
		H ₂	0.4		

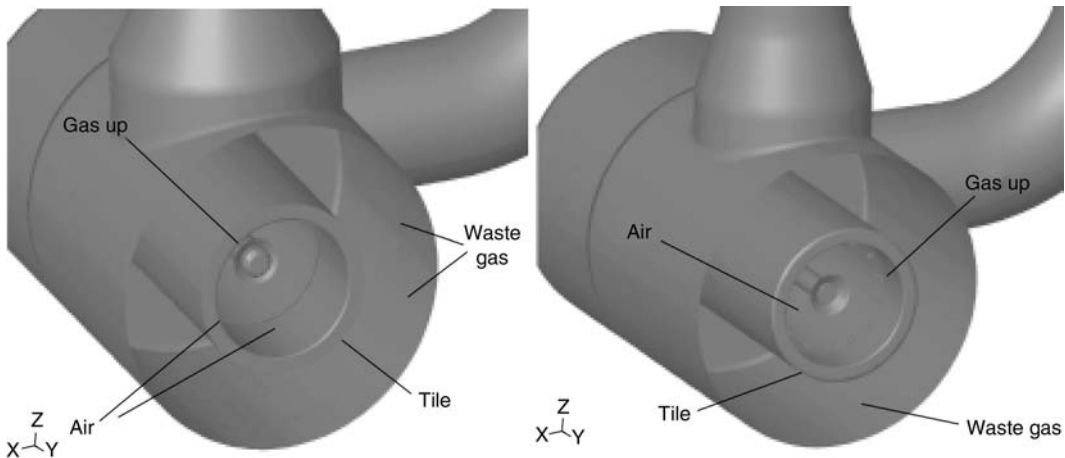


FIGURE 5.19 Existing and proposed burner modifications.

is in units of feet/second. The figure to the right shows the calculated result from the new burner configuration. The flow field now shows a swirling velocity pattern and seems to have a greater percentage of the flow area at a higher velocity.

Figure 5.21 shows the velocity profiles along the vertical mid-plane of the furnace, looking down from the top. The first profile (Figure 5.21a) shows the result from the existing burners. The velocity fields from the two burners combine and seem to form a “jet” that continues out toward the exit of the reactor. The implication is that the full reactor volume is not being utilized. The second profile (Figure 5.21b) shows the effect of the new burners. The overall magnitude of the combined jet is reduced; however, the slip that was occurring in the first case still seems to persist. This result prompted an additional study, with the addition of a choke ring to the reactor downstream of the burners. This addition could be made without major changes to the reactor as it currently existed.

As is shown, the addition of the choke ring significantly modified the flow fields in the reactor. Figure 5.22 shows the calculated temperature profiles from these three cases, and also the increase in field uniformity with the use of the new burners and more so with the choke ring.

The true impact this improvement in mixing has is best demonstrated by the contours shown in Figure 5.23. These represent H₂S mass fractions along the vertical mid-plane of the furnace, looking down from the top. The first, again, is from the simulation of the existing burner/reactor configuration. The second shows the impact of the new burners and indicates, for this particular metric, the addition of the new burners would make little improvement in the reactor’s effectiveness. There appears to be significant slip of the waste gas stream toward the exit. The case with the addition of the choke

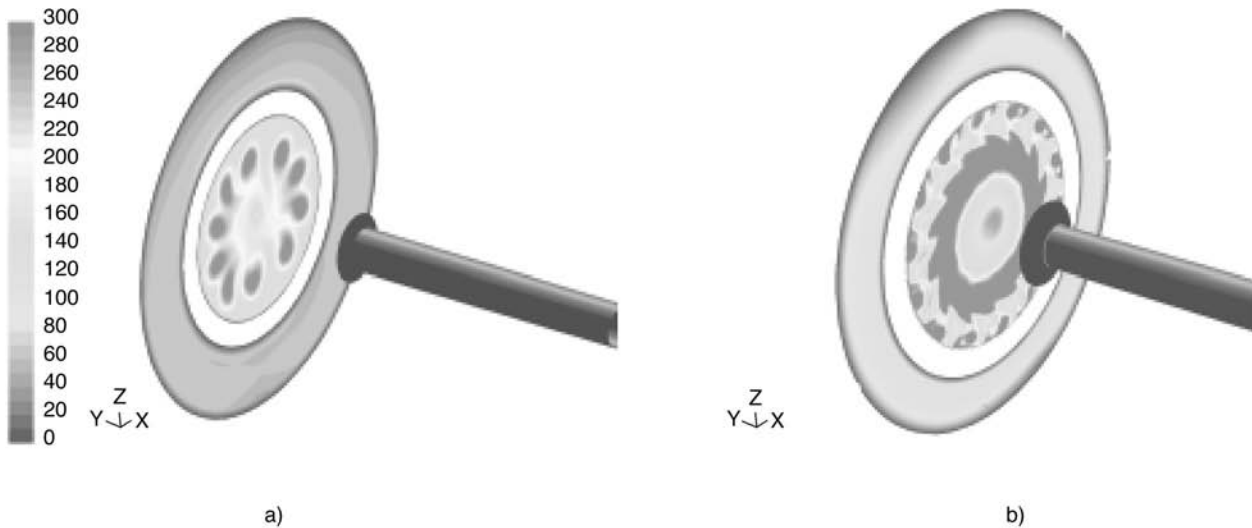


FIGURE 5.20 Velocity profiles near the burner face: (a) current burner and (b) modified burner design.

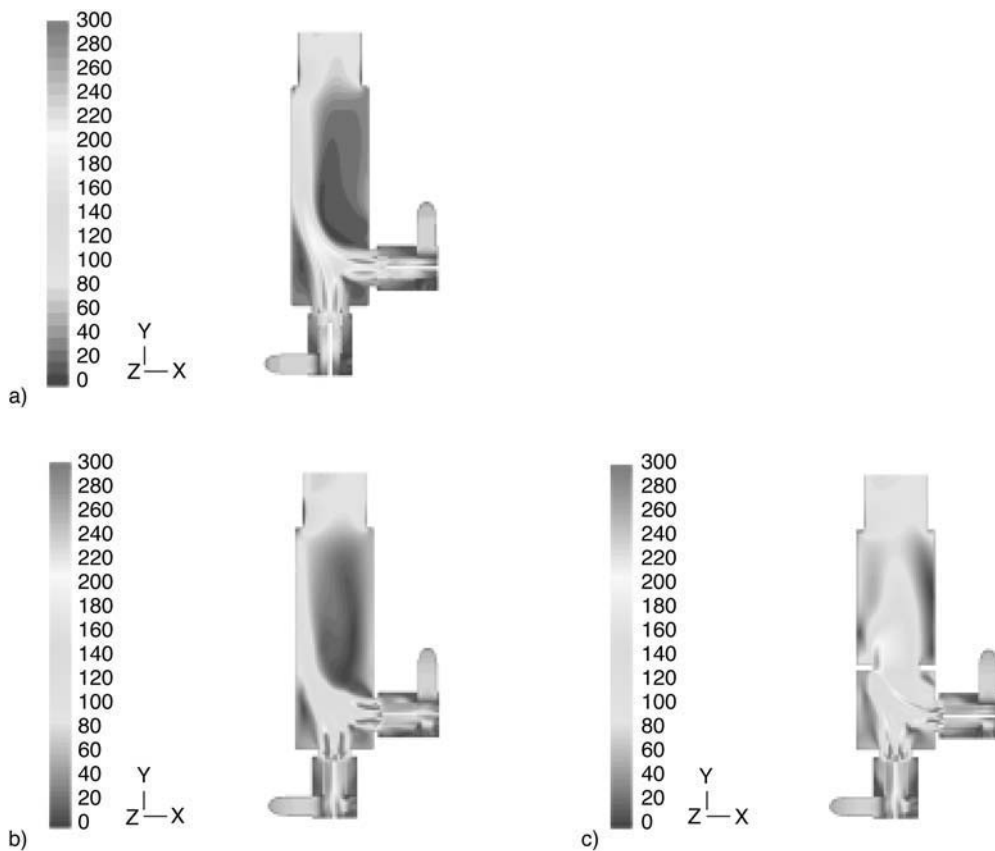


FIGURE 5.21 Velocity magnitude profiles along the reactor's vertical mid-plane (ft/sec): (a) existing burners, (b) new burners, no choke, and (c) new burners with choke.

ring shows the elimination of this slip, due to the increased utilization of the whole reactor volume. As can be seen, the improvement in mixing in the system utilizing the new burners and the choke seems to noticeably reduce the mass fraction of H_2S leaving the reactor. The improvement in mixing in the downstream section of the reactor also results in a more uniform temperature profile along the reactor walls, as shown in Figure 5.24. Figure 5.24a shows the expected temperature profiles from the existing burner configuration. The profiles seem to corroborate data taken during a site visit. Figure 5.24b and Figure 5.24c show that the temperature profiles along the reactor walls, with the addition of the new burners, becomes much more uniform, which should help improve the maintenance of the reactor as a whole.

The conclusion reached from this case study was that the addition of new burners in the existing reactor configuration should greatly improve the localized mixing, thereby helping with the incinerator's overall destruction efficiency. This was based on the calculated temperature and velocity fields from the CFD analysis. The addition of a choke seems to encourage better utilization of the reactor's available volume and subsequently improve the downstream uniformity of the resulting flow and temperature fields, as well as reduce the slip of waste gas from the side burner annulus. Temperature uniformity at the exit was considered important due to the presence of a waste heat boiler immediately downstream from the reactor exit. This improvement in mixing also appears to result in lower H_2S mass fractions leaving the oxidizer section. It was suggested that this addition should be considered an essential portion of the furnace upgrade.

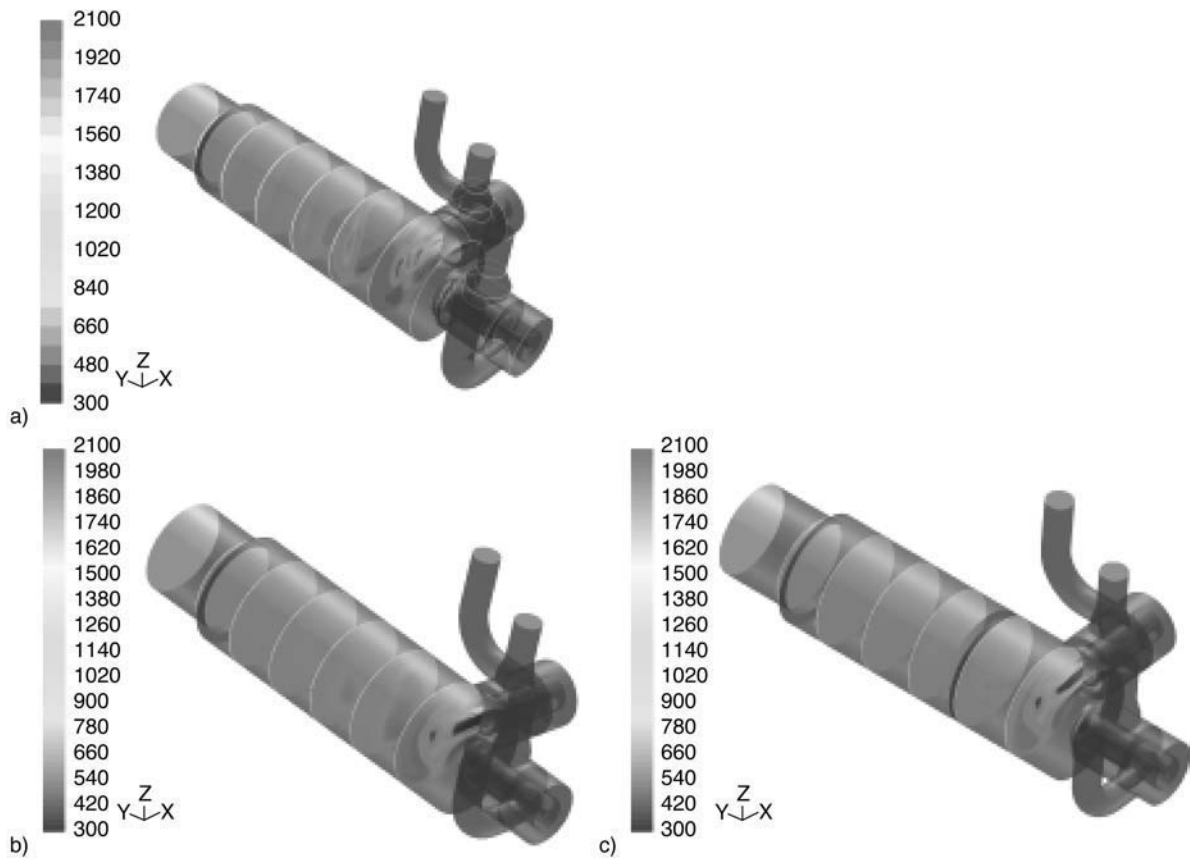


FIGURE 5.22 Temperature contour slices along the reactor axis (K): (a) existing burners, (b) modified burners without choke, (c) modified burners with choke.

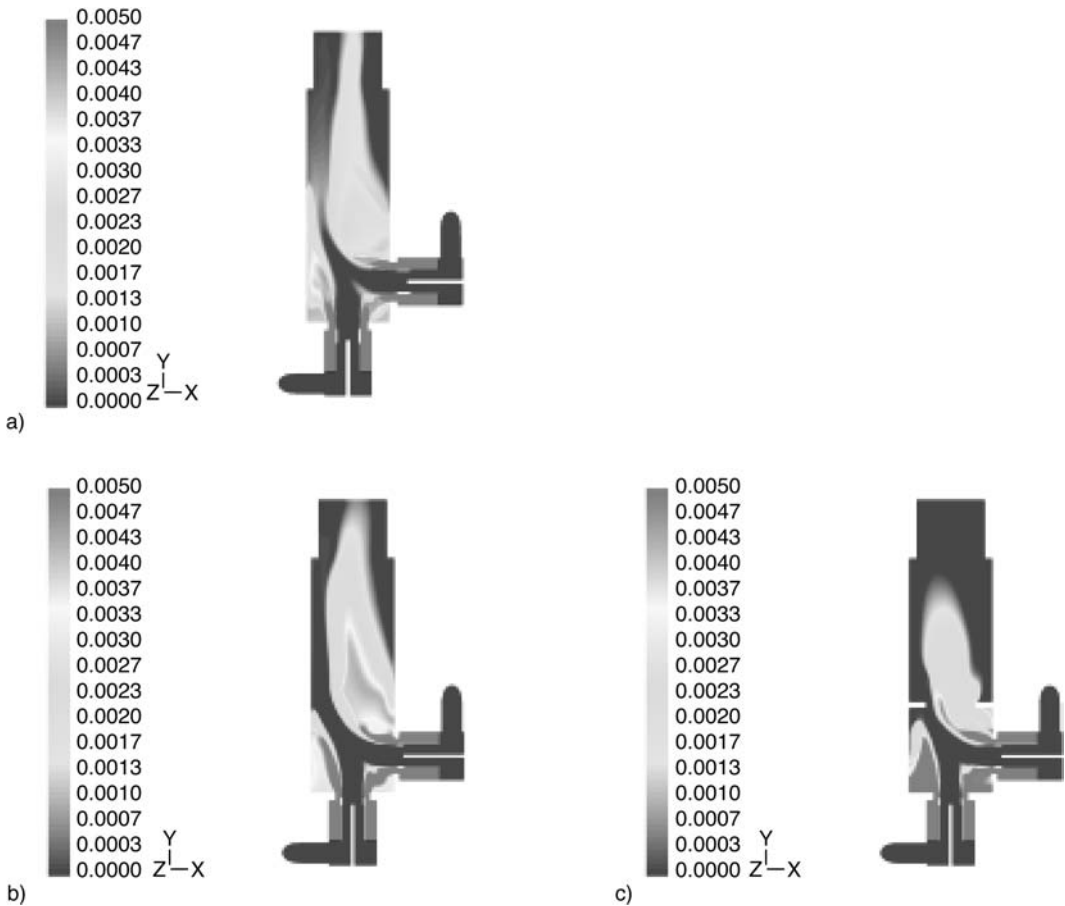


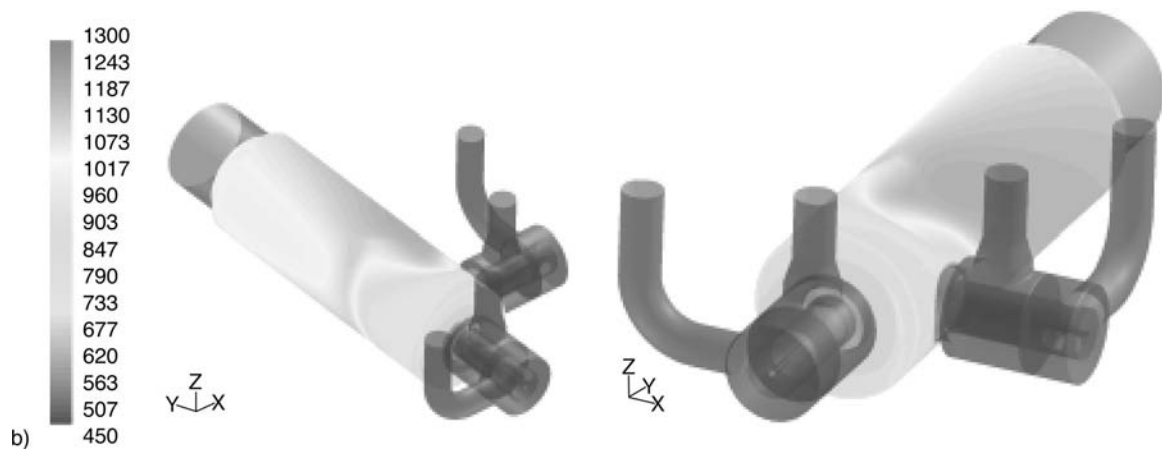
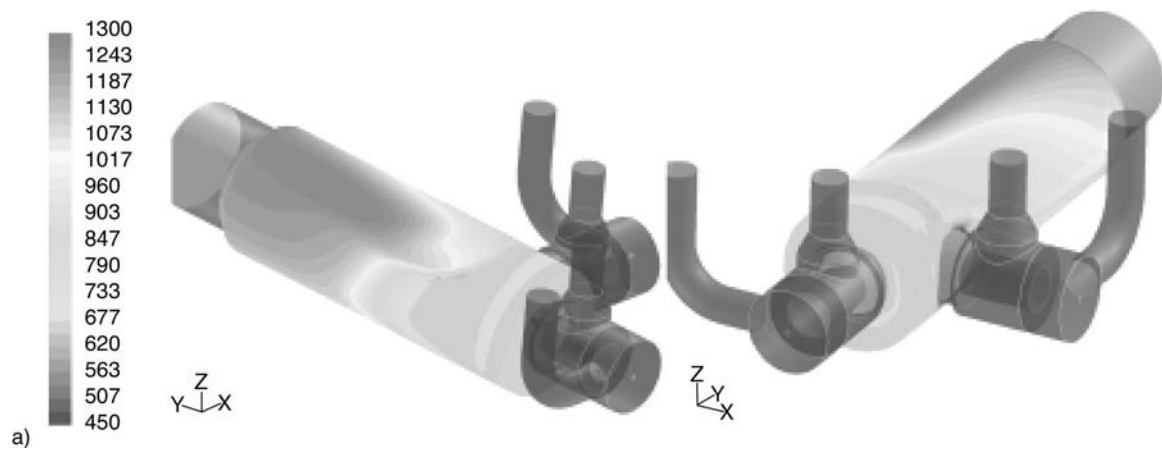
FIGURE 5.23 H₂S mass fraction profiles along the reactor's vertical mid-plane: (a) existing burners, (b) new burners, without choke, and (c) new burners with choke.

5.5 CONCLUSIONS AND SUMMARY

Time and experience in CFD-based combustion analysis have revealed their critical importance to the design and development of next-generation burners for the CPI/HPI. Recent advances in computer architecture, more comprehensive physics, and improved CFD solver algorithms have allowed engineers to address issues such as pollutant generation and equipment reliability. While tomorrow's supercomputers promise to open exciting new doors in the CFD field, today's challenge continues to be simulating fully three-dimensional turbulent reacting compressible flows inside very complex burner/furnace geometries.

Modeling continues to play a vital role in identifying complex problems. This approach provides a foundation to solve difficult problems, which in years past would have been intractable or exorbitantly expensive to address. In the examples presented in this chapter, the goals were to reduce fuel consumption without increasing combustion emissions or compromising burner turndown and carbon burnout at all loads. In each situation, operational improvements enabled the system to function at reduced excess air rates and higher efficiency, which translated into real savings.

Advanced modeling along with experimentation have also been used to address problems related to the thermal performance of ethylene pyrolysis furnaces. CFD has successfully identified and



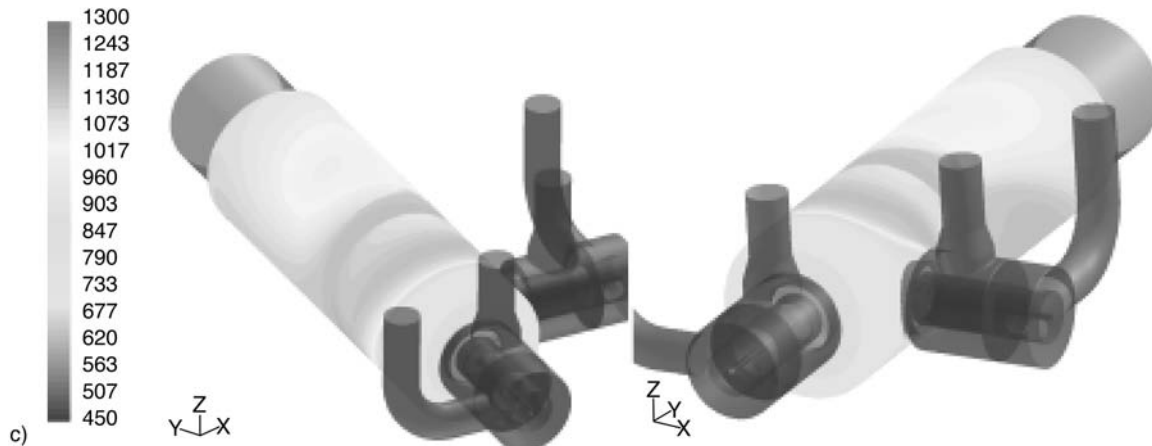


FIGURE 5.24 Temperature contour profiles along the reactor wall (K): (a) existing burners, (b) new burners, without choke, and (c) new burners with choke.

resolved the flame impingement/flame rollover problems in this specific furnace, which was implemented in the field quickly and cost-effectively. This same approach has been used on other similar furnaces with similar success. Solving these types of problems translates into significant cost savings in terms of higher online production rates for the operating unit.

Perhaps most importantly, advanced problem-solving techniques using CFD are making ultra-low emission burner design routine in today's ever-stringent economic and operating environment. This new tool has proven its ability to effectively help industry meet evermore stringent air quality regulations at acceptable costs.

REFERENCES

1. Smith, P. J., Heap, M. P., and Kertamus, N. J., Using Computational Combustion Simulations to Solve Industrial Problems, 92-JPGC-FACT-13, International Power Generation Conference, Atlanta, GA, October 18–22, 1992.
2. Pitts, W. M., Resolution Requirements for Scalar Dissipation Measurements in Turbulent Jets and Flames, 52nd Proceedings, American Physical Society/Division of Fluid Dynamics, November 21–23, 1999, New Orleans, LA, 1999, 37.
3. Smith, J. D. and Webster, T., Using CFD to Solve Challenges of Ultra-Low NO_x Burner Retrofit in Refinery Process Heaters, *Petroleum Technology Quarterly*, July 2002.
4. Henneke, M., Smith, J. D., Jayakaran, J. D., and Lorra, M., Computational Fluid Dynamics (CFD) Based Combustion Modeling, *The John Zink Combustion Handbook*, Baukal, C. E., Ed., CRC Press, Boca Raton, FL, 2001.
5. Engleman, M. S., Computational Fluid Dynamics in the 90's, Technology Trends in Automotive Engineering, Convex Computer Corporation, May 14–15, 1991.
6. Henneke, M., Lewellen, J., and Smith, J. D., Evaluating Burner Replacement Projects Using CFD, *Proceedings of the International Combustion Symposium: AFRC*, Ottawa, Canada, May 8–10, 2002.
7. Anderson, John D., Jr., *Computational Fluid Dynamics — The Basics with Applications*, McGraw-Hill, New York, p. 125, 1995.
8. Casey, M. and Wintergerste, T., Eds., *ERCOTAC Special Interest Group on "Quality and Trust in Industrial CFD" — Best Practice Guidelines*, European Research Community on Flow, Turbulence and Combustion, 2000, 14–15.
9. White, F. M., *Viscous Fluid Flow*, McGraw-Hill, New York, 1974.
10. Wilcox, D. C., *Turbulence Modeling for CFD*, DCW Industries, Inc., La Canada, CA, 1993.
11. Tennekes, H. and Lumley, J. L., *A First Course in Turbulence*, The MIT Press, Cambridge, MA, 1972.
12. Morkovin, M.V., Effects of Compressibility on Turbulent Flow, *The Mechanics of Turbulence*, Gordon and Breach, 1962.
13. Rodi, W., Turbulence Models and Their Application in Hydraulics — A State of the Art Review, *Association for Hydraulic Research*, 3rd ed., Delft, 1993.
14. Baldwin, B. S. and Barth, T. J., A One-Equation Turbulence Transport Model for High Reynolds Number Wall-Bounded Flows, NASA TM-102847, 1990.
15. Spalart, P. R. and Allmaras, S. R., A One-Equation Turbulence Model for Aerodynamic Flows, AIAA Paper 92-439, Reno, NV, 1992.
16. Chou, P. Y., On the Velocity Correlations and the Solution of the Equations of Turbulent Fluctuation, *Quart. Appl. Math.*, Vol. 3, 1945.
17. Davidov, B. I., On the Statistical Dynamics of an Incompressible Fluid, *Doklady AN. SSSR*, Vol. 136, 1961.
18. Harlow, F. H. and Nakayama, P. I., Transport of Turbulence Energy Decay Rate, Los Alamos National Laboratory, University of California Report LA-3854, 1968.
19. Jones, W. P. and Launder, B. E., The Prediction of Laminarization with a Two-Equation Model of Turbulence, *International Journal of Heat and Mass Transfer*, Vol. 15, 1972.
20. Roberson, J. A. and Crowe, C. T., *Engineering Fluid Mechanics*, Houghton Mifflin, Boston, MA, 1975.
21. Kim, S.E. and Choudhury, D., A Near Wall Treatment Using Wall Functions Sensitized to Pressure Gradient, ASME FED Vol. 217, Separated and Complex Flows, ASME, 1995.
22. Oran, E. S., Boris, J. P., *Numerical Simulation of Reactive Flow*, 2nd ed., Cambridge University Press, Cambridge, U.K., 2001.

23. Borghi, R., Turbulent Combustion Modelling, *Prog. Energy Combust. Sci.*, 14, 245–292, 1988.
24. Kee, R. J. et al., *Chemkin II: A FORTRAN Chemical Kinetics Package for the Analysis of Gas-phase Chemical Kinetics*, Sandia Report SAND 89-8009B-UC706, 1989, reprinted 1992.
25. Kee, R. J. et al., *SENKIN: A FORTRAN Program for Predicting Homogeneous Gas Phase Chemical Kinetics With Sensitivity Analysis*, Sandia Report SAND 87-8248UC401, reprinted 1991.
26. Glarborg, P. et al., *PSR: A FORTRAN Program for Modelling Well-Stirred Reactors*, Sandia Report SAND 86-8209UC4, reprinted 1992.
27. Rogg, B., *RUN-1DL: The Cambridge Universal Laminar Flamelet Computer Code*, in *Reduced Kinetic Mechanisms for Application in Combustion Systems*, Appendix C, Peters, N. and Rogg, B., Eds., Springer-Verlag, Berlin, 1993.
28. Rogg, B., *RUN-1DL: The Universal Laminar Flame and Flamelet Computer Code*, User Manual, 1994.
29. Rogg, B., *Numerical Modelling and Computation of Reactive Stagnation-Point-Flows*, in *Computers and Experiments in Fluid Flow*, Carlomagno, G. M. and Brebbia, C. A., Eds., Springer Verlag, Berlin, 1989, 75–85.
30. Spalding, D. B., Mixing and Chemical Reaction in Steady Confined Turbulent Flames, *13th Symp. (Int.) on Combustion*, 1971, 649–657.
31. Magnussen, B. F. and Hjertager, B. H., On Mathematical Modeling of Turbulent Combustion with Special Emphasis on Soot Formation and Combustion, *16th Symp. (Int.) on Combustion*, 1977, 719–727.
32. Magnussen, B. F., Hjertager, B. H., Olsen, J. G., and Bhaduri, D., Effects of Turbulent Structure and Local Concentrations on Soot Formation and Combustion in C₂H₂ Diffusion Flames, *17th Symp. (Int.) on Combustion*, 1978, 1383–1393.
33. Lorra, M., Investigation of NO_x Reduction in Turbulent Exhaust Gas Flows with Reburning Methods Using Experimental and Mathematical Modeling Regarding Detailed Reaction Mechanisms Using the Laminar Flamelet Theory, Ph.D. thesis, Ruhr-Universitaet Bochum, 1999 (in German).
34. Lorra, M. and Kremer, H., Mathematical Modelling and Experimental Evaluation of NO_x Reduction at Glass Melting Furnaces with Reburning, *Proc. 5th Int. Conf. of Combustion Technologies for a Clean Environment*, Lisbon, Portugal, 1999.
35. Lorra, M., Schnepfer, C., and Stephen, S., Investigation of a Duct Burner Design Using CFD Capabilities in Conjunction with Full-Scale Experiments, *Proc. 6th Eur. Conf. on Industrial Furnaces and Boilers*, Estoril, Portugal, 2002.
36. Shuster, A., *J. Astrophys.*, 21, 1, 1905.
37. Hamaker, H. C., *Phillips Research Reports*. Vol. 2, 55, 103, 112, 420, 1947.
38. Field, M. A., Gill, D. W., Morgan, B. B., and Hawksley, P. G. W., Combustion of Pulverized Coal, The British Coal Utilization Research Association, Leatherhead, Surrey, England (1967).
39. Bueters, K. A., Cogoli, J. G., and Habelt, W. E., Performance Prediction of Tangentially Fired Utility Furnaces by Computer Model, *15th Symposium (Int.) on Combustion*, The Combustion Institute, Pittsburgh, PA, 1974, 1245.
40. Lowe, A., Wall, T. F., and Steward, I. McC., A Zoned Heat Transfer Model of a Large Tangentially Fired Pulverized Coal Boiler, *15th Symp. (Int.) on Combustion*, The Combustion Institute, Pittsburgh, PA, 1974, 1261.
41. Hottel, H. C. and Cohen, E. S., Radiative Heat Exchange in a Gas-Fired Enclosure: Allowance for Non-Uniformity of Gas Temperature, *AIChE Journal*, 4, 3–14, 1958.
42. Johnson, T. R. and Beer, J. M., Radiative Heat Transfer in Furnaces: Further Development of the Zone Method of Analysis, *14th Symp. (Int.) on Combustion*, The Combustion Institute, Pittsburgh, PA, 1972, 693.
43. Patankar, S. V. and Spalding, D. B., A Computer Model for Three-Dimensional Flow in Furnaces, *14th Symp. (Int.) on Combustion*, The Combustion Institute, Pittsburgh, PA, 1972, 605.
44. Gosman, A. D. and Lockwood, F. C., Incorporation of a Flux Model for Radiation into a Finite-Difference Procedure for Surface Calculations, *14th Symp. (Int.) on Combustion*, The Combustion Institute, Pittsburgh, PA, 1972, 661.
45. Varma, S. A., Radiative Heat Transfer in a Pulverized Coal Flame, in *Pulverized Coal Combustion and Gasification*, Smoot, L. D. and Pratt, D. T., Eds., Plenum Press, New York, 1979.
46. Steward, F. R. and Cannon, P., The Calculation of Radiative Heat Flux in a Cylindrical Furnace Using the Monte Carlo Method, *Int. J. Heat Mass Transfer*, 14, 245, 1971.
47. Hottel, H. C. and Sarofim, A. F., *Radiative Transfer*, McGraw-Hill, New York, 1967.
48. Fiveland, W. A., Discrete-Ordinates Solutions of the Radiative Transport Equation for Rectangular Enclosures, *ASME J. Heat Transfer*, 106, 699, 1984.

49. Jamaluddin A. S. and Smith, P. J., Radiative Transfer in Axisymmetric Cylindrical Enclosures Using the Discrete Ordinates Method, *Combustion Science and Technology*, 62(4–6), 173, 1988.
50. Jamaluddin A. S. and Smith, P. J., Predicting Radiative Transfer in Rectangular Enclosures Using the Discrete Ordinates Method, *Combustion Science and Technology*, 59, 321, 1988.
51. Jamaluddin, A. S. and Smith, P. J., Discrete-Ordinates Solution of Radiative Transfer Equation in Non-Axisymmetric Cylindrical Enclosures, *Journal of Thermophysics and Heat Transfer*, 6(2), 242, 1992.
52. Adams B. R. and Smith, P. J., Three-dimensional Discrete-Ordinates Modeling of Radiative Transfer in a Geometrically Complex Furnace, *Combustion Science and Technology*, 83, 1–15, 1992.
53. Mie, G., Optics of Turbid Media, *Ann. Phys.*, 25, 377–445, 1908.
54. Yakhot, V. and Orszag, S. A., Renormalization Group Analysis of Turbulence. I. Basic Theory, *J. Scientific Computing*, 1, 1–51, 1986.
55. Yakhot, V. Orszag, S. A., Thangam, S., Gataski, T. B., and Speziale, C. G., Development of Turbulence Models for Shear Flows by a Double Expansion Technique, *Phys. Fluids*, A4(7), 1510–1520, 1992.
56. Carlson, B. G. and Lathrop, K. D., Transport Theory — The Method of Discrete Ordinates, in *Computing Methods in Reactor Physics*, Greenspan, H., Kelber, C. N., and Okrent, D., Eds., Gordon Breach Science Publishers, New York, 1968.
57. Coppalle, A. and Vervisch, P., The Total Emissivities of High-Temperature Flames, *Combustion and Flame*, 49, 101–108, 1983.

Section II

Burner Fundamentals

6 Heat Transfer from Burners

Charles E. Baukal, Jr., Ph.D., P.E.

CONTENTS

- 6.1 Introduction
 - 6.2 Open-Flame Burners
 - 6.2.1 Momentum Effects
 - 6.2.2 Flame Luminosity
 - 6.2.3 Firing Rate Effects
 - 6.2.4 Flame Shape Effects
 - 6.3 Radiant Burners
 - 6.3.1 Perforated Ceramic or Wire Mesh Radiant Burners
 - 6.3.2 Flame Impingement Radiant Burners
 - 6.3.3 Porous Refractory Radiant Burners
 - 6.3.4 Advanced Ceramic Radiant Burners
 - 6.3.5 Radiant Wall Burners
 - 6.3.6 Radiant Tube Burners
 - 6.4 Effects on Heat Transfer
 - 6.4.1 Fuel Effects
 - 6.4.1.1 Solid Fuels
 - 6.4.1.2 Liquid Fuels
 - 6.4.1.3 Gaseous Fuels
 - 6.4.1.4 Fuel Temperature
 - 6.4.2 Oxidizer Effects
 - 6.4.2.1 Oxidizer Composition
 - 6.4.2.2 Oxidizer Temperature
 - 6.4.3 Staging Effects
 - 6.4.3.1 Fuel Staging
 - 6.4.3.2 Oxidizer Staging
 - 6.4.4 Burner Orientation
 - 6.4.4.1 Hearth-Fired Burners
 - 6.4.4.2 Wall-Fired Burners
 - 6.4.4.3 Roof-Fired Burners
 - 6.4.4.4 Side-Fired Burners
 - 6.4.5 Heat Recuperation
 - 6.4.5.1 Regenerative Burners
 - 6.4.5.2 Recuperative Burners
 - 6.4.5.3 Furnace or Flue Gas Recirculation
 - 6.4.6 Pulse Combustion
 - 6.5 In-Flame Treatment
 - References
-

6.1 INTRODUCTION

The primary purpose of a burner is to transfer heat from the combustion products to some type of load. Therefore, it is important to match the burner to the load to ensure heat transfer is maximized in order to maximize the system thermal efficiency. This reduces operating costs and indirectly reduces pollutant emissions because less fuel needs to be combusted for a given production rate. The heat transfer from burners is often a complicated process because of the turbulent fluid flow, high-temperature chemical reactions, and spectral gaseous radiation.

The purpose of this chapter is to consider the heat transfer from different types of burners, without much consideration for the applications of the burners that are discussed in other chapters as they pertain to different burner types. The emphasis here is to give the reader an idea of the general behavior of different types of burners. This information should be useful when considering new applications or reevaluating existing technologies. [Chapter 2](#) contains a general discussion of the modes of heat transfer. Much of this chapter was taken from Baukal (2000).¹

6.2 OPEN-FLAME BURNERS

Open-flame burners are defined here as ones where the flame is not confined, as is the case in radiant tubes (see [Chapter 13](#)), nor are the flames primarily attached to a surface as in porous refractory burners (see [Chapter 14](#)). Open-flame burners are normally visible to the naked eye where the radiant heat from the flame, rather than from a surface heated by the flame, can directly heat the load. Some of the important factors that affect the heat transfer from open-flame burners are considered in this section.

6.2.1 MOMENTUM EFFECTS

There are two aspects to the momentum effects on flames. The first involves the forward momentum normally associated with the average outlet velocity of the combustion products. The second aspect is the lateral momentum caused by swirl. The swirl number is defined as the ratio of the lateral momentum to the forward momentum. Burners with no swirl have a swirl number of zero. Beér and Chigier (1972) defined weak swirl as a swirl number below 0.6 and strong swirl as a swirl number greater than 0.6.⁹ Villasenor and Escalera (1998) studied swirl effects on heavy fuel oil combustion in an air-cooled, high-temperature research furnace.² The experimental results showed that there was a strong dependence between the incident radiation flux and the swirl number. Burners with intermediate swirl numbers (0.1 and 0.4) produced more uniform heat flux profiles than burners with either no swirl, or with higher swirls (0.75 and 1.0). As expected, the burner swirl has an impact on the heat flux distribution from the flame.

6.2.2 FLAME LUMINOSITY

An example of a high-luminosity flame is shown in [Figure 6.1](#).³ An example of a low-luminosity flame is shown in [Figure 6.2](#). The flame luminosity is a function of many variables but is especially dependent on the fuel. Solid and liquid fuels tend to make more luminous flames than gaseous fuels because of particles in the flame that radiate like graybodies. A recent trend in the glass industry has been to make more luminous flames, with natural gas as the fuel, to improve the thermal efficiency of the glass melting process.⁴ The burner design also plays a large role in how luminous the flame will be and how heat is transferred from the flame to the load.⁵

The radiant energy from the flame can be approximated by:⁶

$$q_{\text{rad}} \propto a_p V_f T_f^4 \quad (6.1)$$

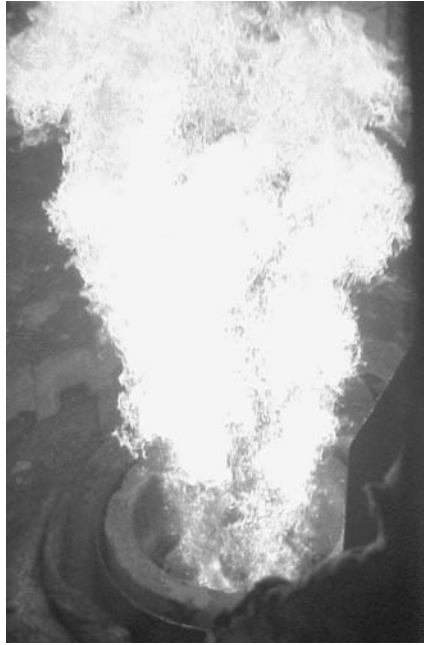


FIGURE 6.1 Example of a high-luminosity oil flame. (Courtesy of John Zink Company, LLC.³)



FIGURE 6.2 Example of a low-luminosity gas flame. (Courtesy of John Zink Company, LLC.³)

where a_p is the Planck-mean absorption coefficient for an optically thin flame, V_f is the flame volume, and T_f is the absolute temperature of the flame. The total heat release by combustion is:

$$q_{\text{total}} = \dot{m}_{\text{fuel}} \Delta H_c \quad (6.2)$$

where \dot{m}_{fuel} is the fuel mass flow rate and ΔH_c is the heat of combustion. The radiant fraction was then defined as the ratio of the radiant heat transfer to the total heat released by combustion:

$$\chi_{\text{rad}} = q_{\text{rad}} / q_{\text{total}} \approx a_p T_f^4 d / u \quad (6.3)$$

where d is the diameter of the nozzle outlet diameter, u is the outlet velocity, and the flame volume was assumed proportional to d^3 and the fuel flow rate to $d^2 u$. Turns and Myhr (1991) studied the interaction between flame radiation and NOx emissions from turbulent jet flames.¹⁶ Radiant fractions were calculated from radiant heat flux measurements made with a transducer having a 150° view angle with a window for free jet flames of C₂H₄, C₃H₈, CH₄, and a blend of 57% CO/43% H₂. A global residence time was defined as:

$$\tau_g = \frac{\rho_f w_f^2 l_f f_s}{3 \rho_0 d^2 u} \quad (6.4)$$

where ρ_f is the flame density, w_f is the flame width, l_f is the flame length, f_s is the fuel mass fraction, and ρ_0 is the cold fuel density. Figure 6.3 shows a plot of the calculated radiant fraction as a function of the global residence time for all four fuels. At small residence times, the radiant fraction is somewhat independent of the fuel composition because the flames are momentum-dominated and nonluminous. As the residence time increases, the radiant fraction becomes dependent on the sooting tendency of the fuel.

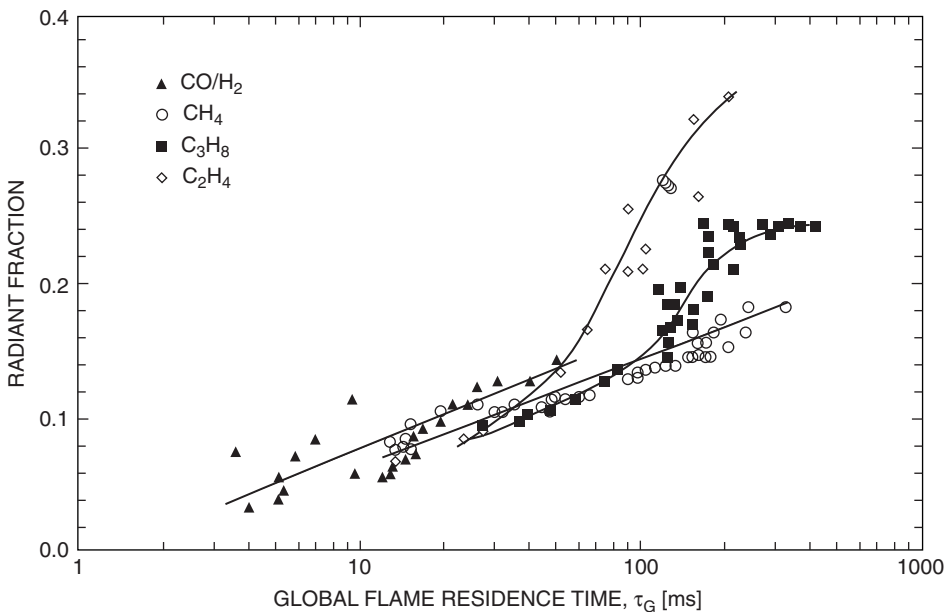


FIGURE 6.3 Flame radiant fractions as functions of global residence time. (Courtesy of The Combustion Institute.¹⁶)

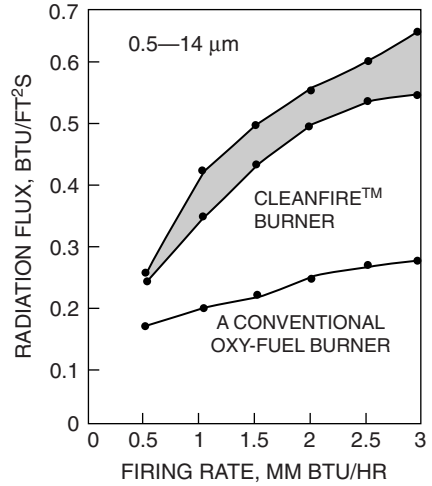


FIGURE 6.4 Comparison of measured flame radiation for a new style oxy/fuel burner Cleanfire™ Burner and a conventional oxy/fuel burner.⁷

Slavejkov et al. (1993) showed that a new style oxy/fuel burner can produce significantly more radiant flux than conventional, older-style designs.⁷ A comparison of the radiant flux as a function of firing rate is shown in Figure 6.4. In some cases, the measured radiant flux was more than doubled using the new burner design.

6.2.3 FIRING RATE EFFECTS

The main concern in industrial combustors is normally to maintain a certain temperature profile in the material being heated, which often equates to a specific temperature profile inside the combustor for a given burner type. It is often necessary to adjust the firing rate to meet the needs of a given application. For example, for an existing combustion system, it may be desirable to increase the material processing rate, which normally means that the firing rate must be increased. The design question to be answered is by how much, because this may or may not be a linear relationship. Another example is the modification of a well-known system design for higher or lower throughput rates. Again, the question is how to do the scaling from the known design.

There are many possible ways to scale a burner according to changes in the firing rate, which is the primary characteristic of interest in most industrial applications. Spalding (1963),⁸ Beér and Chigier (1972),⁹ and Damköhler (1936)¹⁰ looked at numerous dimensionless groups based on considerations of the momentum, energy, and mass balances. Some of these groups include the Reynolds, Froude, and Damköhler numbers. However, it is not possible to maintain all of the dimensionless groups constant simultaneously.

The two most common methods used to scale industrial burners are constant velocity and constant residence time. Constant velocity scaling is, by far, the most popular. The burner thermal input (Q) can be calculated using:

$$Q_0 = K\rho_0 u_0 d_0^2 \quad (6.5)$$

where ρ_0 , u_0 , and d_0 are the inlet average fluid density, characteristic fluid velocity, and characteristic diameter, respectively, and K is a proportionality constant. Assuming that the inlet fluid density is constant, and the characteristic inlet fluid velocity u_0 is held constant, then the constant velocity scaling law can be written as:

$$d_1 \propto (Q_1)^{0.5} \quad (6.6)$$

where the new characteristic burner diameter d_1 is proportional to the square root of the new firing rate. This law simply says that the outlet area of the burner is directly proportional to the firing rate for a constant-velocity scaling law. For round outlets, the area is proportional to the square of the diameter.

The principle for constant residence-time scaling is to maintain the ratio of d_0/u_0 , which has the units of time (typically seconds). This scaling law, sometimes known as the inertial or convective time scale, can then be written as:

$$d_1 \propto (Q_1)^{0.33} \quad (6.7)$$

This approach is not as commonly used because it leads to very low windbox pressures for smaller burners and excessive pressures for larger burners.¹¹

The heat transfer from the flame to the furnace and load is often dominated by radiation close to the burner outlet. Further from the burner outlet, radiation and convection may both be important. Another approach to scaling is based on the radiative characteristics of the flame. Markstein (1976) developed a correlation for buoyancy-dominated turbulent flames.¹² Other correlations have been developed for laminar flames.^{13,14} Works by Buriko and Kuznetsov (1978),¹⁵ Turns and Mayr (1991),¹⁶ Faeth et al. (1989),¹⁷ and Delichatsios et al. (1988, 1992)^{18,19} have quantified radiation from flames for different fuels of different sooting tendencies, using the radiant fraction as a scaling parameter. All of the above were for free jets, without confinement and not inside a hot combustor. The radiation scaling inside a combustor is more complicated because of recirculation effects and reradiation from the furnace walls to the flame gases.

Weber (1996) reported on burner scaling effects for firing rates ranging from 7 kW to 14 MW (24×10^3 to 48×10^6 Btu/hr) or a 2000:1 turndown range.²⁰ The goal of the study, known as the Scaling 400 Study for the nominal turndown of 400:1,²¹ was to determine the proper method for scaling burner sizes. The burner used in that study was a staged mixing burner for primary, secondary, and tertiary air, with variable swirl capability. The primary conclusions of the study were that:

- The fuel-to-air momentum ratio must be maintained.
- The geometrical burner similarity must be maintained (small departures are acceptable).
- The confinement effects of the furnace are secondary if the confinement ratio (furnace-to-burner diameter ratio) is larger than 3.
- The inlet swirl should be reduced by 20 to 30% for laboratory-scale burners with characteristic diameters less than 2 in. (5 cm).

Baukal and Gebhart (1998) studied oxygen-enhanced natural gas flames impinging normal to a water-cooled flat metal disk.²² The firing rate of the burner was one of the parameters studied to determine its effect on the heat transfer to the target. The heat flux was determined by calorimetry to concentric water-cooled rings on the target. The firing rate was varied from 5 to 25 kW (17,000 to 85,000 Btu/hr). The upper limit was a function of the flow control equipment. Figure 6.5 shows contours of the heat flux as functions of both the axial and radial distances from the burner, with 35% total O₂ in the oxidizer ($\Omega = 0.35$). This was the lowest oxidizer composition that could be used which produced an acceptable flame throughout the entire range of firing rates for the burner that was used (see Figure 2.23). These plots show that for small L, the peak heat flux did not occur at the stagnation point, but at about $R_{\text{eff}} = 0.5$ to 0.7. This was caused primarily by a slightly higher heat output from the burner at that radial location.²³ The heat flux increased by 40 to 230%, depending on the axial and radial position, by increasing the firing rate 400% by going from 5 to 25 kW (17,000 to 85,000 Btu/hr). The smallest percentage improvements were for the closest axial ($L = 0.5$) and radial ($R_{\text{eff}} = 0.16$) locations. This was because the heat flux rate was already relatively high there, compared to farther axial and radial locations. The largest percentage improvements

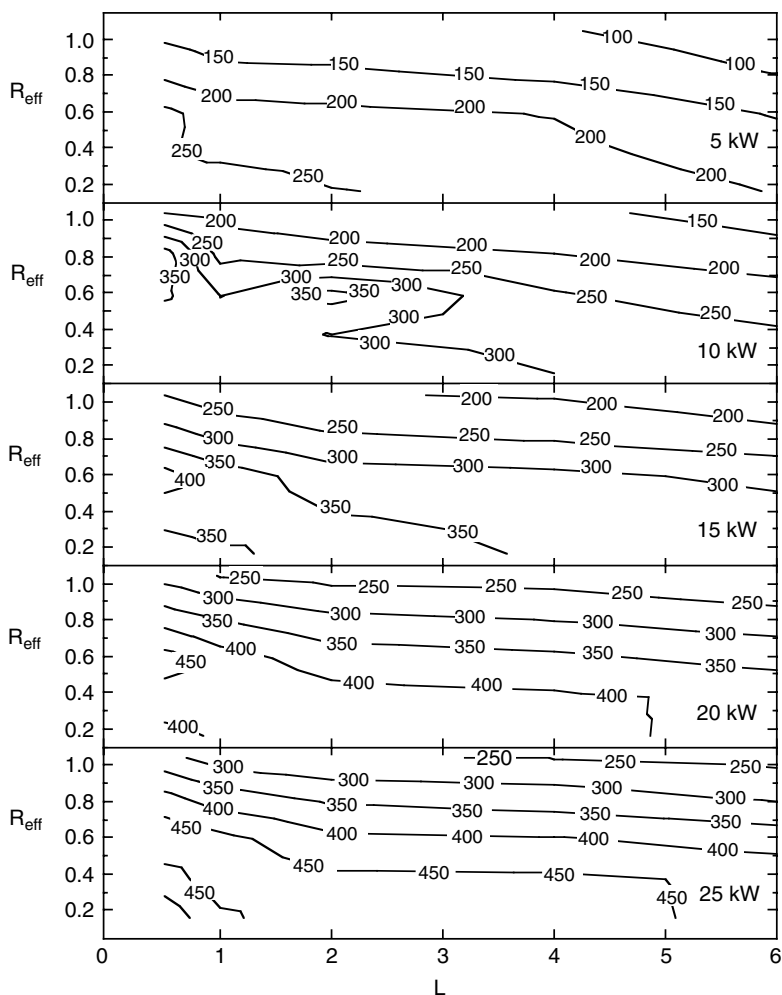


FIGURE 6.5 Contours of the total heat flux, q'' (kW/m^2), from stoichiometric natural gas flames ($\Omega = 0.35$) with various firing rates ($q_f = 5$ to 25 kW) impinging on the surface of an untreated stainless target.²²

occurred at the farthest axial ($L = 6$) and radial ($R_{\text{eff}} = 1.04$) locations, because the heat flux rate was initially so low there. At $q_f = 5$ kW and $R_{\text{eff}} = 1.04$, the heat flux increased by 91% by decreasing the axial spacing from $L = 6$ to $L = 0.5$. However, at $q_f = 25$ kW ($85,000$ Btu/hr) and $R_{\text{eff}} = 0.16$, the heat flux decreased by 14% by decreasing the axial spacing from $L = 6$ to $L = 0.5$. In general, at higher firing rates, the heat flux did not have a strong dependence on the axial distance L between the flame and the target. At the farthest axial location ($L = 6$), the heat flux to the inner calorimeter was approximately double the heat flux to the outer calorimeter. However, at the closest axial spacing ($L = 0.5$), the peak flux occurred at about the middle calorimeter ($R_{\text{eff}} = 0.59$).

Figure 6.6 shows heat flux contours similar to Figure 6.7, but for a pure O oxidizer. The peak fluxes occurred at the stagnation point, except for $q_f = 20$ and 25 kW ($68,000^2$ and $85,000$ Btu/hr) for $L = 0.5$, where a slightly higher flux was measured at $R_{\text{eff}} = 0.37$. The heat flux increased by 78 to 470%, depending on the axial and radial locations, by increasing the firing rate from 5 to 25 kW ($17,000$ to $85,000$ Btu/hr). Again, the largest percentage improvements occurred at the farthest locations while the smallest improvements occurred at the closest locations. Unlike the $\Omega = 0.35$ data in Figure 6.6, the heat flux strictly increased, by 42 to 230%, as the axial spacing decreased

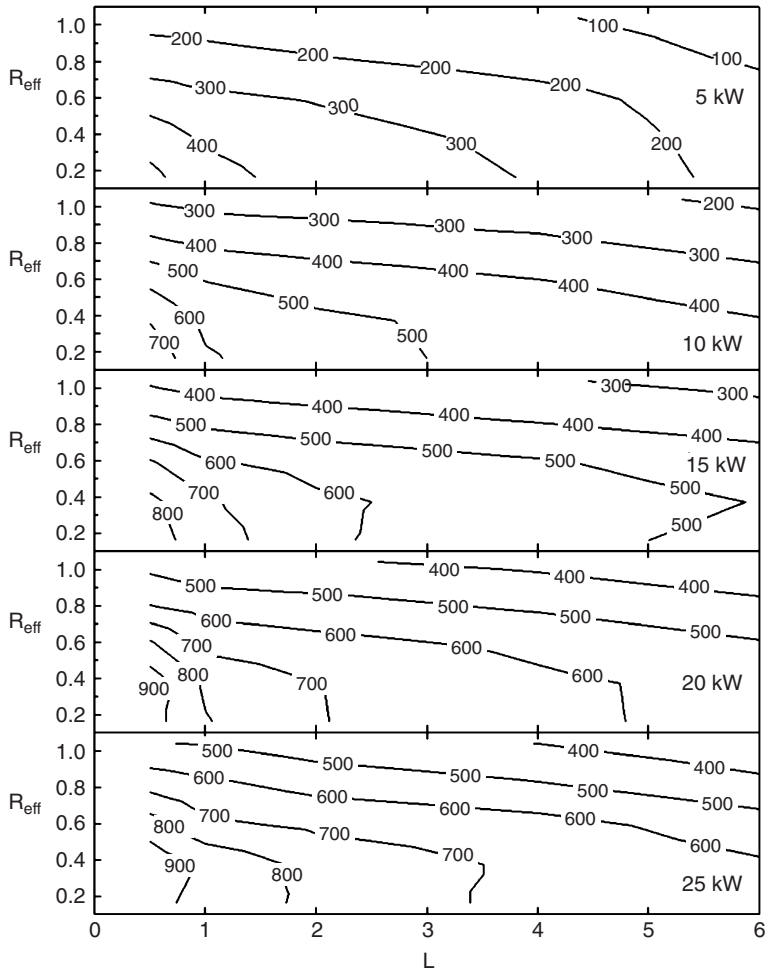


FIGURE 6.6 Contours of the total heat flux, q'' (kW/m^2), from stoichiometric natural gas flames ($\Omega = 1.00$) with various firing rates ($q_f = 5$ to 25 kW) impinging on the surface of an untreated stainless target.²²

for the $\Omega = 1.00$ data in Figure 6.6. Like the $\Omega = 0.35$ data, at large axial spacings, the heat flux to the innermost calorimeter was approximately double the flux to the outermost calorimeter.

Figure 6.7 shows how the heat flux to the innermost calorimeter was affected by the axial location of the target and by the burner firing rate. The heat flux increased with the firing rate and decreased with the axial distance. The shape of the contour lines was significantly different for the $\Omega = 0.35$ flames, compared to the $\Omega = 1.00$ flames. The peak flux occurred at an intermediate axial location ($L \approx 2$) for the $\Omega = 0.35$ flames. For the $\Omega = 1.00$ flames, the heat flux strictly increased as the axial spacing decreased.

Figure 6.8 shows that for $\Omega = 1.00$ and large L , the heat flux increased rapidly with the firing rate. The shape of each curve is similar. In all cases, the heat flux increased with the firing rate and decreased with the axial spacing. The thermal efficiency η was defined as:

$$\eta = \frac{\sum_{i=1}^5 q_i'' A_i}{q_f} \quad (6.8)$$

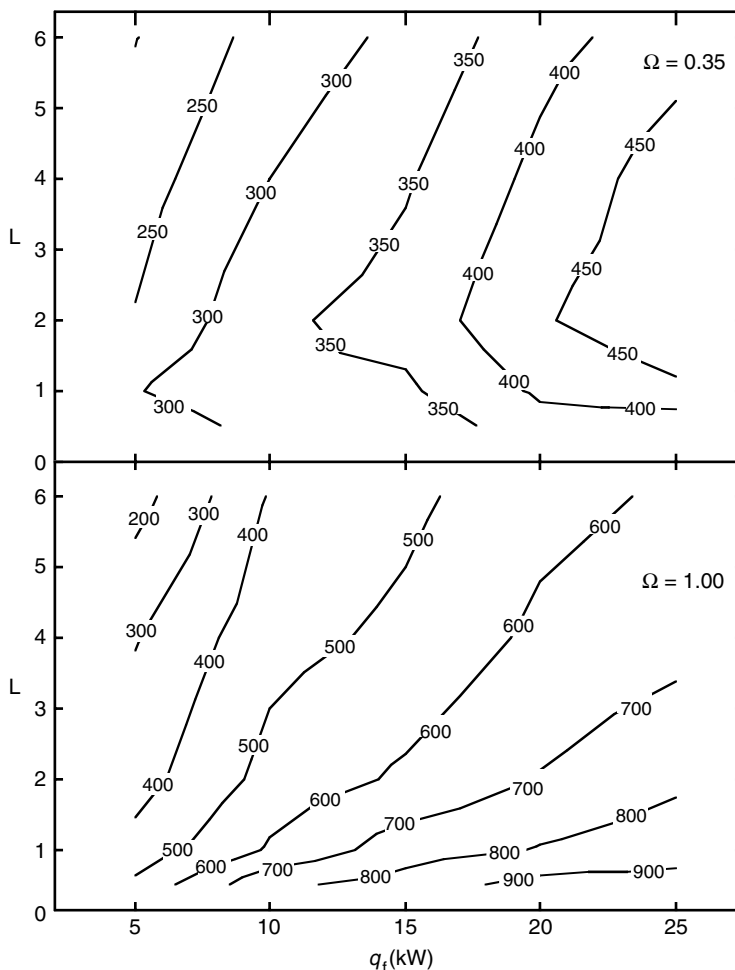


FIGURE 6.7 Contours of the total heat flux, q'' (kW/m²), from stoichiometric natural gas flames of various firing rates ($q_f = 5$ to 25 kW) and oxidizer compositions ($\Omega = 0.35$ and 1.00) to the stagnation point ($R_{\text{eff}} = 0.16$) of an untreated brass target.²²

where q''_i was the calculated heat flux to ring i , A_i was the impingement surface area of ring i , and q_f was the burner firing rate. The efficiency was then the total energy absorbed by the first five calorimeters divided by the burner firing rate. Figure 6.9 shows how the thermal efficiency varied with the firing rate, oxidizer composition, and axial location. The efficiency decreased with L , increased with Ω , and decreased with the firing rate. At $\Omega = 1.00$ and $q_f = 5$ kW (17,000 Btu/hr), the efficiency decreased rapidly from $L = 4$ to $L = 6$, because, at $L = 6$, the visible flame length was less than the distance between the burner and the target. Buoyancy effects were visually evident, as the flame shape was highly transient and wavy. Air infiltration may have significantly reduced the heat flux to the target for that set of conditions.

6.2.4 FLAME SHAPE EFFECTS

Hutchinson et al. (1975) experimentally and numerically showed that a quarl (burner block or tile) shortened the flame on an air/natural gas burner with swirl firing into a water-cooled cylindrical furnace.²⁴ The recirculation zone in the furnace was pulled closer to the burner with the

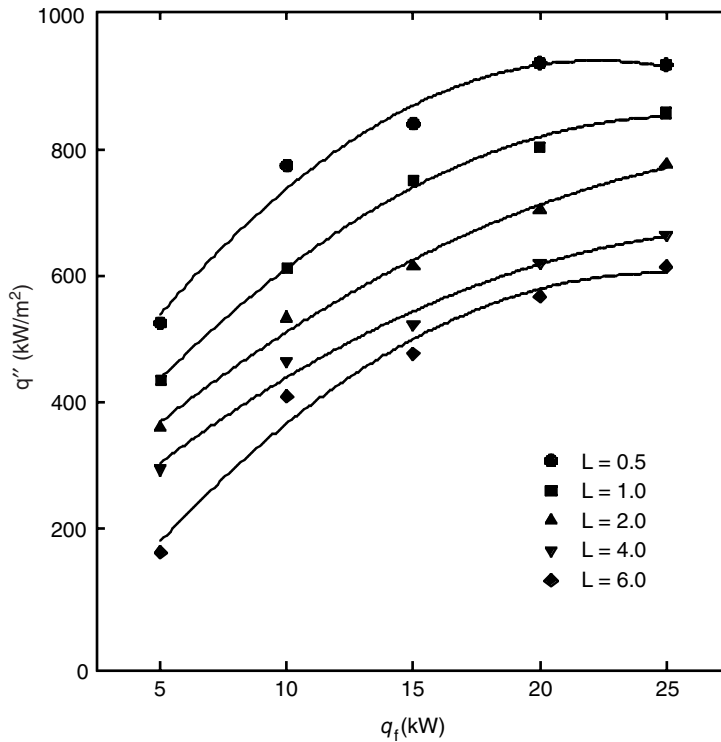


FIGURE 6.8 Total heat flux (q'') from stoichiometric natural gas flames ($\Omega = 1.00$) of various firing rates (q_f) impinging on the stagnation point ($R_{\text{eff}} = 0.16$) of an untreated stainless target.²²

quarl, compared to the same burner without a quarl. Higher temperatures and heat fluxes were measured closer to the burner with the quarl, than without the quarl. The quarl shortened the flame and moved the heat release closer to the burner. The calculations showed that the convective heat transfer and the radiative heat transfer to the furnace wall were of the same order with or without the quarl.

One recent burner development trend in about the last decade has been the development of so-called flat flame burners. This can mean different things, but here it refers to a rectangular flame shape (see Figure 16.29), as opposed to the traditional round flame shape. The goal is to have a higher flame surface area to increase the area that radiates from the flame to the load. This trend in burner design has been particularly evident in the use of oxygen-enriched burners (see Chapters 20 and 21) in the glass and aluminum industries. If the trend continues, this type of flame will likely be applied to other industrial heating and melting applications.

There are numerous examples of the use of flat flames in glass melting (e.g., Figure 20.24). Kirilenko et al. (1988) described a flat flame burner used in a regenerative glass-melting furnace.²⁵ Ibbotson (1991) described a technique for lancing a fan-shaped jet of oxygen under a fuel port in a glass-melting furnace to improve temperature uniformity and minimize hot spots.²⁶

Flat shape flames have also been used in aluminum melting. Yap and Pourkashanian (1996) described a flat flame oxy/fuel burner that they describe as a large aspect-ratio flame.²⁷ The burner was claimed to have more uniform heat transfer rates, compared to conventional round flame burners. The burner also had excellent flame stability, resulting in a wide operating range, low NO_x emissions, and high flame luminosity. The combination of low NO_x emissions and high luminosity, both of which are important in most heating applications, is a unique aspect of the burner.

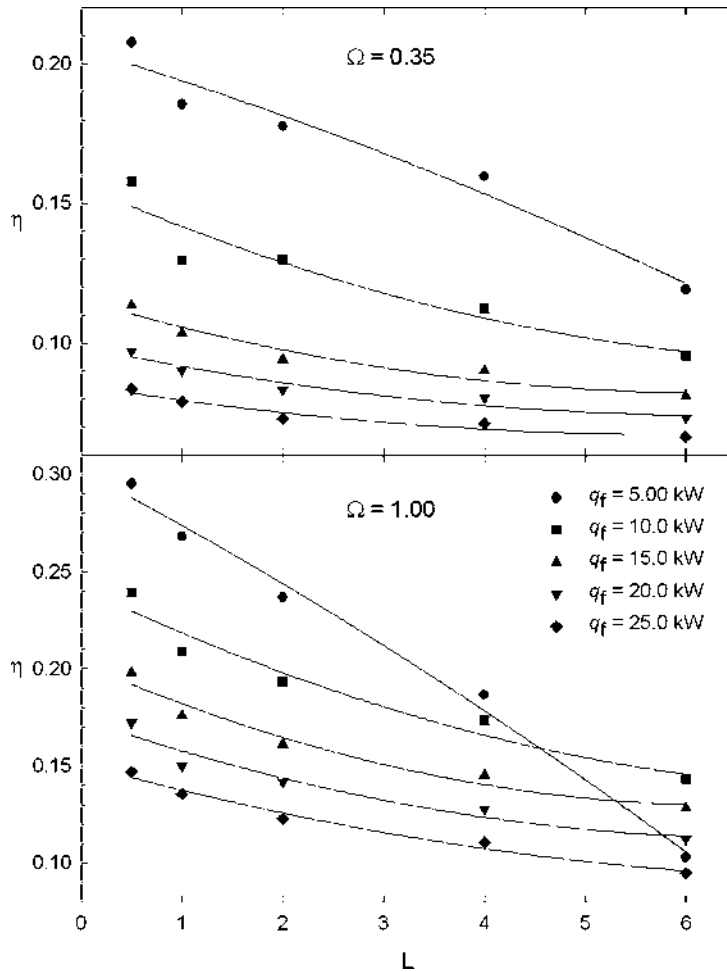


FIGURE 6.9 Thermal efficiency (η) for stoichiometric natural gas flames of various firing rates ($q_f = 5$ to 25 kW) and oxidizer compositions ($\Omega = 0.35$ and 1.00).²²

In addition, the burner minimized oxidation of the molten aluminum, which maximizes the product yield.

The length of the flame influences the heat transfer as longer flames may be more luminous and lower temperature compared to similar flames at the same operating conditions. Blake and McDonald (1993) have correlated visible flame length data for vertical turbulent diffusion flames as follows:²⁸

$$\frac{l_f}{d_f} = \alpha_1 \left(\frac{4J}{\pi \rho_\infty g d_f^3} \right)^{\alpha_2} \quad (6.9)$$

where l_f is the flame length, d_f is the flame diameter, J is the momentum of the source jet, ρ_∞ is the density of the ambient, g is the gravitational constant, and α_1 and α_2 are constants as given in Table 6.1. The fraction inside the parentheses in Equation 6.9 is referred to as the density weighted Froude number.

TABLE 6.1
Constants for Flame Length Equation

$4J/\pi\rho_{\infty}gd_f^3$	α_1	α_2
10^{-9} – 10^{-6}	6.73	0.209
10^{-6} – 10^{-4}	7.79	0.218
10^{-4} – 10^{-1}	7.25	0.184

Source: Adapted from T.R. Blake and M. McDonald, *Comb. Flame*, 94, 426–432, 1993.

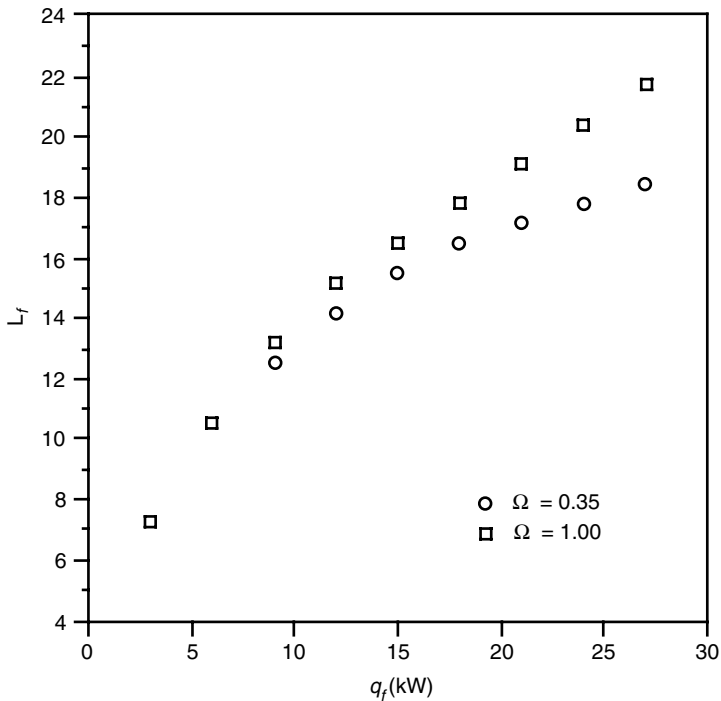


FIGURE 6.10 Flame length as function of firing rate and oxidizer composition for stoichiometric natural gas flames.²⁹

Figure 6.10 shows how the visible flame length for an open-flame diffusion burner varies as a function of the firing rate and oxidizer composition.²⁹ The flame length was nearly the same for lower firing rates. At higher firing rates, the pure O₂ flames ($\Omega = 1.00$) were longer than the lower purity flames ($\Omega = 0.35$). The flame length affects the flame shape, which influences the radiating area of the flame.

6.3 RADIANT BURNERS

Radiant burners operate by combusting a fossil fuel, which heats a solid surface that radiates infrared energy to a load. These burners are used in a number of lower temperature heating and drying applications, including, for example:

- Drying paper and cardboard in a paper mill
- Paper finishing
- Drying wood
- Porcelain frit drying
- Curing ceiling tiles
- Teflon curing
- Drying and curing coatings on paper and metals
- Curing ink on paper and powder coat paints
- Baking in mass food preparation
- Setting dyes in textile and carpet production, sometimes referred to as pre-drying
- Curing lens assemblies in automotive headlamp assembly manufacturing
- Plastics curing

Both gas-fired and electric radiant heaters are commonly used, however, gas-fired radiant burners have lower operating costs due to the difference between the cost of electricity and natural gas in most locations. Pettersson and Stenström (1998) compared gas-fired and electric IR heaters in two paper-coating drying processes.³⁰ The efficiency of the gas-fired and electric dryer was 30% and 40%, respectively. However, there was considerable uncertainty in the measurements due to the difficulty in obtaining accurate moisture measurements of the paper being dried. Even if the efficiencies are correct, the gas-fired system may still be more economical, depending on the cost of electricity vs. natural gas.

Radiant burners (see [Chapter 13](#)) are designed to produce a uniform surface temperature heat source for heating and melting a variety of materials. The uniform surface temperature produces more homogeneous heating of the materials, which normally improves the product quality compared to conventional burners that may produce hot spots. Other advantages of these burners may include:

- High thermal efficiencies
- Low pollutant emissions
- Directional heating
- Very fast response time to load changes
- Very fast heating compared to convective heating
- Burner shape can be tailored to the shape of the heat load to optimize heat transfer
- Ability to segment a burner to produce a nonuniform heat output profile, which may be useful in certain types of heating and drying applications
- Certain types of radiant burners have very rapid heat-up and cool-down times
- No open flames that could ignite certain types of materials (e.g., paper or textiles)
- More control over the heating process because of the known and measurable surface temperature of the radiant surfaces compared to open flames, where the flame temperature is very difficult to measure
- Burners are very modular and can be configured in a wide variety of geometries to accommodate the process heating requirements

The primary parameters of interest for radiant burners are the power density (firing rate per unit area), radiant efficiency (fraction of fuel heating value converted to thermal radiation), heat-up and cool-down time, and pollutant emissions. Other factors of importance include cost, durability, and longevity.

There are also some important limitations of porous refractory burners, compared to more conventional open-flame burners, which may include:

- Relatively low temperature limit for the radiant surface due to the limits of the refractory material
- Fuel and oxidizer must be clean to avoid plugging the porous radiant surface, which essentially precludes the use of fuels such as coal or heavy fuel oil

- Some of the radiant surfaces can be damaged by water or by contact with solid materials that may be prevalent in certain applications
- Holes in the radiant surface can cause flashback because these burners use premix
- Some designs may have high pressure drops, which means that more energy is needed for the blower to flow the combustion air through the ceramic burner material
- Due to the limits in radiant surface temperatures, the firing rate density is usually limited
- Some types of radiant burners using hard ceramic surfaces may have high heat capacities that could ignite certain load materials upon a sudden line stoppage

In these burners, fuel and air are premixed and combusted, either just inside a radiating surface or just above the surface, depending on the operating conditions and specific radiant burner design. If the mixture velocity is too low, flashback or flame extinguishment can occur, depending on the design of the burner. In addition to the operational considerations, flashback is an obvious safety concern. If the mixture velocity is too high, the flame may blow off or the radiant performance may be severely reduced because the burner surface is not being directly heated by the hot exhaust products. Depending on the specific design of the burner, optimum performance is achieved when the flame is stabilized just inside or just above the outer burner outlet.

Howell et al. (1995) refer to the burner material as “porous inert media” and present a review of these types of burners that have been made from a wide variety of ceramics, which often include alumina, zirconia, or silicon carbide.³¹ Hsu and Howell (1993) developed the following equation for the effective thermal conductivity of partially stabilized zirconia (PSZ) (zirconium oxide plus <3% magnesium oxide) for temperatures in the range of 290 to 890K (63 to 1140°F) and for sample pore sizes from 10 to 65 pores per inch (ppi):³²

$$k \text{ (W/m-K)} = 0.188 - 0.0175 d \quad (6.10)$$

where d is the actual pore size of the material (in mm) and $0.3 < d < 1.5$ mm.

Speyer et al. (1997) studied the performance of four different types of commercial gas-fired radiant burners: a metal (Fe-Cr-Al) fiber (~40 μm diameter) burner, a reticulated ceramic burner made of a porous cordierite ($\text{Mg}_2\text{Al}_4\text{Si}_5\text{O}_{18}$), a porous single-unit mullite ($\text{Al}_6\text{Si}_2\text{O}_{13}$) tile burner, and a flame impingement burner where the products of combustion are forced around a metal screen that radiates to the load.³³ The study was sponsored by the Gas Research Institute (Chicago, IL). The thermal efficiencies as a function of the combustion intensity are shown in Table 6.2. The efficiency was determined by measuring the radiant output or radiosity from the burner surface and

TABLE 6.2
Comparison of Thermal Efficiencies for Radiant Burners

Radiant Burner Type	Combustion Intensity (kW/m ²)	Thermal Efficiency Range (%)
Metal fiber		
No perforations	150–540	18–26
With perforations	150–540	16–27
With perforations and front metal screen	100–440	22–38
Reticulated ceramic	150–630	27–39
Ported ceramic	140–520	37–54
Flame impingement	150–430	46–52

Source: Adapted from R.F. Speyer, W.-Y. Lin, and G. Agarwal, *Exp. Heat Transfer*, 9, 213–245, 1996.³³

was calculated using:

$$e = \frac{R_T}{\dot{V}_g \Delta H_c / A} \quad (6.11)$$

where e is the calculated efficiency, R_T is the measured radiosity, \dot{V}_g is the volume flow rate of the fuel, H_c is the heating value of the fuel, and A is the surface area of the burner. The experimental results showed that the peak radiosity measurements as a function of the air-to-fuel mixture ratio occurred for percent excess fuels ranging from 6 to 7.5%, depending on the specific burner design. Similar results were calculated for the radiant efficiencies. Preheating the air/fuel mixture increased both the radiosity and thermal efficiencies essentially in a linear manner for mixture temperatures ranging from 40 to 155°C (100 to 311°F). In most cases, the efficiency declined with combustion intensity, except for the reticulated ceramic and metal fiber with perforations and a front metal screen, both of which had peak efficiencies at intermediate combustion intensities. The flame impingement and ported ceramic burners were the most efficient, while the metal fiber with and without perforations was the least efficient. The study also showed that the thermal efficiency generally increased as the fraction of closed area increased on the burner surface.

The heat transfer coefficient between the hot exhaust products and the radiant burner material is difficult to predict and measure due to the uncertainty in the surface area of the ceramic structure. These coefficients have traditionally been presented in terms of a volumetric coefficient (Btu/hr-°F-ft³ or kW/°C-m³). Chen et al. (1987) assumed the coefficient was large enough that the temperature of the solid was essentially the same as the temperature of the hot flowing gas.³⁴ Sathe et al. (1990) used a value of 2×10^9 W/m³-K (1×10^8 Btu/hr-°F-ft³) computed for cylinders in cross flow.³⁵ Hsu et al. (1993) used 10^7 W/m³-K (5×10^5 Btu/hr-°F-ft³).³⁶ Younis and Viskanta (1993) empirically determined the following correlation for alumina and cordierite ceramic foams with pore diameters ranging from 0.29 to 1.52 mm (0.011 to 0.0598 in.):³⁷

$$\text{Nu} = 0.819 [1 - 7.33 (d/L)] \text{Re}^{0.36[1 + 15(d/L)]} \quad (6.12)$$

where d is the actual pore diameter and L is the thickness of the specimen in the flow direction. Fu et al. (1998) noted the relationship between the volumetric heat transfer coefficient h_v and the convection coefficient h :³⁸

$$h_v = a_v h \quad (6.13)$$

where a_v can be computed using the following empirical equation:

$$a_v = 169.4 \text{ PPC} (\text{m}^2/\text{m}^3) \quad (6.14)$$

where PPC is the number of pores per centimeter for cellular ceramics. Four different choices for the characteristic dimension were identified:

$$\text{The reciprocal of the surface area, } d_a = 1/a_v \quad (6.15)$$

$$\text{The hydraulic diameter, } d_h = 4\phi/a_v \quad (6.16)$$

$$\text{The mean pore diameter, } d_m = \frac{\sqrt{4\phi/\pi}}{\text{PPC}} \text{ (cm)} \quad (6.17)$$

$$\text{The ratio of the inertial to the viscous friction coefficients, } d_r = \beta/\alpha \quad (6.18)$$

where ϕ is the porosity, β is the inertia coefficient in the Reynolds-Forchheimer equation, and α is the viscous coefficient in the Reynolds-Forchheimer equation. The following empirical correlations,

using each of these characteristic dimensions, were developed for specimens having a PPC ranging from 4 to 26:

$$\text{Nu}_v = \left[0.0426 + \frac{1.236}{L/d_m} \right] \text{Re}_{d_m} \quad \text{for } 2 \leq \text{Re}_{d_m} \leq 836 \quad (6.19)$$

$$\text{Nu}_v = \left[0.0730 + \frac{1.302}{L/d_h} \right] \text{Re}_{d_h} \quad \text{for } 3 \leq \text{Re}_{d_h} \leq 1594 \quad (6.20)$$

$$\text{Nu}_v = \left[0.0252 + \frac{1.280}{L/d_a} \right] \text{Re}_{d_a} \quad \text{for } 1 \leq \text{Re}_{d_a} \leq 480 \quad (6.21)$$

$$\text{Nu}_v = \left[0.000267 + \frac{1.447}{L/d_r} \right] \text{Re}_{d_r} \quad \text{for } 0.02 \leq \text{Re}_{d_r} \leq 2.4 \quad (6.22)$$

where Nu_v is the volumetric Nusselt number, defined as:

$$\text{Nu}_v = \frac{h_v l_c^2}{k} \quad (6.23)$$

where l_c is the characteristic pore length and k is the thermal conductivity of the gas. The uncertainty in the correlations was largest for the smaller Reynolds numbers.

One of the challenges of gas-fired infrared burners is determining the radiant efficiencies. Mital et al. (1998) noted that there is a wide discrepancy in the reported radiant efficiencies (varying by more than 200%) for radiant burners.³⁹ Part of the discrepancy was attributed to a lack of a standard measurement technique to determining the efficiency. Other problems include nondiffuse radiation from the burners and nonuniform burner surfaces. They presented a technique that is not sensitive to burner surface nonuniformities. Typical results for a reticulated ceramic foam radiant burner are shown in Figure 6.11. A calorimetric method was used to check the consistency of the data. It was shown that single-point radiation measurements can deviate considerably from more rigorous multi-point measurement techniques. Yetman (1993) described a simple technique for measuring the total radiant output of an infrared burner using a narrow-angle pyrometer.⁴⁰ Johansson (1993) presented a method for measuring the spectral output of radiant burners using an infrared spectrometer.⁴¹

Madsen et al. (1996) measured the spectral radiation from several types of radiant burners.⁴² As can be seen, the spectra are fairly similar that have distinctive peaks around 3 and 4.5 μm . This shows the selective emittance of certain types of radiant burners and the possibility of matching the burner to the load spectral absorptivity to optimize heat transfer efficiency.

6.3.1 PERFORATED CERAMIC OR WIRE MESH RADIANT BURNERS

Examples of these types of burners are shown in Figure 6.12. Perforated or ported ceramic burners may consist of a pressed ceramic plate that may include prepunched holes, where the flames heat the surface directly.⁴³ The surface can be textured to further enhance the radiant efficiency of the burner. New developments in ceramic foams are being applied to this type of burner. These foams are often less expensive to make than perforated ceramics. They provide a higher surface area for radiation and a more uniform heating surface, compared to perforated ceramics. Many shapes are possible with the ceramic foams and the pore size is adjustable. Flanagan et al. (1992) described the use of a ported ceramic burner to achieve low NOx emissions.⁴⁴ However, the burner was

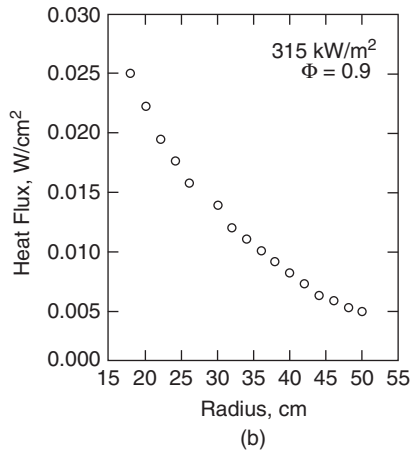
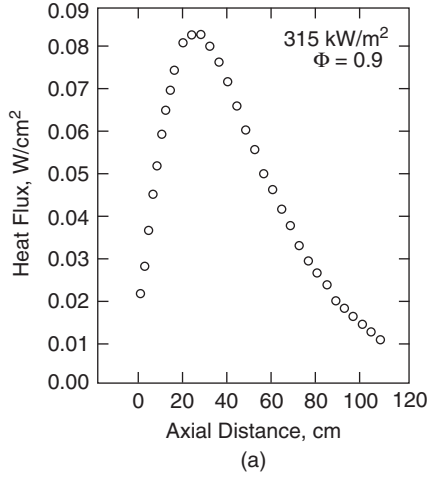


FIGURE 6.11 Heat flux measurements from a ceramic foam radiant burner as a function of (a) the axial distance from the burner surface and (b) the radial distance from the center of the burner. (Courtesy of The Gas Research Institute.³⁹)

actually fired at up to 15 times its normal maximum design firing rate so that the flames were highly lifted and therefore did not radiate from the surface as in normal operation. Mital and Gore (1994) discussed the use of a reticulated ceramic insert to enhance radiation heat transfer in direct-fired furnaces.⁴⁵ The insert was placed downstream of the outlet of a laminar diffusion flame. Experimental results showed up to a 60% improvement in radiative heat flux compared to the case with no insert. There was a significant difference in radiative heat flux with and without the insert. Kataoka (1998) described a new type of high-temperature porous ceramic burner made of aluminum titanate (Al_2TiO_5) capable of surface temperatures up to 1100°C (2000°F).⁴⁶

Wire mesh burners are made from high-temperature-resistant metals, such as stainless steels or inconel. The open area in the mesh serves as the port area for the burner. However, due to the high thermal conductivity of metals, several layers of mesh are often required to prevent flashback. The thermal conductivity between the layers is much less than through the mesh itself because of the contact resistance between the layers. An important problem with wire mesh radiant burners are the lower temperature limits compared to ceramic burners, due to the temperature limits of the metals.

6.3.2 FLAME IMPINGEMENT RADIANT BURNERS

This burner is sometimes referred to as a direct-fired refractory burner. In this type of radiant burner, the flame impinges on a hard ceramic surface, which then radiates to the load. The heat transfer from the flame to the tile is mostly by convection due to the direct flame impingement. The heat



FIGURE 6.12 Examples of porous ceramic and wire mesh radiant burners. (Courtesy of Solaronics.⁴³)

transfer from the burner tile to the load is purely by radiation. The hot exhaust gases from the burner heat up the surrounding wall by convection, but at a much lower rate than to the burner tile. One advantage of this type of burner is that there is no metal matrix with lower temperature limits compared to ceramic that has high temperature limits. Therefore, this type of burner can often be used in higher temperature applications. There also is no matrix of porous ceramic fiber refractory that could get plugged up as in the next type of burner. This type of burner can also fire a liquid fuel as opposed to many other radiant burners that use only gas. A disadvantage is that the heat flux is not as uniform as other types of radiant burners. Another problem is that the burner tile has the typical problem of thermal cycling, which can cause the tile to disintegrate.

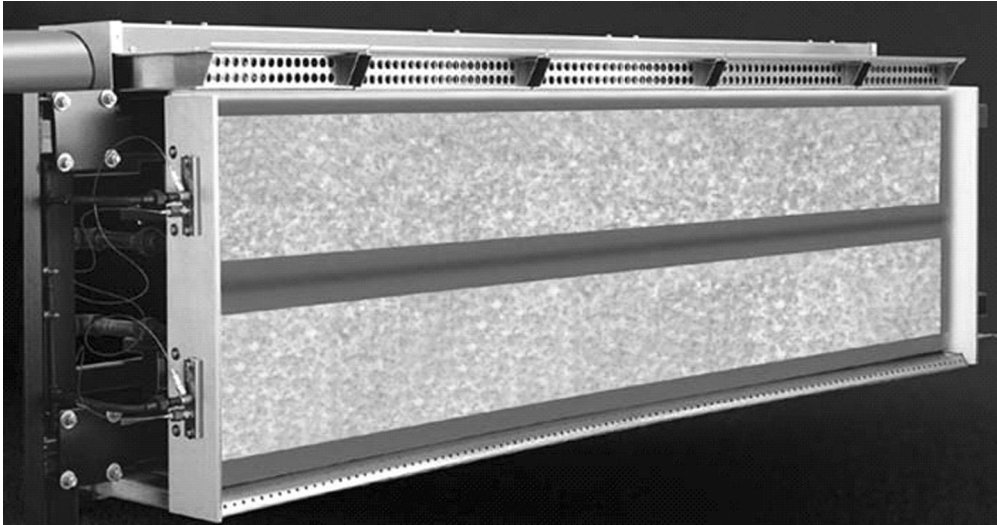


FIGURE 6.13 Flat-panel infrared burner. (Courtesy of Marsden, Inc., Pennsauken, NJ.)

6.3.3 POROUS REFRACTORY RADIANT BURNERS

In this type of burner, the surface is made of a porous ceramic fiber that is often made in a vacuum-forming process. A relatively new type is now available, made from a woven ceramic fiber mesh, similar to the wire mesh radiant burners except that ceramic fiber is used instead of metal. The predominant shape used in porous refractory burners is a flat panel. An example is shown in Figure 6.13.

In addition to flat panels, other shapes are also available. Alzeta Corp. (Santa Clara, CA) makes many cylindrically shaped porous refractory burners.^{47,48} For their Duratherm™ burners, sizes range from as small as 2 in. (5 cm) in diameter by 4.5 in. (11 cm) long, to as large as 30 in. (76 cm) in diameter by 180 in. (460 cm) long. Firing rates range from 23,000 Btu/hr (6.7 kW) to 16.5×10^6 Btu/hr (4.83 MW). Bartz et al. (1992) describe the use of an Alzeta porous refractory radiant burner to incinerate volatile organic compounds (VOCs).⁴⁹ The unique aspect of the combustion system was that the burner was formed into a cylinder and fired inwardly while the VOCs flowed into that inner core with the combustion products where the VOCs were then destroyed. Very high VOC destruction efficiencies were measured.

The American Gas Association made an extensive study of radiant burners, both gas fired and electric.⁵⁰ For the gas-fired burners, they determined what was termed a “Gas Infrared Radiation factor” (GIR), which was determined as follows:

$$\text{GIR} = \frac{W}{\sigma T_b^4} \quad (6.24)$$

where $W = Q/A$ was the total normal infrared radiation from the burner measured by a spectrophotometer, σ is the Stefan-Boltzmann constant, and T_b is the absolute brightness temperature of the burner surface measured with an optical pyrometer. The GIR factor was similar to a burner emissivity. However, for some of the burners, the GIR factor exceeded 1.0. The GIR factor was approximately 15% higher than the true burner surface emissivity. This is due to the gaseous non-luminous radiation in addition to the surface radiation from the burner. For the burners tested, the GIR factor ranged from 0.36 to 1.17, depending on the burner type.

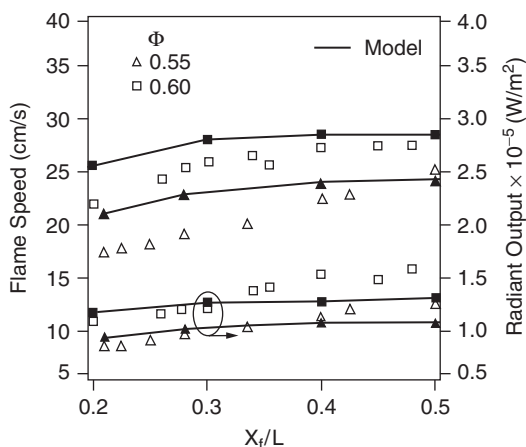


FIGURE 6.14 Measured and predicted flame speed and radiant output for a porous radiant burner. (Courtesy of The Combustion Institute.⁵¹)

Sathe et al. (1990) made experimental measurements and numerical predictions on a porous radiant burner.⁵¹ They used the following correlation for flow over circular cylinders for the convection heat transfer coefficient from the flame to the porous refractory:

$$Nu = 0.989 Re^{0.33} \quad (6.25)$$

where the characteristic length d is the equivalent particle diameter. Figure 6.14 shows a comparison of the measured and predicted result as a function of the axial location of the flame (x_f) normalized by the porous layer length (L). The figure shows that both the radiant output and the flame speed are fairly independent of the flame location, but are dependent on the equivalence ratio. Zabielski et al. (1991) used an optical technique to measure the radiant characteristics of a porous ceramic fiber radiant burner.⁵² The macroscopic emittance of the burner was estimated to be 0.70. Xiong and Viskanta (1992) measured the heat flux and calculated the thermal efficiency of a porous matrix ceramic combustor.⁵³

Jugjai and Sanitjai (1996) presented a concept for a new type of porous radiant burner incorporating internal heat recirculation to increase thermal efficiency.⁵⁴ They studied the effects of the optical thickness of the porous medium on the radiant output of porous radiant burners. The optical thickness was increased by added layers of stainless steel wire mesh that formed the porous medium for the burners tested. The added layers improved the heat transfer from the hot gases to the porous medium.

Mital et al. (1996) claimed to have made the first measurements of temperature and species distributions inside submerged flames stabilized inside porous ceramic burners.⁵⁵ They note the wide discrepancy in the performance of these burners in the literature and in manufacturers' literature.

Rumminger et al. (1996) developed a one-dimensional model of a bilayered reticulated ceramics radiant burner.⁵⁶ The model results showed that for a "submerged flame" where the flame is anchored inside the porous refractory, nearly all of the important reactions occur inside the porous medium. This complicates the study for this type of burner because of the difficulty in making measurements inside the porous medium. They speculate that it is possible the large internal surface area of the porous medium could affect the chemistry, but there is no data at this time to confirm that possibility.

Van der Drift et al. (1997) studied various coatings on porous foam ceramic infrared burners to determine the effects on heat transfer to wet paper and to three colors (white, blue, and black).⁵⁷ They showed that there can be up to a 10% improvement using coated burners compared to a base case metal fiber burner.

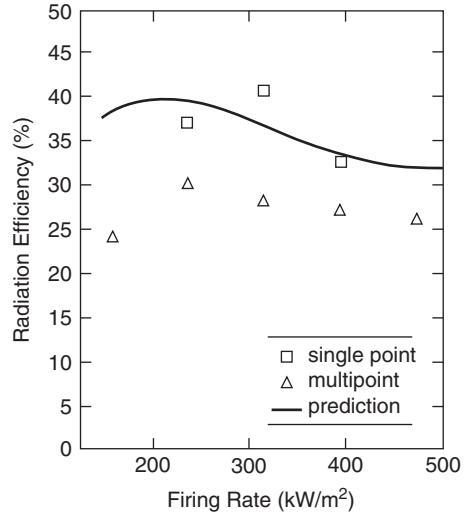


FIGURE 6.15 Predicted and measured radiation efficiency for a porous radiant burner at an equivalence ratio of 0.9. (Courtesy of The Combustion Institute.⁵⁸)

Mital et al. (1998) made experimental measurements on a bilayered reticulated ceramic foam made of Cordierite.⁵⁸ Measurements included radiation efficiency using a heat flux gage and burner surface measurements with a type R thermocouple. Radiation efficiency results are shown in Figure 6.15, which include both single and multi-point measurements and model predictions.

6.3.4 ADVANCED CERAMIC RADIANT BURNERS

Tong et al. (1989) showed through computer modeling that the performance of porous radiant burners can be improved by as much as 109% using sub-micron diameter ceramic fibers.⁵⁹ Bell et al. (1992) described a staged porous ceramic burner that demonstrated low NO_x emissions.⁶⁰ Kendall and Sullivan (1993) studied enhancing the radiant performance of porous surface radiant burners using improved ceramic, high-temperature, high-emissivity fibers.⁶¹ Selective emissivity was achieved by coating a standard ceramic fiber burner with an outer layer of ytterbia. The output of the uncoated vs. the coated burner is shown in Figure 6.16. As can be seen, there is a large spike in the output of the coated burner at around 1 μm . However, there was not a significant improvement in performance and the durability was in question. In certain applications, there may be a need to have a burner with selective radiant emissions corresponding to selective absorption in the load. Potential applications include glass melting, glass bending and lamination, thin film drying, and indirect heating. Xiong et al. (1993) described a porous ceramic surface combustor-heater with a built-in heat exchanger for improving the thermal efficiency.⁶² Ruiz and Singh (1993) described an advanced infrared burner.⁶³ The new burner design has considerably higher radiant outputs than the previous style design. The new burner increased a powder paint drying process by 40% and a paper drying process by 200%. Severens et al. (1995) modeled porous radiant burners.⁶⁴ The one-dimensional model results compared favorably with experimental data for the radiant fraction as a function of the gas velocity through the burner. Bogstra (1998) described a new type of infrared radiant burner, referred to as CHERUB, with a closed surface to separate the combustion exhaust gases from the product being heated.⁶⁵ The burner had an enclosed, flat, multi-burner system that heats a ceramic radiant plate. The burner was reported to have a radiant efficiency of 80%, compared to an efficiency of 40% for conventional high-temperature radiant burners.

As previously discussed, one of the limitations of porous refractory burners is the burner surface temperature. If the firing rate density is to be increased, new refractory materials are needed that can withstand continuous operation at higher temperatures, while maintaining their integrity during thermal cycling. One example of research to develop improved radiant burner materials is by

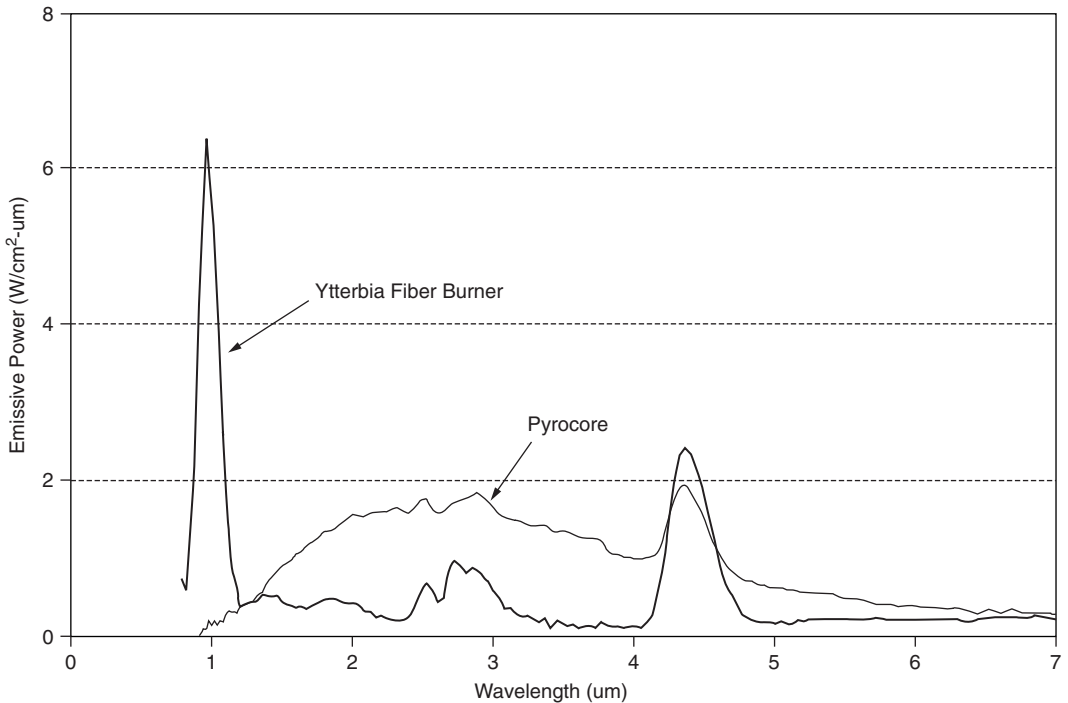


FIGURE 6.16 Emission spectra of ytterbia fiber burner compared to Alzeta (Santa Clara, CA) Pyrocore burner, both operating at 127,000 Btu/hr-ft² (400 kW/m²). (Courtesy of The Gas Research Institute.⁶¹)

Superkinetic, Inc. (Albuquerque, NM) with funding from the U.S. Dept. of Energy.⁶⁶ Three single-crystal ceramic fibers were produced and two fiber materials were successfully made into felt for testing as radiant burner screen surfaces. The materials were alpha-alumina and alpha-silicon carbide, which were successfully bonded with a high-temperature ceramic to form the burner screens that were 95% porous. The purpose of this project was to develop materials capable of radiant burner service near 3000°F (1900K), compared to conventional radiant burner surface temperatures of about 1800°F (1300K). The new materials performed well in actual burner operation, but more research was recommended.

6.3.5 RADIANT WALL BURNERS

A typical radiant wall burner is shown schematically in [Figure 6.17](#). This type of burner is commonly used in process heaters where they heat a refractory wall that radiates heat to tubes parallel to the wall.⁶⁷ The tubes contain a fluid, typically a hydrocarbon, which is being heated. These burners are similar to flame impingement radiant burners except that the flame in a radiant wall burner is directed along the wall and not at the wall or burner tile in the case of impingement burners. The object of a radiant wall burner is to distribute heat as evenly as possible over a fairly wide area. The impingement burner primarily heats its burner tile, which then radiates to the load. This burner is discussed in more detail in [Chapter 15](#).

6.3.6 RADIANT TUBE BURNERS

In some heating processes, it is not desirable to have the products of combustion come in contact with the load. One example is in certain types of heat treating applications where the exhaust gases from a combustion process could contaminate the surface of the parts being heated. In those cases,

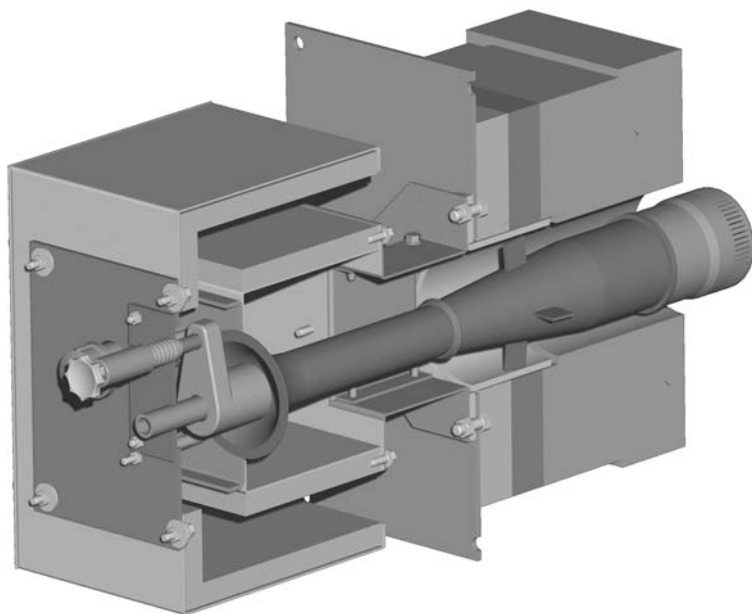


FIGURE 6.17 Typical radiant wall burner. (Courtesy of John Zink Co. LLC.³)

an indirect method of heating is needed. Electric heaters are sometimes used; however, the energy costs are considerably higher than the cost of fossil-fuel-fired heaters. The burner of choice for indirect heating is typically a radiant tube (see [Chapter 14](#)).

The objective of the radiant tube burner is to efficiently transfer heat from the combustion gases to the radiant tube, and then to efficiently radiate that energy to the load. There are several challenges that need to be considered when using radiant tubes. The biggest challenge is the material of construction for the tube itself. Typical tubes are constructed of high-temperature metal alloys or ceramics. Metal alloys can be expensive and typically do not have as high a continuous operating temperature as ceramics. Metal tube burners typically operate at temperatures around 2000°F (1400K). These tubes can fail due a variety of metallurgical problems related to the high-temperature operation and thermal cycling of the burners. Metal tubes are more commonly used than ceramic tubes and research continues into higher temperature metals for use in metallic radiant tube burners.^{68,69} Ceramic tubes tend to have higher temperature operating limits compared to the metal tubes, but are even more susceptible to thermal shock. Research also continues on new ceramic materials for radiant tube burners.⁷⁰⁻⁷² There may also be problems joining the ceramic tubes to the metal burner body due to the differences in thermal expansion that can cause the ceramic tubes to crack. The Institute of Gas Technology (Chicago, IL) is working on a new composite material for radiant tubes that is silicon carbide based and has a working temperature that exceeds 2450°F (1620K).⁷³ These new tubes have excellent shock resistance and are capable of heat flux rates up to 150 Btu/hr-in.² (68 kW/m²), compared to rates of 55 Btu/hr-in.² (25 kW/m²) for metallic radiant tubes. Tube lives can be increased by as much as three times with the new tubes. The Gas Research Institute (1998) has funded many projects related to the use of advanced ceramic composite materials for radiant tube burners.⁷⁴ The GRI estimated that about 40% of the more than 50,000 heat treating furnaces are indirectly heated using an estimated 250,000 radiant tube burners. The new ceramic composites promise higher operating temperatures and longer lives.

There are three common configurations for radiant tube heaters. The first and simplest is known as a straight-through tube, where there is a burner at one end of a tube with the exhaust gases from

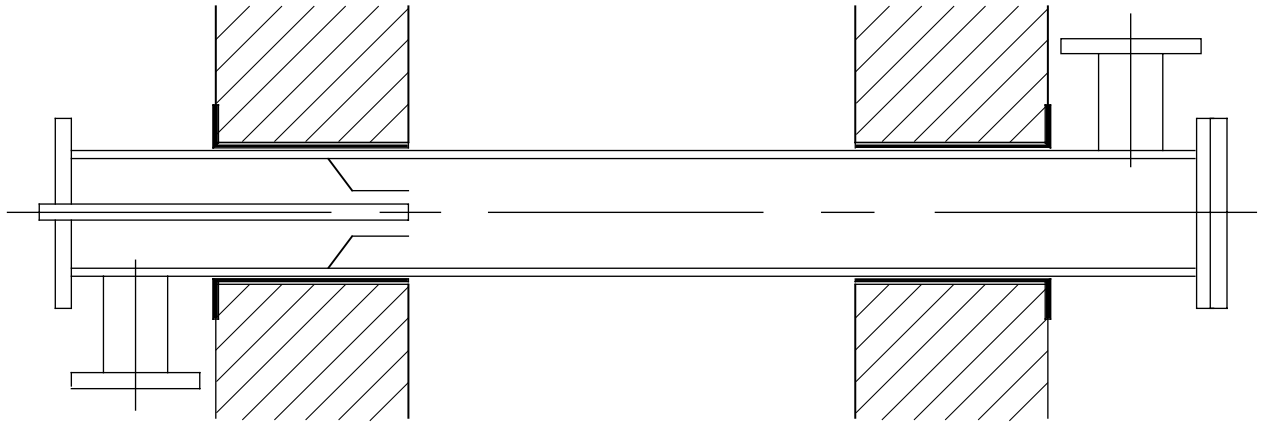


FIGURE 6.18 Straight-through radiant tube burner. (From Ceramic Single Ended Recuperative Radiant Tube (Phase 1), Final Report, NTIS PB91222554, 1990.⁷⁰)

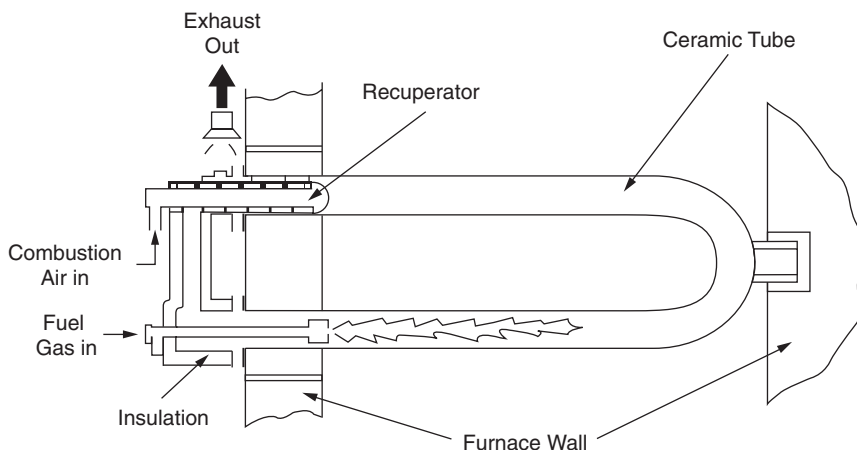


FIGURE 6.19 U-tube radiant tube burner. (Courtesy of American Society of Metals.⁶⁸)

the burner traveling through the tube and exiting at the other end (see Figure 6.18). The challenge when using this geometry is to get efficient heat transfer from the flame gases to the tube, which then radiates to the load. Another potential disadvantage of this type compared to the other two types is that connections for the supply gases are on one side, while the connections for the exhaust gases are on the other side. The second type of radiant tube heater is known as a single-ended recuperative burner. Here, the burner and exhaust are located on the same side of the tube. The burner fires down an inner tube and then returns back to the starting end through an outer annulus. The exhaust gases are used to preheat the incoming fuel and oxidizer, which increases the overall efficiency. A potential difficulty with this design is that the tube is cantilevered from the wall, which puts some additional stress on the tube. Louis et al. (1998) described a single-ended recuperative radiant tube burner for use in a steam-cracking ethylene production plant.⁷⁵ The third radiant tube design is known as a U-tube because of its shape (see Figure 6.19). Again, the supply inlets and exhaust gas outlet are on the same side. One of the difficulties of this design is making a single monolithic U-tube that avoids the need for the 180° elbow where leaks and failures might occur. Abbasi et al. (1998) described an advanced, high-efficiency, low-emissions U-tube radiant tube burner made of either a metal alloy or a ceramic composite.⁷⁶ The new burner promises to have better temperature uniformity and lower pollutant emissions than conventional burners by using internal exhaust gas recirculation.

The heat transfer from radiant tube burners is important because it not only affects the energy transfer to the load, but also the life and performance of the radiant tube. If the heat flux profile along the radiant tube is highly nonuniform, with high- and low-temperature regions along the length of the tube, then the life of the tube will be significantly reduced due to the high thermal stresses and possible overheating. A more uniform heat flux from the tube will give a higher tube life and is normally also more desirable for the load as well to produce uniform heating. The fuel burn-up in the tube is needed to calculate the heat flux from the tube. Ramamurthy et al. (1997) developed fuel burn-up and wall heat transfer correlations for gas-fired radiant tube burners with turbulent flows inside the tube.⁷⁷ They studied several parameters, including the burner area ratio (ratio of the outer annular air inlet port area to the inner circular fuel port inlet area), excess combustion air ratio, combustion air preheat temperature, and the fuel firing rate. The fuel burn-up ratio increased for both high and low burner area ratios, where there was a higher difference between the fuel and combustion air velocities compared to the base case burner area ratio where the velocities were more similar. The fuel burn-up ratio increased with the excess air ratio and with

the air preheat temperature, but decreased as the fuel firing rate increased. The following correlation was developed for the fuel burn-up:

$$\kappa(z) = 1 - \exp \left[-8.24 \times 10^{-4} \frac{A_b^{0.54}}{\phi^{1.53}} \left(\frac{\dot{m}_{\text{air}} \bar{v}_{\text{air},z=0}}{\dot{m}_{\text{fuel}} \bar{v}_{\text{fuel},z=0}} \right)^{0.41} \left(\frac{z}{d} \right)^{1.6} \text{Re}_{\text{AFT}}^{-0.08} \right] \quad (6.26)$$

where κ is the fuel burn-up coefficient (fraction of the fuel that has been consumed), z is the distance from the burner outlet, A_b is the burner area ratio (defined above), ϕ is the fuel equivalence ratio, \dot{m}_{air} is the combustion air mass flow, \dot{m}_{fuel} is the fuel mass flow, $\bar{v}_{\text{air},z=0}$ is the average combustion air velocity at the burner outlet, $\bar{v}_{\text{fuel},z=0}$ is the average fuel velocity at the burner outlet, d is the tube inner diameter, and Re_{AFT} is the Reynolds number of the combustion products at stoichiometric adiabatic flame temperature conditions. They also developed a correlation for the one-dimensional heat flux from the tube to an isothermal bounding wall:

$$q_{\text{rad,1D}} = \frac{\varepsilon_w \sigma (\varepsilon_{\text{CP}} T_{\text{CP}}^4 - \alpha_{\text{CP}} T_w^4)}{1 - (1 - \varepsilon_w)(1 - \alpha_{\text{CP}})} \quad (6.27)$$

where ε_w is the emissivity of the wall, σ is the Stefan-Boltzmann constant, ε_{CP} is the emissivity of the combustion products, T_{CP} is the absolute temperature of the combustion products, α_{CP} is the absorptivity of the combustion products, and T_w is the absolute temperature of the wall. This correlation was then modified for two dimensions by calculating two factors, depending on the temperature of the combustion products compared to the temperature of the isothermal bounding wall:

$$F_1 = \frac{\int_{z=0}^{z=l_1} q_{\text{rad,2D}} dz}{\int_{z=0}^{z=l_1} q_{\text{rad,1D}} dz} \quad \text{for } T_{\text{CP}} < T_w \quad (6.28)$$

$$F_2 = \frac{\int_{z=l_1}^{z=l_2} q_{\text{rad,2D}} dz}{\int_{z=l_1}^{z=l_2} q_{\text{rad,1D}} dz} \quad \text{for } T_{\text{CP}} > T_w \quad (6.29)$$

where $0 \leq l < l_1$ is the length along the tube where $T_{\text{CP}} < T_w$ and $l_1 \leq l < l_2$ is the length along the tube where $T_{\text{CP}} > T_w$. The average values for F_1 and F_2 were found to be 1.39 and 1.26, respectively. There was excellent agreement between the measured and predicted heat fluxes using the two-dimensional correction factors.

Schultz et al. (1992) reported the use of a single-ended radiant tube burner in a vacuum furnace used for heat treating metals.⁷⁸ The radiant flux from the burner was 150 Btu/hr-in.² (68 kW/m²). Mei and Meunier (1997) tested and modeled the single-ended radiant tube.⁷⁹ They used the Reynolds Stress Model to simulate the burner. The results showed that detailed flame chemistry modeling in the near flame region is important to get an accurate representation of the heat release pattern. The model was in good agreement with the measurements for the total heat flux from the outer tube to the environment, but that the choice of a turbulence model was important for getting agreement on the tube wall temperatures.

There are a number of new developments being made to improve radiant tube burners. One concept involves coating the inside of the tube with a catalyst so that the premixed preheated air

and fuel partially burn on the catalyst surface and thermally conduct that energy to the outside of the tube to radiate to the load.⁸⁰ Advantages include more uniform tube heating and lower NO_x emissions. Further research was recommended to find a platinum catalyst with a higher melting point. Huebner et al. (1986) described the results of tests using oxygen-enriched air to enhance the performance of radiant tube burners.⁸¹ The oxygen content in the oxidizer ranged from 21% (air) to 80%, by volume. The furnace temperatures ranged from 1300 to 2400°F (700 to 1315°C) and radiant tube diameters of 4, 7 $\frac{1}{8}$, and 10 in. (10.2, 18.1, and 25.4 cm) were tested. Large improvements in thermal efficiency and relatively little change in the tube temperature were found. Larger efficiency improvements were found for the larger diameter tubes.

6.4 EFFECTS ON HEAT TRANSFER

There are many variables that affect the heat transfer from flames. In this section, the following effects are briefly discussed: fuel and oxidizer composition and temperature, fuel and oxidizer staging, burner orientation, heat recuperation, and the use of pulse combustion.

6.4.1 FUEL EFFECTS

The fuel can have a significant impact on the heat transfer from flames. The three major types of fuels (solids, liquids, and gases) are considered in this section.

6.4.1.1 Solid Fuels

Solid fuels such as coal and coke are well-known for producing luminous flames because of the particles in the flame that radiate (see [Chapter 2](#)). Solid fuels are not often used in industrial combustion applications and are most used in large power generation plants. The solid particles in solid-fuel combustion radiate as graybodies and give a more uniform spectral radiation output than gaseous flames that tend to have discrete wavelength bands for water and carbon dioxide radiation. The luminous radiation from solid fuel combustion tends to make these flames more efficient, although there are challenges to completing combusting the fuel and handling any residues that are generated from the flame.

Another aspect of solid fuels that indirectly impacts the heat transfer in a combustor is the deposition of ash, produced by the combustion of the solid fuel, onto the inside of the combustor.⁸² These deposits may improve the radiant absorptivity of the materials to which they adhere because the emissivity of the deposit is often high. However, the deposits may have a lower thermal conductivity than the base material, particularly when the substrate is a metal tube containing a fluid to be heated, such as water. Then, the deposits can significantly impede the heat transfer to the load and must be periodically removed. Wall et al. (1994) noted that there can actually be a slight increase in the thermal conductivity of the deposit with time as its physical and chemical nature change, but the conductivity is still considerably less than that of the metal tube.⁸²

Books are available on solid fuel combustion, particularly coal combustion, although most of them have very little on heat transfer and tend to focus more on the physics of the combustion process itself.⁸³⁻⁹⁰

6.4.1.2 Liquid Fuels

Boersma (1973) showed that the heat transfer from liquid oil flames can be considerably higher than for comparable gas flames (see [Figure 6.20](#)).⁹¹ This is caused by particle generation in the flames where the particles radiate like graybodies, similar to solid fuel flames. An example of an oil flame is shown in [Figure 6.1](#).

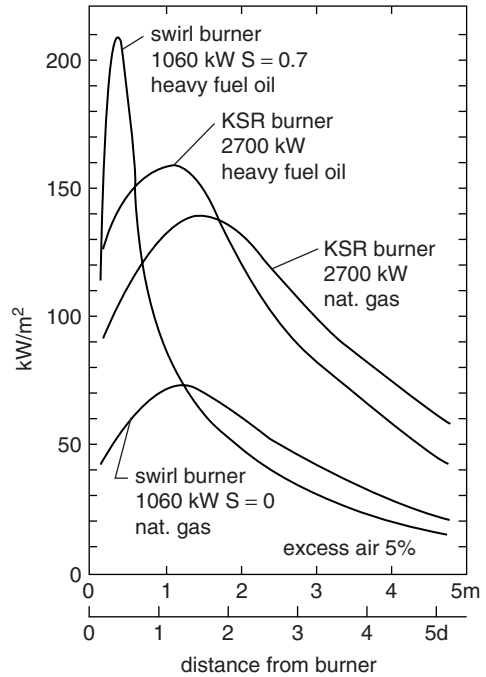


FIGURE 6.20 Measured heat flux rates from different fuels and burners in a cylindrical furnace. (Courtesy of Academic Press.⁹¹)

Zung (1978) has edited a book about the evaporation and combustion of liquid fuels.⁹² However, the book has almost nothing on heat transfer from flames or in furnaces. Williams (1990) has written a book that has a chapter that specifically addresses liquid fuel combustion in furnaces, although there is very little on heat transfer.⁹³

6.4.1.3 Gaseous Fuels

One of the benefits of the gaseous fuels used in industrial combustion applications is that they are very clean-burning and normally generate very few particulates. However, this is a detriment when it comes to heat transfer from flames because gaseous flames are often very nonluminous and may only radiate in a few narrow wavelength bands as discussed in [Chapter 2](#). New burner designs have been introduced in recent years to increase the flame luminosity from natural gas flames. This has improved thermal efficiencies and increased product throughputs. One major way this has been achieved is through staged combustion by making the inner part of the flame closest to the burner to be fuel rich and then to burn out the fuel downstream with staged oxidizer injection. This technique is well-known for NO_x emission reduction as well. Other techniques for increasing the luminosity of gaseous flames include particle injection into the flames, oil injection into the flames, and preheating and cracking the fuel prior to combustion. As discussed in [Chapter 1](#), this continues to be an important area of combustion research.

6.4.1.4 Fuel Temperature

Preheating the fuel influences the flame temperature by increasing the adiabatic flame temperature (see [Figure 6.21](#)). This influences both the radiation and convection from the combustion products to the load. The radiation is often increased because of the higher gas temperature. However, different gas species are often produced at higher temperatures, which also influences the radiant heat flux, especially if more or less soot is produced. Amin et al. (1995) experimentally determined that the radiant fraction from an oxygen enhanced methane flame decreased as the fuel preheat temperature was increased from 300 to 500°C (570 to 930°F).⁹⁴ The measured radiant fraction actually increased

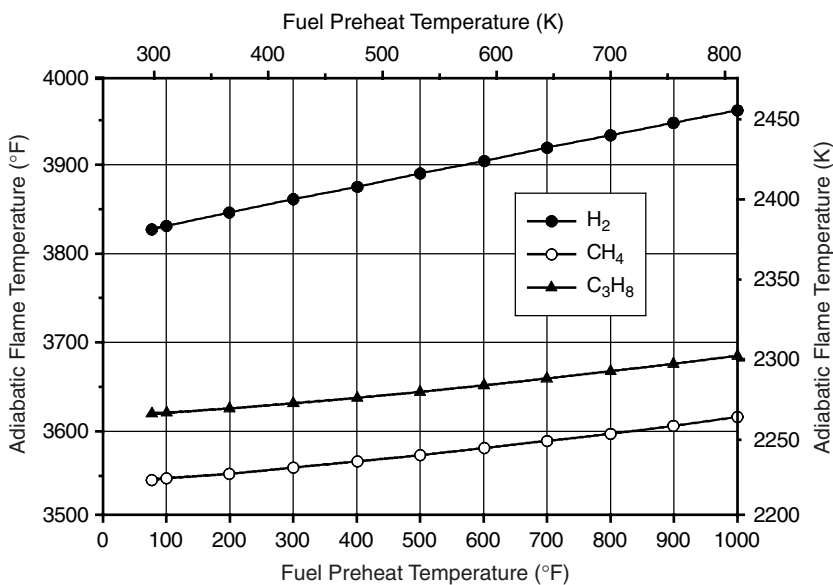


FIGURE 6.21 Adiabatic flame temperature as a function of fuel preheat temperature. (Courtesy of John Zink Co., LLC.³)

slightly by increasing the fuel preheat temperature from 500 to 600°C (930 to 1100°F), due to increased soot production. The convective heat transfer from the combustion products to the load is also influenced by fuel preheating. By preheating the fuel, the transport properties change with both temperature and composition, which directly influence the convective heat transfer coefficient. The gas velocity increases with temperature because of the gas expansion at higher temperatures, which can increase the convective heat transfer to the load.

6.4.2 OXIDIZER EFFECTS

The oxidizer composition and temperature both play important roles in the heat transfer from flames to the load and are briefly discussed next.

6.4.2.1 Oxidizer Composition

This section briefly discusses the effects of the oxidizer composition on the heat transfer from flames. Related discussions are also given in Chapters 2, 20, and 21. Chedaille (1965) showed that an air/oil flame can be enhanced by injecting pure oxygen between the flame and the load.⁹⁵ The experiments were conducted in a tunnel furnace where the load consisted of water-cooled tubes located 7 cm (0.3 in.) below the top of the hearth. The flame was angled, at angles ranging from 16 to 30°, from an end wall down toward the hearth. The total combined oxygen content of the combustion air and lanced O₂ was 30% by volume. The experiments showed that the total heat transfer was highest by injecting the oxygen under the flame, but the heat transfer was more uniform by premixing the oxygen in with the combustion air. Arnold (1967) calculated the heat transfer rates for burners fired on town gas with either air or pure oxygen as shown in Figure 6.22.⁹⁶ The oxy/fuel flames produced heating rates as much as six times higher than the air/fuel flames when the surface temperature of the load was the highest. Kobayashi et al. (1986) showed theoretically how the heat flux to the furnace heat load can be significantly improved using higher levels of O₂ in the oxidizer, as shown in Figure 6.23.⁹⁷ De Lucia (1991) showed that using oxygen to enhance the performance of industrial furnaces can result in some dramatic fuel reductions per unit of output:⁹⁸

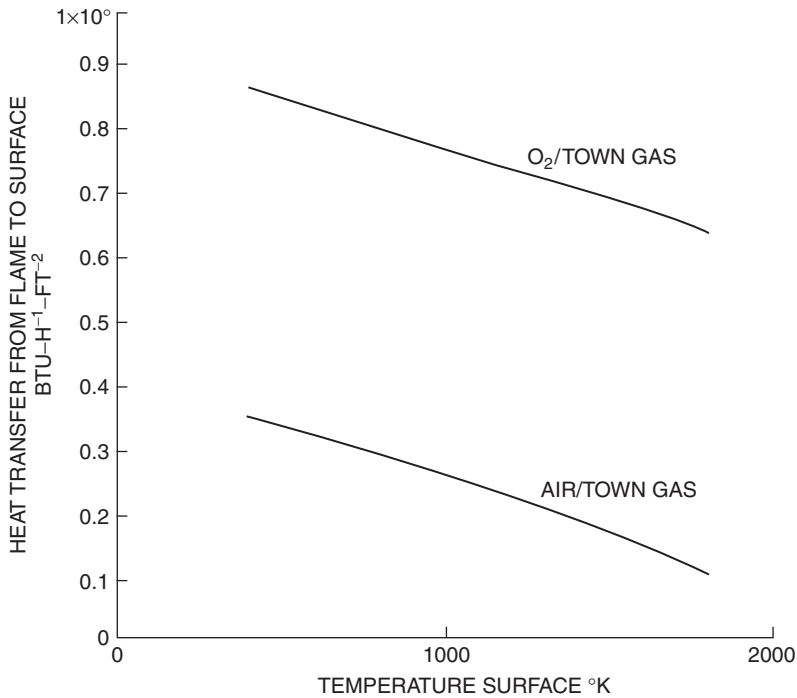


FIGURE 6.22 Calculated heat transfer rates for town gas flames combusted with either air or pure O_2 . (Courtesy of Institute of Energy.⁹⁶)

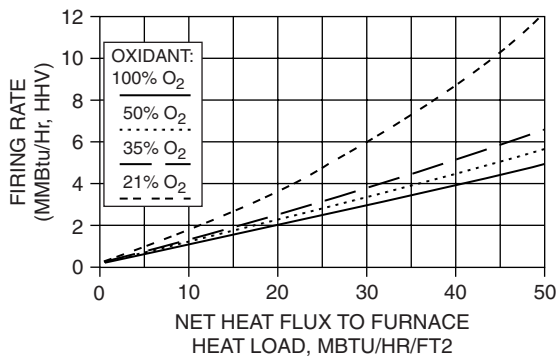


FIGURE 6.23 Calculated heat flux vs. firing rate for different oxidant compositions. (Courtesy of American Society of Metals.⁹⁷)

- 30 to 50% in glass melting
- More than 50% in pig iron melting
- More than 30% in copper alloy production
- As much as 39% in ceramic production

In the study by Baukal and Gebhart discussed above under firing rate considerations, the oxidizer composition was also a parameter of interest.²² Figure 6.24 shows how the heat flux to the target varied as a function of the oxidizer composition and as a function of the geometry. The heat flux intensity increased by 54 to 230% as Ω increased from 0.30 to 1.00. The average improvement was approximately 80%. The largest improvement occurred at $L = 0.5$ and $R_{\text{eff}} = 0.16$. At higher

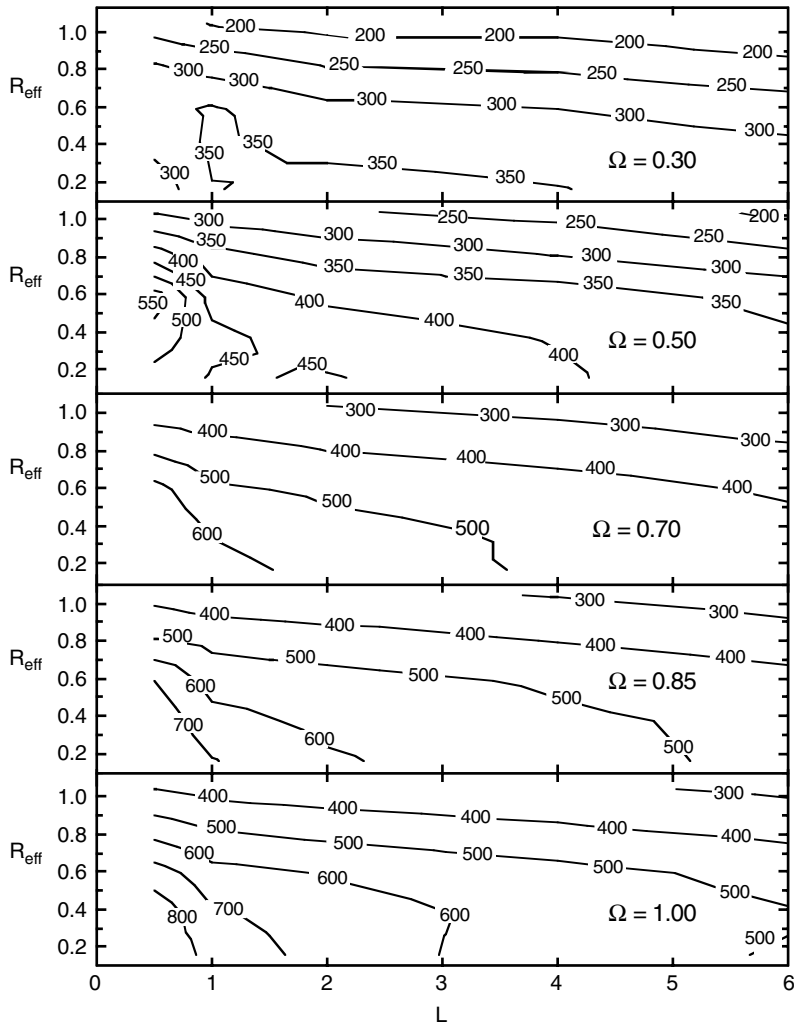


FIGURE 6.24 Contours of the total heat flux, q'' (kW/m^2), for stoichiometric natural gas flames ($q_f = 15.0 \text{ kW}$), with a variable oxidizer composition, impinging on an untreated stainless target.²²

values of Ω , the peak heat flux was measured at the closest axial and radial locations. At lower values of Ω , the peak flux occurred at intermediate axial and radial positions. Therefore, at lower Ω , there was clearly an optimum position to maximize the heat transfer and the thermal efficiency. Figure 6.25 depicts the increase in heat flux intensity as the O_2 content in the oxidizer (Ω) increased. For $L = 0.5$, the heat flux increased by 192% as the O_2 in the oxidizer increased from $\Omega = 0.30$ to $\Omega = 1.00$. As L increased, the oxidizer composition had less influence on the heat flux intensity. The slope of each curve increased as L decreased. Therefore, the oxidizer composition was more important for closer axial spacings. Figure 6.26 shows that the thermal efficiency increased with Ω . This was a consequence of removing the diluent N_2 from the oxidizer. The efficiency decreased with L . The shapes of the curves are similar.

6.4.2.2 Oxidizer Temperature

Preheating the oxidizer is commonly done to recover energy from the exhaust products and to increase the adiabatic flame temperature of the flame as shown in Figure 6.27. Preheating the

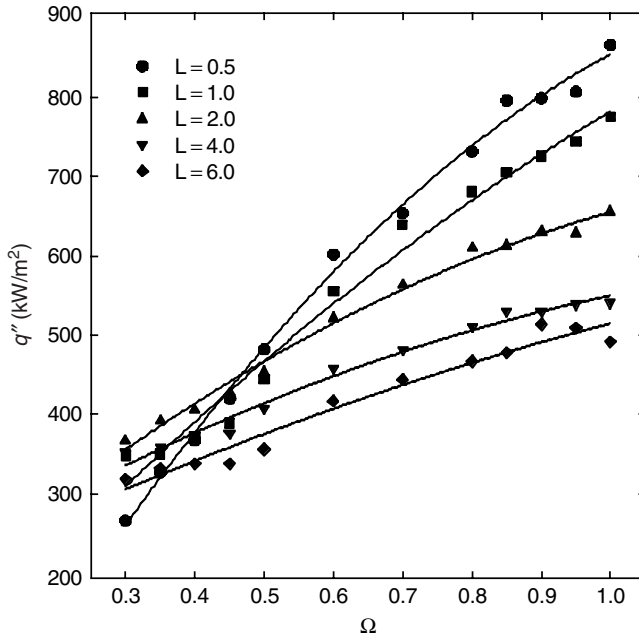


FIGURE 6.25 Total heat flux (q'') to the stagnation point ($R_{\text{eff}} = 0.16$) of an untreated stainless target, for stoichiometric natural gas flames ($q_f = 15.0$ kW) with a variable oxidizer composition (Ω).²²

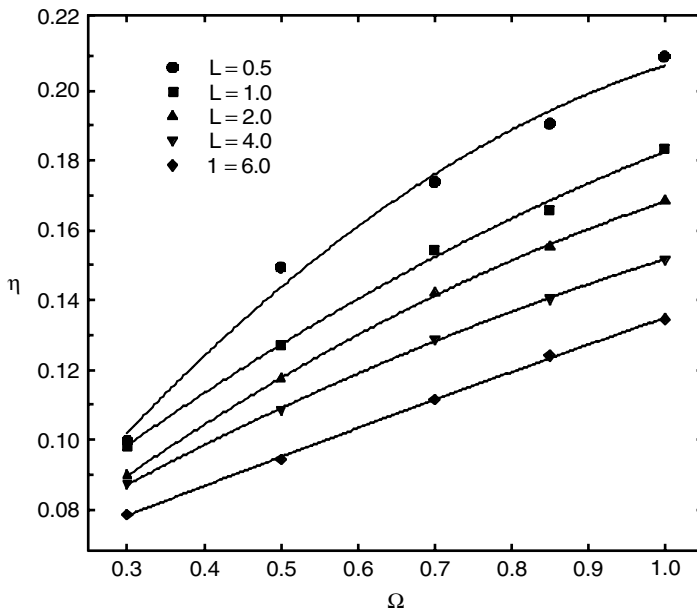


FIGURE 6.26 Thermal efficiency (η) for stoichiometric natural gas flames ($q_f = 15.0$ kW), with a variable oxidizer composition (Ω), impinging on the stagnation point ($R_{\text{eff}} = 0.16$) of an untreated stainless target.²²

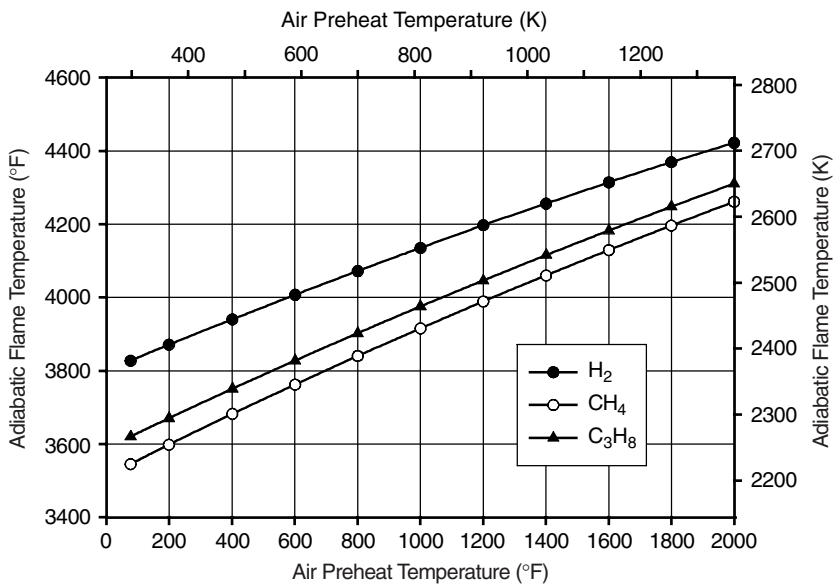


FIGURE 6.27 Adiabatic equilibrium flame temperature vs. air preheat temperature for stoichiometric air/H₂, air/CH₄, and air/C₃H₈ flames. (Courtesy of John Zink Co., LLC.³)

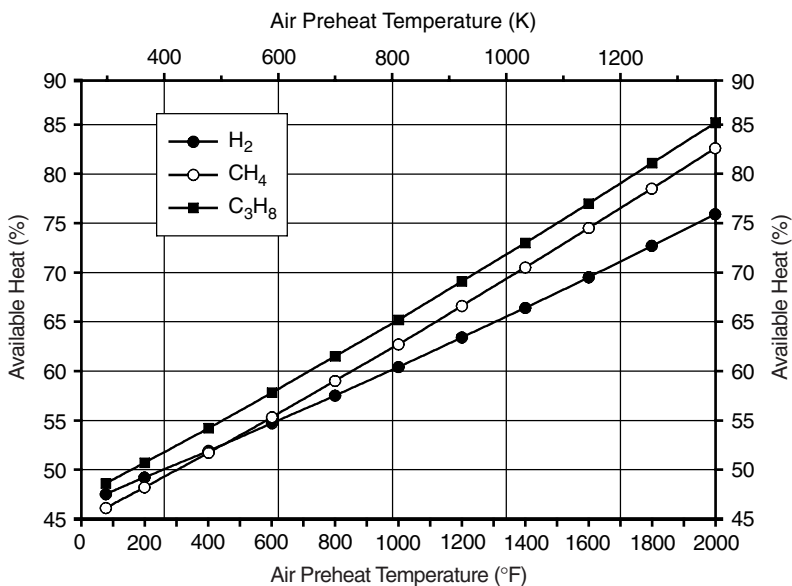


FIGURE 6.28 Available heat vs. air preheat temperature, for equilibrium stoichiometric air/H₂, air/CH₄, and air/C₃H₈ flames at an exhaust gas temperature of 2000°F (1366K). (Courtesy of John Zink Co., LLC.³)

oxidizer also improves the thermal efficiency of a process as shown in Figure 6.28. Higher flame temperatures can dramatically increase the radiant heat flux from the flame because of its dependence on the absolute temperature raised to the fourth power. Guénebaut and Gaydon (1957) studied the effect of air preheating on the shape and radiant output from methane, bunsen-burner-type flames.⁹⁹ As shown in Figure 6.29, preheating the air to 550°C (1020°F) caused the flame to become

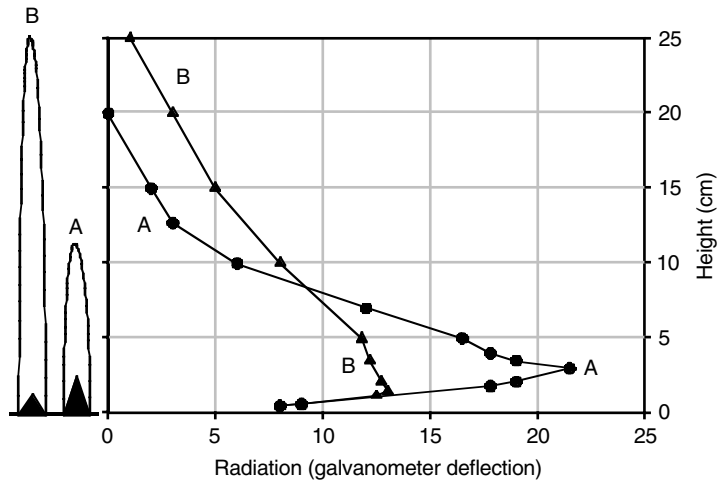


FIGURE 6.29 Flame shapes and radiant heat flux from a methane flame produced by a bunsen burner: (A) no air preheating and (B) air preheated to 550°C (1020°F). (Courtesy of The Combustion Institute.⁹⁹)

twice as long and the radiant heat flux profile to become more uniform compared to the burner with no air preheat.

6.4.3 STAGING EFFECTS

Staging the fuel¹⁰⁰ or the oxidizer^{101,102} are common techniques for reducing NO_x emissions. This staging also impacts the heat transfer of the system, which is briefly considered next. In either type of staging, the flame is usually longer than unstaged flames. It is assumed in the discussions for both types of staging that both the furnace geometry and the heating process permit longer flames without either flame impingement on the walls of the combustor or without damaging the product quality.

6.4.3.1 Fuel Staging

An example of fuel staging is shown in Figure 6.30. Staging the fuel normally means that the inner flame region has excess oxidizer or is fuel lean. Fuel-lean flames tend to be very nonluminous, depending on the mixing and, therefore, generate only gaseous radiation, with little or no soot formation. The balance of the oxidizer is added downstream of the main flame region and normally brings the overall combustion process from very fuel-lean conditions to slightly lean conditions. Again, this does not favor luminous flame radiation even in the secondary flame region. Therefore, fuel staged flames tend to be nonluminous and the heat transfer from these flames is more dominated by forced convection compared to luminous flames. Depending on the application, this may not only be acceptable, but desirable. If putting too much heat near the beginning of the flame can cause overheating, then fuel staging may be an option for stretching out the heat flux over a longer length, while simultaneously reducing the heat flux near the base of the flame. An example would be a counterflow rotary kiln. The material enters the kiln at one end and the burner is located at the other end. This means that the processed material exits at the burner end. Too much heat applied at the material exit could cause slagging, which is partial melting and agglomeration. Pushing the flame more toward the material feed end puts more of the heat where there is much less chance of overheating.

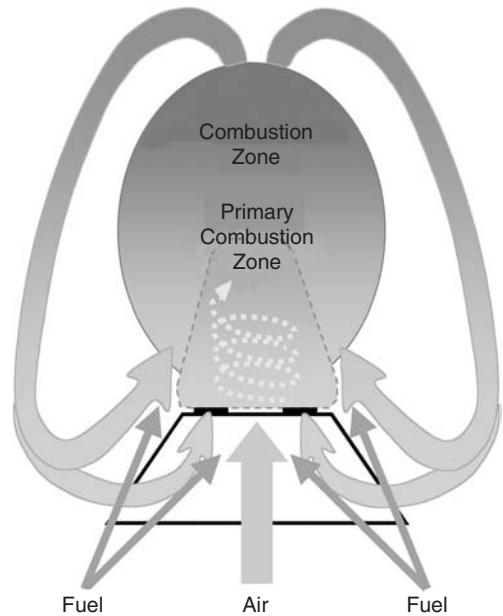


FIGURE 6.30 Schematic of fuel staging. (Courtesy of John Zink Co., LLC.³)

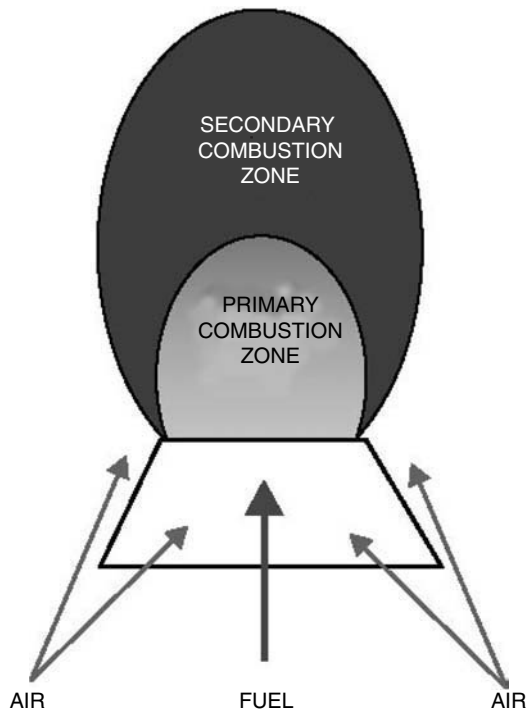


FIGURE 6.31 Schematic of air staging. (Courtesy of John Zink Co., LLC.³)

6.4.3.2 Oxidizer Staging

A schematic of air staging is shown in Figure 6.31. In this type of flame, the main flame region closest to the burner does not have enough oxygen and is fuel rich. This normally produces soot and therefore a luminous flame. This type of flame has a higher heat flux from the flame, although the overall efficiency of the process is still dependent on the system geometry and any heat recovery

devices that have been incorporated into the system. A staged oxygen flame commonly has higher heat flux near the burner outlet than the staged fuel flame. Again, depending on the application, this may be desirable or undesirable. In the counterflow rotary kiln process discussed above, this would be undesirable and could lead to slagging. However, for a co-flow rotary kiln, an initially fuel-rich and luminous flame is often desirable because the incoming cold/wet material can absorb higher heat fluxes without affecting product quality. In the staged oxidizer flame, the secondary flame zone combusts the unburned fuel coming out the primary, fuel-rich, flame region to avoid emitting particulates or CO from the exhaust products. This secondary flame zone helps lengthen the flame and the resulting heat flux profile, compared to an unstaged flame.

6.4.4 BURNER ORIENTATION

The choice of burner orientation can vary widely, depending on the industry. Some examples will suffice to illustrate. In the metals and minerals industries, the burners are usually mounted in the side wall and either fire parallel to or angled toward the materials being heated. In the heat treating industry, the burners may fire over or at a muffle that separates the combustion products from the materials being processed. In the petrochemical industry, a more common configuration is for the burners to be mounted in the floor of the furnaces and fire vertically upward. Several common configurations are briefly discussed in this section to show their impact on the heat transfer in the process.

6.4.4.1 Hearth-Fired Burners

A diagram of a hearth-fired burner is shown in Figure 6.32. Pictures of hearth-fired burner are shown in Figure 6.1 and Figure 6.2. These burners are commonly used in the petrochemical industry and are often natural draft (see Chapter 16). Depending on the heater design, the burners can be arranged in a variety of ways. A smaller cylindrical heater may have a single burner in the middle of the floor, while larger cylindrical heaters usually have multiple burners located at some radius from the centerline, arranged at equal angular distances apart (see Figure 6.33). Rectangular heaters generally have one or more rows of burners in the floor.

The flames from hearth-fired burners are normally directly vertical, in line with the natural buoyancy force. These burners are designed to release the majority of their heating value in the lower part of the furnace or heater in what is usually referred to as the radiant section. Many of these heaters have a convection section near the top, where further heat is released from the combustion products to the tubes in the convection section.

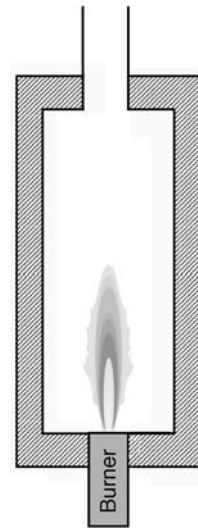


FIGURE 6.32 Elevation view of a hearth-fired burner configuration. (Courtesy of John Zink Co., LLC.³)

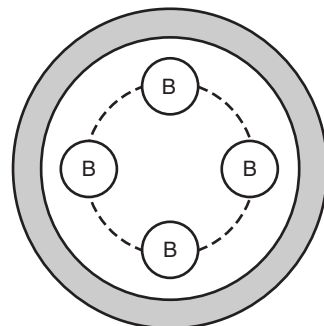


FIGURE 6.33 Cross section of a vertical cylindrical furnace with multiple burners. (Courtesy of John Zink Co., LLC.³)

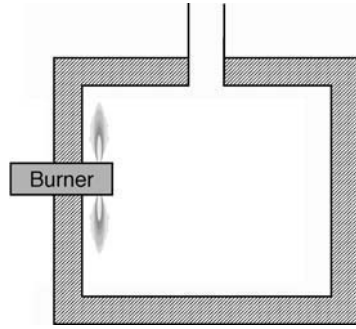


FIGURE 6.34 Elevation view of a perpendicular wall-fired burner configuration. (Courtesy of John Zink Co., LLC.³)

Often, the vertical heat flux profile from hearth-fired burners to the tubes in the radiant section is an important design consideration. An important heat transfer consideration for this type of burner is the distance from the burners to the tubes. If the spacing is too close, then the tubes can fail prematurely due to overheating. If the spacing is too far, then not enough heat will be transferred in the radiant section and too much can be transferred in the convection section. The former reduces productivity, while the latter can cause damage to the tubes in the convection section. The spacing between burners is also important in order to maximize the power density without causing adverse interactions between flames.

6.4.4.2 Wall-Fired Burners

There are a variety of wall-fired burner configurations. A diagram of a perpendicular wall-fired burner is shown in Figure 6.34. A schematic is shown in Figure 6.17. The flame comes out in all angular directions, flowing radially outward from the burner. A variation of this type of burner that is sometimes considered to be a wall burner is an infrared burner (see Chapter 13). In that case, the burner tile (sometimes referred to as a block or quarl) is heated by flames and radiates toward the load. A diagram of a parallel wall-fired burner is shown in Figure 6.35. That is a variation of the hearth-fired burner where the burner is located next to and fires along a vertical wall. A schematic of a terrace-fired burner is shown in Figure 6.36. The schematic shows a single terrace, but furnaces using this technology usually have multiple terraces along the vertical wall. There, the combustion products from lower terrace burners also flow against upper terraces.

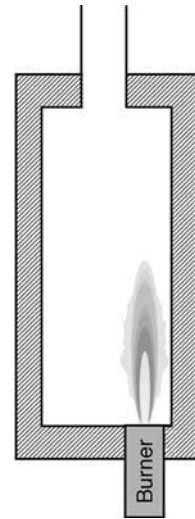


FIGURE 6.35 Elevation view of a parallel wall-fired burner configuration. (Courtesy of John Zink Co., LLC.³)

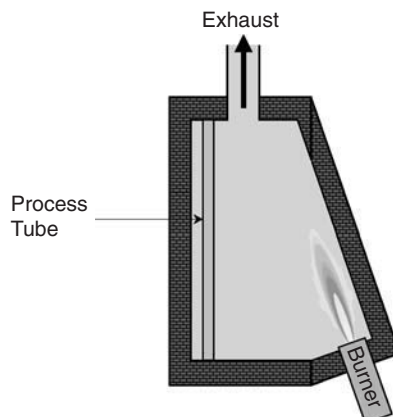


FIGURE 6.36 Elevation view of a terrace-fired burner configuration.



FIGURE 6.37 Example of a down-fired, forced-draft, preheated air burner. (Courtesy of John Zink Co., LLC.³)

The basic principle of wall-fired burners is to heat a refractory wall, which then radiates to the load. It is often important to have fairly uniform heat flux to the walls to prevent overheating the refractory, which could cause the walls to fail prematurely. Uniform heating of the wall is often desired to uniformly heat the load. In vertical wall-fired burners used in the petrochemical industry, there may be a desired heat flux profile along the wall to optimize the heat transfer to the tubes in the radiant section.

6.4.4.3 Roof-Fired Burners

A picture of a roof- or down-fired burner is shown in [Figure 6.37](#). These burners are used in a variety of applications. One application is to supplement electric arc furnaces. There, burners are often mounted in the roof or upper side wall of an electric arc furnace (EAF) and fire down onto the scrap metal (see [Figure 6.38](#)). The flames may impinge directly on the scrap. Another application is in reforming furnaces where the burners are often natural draft. In this type of configuration, the flow of the combustion gases is against the buoyancy force. This can affect the flame shape if there is not adequate draft in the furnace. This configuration is not used in many applications because of the difficulties of mounting burners on the roof of a furnace.

An important heat transfer consideration with this design is to ensure that the roof is not overheated, which could become a safety issue if the hot combustion products leaked through the roof where they could damage the burner or the fuel gas piping. Another challenge is to get the proper heat flux distribution with the desired flame length, especially in a furnace like a down-fired reformer.

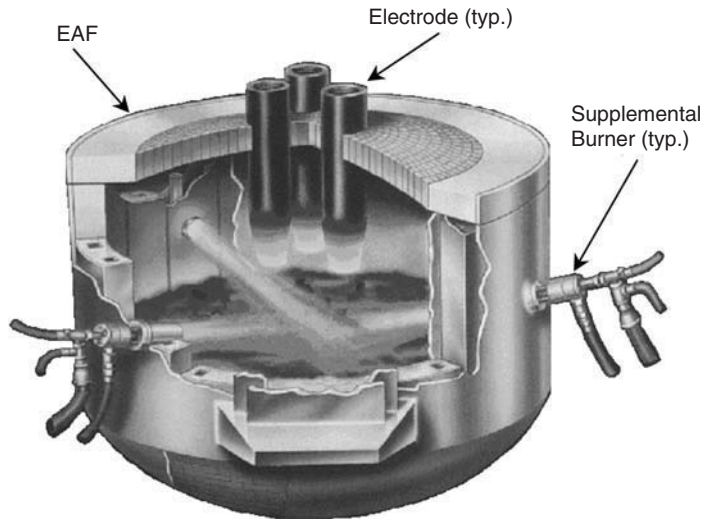


FIGURE 6.38 Supplemental burners firing from the roof of an electric arc furnace.

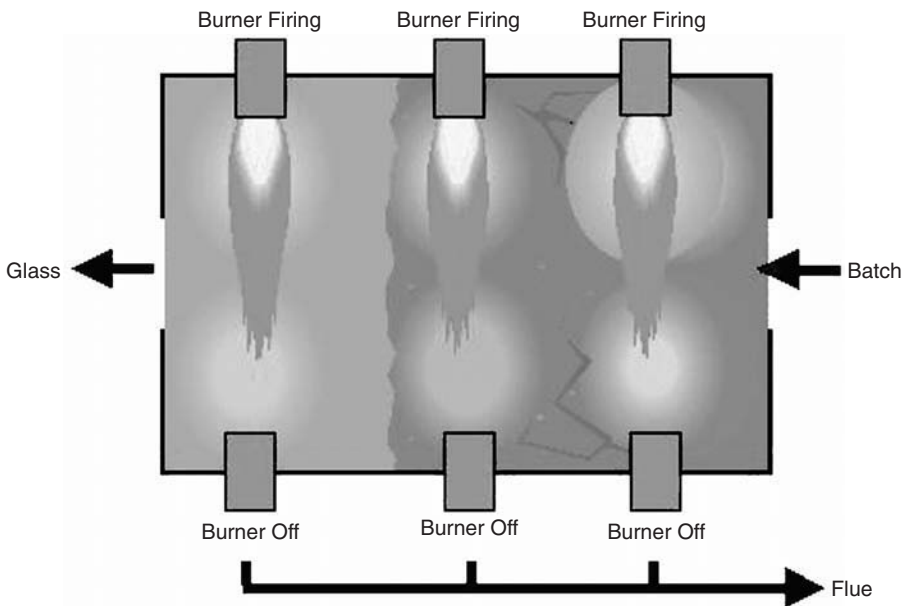


FIGURE 6.39 Example of a side-fired regenerative glass furnace.

6.4.4.4 Side-Fired Burners

This is a common configuration in a wide range of applications. An example is shown in Figure 6.39. The burners are mounted on the side walls and fired perpendicular to those walls, in contrast to wall-fired burners which fire along the wall. Side-fired burners often fire parallel to and over top of the load. The location of the burners on opposing side walls may be either directly opposed, or staggered, depending on the furnace design. Low-momentum flames are often more luminous and have lower NO_x emissions compared to high-momentum flames. However, there are potential problems with

lower momentum flames. Buoyancy effects can lift the flames toward the roof and away from the load. This may reduce the roof refractory life and reduce the heating efficiency to the load. Another problem is that lower momentum flames are also more easily disturbed by neighboring flames. Therefore, the burner design is a balance of many factors affected by flame momentum.

Traditional side-fired burners were and, in many cases, still are round flame designs. A relatively newer side-fired burner is a rectangular design with a wide, fan shape, often referred to as a flat flame burner (e.g., Figure 20.24). The wide part of the flame is parallel to the load below it, to maximize the flame radiation surface area, which maximizes the heat transfer to the load. It is usually desirable to have a fairly uniform heat flux output from the flame and to minimize hot spots in the flame. The flame length and surrounding burners also play important roles in determining the heat flux to the load.

6.4.5 HEAT RECUPERATION

There are two strategies that are commonly used to recuperate heat from the combustion exhaust products. The first strategy is to use those hot gases to preheat an incoming feed stream to the combustor, such as the incoming fuel, oxidizer, both the fuel and the oxidizer, or the raw materials being processed in the combustor. In this strategy, a heat exchanger is used so that the hot exhaust gases do not contact the material they are preheating. This is commonly done using either recuperative or regenerative techniques, which are discussed below. Freeman (1986) compared these two techniques for an innovative air preheating system for use in glass melting furnace, where, in that case, the regenerative system performed slightly better than the recuperative systems, as shown in Figure 6.40.¹⁰³ The second strategy for recuperating heat from the hot exhaust gases is to actually blend them into a feed stream coming into the furnace. This is commonly done by either furnace or flue gas recirculation.

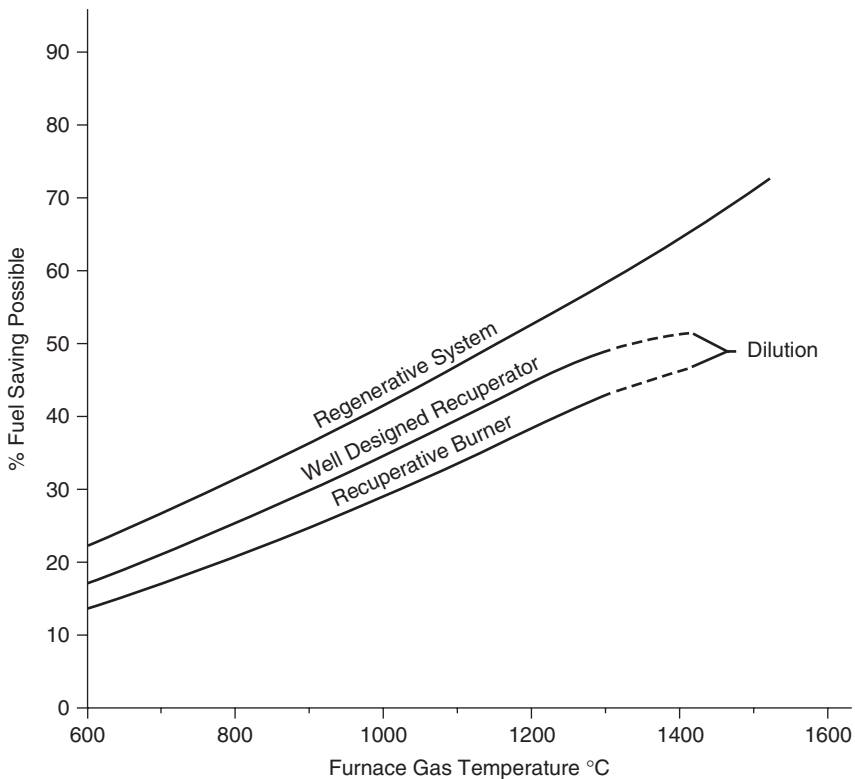


FIGURE 6.40 Calculated fuel savings from regenerative and recuperative systems in a glass-melting furnace. (Courtesy of American Society of Metals.¹⁰³)

There are two primary reasons for recuperating the sensible energy in those exhaust products. The first is simply to improve the thermal efficiency of the combustion system. The increase in the available heat for the stoichiometric combustion of methane by preheating the incoming combustion air is shown in Figure 6.28. The second reason that heat may be recuperated is to increase the flame temperature for processes that need higher temperatures, such as in the melting of raw materials like sand to produce glass. Figure 6.27 shows the adiabatic flame temperature for a stoichiometric air/methane flame increases as the combustion air temperature increases.

Heat recuperation is frequently done using heat exchangers and does not involve the burners at all. However, there are also systems that incorporate heat recuperation in the burner itself. This heat recuperation can have a significant impact on the heat transfer from the flame to the load, which is briefly discussed next for three types of recuperative burners. Brooks and Winters (1990) discussed the use of cellular ceramic materials (CCMs) to recuperate heat in a furnace.¹⁰⁴ Combustion products from burners flow through the CCM, which is separate from the burner and which then radiates energy to the furnace. This is not discussed further here as it is not commercially popular at this time, but it may have merit for future applications.

6.4.5.1 Regenerative Burners

Regenerative burners (see Chapter 12) are designed to fire intermittently, wherein half of the burners are on at any given time while half are off. The exhaust products from the burners that are firing flow through the burners that are off. The burners contain some type of heat storage material, usually some type of porous ceramic or ceramic beads, that remove much of the heat from the hot exhaust products flowing through them. After a certain amount of time, usually on the order of 0.5 to 15 minutes, the firing pattern is reversed. The combustion air flows through the heat storage material and is preheated prior to combustion. As previously shown, the preheated air can significantly raise the flame temperature. Although the level of dissociation may increase in the flame because of the higher temperatures, any dissociated species normally exist in trace quantities so that the bulk composition of the flame gases is essentially the same with or without preheating (see Table 6.3). The main difference is the flame temperature, which affects the radiation from the flame.

TABLE 6.3
Adiabatic Equilibrium Combustion Products
(Mole Fraction) for the Stoichiometric
Combustion of Methane With and Without Air
Preheating

Species	Combustion Air Temperature	
	77°F	2000°F
CO	0.012	0.041
CO ₂	0.103	0.071
H	0.000	0.005
H ₂	0.003	0.011
H ₂ O	0.148	0.129
NO	0.002	0.008
N ₂	0.721	0.699
O	0.000	0.004
O ₂	0.006	0.018
OH	0.003	0.014
Adiabatic Flame Temp. (°F)	3620	4311

Source: Courtesy of CRC Press.¹

Davies (1986) described the use of a regenerative burner for radiant tubes for heating galvanized steel coils.¹⁰⁵ The cycle frequency for switching the firing between burners was 20 seconds. Fuel savings of more than 50% were reported. Newby (1986) reported on an all-ceramic, high-temperature regenerative burner for use in applications requiring temperatures up to 3000°F (1650°C).¹⁰⁶ The burner has been proven to operate in dirty environments without plugging the regenerators or causing corrosion damage in the burner. Examples were given of its use in an open pot glass melting furnace with a reported fuel savings of 20%, an argon-oxygen decarburization vessel preheater, and in (5) small aluminum melting furnaces. Morita (1996) described Japanese research into high-temperature regenerative air preheaters capable of air temperatures exceeding 1000°C (2100°F).¹⁰⁷ Katsuki and Hasegawa (1998) discussed a regenerative preheater for industrial burners capable of air preheats above 1300K (1900°F).¹⁰⁸ Takamichi (1998) described the use of regenerative burners for improving the performance of forging furnaces.¹⁰⁹ Energy savings of up to 40% were reported.

6.4.5.2 Recuperative Burners

In a recuperative burner, a heat exchanger is built into the burner so that the hot combustion products are exhausted through the burner where they preheat either the fuel, the oxidizer, or both. This is a challenging design due to the large temperature and pressure differences in the various streams. Using heat recuperation in the burner has some advantages over using an external heat exchanger for recovering energy from the furnace, which requires a significant amount of large, insulated ductwork. However, the heat exchanger built into the burner may be less efficient than an external exchanger and therefore tends to have lower preheat temperatures. As discussed above, preheating the incoming fuel or oxidizer raises the flame temperature, which enhances flame radiation.

Singh et al. (1986) reported on the use of a recuperator for single-ended radiant tube burners with a mullite outer tube and silicon carbide inner recuperator.¹¹⁰ The heat flux rates from the tube ranged from 55 to 69 Btu/hr-in.² (25 to 31 kW/m²) and had exhaust gas temperatures up to 2000°F (1100°C). Flamme et al. (1998) compared several different types of ceramic heat exchangers for use in self-recuperative burners.¹¹¹ They defined the combustion efficiency (η) as:

$$\eta = \frac{h_{\text{fuel (LHV)}} + h_{\text{air}} - h_{\text{flue gas (inlet)}}}{h_{\text{fuel (LHV)}}} \quad (6.30)$$

where $h_{\text{fuel (LHV)}}$ is the lower heating value of the fuel, h_{air} is the enthalpy of the preheated combustion air, and $h_{\text{flue gas (inlet)}}$ is the enthalpy of the flue gas at the inlet of the recuperator. The relative air preheat rate (ϵ) was expressed as:

$$\epsilon = \frac{T_{\text{air (outlet)}} - T_{\text{air (inlet)}}}{T_{\text{flue gas (inlet)}} - T_{\text{air (inlet)}}} \quad (6.31)$$

where $T_{\text{air (outlet)}}$ is the combustion air temperature at the outlet of the recuperator, $T_{\text{air (inlet)}}$ is the combustion air at the inlet of the recuperator, and $T_{\text{flue gas (inlet)}}$ is the temperature of the flue gas at the inlet of the recuperator. Figure 6.41 shows the relationship between the combustion efficiency and the relative air preheating rate for various flue gas inlet temperatures. Figure 6.42 shows how three different ceramic recuperators were calculated to perform as a function of the flue gas inlet temperature. Louis et al. (1998) described a new self-recuperative single-ended radiant tube burner named CERAJET, which is made of silicon carbide and capable of combustion air preheat temperatures up to 900°C (1650°F) and a thermal efficiency up to 75%.⁷⁵

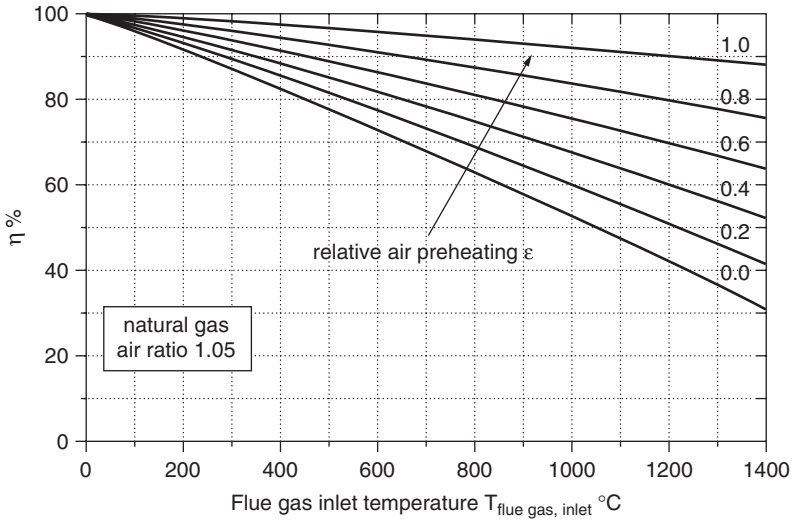


FIGURE 6.41 Combustion efficiency as a function of flue gas temperature at the inlet of the recuperator. (Courtesy of The Gas Research Institute.¹¹¹)

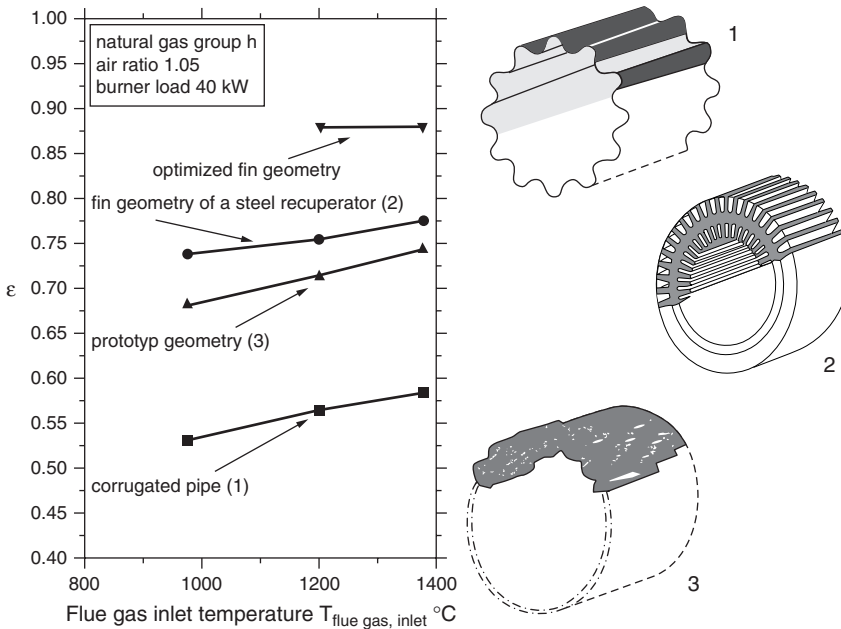


FIGURE 6.42 Calculated relative air preheating rates for different recuperator geometries. (Courtesy of The Gas Research Institute.¹¹¹)

6.4.5.3 Furnace or Flue Gas Recirculation

In flue gas recirculation (see Figure 1.20), some of the hot combustion products from the exhaust stack are recirculated back through the burner. This requires an external fan and insulated ductwork that is often fairly large because of the hot expanded gases and low gas pressures. Although there are added costs for the fan and ductwork, this method has better control as the amount of flue gas recirculation can be controlled independently of the burner.

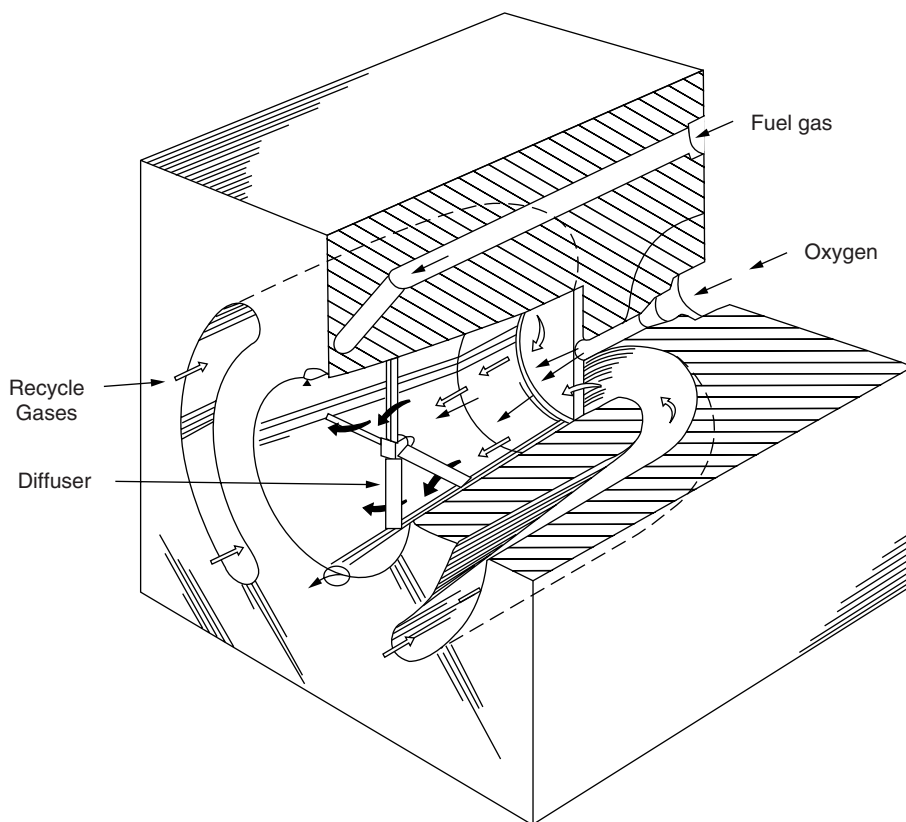


FIGURE 6.43 Oxygen/fuel burner incorporating furnace gas recirculation.¹¹⁴

In furnace gas recirculation, the hot combustion products inside the furnace are recirculated back into either the flame or inside the burner to mix with either the fuel or the oxidizer. An example is given in Wüning and Wüning (1996).¹¹² No external ductwork or fans are required, which makes it much less expensive than furnace gas recirculation. The fluid pumping is accomplished by the design of the burner, where the fuel or the oxidizer flows through a venturi to create a vacuum to induce the furnace gases to flow back toward the burner. This method is less controllable than flue gas recirculation because the amount of recirculated gas is dependent on the burner conditions. Also, at least one of the incoming gases must have a high enough supply pressure to create suction in the venturi. An example of an oxygen/fuel burner¹¹³ utilizing furnace gas recirculation is shown in Figure 6.43.¹¹⁴ The measured heat flux rates from that burner using a total heat flux probe inserted into a pilot scale furnace are shown in Figure 6.44. Plessing et al. (1998) described a combustion system that uses furnace gas recirculation and is known as flameless oxidation (FLOX) where the combustor temperature must be a minimum of 800°C (1500°F) for safe operation.¹¹⁵ The primary advantage of FLOX is low NO_x emissions. Although no specific measurements are given, the radiation from the flame was said to remain the same even though the flame is completely nonluminous. Abbasi et al. (1998) described an advanced U-tube radiant tube burner that uses internal furnace gas recirculation to improve temperature uniformity and lower pollutant emissions.⁷⁶

6.4.6 PULSE COMBUSTION

Pulse combustion refers to the periodic change in the outlet flow of the exhaust products from a combustion process to produce a pulsating flow. Putnam (1971) has written an entire book on the subject.¹¹⁶ The main purpose of that book was how to suppress unwanted, combustion-driven

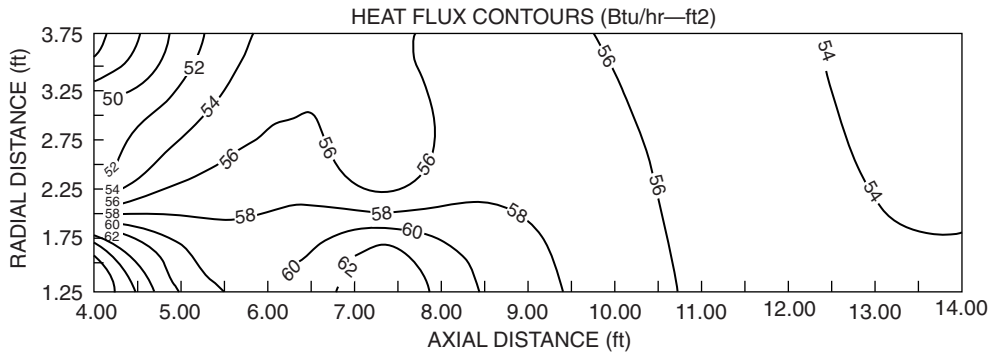


FIGURE 6.44 Measured heat flux rates from an oxygen/fuel burner incorporating furnace gas recirculation.¹¹⁴

oscillations that cause noise and vibration that are detrimental to processes which are not designed to pulse. He discussed how oscillations can be generated in a wide range of industrial combustors. Some of the early papers focused more on the acoustics and fluid dynamics than on the heat transfer from pulse combustion.¹¹⁷

Some of the benefits of combustion specifically designed to pulse include:

- Ability to burn various fuels
- High combustion intensities
- Low NO_x formation
- Low excess air requirements
- Self-aspiration, which eliminates the need for combustion air fans
- Improved heat transfer¹¹⁸

Note that for some pulse combustors, the burner design is integrally linked to the combustion chamber. Therefore, both the burner and, where appropriate, the combustor are considered together here for the sake of consistency and to avoid redundancy. Zinn et al. (1993) described a tunable pulse combustor capable of incinerating waste materials with high efficiencies.¹¹⁹

There are two common types of “pulse” combustion: natural and mechanical. In natural pulsed combustion, the combustion system is designed to deliberately create a resonance that causes the flow to pulse. The heat released in the combustion process excites the fundamental acoustic mode of the combustor. The resulting oscillations interact with the combustion process in such a way as to cause periodic reaction and heat release rates. When the periodicity of the heat release is in phase with the acoustic pressure oscillations, the pulsing process is self-sustaining. There are three common types of natural resonant combustor designs: the quarter wave or Schmidt combustor, the Helmholtz combustor, and the Rijke combustor.¹²⁰ The resonance in the chamber causes the exhaust gases to pulse in a regular and periodic fashion. The pressure initially rises during the first part of the cycle, forcing the exhaust gases out of the tailpipe. After the initial pressure wave, a partial vacuum is created, which pulls in fresh combustion air. The fuel valve (sometimes referred to as a flapper valve) is simultaneously opened by the vacuum pressure and fuel is injected into the incoming combustion air, creating a flammable mixture. The cycle frequency rates may be over 100 Hz and often appear as steady flow to the naked eye and to the ear. Neumeier et al. (1991) discussed modeling of the flapper valve in pulse combustors.¹²¹

The second type of pulse combustor is where a mechanical system causes the flow pulsations. This is often accomplished by opening and closing a valve at fairly high frequencies. One common way is to open and close the fuel valve while keeping a constant flow of oxidizer to a burner. This causes successive regions of fuel-rich and fuel-lean combustion, which can lead to significant reductions in NO_x emissions. This type of pulse combustion has a much lower cycle frequency

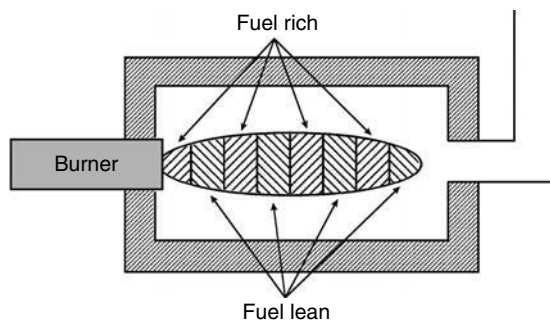


FIGURE 6.45 Alternating fuel-rich and fuel-lean zones in a pulse combustor.¹

and is often detectable by the human eye and ear. Two concerns with this type of pulse combustion system are the life of the mechanical valve because of the number of times it opens and closes, as well as the increase in noise that is often associated with the lower frequency pulsing. George and Putnam (1991) studied the development of a rotary valve for pulse combustors and looked at pulse frequencies from 25 to 90 Hz.¹²² They noted that significant improvements in heat transfer can be expected using a rotary valve pulse combustor. The Institute of Gas Technology (Chicago, IL) has developed an oscillating combustion process that uses a fast cycling valve to pulse the incoming fuel to a burner, while having a steady flow of oxidant.¹²³ By pulsing the fuel, alternating zones of fuel-rich and fuel-lean combustion are produced (see Figure 6.45). The preferred pulse rate is about 5 to 30 cycles per second. The primary reason to do this is to reduce NOx emissions because NOx formation is less favorable under either fuel-rich or very fuel-lean conditions. However, a secondary benefit of the process is often an increase in heat transfer from the flame to the load. This can occur for two reasons. The first is that the fuel-rich regions often produce a luminous flame that radiates heat more efficiently to the load compared to less luminous or nonluminous flames. A second reason is that the oscillating causes the flame gases to pulse, which tends to minimize boundary layer formation and increase convective heat transfer.

In either type of pulse combustion, an important benefit of the process is increased convective heat transfer rates. This is explained by analyzing the flow of the combustion products over a surface (the load). In continuous forced convective flow, a boundary layer builds up as the gases flow over a surface. This boundary layer causes thermal resistance to heat transfer from the gases to the solid surface. In pulsed flow, the boundary layer is continually broken up by the constant changes in flow over the surface. In the higher pressure part of the cycle, the flow goes in one direction, while in the low pressure (vacuum) portion of the cycle, the flow may actually reverse. Breaking up or reducing the thickness of the boundary layer lowers the resistance to heat transfer between the gases and the solid, which enhances the heat transfer rate for a given system compared to nonpulse flow. Hanby (1969) reported heat transfer improvements of up to 100% for an air/propane flame in a straight tube for pulse combustion with a frequency of 100 Hz.¹²⁴ The convective heat transfer coefficient was 15 Btu/hr-ft²-°F (85 W/m²-°C) for steady flow and 35 Btu/hr-ft²-°F (200 W/m²-°C) for pulse flow. Blomquist et al. (1982) measured an improvement in heat transfer ranging from 25 to 40% for a Helmholtz type pulse combustor operating at about 70 Hz and firing on natural gas.¹²⁵ Corliss and Putnam (1986) noted an increase in the convective heat transfer coefficient by as much as 100% using pulse combustion.¹²⁶ The results also showed that when considering both heat and mass transfer, a process can be improved by up to a factor of 5. Brinckman and Miller (1989) reported experimental measurements on methane combustion in a Rijke pulse combustor.¹²⁷ Results showed that pulse combustion could be maintained over a range of fuel flow rates, equivalence ratios, nozzle exit positions, and combustor lengths. Xu et al. (1991) discussed pulse combustion of heavy liquid oil fuels in a Rijke-type pulse combustor.¹²⁸ Arpaci et al. (1993) developed an empirical equation for the convective heat transfer in a pulse combustor tailpipe¹²⁹ to correlate the experimental

data of Dec and Keller (1989).¹³⁰ The Nusselt number increased with combustion chamber pressure (0.5 to 9 kPa) and oscillation frequency (54 to 101 Hz). Barr et al. (1996) described a computational tool for designing pulse combustors.¹³¹ The predicted heat transfer efficiency of a pulse combustion system can be improved by increasing the number of tailpipes in the system. However, there is a diminishing return as the number of tailpipes increases above about 10. Marsano et al. (1998) reported experimental measurements on a 250-kW Helmholtz-type pulse combustor.¹³² Lundgren et al. (1998) analytically showed that a Helmholtz-type combustor can increase the heat transfer by a factor of approximately 2 to 6.¹³³ Grosman et al. (1998) successfully demonstrated the use of an oscillating combustion system using oxygen-enhanced combustion (see [Chapter 21](#)) in a rotary iron melter, ladle preheater, and batch annealing furnace in the steel industry.¹³⁴ In laboratory tests, increases in heat transfer up to 59% were demonstrated.

6.5 IN-FLAME TREATMENT

In some applications, particularly waste incineration, it is possible to inject the material to be heated directly into the flame. The material can be a solid, a liquid, a gas, or a combination of the three. For example, Steward and Guruz (1974) describe the injection of solid particles (alumina or magnesia) into the fuel stream of a burner to study the effects on radiation.¹³⁵ The injected particles had relatively little effect on the measured radiation in the furnace. In many cases, the objective is to fully combust the injected material. For example, Santoleri (1986) describes the incineration of waste liquid fuels injected through a swirl burner, as shown in Figure 6.46.¹³⁶ Although the waste materials in these systems have some heating value, it may be fairly low because of the high water content. This can make the combustion process more difficult due to the high heat extraction from the water. The reason for injecting the waste materials into the flame is to improve the heat and mass transfer processes and more efficiently destruct the waste.

Another type of in-flame treatment involves injecting a solid material into the flame for some type of heat treatment. For example, an inorganic solid can be injected through the flame to be heated and possibly even melted. That type of material is strictly a heat load and does not contribute any heating through combustion reactions. Although the heat transfer to the load can be significantly

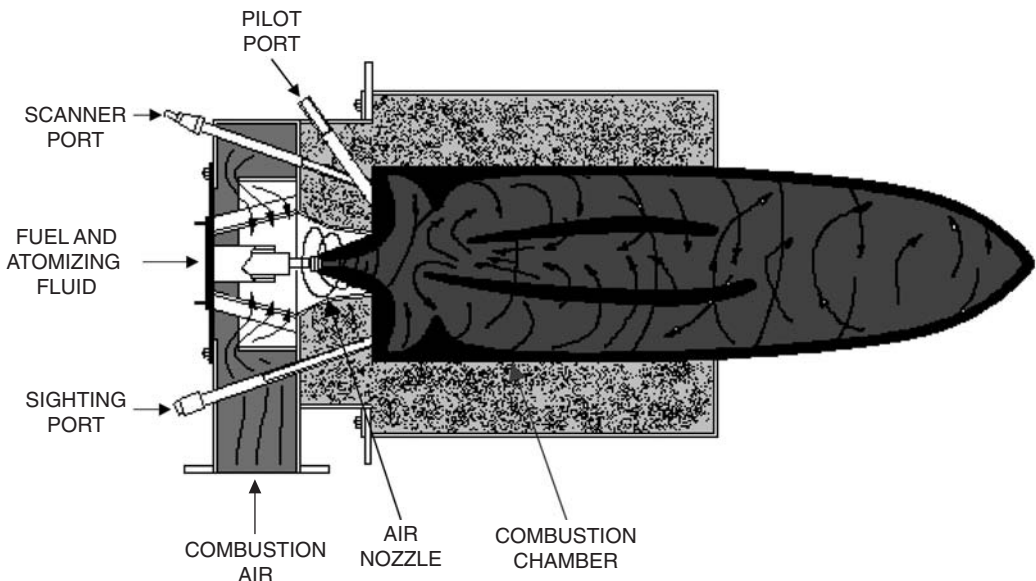


FIGURE 6.46 Swirl burner with waste liquid injection. (Courtesy of American Society of Metals.¹³⁶)

increased using in-flame treatment, because of the intimate contact with the hot exhaust gases, the main challenge is transporting and injecting the solids into the flame. Wagner et al. (1996) describe a process for injecting spent aluminum potliner (SPL) into a cyclonic combustor for destruction of the SPL, which is a hazardous waste.¹³⁷ SPL is a refractory-like substance containing roughly 30% carbon, 15% highly leachable fluoride, and 0.2% cyanide, and is used as the liner in furnaces used to reduce alumina into aluminum in the Hall reduction cell process. The SPL was fed in the top of the cyclonic combustor and traveled through the flame zone, which destroyed the hazardous waste with high efficiency.

Zhang et al. (1996) presented a novel method for incinerating solid wastes by feeding them through a counter-rotating air-oxy/fuel (see Chapter 20) burner.¹³⁸ High temperatures are important in destructing waste materials. The process was tested in a 50-kW (170,000-Btu/hr) pilot-scale furnace using phenolic-coated foundry sand as the waste material to simulate sand reclamation. The furnace had an internal diameter of 0.2 m (0.7 ft) and a height of 2.5 m (8.2 ft). Complete destruction of the resin was demonstrated and clean sand was produced.

REFERENCES

1. C.E. Baukal, *Heat Transfer in Industrial Combustion*, CRC Press, Boca Raton, FL, 2000.
2. R. Villasenor and R. Escalera, A highly radiative combustion chamber for heavy fuel oil combustion, *Int., J. Heat Mass Transfer*, 41, pp. 3087–3097, 1998.
3. C.E. Baukal, Ed., *The John Zink Combustion Handbook*, CRC Press, Boca Raton, FL, 2001.
4. A.G. Slavejkov, C.E. Baukal, M.L. Joshi, and J.K. Nabors, Oxy-fuel glass melting with a high-performance burner, *Ceramic Bulletin*, 71(3), 340–343, 1992.
5. D. Neff, P. Mohr, J. Gaddone, A. Fridman, S. Nester, R. Viskanta, R. Jain, D. Rue, and O. Loo, High-luminosity, low-NOx oxy-natural gas burner for high-temperature furnaces, *IGRC98*, Vol. V: Industrial Utilization, D.A. Dolenc, Ed., Gas Research Institute, Chicago, 1998, 34–44.
6. S.R. Turns, *An Introduction to Combustion*, McGraw-Hill, New York, 1996, chap. 13.
7. A.G. Slavejkov, C.E. Baukal, M.L. Joshi, and J.K. Nabors, Advanced oxygen-natural gas burner for glass melting, *Proc. 1992 International Gas Research Conf.*, H.A. Thompson, Ed., Govt. Institutes, Rockville, MD, 1993, 2269–2278.
8. D.B. Spalding, The art of partial modeling, *Ninth Symposium (International) on Combustion*, Academic Press, New York, 1963, 833–843.
9. J.M. Beér and N.A. Chigier, *Combustion Aerodynamics*, Applied Science Publishers Ltd., London, 1972.
10. G. Damköhler, *Elektrochem*, 42, 846, 1936.
11. C.J. Lawn, T.S. Cunningham, P.J. Street, K.J. Matthews, M. Sarjeant, and A.M. Godridge, in *Principles of Combustion Engineering in Boilers*, C.J. Lawn, Ed., Academic Press, New York, 1987.
12. G.H. Markstein, Scaling of radiative characteristics of turbulent diffusion flames, *Sixteenth Symposium (Int'l) on Combustion*, The Combustion Institute, Pittsburgh, PA, 1976, 1407–1419.
13. G.H. Markstein and J. De Ris, Radiant emission and absorption by laminar ethylene and propylene diffusion flames, *Twentieth Symposium (Int'l) on Combustion*, The Combustion Institute, Pittsburgh, PA, 1984, 1637–1646.
14. J.H. Kent and H.G. Wagner, Temperature and fuel effects in sooting diffusion flames, *Twentieth Symposium (Int'l) on Combustion*, The Combustion Institute, Pittsburgh, PA, 1984, 1007–1015.
15. Y.Y. Buriko and V.R. Kuznetsov, Possible mechanisms of the formation of nitrogen oxides in turbulent diffusional combustion, *Combust. Explos. Shockwaves*, 14(3), 296–303, 1978.
16. S.T. Turns and F.H. Myhr, Oxides of nitrogen emissions from turbulent jet flames. I. Fuel effects and flame radiation, *Comb. Flame*, 87, 319–335, 1991.
17. G.M. Faeth, J.P. Gore, S.G. Chuech, and S.M. Jeng, Radiation from turbulent diffusion flames, *Annu. Rev. Numerical Fluid Mech. & Heat Trans.*, C.L. Tien and T.C. Chawla, Eds., Hemisphere, New York, 1989, Vol. 2, 1–38.
18. M.A. Delichatsios and L. Orloff, Effects of turbulence on flame radiation from diffusion flames, *Twenty Second Symposium (Int'l) on Combustion*, The Combustion Institute, Pittsburgh, PA, 1988, 1271–1279.

19. M.A. Delichatsios, J. De Ris, and L. Orloff, An enhanced flame radiation burner, *Twenty-Fourth Symposium (Int'l) on Combustion*, The Combustion Institute, Pittsburgh, PA, 1992, 1075–1082.
20. R. Weber, Scaling characteristics of aerodynamic, heat transfer, and pollution emissions in industrial flames, *Twenty Sixth Symposium (Int'l) on Combustion*, The Combustion Institute, Pittsburgh, PA, 1996, 3343–3354.
21. R. Weber, J.F. Driscoll, W.J.A. Dahm, and R.T. Waibel, Scaling characteristics of the aerodynamics and low NO_x properties of industrial natural gas burners, The Scaling 400 Study, Part I: Test Plan, Gas Research Institute, Chicago, IL, report GRI-93/0227, 1993.
22. C.E. Baukal, and B. Gebhart, Heat Transfer from Oxygen-Enhanced/Natural Gas Flames Impinging Normal to a Plane Surface, *Exp. Therm. Fluid Sci.*, 16(3), 247–259, 1998.
23. C.E. Baukal, Heat Transfer from Flames Impinging Normal to a Plane Surface, Ph.D. thesis, University of Pennsylvania, Philadelphia, PA, 1996.
24. P. Hutchinson, E.E. Khalil, J.H. Whitelaw, and G. Wigley, Influence of burner geometry on the performance of small furnaces, *2nd European Symp. on Combustion*, 1975, 659–665.
25. V.I. Kirilenko, I.S. Il'yashenko, A.I. Es'kov, I.B. Smulyanskii, and V.I. Basov, Flat-flame combustion of natural gas in a recuperative glass-melting furnace, *Glass & Ceramics*, Nov., 121–123, 1988.
26. A. Ibbotson, Flat-jet oxygen lancing for homogeneous melt, *Glass*, 68(6), 217, 1991.
27. L.T. Yap and M. Pourkashanian, Low-NO_x oxy-fuel flames for uniform heat transfer, *Light Metals 1996*, W. Hale, Ed., Minerals, Metals & Materials Society, 1996, 655–660.
28. T.R. Blake and M. McDonald, An examination of flame length data from vertical turbulent diffusion flames, *Comb. Flame*, 94, 426–432, 1993.
29. C.E. Baukal and B. Gebhart, Oxygen-enhanced/natural gas flame radiation. *Int. J. Heat Mass Transfer*, 44(11), 2539–2547, 1997.
30. M. Pettersson and S. Stenström, Evaluation of gas-fired and electrically heated industrial infrared paper dryers, *Proceedings of the 1998 International Gas Research Conf.*, Vol. V: Industrial Utilization, D.A. Dolenc, Ed., Gas Research Institute, Chicago, 1998, 210–221.
31. J.R. Howell, M.J. Hall, and J.L. Ellzey, Combustion within porous media, in *Heat Transfer in Porous Media*, Y. Bayazitoglu and U.B. Sathuvalli, Eds., ASME, HTD-Vol. 302, 1–27, 1995.
32. P.F. Hsu and J.R. Howell, Measurement of thermal conductivity and optical properties of porous partially stabilized zirconia, *Exper. Heat Transfer*, 5, 293–313, 1993.
33. R.F. Speyer, W.-Y. Lin, and G. Agarwal, Radiant efficiencies and performance considerations of commercially manufactured gas radiant burners, *Exp. Heat Transfer*, 9, 213–245, 1996.
34. Y.-K. Chen, R.D. Matthews, and J.R. Howell, The effect of radiation on the structure of a premixed flame within a highly porous inert medium, in *Radiation, Phase Change Heat Transfer and Thermal Systems*, Y. Jaluria, V.P. Carey, W.A. Fiveland, and W. Yuen, Eds., ASME, HTD-Vol. 81, 35–42, 1987.
35. S.B. Sathe, R.E. Peck, and T.W. Tong, Flame stabilization and multimode heat transfer in inert porous media, a numerical study, *Comb. Sci. Tech.*, 70, 93–109, 1990.
36. P.F. Hsu, J.R. Howell, and R.D. Matthews, A numerical investigation of pre-mixed combustion within porous media, *J. Heat Transfer*, 115(3), 744–750, 1993.
37. L.B. Younis and R. Viskanta, Experimental determination of the volumetric heat transfer coefficient between stream of air and ceramic foam, *Int.J. Heat Mass Transfer*, 36(6), 1425–1434, 1993.
38. X. Fu, R. Viskanta, and J.P. Gore, Measurement and correlation of volumetric heat transfer coefficients of cellular ceramics, *Exper. Thermal Fluid Sci.*, 17, 285–293, 1998.
39. R. Mital, J.P. Gore, and R. Viskanta, A radiation measurement procedure for gas-fired radiant burners, *Proceedings of the 1998 International Gas Research Conf.*, Vol. V: Industrial Utilization, D.A. Dolenc, Ed., Gas Research Institute, Chicago, 1998, 197–209.
40. M.E. Yetman, Evaluation of infrared generators, *Proc. of 1992 International Gas Research Conf.*, H.A. Thompson, Ed., Govt. Institutes, Rockville, MD, 1993, 2401–2409.
41. M. Johansson, Spectral characteristics and efficiency of gas fired infrared heaters, *Proc. of 1992 International Gas Research Conf.*, H.A. Thompson, Ed., Govt. Institutes, Rockville, MD, 1993, 2420–2426.
42. O.H. Madsen, K. Jørgensen, N.B.K. Rasmussen, and A. van der Drift, Improved efficiency heat transfer using selective emittance radiant burners, *Proc. of 1995 International Gas Research Conf.*, D.A. Dolenc, Ed., Govt. Institutes, Rockville, MD, 1996, 2208–2217.
43. F. Ahmady, Gas-fired IR burners are worth considering, *Process Heating*, 1(2), 38–43, 1994.

44. P. Flanagan, K. Gretsinger, H.A. Abbasi, and D. Cygan, Factors influencing low emissions combustion, in *Fossil Fuels Combustion—1992*, R. Ruiz, Ed., ASME PD-Vol. 39, 13–22, 1992.
45. R. Mital and J.P. Gore, An experimental study of laminar diffusion flames with enhanced heat transfer by reticulated ceramic inserts, in *Heat Transfer in Fire and Combustion Systems*, W.W. Yuen and K.S. Ball, Eds., ASME HTD-Vol. 272, 7–12, 1994.
46. A. Kataoka, New type of high temperature surface combustion burner, *Proceedings of the 1998 International Gas Research Conf.*, Vol. V: Industrial Utilization, D.A. Dolenc, Ed., Gas Research Institute, Chicago, 1998, 115–124.
47. W.V. Krill and R. Pam, Industrial applications of the pyrocore burner, in *Industrial Combustion Technologies*, M.A. Lukasiewicz, Ed., American Society of Metals, Materials Park, OH, 1986, 267–271.
48. Alzeta Corp., brochure, Santa Clara, CA, 1998.
49. D.F. Bartz, F.E. Moreno, and P.A. Duggan, Ultra-low, NO_x ultra-high VOC destruction with adiabatic radiant combustors, in *Fossil Fuels Combustion—1992*, R. Ruiz, Ed., ASME PD-Vol. 39, 7–12, 1992.
50. D.W. DeWerth, A Study of Infra-Red Energy Generated by Radiant Gas Burners, American Gas Association Research Bulletin 92, Catalog No. 41/IR, Cleveland, 1962.
51. S.B. Sathe, M.R. Kulkarni, R.E. Peck, and T.W. Tong, An experimental and theoretical study of porous radiant burner performance, *Twenty-Third Symposium (International) on Combustion*, The Combustion Institute, Pittsburgh, PA, 1990, 1011–1018.
52. M.F. Zabielski, J.D. Freihaut, and C.J. Egolf, Fuel/air control of industrial fiber matrix burners using optical emission, in *Fossil Fuel Combustion 1991*, R. Ruiz, Ed., ASME PD-Vol. 33, 41–48, 1991.
53. T.-Y. Xiong and R. Viskanta, A basic study of a porous-matrix combustor-heater, in *Fossil Fuels Combustion—1992*, R. Ruiz, Ed., ASME PD-Vol. 39, 31–39, 1992.
54. S. Jugjai and S. Sanitjai, Parametric studies of thermal efficiency in a proposed porous radiant recirculated burner (PRRB): a design concept for the future burner, *RERIC Int. Energy J.*, 18(2), 97–111, 1996.
55. R. Mital, J.P. Gore, R. Viskanta, and S. Singh, Radiation efficiency and structure of flames stabilized inside radiant porous ceramic burners, in combustion and fire, M.Q. McQuay, W. Schreiber, E. Bigzadeh, K. Annamalai, D. Choudhury, and A. Runchal, Eds., *ASME Proceedings of the 31st National Heat Transfer Conf.*, Vol. 6, ASME HTD-Vol. 328, 131–137, 1996.
56. M.D. Rumminger, R.W. Dibble, N.H. Heberle, and D.R. Crosley, Gas Temperature above a porous radiant burner: comparison of measurements and model predictions, *Twenty Sixth Symposium (Int'l) on Combustion*, The Combustion Institute, Pittsburgh, PA, 1996, 1755–1762.
57. A. van der Drift, N.B.K. Rasmussen, and K. Jorgensen, Improved efficiency drying using selective emittance radiant burners, *Applied Therm. Engrg.*, 17(8–10), pp. 911–920, 1997.
58. R. Mital, J.P. Gore, R. Viskanta, and A.C. McIntosh, An experimental evaluation of asymptotic analysis of radiant burners, *Twenty-Seventh Symposium (International) on Combustion*, The Combustion Institute, Pittsburgh, PA, 1998, 3163–3171.
59. T.W. Tong, S.B. Sathe, and R.E. Peck, Improving the performance of porous radiant burners through use of sub-micron size fibers, in *Heat Transfer Phenomena in Radiation, Combustion, and Fires*, R.K. Shah, Ed., ASME HTD-Vol. 106, 257–264, 1989.
60. R.D. Bell, C. Chaffin, and M. Koeroghlian, Experimental investigation of a staged porous ceramic burner, in *Fossil Fuels Combustion—1992*, R. Ruiz, Ed., ASME PD-Vol. 39, 41–46, 1992.
61. R.M. Kendall and J.D. Sullivan, Selective and Enhanced Radiation from Porous Surface Radiant Burners, Gas Research Institute Report GRI-93/0160, Chicago, 1993.
62. T.-Y. Xiong, M.J. Khinkis, B.M. Kramnik, R. Viskanta, and F.F. Fish, An experimental and theoretical study of a porous-matrix combustor-heater, *Proc. of 1992 International Gas Research Conf.*, H.A. Thompson, Ed., Govt. Institutes, Rockville, MD, 1993, 2013–2024.
63. R. Ruiz and S.N. Singh, Enhanced infrared burner system, *Proc. of 1992 International Gas Research Conf.*, H.A. Thompson, Ed., Govt. Institutes, Rockville, MD, 1993, 2410–2419.
64. P.F.J. Severens, P.H. Bouma, C.J.H. van de Ven, L.P.H. de Goey, and A. van der Drift, Modeling of two-fold flame behavior of ceramic foam surface burners, *J. Energy Resources Tech.*, 117(1), 29–36, 1995.
65. A.N. Bogstra, Development of a new prototype of a flat closed high efficient infrared radiant burner, *Proc. 1998 International Gas Research Conf.*, Vol. V: Industrial Utilization, D.A. Dolenc, Ed., Gas Research Institute, Chicago, 1998, 24–33.

66. Milewski, J.V., Shoultz, R.A., McConnell, M.M.B., and Milewski, E.B., Improved Radiant Burner Material, Superkinetic, Inc., Albuquerque, NM, Final Report, U.S. Dept. of Energy report DOE/EE/15643-T2, 1998.
67. American Petroleum Institute Publication 535: Burners for Fired Heaters in General Refinery Services, First Edition, API, Washington, D.C., July 1995.
68. W.W. Liang and M.E. Schreiner, Advanced materials development for radiant tube applications, in *Industrial Combustion Technologies*, M.A. Lukasiewicz, Ed., American Society of Metals, Materials Park, OH, 1986, 305–311.
69. I. Alliat, R. Rezakhanlou, M. Gutmann, and M. Boussuge, Predictive model of delayed failure of ceramic materials at high temperature, *Proc. 1998 International Gas Research Conf.*, Vol. V: Industrial Utilization, D.A. Dolenc, Ed., Gas Research Institute, Chicago, 1998, 169–177.
70. J.E. Peters, M.Q. Brewster, and R.O. Buckius, Radiative Heat Transfer Augmentation in High Temperature Combustion Systems with Application to Radiant Tube Burners, Gas Research Institute Report GRI-91/0101, Chicago, IL, June 1990.
71. S.S. Singh and L.M. Gorski, Final Report—Ceramic Single Ended Recuperative Radiant Tube (Phase 1), NTIS Document PB91222554, 1990.
72. J.C. Mocsari, H.A. Abbasi, S.M. Nelson, and S.J. Sikirica, Performance evaluation of an advanced hybrid U-tube for industrial heating applications, *Proc. of 1995 International Gas Research Conf.*, D.A. Dolenc, Ed., Govt. Institutes, Rockville, MD, 1996, 2225–2231.
73. Institute of Gas Technology, Composite Radiant Tubes, brochure, Chicago, IL, 1998.
74. S. Sikirica, Benefits of furnace conversions using composite radiant tubes, *Proceedings of the 1998 International Gas Research Conf.*, Vol. V: Industrial Utilization, D.A. Dolenc, Ed., Gas Research Institute, Chicago, 1998, 178–188.
75. G. Louis, J. Peureux, T. Landais, J.P. Burzynski, and C. Busson, A new high temperature furnace technology for application in the steam-cracking area, *Proceedings of the 1998 International Gas Research Conf.*, Vol. V: Industrial Utilization, D.A. Dolenc, Ed., Gas Research Institute, Chicago, 1998, 136–146.
76. H. Abbasi, H. Kurek, M. Khinkis, A.E. Yerynov, and O.M. Semerin, Advanced, high-efficiency, low-emissions burner for radiant tube applications, *Proceedings of the 1998 International Gas Research Conf.*, Vol. V: Industrial Utilization, D.A. Dolenc, Ed., Gas Research Institute, Chicago, 1998, 147–157.
77. H. Ramamurthy, S. Ramadhyani, and R. Viskanta, Development of fuel burn-up and wall heat transfer correlations for flows in radiant tubes, *Num Heat Transfer, Part A*, 31, 563–584, 1997.
78. T.J. Schultz, R.A. Schmall, and I. Chan, Selection of a heating system for a high temperature gas fired soft vacuum furnace, in *Fossil Fuels Combustion—1992*, R. Ruiz, Ed., ASME PD-Vol. 39, 13–22, 1992.
79. F. Mei and H. Meunier, Numerical and experimental investigation of a single ended radiant tube, in *ASME Proceedings of the 32nd National Heat Transfer Conf.*, Vol. 3: Fire and Combustion, eL. Gritz and J.-P. Delplanque, Eds., ASME, New York, 1997, 109–118.
80. J.L. Lannutti, R.J. Schreiber, and M.A. Lukasiewicz, Catalytic radiant tube for industrial process heating applications, in *Industrial Combustion Technologies*, M.A. Lukasiewicz, Ed., American Society of Metals, Materials Park, OH, 1986, 29–37.
81. S.R. Huebner, C.A. Hersch, and M.A. Lukasiewicz, Experimental evaluation of a radiant tube combustion system fired with oxygen enriched combustion air, in *Industrial Combustion Technologies*, M.A. Lukasiewicz, Ed., American Society of Metals, Materials Park, OH, 1986, 49–53.
82. T.F. Wall, L.L. Baxter, G. Richards, and J.N. Harb, Ash deposits, coal blends and the thermal performance of furnaces, *Eng. Foundation Conf. on Coal-Blending and Switching of Low-Sulfur Western Coals*, Snowbird, UT, Sept./Oct. 1993, pp. 453–463, 1994.
83. D. Merrick, *Coal Combustion and Conversion Technology*, Elsevier, New York, 1984.
84. S. Singer, *Pulverized Coal Combustion—Recent Developments*, Noyes Publications, Park Ridge, NJ, 1984.
85. L.D. Smoot and P.J. Smith, *Coal Combustion and Gasification*, Plenum Press, New York, 1985.
86. J. Feng, Ed., *Coal Combustion*, Hemisphere, New York, 1988.
87. D.A. Tillman, *The Combustion of Solid Fuels and Wastes*, Academic Press, San Diego, 1991.
88. L.D. Smoot, *Fundamentals of Coal Combustion*, Elsevier, New York, 1993.
89. J. Tomeczek, *Coal Combustion*, Krieger Pub., Malabar, FL, 1994.
90. A. Williams, M. Pourkashanian, J.M. Jones, and N. Skorupska, *Combustion and Gasification of Coal*, Taylor & Francis, New York, 1999.

91. D. Boersma, Flame stabilization and heat transfer in a cylindrical furnace, in *Combustion Institute European Symposium 1973*, F.J. Weinberg, Ed., Academic Press, London, 1973, 615–620.
92. J.T. Zung, Ed., *Evaporation—Combustion of Fuels*, American Chemical Society, Washington, D.C., 1978.
93. A. Williams, *Combustion of Liquid Fuel Sprays*, Butterworths, London, 1990.
94. E.M. Amin, M. Pourkashanian, A.P. Richardson, A. Williams, L.T. Yap, R.A. Yetter, and N.A. Moussa, Fuel preheat as NO_x abatement strategy for oxygen enriched turbulent diffusion flames, EC-Vol. 3/FACT-Vol. 20, *1995 Joint Power Generation Conf.*, S.M. Smouse and W.F. Frazier, Eds., ASME, 1995, 259–269.
95. J. Chedaille, Experimental Study of the Influence on Heat Transfer of the Injection of Pure Oxygen Under Industrial Oil Flames, International Flame Research Foundation, IJmuiden, The Netherlands, Report K 20/a/28, 1965.
96. G.D. Arnold, Developments in the use of oxy/gas burners, *J. Inst. Fuel*, 40, 117–121, 1967.
97. H. Kobayashi, J.G. Boyle, J.G. Keller, J.B. Patton, and R.C. Jain, Technical and economic evaluation of oxygen enriched combustion systems for industrial furnace applications, in *Industrial Combustion Technologies*, M.A. Lukasiewicz, Ed., American Society of Metals, Materials Park, OH, 1986, 153–163.
98. M. De Lucia, Oxygen enrichment in combustion processes: comparative experimental results from several application fields, *J. Energy Resources Technology*, 113, 122–126, 1991.
99. H. Guénebaud and A.G. Gaydon, The effect of preheating on flame radiation and flame shape, *Sixth Symposium (International) on Combustion*, Reinhold Publishing, New York, 1957, 292–295.
100. B.E. Cain, T.F. Robertson, and J.N. Newby, Reducing NO_x emissions in high-temperature furnaces, *Proc. 1998 International Gas Research Conf.*, Vol. V: Industrial Utilization, D.A. Dolenc, Ed., Gas Research Institute, Chicago, 1998, 237–253.
101. A. Quinqueneau, P.F. Miquel, L.M. Dearden, M. Pourkashanian, G.T. Spence, A. Williams, and B.J. Wills, Experimental and theoretical investigation of a low-NO_x high temperature industrial burner, *Proc. 1998 International Gas Research Conf.*, Vol. V: Industrial Utilization, D.A. Dolenc, Ed., Gas Research Institute, Chicago, 1998, 225–236.
102. D.S. Neff, P.J. Mohr, D. Rue, H. Abbasi, and L. Donaldson, Oxygen-enriched air staging for NO_x reduction in regenerative glass melters, *Proc. 1998 International Gas Research Conf.*, Vol. V: Industrial Utilization, D.A. Dolenc, Ed., Gas Research Institute, Chicago, 1998, 254–261.
103. R.A. Freeman, Some innovative techniques in the glass industry, in *Industrial Combustion Technologies*, M.A. Lukasiewicz, Ed., American Society of Metals, Materials Park, OH, 1986, 273–277.
104. D.L. Brooks and E.M. Winter, Material selection of cellular ceramics for a high temperature furnace, in *Fossil Fuel Combustion Symposium 1990*, S. Singh, Ed., ASME PD-Vol. 30, 117–125, 1990.
105. T. Davies, Regenerative burners for radiant tubes—field test experience, in *Industrial Combustion Technologies*, M.A. Lukasiewicz, Ed., American Society of Metals, Materials Park, OH, 1986, 65–70.
106. J.N. Newby, Regen Regenerative Burner for High Performance, Heat Recovery in Aggressive Environments, in *Industrial Combustion Technologies*, M.A. Lukasiewicz, Ed., American Society of Metals, Materials Park, OH, 1986, 77–85.
107. M. Morita, Present state of high-temperature air combustion and regenerative combustion technology, *Science & Technology in Japan*, No. 58, 11–26, 1996.
108. M. Katsuki and T. Hasegawa, The science and technology of combustion in highly preheated air, *Twenty-Seventh Symposium (International) on Combustion*, The Combustion Institute, Pittsburgh, PA, 1998, 3135–3146.
109. S. Takamichi, Development of high performance forging furnaces, *Proc. 1998 International Gas Research Conf.*, Vol. V: Industrial Utilization, D.A. Dolenc, Ed., Gas Research Institute, Chicago, 1998, 100–112.
110. S. Singh, S. Yokosh, T. Briselden, and S.S. Singh, Improved combustion/thermal efficiency with compact recuperator design, in *Industrial Combustion Technologies*, M.A. Lukasiewicz, Ed., American Society of Metals, Materials Park, OH, 1986, 71–75, 1986.
111. M. Flamme, M. Boß, M. Brune, A. Lynen, J. Heym, J.A. Wünnig, J.G. Wünnig, and H.J. Dittman, Improvement of energy saving with new ceramic self-recuperative burners, *Proc. 1998 International Gas Research Conf.*, Vol. V: Industrial Utilization, D.A. Dolenc, Ed., Gas Research Institute, Chicago, 1998, 88–99.
112. J.A. Wünnig and J.G. Wünnig, Regenerative burner using flameless oxidation, *Proc. 1995 International Gas Research Conf.*, D.A. Dolenc, Ed., Government Institutes, Rockville, MD, 1996, 2487–2495.

113. K.J. Fioravanti, L.S. Zelson, and C.E. Baukal, Flame Stabilized Oxy-Fuel Recirculating Burner, U.S. Patent 4,954,076, issued September 4, 1990.
114. C.E. Baukal, K.J. Fioravanti, and L. Vazquez del Mercado, The Reflex[®] burner, in *Fossil Fuel Combustion—1991*, R. Ruiz, Ed., ASME PD-Vol. 33, 61–67, 1991.
115. T. Plessing, N. Peters, and J.G. Wünnig, Laseroptical (sic) investigation of highly preheated combustion with strong exhaust gas recirculation, *Twenty-Seventh Symposium (International) on Combustion*, The Combustion Institute, Pittsburgh, PA, 1998, 3197–3204.
116. A.A. Putnam, *Combustion-Driven Oscillations in Industry*, Elsevier, New York, 1971.
117. W.W. Sipowicz, N.W. Ryan, and A.D. Baer, Combustion-driven acoustic oscillations in a gas-fired burner, *Thirteenth Symposium (International) on Combustion*, The Combustion Institute, Pittsburgh, PA, 1970, 559–564.
118. B.T. Zinn, Applications of pulse combustion in industry, in *Industrial Combustion Technologies*, M.A. Lukasiewicz, Ed., American Society of Metals, Materials Park, OH, 1986, 55–61.
119. B.T. Zinn, B.R. Daniel, A.B. Rabhan, M.A. Lukasiewicz, P.M. Lemieux, and R.E. Hall, Applications of pulse combustion in industrial and incineration processes, *Proc. 1992 International Gas Research Conf.*, H.A. Thompson, Ed., Government Institutes, Rockville, MD, 1993, 2383–2391.
120. B.T. Zinn, Pulse combustion: recent applications and research issues, *Twenty-Fourth Symposium (International) on Combustion*, The Combustion Institute, Pittsburgh, PA, 1992, 1297–1305.
121. Y. Neumeier, J.I. Jagoda, and B.T. Zinn, Modelling of pulse combustor flapper valves, in *Fossil Fuel Combustion 1991*, R. Ruiz, Ed., ASME PD-Vol. 33, 117–125, 1991.
122. P.E. George and A.A. Putnam, development of a rotary valve for industrial pulse combustors, in *Fossil Fuel Combustion 1991*, R. Ruiz, Ed., ASME PD-Vol. 33, 27–33, 1991.
123. H.A. Abbasi, Fuel Combustion, U.S. Patent 4,846,665, July 11, 1989.
124. V.I. Hanby, Convective heat transfer in a gas-fired pulsating combustor, *Trans. ASME, J. Eng. Power*, 1, 48–51, 1969.
125. C.A. Blomquist and J.M. Clinch, Operational and heat-transfer results from an experimental pulse-combustion burner, *Proc. Pulse-Combustion Applications* Gas Research Institute report GRI-82/0009.2, Vol. 1, Chicago, 1982.
126. J.M. Corliss and A.A. Putnam, Heat-transfer enhancement by pulse combustion in industrial processes, in *Industrial Combustion Technologies*, M.A. Lukasiewicz, Ed., American Society of Metals, Materials Park, OH, 1986, 39–48, 1986.
127. G.A. Brinckman and D.L. Miller, Combustion of methane in a Rijke pulsating combustor, in *Heat Transfer Phenomena in Radiation, Combustion, and Fires*, R.K. Shah, Ed., ASME HTD-Vol. 106, 487–491, 1989.
128. Z.X. Xu, D. Reiner, A. Su, T. Bai, B.R. Daniel, and B.T. Zinn, Flame stabilization and combustion of heavy liquid fuels in a Rijke type pulse combustor, in *Fossil Fuel Combustion 1991*, R. Ruiz, Ed., ASME PD-Vol. 33, 17–26, 1991.
129. V.S. Arpaci, J.E. Dec, and J.O. Keller, Heat transfer in pulse combustor tailpipes, *Comb. Sci. Tech.*, 94(1–6), 131–146, 1993.
130. J.E. Dec and J.O. Keller, Pulse combustor tail-pipe heat-transfer dependence on frequency, amplitude, and mean flow rate, *Comb. Flame*, 77, 359–374, 1989.
131. P.K. Barr, J.O. Keller, and J.A. Kezerle, SPCDC: A user-friendly computation tool for the design and refinement of practical pulse combustion systems, *Proc. 1995 International Gas Research Conf.*, D.A. Dolenc, Ed., Government Institutes, Rockville, MD, 1996, 2150–2159.
132. S. Marsano, P.J. Bowen, and T. O'Doherty, Cyclic modulation characteristics of pulse combustors, *Twenty-Seventh Symposium (International) on Combustion*, The Combustion Institute, Pittsburgh, PA, 1998, 3155–3162.
133. E. Lundgren, U. Marksten, and S.-I. Möller, The enhancement of heat transfer in the tail pipe of a pulse combustor, *Twenty-Seventh Symposium (International) on Combustion*, The Combustion Institute, Pittsburgh, PA, 1998, 3215–3220.
134. R.E. Grosman, M.L. Joshi, J.C. Wagner, H.A. Abbasi, L.W. Donaldson, C.F. Youssef, and G. Varga, Oscillating combustion to increase heat transfer and reduce NO_x emissions from conventional burners, *Proc. 1998 International Gas Research Conf.*, Vol. V: Industrial Utilization, D.A. Dolenc, Ed., Gas Research Institute, Chicago, 1998, 1–14.

135. F.R. Steward and K.H. Guruz, The effect of solid particles on radiative transfer in a cylindrical test furnace, *Fifteenth Symposium (International) on Combustion*, The Combustion Institute, Pittsburgh, PA, 1974, 1271–1283.
136. J.J. Santoleri, Burner/atomizer requirements for combustion of waste fuels, in *Industrial Combustion Technologies*, M.A. Lukasiewicz, Ed., American Society of Metals, Materials Park, OH, 1986, 335–343.
137. J.C. Wagner, H.A. Abbasi, and D. Sager, Thermal treatment of spent aluminum potliner (SPL) in a natural gas-fired slagging cyclonic combustor, *Proc. 1995 International Gas Research Conf.*, D.A. Dolenc, Ed., Government Institutes, Rockville, MD, 1996, 2677–2686.
138. B.L. Zhang, C. Guy, J. Chaouki, and L. Mauillon, Heat treatment of divided solid wastes in an oxy-gas reactor, *Proc. 1995 International Gas Research Conf.*, Vol. II, D.A. Dolenc, Ed., Government Institutes, Rockville, MD, 1996, 2667–2676.

7 Burner Noise

*Mahmoud Fleifil, Ph.D., Jay Karan,
and Wes Bussman, Ph.D.*

CONTENTS

- 7.1 Introduction
- 7.2 Basic Definitions of Sound
 - 7.2.1 Measurement of Sound
 - 7.2.2 Overall Sound Level and How to Add dB Values
- 7.3 Characteristics of Sound Propagation
 - 7.3.1 Absorption of Sound
 - 7.3.1.1 Absorption Coefficient
 - 7.3.1.2 Methods of Evaluating Sound Absorption
 - 7.3.1.3 Factors Affecting the Absorption Coefficient
 - 7.3.2 Reflection of Sound
 - 7.3.2.1 Reflection from Flat Surfaces
 - 7.3.3 Diffraction of Sound
 - 7.3.3.1 Diffraction of Sound Waves by Large and Small Apertures
 - 7.3.3.2 Diffraction of Sound Waves by Obstacles
 - 7.3.3.3 Diffraction of Sound Waves by a Slit
 - 7.3.3.4 Diffraction of Sound by an Acoustic Lens
 - 7.3.4 Refraction of Sound
 - 7.3.5 Diffusion of Sound
 - 7.3.5.1 Steady-State Measurements
 - 7.3.6 Spatial Uniformity of Reverberation Time
 - 7.3.7 Decay Shapes
 - 7.3.8 Microphone Directivity
- 7.4 Sources of Noise in Burners
 - 7.4.1 Low Frequency: Combustion Roar
 - 7.4.2 Low Frequency: Fan Noise
 - 7.4.3 High Frequency: Gas Jet Noise
 - 7.4.3.1 Gas Jet Mixing Noise
 - 7.4.3.2 Shock-Associated Noise
 - 7.4.4 High Frequency: Piping and Valve Noise
- 7.5 Sound Inside Enclosures
 - 7.5.1 Low-Frequency Range
 - 7.5.2 High-Frequency Range
 - 7.5.2.1 Effective Intensity in a Diffuse Sound Field
 - 7.5.2.2 Steady-State Response
 - 7.5.2.3 Transient Response
- 7.6 Noise Radiation from Burner
 - 7.6.1 Multiple-Cavity Model of Furnace-Burner Acoustic System
 - 7.6.2 Evaluation of Acoustic Properties of Internal Surfaces and Walls

- 7.6.3 Effect of Background Noise on Burner Noise Level
- 7.6.4 Noise Level due to Multiple Burners
 - 7.6.4.1 Example
- 7.7 Noise Control and Mufflers
 - 7.7.1 Evaluation of Muffler Insertion Loss
 - 7.7.2 Iterative Design of Mufflers
- 7.8 Glossary
- References

7.1 INTRODUCTION

The sensation of sound is a thing *sui generis*, not comparable with any of our other sensations. No one can express the relation between a sound and a color or a smell. Directly or indirectly, all questions connected with this subject must come for decision to the ear, as the organ of hearing; and from it there can be no appeal. But we are not therefore to infer that all acoustical investigations are conducted with the unassisted ear. When once we have discovered the physical phenomena which constitute the foundation of sound, our explorations are in great measure transferred to another field lying within the dominion of the principles of Mechanics. Important laws are in this way arrived at, to which the sensations of the ear cannot but conform.

— **The Theory of Sound**
by Lord Rayleigh III

According to recent statistics, more than 20 million Americans are exposed to hazardous sound levels on a regular basis. There are approximately 28 million Americans who have some degree of hearing loss: about one third of these — more than 9 million — have been affected, at least in part, by exposure to excessive noise.¹

Combustion equipment and processes are some of the loudest known sources of noise. Ranging from the earliest jet engines, the pulse combustors used on the V-1 bombs (Buzz Bombs) during World War II, and the large rocket engines on the Saturn rockets, down to the humble propane torch, it is obvious that combustion processes create significant to dangerous noise levels. Industrial burners are in the middle of the size range of combustion equipment as a whole, but are a ubiquitous part of all types of industry and, as such, industrial personnel as well as unrelated neighbors experience significant exposure to the noise from industrial burners

Understanding how noise is produced and propagated in industrial burners and associated equipment has grown over the years and has provided the knowledge necessary to apply effective noise control to burners. This chapter attempts to inform the reader of the various factors and mechanisms involved in the production and propagation of burner noise, as well as the techniques and strategies to mitigate its impact on the environment.

7.2 BASIC DEFINITIONS OF SOUND

Webster's Dictionary defines sound as "that which is heard." However, in keeping with Lord Rayleigh's argument that sound follows principles of mechanics in addition to human hearing, the Noise Control Reference Handbook² gives a fuller definition as follows:

Sound is a vibrational disturbance, exciting hearing mechanisms transmitted in a predictable manner determined by the medium through which it propagates. To be audible the disturbance must fall within the frequency range of approximately 20 Hz to 20,000 Hz.

Nobel laureate Lord Rayleigh (John William Strutt, Third Baron of Rayleigh), considered by some to be the father of modern acoustics, outlined most of the fundamentals of acoustics in his historic 1877 text entitled *The Theory of Sound*. In this work, Lord Rayleigh clearly explains the wave propagation of sound.¹

Sound is propagated as waves in solids, liquids, and gases. Waves transmit energy without the translation of matter in the direction of energy flow. An example is the expanding ripples caused when a pebble is dropped in a still pond. The energy is conducted out and away from the source but the particles of water only move up and down in the same place, as can be seen from the up-and-down movement of a piece of wood or leaf floating on the surface.

Lord Rayleigh pointed out that if sound propagation involved gross motion of the air, rather than wave propagation, then a cricket that is heard at considerable distance would need to move a tremendous mass of air, all at once.

Wave motion can be uniquely identified by two of its properties: namely, frequency and amplitude. For sound, frequency defines the pitch or tone of the sound; and sound pressure, which is the amplitude, defines the loudness of the sound. Sound frequency can be measured in cycles per second (cps) and, as with electricity, the commonly used unit is Hertz (1 Hertz [Hz] = 1 cycle per second [cps]). Sound pressure can be quantified in pressure units such as kPa or psig, but is most commonly expressed in units of decibels.

It is important to distinguish between sound power and sound pressure. *Sound power* usually means the capacity or power level of a sound source. *Sound pressure*, on the other hand, is the incident energy reaching any point of interest, some distance from the sound source.⁴ The difference between sound power and sound pressure is easily understood using the analogy of a 100 W light bulb. The power of the source, in the case of the light bulb, is a constant 100 W; however, the incident light energy from the 100 W light bulb at any point of interest depends on the distance from the light source as well as atmospheric conditions. Most of the time, sound pressure is of interest because it is what affects us. However, estimates of the sound power of sources is required to model and calculate the impact of sound on the environment. Sound power can be expressed in terms of power units such as watts (W), but is also most commonly expressed in decibels (dB).

“Decibel,” a term coined in the 1960s by Bell Laboratories for a \log_{10} scale, is used to compress the large range of power or pressure units required to span the various sounds that we deal with every day. The abbreviation for decibel is dB. Figure 7.1 shows how decibel (dB) relates to power

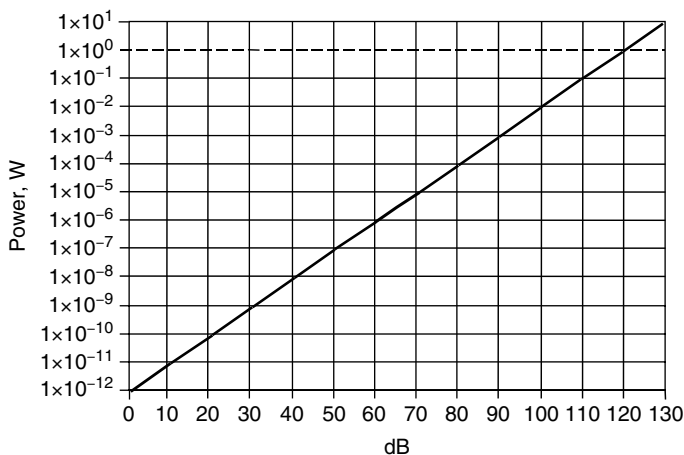


FIGURE 7.1 Relationship between decibels and watts.

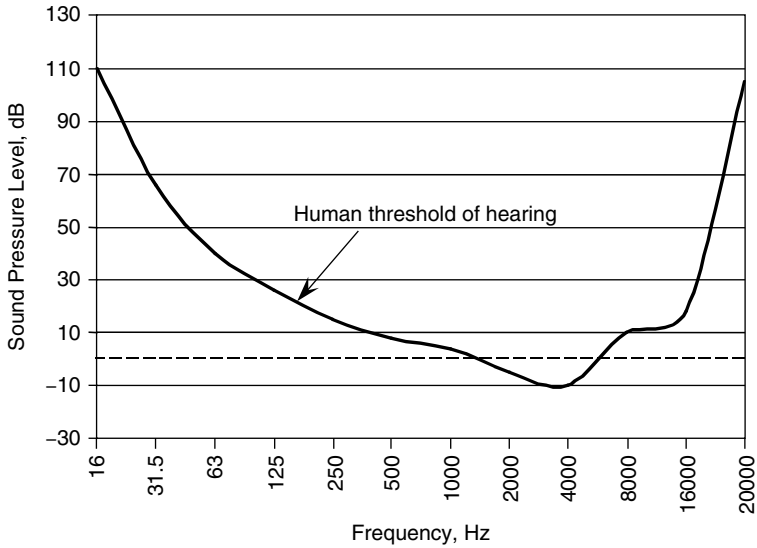


FIGURE 7.2 Hearing threshold in humans.

in watts (W). In this convention, 0 dB relates to a reference power of 1×10^{-12} W, and 1 W is equal to 120 dB.

Sound power level is the acoustic power radiated from a given sound source as related to the reference power level of 1×10^{-12} W, and can be expressed as:

$$L_w = 10 \log(W/10^{-12}) \text{ or } L_w = 10 \log W + 120 \quad (7.1)$$

where W = acoustic power in watts.

Sound pressure level in decibels (dB) is a ratio of the mean square of the actual pressure to the mean square of a reference pressure. The reference pressure, by convention, has been selected to be the threshold of hearing. That is, 0 dB has been chosen to be equal to the quietest audible sound for persons with excellent hearing (i.e., 20 μ Pa).

Human hearing sensitivity extends over a wide range of frequencies; namely, 20 to 20,000 Hz. The human ear is not equally sensitive over this entire range. [Figure 7.2](#) shows the “Threshold of Hearing,” which represents the human ear’s sensitivity curve. The area above the curve is what can be heard. The large range of frequencies of the human hearing range can be divided into octave bands. An octave represents a doubling of frequency and, for the sake of more accurate measurement and analysis, the octave bands can be divided into one-third octave bands. The list of octave bands and the one-third octave bands is shown in [Table 7.1](#). Any of these bands can be conveniently identified by its center frequency. The center frequency is the geometric mean of the range whose upper and lower limits are defined by the ISO and ANSI standards.

The advantages of making broad band analysis of sound using octave or one-third octave band filter sets are that less time is needed to obtain data and the instrumentation required to measure the data is less expensive. The main disadvantage is the loss of detailed information about the sound which is available from narrow band (FFT) analysis.

The upper and lower nominal octave band limits are arrived at by multiplying the center frequency by 1.414 and 0.707, respectively. One-third octave band center frequencies are given by

TABLE 7.1
Octave and One-Third Octave Bands

Band	Lower Band		Upper Band		Upper Band	
	Limit	Center	Limit	Limit	Center	Limit
12	11	16	22	14.1	16	17.8
13				17.8	20	22.4
14				22.4	25	28.2
15	22	31.5	44	28.2	31.5	35.5
16				35.5	40	44.7
17				44.7	50	56.2
18	44	63	88	56.2	63	70.8
19				70.8	80	89.1
20				89.1	100	112
21	88	125	177	112	125	141
22				141	160	178
23				178	200	224
24	177	250	355	224	250	282
25				282	315	355
26				355	400	447
27	355	500	710	447	500	562
28				562	630	708
29				708	800	891
30	710	1000	1420	891	1000	1122
31				1122	1250	1413
32				1413	1600	1778
33	1420	2000	2840	1778	2000	2239
34				2239	2500	2818
35				2818	3150	3548
36	2840	4000	5680	3548	4000	4467
37				4467	5000	5623
38				5623	6300	7079
39	5680	8000	11,360	7079	8000	8913
40				8913	10,000	11,220
41				11,220	12,500	14,130
42	11,360	16,000	22,720	14,130	16,000	17,780
43				17,780	20,000	22,390

$10^{n/10}$, where n is the index number (left column of [Table 7.1](#)) of the one-third octave band. As an example: for 125 Hz, the band index number is 21 and $10^{21/10} = 125.89$. Lower and upper frequencies are a function of $2^{-1/6}$ (0.89) or $2^{1/6}$ (1.12), respectively. As one can see, there is considerable approximation and truncation or round-up being used in handling these numbers. The values shown in the table are the nominal values that are most commonly used.

Sound meters have the capability to measure with equal sensitivity over the entire audible range. However, because humans do not hear with equal sensitivity at all frequencies, the sound meter's measurement needs to be modified to quantify what really affects us. This can be done using correction curves. There are various correction curves: namely, A, B, C, and D (see [Figure 7.3](#)). The most common correction is the A-scale, which is approximately representative of the frequency response of the human ear, which is less sensitive to low-frequency than to high-frequency sound. A-scale decibel levels are expressed as "dBA."

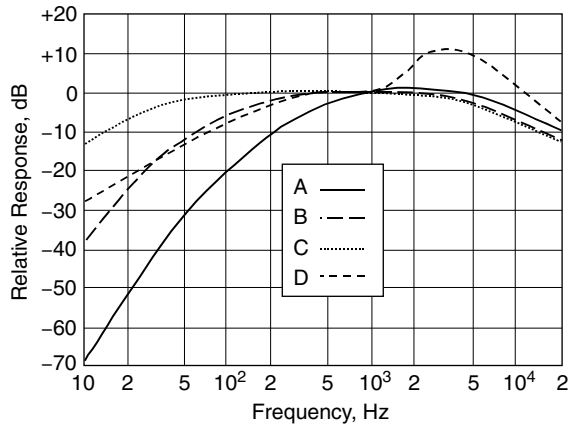


FIGURE 7.3 Weighting curves A, B, C, and D.

7.2.1 MEASUREMENT OF SOUND

Noise meters consist of a microphone, preamplifier, signal processor, output amplifier, and display. Figure 7.4 shows a typical noise meter used for measurements of burner noise. For noise analysis tasks, more sophisticated digital signal processing (DSP) equipped analyzers are used. The more sophisticated analyzers can perform Fast Fourier Transform (FFT) operations that aid accurate narrowband analysis. In general, spectrum analyzers allow the user to map the sound pressure level at different frequencies, that is, generate a curve of the sound over different frequencies. Typical measurements are made with the following resolutions:

1. Octave band measurements (one measurement per octave)
2. One-third octave band measurements (one measurement per one third of an octave)
3. Narrow band measurements (via FFT)

As the name suggests, a one-third octave band instrument makes three measurements in each octave, as opposed to the single measurement of the octave band instrument. A narrow band instrument, on the other hand, uses digital signal processing (DSP) to implement an FFT analysis and, in the current state of the art, FFT analysis allows a given frequency range to be sliced into as many as 128 intervals.

Figure 7.5 provides a comparison of the same sound spectrum as analyzed using three different band intervals: octave band, one-third octave, and narrow band. This comparison shows that the



FIGURE 7.4 Typical noise meter.

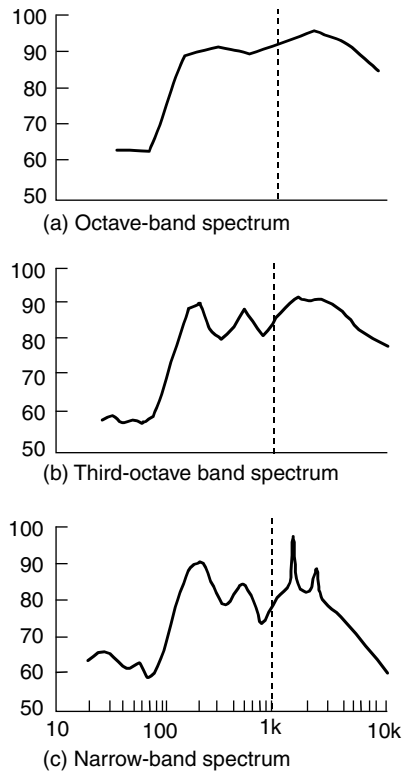


FIGURE 7.5 Same sound spectrum on three different band intervals.

additional resolution provided by narrower band methods is of vital importance. In this example, the level at 1 kHz, as recorded by the octave band instrument is 90 dB; on the one-third octave instrument, it is 85 dB; and on the narrow band instrument it is 70 dB. The lower resolution measurements produce higher measurements because the lack of resolution allows the nearby 1.8-kHz peak to influence the measurement at 1 kHz. Further, in considering implementing some noise control for this source, it is very valuable to know that it is the narrow peak at 1.8 kHz that is driving the maximum noise. This knowledge helps one to zero in on the hardware that may be causing the noise, such as an 1800-rpm motor or pump.

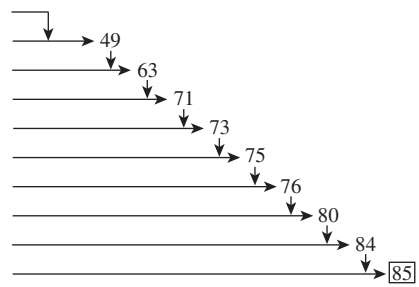
A detailed discussion of measurement issues is beyond scope of this chapter and the reader is urged to use some of the more comprehensive works in the list of references at the end of this chapter. The American Petroleum Institute has issued a recommended practice for measuring noise from fired process heaters.

7.2.2 OVERALL SOUND LEVEL AND HOW TO ADD dB VALUES

Most sounds are composites of several different levels at different frequencies. This is especially true of industrial burner noise. A typical burner noise curve is shown in Figure 7.6. As can be seen, there are significant peaks in two different frequency zones, both of which will contribute to the apparent intensity experienced by a person working in the vicinity of the burner. It is difficult to describe this sound without using either a diagram like the one shown, or a table listing various SPLs occurring in the different octave bands. The *overall sound pressure level*, a single number, has been devised to conveniently represent such composite sound curves. If a single number is to be used to represent the whole curve, then it should adequately represent the peaks in the curve, because the peaks have the most influence on the listener. Consequently, it is not practical to use the average of the various levels in the octave bands, because this number would be less than the levels at the peaks.

TABLE 7.2
Addition Rules

What is the Overall dBA Level?			
Frequency Hz	SPL dB	A-scale CF dB	SPL dBA
31.5	72	-39	33
63	75	-26	49
125	79	-16	63
250	79	-9	70
500	72	-3	69
1000	69	-0	69
2000	68	-1	69
4000	78	-1	79
8000	83	-1	82
16,000	80	-7	73



Notes: Overall sound level = 85 dBA.
Caution: Overall SPL does not = average SPL.

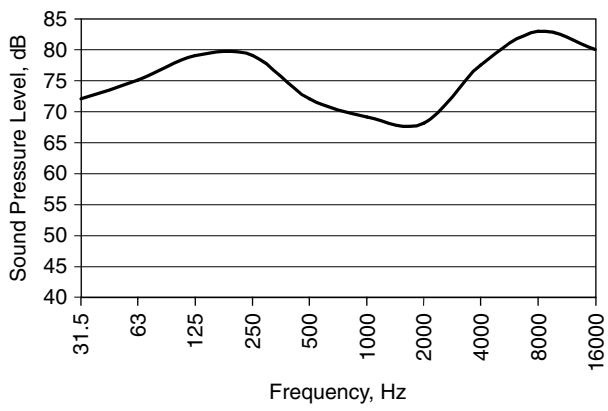


FIGURE 7.6 Typical burner noise curve.

The overall sound pressure level is calculated by adding the individual levels in the various octave bands. In columns 1 and 2 of Table 7.2, the burner sound curve has been split into its component levels in each octave band. In column 3, the A-weighted correction has similarly been split and listed. Column 4 gives the A-scale corrected values for the sound curve by simply subtracting column 3 from column 2. The overall sound pressure level after A-scale correction can now be obtained by adding the values in column 4.

Decibel values cannot be added in a conventional manner due to the influence of the log₁₀ scale. Figure 7.7 shows a chart that can be used to add two dB values. When adding two numbers, first determine the difference between the two numbers. Locate the difference on the x-axis of the chart and determine the corresponding y-axis value and add it to the larger of the two numbers. For numbers that differ by 10 or more, the larger of the two numbers can just be used as the sum because of the decreasing significance in real power level (watts) caused by the log₁₀ scale. It can also be noted that for adding two numbers of equal value, just 3 dB are added. What this translates to is that an increase of 3 dB requires a doubling in the power level.

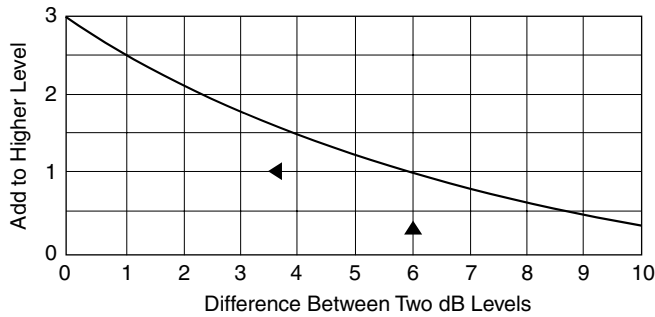


FIGURE 7.7 Graph for adding two dB values.

Alternately, the following formula can be used for dB addition:

$$L_{\text{total}} = 10 \text{ Log}(\sum_{i=1 \text{ to } n} 10^{0.1L_i}) \tag{7.2}$$

where

- L_{total} = overall sound pressure level
- L_i = each individual level
- N = number of levels to be added

And subtraction can be performed using:

$$L_{\text{diff}} = 10 \log(10^{0.1L_2} - 10^{0.1L_1}) \tag{7.3}$$

7.3 CHARACTERISTICS OF SOUND PROPAGATION

There is a great similarity between sound and light. Like light waves, sound waves can be reflected, refracted, diffracted, and diffused.⁵⁻⁷ The only difference between light and sound waves is that the latter cannot be polarized. The material nature of light allows it to be polarized. The following paragraphs present some basic characteristics of sound waves.⁷

7.3.1 ABSORPTION OF SOUND

Hard surfaces such as concrete and metal reflect almost all the sound energy that is incident upon them. However, soft fibrous surfaces, such as slabs of glass fiber or mineral fiber, are poor reflectors and absorb most of the sound energy, converting it into heat as a result of friction that occurs when the sound travels within the small air spaces between the fibers of the material.⁶⁻⁸ The absorption coefficient of a material is used to characterize the fraction of sound energy that is absorbed at the surface of the material. In the following paragraphs the absorption coefficient and the different methods of evaluating it will be discussed in detail. In addition, the factors that influence the absorption coefficient are presented.

7.3.1.1 Absorption Coefficient

The *absorption coefficient* is a material property and is defined as the fraction of incident sound energy absorbed at the surface of the material. The absorption coefficient strongly depends on frequency and varies with the angle of incidence at which the sound strikes the surface. In general, there are two types of absorption coefficients, depending on the direction of the incidence of the sound wave relative to the surface of the material.^{7,9} The normal incidence absorption coefficient is used to characterize the absorption of the sound energy that impinges on the surface in the

normal direction. The random incidence absorption coefficient is used to characterize the absorption of sound energy that impinges on the surface from various directions. Numerically, the random incidence absorption coefficient is larger than the normal incidence absorption coefficient for the same material.

7.3.1.2 Methods of Evaluating Sound Absorption

There are several methods that can be used to measure the absorption coefficient of different materials. Three of these methods are discussed below:⁷

7.3.1.2.1 Reverberation Chamber Method

In this method, a special chamber — a reverberation chamber — is used to perform the measurements. The reverberation chamber is a relatively large room with all surfaces — the walls, ceiling, and floor — being reflective surfaces. The reflective surfaces make the reverberation time of the room very long. The reverberation time is the time taken by the sound pressure level to decrease by 60 dB. After the reverberation time of just the empty room is measured, a piece of the material, for which the absorption coefficient is to be determined, is placed on the floor. Then the reverberation time for the room with the material is measured and the times with and without the specimen are compared. The shorter reverberation time of the room with the specimen is attributed to the absorption of sound by the material and size of the specimen. Comparing the reverberation times of the room with and without the specimen yields the number of absorption units the sample has added to the room. Then the absorption attributed to each square foot of the sample (i.e., the absorption coefficient) can be calculated. Usually, the absorption coefficient is reported for each of the following six frequencies: 125, 250, 500, 1000, 2000, and 4000 Hz.

7.3.1.2.2 Impedance Tube Method

A reverberant chamber is a relatively large room and requires a large piece of the material for the absorption coefficient measurement. An impedance tube, also known as standing-wave tube, is really handy and simple to use to determine the absorption coefficient of a material. It only takes a small piece of the material. The impedance tube is a circular tube with rigid walls and a rigid backing plate at one end. A loudspeaker is mounted at the open end. A slender tube for insertion of the measuring microphone passes through the center of the loudspeaker magnet. The sample is placed close to the backing plate end (either in contact with the plate or with some air gap between material and plate, depending on the intended use of the material). The loudspeaker is fired at different frequencies and for each frequency, the maxima and minima of the corresponding standing wave are determined using the microphone. The ratio of one of the maximum sound pressure to its adjacent minimum sound pressure is used to determine the absorption coefficient of the sample. It is worth noting that the absorption coefficient measured using the impedance tube is the normal incidence absorption coefficient.

7.3.1.2.3 Tone-Burst Method

Another simple and low-cost method for measuring the absorption coefficient at any incidence angle is the tone-burst method. This method allows anechoic chamber measurements to be made in ordinary rooms. Because it takes some time for the unwanted reflection from the walls to reach the measurement location, the tone-burst method utilizes short pulses of sound. A speaker and microphone are placed with some distance (X) between them, and the loudspeaker is fired with a short pulse. The sound pressure level from this short pulse is measured using the microphone. Then, a sample of the material is placed so that the path length of the reflected sound from the sample between the speaker and the microphone is the same as X . A barrier is used to prevent the direct sound path between the speaker and the microphone. Comparing the strength of the reflected pulse to the original direct pulse at distance X , the coefficient of absorption can be determined.

TABLE 7.3
Absorption Coefficients for Some Commonly Used Materials

Material	Octave Band Center Frequency (Hz)					
	125	250	500	1000	2000	4000
Fiber-glass or rock wool blanket						
25 mm thick (typical)	0.18	0.24	0.68	0.85	1.00	1.00
50 mm thick (typical)	0.25	0.83	1.00	1.00	1.00	1.00
Floors						
Wood platform with large space beneath	0.40	0.30	0.20	0.17	0.15	0.10
Concrete or terrazzo	0.01	0.01	0.01	0.02	0.02	0.02
Walls						
Polyurethane foam, 27 kg/m ³ 15-mm thick	0.08	0.22	0.55	0.70	0.85	0.75
Acoustic plaster, 10-mm thick, sprayed on solid wall	0.08	0.15	0.30	0.50	0.60	0.70
Glass, heavy plate	0.18	0.60	0.04	0.03	0.02	0.02
Water	0.01	0.01	0.01	0.015	0.02	0.03

7.3.1.3 Factors Affecting the Absorption Coefficient

There are many factors that influence the absorption coefficient of different materials.⁷⁻⁹ First, the method of mounting the test sample, whether the sample is in contact with the rigid floor of the reverberation room or there is an air gap between them that will affect the measured absorption coefficient. The air gap increases the absorption coefficient of the sample. As mentioned, the absorption coefficient is strongly dependent on frequency and usually is higher at high frequency. Incidence direction is another factor that affects the absorption coefficient. Furthermore, the thickness of the sample also affects the absorption coefficient, but its dependence varies with frequency. The dependence of the absorption coefficient on the density of the material is fairly low except for two extreme cases; namely, very high density and very low density. In both cases, the absorption coefficient is reduced. Table 7.3 gives the absorption coefficients for some commonly used materials.

7.3.2 REFLECTION OF SOUND

When a sound source is activated in an enclosed space, sound travels radially in all directions. As the sound waves encounter obstacles or rigid surfaces, such as walls, their direction of travel is changed (i.e., they are reflected).^{7,9}

7.3.2.1 Reflection from Flat Surfaces

Spherical sound waves that strike a rigid wall will be reflected and return toward the source (see Figure 7.8). As in the case of light on a mirror, the reflected wavefronts act as if they originated from a virtual image of the real sound source, on the other side of the reflecting surface. The image source is located at the same distance behind the wall as the real source is in front of the wall. This is a simple case; that is, a single reflection. In a rectangular enclosed space, there are six surfaces and the source has a virtual image with respect to each of the six surfaces, with the apparent effect of the images sending acoustic energy back to the receiver. In addition, reflected images of the virtual image sources exist and so on, resulting in a more complex situation. It is important to note that, in computing the total sound intensity at a given point, the contribution from all these images must be taken into consideration.⁷

Sound waves are reflected from objects that are large compared to the wavelength of the impinging sound. As a general rule, sound with frequencies of 300 to 400 Hz is best thought of in

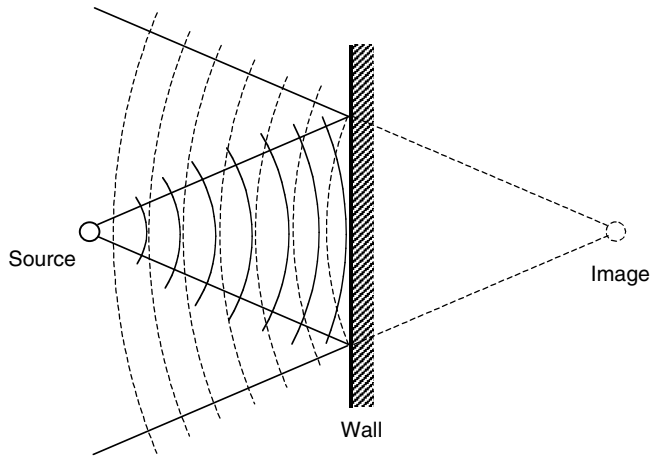


FIGURE 7.8 Reflection of sound from a point source from a flat surface. Incident waves are solid lines and reflected waves are dashed lines. The reflected waves appear to be from a virtual image source.

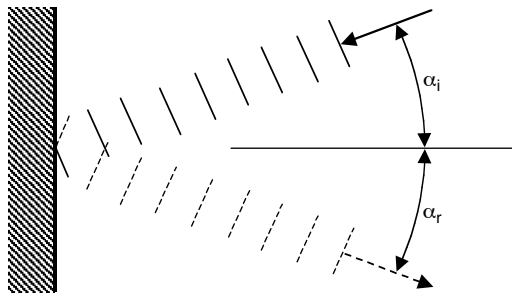


FIGURE 7.9 The angle of incidence α_i is equal to the angle of reflection, α_r .

terms of waves, and sound with frequencies above 300 to 400 Hz is best considered as traveling in rays. When a ray of sound undergoes many reflections as it bounces around an enclosed space with energy being lost at each reflection, the energy loss eventually results in the demise of that ray. Sound reflection follows the same rule as light reflection: the angle of incidence is equal to the angle of reflection^{5,7} (see Figure 7.9).

7.3.2.1.1 Doubling of Pressure at Reflection

Sound pressure on a surface normal to the incident waves is equal to the energy density of the radiation in front of that surface. If the surface is a perfect absorber, the pressure equals the energy density of the incident radiation. On the other hand, if the surface is a perfect reflector, the pressure equals the energy density of both the incident and reflected radiation. Thus, the pressure at the face of a perfectly reflecting surface is twice that of a perfectly absorbing surface. Pressure doubling has more significance in standing waves.

7.3.2.1.2 Reflecting from Convex Surfaces

Sound waves are emitted from a point source as spherical wavefronts and tend to become plane waves when further away from the source.⁷ Reflection of plane wavefronts of sound from a solid convex surface tends to scatter the sound energy in many directions as shown in Figure 7.10 and this effectively diffuses the impinging sound.

FIGURE 7.10 Plane sound waves impinging on a convex surface tend to be dispersed through a wide angle.

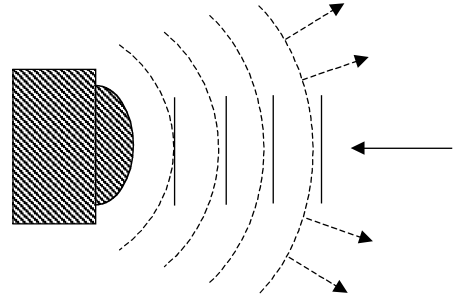


FIGURE 7.11 Plane sound waves impinging on a concave surface tend to be focused if the size of the irregularity is large compared to the wavelength of sound.

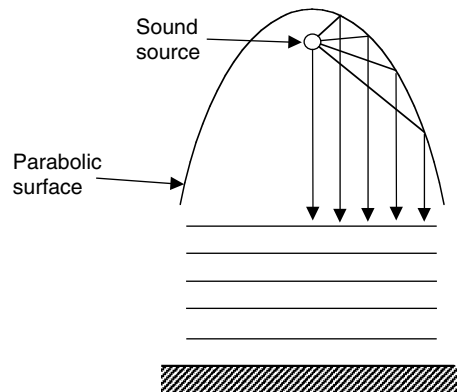
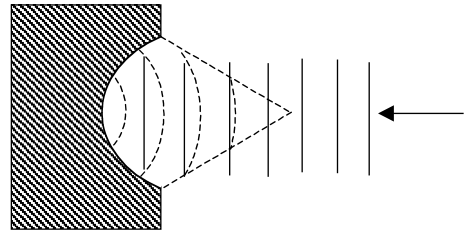


FIGURE 7.12 A parabolic reflector surface can produce plane parallel wavefronts when the sound source is placed at the focal point.

7.3.2.1.3 Reflections from Concave Surfaces

Plane waves of sound when impinging on a concave surface tend to get focused to a point as shown in Figure 7.11. The precision of focusing the sound wave depends on the shape of the concave surface. Spherical surfaces are good examples of concave reflectors. Sometimes, such a reflector is used with a microphone placed at the focal point, in order to make the microphone directional. For a concave surface to be an effective focusing reflector, the size of the reflector has to be larger than the wavelength of the sound to be focused.

7.3.2.1.4 Reflections from Parabolic Surfaces

The parabola has the characteristic of focusing the sound precisely to a point.⁷ The shape of the parabolic surface is generated based on a simple relationship, namely, $y = x^2$. A deep parabolic surface provides much better directional properties than a shallow one. Plane waves striking a parabolic surface would be focused to the focal point as shown in Figure 7.12. Conversely, sound emitted radially from a point source located at the focal point of a parabolic reflector generates plane wavefronts. Lighthouses and searchlights use parabolic mirrors to achieve a straight, low-divergence beam.

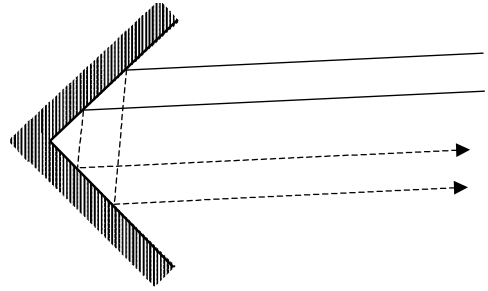


FIGURE 7.13 Sound waves reflected by a 90° corner will always return back in the same direction as the incident wave.



FIGURE 7.14 Large aperture has a very little effect on the plane wavefront that passes through it. Small aperture will turn the plane wavefront that penetrates the hole into a hemispherical wavefront because of the closeness of the new point sources.

7.3.2.1.5 Standing Waves

An important artifact that is a direct result of reflection is the standing wave. When a sound source is located between two parallel walls, sound waves radiated toward the two walls are reflected back. If the distance between the two walls is equal to an integer multiple of half the wavelength of the sound wave, the two waves that travel to the right and to the left will create a standing wave.⁸ This standing wave is stationary, and only sound waves that satisfy the resonance condition (integer multiple of half the wavelength) will establish a standing wave.

7.3.2.1.6 Reflections from Corners

One of the interesting consequences of sound reflection is the reflection from corners. Examine the schematic diagram in [Figure 7.13](#). It can be seen that a sound wave radiated from a source toward a corner will be reflected back to the source. For a corner with 90° , the sound wave is reflected twice and always returns in the direction of the source.⁷

7.3.3 DIFFRACTION OF SOUND

Sound waves travel in straight paths. However, when sound waves encounter an obstruction with certain geometric attributes, they change direction.^{5,7,9} The process by which sound waves change direction is called *diffraction*. The shorter the wavelength, the less is the effect of diffraction. Diffraction can be better explained using Huygens principle, which can be stated as follows: every point on the wavefront of sound that has passed an obstacle or a diffracting edge is considered to be a point source radiating sound energy back into the shadow zone (behind the obstacle).

7.3.3.1 Diffraction of Sound Waves by Large and Small Apertures

When a plane wavefront strikes a wall with an aperture, some of the energy is reflected back by the wall and some of the energy goes through the aperture. If the size of the aperture is larger than the wavelength of the sound, then the wavefront will remain a plane wave with little disturbance (see [Figure 7.14](#)). However, if the aperture size is smaller than the wavelength of the sound, the wavefront of the sound that passes through the aperture will take the form of a hemisphere. The behavior

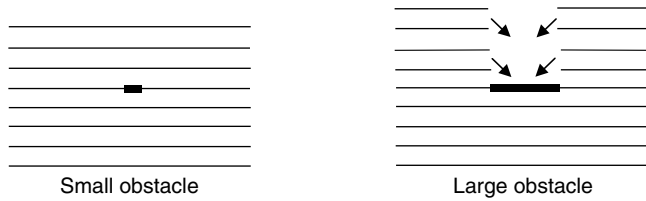


FIGURE 7.15 The small obstacle (relative to the wavelength) has very small effect on the wavefront that passes by the obstacle. The large obstacle (relative to the wavelength) has a definite effect in casting a shadow behind the obstacle.

of the two apertures can be explained with the help of the Huygens principle.⁷ In the case of the large aperture, the new virtual source points on each side of the wavefront are far apart and thus they have little effect on the wavefront; but in case of the small aperture, the new virtual source points are so close to each other that they make the wavefront hemispherical.

7.3.3.2 Diffraction of Sound Waves by Obstacles

When a plane wavefront encounters an obstacle that is small relative to the wavelength of the sound, the wave passes the obstacle with a very small shadow behind the obstacle (see Figure 7.15). In the case of an obstacle that is large with respect to the wavelength of the sound, the obstacle will lead to the generation of a significant acoustic shadow behind the obstacle see Figure 7.15). Again, consulting Huygens principle,⁷ in the case of a small obstacle, the new virtual sources are close and their combined radiation behind the obstacle maintains the plane wavefront. However, in case of the large obstacle, the new virtual sources are far from each other and their radiation behind the obstacle cannot retain the plane wavefront and hence a shadow is cast.

7.3.3.3 Diffraction of Sound Waves by a Slit

A classical experiment conducted with a narrow slit demonstrated that when sound is incident on a narrow slit, the width of the sound beam behind the slit varies inversely with the width of the slit.⁸ Thus, a narrower slit yields correspondingly more diffraction and results in a more divergent sound beam behind the slit, in keeping with the earlier discussion about the formation of a hemispherical wavefront behind a small aperture.

7.3.3.4 Diffraction of Sound by an Acoustic Lens

The acoustic lens consists of a round plate with a set of concentric annular slits.^{5,7} The radii of these slits are such that the paths from the focal point to each slot differ by multiples of $\lambda/2$, where λ is the wavelength of the sound wave (see Figure 7.16). Because these path lengths differ by $\lambda/2$, it means that all the waves will arrive at the focal point at the same time (i.e., in phase) and hence intensify the sound at the focal point.

7.3.4 REFRACTION OF SOUND

Refraction of sound is the mechanism by which the sound wave changes its direction when it propagates from one medium to another medium, when the propagation velocity of sound in the two media is different.⁷ There is a common confusion between diffraction and refraction of sound. Although the similarity of the words may lead to the confusion, the real reason stems from the perceived difficulty in understanding the difference in the two phenomena, because both phenomena

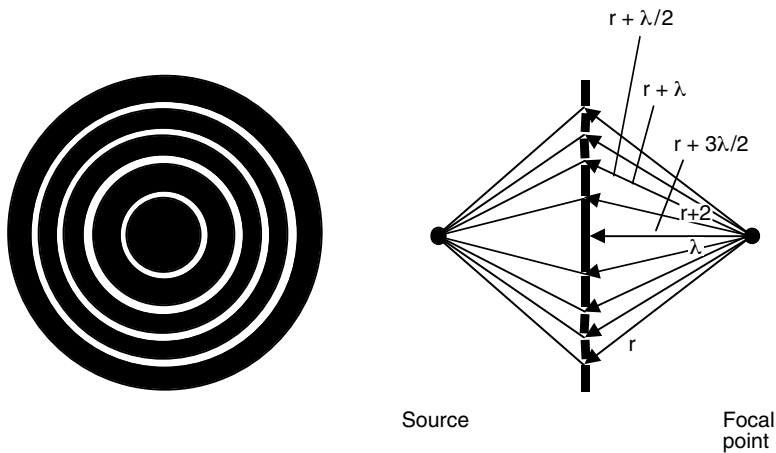


FIGURE 7.16 The slits of the acoustic lens are arranged such that the different path lengths differ by multiples of a half wavelength. Thus, the diffracted sound from all the slits arrive at the focal point in phase.

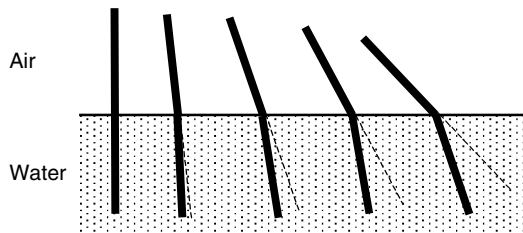


FIGURE 7.17 An immersed stick under water surface demonstrates refraction of light waves. Sound waves are also refracted by changes in the speed of sound in different materials.

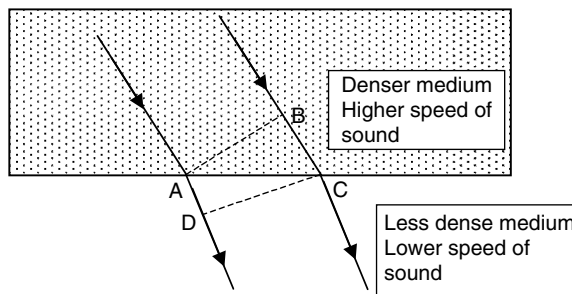


FIGURE 7.18 Sound waves traveling from denser medium.

cause change in the direction of sound waves. A good illustration of refraction is the common observation of the apparent bending of a stick as a part of it is immersed in water (see [Figure 7.17](#)). Of course, this is an illustration of the refraction of light waves.

Sound waves traveling from a denser medium having a certain speed of sound into a less dense medium having a lower speed of sound will result in change of direction of the sound wave; that is, the wavefront AB is not parallel to wavefront DC because of refraction (see [Figure 7.18](#)).

Sound waves exhibit refractive behavior when propagating from a dense solid medium to a less dense medium. The main reason for the refraction is the difference in the speed of sound in

TABLE 7.4
Speed of Sound in Different Media

Medium	Speed of Sound	
	(ft/sec)	(m/sec)
Air	1,130	344
Sea water	4,900	1,500
Wood, fir	12,500	3,800
Steel bar	16,600	5,050
Gypsum board	22,300	6,800

the two media.^{5,7} The speed of sound in the dense solid medium is greater than that in a less dense medium (see Table 7.4) for speed of sound in different media. As illustrated in Figure 7.18, one ray arrives at the boundary between the two media at A while the other ray still has some distance to go. During the time it takes the second ray to travel from B to C, the first ray travels at a slower speed from A to D, a shorter distance, in the new medium. The wavefronts AB and DC represent two different instants in time. The two wavefronts are no longer parallel because the sound has refracted at the interface between two media that have different speeds of sound.

7.3.5 DIFFUSION OF SOUND

When the sound field inside an enclosure meets certain criteria, the sound field is said to be a diffuse field. Physically, the diffuse sound field is a superposition of an infinite number of plane sound waves in which the local sound intensity does not depend on the direction. In a perfectly diffuse sound field, the pressure level is independent of the location. There are six factors that identify whether or not the sound field inside an enclosure is a diffuse sound field.⁷ The first is that the irregularities in the frequency spectrum and in the spatial distribution of the steady-state measurements should be negligible. Second, the beats in the decay characteristics must be negligible. Third, in the decay characteristics, the decay rates must be perfectly exponential; that is, they must be straight lines on a logarithmic scale. Fourth, reverberation time should be the same at all positions in the enclosure. Fifth, the character of the decay must be the same for all frequencies. Sixth and finally, the character of the decay will be independent of the directional characteristics of the microphone.

7.3.5.1 Steady-State Measurements

The frequency response of an enclosure, such as a process furnace, can be obtained by applying a variable frequency signal by means of a loudspeaker and measuring the response of the enclosure using a microphone. Also, the response should be measured at different locations in the enclosure. The typical enclosure frequency response will show some narrow and some wide peaks. The narrow peak is evidence of a single mode, while the wide peak is due to the combined effects of several adjacent modes. These deviations from the flat response of a perfectly diffuse sound field, are evidence of a sound field that is not perfectly diffuse. Also, variations in the enclosure response from one location to another are also evidence of a nondiffuse sound field.

7.3.5.1.1 Decay Beats

The nonsmooth decay response (decay response is explained in the next paragraph) of an enclosure is evidence of nonperfect diffuse sound field. Low frequencies usually exhibit more beats than high frequencies, the reason being that, at low frequencies, the number of resonance modes of enclosure is fewer than at high frequencies. Therefore, the decay at high frequencies is much smoother, resulting from averaging over many resonance modes of the enclosure.

7.3.5.1.2 Exponential Decay

Exponential decay is the characteristic of the impulse response of the enclosure. The impulse response is similar to the steady-state response except that the exciting source is an impulse sound source (a sound source that has enough power throughout the spectrum and is able to deliver a substantial amount of energy in a very short time). In the impulse response test, the impulse source is fired and the enclosure response is measured at different locations for a period of time that ends when the sound pressure level reaches the background level (i.e., all the sound energy from the impulse source has been dissipated by the enclosure). The impulse response of the enclosure is characterized by decay rate or reverberation time. The decay rate is the slope of the plot of sound pressure level vs. time, which is a straight line when the decay is exponential. The reverberation time is the time taken by the sound pressure level to reduce by 60 dB. The decay rate and the reverberation time of an enclosure are related to each other. When the impulse response, sound pressure level vs. time, deviates from being a line, this is evidence of a nonperfect diffuse field. One deviation is known as dual exponential decay, in which the impulse response is characterized by two slopes: a fast decay followed by a slow decay. The slower decay could be due to some modes that encounter low absorption. Another deviation from exponential decay results from the presence of acoustically coupled spaces and is characterized by a concave upward response curve.

7.3.6 SPATIAL UNIFORMITY OF REVERBERATION TIME

The reverberation time of an enclosure should be obtained at different locations in the enclosure. The changes in the reverberation time from one location to another in the enclosure is a sign of deviation from a perfectly diffuse sound field.

7.3.7 DECAY SHAPES

In a perfectly diffuse sound field, the decay character should be the same for all frequencies and the response should be smooth.

7.3.8 MICROPHONE DIRECTIVITY

In a totally homogeneous sound field (perfectly diffuse sound field), a highly directional microphone should register constant signal values irrespective of the direction in which it is pointed.

7.4 SOURCES OF NOISE IN BURNERS

There are four major mechanisms of noise production in burner equipment. They fall into two major categories: high-frequency and low-frequency sources:

1. Low-frequency noise sources:
 - Combustion roar
 - Fan noise
2. High-frequency noise sources:
 - Gas jet noise
 - Piping and valve noise

7.4.1 LOW FREQUENCY: COMBUSTION ROAR

To understand combustion roar, one must consider the mixing process taking place between the fuel and the oxidant on a very small scale. It is known that a well-blended mixture of fuel and oxidant will combust very rapidly if the mixture is within the flammability limits of that fuel.

However, a raw gas fuel stream that depends on turbulence and momentum to mix in the oxidant tends to create a slower combustion process due to the time delay required for mixing. In either case, when regions in the mixing process achieve a flammable mixture and encounter a source of ignition, combustion takes place rapidly.

The speed at which a fuel and oxidant mixture burns depends on the mixture fraction. For example, some hydrocarbons burn most rapidly when the fuel–oxidant mixture is near stoichiometry. The mixture proportion at which the fuel–oxidant mixture burns most rapidly has the maximum flame propagation speed. When combustion occurs at the maximum flame speed, more of the energy release is converted into noise. The rapidly expanding gases in the flame create pressure waves. The rapidly expanding gas pockets behave as acoustic monopoles. That is, they radiate sound very effectively omnidirectionally out from the source. The noise coming from each small region of rapidly combusting mixture adds up to create what we call *combustion roar*. So, combustion roar is largely a function of how rapidly the fuel is being burned. In addition, in the context of burner equipment, usually the larger the fuel flow-rate, the more turbulent the flow in the combustion process. Because turbulence directly influences the mixing rate, high-turbulence processes also produce more combustion roar. Thus, it is more accurate to state that the level of combustion roar generated from a combustion process is a function of the amount of fuel being burned and how rapidly it is burned.

High levels of turbulence in a flame are usually desirable because it helps to reduce the flame length and the tendency to produce smoke. Unfortunately, it increases the combustion roar. The signature of low-frequency combustion roar noise typically consists of a broadband spectrum with a single peak.

A common method for quantifying the *sound pressure level* (SPL) emitted from a burner is to relate the energy released from the combustion of the fuel stream (chemical energy) to the amount of that energy that is converted to noise. The ratio of noise energy released to chemical energy released from the combustion is called the *thermo-acoustic efficiency* (TAE). The TAE typically varies between 1×10^{-9} and 3×10^{-6} . The TAE value largely depends on the turbulent mixing of the fuel with combustion air and is usually determined experimentally.

A burner flame that is highly turbulent may have a TAE on the order of 1×10^{-6} . However, a flame with low levels of turbulence, such as a cigarette lighter, may have a TAE on the order of 1×10^{-9} . For every order of magnitude that the TAE changes, the sound pressure level will change by 10 dB.

Refer back to [Figure 7.6](#) for a plot showing a typical noise spectrum emitted from a burner operating under normal conditions in a furnace. Notice that the noise spectrum has two peak frequencies associated with it. The high-frequency noise contribution is from the fuel gas jets, while the low-frequency contribution is from the combustion roar. Burner combustion roar is associated with a smooth broadband spectrum having relatively low conversion efficiency from chemical energy to noise: in the range of 1×10^{-9} to 1×10^{-6} .

The combustion roar associated with burners can vary in the 200 to 500 Hz range. Burner combustion roar can have a noise spectrum shape and amplitude that can vary with many factors. These factors include the internal shape of the furnace; the design of the burner muffler, plenum, and tile; the acoustic properties of the furnace lining; the transmission of the noise into the fuel supply piping; and the transmissive and reflective characteristics of the furnace walls and stack.

7.4.2 LOW FREQUENCY: FAN NOISE

Fan noise is an issue that impacts burner noise performance in forced-draft systems. The noise emitted from industrial fans typically consists of two noise components: broadband and discrete tones. Vortex shedding from the moving blades and the interaction of the turbulence with the stationary parts of the fan create the broadband noise. This broadband noise is of the dipole type, meaning that the noise is directional. On the other hand, discrete tones are created by the periodic interactions of the rotating blades and nearby upstream and downstream surfaces. Discrete tonal

noise is usually the loudest at the frequency at which a blade passes a given point. The tonal frequency is easily calculated by multiplying the number of blades times the impeller rotation speed in revolutions per second. That is:

$$F = N \times \text{rpm}/60 \quad (7.4)$$

where F is the tonal frequency and N is the number of blades in the impeller.

The broadband and discrete tonal noise emitted from fans can radiate from both the suction and discharge side of a fan and through the fan casing. The noise can radiate downstream through the ducting and discharge into the environment at an outlet, such as a burner. Fan and duct systems should provide means to control this noise if residential areas are located nearby. Installation of mufflers and silencers on the suction and discharge sides of the fan, as well as wrapping the casing and the ducts are common methods of reducing fan noise.

7.4.3 HIGH FREQUENCY: GAS JET NOISE

Gas jet noise is very common in combustion equipment and, in many cases, it can be the dominant source of noise from a burner. The noise that is created when a high-speed gas jet exits into a relatively static ambient gas usually consists of two principal components: gas jet mixing noise and shock-associated noise.

7.4.3.1 Gas Jet Mixing Noise

Studies have shown that a high-speed gas jet, exiting a nozzle, will develop a large-scale orderly pattern as shown in [Figure 7.19](#). This orderly structure is known as the “global instability” or “preferred mode” of the jet. The presence of both the small-scale turbulent eddies within the jet and the large-scale structure is responsible for the gas jet mixing noise.

The source of gas jet mixing noise begins near the nozzle exit and extends several nozzle diameters downstream. Near the nozzle exit, the scale of the turbulent eddies is small and predominantly responsible for the high-frequency component of the jet mixing noise. The lower frequencies are generated further downstream of the nozzle exit where the large-scale orderly pattern of the gas jet exists.

Gas jet mixing creates broadband noise over a range of frequencies. The frequency at which the spectrum peaks depends on several factors, such as the diameter of the nozzle, the Mach number

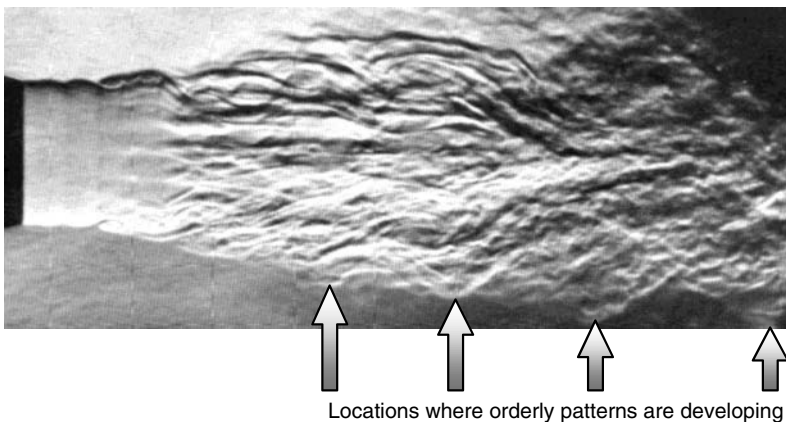


FIGURE 7.19 Development of orderly wave patterns.

of the gas jet, and the angle of observer's position relative to the exit plane of the jet and temperature ratio of the fully expanded jet to the ambient gas.

The maximum overall SPL of gas jet mixing noise occurs at an angle between approximately 15 to 30° relative to the centerline of the gas jet velocity vector. As one moves in either direction from this angle, the noise level can drop off significantly. For example, the overall SPL created by gas jet mixing can be reduced as much as 25 dB when one moves from an angle of maximum noise level to an angle directly behind the nozzle (180° away from the gas jet velocity vector's direction).

7.4.3.2 Shock-Associated Noise

When a burner operates above a certain fuel pressure, a marked change occurs in the structure of the gas jet. Above a certain pressure, called the *critical pressure*, the gas jet develops a structure of shock waves downstream of the nozzle. The critical pressure of a gas jet typically occurs at a pressure of 12 to 15 psig (0.8 to 1 barg), depending on the gas composition and temperature. The structure of shock waves, known as shock cells, consists of compression and expansion waves that repeatedly compress and expand the gas as it moves downstream. Using Schlieren photography, several investigators have seen as many as seven shock cells downstream of a nozzle. These shock cells are responsible for creating two additional components of gas jet noise: screech tones and broadband shock-associated noise.

Screech tones are distinct narrow-band frequency sounds that can be described as a “whistle” or “screech.” The literature reports that these tones are emitted from the fourth and fifth shock cell downstream of the nozzle exit, as shown in Figure 7.20.¹¹ The sound waves from these shock cells propagate upstream where they interact with the shear layer at the nozzle exit. This interaction then creates oscillating instability waves within the gas jet. When these instability waves propagate downstream, they interfere with the fourth and fifth shock cell, causing them to emit the screech tones. Unlike gas jet mixing noise, screech tone noise is not highly directional.

Broadband shock-associated noise occurs when the turbulent eddies within the gas jet pass through shock waves. The shock waves appear to suddenly distort the turbulent eddies, which creates a noise that can range over several octave bands. The broadband shock-associated noise typically peaks at a higher frequency than the screech tone peak frequency.

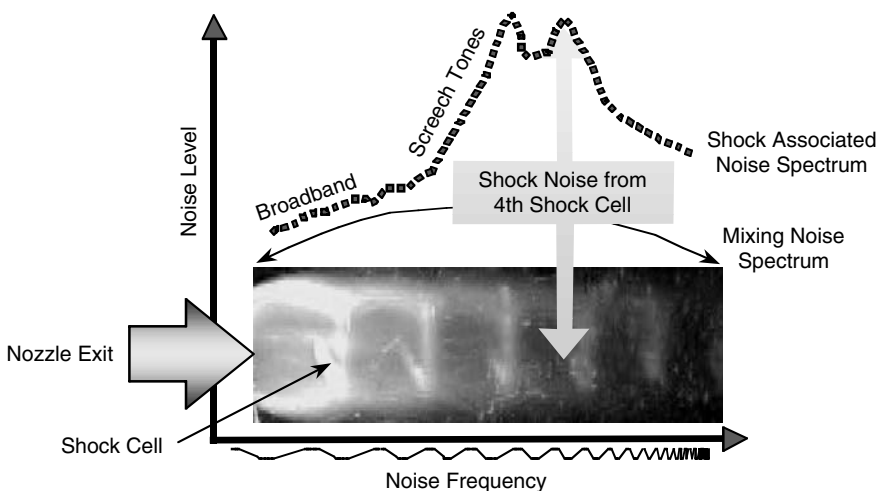


FIGURE 7.20 Location of screech tone emissions.

7.4.4 HIGH FREQUENCY: PIPING AND VALVE NOISE

When a gas flowing steadily in a pipe encounters a valve, a change in the flow pattern and pressure will occur that can create turbulence and shock waves downstream of the valve. Typically, when valves are partially closed, creating a reduction in flow area, the small flow passage behaves much like an orifice and produces jet noise. As discussed, turbulence and shock waves create mixing noise and shock-associated noise. This noise can radiate downstream through the pipe and exhaust into the environment at an outlet and/or radiate through the pipe wall into the space near the valve.

Usually, butterfly valves and ball valves are noisier than globe valves. Butterfly valves and ball valves typically have a smaller vena contracta than a globe valve operating at the same pressure drop, which results in higher levels of mixing and shock-associated noise. As a general guideline, when the pressure ratio across a valve is less than approximately 3, the mixing noise and shock-associated noise are within about the same order of magnitude.¹² With pressure ratios greater than 3, shock noise usually dominates over the mixing noise. There are several methods used for reducing the noise emitted from a valve. These include sound-absorptive wrapping of the pipes and valve casings and the installation of silencers between a valve and the connected pipes.

It should be noted that, just as with the sounding board of a piano or the body of a violin, noise radiation benefits from having a lot of surface area in contact with the source, as is the case with piping. For any sound source of a given power level, the availability of a large radiating surface area will cause the noise to sound louder than if the radiating surface were not available.

7.5 SOUND INSIDE ENCLOSURES

Sound in enclosed space is strongly affected by the reflection from the walls. A sound source in an enclosed space will generate, in general, two kinds of sound fields.⁷⁻¹⁰ The first is the direct sound field, which will dominate the immediate space around the source. The second field is the reverberant field. This field results from the multiple reflection of sound on the walls. It is important to note that the direct sound from the source, once it reflects off a wall, now belongs to the reverberation sound field. One can see that the overall sound pressure level in the cavity is a function of both the direct and reverberant sound fields. Consequently, it is difficult to determine the sound energy distribution and variation with frequency, with precision. Fortunately, there are some approximation and averaging procedures that are accepted and can be used to quantify the sound energy distribution in such sound fields. First, the sound in a reverberant field is divided into two ranges of frequency: low and high frequency.¹⁰ The ratio of the characteristic dimension of the enclosed space to the wavelength of the sound is used to mark, loosely, these two ranges. Usually, a ratio of less than 10 identifies the low-frequency range and a ratio greater than 10 marks the high-frequency range.

7.5.1 LOW-FREQUENCY RANGE

The sound field inside an enclosure in the low-frequency range is mainly governed by the standing waves that have specific characteristic frequencies.⁹ The standing waves occur because the sound travels back and forth in the enclosure due to multiple reflections on the internal surfaces and travel along the same path in opposite directions. At certain frequencies and certain locations, when the waves traveling in opposing directions reach these locations out-of-phase, pressure cancellation occurs and results in a pressure minimum called a *pressure node*. Similarly, when the opposing waves reach these locations in-phase, pressure augmentation occurs and results in a pressure maximum called a *pressure anti-node*. As one would expect, the number of resonance frequencies within a specified frequency band in the low-frequency range is relatively small. Thus, at low frequencies, the response of an enclosure as a function of the frequency and location will be irregular and, in fact, will be characterized by pressure nodes and anti-nodes.

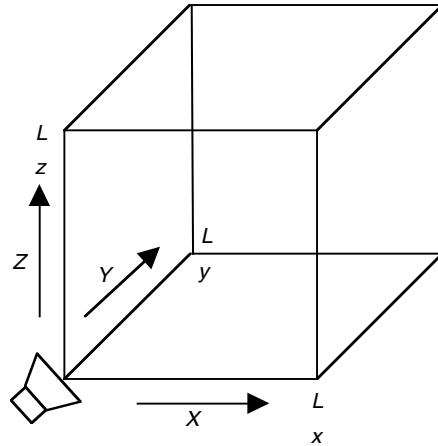


FIGURE 7.21 A schematic diagram for a rectangular enclosure.

Thus far, in the low-frequency range, the dominant response of an enclosure is determined completely by modal response of the enclosed space. It is emphasized that this modal response is by no means unique to rectangular or even other regular-shaped enclosures. In fact, modal response characterizes enclosures of all shapes. It should be understood that irregular or odd numbers of walls will not prevent resonance characterized by nodes and anti-nodes in an enclosure constructed with reasonably reflective inner surfaces.⁹ Also, this peculiar design will not result in a more uniform distribution of the resonance frequencies compared to a regular design of comparable dimensions. The only difference between the regular and irregular design of an enclosure regarding the modal response is the degree of difficulty in computing the frequencies and distributions of these modes. Next, the resonance frequencies of a rectangular enclosure (see Figure 7.21) can be obtained using the following expression:

$$F_n = \frac{c}{2} \sqrt{\left[\frac{n_x}{L_x}\right]^2 + \left[\frac{n_y}{L_y}\right]^2 + \left[\frac{n_z}{L_z}\right]^2} \quad (7.5)$$

where n_x , n_y , and n_z are the particular mode numbers and these numbers can take any positive integer number, including the zero. The subscript n on the frequency is a reference number for each mode, which depends on the mode numbers, and when c is in m/s and L in m the frequency is in hertz (Hz). Spatial and temporal distribution of these normal modes is governed by:

$$p'(x, y, z, t) = p'_o \cos\left[\frac{\pi n_x x}{L_x}\right] \cos\left[\frac{\pi n_y y}{L_y}\right] \cos\left[\frac{\pi n_z z}{L_z}\right] e^{j2\pi F_n t} \quad (7.6)$$

There are three types of normal modes of resonance for an enclosure. These types are categorized according to the corresponding combination of mode numbers, n_x , n_y , n_z , as follows:

1. Axial modes are characterized by only one mode number is nonzero.
2. Tangential modes are characterized by only one mode number is zero.
3. Oblique modes are characterized by no mode number is nonzero.

Consulting Equations (7.5) and (7.6), one can see that axial mode distribution varies in only one direction, and its frequency depends only on the dimension of the rectangular enclosure in that direction, while the tangential mode distribution varies in only two directions, and its frequency depends only on the dimensions of the enclosure in those directions. However, oblique mode varies in all directions, and its frequency depends on all dimensions of the rectangular enclosure. Also, Equation 7.5 shows that as the modes number increases (i.e., in the high-frequency range), the frequencies of the normal modes become much closer to each other than those of the small mode numbers (i.e., in the low-frequency range). That is due to the nature of the square root function in Equation 7.5.

7.5.2 HIGH-FREQUENCY RANGE

In an enclosed space in the high-frequency range, the reverberant sound field can be considered as plane waves propagate in all directions with equal probability.⁸⁻¹⁰ If the mean square amplitude of the acoustic pressure on average is the same in all directions, then the reverberant sound field inside the enclosure is said to be diffuse. This condition for a reverberant sound field to be considered a diffuse sound field can only be achieved in the high-frequency range. That is because in the high-frequency range, the resonance modes are so large that the reverberant sound field approximates uniformity throughout the enclosure. The concept of the diffuse field implies that the net power flow at any given point is negligibly small and that the flow of power is the same in all directions.

7.5.2.1 Effective Intensity in a Diffuse Sound Field

Because the power flow at a given location in a diffuse field is essentially equal in all directions, the intensity at any point in that field is zero. However, an effective intensity in a specified direction characterizing the flow of energy in that direction can be defined.

In a reverberant sound field, consider the sound energy that propagates in a narrow column with a circular cross section, as shown in Figure 7.22. Now let the column encompass a small spherical space in the reverberant field. The ratio of the volume of the spherical region to the

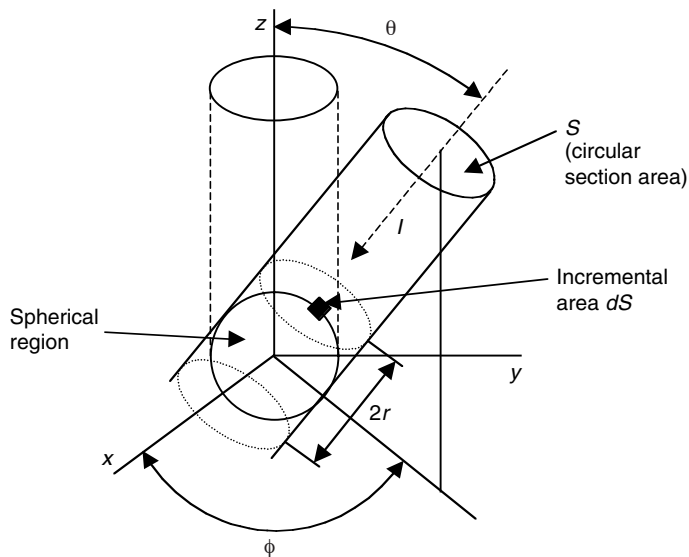


FIGURE 7.22 A schematic for the geometrical illustration for determining the effective intensity in a diffuse sound field.

volume of the cylindrical section of the column that just encloses the spherical region can be obtained as:⁹

$$\frac{4\pi r^3}{3} \cdot \frac{1}{2\pi r^3} = \frac{2}{3} \quad (7.7)$$

That is, the spherical region is occupying two thirds of the volume of the cylinder that encloses it.

In a diffuse sound field, the intensity of the incident beam in any direction would be the same and equal to I (see [Figure 7.22](#)). Now consider a sound beam that has a cross-sectional area S . The time it takes to travel through the spherical region is $2r/c$ (it is the time taken by a sound wave with a propagation speed of c to travel the length of the encompassing cylinder, $2r$). Thus, sound energy in the cylindrical region, E_c due to that beam can be obtained as:

$$E_c = I \cdot S \frac{2r}{c} \quad (7.8)$$

Also, one can compute the sound energy increment contribution from any beam in the spherical region per unit cross-sectional area of the incident beam as:

$$\Delta E = \frac{2}{3} I \frac{2r}{c} \quad (7.9)$$

The incremental area dS of the surface of a sphere with radius r is:

$$dS = r^2 \sin \theta \, d\theta \, d\phi \quad (7.10)$$

Now we can compute the total energy contribution from beams, incident from all directions, in the spherical region by integrating the incremental energy per unit area of the sphere over the whole area of the sphere. Using Equations 7.9 and 7.10, one can obtain the total energy in the spherical region as follows:

$$E = \iint_{\text{Sphere}} \Delta E \cdot dS = \frac{4I}{3c} \int_0^{2\pi} d\phi \int_0^\pi r^3 \sin \theta \, d\theta = \frac{16I\pi r^3}{3c} \quad (7.11)$$

Assume that the energy density at the center of the spherical region is ψ . Then, the total energy in the spherical region can be obtained as:

$$E = \frac{4\pi r^3 \psi}{3} \quad (7.12)$$

Combining Equations 7.11 and 7.12, we can get an expression for the effective intensity I in any direction as a function of the local energy density, ψ :

$$I = \frac{c\psi}{4} \quad (7.13)$$

Now, for a plane wave, it is known that the intensity I_p can be written in terms of the acoustic pressure p' as follows:

$$I_p = \frac{\langle p'^2 \rangle}{(\rho c)} \quad (7.14)$$

where ρ is the mass density of the medium in which the sound is propagating. And an expression for the energy density in terms of the pressure can be obtained:

$$\psi = \frac{\langle p'^2 \rangle}{(\rho c^2)} \quad (7.15)$$

Substituting from Equation 7.15 in Equation 7.13, the effective sound intensity in a diffuse field has the following expression:

$$I = \frac{\langle p'^2 \rangle}{(4\rho c)} \quad (7.16)$$

One can see that if a diffuse sound field has the same intensity as that of a plane sound wave, the acoustic pressure associated with the diffuse field would be, on average, twice that associated with the plane wave. This is consistent with the observation of doubling the acoustic pressure at the face of a perfectly reflective wall.

7.5.2.2 Steady-State Response

In an enclosed space, the acoustic pressure at any point is the combined contribution from both the direct sound field radiated from sound sources and the reverberant field. In general, to get the combined contribution from multiple sound fields, we algebraically add the acoustic energy from each field.¹⁰ Using the notion of directivity D_θ , the acoustic pressure from the direct field at a point, which is located at a distance r from the source, can be computed as:

$$\langle p'^2 \rangle_D = \frac{W_{\rho c} D_\theta}{4\pi r^2} \quad (7.17)$$

where W is the sound power radiated by the source. It is assumed here that the point is indeed in the far field of the source (either r is sufficiently large or the source is sufficiently small). The contribution from the reverberant sound field can be obtained by carrying out sound energy balance. Basically, any sound radiated from the source has to be reflected at least once before it contributes to the reverberant sound field. The fraction of the sound power that enters the reverberant field is $(1 - \bar{\alpha})$, where $\bar{\alpha}$ is the combined absorption and transmission coefficient. By equating the sound power that is added to the reverberant field $(1 - \bar{\alpha})W$ to the sound power absorbed (actually absorbed and transmitted) through the walls while using Equation 7.16 for the sound intensity of the reverberant field, one can get the sound pressure of the reverberant field as:

$$\langle p'^2 \rangle_R = 4W_{\rho c} \frac{(1 - \bar{\alpha})}{\bar{\alpha}S} \quad (7.18)$$

where S is the total area of the enclosed walls. The sound pressure level due to combined effect of the direct and reverberant fields can be written as follows:

$$L_p = L_w + 10 \log_{10} \left\{ \left(\frac{\rho c}{400} \right) \left[\frac{D_\theta}{4\pi r^2} + \frac{4}{R} \right] \right\} \quad (7.19)$$

where $R = \frac{\bar{\alpha}S}{(1-\bar{\alpha})}$ is the constant of the enclosure (room constant). More often, the approximation $\rho c \approx 400$ ($\rho c = 414$ at 20°C) is used to simplify the expression of the sound pressure level to:

$$L_p = L_w + 10 \log_{10} \left[\frac{D_0}{4\pi r^2} + \frac{4}{R} \right] \quad (7.20)$$

One can see in Equation 7.20 that when the enclosure constant R is very small (i.e., the enclosure walls have a low absorption coefficient), the space dominated by the direct field shrinks to a small region around the sound source. On the other hand, with highly absorptive walls, the domain of the dominant direct field expands over a larger region and, at the limit, the enclosure becomes an anechoic enclosure.

7.5.2.3 Transient Response

The reverberation sound field inside an enclosure can be greatly simplified in the high-frequency range. Because the sound field in this frequency range is very close to being a diffuse sound field, it can be described in terms of a simple differential equation.¹⁰ The unsteady sound energy balance in the reverberation field can be formulated as follows: the rate of change of the energy inside the field should equal the rate of supply W_o , less the rate of losses W_a . Thus, one can write this unsteady energy balance as:

$$V \frac{d\psi}{dt} = W_o - W_a = W_o - 0.25\psi Sc\bar{\alpha} \quad (7.21)$$

where V is the volume of the enclosed space and S is the total surface area of the inside walls of the enclosure. A general solution for this first-order differential equation, Equation 7.21 can be written as follows:

$$\psi(t) = \frac{4W_o}{Sc\bar{\alpha}} + g e^{-\frac{Sc\bar{\alpha}}{4V}t} \quad (7.22)$$

where g is a constant to be determined from the initial condition of the energy density in the field. There are two conditions that this solution, Equation 7.22, can be considered. First suppose that initially the sound field was empty; that is, $\psi_o = 0$. Then at time $t = 0$, the sound source is suddenly turned on. Using the initial condition and substituting from Equation 7.15 into Equation 7.22, the response of the sound pressure inside the field can be obtained as follows:

$$\langle p'^2 \rangle = \frac{4W_o\rho c}{S\bar{\alpha}} \left(1 - e^{-\frac{Sc\bar{\alpha}}{4V}t} \right) \quad (7.23)$$

Second, we can consider that the sound field has been established and reached steady state (the sound source is steadily radiating energy to the enclosure). If the the sound source is suddenly turned off, then, at time $t = 0$, the sound power $W_o = 0$; and if the initial sound pressure is $\bar{\alpha}$, Equation 7.22 and Equation 7.29 can be used along with the initial conditions to obtain the following expression for the decaying reverberation sound field:

$$\langle p'^2 \rangle = \langle p_o'^2 \rangle e^{-\frac{Sc\bar{\alpha}}{4V}t} \quad (7.24)$$

or in terms of the sound pressure level:

$$L_{p_o} - L_p = 1.086 \left(\frac{Sc\bar{\alpha}}{V} \right) t \quad (7.25)$$

Equation 7.25 shows that the decay is proportional to the total area of the internal surface of the enclosure, the absorption coefficient, and time, but is inversely proportional to the volume of the enclosure. Now, the reverberation time (T_{60}) is readily calculated from Equation 7.25 as:

$$T_{60} = \frac{55.25 V}{Sc\bar{\alpha}} \quad (7.26)$$

This reverberation time is sometimes called Sabine's reverberation time, referring to the researcher who first introduced it.⁹ The reverberation time obtained in Equation 7.26 is somewhat approximate and that is due to the deviation of the sound field from being a perfectly diffuse field. Another derivation for the reverberation time is based on equal decay rate for all resonance modes of the enclosure. The reverberation time obtained using this approach is:

$$T_{60} = \frac{55.25V}{Sc \log_e (1 - \bar{\alpha}_{st})} \quad (7.27)$$

where $\bar{\alpha}_{st}$ is the statistical absorption coefficient of the internal surface of the enclosure.

7.6 NOISE RADIATION FROM BURNER

Industrial heaters substantially affect the level of the noise that radiates back from the air inlet of the burner (damper section). As discussed in the previous section, the sound field generated by sound sources enclosed in a confined space depends significantly on the acoustic characteristics of the internal surfaces as well as the walls of the enclosure.⁸⁻¹⁰ A burner in a process heater can be represented as a sound source inside an enclosure. Consider a simple process heater, such as the one sketched in Figure 7.23, with a single burner. There are several sound sources associated with the burner, but the major contribution comes from combustion noise and jet noise. In the high-frequency range, the sound field inside the furnace can be considered a diffuse field. For the sake of simplicity, assume that the furnace–burner combination can be represented as a single cavity (multi-cavity considerations will be given later). An acoustic energy balance to obtain the sound pressure immediately on front of the external surface of the enclosure (furnace or burner walls) p'_e can be written as follows:⁹

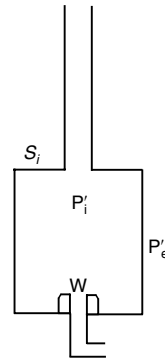


FIGURE 7.23 Schematic diagram for process heater with a single burner.

$$\frac{S_E}{\rho c} \langle p_e'^2 \rangle = W\tau_N + W(1 - \bar{\alpha}_i) \frac{S_E}{\bar{\alpha}_i S_i} \tau \quad (7.28)$$

where S_E and S_i are the external and internal surface areas of the enclosure, respectively; W is the power of all sound sources in the enclosure; τ and τ_N are the average field incidence and normal incidence transmission coefficients of the walls, respectively; and $\bar{\alpha}_i$ is the average absorption coefficient of the internal surface of the enclosure.

Numerically, $\bar{\alpha}_i$ is greater than τ .

7.6.1 MULTIPLE-CAVITY MODEL OF FURNACE-BURNER ACOUSTIC SYSTEM

An acoustic model for the furnace-burner combination will involve more than one cavity. Although all the cavities are physically connected to each other by some passages, dividing the whole internal space into multiple cavities might be required to account for the diverse acoustic properties of the internal surfaces in each cavity. For example, the internal surface of an insulated furnace has a much higher absorption coefficient than that of a burner tile with a hard surface. These cavities interact with each other through the passages that connect them. In the case of a multiple-cavity acoustic system, the whole acoustic model can be derived by applying the single-cavity model on each cavity and then considering the coupling through the interconnecting passages.

7.6.2 EVALUATION OF ACOUSTIC PROPERTIES OF INTERNAL SURFACES AND WALLS

The internal surfaces of the various cavities play an important part in the acoustic model of a furnace burner system. The effective absorption coefficient of the walls is the main property required for the acoustic model. There are many ways to evaluate the absorption coefficient of the internal surface of a cavity.^{10,11} The transient response method is the best-known method for determining the absorption coefficient of the internal surface of a cavity. The different methods of evaluating the absorption coefficient are discussed in the section on the characteristics of sound propagation. Another property required for the acoustic model is the transmission coefficient of the different walls of the cavity. The effective transmission coefficient of a wall composed of different materials can be computed from the individual coefficients of each layer of the wall.

7.6.3 EFFECT OF BACKGROUND NOISE ON BURNER NOISE LEVEL

In addition to combustion equipment, other industrial equipment such as rotating machinery, solids handling equipment, steam traps, and valve actuators emit high levels of noise, contributing to a high background noise level. Background noise creates some challenges in the process of applying noise control. First of all, a noise source that must be measured must have a noise level higher than the background noise level. If the noise source of interest is much lower than the background noise, then it is usually of no concern; but if it is close to the level of the background noise in a given location, it could be a significant contributor that is difficult to measure.

Next, if analysis needs to be performed to identify the noise source's emissions in different frequencies, it should be kept in mind that background noise can mask or provide inaccurate information in frequencies where the noise source's level is comparable to the background noise. The usual approach to tackle background noise interference is to measure close to the noise source such that its noise dominates that of surrounding sources. This may or may not be possible with industrial burners, depending on their proximity to each other and the difference in the noise levels emitted. If the noise from a burner manifests mostly inside the furnace and is poorly transmitted to the exterior of the burner, then the job of identifying, isolating, and measuring the noisy burner becomes more complicated.

It should also be noted that background noise or noise from nearby sources can elevate the noise measured at a given piece of equipment. See next section for an example of the additive effect of nearby noise sources.

7.6.4 NOISE LEVEL DUE TO MULTIPLE BURNERS

Multiple noise sources, such as burners in a furnace, create a higher level of noise than each of the individual sources separately. Of course, this additive effect depends on the number of burners that are within a certain distance of the point of interest. The importance of this effect is that if a certain noise level is to be achieved, say 85 dBA at some distance from the burners, then each individual burner will have to perform at a level lower than 85 dBA to avoid exceeding the limit due to the additive effect.

The following example demonstrates the cumulative effect of noise from neighboring burners using a simple three-burner array. Obviously, having more burners in the array will increase the measured noise, but the impact of the additional burners is reduced proportionately because they are increasingly further away from the point of interest. The formulas shown in the following example take into account the effect of distance and can be used for arrays with any number of sources.

7.6.4.1 Example

A burner manufacturer will typically guarantee a burner noise level at a location 3 ft (1 m) directly in front of the muffler. When several burners are installed in a furnace, however, the noise level 3 ft (1 m) from the burner may be higher than for a single burner due to the noise contribution from surrounding burners. The purpose of this section is to give an example that illustrates the noise level increase due to noise emitted from surrounding burners.

As an illustration, assume a furnace with a simple burner configuration as illustrated in Figure 7.24. If burner B is operating alone and the noise level is 85 dB at location 2, how is the noise level determined at location 2 when all burners are operating? First, find the sound power level L_w emitted from each burner, assuming that the source is emitted at the muffler exit at points 1A, 1B, and 1C. Assume that the noise spreads over a uniform sphere from each of these points. The sound power level can be calculated as follows:

$$L_w = L_p - 10 \log_{10} \left(\frac{1}{4\pi r^2} \right) - 10.5 \quad (7.29)$$

where L_p is the sound pressure level and r is the distance from the source (in feet). The noise level 3 ft (1 m) from burner B (location 2) is 85 dB when it is operating alone. From Equation 7.29 we find that the $L_{wB} = 95.03$ dB. Assuming that all burners are operating at the same conditions, we know that

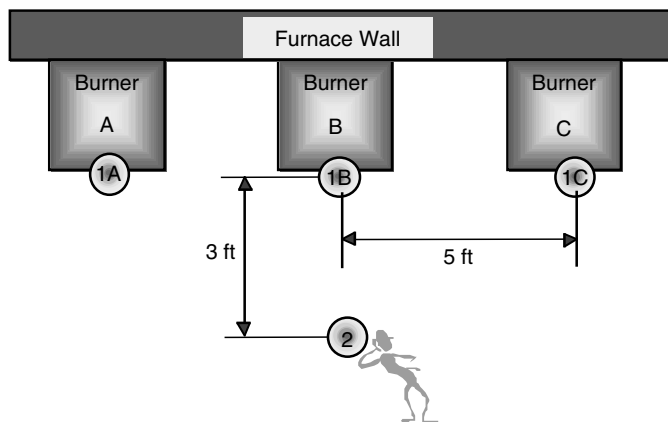


FIGURE 7.24 Burner noise example.

the sound power level must be 95.03 dB for each one. The sound pressure level contribution, L_p can now be calculated at location 2 when burner A is operating alone by solving Equation 7.29 for L_p :

$$L_p = L_w + 10 \log_{10} \left(\frac{1}{4\pi r^2} \right) + 10.5 \quad (7.30)$$

For this case, $L_{wA} = 95.03$ and $r = (5^2 + 3^2)^{0.5} = 5.83$ ft. Substituting these values into Equation 7.30 gives $L_{pA} = 79.2$ dB. This is the sound pressure level contribution emitted from burner A measured at location 2. Because the distance from burner C to location 2 is the same distance away, we know that the sound pressure level contribution from burner C at location 2, L_{pC} , is also 79.2 dB. The total sound pressure level at location 2 can be determined by adding the sound pressure level contribution from each burner (79.2 dB + 79.2 dB + 85 dB). The sound pressure levels can be added by using the following equation:

$$L_{p_{total}} = 10 \log_{10} (10^{L_{pA}/10} + 10^{L_{pB}/10} + 10^{L_{pC}/10}) = 86.8 \text{ dB} \quad (7.31)$$

For this example, the noise level will be approximately 1.6 dB higher when all the burners are operating than if burner B is operating alone.

7.7 NOISE CONTROL AND MUFFLERS

Noise control, obviously, is the desired end result of studying and characterizing noise from industrial burners. Noise control can be implemented either before the fact by including noise control features in the design of the combustion components, or after the fact by applying attenuation devices such as mufflers.

The major requirements that drive the design of industrial burners are, usually, good flame shape and low emissions. The need to achieve good combustion performance usually leaves little opportunity to aggressively design for noise reduction. However, if the opportunity arises, there are certain noise reduction strategies that can be implemented in the design phase.

Jet noise is a major contributor to industrial burner noise and can be addressed at the design phase by using multiple smaller gas orifices instead of one large one. Equation 7.32 gives an empirical relationship between the orifice diameter and the characteristic frequency of the jet noise due to that orifice:

$$F = SU/D \quad (7.32)$$

where F is the characteristic frequency, U is the velocity of the gas jet as it emerges from the orifice, D is the orifice diameter, and S is the struhal number, which is a constant that typically varies between 0.2 and 0.4.

This relationship indicates that as the orifice diameter (the denominator) reduces, the frequency increases. Because gas jet noise produces high-frequency noise, shifting the frequency to a higher realm will tend to move some of the noise out of the audible regime and past the high-frequency threshold of hearing. Figure 7.25 shows the peak noise emissions created by a jet with reference to the threshold of hearing in that range. As the orifice diameter is reduced, the peak shifts to the right and a significant part of the area under the curve is shifted out of the threshold of audibility.

It is also important to note that jet noise, being high-frequency noise, is very directional in nature. That is, the impact of the noise drops off steeply with increasing angle from the axis of the jet. Figure 7.26 shows the decrease in sound pressure level with increasing angular displacement from the axis of the jet. The impact of the directionality of the jet noise is an important parameter

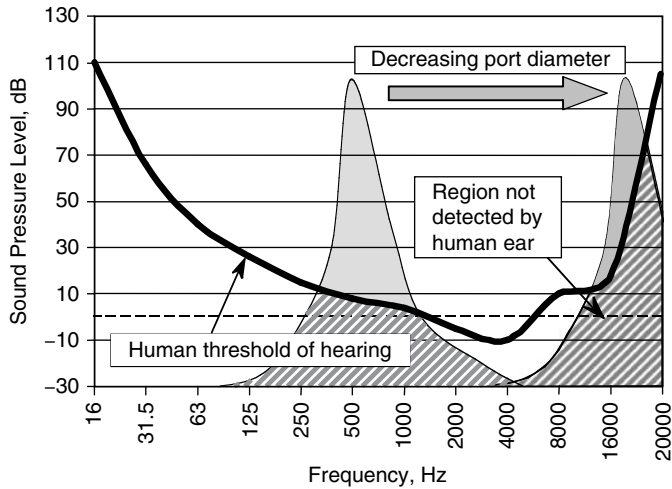


FIGURE 7.25 Threshold of hearing in humans.

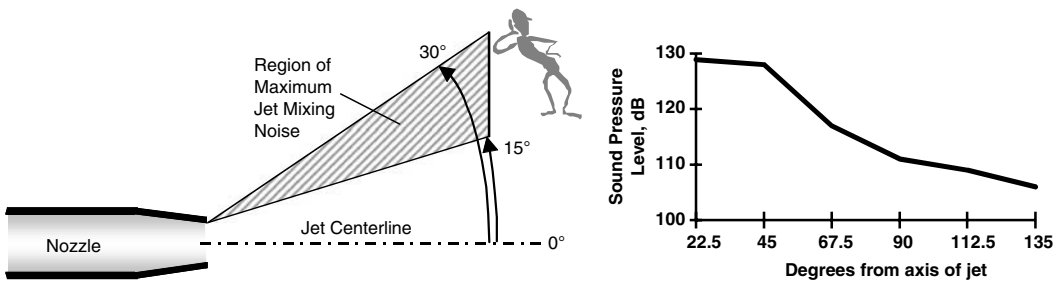


FIGURE 7.26 Region of maximum jet mixing noise and attenuation with angular displacement from axis of jet.

that can be used to reduce noise by introducing convolutions in the air passage to a burner. This use of convolutions or turns to reduce noise is usually implemented in the muffler and air plenum assembly. More information on this is presented further on in the text.

Another mechanism that reduces noise emitted from a flame, specifically combustion noise, is elongation of the flame. That is, when the combustion process is slowed down, either by delayed mixing or by dilution with inerts, the thermo-acoustic efficiency of the flame is reduced. Elongation of the flame or delayed mixing is a technique used to reduce NO_x and so it is typical to find that low-NO_x burners are less noisy than conventional burners. On the other hand, discussion about elongation of the flame is somewhat academic because it is rarely used solely as a noise reduction strategy at the design phase.

The rest of this chapter section is dedicated to discussions about mufflers. Although jet noise can sometimes be controlled through design, most often, the use of a muffler is the main noise control strategy.

A muffler is a barrier and absorber device that attenuates the noise emission from its source.^{8,9} In burner applications, mufflers are needed to meet stringent noise regulations. The muffler, as a barrier, reduces noise by directing and reflecting it away from the listener. Noise reduction in parts of the muffler, such as a bend or the inlet, is achieved through the principles of a barrier. Lined, straight ducts reduce noise by absorption, which is the conversion of acoustic energy into heat by friction in the insulating material, and they are good examples of typical absorbers. Empirical and theoretical models have been developed to predict the attenuation from various types of lined ducts. Designing a muffler to achieve certain noise reduction depends on both the noise source and the

TABLE 7.5
Predicted Octave Band Attenuation for a Rectangular Duct Lined on Two Opposite Sides. Circular or Square Lined Duct on All Four Sides Give Twice the Attenuation Shown Here. Where h is the Half Width of the Airway, and λ is the Sound Wavelength

$2h/\lambda$	0.01	0.02	0.1	0.6	0.9	1.2	2	10
Attenuation rate (dB per h duct length)	0	0	0.06	1.75	2.89	2.83	0.67	0.06

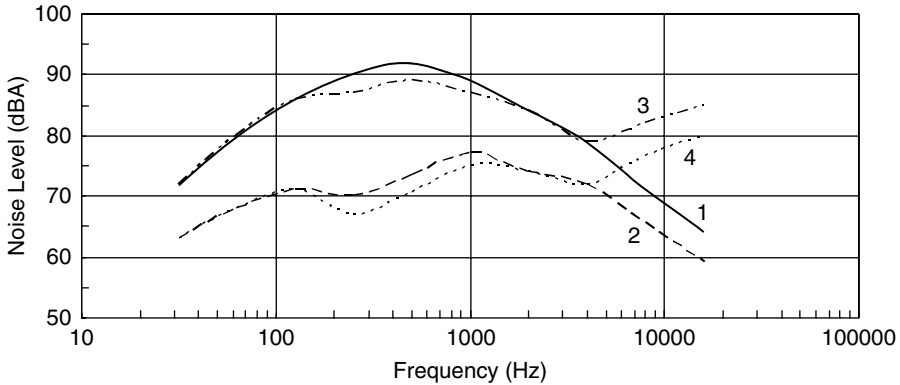


FIGURE 7.27 Noise curves for two burners with the same muffler spectral insertion loss: curve 1 is burner 1 unmuffled with total sound pressure level $L_{p1} = 96.5$ dBA; curve 2 is burner 1 muffled with $L_{p1m} = 81.5$ dBA; curve 3 is burner 2 unmuffled with $L_{p2} = 95$ dBA; and curve 4 is burner 2 muffled with $L_{p2m} = 84$ dBA. The total attenuation for burner 1 is $IL_1 = 15$ dBA, and for burner 2 is $IL_2 = 11$ dBA.

structure of the muffler. The optimal muffler for one noise source may perform poorly with another source. The spectral insertion loss of a muffler, which is the difference between noise levels before and after inserting the muffler in each spectral band, does not depend on the noise spectrum of the noise source. However, the total noise attenuation of the muffler strongly depends on the noise spectrum of the source (see the illustrative example in Figure 7.27). In the example, the overall sound pressure level for burner 1 is 96.5 dBA (curve 1), and for burner 2 is 95 dBA (curve 3); and after inserting the same muffler, the sound pressure level for burner 1 is 81.5 dBA (curve 2) and for burner 2 is 84 dBA (curve 4). Although burner 1 has higher noise, the muffler attenuation in the case of burner 1 (15 dBA) is higher than that of burner 2 (11 dBA). For example, if the muffler was designed to achieve a sound level of 82 dBA when used with burner 1, the muffler cannot achieve the same sound level with burner 2, although burner 2 has a lower sound level than burner 1.

The literature provides some theoretical models that can predict the rate of noise attenuation in straight lined ducts.^{8,9} The rate of attenuation depends on how the sound interacts with the acoustic insulation material, both locally reacting and in a bulk mode. In the local reacting regime, the sound is prevented from propagating in the material in any direction other than normal to the surface by some rigid partitions. In the bulk reacting regime, the sound can propagate in the liner parallel to the surface, and this is more practical to use. Table 7.5 shows predictions for the rate of noise attenuation in a straight duct that is lined on two opposite sides when the liner thickness is equal to one-quarter of the half-width of the airway.⁹ The attenuation rate depends on the nondimensional frequency $2h/\lambda$, the nondimensional liner thickness l/h , and the nondimensional resistance of the liner $R_l l/\rho c$, where h is the half-width of the airway, l is the liner thickness, λ is the wavelength of the sound wave, c is the speed of sound in the duct, ρ is the density of fluid flowing in the duct, and R_l is the liner flow resistivity.

The noise reduction contribution from a bend has been identified in the literature from empirical information. The correction for the bend depends on the condition of the sound that is propagating in the bend as well as the bend configuration. Some of the empirical data that has been reported in the literature⁹ for different bend configurations and sound wave inputs it has been shown that the largest bend attenuation is for the case of a rectangular lined duct and axial plane wave input. A plane wave can result in practical applications because diffuse sound that propagates for some length along the lined duct before it hits the bend, resembles a plane wave. Correction for attenuation for the case of lined duct with rectangular cross-section and diffuse input sound is given in Table 7.6. Experimental evaluations conducted by the authors also indicate a similar contribution by a bend.

Empirical data has been reported in the literature for the duct inlet correction. Because part of the sound is absorbed by the lining, sound that reflects at the wall will be more quickly attenuated than sound that passes at grazing incidence. Thus, sound at all angles of incidence at the entrance to a duct will very rapidly attenuate, until only the portion that is propagating axially remains. It has been determined that such an effect may introduce additional attenuation, the inlet correction. Table 7.7 shows that the inlet correction depends on a nondimensional frequency $S^{0.5}/\lambda$, where S is the cross-sectional area of the duct and λ is the sound wavelength.⁹ Figure 7.28 also shows that the inlet correction is more effective at high frequencies.

Exit loss has been also reported in the literature, and it has been attributed to the sudden change of cross section at the end of a duct flush mounted with a wall or ceiling. Exit loss that has been measured for circular and rectangular ducts in the literature¹⁰ is shown in Figure 7.28. One can see that the attenuation is greater in the low frequency range.

TABLE 7.6
Correction for Attenuation at a 90° Bend with Rectangular Lined Duct and Diffuse Input Sound. S is the Duct Cross-Sectional Area, and λ is the Sound Wavelength

$S^{0.5}/\lambda$	0.1	0.2	0.4	0.6	0.8	1	2	4
Bend Correction (dB)	0	0.667	0.667	11	11.3	11	10	10

TABLE 7.7
Duct Inlet Correction for Random-Incidence Sound. S is the Duct Cross-Sectional Area, and λ is the Sound Wavelength

$S^{0.5}/\lambda$	0.1	0.2	0.4	0.6	0.8	1	2	4
Bend Correction (dB)	0	3	6.834	8.834	9.5	9.8	10	10

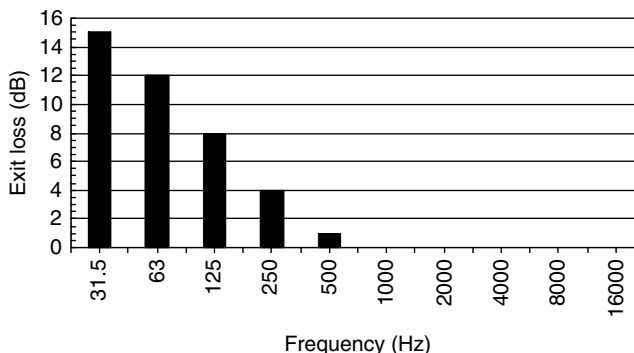


FIGURE 7.28 Exit for rectangular duct size of 0.06 m². Empirical data.

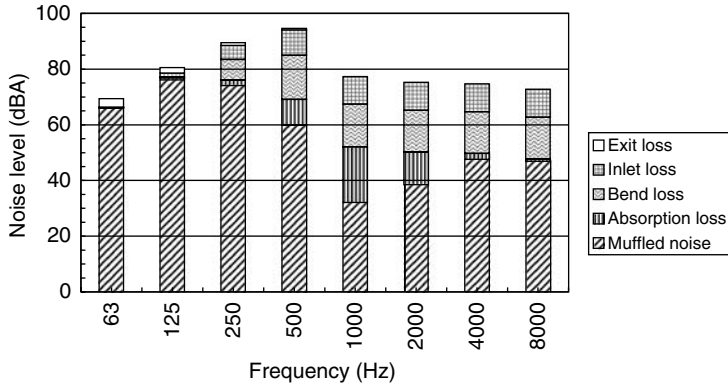


FIGURE 7.29 Insertion loss of a duct muffler with a single bend. The unmuffled noise level is 96 dBA and the muffler insertion loss is 17.5 dB.

7.7.1 EVALUATION OF MUFFLER INSERTION LOSS

Once the configuration and dimensions of a muffler are known, evaluation of the muffler insertion loss (which is the noise reduction due to the muffler insertion) is straightforward. An example of how insertion loss can be determined is shown in Figure 7.29. In this figure, the unmuffled noise in each octave band is at the top value of the column that corresponds to the octave band. To arrive at the muffled noise level—and hence the insertion loss of the muffler’s absorption—bend, inlet, and exit losses must be subtracted from the unmuffled noise level in each octave band. First, the absorption loss can be computed using the width and length of each straight part of the duct as well as the thickness of the insulation. The computation of the absorption loss can be done using Table 7.5. Second, the bend loss for each bend can be determined using the cross-sectional area of the bend and Table 7.6. Third, the inlet loss can be obtained using Table 7.7 and the cross-sectional area of the inlet. Fourth, the exit loss can be obtained using Table 7.6 and the cross-sectional area of the exit. In this example, the unmuffled noise level is 96 dBA and the muffled noise level is 78.5 dBA, making the total muffler insertion loss 17.5 dB.

7.7.2 ITERATIVE DESIGN OF MUFFLERS

Any muffler configuration involves a large number of dimensions, so muffler design is somewhat iterative in nature. Starting by satisfying the constraints that are imposed on the muffler, such as pressure drop and certain dimensional limitations, one can arrive at a rough design for the muffler configuration. Then, by computing the muffled noise level for this configuration, an iterative process can be started where the other dimensions are varied until the required noise level is achieved. It may take three to five trials to reach the final design. In general, as with any design work, the larger the number of constraints imposed on the muffler performance, the more difficult will it be to accomplish the design, and a larger number of trials will be needed.

7.8 GLOSSARY

Absorption: Conversion of sound energy into another form of energy, usually heat, when passing through an acoustical medium.

Absorption coefficient: Ratio of sound absorbing effectiveness, at a specific frequency, of a unit area of acoustical absorbent to a unit area of perfectly absorptive material.

Acoustics: Science of the production, control, transmission, reception, and effects of sound and of the phenomenon of hearing.

Ambient noise: All-pervasive noise associated with a given environment.

Anechoic room: Room whose boundaries effectively absorb all incident sound over the frequency range of interest, thereby creating essentially free field conditions.

Audibility threshold: Sound pressure level, for a specified frequency, at which persons with normal hearing begin to respond.

Background noise: Ambient noise level above which signals must be presented or noise sources measured.

Decibel scale: Linear numbering scale used to define a logarithmic amplitude scale, thereby compressing a wide range of amplitude values to a small set of numbers.

Diffraction: Scattering of radiation at an object smaller than one wavelength and the subsequent interference of the scattered wavefronts.

Diffuse field: Sound field in which the sound pressure level is the same everywhere and the flow of energy is equally probable in all directions.

Diffuse sound: Sound that is completely random in phase; sound which appears to have no single source.

Directivity factor: Ratio of the mean-square pressure (or intensity) on the axis of a transducer at a certain distance to the mean-square pressure (or intensity) that a spherical source radiating the same power would produce at that point.

Far field: The part of the sound field in which sound pressure varies inversely with distance from the source. This corresponds to a reduction of approximately 6 dB in level for each doubling of distance.

Free field: An environment in which there are no reflective surfaces within the frequency region of interest.

Hearing loss: An increase in the threshold of audibility due to disease, injury, age, or exposure to intense noise.

Hertz (Hz): Unit of frequency measurement, representing cycles per second (cps).

Infrasound: Sound at frequencies below the audible range (i.e., below about 16 Hz).

Isolation: Resistance to the transmission of sound by materials and structures.

Loudness: Subjective impression of the intensity of a sound.

Masking: Process by which the threshold of audibility of one sound is raised by the presence of another (masking) sound.

Near field: That part of a sound field, usually within about two wavelengths from a noise source, where there is no simple relationship between sound level and distance.

Noise emission level: dB(A) level measured at a specified distance and direction from a noise source, in an open environment, above a specified type of surface. Generally follows the recommendation of a national or industry standard.

Noise reduction coefficient (NRC): Arithmetic average of the sound absorption coefficients of a material at 250, 500, 1000, and 2000 Hz.

Phon: Loudness level of a sound, numerically equal to the sound pressure level of a 1-kHz free progressive wave, which is judged by reliable listeners to be as loud as the unknown sound.

Pink noise: Broadband noise whose energy content is inversely proportional to frequency (−3 dB per octave or −10 dB per decade).

Power spectrum level: Level of the power in a band 1 Hz wide referred to a given reference power.

Reverberation: Persistence of sound in an enclosure after a sound source has been stopped. Reverberation time is the time (in seconds) required for sound pressure at a specific frequency to decay 60 dB after a sound source is stopped.

Root mean square (RMS): The square root of the arithmetic average of a set of squared instantaneous values.

Sabine: Measure of sound absorption of a surface; 1 metric sabine is equivalent to 1 m² of perfectly absorptive surface.

Sound: Energy that is transmitted by pressure waves in air or other materials and is the objective cause of the sensation of hearing. Commonly called noise if it is unwanted.

Sound intensity: Rate of sound energy transmission per unit area in a specified direction.

Sound level: Level of sound measured with a sound level meter and one of its weighting networks. When A-weighting is used, the sound level is given in dB(A).

Sound level meter: An electronic instrument for measuring the RMS of sound in accordance with an accepted national or international standard.

Sound power: Total sound energy radiated by a source per unit time.

Sound power level: Fundamental measure of sound power defined as

$$L_w = 10 \log \frac{P}{P_0} \text{ dB}$$

where P is the RMS value of sound power in watts, and P_0 is 1×10^{-12} W.

Sound pressure: Dynamic variation in atmospheric pressure. The pressure at a point in space minus the static pressure at that point.

Sound pressure level: Fundamental measure of sound pressure defined as

$$L_p = 20 \log \frac{P}{P_0} \text{ dB}$$

where P is the RMS value (unless otherwise stated) of sound pressure in pascals, and P_0 is 20 μ Pa.

Sound transmission loss: Ratio of the sound energy emitted by an acoustical material or structure to the energy incident upon the opposite side.

Standing wave: A periodic wave having a fixed distribution in space that is the result of interference of progressive waves of the same frequency and kind. Characterized by the existence of maxima and minima amplitudes that are fixed in space.

Thermo-acoustic efficiency: A value used to characterize the amount of combustion noise emitted from a flame. Defined as the ratio of the acoustical power emitted from the flame to the total heat release of the flame.

Ultrasound: Sound at frequencies above the audible range (i.e., above about 20 kHz).

Wavelength: Distance measured perpendicular to the wavefront in the direction of propagation between two successive points in the wave, which are separated by one period. Equals the ratio of the speed of sound in the medium to the fundamental frequency.

Weighting network: An electronic filter in a sound level meter that approximates, under defined conditions, the frequency response of the human ear. The A-weighting network is most commonly used.

White noise: Broadband noise having constant energy per unit of frequency.

REFERENCES

1. Ungar, E.E., Acoustics from A to Z, *Sound and Vibration 35th Anniversary Issue*, January 2002.
2. Hirschorn, M., *Noise Control Reference Handbook*, Industrial Acoustic Company, New York, 1982.
3. Rayleigh, J.W.S., *The Theory of Sound, second edition, Vol. 1*, Dover Publications Inc., 1945.
4. Baukal, C.E., Jr., Ed., *The John Zink Combustion Handbook*, CRC Press, Boca Raton, FL, 2001.
5. Morse, P.M. and Ingard, K.U., *Theoretical Acoustics*, McGraw-Hill, New York, 1986.
6. Everest, F.A., *The Master Handbook of Acoustics*, McGraw-Hill, New York, 1994.
7. Peters, R.J., *The Noise & Acoustics Monitoring Handbook*, Coxmoor Publishing Company, Oxford, U.K., 2002.
8. Beranek, L.L. and Ver, I.L., *Noise and Vibration Control Engineering, Principles and Applications*, John Wiley & Sons, New York, 1992.

9. Bies, D.A. and Hansen, C.H., *Engineering Noise Control, Theory and Practice*, E & FN Spon, New York, 1998.
10. Beranek, L.L., *Acoustics*, Acoustical Society of America, New York, 1996.
11. Shen H. and Tam, C.K.W., Numerical simulation of the generation of axisymmetric mode jet screech tones, *AIAA Journal*, 36(10), 1801, 1998.
12. Beranek, L.L., *Noise and Vibration Control*, McGraw-Hill, New York, 1971.

8 Combustion Controls

Joe Gifford and Zachary Kodesh, P.E.

CONTENTS

- 8.1 Fundamentals
 - 8.1.1 Control Platforms
 - 8.1.1.1 Relay System
 - 8.1.1.2 Burner Controller
 - 8.1.1.3 Programmable Logic Controller (PLC)
 - 8.1.1.4 Distributed Control System (DCS)
 - 8.1.1.5 Hybrid Systems
 - 8.1.1.6 Future Systems
 - 8.1.2 Discrete Control Systems
 - 8.1.3 Analog Control Systems
 - 8.1.4 Failure Modes
 - 8.1.5 Agency Approvals and Safety
 - 8.1.5.1 Double-Block-and-Bleed for Fuel Supply
 - 8.1.5.2 Unsatisfactory Parameter System Shutdown
 - 8.1.5.3 Local Reset Required after System Shutdown
 - 8.1.5.4 Watchdog Timer to Verify PLC Operation
 - 8.1.6 Pipe Racks and Control Panels
- 8.2 Primary Measurement
 - 8.2.1 Discrete Devices
 - 8.2.1.1 Annunciators
 - 8.2.1.2 Pressure Switches
 - 8.2.1.3 Position Switches
 - 8.2.1.4 Temperature Switches
 - 8.2.1.5 Flow Switches
 - 8.2.1.6 Run Indicators
 - 8.2.1.7 Flame Scanners
 - 8.2.1.8 Solenoid Valves
 - 8.2.1.9 Ignition Transformers
 - 8.2.2 Analog Devices
 - 8.2.2.1 Control Valves
 - 8.2.2.2 Thermocouples
 - 8.2.2.3 Velocity Thermocouples
 - 8.2.2.4 Resistance Temperature Detectors (RTDs)
 - 8.2.2.5 Pressure Transmitters
 - 8.2.2.6 Flow Meters
 - 8.2.2.7 Analytical Instruments
- 8.3 Control Schemes
 - 8.3.1 Parallel Positioning

- 8.3.1.1 Mechanical Linkage
- 8.3.1.2 Electronically Linked
- 8.3.1.3 Characterizer Calculations
- 8.3.2 Fully Metered Cross Limiting
- 8.4 Controllers
- 8.5 Tuning
- References

8.1 FUNDAMENTALS

This chapter discusses various control system components, concepts, and philosophies necessary for understanding how control systems work, what the systems are designed to accomplish, and what criteria the controls engineer uses to design and implement a system. The interested reader can find further information on controls in numerous references.¹⁻¹⁰ The American Petroleum Institute has issued a recommended practice concerning instrumentation and control for fired heaters and steam generators.^{11,12}

The purpose of the control system is to start, operate, and shut down the combustion process and any related auxiliary processes safely, reliably, and efficiently. The control system consists of various physical and logical components chosen and assembled according to a control philosophy and arranged to provide the user with an informative, consistent, and easy-to-use interface.

A combustion system typically includes a fuel supply, a combustion air supply, and an ignition system, all of which come together at one or more burners. During system start-up and at various times during normal operation, the control system will need to verify or change the status of these systems. During system operation, the control system will need various items of process information to optimize system efficiency. Additionally, the control system monitors all safety parameters at all times and will shut down the combustion system if any of the safety limits are not satisfied.

8.1.1 CONTROL PLATFORMS

The control platform is the set of devices that monitors and optimizes the process conditions, executes the control logic, and controls the status of the combustion system. There are several different types of platforms and several different ways that the tasks mentioned above are divided among the types of platforms. Following is a list and a brief description of the most commonly used platforms.

8.1.1.1 Relay System

A relay consists of an electromagnetic coil and several attached switch contacts that open or close when the coil is energized or de-energized. A relay system consists of a number of relays wired together in such a way that they execute a logical sequence. For example, a relay system may define a series of steps to start up the combustion process. Relays can tell only if something is on or off and have no analog capability. They are generally located in a local control panel.

Relays have several advantages. They are simple, easily tested, reliable, and well-understood devices that can be wired together to make surprisingly complex systems. They are modular, easily replaced, and inexpensive. They can be configured in fail-safe mode so that if the relay itself fails, combustion system safety is not compromised.

There are also a few disadvantages of relays. Once a certain complexity level is reached, relay systems can quickly become massive. Although individual relays are very reliable, a large control system with hundreds of relays can be very unreliable. Relays also take up a lot of expensive control panel space. Because relays must be physically rewired to change the operating sequence, system flexibility is poor.

8.1.1.2 Burner Controller

A variety of burner controllers is available from several different vendors. They are prepackaged, hardwired devices in different configurations to operate different types of systems. A burner controller will execute a defined sequence and monitor defined safety parameters. They are generally located in a local control panel. Like relays, they generally have no analog capability.

Advantages of burner controllers include the fact that they are generally inexpensive, compact, simple to hook up, require no programming, and are fail-safe and very reliable. They are often approved for combustion service by various safety agencies and insurance companies.

There are also some disadvantages. Burner controllers cannot control combustion systems of much complexity. System flexibility is nonexistent. If it becomes necessary to change the operating sequence, the controller must be rewired or replaced with a different unit. Controllers also require the use of attached peripherals from the same vendor, so some design flexibility is lost.

8.1.1.3 Programmable Logic Controller (PLC)

A programmable logic controller (PLC) is a small, modular computer system that consists of a processing unit and a number of input and output modules that provide the interface to the combustion components. PLCs are usually rack-mounted, and modules can be added or changed (see Figure 8.1). There are many types of modules available. Unlike the relays and burner controllers above, they have analog control capability. They are generally located in a local control panel.

PLCs have the advantage of being a mature technology. They have been available for more than 20 years. Simple PLCs are inexpensive and PLC prices are generally very competitive. They are compact, relatively easy to hook up, and, because they are programmable, they are supremely flexible. They can operate systems of almost any complexity level. PLC reliability has improved over the years and is now very good.

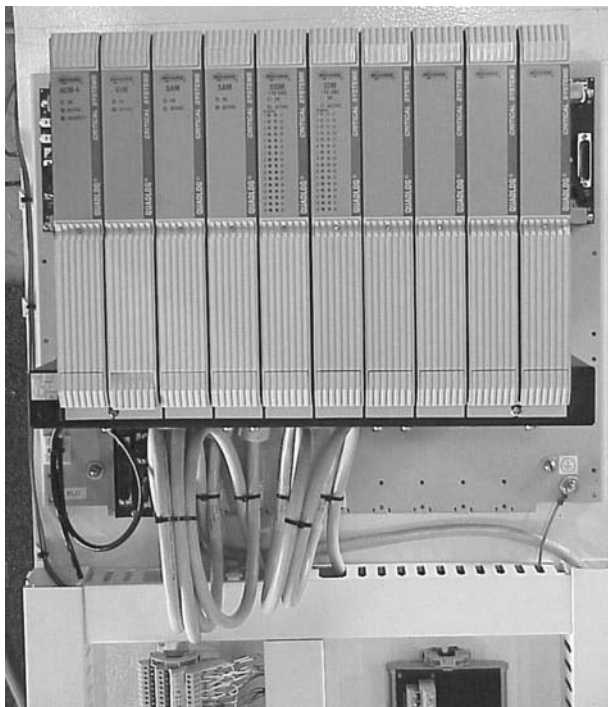


FIGURE 8.1 Programmable logic controller.

Disadvantages of PLCs include having to write software for the controller. Coding can be complex and creates the possibility of making a programming mistake, which can compromise system safety. The PLC can also freeze up, much like a desktop computer freezes up, where all inputs and outputs are ignored and the system must be reset in order to execute logic again. Because of this possibility, standard PLCs should never be used as a primary safety device. Special types of redundant or fault-tolerant PLCs are available that are more robust and generally accepted for this service, but they are very expensive and generally difficult to implement.

8.1.1.4 Distributed Control System (DCS)

A distributed control system (DCS) is a larger computer system that can consist of a number of processing units and a wide variety of input and output interface devices. Unlike the other systems described above, when properly sized, a DCS can also control multiple systems and even entire plants. The DCS is generally located in a remote control room, but peripheral elements can be located almost anywhere.

DCSs have been around long enough to be a mature technology and are generally well-understood. They are highly flexible and are used for both analog and discrete (on-off) control. They can operate systems of almost any level of complexity and their reliability is excellent.

However, DCSs are often difficult to program. Each DCS vendor has a proprietary system architecture, so the hardware is expensive and the software is often different from any other vendor's software. Once a commitment is made to a particular DCS vendor, it is extremely difficult to change to a different one.

8.1.1.5 Hybrid Systems

If you could combine several of the systems listed above and build a hybrid control system, the advantages of each system could be exploited. In practice, that is what is usually done. A typical system uses relays to perform the safety monitoring, a PLC to do the sequencing, and either dedicated controllers or an existing DCS for the analog systems control. Sometimes, the DCS does both the sequencing and the analog systems control, and the safety monitoring is done by a fault-tolerant logic system. Most approval agencies and insurers require the safety monitoring function to be separate from either of the other functions.

8.1.1.6 Future Systems

Over the next decade or so, it is expected that embedded industrial microprocessors using touch-screen video interfaces (see [Figure 8.2](#)) will start to appear in combustion control. The interfaces will communicate with field devices such as valves and switches via a single communications cable. They will use a digital bus protocol such as Profibus or Fieldbus. These systems are becoming common on factory floors around the world. Because establishment of a single standard has not yet happened and combustion standards are slow to change, these systems have not yet achieved widespread acceptance in the combustion world.

8.1.2 DISCRETE CONTROL SYSTEMS

The world of discrete controls is black and white. Is the valve open or shut? Is the switch on or off? Is the button pressed or not pressed? Is the blower running or not running? There are two basic types of discrete devices: (1) input devices (sensors) that have electrical contacts that open or close, depending on the status of what is being monitored; and (2) output devices, or final elements, that are turned on or off by the control system.

In a typical control system, sensors such as pressure switches, valve position switches, flame scanners, and temperature switches do all of the safety and sequence monitoring. These devices

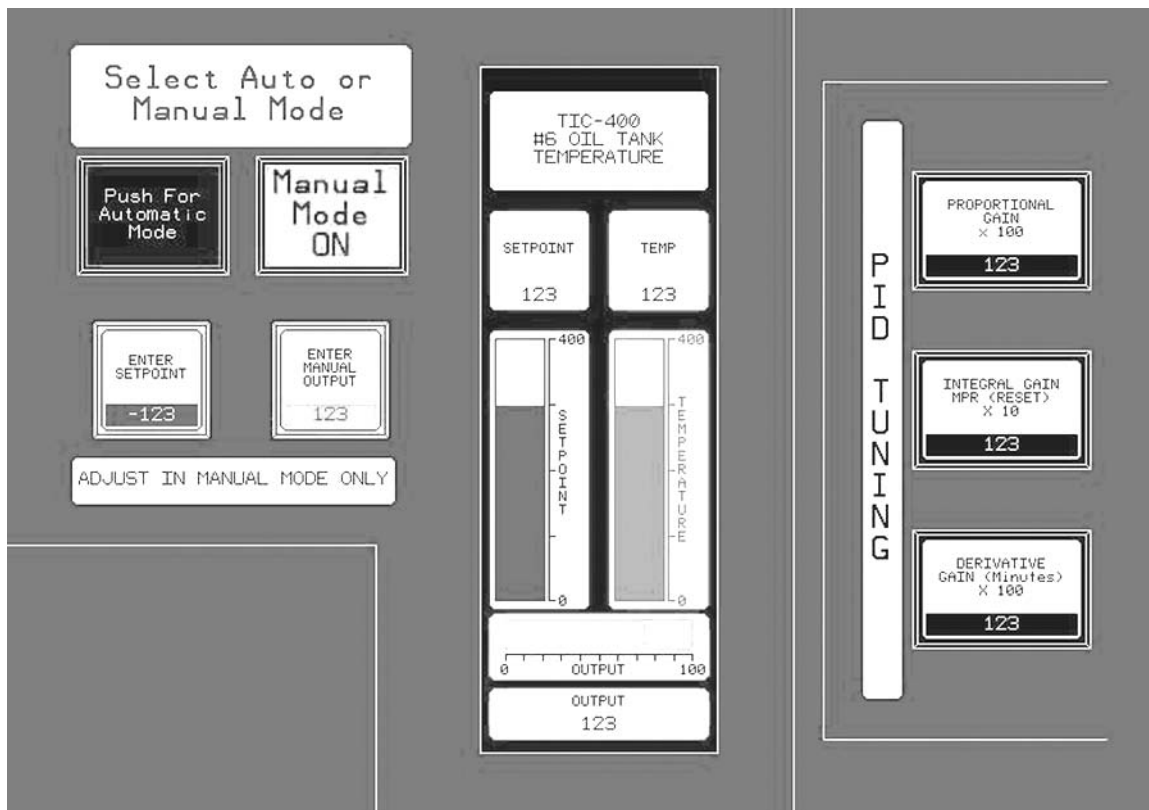


FIGURE 8.2 Touchscreen.

tell the control system what is happening out in the real world. They are described in more detail in the next section.

The final elements carry out the on/off instructions that come from the control system. These are devices such as solenoid valves, relays, indicating lights, and motor starters. These devices allow the control system to make things happen in the real world. They are described in more detail in the next section.

The discrete control system does safety monitoring and sequencing. Typically, the system monitors all the discrete inputs; and if they are all satisfactory, allows combustion system start-up. If a monitored parameter is on when it should be off or vice versa, the start-up process is aborted and the system must be reset before another start-up is permitted. The system also controls such things as which valves are opened in what order, if and when the pilot is ignited, and if and when main burner operation is allowed. Once the system starts, the discrete system has little to do other than monitor safety parameters. If any of the defined safety parameters are not satisfactory, the system immediately shuts down. [Figure 8.3](#) is a simplified flow diagram showing a standard burner light-off sequence.

8.1.3 ANALOG CONTROL SYSTEMS

The world of analog controls is not black and white — it is all gray. How far open is that valve? What is the system temperature? How much fuel gas is flowing?

There are two categories of analog devices with familiar names: (1) sensors, which measure some process variable, such as flow or temperature, and generate a signal proportional to the measured value; and (2) final elements, such as pumps or valves, that change their status (speed or position, for example) in response to a proportional signal from the control system.

In contrast to the discrete control system, the analog control system usually has few tasks to perform until the system completes the start-up sequence and is ready to maintain normal operation. Most analog devices are part of a control loop. A simple loop consists of a sensor, a final element, and a controller. The controller reads the sensor, compares the measured value to its setpoint, set by the operator, and then positions the final element to make the measured value equal the setpoint. [Figure 8.4](#) illustrates a simple analog loop.

In this case, the thermocouple transmits the temperature to the controller. If the temperature is higher than the setpoint, the controller will decrease its signal to the control valve. This will decrease the fuel flow to the burner, thus lowering the temperature. In this way, the loop works to maintain the desired temperature — also known as the setpoint.

The previous illustration is a good example of a simple feedback system. After the controller adjusts the control valve, the resulting change in temperature is fed back to the controller. In this way, the controller “knows” the result of the adjustment and can make a further adjustment if it is required. Another good example of feedback takes place whenever you drive your car. If you get on the expressway and decide to drive at 60 mph, you press your foot on the accelerator and watch the speedometer. When you get near 60 mph, you begin to ease off the accelerator so that you do not overshoot. From then on, you glance at the speedometer every now and then and adjust your foot position as necessary.

Feedback alone is not enough, however. What if there is traffic congestion? You begin to slow down in anticipation. This is called feedforward, which occurs when you change your operating point because some future event is about to happen and you need to prepare for it. Feedforward is commonly used in combustion control systems. A good example from the world of combustion is waste flow. In a combustible waste destruction system, what happens if the waste flow suddenly doubles? There will no longer be enough combustion air in the system to allow destruction of all of the waste. Unburned waste will burn at the tip of the smokestack and clouds of smoke will billow from the stack. Phone calls from irate neighbors will soon begin to accumulate. Using feedforward, as shown in [Figure 8.5](#), the waste flow is measured. When it doubles, the combustion airflow immediately increases by a similar amount, avoiding all the unpleasant consequences listed above.

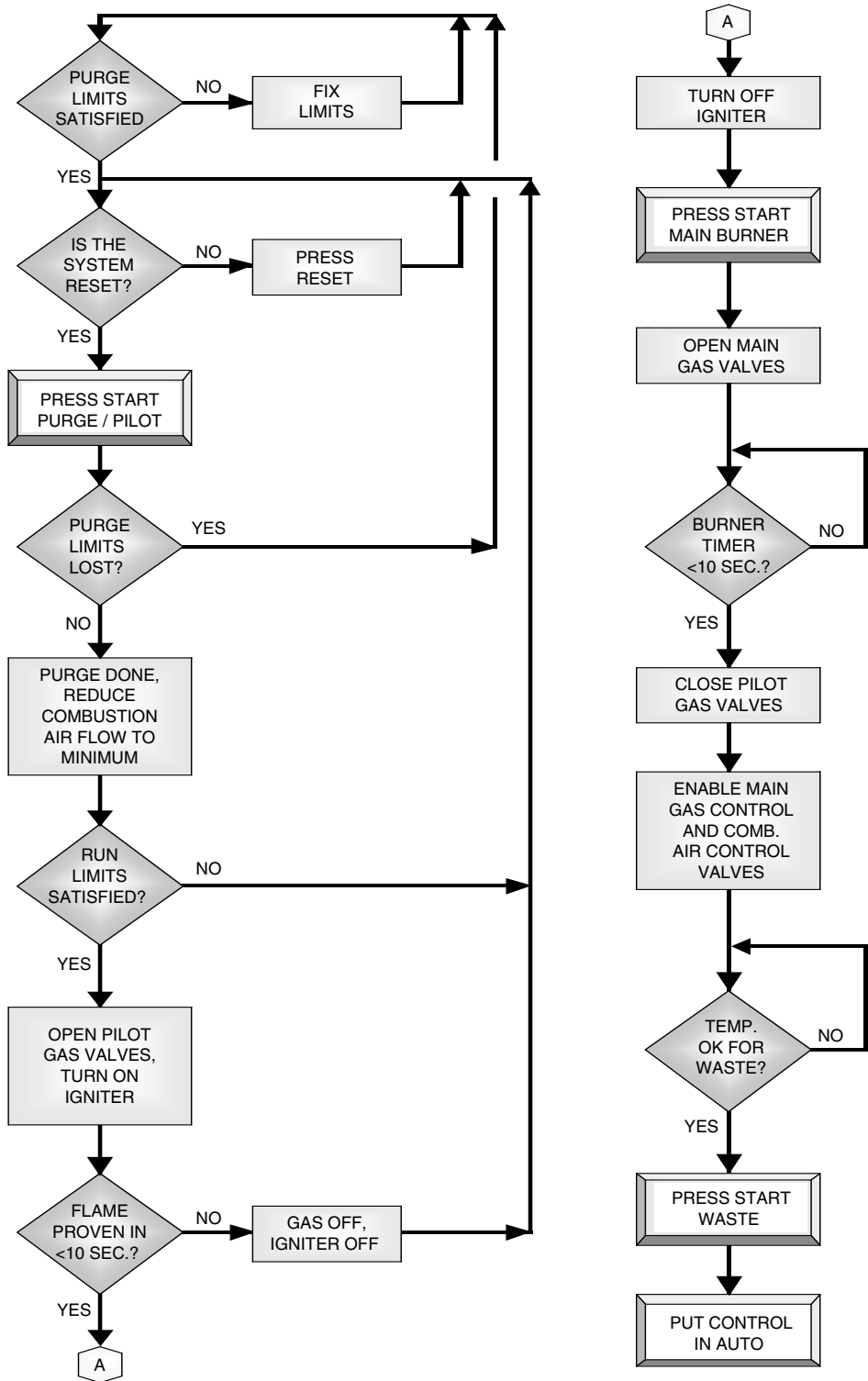


FIGURE 8.3 Simplified flow diagram of a standard burner lightoff sequence.

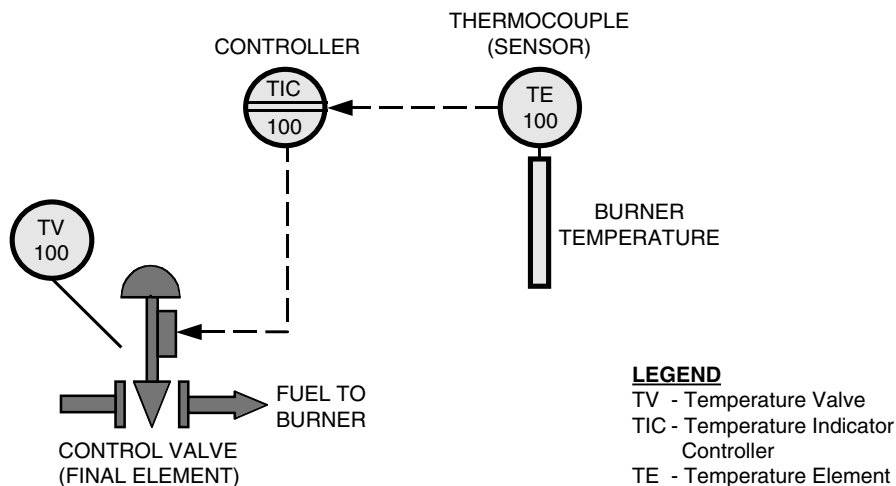


FIGURE 8.4 Simple analog loop.

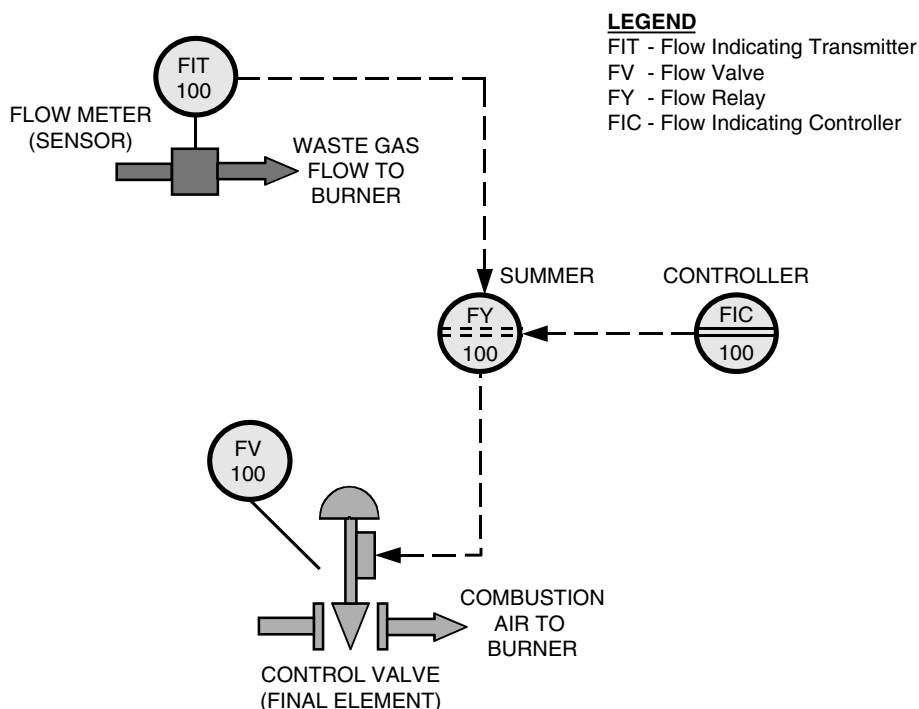


FIGURE 8.5 Feedforward loop.

8.1.4 FAILURE MODES

Almost everything fails eventually. No matter how well the components of a control system are designed and built, some of them will fail from time to time. One of the primary tasks of the controls engineer is to design the controls system so that failure of one or even several components will not cause a safety problem with the combustion system.

All components used in a control system have one or more defined failure modes. For example, if a discrete sensor fails, it will most likely cause the built-in switch contacts to fail open. To design a safe system, the controls engineer will choose and install the sensor so that when an alarm condition is present, the switch contacts will open. Thus, the alarm condition coincides with the failure mode. If it did not, the sensor could fail and the control system would still think everything was normal and attempt to keep operating as before, a condition that could be catastrophic.

In addition to sensors, final control elements also have failure modes. The controls engineer can usually select the desired failure mode. If a burner has an actuated valve that turns the fuel gas supply on and off, the actuator is installed so that the valve will spring closed (fail shut) on loss of air. In addition, assume there is a solenoid valve that turns air to the actuator on and off. The solenoid valve should be selected and installed to rapidly dump air from the actuator on loss of electrical power, thus closing the valve shut. These designs assure that the two most likely circumstances of component failure enhance system safety.

Construction of a well-designed system ensures that every component that can fail is installed so that component failures do not compromise system safety. At its core, that is what controls engineering is all about.

8.1.5 AGENCY APPROVALS AND SAFETY

Worldwide, there are hundreds of private, governmental, and semi-governmental safety organizations. Each ostensibly has the proper implementation of safety at the top of its agenda. Some agencies are concerned with the electrical safety and reliability of the components used in a control system. Other agencies are concerned about preventing explosions caused by sparking equipment in a gaseous atmosphere. Still other agencies are concerned with the proper design of control systems to ensure safe operation of various combustion processes. No single organization does all the things listed above.

The design of combustion systems in the U.S. should include specifications that meet National Fire Protection Association (NFPA) and National Electrical Code (NEC) standards. In accordance with the applicable standards and years of experience in the field, systems should be designed with some or all of the following safety features.

8.1.5.1 Double-Block-and-Bleed for Fuel Supply

This means that there are two fail-shut safety shutoff block valves with a fail-open safety shutoff vent valve located between them, as shown in [Figure 8.6](#). Each of the three safety shutoff valves (SSOVs) in the double block and bleed system has a position switch not shown here. For a system purge to be valid, the block valves must be shut and verified. For burner lightoff, the vent valve is shut. After the vent valve position switch confirms that the valve is shut, the two block valves are opened. If there is a system failure, all three of the valves de-energize and return to their failure positions. Note that if the upstream block valve ever leaks, the leakage will preferentially go through the open vent valve and vent to a safe location rather than into the burner.

8.1.5.2 Unsatisfactory Parameter System Shutdown

An unsatisfactory parameter for any critical input immediately shuts down the system. The control system typically receives critical input information as shown in [Figure 8.7](#). The pressure switch PSSL-100 is wired so that if it fails, the voltage is interrupted to the relay and the programmable logic controller (PLC). The PLC will then shut down the system. If either the switch or the relay fails, the system shuts down.

In addition, the relay has another contact in series with all of the other critical contacts. If any of these contacts open, the power cuts off to all ignition sources (all fuel valves, igniters, etc.), immediately shutting down the combustion system.

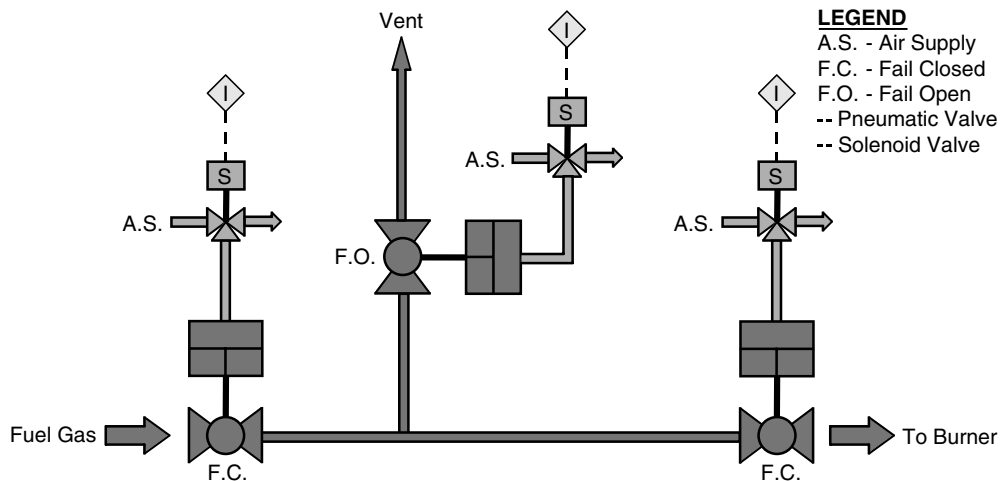


FIGURE 8.6 Double-block-and-bleed system.

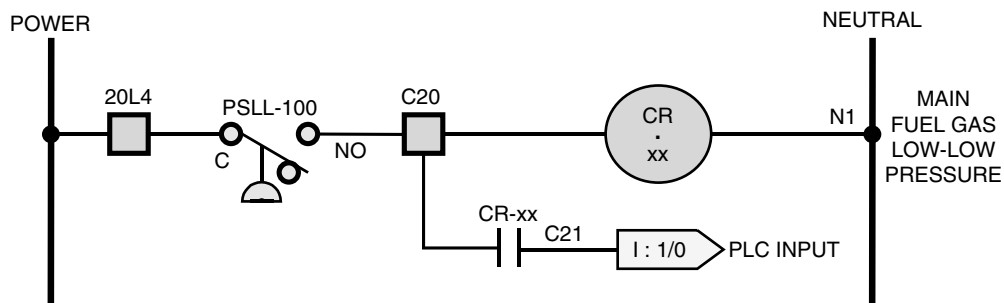


FIGURE 8.7 Failsafe input to PLC.

In Figure 8.8, if there is a failure anywhere in the circuitry, the system shuts down. Even if damage to the PLC occurs, the relays will shut down the system. This is an excellent example of redundancy, fail-safe design principles, and effective design philosophy.

8.1.5.3 Local Reset Required after System Shutdown

After a system shutdown caused by an alarm condition, the system allows a remote restart only after an operator has pressed a reset button located at the combustion system. The operator should perform a visual inspection of the system and verify the correction of the condition that caused the shutdown.

8.1.5.4 Watchdog Timer to Verify PLC Operation

If the PLC logic freezes, a separate timer fails to receive an expected reset pulse from the PLC and shuts down the system.

8.1.6 PIPE RACKS AND CONTROL PANELS

For most combustion control systems, two major assemblies make up the bulk of the system: the pipe rack and the control panel. A pipe rack is shown in Figure 8.9. Sometimes called a skid, the pipe rack is a steel framework that has a number of pipes and associated components attached to it. Usually, most combustion process feeds, such as air, fuel, and waste, have their shutoff and control

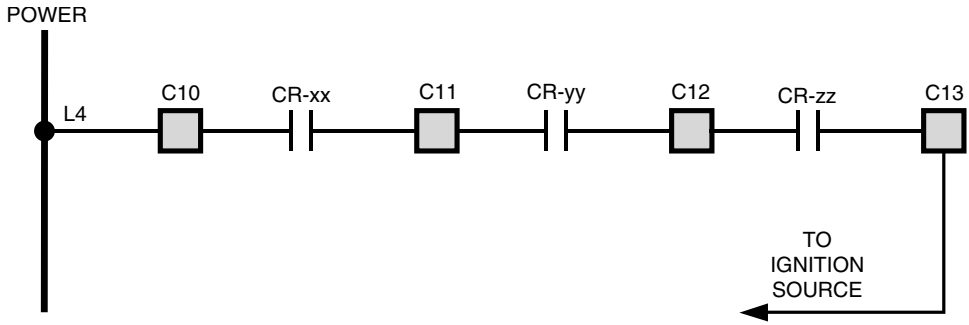


FIGURE 8.8 Shutdown string.

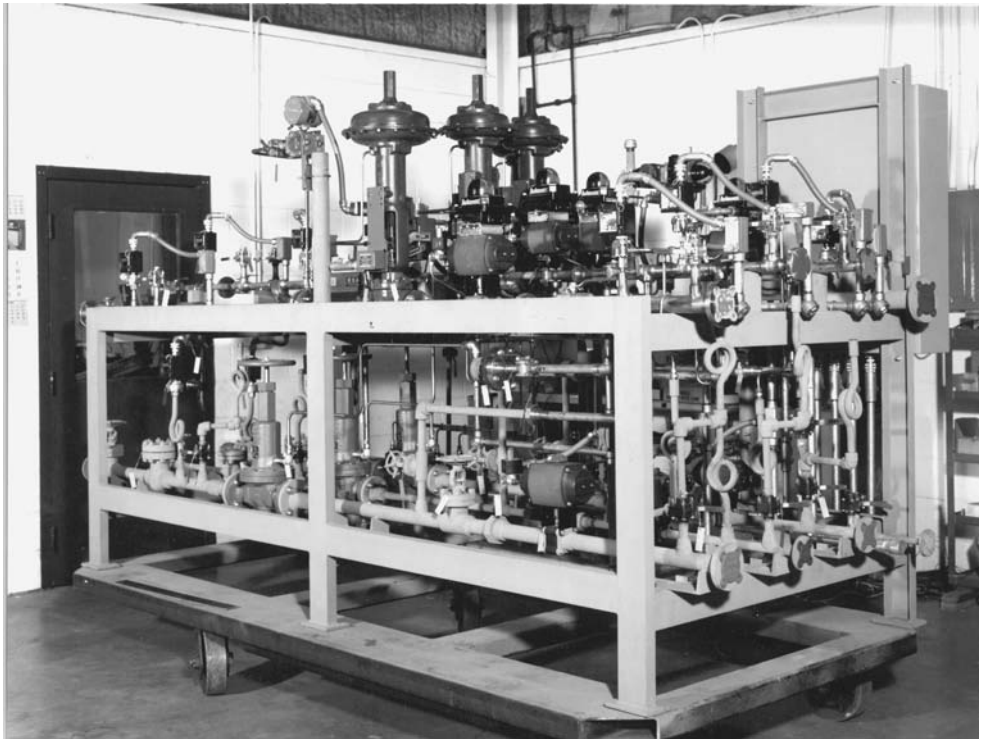


FIGURE 8.9 Typical pipe rack.

elements located on the pipe rack. This makes maintenance and troubleshooting more convenient and reduces the amount and complexity of wiring systems required to connect all of the components.

A typical control panel is shown in [Figure 8.10](#). [Figure 8.11](#) shows the inside of the control panel. The control panel is usually attached to the pipe rack. All of the devices on the pipe rack, as well as the field devices, are electrically connected to the control panel. The control system usually resides inside the control panel. In addition to the wiring, maintenance, and troubleshooting benefits mentioned above, another benefit to packaging the control system is far more important — that the people who designed and built the system can test and adjust it at the factory. When the control system arrives at the job site, installation consists mostly of hooking up utilities and the interconnecting piping, thus minimizing the amount of expensive on-site troubleshooting and tuning.



(a)



(b)

FIGURE 8.10 Control panels: (a) large and (b) small.

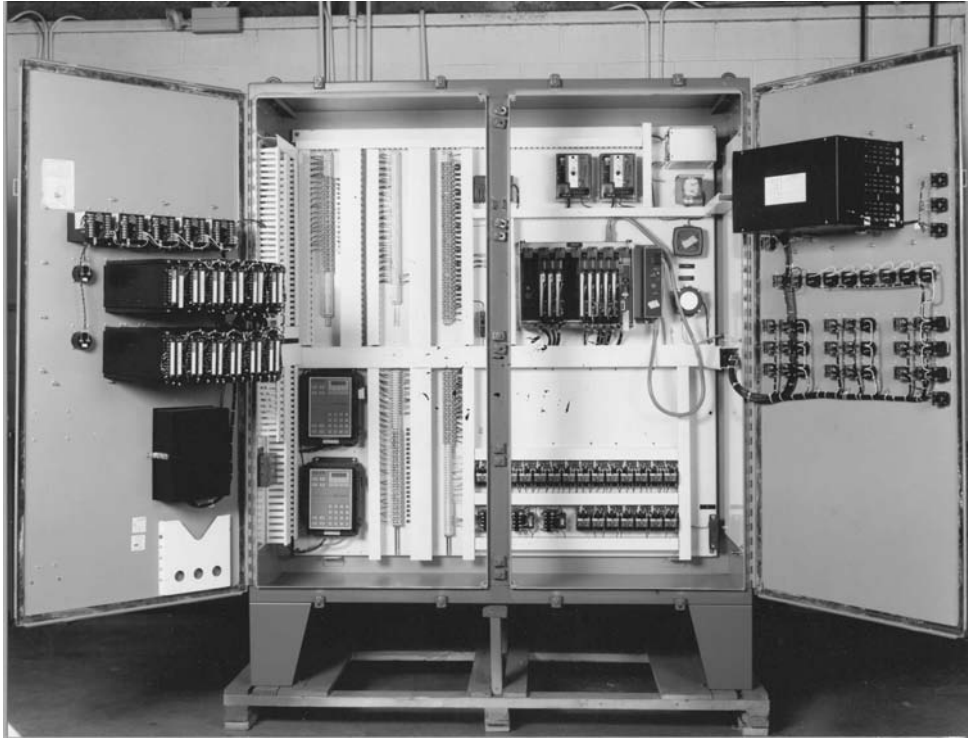


FIGURE 8.11 Inside the control panel.

8.2 PRIMARY MEASUREMENT

This section describes a number of different analog and discrete devices used to provide the interface between combustion systems and control systems. All of these devices are available from numerous suppliers around the world. There are vast differences in price, quality, and functionality among the different devices and suppliers.

8.2.1 DISCRETE DEVICES

8.2.1.1 Annunciators

An annunciator is a centralized alarm broadcasting and memory device. Typically, all the alarms in a control system are routed to the annunciator. When any alarm is triggered, the light associated with that alarm will flash and the annunciator horn will sound. If the annunciator is a “first-out” type, any subsequent alarms that occur will trigger their associated lights to come on solidly — rather than flashing, as the first alarm does. This is very useful for diagnosing system problems. When a safety shutdown occurs, other alarms are usually triggered while the system is shutting down. With a first-out capability, the original cause of the shutdown can be easily determined.

8.2.1.2 Pressure Switches

Pressure switches (see [Figure 8.12](#)) are sensors that attach directly to a process being measured. They can be used to detect absolute, gage, or differential pressure. The switches generally have a pressure element such as a diaphragm, tube, or bellows that expands or contracts against an adjustable spring as the pressure changes. The element attaches to one or more sets of contacts



(a)



(b)

FIGURE 8.12 Pressure switch.

that open or close upon reaching the setpoint. The devices are used in a number of ways, but in combustion systems they are usually used to test for high and low fuel gas pressure. They are normally set so the contacts are open when in the alarm condition.

8.2.1.3 Position Switches

Also called limit switches, these sensors attach to or are built into valves, insertable igniters, and other devices. Position switches usually employ a mechanical linkage, but proximity sensors are also quite common. They are adjustable, and can tell the control system if a valve is open, closed, or in some defined intermediate position. Position switches are not usually used for alarms. In combustion systems, they are generally used to check valve positions during purges and burner lightoff sequences. Position switches are often used with integrated beacons and other visual devices. They are normally installed so that their contacts are closed only when the valve is in the desired safety position.

8.2.1.4 Temperature Switches

Temperature switches are usually attached to auxiliary equipment such as tanks or flame arresters. These sensors generally do not have the range to test for combustion system temperatures, so those applications use other devices. The switches usually use a bimetallic element, where the differential expansion of two different metals generates physical movement. The movement opens or closes one or more sets of contacts. The failure mode of temperature switches is not always predictable. Generally, installation requires open contacts when the switch is in the alarm condition.

8.2.1.5 Flow Switches

Flow switches are sensors that generally insert into the pipe or duct in which flow is measured. Because of the lack of a quantitative readout and the improved reliability of analog transmitters in this service, these devices are becoming less common. Their failure mode is not always predictable. Usual installation requires open contacts when the switch is in the alarm condition.

8.2.1.6 Run Indicators

A run indication sensor shows whether a pump or fan is running. The sensor is especially important when outlet pressure indication of the device may not be definitive. It is usually possible to order a motor starter with a built-in set of signal contacts that close when the starter motor contacts are closed. However, that does not always ensure that the pump is running and pumping fluid. A magnetic shaft encoder rotates a magnetic slug past a pickup sensor every revolution and provides positive indication of shaft revolution, but that too does not always ensure that the pump is pumping fluid. It is usually preferable to have a pressure or flow indicator that shows that the system is functioning normally and moving fluid.

8.2.1.7 Flame Scanners

Flame scanners are crucial to the safe operation of a combustion system. If the flame is out, the fuel flow into the combustion enclosure is stopped and the area is purged before a re-light can be attempted. Flame scanners come in two main varieties: infrared and ultraviolet. The name tells which section of the electromagnetic spectrum it is designed to see. Generally, ultraviolet scanners are preferred because they are more sensitive and quicker to respond. The detector is a gas-filled tube that scintillates in the presence of flame and gives off bursts of current, called an avalanche, several hundred times per second as long as the flame continues. When the flame stops, the current stops. There is a 2- to 4-second delay, to minimize spurious shutdowns, and then the contacts open

to designate the alarm condition. Most systems have two flame scanners. To achieve system shutdown, both scanners must fail. Use of infrared scanners is desirable if there is a waste stream, such as sulfur, which absorbs ultraviolet light and makes operation of ultraviolet scanners unreliable. Self-checking scanners are usually used. They have output contacts that open on either loss of flame or failure of the self-check. Usually, the contacts are part of an amplifier/relay unit located in the control panel, but some newer systems have everything located in the scanner housing, which mounts on the burner endplate. One limitation with flame scanners is the possibility of the power wire to the scanner inducing false flame indications in the signal wire from the scanner. If there are separate wires for scanner power and scanner signal, they must run in separate conduit or shielding to prevent false signals caused by induction.

8.2.1.8 Solenoid Valves

Solenoid valves are turned on or off by the presence or absence of voltage from the control system. A solenoid valve has a relay coil that links mechanically to a valve disc mechanism. Energizing the solenoid causes the linkage to push against a spring to reposition the valve disc. De-energizing the solenoid allows the spring to force the valve to the failure position. The most common types of solenoid valves are two-way and three-way valves. Two-way valves have two positions; they allow flow or they do not. They are often used to turn pilot gas on and off. Three-way solenoid valves have three ports but still only two positions. If ports are labeled A, B, and C, energizing the valve may allow flow between ports A and B, while de-energizing the valve may allow flow between ports A and C. It is very important to carefully select, install, and test three-way solenoid valves. Three-way solenoid valves typically attach to control valves and safety shutoff valves (SSOVs). In the case of control valves, when the solenoid valve is energized, the control valve is enabled for normal use. When the solenoid valve is de-energized, the instrument air is dumped from the control valve actuator diaphragm, causing the control valve to go to its spring-loaded failure position. For safety shutoff valve (SSOV) service, the solenoid valve is hooked up so that when energized, instrument air is allowed to reposition the SSOV actuator away from its spring-loaded failure position. When the solenoid valve is de-energized, the air is dumped from the SSOV actuator, causing the control valve to go to its spring-loaded failure position. The failure modes of the solenoid valve, control valve, and SSOV are coordinated to maximize system safety no matter what component fails.

8.2.1.9 Ignition Transformers

Ignition transformers supply the high voltage necessary to generate the spark used to ignite the pilot flame during system lightoff. The type of transformer usually used converts standard AC power to a continuous 6000 VDC. This voltage then continuously jumps the spark gap at the igniter, which is located at the head of the pilot burner. High-energy igniters provide a more intense spark. A high-energy igniter is similar to the transformer mentioned above except that capacitors are included to store up energy and release it in spurts, resulting in a more intense spark. Both types of transformers are usually located close to the burner in a separate enclosure and hooked to the igniter using coaxial cable similar to the sparkplug wire used in cars.

8.2.2 ANALOG DEVICES

8.2.2.1 Control Valves

Control valves are among the most complex and expensive components in any combustion control system. Numerous extensive books document the nearly infinite variety of valves. Misapplication or misuse of valves compromises system efficiency and safety. Controls engineers cannot simply pick control valves from a catalog because they are the right size for the line where they will be used. Control valves must be engineered for their specific application. A typical pneumatic control valve is shown in [Figure 8.13](#).

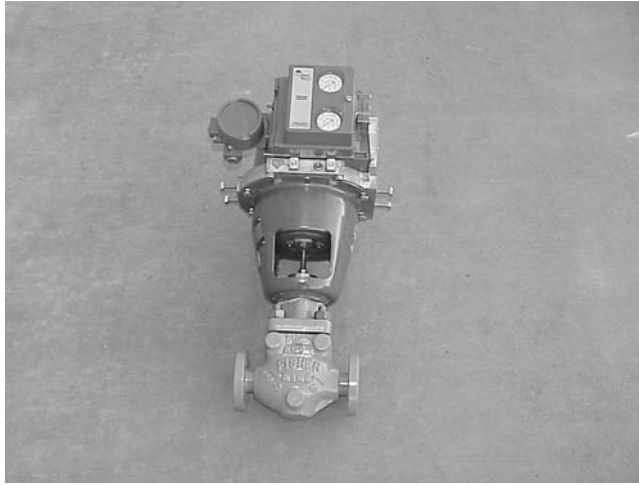


FIGURE 8.13 Pneumatic control valve.

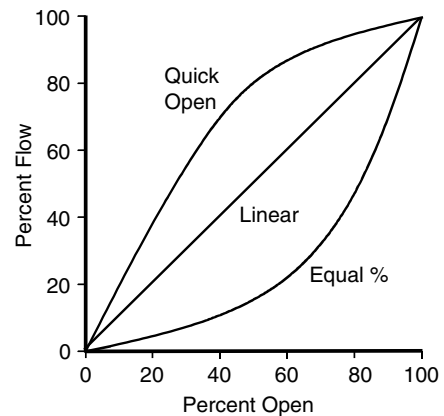


FIGURE 8.14 Control valve characteristics.

As shown in Figure 8.14, the type of service and control desired determines the selection of different flow characteristics and valve sizes. Controls engineers use a series of calculations to help with this selection process. A typical control valve consists of several components that are mated together before installation in the piping system:

8.2.2.1.1 Control Valve Body

The control valve body can be a globe valve, a butterfly valve, or any other type of adjustable control valve. Usually, special globe valves of the equal percent type are used for fuel gas control service or liquid service. Control of combustion air and waste gas flows generally require the use of butterfly valves — often the quick-opening type. Because the combustion air or waste line usually has a large diameter, and the cost of globe valves quickly becomes astronomical after the line size exceeds 3 or 4 inches, butterfly valves are usually the most economical choice. In Chapter 8.3, a discussion of parallel positioning describes how controls engineers use a globe valve and a butterfly valve to work smoothly together for system control.

8.2.2.1.2 Actuator

The actuator supplies the mechanical force to position the valve for the desired flow rate. For control applications, a diaphragm actuator is preferred because, compared to a piston-type actuator,

it has a relatively large pressure-sensitive area and a relatively small frictional area where the stem is touching the packing. This ensures smooth operation, precision, and good repeatability. Proper selection of the actuator must take into account valve size, air pressure, desired failure mode, process pressure, and other factors. Actuators are usually spring-loaded and single-acting, with control air used on one side of the diaphragm and the spring on the other. The air pressure forces the actuator to move against the spring. If air pressure is lost, the valve fails to the spring position thus, the actuator is chosen carefully to fail to a safe position (i.e., closed for fuel valves, open for combustion air valves).

8.2.2.1.3 Current-to-Pressure Transducer

The current-to-pressure transducer, usually called the I/P converter, takes the 24 VDC (4 to 20 milliamps) signal from the controller and converts it into a pneumatic signal. The signal causes the diaphragm of the actuator to move to properly position the control valve.

8.2.2.1.4 Positioner

The positioner is a mechanical feedback device that senses the actual position of the valve as well as the desired position of the valve. It makes small adjustments to the pneumatic output to the actuator to ensure that the desired and the actual position are the same. Current conventional wisdom states that positioners should be used only on “slow” systems and not on “fast” systems, where they can actually degrade performance. There is not a defined border between “fast” and “slow,” but virtually all combustion control applications are considered “slow,” so positioners are almost always used in these systems.

8.2.2.1.5 Three-Way Solenoid Valve

When energized, the three-way solenoid valve admits air to the actuator. When de-energized, it dumps the air from the actuator. Because single-acting actuators are generally used, the spring in the actuator forces the valve either fully open or fully closed, depending on the engineer’s choice of failure modes when specifying the valve. Obviously, a control valve that supplies fuel gas to a combustion system should fail closed, while the control valve that supplies combustion air to the same system should fail open. In an application in which the failure mode of the valve is irrelevant, and there are some, solenoid valves are not used.

8.2.2.1.6 Mechanical Stops

Mechanical stops are used to limit how far open or shut a control valve can travel. If it is vital that no more than a certain amount of fluid ever enters a downstream system, an “up” stop is set. If it is necessary to ensure a certain minimum flow, for cooling purposes for example, a “down” stop is set. In the case of a fuel supply control valve, the “down” stop is set so that during system lightoff, an amount of fuel ideal for smooth and reliable burner lighting is supplied. After a defined settling interval, usually 10 seconds, the three-way solenoid valve is energized and normal control valve operation is enabled.

8.2.2.2 Thermocouples

Whenever two dissimilar metals come into contact, current flows between the metals and the magnitude of that current flow and the voltage driving it, vary with temperature. This phenomenon is called the Seebeck effect. If both of the metals are carefully chosen and are of certain known alloy compositions, the voltage will vary in a nearly linear manner with temperature over some known temperature range. Because the temperature and voltage ranges vary depending on the materials employed, engineers use different types of thermocouples for different situations. In combustion applications, the “K” type thermocouple (0 to 2400°F or –18 to 1300°C) is usually used. When connecting a thermocouple (see [Figure 8.15](#)) to a transmitter, the transmitter should



FIGURE 8.15 Thermocouple.



FIGURE 8.16 Thermowell.

be set up for the type of thermocouple employed. Installing thermocouples in a protective sheath known as a thermowell (see Figure 8.16) prevents the sensing element from suffering the corrosive or erosive effects of the process being measured. However, a thermowell also slows the response of the instrument to changing temperature and should be used with care.

8.2.2.3 Velocity Thermocouples

Also known as suction pyrometers, the design of velocity thermocouples attempts to minimize the inaccuracies in temperature measurement caused by radiant heat. Inside a combustor, the thermocouple measures the gas temperature. However, the large amount of heat radiated from the hot surroundings significantly affects the measurement. A velocity thermocouple (see Figure 8.17) shields the thermocouple from radiant heat by placing it in one or more concentric hollow pipes. Hot gas is induced to flow across the thermocouple, producing a gas temperature reading without a radiant component.

8.2.2.4 Resistance Temperature Detectors (RTDs)

Resistance of any conductor increases with temperature. For a specific material of known resistance, it is possible to infer the temperature. Similar to the thermocouples described above, the linearity of the result depends on the materials chosen for the detector and their alloy composition. Engineers sometimes use RTDs instead of thermocouples when higher precision is desired. Platinum is a

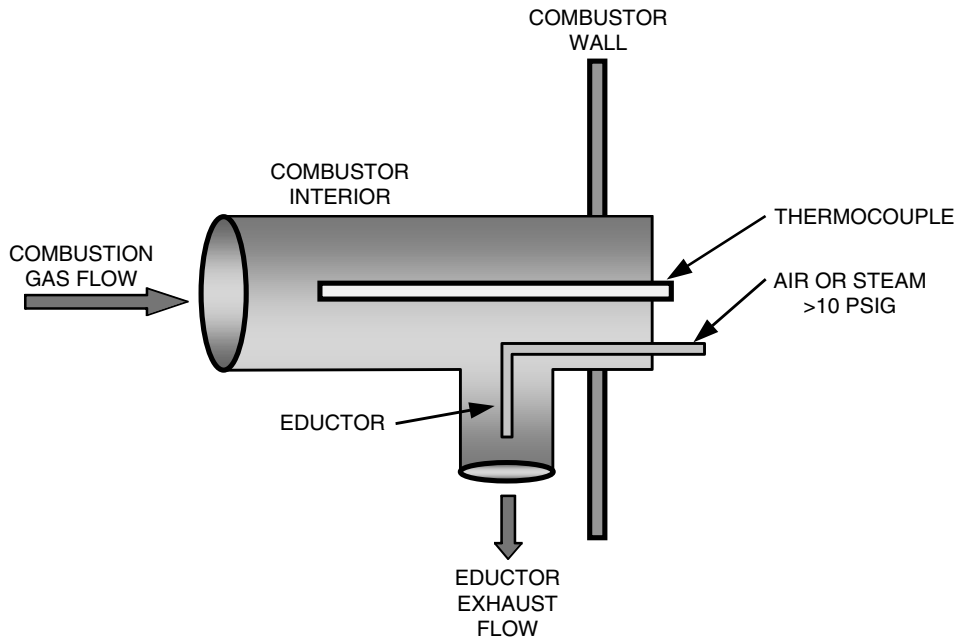


FIGURE 8.17 Velocity thermocouple.

popular material for RTDs because it has good linearity over a wide temperature range. Like thermocouples, installation of RTDs in thermowells is common.

8.2.2.5 Pressure Transmitters

A pressure transmitter (see [Figure 8.18](#)) is usually used to provide an analog pressure signal. These devices use a diaphragm coupled to a variable resistance, which modifies the 24 VDC loop current (4 to 20 milliamps) in proportion to the range in which it is calibrated. In recent years, these devices have become enormously more accurate and sophisticated, with onboard intelligence and self-calibration capabilities. They are available in a wide variety of configurations and materials and can be used in almost any service. It is possible to check and reconfigure these “smart” pressure transmitters remotely with the use of a handheld communicator.

8.2.2.6 Flow Meters

There are many different types of flow meters and many reasons to use one or another for a given application. The following is a list of several of the more common types of flow meters, how they work, and where they are used.

8.2.2.6.1 Vortex Shedder Flow Meter

A vortex shedder places a bar in the path of the fluid. As the fluid goes by, vortexes (whirlpools) form and break off constantly. An observation of the water swirling on the downstream side of bridge pilings in a moving stream reveals this effect. Each time a vortex breaks away from the bar, it causes a small vibration in the bar. The frequency of the vibration is proportional to the flow. Vortex shedders have a wide range, are highly accurate, reasonably priced, highly reliable, and useful in liquid, steam, or gas service.



FIGURE 8.18 Pressure transmitter (left) and pressure gauge (right).

8.2.2.6.2 *Magnetic Flow Meter*

A magnetic field, a current carrying conductor, and relative motion between the two creates an electrical generator. In the case of a magnetic flow meter, the meter generates the magnetic field and the flowing liquid supplies the motion and the conductor. The voltage produced is proportional to the flow. These meters are highly accurate, very reliable, have a wide range, but are somewhat expensive. They are useful with highly corrosive or even gummy fluids as long as the fluids are conductive. Only liquid flow is measured.

8.2.2.6.3 *Orifice Flow Meter*

Historically, almost all flows were measured using this method and it is still quite popular. Placing the orifice in the fluid flow causes a pressure drop across the orifice. A pressure transmitter mounted across the orifice calculates the flow from the amount of the pressure drop. Orifice meters are very accurate but have a narrow range. They are reasonably priced, highly reliable, and are useful in liquid, steam, or gas service.

8.2.2.6.4 *Coriolis Flow Meter*

The Coriolis flow meter is easily the most complex type of meter to understand. The fluid runs through a U-shaped tube that is being vibrated by an attached transducer. The flow of the fluid will cause the tube to try to twist because of the Coriolis force. The magnitude of the twisting force is proportional to flow. These meters are highly accurate and have a wide range. They are generally more expensive than some other types.

8.2.2.6.5 *Ultrasonic Flow Meter*

When waves travel in a medium (fluid), their frequency shifts if the medium is in motion relative to the wave source. The magnitude of the shift, called the Doppler effect, is proportional to the relative velocity of the source and the medium. The ultrasonic meter generates ultrasonic sound

waves, sends them diagonally across the pipe, and computes the amount of frequency shift. These meters are reasonably accurate, have a fairly wide range, are reasonably priced, and are highly reliable. Ultrasonic meters work best when there are bubbles or particulates in the fluid.

8.2.2.6.6 *Turbine Flow Meters*

A turbine meter is a wheel that is spun by the flow of fluid past the blades. A magnetic pickup senses the speed of the rotation, which is proportional to the flow. These meters can be very accurate but have a fairly narrow range. They must be very carefully selected and sized for specific applications. They are reasonably priced and fairly reliable. They are used in liquid, steam, or gas service.

8.2.2.6.7 *Positive Displacement Flow Meters*

Positive displacement flow meters generally consist of a set of meshed gears or lobes that are closely machined and matched to each other. When fluid is forced through the gears, a fixed amount of the fluid is allowed past for each revolution. Counting the revolutions reveals the exact amount of flow. These meters are extremely accurate and have a wide range. Because there are moving parts, the meters must be maintained or they can break down or jam. They also cause a large pressure drop, which can be important for certain applications.

8.2.2.7 **Analytical Instruments**

There are many different types of analytical instruments used for very specific applications. Unlike the sensors described previously, these devices are usually systems. They are a combination of several different sensors linked together by a processor of some sort that calculates the quantity in question. Unlike a pressure transmitter, most analytical instruments sample and chemically test the process in question. Because the process takes time, the engineer, when designing the system, must plan for a delayed response from the analytical instrument. A detailed discussion of the design and operation of analytical instruments is beyond the scope of this book. Below is a list of several of the more common types and their uses.

8.2.2.7.1 *pH Analyzer*

Almost any combustion system occasionally requires the scrubbing of effluent or other similar processes. pH monitoring is needed to assure that the water going into the scrubber is the correct pH to neutralize the acidity or alkalinity of the effluent. The analyzer sends information to a controller that is responsible for opening or closing valves that add alkaline chemicals to the water to raise pH.

8.2.2.7.2 *Conductivity Analyzer*

Conductivity analyzers are often used in conjunction with pH analyzers. Where the pH analyzer system functions to raise pH, the output from the conductivity analyzer is usually sent to a controller responsible for opening or closing valves that dilute salt concentration in the water.

8.2.2.7.3 *O₂ Analyzer*

O₂ or combustibles analyzers monitor the amount of oxygen or combustibles in the exhaust of a combustion system. The analyzer sends data back to the control system that uses it to tightly control the amount of combustion air coming into the system. This has the dual result of making the system more efficient and reducing the amount of pollutants that result from the combustion process. Different models have varying methodologies, accuracies, and sample times, but there are two major types: (1) *in situ* analyzers carry out the analysis at the probe; and (2) extractive analyzers remove the sample from the process and cool it before analysis.

8.2.2.7.4 Nitrogen Oxides (NO_x) Analyzer

Nitrogen oxides (NO, NO₂, etc.; see Chapter 6) are one of the main components of smog and the result of high-temperature combustion. Noxidizers are combustion systems that use an extended low-temperature combustion process designed to minimize the formation of nitrous oxide compounds. Noxidizers use NO_x analyzers. To properly control the process, the NO_x analyzer output goes to a controller that controls airflow into the system, minimizing NO_x formation.

8.2.2.7.5 Carbon Monoxide (CO) Analyzer

CO is also an undesirable pollutant and is a product of incomplete combustion. The output of the CO analyzer is often used in the analysis of system efficiency or to control airflow to the combustion system.

8.3 CONTROL SCHEMES

Other chapters of this book present the combustion process and the definition of the terms used to describe it. This section describes methods used to control the process. Generally, controlling the process means controlling the flow of fuels and combustion air.

8.3.1 PARALLEL POSITIONING

Designers use analog control schemes to modulate valve position and control fan and pump speeds to achieve the required mix of fuel and oxygen in a combustion system. Simple systems often use parallel positioning of fuel and air valves from a single analog signal.

8.3.1.1 Mechanical Linkage

A common method of parallel positioning is to mechanically link the fuel and air valves to a single actuator. Adjustment of a cam located on the fuel valve supplies the proper amount of fuel throughout the air valve operating range. Figure 8.19 shows the arrangement.

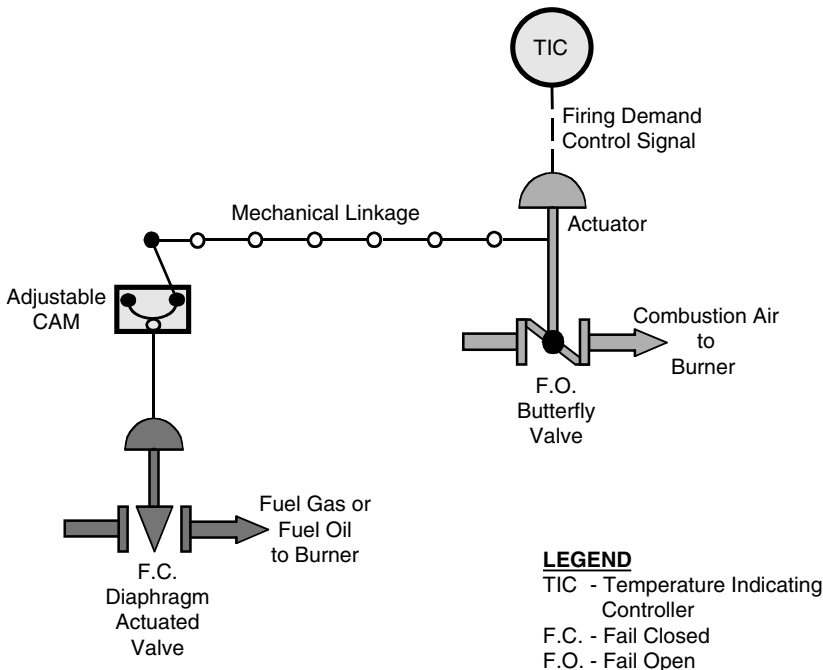


FIGURE 8.19 Mechanically linked parallel positioning.

In the figure, the temperature indicating controller (TIC) operates an actuator attached to the air valve. A mechanical linkage and an adjustable cam operates the fuel valve in parallel with the air valve. Springs or weights attached to the air valve shaft force a full open position of the air valve if the mechanical connection to the air valve fails. The system uses a fail-closed actuator to ensure that a low fire failure mode results from loss of signal or loss of actuator power.

Mechanical linkage is simple in operation but requires considerable adjustment at start-up to obtain the correct fuel/air ratio over the entire operating range. Predictable flow rates of fuel and air throughout valve position require a fixed supply pressure to the valves and constant load geometry downstream of the valves. Analytical feedback to control fuel gas or combustion air supply pressure can make dynamic corrections for fuel variations, temperature changes, and system errors. Dynamic adjustments should be small trimming adjustments rather than primary control parameters.

8.3.1.2 Electronically Linked

Electronically linked fuel and combustion air valves for parallel positioning have many advantages over mechanically linked valves. Figure 8.20 illustrates the scheme.

In the example, a TIC generates a firing rate demand. The controller applies an output of 4 to 20 milliamps to the fuel valve and to a characterizer in the air valve circuit. Electronic shaping of the characterizer output positions the air valve for correct airflow. Predictable and repeatable valve positions require the use of positioners at each valve. Without positioners, valve hysteresis causes large errors in flow rate.

Signal inversion ($1 - \text{the value being measured}$) is sometimes integral to the characterizer. Signal inversion is necessary because the air valve fails open and the fuel valve fails closed. Safety concerns dictate failure modes. Fuel should always fail to minimum and air should fail to maximum.

Electronically linked parallel positioning works well if properly designed. Good design requires valves with known coefficients throughout valve position and use of high-performance positioners. Supply pressure of fuel and air to each valve must be constant or repeatable. System load

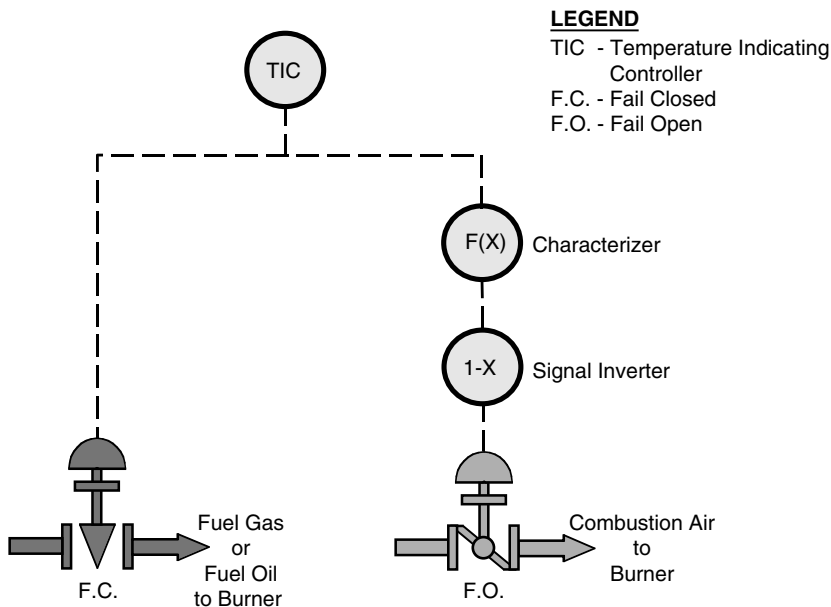


FIGURE 8.20 Electronically linked parallel positioning.

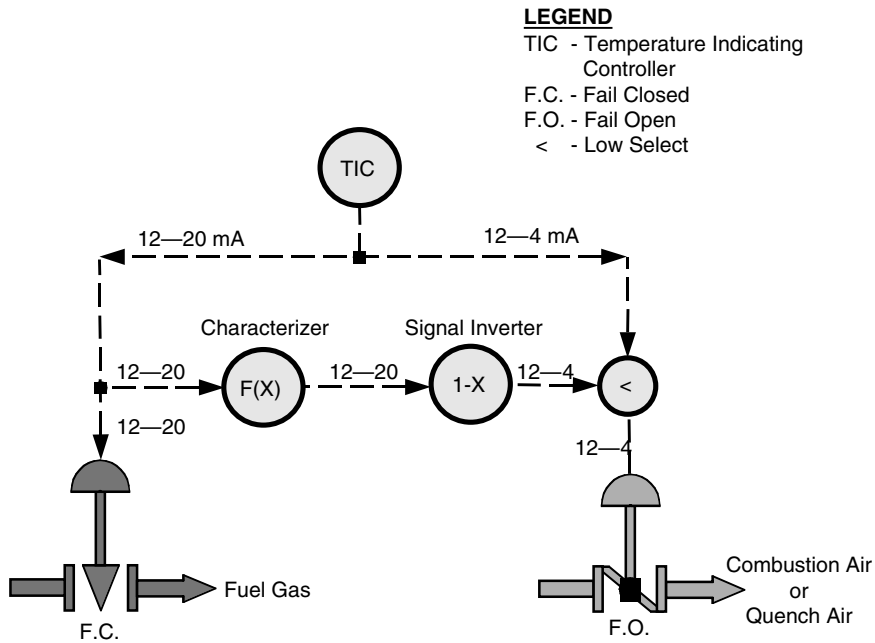


FIGURE 8.21 A variation of parallel positioning.

downstream of the valves must be of fixed geometry. Chapter 8.3.1.3 shows an example of how to calculate and configure a characterizer for the air valve.

Figure 8.21 shows a variation of parallel positioning that permits use of the combustion air valve for the multiple purposes of (1) supplying combustion air during normal operation, (2) supplying quench air when burning exothermic waste, or (3) using another heat source requiring quench air. When showing a range of milliamp signals, the first value is the minimum valve position and the second value is the maximum valve position. This convention aids system analysis and is especially useful for complex systems. The TIC output is split-ranged. The top half, 12 to 20 mA, is used for firing fuel gas. When burning exothermic waste requiring quench air, the temperature controller output decreases, providing low fire fuel at 12 mA, then quench air below 12 mA.

The TIC output is actually 4 to 20 mA. The description of the action of the receivers uses the term “split-ranged.” For example, the TIC applies the entire 4- to 20-mA range to the fuel gas valve but the valve is configured to respond only to the partial range of 12 to 20 mA.

8.3.1.3 Characterizer Calculations

Parallel positioning of a globe-type fuel gas valve and a butterfly type combustion air valve requires characterizer calculations as described below. Figure 8.20 shows the control scheme.

Three general steps are required to define the characterizer:

Step 1: Calculate and graph fuel flow rate vs. control signal.

Step 2: Calculate and graph combustion air flow rate vs. control signal.

Step 3: Tabulate and graph air valve characterizer.

8.3.1.3.1 Step 1: Fuel Flow Rate vs. Control Signal

Predictable and repeatable calculations of fuel gas flow rate vs. control valve position require:

Pressure regulator upstream of control valve to provide constant inlet pressure. Varying inlet pressure can be used only if it is repeatable with flow rate.

1. Constant temperature and composition of fuel gas
2. High-quality positioner on the control valve to eliminate hysteresis and to ensure that valve percent open equals percent control signal
3. Knowledge of valve coefficient vs. valve position throughout the control valve range, including the pressure recovery factor
4. Fixed and known pressure drop geometry downstream of the control valve
5. Subsonic regime throughout the flow range

Results of Step 1 are shown in Figure 8.22 for a typical fuel gas valve with equal percent trim. Low fire position of the valve is approximately 25% open for many applications. Maximum firing rate occurs between 70 and 80% open, resulting in a near linear function of flow rate vs. valve position throughout the firing range. The linear function is not necessary for configuring a combustion air characterizer but is useful for the application of a dynamic fuel/air ratio correction to the control circuit.

Use of a positioner on the fuel gas valve establishes equality between percent control signal and percent valve opening. Columns 1 and 2 of Table 8.1 show gas valve data.

8.3.1.3.2 Step 2: Air Flow Rate vs. Air Valve Position

Calculation of air flow rate vs. valve position that is predictable and repeatable requires:

1. Known and repeatable valve inlet pressure vs. flow rate
2. Near-constant temperature
3. High-quality positioner on the valve

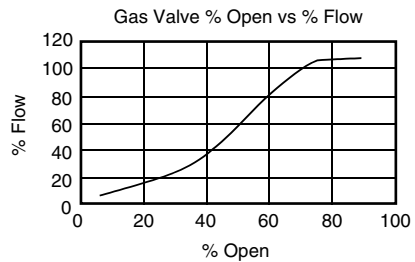


FIGURE 8.22 Fuel flow rate vs. control signal.

TABLE 8.1
Gas Valve Data

Control Signal TIC Output%	Gas Valve % Open	Fuel Gas Flow Rate%
10	10	10
20	20	16
30	30	25
40	40	39
50	50	58
60	60	83
70	70	100
80	80	107
90	90	109
100	100	110

4. Knowledge of valve coefficient and pressure recovery factor of the air valve at all valve positions
5. Fixed and known flow (pressure drop) geometry downstream of the control valve

Figure 8.23 shows the results of a typical butterfly type valve calculation for Step 2. The low fire mechanical stop is normally set at approximately 20% open.

8.3.1.3.3 Step 3: Air Valve Characterizer

Table 8.2 combines data from Figure 8.23 with data from Table 8.1. Air valve graph data are tabulated in columns 3 and 4. Figure 8.24 is a plot of the data from columns 1 and 4 and represents the required shape of the air valve characterizer. The TIC output signal is the characterizer input and is plotted on the x-axis. The characterizer output is the percent open of the air valve and is shown on the y-axis. Many characterizer instruments are available that will model a curved response using straight line segments. This characterizer is sufficiently defined using three segments.

TABLE 8.2
Data for Characterizer

Control Signal TIC Output%	Fuel Gas Flow Rate%	Combustion Air Flow Rate%	Air Valve% Open
10	10	10	5
20	16	16	13
30	25	25	22
40	39	39	29
50	58	58	33
60	83	83	41
70	100	100	46
80	107	107	48
90	109	109	49
100	110	110	50

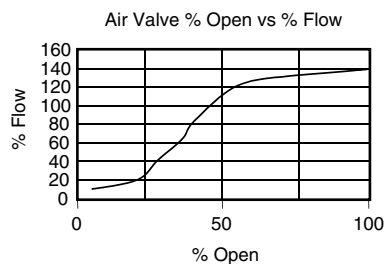


FIGURE 8.23 Typical butterfly type valve calculation.

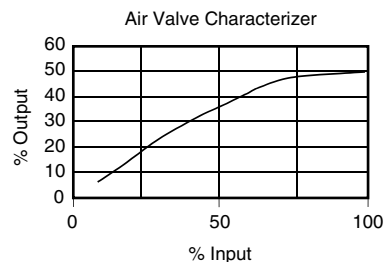


FIGURE 8.24 The required shape of the air valve characterizer.

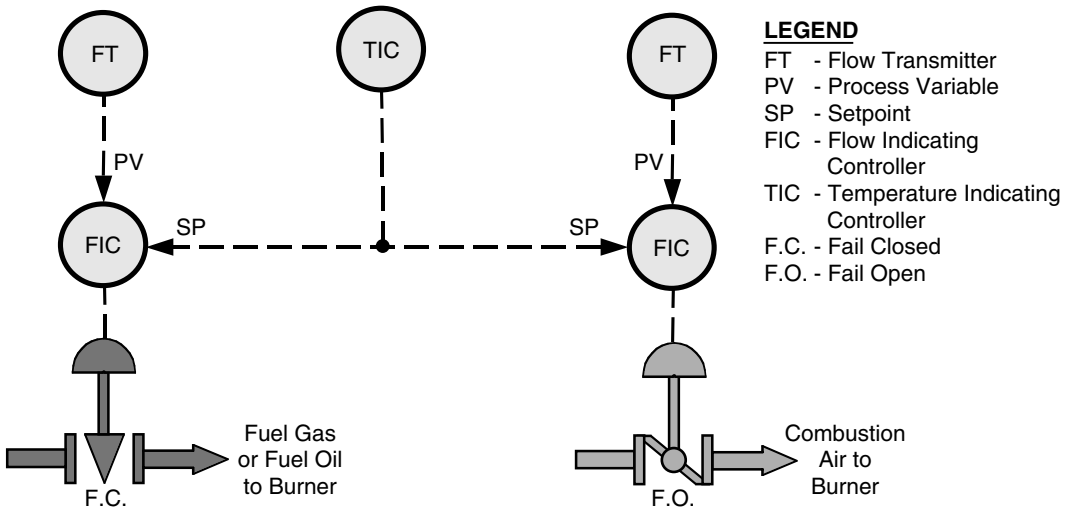


FIGURE 8.25 Fully metered control.

8.3.2 FULLY METERED CROSS LIMITING

Development of a fully metered control scheme for modulating fuel and air to a burner begins with the parallel positioning electronically linked scheme as previously shown in [Figure 8.20](#). [Figure 8.25](#) adds flow meters and flow controllers.

Flow meters are linear with flow rate. Meter output signal scaling provides the firing rate and air/fuel ratio required for the application. The combustion air characterizer used for parallel positioning is not required because the transmitters are linear with flow rate.

In the illustration, temperature controller TIC output sets the firing rate by serving as the setpoint to each flow controller. Signal inversion, shown as $(1 - \text{parameter value})$ in the parallel positioning scheme, is not required. Instead, the controller output mode is configured to match the valve failure mode.

Controller output mode, reverse or direct acting, defines the change in output signal direction with respect to process variable changes. For example, if the controller output increases as the process variable increases, the controller mode is direct-acting. In combustion control schemes, fail-closed fuel valves require a reverse-acting flow controller, while fail-open combustion air valves require direct-acting flow controllers. From controller mode definitions, it is clear that the temperature controller TIC should be reverse-acting. That is, the TIC output should decrease, reducing the firing rate, in response to an increase in temperature, the process variable.

Addition of high and low signal selectors provides cross limiting of the fully metered control scheme as shown in [Figure 8.26](#). The low signal selector ($<$) compares demanded firing rate from the TIC to the actual combustion air flow rate and applies the lower of the two signals as setpoint to the fuel flow controller. The low signal selector ensures that the fuel setpoint cannot exceed the amount of air available for combustion.

The high signal selector compares the demanded firing rate from the TIC to the actual fuel flow rate and applies the higher of the two signals as the setpoint to the airflow controller. This ensures that the air setpoint is never lower than required for combustion of actual fuel flow rate.

Together, the high and low signal selectors ensure that unburned fuel does not occur in the combustion system. Unburned fuel accumulations can cause explosions. Cross limiting by the signal selectors causes air flow to lead fuel flow during load increases and air flow lags fuel flow during fuel decreases. This lead-lag action explains why the fully metered cross-limiting control system is often called “Lead-Lag” control. Whatever the name, the system performs the function of maintaining

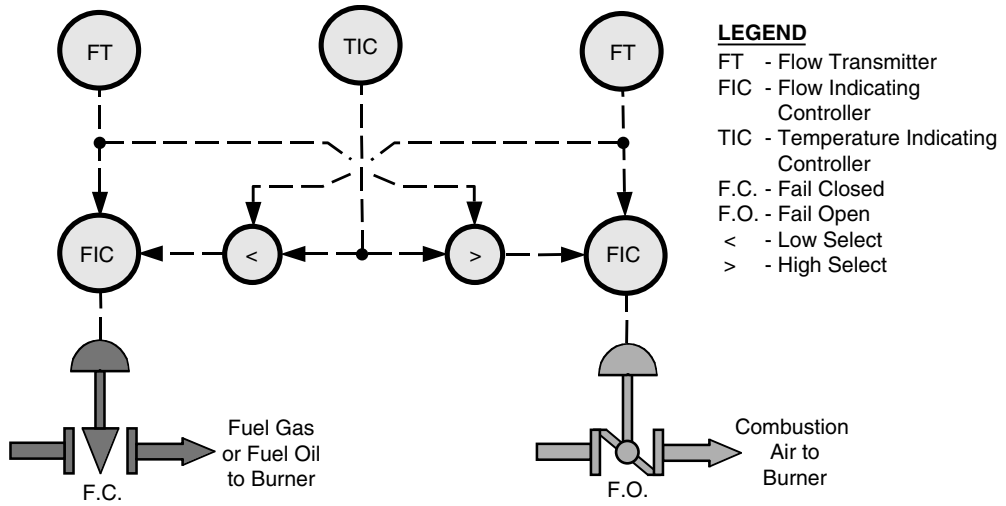


FIGURE 8.26 Fully metered with cross limiting.

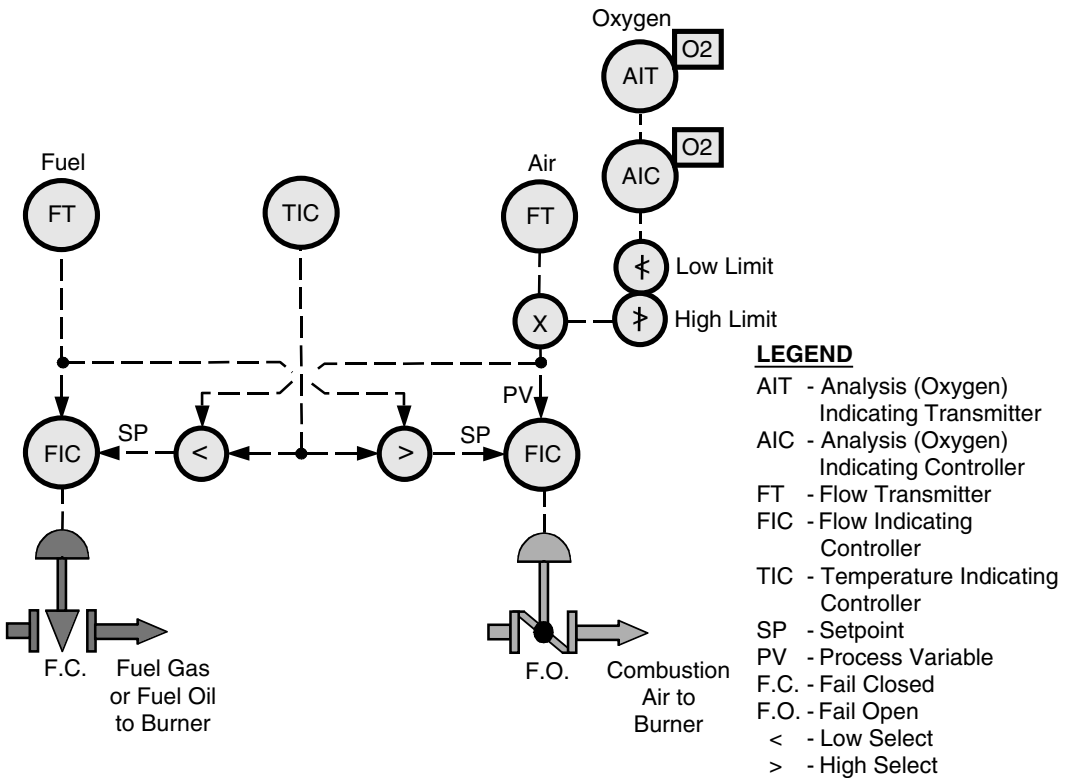


FIGURE 8.27 O₂ trim of air flow rate.

the desired air/fuel mixture during load changes. The system also provides fuel flow rate reduction in the event airflow is lost or decreased.

It is possible to trim the control scheme by measuring the flue gas oxygen content, as in Figure 8.27. For most systems, the oxygen signal should be used to “trim” and not be a primary control. Many oxygen analyzers are high maintenance and/or too slow in response to be used as

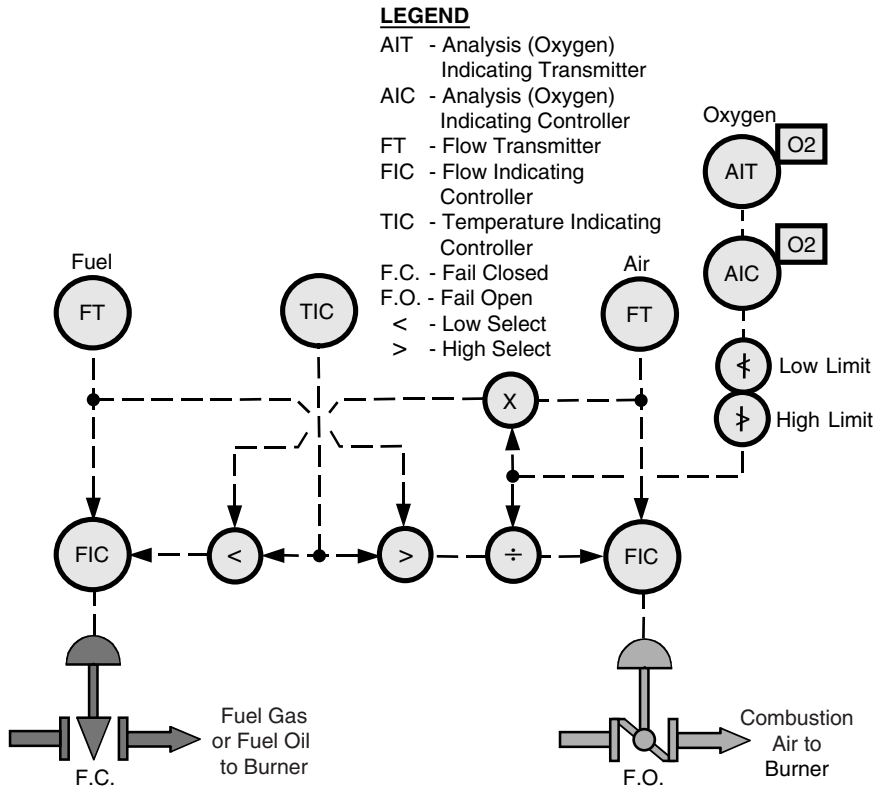


FIGURE 8.28 O₂ trim of air setpoint.

primary control in the combustion process. As shown, the oxygen controller is utilized for setpoint injection and provides tuning parameters to help process customization. High and low signal limiters restrict the oxygen controller output to a trimming function, normally 5 to 10% of the normal combustion air flow rate.

A multiplication function (×) in the combustion airflow transmitter signal makes the oxygen trim adjustment. The multiplier gives a fixed trim gain. Substituting a summing function for the multiplier would result in high trim gain at low flow rates and could produce a combustion air deficiency.

Oxygen trim can be applied to the combustion airflow controller setpoint rather than the flow transmitter signal. If this technique is used, the airflow signal to the low signal selector must retain trim modification. See [Figure 8.28](#) for the scheme.

Multiple fuels and oxygen sources are accommodated by the cross-limiting scheme as shown in [Figure 8.29](#). When multiple fuels are used, heating values must be normalized by adjusting flow transmitter spans or by addition of heating value multipliers. Similar methods are used to normalize oxygen content for multiple air sources.

8.4 CONTROLLERS

Controllers have historically been called analog controllers because the process and I/O signals are usually analog. Controller internal functions performed within a computer or microprocessor by algorithm are sometimes called digital controllers although the I/O largely remains analog. Some digital controllers communicate with other devices via digital communication, but for the most part, controllers connect other devices by analog signals. The analog signal is usually 4 to 20 milliamps, DC.

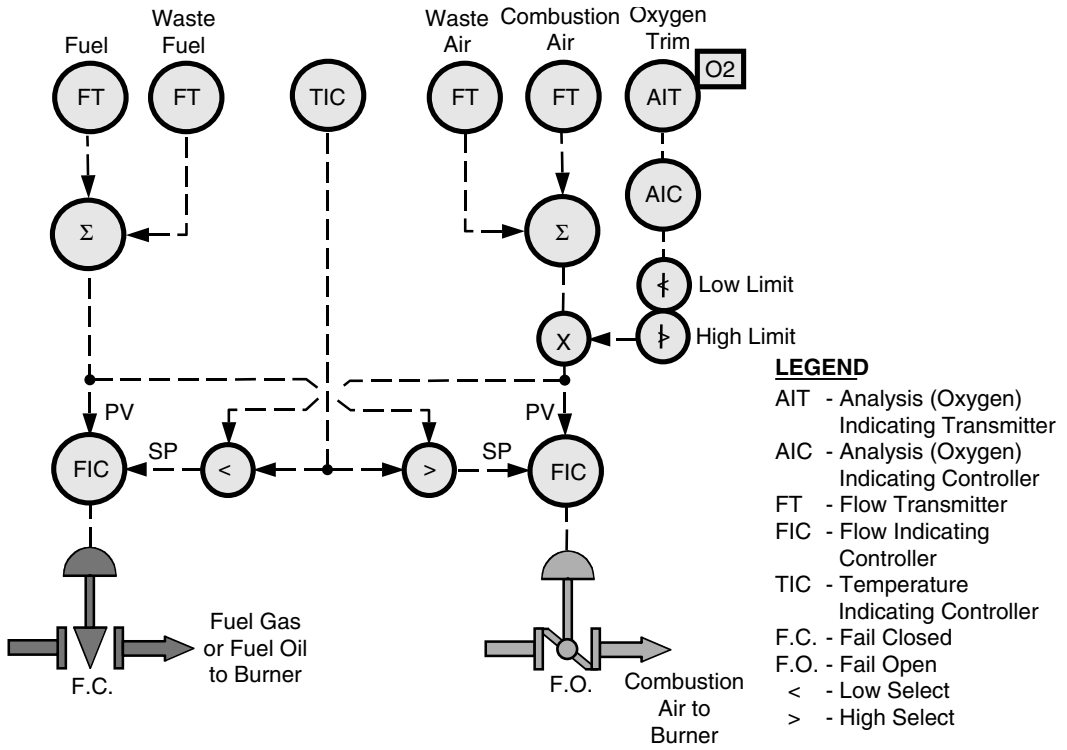


FIGURE 8.29 Multiple fuels and O₂ sources.

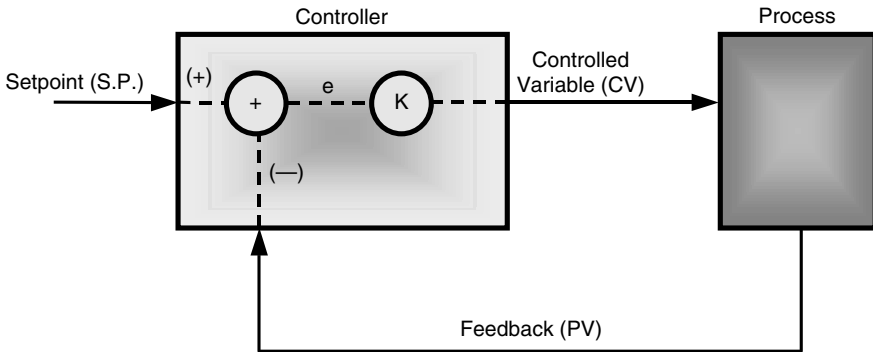


FIGURE 8.30 Controller.

In Figure 8.30, the setpoint is a signal representing the desired value of a process. If the process is flow rate, setpoint is the desired flow rate. Setpoint signals can be generated internally within the controller, called the local setpoint, or can be an external signal, called the remote setpoint.

Controller output, called the controlled variable (CV) or the manipulated variable (MV), connects to a final element in the process. In our example of flow control, the final element is probably a control valve. Feedback from the process, called the process variable (PV) in our example, could be the signal from a flow meter.

The CV is generated within the controller by subtracting the feedback (PV) from the setpoint (SP), generating an error signal “ e ,” which is multiplied by a gain “ K .” The product eK is the controller output (CV).

$$\text{Output (CV)} = (\text{SP} - \text{PV})(K) = eK \tag{8.1}$$

This simple controller is an example of the first controller built early in the 20th century and is called a proportional controller. The output is proportional to the error signal. The proportional factor is the gain K . Proportional controllers require an error (e) to produce an output. If the error is zero, controller output is zero. To obtain an output that produces the correct value of the process variable, the operator is required to adjust the setpoint higher than the desired process variable in order to create the requisite error signal. Reduction of error by increasing controller gain is limited by controller instability at high gain.

Offset is the term given to the difference between the setpoint and process variable. Correction of offset was the first improvement made to the original controller. Offset correction was accomplished by adding bias to the controller output.

$$\text{Output (CV)} = eK + \text{Bias} \tag{8.2}$$

Bias adjustment required operator manipulation of a knob or lever on the controller, which added bias until setpoint and process variables were equal. The operator considered the controller “reset” when equality occurred. Each setpoint change or process gain change required a “manual reset” of the controller. Figure 8.31 illustrates the proportional controller with manual reset.

Many operators prefer the term “proportional band” when describing controller gain. Proportional band is defined as:

$$\text{Proportional band (PB)} = \frac{100}{\text{Gain}} = \frac{100\%}{K} \tag{8.3}$$

Proportional band (PB) represents the percent change in the process variable (PV) required to change the controller output 100%. For example, a controller gain of 1 ($K = 1.0$) requires a PV change of 100% to obtain a 100% change in controller output. Proportional bands for combustion process variables are generally in the range of 1000% to 20% (Gain = 0.1 to 5.0). Flow controller gains are always less than unity. Temperature controller gains vary from 0.1 to 3.0, depending on the process gain. Pressure controllers generally have gains higher than those of flow or temperature controllers. Controller output becomes unstable (oscillatory) when gain is too high. When instability occurs, the controller operating mode must be changed from automatic to manual to stabilize the

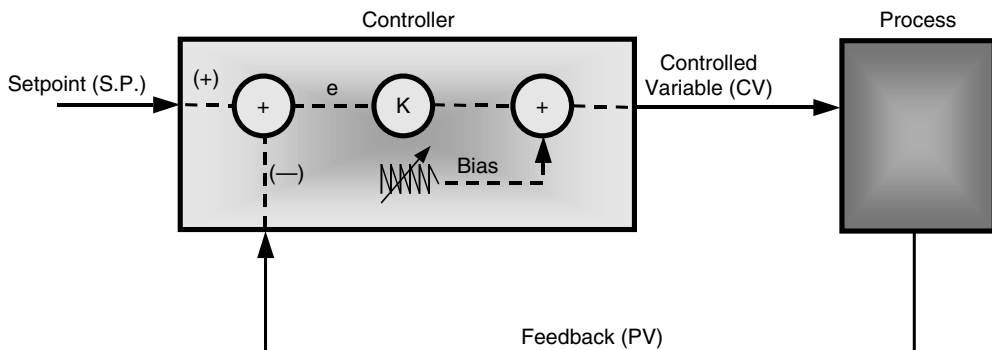


FIGURE 8.31 Analog controller with manual reset.

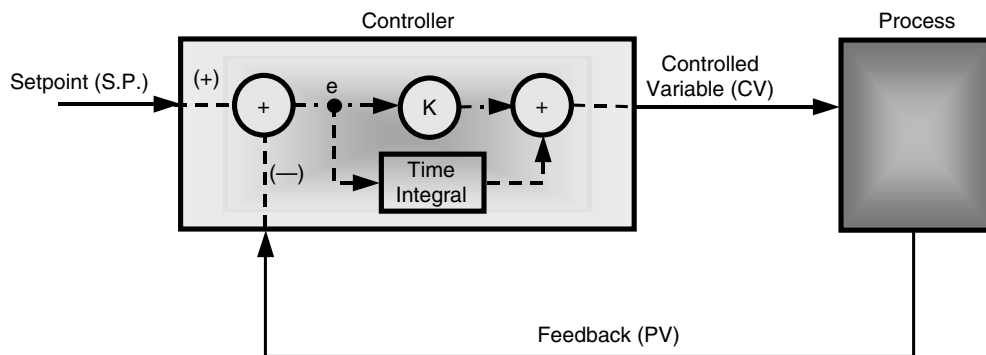


FIGURE 8.32 Analog controller with automatic reset.

process and prevent equipment damage. A reduction of controller gain must occur before a return to automatic mode.

Automatic reset was the next improvement to the process controller. This was a most welcome addition that eliminated the need for manual reset. Automatic reset is a time integral of the error signal, summed with the proportional gain signal, to produce the controller output. Integral gain (controller reset) is highest with large errors and continues until the error is reduced to zero. [Figure 8.32](#) illustrates automatic reset.

Automatic reset is the “I” component of a PID (three-mode) controller. P is proportional gain and D is derivative (rate) gain. I is expressed as repeats per minute (RPM), or as minutes per repeat (MPR), depending on the controller manufacturer’s choice of terms. Some controllers permit user selection of the term. Controller output is the same regardless of terminology, but the operator must know and apply proper tuning constants. For example, if tuning requires an I of 2 RPM, the operator must enter 0.5 MPR into the controller if MPR is the terminology in use. An integral gain of 0.5 minutes per repeat means that automatic reset equal to the proportional gain will be applied at the controller output each 30 seconds. Integral gain is a smooth continuous process that contributes phase lag to the system. Additional phase lag contributes to system instability (oscillation), which prohibits high values of integral gain.

Derivative gain is a function of how fast the process variable is changing. For slow-changing processes, derivative gain is of little use. Derivative gain is not used on flow control loops with head meters or on other loops with noisy process variable signals. High noise levels will drive derivative gain to instability. Derivative gain contributes phase lead that can sometimes be beneficial.

Controllers have many modes of operation. P, I, D, automatic, and manual modes have been discussed. Reverse or direct mode is another choice that must be configured to match the process. Reverse or direct describes the change in direction of controller output when the process variable changes. Reverse-acting means the controller output decreases if the process variable increases. An example illustrates how to select reverse or direct.

In our example of flow control, the process variable (flow rate) increases when the final element (control valve) opens. In addition, the flow meter output or process variable (PV) increases with increased flow rate. If the control valve fails closed and opens on increasing signal (increasing controller output), the controller mode must be reverse-acting. That is, if PV increases, the controller output must decrease to close the valve and restore the flow rate to the correct value. If the control valve fails open (closes on increasing signal), the controller mode must be direct-acting. This example illustrates the need to know if each element in a control loop is reverse- or direct-acting, including transmitters, isolators, transducers (such as I/Ps), positioners, and actuators. Proper selection and configuration of loop elements provide not only proper operation, but also proper failure mode. Reversal of any two elements within a loop will not affect loop response, but failure modes will change.

8.5 TUNING

Many modern controllers have automatic tuning routines built in. Tuning parameters calculated automatically require a loop upset to enable calculation. Parameters are normally de-tuned considerably from optimum because process gains are often nonlinear. Variable loop gain can also be a problem for manual tuning. A controller tuned at low flow rates or low temperature could become unstable at high flow rates or high temperatures. Control of most process loops benefit from addition of feed forward components that relieve the feedback controller of primary control. Operation improves if the feedback controller functions as set point injection and error trimming of the feedforward system.

Many processes controlled by a current proportional controller successfully use the tuning procedure below. The process must be upset to produce oscillations of the process variable. A graphic recorder should be used to determine when the oscillations are constant and to ascertain the time for one cycle (oscillation).

1. In manual mode, adjust the output to bring the process variable (PV) near the desired value.
2. Set the Rate time to 0 minutes and set the Reset time to the maximum value (50.00 minutes), or set repeats per minute to the minimum value to minimize reset action.
3. Increase gain (decrease proportional band PB) significantly. Try a factor of 10.
4. Adjust the local setpoint to equal PV and switch to automatic mode.
5. Increase the setpoint by 5 or 10% and observe PV response.
6. If the process variable oscillates, determine the time for one oscillation. If it does not oscillate, return to the original setpoint, increase the gain again by a factor of two, and repeat Step 5.
7. If the oscillation of Step 6 dampens before the cycle time is measured, increase the gain slightly and try again. If the oscillation amplitude becomes excessive, decrease the gain slightly and try again.
8. Record the current value of gain, and record the value for one completed oscillation of PV.
9. Calculate Gain, Reset, and Rate:
 - a. For PI (two-mode controller):
Gain = Measured gain \times 0.5
Reset Time = Measured time/1.2 (MPR)
 - b. For PID (three-mode controller)
Gain = Measured gain \times 0.6
Reset Time = Measured time/2.0 (MPR)
Rate = Measured time/8.0 (minutes)
10. Enter the values of Gain, Reset, and Rate into the controller.
11. Make additional trimming adjustments, if necessary, to fine-tune the controller.
12. To reduce overshoot: less gain, perhaps a longer rate time.
13. To increase overshoot or increase speed of response: more gain, perhaps shorter rate time.

The above method is known as a closed-loop method because the controller is dynamically affecting the process. Another method that can be used is an open-loop method in which the controller is taken out of automatic operation and placed in manual mode. A data logger should be utilized to record the process variable and the controller output. Care should be taken prior to using this method to ensure that the operator can maintain control of the process while the controller is in manual mode.

1. Place the controller in manual mode.
2. When the process is stable, make a step change in the controller output.

3. The information obtained from this step change includes apparent dead time and slope. The apparent dead time is the time from when the controller output step change is executed to when the process variable begins to react. The slope is the initial slope of the process variable once it begins to react. The slope is the change per minute of the process variable (expressed as a percentage of the transmitter span) divided by the step change (expressed as a percentage of the controller output span).
4. Calculate Gain, Reset, and Rate:
 - a. Gain = $1/(\text{Rate} \times \text{Dead time})$, aggressive
 - b. Gain = $1/(2 \times \text{Rate} \times \text{Dead time})$, conservative
 - c. Reset time = $5 \times \text{Dead time}$
 - d. Rate = $\text{Dead time}/2$
5. Enter the Gain, Reset, and Rate values into the controller and place it into automatic mode.
6. Make small setpoint changes and observe the response.
7. Make additional trimming adjustments, if necessary, to fine-tune the controller.
8. To reduce overshoot: less gain, perhaps a longer rate time.
9. To increase overshoot or increase speed of response: more gain, perhaps shorter rate time.

REFERENCES

1. Joel O. Hougren, *Measurement and Control Applications for Practicing Engineers*, CAHNERS Books, Barnes & Noble Series for Professional Development, 1972.
2. *Combustion Control*, 9ATM1, Fisher Controls, Marshalltown, IA, 1976.
3. Boiler Control, Application Data Sheet 3028, Rosemount Inc., Minneapolis, MN, 1980.
4. Instrumentation Symbols and Identification, ANSI/ISA – S5.1 – 1984, Instrument Society of America, Research Triangle Park, NC, 1984.
5. Temperature Measurement Thermocouples, ANSI – MC96.1 – 1984, Instrument Society of America, Research Triangle Park, NC, 1984.
6. F.G. Shinskey, *Process Control Systems, Application, Design, and Tuning*, 3rd edition, McGraw-Hill, New York, 1988.
7. Michael J. Gilbert Polonyi, PID controller tuning using standard form optimization, *Control Engineering Magazine*, March, 1989, 102–106.
8. David W. St.Clair, Improving control loop performance, *Control Engineering Magazine*, Oct., 141–143, 1991.
9. Controller Tuning, Section 11, UDC 3300 Digital Controller Product Manual, Honeywell Industrial Automation, Fort Washington, PA, 1992.
10. Fred Y. Thomasson, Five steps to better PID control, *CONTROL Magazine*, April, 65–67, 1995.
11. API Recommended Practice 556: Instrumentation and Control Systems for Fired Heaters and Steam Generators, First Edition, American Petroleum Institute, Washington, D.C., May 1997.
12. David W. St.Clair, PID Tuning: it's the method, not the rules, *INTECH*, Dec., 26–30, 1994.

9 Burner Testing

*Jeffrey Lewallen, P.E., and
Charles E. Baukal, Jr., Ph.D., P.E.*

CONTENTS

- 9.1 Introduction
 - 9.2 Thermal Environment
 - 9.2.1 Open Air
 - 9.2.2 Pilot Furnace
 - 9.2.3 Field Testing
 - 9.3 Burner Test Setup
 - 9.3.1 Application
 - 9.3.2 Test Furnace Selection Criteria
 - 9.3.3 Selection of Test Fuels
 - 9.4 Instrumentation and Measurements
 - 9.4.1 Combustion Inputs
 - 9.4.1.1 Fuel Flow Rate
 - 9.4.1.2 Combustion Air Flow Rate
 - 9.4.2 Combustor Conditions
 - 9.4.2.1 Furnace Temperature
 - 9.4.2.2 Burner Conditions
 - 9.4.2.3 Draft
 - 9.4.2.4 Flame Characteristics
 - 9.4.2.5 Heat Flux
 - 9.4.3 Emissions Measurements
 - 9.4.3.1 Exhaust Gas Flow Rate
 - 9.4.3.2 Exhaust Gas Temperature
 - 9.4.3.3 NO_x
 - 9.4.3.4 Carbon Monoxide
 - 9.4.3.5 O₂ (Wet and Dry)
 - 9.4.3.6 Unburned Hydrocarbons (UHCs)
 - 9.4.3.7 Particulates
 - 9.4.3.8 Noise
 - 9.5 Test Matrix (Test Procedure)
 - 9.5.1 Heater Operation Specifications
 - 9.5.2 Performance Guarantee Specifications
 - 9.5.2.1 Emissions Guarantees
 - 9.5.2.2 Noise
 - 9.5.2.3 Fuel and Air-Side Pressure Drop
 - 9.5.2.4 Flame Dimension Guarantees
 - 9.5.3 Data Collection
 - 9.6 Conclusion
 - References
-

9.1 INTRODUCTION

Burner testing provides an opportunity to gather and verify valuable information such as operating parameters, pollutant emissions, flame dimensions, heat flux profile, safety limitations, and noise data. Information from test data is often essential for performance verification of customer applications as well as being vital to research and development efforts. Empirical data collected from burner testing is a valuable source of information that can be used to improve the predictive capabilities of CFD models (see Chapter 5 and Reference 1), which are becoming more prevalent tools used in the research, development, and design of combustion equipment at the forefront of technology in the industry. At state-of-the-art test facilities as shown in Figure 9.1, testing is done year-round to provide customers the data they need to improve heater designs and operate their heaters and furnaces more efficiently and to develop new technology to meet the ever-increasing demands of customer processes and environmental regulation.

While designing a burner appears to involve relatively simple calculations, it is difficult to predict how a burner will operate over a broad range of operating conditions. Consider the multitude of heater and furnace applications, the wide range of available fuels and oxidants, the required pollutant levels to be met, and the different furnace operating conditions. The variations between burner designs are numerous. Through full-scale testing, specific conditions can be simulated and the actual operational performance of a burner can be measured accurately. Testing allows a burner manufacturer to optimize a burner design to closely meet the requirements of a specific application.

An important operating parameter that can be obtained through testing includes the heat release range of the burner. Burners are sized for a maximum heat release with a specified turndown, or the minimum rate at which a burner can be safely operated. Turndown is defined as the ratio of maximum heat release to minimum heat release:

$$\text{turndown} = \frac{\text{maximum firing rate}}{\text{minimum firing rate}} \quad (9.1)$$

For example, if the maximum heat release of a burner is 5×10^6 Btu/hr and the minimum heat release of that burner is 1×10^6 Btu/hr, then the turndown is 5:1. Another variable that operators and engineers may need to know is what happens to a burner if it is fired beyond its maximum designed heat release. With this performance information, a customer can set a target oxygen level in the flue gas to stay above or set an upper pressure limit for a given fuel to stay below to ensure that the burner does not exceed the designed parameters. More important, test data can determine the upper heat release value at which a burner can be safely operated for short durations until a process upset can be corrected.

An operator also needs to know the point at which a burner will become unstable if fired below the minimum heat release. The rate at which a burner can be fired below the designed minimum heat release is defined as the absolute minimum. A lower pressure limit can be set as a safety limit for the fuel gas to ensure safe heater operation. This information is especially useful in determining how many burners should be fired, and at what heat release, for special operations.

Along with defining the firing envelope of a burner, the combustion air settings can be determined through testing to ensure the efficient operation of a heater or furnace by controlling the excess oxygen in the flue gas. By running at lower oxygen concentrations, fuel savings can be realized, thus leading to higher heater efficiency. In complex furnaces such as ethylene heaters, which may have hundreds of burners in operation at once, advanced knowledge of air door settings for various operating conditions can save valuable time in trimming the excess air during actual operation.

Other information that can be collected during a burner test or demonstration is the emissions of pollutants such as NO_x, CO, and unburned hydrocarbons (UHC). While it is easy to predict emissions for a single fuel, modern burners are often expected to operate acceptably on a wide



FIGURE 9.1 John Zink Co. LLC. R&D Test Center, Tulsa, Oklahoma. (Courtesy of John Zink Co., LLC.²¹)

range of fuels. As a result, some fuels may not be fired at their optimum pressures, and variables such as fuel pressure can significantly affect the emission performance of a burner. By testing a burner in an operating furnace prior to final installation, the expected emissions for different operating conditions can be predicted and anticipated with a greater degree of accuracy.

When firing burners on a wide variety of fuels, flame dimensions can change, depending on the fuel fired, the operating fuel pressure, and the heat release, because the mixing energy available can significantly affect the volume or shape of a flame. By conducting a burner test over the normal operating envelope of a burner, the dimensions of the flame can be determined for all conditions. The flame dimensions are important to ensure that there is proper heat distribution in the combustion and that the flames do not impinge undesirably on anything in the combustor.

Another valuable piece of data that can be collected is noise. New and existing plants are being more strictly regulated and are required to reduce noise levels. Depending on the severity of the requirement, mufflers can be designed to attenuate the burner noise to acceptable levels (see Chapter 7).

Some burners are designed to heat a furnace wall. For these burners, heat flux profiles can be determined through testing to provide heater manufacturers with information about the transfer of heat radiated from the wall to the process tubes. By optimizing the heat flux profile, the heat transfer to the load can be optimized to maximize the overall system thermal efficiency.

Testing can provide a variety of data concerning a burner's performance. But without a proper setup, the correct instrumentation and measurement methods, and a well-defined test procedure (test matrix), the data collected during a test may have little or no meaning. This chapter discusses the proper elements required for conducting a test. Items discussed include identifying the application of the burner, selecting the correct test environment, and determining the test fuels to be utilized during testing.

This chapter also discusses the instrumentation necessary to record consistent and accurate data. This includes the concentration of NO_x, CO, O₂ (wet and dry), unburned hydrocarbons (UHC), and particulates in the flue gas; heat flux; and noise emissions from the burner. Fuel flow metering and flame measurement are also discussed.

With input from the furnace manufacturer and end user, a meaningful test procedure can be put together that will yield valuable data in determining a burner's performance under different operating conditions. The test procedure is designed to answer a specific set of questions regarding the performance of the burner. By closely matching the conditions of operation expected in the field, data can be collected that will aid operators in running their furnaces.

Finally, this chapter discusses data analysis. Once a test is run, it must be determined if the burner has met the criteria outlined in the test procedure. The criteria include performance guarantees and operating parameters. With the data collected, the test engineer can optimize the burner to improve emissions, flame dimensions, stability, and air flow distribution.

Armed with the knowledge described above, customers will have a greater understanding of what to expect from a burner test, as well as what goes into setting up and conducting a test that will provide meaningful data. API 535 gives some good guidelines for specifications and data required for burners used in fired heaters.²

Several excellent general references have been published concerning combustion diagnostics. An early book by Beér and Chigier (1972)³ gives detailed descriptions and diagrams of different probes used to make measurements in industrial-scale flames. The report by Okoh and Brown (1988)⁴ reviews and compares many techniques for the measurement of a wide range of variables in combustion systems. It also includes equipment specifications and suppliers. The books edited by Durão et al. (1992)⁵ and Taylor (1993)⁶ contain chapters on the use of both physical probes and optical techniques. Fristrom (1995)⁷ has several chapters devoted to probe and optical measurements in flames. The books by Eckbreth (1988)⁸ and Chigier (1991)⁹ focus specifically on optical techniques for diagnosing flames. The articles by Fristrom (1976),¹⁰ Bowman (1977),¹¹ Gouldin (1980),¹² and Becker (1993)¹³ review probe measurements in flames. Newbold et al. (1996)¹⁴ gave a good example of making probe measurements of velocity, species, radiation, and gas temperature in an

industrial, gas-fired, flat-glass furnace. Solomon et al. (1986)¹⁵ reviewed Fourier transform infrared (FTIR) optical techniques for measuring particles, species concentrations, and temperature in combustion processes. Articles are available on the use of laser diagnostics in combustion systems.^{16–20} Lewallen et al. (2001)²¹ have written a book chapter on burner testing for the hydrocarbon and petrochemical industries.

9.2 THERMAL ENVIRONMENT

There are three common thermal environments used to test burners: open air testing, a test or pilot furnace test (usually a single burner test), or testing in the actual application or furnace. Each method offers its own set of advantages and disadvantages.

9.2.1 OPEN AIR

While testing in open air can provide a stunning visual observation of the burner's flame and its characteristics, open air testing provides very limited information required to evaluate a burner's suitability for its intended operation. In essentially all industrial combustion applications, the burners are fired in some type of combustor. As an example, burners designed for petrochemical and refining industries operate under vessel pressures that are slightly less than atmospheric pressure or are fired into pressurized vessels. In both cases, the equipment is fired into a controlled volume so that the heat generated can be transferred to the heat load. Therefore, an important limitation of open air firing is the lack of an enclosure. As government agencies continue to work on the problem of clean air, the demand for burner equipment that produces lower and lower levels of NO_x, CO, unburned hydrocarbons (UHCs or VOCs), and particulate emissions continually pushes equipment manufacturers to come up with innovative ways to reduce emissions. As a result, burner testing must be conducted in a combustor that allows the firing of fuel mixed with an oxidant (ambient air, preheated air, turbine exhaust gas, oxygen-enriched air, or pure oxygen) through the burner and out of an exit to pass the flue products out.

The stack of a furnace is sampled to measure the pollutants mentioned earlier (NO_x, CO, UHC, etc.) in order to determine if the equipment is meeting the permitted levels required by the local environmental agency. To test burner equipment, most manufacturers have testing facilities that allow the burner equipment to be tested so that emission data can be collected.

9.2.2 PILOT FURNACE

Pilot furnaces provide an enclosure for burners to be fired in. Burner manufacturers are interested in testing the equipment for a number of reasons. These include confirming capacity (heat release rate), ensuring air and fuel metering is at the desired pressure drop, verifying flame shape (or heat flux profile), and analyzing the pollutants produced by the burner. Pilot or test furnaces are typically sized to handle a limited range of heat input and burner configurations (up-fired, down-fired, fired adjacent to a wall, or fired radially against a wall). The test furnace gives accurate information on how a single burner operates, whereas many industrial furnaces use multiple burners.

This pilot-scale furnace data is then used to predict the performance in a given application. Due to the wide range of commercial applications, single burner pilot furnaces are attractive for their flexibility. Test setups can be implemented and dismantled for a relatively low cost compared to testing multiple pieces of equipment at the same time. Depending on the application, testing more than one burner can create problems for adequately cooling the furnace to the desired operating conditions. Most test furnaces are water cooled, either by passing water (or other heat-absorbing media) through tubes or encapsulating the furnace with a water jacket. Most of the heat generated during pilot testing is waste heat as no product is being processed during testing.

Another significant limitation to pilot testing or single-burner testing is the impact of the proximity of multiple burners in an actual application, or the furnace fluid dynamics. Depending on the configuration of the actual furnace, the circulation of flue products within the furnace can be dramatically different than the circulation pattern in a test furnace. This can result in poor flame quality, higher emissions, and the added risk of improper heat transfer in the actual application. To compensate for the differences in pilot furnaces compared to operating furnaces, other tools must be used in conjunction with a burner test to gain insight into and a predictive capability of how a burner or multiple burners will perform. Additional avenues include computational fluid dynamics or CFD (see Chapter 5), physical testing (see Chapter 10), and field-testing (discussed below).

9.2.3 FIELD TESTING

Simply put, field testing is collecting available data from furnaces in operation to evaluate the performance of burners. There are many advantages to field testing. Here, this refers to testing in actual furnaces that are test sites designed to demonstrate feasibility. These test sites may or may not be eventual end users. Field test furnaces are generally representative of typical furnaces for a given application, including multiple burner operation. The data collected is extremely valuable as it validates the calculations that burner manufacturers use to predict burner performance. The impact of burner-to-burner proximity (or spacing) can be evaluated as can the effect of the flue gas currents within the furnace on the flame envelope.

There are also some disadvantages to field testing. One is the confidentiality of the data collected. Most industries are extremely competitive and rival companies are reluctant to share data that may or may not be giving them a competitive edge in the market. Also, furnaces, with the passage of time, begin to “leak.” Leaks are, by definition, any area in a furnace where air is allowed to enter the vessel other than through the air entry of the burner. This problem is often not easily detected. Most furnaces are outfitted with an oxygen analyzer that monitors the percentage of oxygen in the flue gases exiting the stack. For most applications this is approximately 2 to 3% oxygen (volume, dry) in the flue gas. With excessive leakage of an air source, the uncontrolled air may negate the pollutant-reducing technology employed by the burners. Another limitation is often a lack of instrumentation. Outfitting an actual operating furnace with analytical equipment to measure emissions, fuel and air flow, and process conditions can be very expensive. Due to the limitations of economics, furnaces are typically fitted with the minimum amount of required instruments to safely operate and produce products. Finally, the sole reason for the existence of furnaces is for generating product and producing a profit. Supply and demand dictates at what condition the heater is operating and it is difficult to coordinate a time that the heater will be operating at design conditions for a period of time sufficiently long enough to record a complete set of data that gives an accurate representation of the burner’s performance.

9.3 BURNER TEST SETUP

One of the most important aspects of a burner test is the setup. This includes the selection of a test combustor, which is determined by the type of burner to be tested and its installation configuration. Typically, test furnaces are built with one of two common methods of cooling: a water-cooled jacket or a series of water-cooled tubes. A water jacket is simply a furnace surrounded by two shells (an inner and outer) of carbon steel that contains circulating water between the shells. This keeps cooling water on the four vertical surfaces to transfer heat. The other method utilizes cooling tubes that run either horizontally or vertically along one or two of the furnace walls.

Burners are designed to cover a wide range of applications. They are vertically up-fired, vertically down-fired, or horizontally fired. They can have round or rectangular flames and can be free-standing (away from the walls) or fired along a refractory wall. The criteria for selecting a burner normally includes the fuel to be fired, oxidant (typically air) supply method, emission

requirements, and heater configuration. Fuels can be gas, oil, waste gas, or some combination of the three. The combustion air supply can be either natural (induced) draft, forced draft, turbine exhaust gas, or other sources of oxygen. Emission requirements are primarily based on NO_x but can include unburned hydrocarbons, carbon monoxide, SO_x, and particulates.

The test fuel blend is an important component of a successful test, particularly those for burners used in petrochemical applications. Without the proper blend, a simulated fuel may or may not provide data that will aide engineers and operators when starting up new units or evaluating the performance of new burners installed in an existing unit. Test fuels are typically blended to closely simulate the heating value, flame temperature, specific gravity, and major components of the fuels to be used in the actual application. Another example of the importance of the test fuel is the case where fuel oil is used. The nitrogen content in heavy fuel oils is very important in determining NO_x emissions. In some cases, chemicals such as pyridine may need to be added to the test fuel to match the nitrogen content in the actual fuel.

9.3.1 APPLICATION

Although any fuel (solid, liquid, or gas) can be used in a burner designed for a specified fuel type, this chapter is limited to gas and liquid fuel firing because they are, by far, the most common found in most industrial applications. When firing a fuel, the normal products of combustion are CO₂, H₂O, N₂, O₂, and the energy or heat released during a combustion process. Unfortunately, there are also other less desirable products that can be released. These commonly include unburned hydrocarbons (UHCs), particulates, NO_x, SO_x, and CO.

9.3.2 TEST FURNACE SELECTION CRITERIA

The selection of a test furnace is important. The furnace should be big enough to contain the flame without impingement on the walls or ceiling of the furnace. Also, it is important to select the proper furnace to keep the furnace temperature close to the customer's expected furnace temperature. The following figures show some typical furnaces used for burner testing.

The furnace shown in [Figure 9.2](#) can be tested in a variety of configurations. Wall-fired burners can be tested at the floor level and radiant wall burners can be tested at higher elevations in the furnace to match the end-use configuration. The number of burners can be changed to simulate the setup in the field as well as to achieve a certain furnace temperature.

The furnaces shown in [Figure 9.3](#) can be tested in the down-fired configuration to simulate certain types of reformers in the petrochemical industry where the burners are installed on the roof of the furnace and fired down in between the process tubes. Another type of furnace is a vertical cylindrical water-jacketed furnace as shown in [Figure 9.4](#).

Because test facilities are not built for the purpose of heating an actual load (e.g., a hydrocarbon fluid in a petrochemical application) to a desired temperature or creating products, the heat released from the burners must be absorbed by some method. The furnace shown in [Figure 9.4](#) is surrounded by a shell filled with water. [Figure 9.5](#) shows a test furnace used to demonstrate burners for terrace wall reformers.

9.3.3 SELECTION OF TEST FUELS

The main criteria for fuel selection include the similarity in combustion characteristics with the actual fuel specified for the application, economics, availability, and compatibility with the systems, operations, and equipment. [Figure 9.6](#) shows both permanent and portable fuel storage tanks. Portable tanks can be used when testing is required on specialty fuels.

Probably the most critical component of successfully testing a burner is the selection of the test fuel. Without matching key components in the customer's fuel, the emissions, stability, and flame shape shown during a burner test may vary greatly when compared to the field results.



FIGURE 9.2 Test furnace for simulation of ethylene furnaces. (Courtesy of John Zink Co., LLC.²¹)

Fuel can be blended to the heating value or molecular weight as specified or as mutually agreed upon with the customer. Fuel and the diluent content of the fuel gas blend should be similar in volumetric proportion as in the specified actual service fuel gas if these proportions significantly impact burner performance. The Wobbe index is often used when reviewing a test blend that will be used to simulate a fuel. The Wobbe index is the higher heating value (HHV) of a fuel, divided by the square root of its specific gravity (SG):

$$\text{Wobbe index} = \frac{HHV}{\sqrt{SG}} \quad (9.2)$$

The specific gravity (SG) for a gas is the ratio of the molecular weight of a gaseous fluid to the molecular weight of air. The specific gravity for a liquid is the ratio of the density of a liquid to the density of water. It is important to note that the two fluids must be compared at the same temperature. Two fuels will provide the same heat release from a gas tip at a given supply pressure if the Wobbe index is the same.



FIGURE 9.3 Test furnace for simulation of downfired tests. (Courtesy of John Zink Co., LLC.²¹)



FIGURE 9.4 Test furnace for simulation of upfired tests. (Courtesy of John Zink Co., LLC.²¹)

While the Wobbe index is a good indicator to see if a fuel is similar, it is important to try and match the lower heating value (LHV), molecular weight, and adiabatic flame temperature to ensure a good simulation. Commonly available gaseous fuels for blending at well-equipped test facilities include natural gas, propane, propylene, butane, hydrogen, nitrogen, and carbon dioxide. The composition of natural gas varies by geographic location. As an example, Tulsa natural gas has a typical composition as shown in [Table 9.1](#).

[Table 9.2](#) illustrates a typical refinery gas and the points of interest in determining a test blend that will effectively simulate the fuel handling properties, burning characteristics (tendency of a fuel to coke, etc.), and emission levels of the customer's fuel composition.

Based on the available fuels for blending, the hydrogen content is matched, propylene is used to substitute the ethylene content, and Tulsa natural gas (TNG) is used to simulate the methane content. By holding the hydrogen content fixed at 38%, TNG and propylene are balanced to obtain a match of the lower heat value (LHV) and molecular weight. By attempting to balance the LHV, molecular weight, and adiabatic flame temperature, a test fuel blend of 34% TNG, 28% C_3H_6 , and 38% H_2 would be acceptable to simulate the refinery fuel gas illustrated in [Table 9.2](#). [Table 9.3](#) gives a side-by-side comparison of the fuel properties.

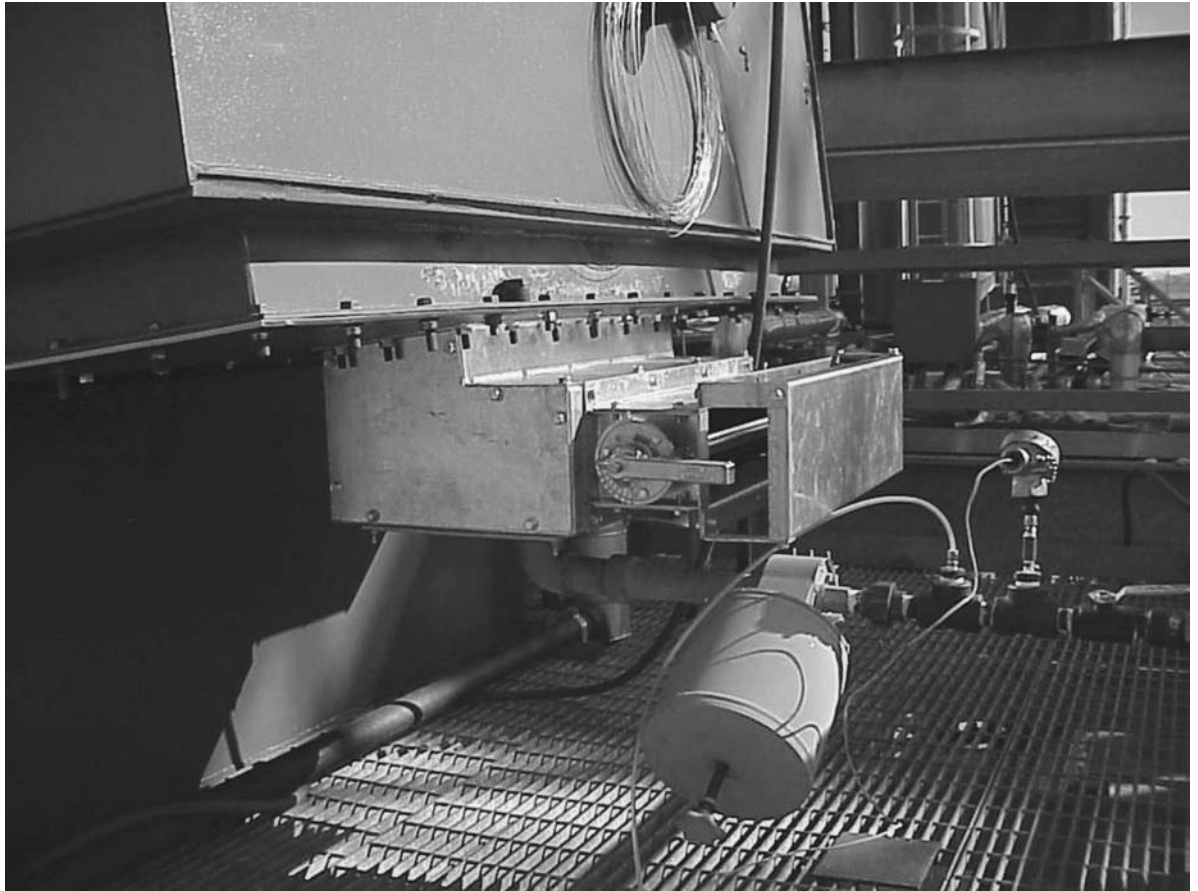


FIGURE 9.5 Test furnace for simulation of terrace wall reformers. (Courtesy of John Zink Co., LLC.²¹)



FIGURE 9.6 Test fuel storage tanks. (Courtesy of John Zink Co., LLC.²¹)

TABLE 9.1
Tulsa Natural Gas Nominal Composition and Properties²¹

CH ₄ (volume%)	93.4	C ₄ H ₁₀ (volume%)	0.20
C ₂ H ₄ (volume%)	2.70	CO ₂ (volume%)	0.70
C ₃ H ₈ (volume%)	0.60	N ₂ (volume%)	2.40
LHV (Btu/scf)	913	HHV(Btu/scf)	1012
Molecular weight	17.16	Specific heat ratio @ 60°F	1.3
Adiabatic flame temperature (°F)	3452		

TABLE 9.2
Typical Refinery Gas²¹

Fuel Component		
Name	Formula	volume %
Methane	CH ₄	8.13
Ethane	C ₂ H ₆	19.9
Propane	C ₃ H ₈	0.30
Butane	C ₄ H ₁₀	0.06
Ethylene	C ₂ H ₄	32.0
Propylene	C ₃ H ₆	0.78
Butylene	C ₄ H ₈	0.66
1-Pentene	C ₅ H ₁₀	0.07
Benzene	C ₆ H ₆	0.12
Carbon Monoxide	CO	0.22
Hydrogen	H ₂	37.8

Balance of fuel is primarily methane and ethane.

Note: level of olefins in the fuel.

Note: hydrogen content

TABLE 9.3
Comparison of Refinery Gas to Test Blend²¹

	Refinery Fuel	Test Fuel
LHV (Btu/sch)	1031	1026
HHV (Btu/scf)	1124	1121
Molecular Weight	18.09	18.38
Specific heat ratio @ 60°F	1.27	1.26
Adiabatic flame temperature (°F)	3481	3452
Wobbe Index	1422	1407

With the test fuel(s) established, it is time to determine what measurements will need to be taken and what instruments will be required.

9.4 INSTRUMENTATION AND MEASUREMENTS

Measurements generally required during testing include (but not limited to) fuel pressure and temperature, air pressure drop and temperature, fuel flow rates, flame dimensions, and emissions measurements.

9.4.1 COMBUSTION INPUTS

Combustion is the mixing of fuel and air to generate a reaction that produces energy. To conduct a successful test, many variables have to be measured throughout testing. The properties of the air and fuel must be measured, as well as the flue gas products resulting from combustion. In addition,

the operating conditions of the furnace must be measured in order to use the data collected. All test data must be corrected to the actual conditions that will be seen in the actual customer furnace.

9.4.1.1 Fuel Flow Rate

One of the most important aspects of burner testing is fuel metering. When firing a natural-draft burner, it is difficult to measure the flow rate of combustion air. Therefore, accurately metering the flow rate of each individual component used to make up a fuel blend is necessary to measure the heat release of the burner and its performance. There are many ways to measure flow, including differential pressure, magnetic, mass, oscillatory, turbine, and insertion flow meters just to name a few. For purposes of burner testing, the differential pressure flow meter will be discussed. Even limiting this discussion to differential flow meters, there are still several different methods of measurement available. Measuring the differential pressure across a known orifice plate is a common method to measure the gaseous fuel and steam flow. For liquid fuel firing, a coriolis meter is often used.

The orifice plate is the most commonly applied method of measuring flow.²² The advantage of using orifice plates (see Figure 9.7) is that they are versatile and can be changed to match a flow rate and fuel to be metered. Also, there is a significant amount of data concerning measuring fuel flow via an orifice plate. Finally, there are no moving parts to wear out. The drawbacks to orifice plates are that they are precision instruments and the following must be considered: the flatness of the plate, smoothness of the plate surface, cleanliness of the plate surface, sharpness of the upstream orifice edge, diameter of the orifice bore, and the thickness of the orifice edge. The critical inaccuracies due to these items can be alleviated by the purchase of ASTM-approved plates, rather than machining the plates. Another drawback is loss of accuracy when measuring flow rates of dirty



FIGURE 9.7 Orifice plate flow meter.

fuels. While dirty fuels are a way of life for the refining industry, test fuels are clean (no liquid or solid particles in the gaseous fuels) and such concern is minimized. Two items that should be verified when testing with orifice plates are that they are installed in the right direction (the paddle usually indicates the inlet side) and that the correct orifice bore is in the correct flow run.

While orifice plates can be used to meter liquids, coriolis meters are often preferred for measuring liquid fuel flow such as no. 6 oil or diesel oil. The coriolis meter operates on the basic principle of motion mechanics.²² The coriolis meter is able to measure the mass by measuring the amount of vibration the tube carrying the fluid is undergoing. The coriolis meter is a more expensive means of measurement, but this is often offset by its degree of accuracy and its low maintenance requirements.

9.4.1.2 Combustion Air Flow Rate

Combustion air flow rates are probably the most difficult measurements to make. Most applications are natural-draft applications where the differential pressure between the furnace and the external (or atmospheric air) to the combustion chamber creates air flow. This differential is usually less than an inch of water column. Because so little energy is available for metering and mixing the air flow, devices for measuring air are not practical due to their intrusive nature and energy requirements. In forced-draft (air supplied by a blower or fan) testing and turbine exhaust gas (TEG) testing, the combustion air is supplied via ducting to the burner. With this type of testing, air flow can be measured using devices such as venturi meters, the use of a Pitot tube, or a hot wire anemometer. Usually, the air flow is a calculated variable based on the fuel flow, which is measured, the fuel composition and the percentage of oxygen in the flue products. Due to the difficulties in air flow measurement, it is critical to ensure proper metering and measurement of the flue products and fuel properties.

9.4.2 COMBUSTOR CONDITIONS

The conditions within the combustor or furnace also provide critical information in determining the performance of a burner. Some of the information collected from the combustor includes the furnace gas temperatures at different locations. Typically, it is good practice to collect the furnace gas temperatures at the elevation of the burner, midway through the combustion chamber, and at the exit of the fired chamber. This is usually measured with a velocity thermocouple.

9.4.2.1 Furnace Temperature

A suction pyrometer (also known as a suction thermocouple or velocity thermocouple) is widely considered the preferred method for obtaining gas temperature measurements in the harsh environment of an operating furnace. If a bare thermocouple is introduced into a hot furnace environment for the measurement of gas temperature, measurement errors can arise due to the radiative exchange between the thermocouple and its surroundings. A suction pyrometer (see [Figure 9.8](#)) is typically comprised of a thermocouple recessed inside a radiation shield. An eductor rapidly aspirates the hot gas across the thermocouple. This configuration maximizes the convective heat transfer to the thermocouple while minimizing radiation exchange between thermocouple and its surroundings, ensuring that the equilibrium temperature is nearly that of the true gas temperature.

9.4.2.2 Burner Conditions

There are several burner conditions that should be recorded during testing. These mainly concern the configuration of the burner, such as the position of the combustion air inlet damper and the fuel injectors. The burner tile or quarl geometry should be recorded. Pressures and temperatures inside the burner at one or more locations are often of interest.



FIGURE 9.8 Suction pyrometer with noise muffler.

9.4.2.3 Draft

The combustion air for natural-draft burners (see Chapter 16) is induced through the burner, either by the negative pressure inside the firebox or by fuel gas pressure that educts the air through a venturi. Natural-draft burners are the simplest and least expensive burners, and most commonly found in the hydrocarbon and petrochemical industries. Because the energy available to draw air into the burner is relatively low, it is difficult to measure the air flow through the burner. As a result, the temperature of the air, the ambient air pressure, the fuel flow, and the excess air measurements are critical in accurately calculating the air flow through a natural-draft burner.

Forced-draft burners are supplied with combustion air at a positive pressure. The air is supplied by mechanical means (air fans/blowers). These burners normally operate at an air-side delivery pressure that can be in excess of 2 inches of water column (0.5 kPa). They utilize the air pressure to provide a superior degree of mixing between fuel and air. Also, with forced-draft systems, air control can be better maintained, thus allowing furnaces to operate at lower excess air rates over a wide firing range and allowing the operator to realize economic savings. [Figure 9.9](#) shows an example of a mobile air preheater used during forced draft testing.

With the use of an air delivery system, the air flow can be measured to provide a secondary method of measuring the air flow to validate the primary measurement. Fuel flow metering is still used to regulate the air flow. By knowing the amount of fuel burned and the excess air exiting the furnace, the amount of air consumed by the burner can be calculated.

9.4.2.4 Flame Characteristics

The flame shape and dimensions are determined by the burner tile, the drilling of the gas tip, the fuel, and the aerodynamics of the burner. Round burner tiles are used to produce a conical or cylindrical shape. Flat flame burners are designed with rectangular burner tiles and produce fishtail-shaped flames. Many of the liquid fuel burners are designed with round burner tiles and produce a conical



FIGURE 9.9 Forced-draft air preheater. (Courtesy of John Zink Co., LLC.²¹)

flame. The drilling of the oil tip determines the shape and length of the flame. Reducing the angle produces a longer, narrower flame. Increasing the angle produces a shorter, bushier flame. Forced-draft burners produce a shorter flame because of the better mixing between the fuel and the air. Firing in combination with both liquid and gas fuels will increase the length and volume of the flame and can cause coking of the oil and gas burner nozzles.

Another characteristic of a burner flame is its stability. Stability is a controversial and subjective measurement. Stability can be defined as erratic motion at the flame front (point of ignition), by vibrations in the furnace, or by CO measurements within and around the flame envelope. Industry practice defines flame shape as the envelope that is in the visual spectrum. As can be imagined, two people viewing a flame will arrive at different dimensions, thus making flame shape very subjective. To compensate for this inaccuracy, testing has fallen back to measuring the CO to determine the point at which combustion is nearly complete. It is widely debated as to whether the CO measurement for defining a flame shape is 500, 1000, 2000 ppm, or some other level. Flame intensity is how bright a flame is to the naked eye. Oil-fired burner equipment typically produces an intense flame that is bright yellow and opaque. Gas-fired equipment typically produces a blue, less intense translucent flame.

9.4.2.5 Heat Flux

Several techniques have been developed to measure heat flux levels at different locations within a furnace. The instruments designed to successfully obtain heat flux data in the hostile environment of a full-scale furnace are typically water-cooled probes inserted through a furnace port at the location of interest. The probes may utilize pyrometers that measure radiant or total (radiant + convective) heat flux levels. The sensing element is typically composed of a thermopile-type sensor that outputs a voltage proportional to the temperature difference between the area of the element exposed to heat transfer from the furnace and the area that is cooled and kept at a relatively constant temperature per the element design. Sensor element designs differ chiefly between the geometry

and configuration of the thermopile-type sensing element. Common designs utilize a plug-shaped thermopile element with the exposed face at one end and the opposite end cooled by contact with a heat sink (see Figure 9.10). Others use a disk-shaped sensor with the temperature gradient existing between the center of the disk receiving radiant energy and the radial edge that is cooled by contact with a heat sink. A sensor designed to measure only the radiant component of heat flux (radiometer) may utilize a crystal window, gas screen, or a mirrored ellipsoidal cavity (see Figure 9.11) to negate convective heat transfer to the sensor. A radiometer is also often equipped with a gas purge in an effort to keep the crystal window or mirrored ellipsoidal cavity clean and free from fouling. Critical parameters to consider when using a heat flux meter include the ruggedness, sensitivity, calibration method, and view angle of the instrument.

9.4.3 EMISSIONS MEASUREMENTS

Emissions analysis is an important criterion for burner testing. The main pollutants in the combustion products are NO_x, CO, unburned hydrocarbons, and particulates. There are several parameters that are typically measured to determine the pollution emission rate. These are discussed in this section. A more comprehensive discussion is given elsewhere.²³

There are two methods for obtaining gas samples: extractive and *in situ*. In extractive sampling, the exhaust gas is withdrawn from the sample point and conveyed to a gas sampling system (see Figure 9.12) typically located in a conditioned building. The extracted sample must be conveyed in such a way as to preclude any changes in the composition prior to reaching the analysis equipment. This typically involves heat traced sample lines to prevent water from condensing out of the sample, which could cause a scrubbing effect on some of the other components. Extractive systems can have a significant time delay between extracting a given sample and determining its composition, depending on how far the sample is being transported.

In situ sampling means that the sample probe is located directly in the exhaust gas stream. *In situ* sampling involves analyzing the exhaust gases in the exhaust stack without extracting them. *In situ* analyzers are available for SO₂, CO, O₂, NO_x, and CO₂. They are also available for measuring opacity and particulates. There is essentially no time delay in getting an analysis. However, the sensor is often subjected to high exhaust gas temperatures and any particulates in the stream that could cause plugging. The electronics are also typically subject to the weather conditions which can increase maintenance costs. The physical location of the equipment, typically on the side of an exhaust stack, may make maintenance more difficult.

9.4.3.1 Exhaust Gas Flow Rate

The exhaust gas flow is usually not directly measured but is often determined through a combination of measurements, calculations, and assumptions. For example, the gas velocity is measured at one or more points across the exhaust duct. Because it is not known *a priori*, if the gas sample is homogeneous, it must be assumed, until proven otherwise, that there is some variation across the exhaust gas duct. This is done by making multiple traverses across the duct. The cross-sectional area of the duct is subdivided into smaller areas for the purpose of making measurements. The gas velocity in each sub-area is assumed to be constant. Then the gas flow rate through that sub-area is simply:

$$Q_i = \frac{v_i}{A_i} \quad (9.3)$$

where Q_i is the gas flow rate through sub-area i , v_i is the gas velocity through the sub-area, and A_i is the area. The sum of all the sub-areas equals the total cross-sectional area of the duct:

$$A = \sum_{i=1}^n A_i \quad (9.4)$$

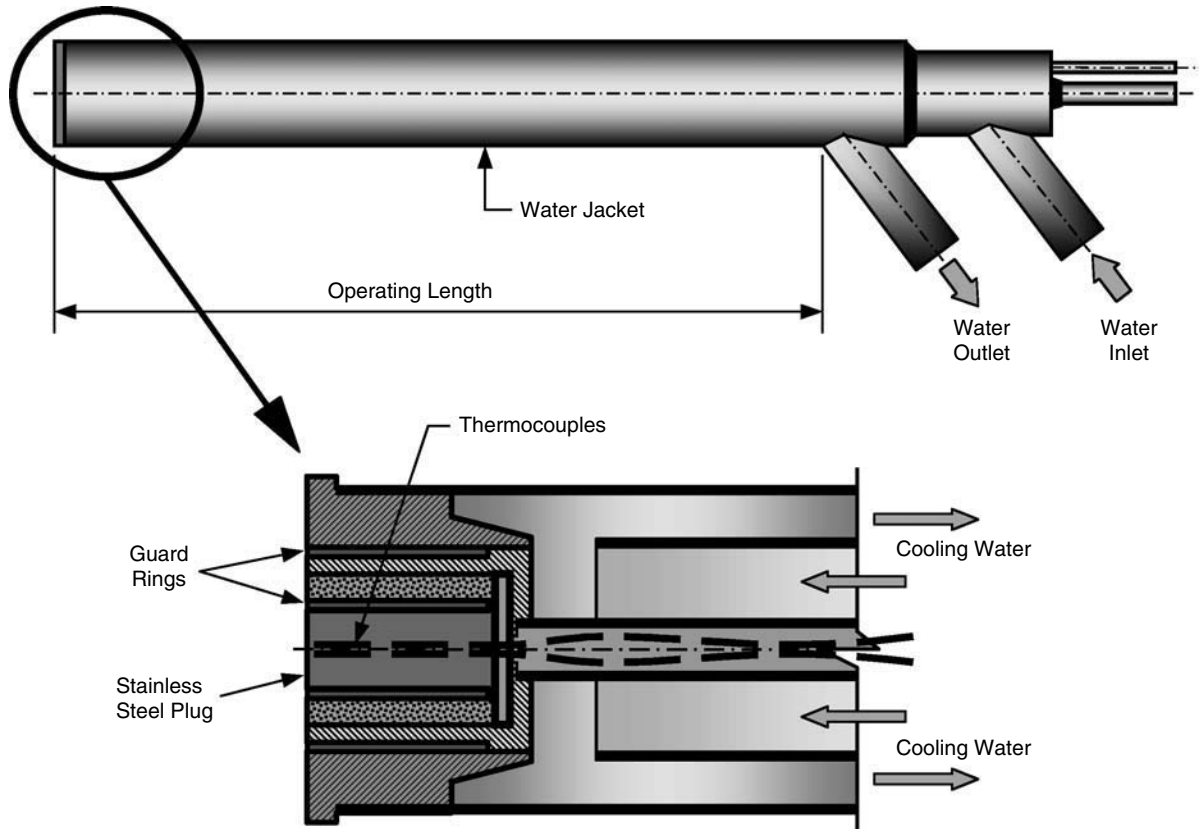


FIGURE 9.10 Schematic of a heat flux probe. (Courtesy of John Zink Co., LLC.²¹)

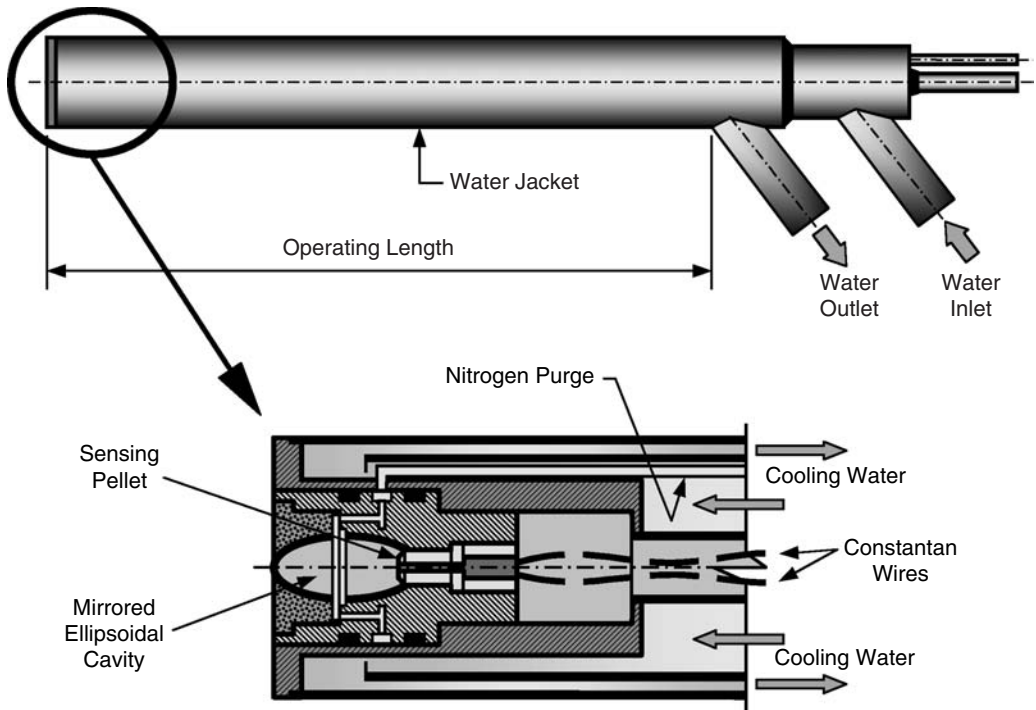


FIGURE 9.11 Schematic of an ellipsoidal radiometer. (Courtesy of John Zink Co., LLC.²¹)



FIGURE 9.12 Gas sample analysis system.

where A is the total duct cross-sectional area and n is the total number of sub-areas. Then, the total exhaust gas flow rate equals the sum of the individual gas flow rates:

$$Q = \sum_{i=1}^n Q_i \quad (9.5)$$

EPA Method 2 discusses how to determine the volumetric stack gas flow rate using an S-type Pitot tube that includes a temperature sensor (see Figure 9.13).²⁴ The method only applies to flows that are not swirling or cyclonic. This method combines measurements and calculations to determine the gas flow rate. Specific guidelines are given for what materials should be used and that dimensions are critical. Each Pitot probe must be calibrated with a known coefficient that should be engraved on the probe. The static and dynamic measuring holes on the probe must not be plugged; that might be a problem in particulate-laden flows. The pressure “head” or difference between the static and dynamic measurements is typically very small and can be measured with an inclined manometer (see Figure 9.14) or a similar device such as a magnehelic gage. Both of these need to be calibrated to ensure accuracy.

According to EPA Method 2, the average stack gas velocity can be calculated for an S-type Pitot tube using:

$$v_s = K_p C_p \sqrt{\frac{(p_t - p_{st})T_s}{P_s M_s}} \quad (9.6)$$

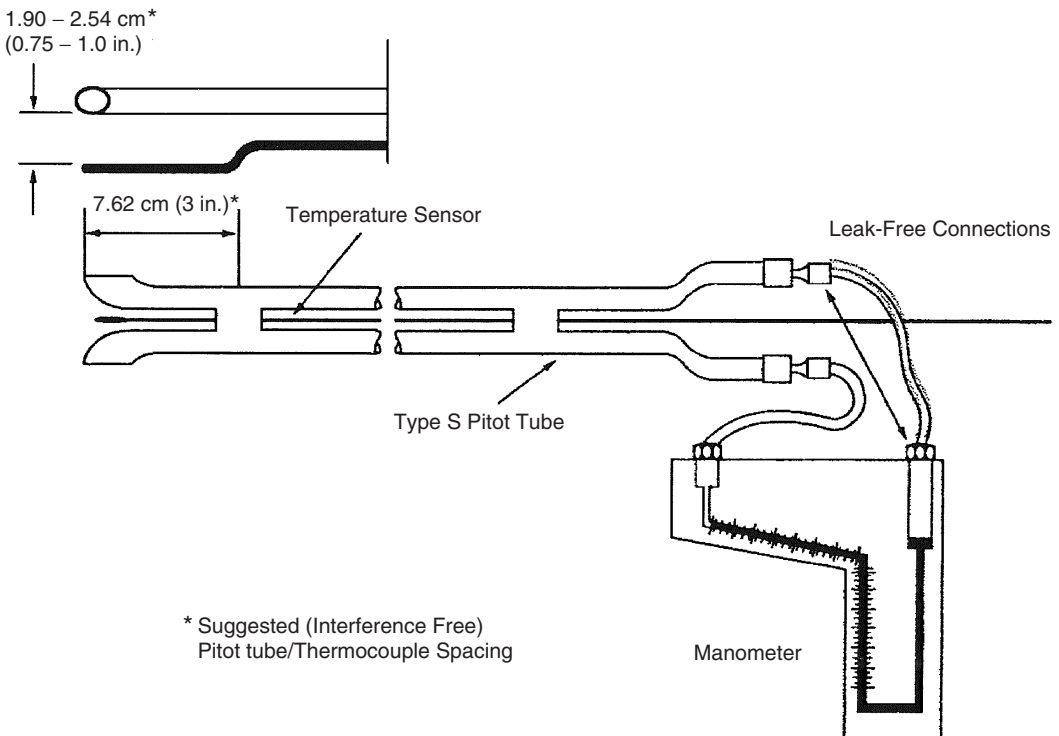


FIGURE 9.13 S-type Pitot tube manometer assembly for measuring gas velocity. (From U.S. EPA.²⁴)



FIGURE 9.14 Inclined manometers for measuring differential pressure.

where

- v_s = average stack gas velocity (ft/s)
- K_p = velocity equation constant
- C_p = Pitot tube probe constant
- $p_t - p_{st}$ = difference between total and static pressures measured with Pitot tube (in. H₂O)
- T_s = absolute stack temperature (°R)
- P_s = absolute stack pressure (in. Hg)

$$M_s = M_d(1 - B_{ws}) + 18B_{ws} \quad (9.7)$$

where

- M_s = molecular weight of wet stack gas (lb/lb-mole)
- M_d = molecular weight of dry stack gas (lb/lb-mole)
- B_{ws} = fraction by volume of water in the gas stream (determined by Methods 4 or 5)

According to EPA Method 2, the average dry stack gas volumetric flow rate is calculated as follows:

$$Q = 3600(1 - B_{ws})v_s A \left[\frac{T_{std} P_s}{T_s P_{std}} \right] \quad (9.8)$$

where

- Q = volumetric flow rate in dry standard cubic feet per hour (dscf/hr)
- B_{ws} = fraction by volume of water in the gas stream (determined by Methods 4 or 5)
- v_s = average stack gas velocity (ft/s)
- A = cross-sectional area of the stack (ft²)

T_{std} = standard absolute temperature = 528°R
 P_{s} = absolute stack pressure (in. Hg)
 T_{s} = absolute stack temperature (°R)
 P_{std} = standard absolute pressure (29.92 in. Hg)

EPA Method 2A discusses the direct measurement of the gas volume flow rate through pipes and small ducts. These devices include, for example, positive displacement meters and turbine meters. This is a much simpler and faster technique than measuring multiple traverse points in the exhaust gas stack and then computing the flow rate based on several different types of measurements (e.g., pressure difference, gas temperature, barometric conditions, and moisture in the stack gases). Direct measuring devices must also be properly calibrated to ensure accuracy. These usually cost much more than the using Pitot tubes and manometers but require far less labor to operate. They can also mitigate the problem of varying conditions across the exhaust duct. However, they are typically used only on smaller diameter ducts and they may introduce a significant pressure drop in the exhaust system that may require either additional fan power or a reduction in the exhaust gas volume flow rate, which is usually not desirable.

In some cases, the simplest and most straightforward method to determine the exhaust gas flow rate is to calculate it based on the incoming fuel and combustion air flows and measured exhaust gas composition. This is often of sufficient accuracy for many situations. This method uses a combination of measurements, assumptions, and calculations to determine the gas flow rate. There are also some variations of the technique. However, in general, the technique involves calculating the gas flow rate based on either the measured input flow rates, the measured stack gas composition, or a combination of the two as a check to make sure the results make sense.

9.4.3.2 Exhaust Gas Temperature

A common method for measuring the exhaust gas temperature is with a suction pyrometer (see [Figure 9.8](#)). At the desired measurement location, gases are extracted from the flame through a sampling tube. A thermocouple is positioned just inside this tube, typically made of a ceramic or high-temperature metal, which acts as a radiation shield. This technique is particularly useful when measuring gas temperatures in hot-surfaced enclosures. Surface radiation from the walls to an unshielded thermocouple may introduce large errors in the gas temperature measurement. Chedaille and Braud (1972)²⁵ and Goldman (1987)²⁶ specifically discuss the use of a suction pyrometer to measure gas temperatures in combustors. This device has been successfully used to measure gas temperatures in excess of 2200K (3500°F).

The use of a thermocouple that is not shielded from radiation effects is not recommended unless appropriate corrective calculations are applied (see Reference 27). These corrections can be on the order of 200°F (110°C), or even more in certain cases. Unshielded thermocouples tend to underestimate the actual gas temperature because of radiant and conductive losses from the thermocouple junction. This is significant because NO_x emission guarantees are often based on the measured combustor temperature. If the measured temperature is 200°F (110°C) less than the actual temperature, then the NO_x may be significantly higher than expected because of its exponential dependence on gas temperature. Therefore, it is important to have a reasonably accurate furnace gas temperature.

9.4.3.3 NO_x

The chemiluminescent method is most widely used for NO_x analysis.²⁸ The method is capable of measuring oxides of nitrogen from sub-parts per million to more than 5000 ppm. Newer detector models are free from disadvantages inherent in analog systems and provide for increased stability,

accuracy, and flexibility. The principle of operation of these analyzers is based on the reaction of nitric oxide (NO) with ozone:



The sample, after it is drawn in the reaction chamber, reacts with the ozone generated by the internal ozonator. The above reaction produces a characteristic luminescence with an intensity proportional to the concentration of NO. Specifically, light emission results when electronically excited NO₂ molecules decay to lower energy states. The light emission is detected by a photomultiplier tube, which, in turn, generates a proportional electronic signal. The electronic signal is processed by the microcomputer into an NO concentration reading. To measure the NO_x (NO + NO₂) concentration, NO₂ is transformed to NO before reaching the reaction chamber. This transformation takes place in a converter heated to about 625°C (1160°F). Upon reaching the reaction chamber, the converted molecules along with the original NO molecules react with ozone. The resulting signal represents the NO_x. Further details of the workings of a chemiluminescent gas analyzer can be found in any standard text.

9.4.3.4 Carbon Monoxide

The carbon monoxide (CO) exiting a burner will initially increase slowly as the excess air rate decreases. The increase will accelerate as excess air levels continue to decline to near zero. Typical control points range between 150 and 200 ppm CO. This range usually results in the best overall heater efficiency. Certain localities may require lower emission levels. The presence of unsaturated hydrocarbons can lead to pyrolysis and polymerization reactions, resulting in a greater possibility that CO will be produced. Burners with greater swirl and/or higher combustion air pressure drop (such as forced-draft burners) typically have lower CO emissions at equivalent excess air levels. The reason is that these burners provide a superior degree of mixing to allow improved combustion at lower excess air levels.

Although CO can be continuously monitored by chromatographic analysis using thermal conductivity detectors or by FTIR spectroscopic methods, individual analysis is best accomplished using a nondispersive infrared technique. The main advantages of this technique is that it is highly specific to CO, and has lower ranges with a wider dynamic range, increased sensitivity and stability, and easy operation because of microcomputer control diagnostics. An added advantage of the technique is that the changes in temperature and pressure of the sample gas are immediately compensated by the microcomputer and the results are thus not affected by fluctuations in the operating conditions. The basic principle of these analyzers is based on the radiation from an IR source passing through a gas filter alternating between CO and N₂ due to rotation of the filter wheel. The CO gas filter acts to produce a reference beam which cannot be further attenuated by CO in the sample cell. The N₂ side of the filter wheel is transparent to the IR radiation and therefore produces a measure beam that can be absorbed by CO in the cell. These analyzers can measure 0.1 to 1000 ppm CO under well-controlled conditions. The detailed working of an IR analyzer can be obtained from a standard text on the subject.

9.4.3.5 O₂ (Wet and Dry)

The oxygen concentration is also conveniently measured by chromatographic techniques using thermal conductivity detectors and also by low-resolution FTIR spectroscopy. Individual measurements of oxygen concentration are most widely done by analyzers based on standard paramagnetic analyzers. The detailed working of such analyzers can be found in related texts.

9.4.3.6 Unburned Hydrocarbons (UHCs)

The unburned hydrocarbons (UHCs) increase as the excess air rate decreases. The combustion of hydrogen and paraffin-rich fuel will produce a minimum of combustibles. The presence of unsaturated hydrocarbons leads to pyrolysis and polymerization reactions, resulting in more combustibles. Unsaturated hydrocarbons, chlorides, amines, and the like can plug or damage burner tips, disrupting the desired fuel/air mixing. This can cause a further increase in the combustibles level. Heavy oils are more likely to produce greater levels of combustibles than lighter oils. Heavier components are not as easily atomized and ignited and, therefore, polymerization and pyrolysis reactions are more likely to occur. Forced-draft burners provide better mixing of the fuel/air mixture and therefore produce reduced combustibles at equivalent excess air rates.

Chromatographic techniques are the most widely used for VOC determination in the refinery off-gases. Their use as a multi-component, completely automated, and continuous emissions monitor is not documented in the literature. Coleman et al.²⁹ (1996) have discussed the use of gas chromatography-based continuous emission monitoring system for the measurement of VOCs using a dual-column (with DB-5 and PoraPlot U, respectively) gas chromatograph equipped with thermal conductivity detectors, in which separation was optimized for fast chromatography. In this system, nine different VOCs plus methane and CO₂ were separated and analyzed every 2 minutes. Because the permits are issued to report emission in pounds or tons of pollutants emitted and not on the basis of parts per million (ppm), the setup was equipped with a continuous mass flow measurement device. The data thus collected can be converted to pounds or mass of VOCs emitted. The column DB-5 separates ethanol, isopropanol, n-propanol, methyl ethyl ketone, isopropyl acetate, heptane, n-propyl acetate, and toluene. The PoraPlot U separates methane and carbon dioxide. A chromatographic technique using two fused silica columns — one with Dura-Bond and the other with Gas Solid-Q-PLOT — equipped with flame ionization detector was used by Viswanath (1994) to measure VOCs in air.³⁰

A technique reported by Pleil et al. (1988)³¹ uses the fact that the compounds once identified by retention time in the chromatographic analysis can be confirmed by determining a second dimension, such as its mass fragmentation pattern or its IR absorption spectrum from a highly specific detector such as a mass selective detector (MSD) or a Fourier transform infrared (FTIR) system. Even with this combination, care should be taken to avoid occasional confusion among isomeric, co-eluting compounds with similar, strongly absorbing functional groups. Using this technique, Pleil et al.³¹ were able to identify and successfully determine more than 40 compounds in the VOCs. They used cross-linked methyl silicon megabore capillary columns with both flame ionization detector (FID) and electron capture detector (ECD) simultaneously. A similar study of VOCs was reported by Siegel et al. (1992).³² They used a DB-1 column with a flame ionization detector and a mass selective detector (GC/MSD).

The U.S. EPA guidelines as presented in “Compendium of Methods for the Determination of Toxic Organic Compounds in Ambient Air, Method TO-14” is slowly becoming the criterion for VOCs (Pleil et al., 1991).³³ The recommended method uses cryogenic pre-concentration of analytes with subsequent gas chromatographic separation and mass spectrometric detection. The methodology requires detecting nanogram and sub-nanogram quantities. To get this high sensitivity, the method TO-14 recommends the use of a selective ion monitoring (SIM) spectrometric technique. The details of the method were discussed by Pleil et al. (1991).³³ Evans et al. (1992)³⁴ have also discussed the use of a cryogenic GC/MSD system to measure the VOCs in air in different parts of the country. The sample first passes through a fused silica column to resolve the target compounds. The column exit flow splits, such that one third of the flow is directed to the chromatographic column (with flame ionization detector) and two thirds of the flow goes to the mass selective detection system (MSD). The method was found to effectively detect 0.1 ppb by volume of about 25 VOCs.

Larjava et al. (1997)³⁵ have recently reported a comprehensive technique for the determination of nitric oxide (NO), sulfur dioxide (SO₂), carbon monoxide (CO), carbon dioxide (CO₂), and total hydrocarbons (C_xH_y) in the air. The technique used single-component gas analyzers in parallel with a low-resolution Fourier transform infrared (FTIR) gas analyzer. The technique successfully demonstrated that the results obtained by single-component analyzers and the FT-IR were very close. Online analysis of stack gases with FTIR spectrometry has received considerable attention recently because of the multi-component analysis capability and sensitivity of the method (Larjava et al., 1997; Wübern, 1992;³⁶ and Demirgian and Erickson, 1990).³⁷ A typical low-resolution FTIR spectrometer uses spectral resolution, BaF₂ optics, a Peltier-cooled semiconductor detector, and a temperature-controlled multi-reflection gas cell. The advantages of low-resolution FTIR over conventional high-resolution FTIR are its rugged design, high signal-to-noise ratio without liquid nitrogen-cooled detectors, reduced data storage requirements, and increased dynamic range for quantitative analysis (Larjava et al., 1997).³⁵

Jayanti and Jay (1990)³⁸ have summarized studies on estimating VOCs by different techniques employed by different workers.

9.4.3.7 Particulates

Proper combustion of gaseous fuels does not generate significant quantities of combustion-generated particulates. Particulate emissions generally occur with the burner of heavy fuel oils. Burners with greater swirl and/or higher combustion air pressure (such as forced-draft burners) are less likely to produce particulates. They provide a superior degree of mixing to reduce the formation of particulates. Greater atomization of fuel oil into finer particles will reduce particulate emissions. High-intensity burners can considerably reduce particulates. The high degree of swirl, coupled with the high-temperature reaction zone, induces superior combustion of the particulates. However, these burners also emit an increased amount of NO_x.

The particulates from the hydrocarbon industries are the pollutants that are emitted by the effluent gases. The most important criterion for the evaluation of particulates is the particle size. It has been observed that different results are obtained using different techniques of collection and analysis.

The U.S. EPA (1971)³⁹ recommended procedures suggest that sampling ports be located at least eight duct diameters downstream and two diameters upstream from any flow disturbance. Flue gas should be drawn through the EPA sampling train. It is important to maintain isokinetic sampling conditions. The EPA defines isokinetic sampling as “sampling in which the linear velocity of the gas entering the sampling nozzle is equal to that of the undisturbed gas stream sample point.”⁴⁰ This is particularly important when measuring larger particulates, especially those greater than about 5 μm. A schematic of an isokinetic sample probe is shown in [Figure 9.15](#).

Particles can be collected by filtration, impaction, and impingement. Glass fiber and membrane filters are efficient for 0.3-μm particles. These filters can be used in an inline filter holder. The filter holder can be kept inside the sampling port such that the filter attains the temperature of the gas stream.

For particulates collection by impaction, an Anderson type in-stack sampler is used. In cases where the sampler cannot be accommodated inside the sampling port flange, it can be put outside, with an arrangement to heat it to prevent condensation within the sampler. In this type of sampler, the collecting plates are coated with a thin film of silicone grease formed by immersing them in a 1% solution of silicone grease dissolved in benzene and dried overnight at 100°C (212°F).

The collection of particulates by impingement consists of using a series of three or four liquid impingers. These impingers each contain 250 ml of distilled water. A common practice is to use impaction and impingement techniques followed by glass fiber back-up filters.

Sampling times also vary according to the technique employed. One- to five-minute samples are common for filters and Anderson-type units, while 20 minutes are needed for impingers.

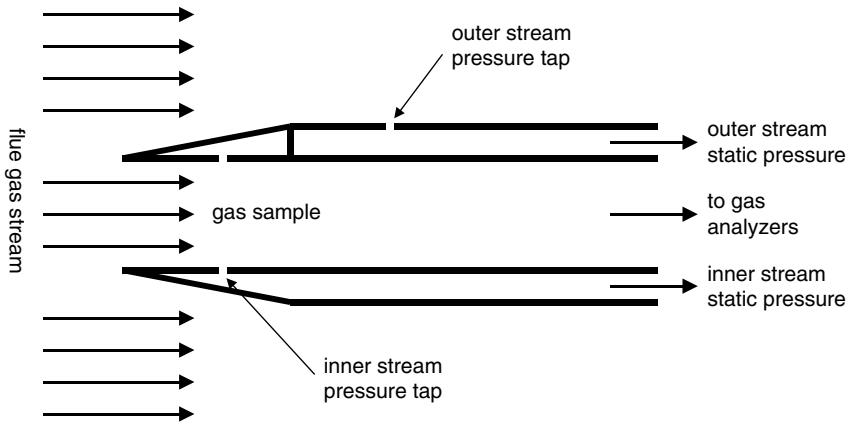


FIGURE 9.15 Nozzle for isokinetic sampling probe (not to scale).

Filter samples are analyzed by light microscopy and scanning electron microscopy (SEM). The liquid samples from the wet impingement device are filtered onto 0.2- μm membrane filters and examined by SEM. The samples from the Anderson sampler can be analyzed by the recommended procedure or by calculations based on Ranz and Wong equations. The Anderson plates can also be examined by SEM to determine the range of particles trapped on the plates. Particle counts can be determined by light microscopy using an oil-immersion lens system (Byers, 1973).⁴¹ Individual particles are compared on the basis of equal area to previously calibrated circle sizes contained on a size comparator. In an exhaustive study, Byers⁴¹ took data on particulates from a refinery effluent and suggested that membrane filters should be preferred when the gas being sampled is at a temperature less than 300°F (150°C). For higher temperatures, the Anderson sampler is suitable, provided the plates are suitably coated. Sampling techniques causing agglomeration, such as glass fiber filters, wet collection, bulk grab samples, and scrapping of deposits from collecting surfaces, should be avoided.

9.4.3.8 Noise

Noise is discussed in more detail in Chapter 7 and therefore will only be considered briefly here. Figure 9.16 shows a commonly used device for measuring industrial noise. A noise measurement system consists primarily of some type of microphone to receive the sound, some type of transducer to convert the sound waves into a usable signal typically digital, and a meter to convert the signals into the proper weighting system and to display and record the signals.



FIGURE 9.16 Bruel & Kjaer, sound level meter. (Courtesy of Bruel & Kjaer.)

The American Petroleum Institute Recommended Practice 531M gives information on measuring noise from process heaters.⁴² Recommendations are given for making field measurements, as well as procedures for sound-level measurement, including correcting for background noise. Measurements are suggested to be made at 1 m (3.3 ft) from the outside heater walls at various locations, depending on the configuration.

Hassall (1998)⁴³ lists the following procedural steps when making noise measurements:

1. Determine what quantities are to be measured.
2. Select the instruments, including the type of microphone to be used.
3. Determine the minimum number of microphone positions and their locations, including a diagram of the arrangement (multiple microphones are necessary to measure the sound field).
4. Check the system sensitivity.
5. Measure the acoustical and electrical noise level.
6. Measure the source sound levels.
7. Correct the measurements as appropriate (e.g., subtracting background noise).
8. Record the data.

Lang (1998)⁴⁴ discusses how to make sound power level measurements, typically used as a descriptor for stationary equipment. These measurements can be used to calculate the sound pressure level at a given distance from equipment, compare the noise radiated by equipment of the same type and size, compare the noise radiated by equipment of different types and sizes, determine whether equipment complies with a specified upper sound emission limit, determine the amount of noise reduction required for a particular circumstance, and develop quieter equipment. This type of measurement requires a three-dimensional array of microphones and therefore is not commonly used when measuring combustion noise.

Measuring sound intensity can be challenging as multiple types of probes are required to measure both the sound pressure and the particle velocity.⁴⁵ This is often done using two microphones and performing appropriate calculations to determine the particle velocity. This type of measurement is also not commonly done for industrial combustion systems.

There are a number of factors that can affect noise measurements and instrument performance, including temperature, humidity, atmospheric pressure, wind or dust, and even magnetic fields.⁴⁶ Instruments should be calibrated according to the manufacturer's instructions before and after each day of use and whenever the temperature or relative humidity changes significantly. Zahringer et al. (2000)⁴⁷ experimentally demonstrated the effectiveness of using microphones combined with an intensified camera system to measure acoustic oscillations in a boiler.

9.5 TEST MATRIX (TEST PROCEDURE)

9.5.1 HEATER OPERATION SPECIFICATIONS

Some of the parameters normally measured in burner testing are fuel pressure, air-side pressure drop, noise emissions, NO_x emissions, CO emissions, UHC emissions, particulate emissions, heat flux profiles, flame dimensions, and some subjective burner characteristics such as flame stability and color.

9.5.2 PERFORMANCE GUARANTEE SPECIFICATIONS

The primary reasons for conducting a burner test are to determine the operating envelope of the burner and the emissions performance. With this data collected, the burner's performance in the field will be more predictable and easier to operate.

9.5.2.1 Emissions Guarantees

It is important to identify which fuels are the operation or on-line fuels and which fuels are for start-up or emergency use only. By identifying which fuels the emissions guarantees apply to, the burner can be better optimized to run on the operation fuels.

9.5.2.2 Noise

Noise emissions are becoming as important as stack emissions. With some industrial plants located near populated areas, it is important to keep noise to a minimum. Burner testing is usually conducted on a single burner, and noise emissions are usually measured at 1 meter (3 ft) from the burner. Data collected during the test include an overall dBA measurement and an octave band measurement ranging from 31.5 to 8000 Hz. When collecting noise data, it is important to measure it with the burner operating, and without it operating, to obtain the background noise which may or may not be required to determine the noise contributed from the burner.

9.5.2.3 Fuel and Air-side Pressure Drop

The fuel and air-side pressure drop also need to be verified during the test. The test confirms that the burner will have the correct capacity for proper operation. The fuel-side pressure drop will be displayed during the test. It is important that the test engineer ensure that the customer's fuel will meet the design pressure requirement based on the data collected on the test fuels. When verifying the air-side pressure drop, the test engineer must determine the elevation and the range of the ambient air temperatures that the burners will be subjected to once installed in the field.

9.5.2.4 Flame Dimension Guarantees

Flame dimensions in a full-scale furnace are typically made by subjective measurement. The flame envelope is most often determined by visual observation. These visual observations will often vary somewhat, depending on the observer and also on the operating conditions. For example, in an outdoor test furnace, the reflection of the sun off the sight ports can make it difficult to determine an approximate flame length. The hotter the test furnace, the more difficult for the human eye to distinguish between the hot furnace walls and the flame.

This operating parameter is important in ensuring that the flame will not impinge on the furnace process tubes or interact with another burner's flame. Flame impingement on the tubes can damage the process tubes and cause the furnace to prematurely shut down for repairs — at great expense to the operator. Flame interaction between two or more burners can result in longer, more uncontrollable flames and higher emissions. It is important to identify the burner spacing, the furnace dimensions, and the customer's desired flame dimensions. With this information, the test engineer can fine-tune the flame envelope to improve the burner's performance in the customer's heater.

9.5.3 DATA COLLECTION

Prior to installation and testing a burner, a test matrix (test procedure) must be developed. A sample fuel gas specification is shown in [Table 9.4](#). A typical test procedure might resemble that shown in [Table 9.5](#). With a well-developed test procedure, the data collected from a test will be meaningful and will assist the operator in running the furnace and predicting the performance from the furnace.

The data should be recorded in an orderly fashion, preferably with a computer data acquisition system or by hand on a well-conceived data entry form. It is important to record not only all the

TABLE 9.4
Test Procedure Gas Specification Sheet²¹

JOHN ZINK COMPANY TULSA, OK			BURNER PERFORMANCE DEMONSTRATION BURNER SPECIFICATION (GAS)			
Date:	2/4/00	Rev. No:	0	J.Z. Quote No:		
Customer:				Customer P.O. No:		
Burner:	PSFFG-45M			J.Z. Sales Order No:		
Drawing:				Capacity Curve No:		
User:				Project Engineer:		
Jobsite:				Test Engineer:		
CUSTOMER HEATER DATA						
Spec Reference:				Direction of Firing:		
Item No:				Setting Thickness:		
Quantity of Burners:	60			Burner Spacing:	39 inches (1 meter)	
Type of Heater	Ethylene			Pilot:	ST-1S manual pilot	
Firebox Dimensions:				Elevation:	<1000 feet ASL	
Draft Type	Induced					
SPECIFICATIONS						
Fuel Composition	LHV	MW	FUEL A	FUEL B	TMG	
Component:	Btu/scf	## mol	vol%	vol%	vol%	vol%
Tulsa natural gas	913.0	17.160	34.00	80.00	100.00	
Hydrogen	273.8	2.022	38.00	20.00		
Propane	2314.9	44.100				
Propylene	2181.8	42.080	28.00			
Carbon Dioxide		44.010				
Butane	3010.6	58.120				
Lower Heating Value:	Btu/scf					
Molecular Weight:	## mol		18.385	14.132	17.180	
Isentropic Coefficient:	(Cp/Cv)		1.2600			
Temperature:	(degF)		60	60	60	
Pressure Available:	usig		20.0	20.0	20.0	
Heat Release per Burner:						
Design Maximum:	(MMBtu/hr)		6.800	6.800	6.800	
Normal:	(MMBtu/hr)		5.913	5.913	5.913	
Minimum:	(MMBtu/hr)		1.360	1.360	1.360	
Flame Dimensions: @ ft						
Cross Section (Dia):			4.000	4.000	4.000	
Length:			16.000	16.000	16.00	
Turndown:			5:1	5:1	5:1	
Excess Air @ Design:			10	10	10	
Conditions @ Burner:						
Heater Draft Available:	(w.c.)		0.80	0.80	0.80	
Burner dP @ Design:	(w.c.)		0.80	0.80	0.80	
Combustion Air Temp:	(degF)		100	100	100	
Guarantees:						
NOx	ppm(vd)		100	100	100	
CO:	ppm(vd)		50	50	50	
Note 1 Particulate:	#MMBtu (hv)					
Note 1 UHC:	#MMBtu (hv)					

TABLE 9.4
Test Procedure Gas Specification Sheet (Continued)

JOHN ZINK COMPANY TULSA, OK		BURNER PERFORMANCE DEMONSTRATION BURNER SPECIFICATION (GAS)			
	(English)				
DSCF / MMBtu @ 3% O ₂ (d)	(hv)				
Noise:	dBA (spi) @ 3 ft.	85	85	85	
Conditions of Guarantees:					
% Oxygen Corrected to:		3	3	3	
Combustion Air Temp:	(degF)	100	100	100	
Heat Release:	(MMBtu/hr)	4.500	4.500	4.500	
Furnace Temperature:	(degF)	2100	2100	2100	
COMMENTS: General – Heat Releases are shown as Net or Lower Heating Value. <i>Note 1:</i> Particulate and UHC are NOT measured during Test Demonstration.					

relevant operating parameters (e.g., temperatures, pressures, and flow rates), but also the conditions of both the burner and the combustor. For example, if the insulation pattern changes inside the test furnace from test to test, then this should be recorded for future reference. If, for example, orifice plates are used to measure gas flows, then these need to be recorded for a given test in case verification is needed later. Any unusual features of the test should also be recorded, including photos where appropriate. For example, if a structure such as an internal wall is temporarily built inside the test furnace, this should be documented. Therefore, it is recommended that a comprehensive checklist be developed to ensure that all the appropriate information is recorded for a given test.

The test data should be put into some type of test report to summarize the results of the test. Enough information must be included so that the test can be replicated if necessary and that proper analysis can be done at a later time if desired. For example, CFD analysis (see Chapter 5) will only be meaningful if enough data has been collected for proper comparison between the measurements and computer predictions. The data should be presented in tabular or graphical form to make it easier for the reader to both find and compare the data. The data should also be presented in the proper units or, in some cases, multiple units (e.g., English and SI). This may include converting some of the measurements to other units. For example, raw NO_x emissions are typically measured in ppm (parts per million) at some oxygen level in the exhaust stack. These are usually converted to ppm at a specific oxygen level (e.g., 3% O₂) and often to another unit, such as lb NO_x per million Btus (lb NO/MMBtu). Noise measurements may need to be filtered by subtracting the background readings if they are significant. Both the raw and corrected data should be included in the report in case any future analysis is required. (The raw data is often included in an appendix for the interested reader.)

The test report should be written in such a way that someone who is not necessarily an expert on testing or is not intimately familiar with the test apparatus can understand the data collected and the data analysis. The report should be a permanent record of the findings from a particular test. The test report is one of the most important outputs from a burner test.

9.6 CONCLUSION

While burner testing is mostly a well-defined process, there is still a considerable amount of both art and discretion used. Part of the art of testing is to determine the appropriate operating conditions in a pilot test furnace that best represent those in the actual end-use furnace. It also includes making some subjective measurements such as flame shape and stability. It is nearly impossible to exactly

TABLE 9.5
Example Test Procedure²¹

JOHN ZINK COMPANY			BURNER PERFORMANCE DEMONSTRATION				Date:	2/4/00	
TULSA, OK		(English)	BURNER TEST PROCEDURE				Rev. No.		
J.Z.80 No: Burner.	PSFFG-45M	Customer P.O. No.					User Jobsite:	Burner Drawing No:	Furn.
Data Point	Fuel	Liberation (MMBtu/hr)	Air Temp. (degF)	Excess O ₂ (%O ₂ (day))	Draft (w.t)	deltaP (w.t)	DESCRIPTION/COMMENTS		
1	TNG		60		0.80		Burner light off on Tulsa natural gas (TNG).		
2	A	6.800	60	2.0	0.80		Maximum heat release, set air to 10% excess air, record noise and heat flux profile.		
3	A		60		0.80		Above maximum heat release, increase fuel flow until CO > 250 ppm.		
4	A	5.910	60	2.0	0.80		Reduce heat release to normal heat release, set air damper to maintain 10% excess air.		
5	A	1.360	60		0.80		With damper set for normal heat release, reduce fuel flow to minimum heat release.		
6	A		60		0.80		Determine absolute minimum heat release.		
7	B	6.800	60	2.0	0.80		Maximum heat release, set air to 10% excess air, record noise and heat flux profile.		
8	B		60		0.80		Above maximum heat release, increase fuel flow until CO > 250 ppm.		
9	B	5.910	60	2.0	0.80		Reduce heat release to normal heat release, set air damper to maintain 10% excess air.		
10	B	1.360	60		0.80		With damper set for normal heat release, reduce fuel flow to minimum heat release.		
11	B		60		0.80		Determine absolute minimum heat release.		

GENERAL COMMENTS:		DATA TO BE RECORDED:			
1) Refer to the schematic of the equipment set-up for approximate instrument and sight point locations.		Fuel Flow	X	Burner dP	X
2) The firebox temperature will be within the range of 1900°F and 2100°F for Normal and Maximum Heat Release. It will be lower at reduced rates.		Fuel Press.	X	NOx	X
3) Once the O ₂ has stabilized, at the target value for a given test point, data will be recorded and adjustments for the next point will begin.		Fuel Temp.	X	CO	X
4) All data points will be run with the furnace draft as specified, controlling excess O ₂ with the blower (forced draft), or with the damper (register(s)) (natural draft).		Air Temp.	X	O₂	X
5) The proposed time frame for the duration of the test is approximate and could be longer, or shorter, depending on equipment operation and/or weather.		Draft	X	Noise	X
6) Standard tolerances on measurements will be as follows: Air Temp. +/-20°F, Fuel Temp. +/-20°F, O ₂ +/-0.2%. Draft or dP +/-6% of specified.		Box Temp.	X		
Test Procedure Acceptance:					
<u> </u> Approved <u> </u> Approved as Noted:	Company:	Signature:		Date:	
Test Acceptance:					
Name:	Company:	Signature:		Date:	

replicate field conditions in a test furnace; therefore, compromises are necessary. One example is in the test fuel composition. In petrochemical applications, the actual fuel may have ten or more components, although many are in very small concentrations. These fuels are typically simulated by blending a handful of components.

Probably the largest compromise in pilot-scale testing is either using a reduced burner size or a reduced number of burners. The latter is particularly an issue when burner-to-burner interactions play an important role in the actual field furnace. It is nearly impossible for burner manufacturers to have full-size test furnaces, given the cost and variety of furnaces in any given field of industrial combustion. Therefore, the skill of the test engineer is required to first make the pilot testing as close as possible to the actual end-use conditions, and then to make the appropriate corrections and adjustments so that the test results are meaningful. Fortunately, tools such as computational fluid dynamic modeling (Chapter 5) and physical modeling (Chapter 10) can be used to assess the validity of pilot-scale burner testing and extend the test results to the actual furnace conditions.

REFERENCES

1. C.E. Baukal, V.Y. Gershtein, and X. Li, *Computational Fluid Dynamics in Industrial Combustion*, CRC Press, Boca Raton, FL, 2001.
2. American Petroleum Institute, Burners for Fired Heaters in General Refinery Services, API Publication 535, First Edition, American Petroleum Institute, Washington, D.C., July 1995.
3. J.M. Beér and N.A. Chigier, *Combustion Aerodynamics*, Applied Science Publishers, London, 1972.
4. C.I. Okoh and R.A. Brown, *Combustion Experimentation Handbook*, Gas Research Institute Report GRI-88/0143, Chicago, IL, 1988.
5. D.F.G. Durão, M.V. Heitor, J.H. Whitelaw, and P.O. Witze, *Combusting Flow Diagnostics*, Kluwer Academic Publishers, Dordrecht, 1992.
6. A.M.K.P. Taylor, *Instrumentation for Flows with Combustion*, Academic Press, London, 1993.
7. R.M. Fristrom, *Flame Structure and Processes*, Oxford University Press, New York, 1995.
8. A.C. Eckbreth, *Laser Diagnostics for Combustion Temperature and Species*, Abacus Press, Cambridge, MA, 1988.
9. N. Chigier, *Combustion Measurements*, Hemisphere Publishing, New York, 1991.
10. R.M. Fristrom, Probe measurements in laminar combustion systems, in *Combustion Measurements — Modern Techniques and Instrumentation*, R. Goulard, Ed., Academic Press, New York, 1976.
11. C.T. Bowman, Probe measurements in flames, *Prog. Astr. Aero.*, 53, 1–24, 1977.
12. F.C. Gouldin, Probe measurements in multi-dimensional reacting flows, in *Testing and Measurement Techniques in Heat Transfer and Combustion*, AGARD CP-281, paper #4, 1980.
13. H.A. Becker, Physical probes, in *Instrumentation for Flows with Combustion*, A.M.K.P. Taylor, Ed., Academic Press, London, 1993, 53–112.
14. J. Newbold, M.Q. McQuay, B.W. Webb, and A.M. Huber, The experimental characterization of the combustion process in an industrial, gas-fired, flat-glass furnace, *29th Int. ISATA Conf. — Automotive Technology & Automation*, Florence, Italy, June, Automotive Assoc. Ltd., Vol. 2, pp. 967–976, 1996.
15. P.R. Solomon, P.E. Best, R.M. Carangelo, J.R. Markham, P-L Chien, R.J. Santoro, and H.G. Semerjian, FT-IR emission/transmission spectroscopy for *in situ* combustion diagnostics, *Twenty-First Symposium (International) on Combustion*, The Combustion Institute, Pittsburgh, PA, 1986, 1763–1771.
16. A.C. Eckbreth, Recent advances in laser diagnostics for temperature and species concentrations in combustion, *Eighteenth Symposium (International) on Combustion*, The Combustion Institute, Pittsburgh, PA, 1980, 1471–1488.
17. S.S. Penner, C.P. Wang, and M.Y. Bahadori, Laser diagnostics applied to combustion systems, *Twentieth Symposium (International) on Combustion*, The Combustion Institute, Pittsburgh, PA, pp. 1149–1176, 1984.
18. R.K. Hanson, Combustion diagnostics: planar imaging techniques, *Twenty-First Symposium (International) on Combustion*, The Combustion Institute, Pittsburgh, PA, 1986, 1677–1691.

19. N.R. Fornaciari, R.W. Schefer, P.M. Walsh, and L.E. Claytor, Application of laser-based diagnostics to industrial scale burners, *Proc. 1995 International Gas Research Conf.*, D.A. Dolenc, Ed., Government Institutes, Rockville, MD, 1996, 2398–2405.
20. M. Perrin, J. Imbach, S. Albert, J. Mariasine, and A. Quinqueneau, Application of advanced instantaneous in-flame measurements techniques in an industrial flame with preheated air, *Proc. 1995 International Gas Research Conf.*, D.A. Dolenc, Ed., Government Institutes, Rockville, MD, 1996, 2406–2415.
21. J. Lewallen, R. Hayes, P. Singh, and R.T. Waibel, Chapter 14: Burner Testing, in *The John Zink Combustion Handbook*, C.E. Baukal, Ed., CRC Press, Boca Raton, FL, 2001.
22. D.W. Spitzer, *Practical Guides for Measurement and Control*, Instrument Society of America, Research Triangle Park, NC, 1991.
23. C.E. Baukal, *Industrial Combustion Pollution and Control*, Marcel Dekker, New York, to be published in 2004.
24. EPA. 40 CFR 60 – Standards of Performance for New Stationary Sources, U.S. Environmental Protection Agency, Washington, D.C., 2001.
25. J. Chedaille and Y. Braud, *Vol. 1: Measurements in Flames*, Crane, Russak & Co., New York, 1972.
26. Y. Goldman, Gas temperature measurement in combustors by use of suction pyrometry, in *Heat Transfer in Furnaces*, C. Presser and D.G. Lilley, Eds., ASME HTD-Vol. 74, 1987, 19–22.
27. C.E. Baukal, *Heat Transfer in Industrial Combustion*, CRC Press, Boca Raton, FL, 2000.
28. B.K. Gullett, M.L. Lin, P.W. Groff, and J.M. Chen, NO_x removal with combined selective catalytic reduction and selective non catalytic reduction: pilot scale test results, *J. Air & Waste Manag. Assoc.*, 44, 1188, 1994.
29. W.M. Coleman, L.M. Dominguez, and B.M. Gordon, A gas chromatographic continuous emission monitoring system for the determination of VOCs and HAPs, *J. Air & Waste Manag. Assoc.*, 46, 30, 1996.
30. R.S. Viswanath, Characteristics of oil field emissions in the vicinity of Tulsa, Oklahoma, *J. Air & Waste Manag. Assoc.*, 44, 989, 1994.
31. J.D. Pleil, K.D. Oliver, and W.A. McClenny, Ambient air analyses using nonspecific flame ionization and electron capture detection compared to specific detection by mass spectroscopy, *J. Air & Waste Manag. Assoc.*, 38, 1006, 1988.
32. W.O. Siegl, R.W. McCabe, W. Chun, E.W. Kaiser, J. Perry, Y.I. Henig, F.H. Trinker, and R.W. Anderson, Speciated hydrocarbon emission from the combustion of single component fuels. I. Effect of fuel structure, *J. Air & Waste Manag. Assoc.*, 42, 912, 1992.
33. J.D. Pleil, T.L. Vossler, W.A. McClenny, and K.D. Oliver, Optimizing sensitivity of SIM mode of GC/MS analysis for EPA's TO-14 air toxics method, *J. Air & Waste Manag. Assoc.*, 41, 287, 1991.
34. G.F. Evans, T.A. Lumpkin, D.L. Smith, and M.C. Somerville, Measurement of VOCs from the TAMS network, *J. Air & Waste Manag. Assoc.*, 42, 1319, 1992.
35. K.T. Larjava, K.E. Tormonen, P.T. Jaakkola, and A.A. Roos, Field measurements of flue gases from combustion of miscellaneous fuels using a low resolution FTIR gas analyzer, *J. Air & Waste Manag. Assoc.*, 47, 1284, 1997.
36. K. Wülbern, On line messung von rauchgasen mit einen FTIR spektrometer, *VGB Kraftwerkstechnik*, 72, 985, 1992.
37. J.C. Demirgian and M.D. Erickson, The potential of continuous emission monitoring of hazardous waste incinerators using FTIR spectroscopy, *Waste Management*, 10, 227, 1990.
38. R.K.M. Jayanty and B.W. Gay, Jr., Measurement of toxic and related air pollutants, *J. Air & Waste Manag. Assoc.*, 40, 1631, 1990.
39. *Standard Performance for New Stationary Sources*, Environmental Protection Agency, Federal Register, Vol. 36, # 247, December 23, 1971.
40. Office of the Federal Register, 60.2 Definitions, U.S. Code of Federal Regulations Title 40 Part 60. U.S. Government Printing Office, Washington, D.C., 2001.
41. R.L. Byers, Evaluation of effluent gas particulate collection and sizing methods, *API Proc. Division of Refining*, 53, 60, 1973.
42. API, Measurement of Noise from Fired Process Heaters, Recommended Practice 531 M., American Petroleum Institute, Washington, D.C., reaffirmed August 1995.
43. J.R. Hassall, Noise measurement techniques, in *Handbook of Acoustical Measurements and Noise Control, Third Edition*, C.M. Harris, Ed., Acoustical Society of America, Woodbury, NY, 1998.

44. W.W. Lang, Measurement of Sound Power, in *Handbook of Acoustical Measurements and Noise Control, Third Edition*, C.M. Harris, Ed., Acoustical Society of America, Woodbury, NY, 1998.
45. M.J. Crocker, Measurement of sound intensity, in *Handbook of Acoustical Measurements and Noise Control, Third Edition*, C.M. Harris, Ed., Acoustical Society of America, Woodbury, NY, 1998.
46. U.S. Occupational Safety & Health Administration (OSHA), OSHA Technical Manual — Section III: Chapter 5, Noise Measurement, www.osha.gov/dts/osta/otm/otm_iii/otm_iii_5.html, 2002.
47. K. Zahringer, J-C Rolon, J-P Martin, S. Candel, O. Gicquel, and S. Arefi, Optical diagnostics for analysis of acoustic coupling in domestic gas boilers, *Proc. of 5th European Conf. on Industrial Furnaces and Boilers*, Portugal, Vol. 1, 679–688, 2000.

10 Burner Physical Modeling

John P. Guarco and Tom Eldredge, Ph.D

CONTENTS

- 10.1 Introduction
 - 10.2 Methods of Dimensional Analysis
 - 10.2.1 Buckingham Pi Theorem
 - 10.2.2 Method for Determining the Π Groups
 - 10.2.3 Application of the Buckingham Pi Theorem
 - 10.3 Dimensional Analysis and Model Studies
 - 10.4 Airflow Requirements for Proper Burner Operation
 - 10.5 Using Scaled Modeling for Achieving Proper Burner Airflow
 - 10.6 Characterization of Burner Swirl
 - 10.7 Techniques for Burner Modeling
 - 10.7.1 The Thring-Newby Method for Burner Modeling
 - 10.7.2 The Zelkowski Method for Burner Modeling
 - 10.7.3 The Davidson (Gauze) Method for Burner Modeling
 - 10.7.3.1 Case A: Free Jet
 - 10.7.3.2 Case B: Confined Jet
 - 10.8 Scaled Modeling of Flow-Induced Vibration Phenomena
- References

10.1 INTRODUCTION

Even with the advent of very fast digital computers and algorithms for solving the Navier-Stokes equations, engineering fluid mechanics still rely to a large extent on empiricism. For example, the majority of flows of practical interest are turbulent in nature. With the technology of today, the Navier-Stokes equations can actually be directly solved for some turbulent flows (typically, low Reynolds number) using direct numerical simulation (DNS) algorithms. But for most flows of engineering interest, DNS methods are not practical, and solving the Navier-Stokes equations requires an empirically derived turbulence model. Therefore, the point to be made here is that for the foreseeable future, empirical methods will likely continue to hold an important place in engineering fluid mechanics.

A powerful method for analyzing complex flows is scaled physical modeling. In some cases, scaled physical modeling can be conducted more quickly and cost effectively than computational fluid dynamics (CFD) modeling. Often, scaled physical modeling and CFD modeling can be used to complement one another, so that by using them together, problems can be solved that would be either too difficult or too costly to solve using either physical or CFD modeling alone.

Scaled physical modeling relies on the techniques of dimensional analysis, which predate numerical methods for solving the Navier-Stokes equations by at least 50 years. The primary benefit of using dimensional analysis is that of reducing the number of experiments required to characterize a flow phenomenon using physical modeling. The following example illustrates the power of dimensional analysis to reduce what could be a formidable task into a manageable one.

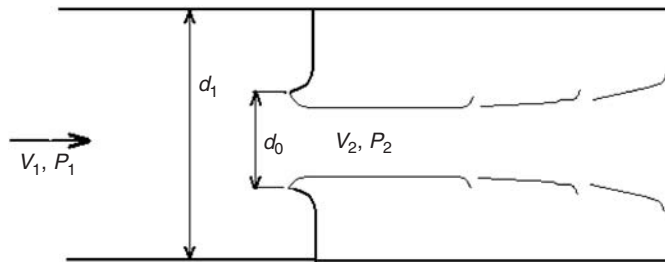


FIGURE 10.1 Flow through an inverted nozzle.

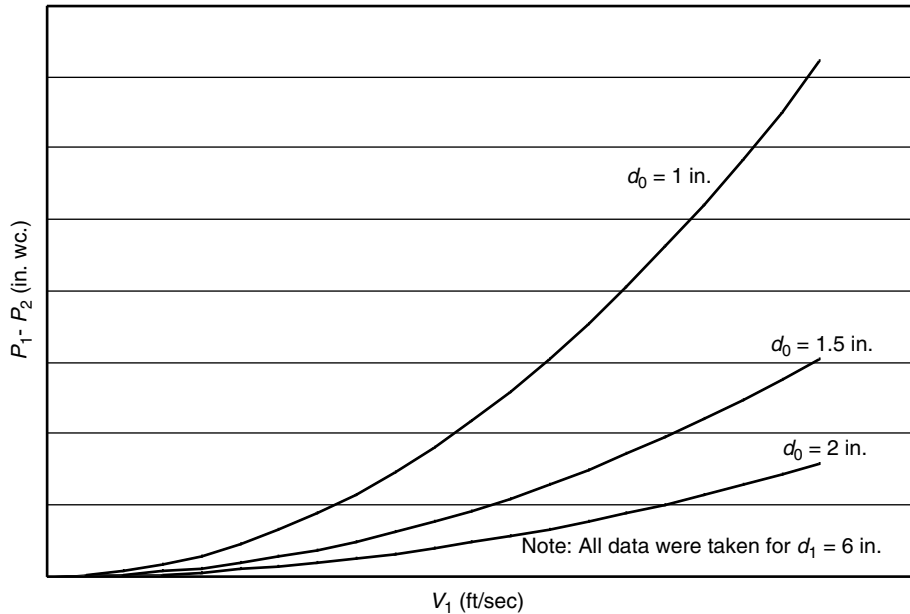


FIGURE 10.2a Pressure-velocity-diameter relationship.

To characterize the static pressure drop ($P_1 - P_2$) through an inverted nozzle, such as shown in Figure 10.1, a brute-force approach would be to conduct a large number of experiments varying d_0 , d_1 , and V_1 , while measuring P_1 and P_2 for each experiment. The result would be developing numerous curves as shown in Figure 10.2a, where each curve represents a large number of tests for fixed values of $d_0 d_1$. If d_1 were varied, then the set of curves shown in Figure 10.2a would need to be regenerated. It can easily be seen that to characterize the system for a wide range of the correlating parameters (d_0 , d_1 , V_1 , P_1 , and P_2), a very large number of tests would be required.

A better approach, which would eliminate many experiments while accomplishing the same objective, is to nondimensionalize the governing equation and define a pressure coefficient. The governing equation for flow through the inverted orifice is the energy equation with a loss term, which is equivalent to Bernoulli's equation with an energy loss term:

$$P_1 + \frac{1}{2}\rho V_1^2 = P_2 + \frac{1}{2}\rho V_2^2 + K_L \frac{1}{2}\rho V_1^2 \quad (10.1)$$

The velocity ratio V_2/V_1 is a function of d_1/d_0 , and the loss coefficient K_L is essentially only a function of d_1/d_0 and the Reynolds number ($\rho V_1 d_0/\mu$). A dimensionless pressure coefficient C_p can be defined as:

$$C_p = \frac{P_1 - P_2}{\frac{1}{2} \rho V_1^2} \quad (10.2)$$

Therefore, Equation 10.1 can be expressed as:

$$C_p = \frac{P_1 - P_2}{\frac{1}{2} \rho V_1^2} = f_1\left(\frac{d_1}{d_0}\right) - 1 + f_2\left(\frac{d_1}{d_0}, \frac{\rho V_1 d_0}{\mu}\right) \quad (10.3)$$

where:

- V_1 = velocity of the fluid upstream of nozzle
- ρ = density of the fluid
- μ = dynamic viscosity of the fluid
- d_0, d_1 = dimensions shown in [Figure 10.1](#)

and C_p is seen to be only a function of d_1/d_0 and Reynolds number ($\rho V_1 d_0/\mu$). The dimensionless pressure coefficient (C_p) represents the ratio of pressure forces to inertial forces.

Instead of conducting many experiments varying $d_0, d_1,$ and V_1 to develop families of curves, fewer curves can be developed requiring significantly fewer tests. The curve in Figure 10.2b was generated at a constant Reynolds number, and it contains similar information as shown in Figure 10.2a, except that it is expressed in a nondimensional fashion. By nondimensionalizing the problem, the number of correlating parameters can be reduced from five ($d_0, d_1, V_1, P_1,$ and P_2) to three

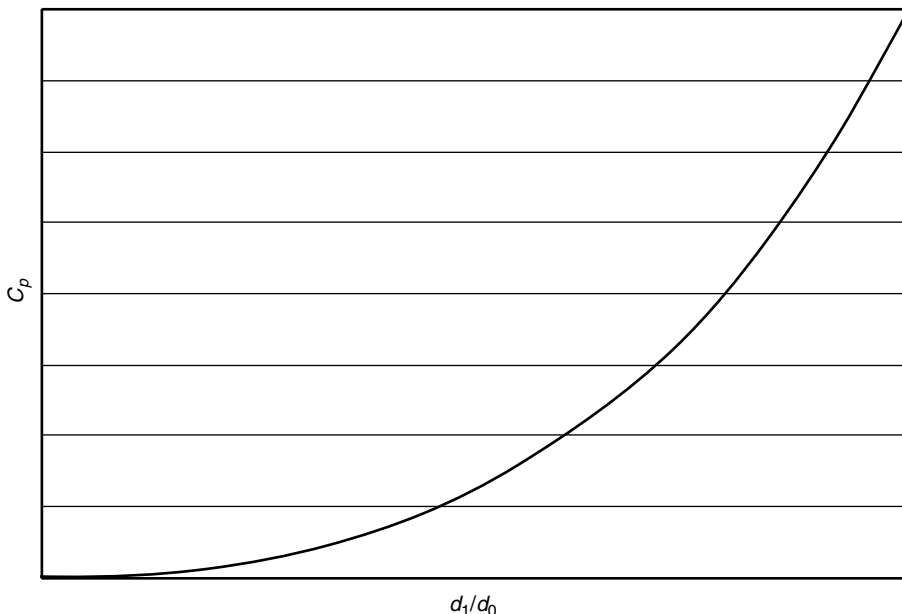


FIGURE 10.2b Nondimensional pressure coefficient.

(C_p , Reynolds number, and d_1/d_0). This example demonstrates the power of dimensional analysis to reduce the number of correlating parameters to the minimum required, and also to significantly reduce the number of tests required to characterize a flow problem. As discussed in the following chapter sections, above a certain Reynolds number, C_p does not vary significantly with Reynolds number for many geometries.

10.2 METHODS OF DIMENSIONAL ANALYSIS

The example of the previous section clearly illustrates the need for using dimensional analysis to conduct flow-modeling studies. There are several good references on dimensional analysis, such as Fox and McDonald¹ and De Nevers.² The Buckingham Pi theorem provides the framework and methodology for determining the pertinent dimensionless parameters for a given flow scenario.

10.2.1 BUCKINGHAM PI THEOREM

For a physical fluid flow problem where a dependent variable is a function of $n - 1$ independent parameters, the relationship between the parameters can be expressed as:

$$q_1 = f(q_2, q_3, q_4, \dots, q_n) \quad (10.4)$$

where, q_1 is the dependent parameter and $q_2, q_3, q_4, \dots, q_n$ are independent parameters. The relationship can be expressed equivalently as:

$$g(q_1, q_2, q_3, q_4, \dots, q_n) = 0 \quad (10.5)$$

The Buckingham Pi theorem says that when a relationship such as Equation 10.5 exists between n parameters, the parameters may be grouped into $n - m$ dimensionless and independent ratios (Π parameters). A set of Π parameters is not independent if any of them can be expressed as a product or quotient of the others.

In addition, the Buckingham Pi theorem states that these $n - m$ dimensionless ratios can be expressed in either of the following functional forms:

$$G_1(\Pi_1, \Pi_2, \Pi_3, \Pi_4, \dots, \Pi_{n-m}) = 0$$

or

$$\Pi_1 = G_2(\Pi_2, \Pi_3, \Pi_4, \dots, \Pi_{n-m})$$

The number m is often, but not always, the minimum number of independent (or primary) dimensions required to specify the dimensions of the $q_1, q_2, q_3, \dots, q_n$ parameters. Examples of independent (or primary) dimensions are mass, length, and time. Force and energy are not primary dimensions because they can be expressed as products and quotients of mass, length, and time. The Buckingham Pi theorem does not state what the function form of the $\Pi_1, \Pi_2, \Pi_3, \Pi_4, \dots, \Pi_{n-m}$ parameters will be. This functional form must be determined through experimentation.

10.2.2 METHOD FOR DETERMINING THE Π GROUPS

The following is a systematic method for determining the Π groups:

Step 1. Develop a list of all pertinent parameters. If it is questionable whether or not a parameter is involved, it is prudent to list it, thereby reducing the likelihood of missing pertinent

parameters. One of the parameters will be the dependent parameter, and it should be identified. Let n be defined as the number of pertinent parameters.

Step 2. Define the primary dimensions (mass, length, time, etc.) for the problem.

Step 3. Express each parameter in terms of its primary dimensions. Let r be defined as the number of primary dimensions required to define the problem.

Step 4. From the list of dependent parameters (**Step 1**), find a number of repeating parameters equal to the number of primary dimensions r . These repeating parameters should include all the primary dimensions from **Step 2**. The repeating parameters should be selected such that they cannot be combined internally into a dimensionless group.

Step 5. Combine the repeating parameters with each of the remaining parameters to form $n - m$ dimensionless groups (Π parameters). Usually, m is equal to the number of primary dimensions r .

Step 6. Verify that each Π parameter is dimensionless.

10.2.3 APPLICATION OF THE BUCKINGHAM PI THEOREM

This section applies the Buckingham Pi theorem to the previously discussed problem for characterizing pressure drop for flow through an inverted nozzle shown in [Figure 10.1](#).

Step 1. Dependent parameter: ΔP , where $\Delta P = P_1 - P_2$

Independent parameters: V, ρ, d_0, d_1, μ ($n = 6$ parameters)

V = velocity of the fluid

ρ = density of the fluid

μ = dynamic viscosity of the fluid

d_0, d_1 = dimensions shown in [Figure 10.1](#)

Step 2. Primary dimensions: M (mass), L (length), t (time) ($r = 3$ dimensions)

Step 3. Expressing each parameter in terms of its primary dimensions:

$$\Delta P: \frac{M}{Lt^2} \quad V: \frac{L}{t} \quad \rho: \frac{M}{L^3} \quad d_0, d_1: L \quad \mu: \frac{M}{Lt}$$

Step 4. Find r repeating parameters: $V, \rho,$ and d_0

Step 5. Combine the repeating parameters with the remaining parameters to form $n - m$, where $m = r$, dimensionless groups or Π parameters.

$$\Pi_1 = (\Delta P)\rho^a V^b d_0^c$$

Substituting primary dimensions for each parameter, $\Pi_1 = \left(\frac{M}{Lt^2}\right)\left(\frac{M}{L^3}\right)^a \left(\frac{L}{t}\right)^b (L)^c$

Step 6. To make Π_1 dimensionless, the exponents for each primary dimension are summed and equated to zero:

$$M: a + 1 = 0$$

$$L: -1 - 3a + b + c = 0$$

$$t: -2 - b = 0$$

Therefore, $a = -1$, $b = -2$, and $c = 0$, and the first Π parameter is shown below:

$$\Pi_1 = \frac{\Delta P}{\rho V^2}$$

Typically, ΔP is made nondimensional by dividing by dynamic pressure; therefore:

$$\Pi_1 = \frac{\Delta P}{\frac{1}{2}\rho V^2}$$

A similar process is conducted for the remaining Π parameters,

$$\Pi_2 = \mu \rho^a V^b d_0^c \quad \text{and} \quad \Pi_3 = d_1 \rho^a V^b d_0^c$$

The remaining Π parameters become:

$$\Pi_2 = \frac{\rho V d_0}{\mu} \quad \text{and} \quad \Pi_3 = \frac{d_1}{d_0}$$

The Π_1 parameter is the pressure coefficient (C_p), Π_2 is the Reynolds number, and Π_3 is the diameter ratio for the orifice. Therefore, $C_p = F(\text{Re No.}, \frac{d_1}{d_0})$, where the functional relationship must be determined through experimentation.

10.3 DIMENSIONAL ANALYSIS AND MODEL STUDIES

When performing a scaled model study of fluid flow phenomena, the model test should yield useful information on forces, pressures, and velocity distributions that would exist in the full-scale prototype. For the model to produce useful information on forces, pressures, and velocities, it must be similar to the prototype in certain respects. There are three similarity types that can be required of a model with respect to the prototype: geometric similarity, kinematic similarity, and dynamic similarity.

Geometric similarity requires that the model and prototype be of the same shape. In addition, the ratio of model dimension to prototype dimension should be a constant scale factor throughout the geometry.

Kinematic similarity requires that velocities be in the same direction at all points in the model and prototype. An additional requirement is that the ratio of model velocity to prototype velocity be a constant scale factor for all locations in the geometry, so that flows that are kinematically similar have similar streamline patterns. Because boundaries of the geometry determine the bounding streamlines, flows that are kinematically similar must also be geometrically similar.

The third type of similarity is dynamic similarity, which exists when model and prototype force distributions are in the same direction (i.e., parallel) and the ratio of the magnitudes is a constant scale factor. Dynamic similarity requires that both geometric and kinematic similarity exist between the model and prototype. To achieve dynamic similarity, all forces (pressure, viscous, surface tension, etc.) acting on the fluid must be considered. The dimensionless groups determined by applying the Buckingham Pi theorem can be shown to be ratios of forces (e.g., the Reynolds number is the ratio of the inertia force to the viscous force). This implies that to achieve dynamic similarity, all of the pertinent dimensionless groups must be matched between the model and the prototype (For example, $\text{Re No.}_{\text{model}} = \text{Re No.}_{\text{prototype}}$). As discussed in a subsequent section, in practicality for many model studies, complete dynamic similarity cannot be achieved but it is still possible to use the model test results to accurately predict forces and pressures in the prototype.

10.4 AIRFLOW REQUIREMENTS FOR PROPER BURNER OPERATION

Up to this point, the need for dimensional analysis and the associated methods and theory have been discussed in some detail. Additionally, Chapter 10.3 discussed how dimensionless analysis is applied in conducting physical flow modeling studies. This section discusses the application of flow model studies for burner design.

There are three very important factors related to airflow for burner designers:

1. For multiple burner units, each burner should receive an equal amount of airflow. For units with FGR (flue gas recirculation), this implies that each burner should also receive the same amount of FGR.
2. The velocity distribution entering each burner should be uniform around the periphery of the air inlet.
3. The airflow in the burner should not have swirl caused by the conditions of the air as it enters the burner. Most burners, by design, generate swirl in the air after it has entered the burner, but the airflow inlet conditions should not generate swirl.

As a result of many observations of multiple-burner, oil and gas firing equipment, on a wide range of boiler designs, it has been concluded that the proper airflow distribution to each burner is essential in order to control flame shape, flame length, excess air level, and overall combustion efficiency. Proper airflow distribution consists of equal combustion airflow between burners, uniform peripheral velocity distributions at the burner inlets, and the elimination of tangential velocities within each burner. If the unit has been designed with windbox FGR, the O_2 content must be equal between the burners, and this is accomplished by balancing the FGR distribution to each burner. Considering that air in the combustion process accounts for approximately 94% of the mass flow, numerous observations on boiler combustion systems have shown that correct airflow distribution is a key factor in the achievement of high performance (low NO_x , low O_2 , and low CO). The concept of equal stoichiometry at each burner results in the minimum O_2 , NO_x , and CO. The most direct way to achieve this is to ensure equal distribution of air and fuel to each burner. Airflow distribution is difficult because it requires a reliable and repeatable flow measuring system in each burner, and a means to correct the airflow without disrupting the peripheral inlet distribution or adding swirl to the airflow.

The remainder of this section explains how each of the three airflow factors relates to a specific burner performance parameter. To achieve the lowest emissions of NO_x , CO, opacity, and particulate, at the minimum excess O_2 , equalization of the mass flow of air to each burner is required. Mass flow deviations should be minimized to enable lower post-combustion O_2 , CO, and NO_x concentrations. The lowest post-combustion O_2 concentration possible is constrained by the burner most starved for air. This starved burner will generate a high CO concentration and, consequently, the total O_2 must be raised to minimize the formation of CO in that burner. By equalizing the airflow to each burner and ensuring that the fuel flow is equal, the O_2 can be lowered until the CO starts to increase equally for all burners. Lower O_2 not only lowers NO_x formation, but also results in higher thermal efficiency. The goal is to reduce the mass flow differences between burners (in the model) to within $\pm 2\%$ of mean. Obviously, this goal becomes inconsequential if the boiler has only one burner.

Flame stability is a very important aspect of the burner and one that appeals to the boiler operator. Flame stability is enhanced in the model by controlling two parameters: peripheral distribution of airflow at the inlet and the inlet swirl number. Flame stability is primarily controlled in the burner design but must be supported by proper inlet conditions. The equalization of the peripheral air velocity at the burner inlet will result in equal mass flow of air around and through the periphery of the flame stabilizer. The flame stabilizer will tend to equalize any remaining flow deviations because of the high velocity developed in this region of the burner throat. The result of

an equal air mass flow distribution through and around the flame stabilizer will be a fully developed and balanced vortex at the center of the outlet of the flame stabilizer. Flame stability and turndown of the burner depend on the condition of this vortex and its attachment to the flame stabilizer. Nonuniform peripheral inlet velocities result in an asymmetrical vortex, which can lead to a multiplicity of problems. An asymmetrical vortex behind the flame stabilizer can lead to a flame that has poor combustion performance and is more sensitive to operating conditions: turndown might be limited, combustion-induced vibrations might be experienced, FGR might cause flame instability at lower loads, light-off by the ignitor might be more difficult, and flame scanning might show increased sensitivity. Another consideration is that low-NO_x burners rely on injection of fuel at precise locations within the burner airflow, and thus it is imperative that the proper airflow be present at the injection locations. A goal in the model is to reduce peripheral airflow deviations to $\pm 10\%$ at each burner entrance.

Swirl number is an indication of the rotational flow entering the burner. The creation of swirling air is a fundamental requirement of all burners. Louvered burners create this swirl by rotating the entire air mass. Unfortunately, this creates a problem at high turndown rates. At low loads (e.g., 10% of full load heat input), excess O₂ is typically 11 to 13%. By swirling the entire air mass, the fuel is diluted to the point where flame stability becomes marginal. Swirling air entering louvered burners (not created by the burner louvers) can result in different burner-to-burner register settings to obtain uniform swirl intensity at each burner. The differing register positions consequently affect the air mass flow at each burner.

An axial flow burner operates on the principle of providing axial airflow through the burner and developing a controlled swirling vortex of primary air at the face of the smaller, centrally located flame stabilizer (or swirler). This concept maintains a stable flame at the core of the burner by limiting dilution at high turndown rates. The secondary air that passes outside the flame stabilizer, however, is most effective if it is not swirling (which is the concept behind “axial flow” burners). Swirling secondary air increases the dilution of the fuel and limits turndown. A goal in the model, for both the louvered burner and the axial flow burner, is to eliminate any tangential velocities entering the burner. The only swirl present must be that created by the burner itself.

The thermal NO_x from a burner increases exponentially with an increase in flame temperature. The introduction of FGR into the combustion air increases the overall mass of the reactants, and hence the products, in the combustion process. The increased mass, as well as the increased reactant diffusion time requirement, reduce the overall flame temperature. The burner with the least amount of FGR will theoretically have the highest flame temperature and will therefore have the highest NO_x. Likewise, the burner with the highest amount of FGR will theoretically have the lowest flame temperature and lowest NO_x. However, due to the exponential nature of the NO_x-temperature relationship, given an equal FGR deviation (e.g., $\pm 10\%$) between two burners, the higher NO_x values from the low FGR burner will outweigh the lower NO_x values from the high FGR burner. Minimizing the FGR deviations will even out the flame temperatures and therefore minimize the overall NO_x formation rate.

To achieve the goals described above, a scaled aerodynamic simulation model, similar to the one shown in [Figure 10.3](#), can be constructed and tested, based on the physical dimensions and flow rates within the field unit. The model shown in [Figure 10.3](#) is for a 24-burner opposed wall-fired utility unit, equipped with FGR and over-fire air (OFA). A scale model constructed of Plexiglas allows for full visualization of the airflow within the windbox/burner configuration and existing ductworks. The goals of the model are primarily accomplished by installing secondary air duct and windbox baffles. The modeler determines the location of baffles and turning vanes within the combustion air/FGR supply system. An additional goal of the modeling is to have minimal impact on the combustion air/FGR supply system pressure drop. This minimizes the effects on the unit fan performance.

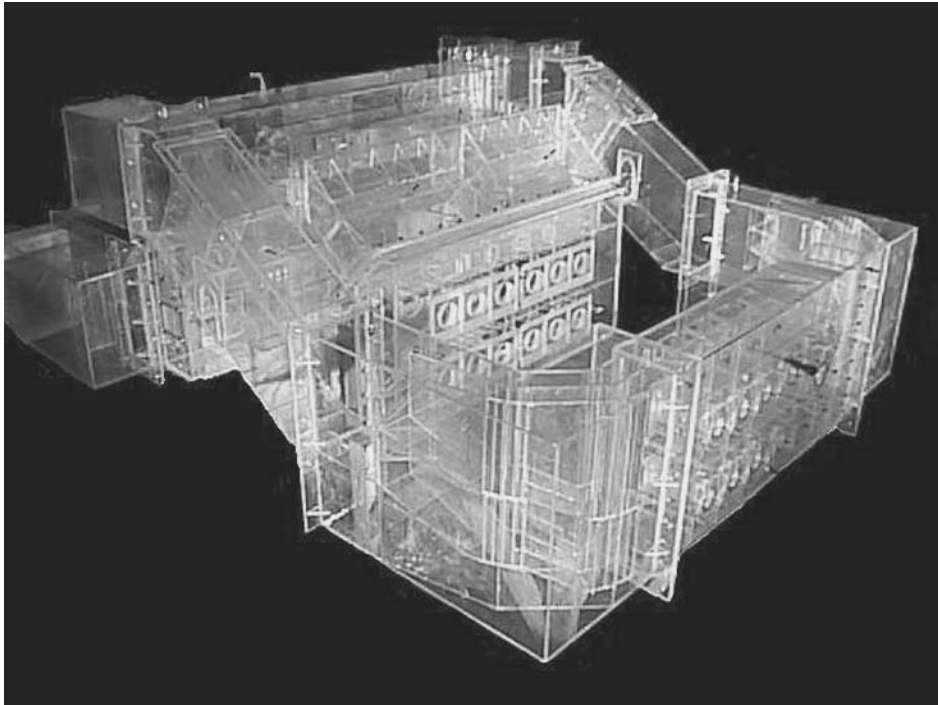


FIGURE 10.3 Windbox model for 24-burner utility boiler.

In summary, the airflow modeling should have four primary goals:

1. To reduce the mass flow differences between burners (in the model) to within $\pm 2\%$ of mean
2. To reduce peripheral airflow deviations to $\pm 10\%$ at each burner entrance
3. To eliminate any tangential velocities entering the burner, so that the only swirl present must be that created by the burner itself
4. To accomplish the first three modeling objectives with minimal impact on overall combustion air/FGR supply system pressure drop

Mass flow deviations from average are shown in [Figure 10.4](#) for a 24-burner utility boiler, and the modeled deviations were within $\pm 2\%$. Also shown in [Figure 10.4](#) are field results on the boiler after correcting the windbox airflow, and mass flow deviations measured in the field were within approximately $\pm 5\%$. A result of meeting the four airflow modeling goals described above is flame-to-flame similarity. [Figure 10.5](#) shows modeled peripheral velocity distribution results for a boiler before and after correction. As seen, the peripheral velocity distribution was very poor before correction. Also shown in [Figure 10.5](#) are flame photographs before correction, and there is a direct correlation between the airflow maldistribution and an unevenly distributed flame shape.

10.5 USING SCALED MODELING FOR ACHIEVING PROPER BURNER AIRFLOW

No modeling work can produce an exact model of reality unless an exact model of the full-scale situation (i.e., another boiler) is made. As discussed in Chapter 10.3, to achieve dynamic similarity, all pertinent dimensionless groups must be matched between the model and the prototype. For airflow modeling of the windbox, connected ductwork, and the burners, geometric and kinematic

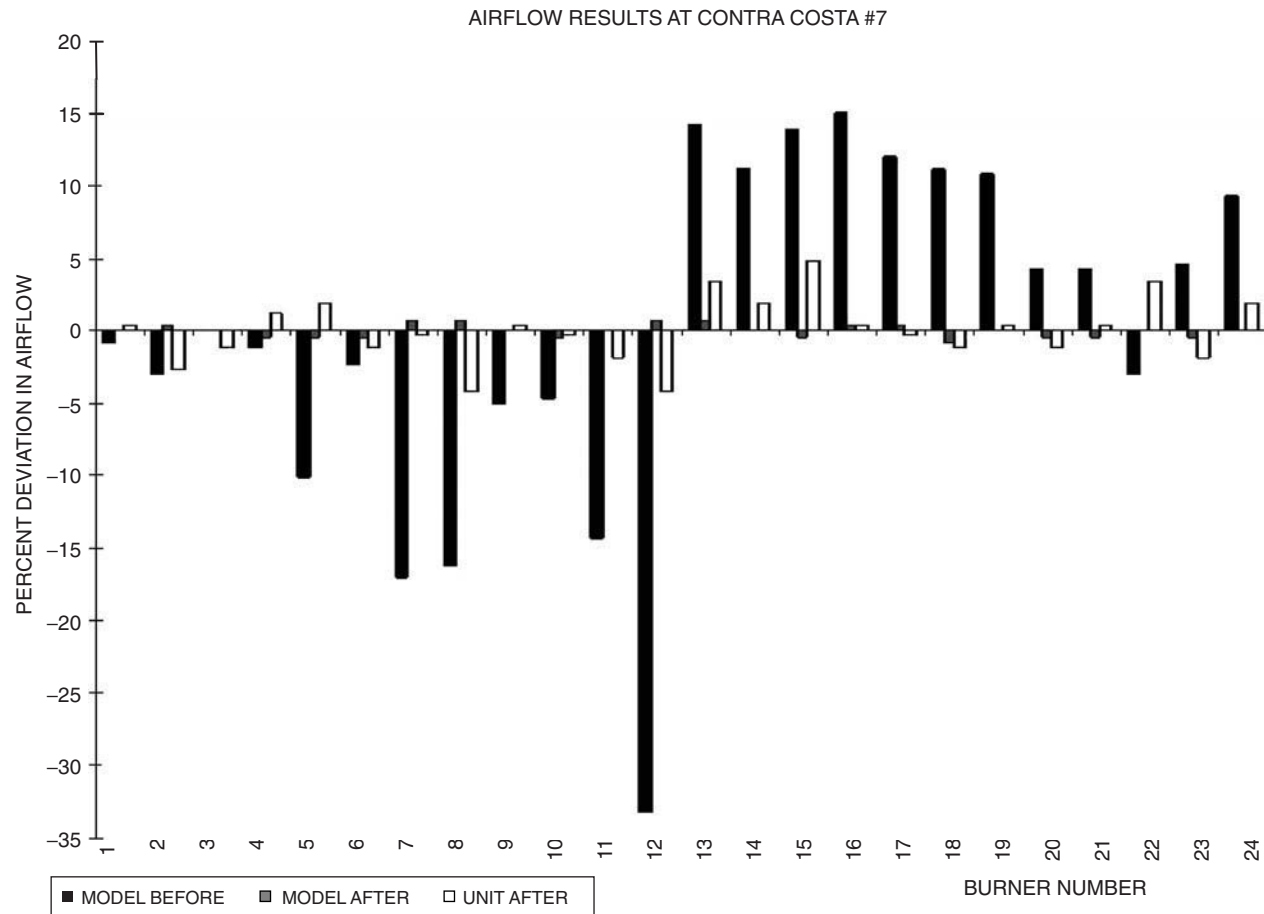


FIGURE 10.4 Improvement of airflow distribution to burners.

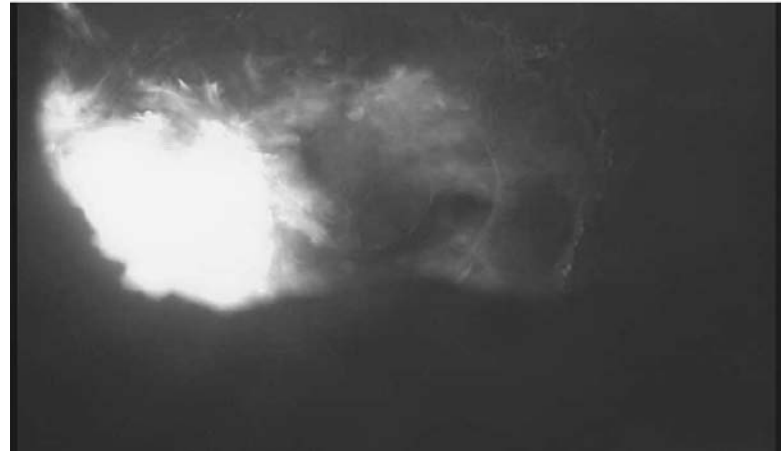
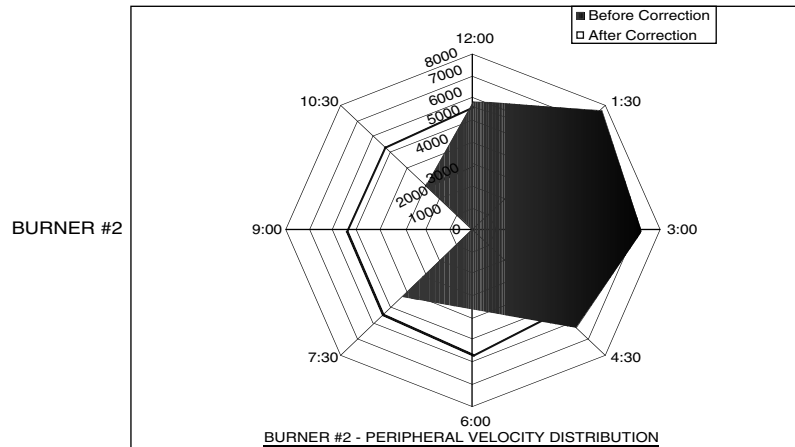
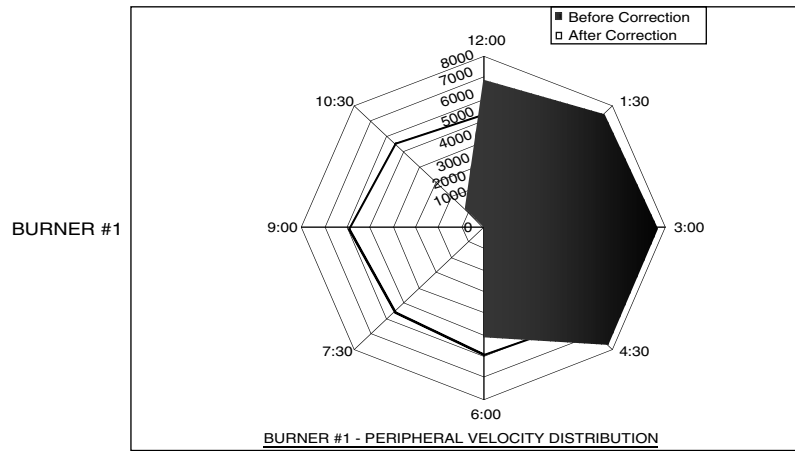


FIGURE 10.5 Effect of peripheral airflow distribution on flame shape.

similitude should be achieved with the scaled model. To achieve dynamic similitude, there are two dimensionless parameters that must be matched: the Reynolds number and the pressure coefficient C_p . This can be verified by applying the Buckingham Pi theorem, which results in Equation 10.6:

$$\text{Re No.}_{\text{model}} = \text{Re No.}_{\text{prototype}} \quad \text{and} \quad C_{p \text{ model}} = C_{p \text{ prototype}} \quad (10.6)$$

where:

$$\text{Re No.} = \frac{\rho V L}{\mu} \quad \text{and} \quad C_p = \frac{\Delta P}{\frac{1}{2} \rho V^2}$$

Air is typically used as the working fluid in the model and the prototype. The model air temperature is typically around 100°F and the prototype air temperature is typically around 530°F (for preheated air). Equating Reynolds numbers, this yields the following relationship between velocities and geometrical dimensions for the model and prototype:

$$\frac{V_{\text{model}}}{V_{\text{prototype}}} \cong 0.37192 \left(\frac{L_{\text{prototype}}}{L_{\text{model}}} \right) \quad (10.7)$$

Model scale is usually around 1/12 ($L_{\text{prototype}}/L_{\text{model}} = 12$) because of physical size constraints, which suggests that:

$$\frac{V_{\text{model}}}{V_{\text{prototype}}} \cong 4.5$$

Prototype duct velocities are typically around 50 ft/sec; this suggests that the model velocity would be in excess of 200 ft/sec to achieve complete dynamic similitude. An air velocity of 200 ft/sec becomes a bit impractical for Plexiglas model construction, and 200 ft/sec would introduce unwanted compressibility effects into the test results. Compressibility effects would result in the model and prototype no longer being kinematically similar, and would require that pitot tube measurements be corrected. For most, if not all, of the losses encountered in windbox and burner geometries, the loss coefficients are relatively constant above a certain Reynolds number. The airflows for windboxes, burners, and associated ductwork are well into the turbulent regime, and it is reasonable to assume that loss coefficients are relatively constant. Therefore, an approach that has been used successfully on many modeling studies is to operate the model at the same velocity as the prototype. The result is that the pressure coefficient C_p will be the same for the model and prototype, which implies that the pressure losses in the model will match those in the prototype. Therefore, experience has shown that although complete dynamic similarity cannot be achieved, it is still possible to use the model test results to accurately predict forces and pressures in the prototype.

10.6 CHARACTERIZATION OF BURNER SWIRL

As discussed, it is important to eliminate the swirl in the burner caused by swirl in the air entering the burner or by a nonuniform peripheral velocity distribution at the inlet. To characterize burner swirl, a swirl number can be computed based on the ratio of angular momentum to the axial momentum. Beer³ recommends an equation for swirl number as given by:

$$S_n \equiv \frac{\int_0^R (Wr) \rho U 2\pi r dr}{R \int_0^R U \rho U 2\pi r dr} \quad (10.8)$$

where:

- W = tangential velocity
- U = axial velocity
- ρ = fluid density
- R = burner radius
- S_n = swirl number

Experimental studies have shown that the swirl number, as shown above, is an appropriate similarity criterion for swirling jets, produced by geometrically similar swirl generators. Therefore, the swirl number (S_n) as given by Equation 10.8 can be used to characterize swirl intensity in the burner. As discussed, the swirl number can have a significant effect on the flame behavior. The North American Combustion Handbook⁴ provides the following approximate rules, applicable to gas and oil burners. The change in swirl from one category to the next typically has a significant effect on flame shape.

- $S_n \sim 0.3$ (Moderate Swirl)
- $S_n > 0.6$ (Considerable Swirl)
- $S_n > 1$ (High Swirl)
- $S_n > 2$ (Very High Swirl)

10.7 TECHNIQUES FOR BURNER MODELING

The discussion of scaled modeling to this point has focused on simulating airflow within the windbox and through the burner without regard for what happens downstream of the burner. Care must be taken to accurately model the jet leaving a burner where combustion takes place. An abrupt change in density occurs as a result of burning the fuel/air mixture. This change in density significantly affects the jet momentum and its rate of entrainment and, therefore, the shape of the jet, as shown in Figure 10.6. Without combustion, capturing the physics in the scaled model poses a problem. Three techniques will be discussed for modeling the important fluid mechanical characteristics of a combusting jet with a scaled isothermal jet:

1. In the Thring-Newby⁵ method, it is assumed that the momentum of the burnt gases controls the fluid mechanics in the furnace. To achieve this hot gas momentum with an isothermal model at room temperature, the model nozzle is exaggerated.
2. The Zerkowski⁶ method attempts to improve upon the Thring-Newby method by using a nozzle that is not as exaggerated, but is displaced back a certain distance.
3. The Davison⁷ method (or Gauze method) uses a strategically placed wire mesh with a certain resistance to artificially create the correct jet shape. The model nozzle is scaled geometrically.

Based on experimental evidence, the Gauze method tends to produce the most accurate results. Therefore, more discussion will be devoted to this method.

10.7.1 THE THRING-NEWBY METHOD FOR BURNER MODELING

As shown in Figure 10.6, the flame front causes the jet to expand, which increases the jet momentum. The Thring-Newby⁵ method assumes conservation of momentum and attempts to account for this increase in jet momentum by enlarging the nozzle area. Using dimensional analysis, the two important dimensionless groups are:

$$\text{Re No.} = \frac{\rho V D}{\mu} \quad \text{and} \quad \frac{L^2 \rho_f}{A \rho_0}$$

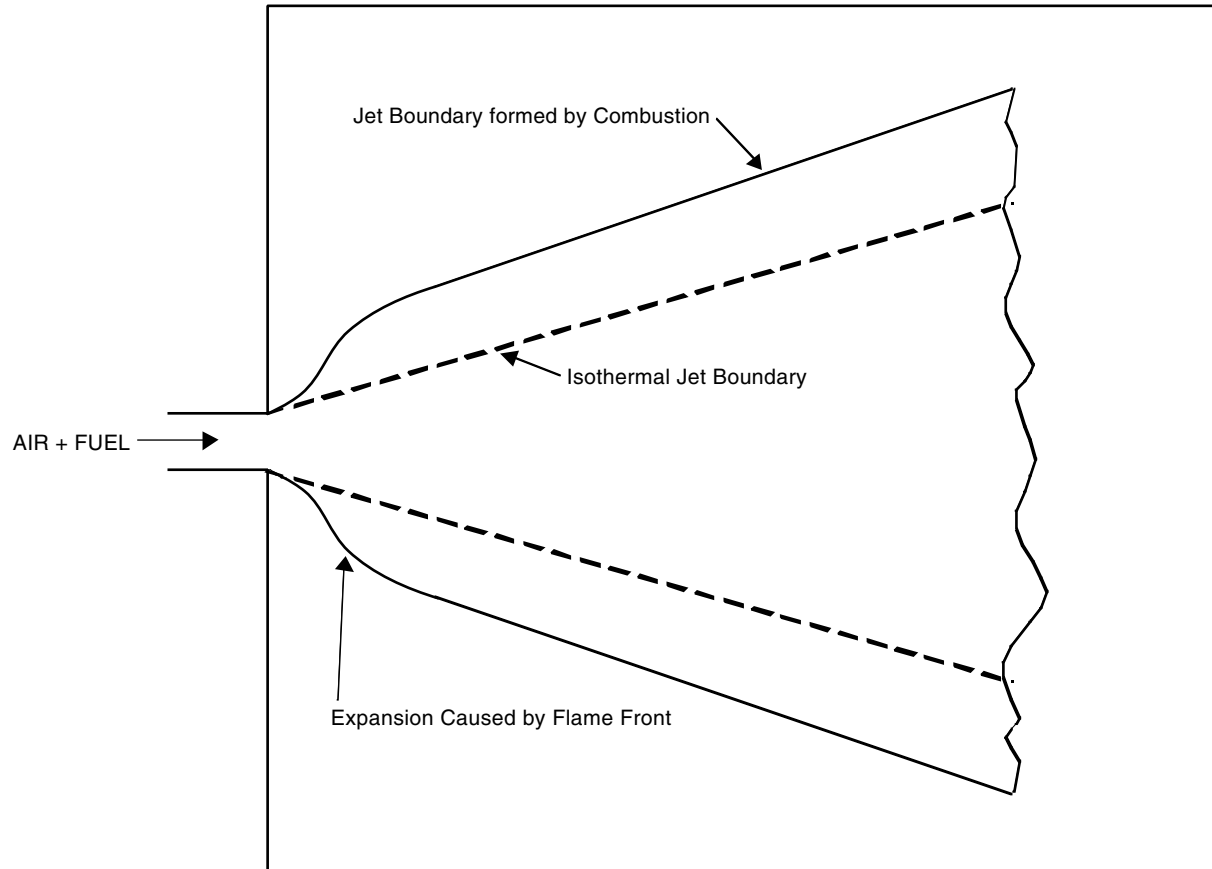


FIGURE 10.6 Combustion jet and isothermal jet boundaries.

where:

- L = characteristic dimension
- A = model nozzle area
- ρ_f = gas jet density at the flame front
- ρ_0 = gas density at the nozzle

Anson⁸ indicates that $(\text{Re No.})_{\text{model}}$ can be smaller than $(\text{Re No.})_{\text{prototype}}$ by a factor of 50 with no significant effect on results. Therefore, it is possible to neglect the Reynolds number and only consider the remaining dimensionless group. Neglecting the Reynolds number, the similarity requirement is given by Equation 10.9:

$$\left(\frac{L^2 \rho_f}{A \rho_0} \right)_{\text{model}} = \left(\frac{L^2 \rho_f}{A \rho_0} \right)_{\text{prototype}} \quad (10.9)$$

The model scale factor is defined by:

$$\text{SF} = \frac{L_{\text{prototype}}}{L_{\text{model}}}$$

The working fluid in the model is air; thus, for the model, $\rho_f = \rho_0$. This results in the following relationship for enlarging the nozzle size using the Thring-Newby method:

$$\frac{A_{\text{model}}}{A_{\text{prototype}}} = \frac{1}{(\text{SF})^2} \left(\frac{\rho_0}{\rho_f} \right)_{\text{prototype}} \quad (10.10)$$

The model inlet velocity is typically the same as in the prototype, so that with the enlarged inlet area, the Thring-Newby jet maintains the same momentum of the hot combustion gases at the flame front. Figure 10.7 shows a schematic comparing the Thring-Newby jet with a typical flame shape. The velocity profile at a given cross section is a function of the centerline velocity, which depends on the length of the potential core of the jet. The length of the potential core depends on the nozzle size. Therefore, because of the enlarged nozzle size, the velocity profiles from using the Thring-Newby⁵ method are in error.

10.7.2 THE ZELKOWSKI METHOD FOR BURNER MODELING

Because the nozzle is enlarged with the Thring-Newby method, the length of the potential core is considerably longer than for the actual burner jet. This results in an error in the Thring-Newby velocity profile, which has been estimated by Zelkowski.⁶ Figure 10.8 shows the velocity profile error as suggested by Zelkowski, and Equation 10.11 shows how the velocity error can be calculated. Zelkowski developed a new model to minimize the error as shown by Equation 10.11:

$$\text{VELOCITY ERROR} = \frac{\left[\int_0^{A/r_0} \left(\frac{V_c}{V_0} \right) d \left(\frac{X}{r_0} \right) \right]_{\text{model}}}{\left[\int_0^{A/r_0} \left(\frac{V_c}{V_0} \right) d \left(\frac{X}{r_0} \right) \right]_{\text{actual}}} - 1 \quad (10.11)$$

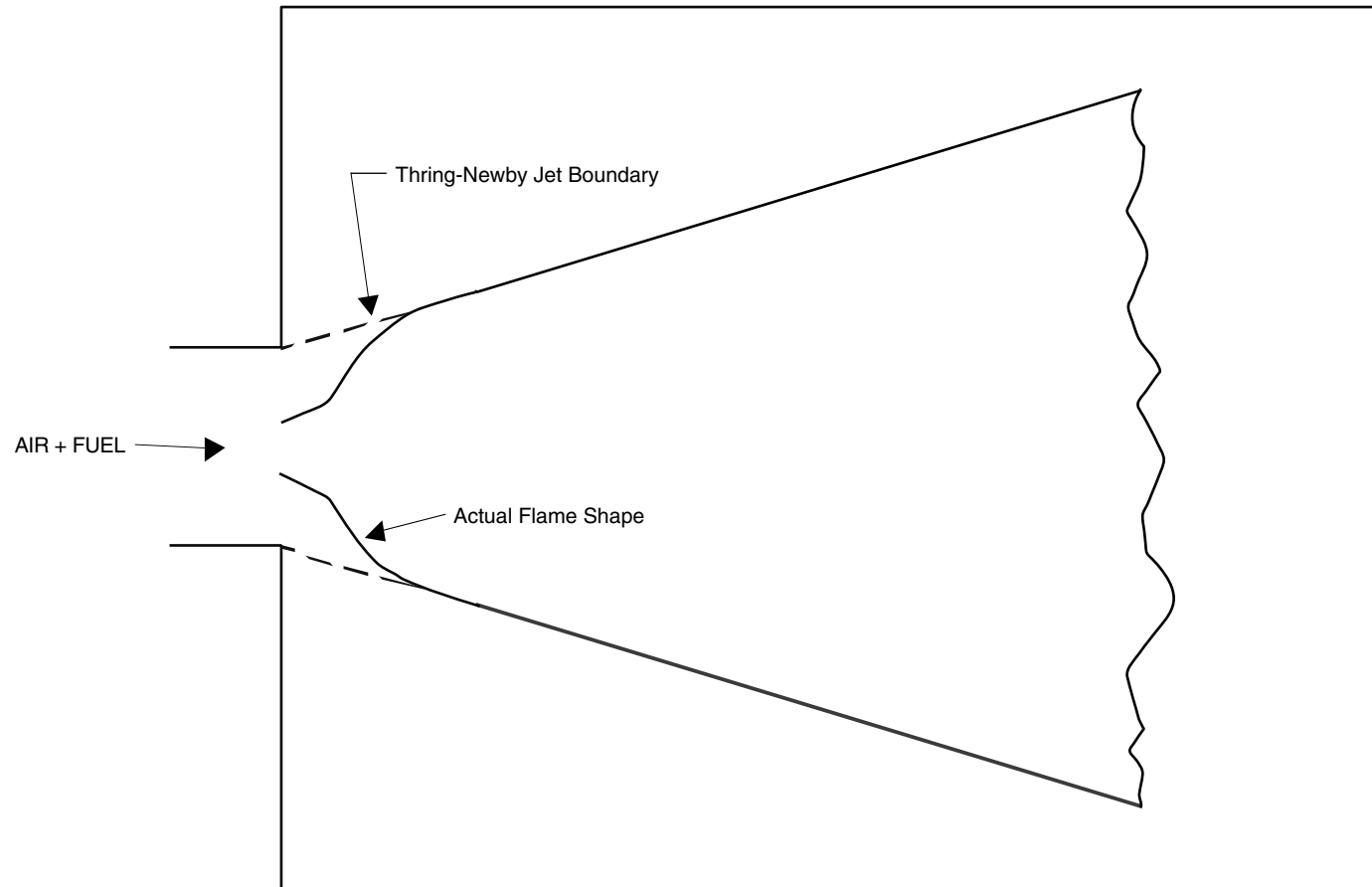


FIGURE 10.7 Thring-Newby jet boundaries.

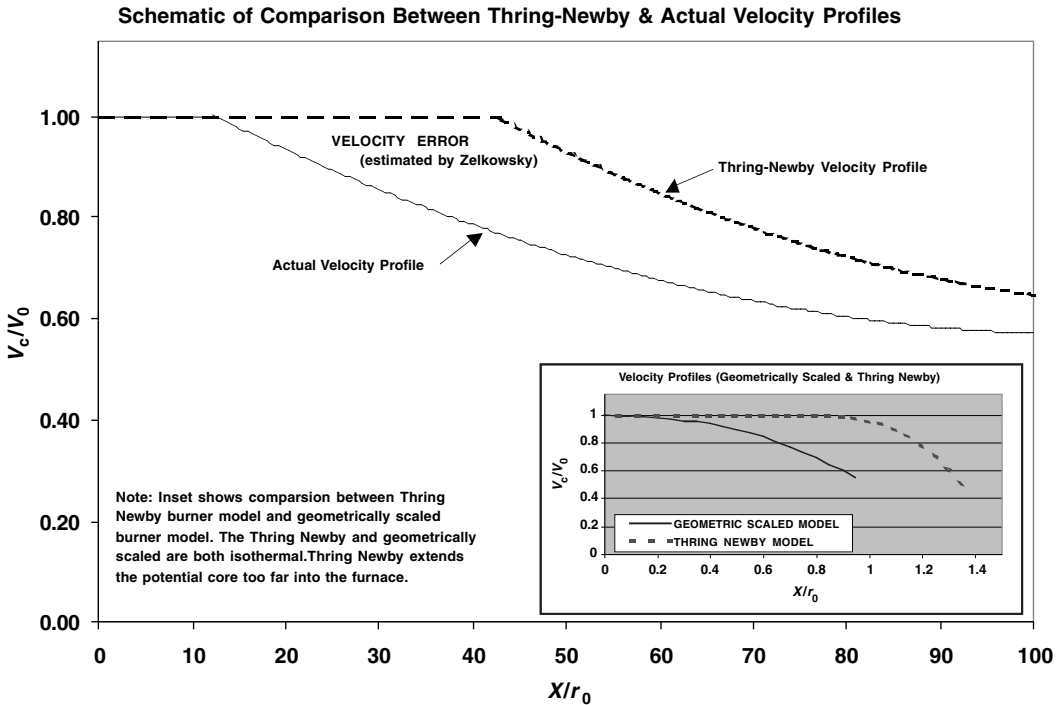


FIGURE 10.8 Thring-Newby velocity errors.

The new model uses a nozzle smaller than that used by Thring-Newby and the nozzle is displaced a certain distance behind the geometrically scaled location. Zelkowsky has put the actual velocity profile, shown in Figure 10.8, and a new parameterized model velocity profile into Equation 10.11, and then found parameters for the new profile that minimize the velocity error (Equation 10.11). Included in the parameters solved for are nozzle size and the distance displaced behind the actual location.

10.7.3 THE DAVIDSON (GAUZE) METHOD FOR BURNER MODELING

The Davison method (or Gauze method)⁷ uses a strategically placed wire mesh with a certain resistance to artificially create the correct jet shape. In the following discussion, two limiting cases are discussed. The first case is a confined jet, and the second case is an effectively free jet, as shown in Figure 10.9 and Figure 10.10, respectively. The wire grid causes the jet to expand which simulates the expansion created by the flame or combustion front. As stated above, in the Gauze method, the model nozzle is scaled geometrically. The authors recommend maintaining the same nozzle velocity in the model and prototype, as shown in Equation 10.12:

$$V_{0,model} = V_{0,prototype} \quad (10.12)$$

The primary reason for this is to prevent significant compressibility effects from occurring. Davison seems to recommend scaling the prototype nozzle velocity ($V_{0,prototype}$) by the density ratio (ρ_0/ρ_f). A typical value of $V_{0,prototype}$ is 100 to 150 ft/sec; therefore, $V_{0,model}$ would easily be around 500 ft/sec, which would introduce significant compressibility effects.

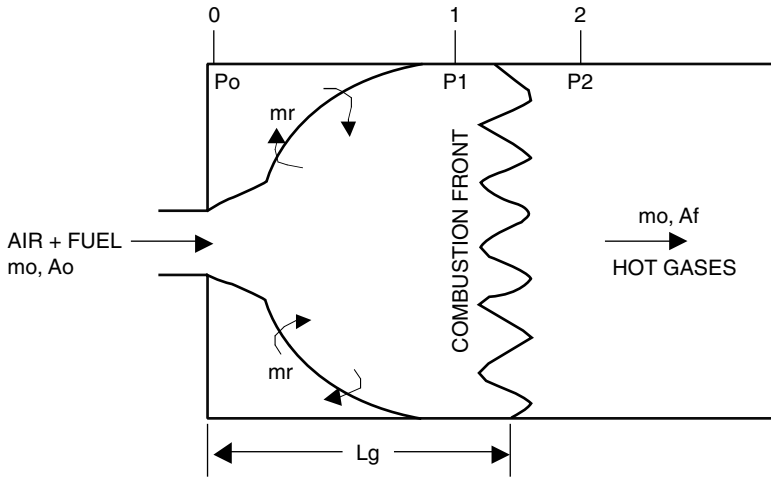


FIGURE 10.9 Confined combustion jet.

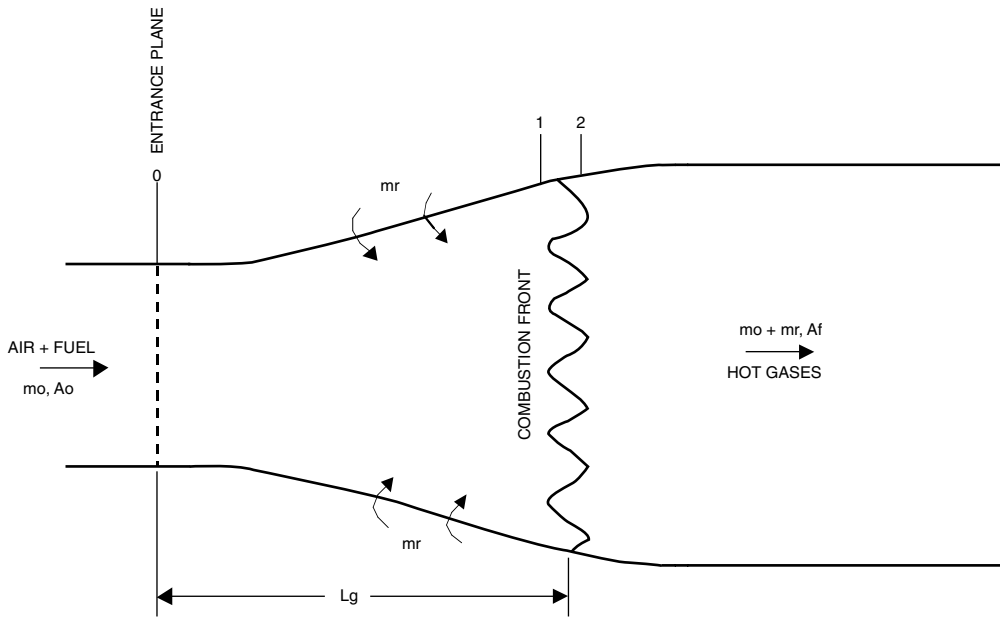


FIGURE 10.10 Free combustion jet.

10.7.3.1 Case A: Free Jet

In the free jet (Figure 10.10), the static pressures at locations 0, 1, and 2 are all equal. The jet is isothermal for the distance (L_g) from the entrance plane to the combustion front. The fluid momentum within the isothermal region entrains surrounding fluid into the jet boundary. The flame causes the gases to expand, which creates a drag force within the jet. The effect of the expansion is similar to placing an obstruction in the jet flow field, as shown in Figure 10.11. If the momentum equation is applied to a control volume around the obstruction, the drag force exerted on the fluid is given

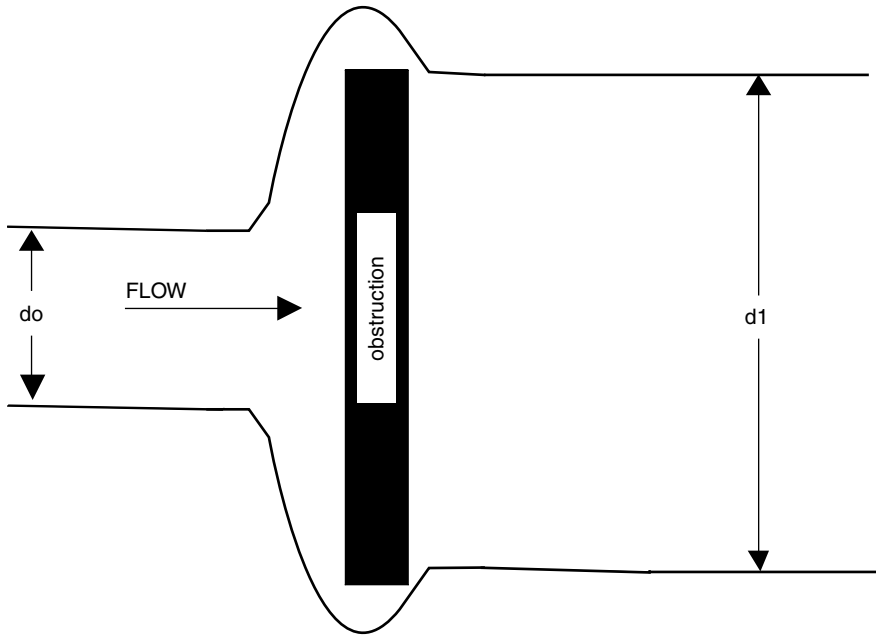


FIGURE 10.11 Jet flow field around an obstruction.

by Equation 10.13, which shows that the drag force on the fluid is a function of the flow areas upstream and downstream of the obstruction.

$$\frac{D}{G_0} = 1 - \frac{A_0}{A_1} = 1 - \frac{d_0^2}{d_1^2} \quad (10.13)$$

where:

- D = drag force exerted on fluid by obstruction
- G_0 = upstream momentum flux (product of mass flow rate and velocity)
- A_0, A_1 = flow areas upstream and downstream of obstruction, respectively
- d_0, d_1 = diameters upstream and downstream of obstruction, respectively

As stated above, for the free jet case, as depicted in [Figure 10.10](#), the pressures at planes 0, 1, and 2 are equal. Therefore, for the free jet, the flow area at plane 2 is inversely proportional to the density, $\rho_2 = \rho_f \sim 1/A_2$. Using this result in Equation 10.13 provides a relationship for the drag force of the wire grid, as shown in Equation 10.14:

$$\frac{D}{G_0} = 1 - \frac{\rho_f}{\rho_0} \quad (10.14)$$

where:

- ρ_0 = density of nozzle gas in prototype
- ρ_f = density of hot gases downstream of the combustion front in prototype

At this point, an analysis will be applied to the model with the wire grid in place. An assumption is made that the entrained flow be neglected. Referring to [Figure 10.12](#), the jet boundaries form

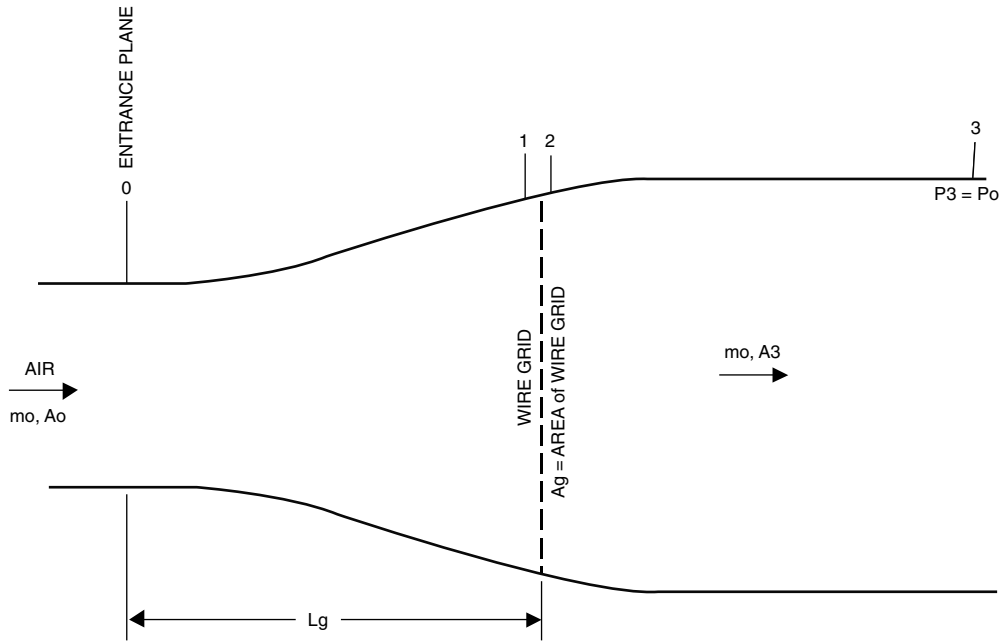


FIGURE 10.12 Modeled isothermal free jet with wire grid.

stream tubes and Bernoulli's equation can be applied between planes 0 and 1, and then between planes 2 and 3. This is shown in Equations 10.15 and 10.16:

$$P_1 - P_0 = \frac{m_0^2}{2\rho_0} \left(\frac{1}{A_0^2} - \frac{1}{A_g^2} \right) \quad (10.15)$$

$$P_3 - P_2 = \frac{m_0^2}{2\rho_0} \left(\frac{1}{A_g^2} - \frac{1}{A_3^2} \right) \quad (10.16)$$

Applying the momentum equation to a control volume bounded by planes 0 and 3, and recalling that $P_0 = P_3$, yields Equation 10.17:

$$\frac{m_0^2}{\rho_0 A_3} - \frac{m_0^2}{\rho_0 A_0} = -D \quad (10.17)$$

where D is the drag force caused by wire grid.

If the momentum equation is applied to a control volume just surrounding the wire grid, bounded by planes 1 and 2, Equation 10.18 is obtained:

$$P_1 - P_2 = \frac{D}{A_g} \quad (10.18)$$

If a resistance coefficient K is defined for the wire grid, the loss across the grid can be expressed by Equation 10.19:

$$P_1 - P_2 = \frac{K}{2} \frac{m_0^2}{\rho_0 A_g^2} \quad (10.19)$$

Combining Equations 10.14 through 10.19 results in a relationship for the wire grid resistance coefficient K in terms of the density ratio, ρ_f/ρ_0 , shown in Equation 10.20:

$$\frac{K}{2} = \frac{2\left(1 - \frac{\rho_f}{\rho_0}\right)}{\left(1 + \frac{\rho_f}{\rho_0}\right)} \quad (10.20)$$

Davison showed that Equation 10.20 is valid by demonstrating favorable comparisons with experimental data. Therefore, the above assumption of neglecting entrained mass flow in the analysis is acceptable.

10.7.3.2 Case B: Confined Jet

For this case, the jet is constrained by its surroundings, and the pressures at planes 0, 1, and 2 are not equal. Referring to Figure 10.9, the net mass entrainment (m_f) is zero because the jet is constrained by its walls. By applying the momentum equation between planes 1 and 2, a relationship for the pressure drop across the combustion front is obtained. This relationship is given by Equation 10.21:

$$P_1 - P_2 = \frac{m_0^2}{\rho_0 A_f^2} \left(\frac{\rho_0}{\rho_f} - 1 \right) \quad (10.21)$$

The pressure drop across the wire grid in the model can also be related to a resistance coefficient, as given by Equation 10.22:

$$P_1 - P_2 = \frac{K}{2} \frac{m_0^2}{\rho_0 A_f^2} \quad (10.22)$$

Equating Equations 10.21 and 10.22 gives a relationship for the wire grid resistance coefficient:

$$\frac{K}{2} = \frac{\rho_0}{\rho_f} - 1 \quad (10.23)$$

The results in Equations 10.20 and 10.23 assume that the nozzle density in the prototype and the model are the same. If they are significantly different, then Equations 10.20 and 10.23 should be corrected accordingly.

It should be noted that the two cases considered—the free jet and the confined jet—are limiting cases. Many practical cases will likely lie somewhere between these two limiting cases. For example, in the case of a large furnace with multiple burners, adjacent burners will impose some confinement, but there will also be free jet expansion. Figure 10.13 shows a comparison between the resistance coefficients for the two limiting cases discussed above. Figure 10.13 shows that only for small density ratios (ρ_0/ρ_f), the wire grid resistance coefficients for the two limiting cases are reasonably close to one another.

The authors are aware of at least one experimental investigation comparing the Thring-Newby,⁵ Zelkowski,⁶ and Davison⁷ (Gauze) methods. Based on this study, it was concluded that the Gauze model data was in good agreement with the Desbois⁹ model of vortex flow phenomena, applied to corner fired furnaces. Additionally, the Gauze model data agreed reasonably well with visualization photographs of flow in the lower furnace regions of a prototype furnace. The Gauze method appears to produce more realistic results than the Thring-Newby and Zelkowski methods.

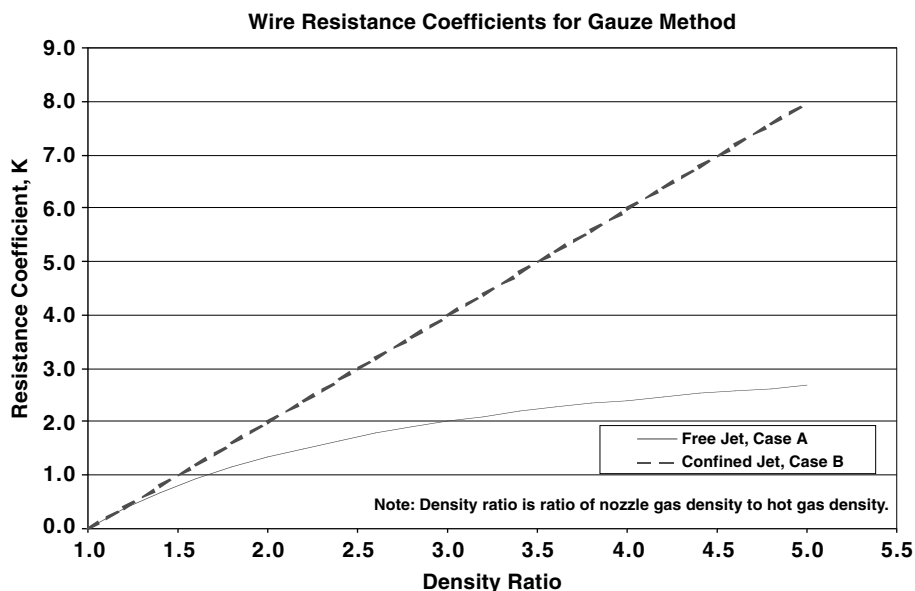


FIGURE 10.13 Gauze method resistance coefficients.

10.8 SCALED MODELING OF FLOW-INDUCED VIBRATION PHENOMENA

An in-depth discussion of flow-induced vibration is beyond the scope of this chapter; however, scaled modeling can be used for diagnosing a type of flow-induced vibration problem. Therefore, a brief discussion is given on this type of modeling. Flow-induced vibration problems can occur when either the structure is excited at one or more of its natural frequencies or when a volume of gas is excited at one or more of its resonance or natural acoustic frequencies. This section discusses flow modeling of flow-induced vibration when the natural acoustic frequencies are excited by vortex shedding.

Most steady flows (constant free stream velocity) over a bluff body, like a cylinder, typically shed vortices at some periodic frequency in the wake of the object. An exception is if the flow does not separate as it passes over the object. For example, for flow over a smooth circular cylinder, periodic vortices are not shed for a Reynolds number below about 40. But for most practical flows dealing with gases, periodic vortices will be shed. The vortices result in pressure fluctuations in the flow field. The nondimensional parameter that governs the shedding frequency is the Strouhal number S_t given by Equation 10.24:

$$S_t = f_s D / U \quad (10.24)$$

where:

f_s = frequency of periodic vortex shedding

D = diameter of bluff body member

U = steady free stream velocity

The Strouhal number varies somewhat with the Reynolds number and depends on the shape of the object. Blevins¹⁰ provides a summary of data showing the effects of Reynolds number and geometric shape on Strouhal number.

As stated, a volume of gas can be excited at one or more of its natural acoustic frequencies. When this condition occurs, sound waves reflect off duct walls to create a pattern of standing waves, and this condition is referred to as acoustic resonance. Baird¹¹ reported this phenomenon in 1954, occurring in a heat exchanger at the Etiwanda Steam Power Station when the power output reached certain megawatt (MW) levels. Baird reported that "... The vibration was accompanied by intense sound which could easily be heard in the concrete control room some distance away." Based on this example and others, the vibration energy and potential for damage is high when acoustic resonance occurs.

Acoustic resonance occurs when the gas is excited at one of its transverse natural acoustic frequencies. Transverse directions are perpendicular to the duct axis and the primary flow direction. The following equations, given by Blevins, can be used to compute the transverse natural acoustic frequencies in rectangular and round ducts.

$$f_{a,j} = \frac{cj}{2b}, \quad j = 1, 2, 3, \dots \text{ rectangular volume} \quad (10.25)$$

$$f_{a,j} = \frac{c\lambda_j}{2\pi R}, \quad j = 1, 2, 3, \dots \text{ cylindrical volume} \quad (10.26)$$

where:

- b = width (or height) of the rectangular duct transverse to the primary flow direction
- R = radius of the cylindrical duct
- c = speed of sound in gas (at the conditions in the duct)
- λ_j = dimensionless frequency parameters
- $\lambda_1 = 1.841, \lambda_2 = 3.054$

When one of the natural acoustic frequencies matches the vortex shedding frequency (Equation 10.24), within some tolerance, the probability of acoustic resonance is high.

Investigations by Blevins¹² has shown that scaled modeling can be used to reproduce the acoustic resonance condition. For a geometrically scaled model, the two parameters that must be matched are Mach number and the acoustic reduced velocity. Equations 10.27 and 10.28 define these two parameters:

$$\text{Mach number:} \quad \left(\frac{U}{c}\right)_{\text{model}} = \left(\frac{U}{c}\right)_{\text{prototype}} \quad (10.27)$$

$$\text{Acoustic reduced velocity:} \quad \left(\frac{U}{fL}\right)_{\text{model}} = \left(\frac{U}{fL}\right)_{\text{prototype}} \quad (10.28)$$

where:

- U = flow velocity
- c = speed of sound in gas
- f = acoustic natural frequency
- L = characteristic length

REFERENCES

1. R.W. Fox and A.T. McDonald, *Introduction to Fluid Mechanics, fourth edition*, John Wiley & Sons, New York, 1992.
2. N. De Nevers, *Fluid Mechanics*, Addison-Wesley, Reading, MA, 1970.
3. J.M. Beer and N.A. Chigier, *Combustion Aerodynamics*, Krieger Publishing, Malabar, FL, 1983.
4. R.J. Reed, *North American Combustion Handbook*, third edition, Vol. II, Cleveland, OH, 1995.
5. M.W. Thring and M.P. Newby, Combustion Length of Enclosed Turbulent Flames, *Fourth (International) Symposium on Combustion*, The Combustion Institute, 1953.
6. J. Zelkowski, Modelluntersuchungen uber die Stromung in Feuerraumen, *Brennst. – Wärme – Kraft* 25, 1973.
7. F.J. Davison, Nozzle scaling in isothermal furnace models, *Journal of the Institute of Fuel*, pp. 470–475, 1968.
8. D. Anson, Modeling experience with large boilers, *Journal of the Institute of Fuel*, 40, 20–25, 1967.
9. G.P. Debois, A Study of the Vortex Flow Phenomenon as Applied to Corner Fired Furnace, Masters' project, Sir George Williams University, Montreal, Quebec, 1970.
10. R.D. Blevins, *Flow-Induced Vibration, second edition*, Krieger Publishing, Malabar, FL, 2001.
11. R.C. Baird, pulsation-induced vibration in utility steam generation units, *Combustion*, 25, 38–44, 1954.
12. R.D. Blevins and M.K. Au-Yang, Flow Induced Vibration with a New Calculations Workshop, Continuing Education Short Course Notes, American Society of Mechanical Engineers, New York, 2002.

Section III

Burner Designs

11 High-Velocity Burners

Tom Robertson, Todd A. Miller, and John Newby

CONTENTS

- 11.1 Introduction
- 11.2 Types of High-Velocity Burners
 - 11.2.1 Premix Burners
 - 11.2.2 Conventional Nozzle Mix Burners
 - 11.2.3 Iso-Jet Burner
 - 11.2.4 Air-Staged Nozzle Mix High-Velocity Burner
 - 11.2.4.1 “Jet Can” Burner
 - 11.2.4.2 “Cup” Burner
 - 11.2.5 “Tube Burners” with Thin-Walled, Self-Supporting Tiles
- 11.3 Jet Theory
 - 11.3.1 Free Turbulent Jets
 - 11.3.2 Some Example Calculations
 - 11.3.3 High-Velocity Burner Installation and Chamber Effects
 - 11.3.3.1 Recessed Burners
 - 11.3.3.2 Tile Exit Geometry
 - 11.3.4 Effect of Multiple Burners
 - 11.3.4.1 Centerline Spacing
 - 11.3.4.2 Opposed vs. Staggered Wall Placement
- 11.4 High-Velocity Burner Design
 - 11.4.1 Delayed Mixing/Cup Style Air Staging Designs
 - 11.4.2 Fast Mixing Designs
 - 11.4.3 Ignition: Direct Spark, Premix Pilots
 - 11.4.4 Flame Supervision
 - 11.4.5 Tiles
 - 11.4.6 Light Oil, High-Velocity Burners
- 11.5 Heat Transfer
 - 11.5.1 Burner Selection and Sizing
 - 11.5.2 Material Heating Approaches with High-Velocity Burners
 - 11.5.2.1 Solid and Large-Shape Heating
 - 11.5.2.2 Densely Packed Loads
 - 11.5.2.3 Well-Spaced Loads or Open Settings
 - 11.5.2.4 The Fired Chamber as the Load
- 11.6 Control of High-Velocity Combustion Systems
 - 11.6.1 Fuel/Air Ratio Control
 - 11.6.2 Fixed Fuel/Air Ratio Turndown (On Ratio Turndown)
 - 11.6.3 Variable Ratio or “Thermal” Turndown
 - 11.6.4 Pulse-Firing Input Control
 - 11.6.5 High-Velocity Oil Burner Control

References

11.1 INTRODUCTION

The term “high-velocity burner” typically implies a burner with a tile outlet port sized to provide an exit velocity exceeding 300 ft/s to the combustion products passing through it, with nominal values in the 400- to 500-ft/s range for commercial products. A high-velocity burner system is usually configured to allow the momentum of the burner’s exit combustion product stream to entrain fully reacted products of combustion (POCs) from the fired chamber. This promotes POC circulation within the fired chamber with the aim of enhancing temperature uniformity and heat transfer.

High-velocity burners have been extensively used in metallurgical, ceramic, and process applications since the 1960s. For gas burners, both premix and nozzle-mixing configurations have been developed and deployed, while oil burners are only made with nozzle-mixing configurations.

Although high-velocity burners are often thought of as providing more benefits in low-temperature applications where the convective heat transfer component is dominant, they have shown themselves to be equally capable of providing value to high-temperature processes. Fuel efficiency, particularly expressed in terms of specific fuel consumption (BTU/lb), or specific fuel consumption rate (BTU/lb/h), is frequently enhanced over conventionally fired systems. This is especially true where the final exhaust gas temperatures leave the fired chamber closer to the load temperature. In addition, heating is often accomplished more quickly because the time required for the coldest part of the load to reach target temperature is reduced.

Economic drivers for the adoption of high-velocity burners include system capital and maintenance costs in addition to the efficiency, productivity, and quality aspects from improved heat transfer and temperature uniformity. In many cases, fewer strategically placed high-velocity burners can provide equivalent or better performance than conventional low- to medium-velocity burner systems. Given that the costs of the necessary flame supervision and safety controls of a burner system are a significant part of both the capital and ongoing maintenance costs, this potential reduction in the number of burners alone can provide justification for their use.

Modern nozzle mix burners may use excess air to provide a “low-temperature head” jet of combustion products to heat and stir a low-temperature application. With high-velocity burners, less excess air is required than would be needed with low- or medium-velocity burners in such an application, because the high-velocity burner’s jet temperature is diluted faster by entrainment of cooler products of combustion from the furnace. The momentum of the gas stream from a high-velocity burner can be used to drive heat into closely packed loads such as brick hacks or piles of aluminum scrap. It can also be used to advantage to promote jet mixing with surrounding gases in such applications as cupola afterburners and other fume incineration processes.

Transportable high-velocity burner systems are widely used for the on-site dryout and preheat of refractory structures such as glass tanks after reconstruction, and the on-site heat treatment of large, welded steel structures such as high-pressure gas storage tanks, where the steel structure is externally insulated with slab or blanket and the burner fired inside the vessel, essentially turning the workpiece into the furnace.

High-velocity burners present challenges to the burner designer. Designers must consider the characteristics of the required combustion product jet. Many factors influence the design of the burner and the selection of its materials of construction, including the temperature of the outlet stream, the size of the flame envelope in the fired chamber, the jet momentum required to provide the target process heating, and the target emissions level for NO_x, CO, VOCs and HCs for the burner and the resulting fired process. High temperatures and/or pressures within the burner are significant considerations both for the burner construction and the design and configuration of its mounting into the fired structure. Burner tile outlet shapes other than the conventional round port can be used to impart specific characteristics to the jet.

To take advantage of the jet characteristics requires study of the aerodynamics within the fired chamber and also of its thermal characteristics. The aerodynamics will be influenced by the size and shape of the chamber and the load to be heated, the placement of the burners and exhaust ports

leading to the flues, and the control strategy employed. The thermal characteristics will be influenced by the heat capacity and losses of the furnace and the load, their distribution relative to the heat source provided by the burners, the placement and nature of the sensors used to provide the inputs to the control system, and the actions of the outputs of that system. Optimization of the design and operation of a high-velocity burner system requires appropriate synergy between all these elements.

Although capable of effective use with most conventional thermal input and fuel/air ratio control strategies, special systems have been designed to complement the characteristics of the high-velocity burner's jet — generically known as “pulse firing systems.” They are available with many proprietary algorithms to enhance the heating and uniformity of the fired application. Special flow control hardware has been developed to reliably translate the output of these control systems into air and fuel flows fed to the high-velocity burners.

Other high-velocity burner characteristics that may be useful to the user include the high excess air capability of many of the nozzle-mixing designs, which allows their use as self-contained direct fired air heaters, or the “integral combustion chamber” configuration that can provide assured high levels of completion of combustion for sub-stoichiometric firing applications such as those where significant free oxygen in the combustion products has an undesirable reaction with the load.

11.2 TYPES OF HIGH-VELOCITY BURNERS

11.2.1 PREMIX BURNERS

In the early 1900s, gas became widely available, and with that came “aerated burners” for higher input industrial use. Premix (or “air blast”) gas burners were one of the early practical types of high-input, high-stability burners — with 100% of air and fuel intimately mixed before the point of ignition and flame attachment within the burner.

The sealed tile premix burner, often called a “tunnel burner” (Figure 11.1) contains the great majority of the combustion within the tile and thus has a very high outlet temperature for its combustion gases. The high volume resulting from the high-temperature expansion imparts a high velocity to the gas stream. Hence, premix burners may be said to be inherently high-velocity burners. However, they are of limited size, turndown range, and stability and have the disadvantage that the high heat release inside the tile is taxing for the refractory. The size limitation typically leads to the use of large numbers of premix burners in a given application. The risk of flashback into large premix manifolds has made such burner systems unpopular except for applications where their ability to provide predictably reacted combustion product streams has value. One such application is a copper shaft melting furnace, running with a sub-stoichiometric fuel/air ratio, where any significant level of free O_2 in the products of combustion must be avoided.

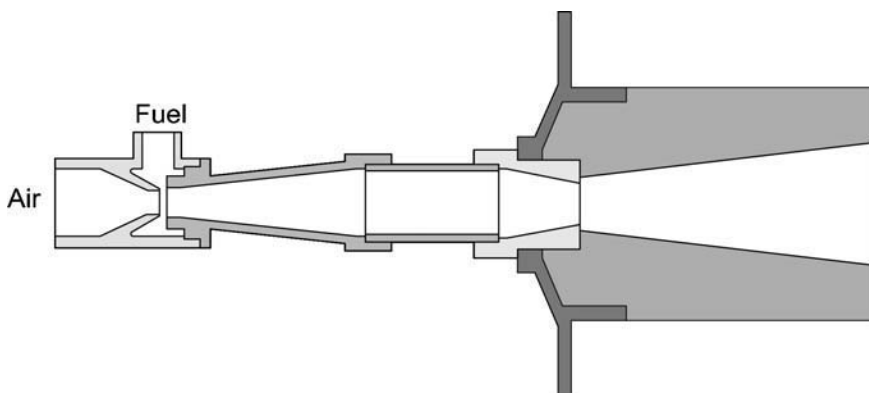


FIGURE 11.1 Premix tunnel burner.

11.2.2 CONVENTIONAL NOZZLE MIX BURNERS

The introduction of nozzle mix burners greatly simplified the control and construction of industrial combustion systems and furnaces over those using premix burners, because they had a much wider operating range and could be safely used at much larger thermal inputs.

All burners must operate within the flammability limits of the fuel they are burning. While true premix burners must operate in a single, narrow flammability window, nozzle mix burners (Figure 11.2) can have many fuel/air ratio regions within the combustion space of their tiles, with only the region at the point of ignition being required to be within the flammability limits. Heat released from regions within flammability limits broadens the limits of adjacent fuel/air regions permitting them to also burn. It can thus appear that a nozzle mix burner is operating outside the normal flammability limits of the supplied fuel based on the total fuel and air supplied to the burner.¹

Because nozzle mix burners can run under significant excess air conditions, the burner's air supply can be set at the maximum setting and the gas flow simply reduced to meet the temperature demand. The burner air and gas may still have to be turned down during times of low heat demand, but adding excess air will provide higher velocity than is possible with an equivalent premix burner at low fire. When fuel was inexpensive, there were few objections to the resulting low efficiency of heating large amounts of excess air to process temperature. Combustion system designers enjoyed the excess air capability of nozzle mix burners, because the extra velocity allowed the use of fewer burners to achieve temperature uniformity, reducing costs for larger furnaces. Combustion system designers also enjoyed the wider stability range of the nozzle mix burners that introduced a cushion to the previously difficult issue of accurately sizing a combustion system within the limited turndown range of the premix burner. Nozzle mix burners also introduced the possibility of firing oil in the same burner structure as gas, resulting in the development of both oil and dual fuel versions.

In the early to mid-1960s, burner manufacturers started to add restrictions to the tile exits of their conventional nozzle mix burners (Figure 11.3) to increase exit velocities.² The higher tile exit velocity increased the POC circulation in the furnace by entrainment, reducing the amount of excess air required to achieve good temperature uniformity over that of the conventional nozzle mix burner. Many nozzle mix burners of this type had very fast fuel/air mixing and provided a clean-burning, well-defined flame. This is a very desirable characteristic for the heating process but puts a great deal of thermal stress on the tile refractory. The conventional way of overcoming this problem is to use an alloy jacket around the tile to contain, support, and seal the refractory against cracks and leakage of hot gases into the surrounding furnace structure.

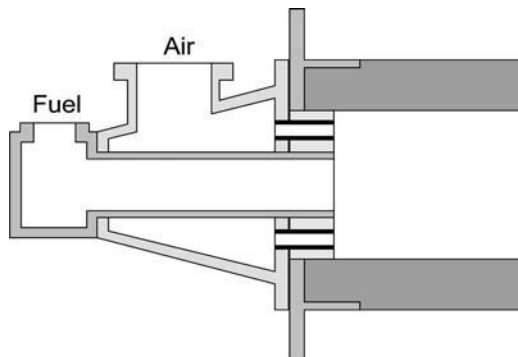


FIGURE 11.2 Nozzle mix jet tube burner.

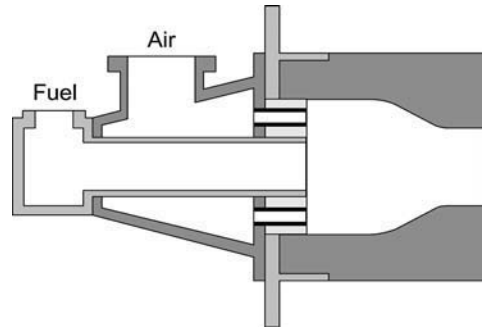


FIGURE 11.3 Nozzle mix burner with restricted tile exit.

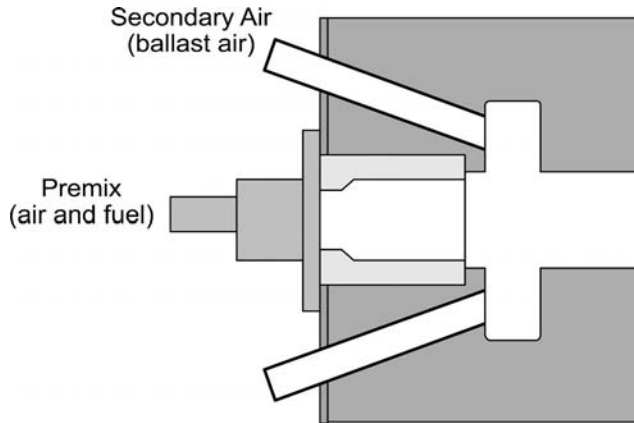


FIGURE 11.4 Iso-Jet (premix core). (Courtesy of Nutec Bickley.³ With permission.)

11.2.3 ISO-JET BURNER

In 1958, the Bickley Iso-Jet[®] (Nutec Bickley, Philadelphia, PA) burner was introduced as an integral component of Bickley's batch kilns.³ The original Iso-Jet consisted of a premix burner core with secondary air piped through a surrounding tile structure (Figure 11.4) that tempered the hot products of combustion from the premix core during lower-temperature operations. The resulting high-velocity jet provided high convective heating and excellent temperature uniformity with a maximum tile velocity much higher than the nozzle mix burners of the day.

To adjust the furnace temperature, the burner's control system would balance the premix and secondary air flows. Gradually reducing the secondary air flow would increase the chamber temperature. To reach high furnace temperatures, the secondary air was turned completely off, while the premix core continued to operate alone. In this mode, the high-velocity feature was not available, and temperature uniformity was largely dependent on radiation. This made the Iso-Jet best suited for batch furnaces with firing schedules requiring long cycle times at low furnace temperatures. The premix burner core of the Iso-Jet was later replaced with a nozzle mix design to widen its operating capabilities (Figure 11.5).

11.2.4 AIR-STAGED NOZZLE MIX HIGH-VELOCITY BURNER

11.2.4.1 "Jet Can" Burner

In the early 1960s, a significant amount of development of high-velocity air-staged nozzle mix burners was carried out by the gas industry in Britain. A commercial burner arising from this work was the Hotwork High Velocity Burner.⁴ Based on a design concept similar to a gas turbine combustion

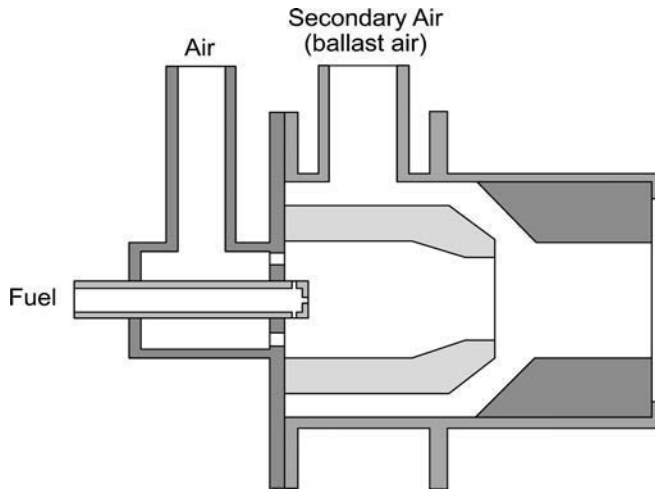


FIGURE 11.5 Iso-Jet III (nozzle mix core). (Courtesy of Nutec Bickley.³ With permission.)

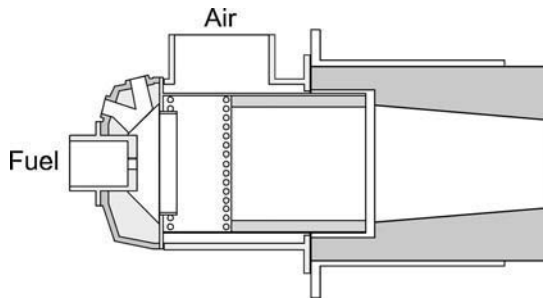


FIGURE 11.6 Jet can burner. (Courtesy of Hotwork Combustion Technology Ltd.⁴ With permission.)

chamber, the burner consists of an air body containing a perforated high-temperature alloy can with a refractory lining followed by a metal-encased high-temperature refractory tile (Figure 11.6). All fuel enters from the rear of the can where it mixes with a portion of the air circulating from the impinging jets formed by the rows of perforations in the metal can. The impinging air jets create a high degree of internal recirculation of the combusting products as they move forward to meet further air introduced to the can. This design is highly stable and operates at a very high combustion intensity. The entire structure is designed to complete approximately 85% of the combustion of a gaseous fuel before the tile exit, and 60% for diesel oil. The hot combustion product stream exits the reduced port tile at a design velocity around 450 ft/s, with significant momentum and a high entrainment capability. This produces high potential recirculation of the gases within the furnace with a relatively small flame envelope. These attributes allowed small numbers of these burners to be used to replace large numbers of then-conventional burners on high-performance furnaces requiring good temperature uniformity. The high excess air capability of the burner also allows it to be used as a high-velocity hot gas generator for drying and preheating applications.

11.2.4.2 “Cup” Burner

In 1969, the authors’ company introduced the Tempest[®] (The North American Manufacturing Company, Ltd.) high-velocity burner. Similar to earlier high-velocity burners, it was a nozzle mix burner with a restricted tile exit, which made it possible to produce good temperature uniformity with less excess air at high fire, but with a number of unique features.

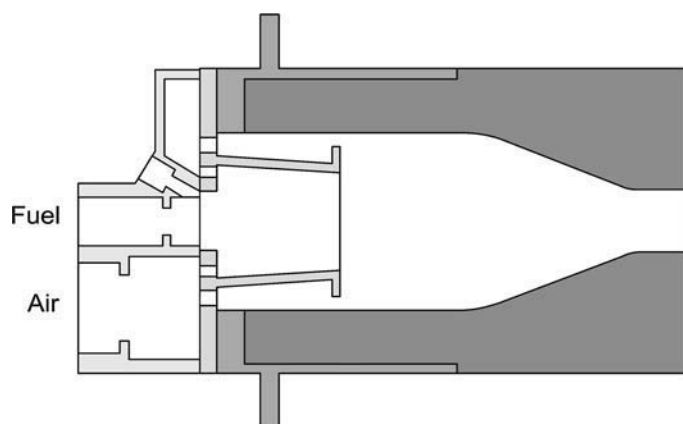


FIGURE 11.7 Nozzle mix cup burner.

The Tempest burner was relatively inexpensive, had a square refractory tile, and integral air and gas flow metering elements to reduce installation costs. The tile was partially jacketed with metal to prevent hot gases from leaking out into the surrounding refractory of the furnace. An internal cup-shaped stabilizer shielded the refractory from the base flame, and staged the air introduction to the fuel inside the tile (Figure 11.7). As the overall fuel/air ratio approached stoichiometric, more of the combustion would take place outside the tile in the furnace, which suppressed internal temperatures and reduced the duty requirement of the tile refractories over those of a design such as the “Jet Can” described above. The excess air limit was also very high, making it possible to hold a furnace temperature below 200°F simply by reducing the fuel rate (thermal turndown) while the air remained at its maximum setting.

During the 1970s, the Tempest burner became very popular for firing tunnel kilns in brick manufacture because the burner’s jet flame could penetrate and release heat deep into a brick hack. This meant wider furnaces and kilns could be built without temperature uniformity sacrifices. Tempests have also been used as auxiliary “stirring” burners while larger, more luminous flame burners provide the majority of the heat input to the furnace. During the 1980s and 1990s, most manufacturers of high-velocity burners embraced the high-velocity cup burner concept and developed similar designs that continue to be popular. New features of updated Tempests and similar burners include self-supporting tiles, metal tiles, shaped tile exits, and dual fuel capability.

11.2.5 “TUBE BURNERS” WITH THIN-WALLED, SELF-SUPPORTING TILES

Ceramic fiber wall construction became an alternative to hard refractory walls in the 1970s. Ceramic fiber is unable to support a conventional refractory burner tile, requiring the use of tile jackets or other similar measures. Advances in ceramic materials and fabrication techniques have made it possible to produce thin-section, self-supporting high-velocity burner tiles. Thin and uniform tile sections are much more resistant to thermal shock than thick nonuniformly walled ceramic structures. The new ceramic materials are denser, stronger, and have lower porosity than traditional refractory, which makes them ideal for containing the hot reacting gases produced inside high-velocity burners. Reaction-bonded silicon carbide and alumina composites are the most often used materials for self-supporting tiles. Heat-resisting metal alloys are also used in low-temperature applications.

The self-supporting tile is also used to reduce the overall size and weight of the extended-length burners required for thick-walled structures such as those typical of tunnel kilns. The geometry of the flame stabilizer in a “tube burner” is best described as a disk centered in the tile with one or

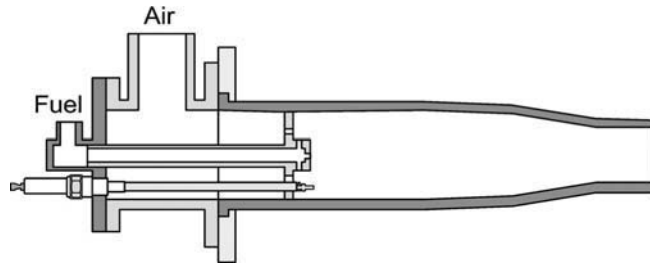


FIGURE 11.8 Nozzle mix tube burner with self-supporting tile.

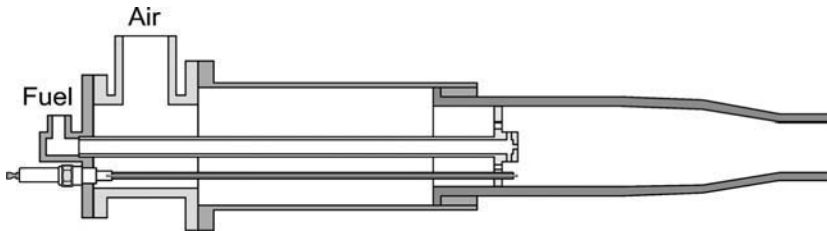


FIGURE 11.9 Nozzle mix tube burner with extended self-supporting tile.

more rows of holes through it and air passages around it. A central fuel nozzle supplies fuel to the burner head. In some respects, these burners' flame stabilizers and resultant flames are similar to those of the early nozzle-mix high-velocity burners previously discussed. They have similar excess air limits and burn a similar proportion of the fuel within their tiles, but their designs are much more refined and they are of much lighter weight (Figure 11.8).

Ignition and flame detection must take place in front of the flame stabilizer disk. For ignition, long, single-electrode spark igniters are fed through from the burner back plate to the front of the stabilizer with the spark gap grounding to the stabilizer or fuel tube. Flame rods for ionization flame detection are common with tube burners and are of similar construction to the spark igniter, but with an electrode typically extending further past the stabilizer air disk.

Most high-velocity burners are designed to fit 9- to 12-inch-thick walls. Extended-length burners are available for mounting in thicker furnace walls. These burners have a design emphasis on small-diameter extension tubes and tiles to simplify installation. Standard insertion lengths vary from 12 to 48 inches, with longer special lengths available. Extended-length tube burners can have an extended metal body, an extended self-supporting tile, or both, to pass through these thick walls (Figure 11.9). To reduce the heated length of the assembly, the burner's stabilizer may be well inside the tile. The length of the tube may be engineered to fit a specific wall thickness, or made with some means of adjusting the length.

Extended-length burners can be retrofitted to existing thick-wall kilns with little or no downtime by normal core-drilling techniques. These eliminate the need for access to the inside of the kiln or furnace for refractory modifications.

11.3 JET THEORY

The foundation of all benefits associated with high-velocity burners is rooted in fluid dynamics and, more specifically, in turbulent jet theory. While it is not within the scope of this text to fully develop the mechanics of free turbulent jet flow, it is important to provide the reader with a fundamental understanding of the fluid behavior. More thorough treatment can be found in reference texts⁵⁻¹⁰ on this subject.

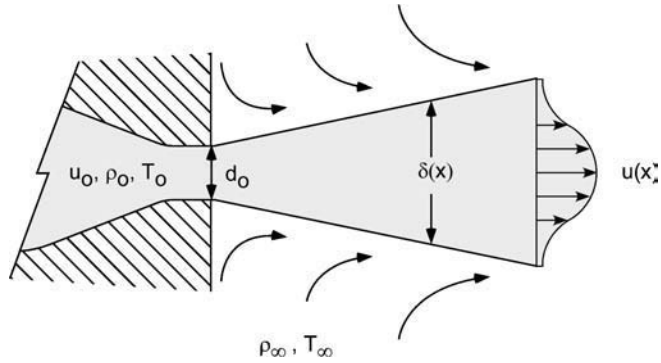


FIGURE 11.10 Diagram of a free turbulent jet.

11.3.1 FREE TURBULENT JETS

To simplify this presentation, certain assumptions must be made regarding the character of the jet flow. Free jets are those that are not acted upon by their surroundings. Other than that through which the jet emanates, there are no walls or surfaces that can constrain the flow field. A typical arrangement for a free turbulent jet is shown in [Figure 11.10](#).

As shown, the emerging jet carries with it some of the surrounding fluid, which was originally at rest, due to the friction developed on its periphery. The turbulent shear created by the two fluids moving at different velocities defines the jet boundary. As the flow progresses in the x -direction, the mass flow within the jet boundary increases due to the turbulent shear. As the same time, the centerline velocity decays with distance. The jet itself is the only source of momentum in the flow field and that momentum must be conserved at each point. Hence, as the jet spreads out, its mass flow increases and its velocity decreases, but the total jet momentum remains constant. For a given application, the most interesting parameters to determine are the centerline velocity $u(x)$, the width of the jet $\delta(x)$, the mass flow $m(x)$, and the entrainment rate $E(x)$.

While the near-field area of a jet can be quite complex, looking at the far-field flow dynamics results in a powerful simplifying assumption. In this case, the density ρ is assumed equal to the entrained fluid density ρ_∞ . The conservation of the source momentum flux J_0 then dictates the other properties as a function of distance from the nozzle. From the cited reference sources,^{5,8,9} we have:

$$u(x) = 7.2 \left(\frac{J_0}{\rho_\infty} \right)^{1/2} x^{-1} \quad (11.1)$$

The flow width is proportional to distance x , and specifically:

$$\delta(x) = 0.44 x \quad (11.2)$$

Also, the decay of the centerline velocity is:

$$\frac{u(x)}{u_0} = 6.5 \left(\frac{x}{d^*} \right)^{-1} \quad \text{where} \quad d^* = \frac{2m_0}{(\pi\rho_\infty J_0)^{1/2}} \quad (11.3)$$

Any arbitrary source produces a far-field flow equivalent to that produced by a circular nozzle of diameter d^* issuing fluid at a uniform velocity u_0 and density ρ . When the jet is circular with a uniform exit velocity profile, the expression for d^* reduces to:

$$d^* = \left(\frac{\rho_0}{\rho_\infty} \right)^{1/2} d_0 \quad (11.4)$$

Also, the resultant mass $m(x)$ and entrainment relationships can be determined:

$$m(x) = 0.282(\rho_\infty J_0)^{1/2} x \quad (11.5)$$

$$E(x) \equiv \frac{m(x + dx) - m(x)}{dx} = \frac{d}{dx} m(x) = 0.282(\rho_\infty J_0)^{1/2} \quad (11.6)$$

An often-surprising result is that the entrainment rate is independent of position downstream of the nozzle.

Finally, by shifting coordinates upstream in the flow field from the plane of the jet exit, a single point source can be defined. This point source is called the virtual origin of the jet. It is located at a position $x = 3.14 d^*$ upstream from the jet exit plane.

One other defined jet parameter that is frequently used is the potential core length. It is essentially the point downstream of the jet exit plane at which the centerline velocity begins to decay. This point is typically five to eight jet diameters downstream of the exit, depending on the geometry of the jet exit. These jet parameters are illustrated in Figure 11.11.

While the formulas and calculations can be daunting, the insights gained from them are powerful. Perhaps the first and simplest involves the jet spread $\delta(x)$. Looking at the inverse tangent of 0.44 (Equation 11.2), the free jet expands at an angle of just over 23° or an 11.5° half angle. This expansion becomes important when looking at burner-to-burner interactions as well as when making quick estimations of impingement locations in confined jet problems.

11.3.2 SOME EXAMPLE CALCULATIONS

Now that the basis for high-velocity burner flow fields is defined, a few specific examples should help quantify the implications of the theory.

For the base case, mass flow and jet exit pressure are representative of conditions found in a 1.0-MMBTU/h high-velocity burner operating with 10% excess air at 60°F with 0.5 psig of upstream nozzle pressure. Case 5 is a simplified example of a partially combusted high-velocity burner, much

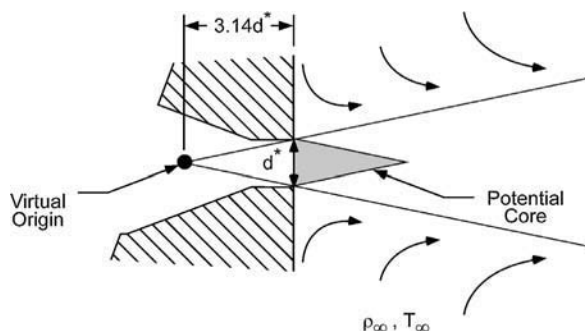


FIGURE 11.11 Virtual origin and potential core of a free jet.

like the cup burner described previously. Likewise, Case 6 represents the “jet can” burner. It is important to note that the continuing chemical reaction alters the rate of entrainment along the burner axis and these changes are not predicted by the cases shown below. They do, however, provide directional insights into burner behavior. Readers are referred to Tachina and Dahm⁹ for a more complete theoretical development of reacting jet flows.

The base parameters for each case are defined in Table 11.1. Making the calculations for mass flow and centerline velocity results in the derived data of Table 11.2. Table units are mass flow, slugs/s; velocity, ft/s; distance, ft; pressure, psig; temperature, °F.

Cases 1 through 3 are all isothermal so $d = d^*$ for each. The jet parameters are self-similar and scale directly with x/d . For each case, the velocity drops by half at $x/d = 9.6$ and the mass flow doubles at $x/d = 3.14$. Case 4 shows the jet change that occurs when a cold jet penetrates a hot environment. The centerline velocity maintains a higher value for a greater distance compared to the base case. Additionally, it takes a much greater distance to achieve the same mass ratio between the jet fluid and the entrained fluid. Compared to the base case, the jet entering an 1800°F environment must travel 2.08 times further to achieve similar effects. This entire change is seen in the scaling translation from d to d^* .

TABLE 11.1
Sample Jet Configurations

Case	Description
1. Base case	1.0 MMBTU/h fuel with 10% excess air, nonreacting, delivered to a nozzle at 60°F and 0.5 psig upstream pressure into a 60°F furnace environment
2. Low velocity	Same as base but with velocity equal to one half of base case exit velocity
3. Increased mass flow	Same as base but with mass increased to represent 4.0 MMBTU/h
4. Hot furnace	Same as base but with an 1800°F furnace environment
5. Low reaction progress	Same as base but with a partially reacted 900°F gas mixture, 17% of stoichiometric fuel combusted at tile exit
6. High reaction progress	Same as base but with a mostly reacted 2600°F gas mixture, 63% of the stoichiometric fuel combusted at tile exit

TABLE 11.2
Mass and Velocity Calculations for Sample Jet Configurations

	1. Base Case	2. Low Velocity	3. Increased Mass Flow	4. Hot Furnace	5. Low Reaction Progress	6. High Reaction Progress
Mass Flow, m_o	0.007212	0.007212	0.028848	0.007212	0.007212	0.007212
Velocity, u_o	200	100	200	200	325	487
Nozzle ID, d_o	0.1416	0.2006	0.2832	0.1416	0.1801	0.2206
Nozzle Pressure	0.5	0.125	0.5	0.5	0.5	0.5
T_o	60	60	60	60	900	2600
T_{inf}	60	60	60	1800	1800	1800
J_o	1.4467	0.7215	5.7869	1.4467	2.3419	3.5128
d^*	0.1416	0.2006	0.2832	0.2952	0.2322	0.1896
Virtual origin	-0.445	-0.630	-0.889	-0.927	-0.729	-0.595
x at $u = u/2$	1.36	1.92	2.72	2.84	2.23	1.82
x at $m = 2^* m_o$	0.446	0.631	0.89	0.929	0.73	0.596
x at $m = 5^* m_o$	1.78	2.52	3.56	3.71	2.92	2.38

Cases 5 and 6 are representations of actual high-velocity burners. Different high-velocity burner designs use different stabilizing techniques that result in widely varying combustion reaction progress, or degree of completion, at the tile exit. In the cup-stabilized burner, only about 15 to 30% of the combustion is complete at the tile exit, whereas a jet can type burner may have over 60% complete. As the reaction progress goes up, the tile exit diameter must also increase. This is due to the initial requirement of a constant upstream pressure; thus, the greater the degree of reaction completeness, the larger the exit diameter. However, at the same time, the exit velocity increases. All these changes are reflected appropriately in d^* ; the greater the degree of reaction completion, the smaller the value of d^* . As shown in the Table 11.2, there is a big difference in performance between these cases and Case 4. At every point downstream, the jet with the higher exit temperature has entrained more mass and maintained a higher centerline velocity.

11.3.3 HIGH-VELOCITY BURNER INSTALLATION AND CHAMBER EFFECTS

While the free turbulent jet analogy provides useful insight, the application of high-velocity burners in operating furnaces creates additional challenges. In many of these applications, temperature uniformity, without product overheating, is the desired objective. In these cases, entrainment of large volumes of furnace gas limit the temperature of the overall flame envelope while providing enhanced convective heat transfer. Optimization of these effects must be considered on a case-by-case basis, but there are some universal approaches to maximizing the benefit.

11.3.3.1 Recessed Burners

In many applications, the distance from the burner outlet to the product being heated is very short. This is typically due to efficient furnace construction and loading where little chamber volume is wasted. In these applications, burners are frequently recessed into the burner wall. This approach effectively moves the virtual origin and exit plane of the burner away from the work and allows for a greater amount of entrainment in the limited space available. This results in a lower overall temperature of the combustion product gas, but with greater mass flow, impacting the load. Based on typical wall thickness, a recess distance of as much as 12 in. can be achieved.

There are several limitations that must be considered with this technique. First, the technique is best used when the jet is free to entrain the furnace atmosphere from all directions. If any lateral confinement of the jet is present near the original jet exit position, it may not be possible to entrain additional products of combustion. Second, the recess cannot be so deep as to permit the jet to fully expand into the space created by the exit relocation. For example, let's look at a 1-in. diameter circular jet, retracted 6 in. into a wall, but with only a 3-in. diameter hole at the wall plane (Figure 11.12a).

Using the rule-of-thumb for jet expansion (23°), such a jet would expand and impinge inside the recess at a position roughly 5 in. from the jet exit. Once this occurs, all of the initial jet mass requirements are fulfilled by the recirculation of the jet itself, not by outside combustion product gases. Additionally, instead of having a high-velocity, 1-in. diameter jet emanating from the wall, we now have a 3-in. diameter, low-velocity jet producing far less bulk fluid motion and resulting in an elevated flame temperature. The condition of jet attachment within the burner recess must be prevented or, not only will the benefits of recessing be lost, but performance will be reduced beyond that of the base case. Figure 11.12b shows a burner properly recessed in the chamber wall. In some cases, a divergent taper in the sides of the recess can be advantageous. Not only does it eliminate jet attachment, but also opens up the area around the exit, allowing more combustion product gases to have access to the base of the burner jet. Finally, when considering a recessed jet, the chamber wall operating temperature capability must be considered. "Pulling the flame back" within the wall to a new position without appropriate adjacent insulating material can cause localized furnace wall and shell material overheating.

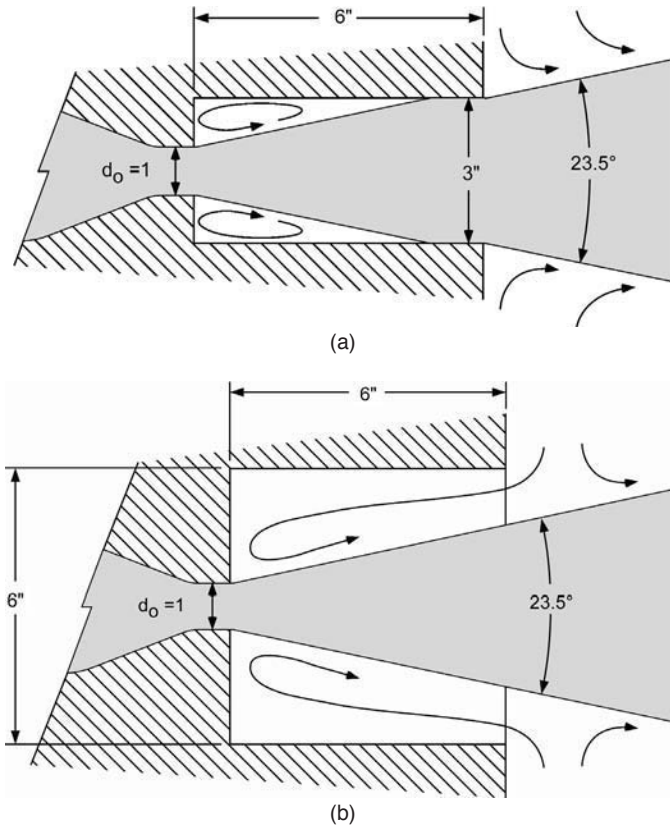


FIGURE 11.12 Schematic of a recessed burner installation.

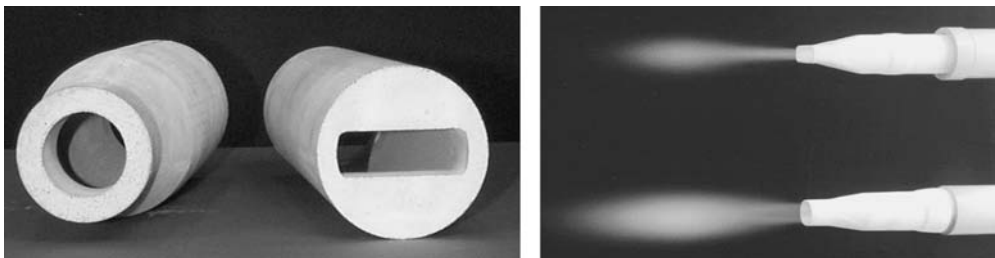


FIGURE 11.13 Round and slotted high-velocity burner tile exits.

A further caution on this technique is the need to consider the possibility of the deposition of material from the furnace gases drawn into the recess in front of the jet. Not only can such accumulation render further recirculation impossible, but it can also cause the concentration of undesirable elements or compounds in a hot environment and lead to corrosion damage of the surrounding materials.

11.3.3.2 Tile Exit Geometry

Local entrainment can be increased by jet exit geometry changes and exit treatments. The most common exit geometry change is from a round burner jet discharge to a slotted shape (Figure 11.13). This change to the exit shape maintains the jet mass and momentum, but redistributes it in another configuration. As higher aspect ratio designs are considered, the ratio of jet perimeter to area increases. Consider

a 1-in. diameter jet exit with an area of .785 sq. in. Creating a slot of the same area with an aspect ratio of 5:1 results in an increase of jet discharge perimeter of over 50% compared to the round exit. This results in quicker dissipation of the potential core and faster jet breakup. The effects of entrainment act more quickly on the long side of the exit while reducing entrainment on the short side.

The slotted exit is ideal for several chamber geometries. If constraints such as walls or supports are present in the chamber, the slot can optimize the product gas entrainment along an axis normal to the direction of confinement. One example is a case where burner-to-burner spacing is too close and jets tend to interfere with one another. If sufficient room is present above and below the burner exit, a slotted tile can be used to draw more product gas from these regions and reduce the burner interference. Another example is a case where the work is arranged in narrow firing lanes and tight temperature uniformity is required. A slotted exit can be used to entrain greater quantities of product gas in the direction of the work, reducing the temperature of the gases in contact with the load. This both promotes uniformity and prevents product overheating. Shaped exits are not as good as round exits for penetrating dense loads and firing wide furnaces.

With the improvements in materials technology during the past few years, new approaches to jet breakup and enhanced entrainment continue to be explored. Many of these techniques use tabs or other small devices to introduce vortices into the jet flow at the burner exit plane. Even small serrations applied to a round exit can have an effect on the core breakup.

11.3.4 EFFECT OF MULTIPLE BURNERS

The full benefits of enhanced convective heat transfer and a high level of temperature uniformity can only be achieved by proper burner placement. Our analysis thus far has been limited to a single free jet. But as we look to apply jet dynamics to our heating system, burner placement and burner-to-burner effects, as well as the geometry of the chamber and properties of the material to be heated, must all be considered. It is important to properly space the burners in both the horizontal and vertical planes of the chamber in order to get as even heating as possible.

11.3.4.1 Centerline Spacing

The first consideration in placing burners on an application is the development of the reacting gas jet. In the sections above, it was demonstrated that a typical free jet expands with $\delta(x) = 0.44x$, or just over a 23° included angle. This parameter is used to set burner-to-burner centerline spacing in high-velocity applications.

Looking first at the effect of burners adjacent to each other, either horizontally or vertically, where the intersection of the jet streams will determine the overall effectiveness of the burner velocities. [Figure 11.14](#) shows the positions of paired burners on three different centerline spacings.

At a burner centerline spacing of 2 ft, the hot gas “cones” meet approximately 4.5 ft from the hot face of the burner tile, assuming a point source. In real jets, the spacing will be reduced by the diameter of the actual jet initial diameter, shortening the intersection distance. As the streams merge, they are unable to entrain additional product gas at the intersection point and temperatures will not diminish as rapidly. This can create hot spots in the load. Further, depending on the location of the load, the two jets may begin to look much more like a single, low-velocity jet. In fact, this is exactly how such an arrangement is treated on a theoretical basis. The two jets merge together as one, with a combined mass flow based on the total mass at the point of intersection and new virtual origin. At burner centerlines of 3 ft and 4 ft, the jet intersection distances are 6.8 ft and 9.1ft, respectively.

It is important to note that the region between burners does not provide for good recirculation and reduction in temperature for either of the two jets. Each jet has its own mass entrainment requirements and the two compete for this particular volume. In satisfying this requirement, the jets will tend to turn toward each other and, in the case of a burner jet, recirculate hot, reacting

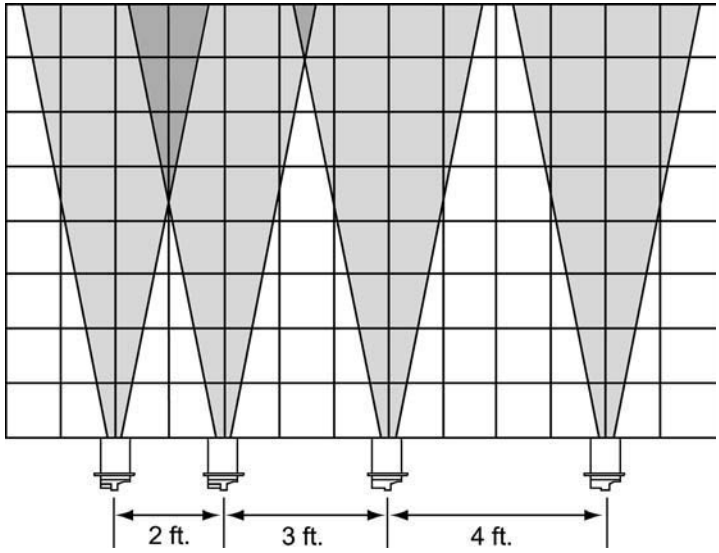


FIGURE 11.14 Effect of burner centerline spacing.

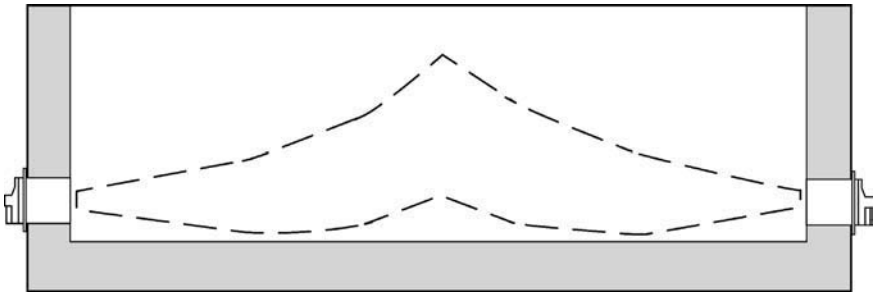


FIGURE 11.15 Typical buoyant jet pattern of an unopposed burner.

gases back into the flame envelope. Experimental studies^{3,5} have shown that if burner nozzles are separated by at least 18 nozzle diameters, no interaction in the flame front will occur. More recent work has shown that this actually depends on the fuel type, and it has also been shown⁷ that at least 26 diameters are required for methane fuel.

11.3.4.2 Opposed vs. Staggered Wall Placement

Under all conditions, the location of burners relative to the load and to each other is important in achieving the most benefit from the investment in high-velocity burners. For many years, one practice had been to oppose high-velocity burners to promote a vertical circulation of the hot gases through the center of the chamber. This works well if the furnace is wide and the burners have been properly sized to allow the gases to turn upward as they meet (Figure 11.15).

However, in a narrow furnace chamber, the gases impact upon each other, resulting in a stagnant flow area at the center of the furnace. The impacting gases are the high-temperature, centerline portion of the combustion jet, resulting in an overheated region of the furnace. For this reason, it is often advantageous to offset or stagger the burner placement to allow the burner gases to sweep the full distance across the chamber and be recirculated for improved temperature distribution.

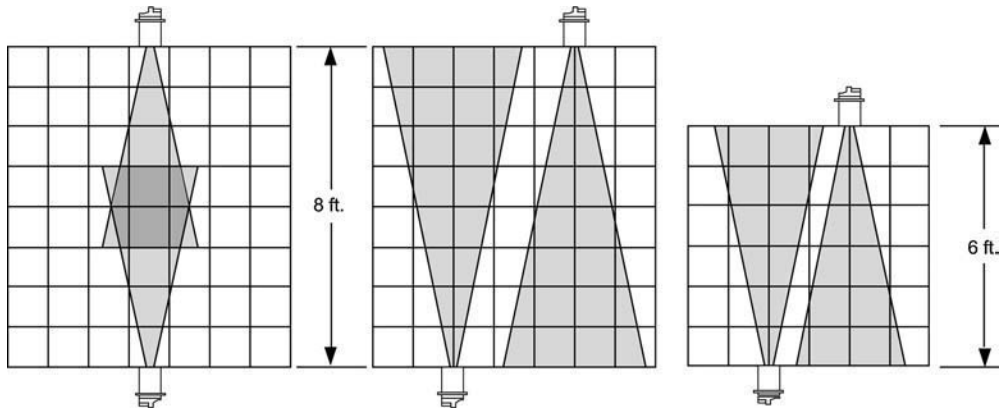


FIGURE 11.16 Effect of centerline spacing on opposed burners.

Figure 11.16 shows this effect on burners located across the chamber from each other, on 3-ft and 4-ft centerlines and at 8-ft and 6-ft chamber widths. It shows the relative positioning that must be considered for the burners to promote good flow across the kiln and load. If the burners are too close together in either of the arrangements, interference from the turbulent interaction of the gas streams can be counterproductive to the goals of high-velocity heating. When firing large open volumes, it is important to remember that staggering the burners will not always provide the best result. Burners on opposite walls still create dead zones, where gases move slowly or are stagnant in the region between staggered expanding jets. In this particular case, locating burners to promote bulk motion of the gases typically provides the best result.

It is also very important to examine the load setting when placing high-velocity burners. Too little space between the wall and the work will not allow for proper recirculation of the product gases. Raising the work off the floor also helps promote good gas recirculation and even heating. Appropriate product spacing is also important to achieving improved product temperature uniformity by enhanced entrainment and gas recirculation.

Proper flue locations are also critical. Essentially, one must consider the “sinks” in the flow field as well as the “sources.” A poor flue location can cause the high-velocity streams to short-circuit the furnace chamber, effectively heating only the flue. High-velocity combustion can offer many benefits, but can only be brought to fruition by a well-designed heating process.

11.4 HIGH-VELOCITY BURNER DESIGN

High-velocity burner design is an exercise in compromise. The most basic difference between the various designs lies in how the high velocity is achieved. All high-velocity burners have some amount of tile restriction after the flame stabilizer arrangement. Making the tile exit smaller increases the exit velocity. The reaction progress inside the tile also affects the exit velocity. As more combustion is completed in the tile, the gas temperature rises and the gas volume expands, which increases velocity. The optimum balance between tile exit size and the amount of combustion allowed to complete in the tile is application and control system specific.

The amount of the fuel combusted within the burner before the tile exit is a function of the design of the mixing and flame stabilizing sections of the burner. While more intense mixing will increase gas outlet temperatures and provide a higher-velocity flame, the internal tile pressure will also rise, requiring higher inlet pressures for air and fuel to maintain the same flow rate. So, as fuel is throttled off, airflow through the burner will increase due to lower pressures in the tile. The differences in firing vs. not-firing airflow rates are greater in burners that have higher percentages of combustion taking place in their tile.

Because of the airflow changes due to the ratio settings, high-velocity burners are typically installed with air and gas flow meters to aid in setting the fuel/air ratio. Orifice meters can be built into the burner, but external meters are normally more accurate because “flow-smoothing” space is not restricted.

11.4.1 DELAYED MIXING/CUP STYLE AIR STAGING DESIGNS

All delayed mixing or cup style high-velocity burners have at least one central stabilizer cup where all of the gas is mixed with a portion of the combustion air. The flame that exits the cup tends to stay fuel-rich in the center of the tile as it meets the remaining air passing around the outside of the cup stabilizer. Most of the individual air and gas jets inside the burner run substantially parallel to each other, slowing the fuel/air mixing. The amount of burning that takes place in the tile depends on the tile volume and the geometry of the stabilizer. The reacted products and the remaining fuel and air exit the tile and entrain furnace atmosphere while the balance of the combustion takes place in the furnace.

The stabilizer cup allows the burner to achieve very high excess air rates by initially shielding the gas from most of the air. Even with the airflow at a high rate, the fuel can be reduced to a rate where the flame will shift completely into the base of the cup and remain stable. The air outside the cup and the hot gases from inside the cup are mixed in the tile before exiting. Excess air capabilities for delayed mixing burners are typically in the range of 3000 to 5000% excess air (equivalence ratio = 0.03–0.02).

Allowing combustion to complete in the furnace has a number of advantages. Because the delayed mixing design is less dependent on expanding combustion products, the tile exit velocity will not fall off markedly when running at high excess air rates. The tile and the burner’s internal parts are also less thermally stressed as the air passing around the outside of the cup cools the cup and shields the inside surface of the tile from the centrally concentrated flame. Combustion is completed in an environment containing entrained products of combustion from the furnace chamber resulting in inherently low NO_x emissions.

Designing for significant combustion outside a high-velocity burner has the potential disadvantage that the combustion reaction may be quenched when the fired chamber is cold, resulting in incomplete combustion of the fuel, with the presence of fuel fragments, CO, and aldehydes in the combustion product gases.

11.4.2 FAST MIXING DESIGNS

Fast mixing high-velocity burners are designed to burn as much of their fuel in the tile as possible. This may be achieved with either the “jet can” style burner or with a disk-shaped stabilizer, combined with an appropriate internal volume. The fast mixing designs require a high-integrity tile structure of low porosity and high resistance to thermal shock. Self-supporting, reaction-bonded silicon carbide tiles are often used because they meet these requirements and have a high thermal conductivity. A cast refractory tile for this duty will typically be contained in a heat-resisting alloy jacket to maintain the refractory under compression and minimize the potential for the escape of the very hot internal gases into the surrounding structure through cracks.

The disk stabilizer style has fewer stabilizing zones than the “can type” stabilizer, leading to more limited excess air capabilities typically in the 500 to 1000% air range (equivalence ratio = 0.17–0.09). Burners of this style can be controlled by pulse firing or time-proportioned control systems that do not rely on high excess air capability for the complete combustion system to provide a high level of turndown.

Allowing more of the fuel and air to mix and combust within the burner has the advantage of a higher tile exit velocity for a given exit diameter. It also suppresses the potential for CO, aldehyde, and other unburned hydrocarbon emissions when run with an excess of air, although NO_x emissions can increase as a result of the higher internal tile temperatures and the lack of dilution from cooled

combustion products. The fast mixing style is the burner of choice for sub-stoichiometric firing applications where the burner is required to operate as a reactor and provide a hot, low-oxygen combustion product stream to the fired process.

11.4.3 IGNITION: DIRECT SPARK, PREMIX PILOTS

High-velocity burners require an ignition source inside the burner to ignite the fuel/air mixture. The high velocity at the restriction of the tile exit typically prevents an external flame from propagating back through the tile port to the burner's intended stabilization zone. Hot furnaces, externally applied torches, (and flaming oily rags) will not reliably light high-velocity burners. Attempting torch lighting through a shutter at the back of the burner is not recommended, because the high internal tile pressure inside a high-velocity burner may cause a "stinger" — a direct flame risk to the operator.

The most common methods of lighting high-velocity burners are direct spark igniters and premix pilots. Direct spark ignition is the most popular for gas burners. It has the advantages of simplicity and lower cost over premix pilot systems, but the location of the spark gap inside the burner is critical to achieving reliable lighting. As the best location may be in an area of continuous combustion, the igniter design for long life can be challenging.

Premix pilot burners deliver much more energy than spark igniters and have a much larger zone of influence. Being burners in their own right, they project a flame into the combustion space of the high-velocity burner, and may be located external to the main combustion space and thus less subject to thermal deterioration. Accordingly, they are chosen for larger-capacity gas burners and most oil burners. The fuel supplying a premix pilot must be turned off once the main burner is ignited (an "interrupted pilot") for safe operation of any burner system with flame supervision. Doing so also allows the pilot combustion air to cool the pilot tip.

There are many different styles of direct spark igniters, most specific to the burner in which they are being used. They range from simple industrial spark plugs (Figure 11.17) to extended versions that perform as flame rod flame detectors when the burner is lit (Figure 11.18).

11.4.4 FLAME SUPERVISION

Note: This section is not intended to act as a specific guide to the use of flame supervision systems for high-velocity (or any other) burners. The reader is referred to the applicable international, national, local, and insurance industry codes, standards, requirements, etc. for appropriate information on this subject.

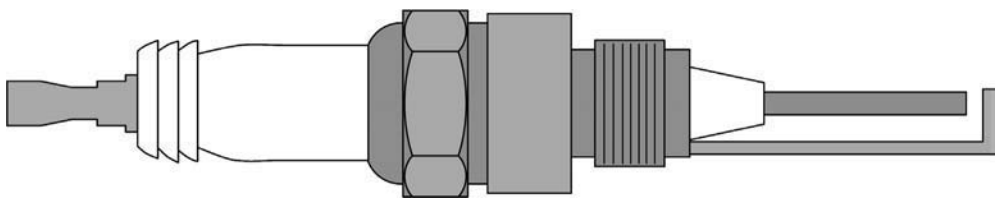


FIGURE 11.17 Industrial spark plug.



FIGURE 11.18 Combination flame rod igniter.

A reliable flame supervision system will reduce the incidence of combustion-related accidents. At the most basic level, well-sighted observation ports will allow operating personnel to confirm ignition and the establishment of combustion. The geometry of the burner will dictate how good the observation will be, shorter burners typically having better observation capability than the long tube-style burners. Care should be taken during burner installation to ensure that the operator's view down a burner observation port is not restricted by piping or other obstructions.

The most common methods of electronic flame supervision are the use of ultraviolet (UV) scanners and flame rods. Some high-velocity burners are designed to have the capability to use either, leaving the choice to the system designer. Other designs can use only one.

UV scanners have the advantage that they mount externally to the burner and need only a UV source in their line of sight. Their disadvantages are higher initial system costs and their potential for failure into an unsafe "flame detected" condition. Codes and standards typically require that "self-checking" UV scanners be used for continuously operating burners, or mandate a frequent safety check of "non-self-checking scanners" to reduce the risk of undetected failure. A UV scanner's "eye" must be kept clear of obstruction (such as dirt and water vapor) to prevent nuisance shutdowns. It should also be recognized that water vapor, CO₂, and many gaseous fuels absorb UV light. UV scanners will not reliably detect flame through long columns of these gases, making them unsuitable for use with burner designs where this condition might arise.

Flame rods cost less than UV cells and fail a "no flame detected mode." Most burners must be specifically designed to permit the use of a flame rod, normally require the use of a flame rod specific to the burner, and incorporate an appropriate electrical grounding path for the flame. Many tube-style, high-velocity burners have "twin igniter/flame rods" where the igniter and flame rod are identical electrode structures and are thus interchangeable. Some electronic flame ignition/detection systems allow a single rod to be used as the igniter and the flame rod with an appropriately designed burner.

11.4.5 TILES

The tile serves as the interface between the burner flame holder and the furnace. The restricted exit is the most obvious common feature in all high-velocity burners.

A tile of high integrity is a prime requirement for a high-velocity burner to prevent the high-temperature, high-pressure combusting gases within the tile from reaching the surrounding furnace structure. High thermal shock resistance is required to minimize reliance on the conduction of the surroundings to reduce the material stress effects of sudden tile material temperature changes.

There are many tile material choices available for high-velocity burner applications, each having advantages in different situations. They include molded refractory, cast refractory concrete, high-performance ceramics (for self-supporting tiles), and cast or fabricated heat-resisting metal.

Molded refractory and cast refractory concrete tiles are relatively inexpensive and can be made with simple tooling. Properly designed and manufactured, they can withstand very high temperatures and have some resistance to mechanical stress and abuse. Refractory material is very dense and somewhat subject to stress cracking. For these reasons, refractory tiles typically rely on external support for integrity. There are a number of ways to reduce the chance of hot combusting gases leaking out through cracks in the tile. Simply making the tile walls thicker will help, but the tile will become heavier and take up more space. Adding a metal jacket to the outside of the tile is very effective at stopping leaks by keeping the refractory under compression and providing support. However, the jacket may be subject to rapid degradation from the furnace environment by conduction through the walls or direct exposure to products of combustion from gaps in the insulation structure. In most cases, jackets are designed to stop short of the hot face of the furnace wall, leaving some portion of the refractory concrete tile unprotected.

Round refractory tiles with their uniform wall thickness are not as prone to stress cracking as square tiles of the same material. However, square refractory tiles have been a popular choice for

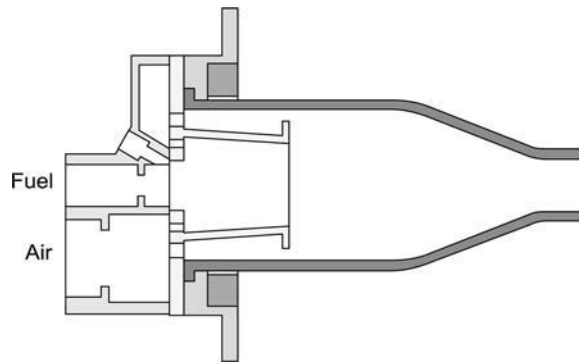


FIGURE 11.19 High-performance self-supporting ceramic tile.

smaller-capacity, high-velocity burners, especially for installation in furnaces built from brick where special cutting is reduced. In both cases, these tiles are typically made from very dense refractory concrete cast directly into a metal mounting plate or box, or from a preformed tile cemented into a mounting.

High-performance self-supporting ceramic tiles (Figure 11.19) are light in weight with relatively thin, uniform wall thickness. No external support is required for these materials other than that of the fixing of the burner mounting plate to the furnace wall. They are well suited for use in ceramic fiber-lined furnaces.

Such tiles are typically produced from reaction-bonded silicon carbide or other ceramic composites that resist high-temperature oxidation and thermal shock. The reaction-bonded silicon carbide tiles have very low porosity and high thermal shock resistance — ideal for containing the high-temperature products of combustion in high-velocity burner tiles. They also permit stabilizer designs that allow more combustion inside the tile without risk of damage to it. They are more expensive than refractory tiles and are more susceptible to mechanical damage. Silicon carbide tiles may require an air gap between the tile and furnace wall to prevent overheating the tile material.

Rolled heat-resistant stainless steel, heat-resistant cast iron, or investment cast alloys can be used for high-velocity tiles in lower-temperature applications. Metal tiles have the advantage of high resistance to mechanical damage and do not have porosity or thermal shock issues. Not only are they self-supporting, but they can be designed to support the entire weight of the burner. High-velocity burners with cup-style stabilizers are well suited for metal tiles, because they release less heat inside the tile, and the same air that keeps the cup cool also helps control the temperature of the tile. Some designs are fabricated with double skins with forced air-cooling between them. Metal tiles need to be chosen carefully, depending on the intended application temperature. They are not generally thought suitable for “clean” applications where metal oxide shed from the surface would spoil the product being heated.

11.4.6 LIGHT OIL, HIGH-VELOCITY BURNERS

Although most high-velocity burners are gas fired, oil-fired high-velocity burners are available. Most of them are “dual-fuel” versions with the ability to fire with diesel oil or gas (Figure 11.20). Air atomization is used to provide suitably fine oil droplets to the combustion process to reduce the potential for carbon formation in the reduced port tiles. Both compressed air and low-pressure air at pressures around 1.5 psig are commonly used for this atomization.

When compared with gas-fired high-velocity burners, their oil-fired versions have less turndown capability, are very difficult to light reliably with direct spark ignition, have significantly less excess air capability, and are prone to carbon formation in the tile if the appropriate fuel/air ratios are not

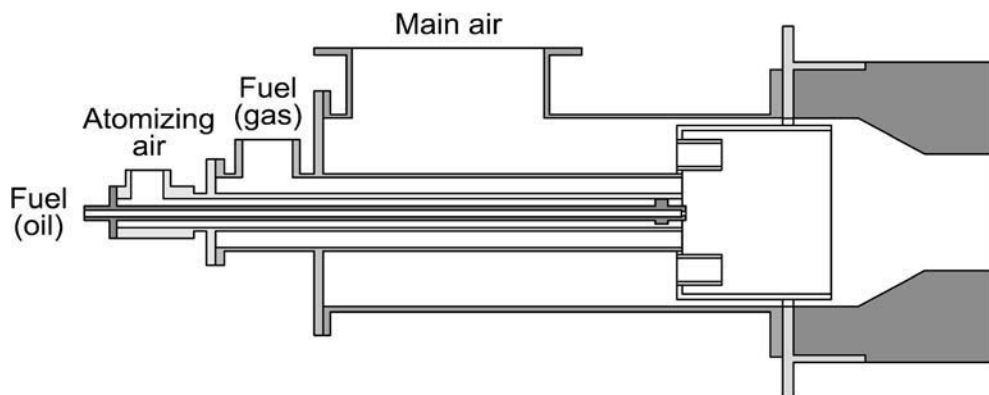


FIGURE 11.20 High-velocity dual-fuel burner.

maintained. Low atomizing air pressure and oil of much greater viscosity than diesel can also lead to carbon formation in the tile.

11.5 HEAT TRANSFER

Most of the impetus for applying high-velocity burners revolves around increased convective heat transfer. Increasing convection results in better temperature uniformity in the fired chamber, localized uniformity improvements in the heated work, and can result in improvement in product quality and reduced cost of production. The purpose of this section is to provide the framework to achieve these benefits for various heating applications.

11.5.1 BURNER SELECTION AND SIZING

Earlier sections indicated the importance of relative burner placement for optimum performance in a given application. The selection of the number of burners and their individual heat input requirement is inevitably linked to the final system performance by those considerations. The total number of burners used in a furnace is determined by factoring the furnace input capability and the input of the particular burner sized for optimum firing of the product. A larger burner will tend to throw heat a greater distance while a smaller burner will have the centerline velocity dissipate more quickly. To choose the optimum burner size, the length of the fired path on the burner axis must be considered. These choices, in conjunction with the reaction progress at tile exit and associated exit velocity, determine the heat flux profile from the burner.

Selection of an oversized burner can create significant problems in the heating application. One area of particular concern is the opposite (or target) wall across the furnace from the burner. Excessive centerline velocity and temperature will create hot spots on the refractory surfaces opposite the burner. This can result in refractory damage as well as localized overheating of the product due to re-radiation. Additionally, furnace seals can be over-pressured, potentially directing hot gases into undesirable areas, such as between the wall plates and refractories or into areas where structural members are located. Over time, this might lead to a catastrophic failure of the furnace.

With oversized burners, it is not simply a matter of turning down the burner firing rate. At turndown, the velocity of the burners is reduced, resulting in reduced entrainment of furnace gases with a connected loss of convective heat transfer capability. Oversized burners can also degrade product quality, counteracting one of the primary benefits of high-velocity firing.

If burners are undersized based on the width of the chamber, although they have sufficient total input among them, the area of optimal heat release may not be located in the proper part of the

load. For example, the burners may dissipate most of their heat in the near field, leaving the hard-to-heat areas cold, such as the bottom center of a brick hack.

11.5.2 MATERIAL HEATING APPROACHES WITH HIGH-VELOCITY BURNERS

11.5.2.1 Solid and Large-Shape Heating

High-velocity combustion is often utilized to heat large shapes to uniform temperatures. One example is the heating of steel ingots prior to forging. In demanding aerospace applications, the temperature uniformity requirement may be as tight as $\pm 15^{\circ}\text{F}$ throughout the entire chamber volume. These applications can use high-velocity burners to stir the products of combustion and produce very uniform temperatures. Although most of the heating at the target temperatures occurs by radiation, high-velocity burners bring all the radiating refractory and metal surfaces to a uniform temperature.

When heating solids, the best strategy is often large-scale (“bulk”) furnace gas movement. A row of high-velocity burners mounted on one furnace wall at a high level above the work can create the desired recirculation. If the work can be elevated on piers or other furniture above the hearth, a second row of smaller high-velocity burners can be added at hearth level on the wall opposite the other burners (Figure 11.21). Careful consideration should be given to the position of the flue exit ports from the furnace. Wherever possible, the flue ports should be located low in the furnace wall. This will ensure that good furnace pressure is maintained and that the furnace exhausts the coolest gases for best fuel efficiency. This approach eliminates the infiltration of ambient air, which affects temperature uniformity and fuel economy. It also helps overcome any buoyancy effects of hotter gases that exist, despite the stirring of the high-velocity burners. This combination will reinforce the bulk recirculation pattern and aid in increasing the convective heat transfer to the piece and creating the most uniform refractory temperature possible. Although much of this heating may occur at relatively high temperatures, some variation in excess air level can still be utilized to create even greater temperature uniformity, where the value of the load and elimination of rejects may far outweigh the fuel cost associated with increased excess air.

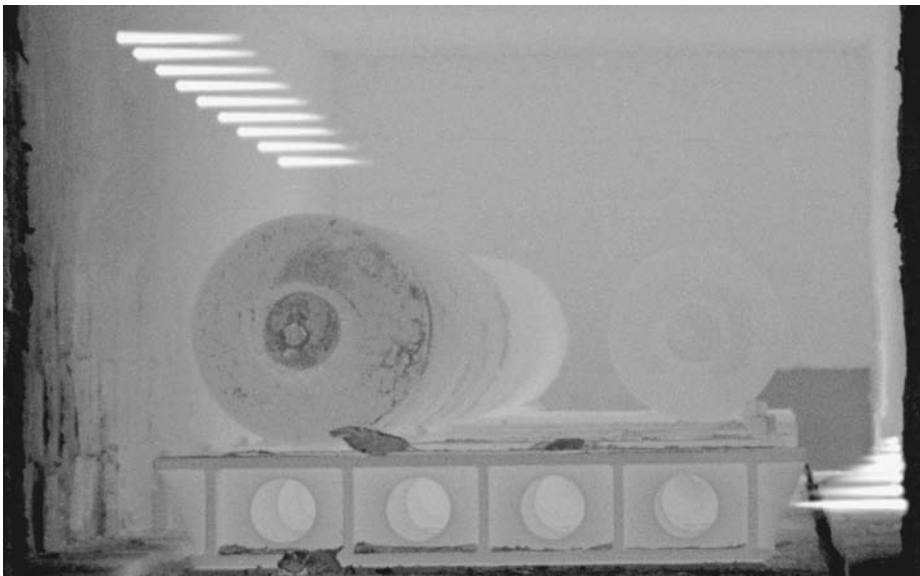


FIGURE 11.21 High-temperature heating of a large shape.



FIGURE 11.22 Typical tunnel kiln for brick production.

11.5.2.2 Densely Packed Loads

Another common application for high-velocity burners is the firing of densely packed loads, such as brick hacks. The heating of brick must follow a very specific time and temperature profile to achieve organic material burnout and proper ceramic bonding. A single brick can be fired to the desired properties in a very short time in a laboratory test furnace — typically less than 2 hours. However, production at industrial levels requires the firing of large hacks of formed and dried bricks in tight stacking arrangements. Every brick within these hacks must follow the same prescribed time and temperature profile. This creates significant difficulty as exterior bricks are heated more quickly than those in the interior of the hack. The time to successfully fire a brick hack increases substantially over the laboratory cycle, often to 40 to 60 hours, dependent on the actual time to heat the coldest brick in the hack.

Because they drive hot combustion products to the innermost bricks of a hack, high-velocity burners have become the burner of choice for firing brick tunnel kilns (Figure 11.22). Without the velocity from the burners, interior bricks would essentially be heated only by conduction, a very slow and inefficient means. The majority of the burners in the firing zones of a tunnel kiln are typically mounted low in the sidewalls, with a combination of staggered and opposed arrangements. The opposed burners provide heat release in the center of the load while the staggered burners sweep across the hacks, distributing heat across the setting. The intent is to get the heat to penetrate the load evenly, especially to the normally cold bottom of the hack. This is difficult to impossible with conventional low- or medium-velocity burners, regardless of the position of burners or type of control system.

A smaller quantity of high-velocity burners placed at intervals in the upper sidewall can also help in breaking up “crown drift” in tunnel kilns. This phenomenon occurs when hot products of combustion migrate to the low-flow-resistance area at the roofline of the kiln above the hacks and travel toward the exhaust at the cold end of the kiln, thus “bypassing” the area of the kiln cross section occupied by the hacks. It reduces the overall efficiency of the heating process and can affect the optimum control of the kiln. High-velocity burners placed high in the side walls, firing above the hacks, will entrain these stratified products of combustion and push them downward at the opposite wall to be entrained by the lower burners and allow their heat content to be put to useful work within the hacks. High-velocity burners firing vertically downward from the roof can also be

used for a similar purpose, particularly in wide kilns where side-mounted burners do not have the drive to create significant recirculation across the full width of the kiln.

High-velocity burners are also very effective in the low-temperature preheat zone at the entry end of a tunnel kiln.¹¹ These burners are typically fired at elevated excess air rates to achieve the lowest possible temperature difference between the resulting entrained gases and the bricks, while providing the required heat input to match the curve. This approach ensures that the bricks will be uniformly heated in an oxidizing environment conducive to the controlled burnout of any organic material in the clay. The entire hack can then pass into a more highly fired zone without risk of affecting product quality and yield of saleable product from the kiln. Adding high velocity burners to tunnel kiln zones, which previously relied on recirculating fans, can significantly increase the production capability of a brick kiln. By maintaining better temperature uniformity throughout the brick hacks in the preheat zones, less time is required to heat the interior bricks in the high temperature heating zones. Therefore, if the burners in the early part of kiln properly condition the load, the hot zone burners need only to maintain the temperatures required for the final material properties to develop.

11.5.2.3 Well-Spaced Loads or Open Settings

Firing of ceramics such as dinnerware, cookware, sanitary ware, and technical materials typically falls into the category of heating a well-spaced load. In these instances, the individual pieces are spaced on support structures without piece-to-piece contact. This minimizes imperfections in the fired part and allows for the high degree of temperature uniformity desired in these applications. Because nearly all of the surface area of the load is swept by combustion product gases, uniformity as close as $\pm 10^{\circ}\text{F}$ can be achieved. High-velocity burners, often running with excess air, move large volumes of products of combustion between and across the pieces of the load. Because the support structures form part of the load to be heated, the quantity of supports and the spacing between the parts must be minimized for best economic use of the kiln interior space and fuel utilization (Figure 11.23).

These applications frequently arrange the material into lanes, several pieces high. When firing such an arrangement, it is important to understand the spread of the high-velocity burner jet and its rate of entrainment of surrounding gases in order to reduce hot spots on the load. The combustion envelope must not overheat pieces sitting close to the burner wall. The combination of excess air,



FIGURE 11.23 Typical china setting.

distance to the part, jet spread, and spaces between the parts affects the temperature of the products of combustion as they sweep across the fired piece. High-velocity burners with slotted tile exits may offer distinct advantages in firing narrow lanes in such circumstances. Its elevated rate of near-field entrainment and preferential vertical entrainment can aid in the movement of gases through the kiln while minimizing the temperature gradients at the work.

11.5.2.4 The Fired Chamber as the Load

The high excess air capability and high-velocity combustion product jets of lightweight, air-cooled tile, high-velocity burners are the accepted method of dryout and preheat of large refractory structures and are also applied to the on-site heat treatment of large welded structures. The equipment and technology for such applications is generally provided by refractory dryout/heat treatment specialist companies as a contract service.

Using temporarily mounted lightweight 10 million BTU/hr burners of the jet-can type with double-skinned air cooled outlets, jets of dilute POC from 200°F to 2500°F are projected into the structure to be heated, the jet temperature being controlled according to the required program for the particular treatment. The number of burners to be used is evaluated based on the heat requirement of the cycle determined by the temperature curve to be followed, the size and shape of the space being heated, and the amount of water vapor to be removed in case of a dryout. The temporary burners are configured to produce a POC circulation pattern conducive to achieving the best temperature uniformity in the volume of the fired space. As the burners' access points to the interior of the structure are frequently not in "ideal" locations, the art and ingenuity of the contractor's experience is an important element in the configuration exercise. A means of controlling the exhaust rate from the space is installed so that the volume can be pressurized relative to atmospheric pressure to prevent the ingress of ambient air in the interests of control of uniformity and elimination of waste of the fired fuel.

For a refractory dryout, large volumes of water can be removed at low temperature differences with the refractory surface, thus allowing a closely controllable rate of temperature increase to eliminate explosive spalling caused by trapped steam.

In the heatup of sensitive materials such as the silica bricks and fused-cast refractories used in glass tank construction, close control of temperature uniformity is required to prevent damage to the structure from differential thermal expansion and/or spalling. The convective heating provided by the high-velocity burner jets and their entrainment of circulating products of combustion gives operators the ability to control the rate of change of temperature to a few degrees per hour with single-digit temperature differentials at the materials' transition points.

Large, fabricated structures such as gas storage tanks, chemical process equipment, and pressure vessels frequently require stress relieving *in situ*. The use of high-velocity burners offers an alternative to the highly labor-intensive and expensive electrical method of strapping resistance heaters to the exterior surface. The subject structure is temporarily externally insulated, and one or more burners installed to fire into the internal space. In some extreme cases of thin-walled vessels and high-temperature treatments, the internal pressure created by the combustion process has been consciously employed to prevent collapse of the vessel.

Figure 11.24 shows the use of a single burner on an aluminum melter heatup, and Figure 11.25 shows multiple burners in use on the heatup of a steel plant coke oven battery.¹²

11.6 CONTROL OF HIGH-VELOCITY COMBUSTION SYSTEMS

Burner control techniques have evolved along with furnaces and high-velocity burners. To best utilize the high-velocity burner's jet properties, the heat input and fuel/air ratio control system should generally be chosen to operate the burner(s) at the maximum input rate for the longest possible time in any heating cycle. The particular application will dictate the best choice for a given furnace, considering the type of product being heated, the type of furnace, the degree of temperature

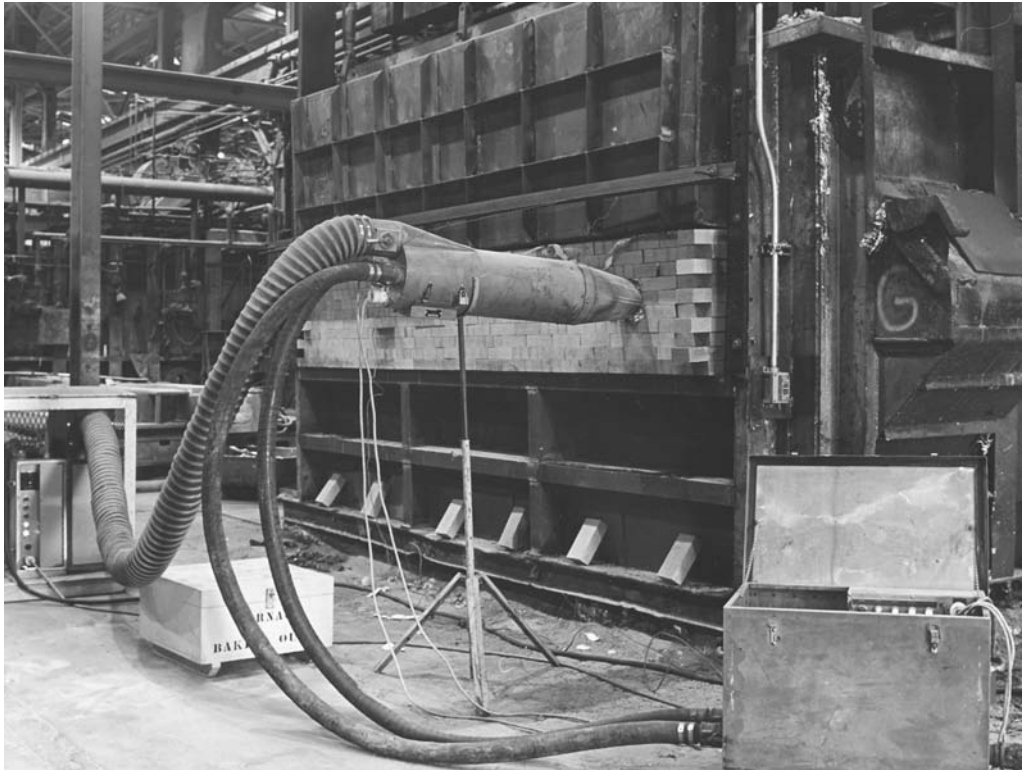


FIGURE 11.24 A single temporary burner on an aluminum melter heatup. (Courtesy of Hotwork—Division of Fosbel, Inc. With permission.)

uniformity required, the desired atmospheres, and the prevailing economics (usually an evaluation of product value and quality vs. the cost of the energy to produce it).

Most modern furnaces have multiple control zones, each monitored by a temperature-measuring element such as a thermocouple or infrared scanner. Each zone may have multiple burners controlled as a group to meet the demands of the zone controller. The fuel input to the burners is varied, either by continuous modulation or pulse-width modulation, to maintain a desired furnace temperature.

All burners have some capability to operate at lower fuel rates than their design maximum. The amount a burner can turn down is often referred to as its “turndown ratio,” defined as the maximum firing rate divided by the minimum firing rate. With continuous modulation, the higher the turndown ratio, the greater the range of temperatures that can be maintained in the furnace. For pulse-width modulation, the burners are typically operated at a fixed rate, and the firing time at that rate is adjusted to change the heat input. Differences in the control methods affect the means by which the output of a group of burners is reduced within a control zone.

All of the piping examples shown in this section are intended to illustrate control concepts only. They do not show flow meters, manual or electrical shutoff valves, and other components needed for normal operation or to meet applicable safety codes. Valves must be “approved” for fuel shutoff service as required by the regulatory authority having jurisdiction.

11.6.1 FUEL/AIR RATIO CONTROL

Each control zone or individual burner must have a means of fuel/air ratio control for efficient operation. While electronic controls are available for this purpose, the most prevalent method of fuel/air ratio control is the cross-connected ratio regulator.

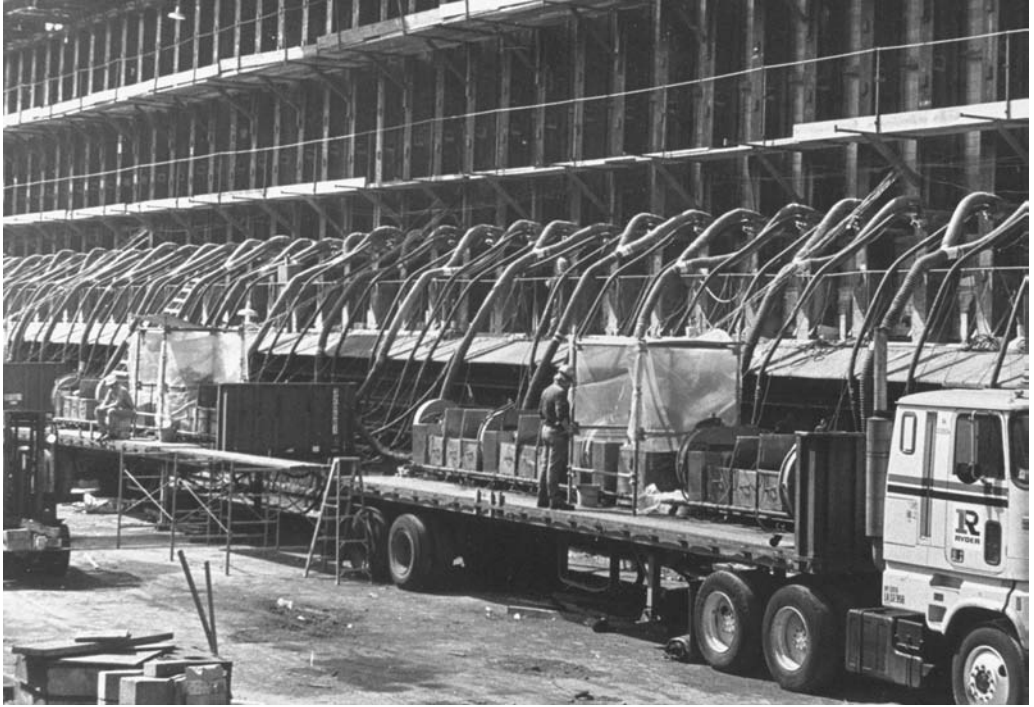


FIGURE 11.25 Multiple temporary burners in use on the heatup of a steel plant coke oven battery. (Courtesy of Hotwork—Division of Fosbel, Inc. With permission.)

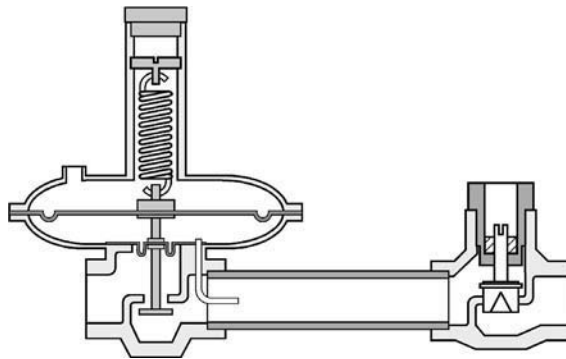


FIGURE 11.26 Cross-connected ratio regulator with limiting orifice valve.

The function of a cross-connected ratio regulator system is based on the principle that the internal air and gas orifices of a burner are fixed resistances to flow, such that the flow and pressure are related by the “square root law:”¹³

$$\frac{Q_1}{Q_2} = \sqrt{\frac{\Delta P_1}{\Delta P_2}} \quad (11.7)$$

The cross-connected ratio regulator (Figure 11.26) is designed to maintain a fuel outlet pressure that matches the combustion air pressure to the burners. A pressure sensing line is run from the burner combustion air line to the regulator’s main diaphragm case to provide an opening force to the regulator’s gas valve. An internal gas outlet pressure sensing port applies that gas pressure to

the other side of the main diaphragm as an opposing, closing force. A plug valve attached to the diaphragm adjusts the gas pressure exiting the regulator to maintain a pressure balance. As the regulator only controls pressure directly — not the actual flow — a downstream variable resistance, such as a limiting orifice valve, is required in the gas line to adjust the actual flow at the high fire rate.

A biasing spring in the regulator is used to set the low-fire fuel/air ratio. A negative bias can be applied to the ratio regulator by tensioning the diaphragm spring. This makes the fuel/air ratio “leaner” at low fire without significantly affecting the high-fire setting.

Some high-velocity burners have gas pressure requirements that are higher than their air pressure requirements. The simple cross-connected regulator described above, supplying fuel at the same pressure as the air, will not be able to supply sufficient gas pressure to operate the burner near the stoichiometric conditions. There are a number of options for ratio control in these cases. Multiplying regulators that provide gas pressure at a multiple of the air pressure, or electronic fuel/air ratio systems, can be used. If there is sufficient air pressure available, an orifice can be put in the burner air supply to raise the air pressure to the point where it is at least 25% greater than the required fuel pressure, allowing a simple cross-connected regulator to function properly.

It is common to use a single cross-connected regulator to control the gas flow for an entire zone of premix or conventional nozzle mix burners. However, the restricted tile outlets and tile back pressures of high-velocity burners will accentuate any pressure variations occurring in the tile as a result of combustion. These are manifested as variations in air and fuel flows to the burner, and, when high-velocity burners are on a common control manifold, a pressure disturbance in one burner can affect the others. This may initiate additional sympathetic pressure variations to the degree that the entire group of burners will display erratic behavior. The effect of feedback of tile pressure fluctuations can be minimized by using an individual ratio regulator for each high-velocity burner, and by placing the limiting orifice valve as close as possible to the burner gas inlet and taking the highest possible pressure drops allowed by the system across it and the burner air valve.

11.6.2 FIXED FUEL/AIR RATIO TURNDOWN (ON RATIO TURNDOWN)

Fixed fuel/air ratio control using cross-connected regulators is the most prevalent control system style for high-velocity burners. This is the only control method available for the early premix systems that required the fuel/air ratio to be set near stoichiometric at all firing rates and is often called “on ratio turndown.” In this control scheme (Figure 11.27), the zone temperature controller positions a motorized air valve to vary the airflow into the burner. The ratio regulator delivers fuel to maintain the appropriate fuel/air ratio at any airflow rate. The air valve can be continuously modulated or operated in a high/low mode.

Fixed fuel/air ratio systems optimize fuel efficiency but do not maximize the potential of the high-velocity burner. Velocity decreases as the burner turns down and the entrainment capability of the jet is reduced. A common way to maximize the time at high fire is the use of “high/low”

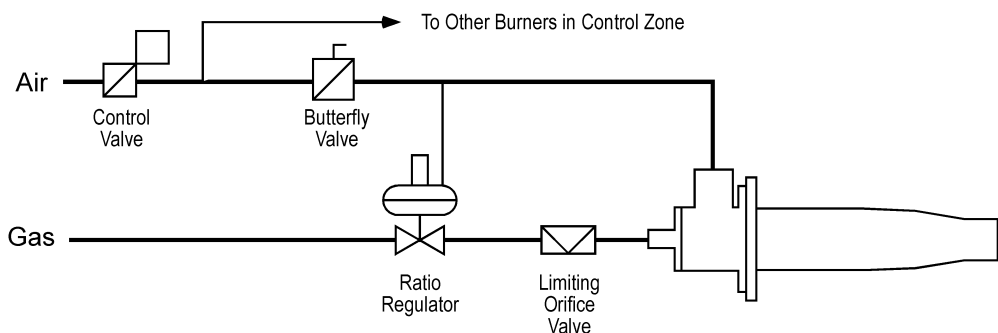


FIGURE 11.27 Fixed fuel/air ratio control schematic.

control, where the motorized air control valve is either at the maximum setting or the minimum. This method of control maximizes the time the burners are at high fire, which maximizes the entrainment and recirculation benefits, but may create difficulties for furnace pressure control, as all the burners in a control zone cycle firing rates simultaneously.

11.6.3 VARIABLE RATIO OR “THERMAL” TURNDOWN

Nozzle mix high-velocity burners have a wide fuel/air ratio capability that can be used to advantage in ratio control systems. To maintain burner nozzle velocity with reducing input requirement, the fuel flow can be reduced faster than the airflow, the increase in the excess air rate resulting in a lower temperature flame. If there is enough burner capacity available, the high fire ratio can be made “leaner” to force the burner to spend more time at high fire where the velocity is highest. This concept taken to its extreme is known as thermal turndown.

In the extreme thermal turndown system, the airflow remains fixed at the maximum setting while only the fuel flow is reduced when temperature demand drops. This method of control maintains the highest velocity for any firing rate and is useful for applications that require the ultimate temperature uniformity. At intermediate firing rates, the hot-mix temperature exiting the burner may only be a few degrees higher than the furnace setpoint, which provides for very even heating. Furnace pressure control is simplified because the amount of air introduced into the furnace remains relatively constant at all firing rates. The disadvantage of thermal turndown systems is the loss in fuel efficiency resulting from heating the excess air to the furnace temperature.

To use a thermal turndown control system, the burner must be capable of running at high enough excess air rates that the minimum temperature requirement for the furnace can be maintained without overshooting. The Bickley Iso-Jet burner described previously is an exception in that it has a premix or nozzle mix core (depending on the vintage) that runs close to stoichiometric ratio while additional air is added around the primary burner to temper the resulting hot mixture to the desired temperature.

There are a number of ways to set up a zone of burners with thermal turndown control. One popular method is to pipe the burners in the same manner as for on ratio control but to control temperature with a motorized control valve that bleeds off some of the impulse pressure feeding the cross-connected regulator instead of a motor that reduces main air flow (Figure 11.28). Note that a main air control valve may still be required to meet an enforced low-fire start requirement of a safety code.

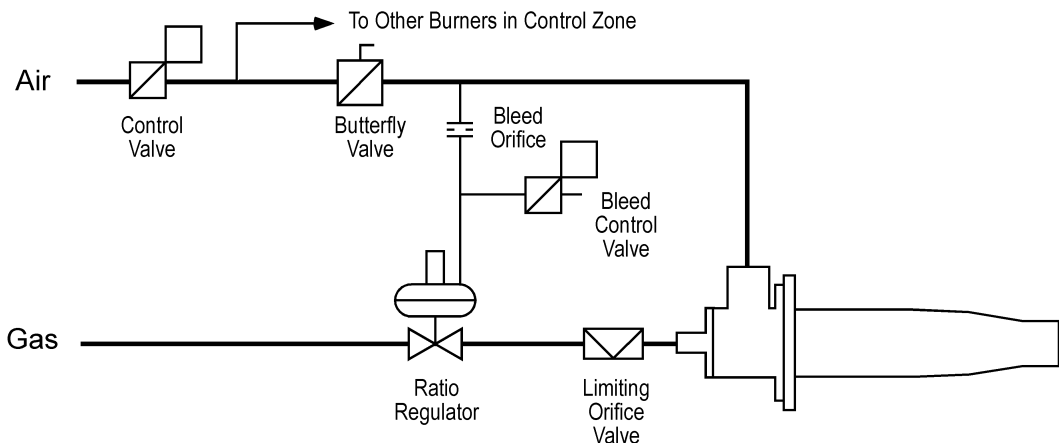


FIGURE 11.28 A typical method of thermal turndown control schematic.

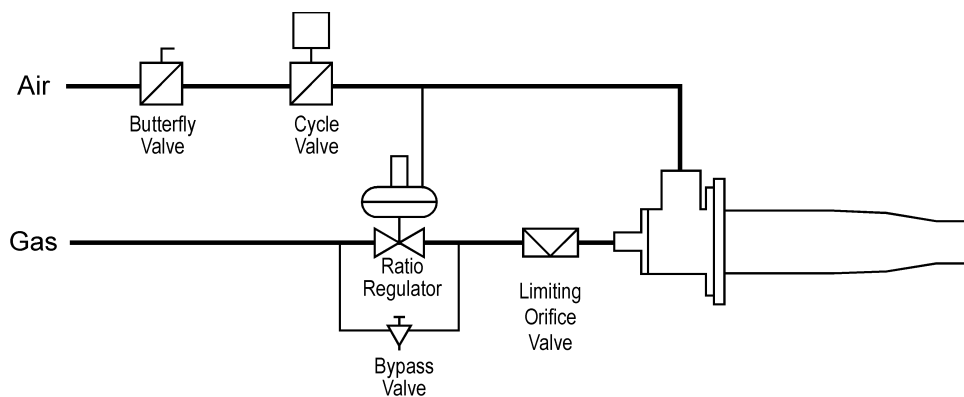


FIGURE 11.29 Typical pulse firing control schematic.

11.6.4 PULSE-FIRING INPUT CONTROL

As earlier stated, high-velocity burners are most effective when operated at high fire where the velocity and mass flow are the highest. A pulse-firing system reduces input in a zone by selectively turning down individual burners in the zone to low fire while the other burners remain at their maximum firing rate. As the required input decreases, more burners are turned off and fewer are left on. One such example would be that at 50% firing rate, half the burners will be at their full firing rate and the other half at low fire. The selection of high and low firing burners is continuously changed by the pulse-firing system logic in order to step the required heat input around the total number of burners and create temperature uniformity in the fired chamber.

Pulse-firing has the advantages of better potential temperature uniformity and more consistent furnace pressure control than modulated or high/low fixed fuel/air ratio control systems, and has better fuel efficiency than thermal turndown systems.

Pulse-fired systems use fast operating air cycle valves to switch from high fire to low fire. A small amount of air is allowed to pass through or around the closed valve position to provide the low fire air. Fuel is commonly controlled with a conventional cross-connected regulator having its spring set for a negative bias to close the valve seat at low fire, with a low-capacity bypass to set the low-fire gas rate (Figure 11.29). This arrangement typically provides more consistent minimum flow conditions than does relying on the regulator to accurately position for very low flows. Cross-connected ratio regulators are designed to constantly adjust gas flow, so they are well-suited for use as cycle valves in applications that do not require a gas-tight seal in the closed position. This may eliminate the use of a dedicated electrical or pneumatic valve where individual automatic gas valves have not been used to interrupt the gas flow for the pulse-firing system.

11.6.5 HIGH-VELOCITY OIL BURNER CONTROL

While high-velocity oil burners can be controlled by methods similar to those described above, oil burners do not typically have turndown capabilities as high as gas burners.¹⁴ Their low-fire input cannot be turned down as far using fixed fuel/air ratio control, nor do they have wide excess air capability, thereby limiting the degree to which thermal turndown can be employed. It may be necessary to use a high/low/off control with oil burners if high turndown is required. Spark-ignited gas pilots are often used for improved reliability over direct-spark ignition.

REFERENCES

1. *North American Combustion Handbook, Volume 2*, third edition, The North American Manufacturing Company, Ltd., Cleveland, OH, 1995.
2. Watson, J., Personal communication, 2002.
3. Gray, M., Personal communication, Nutec-Bickley, 2002.
4. Crowther, B., Personal communication, Hotwork Combustion Technology Limited, 2002.
5. Beer, J. M. and Chigier, N. A., *Combustion Aerodynamics*, Robert E. Krieger, Malabar, FL., 1983.
6. Dahm, W. J. A. and Dimotakis, P. E., Measurements of entrainment and mixing in turbulent jets, *AIAA J.*, 25, 1216–1223, 1987.
7. Dahm, W. J. A., Personal communication, University of Michigan, 2002.
8. Eickhoff, H. and Lenze, B., Grundformen von strahlammen, *Chemie Ingeniuer Technik* 20, 1095–1099, 1969.
9. Schlichting, H., *Boundary Layer Theory*, seventh edition, McGraw-Hill, New York, 1987.
10. Tachina, K.M. and Dahm, W. J. A., Effects of heat release on turbulent shear flows. 1. A general equivalence Principle for non-buoyant flows and its application to turbulent jet flames, *J. Fluid Mech*, 415, 23–44, 2000.
11. Lukacs, J. J., Personal communication, The North American Manufacturing Company, Ltd., 2002.
12. Cobane, I., Personal communication, Hotwork—Division of Fosbel Inc., 2002.
13. *North American Combustion Handbook, Volume 1*, third edition, The North American Manufacturing Company, Ltd., Cleveland, OH, 1986.
14. *Fuel Oils for Industrial Burners*, The North American Manufacturing Company, Ltd., Cleveland, OH, Handbook Supplement 113, 1998.

12 Regenerative Burners

Russ Lang, Bruce B. Abe, Clive Lucas, and John Newby

CONTENTS

- 12.1 Introduction
- 12.2 Efficiency in the Context of High-Performance Heat Recovery from Combustion Products
 - 12.2.1 Available Heat
 - 12.2.2 Evaluating Fuel Savings Potential from Air Preheating
- 12.3 The Regenerator Principle
 - 12.3.1 The Regenerator
 - 12.3.2 The Modern Compact Regenerative Burner
 - 12.3.3 The Principle of the Compact Regenerative Burner
 - 12.3.4 Types and Styles of Regenerative Burners
 - 12.3.5 Heat Transfer Media
 - 12.3.6 Heat Transfer Characteristics for Compact Regenerator Media
 - 12.3.7 The Performance of Compact Regenerative Burners
- 12.4 Types of Regenerator for Compact Regenerative Burners
 - 12.4.1 Basic Shapes
 - 12.4.2 Regenerators with Removable Packing
 - 12.4.3 Remote Regenerators
 - 12.4.4 Rotary Regenerators
- 12.5 Controls for Regenerative Burners
 - 12.5.1 Safety Systems
 - 12.5.2 Exhaust Fan Proving
 - 12.5.3 Pre-purge
 - 12.5.4 Air/Fuel Ratio
 - 12.5.5 Flow Measurement and Control
 - 12.5.6 Ratio Control Special Functions
 - 12.5.7 Furnace Pressure and Regenerator Exhaust
 - 12.5.8 Regenerator System Reversals
 - 12.5.9 Reversing Valve Types and Operation
 - 12.5.10 Reversal Valves Sequencing
 - 12.5.11 Confirmation of Reversal Valve Operation
 - 12.5.12 Flame Supervision and Reversals
- 12.6 Emissions
 - 12.6.1 CO₂ Emissions
 - 12.6.2 NO_x Emissions
 - 12.6.3 NO_x Reduction Methods for Regenerative Burners
- 12.7 Some Regenerative Burner Applications
 - 12.7.1 Well-Charged Aluminum Melter
 - 12.7.2 Direct-Charged Aluminum Melter
 - 12.7.3 Steel Reheat Furnace Applications

- 12.7.3.1 New Reheat Furnace Designed for Regenerative Firing
- 12.7.3.2 Addition of Booster Zone to Existing Furnace
- 12.7.3.3 Addition of Booster Zone to Existing Furnace

References

12.1 INTRODUCTION

In 1858, William Siemens built the first experimental furnace using the regenerative principle to achieve high temperatures¹. Two years later, he built and patented the first practical furnace using regenerators for the melting of glass. The significant advantages of the principle of regeneration were quickly understood, and it was quickly adopted in furnaces for zinc distillation, the puddling of iron, the reheating of iron and steel, and for the melting of steel. From these applications evolved the Siemens Martin Basic Open Hearth Furnace, used in the making of steel until displaced by the electric arc furnace, and the Glass Melting Tanks used today for all large-scale glass production.

The regenerators of today's glass melter are large refractory structures containing a refractory checkerwork heat storage mass — usually substantially larger than the actual glass-melting furnace section itself. Reversal times of 40 to 50 minutes between the heating and cooling functions are common, with 2-minute firing interruptions for valve cycling to take place.

In the early 1980s, attention was turned from the use of the compact self-recuperative burner that was then the leading high-efficiency, small-to-medium capacity, direct-firing burner technology to the development of compact regenerative burners to bring the inherently high regenerator efficiency to furnace plant and processes previously considered unsuitable for the application of regenerators. It is the combination of a high air preheat temperature burner and a compact high-efficiency heat recovery device to which this chapter is devoted.

12.2 EFFICIENCY IN THE CONTEXT OF HIGH-PERFORMANCE HEAT RECOVERY FROM COMBUSTION PRODUCTS

Industrial combustion produces hot gases to be utilized in the transfer of heat to another body. The primary attributes of the hot gases in achieving this transfer are temperature and heat content, with the secondary properties of heat emissivity and chemical characteristics such as oxidizing or reducing potential.

This chapter is primarily devoted to the production and use of those gases where they are directly in contact with the material to be heated, but the principles of this section apply also in the case where the fuel is combusted in an enclosure separated from the work by a partition, such as muffle furnaces or those fired with radiant tubes.

The process of utilization of the heat of the combustion gases involves some waste. Only part of the heat is used in heating the work; part is used in heating the work enclosure, part will be lost from that enclosure, and part will exit at the full process temperature in the exhaust gases from the work enclosure. The regenerative burner is devoted to the combination functions of producing the hot combustion gases and recovering a significant portion of that heat leaving the process at full process temperature.

The basic Sankey diagram in [Figure 12.1](#) illustrates the relationship of the gross heat input of the fuel to the useful heat output.

The process efficiency can be calculated as:

$$\% \text{Process Efficiency} = \left[\frac{\text{Usable Heat To Load}}{\text{Gross Heat Input}} \right] \times 100 \quad (12.1)$$

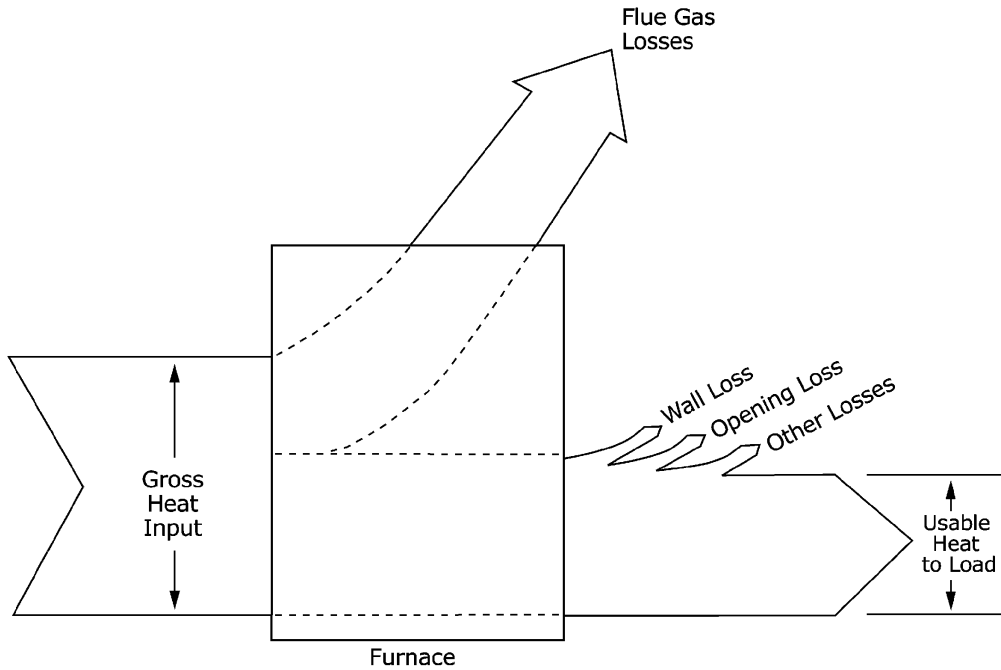


FIGURE 12.1 Basic Sankey diagram.

Because the Usable Heat to Load, Wall Loss, Opening Loss, and Other Losses are all functions of the particular furnace and load in process and not related to the combustion process, the efficiency related to combustion can be calculated as:

$$\% \text{Combustion Efficiency} = \left[\frac{(\text{Gross Heat Input} - \text{Flue Gas Losses})}{\text{Gross Heat Input}} \right] \times 100 \quad (12.2)$$

The amount of heat derived from (Gross Heat Input – Flue Gas Losses) is commonly referred to as the “Available Heat to the process,” and the % Combustion Efficiency from Equation 12.2 as the “% Available Heat.”

12.2.1 AVAILABLE HEAT

Most fuel-fired industrial heating applications can increase their overall heating efficiency and reduce fuel consumption by preheating of the combustion air. Preheating combustion air requires less of the chemical energy derived from the fuel to be used to raise the air to furnace temperature.

$$\text{Available Heat} = [\text{Gross Heat Input} - (\text{Moist Loss} + \text{Dry Loss})] \quad (12.3)$$

The moist flue loss is the heat given up by the water vapor in the combustion products as it cools to the base temperature at which the calorific value of the fuel was determined. It is mainly the latent heat of condensation of the water vapor formed by combustion of the hydrogen in the fuel. The dry flue loss is the amount of heat given up by the dry combustion products as they cool to the base temperature at which the calorific value of the fuel was determined.

The available heat can be calculated for each specific fuel and oxidant, cold or preheated combustion air, oxygen enriched air, and oxy-fuel, for specific air/fuel ratios at, above (excess air), or below (excess fuel) the ideal stoichiometric ratio, at any flue gas temperature.

The Sankey diagram in Figure 12.2 expands on the basic diagram of Figure 12.1 to include the additional components previously described. The Sankey diagram of Figure 12.3 expands on Figure 12.2 by including the illustration for recovered heat from the flue gases to the combustion air.

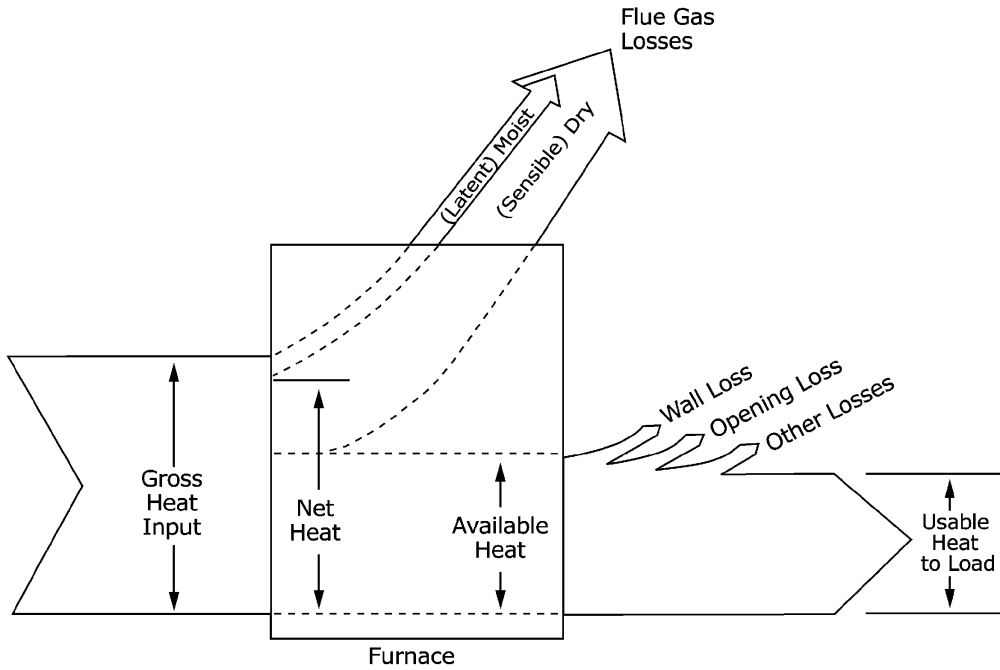


FIGURE 12.2 Expanded Sankey diagram to include the moist flue gas loss.

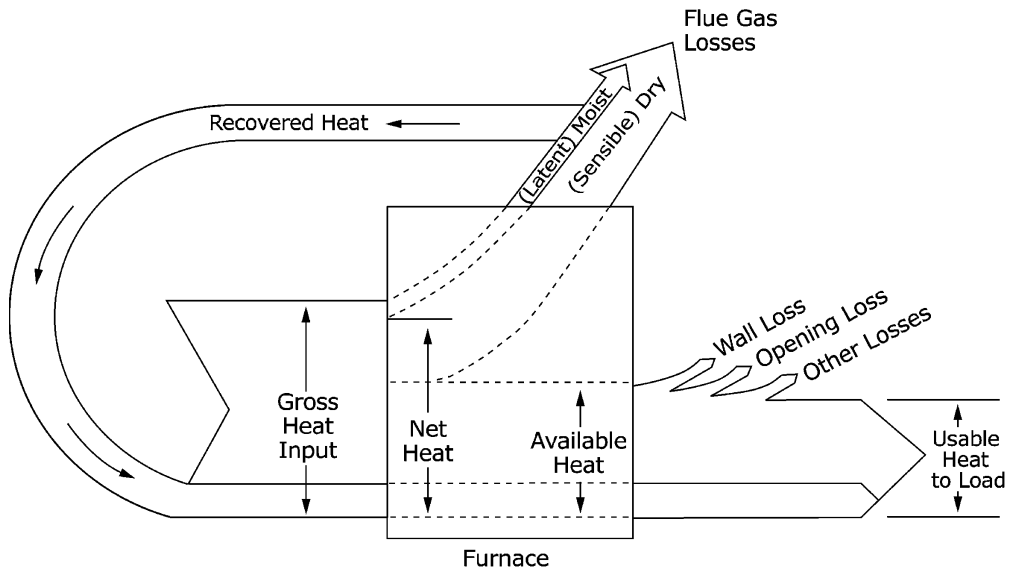


FIGURE 12.3 Sankey diagram, including recovered exhaust heat.

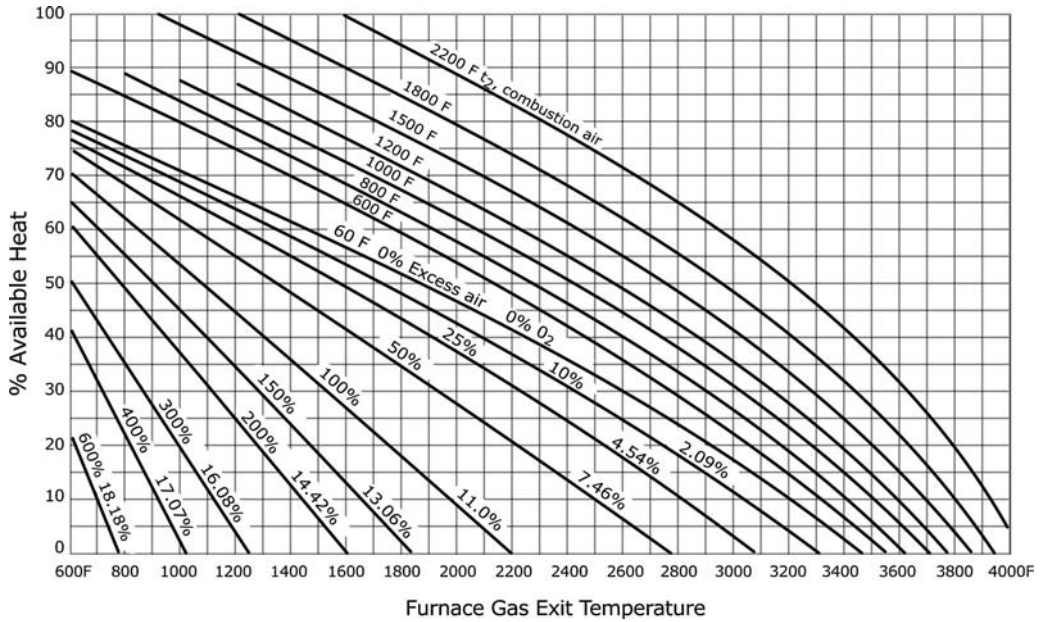


FIGURE 12.4 Available heat for 1000 BTU/ft³ natural gas at various furnace temperatures and air preheat levels.

Figure 12.4 is a typical chart-plotting % Available Heat against flue gas temperature for both cold and preheated air for a typical natural gas.

The following example demonstrates the use of Figure 12.4. The intersection of a 2000°F furnace temperature with cold (unheated) combustion air at 10% excess air shows an available heat of 42%. The intersection of combustion air preheated to approximately 1660°F with a furnace temperature of 2000°F shows 75% available heat. It can be seen that preheating the combustion air results in higher combustion efficiency as only 25% (100% minus 75%) of the gross heat input is lost to the flue gases compared to 58% (100% minus 42%) when using cold combustion air.

12.2.2 EVALUATING FUEL SAVINGS POTENTIAL FROM AIR PREHEATING

The available heat concept can be used to evaluate the fuel saving resulting from preheating the combustion air (or changing the amount of excess air in use):

$$\% \text{Fuel Saved} = \left[1 - \left(\frac{\text{Original \% Available Heat}}{\text{New \% Available Heat}} \right) \right] \times 100 \quad (12.4)$$

Applying Equation 12.4 to the previously referenced values for a 2000°F furnace yields:

$$\% \text{Fuel Saved} = \left[1 - \left(\frac{42}{75} \right) \right] \times 100 = 44\% \quad (12.5)$$

The higher the furnace operating temperature, the greater the potential fuel savings can be with preheated combustion air. The 75% available heat value is indicative of that typically realized by regenerative burners.

12.3 THE REGENERATOR PRINCIPLE

The principle of the regenerator, the alternate heating of a heat storage mass by flowing exhaust gas and subsequent cooling of it by the combustion air on its way to the burner, with the units applied in pairs to allow a virtually continuous firing process interrupted only by reversal of the functions of the two regenerators, is a highly efficient means of heat recovery from exhausting combustion products. Because the heating/cooling process is in counter flow, and the hot end of the heat storage mass reaches the full temperature of the gases exhausted from the furnace, the combustion air can be heated to a temperature very close to that of the furnace. The inherent heat recovery effectiveness of a regenerator can approach 90%, compared with ~40% for a typical recuperator.

12.3.1 THE REGENERATOR

The regenerative principle was first developed by the prolific inventor William Siemens and employed in the construction of steam engines, although later abandoned for this use as a result of the severe wear to the cylinders from the high temperatures attained. In 1858 Siemens built his first experimental furnace with regenerators to elevate the combustion air temperature in order to achieve higher flame temperatures. Two years later, he built and patented the first practical gas-fired regenerative furnace, used in melting glass. It was soon established that the use of regenerators would provide significant fuel savings in high-temperature furnaces, leading to their adoption in zinc distillation furnaces, for the puddling of iron, the reheating of iron and steel, and in the well-known Siemens Martin Basic Open Hearth Furnace for the making of steel and the Glass Melting Tank still used today for all large-scale glass production.

An example of a traditional regenerator is shown in Figure 12.5.² It can be seen that the regenerators are of significant size relative to the furnace.

Refractory checkerwork is used as the heat transfer mass, and a series of valves and dampers are used to control the direction of combustion air and waste gas flows. In the example of Figure 12.5,

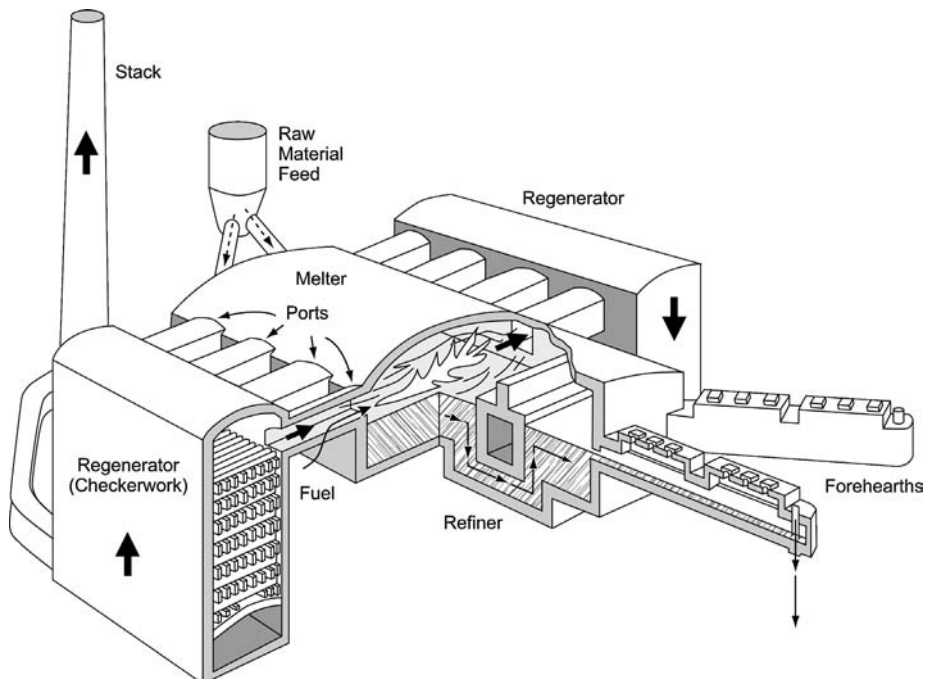


FIGURE 12.5 A regenerative side-port glass melting furnace.

there are four air/exhaust ports on each side of the furnace. Only the ports on one side fire at any one time, fuel being injected into the air stream adjacent to the furnace end of the air port. During the first cycle, products of combustion (POC) from the firing side are carried through the opposite brick checkerwork after they exit the furnace. As the POC travel through the cool checkerwork, they lose heat to the refractory and drop in temperature. After a period as long as 40 to 50 minutes, the valves and dampers are reversed to change the direction of flow. Cold combustion air is now directed through the previously heated checkerwork, absorbing the heat from the refractory and rising in temperature before reaching the ports now to be fired.

The choice of individual shapes, their refractory composition, and the arrangement of the shapes in a conventional regenerator checkerwork packing are strongly influenced by the temperature and constituents of the flue gas from the fired process, as well as the desire for high-performance heat recovery. Depending on the furnace charge and the heat processing, the hot exhaust products exiting the furnace may not only contain the normal products of combustion, but also may contain volatilized compounds and particulates emanating from the charge and the furnace structure. The fuel fired in the furnace may also be a source of elements such as sulfur and vanadium.

As the exhaust gases cool, these various “passengers” will have the potential to combine, condense, and deposit on the packing, depending on their nature. The chemistry of the packing must be chosen taking into consideration the potential for any corrosion attack by the deposits. The shape and size of the gas passages in the packing must be selected with an eye toward the heat transfer and the resistance to flow (affecting the power required to move the gases through the regenerator), and also with the aspects of the potential degradation to performance caused by any fouling, and the possible removal of the fouling to maintain heat transfer performance or keep air and exhaust gas pressure drops within the bounds of the capability of their flow-producing devices.

Using the glass melting furnace as an example, the typical soda-lime glass container tank exhaust gases will be carrying at least volatile sodium sulfate and some fine, but sticky, batch material particles. The accumulation of these will cause fouling and give rise to the potential of slagging of the refractory materials of the packing. Although the regenerator packings are designed to minimize the effect of accumulation and corrosion on regenerator efficiency and availability, it is common practice in the industry to utilize special portable burner equipment and trained crews to “melt out” glass tank regenerator accumulations *in situ* in cases where resistance to flow has become extreme.

Traditional regenerators use large refractory shapes in the packing that are placed according to a pattern to create gas flow passages of the desired hydraulic and thermal properties. Different materials can be used at different levels in the packing according to the design conditions of temperature, corrosion potential, and mechanical loading at the particular location.

12.3.2 THE MODERN COMPACT REGENERATIVE BURNER

In the early 1980s, work began on the development of compact regenerative burners. Although difficult to track exactly, it seems that it may have begun almost simultaneously in the U.K. at what was then British Gas,³ in conjunction with the British combustion company Hotwork Development, and in the U.S. at the authors’ company, The North American Manufacturing Company.⁴ Certainly, the first commercial installation, in February 1983, was a 1 MMBtu/hr, 1400°C, open pot glass melting furnace.^{3,5} From that small beginning in Wakefield, England, have come hundreds of installations spanning the steel, aluminum, glass, and ceramic industries, with standard burners from 100,000 Btu/hr to close to 50 MMBtu/hr in individual heat input capacity, across the globe. In Japan where high fuel prices and a government-sponsored energy/emissions initiative spurred adoption,^{6,7} in Europe with high energy prices and emissions concerns, and in the U.S. where a high initial adoption rate was influenced by the rise and decline of energy prices, the regenerative burner constitutes the leading technology for the firing of high-temperature, high-efficiency, low emissions, industrial furnaces.

12.3.3 THE PRINCIPLE OF THE COMPACT REGENERATIVE BURNER

The compact regenerative burner, a high-temperature preheated air burner close-coupled to a compact, fast-cycle ceramic regenerator, can provide air preheat in excess of 85% of the process temperature in fuel-fired applications up to 3000°F.

The average 90% effectiveness of the compact regenerator gives close-to-ultimate performance for any combustion air preheater recovering heat from exhaust gas. The high preheat level and insensitivity to the operating environment combine to provide good economics with trouble-free, low-maintenance operation.

The burner serves double duty, acting also as the exhaust port and flueway from the fired chamber. One complete compact regenerative burner set comprises two burners, two regenerators, reversing valves, and the reversing logic.

Each burner has a compact heat storage regenerator containing a bed of ceramic balls. Operating in pairs, one burner fires with cold air fed to the base of its regenerator, and the other burner acts as the exhaust from the fired chamber. Combustion air is preheated as it passes through the bed of the firing burner by removing heat stored in the ceramic balls. At the same time, hot furnace gases give up heat to the ceramic balls in the regenerator of the exhausting burner. Burner duties are reversed within an application-specific time period on the basis of time, or a combination of exhaust temperature and time. The burners continuously cycle between firing and exhausting when the fired process demands heat. A simple representation of this can be seen in Figure 12.6 and Figure 12.7.

12.3.4 TYPES AND STYLES OF REGENERATIVE BURNERS

There are two major components of a regenerative burner: (1) a high-temperature preheated air burner that can do double duty as an exhaust port, and (2) its companion heat-storage-medium-containing regenerator.

Mostly influenced by the heat input capacity of the unit, there are two basic styles – the generally smaller-capacity unit where the burner and the regenerator share the same housing and the regenerator has a horizontal flow path, and the generally larger-capacity unit where the burner has an appearance not unlike a conventional hot air burner, but is connected by high-temperature ductwork to a regenerator having vertical gas flow through the regenerative medium. For the sake of ease of distinction between the two types, the authors will use the convenient terminology one of them first heard in Japan to describe them: “one-box” and “two-box,” respectively.

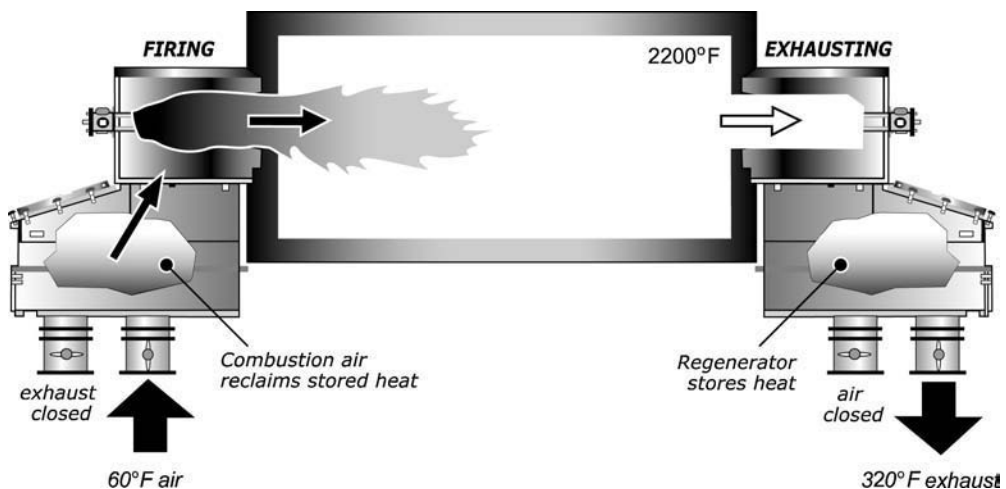


FIGURE 12.6 Regenerative burner operation: first half of cycle.

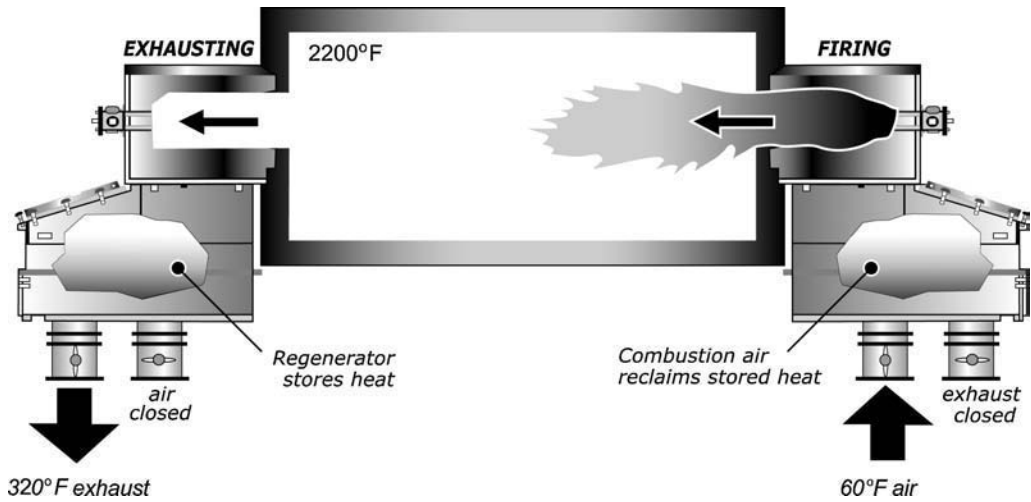


FIGURE 12.7 Regenerative burner operation: second half of cycle.

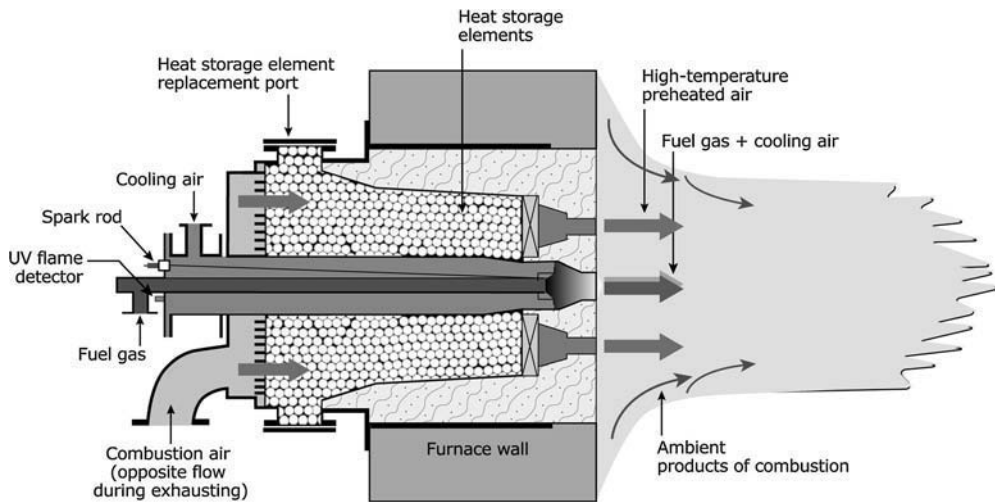


FIGURE 12.8 Cross section of Tokyo Gas FFR burner. (Courtesy of Tokyo Gas Co. Ltd.⁹ With permission.)

Both types exist as direct-fired units, wherein the products of combustion come directly into contact with the work being heated in the fired chamber. The one-box type is also used as a regenerative radiant tube burner, where the products of combustion are separated from the work by a tube that contains the combustion and radiates heat to the furnace workload. This regenerative burner application is covered in another chapter in this book.

The one-box burner design of Tokyo Gas Company⁸ is shown in Figure 12.8. With a range of capacities from 0.5 to 2.5 MMBtu/hr, it can be seen that this unit has the horizontal flow regenerator directly behind the burner tile ports that alternately carry the preheated air to the furnace and the exhaust gas into the regenerator. The ceramic ball regenerator packing is contained and supported at the hot end by a series of perforated SiC discs, and a perforated metal plate at the cold end. The burner's fuel tube passes down the center of the regenerator to the fuel port in the burner tile.

The standard two-box burner design of the author's company is shown in Figure 12.9. With standard capacities ranging from 3.0 to 30 MMBtu/hr, this unit has a high-temperature preheated

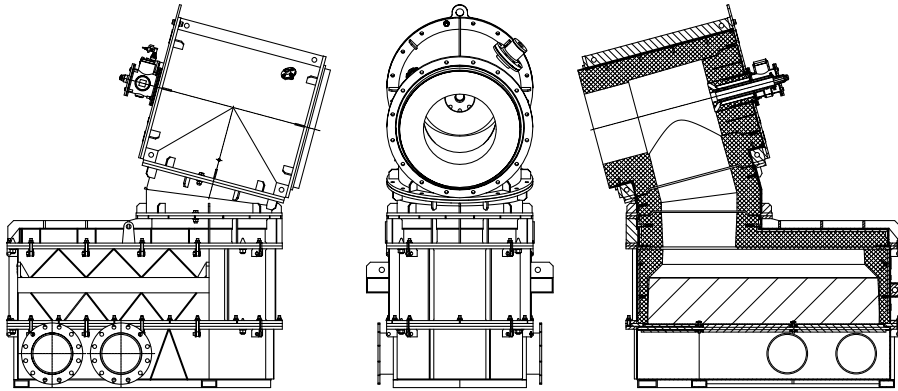


FIGURE 12.9 TwinBed® II (The North American Manufacturing Company, Ltd.) regenerative burner.

air burner connected to a separate refractory-lined regenerator housing containing the ceramic ball regenerator media. It will be appreciated that the vertical flow regenerator needs no containment for the hot end of the packing, merely a support structure for the cold end that will allow even gas flow through the cold face.

The burner head on the example two-box burner is a simple high-temperature insulating refractory-lined unit with no internal obstructions to air or exhaust flow through it, unlike most conventional burners which contain air and gas porting and mixing promotion elements. The necessity of passage of high-temperature exhaust gases through the compact regenerative burner dictates the simplest burner head structure possible. In this case, the fuel tube is mounted on the burner backplate and discharges into the void of the burner body, with mixing and stabilization being achieved by the aerodynamic design of air and gas flows within the burner head.

Both the one-box and two-box burner designs depicted here are provisioned on the burner head for ignition and flame detection devices, as with conventional burners.

At the time of writing, the marketplace for the compact regenerative burner has driven the majority of the development work to be centered on gas firing, for which both the one- and two-box versions are commonly available. With some limitations on their operation over the gas-fired versions, oil-fired systems using the two-box version have been successfully applied.

12.3.5 HEAT TRANSFER MEDIA

The most common type of heat transfer medium used in compact regenerative burners today is alumina balls. With a melting temperature of over 3700°F, alumina provides excellent durability for the high-temperature service it must endure. It is also highly corrosion resistant to the more common contaminants found in industrial furnace exhaust streams. While not normally noted for good thermal shock resistance, it can be appreciated that alumina is suitable for use in compact regenerators when one considers that, despite the fact that typical cycle times from exhausting to air heating are between 20 sec and 3 min, each individual element of the packing only changes its temperature by a small amount during each cycle. Alumina balls used in typical compact regenerators range in size from 3/8 up to 1 in. Although the most common shape today is spherical, alumina can also be used in other shapes, such as nuggets and saddles. For glass applications where alumina will be subject to hot corrosion from contaminants in the exhaust gas, nuggets of zirconia–mullite are successfully used.

The previously described packing materials are purchased in bulk and may be “poured” into a regenerator housing (Figure 12.10) to achieve statistically consistent packing density, thus with statistically consistent thermal and hydraulic characteristics. This placement ability is significant in certain types of applications and is discussed later in this chapter.

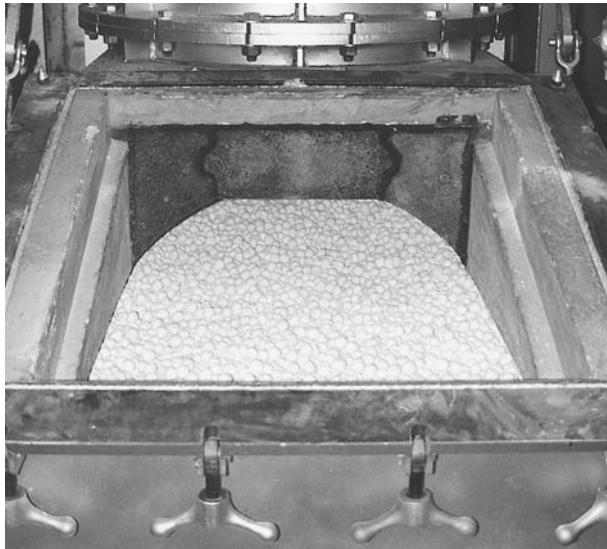


FIGURE 12.10 Open regenerator showing alumina balls.

An alternative approach that has been successfully applied to small input burners in nonfouling exhaust gas streams is to use an engineered packing of high surface-to-mass ratio ceramic components. Examples of such packings are cordierite or SiC honeycomb blocks having very small gas passages separated by very thin ceramic walls. These blocks may be monoliths shaped to fit a particular regenerator box cross section, or a packing may be made up of a series of small blocks placed to ensure that their gas passages are all aligned in the desired direction of flow. For suitable applications, this type of packing has proved itself amenable to the production of very compact, high-performance regenerators, although lacking the flexibility of the “pour to place” packing earlier described.

12.3.6 HEAT TRANSFER CHARACTERISTICS FOR COMPACT REGENERATOR MEDIA

In the convective heat transfer process, the amount of heat transferred from the hot products of combustion to the media, and likewise the heat transferred from the media to the cold combustion air, is directly proportional to the surface area of the media. For this reason, it is desirable to maximize the amount of surface area available for a given volume. When spheres are theoretically nested, regardless of their diameter, they will take up the same volume within the box. (Although the void between smaller diameter balls is smaller, there are more of them, such that the sum of the volume of the voids adds up to the same total volume for all ball diameters.) The void fraction (percent of open volume in the media bed) for balls is 37 to 39%. When comparing the commercially available 3/8-in. diameter balls to 3/4-in. diameter balls, the surface-area-to-volume ratio for the 3/8-in. balls is twice that of the 3/4-in. balls, resulting in more surface area and therefore a potential gain in heat recovery performance. However there are downsides to using smaller balls, the main two being increased pressure drop and a greater potential for plugging. The smaller voids create greater frictional losses, increasing the pressure loss through the media bed. Smaller voids also create more of a filtering effect, increasing the likelihood of trapping particles in applications where the products of combustion contain contaminants. The two common compact regenerative burner applications most likely to have a greater potential for plugging are aluminum melting where fluxing salts are used and glass melting where there are volatiles and particulates in the furnace atmosphere. In these cases, it may be more practical to select a larger-sized medium to reduce the opportunity for plugging.

Similar considerations on the thermal and hydraulic performance, and the potential for fouling, apply to the use of monolithic material structures as regenerator medium. These have very high surface-area-to-mass ratios and thus high heat recovery potential, but typically very small passages for air and waste gas.

12.3.7 THE PERFORMANCE OF COMPACT REGENERATIVE BURNERS

A common method for analyzing and comparing the thermal performance of various heat exchangers is their heat transfer effectiveness e , expressed as:

$$e = \frac{\text{heat_transferred}}{\text{maximum_heat_available_to_be_transferred}}$$

$$= \frac{C_h(t_{h,\text{in}} - t_{h,\text{out}})}{C_{\min}(t_{h,\text{in}} - t_{c,\text{in}})} = \frac{C_c(t_{c,\text{out}} - t_{c,\text{in}})}{C_{\min}(t_{h,\text{in}} - t_{c,\text{in}})} \quad (12.6)$$

where:

- $t_{h,\text{in}}$ and $t_{h,\text{out}}$ are the hot fluid entrance and exit temperatures
- $t_{c,\text{in}}$ and $t_{c,\text{out}}$ are the cold fluid entrance and exit temperatures
- $C_h = (MC_p)_h$ is the hot fluid capacity rate
- $C_c = (MC_p)_c$ is the cold fluid capacity rate

For natural gas combustion products with air, the cold fluid capacity rate has a value of about 79% of the hot fluid capacity rate (mass of air is less, specific heat of air is less, maximum possible air temperature is that of the incoming exhaust gas). Accordingly, there is no benefit to extracting more than approximately 80% of the products of combustion through the regenerators because the air cannot carry more heat away. Extracting more than 80% will only elevate the exhaust gas temperature leaving the regenerator and necessitate higher service duty for downstream components, including increasing the size and power consumption of the exhaust fan. The benefits of limiting the extracted rate to 80% thus include lower exhaust temperatures out of the regenerator, a smaller exhaust fan, and providing smoother furnace pressure control through the use of a dampered direct flue from the fired chamber.

Figure 12.11 shows the effectiveness of regenerative and recuperative systems for heating 60°F combustion air. It can be seen in the figure that a regenerative system is nearly twice as effective as even the best typical recuperative system.

Table 12.1 and Figure 12.12 are taken from a record of a laboratory trial of a pair of regenerative burners operating in a test furnace.

12.4 TYPES OF REGENERATOR FOR COMPACT REGENERATIVE BURNERS

The typical regenerator's entire packing is cycled back and forth between hot and cold gases. Unlike the rotational regenerators addressed in Chapter 12.4.4, these regenerators are operated in physical or logical pairs if the process firing is to be substantially continuous. At any given moment, one regenerator will be heating combustion air and the other will be storing heat being recovered from the waste gas. A combination of valves is used to direct gases in the appropriate manner.

TABLE 12.1
Actual Performance Data from Laboratory Trial

Furnace Temp. (°F)	Available Heat (cold air) (%)	Air Preheat Temp. (average) (°F)	Exhaust Gas Temp. at 90% Bed Extraction (°F)	TwinBed Available Heat (average) (%)	Fuel Saving over Cold Air Operation (%)
1470	57	1220	270	82	30
1830	47	1560	330	79	42
2190	37	1900	370	77	52
2640	23	2280	460	74	69

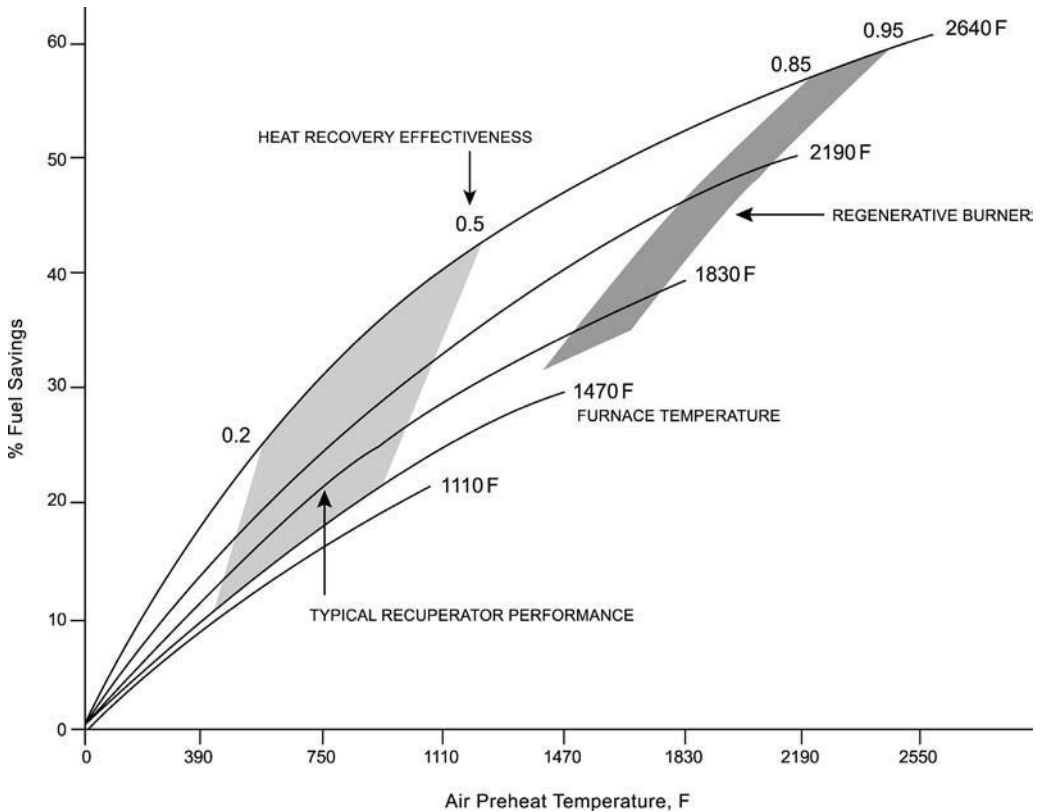


FIGURE 12.11 Comparative performance of regenerative burners and recuperators.

12.4.1 BASIC SHAPES

The most common regenerator shapes adopted for compact regenerative burners are rectangular and cylindrical. Both shapes have their advantages and disadvantages. The simplest to manufacture is the cylindrical regenerator. The necessary refractory lining of the cylindrical regenerator will suffer less natural thermal stresses and, depending on its diameter and lining thickness, less chance of lining collapse because of the natural “keying” of the wall. The cylindrical design will have lower wall heat losses than a rectangular version of the same area, because it has a lower wall-surface-to-regenerator-area ratio and does not have “corner losses.” The reduced perimeter also provides for less “bypass loss” from the edge effect of the increased voidage where packing rests

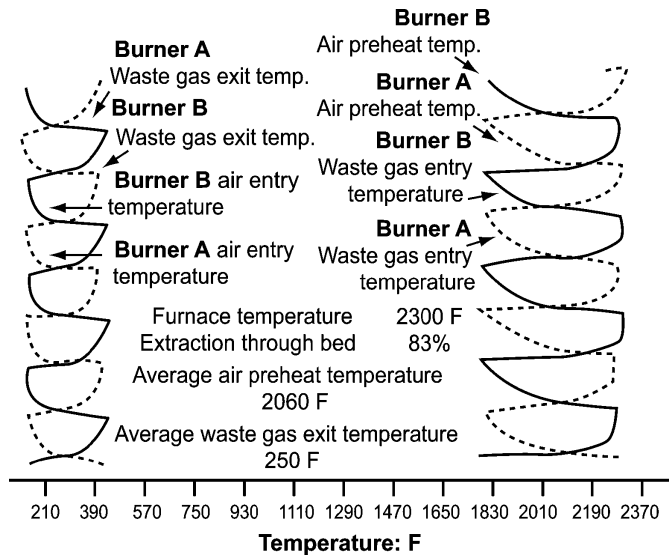


FIGURE 12.12 Combustion air and exhaust gas temperatures measured during laboratory trial.



FIGURE 12.13 An aluminum melter's cassette regenerator being removed by forklift truck.

against a plane wall. The primary advantage of a square or rectangular regenerator is that of efficient use of real estate. The aspect ratio can be easily changed to accommodate available space.

12.4.2 REGENERATORS WITH REMOVABLE PACKING

In applications such as aluminum and glass melting, fouling of the regenerator packing is common. In the aluminum application, for example, fluxing salts will enter the regenerator in the form of a vapor, condense/sublime as they pass through the cold media bed, and deposit on the media surface. Because the rate of accumulation is strongly temperature dependent, the deposition is typically over a particular stratum in the height of the packing, forming a hardened layer that is sometimes difficult to break.

In such cases where frequent cleaning of the media is required, the regenerator can be designed for fast removal and replacement of the packing, or in "cassette" form such that the media section of the regenerator can be quickly removed and replaced, as is shown in Figure 12.13. Spare cassettes can be preloaded with clean media, allowing for a quick exchange as shown in Figure 12.14. As with

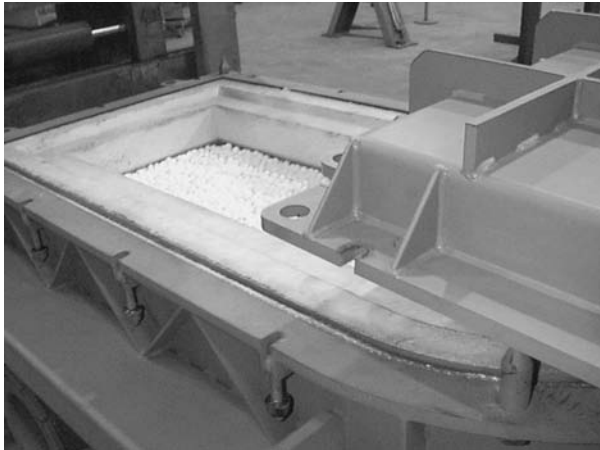


FIGURE 12.14 Putting a fresh media cassette in place.

all regenerative burners, media changes should be performed at the same time for both burners of a pair in order to maintain balanced performance.

Appropriate choice of media form for dirty applications will allow the fouled media to be cleaned and reused. Alumina balls, for example, can be cleaned by methods such as tumbling or high-pressure washing.

12.4.3 REMOTE REGENERATORS

Although the typical compact regenerative burner uses a close-coupled regenerator, if space is restricted, the regenerator can be remotely mounted from its associated burner. Considerations in these instances include allowance for the thermal expansion of the hot duct carrying the exhaust and air back and forth between the regenerator and burner. Appropriate timings of the reversal control system to ensure purging on switching from exhausting to firing modes are also required to compensate for the increased swept volume. [Figure 12.15](#) shows remote regenerators mounted on the roof of a steel reheat furnace. Five other such burner and regenerator combinations are located on the opposite side of the furnace.

12.4.4 ROTARY REGENERATORS

First conceived in the 1930s, the rotary regenerator (often called a “heat wheel;” [Figure 12.16](#)) consists of a cylindrical drum packed with heat storage media in such a way that gases can flow parallel to the axis, but divided (commonly into segments) such that they cannot flow circumferentially. The drum is rotated on its axis between two stationary sections. Each stationary section has two chambers, sealed from each other by sealing surfaces close to the surface of the drum. Exhaust gases enter and leave from the corresponding chambers at each end of the drum, and combustion air through the other pair of corresponding chambers. The rotation of the drum between the stationary sections continuously presents “cold” and “hot” segments of the media in the drum to the air and waste gas streams. The exhaust gas flows through a cold section and preheats the media. That hot section then proceeds into the air path where it preheats the air as the media is cooled. This process occurs without the need for interruption of the air and gas flows, as occurs with the fixed regenerator system, and thus, the burner system can fire continuously.

Heat wheels of metallic construction are in common use in boilers and the process industries with low-temperature waste gas streams.¹⁰ In the late 1970s and early 1980s, newly developed ceramic materials and fabrication techniques allowed monolithic wheels to be made of cordierite and silicon

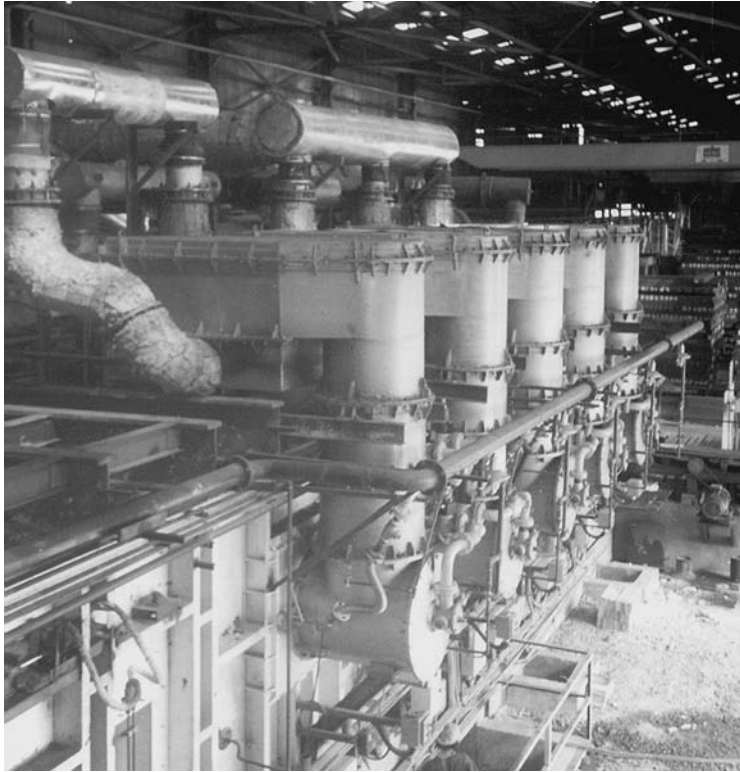


FIGURE 12.15 Remote regenerators on the roof of a steel reheat furnace.

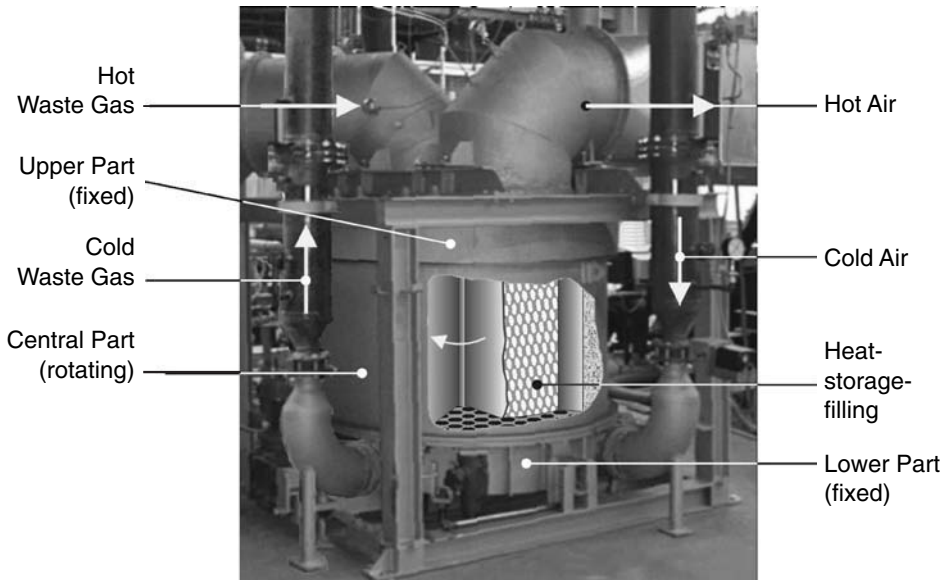


FIGURE 12.16 The EcoReg[®] (Jasper GmbH) rotary regenerator. (Courtesy of Jasper GmbH.¹¹ With permission.)

carbide and tested in higher temperature industrial applications. However, in addition to material shortcomings leading to short life of the wheel structure, they developed a reputation for excessive seal leakage between the air and waste gas chambers, and their use was substantially abandoned.

In the late 1980s and through the 1990s, development of these devices continued in Europe and Japan. In Europe, there are systems operating with exhaust gas temperatures as high as 2800°F, preheating air up to some 90% of the temperature of the inlet waste gas.¹¹ These latest practical manifestations of the high-temperature heat wheel use packings similar to those previously described for the conventional compact regenerators. They have sealing technologies capable of sustainable practical performance at pressure differences between combustion air and exhaust gas suitable for industrial combustion applications, although with lower hot combustion air pressures that require the use of larger insulated burner structures than the fixed regenerator technology. They have been successfully applied to such applications as clean aluminum melting and steel billet reheating furnaces.

12.5 CONTROLS FOR REGENERATIVE BURNERS

Of all industrial burner controls, in these authors' experience none is more challenging than the control required for regenerative burners. In addition to the safety and fuel/air ratio requirements of conventional industrial burners, the control system must deal with burners switching from being a "burner" to being a "flue" as often as twice a minute.

In the firing periods between switching events, both the firing and exhausting regenerators' temperature profiles change. As the temperatures are changing, the regenerators' flow resistances (flow with respect to pressure drop) are changing. The control system needs to be able to correct the fuel/air ratio and maintain a balance between the firing rate and the exhaust extracted (control the furnace pressure) throughout the reversing regenerative cycle.

Most compact regenerative burner systems fire into a chamber having a conventional flue. That flue can be sized for that part of the exhaust gases from which heat cannot be recovered (see Chapter 12.5.7), or it can be sized to accept the exhaust gases of one or more of the burners firing in a "direct" (nonreversing) mode. This flue will have a damper of some type that needs to be controlled as part of the furnace pressure control loop.

Maintaining control of all of these variables to simultaneously optimize efficiency, in-furnace conditions, and emissions is a complex control problem. The following sections identify control system requirements peculiar to regenerative burner systems when compared with conventional burner systems in industrial practice.

12.5.1 SAFETY SYSTEMS

Regenerative burner systems must meet the same insurance and regulatory standards for safety and flame monitoring as a conventional burner applied to the same process. In general, the furnace temperature, combustion air, and main fuel limits are handled in the same way as with any non-regenerative system. The system's main safety shutoff valving is also the same as that for conventional burners. Most regulatory standards do not allow the function of individual burner fuel safety shutoff valves to be combined with that of the regenerative system's fuel reversal valving, requiring additional valves for this purpose.

The requirements for fuel reversal valving and flame monitoring are discussed later in this chapter. Figure 12.17 shows a typical schematic of a single pair regenerative control system.

12.5.2 EXHAUST FAN PROVING

Most regenerative systems require an exhaust fan to pull the products of combustion through the regenerators. The operation of that fan requires proving. This can be accomplished with a pressure (suction) switch connected to the exhaust header between the exhaust fan inlet and any exhaust

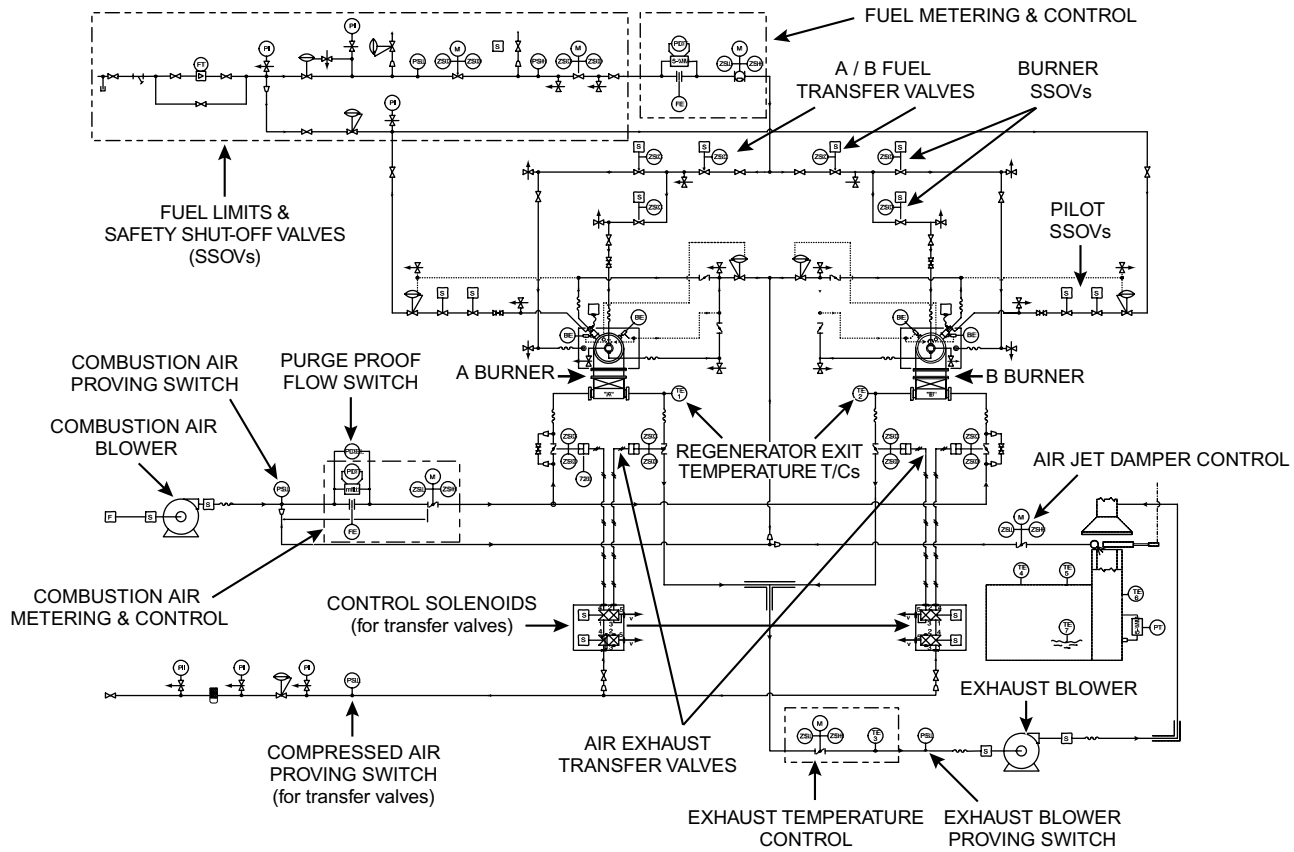


FIGURE 12.17 Typical single pair control schematic.

flow control or regenerator switching valve. As with other critical fans, most regulatory agencies also require that there be a contact from the fan motor starter in the checked limit string.

Some regenerative burner applications provide the ability to fire the burners “direct” as conventional cold air burners, either for process reasons or to maintain operation if there is a failure of the exhaust system. In such cases, the implications of the direct vs. conventional cycling regenerative modes need to be considered in the design of the limits and purge circuitry.

12.5.3 PRE-PURGE

When considering the issue of purging, it is important to remember that you are purging two different flow paths: one through the regenerators and their associated exhaust system and fan, and one through a conventional flue from the furnace chamber. For safety, both paths must be adequately purged of potentially combustible gases. In most applications, purging can be accomplished in the cycling regenerative mode as long as continuous airflow is proven. The purge air will exit via both the regenerative burner exhaust system and the conventional flue from the furnace chamber. If the direct mode is chosen for process reasons, special consideration will be needed to ensure purging of the regenerative burner exhaust system. If the exhaust fan is on during a direct-mode purge, the typical leakage past the air and exhaust cycle valves will pull some air through the exhaust system, requiring only a purge of sufficient duration to ensure no combustible gases remain in the exhaust system.

12.5.4 AIR/FUEL RATIO

From an efficiency standpoint, running a regenerative system with excess air is not as detrimental to efficiency as it is with a cold-air combustion system — the excess air is preheated close to the process temperature. Excess air (O_2) is, however, detrimental to achieving low NO_x generation and to product quality in many processes, so it is generally minimized.

The fuel/air ratio system must use airflow, rather than pressure, as its reference base because the regenerators’ resistance to flow changes with temperature and/or fouling. Ratio control is typically performed on a physical or logical “per pair,” rather than zone (multiple pair) basis to better compensate for the changing resistance of the regenerators. Ratio control on a per-burner basis can be advantageous in some situations — to eliminate long piping runs on large furnaces, for example.

Because most systems meter the combustion air flow at ambient temperature, thus requiring no temperature compensation, regulator-based mass flow ratio systems may be adequate for some applications using small-capacity burners. However, given the limited capacity of suitable regulators and the greater flexibility and accuracy of fully metered air and fuel flow systems, the latter are the control systems of choice for the high heat input capability of most applications using regenerative burners.

12.5.5 FLOW MEASUREMENT AND CONTROL

During the transition of a burner from firing to fluing, there are step changes in flows of air, exhaust, and fuel. The resistance of the regenerators of a physical or logical burner pairing will be different, depending on their respective temperatures and fouling levels. It is important that the flow measuring system be able to quickly determine the flows, and that the flow control system’s components be able to quickly position themselves to control the newly determined required flow after the step change.

12.5.6 RATIO CONTROL SPECIAL FUNCTIONS

Logic to limit air or exhaust flow may be required to prevent overfiring the burners or overloading the blowers when the regenerators are cold and thus at their highest-flow-for-lowest-pressure-drop condition.

Electronic ratio systems can incorporate a function to hold the flow control valve actuators during reversal, and for a short duration after reversal, until the flows stabilize. The duration of such holds will depend on the specific system's response to step changes in flow.

12.5.7 FURNACE PRESSURE AND REGENERATOR EXHAUST

No control function associated with regenerative burners has more influence on the ultimate efficiency of the system than that which determines the balance of the exhaust flow between the regenerators and the hot flue. Typically, a combination of one exhaust control loop per pair of burners and one furnace pressure control loop is used.

Systems with a direct-firing capability require a high turndown or multi-stage damper system. The hot flue of a regenerative furnace needs to be able to controllably handle as little as less than 20% of the POC from one burner in a pair firing at turndown, to as high as 100% of the POC of the full-design firing rate of all the burners in the system allowed to fire simultaneously. A form of split range output function should be used in the furnace pressure control loop. Figure 12.19 shows a flue that utilizes both a "hard" damper and an auxiliary air jet damper. Increased flow from the air jet acts to form a curtain across the opening, adding resistance to fluing gases. The air jet has two advantages: (1) it has the ability to "fine-tune" the flue dampening and (2) it is more forgiving of sudden pressure spikes. The jet and damper combination should be designed such that the curtain of air covers all open areas created when the damper opens. A jet damper will work best when used in conjunction with a sliding damper as shown in the Figure 12.18.

The first action to increase furnace pressure (decrease flue area) should be to close the auxiliary (hot) flue damper and increase the air jet flow (if one is used). Once it is at or near its minimum open (fluing) position, the control action should be to decrease the regenerator exhaust flow (also decreasing the total effective flue area). If the regenerative burner exhaust system can be allowed to satisfy its needs without regard to the furnace pressure, the exhaust fan is likely to pull the furnace chamber negative. This will draw cold air through any crack or opening, possibly even reversing the flow in the hot flue, with corresponding influence on the fuel/air ratio and the system efficiency. Figure 12.19 expresses the logic used to maintain furnace pressure control.

During regenerator reversals, the furnace pressure transmitter will experience a rapid decrease in pressure as a firing burner stops firing, followed by a pressure spike as the new burner starts to fire. The magnitude of these spikes will be influenced by that proportion of the total input represented by the firing rate of the reversing burners. The exhaust system will not be able to respond to this pressure spike, nor should it be allowed to try to do so. The furnace pressure controller should have an input averaging feature to minimize the effects of such spikes on its control output.

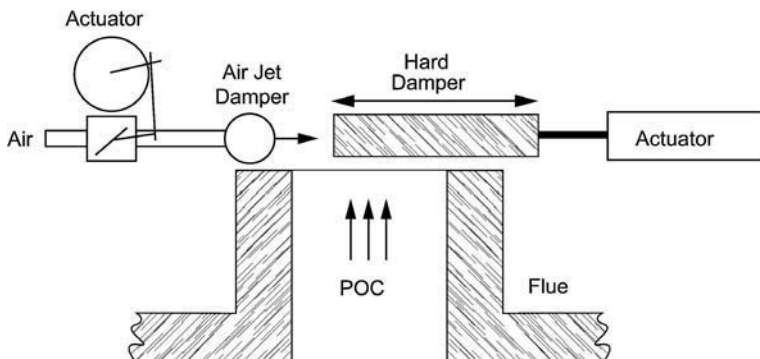


FIGURE 12.18 Two-stage flue damper for a regenerative burner system.

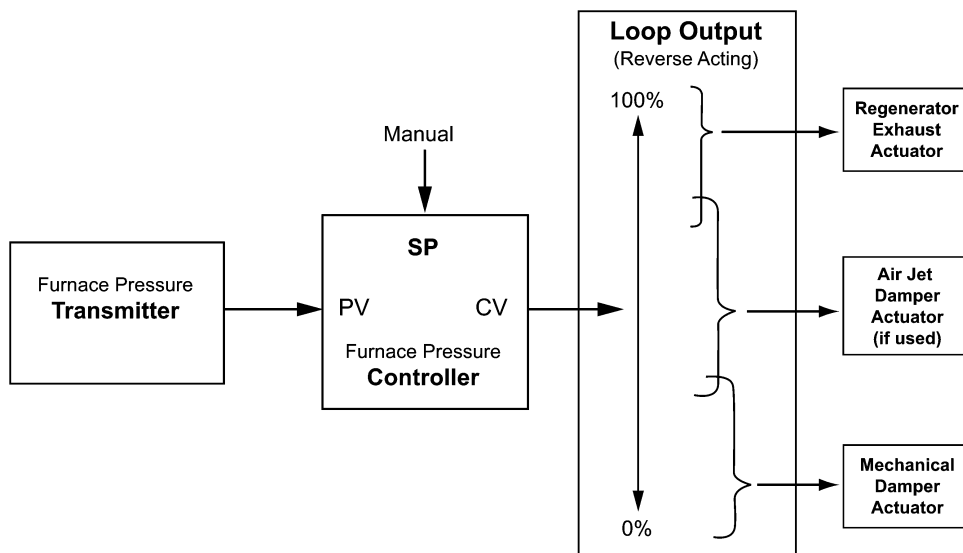


FIGURE 12.19 Regenerative burner furnace pressure control logic.

12.5.8 REGENERATOR SYSTEM REVERSALS

Regenerator reversals can be based on time, on exhaust temperature, or on a combination of both time and temperature.

Time-based systems work well for processes that are relatively steady-state — each burner in a pair fires and exhausts on a constant predetermined time base with each burner firing and exhausting for the same amount of time.

In temperature-based systems, the time one burner of a pair fires while the other burner is exhausting is determined by the temperature of the exhaust of the exhausting regenerator.

Time-and temperature-based systems switch at a predetermined exhaust temperature within a minimum and maximum exhaust time window, as shown in [Figure 12.20](#).

The optimal times and temperatures are determined based on regenerator efficiency, process temperature, and flow through the regenerator. Additionally, the optimal temperature setting varies with sensor location and response time.

To minimize the furnace pressure spike during reversals, multi-pair systems can incorporate anti-coincidence logic to prevent more than one pair from reversing simultaneously.

12.5.9 REVERSING VALVE TYPES AND OPERATION

Listed and approved high-duty cycle safety shutoff valves are used to interrupt the flow path of the fuel to the burners. Each burner will have one or more of these valves based on local codes, insurance underwriter requirements, and regulatory standards. In general, the valves used for fuel reversal control cannot do double-duty as the burners' safety shutoff valves even if they are listed as safety shutoff valves.

Many of the early compact regenerative burner systems used a single actuator and a multi-port five-port spool valve to switch the air and exhaust flow paths for a pair of burners. In one position, it closed the exhaust flow and opened combustion airflow to the first burner in the pair as it opened the exhaust and closed the air to the second burner. The combustion air and exhaust flow paths could not get out of synchronization. It had the disadvantage that it would neither permit the burners to fire in the nonregenerative mode required by some processes, nor would it simultaneously shut off the air and exhaust flows of all the burners.

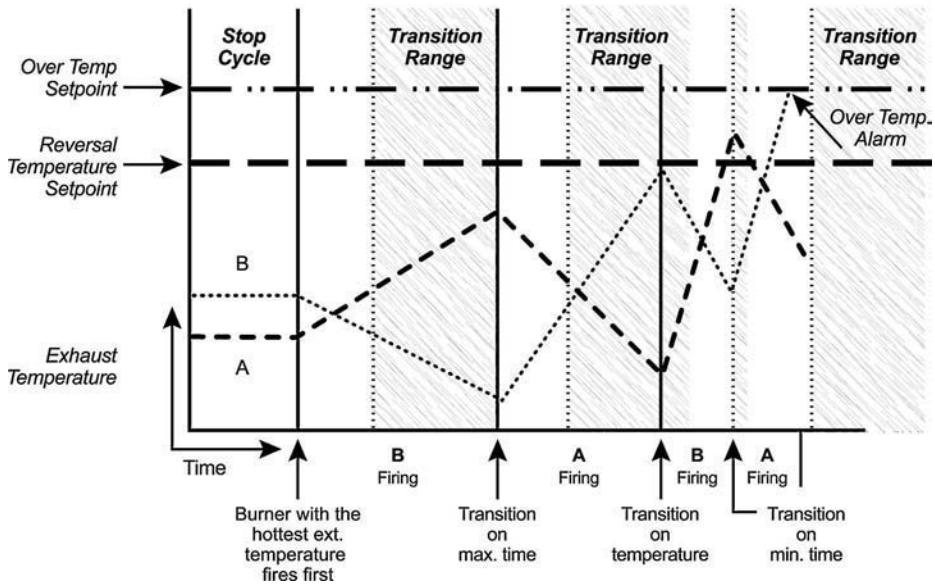


FIGURE 12.20 Combination time and temperature reversing sequence.

Most direct-fired (nonradiant tube) regenerative burner systems today use four valves per pair for the air and exhaust switching function. Each regenerator has a valve and actuator combination for each of the air and for the exhaust. This arrangement allows each burner in a pair to operate independently if required. A pair can be operated with one burner on, both on, or both off, in addition to running in the conventional reversing regenerative mode.

A burner firing as a cold air burner (i.e., firing in “direct mode”) can be used to continue heating the process in the event the other burner in the pair is inoperable or the exhaust system is down. Direct mode is commonly used, by design, at certain points in the normal operation of some heating processes; for example, in aluminum melters at times when they are producing particularly “dirty” flue products that could very rapidly plug the regenerators.

If a regenerator becomes plugged, a system with direct-mode capability will allow it to be cleaned or changed with the other burner in the pair still firing on cold air to maintain production.

Direct-mode firing of both burners in a pair can be used to “boost” the fuel input of a system during the early, cool stages of some batch processes to allow for faster building of a required heat head in the fired chamber.

Both burners off, all reversing valves closed, is used as a standard control mode to extend system input turndown, particularly for batch processes. Some systems that can benefit from the effect of high rates of POC recirculation in the fired chamber are operated in this essentially on/off mode, with pulse-width modulated input control superimposed upon the reversing controls.

12.5.10 REVERSAL VALVES SEQUENCING

When in the regenerative mode, most control systems sequence the simultaneous actuation of the air and exhaust reversing valves for each pair. Air is opened to one burner as it is closed to the other. At the same time, exhaust is closed to one as it is opened to the other. The fuel reversing valves are generally closed prior to the air and exhaust valve movement to provide a short, “post purge” of the firing burner. The fuel reversing valves are generally opened after the air and exhaust valves’ new positions are confirmed, providing safe operation and sufficient time for the airflow to pre-purge the regenerator on the burner about to be fired.

12.5.11 CONFIRMATION OF REVERSAL VALVE OPERATION

The control system should check the operation of all air, exhaust, and fuel valves used for reversing control to ensure they are in the proper position for the firing mode of the burner that they supply. This requires the air and exhaust valves to have position switches to indicate both the open and closed positions. The fuel valves require a switch to prove the closed position.

When a burner is to be firing, its air valve should be proven open and its exhaust valve proven closed. If the exhaust valve is not closed, some or all of the combustion air that is being metered by the fuel/air ratio control will bypass the regenerator directly to the exhaust system, causing the burner to be fuel-rich.

When a burner is to be exhausting, its exhaust valve should be proven open and its air and fuel valves closed. If the air valve is not closed, a portion of the combustion air that is being metered by the fuel/air ratio control will bypass the firing burner, causing the firing burner to be fuel-rich.

12.5.12 FLAME SUPERVISION AND REVERSALS

Note: This section is not intended to act as a specific guide to the use of flame supervision systems for regenerative or any other burners. The reader is referred to the applicable international, national, local, and insurance industry codes, standards, requirements, etc. for appropriate information on this subject.

Flame monitoring and the reversal sequence are handled in a variety of ways, depending on the design of the specific burner and the local code requirements. In the authors' company case, each burner of a pair has two UV flame detectors. One detector monitors the pilot and a separate detector monitors the main flame. The detector mounting locations are such that the main flame detector cannot sight the pilot flame under any conditions. The pilot is burning in all modes when its burner has permission to be fired. When a burner is actually to be firing, the flame detector for the main flame is active and the pilot detector is switched out of the monitoring circuit. Loss of the main flame will shut down the burner. When a burner is acting as the exhaust, the flame detector for the pilot is switched back into the monitoring circuit. Loss of the pilot flame while exhausting shuts down the burner. Loss of either flame as described requires resetting the flame monitoring system and restarting the burner in the same manner as with nonregenerative burners.

12.6 EMISSIONS

The primary products of combustion are carbon dioxide (CO_2), water vapor (H_2O), oxygen (O_2), and nitrogen (N_2). CO_2 reduction is being pursued in many countries because, although not harmful to human health, CO_2 is considered the most significant "greenhouse gas" due its abundance in the lower atmosphere. Trace species that are harmful pollutants include nitric oxide (NO), nitrogen dioxide (NO_2), carbon monoxide (CO), sulfur dioxide (SO_2), and particulates.¹² This discussion includes NO and NO_2 — collectively referred to as NO_x — and CO_2 as those most directly involved with use of regenerative burners. SO_2 is not discussed here, because it is most directly related to the use of heavy fuel oil, a fuel used by only a very small number of the world's regenerative burner installations.

12.6.1 CO_2 EMISSIONS

To deal with the easiest pollutant emission subject first, as stated above — CO_2 is considered the most significant "greenhouse gas" although it is not harmful to human health. The use of regenerative burners is extremely helpful in reducing CO_2 emissions. The amount of CO_2 produced is directly related to the amount of fuel burned in a process. The energy saved by the application of a regenerative burner system will produce a commensurate reduction in the amount of CO_2 emitted into the atmosphere. Given the significant energy reductions available from the use of regenerative burners in high-temperature processes, they may be regarded as a significant "green" product in the reduction of CO_2 .

12.6.2 NO_x EMISSIONS

When fossil fuels are burned using air as the oxidant source, virtually all the nitrogen contained in the air (approximately 79% by volume) goes through the process as an inert. However, under the extremely high temperatures experienced during combustion, a relatively small portion of nitrogen reacts with oxygen to form NO and NO₂. The very highly preheated air of a regenerative burner results in high peak flame temperatures and leads to potentially high NO_x emissions.¹²

12.6.3 NO_x REDUCTION METHODS FOR REGENERATIVE BURNERS

To reduce the primary cause of NO_x emissions with regenerative burners — the high peak flame temperatures — NO_x reduction methods employ various techniques to reduce the reaction rate between the fuel and the highly preheated air, and/or reduce its temperature.

Flue gas recirculation (FGR) is a common and fairly simple method of NO_x reduction. FGR is the process of returning a portion of the POC to the combustion zone, most commonly done by mixing with the combustion air supply to the burner. Other means of introducing POC are to mix with the fuel, add directly to the burner through a separate connection, or to use self-recirculated FGR where the energy in the flame front itself induces POC into the combustion zone. All methods using FGR, except the last one mentioned, have potential costs, such as additional piping, increased burner size, larger blowers to handle the extra volume or possibly an additional blower to transport the FGR, increased maintenance, and reduced efficiency. The quality of the FGR is also important; it should be of the lowest feasible oxygen content and, for systems using external piping and components, as clean as possible to prevent problems such as fouling and corrosion. Condensation of water is also possible if the FGR becomes cold.

Regenerative burners might be considered ideal candidates for the application of FGR for NO_x reduction. The exhaust gas at the outlet of the regenerators is cool FGR. The cool FGR available at the outlet of the exhaust fan can be led back to the burner, possibly via an additional FGR blower, and mixed with the combustion air. It can be mixed with the air at the inlet to the regenerator, likely requiring an increase in regenerator size to handle the increased volume without an excessive pressure requirement. In this case, however, all the FGR is heated as it passes through the regenerator with the combustion air and will thus place only a minimal system efficiency penalty on the use of FGR. Alternatively, the cool FGR can be fed directly to the hot air stream entering the burner. In this case, there will be no effect on the performance or the required size of the regenerator, but the cool FGR will have to be heated to furnace temperature, resulting in a larger loss in efficiency. A further means of introducing FGR is to mix it with the fuel entering the burner. This is an effective means of using FGR, requiring less FGR per unit NO_x reduction than addition to the air.

Air staging and fuel staging are other common methods of reducing NO_x emissions. Staging is performed by splitting one of the reactants — either the air or the fuel — into two or more separate streams. Part of one of the reactants is mixed and combusted with all of the other reactants in a primary zone. The remainder of the split reactant is then introduced downstream of the primary zone. The use of these methods requires complex burner structures to keep the various flows separated. Such structures may not be favored in the construction of regenerative burners that operate with very highly preheated air and must also be capable of handling the full-temperature exhaust gases from the furnace.

The NO_x reduction technique used with the regenerative burners of the authors' company is a dilute gas combustion scheme called "fuel direct injection" (FDI).¹³⁻¹⁵ It was developed by Tokyo Gas Co. in the late 1980s.

As the exclusive licensee, the authors' company has developed and widely applied low-NO_x regenerative burners based on this technology. Known as the Low-NO_x Injection (LNI) technique, it has been used in the aluminum, steel, and glass industries and has demonstrated outstanding low-NO_x performance.¹⁶ An LNI-equipped regenerative burner operates as a conventional nozzle-mixing regenerative burner when the furnace temperature is below 1450°F. Above 1450°F, fuel is switched

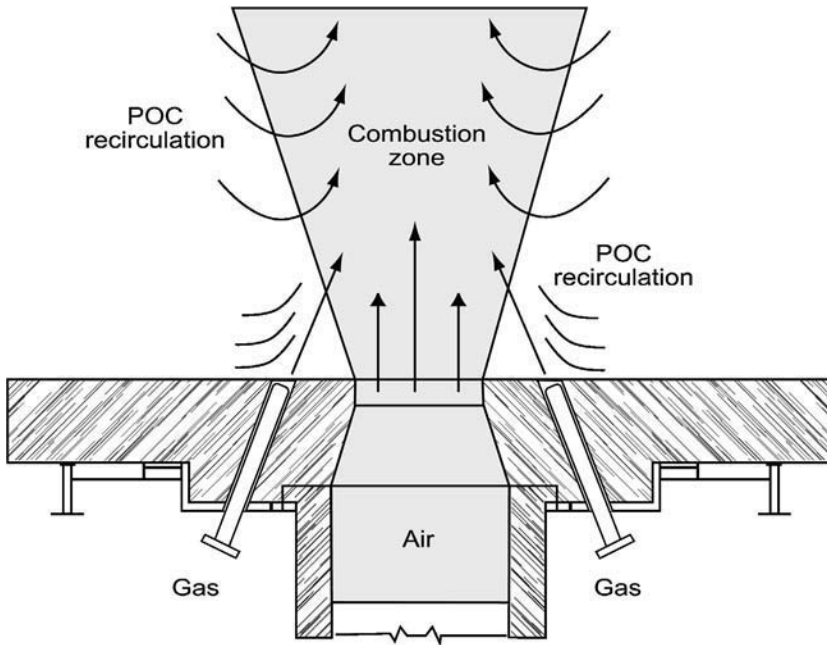


FIGURE 12.21 LNI burner arrangement.

to one or more strategically positioned nozzles adjacent to the burner tile port. These injectors are displaced from the burner tile exit inside the furnace (Figure 12.21). Fuel and preheated air streams mix thoroughly with furnace gases, becoming extremely dilute before combining in front of the burner tile. The dilute gas streams auto-ignite and achieve complete combustion within the furnace environment. In the flame envelope, entrained gases limit maximum in-flame combustion temperatures that generate high NO_x emissions.

The low NO_x emissions realized using the LNI technique are displayed in Figure 12.22, where NO_x emissions are presented for a conventionally fired nozzle-mix regenerative burner vs. LNI firing, for natural gas and fuel oil.

12.7 SOME REGENERATIVE BURNER APPLICATIONS

12.7.1 WELL-CHARGED ALUMINUM MELTER

This furnace was converted from conventional cold-air burners to regenerative burners using LNI technology with the aim of reducing the specific fuel consumption and at the same time providing the low emissions mandated for the Los Angeles area.

Originally fired with 41 MMBtu/hr through three high-velocity burners, the new installation comprised one pair of regenerative burners with an input capacity of 25 MMBtu/hr. A plan view of the furnace is shown in Figure 12.23.

With an operating roof temperature setpoint of 2075°F and a bath setpoint temperature of 1350°F, the target melt rate was 12500 lb/hr with a charge of 70% continuously fed used beverage cans, 30% sow and coil. The target-specific fuel consumption was 1050 Btu/lb of aluminum, and NO_x emissions of 58 ppm, corrected to 3% oxygen. The required average air preheat level for the regenerative burners in this installation would be above 1590°F in order to attain the desired melt rate and commensurate fuel input rate.

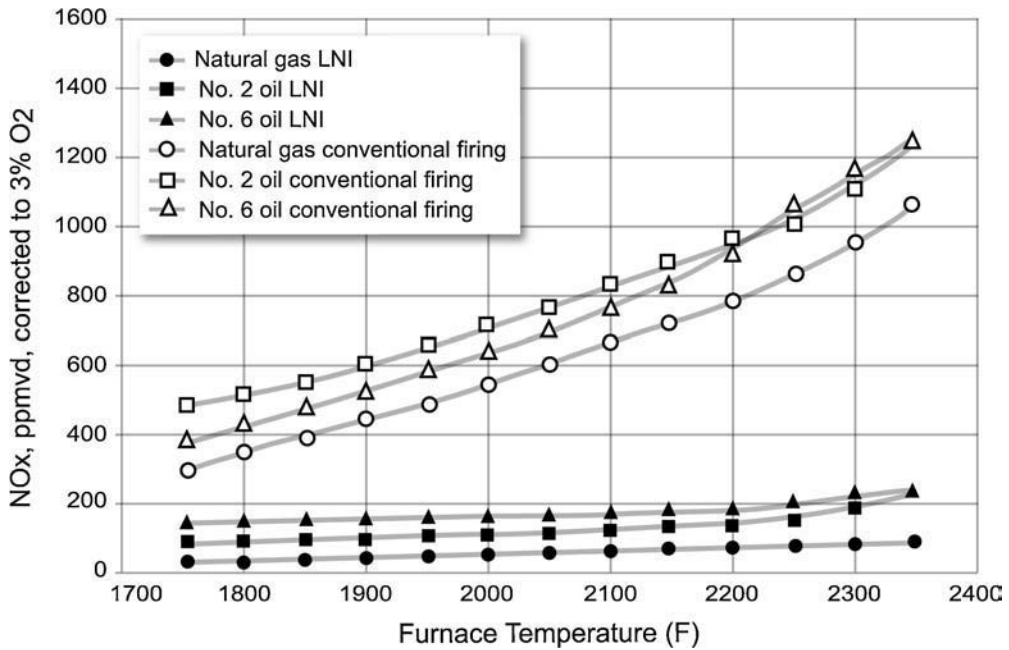


FIGURE 12.22 LNI regenerative burner NO_x performance.

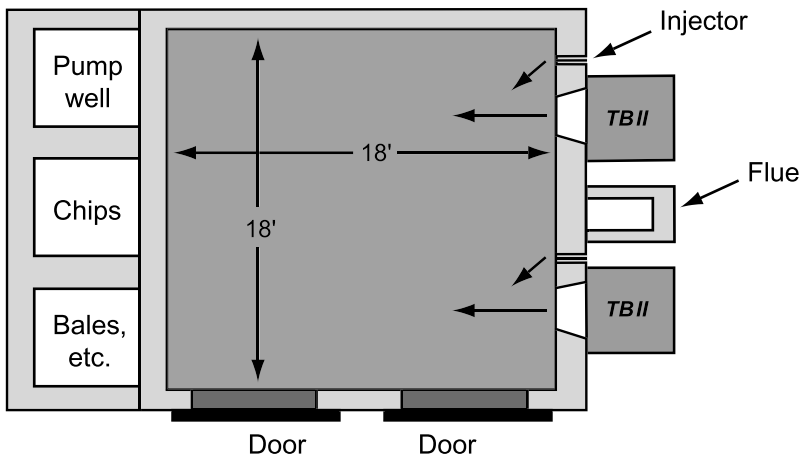


FIGURE 12.23 Plan view of well-charged aluminum melting furnace.

NO_x and specific fuel consumption targets were both met with this arrangement, and a successful compliance test completed. Table 12.2 shows a side-by-side comparison of before and after the conversion to the regenerative system.

12.7.2 DIRECT-CHARGED ALUMINUM MELTER

The furnace shown in Figure 12.24 is a direct-charged rectangular tilting aluminum melter with a capacity of 66,150 lb and a melt rate of 22,050 lb/hr. The unit is charged with 70% extrusion scrap and 30% ingot. The basic internal furnace dimensions are 24.7 ft wide × 16.9 ft deep × 5.4 ft from top of bath to roof.

TABLE 12.2
Before and After Comparison of Regenerative Conversion

Parameter	Cold Air System	Regenerative System
Combustion air temperature	Ambient	1620°F average
Available heat	41%	71%
Specific fuel consumption	1960 Btu/lb	1050 Btu/lb
NOx emissions	60 ppmvd @ 3% O ₂	58 ppmvd @ 3% O ₂
NOx emissions per ton aluminum	0.28 lb	0.15 lb
CO ₂ emissions per ton aluminum	494 lb	265 lb

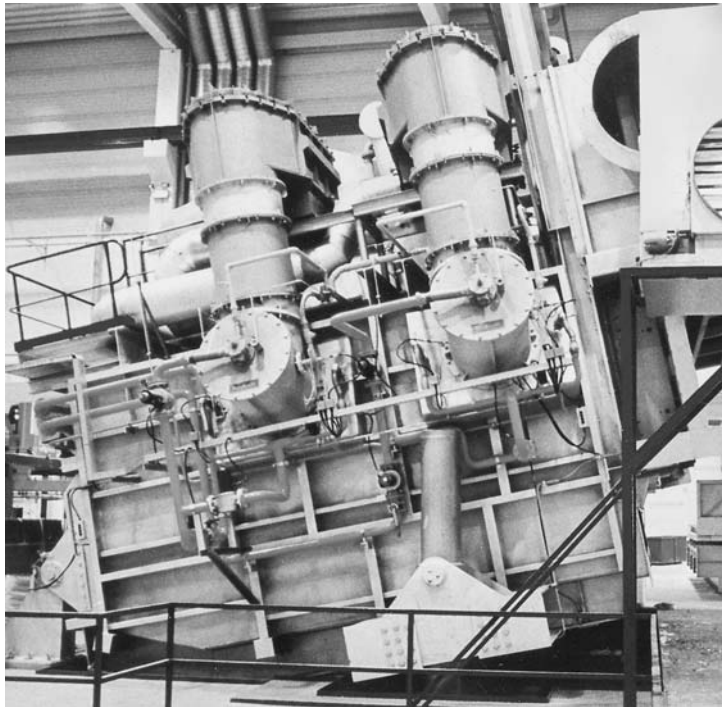


FIGURE 12.24 Tilting aluminum melter.

The furnace is fired with two pairs of regenerative burners, one pair mounted on each 17-ft wall, with burners angled downward to the bath surface at 15°. Each burner pair is rated at a capacity of 13 MMBtu/hr.

The nominal furnace operating temperature is 1700°F and the specified NOx target was a generous 225 ppm, corrected to 3% oxygen. The actual emissions performance was measured at 55 ppm NOx, with 51 ppm CO (both corrected to 3% oxygen).

Table 12.3 shows comparative data from three similar furnaces by the same manufacturer:¹⁷ one cold air, one low-NOx recuperative with 750°F preheated combustion air, and the subject regenerative furnace (average, 1395°F preheated combustion air). It can be seen from Table 12.3 that furnaces equipped with low-NOx regenerative burners can produce NOx levels similar to ambient air burners.

TABLE 12.3
Comparative Emissions Data for Three Similar Aluminum Melters

Burner Type	Flue Gas Temp. (°F)	NOx (ppmv @ 3% O ₂)	CO (ppmv @ 3% O ₂)
Cold Air	1670	66	401
Recuperative	1650	143	401
Regenerative	1680	55	51

TABLE 12.4
Efficiency and Emissions Data Summary for Three Similar Aluminum Melters

Burner Type	Energy Consumption (Btu/lb of aluminum)	NOx (lb NOx/ton of aluminum melted)
Cold Air	1305	0.2
Recuperative	1045	0.36
Regenerative	835	0.11

However, the energy efficiency of the ambient air burner system is low compared with the regenerative system. To compensate for this, more fuel is consumed but still producing the same volumetric value of NOx. When the amount of NOx generated per pound of aluminum melted is computed, it can be seen that the regenerative system, even with its high-temperature combustion air, produces less NOx for the operation of the furnace. The results are tabulated in [Table 12.4](#).

12.7.3 STEEL REHEAT FURNACE APPLICATIONS

Steel reheat furnaces can be an excellent platform for regenerative burners as they operate at high temperatures and allow the opportunity to achieve substantial fuel savings.

The highly effective heat exchange capability (low final exhaust temperatures) of regenerative burners allows them to be located right up to the charge door of a pre-heat zone, eliminating the traditional unfired section and thus saving construction cost in a new furnace designed for their use. An existing furnace can have regenerative burners added in its unfired front section to increase production capability without suffering any significant decrease in efficiency, and sometimes even allowing a slight gain.

12.7.3.1 New Reheat Furnace Designed for Regenerative Firing

The four-zone steel reheat furnace shown in [Figure 12.25](#) and [Figure 12.26](#) was specifically designed to be fired using regenerative burners. Furnace heating curves were developed to calculate the overall length of 52.5 ft and width of 28 ft, and to determine the zone lengths and heat inputs. The Top and Bottom Preheat zones are each fired with a design input of 57.6 MMBtu/hr. The Top fired Heat zone has a design input of 18 MMBtu/hr and the soak zone 16 MMBtu/hr. The furnace that it replaced had a specific fuel consumption of 2.11 MMBtu/ton. The regenerative furnace operates at an average of 1.15 MMBtu/ton. A fuel efficiency of 78% was been achieved heating 121 tons/hr to a temperature of 2150°F with a uniformity of $\pm 25^\circ\text{F}$.

12.7.3.2 Addition of Booster Zone to Existing Furnace

As previously mentioned, regenerative burners can be added to existing furnaces to increase production. The walking beam furnace shown in [Figure 12.27](#) was purchased for a production rate of 73 tons/hr of 4.5 in. \times 4.5 in. \times 24 ft long billets using hot-air flat-flame burners. The objective of

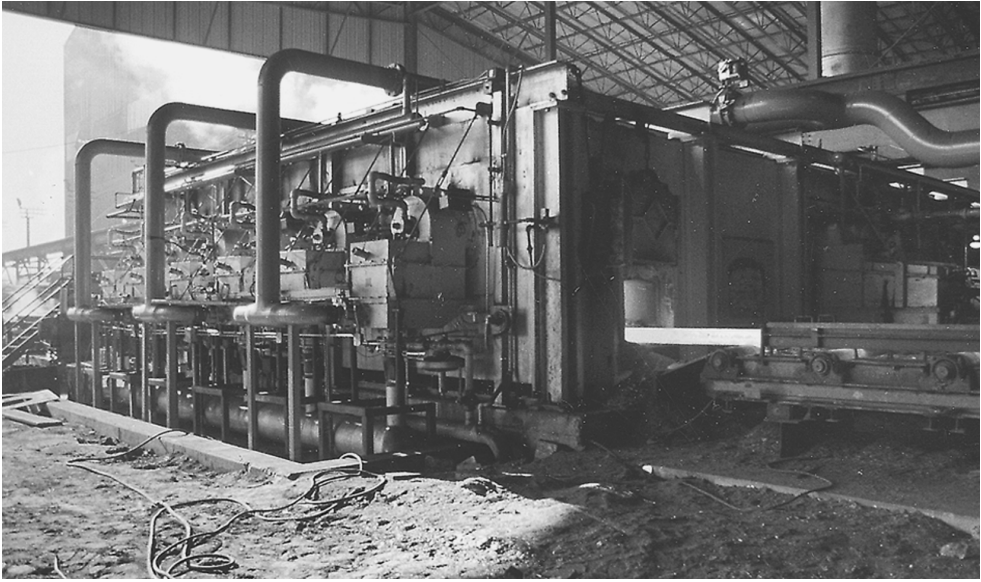


FIGURE 12.25 A 52.5-ft steel reheat furnace.

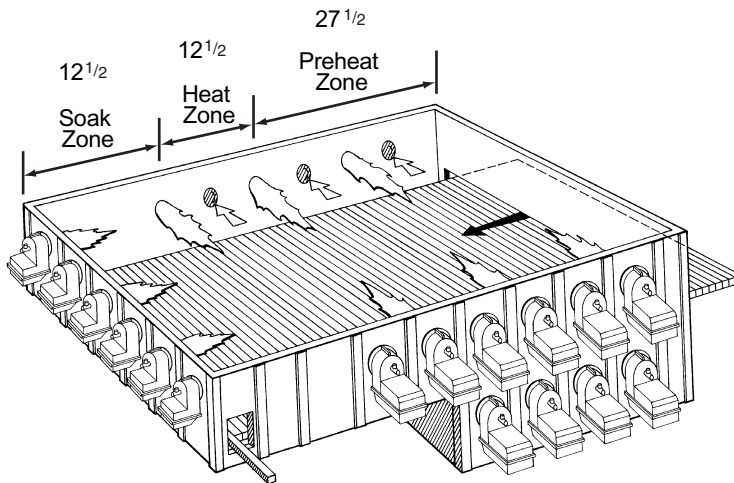


FIGURE 12.26 Model of 52.5-ft steel reheat furnace.

adding four pairs of regenerative burners to the furnace was to increase the production rate to at least 80 tons/hr.

The pre-conversion specific fuel consumption of the furnace was 1.3 MMBtu/ton. With the regenerative burners, production capacity was increased to 92 tons/hr and the specific fuel consumption reduced to 1.1 MMBtu/ton.

12.7.3.3 Addition of Booster Zone to Existing Furnace

A further example of adding regenerative burners to an unfired section is the addition of a pair of heavy fuel oil-fired compact regenerative burners to the front end of the first heating zone of a 30-year-old, three-zone walking hearth reheating furnace in order to increase the production rate

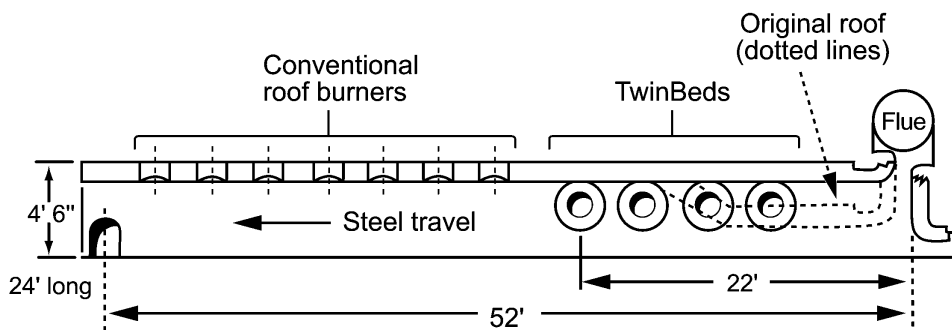


FIGURE 12.27 Addition of booster zone to walking beam furnace.

reported by Nordell and Fredriksson.¹⁸ The addition of regenerative burners was chosen as the existing recuperator was already operating at its maximum capability and could not accept additional hot flue gases from conventional burners. From this, the desired production capacity of 72 ton/hr, from 66 ton/hr, was achieved.

REFERENCES

1. Camp, J.M. and Francis, C.B., *The Making, Shaping, and Treating of Steel*, Carnegie Steel Company, 4th ed., Pittsburgh, PA, 1925, 289.
2. The North American Manufacturing Company, Ltd., *Handbook Supplement 128 – Combustion in the Glass Industry*, 1972.
3. Webb, R., On the Road to Recovery, in *MRS Relay*, British Gas, September 1983, 9–11.
4. Davies, T., Regenerative burners for radiant tubes — field test experience, in *Industrial Combustion Technologies*, Lukasiewicz, M.A., Ed., American Society of Metals, Warren, PA, 1986, 65–70.
5. Newby, J.N., The reGen Regenerative Burner — Principles, Properties and Practice, in *Industrial Heat Exchangers*, Hayes, A.J. et al., Eds., American Society of Metals, Warren, PA, 1985, 143–152.
6. New Energy and Industrial Technology Development Organization (NEDO), *High Performance Industrial Furnaces Development Project Report*, Japan, annual.
7. Tanaka, R. et al., Advances in High Temperature Combustion Technology — New Combustion Technology for Reducing CO₂ Emissions, in *National Project Reports, High Performance Industrial Furnace Development Project, High Temperature Air Combustion*, The Japan Industrial Furnace Manufacturers Association, March 1997, 3–9.
8. Nakamachi, I. et al., U.S. Patent No. 5,571,006, Regenerative Burner, Burner System and Method of Burning, Nov. 5, 1996.
9. Kurihara, T., Reducing NO_x emissions in High Temperature Furnaces, *AFRC/JFRC International Symposium*, Maui, Hawaii, 1998.
10. The North American Manufacturing Company, Ltd., *Handbook Supplement 177 — Thinking Man's Guide to Preheated Air Systems*, 1980.
11. Jasper, H.D., Personal communication, Jasper GmbH, 2002.
12. Reed, R.J., *North American Combustion Handbook*, third edition, Vol. II, The North American Manufacturing Company, Ltd., 1997, 153–176.
13. Nakamachi, I. et al., U.S. Patent No. 4,945,841, Apparatus or Method for Carrying Out Combustion in a Furnace, Aug. 7, 1990.
14. Shigeta, E. et al., Low-NO_x Combustion Technique for High-Temperature Furnace, *AFRC/JFRC International Conference on Environmental Control of Combustion Processes*, Honolulu, Hawaii, 1991.

15. Saiki, N. and Koizumi, T., Application of Low-NO_x Combustion Technique for Regenerative System, *AFRC/JFRC Pacific Rim International Conference on Environmental Control of Combustion Processes*, Maui, Hawaii, 1994.
16. Cain, B. et al., The Development and Application of Direct Fuel Injection Techniques for Emissions reduction in High Temperature Furnaces, *2nd International Seminar on High Temperature Combustion in Industrial Furnaces*, Stockholm, Sweden, 2000.
17. de Groot, J., Personal communication, Thermcon Ovens B.V., 1999.
18. Nordell, K. and Fredriksson, J., Experiences of Regenerative Burners in Billet Reheating Furnace at Fundia Dalsbruck, *2nd International Seminar on High Temperature Combustion in Industrial Furnaces*, Stockholm, Sweden, 2000.

13 Thermal Radiation Burners

Thomas M. Smith and Charles E. Baukal, Jr., Ph.D., P.E.

CONTENTS

- 13.1 Introduction
 - 13.2 Applications
 - 13.2.1 Predryers
 - 13.2.2 Dryers
 - 13.3 Industries
 - 13.3.1 Paper Industry
 - 13.3.2 Printing and Publishing
 - 13.3.3 Textile Manufacturing
 - 13.4 Burner Types
 - 13.4.1 Porous Ceramic Burners
 - 13.4.2 Ported Ceramic Burners
 - 13.4.3 Ported Metal Burners
 - 13.4.4 Fiber Metal Burners
 - 13.4.5 Flame Impingement Radiant Burners
 - 13.4.6 Catalytic Burners
 - 13.4.7 Advanced Ceramic Radiant Burners
 - 13.5 Testing and Characterization
 - 13.5.1 Radiation Efficiency
 - 13.5.2 Heat Transfer Coefficient
 - 13.6 Conclusion
- References

13.1 INTRODUCTION

Thermal radiation burners refers here to a class of burners designed specifically to transfer heat by thermal radiation, primarily infrared (IR), to the load. This does not include radiant tube burners (Chapter 14) or radiant wall burners (Chapter 15), which are discussed elsewhere and designed for some specific applications. The burners discussed here are generally designed for loads at lower temperatures, often for drying applications.

These burners generally have a rectangular plenum with four sidewalls and a back wall with an inlet for the introduction of a gaseous fuel and a porous plate enclosing the open mouth of the plenum. The porous plate may contain a series of small (<3 mm diameter) fuel injection holes or may contain a fibrous material having microscopic passages for the fuel. In the case of surface combustion and sub-surface combustion thermal radiation burners, the porous plate is also the primary IR emitter as the fuel combusts on, or within, the porous plate surface to heat it. Impingement burners have a secondary plate(s) constructed of metal or ceramic onto which the combusting fuel ejected from the porous plate holes impinges to heat the secondary plate.

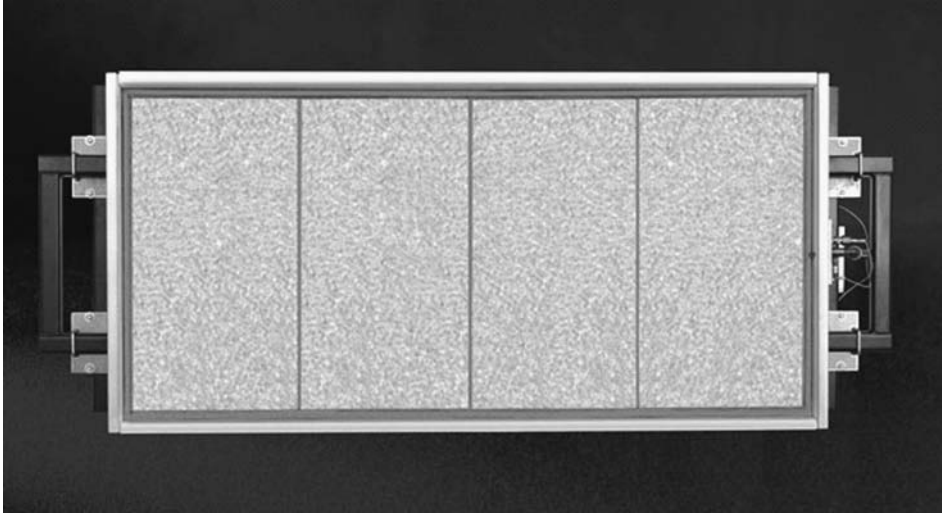


FIGURE 13.1 Uniform surface temperature of thermal radiation burner. (Courtesy of Marsden, Inc.)

Thermal radiation burners are designed to produce a uniform surface temperature (see [Figure 13.1](#)) heat source for heating and melting a variety of materials. The uniform surface temperature produces more homogeneous heating of the materials, which normally improves the product quality compared to conventional burners that may produce hot spots. Other advantages of these burners can include:

- High thermal efficiencies
- Low pollutant emissions
- Directional heating
- Very fast response time to load changes
- Very fast heating compared to convective heating
- Burner shape can be tailored to the shape of the heat load to optimize heat transfer
- Ability to segment a burner to produce a nonuniform heat output profile that might be useful in certain types of heating and drying applications
- Certain types of radiant burners have very rapid heat-up and cool-down times
- More control over the heating process because of the known and measurable surface temperature of the radiant surfaces compared to open flames where the flame temperature is very difficult to measure
- Burners are very modular and can be configured in a wide variety of geometries to accommodate the process heating requirements

The primary parameters of interest for radiant burners are the power density (firing rate per unit area), radiant efficiency (fraction of fuel heating value converted to thermal radiation), heat-up and cool-down time, and pollutant emissions. Other factors of importance include cost, durability, and longevity.

There are also some potential limitations of porous refractory burners, compared to more conventional open-flame burners, which may include:

- There can be a relatively low temperature limit for the radiant surface due to the limits of the refractory material.
- The fuel and oxidizer must be clean to avoid plugging the porous radiant surface, which essentially precludes the use of fuels such as coal or heavy fuel oil.

- Some radiant surfaces can be damaged by water or by contact with solid materials that may be prevalent in certain applications.
- Holes in the radiant surface can cause flashback because these burners use premix.
- Some designs may have high pressure drops, which means that more energy is needed for the blower to flow the combustion air through the ceramic burner material.
- Due to the limits in radiant surface temperatures, the firing rate density is usually limited.
- Some types of radiant burners using hard ceramic surfaces may have high heat capacities that could ignite certain flammable load materials upon a sudden line stoppage.

In these burners, fuel and air are premixed and combusted either just inside a radiating surface or just above the surface, depending on the operating conditions and specific radiant burner design. If the mixture velocity is too low, flashback or flame extinguishment can occur, depending on the design of the burner. In addition to the operational considerations, flashback is an obvious safety concern. If the mixture velocity is too high, the flame may blow off or the radiant performance may be severely reduced because the burner surface is not being directly heated by the hot exhaust products. Depending on the specific design of the burner, optimum performance is achieved when the flame is stabilized just inside or just above the outer burner outlet.

Howell et al. (1995) refer to the burner material as “porous inert media” and present a review of these types of burners, which have been made from a wide variety of ceramics that often include alumina, zirconia, or silicon carbide.¹

13.2 APPLICATIONS

Thermal radiation burners are used for a wide variety of applications. These are generally some type of heating, drying, or curing process, including, for example:

- Drying paper and cardboard in a paper mill
- Paper finishing
- Drying wood
- Porcelain frit drying
- Curing ceiling tiles
- Heating flooring products
- Curing coatings on carpet backs
- Teflon curing
- Paint drying
- Drying and curing coatings on paper and metals
- Curing ink on paper and powder coat paints
- Baking in mass food preparation
- Setting dyes in textile and carpet production, sometimes referred to as predrying
- Curing lens assemblies in automotive headlamp assembly manufacturing
- Plastics curing

Thermal radiation burners are often used to heat webs moving at high speeds (see [Figure 13.2](#)).

An important consideration for the choice of oven or dryer type for the specific application depends on whether direct or indirect heating is needed.² Direct heating means that the product is exposed directly to the flame (see [Figure 13.3](#)), while indirect heating means that the products of combustion do not come in contact with the material being heated (see [Figure 13.4](#)). In indirect heating, an intermediate carrier or type of heat exchanger is used to transfer the heat. Normally, an intermediate medium between the flame and the load reduces the thermal efficiency compared to direct heating. The most common reason for keeping the exhaust products separate from the heat load is for product quality reasons where the product could be contaminated by the exhaust gases.

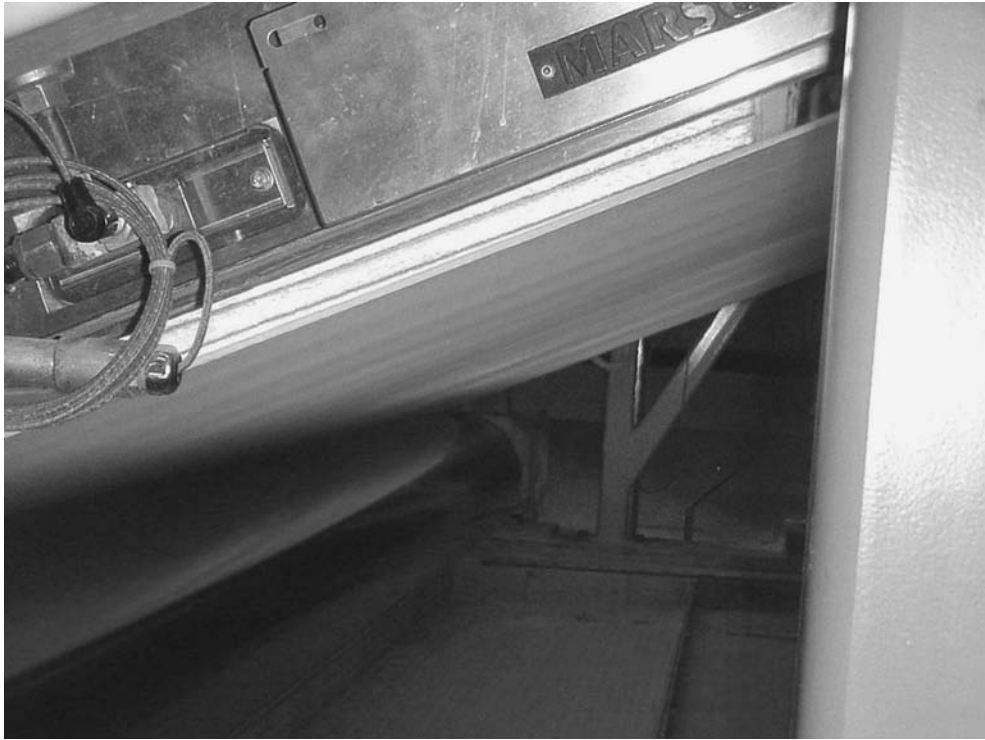


FIGURE 13.2 Example of a thermal radiation burner heating a moving web. (Courtesy of Marsden, Inc.)

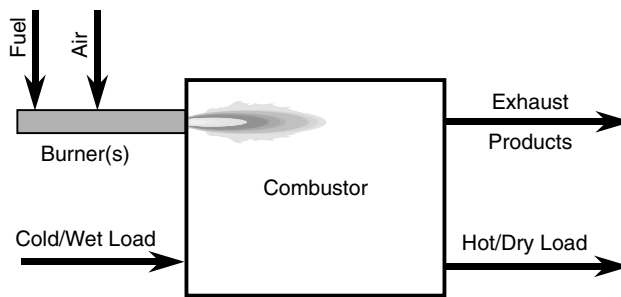


FIGURE 13.3 Schematic of direct heating system.

Another reason is that the product may be emitting combustible volatile vapors that could be ignited if they came into contact with open flames. Still another reason might be that exhaust gases could carry fine particles from the load out of the combustor. These particles would then have to be scrubbed out of the exhaust before the exhaust enters the atmosphere. That means that not only are the raw material costs higher, but there is also the added cost of removing the unused raw materials in the exhaust. As expected, the heat transfer mechanisms will be different, depending on the type of heating used in a given process.

There are some lower-temperature drying applications employing industrial combustion that are briefly considered here. These include the paper, printing and publishing, textile manufacturing, and food processing industries. Drying is defined as “a process in which a wet solid is heated or contacted with a hot gas stream, causing some or all of the liquid wetting the solid to evaporate.”³ Kudra and Mujumdar (2002) have written a book⁴ on advanced drying technologies that covers a

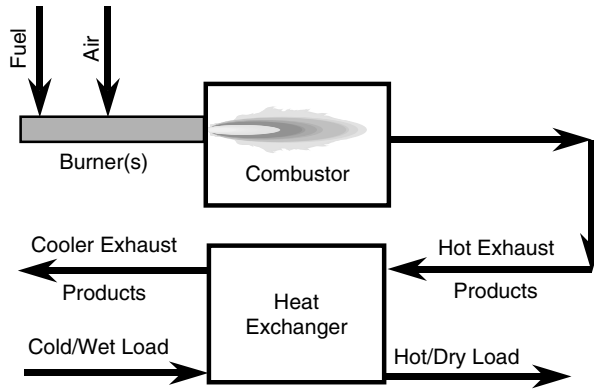


FIGURE 13.4 Schematic of indirect heating system.

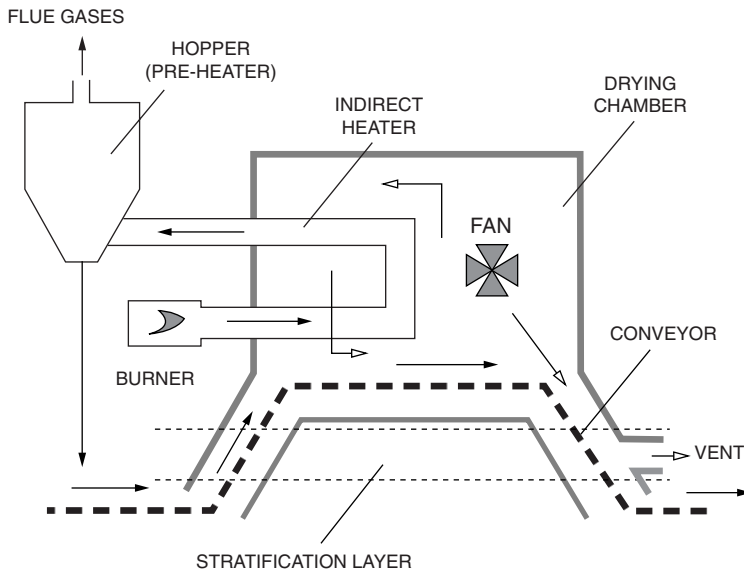


FIGURE 13.5 Continuous airless dryer. (Courtesy of Marcel Dekker.⁴)

wide range of industries, including those discussed in this chapter. Some of the more advanced drying techniques include impinging steam dryers, pulsed fluid beds, airless dryers (see Figure 13.5), sonic dryers, plasma torch dryers, slush drying, and a variety of hybrid methods. The authors call for more R&D and innovation to advance the state-of-the-art in dryers, which have received much less attention than other types of heating equipment, and has been mostly evolutionary up until fairly recently. Table 13.1 shows a classification of typical dryers.

13.2.1 PREDRYERS

Predryers are used in some applications prior to final drying of the product. An example of this type of application is the use of infrared (IR) burners to set the dyes in the dyeing of fabrics in textile manufacturing.⁵ After the dyes are applied to the fabric, they must be set prior to contact with the dryer; otherwise, the dyes will migrate to drier areas of the fabric, which reduces the quality of the textile. The IR burners in the predryer are used to rapidly set the dyes without the need to contact the material, as would be the case with, for example, a steam-heated drum dryer.

TABLE 13.1
Classification of Dryers

Criterion	Types
Mode of operation	Batch Continuous ^a
Heat input-type	Convection, ^a conduction, radiation, electro-magnetic fields, combination of heat transfer modes Intermittent or continuous ^a Adiabatic or nonadiabatic
State of material in dryer	Stationary Moving, agitated, dispersed
Operating pressure	Vacuum ^a Atmospheric
Drying medium (convection)	Air ^a Superheated steam Flue gases
Drying temperature	Below boiling temperature ^a Above boiling temperature Below freezing point
Relative motion between drying medium and drying solids	Concurrent Countercurrent Mixed flow
Number of stages	Single ^a Multistage
Residence time	Short (<1 min) Medium (1–60 min) Long (>60 min)

^aMost common in practice.

Source: Courtesy of Marcel Dekker.⁴

IR predrying in the paper industry occurs in several areas. After the last wet press and before the first steam cylinder contact dryer, IR is used to evaporate the surface water to minimize “picking.” Picking is caused by the explosive evaporation of the surface water and dislodging of surface fibers when the paper meets the hot cylinder surface. The dislodged fibers start to coat the drying cylinder, reducing its heat transfer ability. Another area is where IR burners are installed after the coating machine and are used to set the coatings on the paper prior to the paper contacting a steam-heated cylinder drum dryer or the hot air “floater” dryer, used to complete the drying (see next section).⁶ The IR predryer is primarily used to increase productivity and improve the paper coating quality. The productivity is increased because of the additional drying. The quality is improved because the rapid drying minimizes binder migration from the coating into the paper, which minimizes or eliminates mottle. Also, the IR energy does not physically disturb the coating as convection or conduction heat transfer methods might. Figure 13.6 shows the typical spectral radiant transmissivity for uncoated paper. The paper is more absorbent (less transmissive) at longer wavelengths and less absorbent (more transmissive) at shorter wavelengths. Because IR burners typically have their peak radiant output at wavelengths less than 3 μm, this leads to good thermal efficiencies because the paper is highly absorbent at those wavelengths. Mottle is a measure of the quality of the finished paper product and refers to the finish. Higher mottle means the paper has more blemishes on the surface than lower mottle. Figure 13.7 shows how mottle, measured by a surface image analyzer, was affected by the evaporation rate (related to the firing rate of the burners) and the type of heat source. This shows that gas-fired IR burners produced less mottle and, therefore, higher quality paper, than electric IR burners.

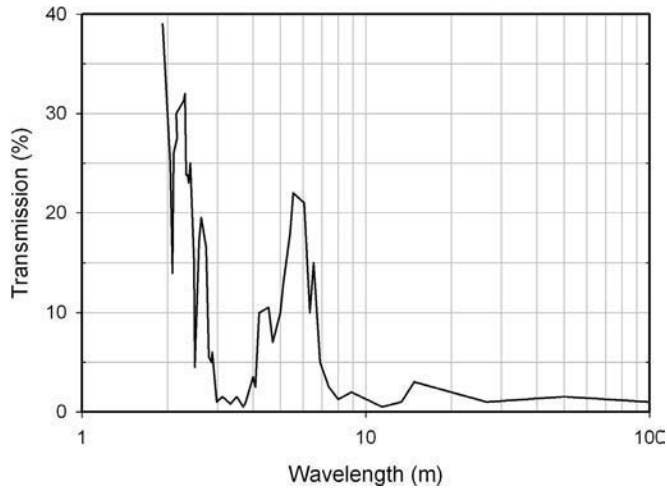


FIGURE 13.6 Spectral transmissivity for typical uncoated paper. (Adapted from Reference 6.)

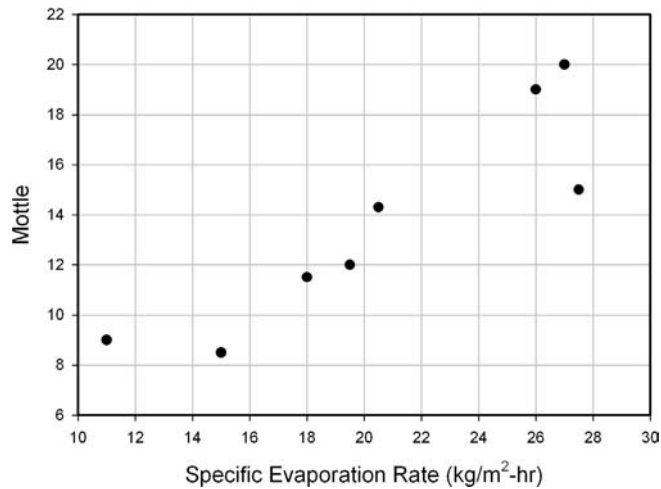


FIGURE 13.7 Mottle as a function of evaporation rate and heat source type. (Adapted from Reference 6.)

Pettersson and Stenström (1998) compared the use of gas-fired and electric infrared burners used to set the coating before the paper reached the next cylinder in a paper line.⁷ Figure 13.8 shows the IR heaters between the coating station and the next steel cylinder in the paper machine. IR burners are preferred in this application, instead of convective or conductive dryers, because they are noncontact and have high power densities (10 to 40 kW/m² or 3000 to 13,000 Btu/hr-ft²). The thermal efficiencies were calculated as 30 and 40%, respectively, for the gas-fired (propane) and electric IR burners. However, the burners were tested on two different machines and there was some uncertainty in the measurements. That being said, the gas-fired IR burners may still be more economical than the electric IR burners, because electricity is often much more expensive than natural gas on an equal energy basis. It is noted that some thermal radiation burners are capable of power densities up to 120 kW/m² and total efficiencies of 50%.⁸

Riikonen et al. (1987) developed a computer model to simulate both the convection and radiation heat transfer in IR heating systems used in paper drying.⁹ Experiments were conducted to test the model. The model significantly underpredicted the time for the sample to dry. The error in the calculations was identified as the moisture isotherm predictions. The explanation was that IR heating

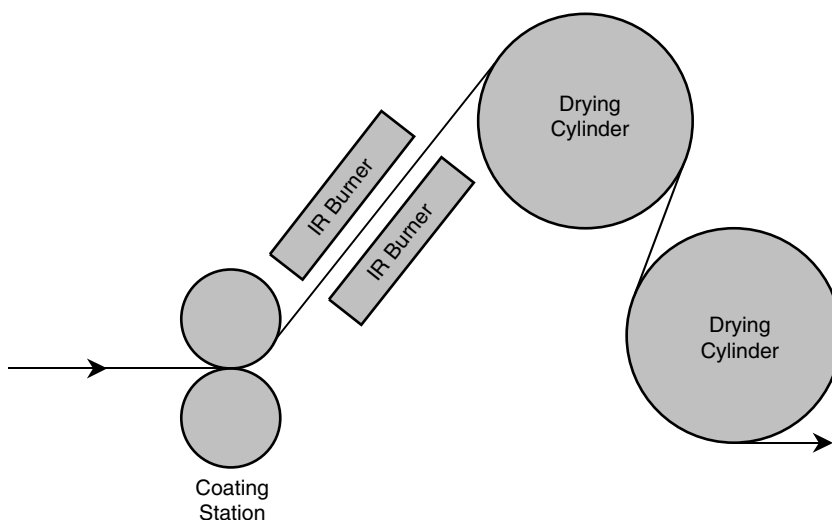


FIGURE 13.8 Schematic of IR heaters used to set coating in a paper machine where the paper is traveling from left to right.

quickly removes the bound water between fibers but more slowly removes water inside the fibers. A suggested correction was to use an apparent diffusivity to correct for the difference in moisture evaporation rates in and around the pulp fibers.

The difference in heat transfer requirement at low moisture contents is the higher temperature required to free the bound water from the fiber, which requires that the paper mass as well as the water mass must be heated to the higher temperature. In the constant rate period, the paper/water temperature remains fairly constant at 60 to 89°C (140 to 190°F). At moisture contents below about 15%, the paper temperature rises. Because the percent water decreases and the percent fiber increases at lower moisture contents, the additional energy required for drying per unit mass of water increases as well.

13.2.2 DRYERS

Dryers are commonly used to remove moisture from products during the manufacturing process. Common industries using dryers include the color, pigment, and dyestuff industries; the pharmaceutical and fine chemicals industry; natural ores, minerals, and heavy chemicals; paper and allied products; foodstuffs and agricultural products; and the ceramics and textile industries.¹⁰ If the heat source is some type of burner, dryers can be directly fired or indirectly fired, depending on the application. Dryers can also be batch or continuous.¹¹ Figure 13.9 shows some examples of continuous dryers. Sloan (1967) reviewed the following classes of dryers: air-suspended systems that rely primarily on using air for mass transfer, direct-heat continuous systems, direct-heat batch systems, indirect-heat continuous systems, and indirect-heat batch systems.¹² IR burners can be used to boost the performance of conventional hot-air convective dryers.¹³ Direct flame impingement is even used in limited cases, such as drying refractory-lined vessels and moulds used in metals and minerals production.¹⁴

There are commonly three periods in the drying process, as shown in Figure 13.10. The period from A to B is the warming-up period where the material is heated up to the evaporation temperature. The period from B to C is referred to as the constant rate period, where the drying rate is constant. The rate of drying is essentially that for the liquid and behaves as if there were no solid present. The liquid wicks rapidly during this period. The period from C to D is referred to as the falling rate period, where the free liquid has been essentially removed and the remaining liquid must move to the surface by diffusion and capillarity. During that period, the solid is an impediment to the liquid removal.

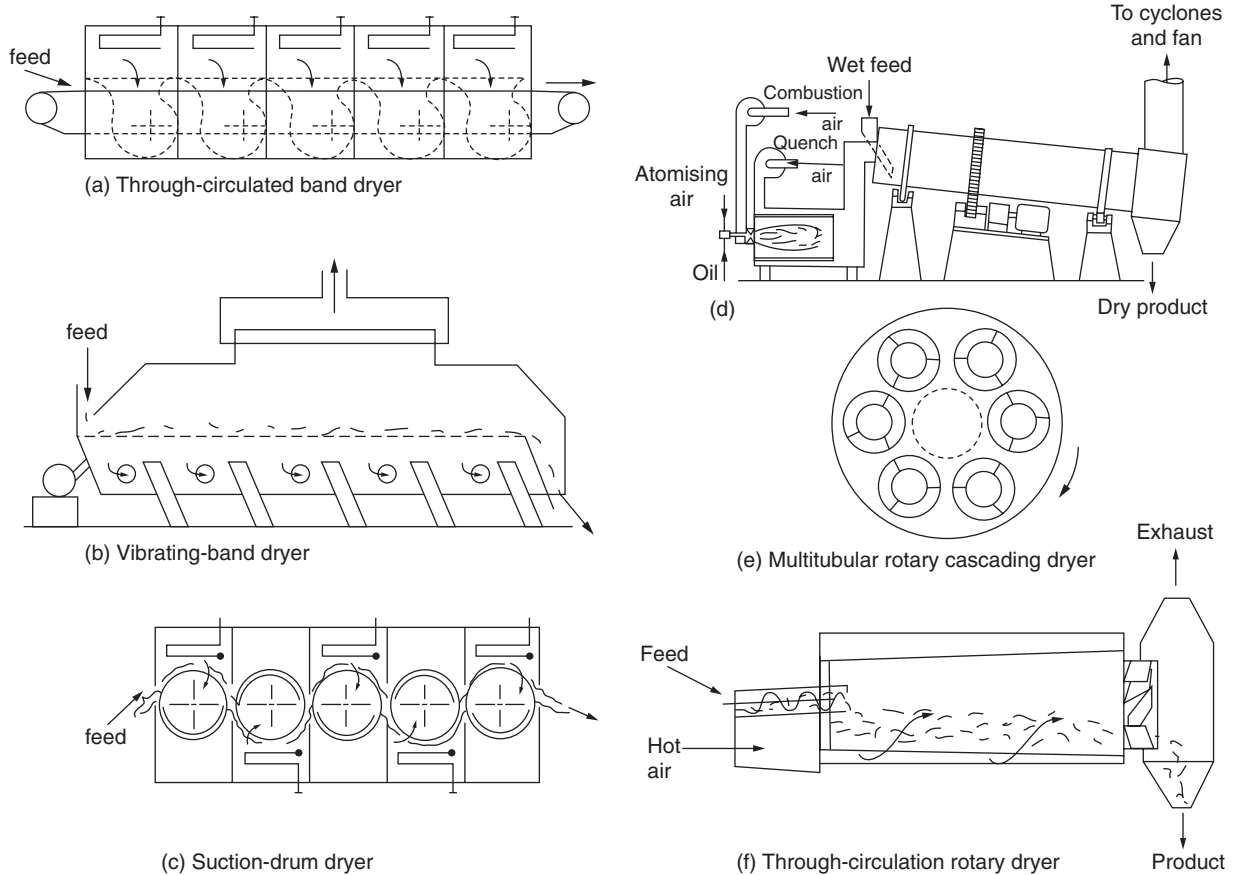


FIGURE 13.9 Examples of continuous dryers.¹¹

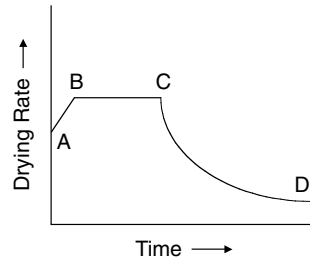


FIGURE 13.10 Periods of drying.¹⁹

Dryers are sometimes classified by the predominant heat transfer mechanism: convection, conduction, or radiation. They are then sub-classified into batch and continuous dryers. An example of a batch convection dryer is a tray dryer. Continuous convection dryers include truck-and-tray tunnels, continuous through-circulation, rotary dryers, fluid bed dryers, spray dryers, and pneumatic or flash dryers. Batch conduction dryers include vacuum tray dryers, vacuum double cone dryers, trough dryers, pan dryers, and rotary dryers. Continuous conduction dryers include film drum or roller dryers, cylinder or can dryers, rotary dryers, and trough dryers. There are both batch and continuous radiation dryers that use IR heating. While not all of these dryers use combustion, many of the convection dryers preheat the air with burners and the radiation dryers often use gas-fired IR burners.

Dryers are usually low-temperature applications as the material is usually no more than about 300°F (400°K). One example is in the drying of paper and board in a paper mill. The paper products are made from pulp in a slurry that has a very high moisture content. The paper is then dried in one of several ways. First, as much water as possible is removed mechanically, typically with some type of press. The remaining moisture is removed by heating, using some type of dryer.

Another type of dryer uses very-high-velocity hot air impingement on both sides of a moving web. The web “floats” through the nozzles, which is where this type of dryer gets its name — *floaters dryer*. The primary mode of heat transfer for this dryer is convection. This technique combines heat and mass transfer in the same apparatus, as the hot air both heats the web and carries away the moisture that evolves from it. This type of dryer has several potential advantages over other types of dryers. No additional systems are needed to remove the volatiles vaporizing from the material being dried. There is no direct contact with the product that could reduce the quality. It is possible to segment this type of dryer to vary the moisture removal rate across the width, although the reaction time is slow compared to IR dryers. There are also potential disadvantages. The air nozzles can become plugged because they are typically fairly small to achieve the high gas velocities. In drying materials such as papers and textiles, this method also ultimately relies on conduction for the energy to get to the core of the product whose thermal conductivity decreases as the moisture content decreases. Another version of an air dryer is where heated air is blown only onto one side of a paper web traveling through a dryer where a coating is to be dried, as shown in [Figure 13.11](#).¹⁵ In hot air dryers, burners are used to heat the air blown onto the material being dried.

13.3 INDUSTRIES

Some of the common industries that use thermal radiation burners are briefly considered here. These include the paper, printing and publishing, and textile manufacturing industries.

13.3.1 PAPER INDUSTRY

The paper industry is composed of two primary sectors:¹⁶

- Pulp and paper mills, which produce mechanical, thermomechanical, and chemical pulps and process these pulps to form paper, paperboard, or building papers
- Converting operations, which manufacture boxes, tablets, and other finished paper products

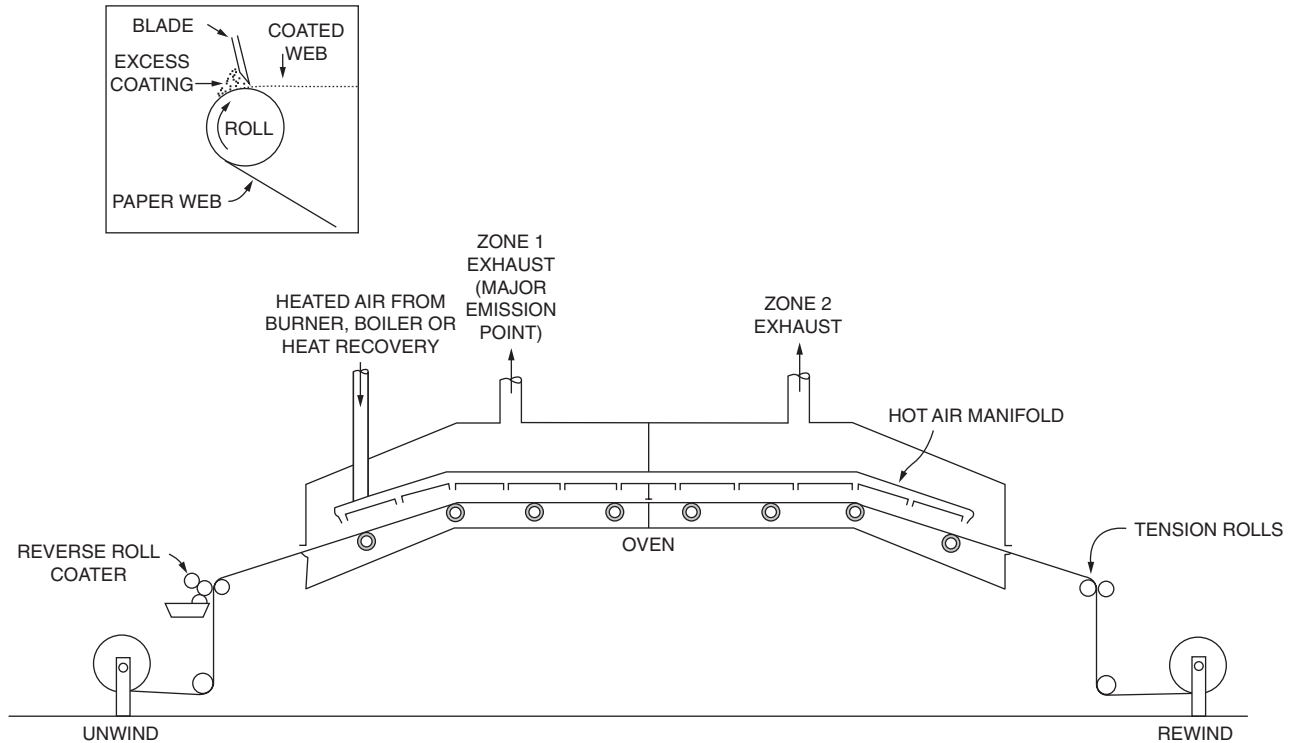


FIGURE 13.11 Schematic of a paper coating dryer. (Source: U.S. EPA.)

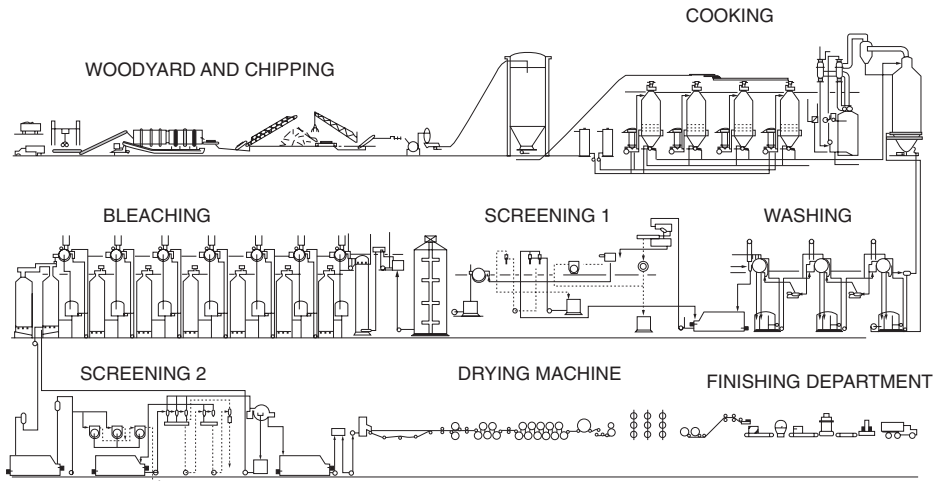


FIGURE 13.12 Integrated paper mill. (Source: U.S. EPA.¹⁷)

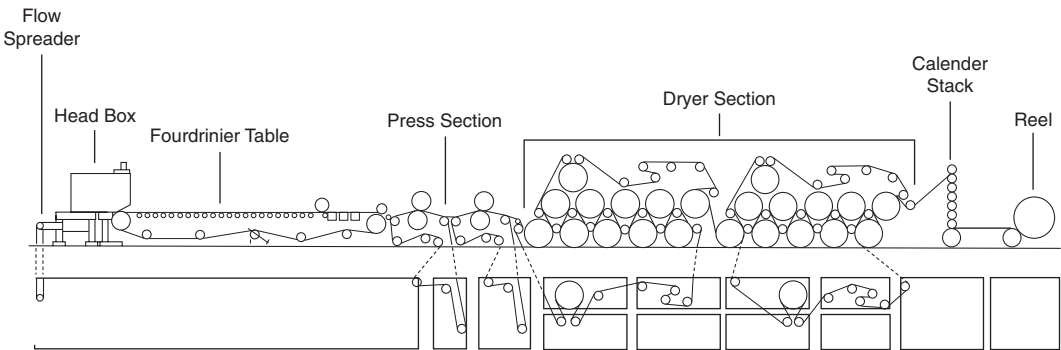


FIGURE 13.13 Fourdrinier paper machine. (Source: U.S. EPA.¹⁷)

The first sector involves production of paper products from raw wood while the second sector involves converting those initial products into more specialized end products. The pulp and paper industry produces commodity grades of wood pulp, primary paper products, and paper board products such as: printing and writing papers, sanitary tissue, industrial-type papers, container board and boxboard.¹⁷ Figure 13.12 shows a schematic of an integrated paper mill. The only part of the mill that uses industrial combustion is the drying machine. Even there, it is only supplemental to the steam-heated cylinders, which do the bulk of the drying. Figure 13.13 shows an elevation view of a Fourdrinier paper machine commonly used to make paper. A steam-heated cylinder in the drying section can be seen in more detail in Figure 13.17. Figure 13.14 shows a schematic of the Kraft process for handling the pulp and bark used to make the paper, including the treatment of the chemicals in the various reactors that are considered in more detail below.

Paper is commonly dried using the three primary modes of heat transfer: convection, conduction, or radiation (see Chapter 2). Convection dryers use heated air. Conduction drying is done with steam-heated cylinders. Radiation drying is done with thermal radiation burners. These three methods are sometimes used in combination. The most common way to dry paper traveling at high velocities is by contact with steam-heated cylinders. The paper wraps around the drums in a serpentine fashion to maximize the contact area with the drum. In this type of dryer, the primary method of drying is by thermal conduction.¹⁸ One problem with this technique is that as the paper

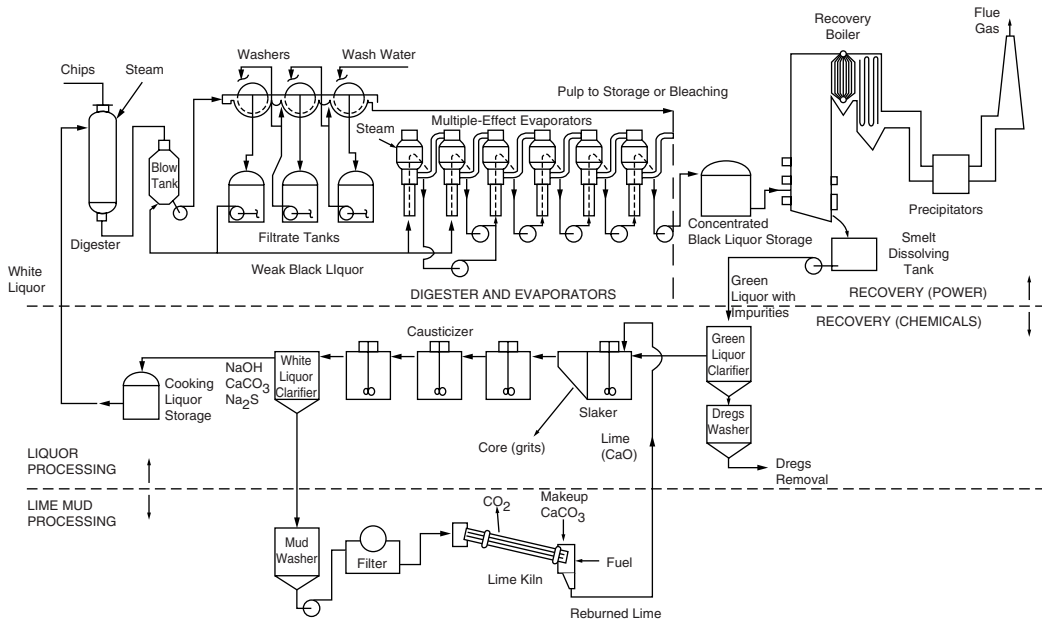


FIGURE 13.14 Kraft process flow diagram. (Source: U.S. EPA.¹⁷)



FIGURE 13.15 Infrared burner heating a continuously moving paper web. (Courtesy of Marsden, Inc.¹⁹)

dries, the thermal conductivity goes down, which makes it more difficult to conduct the heat into the paper. As previously discussed, this is known as the “falling rate period,” where the downstream steam cylinders are much less effective at removing moisture than the upstream cylinders.

In many drying processes, moisture is removed from paper webs often traveling at high speeds. Radiant heating (see Figure 13.15) is often used to supplement steam-heated cylinder drying or

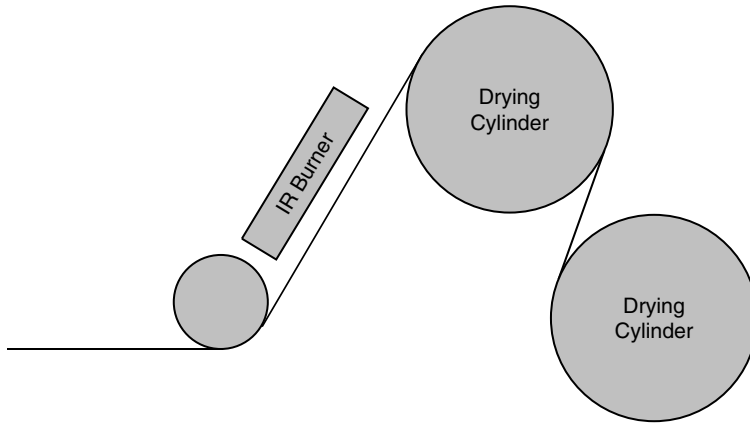


FIGURE 13.16 Schematic of an IR burner located before a steam cylinder in a paper drying process.



FIGURE 13.17 Supplemental IR burners for paper drying located over steam cylinders. (Courtesy of Marsden, Inc.)

high-velocity hot air dryers.¹⁹ The radiant heaters are either electric or fired with a fuel such as natural gas. These supplemental heaters may be located before the steam-heated cylinders (see [Figure 13.16](#)), in between cylinders, over cylinders (see [Figure 13.17](#)), and/or after the cylinders.

The heaters can also be partitioned across the machine to vary the drying capacity. The moisture content of the paper web often varies across the machine direction. Some streaks may be significantly wetter than others and therefore require more drying energy. A fictitious example is shown in [Figure 13.18](#) where the peak moisture content is near 15% while the minimum is at 10%. The paper is normally specified to have a maximum moisture content. Assume for the sake of argument

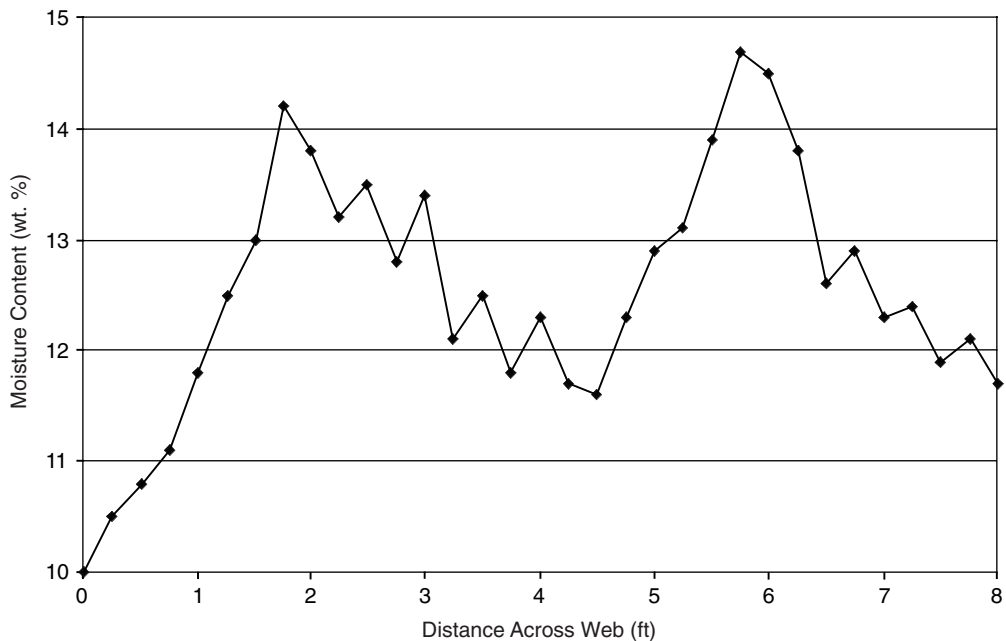


FIGURE 13.18 Moisture profile across a paper web prior to drying.

that it is 4%. This means that the entire paper must be dried so that the wettest streaks are at or below the maximum allowable moisture content. If the heating is uniform across the web, then enough energy must be supplied to reduce the moisture streak of nearly 15% water content down to 4%. This means that the section of the web at 10% will be dried well below 4%. However, this is detrimental for several reasons. Because paper is sold by weight, removing more moisture than necessary in drier sections of the paper reduces profitability. More fuel than necessary is used to dry some sections well below the maximum allowable moisture limit. The paper quality also suffers when some sections of the paper are overdried, which causes handling problems for machines such as printers and copiers. Some paper manufacturers actually spray water back onto the drier streaks to make the profile more uniform. This is energy inefficient as energy was spent removing the moisture, which is then re-added. So-called moisture profiling is where the radiant output of the burners varies across the machine direction (see [Figure 13.19](#)) to match the moisture levels. This fixes the problems of overdrying some sections that occurs with a uniform radiant heating level. This is much more fuel efficient and economic because more moisture can be sold and the product quality is also improved.

Infrared dryers can have significantly higher evaporation rates for removing moisture from paper webs, compared to steam cylinders and air dryers. Longacre (1997) has shown that typical evaporation rates using steam cylinders, air dryers, and infrared dryers are 5, 8, and 20+ lb/ft²/hr, respectively.²⁰

Another example of predrying is in the paper industry where IR burners are installed after the coating machine and are used to set the coatings on the paper prior to the paper contacting a steam cylinder drum dryer which is used to complete the drying.²¹ The IR predryer is primarily used to increase productivity and improve the paper coating quality. The productivity is increased because of the added heat. The quality is improved because the IR energy does not disturb the coating as convection or conduction heat transfer methods could, which lets the coating set on the paper prior to contact with the steam cylinder which relies on thermal conduction heat transfer.

IR burners (see [Figure 13.20](#)) are often used to supplement these dryers because the IR radiation sees 100% of the surface area and thus is better able to penetrate into the paper. Steam cylinder

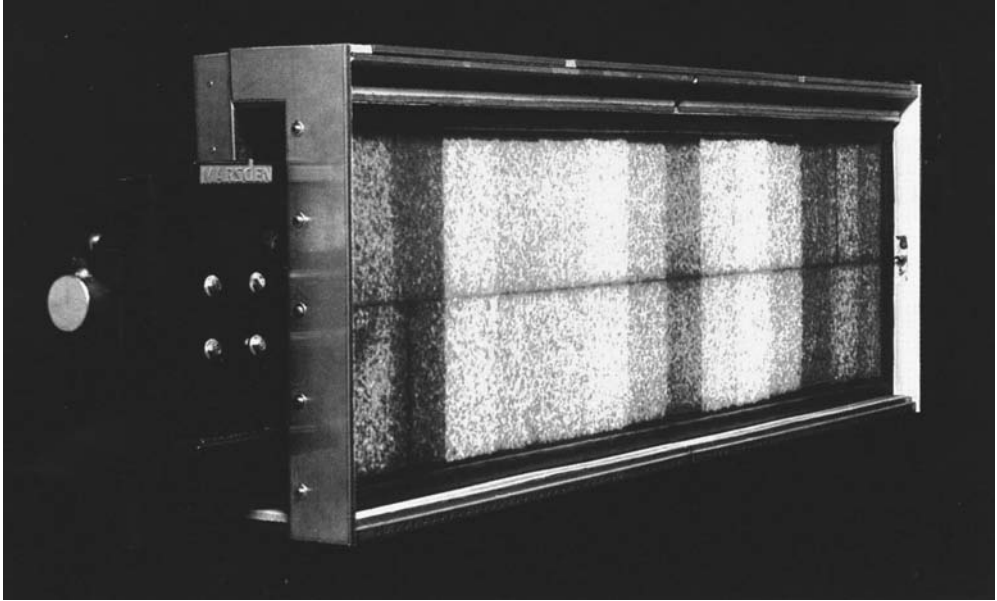


FIGURE 13.19 IR burners designed for moisture profiling. (Courtesy of Marsden, Inc.)

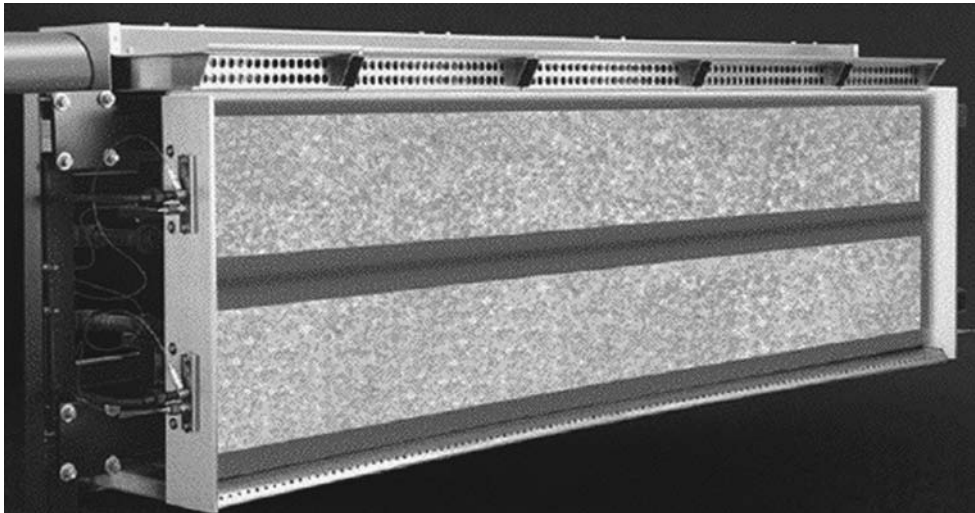


FIGURE 13.20 Example of a flat-panel gas-fired infrared burner. (Courtesy of Marsden, Inc.¹⁹)

dryers only contact the fibers on the top of the fiber matrix, which is a comparatively small area. Compounding the conductive heat transfer problem is that the fibers on the surface have been dried by previous contact and now are good heat insulators. In a survey of paper makers by the Gas Research Institute (Chicago, IL), respondents believed the best place to install infrared burners on a paper drying line is in the pre-heat zone.²² This is undoubtedly because early gas IR dryers cooled very slowly and often set the paper on fire, but there is much less danger of fire in the beginning of the paper machine where the paper is wet. In actual fact, using IR on the dry end of the paper machine makes for better utilization of the whole drying system. As previously discussed, contact

dryers are most effective in the constant rate period of the dryer where there is sufficient water movement to keep the paper surface moist. IR, with its better heat transfer ability, is best utilized where the contact dryers are least effective. If the IR is added to increase speed, putting it in the dry end of the paper machine provides for a bonus effect because the end of the constant rate period moves toward the end of the machine and some cylinders move from the falling rate to the constant rate drying period. If IR is added somewhere in the middle of the machine, trailing cylinders move from the constant to the falling rate period of drying. Other locations identified in the survey included in the forming section, above and below the steam cylinders in the constant rate zones, and above and below the steam cylinders in the falling rate zone.

One reason for the popularity of steam cylinder dryers is that there is usually plenty of steam available in paper mills because much of the waste bark and liquor from the trees used to make the paper is burned in hog fuel boilers. Another reason is that the cylinders help guide and transport the paper. Contact dryers generally help smooth the paper surface and minimize shrinking. One disadvantage includes the large thermal inertia of the metal (typically cast iron) cylinders, which causes longer start-up times and a reduced ability to quickly change the drying rate. An important disadvantage is the reduced drying effectiveness as the moisture content of the paper decreases because of the reduction in the thermal conductivity. These dryers do not typically have the capability to vary the drying capacity across the width of the paper. Also, for thicker materials, the drying rate is reduced because the evolving water vapor is trapped between the cylinder and the paper as it is unable to come out the side of the paper in contact with the cylinder.

Hannum et al. (2000) discuss the development of a high-intensity lean premix combustion system with low NO_x emissions for use in drying applications such as tissue and plasterboard drying.²³ The burner was used to heat air for use in drying in a loop drying system. Measured NO_x emissions were below 10 ppmvd (3% O₂).

In most paper drying applications, the only pollutant of significant concern is NO_x. Carbon monoxide emissions are relatively easy to minimize due to the high degree of control of the combustion process. The gaseous fuels used, such as natural gas, contain little or no sulfur to produce SO_x. These clean fuels and moist webs generate little if any particulates. There are no VOCs in the process. There is very little noise produced. While there are significant levels of thermal radiation, this is directed at the paper and is not usually a problem for personnel operating the equipment. Even NO_x emissions are typically low because of the relatively low operating temperatures.

13.3.2 PRINTING AND PUBLISHING

Web offset lithography is used to produce about 75% of books and pamphlets as well as an increasing number of newspapers.²⁴ Dryers and ovens are sometimes used to dry ink in the printing and publishing industry.²⁵ One of the major environmental concerns related to the printing and publishing industry is VOC emissions. VOCs are used in ink to promote fast drying. This ink is commonly referred to as “heatset” ink. In many applications, no ovens or dryers are required to dry the ink during the production process because of the rapid vaporization of the VOC solvents in the ink compared to the slower speed of the production process. However, high-speed paper webs are used in some printing applications where dryers are required to set the ink before it contacts downstream rollers that would cause the ink to smear if it were not set. [Figure 13.21](#) shows a schematic of a webfed high-speed rotary flexographic press with a printing and drying section used to dry the ink on the paper.²⁶

These printing presses are often of multiple colors, which means that each color must be individually set before the next color can be applied; otherwise, the colors will smear. The heater to set the ink may be as simple as an electric infrared or ultraviolet lamp. [Figure 13.21](#) shows a heater between each color application of the roller ink system. In some cases, natural-gas-fired burners may be used because of their lower operating costs compared to using electricity. Whichever technology

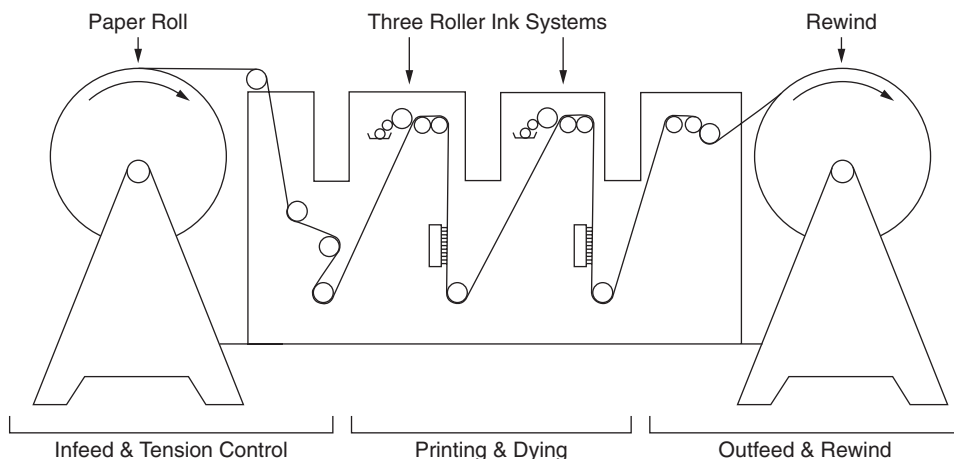


FIGURE 13.21 Schematic of a webfed rotary flexographic press. (Source: U.S. EPA.²⁶)

is used, the heater must either be capable of very rapid cool-down or some type of shielding from the web in the event of a sudden line stoppage, in order to prevent the paper from catching fire.

However, because of the increased concern about VOC emissions, inks are being made with less VOCs and with more aqueous-based solvents that require heat to set. The heaters can be gas-fired infrared burners. For larger and higher-speed presses, gas-fired ovens can be used where air is heated and blown at high velocity onto the paper to both dry the paper and remove the vaporized solvents. These ovens are often designed to float the paper by having air nozzles on both sides of the paper. The floater dryer temperature is in the range of 400 to 500°F (200 to 290°C). One or more burners are fired in the dryer to maintain a given air temperature. An afterburner may also be included in the drying system if there are significant VOC emissions in the recycled air containing ink solvents.

Other than VOCs, there are no other significant pollutants produced by the dryer. The fuel is typically natural gas, which contains little or no sulfur to produce SO_x. There are no significant sources for particulate emissions. Noise may be an issue for hot air dryers because of the fans and high gas velocities. Thermal radiation exposure to personnel could be a consideration if radiant burners are used to set the ink.

13.3.3 TEXTILE MANUFACTURING

The textile manufacturing industry consists of the following segments:²⁷

- Broad woven fabric mills and wool mills, including dyeing and finishing
- Knitting mills and knit goods finishing
- Other dyeing and finishing textile mills
- Floor covering mills, including dyeing and finishing

Predryers are used in some applications prior to the final drying of the product. An example of this type of application is the use of IR burners to set the dyes in the dyeing of fabrics in textile manufacturing.²⁸ After the dyes are applied to the fabric, they must be set or dried uniformly (typically to 30% wet pick-up) prior to contact with the dryer (tenter); otherwise, the dyes will migrate to drier areas of the fabric, which causes shading that reduces the quality of the textile. The IR burners in the predryer are used to rapidly set the dyes without the need to contact the material, as would be the case with, for example, a drum dryer.²⁹ Dryers and ovens are also used to cure inks used in textile printing, as shown in [Figure 13.22](#).³⁰

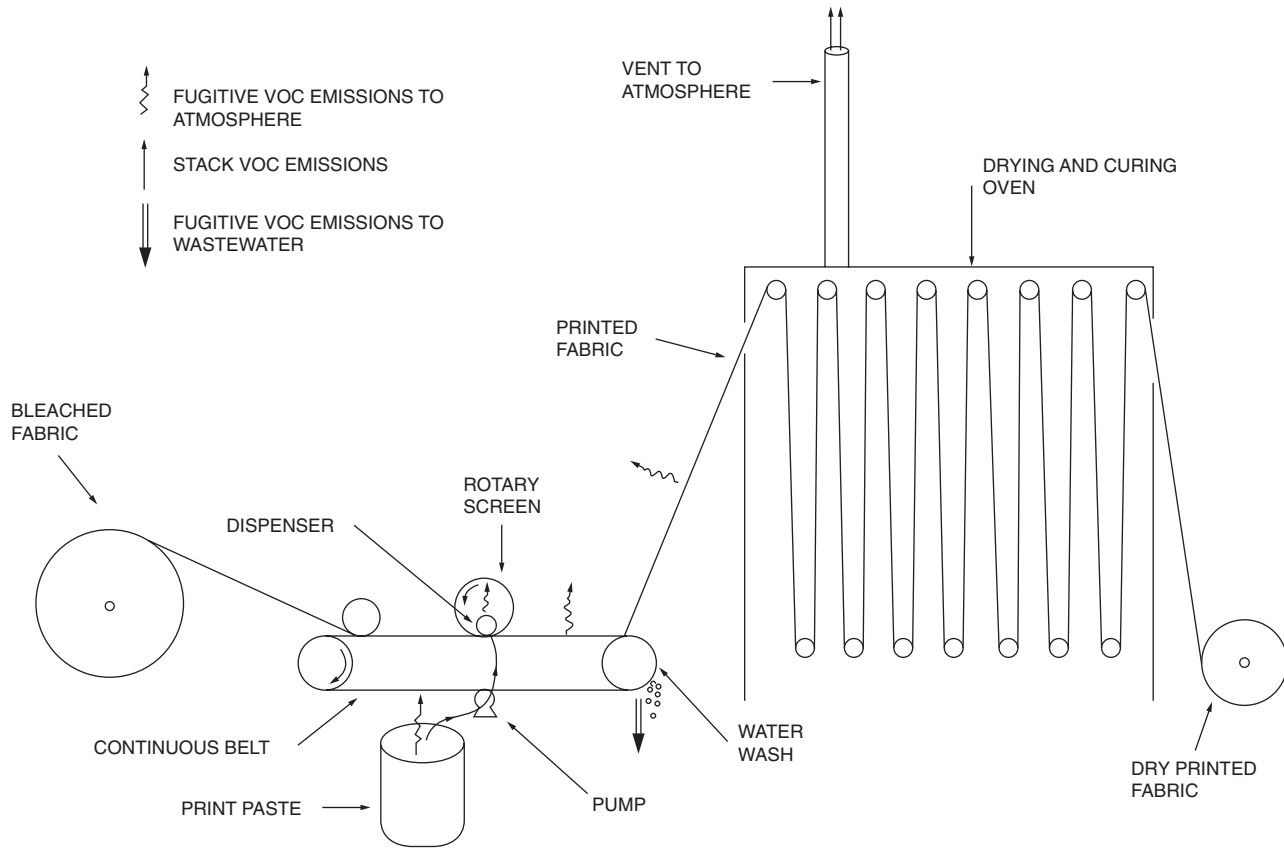


FIGURE 13.22 Schematic of a textile printing process. (Source: U.S. EPA.³⁰)

TABLE 13.2
Comparison of Thermal Efficiencies for Radiant Burners³⁵

Radiant Burner Type	Combustion Intensity (kW/m ²)	Thermal Efficiency Range (%)
Metal fiber		
No perforations	150–540	18–26
With perforations	150–540	16–27
With perforations and front metal screen	100–440	22–38
Reticulated ceramic	150–630	27–39
Ported ceramic	140–520	37–54
Flame impingement	150–430	46–52

13.4 BURNER TYPES

Speyer et al. (1997) studied the performance of four different types of commercial gas-fired radiant burners: a metal (Fe-Cr-Al) fiber (~40 μm diameter) burner, a reticulated ceramic burner made of a porous cordierite (Mg₂Al₄Si₅O₁₈), a porous single-unit mullite (Al₆Si₂O₁₃) tile burner, and a flame impingement burner where the products of combustion are forced around a metal screen that radiates to the load.³¹ The study was sponsored by the Gas Research Institute (Chicago, IL). The thermal efficiencies as a function of the combustion intensity are shown in Table 13.2. The efficiency was determined by measuring the radiant output or radiosity from the burner surface and was calculated using:

$$e = \frac{R_T}{\dot{V}_g \Delta H_c / A} \quad (13.1)$$

where e is the calculated efficiency, R_T is the measured radiosity, \dot{V}_g is the volume flow rate of the fuel, H_c is the heating value of the fuel, and A is the surface area of the burner. The experimental results showed that the peak radiosity measurements as a function of the air-to-fuel mixture ratio occurred for percent excess fuels ranging from 6 to 7.5%, depending on the specific burner design. Similar results were calculated for the radiant efficiencies. Preheating the air/fuel mixture increased both the radiosity and thermal efficiencies, essentially in a linear manner for mixture temperatures ranging from 40 to 155°C (100 to 311°F). In most cases, the efficiency declined with combustion intensity, except for the reticulated ceramic and metal fiber with perforations and a front metal screen, both of which had peak efficiencies at intermediate combustion intensities. The flame impingement and ported ceramic burners were the most efficient, while the metal fiber with and without perforations was the least efficient. The study also showed that the thermal efficiency generally increased as the fraction of closed area increased on the burner surface. Porous ceramic fiber emitters were not included in this report.

13.4.1 POROUS CERAMIC BURNERS

There are two main types: reticulated ceramic and ceramic fiber burners. Reticulated ceramic burners have lightweight, foam-like rectangular blocks attached to a metal plenum. The length and width dimensions are normally less than 250 mm (9.8 in.) to minimize problems due to thermal expansion and contraction. They are designed as a surface combustion burner. They may also have a silicon carbide (SiC) coated ceramic lace-like topcoating or metal screen to increase heat transfer to the emitter surface. The heat-up and cool-down time is in the 15- to 30-s range.

Ceramic fiber burners are generally molded into flat rectangular blocks from a mixture of refractory fibers and binders. They are then machined to smooth the surfaces and meet thickness requirements. Some types have the firing surface coated with a high-emissivity material while another type has a molded-in opacifier. Ceramic fiber burners can be molded into cylindrical, conical, or compound shapes to suit special applications. Most ceramic fiber burners are surface combustion burners. One type, manufactured by Marsden, Inc. (Pennsauken, NJ), has an integral opacifier that permits the combustion process to occur about 3 mm (0.12 in.) below the outer surface. This greatly enhances the conversion to radiation efficiency by increasing the surface area and the time for the hot gas molecules to exchange energy to the emitter material. This, in turn, lowers the flame temperature and eliminates the formation of NO_x. An advantage of ceramic fiber burners is the low mass at radiant temperature that permits rapid heat-up (5 s) and instantaneous cool-down (1 s).

In this type of burner, the surface is made of a porous ceramic fiber that is often made in a vacuum-forming process. A relatively new type is now available and is made from a woven ceramic fiber mesh, similar to the wire mesh radiant burners except that ceramic fiber is used instead of metal. The predominant shape used in porous refractory burners is a flat panel. An example is shown in Figure 13.20.

In addition to flat panels, other shapes are also available. Alzeta Corp. (Santa Clara, CA) makes many cylindrically shaped porous refractory burners.^{32,33} For their Duratherm™ burners, sizes range from as small as 2 in. (5 cm) in diameter by 4.5 in. (11 cm) long, to as large as 30 in. (76 cm) in diameter by 180 in. (460 cm) long. Firing rates range from 23,000 Btu/hr (6.7 kW) to 16.5×10^6 Btu/hr (4.83 MW). Bartz et al. (1992) describe the use of an Alzeta porous refractory radiant burner to incinerate volatile organic compounds (VOCs).³⁴ The unique aspect of the combustion system was that the burner was formed into a cylinder and fired inwardly while the VOCs flowed into that inner core with the combustion products where the VOCs were then destroyed as shown in Figure 13.23. Very high VOC destruction efficiencies were measured.

In the early 1960s, the American Gas Association made an extensive study of radiant burners, both gas-fired and electric.³⁵ For the gas-fired burners, they determined what was termed a Gas Infrared Radiation factor (GIR), which was determined as follows:

$$\text{GIR} = \frac{W}{\sigma T_b^4} \quad (13.2)$$

where $W = Q/A$ is the total normal infrared radiation from the burner measured by a spectrophotometer, σ is the Stefan-Boltzmann constant, and T_b is the absolute brightness temperature of the

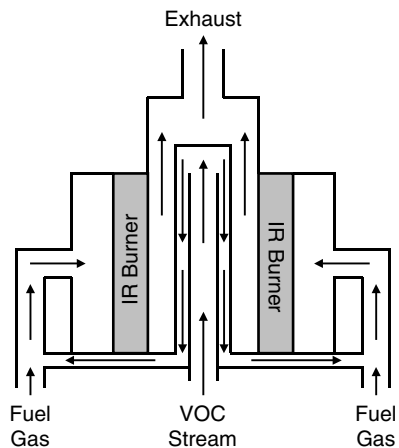


FIGURE 13.23 Inwardly fired porous refractory radiant burner, with heat recovery, for VOC destruction. (Adapted from Reference 34.)

TABLE 13.3
Results of Gas-Fired Infrared Burner Studies

Infrared Burner Type	Emitting Surface	Operating Red Brightness Temperature (°F)	Total Normal Radiation (Btu/hr-ft ²)	GIR Factor
Atmospheric	Ceramic tile or inconel	1400–1650	17,800–32,600	0.51–1.06
Powered	Cordurite, low-density refractory, refractory brick, or inconel	1500–2300	18,000–62,800	0.63–1.17
Catalytic	Glass wool	600–800	800–3300	0.36–0.65

Adapted from Reference 35.

burner surface measured with an optical pyrometer. The GIR factor was similar to a burner emissivity. However, for some of the burners, the GIR factor exceeded 1.0. The GIR factor was approximately 15% higher than the true burner surface emissivity. This is due to the gaseous non-luminous radiation in addition to the surface radiation from the burner. For the burners tested, the GIR factor ranged from 0.36 to 1.17, depending on the burner type. Table 13.3 shows the GIR factors for several types of gas-fired infrared burners, in addition to some other useful operating data. The red brightness temperature was determined using a spectrophotometer in comparison with a blackbody. The study concluded that the flue gas layer contributes up to 18% of the energy input to the useful radiant output and that the layer radiates more than it absorbs. Gas-fired IR burners emit primarily in the 2- to 6-micron region of the IR spectrum. Proper selection of a surface coating for a burner can improve the radiant output. The study also investigated electric IR burners and the spectral absorption characteristics of various loads (e.g., paints, food types, inks, and building materials) heated with IR burners.

Sathe et al. (1990) made experimental measurements and numerical predictions on a porous radiant burner.³⁶ They used the following correlation for flow over circular cylinders for the convection heat transfer coefficient from the flame to the porous refractory:

$$\text{Nu} = 0.989 \text{Re}^{0.33} \quad (13.3)$$

where the characteristic length d is the equivalent particle diameter. Figure 13.24 shows a comparison of the measured and predicted result as a function of the axial location of the flame (x_p) normalized by the porous layer length (L). The figure shows that both the radiant output and the flame speed are fairly independent of the flame location, but are dependent on the equivalence ratio. Zabielski et al. (1991) used an optical technique to measure the radiant characteristics of a porous ceramic fiber radiant burner.³⁷ The macroscopic emittance of the burner was estimated to be 0.70. Xiong and Viskanta (1992) measured the heat flux and calculated the thermal efficiency of a porous matrix ceramic combustor.³⁸ The thermal efficiency declined with firing rate. The heat transfer rate increased with firing rate up to about 45 kW and then slightly declined at a higher firing rate.

Jugjai and Sanitjai (1996) presented a concept for a new type of porous radiant burner incorporating internal heat recirculation to increase thermal efficiency.³⁹ They studied the effects of the optical thickness of the porous medium on the radiant output of porous radiant burners. The optical thickness was increased by added layers of stainless steel wire mesh that formed the porous medium for the burners tested. The added layers improved the heat transfer from the hot gases to the porous medium.

Mital et al. (1996) claimed to have made the first measurements of temperature and species distributions inside submerged flames stabilized inside porous ceramic burners.⁴⁰ They noted the wide discrepancy in the performance of these burners in the literature and in manufacturers' literature.

Rumminger et al. (1996) developed a one-dimensional model of a bilayered reticulated ceramics radiant burner.⁴¹ The model results showed that for a "submerged flame" where the flame is anchored

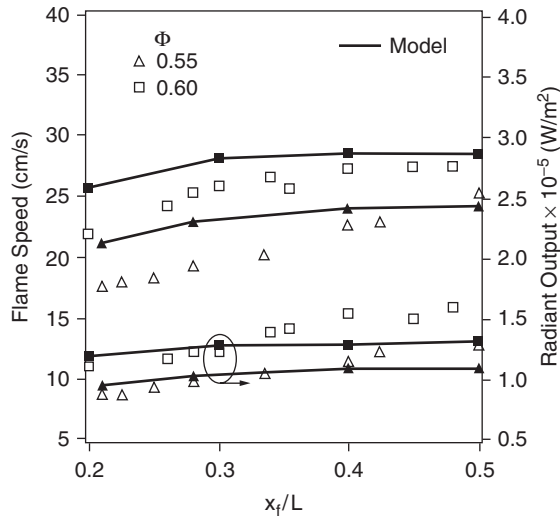


FIGURE 13.24 Measured and predicted flame speed and radiant output for a porous radiant burner. (Courtesy of The Combustion Institute.³⁶)

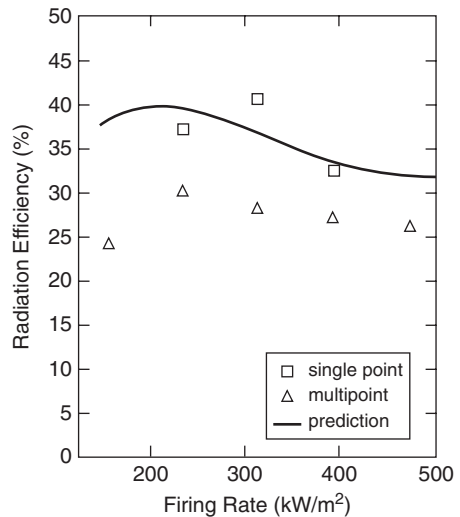


FIGURE 13.25 Predicted and measured radiation efficiency for a porous radiant burner at an equivalence ratio of 0.9. (Courtesy of The Combustion Institute.⁴³)

inside the porous refractory, nearly all of the important reactions occur inside the porous medium. This complicates the study for this type of burner because of the difficulty in making measurements inside the porous medium. They speculated that it is possible that the large internal surface area of the porous medium could affect the chemistry, but there is no data at this time to confirm that possibility.

Van der Drift et al. (1997) studied various coatings on porous foam ceramic IR burners to determine the effects of heat transfer to wet paper and to three colors (white, blue, and black).⁴² They showed that there can be up to a 10% improvement using coated burners compared to a base case metal fiber burner.

Mital et al. (1998) made experimental measurements on a bilayered reticulated ceramic foam made of cordierite.⁴³ Measurements included radiation efficiency using a heat flux gage and burner surface measurements with a type-R thermocouple. Radiation efficiency results are shown in Figure 13.25, which include both single and multi-point measurements and model predictions.

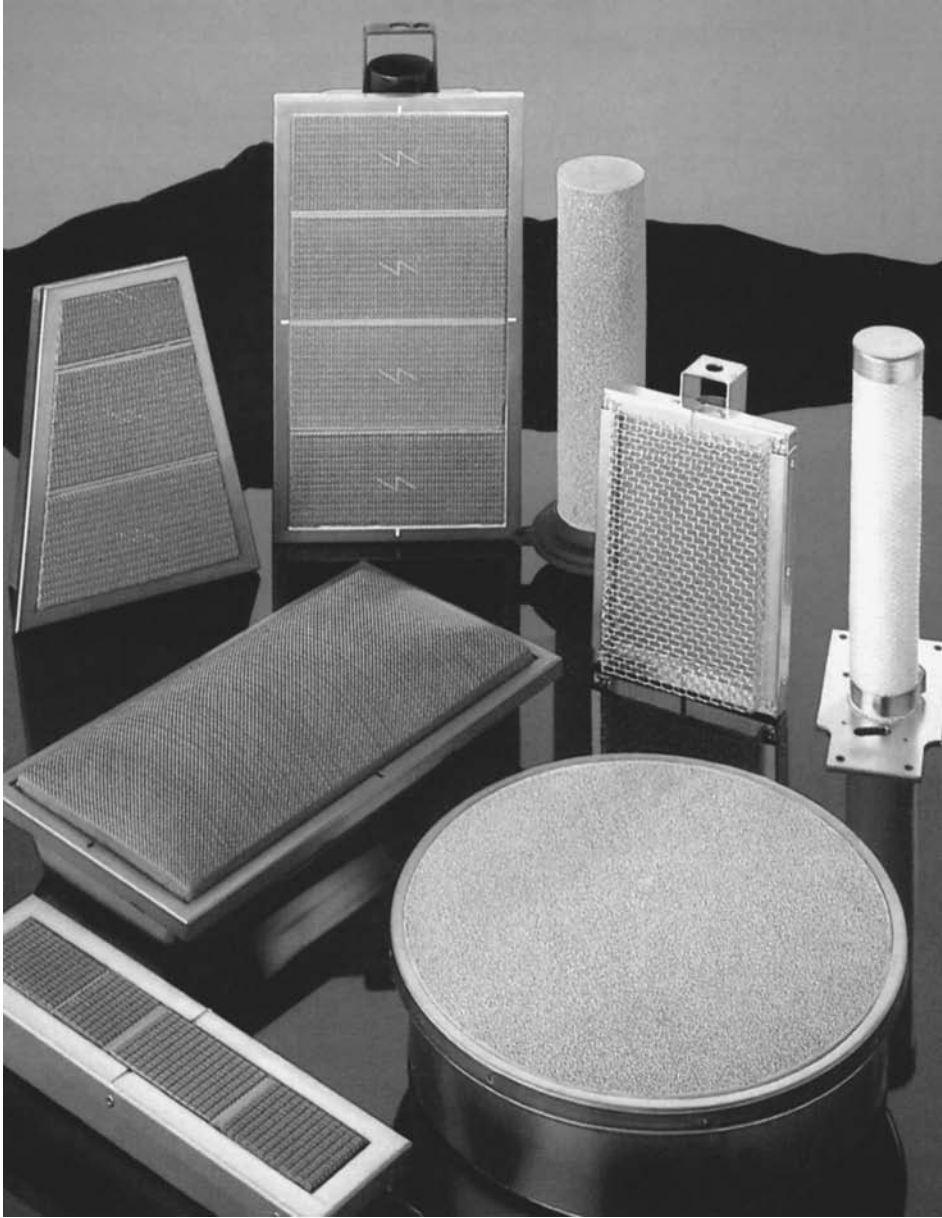


FIGURE 13.26 Examples of porous ceramic and wire mesh radiant burners. (Courtesy of Solaronics.⁴⁴)

13.4.2 PORTED CERAMIC BURNERS

Ported or perforated ceramic burners have a plenum across the open mouth that is mounted to a cast ceramic plate (approximately 12 mm or 0.5 in. thick) with a multitude of very small holes (about 2 mm or 0.08 in.) (12 to 16 holes/cm²). Ported ceramic burners are surface combustion types. They are often fitted with a metal screen to improve their conversion to radiation efficiency, in which case they become a combination surface combustion and impingement type. The relatively high mass produces slow heating and cooling times that are further exacerbated by the metal screen.

Examples of these types of burners are shown in Figure 13.26. Perforated or ported ceramic burners may consist of a pressed ceramic plate, which may include prepunched holes, where the

flames heat the surface directly.⁴⁴ The surface can be textured to further enhance the radiant efficiency of the burner. New developments in ceramic foams are being applied to this type of burner. These foams are often less expensive to make than perforated ceramics. They provide a higher surface area for radiation and a more uniform heating surface, compared to perforated ceramics. Many shapes are possible with the ceramic foams and the pore size is adjustable. Flanagan et al. (1992) described the use of a ported ceramic burner to achieve low NO_x emissions.⁴⁵ However, the burner was actually fired at up to 15 times its normal maximum design firing rate so that the flames were highly lifted and therefore did not radiate from the surface as in normal operation. Mital and Gore (1994) discussed the use of a reticulated ceramic insert to enhance radiation heat transfer in direct-fired furnaces.⁴⁶ The insert was placed downstream of the outlet of a laminar diffusion flame. Experimental results showed up to a 60% improvement in radiative heat flux compared to the case with no insert. The radiative heat flux as a function of radius increased with the insert. Kataoka (1998) described a new type of high-temperature, porous ceramic burner made of aluminum titanate (Al₂TiO₅) capable of surface temperatures up to 1100°C (2000°F).⁴⁷

Wire mesh burners are made from high-temperature-resistant metals, such as stainless steels or inconel. The open area in the mesh serves as the port area for the burner. However, due to the high thermal conductivity of metals, several layers of mesh are often required to prevent flashback. The thermal conductivity between the layers is much less than through the mesh itself because of the contact resistance between the layers. An important problem with wire mesh radiant burners are the lower temperature limits compared to ceramic burners, due to the temperature limits of the metals.

13.4.3 PORTED METAL BURNERS

Ported metal burners are similar to the ported ceramic burners discussed above. Ported metal burners can be classified as surface combustion, impingement, or a combination of the two, depending on design and manufacturer. Due to the high metal mass, the heat-up and cool-down times are measured in minutes. The maximum operating temperature is limited by metal oxidation at the higher temperatures.

13.4.4 FIBER METAL BURNERS

Fiber metal burners use a thin (<2 mm or 0.08 in.) knitted or sintered metal fiber pad as the emitter. They were originally developed as a low NO_x nonradiant burner. These are surface combustion burners and have the lowest conversion to radiation efficiency of all the types above (<20%) at maximum radiant temperatures of about 935°C (1715°F).

13.4.5 FLAME IMPINGEMENT RADIANT BURNERS

This burner is sometimes referred to as a direct-fired refractory burner. An example of this type of burner is shown schematically in [Figure 13.27](#). An actual burner is shown in [Figure 13.28](#). In this type of radiant burner, the flame impinges on a hard ceramic surface, which then radiates to the load. The heat transfer from the flame to the tile is mostly by convection due to the direct flame impingement. The heat transfer from the burner tile to the load is typically purely by radiation. The hot exhaust gases from the burner heat up the surrounding wall by convection, but at a much lower rate than to the burner tile. One advantage of this type of burner is that there is no metal matrix with lower temperature limits compared to ceramic, which has high temperature limits. Therefore, this type of burner can often be used in higher-temperature applications. There also is no matrix of porous ceramic fiber refractory that could get plugged up as in the next type of burner. This type of burner can also fire a liquid fuel, as opposed to many other radiant burners that use only gaseous fuels. A disadvantage is that the heat flux is not as uniform as other types of radiant burners. Another problem is that the burner tile has the typical problem of thermal cycling, which can cause the tile to disintegrate over time and become a maintenance issue.

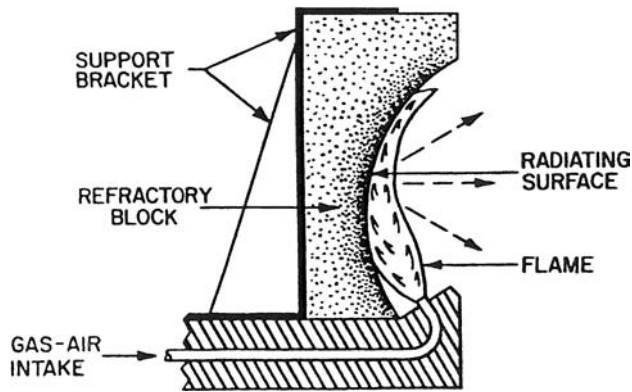


FIGURE 13.27 Schematic of a flame impingement radiant burner. (Courtesy of American Gas Association.³⁵)

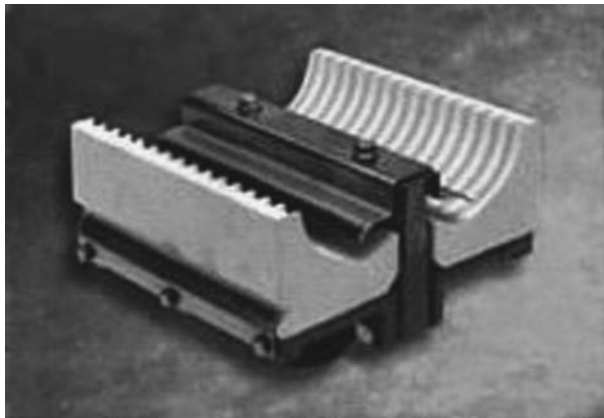


FIGURE 13.28 InfraRad ceramic radiant infrared burner. (Courtesy of Eclipse, Rockford, IL.)

13.4.6 CATALYTIC BURNERS

Catalytic heaters operate at comparatively low temperature ($<475^{\circ}\text{C}$ or $<887^{\circ}\text{F}$). Non-aerated fuel gas is introduced into a plenum behind a catalytically doped fiber pad. An electric heating coil is layered within the fiber pad to preheat it so the catalytic reaction can proceed between the introduced fuel gas, the catalyst, and oxygen in air, which diffuses into the pad from its outer surface. Very low radiant power is generated because of the low operating temperature ($<15\text{ kW/m}^2$ or $4800\text{ Btu/ft}^2\text{-hr}$).

13.4.7 ADVANCED CERAMIC RADIANT BURNERS

Tong et al. (1989) showed through computer modeling that the performance of porous radiant burners can be improved by as much as 109% using sub-micron diameter ceramic fibers.⁴⁸ Bell et al. (1992) describe a staged porous ceramic burner that demonstrated low NO_x emissions.⁴⁹ Kendall and Sullivan (1993) studied enhancing the radiant performance of porous surface radiant burners by using improved ceramic, high-temperature, high-emissivity fibers.⁵⁰ Selective emissivity was achieved by coating a standard ceramic fiber burner with an outer layer of ytterbia. The output of the uncoated vs. the coated burner is shown in Figure 13.29. As can be seen, there is a large spike in the output of the coated burner at around $1\text{ }\mu\text{m}$. However, there was no significant improvement

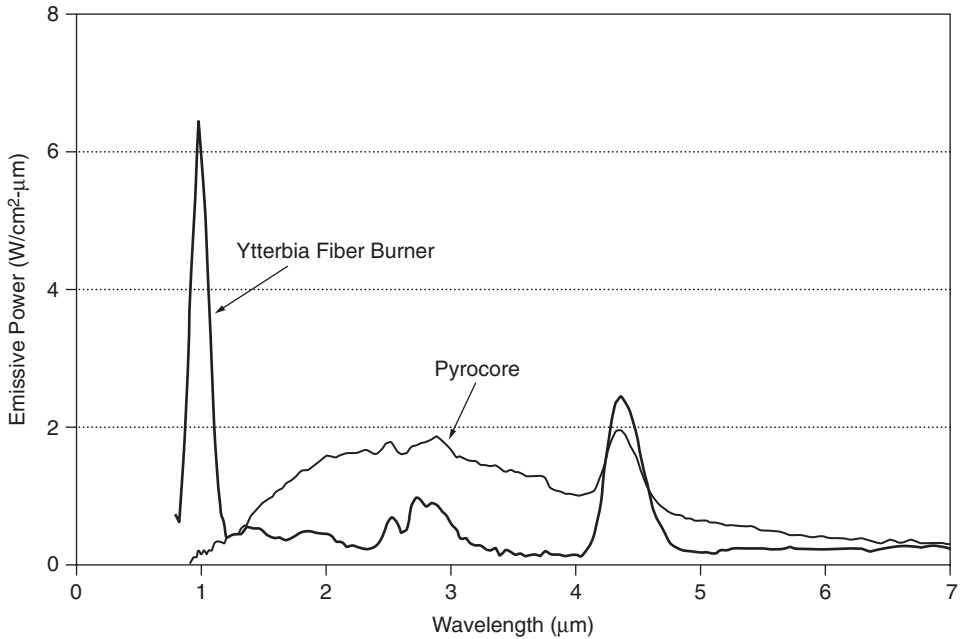


FIGURE 13.29 Emission spectra of ytterbia fiber burner compared to Alzeta (Santa Clara, CA) Pyrocore burner, both operating at 127,000 Btu/hr-ft² (400 kW/m²). (Courtesy of GRI.⁵⁰)

in performance and the durability was in question. In certain applications, there may be a need to have a burner with selective radiant emissions corresponding to selective absorption in the load. Potential applications include glass melting, glass bending and lamination, thin-film drying, and indirect heating. Xiong et al. (1993) described a porous ceramic surface combustor-heater with a built-in heat exchanger for improving the thermal efficiency, as shown in Figure 13.30.⁵¹ Ruiz and Singh (1993) described an advanced IR burner.⁵² The new burner design had considerably higher radiant outputs than the previous style design. The new burner increased a powder paint drying process by 40% and a paper drying process by 200%. Severens et al. (1995) modeled porous radiant burners.⁵³ The one-dimensional model results compared favorably with experimental data for the radiant fraction as a function of the gas velocity through the burner. Bogstra (1998) described a new type of IR radiant burner, referred to as CHERUB, with a closed surface to separate the combustion exhaust gases from the product being heated.⁵⁴ The burner had an enclosed, flat, multi-burner system that heats a ceramic radiant plate. The burner was reported to have a radiant efficiency of 80%, compared to an efficiency of 40% for conventional high-temperature radiant burners.

As previously discussed, one of the limitations of porous refractory burners is the burner surface temperature. If the firing rate density is to be increased, new refractory materials are needed that can withstand continuous operation at higher temperatures, while maintaining their integrity during thermal cycling. One example of research to develop improved radiant burner materials is by Superkinetic, Inc. (Albuquerque, NM) with funding from the U.S. Dept. of Energy.⁵⁵ Three single-crystal ceramic fibers were produced and two fiber materials were successfully made into felt for testing as radiant burner screen surfaces. The materials were alpha-alumina and alpha-silicon carbide, which were successfully bonded with a high-temperature ceramic to form the burner screens that were 95% porous. The purpose of this project was to develop materials capable of radiant burner service near 3000°F (1900°K), compared to conventional radiant burner surface temperatures of about 1800°F (1300°K). The new materials performed well in actual burner operation, but more research was recommended.

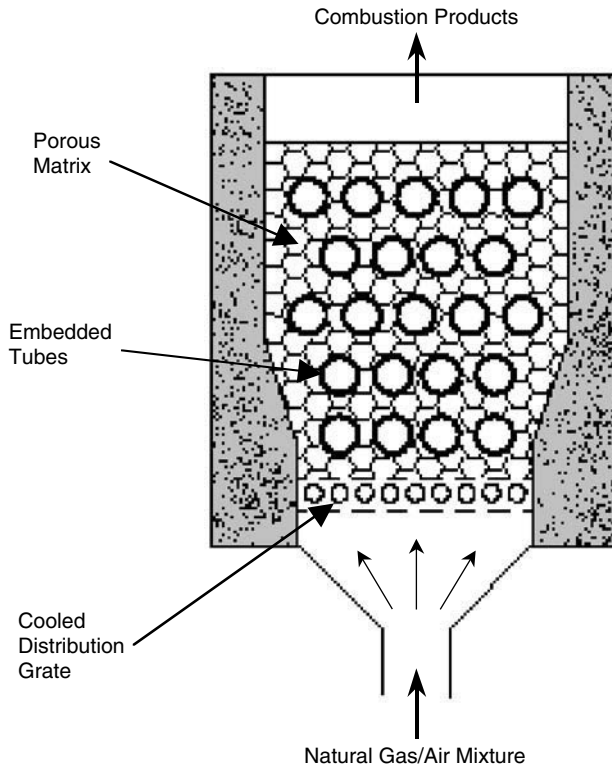


FIGURE 13.30 Surface combustor-heater concept. (Adapted from Reference 51.)

13.5 TESTING AND CHARACTERIZATION

13.5.1 RADIATION EFFICIENCY

One of the challenges of gas-fired IR burners is determining the radiant efficiencies. Mital et al. (1998) noted that there is a wide discrepancy in the reported radiant efficiencies (varying by more than 200%) for radiant burners.⁵⁶ Part of the discrepancy was attributed to a lack of a standard measurement technique to determine the efficiency. Other problems include nondiffuse radiation from the burners and nonuniform burner surfaces. They presented a technique that is not sensitive to burner surface nonuniformities. A calorimetric method was used to check the consistency of the data. It was shown that single-point radiation measurements can deviate considerably from more rigorous multi-point measurement techniques. Yetman (1993) described a simple technique for measuring the total radiant output of an IR burner using a narrow angle pyrometer.⁵⁷ Johansson (1993) presented a method for measuring the spectral output of radiant burners using an IR spectrometer.⁵⁸

Madsen et al. (1996) measured the spectral radiation from several types of radiant burners.⁵⁹ The spectra were fairly similar, with distinctive peaks around 3 and 4.5 μm . This shows the selective emittance of certain types of radiant burners and the possibility of matching the burner to the load spectral absorptivity to optimize heat transfer efficiency.

Radiation efficiency is a controversial measurement that is often overstated in manufacturers' literature. The true measure of radiation efficiency (conversion to thermal radiation efficiency) measures the global thermal radiation output according to accepted formulas and measurement means and divides it by the gross fuel input:

$$\eta_{\text{rad}} = \frac{\text{Radiant output}}{\text{Gross fuel input/Unit area}} \quad (13.4)$$

Example 13.1

Given: 20 kW/m² radiant output at 100 kW fuel input, 1 m² burner output area.

Find: Radiation efficiency.

Solution:

$$\eta_{\text{rad}} = \frac{\text{Radiant output}}{\text{Gross fuel input/Unit area}} = \frac{20 \text{ kW/m}^2}{100 \text{ kW/1m}^2} = 0.20 = 20\%$$

The performance of a gas thermal radiation burner is often optimistically given as “combustion intensity” or “energy release,” which is actually either the gross energy input or total thermal radiation plus conductive/convective output. Neither of these are the true measure of radiation efficiency.

Testing methods can be very sophisticated, utilizing expensive equipment. A reasonably accurate conversion to radiation efficiency can be obtained by measuring the emitter radiant face temperature using an infrared thermometer (see Figure 13.31) set for 1.0 emissivity, measuring the fuel gas input with a flow meter and measuring the actual radiant area of the emitter not including nonradiant perimeter frames, clamps, etc. The thermal radiation heat flux between surfaces can be calculated according to the formula:

$$q_r \text{ (kW/m}^2\text{)} = \sigma * \{T_s^4 - T_r^4\} * F_s * F_r * A \quad (13.5)$$

where q_r is the thermal radiation heat flux between the source and the receiver in kW/m²; $\sigma = 5.669 \times 10^{-8}$ W/m²-K⁴ (Stephan-Boltzmann constant); T_s and T_r are the absolute temperatures of the source



FIGURE 13.31 Example of an infrared pyrometer measuring the surface temperature of a porous refractory matrix burner.¹⁹

and receiver in degrees Kelvin, respectively; F_s and F_r are the emittances of the source and receiver, respectively; and A is the arrangement or view factor.

Example 13.2

Given: Source or emitter temperature = 836°C, the receiver (sink or load) temperature = 40°C, the source (emitter) emittance is 0.97, the receiver (sink or load) emittance is 0.90, and the arrangement factor is 0.95.

Find: Radiant flux from the source to the receiver.

$$\text{Solution: } q_r = (5.669 \cdot 10^{-8})[(836 + 273.15)^4 - (40 + 273.15)^4](0.97)(0.90)(0.95) = 70,700 \frac{\text{kW}}{\text{m}^2}$$

The radiant area in square meters (m^2) is then multiplied by the calculated thermal radiation output/ m^2 to obtain the emitter's thermal radiation output in kilowatts (kW). The emitter's thermal radiation output is then divided by the fuel gas energy input (in kW) to obtain the emitter's conversion to radiation efficiency. The actual heat flux between the emitter and a target to be heated is then a factor of the target's temperature, emissivity, and view angle.

The thermal radiation thermometer when set for an emissivity of 1.0 will give the temperature of the emitter as if the emitter's emissivity were 1.0. The actual emitter temperature will be greater and the emitter's emissivity will be lower. By setting the thermometer emissivity at 1.0, the actual thermal radiation output of the emitter is equated to the formula calculation to obtain a reasonably accurate result.

13.5.2 HEAT TRANSFER COEFFICIENT

The heat transfer coefficient between the hot exhaust products and the radiant burner material is difficult to predict and measure due to the uncertainty in the surface area of the ceramic structure. These coefficients have traditionally been presented in terms of a volumetric coefficient (Btu/hr-°F-ft³ or kW/°C-m³). Chen et al. (1987) assumed the coefficient was large enough that the temperature of the solid was essentially the same as the temperature of the hot flowing gas.⁶⁰ Sathe et al. (1990) used a value of 2×10^9 W/m³-K (1×10^8 Btu/hr-°F-ft³) computed for cylinders in cross flow.⁶¹ Hsu et al. (1993) used 10^7 W/m³-K (5×10^5 Btu/hr-°F-ft³).⁶² Younis and Viskanta (1993) empirically determined the following correlation for alumina and cordierite ceramic foams with pore diameters ranging from 0.29 to 1.52 mm (0.011 to 0.0598 in.):⁶³

$$\text{Nu} = 0.819 [1 - 7.33 (d/L)] \text{Re}^{0.36[1 + 15(d/L)]} \quad (13.6)$$

where d is the actual pore diameter and L is the thickness of the specimen in the flow direction. Fu et al. (1998) noted the relationship between the volumetric heat transfer coefficient h_v and the convection coefficient h .⁶⁴

$$h_v = a_v h \quad (13.7)$$

where a_v can be computed using the following empirical equation:

$$a_v = 169.4 \text{ PPC} (\text{m}^2/\text{m}^3) \quad (13.8)$$

where PPC is the number of pores per centimeter for cellular ceramics. Four different choices for the characteristic dimension were identified: the reciprocal of the surface area,

$$d_a = 1/a_v \quad (13.9)$$

the hydraulic diameter,

$$d_h = 4\phi/a_v \quad (13.10)$$

the mean pore diameter,

$$d_m = \frac{\sqrt{4\phi/\pi}}{\text{PPC}} \text{ (cm)} \quad (13.11)$$

and the ratio of the inertial to the viscous friction coefficients,

$$d_r = \beta/\alpha \quad (13.12)$$

where ϕ is the porosity, β is the inertia coefficient in the Reynolds-Forchheimer equation, and α is the viscous coefficient in the Reynolds-Forchheimer equation. The following empirical correlations, using each of these characteristic dimensions, were developed for specimens having a PPC ranging from 4 to 26:

$$\text{Nu}_v = \left[0.0426 + \frac{1.236}{L/d_m} \right] \text{Re}_{d_m} \text{ for } 2 \leq \text{Re}_{d_m} \leq 836 \quad (13.13)$$

$$\text{Nu}_v = \left[0.0730 + \frac{1.302}{L/d_h} \right] \text{Re}_{d_h} \text{ for } 3 \leq \text{Re}_{d_h} \leq 1594 \quad (13.14)$$

$$\text{Nu}_v = \left[0.0252 + \frac{1.280}{L/d_a} \right] \text{Re}_{d_a} \text{ for } 1 \leq \text{Re}_{d_a} \leq 480 \quad (13.15)$$

$$\text{Nu}_v = \left[0.000267 + \frac{1.447}{L/d_r} \right] \text{Re}_{d_r} \text{ for } 0.02 \leq \text{Re}_{d_r} \leq 2.4 \quad (13.16)$$

where Nu_v is the volumetric Nusselt number, defined as:

$$\text{Nu}_v = \frac{h_v l_c^2}{k} \quad (13.17)$$

where l_c is the characteristic pore length and k is the thermal conductivity of the gas. The uncertainty in the correlations was largest for the smaller Reynolds numbers.

13.6 CONCLUSION

Thermal radiation burners are used in a wide range of heating and drying applications. They have a number of unique properties compared to other burners, including very uniform surface temperatures, high conversion of fuel energy to thermal radiation, flat shapes, very low pollutant emissions, and some have the ability to heat up and cool down very rapidly. These burners can be used to supplement other heating and drying techniques, or they can be the primary source of heat. They are commonly

fired on fuel gases such as natural gas. They offer the end user considerable flexibility in how they are applied and operated. They will continue to play an important role in industry.

REFERENCES

1. J.R. Howell, M.J. Hall, and J.L. Ellzey, Combustion within porous media, in *Heat Transfer in Porous Media*, Y. Bayazitoglu and U.B. Sathuvalli, Ed., ASME, HTD-Vol. 302, 1–27, 1995.
2. D. Traub, Indirect vs. direct: the heat transfer method does affect the process, *Process Heating*, 6(2), 26–29, 1999.
3. R.M. Fedler and R.W. Rousseau, *Elementary Principles of Chemical Process*, third edition, John Wiley & Sons, New York, 2000.
4. T. Kudra and A.S. Mujumdar, *Advanced Drying Technologies*, Marcel Dekker, New York, 2002.
5. Anonymous, Ceramic tile burner improves performance of infrared predryer, *Process Heating*, 4(7), 43–45, 1997.
6. P. Mattsson, J. Perkonen, and A. Riikonen, Infrared drying of coated paper, *Proc. 1989 International Gas Research Conf.*, T.L. Cramer, Ed., Government Institutes, Rockville, MD, 1989, 1308–1316.
7. M. Pettersson and S. Stenström, Evaluation of gas-fired and electrically heated industrial infrared paper dryers, *Proc. 1998 International Gas Research Conf.*, Vol. V: Industrial Utilization and Power Generation, D. Dolenc, Ed., Government Institutes, Rockville, MD, 1998, 100–112.
8. Thomas M. Smith, *Heat Transfer Dynamics*, TAPPI 1994 Non-Woven Conference.
9. J. Riikonen, E. Härkönen, and S. Palosaari, Modeling of Infrared Drying of Pulp, in *Drying '87*, A.S. Majumdar, Ed., Hemisphere, Washington, D.C., 1987, 18–23.
10. A. Williams-Gardner, *Industrial Drying*, Leonard Hill, London, 1971.
11. R.B. Keey, Dryers, in *International Encyclopedia of Heat & Mass Transfer*, G.F. Hewitt, G.L. Shires, and Y.V. Polezhaev, Eds., CRC Press, Boca Raton, FL, 1997, 337–342.
12. C.E. Sloan, Drying Systems and Equipment, *Chem. Eng.*, 74(14), 169–200, 1967.
13. B.J. Ezerski and G.P. Megan, Boosting the performance of your convection oven, *Process Heating*, 7(1), 22–26, 2000.
14. J.R. Cornforth, Ed., *Combustion Engineering and Gas Utilisation*, E&FN Spon, London, 1992.
15. U.S. EPA, *Compilation of Air Pollutant Emission Factors, Vol. I: Stationary Point and Area Sources*, Section 4.2.2.6: Paper Coating, fifth edition, U.S. Environmental Protection Agency report AP-42, Washington, D.C., 1995.
16. U.S. EPA, Paper Industry, Report EPA/530-SW-90-027o, U.S. Environmental Protection Agency, Washington, D.C., 1990.
17. U.S. EPA, Profile of the Pulp and Paper Industry, Report EPA/310-R-95-015, U. S. Environmental Protection Agency, Washington, D.C., 1995.
18. T. Berntsson, P-A Franck, and A. Åsblad, *Learning from experiences with Process Heating in the Low and Medium Temperature Ranges*, CADDET Energy Efficiency, Sittard, the Netherlands, 1997.
19. C.E. Baukal, *Heat Transfer in Industrial Combustion*, CRC Press, Boca Raton, FL, 2000.
20. S. Longacre, Using infrared to dry paper and its coatings, *Process Heating*, 4(2), 45–49, 1997.
21. P. Mattsson, J. Perkonen, and A. Riikonen, Infrared Drying of Coated Paper, *Proc. 1989 International Gas Research Conf.*, T.L. Cramer, Ed., Government Institutes, Rockville, MD, 1989, 1308–1316.
22. C.E. Bean and J.M. Cocagne, Assessment of Gas-Fired Infrared Heaters in the Paper Industry, Gas Research Institute report GRI-96/0087, Chicago, IL, 1996.
23. M. Hannum, T. Robertson, J. Winter, B. Schmotzer, and T. Neville, High Intensity Lean Premix Combustion Systems for Drying Applications, *Proc. 5th European Conf. on Industrial Furnaces and Boilers*, Portugal, Vol. 1, 455–464, 2000.
24. U.S. EPA, *Compilation of Air Pollutant Emission Factors, Vol. I: Stationary Point and Area Sources*, Section 4.9.1: General Graphic Printing, fifth edition, U.S. Environmental Protection Agency report AP-42, Washington, D.C., 1995.
25. U.S. EPA, Profile of the Printing and Publishing Industry, U.S. Environmental Protection Agency Report EPA/310-R-95-014, Washington, D.C., 1995.
26. U.S. EPA, Printing Industry and Use Cluster Profile, U.S. Environmental Protection Agency Report EPA/744-R94-003, Washington, DC, 1994.

27. U.S. EPA, Textile Manufacturing. Report EPA/530-SW-90-027e, U.S. Environmental Protection Agency, Washington, D.C., 1990.
28. Anonymous, Ceramic tile burner improves performance of infrared predryer, *Process Heating*, 4(7), 43–45, 1997.
29. T.M. Smith and C.E. Baukal, Space-age refractory fibers improve gas-fired infrared generators for heat processing textile webs, *J. Coated Fabrics*, 12, 160–173, 1983.
30. U.S. EPA, *Compilation of Air Pollutant Emission Factors, Vol. I: Stationary Point and Area Sources*, Section 4.11: Textile Fabric Printing, fifth edition, U.S. Environmental Protection Agency Report AP-42, Washington, D.C., 1995.
31. R.F. Speyer, W-Y Lin, and G. Agarwal, Radiant efficiencies and performance considerations of commercially manufactured gas radiant burners, *Exp. Heat Transfer*, 9, 213–245, 1996.
32. W.V. Krill and R. Pam, Industrial applications of the pyrocore burner, in *Industrial Combustion Technologies*, M.A. Lukasiewicz, Ed., American Society of Metals, Warren, PA, 1986, 267–271.
33. Alzeta Corp., brochure, Santa Clara, CA, 1998.
34. D.F. Bartz, F.E. Moreno, and P.A. Duggan, Ultra-low, NO_x ultra-high VOC destruction with adiabatic radiant combustors, in *Fossil Fuels Combustion – 1992*, R. Ruiz, Ed., ASME PD-Vol. 39, 7–12, New York, 1992.
35. D.W. DeWerth, A Study of Infra-Red Energy Generated by Radiant Gas Burners, American Gas Association Research Bulletin 92, Catalog No. 41/IR, Cleveland, 1962.
36. S.B. Sathe, M.R. Kulkarni, R.E. Peck, and T.W. Tong, An Experimental and Theoretical Study of Porous Radiant Burner Performance, *Twenty-Third Symposium (International) on Combustion*, The Combustion Institute, Pittsburgh, PA, 1990, 1011–1018.
37. M.F. Zabielski, J.D. Freihaut, and C.J. Egolf, Fuel/air control of industrial fiber matrix burners using optical emission, in *Fossil Fuel Combustion 1991*, R. Ruiz, Ed., ASME PD-Vol. 33, 41–48, New York, 1991.
38. T.-Y. Xiong and R. Viskanta, A basic study of a porous-matrix combustor-heater, in *Fossil Fuels Combustion – 1992*, R. Ruiz, Ed., ASME PD-Vol. 39, 31–39, New York, 1992.
39. S. Jugjai and S. Sanitjai, Parametric studies of thermal efficiency in a proposed porous radiant recirculated burner (PRRB): a design concept for the future burner, *RERIC Inter. Energy Journal*, 18(2), 97–111, 1996.
40. R. Mital, J.P. Gore, R. Viskanta, and S. Singh, Radiation efficiency and structure of flames stabilized inside radiant porous ceramic burners, in *Combustion and Fire*, M. Q. McQuay, W. Schreiber, E. Bigzadeh, K. Annamalai, D. Choudhury, and A. Runchal, Eds., *ASME Proceedings of the 31st National Heat Transfer Conf.*, Vol. 6, ASME HTD-Vol. 328, 131–137, New York, 1996.
41. M.D. Rumminger, R.W. Dibble, N.H. Heberle, and D.R. Crosley, Gas Temperature above a porous radiant burner: comparison of measurements and model predictions, *Twenty-Sixth Symposium (Int'l) on Combustion*, The Combustion Institute, Pittsburgh, PA, 1996, 1755–1762.
42. A. van der Drift, N.B.K. Rasmussen, and K. Jorgensen, Improved efficiency drying using selective emittance radiant burners, *Applied Therm. Eng.*, 17(8–10), 911–920, 1997.
43. R. Mital, J.P. Gore, R. Viskanta, and A.C. McIntosh, An experimental evaluation of asymptotic analysis of radiant burners, *Twenty-Seventh Symposium (International) on Combustion*, The Combustion Institute, Pittsburgh, PA, 1998, 3163–3171, 1998.
44. F. Ahmady, Gas-Fired IR Burners Are Worth Considering, *Process Heating*, 1(2), 38–43, 1994.
45. P. Flanagan, K. Gretsinger, H.A. Abbasi, and D. Cygan, Factors influencing low emissions combustion, in *Fossil Fuels Combustion – 1992*, R. Ruiz, Ed., ASME PD-Vol. 39, 13–22, New York, 1992.
46. R. Mital and J.P. Gore, An experimental study of laminar diffusion flames with enhanced heat transfer by reticulated ceramic inserts, in *Heat Transfer in Fire and Combustion Systems*, W. W. Yuen and K. S. Ball, Eds., ASME HTD-Vol. 272, 7–12, New York, 1994.
47. A. Kataoka, New Type of high temperature surface combustion burner, *Proc. 1998 International Gas Research Conf.*, Vol. V: Industrial Utilization, D.A. Dolenc, Ed., Gas Research Institute, Chicago, 1998, 115–124.
48. T.W. Tong, S.B. Sathe, and R.E. Peck, Improving the performance of porous radiant burners through use of sub-micron size fibers, in *Heat Transfer Phenomena in Radiation, Combustion, and Fires*, R.K. Shah, Ed., ASME HTD-Vol. 106, 257–264, New York, 1989.
49. R.D. Bell, C. Chaffin, and M. Koeroghlian, Experimental Investigation of a Staged Porous Ceramic Burner, in *Fossil Fuels Combustion – 1992*, R. Ruiz, Ed., ASME PD-Vol. 39, 41–46, New York, 1992.

50. R.M. Kendall and J.D. Sullivan, Selective and Enhanced Radiation from Porous Surface Radiant Burners, Gas Research Institute Report GRI-93/0160, Chicago, 1993.
51. T.-Y. Xiong, M.J. Khinkis, B.M. Kramnik, R. Viskanta, and F. F. Fish, An experimental and theoretical study of a porous-matrix combustor-heater, *Proc. 1992 International Gas Research Conf.*, H. A. Thompson, Ed., Government Institutes, Rockville, MD, 2013–2024, 1993.
52. R. Ruiz and S.N. Singh, Enhanced infrared burner system, *Proc. 1992 International Gas Research Conf.*, H.A. Thompson, Ed., Government Institutes, Rockville, MD, 1993, 2410–2419.
53. P.F.J. Severens, P.H. Bouma, C.J.H. van de Ven, L.P.H. de Goey, and A. van der Drift, Modeling of twofold flame behavior of ceramic foam surface burners, *J Energy Resources Tech.*, 117(1), 29–36, 1995.
54. A.N. Bogstra, Development of a new prototype of a flat closed high efficient infrared radiant burner, *Proc. 1998 International Gas Research Conf.*, Vol. V: Industrial Utilization, D. A. Dolenc, Ed., Gas Research Institute, Chicago, 1998, 24–33.
55. Milewski, J.V., Shoultz, R.A., McConnell, M.M.B., and Milewski, E. B., Improved Radiant Burner Material, Superkinetic, Inc., Albuquerque, NM, Final Report, U.S. Dept. of Energy report DOE/EE/15643-T2, 1998.
56. R. Mital, J. P. Gore, and R. Viskanta, A radiation measurement procedure for gas-fired radiant burners, *Proc. 1998 International Gas Research Conf.*, Vol. V: Industrial Utilization, D. A. Dolenc, Gas Research Institute, Chicago, 1998, 197–209.
57. M. E. Yetman, Evaluation of Infrared Generators, *Proc. 1992 International Gas Research Conf.*, H. A. Thompson, Ed., Government Institutes, Rockville, MD, 1993, 2401–2409.
58. M. Johansson, Spectral characteristics and efficiency of gasfired infrared heaters, *Proc. 1992 International Gas Research Conf.*, edited by H. A. Thompson, Govt. Institutes, Rockville, MD, pp. 2420–2426, 1993.
59. O.H. Madsen, K. Jørgensen, N.B.K. Rasmussen, and A. van der Drift, Improved efficiency heat transfer using selective emittance radiant burners, *Proc. 1995 International Gas Research Conf.*, D.A. Dolenc, Ed., Government Institutes, Rockville, MD, 1996, 2208–2217.
60. Y.-K. Chen, R.D. Matthews, and J.R. Howell, The effect of radiation on the structure of a premixed flame within a highly porous inert medium, in radiation, *Phase Change Heat Transfer and Thermal Systems*, Y. Jaluria, V. P. Carey, W. A. Fiveland, and W. Yuen, Eds., ASME, HTD-Vol. 81, 35–42, 1987.
61. S.B. Sathe, R. E. Peck, and T.W. Tong, Flame stabilization and multimode heat transfer in inert porous media: a numerical study, *Comb. Sci. Tech.*, 70, 93–109, 1990.
62. P.F. Hsu, J.R. Howell, and R.D. Matthews, A numerical investigation of pre-mixed combustion within porous media, *J. Heat Transfer*, 115(3), 744–750, 1993.
63. L.B. Younis and R. Viskanta, Experimental determination of the volumetric heat transfer coefficient between stream of air and ceramic foam, *Int. J. Heat Mass Transfer*, 36(6), 1425–1434, 1993.
64. X. Fu, R. Viskanta, and J.P. Gore, Measurement and correlation of volumetric heat transfer coefficients of cellular ceramics, *Exper. Thermal Fluid Sci.*, 17, 285–293, 1998.

14 Radiant Tube Burners

Dennis E. Quinn and John Newby

CONTENTS

- 14.1 Introduction
 - 14.2 Types of Radiant Tubes
 - 14.2.1 Nonrecirculating Tube Types
 - 14.2.2 Recirculating Tube Types
 - 14.2.3 A Brief History of the Application of “Integral” Exhaust Heat Recovery to Radiant Tubes
 - 14.3 Radiant Tube Burners
 - 14.3.1 Inspirator and Pull-Through Burners
 - 14.3.2 Forced-Draft Radiant Tube Burners for Nonrecirculating Tubes
 - 14.3.2.1 Forced-Draft Burners without Integral Heat Recovery
 - 14.3.2.2 Regenerative Burners
 - 14.3.3 Forced-Draft Burners for Recirculating Tubes
 - 14.3.3.1 Single-Ended Radiant Tube Burners
 - 14.3.3.2 Self-Recuperative Burners
 - 14.4 Energy Recovery Methods for Radiant Tubes
 - 14.4.1 Recuperators
 - 14.4.1.1 Insertion-Type Recuperators
 - 14.4.1.2 External Recuperators
 - 14.5 Emission Reduction Techniques
 - 14.6 Heat Transfer Considerations
 - 14.7 Radiant Tube Material Considerations
 - 14.7.1 Metallic Radiant Tubes
 - 14.7.2 Ceramic Radiant Tubes
 - 14.8 Application Considerations
 - 14.9 Combustion Controls for Radiant Tube Burners
 - 14.9.1 Input and Air/Fuel Ratio Control
 - 14.9.2 Flame Supervision
- References

14.1 INTRODUCTION

Indirect firing of the heat processing equipment is essential for many heat treatment processes where the work must not come into contact with the products of combustion or the flame. While separation can be achieved by such means as using an externally heated muffle or saggars to enclose the work, the radiant tube offers many advantages as a source of indirect heating and has become firmly established in the metallurgical heat treatment field. For processes requiring special atmospheres or scrupulously clean conditions in the furnace, it provides very even heat distribution at high intensity. Radiant tubes are normally gas-fired, although oil-fired burners are available.

A radiant tube furnace has one or more radiant tubes inside which the combustion process is completely contained. Heat is given up to the inside wall of the tube, conducted through the wall, and radiated to the work in the furnace. In some cases where a special atmosphere is recirculated within a furnace, heat is also dissipated by convection, but the typical main function of a radiant tube is that of a radiant heat source. There are many different types of radiant tubes for industrial furnaces, but they can generally be subdivided into “straight-through” and “single-ended” types.

14.2 TYPES OF RADIANT TUBES

The straight-through types principally comprise straight, “U”-shaped or “W”-shaped tubes, each of which can be fitted with internal or external recuperators or regenerative burners. The “U”- and “W”-types provide a greater heating path length with consequent increases in heat transfer area and potential efficiency. A specific process or equipment configuration need may dictate that radiant tubes have another geometry.

The single-ended tube type has the burner and flue combined at one end and utilizes an internal tube or structure that takes the hot combustion gases down the tube axis to the closed end of the outer tube, where they are diverted back along the external annulus in a counter-flow direction. A refinement of this principle incorporates a recuperative section closely coupled to the burner head — a single-ended self-recuperative radiant tube (commonly designated SERT).

Radiant tubes are designed to effectively transfer the heat from the combustion products to the radiant tube and subsequently to the load. The tube geometry is based on the load to be heated, the available space to locate the radiant tubes, and the tube material characteristics and limits. It is also important that the temperature of the radiant tube be as uniform as possible to optimize the heating capabilities of the radiant tube and to ensure that no part of the tube is significantly above the mean tube temperature, with that mean being comfortably within the design limits of the tube material selected for the application.

To meet these radiant tube design requirements, two firing system concepts have evolved — *nonrecirculating* and *recirculating* — as designated by Pritchard et al.,¹ each being used in various ways with both straight-through and single-ended designs.

Nonrecirculating radiant tubes are the most common. The distinguishing feature of these tubes is that the combustion products make a single pass through the tube. For a straight-through tube, a burner fires at one end and the products of combustion are exhausted at the other end. In the case of a nonrecirculating, single-ended radiant tube, the burner inlet and radiant tube outlet are located coaxially on the same end of the tube, typically with an annular exhaust surrounding the burner. Nonrecirculating radiant tubes rely on the burner design and adjustment to distribute the heat uniformity over the surface of the tube.

Recirculating radiant tubes use high-velocity burners to entrain combustion products from the exhaust leg of the radiant tube with the jet action of a high-velocity burner, and pump the combined mass of fresh and recirculated products of combustion through the tube. Adding the recirculated products reduces the peak temperature of the burner’s flame envelope and thus the potential for tube hot spots.

14.2.1 NONRECIRCULATING TUBE TYPES

Non-recirculating tubes are manufactured in a number of geometries, as shown in [Figure 14.1](#).

Straight radiant tubes are the simplest to manufacture. These tubes enter the chamber to be heated through one wall and exit on the opposite wall. Straight tubes are typically fixed at the inlet end, with the exit end floating through a gland to allow for differential expansion. Both “U”- style and “W”-style radiant tubes enter and exit the chamber on the same side, usually configured with both entrance and exit legs passing through a single insulated plate (a “bung”) that is either bolted or welded to the furnace casing. The expansion of the tube is allowed for in the method of mounting of the tube to the bung. The “U”- and “W”-styles have the advantage of increasing the exposed

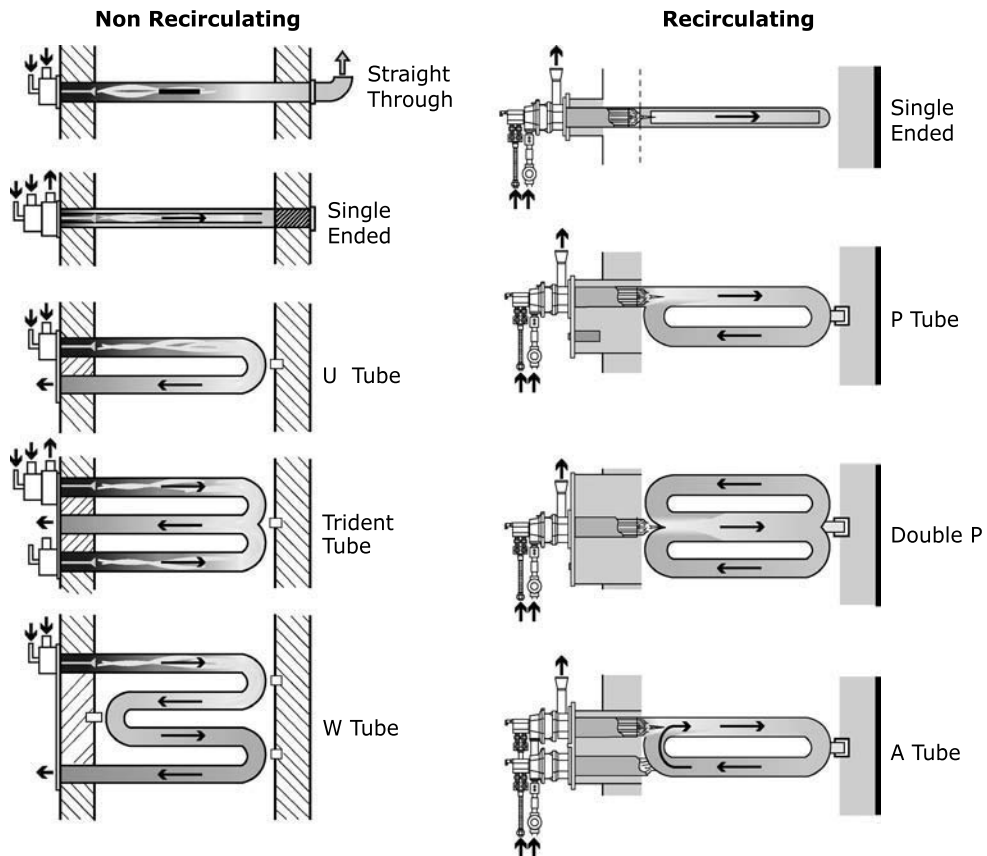


FIGURE 14.1 Nonrecirculating and recirculating radiant tube configurations. (Courtesy of Joachim G. Wunning, WS Thermal Process Technology, Inc., Elyria, OH. With permission.)

heating length and therefore tend to be more efficient than straight-through tubes, as well as reducing the number of penetrations in the furnace casing. The “trident-style” radiant tube was developed to increase the effective total heat transfer from the tube surface. In this type of radiant tube, two burners share a common radiant tube exhaust leg, thereby optimizing the heat transfer of the system. The challenge with the longer radiant tubes is to provide adequate temperature uniformity to avoid local overheating of the tube material. As the length of the radiant tube increases, such as in large “U”- and “W”-type radiant tubes, there is greater potential of deviation in the temperature along the length of the radiant tube. Regenerative burners can greatly improve the temperature uniformity of large nonrecirculating radiant tubes.

The single-ended radiant tube can be built as a nonrecirculating radiant tube. The single-ended tube type has burner and flue combined at one end and utilizes an internal tube or structure that takes the hot gases to the closed end of the outer tube where they are diverted back along the annulus in a counter-flow direction. A refinement of this principle incorporates a recuperative section closely coupled to the burner head — the single-ended self-recuperative radiant tube (commonly designated SERT) — to provide energy savings.

14.2.2 RECIRCULATING TUBE TYPES

Recirculating radiant tubes are produced in several configurations, also shown in [Figure 14.1](#). The most common current configuration is the recirculating single-ended radiant tube where the central tube structure conveying the burner products of combustion is constructed to allow a portion of

the exhausting products to pass from the annulus into the center. However, recent adaptations of 1950s U.K. designs, such as the Wellman Furnaces “Jetube” to include recuperative burners, have produced other configurations such as the “P” tube, the double “P” tube, and the “A” tube for use with regenerative burners.

The main advantage of the recirculating type of radiant tube is that the combustion process is highly dilute, leading to lower flame temperatures and the minimization of hot spots near the flame envelope. Additionally, high recirculation ratios within the tube result in improvement in gas temperature uniformity and correspondingly more uniform tube wall temperatures. A further advantage of recirculating radiant tubes with their inherent flame temperature reduction is a corresponding reduction in thermal NO_x emissions. The mixing of the flame and recirculated, cooled, exhausting products of combustion limits the peak flame temperature and exploits the well-known potential of the use of the recirculated products to reduce the NO_x emissions of the radiant tube — commonly known as the use of flue gas recirculation (FGR). With increasing environmental quality pressures, recirculating radiant tubes are enjoying growth in popularity.

14.2.3 A BRIEF HISTORY OF THE APPLICATION OF “INTEGRAL” EXHAUST HEAT RECOVERY TO RADIANT TUBES

Not a great deal has been written about the history of the radiant tube, but it has been reported² that the first straight, single-ended recuperative radiant tube was developed in Germany in the 1940s. A developmental form of recuperative tube is described in a 1955 paper by Anderson and Broome.³ In the early 1960s, two British gas industry groups pursued its further development. Licensing to manufacturers produced a flood of successful industrial applications in batch and continuous heat treatment furnaces in the U.K. Rapid popularity followed throughout high-fuel-cost industrial Europe and gave rise to further development utilizing the ever-growing base of metallic and ceramic high-temperature materials. Similar developments took place in Japan in the 1970s and 1980s. The use of the single-ended self-recuperative radiant tube is now considered an “industry standard” application.

In the late 1980s, the authors’ company developed and successfully applied compact ceramic regenerators to “U” and “W” tube designs in several large U.S. steel-industry strip line installations.⁴ These led to licensing to Tokyo Gas of Japan and similar applications there in the 1990s, and to local Japanese manufacturers also picking up the regenerative design challenge.

The performance and features of these designs are discussed in later sections of this chapter.

14.3 RADIANT TUBE BURNERS

There are a number of burner options for radiant tubes. Typically, these burners are classified as cold (ambient) air burners, preheated air burners, self-recuperative burners, and regenerative burners. Cold air burners are generally used for lower process temperatures and tube firing rates, where the fuel economies provided by heat recovery cannot be economically justified. At higher temperatures and/or high tube firing rates, recuperators, self-recuperative burners, or regenerative radiant tube burners can be justified. It is important to note that these “lower” and “higher” temperature references are to the temperatures of the exhaust gases of the radiant tube, *not* the heated-process temperature.

Burners for radiant tubes need to provide a uniform heat release profile along the length of the radiant tube to promote an even temperature distribution. A typical limiting factor for radiant tubes is the maximum temperature that the tube material can withstand, given the imposed mechanical load, thermal stresses arising from the heat flux through the tube wall, and the limiting creep stresses. Uneven heat release from the flame and/or combustion products along the length of the radiant tube results in local hot spots: these will either lead to premature tube failure or limit the output for a given radiant tube to that of the lower average temperature. Uniform heat flux from the radiant tube will also likely improve the load temperature uniformity and offer

quality improvement. In practice, few designs come close to providing a uniform heat flux — the exceptions are regenerative burners and highly recirculating tubes.

Before considering the details of the specific types of burners available for radiant tubes, it is appropriate to discuss some system design factors that significantly influence the choice of burner for an application.

Just as with any other fired system, the radiant tube's internal space that forms the combustion chamber can be chosen to be fired under suction, under pressure, or "neutral," compared with the atmospheric pressure or the pressure in the chamber that the tube is heating. A combination of factors can affect this choice. A major consideration for furnaces using a controlled atmosphere to produce specific qualities in the heated product can be the effect of a ruptured tube on the atmosphere: if a pressurized tube ruptures, combustion products will leak out and mix with the furnace atmosphere if the tube pressure is higher than the internal atmosphere pressure in the furnace. In such a case, it is common for the furnace designer to specify a suction or neutral pressure condition inside the tube, such that furnace atmosphere will be drawn into the tube if a crack develops in the tube, and it will not be necessary to shut down the furnace to find "a leaker." These systems can be provided as suction-only systems with no pressure air supplied, or as "push-pull systems" that use a combination of forced air supply to the burner and induced exhaust at the outlet such that the resulting tube internal pressure is slightly negative to the furnace internal pressure.

Another influence on the system choice can be the furnace layout or physical space constraints. Forced-draft systems, with burners supplied with pressure air and fuel, are conventionally preferred because of the fine degree of control that can easily be exerted over the fuel input and burner air/fuel ratio. Such a system, however, requires air, fuel, and exhaust piping to each radiant tube in the system. If space is tight, or for economic considerations, it might be prudent to use an all-suction system in which the exhaust is directly coupled to a draft-producing device and the combustion air is pulled in as ambient air from the furnace surroundings, thereby eliminating the need for a forced combustion air supply. This situation is also most applicable to vertical radiant tube-fired furnaces where tubes are installed at many elevations and the system designer is faced with the effects of buoyancy in considering the distribution of flows in vertical manifolds. For "basic" systems, although not popular today because of their inherent lack of ability to closely control air/fuel ratio, high-pressure fuel can be used to inspirate ambient air into the burner inlet and eliminate the need for combustion air piping, when a low-resistance tube and exhaust system is in use.

The following discusses burners applicable to these various scenarios.

Most radiant tube burners are of nozzle-mixing design and have long flames resulting from delayed combustion. The common approach to achieve a delay in the combustion of the fuel is to have multiple air entry points that stage the mixing of the air into the fuel within the tube. This design approach allows greater control of the heat release within the radiant tube. Burners designed specifically for recirculating-style tubes will typically use a high-velocity burner rather than a delayed combustion design in order to have sufficient burner jet energy to promote recirculation. Thermal efficiency must also be considered in the design and selection of radiant tube burners. Incorporation of an exhaust heat recovery means is the standard approach to enhancement of thermal efficiency.

14.3.1 INSPIRATOR AND PULL-THROUGH BURNERS

Inspirator and pull-through burners are designed to be used without a pressure combustion air supply. In the inspirator style, all the combustion air is pulled in by the entrainment action of a high-pressure fuel jet, although sometimes with the assistance of the "pull" created by a vertical exhaust stack on the tube or by a close-coupled induced draft system. Pull-through burners use only an induced draft system to pull the combustion air into the burner. Adjustable shutters on the entrance of the burner can be used to adjust the flow of combustion air relative to the applied suction. [Figure 14.2](#) illustrates a typical pull-through radiant tube burner.



FIGURE 14.2 “Pull-through” radiant tube burner.

The main advantage of the inspirator and pull-through radiant tube burners is the simplicity of the combustion system. Requiring only that the fuel supply be connected to the burner, combustion air piping is eliminated and installation costs are low.

Because the combustion air is not metered in an inspirator or pull-through burner design, it is difficult to maintain the optimum fuel/air ratio for combustion. The fuel/air ratio is subject to the local ambient conditions, including temperature and humidity fluctuations as well as the inherent ratio characteristics of the air entraining feature. Many of the environments in which radiant tube burners are installed are dirty, any plugging of the air passages leading to a change in the fuel/air ratio.

The low-pressure drop style of fuel and air mixing inherent in a typical simple inspirator or pull-through burner limits the degree to which control over mixing can influence the production of a uniform temperature profile along the length of the radiant tube.

These limitations of the simple inspirator and pull-through burner designs are largely eliminated by forced-draft radiant tube burners.

14.3.2 FORCED-DRAFT RADIANT TUBE BURNERS FOR NONRECIRCULATING TUBES

Forced-draft burners receive combustion air from an external source, typically a low-pressure (1 psig or less) combustion air blower. Pressurizing the combustion air supplied to the burner allows for a variety of combustion controls to be applied to maintain the desired fuel/air ratio over a range of burner firing rates. With pressure combustion air and metering, the potential firing efficiency of this type of radiant tube burner is higher than its pull-through counterpart.

14.3.2.1 Forced-Draft Burners without Integral Heat Recovery

Forced-draft burner designs are available for both ambient air and preheated combustion air from an external recuperator. In many cases, the burner design is the same for both but uses different materials of construction to accommodate the higher burner body and flame stabilizer temperatures from the use of preheated air.

Forced-draft burners often incorporate a means to adjust the flame length to allow it to be matched to a particular radiant tube length or configuration. An old rule of thumb often used for “U” tubes is to adjust the flame length so that it can just be seen coming around the U bend when looking up the exhaust leg. Some burner designs require mechanical adjustment of the flame stabilizer location during installation of the radiant tube burner in order to change flame length. A more desirable method is to provide separate combustion air paths to a primary, secondary, and

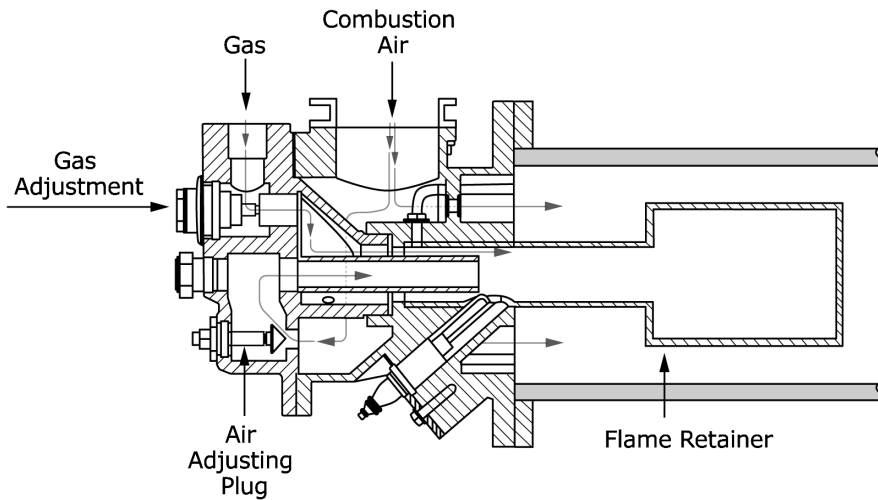


FIGURE 14.3 Forced-draft radiant tube burner.

sometimes tertiary combustion zone, with adjustment of the relative flow rates to each. This approach allows for the rate of mixing and combustion to be controlled in each zone with resulting variation of the flame characteristics. Burners of this design typically have an external adjustment to vary the portion of air introduced into the primary zone, having the advantage of adjustment capability with the burner in operation, allowing visual fine-tuning of the flame characteristics. [Figure 14.3](#) illustrates a typical forced-draft radiant tube burner.

14.3.2.2 Regenerative Burners

Regenerative burners combine both the burner and the heat recovery device into a single package and are capable of providing the highest thermal efficiencies of all the radiant tube burner styles. Thermal efficiencies on an HHV-available-heat basis range from 75 to 85% for regenerative burners.

Within the burner structure is a heat storage bed. One such burner is mounted on each end of the nonrecirculating radiant tube. One burner will fire while the companion burner will exhaust the products of combustion from the tube for a specific period, typically from 20 to 60 s. At the end of the period, the operation is reversed: the burner that was previously firing is placed in exhaust mode while the burner that was previously exhausting is placed in firing mode. The periodic cycling continues while there is a demand for heat by the process.

The combustion air to the firing burner is heated within the heat storage bed by recovering the heat stored in the bed material during the previous exhaust cycle. The resulting air temperature is typically within 200°F of the temperature of the radiant tube exhaust gases. The preheated combustion air is then delivered to the burner nozzle where fuel is introduced, mixing occurs, and combustion is initiated by a pilot burner. In the exhausting mode, the hot exhaust gases from the radiant tube pass the burner nozzle to enter the regenerative bed. These gases heat the bed material that was previously cooled during the firing cycle. The cooled exhaust gases are then either vented to atmosphere or taken away by a directly connected exhaust collection system, depending on the particular combustion system configuration. Some portion of the cooled exhaust gas may be directly recirculated to the firing burner for NO_x emission reduction purposes.

The regenerative bed typically takes the form of either loose packing such as balls, or a monolithic design of supported webs with through-gas passages, both normally of ceramic material. Loose packing is housed in a container that allows either vertical or horizontal flow through the bed, depending on the burner configuration. [Figure 14.4](#) illustrates a typical regenerative burner

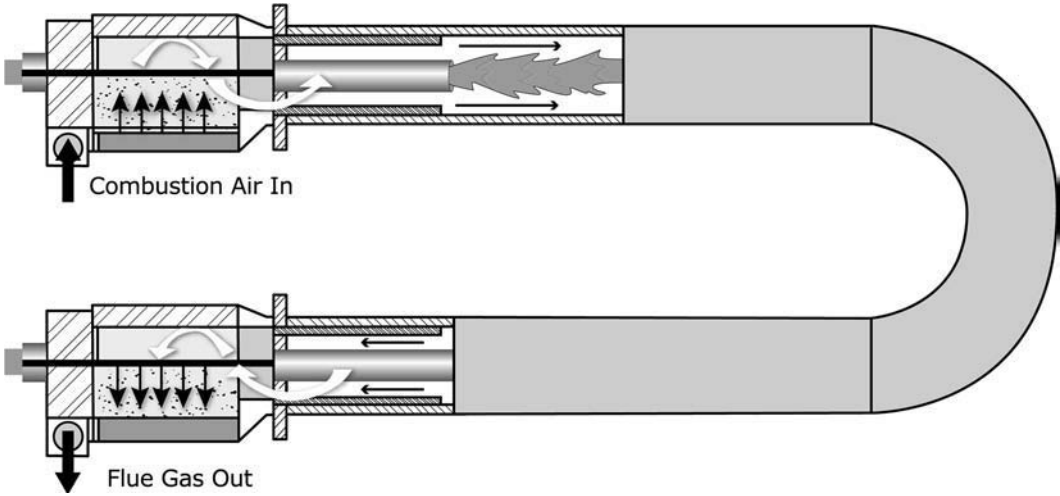


FIGURE 14.4 Regenerative radiant tube burner.

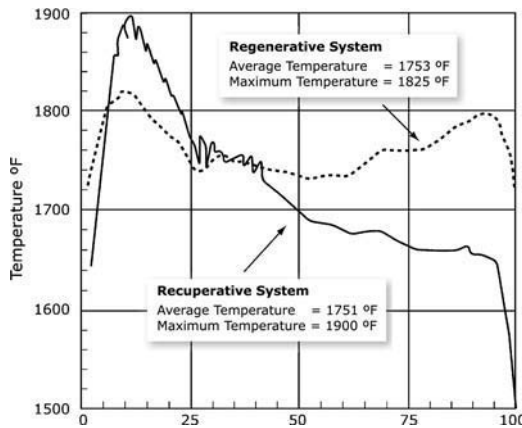


FIGURE 14.5 Comparison of actual tube temperature profiles for recuperative and regenerative tubes at an average temperature of 1750°F.

employing a loose-packed bed. The vertical flow path has the advantage that gravity maintains the bed material location, which is critical to maintaining thermal performance over time. For horizontal packing geometries, the bed housing and interior baffles are used to ensure that material settlement due to thermal cycling and vibrations typical around most industrial furnaces do not allow the products of combustion or the air to bypass the storage bed.

Regenerative burners offer several advantages in the firing of radiant tubes. The inherently high thermal efficiency leads to the highest possible fuel savings and thus to reduced operating costs. Potentially even more significant is the improvement in the temperature uniformity of the radiant tube provided by the alternate firing from each end of the tube, especially on large, long tubes. Figure 14.5 compares the temperature distribution of a regeneratively fired tube and a conventional forced-draft burner-fired recuperated tube.

The improved tube temperature uniformity inherent with regenerative burners leads directly to improved radiant tube life. Small reductions in peak tube temperature result in operating the tube material at the higher creep strength of the average operating temperature of the radiant tube. A second benefit of an improvement of the temperature uniformity for a given radiant tube is that

more heat can be transferred for a given average temperature, and thus more transferred while not exceeding the maximum tube temperature service limit. The advantage of improving the temperature uniformity can be realized through an increase in the heating capability of an existing furnace without negative impact on the tube life, or in a reduction in the size of the heating zone at the design stage of a new furnace. Finally, improvement in the thermal profile can be expected to have a positive impact on the heating quality of the load.

14.3.3 FORCED-DRAFT BURNERS FOR RECIRCULATING TUBES

Although ambient air burners have been used with recirculating tubes, self-recuperative burners have become the accepted means of firing these tubes.

14.3.3.1 Single-Ended Radiant Tube Burners

Early single-ended radiant tubes used ambient air burners. However, self-recuperative burners are now more commonly used, given the proximity of burner and exhaust. Single-ended radiant tube burners fire into small-diameter tubes or tubular structures mounted on the axis of a larger-diameter, outer tube capped at one end. The products of combustion from the combustion process in the inner tube return in an annulus around the inner tube and exhaust around the burner. The relative location of the outer flue gases makes for an ideal match with the self-recuperative burner geometry (Figure 14.1).

Single-ended radiant tube burners must provide combustion of a relatively low-intensity within the inner tube, especially when used with nonrecirculating style tubes. The operating temperature limit of the center tube material is a limiting factor.

14.3.3.2 Self-Recuperative Burners

Self-recuperative burners are commonly used on single-ended style radiant tubes and on some of the newer styles of recirculating radiant tubes. These burners integrate the burner components and a heat exchanger into a single package. Because the burner nozzle is mounted directly on the end of the air side of the recuperator, there are no air-side heat losses. Accordingly, self-recuperative burners often have higher efficiencies than their remote-recuperator counterparts. Typical thermal efficiencies of 65 to 72% on an HHV-available-heat basis are achieved. Figure 14.6 illustrates a typical self-recuperative radiant tube burner.

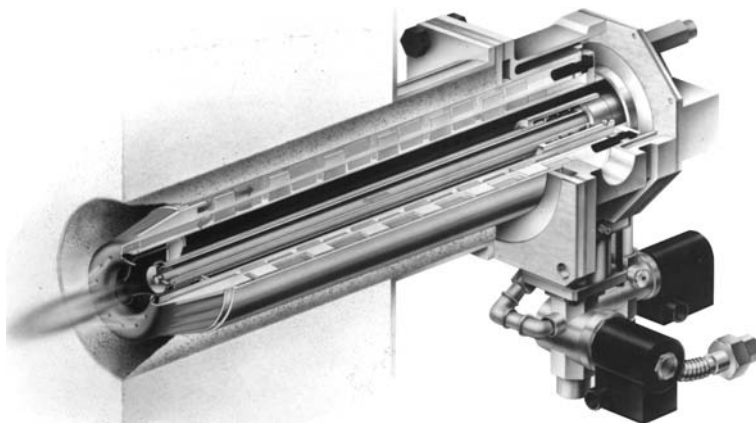


FIGURE 14.6 Self-recuperative radiant tube burner. (Courtesy of Joachim G. Wunning, WS Thermal Process Technology Inc., Elyria, OH. With permission.)

14.4 ENERGY RECOVERY METHODS FOR RADIANT TUBES

Regenerators and recuperators integrated with burners were described in Chapter 14.3. Non-integrated heat recovery devices are described below.

14.4.1 RECUPERATORS

Recuperators using radiant heat transfer from the exhaust gas to the heat transfer partition, in conjunction with preheated air burners, are the typical choice for radiant tube applications. These recuperators can be an insertion type (also known as “plug-in”) in the exhaust end of the radiant tube itself, or externally mounted and connected to the tube by a short section of insulated ductwork.

14.4.1.1 Insertion-Type Recuperators

The insertion-type recuperator (Figure 14.7) is placed into the exhaust leg of the tube. Typical thermal efficiencies on an HHV-available-heat basis for this class of recuperator are 50 to 55%.

A typical design has the exhaust gases passing through an outer annulus formed by the outside wall of the recuperator partition and the inside wall of the radiant tube exhaust leg. It will include fins, sometimes staggered, to increase the heat transfer on one or both sides of the partition. The air side of the recuperator will consist of two passes: one to deliver the combustion air to the recuperator and the other to return the air to the exit of the recuperator, although only one of them truly constitutes a heat transfer pass with the exhausting products of combustion. The preheated air is then connected to the companion burner, usually on the other end of the same radiant tube, although it may be on an adjacent tube in the same firing group if more convenient in the particular physical layout.

Located within the exhaust leg of the radiant tube as it passes through the furnace wall, the insertion-type recuperator minimizes external space requirements. Additionally, ambient losses are minimized by containment within the furnace wall. However, care must be taken so that the end of the insertion-type recuperator does not extend within the heated interior of the furnace chamber. Should the recuperator be allowed to extend past the wall and into the part of the radiant tube within the furnace chamber, then useful energy that would otherwise be available for heating the load will be extracted into the recuperator, both limiting the heat available to the furnace and reducing the effectiveness of the recuperator.

14.4.1.2 External Recuperators

An alternative to the internal recuperator is an externally mounted recuperator. For best efficiency, external recuperators are normally of the counter-flow type, with the cold combustion air entering near the flue gas outlet and the preheated combustion air exiting near the flue gas inlet. The preheated air is then connected to the companion burner. Figure 14.8 illustrates a typical externally mounted recuperator configuration. Typical thermal efficiencies on an HHV-available-heat basis for this class of recuperator are 55 to 65%.

The external recuperator can take advantage of greater space availability for heat exchange surface area than the internal designs, leading to the potential for greater thermal efficiency. Flow passages can be made larger on external recuperators for much lower fluid pressure losses in the system. Locating the recuperator externally minimizes the potential of extraction of useful heat from the radiant tube. The advantages of the external recuperator can be offset by the recuperator size, which can be an issue in some installations. Further, external recuperators and their associated hot piping will require external insulation to minimize ambient losses.

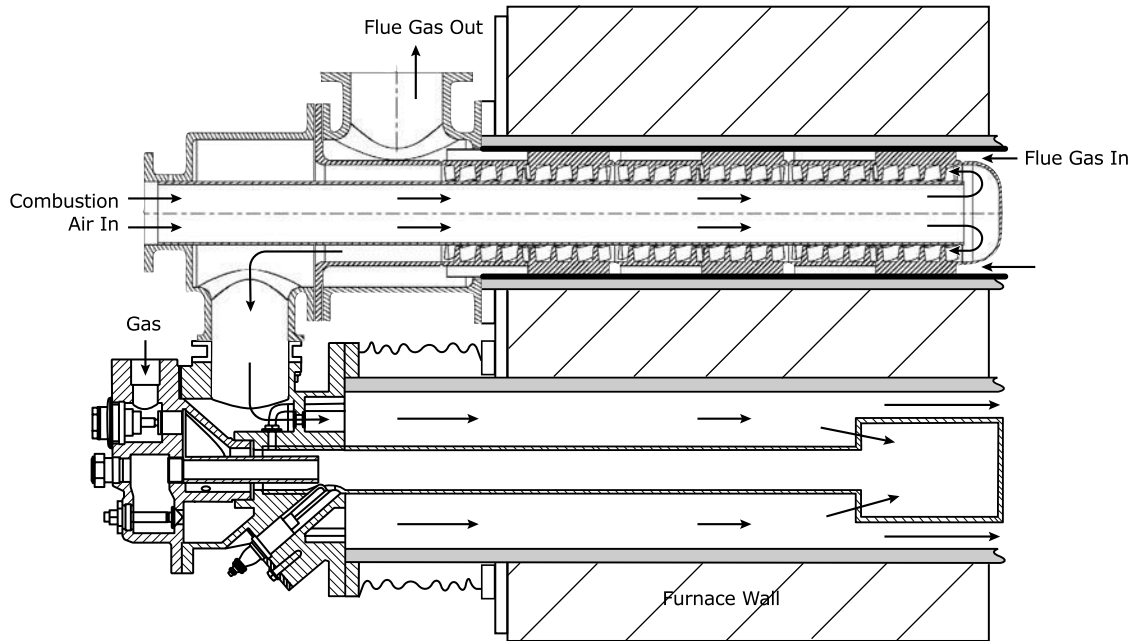


FIGURE 14.7 Insertion type recuperator.

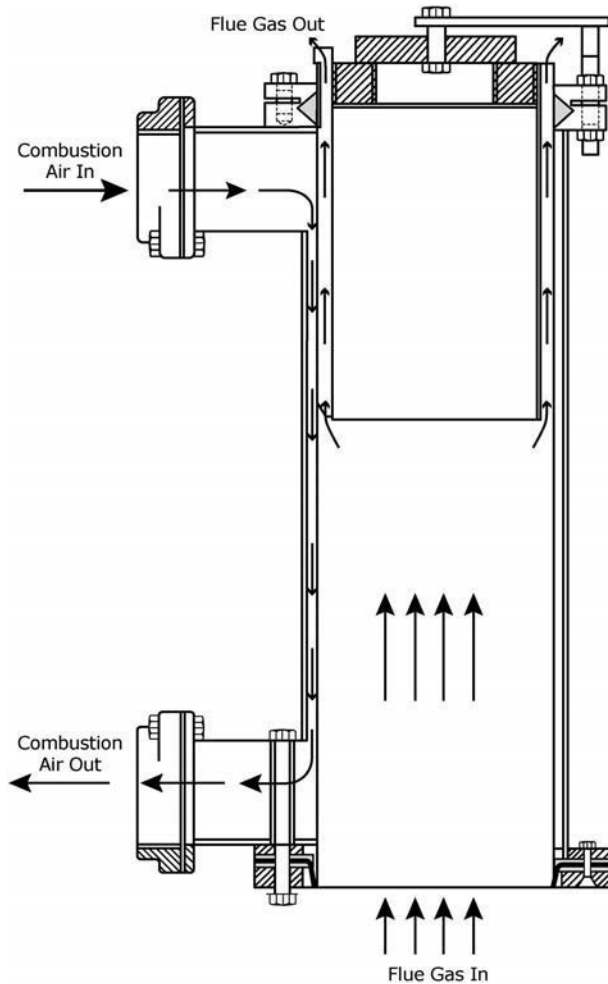


FIGURE 14.8 External recuperator.

14.5 EMISSION REDUCTION TECHNIQUES

Radiant tube burners fire into a confined hot space, limiting the range of techniques available for direct emissions control. External centralized control can be applied but requires that the exhaust collection system be designed and maintained to eliminate in-leakage of ambient “tramp” air if the size and operating cost of the emission post-treatment device is to be minimized. Accordingly, the burners and associated local equipment configurations generally directly incorporate emissions-reduction measures such as the previously mentioned use of recirculation and FGR.

For typical gaseous fuels used in radiant tube burners, NO_x formation is dominated by the thermal mechanism and is therefore dominated by flame temperature. This final flame temperature is a function of the fuel composition, the temperature of the combustion air, and the relative thermal loading on the radiant tube. NO_x reduction techniques for radiant tubes focus on minimizing this flame temperature while fulfilling the thermal requirements of the heating process.

One technique is to break the combustion process up into multiple stages. In this process, an initial portion of the combustion reactants are mixed and combusted. The portion that is combusted is allowed to transfer a portion of the heat of reaction to the process. The resulting combustion products are then delivered to a second combustion zone where either additional air or fuel is

injected, depending on whether the first stage was fuel-rich or fuel-lean. As a portion of the heat of the first reaction has been released, the subsequent flame temperature will be lower than that of a single combustion stage. Multiple stages can be employed by various designs.

A second common technique is to dilute the combustion process by the addition of a nonreactive medium to reduce the ultimate flame temperature and hence NO_x formation. The most common and effective diluent is flue gas from the combustion process and is referred to as flue gas recirculation (FGR). In this technique, combustion products are recirculated into the combustion zone.

There are several variations of the use of FGR. A common approach is to provide the FGR to the burner from a central external blower. In this application, the exhaust from a zone of radiant tubes is connected to a central blower that feeds into the combustion air. This system can be easily applied to a push-pull design with both exhaust and combustion air headers in place. When using FGR, which requires a close coupled exhaust to ensure that the FGR is of “good quality” (low O₂ content), serious consideration must be given to the safety implications of an “explosion-proof system” with no pressure relief — see the comments later in this chapter on safety requirements.

A simpler method is to use an in-burner fuel- or air-driven jet pump to directly inspirate and recirculate the flue gases from the exit of the radiant tube to the burner, relying on the momentum of the jet to provide the motive force to overcome the pressure losses in the recirculating FGR loop.

By design, a recirculating radiant tube provides significant dilution of the combustion zone by hot FGR. Significant quantities of recirculated combustion products (FGR) can be introduced into the combustion zone in such a tube design. However, as the root of the combustion zone is upstream of the point of FGR introduction, substantial thermal NO_x may already have been generated, depending on the specific burner design.

14.6 HEAT TRANSFER CONSIDERATIONS

Optimizing the performance of a radiant tube involves balancing the heat transfer from the flame and products of combustion to the inner surface of the tube, its conduction through the tube wall, and the emission from the outer surface of the tube, while respecting the tube material limitations. Neglecting this balance can result in premature tube failure from thermally induced stresses and material creep. In the authors’ experience, the opportunity costs of lost production generally far outweigh any costs associated with more conservative design of the radiant tube heat transfer area for increased tube life.

Heat is transferred to the inside of a radiant tube by a combination of gas radiation, flame radiation, and convection. Heat is then conducted through the radiant tube material to the outer surface where it is transferred to the load by radiation. Some furnace designs use recirculating fans to improve temperature uniformity and provide convection heating of the load. For these furnaces, there may also be a significant convection component in the transfer of heat from the exterior surface of the radiant tube.

In the case of the more common nonrecirculating tube designs, it is desirable for the burner flame to be long to reduce the potential for local hot spots and to distribute the heat along the length of the tube. The requisite slow heat release flame is created by diffusion mixing of the fuel and air. For the purposes of analysis, it is beneficial to be able to predict the heat release as a function of distance along the axis of the radiant tube. The composition of the combustion products within the radiant tube at any point is actually a mixture of unreacted fuel, combustion air, and reacted combustion products. Ramamurthy et al.⁵ investigated a “fuel burn-up rate” — that proportion of the total input fuel reacted related to the axial distance from the burner nozzle. They expressed this correlation by Equation 14.1.

$$\kappa(z) = 1 - \exp\left[-8.24 \times 10^{-4} \frac{AR^{0.54}}{\Phi^{1.53}} P_{\tau}^{0.41} \left(\frac{z}{D}\right)^{1.6} Re_{\tau}^{-0.08}\right] \quad (14.1)$$

where κ is the fuel burn-up coefficient, z is the distance from the burner outlet, AR is the area ratio (ratio of the annular air inlet port area to the inner circular fuel inlet port area), Φ is the fuel

equivalence ratio, $P_{\dot{v}}$ is the momentum ratio of air to fuel taken at $z = 0$, D is the inside diameter of the radiant tube, and Re_{FT} is the Reynolds number of the combustion products evaluated at adiabatic flame temperature conditions at the stoichiometric fuel/air ratio conditions. This fuel burn-up coefficient can be used to estimate the temperature and composition of the combustion products along the length of a radiant tube.

When the temperature and composition of the combustion products are known within the radiant tube, the rate of heat transfer to the inner surface can be calculated. The heat transfer to the inner surface of the radiant tube is both by convection and by radiation. The local one-dimensional heat convection heat transfer can be expressed by Equation 14.2.

$$q_{\text{conv}} = h(T_{cg} - T_w) \quad (14.2)$$

where h is the local convective heat transfer coefficient, T_{cg} is the local combustion gas temperature, and T_w is the local tube wall temperature.

Ramamurthy et al.⁵ found reasonable agreement with the Gnielinski correlation for the local Nusselt number Nu_D proposed for fully developed noncombusting flows in the range of $2300 < Re_D < 5 \times 10^6$ represented by Equation 14.3.

$$Nu_D = \frac{hD}{k} = \frac{(f_D/8)(Re_D - 1000)Pr}{1 + 12.7(f_D/8)^{1/2}(Pr^{2/3} - 1)} \quad (14.3)$$

where the Darcy friction factor f_D is calculated from Equation 14.4:

$$f_D = (0.79 \ln Re_D - 1.64)^{-2} \quad (11.4)$$

Ramamurthy et al.⁵ also investigated the correlation of the radiant heat transfer to the inner surface of the radiant tube for the one-dimensional case. The Hottel⁶ expression for an isothermal gas in a tube is given as:

$$q_{\text{rad}} = \frac{\epsilon_w \sigma (\epsilon_{cg} T_{cg}^4 - \alpha_{cg} T_w^4)}{1 - (1 - \epsilon_w)(1 - \alpha_{cg})} \quad (11.5)$$

where ϵ_{cg} and α_{cg} are the combustion gas emissivity and absorptivity, respectively, for the combustion gases as described by Hottel, and ϵ_w is the surface emissivity of the interior wall. Application of Equations 12.1 through 12.5 will allow one to estimate the total heat exchange to the inner surface of the tube for a given a tube temperature profile.

Radiant tubes are generally used in chambers where very low or static flow conditions result in low convective heat transfer coefficients. Convective heat transfer is typically ignored for the case of a furnace chamber without forced circulation in view of the high radiation component. Radiant tubes are commonly located adjacent to a refractory furnace wall or roof. It is common to locate several tubes adjacent to a surface, thus forming a tube bank. To reduce the complexity of the evaluation of the radiant heat exchange, Hottel⁷ suggests a gray plane method where the refractory backed bank of tubes can be replaced by an equivalent “gray plane” having an effective emissivity of ϵ_p where the subscript P refers to an effective plane area. The total radiation exchange presented by Hottel for the effective plane is as given in Equation 14.6:

$$\dot{Q}_{\text{net}} = A_p (E_p - E_T) \left[\frac{1}{\frac{1}{F_{PT}} + \frac{C}{\pi D} \frac{\rho_T}{\epsilon_T}} \right] \quad (11.6)$$

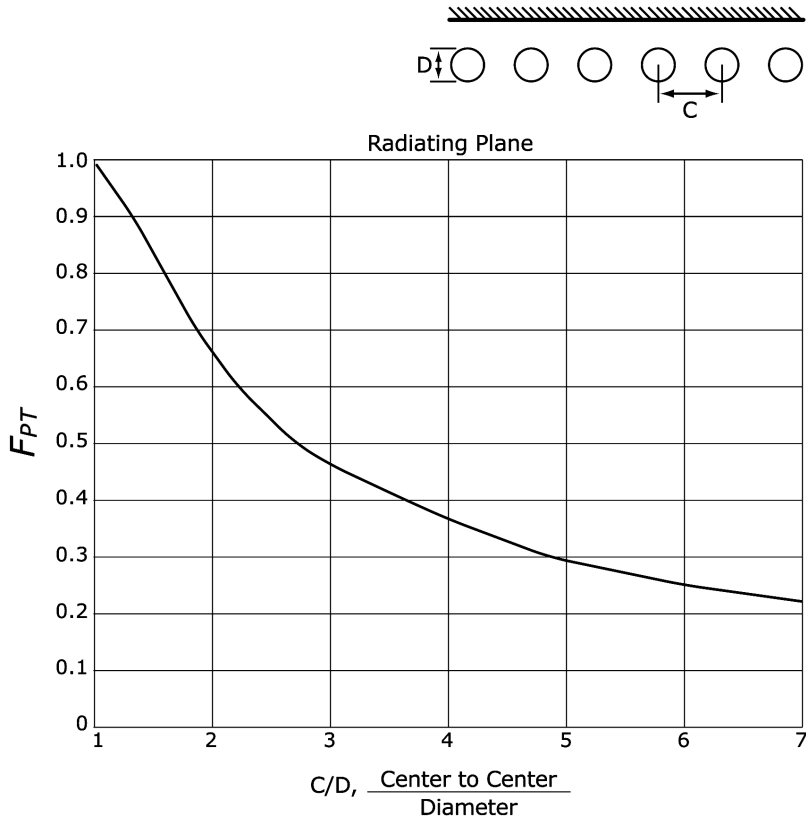


FIGURE 14.9 Total view factor for refractory backed single row of tubes. (Adapted from Hottel, H.C. and Sarofim, A.F., *Radiative Transfer*, McGraw-Hill, New York, 1967. With permission.)

where A_p is an effective black plane parallel to the tube surface and refractory covered wall, and E_p and E_T represent the emissive power for the black plane and the tube surface, respectively. The term in square brackets represents an interchange factor between the refractory-backed tube plane and the effective black plane A_p . Within the square brackets, F_{PT} is the total view factor, C is the center-to-center spacing of the tube banks, ρ_T is the tube reflectance, and ϵ_T is the tube surface emissivity.

F_{PT} depends on the ratio of tube center-to-center spacing to the tube diameter. For a single row of tubes in front of a refractory wall, Hottel presents F_{PT} as shown in [Figure 14.9](#).

14.7 RADIANT TUBE MATERIAL CONSIDERATIONS

There are two major classes of materials that are typically applied to radiant tubes. Metallic radiant tubes of Fe-Cr-Ni alloys in various grades are commonly used on process temperatures up to 1900°F, although some proprietary grades are capable of slightly higher temperatures. Ceramic radiant tubes capable of surface temperatures up to 2450°F are utilized to process temperatures up to 2250°F. Most commercially available ceramic radiant tubes are produced from the SiC (silicon carbide) material family.

Interested readers are encouraged to consult specialist texts for detailed information on the materials aspects of radiant tubes. Some general information follows.

14.7.1 METALLIC RADIANT TUBES

Selection of metallic radiant tube material for optimal performance requires knowledge of the operating temperature of the tube material and the atmosphere of the heating process. These influence creep rate, the rate of corrosion, and the general long-term stability of the material.

Creep is the slow deformation of the tube material resulting from applied stress. Creep failure can result in reduction of the tube cross section and burner flame impingement leading to tube rupture and is a major element in the failure of radiant tube supports. A material's creep strength typically limits the ultimate performance of a radiant tube design because it is much less than the yield strength of the same material. Because creep strength is logarithmic with temperature, small increases in tube temperature at normal operating conditions result in significant reduction of creep strength.

Radiant tubes are subject to the stresses of the applied mechanical loads and from thermally induced stress. Classical mechanical design methods can be used to estimate mechanical loads from the weight of the radiant tube itself and the concentrated loads from the radiant tube's supports. Thermally induced stresses result from hot spots with high local heat flux rates, poor overall temperature distribution along the length of the radiant tube, and periodic loads due to thermal cycling.

High temperature gradients from the inside to the outside of the tube result in thermally generated hoop stresses in the tube wall. In areas of high heat flux loading, consideration must be given to this stress and attempts made to minimize the wall thickness, while at the same time considering the stress due to applied mechanical loads as the mechanical and thermally generated loads must be superimposed upon each other.

Additional thermal stresses result from uneven axial and circumferential temperature distributions. However, Irfan and Chapman⁸ have shown that uneven temperatures along the length of the tube have to be significant in order to result in significant thermally induced stresses. Likewise, unevenness in circumferential temperatures generally does not create significant stress unless the local temperature differences exceed 75°F. This is not to say that there is no loss in strength resulting from these temperature maldistributions, and every attempt should be made to avoid them. Moreover, uneven temperature distributions lead to high tube surface temperatures (creep failure) and less effective use of the available tube surface area.

Corrosion results from interaction of the tube material with the furnace atmospheres and combustion products, starting on the outer and inner surfaces, respectively, and then migrating through the grain structure deeper within the tube wall. Corrosion will result in the loss of mechanical strength and lead to ultimate failure of the radiant tube. Therefore, it is very important that the atmospheres to which it will be exposed be considered in the selection of the radiant tube material.

Metallic radiant tubes are alloyed with high levels of chromium, typically on the order of 25%(wt.), to provide resistance to oxidation. The chromium reacts with local oxygen to form a protective layer of chromium oxide (Cr_2O_3) on the surface of the tube. This protective layer reduces and eventually effectively prevents further direct combination of the metal with the atmosphere. The protective oxide film is, however, subject to breakdown from the expansion and contraction of the base metal, causing exposure of the underlying material to the atmosphere. Minor alloying with silicon or aluminum improves the oxidation resistance of nickel-based alloys, especially when added in combination with rare earth metals.⁹

Radiant tubes frequently operate in carburizing atmospheres. In these processes, carbon is adsorbed and diffused into the metal, where, at sufficiently high temperatures, chromium, iron, and nickel carbides are formed. The precipitation of chromium carbides removes chromium from the alloy matrix, potentially increasing oxidation. Nickel carbides increase the hot strength of the material but decrease ductility. Silicon additions delay the carburization by preventing carbon absorption, and stable carbide formers such as tungsten can be added to increase resistance to the

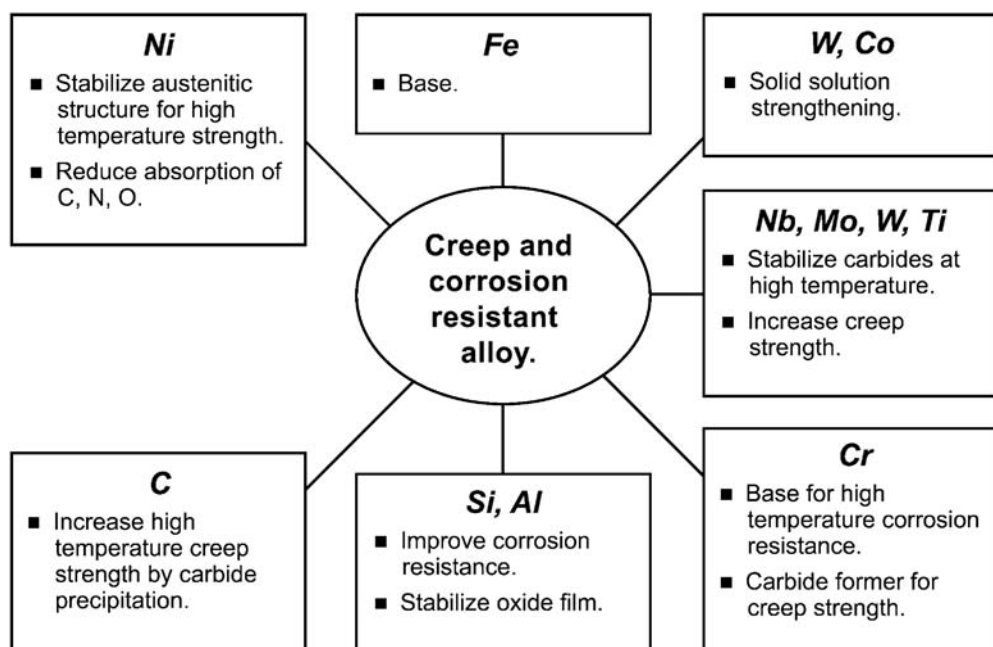


FIGURE 14.10 Major alloying elements in cast heat resistant alloys. (Courtesy of Kubota Metal Corporation, Fahramet division.⁹ With permission.)

effects of carburization. Larger concentrations of chromium reduce the diffusion rates of both carbon and chromium in nickel-based alloys.

Nitridation can also occur at temperatures in the range of 1800°F with nitrogen-containing or ammonia-based atmospheres. High nickel content alloys with low iron content perform well under nitriding conditions.

Figure 14.10 provides an overview of common alloying elements and the result of the use of each. It is recommended that the tube material manufacturer be consulted for the particular application.

14.7.2 CERAMIC RADIANT TUBES

The inherent heat flux limitations of metallic radiant tubes have led to increased popularity of ceramic radiant tubes over the past 20 years, and spurred development of materials and structures for this application. Typically constructed from the SiC family of ceramics, such radiant tubes exhibit great resistance to creep, improved resistance to carburization, and higher temperature capabilities. Current commercial ceramic radiant tube suppliers limit their tube material to 2450°F and process temperatures to 2250°F.

Several forms of SiC are commercially used in the manufacture of radiant tubes. The common forms are Nitride Bonded, Reaction Bonded, and Composites, each term referring to the method of bonding of the larger SiC particles within the matrix. Nitride-bonded SiC uses silicon nitride to bond SiC particles together. It has good resistance to oxidation but has lower thermal conductivity than its reaction bonded counterpart. The reaction bonded SiC is formed by covalently bonding a range of sizes of SiC particles together. This material is very durable, providing excellent high-temperature strength, excellent creep resistance, and good resistance to oxidation. The composite SiC materials integrate SiC particles in a matrix of another material such as silicon. Some examples of this class of material use reinforcement by SiC whiskers or other, similar high-temperature “fiber” materials.

14.8 APPLICATION CONSIDERATIONS

The application of radiant tubes to a specific furnace involves consideration of many factors. The required heat input to the furnace, available space for location of the tubes, required tube temperature to provide the heat transfer to the load, support locations for the radiant tube, material of the radiant tube, and overall costs must all be considered. Future operating and maintenance costs must be factored in to optimize the combined radiant tube and burner selection.

The common starting point is to establish the required heat input to the load and to balance losses from the furnace walls, to a flowing atmosphere, to water cooling, etc. Further, if the application is a batch-type process, the required heat-up time must also be considered. All these factors contribute to what is referred to as the *required available heat* for the process.

Once the required available heat is determined, attention must turn to the space in which the radiant tubes are to be located, giving consideration to the operating temperature of the furnace and the selected tube material. The common approach to determining the required radiant tube surface area is to apply heat flux guidelines. If the furnace temperature is high, heat flux from the tube must be limited to keep tube temperature down and provide acceptable life. In lower temperature furnaces, or if heat transfer from the surface of the tube is enhanced by convection, it may be possible to use high heat flux rates without significant compromise in tube life.

Typically, the heat flux is evaluated as an average over the length of the radiant tube. This average is determined by dividing the required available heat by the number of radiant tubes, and then by the exposed (inside the heating chamber) surface area of the radiant tubes. The heat flux rate is then compared to common values based on past experience with the particular process temperature and tube material. If the heat flux is higher than the experience-based numbers, either the exposed tube area must be increased or higher-grade tube material, allowing higher tube operating temperatures, must be considered. In some cases, the furnace chamber size may need to be increased to allow more space to install the radiant tubes. Table 14.1 shows common heat flux values for metallic radiant tubes. The use of ceramic radiant tubes can increase these values to 100 to 150 Btu/in², depending on the process temperature.

Although the average heat flux approach to specifying radiant tubes is commonly used throughout industry, this approach does not factor in the influence that radiant tube temperature distribution has on the heat flux.

Considerable research and development has obtained more even temperature distribution along the length of the tube by eliminating hot spots or reducing them to a minimum. The resulting consistent heat flux with respect to length allows maximization of tube life by operating with the lowest possible tube temperature for a given total heat flux. For a cold-air or recuperative tube, the challenge is to extend the combustion reaction such that it releases heat evenly along the tube length. The reversing action of the burners mounted at each end of a regeneratively fired tube achieves this objective as a natural outcome of the design, as previously mentioned.

Highly rated single-ended tubes are frequently rotated 180° as part of normal maintenance to allow gravity to correct the effects of sagging. This is generally not possible or practical with “U” or “W” tubes, enhancing the need for even temperature distribution to optimize the life of the tubes.

TABLE 14.1
Commonly Used Heat Flux Rates for Metallic Radiant Tubes

U-Tube Leg Length (ft)	Furnace Temperature (°F)		
	1100–1300	1300–1600	1600–1750
< 3	100	60	30
3 to 6	80	50	20
6 to 10	60	40	10

14.9 COMBUSTION CONTROLS FOR RADIANT TUBE BURNERS

Combustion controls play an important role in the successful application of radiant tubes. Stated elsewhere in this chapter is the importance of maintaining uniform radiant tube surface temperature. Because the mixing energy of a burner is a function of the burner firing rate, it is extremely important that the turndown requirements and low firing rate conditions are reviewed. Moreover, on preheated air burner systems, the temperature of the preheated air most likely increases as a function of turndown — as the flows go down, the heat recovery device efficiency increases. If consideration is not given to this aspect, local overheating of the radiant tube at low firing rates may result in early failure of the tube.

14.9.1 INPUT AND AIR/FUEL RATIO CONTROL

The most prevalent air/fuel ratio control system for radiant tubes uses the pressure-balanced (“cross-loaded”) regulator. The most common for ambient air burners is the single-diaphragm cross-connected regulator shown in [Figure 14.11](#). In this system, the air pressure to the burner is applied to one side of a diaphragm. The regulator’s outlet (downstream) gas pressure is applied to the other side of the diaphragm. As the pressure of the air varies, the regulator opens until the gas pressure “balances” the force of the air pressure plus whatever spring forces that are applied to the regulator diaphragm. Because the flows of both the fuel and the air follow a square-root relationship with their pressures, the two flows will modulate and maintain the desired ratio proportions.

In preheated air systems, the combustion air flow is both a function of pressure and temperature. For this application, a double-diaphragm regulator [Figure 14.12](#), uses differential pressures produced from the air and gas flows to provide its valve positioning forces. A restricting orifice is installed in the combustion air line and the pressure of upstream and downstream taps connected to each side of the regulator air diaphragm. An opposing force is created by connecting a differential pressure from a restriction in the fuel line to a second diaphragm. This differential force is typically created by installing an adjustable orifice downstream of the regulator.

The double-diaphragm regulator’s air flow differential device is installed upstream of the air preheating device where the air density is constant. The signal to the regulator will thus always be proportional to the air flow, and not affected by the change of the temperature of the air as it passes through the air preheating device.

There are several system heat input control philosophies applied to radiant tubes that allow good fuel/air ratio control and aid in maximizing the potential life of the tubes. Systems are typically classified as modulating, high/low, on/off, and combined mode.

In a modulating system, the fuel and air inputs are controlled (“modulated”), as required, to maintain the required process temperature — to match the radiant tube’s heat input to the load requirements. This modulation occurs down to a minimum firing rate, typically between 3:1 and 5:1

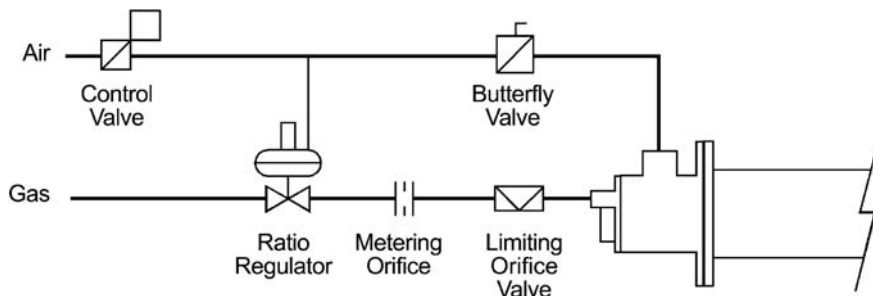


FIGURE 14.11 Pressure-balanced regulator system.

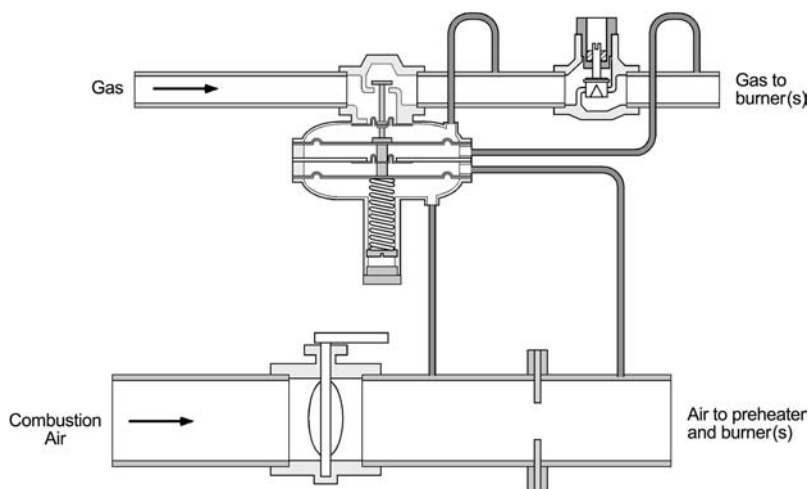


FIGURE 14.12 Double diaphragm regulator.

turndown from the maximum firing rate. Modulating systems have the inherent disadvantage of poorly distributing the heat release at the minimum firing rate where the mixing energy is minimal.

With high/low systems, the firing rate is either at the maximum firing condition (high) or the minimum firing condition (low), depending on the demand of the process temperature controller, with minimum transition time between these two states. If the process temperature is not met, the control places the burner in the high fire mode. Once the temperature is satisfied, the control drives the system to the low fire condition. The high/low control system minimizes the variation in thermal profiles between the two extreme conditions by allowing the two extreme conditions to be set in a predictable manner. However, for many processes, especially in batch operations, the heat input at an acceptable low firing rate may exceed the minimum process requirements.

The on/off control philosophy is similar to high/low as described above, with low rate replaced by turning the burner off. Using the off mode in place of the low fire mode allows a theoretically infinite turndown to be achieved. However, this control mode requires that the burner be re-ignited by a pilot or direct spark igniter each time the input controller calls for heat. A variation is a combination of high/low and on/off known as high/low/off. This allows for the infinite turndown capabilities of the on/off method to be achieved but requires less frequent re-ignition of the burner.

“Pulse firing,” a form of on/off control, can be used on cold-air or recuperative systems to control input with simultaneous enhancement of tube temperature uniformity by firing only at the burner’s maximum rate. In this control mode, the relative durations of the high fire and off pulses will be varied to achieve the desired heat input rate.

Combined control modes can mix any of the modes discussed above.

Regenerative radiant tube burner systems use a variation of pulse firing for input control. Both the combustion air and the fuel must cycle on and off frequently to perform the reversing action required of the burner operation. Pulse width modulated input control can be superimposed on the reversing action. In these systems, fast-acting pneumatic on/off valves are used to instantly turn on both the air and fuel to their maximum flow or off conditions. To compensate for natural system dynamics, it is common for the fuel opening to lag the combustion air opening, and the fuel closing to precede the combustion air closing, by a short interval, ensuring that the burner does not fire in a rich condition. Pulse firing, when applied to regenerative burners, ensures the best possible radiant tube temperature distribution as the burners fire only at the maximum design rate.

14.9.2 FLAME SUPERVISION

Note: This section is not intended to act as a specific guide to the use of flame supervision systems for radiant tube or any other burners. The reader is referred to the applicable international, national, local, and insurance industry codes, standards, requirements, etc. for appropriate information on this subject.

There are many radiant tube combustion systems installed that do not incorporate provisions for flame supervision. At the time of this writing, the U.S. National Fire Protection Agency (NFPA) covers the installation of metallic radiant tubes without flame safety when the system is “explosion proof.” For the explosion-proof determination, the entire combustion and radiant tube system should be reviewed, including any exhaust collection system that might be connected to the radiant tube. If any part of the system is determined not to be “explosion proof,” then an appropriate flame proving system should be installed. System designers should recognize that many areas in the world require flame proving on all systems and that some users require flame proving as a matter of practice.

Two alternatives are commonly employed when flame supervision is required with radiant tube systems. The most common is the use of a standard ultraviolet sensor or a flame rod to monitor the presence of a flame. In cases where direct flame detection may not be feasible, an acceptable alternative may be to monitor the exhaust system for the presence of combustible gases with an appropriately selected exhaust gas analyzer, usually limiting the operation to a conservative percentage of the lower explosive limit (LEL) of carbon monoxide before safety shutdown.

REFERENCES

1. Pritchard, R., Guy, J.J., and Connor, N.E., *Industrial Gas Utilization — Engineering Principles and Practice*, Bowker Publishing, Epping, Essex, 1977, 288.
2. The Gas Council, *Gas Fired Radiant Tubes*, reprinted from *Flambeau*, 6(2), 1968.
3. Anderson, R.H. and Broome, C.G., Immersion and radiant tube heating, presented at the *Ayr Gas Sales and Service Conference of the Gas Council (U.K.)*, September 1955.
4. Davies, T., Regenerative burners for radiant tubes — field test experience, in *Industrial Combustion Technologies*, Lukasiewicz, M.A., Ed., American Society of Metals, Warren, PA, 1986, 65–70.
5. Ramamurthy, H., Ramadhyani, S., and Viskanta, R., Development of fuel burn-up and wall heat transfer correlations for flows in radiant tubes, *Numerical Heat Transfer*, Part A 31, 563–584, 1997.
6. H.C. Hottel, Radiation from Carbon Dioxide, Water Vapor and Soot, presented to the American Flame Research Committee, 1985.
7. Hottel, H.C. and Sarofim, A.F., *Radiative Transfer*, McGraw-Hill, New York, 1967, 113–114.
8. Irfan, M.A. and Chapman, W., Thermal Stresses in Radiant Tubes Due to Axial, Circumferential and Radial Temperature Distributions, unpublished paper, 1998.
9. Magnan, J., Materials Selection for Radiant Heaters, presented at *2000 Galvanizer’s Association Conference*, Toronto, 2000.

15 Radiant Wall Burners

*Demetris Venizelos, Ph.D., R. Robert Hayes,
and Wes Bussman, Ph.D.*

CONTENTS

- 15.1 Introduction
 - 15.2 Burner Description
 - 15.2.1 Burner Components and Design Parameters
 - 15.2.1.1 Entrainment of an Eductor System
 - 15.2.1.2 Venturi Inlet Bell
 - 15.2.1.3 Venturi Throat
 - 15.2.1.4 Venturi Diffuser
 - 15.2.1.5 Downstream Section
 - 15.2.1.6 Premix Burner Tip and Internal Baffle
 - 15.2.1.7 Burner Tile
 - 15.2.1.8 Muffler/Rain Shield
 - 15.2.1.9 Air Doors
 - 15.2.1.10 Staged Fuel Riser and Tip Assembly
 - 15.3 Design Considerations
 - 15.3.1 Fuels
 - 15.3.2 Flame Stability
 - 15.3.2.1 Flashback
 - 15.3.2.2 Flame Attachment and Liftoff
 - 15.3.3 Emissions
 - 15.3.4 Burner Spacing
 - 15.4 Retrofit Considerations
 - 15.5 Operation and Troubleshooting
 - 15.5.1 Operation
 - 15.5.2 Troubleshooting
 - 15.5.2.1 Burner Tip Plugging/Coking
 - 15.5.2.2 Furnace Air Leakage
 - 15.6 Conclusion
- References

15.1 INTRODUCTION

Radiant wall burners, as discussed in this chapter, refer to burners that are typically designed to be installed in several rows along a furnace wall, as shown in [Figure 15.1](#). They typically fire radially outward along the furnace wall providing heat, which is transferred to the process tubes chiefly by thermal radiation from the wall and hot gases. This type of configuration is usually designed to provide uniform heat input to the process from the wall area comprising the radiant wall burner matrix.



FIGURE 15.1 Radiant wall burners (natural draft) firing in an ethylene-cracking furnace. (Courtesy of John Zink Co., LLC.)

Historically, radiant wall burners have been used in many hydrogen-reforming and ethylene-cracking heater applications.¹ These furnaces typically operate in the temperature range between 1900°F and 2300°F. The process fluid is circulated through process tubes, which are usually suspended in the middle of the furnace, and is heated to the required application temperature, with radiative heat transfer from the refractory side walls being dominant. The heat transfer from the furnace to the tubes (and the use of a catalyst in some applications) converts the process fluid to the final product via the appropriate chemical reactions. As one can expect, the product yield efficiency of the process in these furnace operations depends heavily on the heat transfer. Through the years, furnace and burner manufacturers have devoted considerable research efforts to determine the optimum heat flux profiles in various furnace-burner configurations to optimize product yields.

The two most common burner configurations used in furnaces with radiant wall burners are the following: (1) heat input from a combination of hearth burners located on the floor firing vertically upward along the wall, and radiant wall, burners located on the wall above the hearth burner flames, and (2) heat input entirely by radiant wall burners configured in a matrix that extends from the top to the bottom of the furnace radiant section. An illustration of each of these configurations is shown in Figure 15.2. In both burner-furnace configurations described above, the radiant wall burners are arranged in several rows located at different elevations on the furnace wall. The heat release, spacing, and spacing pattern (grid pattern) of the radiant wall burner matrix are designed to suit the radiant heat flux distribution needs of the particular process. Figure 15.3 shows typical heat flux profiles in a furnace operating with hearth (floor) burners only, and with both hearth and radiant wall burners firing.

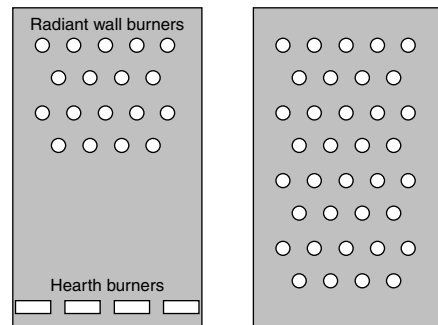


FIGURE 15.2 Common radiant wall burner application furnace configurations.

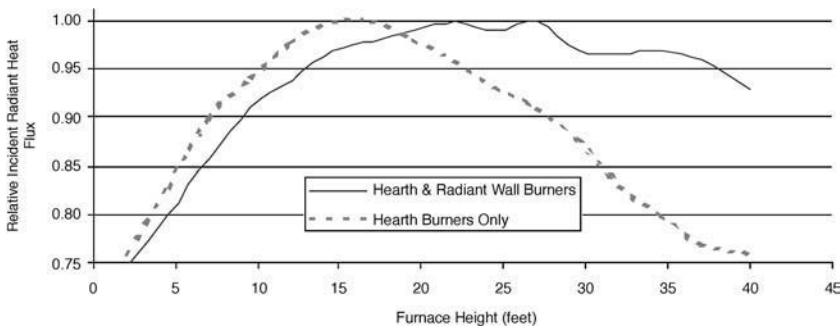


FIGURE 15.3 Heat flux profiles with and without radiant wall burners.



FIGURE 15.4 Forced-draft radiant wall burners in an ethylene-cracking furnace. (Courtesy of John Zink Co., LLC.)

There are many different designs of radiant wall burners, including premix and raw-gas radiant wall burners, as well as forced- and natural-draft burners. A row of forced-draft radiant wall burners in operation is shown in Figure 15.4. The discussion in this chapter focuses mainly on natural-draft, premix, radiant wall burners, as they are the most widely used in cracking and reforming heaters. Descriptions of the components of these burners are given, along with design and operational considerations.

15.2 BURNER DESCRIPTION

15.2.1 BURNER COMPONENTS AND DESIGN PARAMETERS

Figures 15.5a and 15.5b illustrate typical radiant wall burners. These types of burners are usually mounted horizontally through the heater steel and burner tile along the furnace wall. The main components of these burners include:

1. Primary fuel nozzle (spud)
2. Venturi section (inlet, throat, and diffuser)
3. Premix burner tip
4. Primary air door assembly
5. Secondary air door assembly
6. Burner tile
7. Muffler/rain shield
8. Staged fuel riser and tip assembly

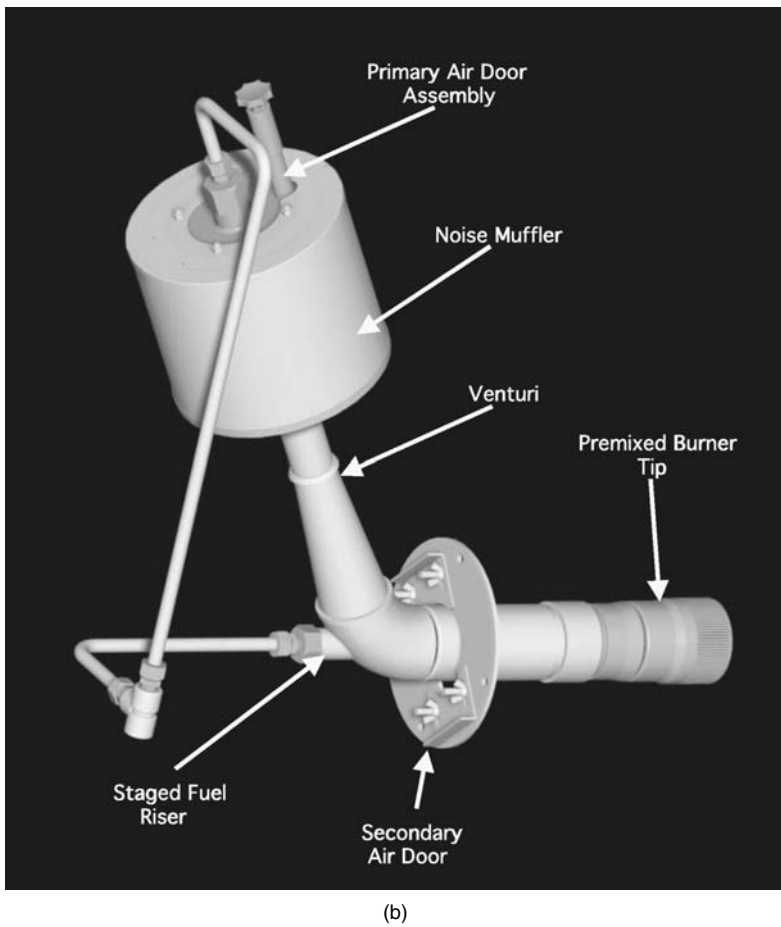
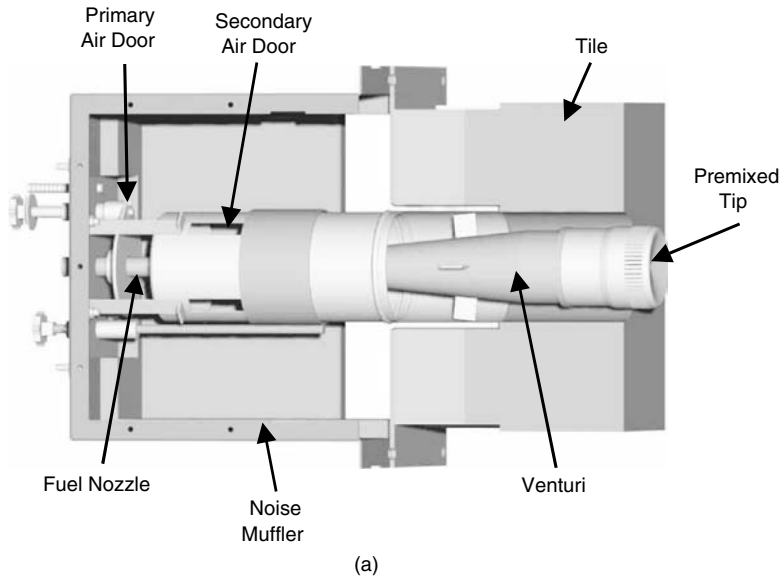


FIGURE 15.5 Solid model illustrating (a) a radiant wall burner and (b) a radiant wall burner with fuel staging. (Courtesy of John Zink Co., LLC.)

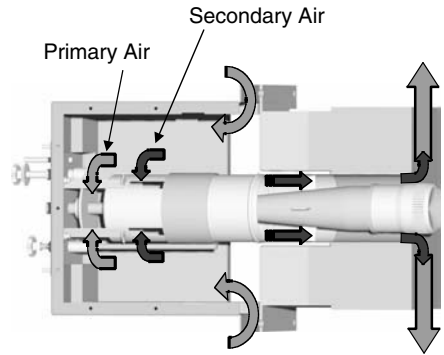


FIGURE 15.6 Illustration of the primary and secondary air flows through a radiant wall burner.

A typical radiant wall burner operates as a premixed burner. The objective in a natural-draft premixed burner is to use the energy from a fuel jet as the motive force to educt combustion air and transfer the fuel/air mixture through the burner and into the furnace where the combustion occurs. Forced-draft burners operate the same as natural-draft burners, with the exception that they can utilize the energy of the forced incoming air stream. Secondary air openings can also be used to inspirate air for combustion by means of the furnace draft. A diagram showing pathways of primary and secondary air flow is shown in Figure 15.6.

The fuel is injected at high velocities from a port on the primary fuel orifice (or primary fuel spud) into the venturi throat where it mixes thoroughly with the educted air. The fuel/air mixture then flows through the diffuser and the downstream section before entering the premix burner tip. The flow then turns and exits through openings in the burner tip in a radial direction near the furnace wall. Depending on the burner manufacturer, these openings can have different shapes and sizes.

In a staged fuel radiant wall burner configuration, the stage fuel riser(s) supplies(y) the stage tip(s) with fuel. The location of the staged fuel tip(s) can vary, depending on the manufacturer and type of burner. Each component of this type of burner design, along with many other operating parameters, are important in providing maximum air entrainment and optimum performance. Understanding the importance of the venturi eductor and premix burner tip geometries allows one to design an optimal burner system. The remainder of this section discusses each component in additional detail.

15.2.1.1 Entrainment of an Eductor System

When a fuel exits a port, it will interact with the surrounding gas. The fuel jet will entrain the surrounding gas and mix as it flows downstream of the port. This process is called *free jet entrainment*. A premixed burner simply consists of a free jet with a venturi located just downstream. The fluid dynamic principles that apply to free jet entrainment also apply to an eductor system. However, the amount of surrounding gas entrained is reduced compared to free jet entrainment. The reduction in entrainment performance is due to momentum losses associated with the flow-restricting geometry of the venturi and burner tip system. Minimizing the momentum losses associated with the venturi system is an important aspect of premix burner design. Some premix burners require a design that achieves maximum entrainment performance for successful operation. The challenge in many instances is to optimize the burner design that will maximum entrainment performance.

15.2.1.2 Venturi Inlet Bell

The inlet to the venturi is typically designed as a well-rounded bell entrance. A well-rounded inlet bell helps minimize momentum losses through the venturi system. Idelchik⁷ reports values for the hydraulic resistance for flows through the inlet of a bell entrance. Typically, in the burner industry,

the bell inlet is designed with a radius r with a value that is at least 20% of the hydraulic diameter D_h of the throat ($r/D_h \geq 0.20$). One should keep in mind that the air door, spud holder, and fuel spud will also introduce additional restrictions to the air flow and can reduce entrainment performance.

The position of the primary fuel spud with respect to the venturi inlet bell also affects the entrainment performance. Depending on the venturi design, the entrainment performance is usually optimized when the fuel spud is located near the entrance plane of the inlet bell.

15.2.1.3 Venturi Throat

The area of the venturi throat can have a significant influence on the entrainment performance of a premix burner. The throat diameter required to achieve maximum entrainment performance depends on the overall design of the burner. For example, premix burners that consume a large pressure drop through the tip exit will require a smaller venturi throat diameter to achieve optimum entrainment performance. As the venturi throat diameter increases, for a given burner design, the entrainment performance increases until the throat diameter reaches an optimum value, beyond which any increase in throat diameter will result in a reduction of entrainment performance, as illustrated in Figure 15.7.

The throat length is another important parameter in venturi design. It is generally recommended that the length of the venturi throat should be approximately 7 times the throat diameter for maximum entrainment performance.

15.2.1.4 Venturi Diffuser

Located downstream of the venturi throat is the diffuser. The diffuser is a conical section that provides a gradual transition, increasing in diameter from the throat to the downstream section of the burner. To reduce momentum losses, it is recommended that the total divergence angle of the diffuser section be less than 10° . Designing diffuser angles with larger values will result in the formation of recirculation zones in this section of the venturi that can significantly reduce entrainment performance.

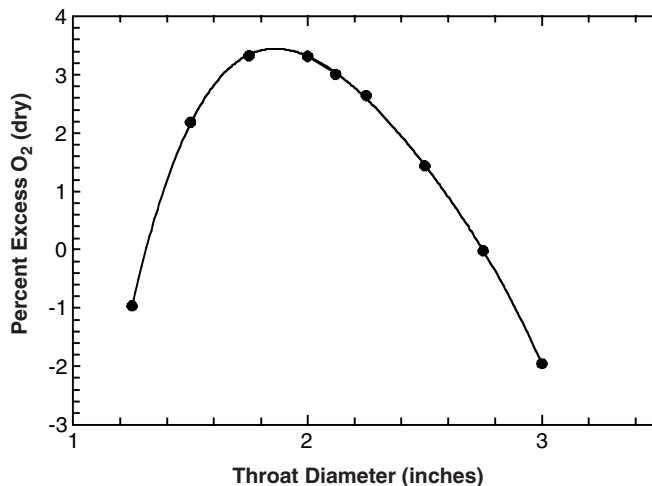


FIGURE 15.7 Effect of throat diameter sizing on air entrainment with other parameters held constant, for a given radiant wall burner design.

15.2.1.5 Downstream Section

The downstream section of the burner is typically a straight pipe that connects the exit of the diffuser section with the burner tip. The length of the downstream section usually varies, depending on the mechanical design requirements. Typically, the downstream section length is determined by the thickness of the furnace wall and mounting or platform requirements.

As shown previously in [Figure 15.5b](#), some premix burners are designed with a bend in the downstream section to accommodate these requirements. The elbow in the downstream section will introduce additional momentum losses. Using long-radius elbows with shallower angles can reduce these losses and improve entrainment performance. After a turn in a pipe, the flow downstream will be highly skewed toward the outer side of the elbow. Depending on the elbow geometry, a longer downstream straight section should be used to allow the gas mixture flow profile to distribute evenly before exiting the burner tip. A nonuniformly distributed flow at the burner tip exit could create problems with flame quality and flashback during operation.

15.2.1.6 Premix Burner Tip and Internal Baffle

As previously shown in [Figures 15.5a](#) and 15.5b, the premix radiant wall burner tip can be comprised of many thin slots or, as shown in [Figure 15.8](#), the tip can utilize fewer larger openings at the exit. A turning baffle located inside the tip to assist in turning the flow can be utilized to help provide more uniform flow profiles at the tip exit and minimize pressure losses.

15.2.1.7 Burner Tile

The burner tile in which the burner insert is mounted provides protective insulation for the burner internals, and the fired tile surface provides a region for flame stabilization and radiant heat transfer

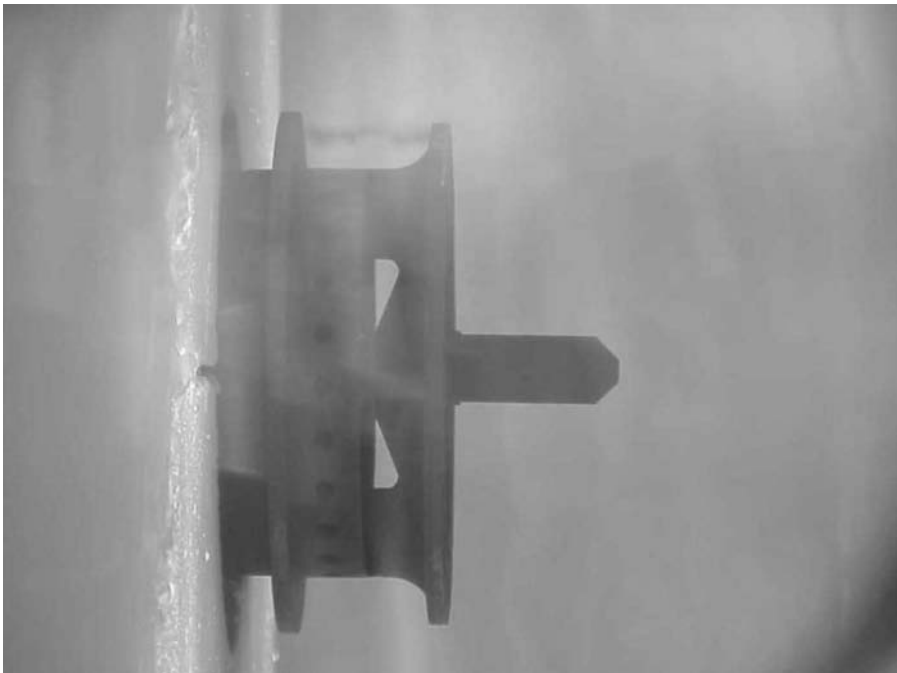


FIGURE 15.8 Photograph of radiant wall burner firing in a test furnace. (Courtesy of John Zink Co., LLC.)

to the process tubes. Tile materials typically consist of hard refractory rated for very high temperatures as the face is exposed to direct contact with the flame.

15.2.1.8 Muffler/Rain Shield

The burner muffler serves the purpose of reducing noise emissions and keeping precipitation and foreign materials from entering the burner inlet. The muffler typically consists of a thin metal liner insulated with noise-attenuating fiber material. The muffler is designed to be large enough so that pressure losses through the inlet and required turns are minimized, to provide maximum capacity for a given venturi system.

15.2.1.9 Air Doors

The primary air doors are used to control the amount of air entrained in the venturi that is premixed with the primary fuel gas. The secondary air door/damper controls the amount of airflow through the burner openings external to the venturi system. The secondary air, inspired by the furnace draft, is not premixed with any fuel prior to entering the combustion zone.

15.2.1.10 Staged Fuel Riser and Tip Assembly

Staged fuel risers and tip assemblies can be utilized in some burner designs. The staged fuel is typically injected at locations where it is allowed to mix with inert furnace gases prior to combustion. The location and method of staged fuel injection varies according to design to reduce NO_x emissions and achieve desired flames shape.

15.3 DESIGN CONSIDERATIONS

Similar to any other combustion system, a successful radiant wall burner design requires understanding of the fundamentals and principles in a wide range of fields, including combustion, fluid dynamics, heat transfer, physics, chemistry, and materials. The importance of some of the different considerations relevant to the design of a premixed radiant wall burner are discussed in this section.

15.3.1 FUELS

An important parameter in the successful design and operation of a radiant wall burner is the available fuel pressure and specified fuel compositions that will be fired. In many petrochemical and refinery applications, the fuel gas composition that a radiant wall burner is required to fire can vary widely because it is made up of various gas streams from different processes that change with time. A burner may be required to operate on both very heavy fuels with high heating value contents and very light fuels containing high levels of hydrogen during periods of start-up, normal operations, or upset conditions. This poses a significant design challenge because the fuel is used as the primary motive force to inspire the required combustion air. Variability in fuel gas compositions can significantly affect the amount of air that can be inspired and premixed. If a wide range of possible fuel compositions is required, the burner should be designed to be optimized for the typical fuel gas composition. This often limits the achievable firing rates for very high or low Btu content fuels. For high Btu content fuels (heavy fuels), the limit is often due to constraints in air education; while for low Btu content fuels (light fuels), the firing rate may be limited due to the maximum available fuel pressure.

15.3.2 FLAME STABILITY

15.3.2.1 Flashback

Flashback is a phenomenon that occurs in premix burners when the flame front propagates through the burner tip and into the venturi, as illustrated in [Figure 15.9](#). This phenomenon occurs when the local flame speed of the burning mixture outside the burner tip exceeds the velocity of the mixture exiting the tip. When a flashback occurs, the flame will typically stabilize inside the burner tip or just downstream of the primary fuel orifice.

Usually, flashback is easily recognized by an intermittent appearance of flame at the fuel orifice and a loud distinct noise. If flashback occurs and is left uncorrected, the venturi and/or burner tip can be quickly damaged due to overheating. When a flashback is detected, the operator should immediately shut off the burner and determine what actions must be taken to eliminate the unsafe operating condition. Several factors governing the flashback potential of a natural-draft premix burner include: (1) fuel composition, (2) air-to-fuel ratio, and (3) tip design.

The fuel gases most susceptible to causing flashback are the ones with higher flame speeds, such as hydrogen or ethylene. These fuels have characteristic flame speeds that are about 5 to 10 times greater than the characteristic flame speed of methane.

In addition, the flame speed of a fuel largely depends on the local air/fuel ratio. For example, the flame speeds of hydrogen for various volumetric air/fuel ratios are listed in [Table 15.1](#).

Notice that the flame speed for hydrogen varies significantly with the air/fuel ratio. For most typical fuel gas components, maximum flame speed levels generally occur near stoichiometric or slightly sub-stoichiometric (fuel-rich) conditions. The local temperature of the flame region also affects flame speed. For example, higher furnace operating temperatures or higher inlet air temperatures result in increased flame velocities.

The design of the premix burner tip is critical in preventing flashback. There are several factors that should be considered when designing the geometry of a premix burner tip to avoid flashback.

TABLE 15.1
Variation of Laminar Flame Speed of Hydrogen

Volumetric Air/ Fuel Ratio	Laminar Flame Speed at 60°F (ft/s)
1.19	5.9
1.70	9.2
2.38 (stoichiometric)	6.9
4.77	1.3

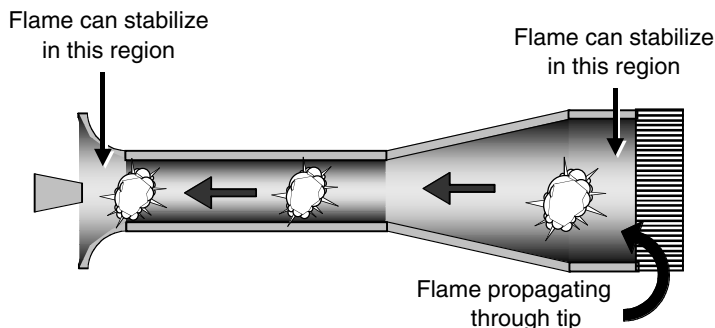


FIGURE 15.9 Illustration of the flashback phenomenon.

These factors include: (1) maximize tip exit velocity of the air/fuel mixture, (2) provide uniform velocity profile of the air/fuel mixture at the tip exit plane, (3) promote laminar flow at the tip exit plane, and (4) provide sufficient quenching distance.

15.3.2.2 Flame Attachment and Liftoff

The flame from a premix burner can be stabilized in a region where it attaches to the tip, as shown in Figure 15.10. This photograph clearly shows that the position of the flame front is located near the burner tip exit plane and is typically referred to as *flame attachment*. In the flame attachment

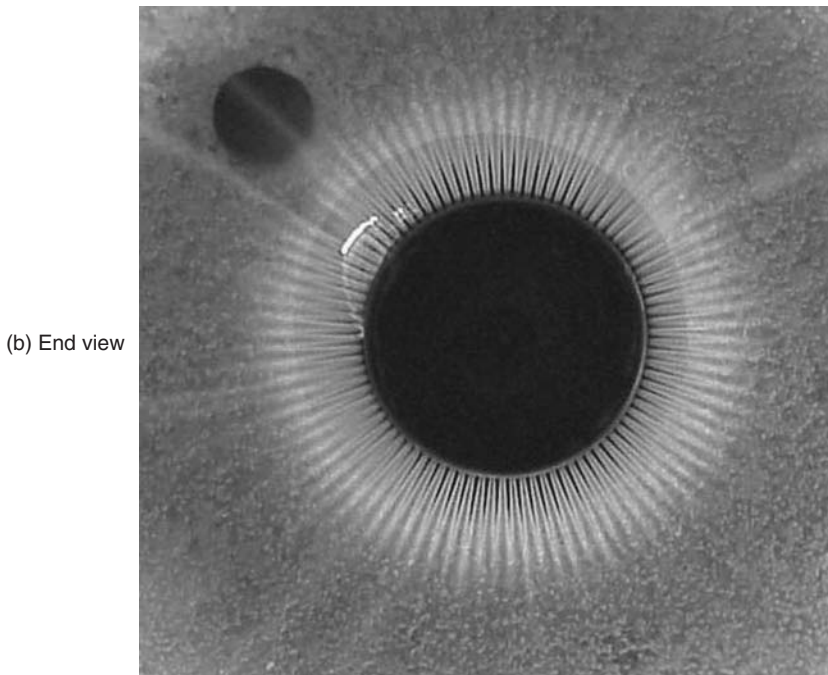
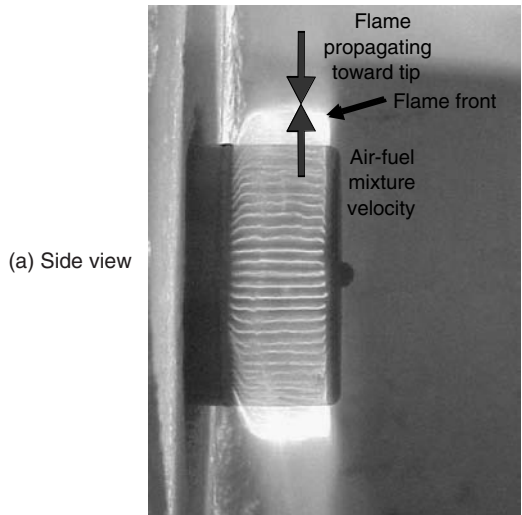


FIGURE 15.10 Photograph of flame attachment on a radiant wall burner tip. (Courtesy of John Zink Co., LLC.)

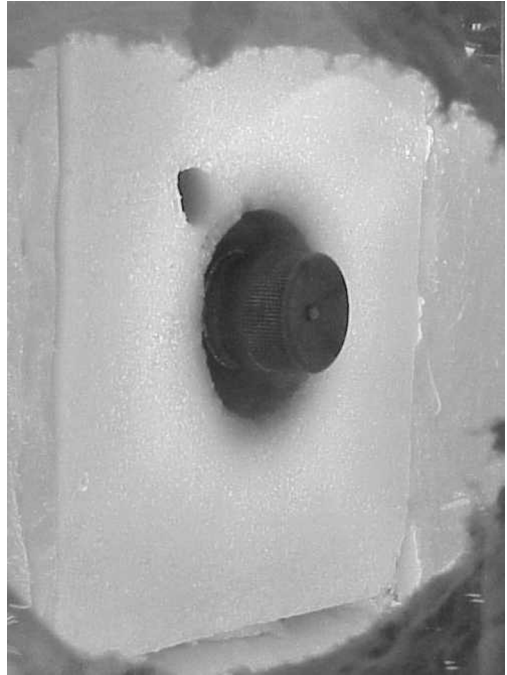


FIGURE 15.11 Photograph of flame detachment on a radiant wall burner tip. (Courtesy of John Zink Co., LLC.)

mode, the velocity of the air/fuel mixture exiting the tip prevents the flame front from propagating through the premix burner tip openings causing a flashback.

Radiant wall burners are also often designed to operate with the flame stabilized in a region some distance away from the premix tip exit along the hot surface of the fired wall. This detached flame is stabilized by radiant heat emitted from the refractory wall. Figure 15.11 shows a burner operating in this detached mode. This mode is typically desirable during hot furnace operation and can result in the reduction of NO_x emissions, as inert furnace gases are entrained into the mixture prior to combustion. However, if local exit velocities of the mixture substantially exceed local flame velocities and/or local temperatures are not maintained at levels high enough to sustain stable combustion, it is possible that the flame could lift off and blow out.

15.3.3 EMISSIONS

Historically, early radiant wall burners were designed with the primary goals of having stable, complete combustion (low CO and unburned fuel emissions), and providing desired heat transfer characteristics. These radiant wall burners were commonly partially premixed burners — meaning that the primary air educted through the burner was not sufficient for complete combustion of the fuel (i.e., fuel-rich mixture). Additional air (secondary air) was supplied through the space between the burner venturi/tip assembly and the tile and was controlled with secondary air doors as previously illustrated in [Figure 15.5a](#). The nitrogen oxide (NO_x) emissions from these previous burner designs are relatively high, due to relatively high peak flame temperatures.

As requirements for lower NO_x emissions arose, radiant wall burners were developed that utilized different fuel staging schemes to lower NO_x emissions. In some configurations, secondary fuel (staged fuel) risers were used to stage the fuel between the primary premixed flame and the furnace wall to reduce NO_x emissions. In other configurations, the fuel was staged on the furnace side, rather than the wall side, of the primary premixed flame. As in other types of burners, staged fuel technology can be used to reduce emissions by reducing the peak flame temperatures in the fuel-rich, staged-flame zones by entrainment of inert furnace gases prior to combustion. Typically, less than 25% of the fuel was staged in these types of radiant wall burners. Although staging a

portion of the fuel is an effective technique to reduce NOx emissions, less fuel is available in the primary zone to entrain the required air for complete combustion. Additional air required for combustion could be supplied through secondary air openings, but this can also result in detrimental increases in flame temperatures and NOx emissions, due to early mixing and reacting of the secondary air with the staged fuel.

In recent years, federal and state regulations in the U.S. have required further reductions in NOx emissions from hydrogen-reforming and ethylene-cracking heaters employing radiant wall burners. New technology employed to achieve these desired emission levels combines a very fuel-lean premixed primary flame with fuel staging.^{4,5} Lean premixed combustion has been the subject of research in academia and industry to successfully reduce NOx emissions. Lean premixed combustion results in very low peak flame temperatures in the primary premixed flame zone as the stoichiometry in this region approaches the limits of flammability, as illustrated in Figure 15.12. Highly efficient venturi systems are employed to achieve the required stoichiometry in the primary fuel/gas mixture. Currently, the best available radiant wall burner technology can achieve entrainment and mixing of 100 to 115% of the total required air for complete combustion with a portion of the fuel. The remainder of the fuel is staged, with little or no secondary air required. Typical NOx levels achievable with the different radiant wall burner technologies discussed are shown in Table 15.2.

TABLE 15.2
Typical NOx Emissions with Described Radiant Wall Burner Technologies

	Early Designs with Secondary Air	Staged Fuel Designs	Lean Premixed Designs
Premixed mixture	100% fuel/<100% air	75–90% fuel/<100% air	40–70% fuel/100% air
Secondary air	Yes	Yes	No
Staged fuel	No	Yes	Yes
Typical NOx emissions (1900–2250°F firebox)	75–120 ppm	40–75 ppm	20–35 ppm

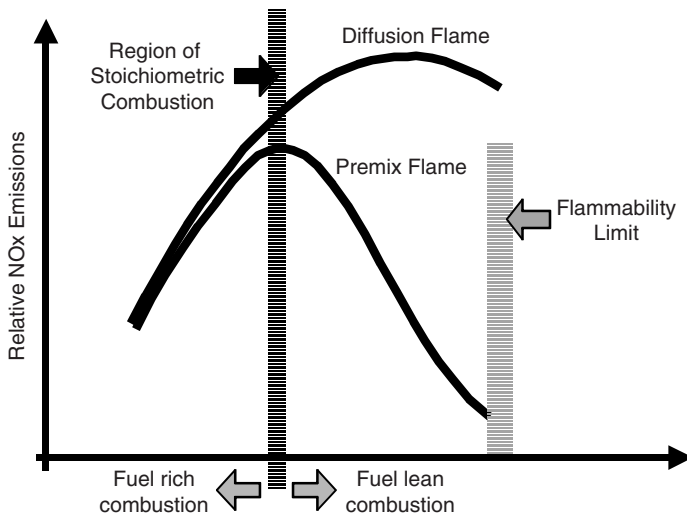


FIGURE 15.12 Effects of stoichiometry on NOx emissions.

15.3.4 BURNER SPACING

Burner location and spacing along the heater wall can play an important role in determining operating performance of the furnace. In typical applications, the desire is to evenly heat the wall to relatively high temperatures without causing local overheating of the process tubes. Overheating can cause fouling or coking of the tubes and decrease product yields and unit run lengths. When burners are spaced too closely together, the burner flames can interact significantly, causing local hot spots and increased NO_x emissions. If they are spaced too far apart, the unit efficiency might be negatively impacted by not providing the maximum levels of heat transfer to the process tubes achievable with the given furnace geometry.

15.4 RETROFIT CONSIDERATIONS

In new heater installations, there is more flexibility for collaboration between the burner and heater manufacturers to provide burner and furnace configurations that complement each other for optimal process performance. However, in existing heaters, many constraints for retrofit with newer burner technologies may be present. This is due to the furnaces being originally designed with geometries optimized for older-technology burners. Several parameters, such as existing burner cutouts, heater dimensions, the distance between the process tubes and the refractory walls, the size of the hole in the tile through which the burner is inserted, the space limitations for personnel access to the burners outside the furnace, or the maximum available fuel pressure, can place many constraints on a burner designed for retrofit to meet new emissions requirements.

15.5 OPERATION AND TROUBLESHOOTING

15.5.1 OPERATION

Proper operation of radiant wall burners during cold light-off, normal operation, and turndown conditions is important in achieving the desired performance. Typically, cold light-off is achieved by inserting a lighting torch near the burner tip exit to provide an ignition source as the fuel gas is opened to flow through the burner. When lighting burners in cold furnace conditions, the air flow is adjusted (typically by positioning the burner air doors or dampers) to provide for a stable flame that is positioned close to the burner tip exit (i.e., attached flame) — see [Figure 15.10](#). As the furnace warms up and the fired wall temperature increases, the burner can be adjusted so that the flame lifts further away from the burner tip and stabilizes along the surface of the hot fired refractory wall. During normal operation, burner air doors should be adjusted appropriately at the different burner elevations to achieve the desired excess air levels locally and globally that optimize combustion efficiency and NO_x emissions. During turndown conditions, fuel flow is reduced, which can lead to flashback conditions if mixture exit velocities become less than the local flame speed at the burner tip exit.

15.5.2 TROUBLESHOOTING

15.5.2.1 Burner Tip Plugging/Coking

Fuel ports can become plugged from particulates in the fuel lines, such as pipe scale, salts, dirt, materials dissolved in liquids in the fuel, or from hydrocarbon liquids in the fuel that crack when they encounter the hot surface of the fuel port, leaving behind coke. If plugging occurs, the firing capacity of the furnace will be reduced for a given fuel pressure. Plugged ports can also create uneven flame patterns within the furnace, flame instability, flashback, or coking of the burner tip.

Coke is a black, solid, carbon-based material that can build up on the inside of a burner tip. Coke buildup usually occurs when fuel containing heavy hydrocarbons, unsaturates, or liquids

comes in contact with the hot metal surface of the burner tip. When the fuel encounters the surface of the tip, and temperatures are elevated above acceptable levels, the fuel gas can crack, creating soot and coke buildup. This buildup can block off the premix burner tip, resulting in a reduction in the entrainment performance of air through the burner. As the coke continues to build up inside the tip, the air flow becomes more restricted, causing the tip temperatures to continue to rise. Eventually, the tip can be destroyed due to the lack of air flowing through and cooling it.

Filtration of fuel stream to remove liquids and/or particulates is recommended to prevent burner tip from plugging/coking. Burner tips should be regularly inspected and cleaned or replaced, if necessary, to maintain optimal burner performance.

15.5.2.2 Furnace Air Leakage

In the typical operation of a heater, the excess air for the entire heater is monitored and appropriately adjusted for the specific process to meet a global target (typically 2 to 3% excess O₂ in reforming and ethylene-cracking applications). If air is unintentionally being pulled into the heater by the furnace draft through openings other than the burners, local air/fuel ratio conditions at the burners and in the flame zones may be very different from those designed (i.e., optimal). This can result in incomplete combustion or increases in NO_x emissions.

15.6 CONCLUSION

Radiant wall burners are an important, widely used component in petrochemical industries. They are utilized to achieve specific heat flux conditions in relatively high temperature furnace applications, such as reformers or ethylene-cracking units. Historically, the design of these burners has changed to meet increasingly stringent emissions requirements. Proper design of the burner components and consideration of a variety of factors are necessary, combined with proper operation, to achieve the best burner performance. This will consequently have a significant impact on heater performance with regard to process efficiency and yield, equipment durability, and emissions.

REFERENCES

1. Baukal, C.E., Ed., *The John Zink Combustion Handbook*, CRC Press, Boca Raton, FL, 2001.
2. Keenan, J.H. and Neumann, E.P., A simple air ejector, *Journal of Applied Mechanics*, A-75, 1942.
3. Bussman, W., A Preliminary Study of the Mixing and Inspiration Performance of a Venturi Eductor System, John Zink Company Research Study, Paper No. 92-03, 1992.
4. Venizelos, D., Bussman, W., Hayes, R., and Poe, R., High Capacity/Low NO_x Radiant Wall Burner, U.S. Patent Application 20020076668, Patent Pending, 2001.
5. Venizelos, D., Hayes, R., Waibel, R., and Bussman, W., Low NO_x Premix Burner Apparatus and Methods, U.S. Patent Application 20020064740, Patent Pending, 2000.
6. Bussman, W., Premixed Burner Model Engineering Program, Proprietary John Zink Company Engineering Design Tool, 1999.
7. Venizelos, D. T., A Report on Testing of the COOLMIX-100 Burner, Internal John Zink Report, February 2000.
8. Idelchik, I. E., *Handbook of Hydraulic Resistance*, second edition, 1986, chap. 3, 113-143.

Footnote

U.S. Patent No. 4702691 and 5180302, U.S. and International patents pending.

16 Natural-Draft Burners

*Charles E. Baukal, Jr., Ph.D., P.E.,
Richard T. Waibel, Ph.D., and Michael Claxton*

CONTENTS

- 16.1 Introduction
- 16.2 Hydrocarbon and Petrochemical Industries
- 16.3 Fired Heaters
 - 16.3.1 Reformers
 - 16.3.2 Process Heaters
- 16.4 Burner Design
 - 16.4.1 Metering the Fuel
 - 16.4.1.1 Gaseous Fuel
 - 16.4.1.2 Liquid Fuel
 - 16.4.2 Metering the Air
 - 16.4.3 Mixing the Fuel and Air
 - 16.4.4 Maintaining Ignition
 - 16.4.5 Molding the Flame Shape
 - 16.4.6 Minimizing Pollutant Emissions
- 16.5 Burner Types
 - 16.5.1 Premix and Partial Premix Gas
 - 16.5.2 Raw-Gas or Nozzle-Mix
 - 16.5.3 Oil or Liquid Firing
 - 16.5.3.1 High-Viscosity Liquid Fuels
 - 16.5.3.2 Low-Viscosity Liquid Fuels
- 16.6 Burner Configuration
 - 16.6.1 Round-Flame Burner
 - 16.6.2 Flat-Flame Burner
 - 16.6.2.1 Wall-Fired Flat-Flame Burners
 - 16.6.2.2 Free-Standing Flat-Flame Burners
 - 16.6.3 Radiant Wall Burners
 - 16.6.4 Down-fired Burners
- 16.7 Materials Selection
- 16.8 Conclusions
- References

16.1 INTRODUCTION

Natural-draft burners are used in a wide range of residential and commercial applications, including gas-fired furnaces, water heaters, cooking ranges, and ovens. However, these burners are somewhat unique in industry. Most burners used in industrial combustion applications are forced or mechanical draft, where the combustion air is supplied to the burner with a fan or blower. In natural-draft burners, the combustion air is induced or drawn into the burner via the suction created by the

incoming fuel jets and via the buoyancy forces inside the furnace that create an updraft. These burners are predominantly used in the chemical process industry (CPI) and the hydrocarbon process industry (HPI). They are fired in a variety of configurations on a variety of fuel compositions that are mostly gaseous, but are sometimes liquid. There are many unique aspects of natural-draft burners, compared to forced-draft burners, discussed in this chapter.

There are some good resources available for the interested reader on the subject of natural-draft burners. A book by Robert Reed (1981), which is now out of print, had been the standard in the industry on the subject of combustion in the hydrocarbon and petrochemical processing industries, including the topic of natural-draft burners (particularly Chapter 5).¹ A recent book written by the John Zink Co., LLC (Tulsa, OK) is the most comprehensive publication of its type on the subject of combustion in HPI and CPI applications.² It includes extensive treatments of natural-draft burners, which are the workhorses for those industries. Much of this chapter was adapted from chapters in that book.^{3,4} The American Petroleum Institute has some good resources that include discussions of natural-draft burners, although less extensive than the previous publications.^{5,6}

16.2 HYDROCARBON AND PETROCHEMICAL INDUSTRIES

The hydrocarbon and petrochemical industries present unique challenges to the combustion engineer, compared to other industrial combustion processes. One of the more important challenges in those industries is the wide variety of fuels,⁷ which are usually off-gases from the petroleum refining processes that are used in a typical plant (see [Figure 16.1](#)). This differs significantly from most other industrial combustion systems, which normally fire a single purchased fuel such as natural gas or fuel oil. Another important challenge is that many of the burners commonly used in the hydrocarbon and petrochemical industries are natural draft which are not as easy to control as forced-draft burners, and are subject to things such as the wind, which can disturb the conditions in a process heater.

According to the U.S. Department of Energy (U.S. DOE), petroleum refining is the most energy-intensive manufacturing industry in the U.S., accounting for about 7% of total U.S. energy consumption in 1994.⁸ [Table 16.1](#) shows the major processes in petroleum refining, most of which require combustion in one form or another. [Figure 16.2](#) shows the process flow through a typical refinery.

The U.S. DOE Office of Industrial Technologies has prepared a Technology Roadmap for industrial combustion.⁹ For process heating systems, some key performance targets for the year 2020 have been identified for burners and for the overall system. For the burners, the targets include reducing criteria pollutant emissions by 90%, reducing CO₂ emissions to levels agreed upon by the international community, reducing specific fuel consumption by 20 to 50%, and maximizing the ability to use multiple fuels. The following were identified as top-priority R&D needs for burners in process heating: burners capable of adjusting operating parameters in real-time, advanced burner stabilization methods, robust design tools, and economical methods to premix fuel and air. The process heaters are considered briefly next.

16.3 FIRED HEATERS

Fired or tubestill heaters are used in the petrochemical and hydrocarbon industries to heat fluids in tubes for further processing. In this type of process, fluids flow through an array of tubes located inside a furnace or heater. The tubes are heated by direct-fired burners. Using tubes to contain the load is somewhat unique compared to the other types of industrial combustion applications. It was found that heating the fluids in tubes has many advantages over heating them in the shell of a furnace.¹⁰ Advantages include better suitability for continuous operation, better controllability, higher heating rates, more flexibility, less chance of fire, and more compact equipment.



FIGURE 16.1 Typical petroleum refinery. (Courtesy of John Zink Co., LLC.³)

TABLE 16.1
Major Petroleum Refining Processes

Category	Major Process
Topping (separation of crude oil)	Atmospheric distillation Vacuum distillation Solvent deasphalting
Thermal and catalytic cracking	Delayed coking Fluid coking/flexicoking Visbreaking Catalytic cracking Catalytic hydrocracking
Combination/rearrangement of hydrocarbons	Alkylation Catalytic reforming Polymerization Isomerization Ethers manufacture
Treating	Catalytic hydrotreating/hydroprocessing Sweetening/sulfur removal Gas treatment
Specialty product manufacture	Lube oil Grease Asphalt

Source: U.S. Dept. of Energy.⁸

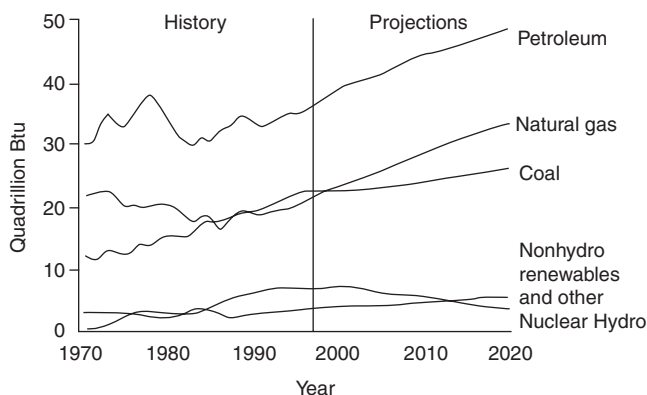


FIGURE 16.2 Typical refinery flow diagram. (Source: U.S. Dept. of Energy.⁸)

One of the problems encountered in refinery-fired heaters is an imbalance in the heat flux in the individual heater passes.¹¹ This imbalance can cause high coke formation rates and high tube metal temperatures, which reduce a unit's capacity and can cause premature failures. Coke formation on the inside of heater tubes reduces the heat transfer through the tubes, which leads to the reduced capacity. One cause of coking is flame impingement directly on a tube, which causes localized heating and increases coke formation there. This flame impingement may be caused by operating without all of the burners in service, insufficient primary or secondary air to the burner, operating the heater at excessive firing rates, fouled burner tips, eroded burner tip orifices, or insufficient

draft. The problem of flame impingement shows the importance of proper design¹² to assure even heat flux distribution inside the fired heater.

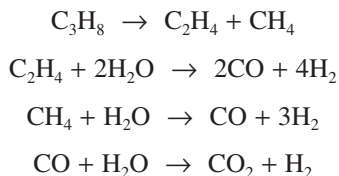
Recently, the major emphasis has been on increasing the capacity of existing heaters rather than installing new heaters. The limitations of over-firing a heater include:

- High tube metal temperatures
- Flame impingement, causing high coke formation rates
- Positive pressure at the arch of the heater
- Exceeding the capacity of induced-draft and forced-draft fans
- Exceeding the capacity of the process fluid feed pump

Garg (1988)¹³ noted the importance of good heater specifications to ensure suitable performance for a given process. Some of the basic process conditions needed for the specifications include heater type (cabin, vertical cylindrical, etc.), number of fluid passes, the tube coil size and material, fluid data (types, compositions, properties, and flow rates), heat duty required, fuel data (composition, pressure, and temperature), heat flux loading (heat flux split between the radiant and convection sections), burner data (number, type, arrangement, etc.), draft requirement, required instrumentation, as well as a number of other details, such as the number of peepholes, access doors, and platforms.

16.3.1 REFORMERS

As the name indicates, reformers are used to reformulate a material into another product. For example, a hydrogen reformer takes natural gas and reformulates it into hydrogen in a catalytic chemical process that involves a significant amount of heat. A sample set of reactions is given below for converting propane to hydrogen:¹⁴



The reformer is a direct-fired combustor containing numerous tubes, filled with catalyst, inside the combustor.¹⁵ The reformer is heated with burners, firing either vertically downward or upward, with the exhaust on the opposite end, depending on the specific design of the unit. The raw feed material flows through the catalyst in the tubes which, under the proper conditions, converts that material to the desired end product. The burners provide the heat needed for the highly endothermic chemical reactions. The fluid being reformulated typically flows through a reformer combustor containing many tubes (see [Figure 16.3](#)). The side-fired reformer has multiple burners on the side of the furnace, with a single row of tubes centrally located. The heat is transferred primarily by radiation from the hot refractory walls to the tubes. Top-fired reformers have multiple rows of tubes in the firebox. In that design, the heat is transferred primarily from radiation from the flame to the tubes. [Figure 16.4](#) shows a down-fired burner commonly used in top-fired reformers. In a design sometimes referred to as *terrace firing*, burners are located in the side wall but firing up the wall at a slight angle (see [Figure 16.5](#)). Foster Wheeler uses terrace wall reformers in the production of hydrogen by steam reformation of natural gas or light refinery gas.¹⁶

The reformer tubes are a critical element in the overall design of the reformer. Because they operate at pressures up to 350 psig (24 barg), they are typically made from a high-temperature and pressure nickel alloy, such as inconel, to ensure that they can withstand the operating conditions inside the reformer. Failure of the tubes can be very expensive because of the downtime of the unit, lost product, damaged catalyst, and possibly, damaged reformer. New reactor technologies are being developed to improve the process for converting natural gas to precursor synthesis gas (syngas).¹⁷

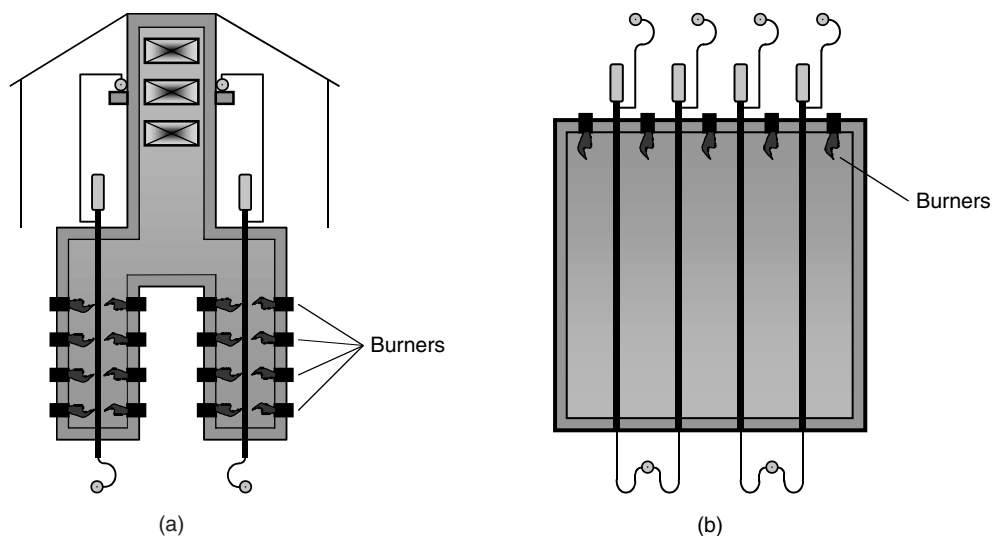


FIGURE 16.3 Side- and top-fired reformers. (Courtesy of Marcel Dekker.¹⁵)



FIGURE 16.4 Down-fired burner commonly used in top-fired reformers. (Courtesy of John Zink Co., LLC.³)

16.3.2 PROCESS HEATERS

Process heaters are sometimes referred to as process furnaces or direct-fired heaters. They are heat transfer units designed to heat petroleum products, chemicals, and other liquids and gases flowing through tubes. Typical petroleum fluids include gasoline, naphtha, kerosene, distillate oil, lube oil, gas oil, and light ends.¹⁸ The heating is done to raise the temperature of the fluid for further processing downstream or to promote chemical reactions in the tubes, often in the presence of a catalyst. Kern¹⁸ noted that refinery heaters can carry liquids at temperatures as high as 1500°F (810°C) and pressures up to 1600 psig (110 barg). The primary modes of heat transfer in process heaters are radiation and convection. The initial part of the fluid heating is done in the convection section of the furnace, while the latter heating is done in the radiant section (see Figure 16.6). Each section has a

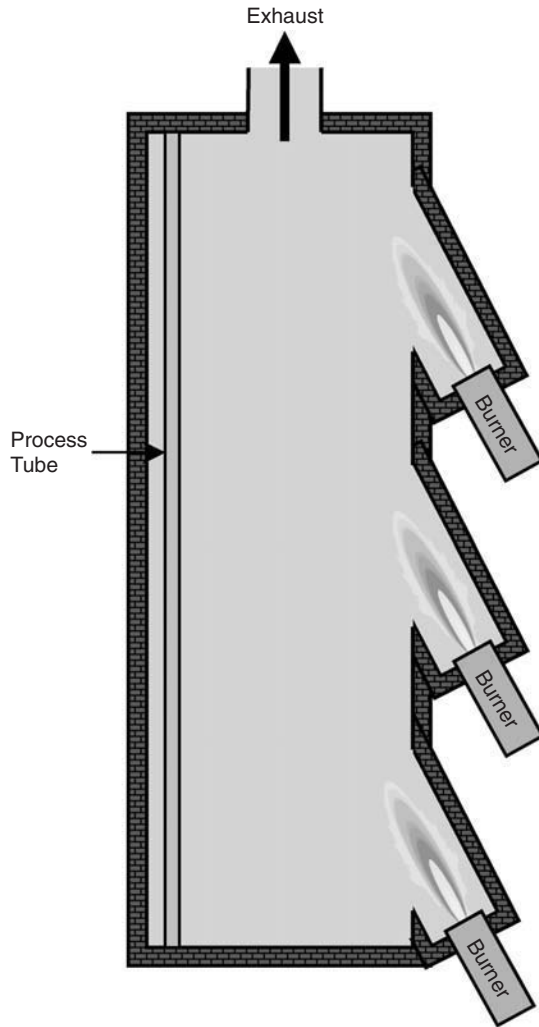


FIGURE 16.5 Terrace firing furnace.

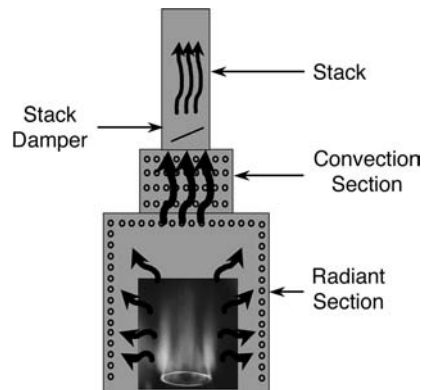


FIGURE 16.6 Schematic of the heating zones in a process heater. (Courtesy of John Zink Co., LLC.³)

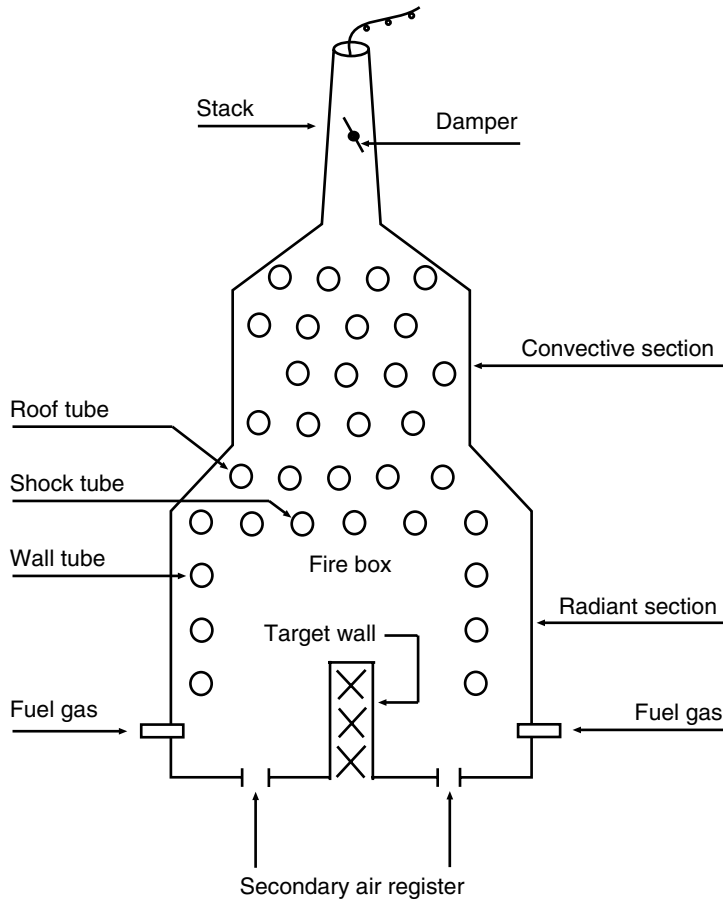


FIGURE 16.7 Typical process heater. (Courtesy of PennWell.¹⁹)

bank of tubes in it through which the fluids flow, as shown in [Figure 16.7](#).¹⁹ Early heater designs had only a single bank of tubes that failed prematurely because designers did not understand the importance of radiation on the process.¹⁰ The tubes closest to the burners would overheat. Overheating caused the hydrocarbons to form coke inside the tube. The coke further aggravated the problem by reducing the thermal conductivity through the coke layer inside the tube. The reduced thermal conductivity prevented the process fluids from absorbing adequate heat to cool the tubes, resulting in overheating and failure of the tubes. One of the key challenges for the heater designer is to get even heat distribution inside the combustor to prevent coking inside the tubes. Bell and Lowy (1967)²⁰ estimated that approximately 70% of the energy is transferred to the fluids in the radiant section of a typical heater and the balance in the convection section. The tubes in the convection section often have fins to improve convective heat transfer efficiency. These fins are designed to withstand temperatures up to about 1200°F (650°C). If delayed combustion occurs in the convection section, the fins can be exposed to temperatures up to 2000°F (1100°C), which can damage the fins.¹⁹

Kern noted that process heaters are typically designed around the burners.¹⁸ There may be anywhere from one to over a hundred burners in a typical process heater, depending on the design and process requirements. In the refinery industry, the average number of burners in a heater varies by the heater type, as shown in [Table 16.2](#).²¹ On average, mechanical draft burners have higher firing rates than natural draft. For forced-draft systems, burners with air preheat typically have higher heat releases than burners without air preheat. According to one survey, 89.6% of the burners in oil refineries are natural

TABLE 16.2
Average Burner Configuration by Heater Type

Heater Type	Avg. No. of Burners	Avg. Design Total Heat Release (10 ⁶ Btu/hr)	Avg. Firing Rate Per Burner (10 ⁶ Btu/hr)
Natural draft	24	69.4	2.89
Mechanical draft, no air preheat	20	103.6	5.18
Mechanical draft, with air preheat	14	135.4	9.67

Source: U.S. EPA.²¹

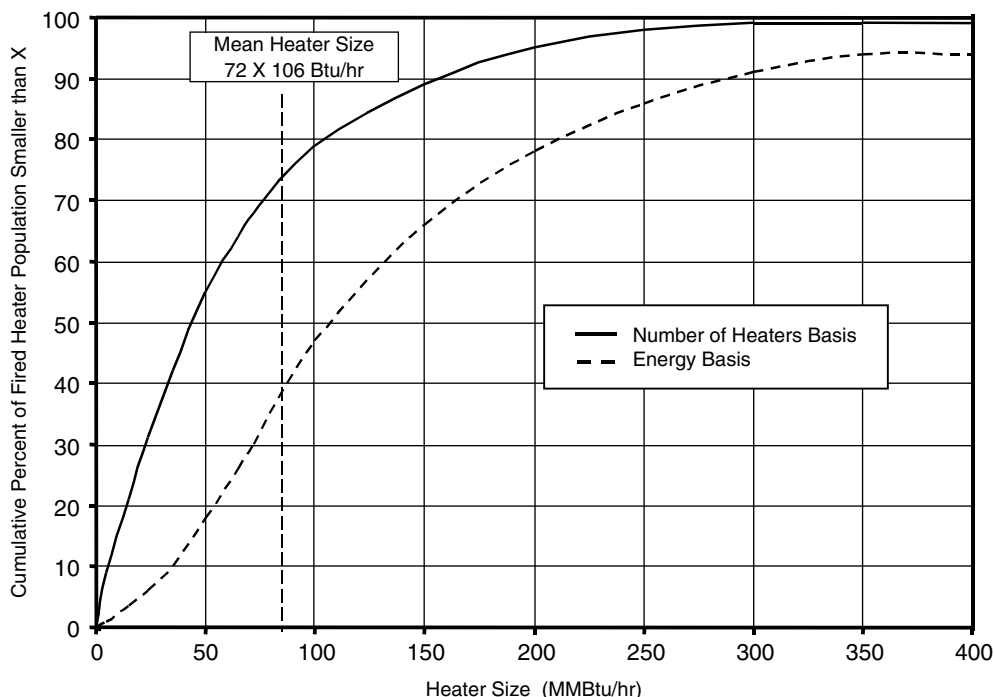


FIGURE 16.8 Fired heater size distribution. (Source: U.S. EPA.²¹)

draft, 8.0% are forced draft with no air preheat, and 2.4% are forced draft with air preheat.²² The mean size of all process heaters is 72×10^6 Btu/hr (21 MW), which are mostly natural draft. The mean size of forced-draft heaters is 110×10^6 Btu/hr (32 MW). Figure 16.8 shows the distribution for the overall firing rate for fired heaters. Table 16.3 shows the variety of processes in a refinery that uses fired heaters.

Table 16.4 shows the major applications for fired heaters in the chemical industry. These can be broadly classified into two categories: (1) low and medium firebox temperature applications such as feed preheaters, reboilers, and steam superheaters; and (2) high firebox temperature applications such as olefins pyrolysis furnaces and steam-hydrocarbon reformers. The low and medium firebox temperature heaters represent about 20% of the chemical industry requirements and are similar to those in the petroleum refining industry.²³ The high firebox temperature heaters represent the remaining 80% of the chemical industry heater requirements and are unique to the chemical industry.

Berman (1979)²⁴ discussed the different burner designs used in fired heaters, Burners may be located in the floor, firing vertically upward. In vertical cylindrical (VC) furnaces, those burners

TABLE 16.3
Major Refinery Processes Requiring a Fired Heater

Process	Process Description	Heaters Used	Process Heat Requirements		Feedstock Temperature Outlet of Heater, (°F)
			KJ/liter	(10 ³ Btu/bbl feed)	
Distillation					
Atmospheric	Separates light hydrocarbons from crude in a distillation column under atmospheric conditions.	Preheater, reboiler	590	89	700
Vacuum	Separates heavy gas oils from atmospheric distillation bottoms under vacuum.	Preheater, reboiler	418	63	750–830
Thermal Processes					
Thermal cracking	Thermal decomposition of large molecules into lighter, more valuable products.	Fired reactor	4650	700	850–1000
Coking	Cracking reactions allowed to go to completion. Lighter products and coke produced.	Preheater	1520	230	900–975
Visbreaking	Mild cracking of residuals to improve their viscosity and produce lighter gas oils.	Fired reactor	961	145	850–950
Catalytic Cracking					
Fluidized catalytic cracking	Cracking of heavy petroleum products. A catalyst is used to aid the reaction.	Preheater	663	100	600–885
Catalytic hydrocracking	Cracking heavy feedstocks to produce lighter products in the presence of hydrogen and a catalyst.	Preheater	1290	195	400–850
Hydroprocessing					
Hydrosulfurization	Remove contaminating metals, sulfur, and nitrogen from the feedstock. Hydrogen is added and reacted over a catalyst.	Preheater	431	65 ^a	390–850
Hydrotreating	Less severe than hydrosulfurization. Removes metals, nitrogen, and sulfur from lighter feedstocks. Hydrogen is added and reacted over a catalyst.	Preheater	497	75 ^b	600–800
Hydroconversion					
Alkylation	Combination of two hydrocarbons to produce a higher molecular weight hydrocarbon. Heater used on the fractionator.	Reboiler	2500	377 ^c	400
Catalytic reforming	Low-octane naphthas are converted to high-octane, aromatic naphthas. Feedstock is contacted with hydrogen over a catalyst.	Preheater	1790	270	850–1000

^aHeavy gas oils and middle distillates

^bLight distillate

^cBtu/bbl of total alylate

Source: U.S. EPA.²¹

TABLE 16.4
Major Fired Heater Applications in the Chemical Industry

Chemical	Process	Heater Type	Firebox Temperature (°F)	1985 Fired Heater Energy Requirement (10 ¹² Btu/yr)	% of Known Chemical Industry Heater Requirements
Low and Medium Temperature Applications					
Benzene	Reformate extraction	Reboiler	700	64.8	9.9
Styrene	Ethylbenzine dehydrogenation	Steam superheater	1500–1600	32.1	4.9
Vinyl chloride monomer	Ethylene dichloride cracking	Cracking furnace	N/A	12.6	1.9
<i>P</i> -Xylene	Xylene isomerization	Reactor fired preheater	N/A	13.0	2.0
Dimethyl terephthalate	Reaction of <i>p</i> -xylene and methanol	Preheater, hot oil furnace	480–540	11.1	1.7
Butadiene	Butylene dehydrogenation	Preheater, reboiler	1100	2.6	0.4
Ethanol (synthetic)	Ethylene hydration	Preheater	750	1.3	0.2
Acetone	Various	Hot oil furnace	N/A	0.8	0.1
High-Temperature Applications					
Ethylene/propylene	Thermal cracking	Pyrolysis furnace	1900–2300	337.9	51.8
Ammonia	Natural gas reforming	Steam hydrocarbon reformer	1500–1600	150.5	23.1
Methanol	Hydrocarbon reforming	Steam hydrocarbon	1000–2000	25.7	4.0
Total Known Fired Heater Energy Requirement				652.4	100.0

Source: U.S. EPA.²¹

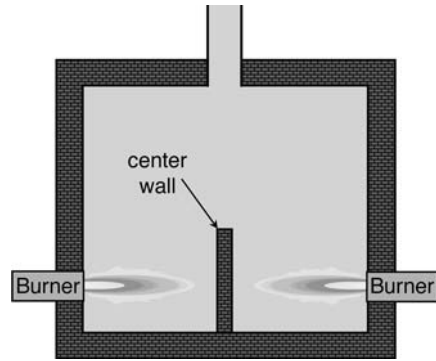


FIGURE 16.9 Sketch of center or target wall firing configuration. (Courtesy of John Zink Co., LLC.³)

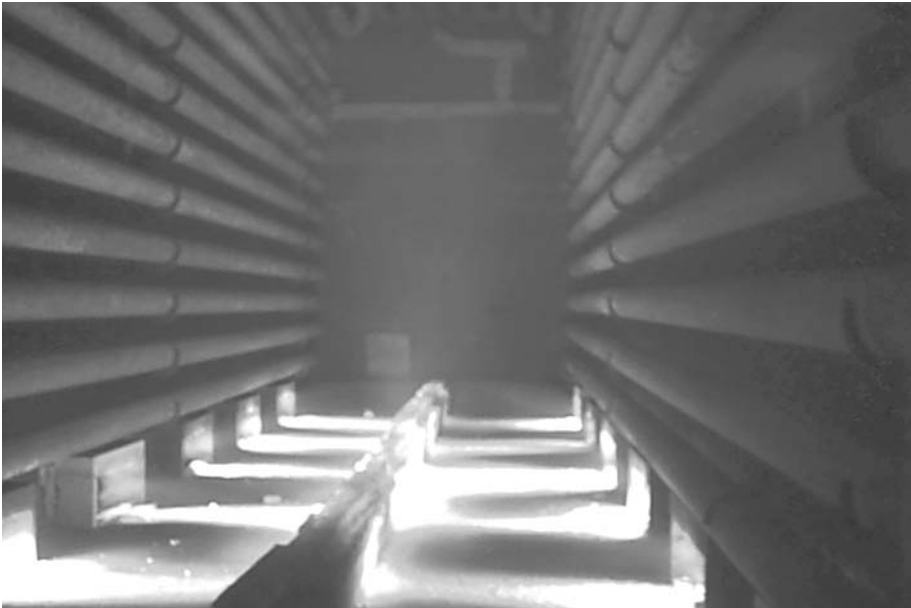


FIGURE 16.10 Horizontal floor-fired burners firing toward a center wall. (Courtesy of John Zink Co., LLC.³)

are located in a circle in the floor of the furnace. The VC furnace itself serves as part of the exhaust stack to help create draft to increase the chimney effect.²⁵ In cabin heaters, which are rectangular, there are one or more rows of burners located in the floor. Burners may be at a low-level, firing parallel to the floor. In that configuration, they may be firing from two opposite sides toward a partial wall in the middle of the furnace that acts as a radiator to distribute the heat (see [Figure 16.9](#) and [Figure 16.10](#)). Burners may be located on the wall, firing radially along the wall (see [Figure 16.11](#)), which are referred to as radiant wall burners (see Chapter 15). There are also combinations of the above in certain heater designs. For example, in ethylene production heaters, both floor-mounted, vertically fired burners (see [Figure 16.12](#)) and radiant wall burners are used in the same heater.

Typical examples of process heaters are shown in [Figure 16.13](#) and [Figure 16.14](#).²⁶ A cabin heater is shown in [Figure 16.15](#). Burners firing in a crude unit are shown in [Figure 16.16](#). Typical burner arrangements are shown in [Figure 16.17](#). Berman (1979)²⁷ noted the following categories of process heaters: column reboilers; fractionating-column feed preheaters; reactor-feed preheaters, including reformers; heat supplied to heat transfer media (e.g., a circulating fluid or molten salt); heat supplied to viscous fluids; and fired reactors, including steam reformers and pyrolysis heaters. Six types of vertical cylindrical fired heaters were given: all radiant, helical coil, crossflow with convection section, integral

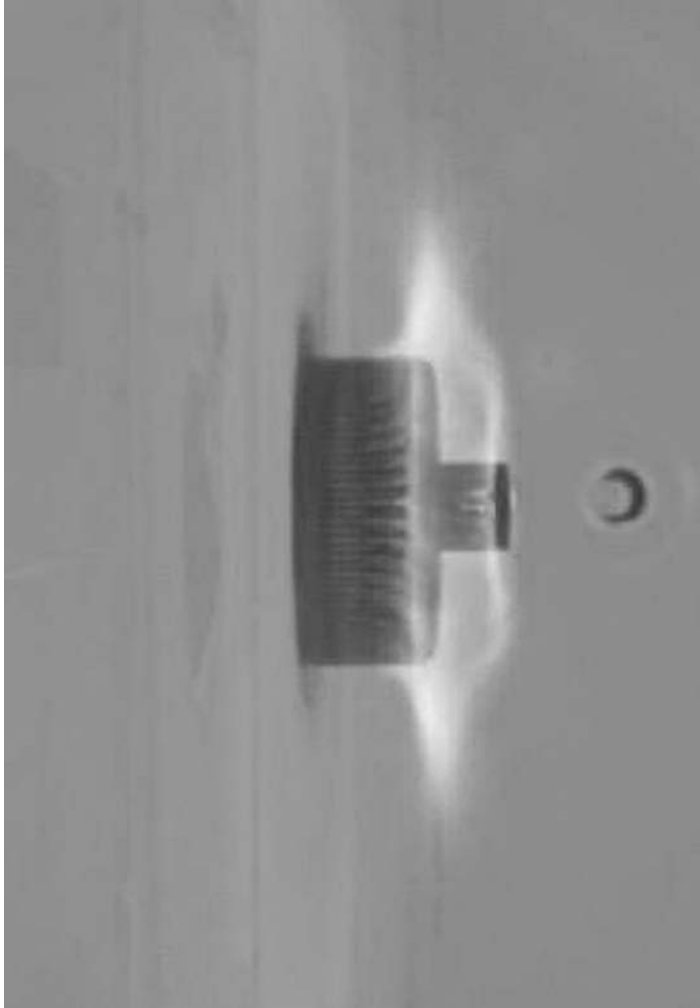


FIGURE 16.11 Wall-fired burner (side view). (Courtesy of John Zink Co., LLC.)

convection section, arbor or wicket type, and single-row/double-fired. Six basic designs were also given for horizontal tube fired heaters: cabin, two-cell box, cabin with dividing bridgewall, end-fired box, end-fired box with side-mounted convection section, and horizontal-tube/single-row/double-fired.

Many commonly used process heaters typically have a radiant section and a convection section. Burners are fired in the radiant section to heat up the tubes. Fluids flow through the tubes and are heated to the desired temperature for further processing. The fluids are preheated in the convection section and heated to the desired process temperature in the radiant section. Radiant heat transfer from the flames to the tubes is the most critical aspect of this heater because overheating of the tubes leads to tube failure and shutdown of the heater.²⁸ The tubes may be horizontally or vertically oriented, depending on the particular heater design.

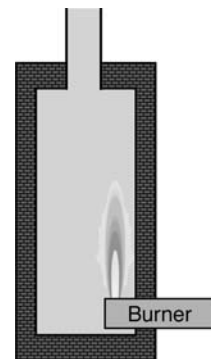


FIGURE 16.12 Sketch of a horizontally-mounted, vertically-fired burner configuration. (Courtesy of John Zink Co., LLC.³)

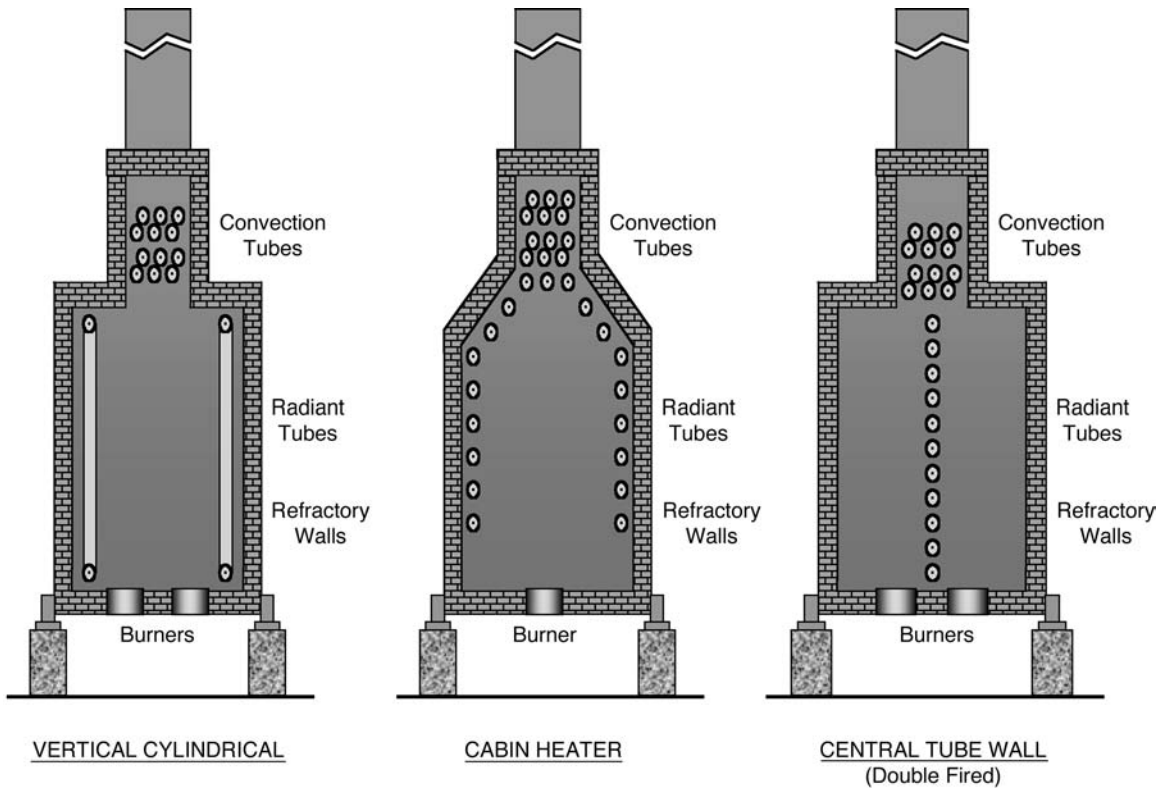


FIGURE 16.13 Examples of process heaters.²⁶

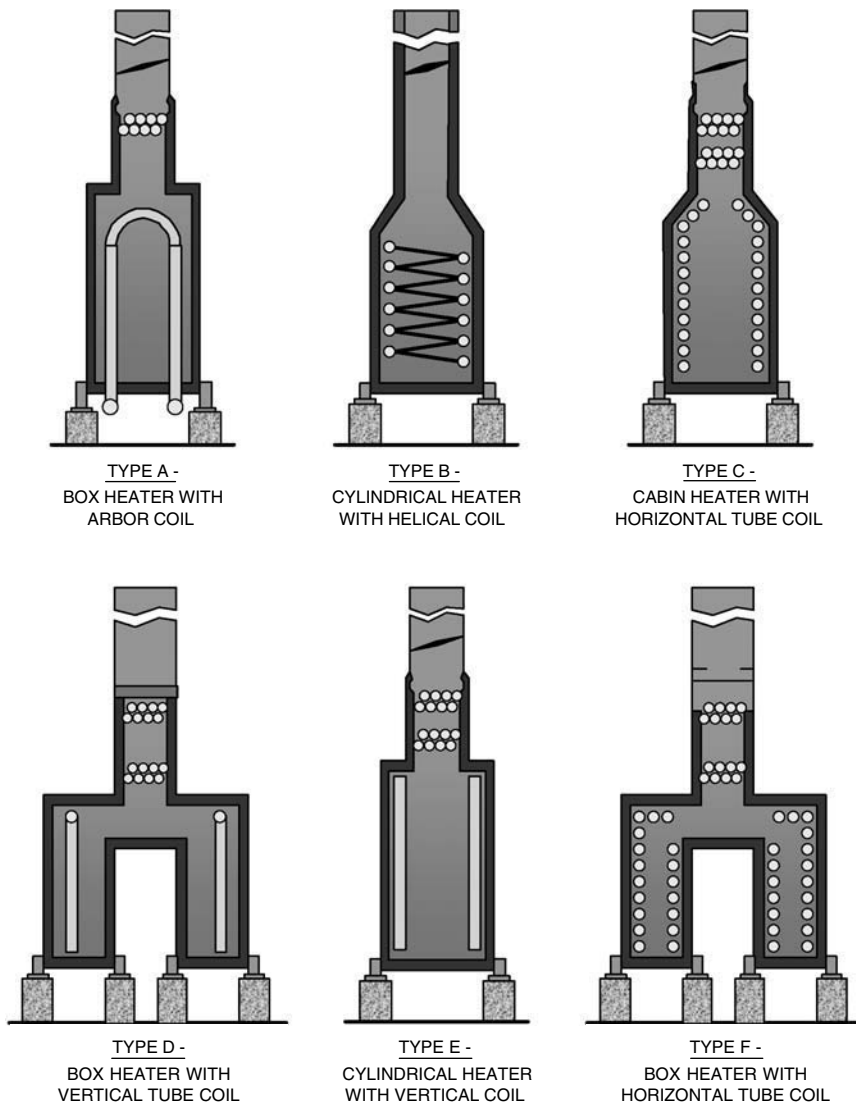


FIGURE 16.14 Typical heater types.²⁶

A unique aspect of process heaters is that they are often natural draft. Another unique aspect of these heaters is the wide range of fuels that are used, which are often byproducts of the petroleum refining process. These fuels may contain significant amounts of hydrogen, which has a large impact on the burner design. It is also fairly common for multiple fuel compositions to be used, depending on the operating conditions of the plant at any given time. In addition to hydrocarbons ranging up to C_5 , the gaseous fuels may also contain hydrogen and inerts (such as CO_2 or N_2). The compositions can range from gases containing high levels of inerts to fuels containing high levels of H_2 . The flame characteristics for fuels with high levels of inerts are very different than for fuels with high levels of H_2 . Add to that the requirement for turndown conditions and it becomes very challenging to design burners that will maintain stability, low emissions, and the desired heat flux distribution, over the range of conditions that are possible. Some plants use liquid fuels, like no. 2 to no. 6 fuel oil, sometimes by themselves and sometimes in combination with gaseous fuels. So-called



FIGURE 16.15 Cabin heater. (Courtesy of John Zink Co., LLC.³)

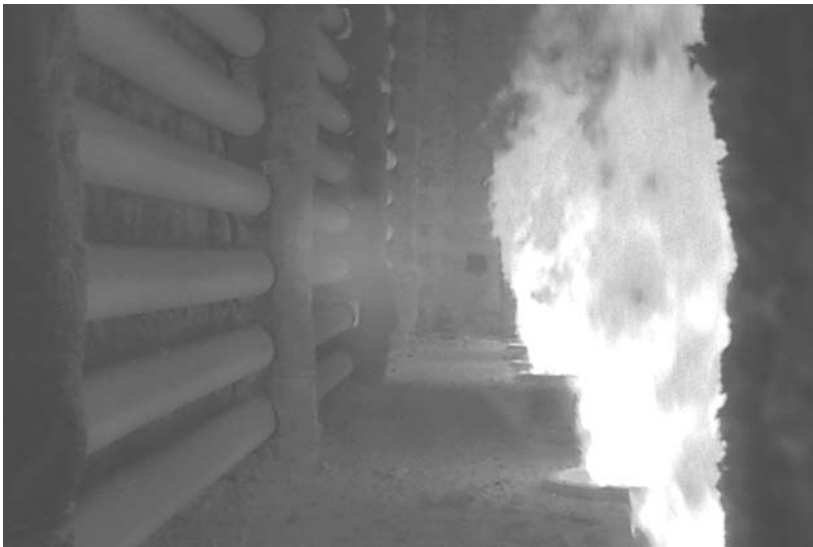


FIGURE 16.16 Crude unit burners. (Courtesy of John Zink Co., LLC.³)

combination burners use both a liquid and a gaseous fuel, which are normally injected separately through each burner. The various aspects of natural-draft burners are considered next.

16.4 BURNER DESIGN

The burner is the device used to combust the fuel with an oxidizer to convert the chemical energy in the fuel into thermal energy. A given combustion system may have a single burner or many burners, depending on the size and type of the application. For example, in a vertical cylindrical

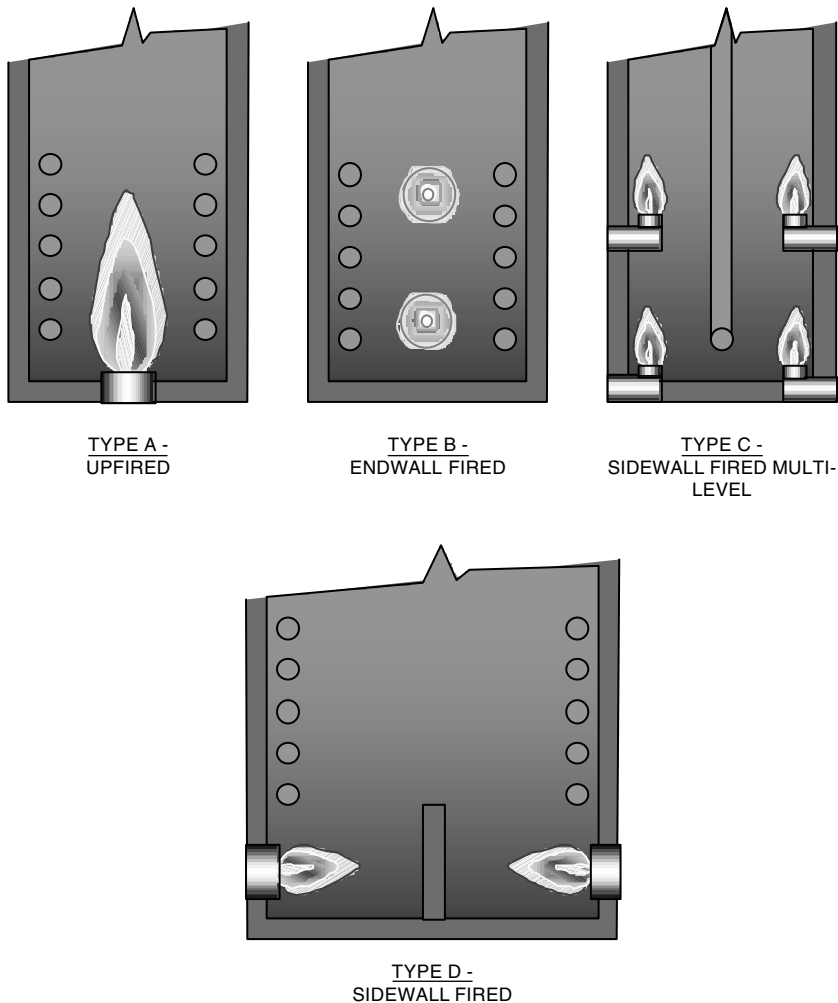


FIGURE 16.17 Typical burner arrangements. (Courtesy of John Zink Co., LLC.³)

furnace, one or more burners are located in the floor of a cylindrically shaped furnace (see [Figure 16.18](#)). The heat from the burner radiates in all directions and is efficiently absorbed by the tubes. Another type of heater geometry is rectangular (see [Figure 16.19](#)). This type of system is generally more difficult to analyze because of the multiplicity of heat sources and because of the interactions between the flames and their associated products of combustion.

Specialization of processes and furnace designs to meet the demands of those processes has resulted in the necessity for specialized burners. A burner is designed to provide stable operation and an acceptable flame pattern over a specific set of operating conditions. In addition, there may be a specified maximum level of pollutant emissions that can be generated through the combustion process. The American Petroleum Institute gives some guidelines for burners used in fired heaters.⁵ Specifications of operating conditions include:

- Specific types of fuels
- Specific range of fuel compositions
- Maximum, normal, and minimum heat release rates

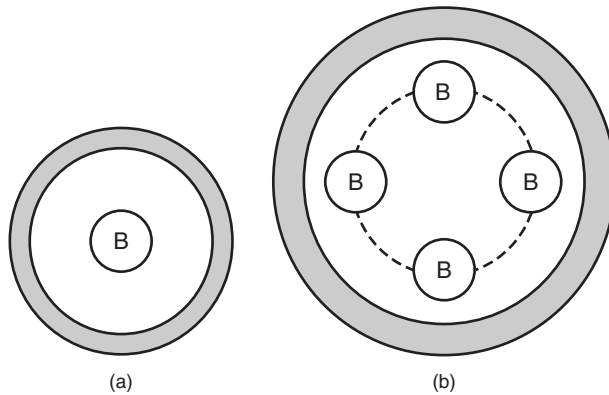


FIGURE 16.18 Burner (B) arrangement in the floor of vertical cylindrical furnaces: (a) small-diameter furnace with a single centered burner and (b) larger-diameter furnace with four burners symmetrically arranged at a radius from the centerline. (Courtesy of John Zink Co., LLC.³)

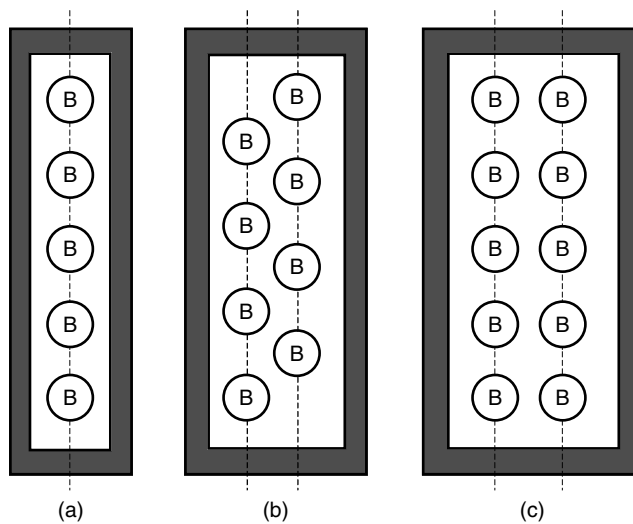


FIGURE 16.19 Burner (B) arrangement in the floor of rectangular cabin heaters: (a) single row of burners in a narrower heater, (b) two rows of staggered burners in a slightly wider heater, and (c) two rows of parallel burners in an even wider heater. (Courtesy of John Zink Co., LLC.³)

- Maximum fuel pressures available
- Maximum atomizing medium pressures available for liquid firing
- Fuel temperature
- Oxidant source, either ambient air, exhaust gases, or enriched
- Available combustion air pressure, whether forced (positive) or induced (negative)
- Combustion air temperature (ambient or preheated)
- Furnace firebox temperature
- Furnace dimensions for flame size restrictions
- Type of flame (configuration or shape)

To provide acceptable operation, the burner must be designed to perform the 5-Ms:

1. Meter the fuel and air into the flame zone
2. Mix the fuel and air to efficiently utilize the fuel
3. Maintain a continuous ignition zone for stable operation over the range
4. Mold the flame to provide the proper flame shape
5. Minimize pollutant emissions

16.4.1 METERING THE FUEL

Typically, the furnace operating system is able to monitor only the total flow of fuel to a furnace. A typical process heater has multiple burners installed to provide the proper heat distribution. The fuel system must then be designed to ensure that the fuel is properly distributed to all burners, because there are not typically individual fuel controls to each burner. Uniform fuel pressure to each burner is critical to the proper operation of the burners. The burner designer then ensures that each burner takes the correct amount of fuel from the system. Controlling the proper amount of fuel flow is accomplished through a system of metering orifices designed for each burner. These ports are specifically designed to act as metering and limiting orifices, passing a specified and known amount of fuel at a given fuel pressure.

16.4.1.1 Gaseous Fuel

A fuel capacity curve is developed for a burner based on the number and size of ports or orifices in the burner. This curve specifies the heat release vs. pressure for a given fuel composition and temperature. For gaseous fuels and compressible or incompressible flow, the calculations for the mass flow through a given orifice depends on:

- P_o the fuel pressure immediately upstream of the orifice
- P_a downstream pressure, generally atmospheric pressure
- T_o fuel temperature upstream of the orifice
- K fuel's ratio of specific heats, which depends on the composition of the fuel and is a factor used in calculating the compressibility of the fuel gas
- A area of the port
- C_d discharge coefficient, which depends on the design of the orifice port

The equations for calculating the flow through an orifice are given in Chapter 3.

The fuel metering orifices for gaseous fuels in raw-gas burners are typically installed at the point where the flame is formed. This is generally located in a region of the burner tile often termed the "burner throat." The fuel injector tips with the fuel orifices may be centered in the burner throat, located on the periphery, or a combination of both. [Figure 16.20](#) shows typical raw gas burner tips.

For premix or partial premix burners, the metering orifice serves two functions: to meter the fuel and to entrain combustion air into the venturi. This orifice is generally a single port located at the entrance of a venturi eductor. A typical premix metering orifice spud and air mixer assembly is shown in [Figure 16.21](#).

Fuel capacity curves are generally presented in terms of heat release vs. fuel pressure. The heat release is calculated from the mass (or volume) flow of the fuel multiplied times the heating value per unit mass (or volume) of the fuel. [Figure 16.22](#) shows a typical set of gaseous fuel capacity curves for three different heating values.

16.4.1.2 Liquid Fuel

Liquid fuels must be vaporized in order to burn efficiently. Burners designed for firing liquid fuels include an atomizer designed to produce a spray of small droplets that enhances the vaporization of the fuel. The design of the atomization system will have a significant impact on the liquid fuel flow

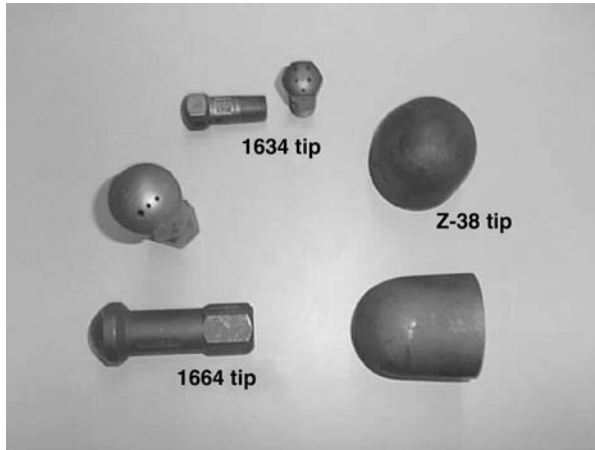


FIGURE 16.20 Typical raw gas burner tips. (Courtesy of John Zink Co., LLC.⁴)

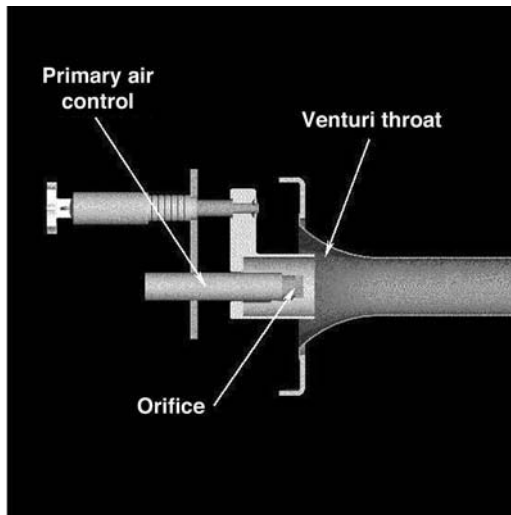


FIGURE 16.21 Typical premix metering orifice spud and air mixer assembly. (Courtesy of John Zink Co., LLC.⁴)

metering of the burner. With liquid fuels, the metering design is more complicated because of the need to “mix” the oil with an atomizing medium, such as steam or compressed air. This results in fuel metering orifices and atomizing media metering orifices in combination with orifices designed to flow the mixture. Figure 16.23 shows three typical liquid fuel atomizer/spray tip configurations.

Many factors are important in a liquid fuel atomization system. Variations in any of a number of factors must be considered when designing the system of ports for the metering of flow for a liquid fuel; those factors include:

- Viscosity as a function of temperature for the fuel
- Atomization medium and its temperature
- Fuel/atomizing medium pressure ratio
- Vaporization temperature for the fuel

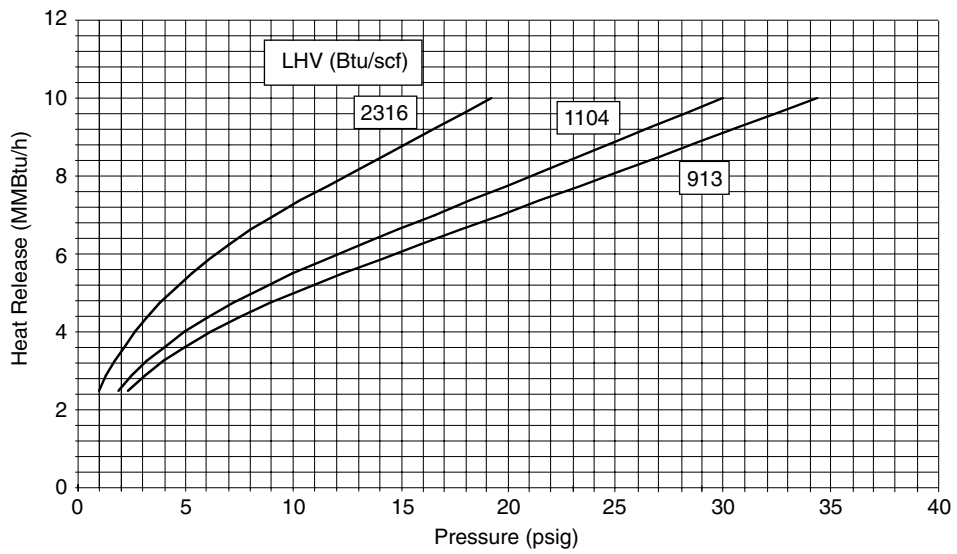


FIGURE 16.22 Typical gas fuel capacity curve. (Courtesy of John Zink Co., LLC.⁴)

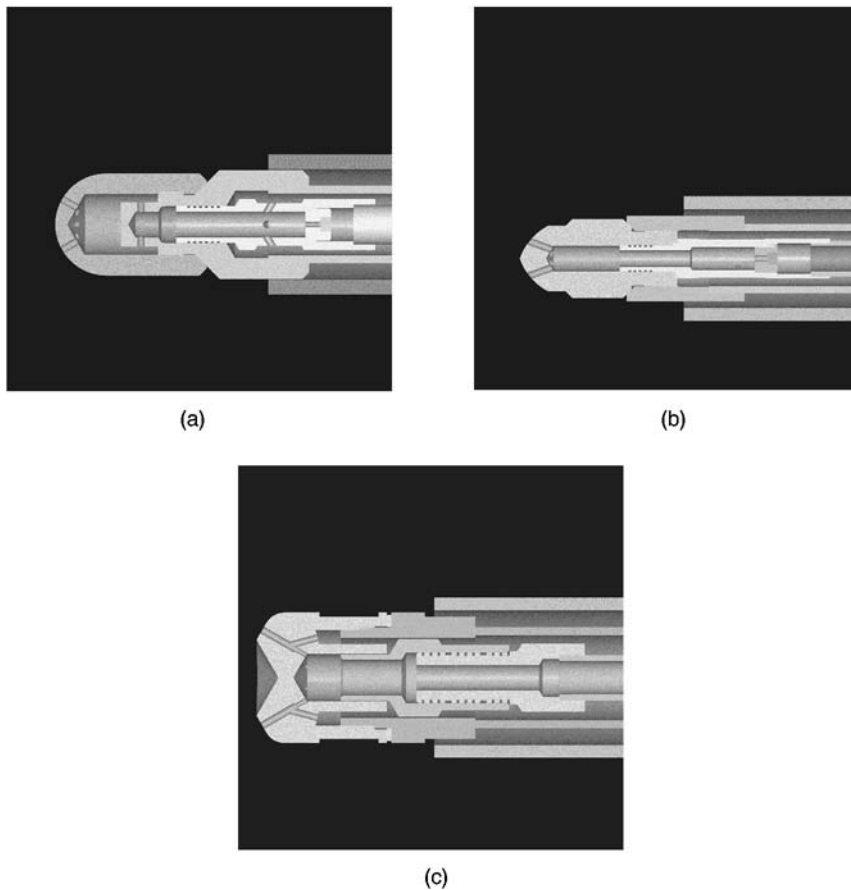


FIGURE 16.23 Typical liquid fuel atomizer/spray tip configurations. (Courtesy of John Zink Co., LLC.⁴)

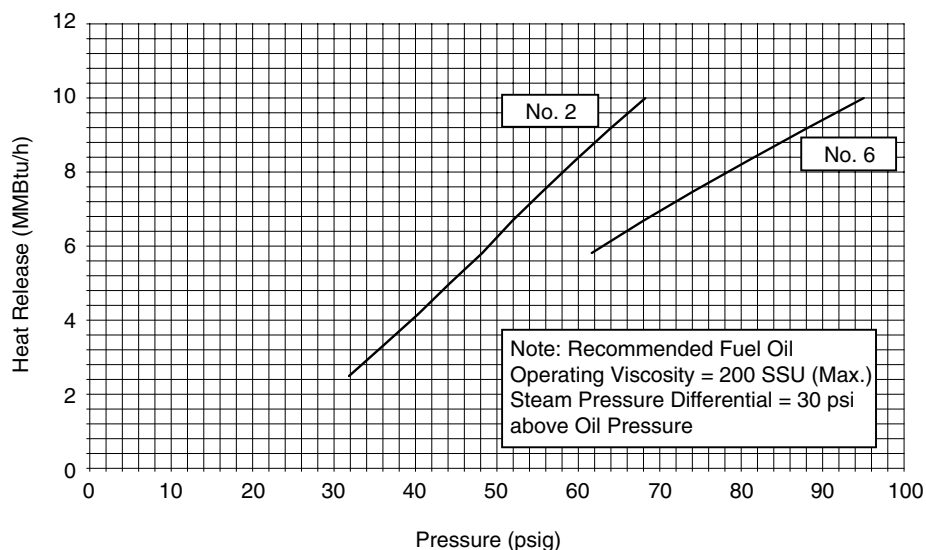


FIGURE 16.24 Typical liquid fuel capacity curve. (Courtesy of John Zink Co., LLC.⁴)

Fuel capacity curves are generally presented in terms of heat release vs. fuel pressure. The heat release is calculated from the mass/volume capacity of the system times the heating value per unit mass of fuel. Figure 16.24 shows a typical liquid fuel capacity curve.

16.4.2 METERING THE AIR

The burner must be designed for the required air flow for the operating conditions, particularly the air pressure that is available. The design of the burner throat is critical for two independent reasons. First, the throat must be capable of achieving the proper flow of combustion O_2 to meet the demands of the fuel. Second, the burner throat is designed to control the shape of the flame.

The primary air flow metering point where most of the available air pressure drop occurs is designated as the “throat.” In most burners, especially raw-gas or nozzle-mix and liquid fuel burners, it is the point at which the fuel is first injected into the air stream. In a premix or partially premixed burner, it is the point at which the fuel/air mixture is injected and, if necessary, secondary or completion air is introduced. In all cases, it is the location at which the initiation of combustion, or ignition, occurs. Figure 16.25 shows the throat for a typical raw-gas (pure diffusion or non-premixed) burner.

Natural-draft burners use the natural suction created in a furnace as the motive force for drawing combustion air through the burner. This negative pressure is typically less than 1 inch water column (<1.0 in. w.c.) at the burner location. Draft is naturally created in a furnace due to the buoyant forces of the hot and lighter combustion products compared to the cool and heavier ambient air outside the furnace (see Chapter 3). This draft is slightly more complicated in process heaters and furnaces used in the chemical and petrochemical industries that have a convection section near the outlet. This convection section is designed to further extract energy out of the combustion products before they are exhausted to the atmosphere. It typically consists of a band of tubes where the fluid is some type of hydrocarbon. There is some pressure drop across this band of tubes that must be taken into account when determining the available draft at the burner. The available draft at the burner is a function of the height of the combustor, the average temperature inside the combustor, and the pressure drop across the convection section. The burner must be adequately sized for the given available draft to induce enough ambient air for the maximum heat release.

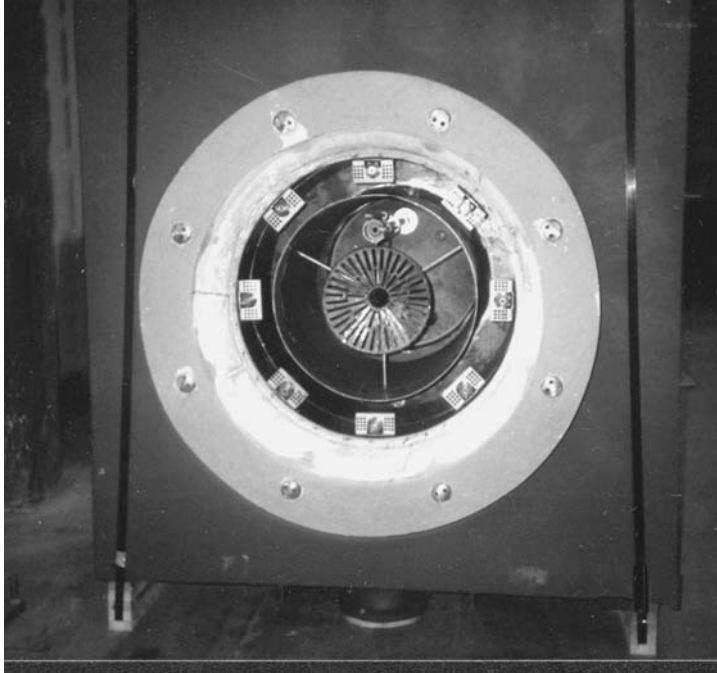


FIGURE 16.25 Typical throat of a raw gas burner. (Courtesy of John Zink Co., LLC.⁴)

In raw-gas (diffusion or nonpremixed) or liquid fuel burners, the principle combustion air flow metering point is the burner throat. In partially premixed burners, the secondary or completion air metering point is the burner throat. As a primary metering restriction, the majority of the pressure loss is expected to be taken across the throat. Engineering groups such as the American Petroleum Institute (API),^{5,6} process design companies, and some furnace manufacturers provide burner design guidelines that define the use of the available airside pressure drop at that point. These guidelines often require that 75 to 90% of the available draft be taken across the burner throat to enhance air control. There are practical limitations to the control range for natural-draft burners. The percentage of available draft utilized for throat metering can leave little room for an adequate air control mechanism.

Example 16.1

Given:

Fuel gas:	1200 Btu/scf (47.27 MJ/Nm ³ , 11,300 kcal/Nm ³)
Maximum design duty:	10.0×10^6 Btu/hr (2.93 MW, 2.52×10^6 kcal/hr)
Normal duty:	8.0×10^6 Btu/hr (2.3 MW, 2.0×10^6 kcal/hr)
Minimum design duty (turndown):	2.0×10^6 Btu/hr (0.586 MW, 0.504×10^6 kcal/hr)
Available furnace draft:	0.5 in. w.c. (120 Pa, 1.25 mbar, 12.7 mm H ₂ O)
Excess air:	20% design, 10% operation
Design standards:	API 560 and 535

API 560 Section 10.1.12 states that “The burner shall be selected to use no less than 90 percent of the maximum draft available for the maximum specified heat release.” API 560 Appendix A (Equipment Data Sheets), Section b (Burner data sheets, Sheet 3 of 3), Note 1 states that “At design condition, minimum of 90% of the available draft with the air register fully open shall be utilized across the burner. In addition, a minimum of 75% of the airside pressure drop with the air registers full open shall be utilized across burner throat.” API 535 Section 8.2 (Dampers and Registers) states

that “Dampers and burner registers shall be sized such that the air rate can be controlled over a range of at least 40–100% of burner capacity.” Assume that the burner requires between the specified 90% to 100% of the available draft, and that the specified 75% is measurable as static loss across the throat. [Table 16.5](#) and [Table 16.6](#) (developed for Example 16.1) indicate the:

- Operating heat release (1)
- Desired operational excess air (2)
- Required pressure loss across the throat (3)
- Required pressure loss across the register or air control device (4)
- Ratio percentage of register or damper opening required (5)

[Table 16.5](#) shows the theoretical percentage of air control opening based on no change in control flow coefficient and 3% leakage in the full closed position. [Table 16.6](#) is based on 6% leakage. These tables assume that the variable orifice, which is the air control mechanism (often referred to as an air register or damper), has a constant discharge coefficient throughout its full range of operation. This is a simplification that is not strictly correct in practical application. These tables provide insight into the problem of excess design capacity. Many who specify combustion equipment seek to provide excess capacity as a cushion against reduced operation with burners out of service, upset operation, process design contingencies, and future desired capacity. The problem is the ability to control excess air and utilize the available pressure drop for the normal operation. At lower firing rates, the air and fuel pressures are both reduced in the mixing zone and the resulting flame quality often suffers because of the reduced control.

16.4.3 MIXING THE FUEL AND AIR

“Mixing” is a general term used to describe the function of bringing the fuel (reactant) in close proximity with the air (oxidant). The higher the level of turbulence and shear between the streams, the more uniform the fuel and air mixture, which makes the combustion reaction more rapid and complete. It is generally accepted that the higher the level of mixing, the more intense, complete, and enhanced the combustion. However, there are a number of conditions and factors that should be considered, including flame shaping and control of pollutant emissions that lead to some exceptions to this rule. Intimate mixing does not always produce the most desirable results.

Designing a combustion system for special applications such as high inert composition fuels can also set limitations on the desired level of mixing. All combustion reactions have a rate at which they will proceed and a minimum temperature that is required to initiate or sustain that reaction. The introduction of inert components to the fuel can generate two conditions that will affect burner stability. First, the inert components slow the reaction, which slows the flame speed and can result in the stabilization point being moved out of the desired position (e.g., at the flameholder). Second, the inerts introduce a heat absorption component that narrows the flammability limits and reduces the flame temperature. Quenching of the flame to extinction is an important consideration when inert components are present in the fuel or the combustion O_2 stream.

Many combustion oxidant streams with greater inert compositions than ambient air are often the result of some type of flue gas recirculation process and are typically at an elevated temperature. This elevated temperature will often partially offset the potential quench effect of the elevated inert levels.

An effective form of emissions control is through the delaying of the combustion process. Highly mixing the fuel and the oxidant in the proper proportions will generate the maximum flame temperatures. This enhances the formation of large quantities of oxides of nitrogen (NO_x), which is a highly regulated pollutant. Certain burner designs reduce the level of fuel and air mixing, sometimes referred to as delayed mixing, which extends the reaction zone to achieve reductions in these emissions. Fuel and air staging are well-known techniques for delaying mixing to reduce NO_x emissions.

TABLE 16.5

Theoretical Air Control Opening, Based on No Change in Control Flow Coefficient and 3% Leakage at the Full Closed Position

Heat Release (1) MMBtu/hr	Percent Design %	Percent X-Air (2) %	Throat Drop		Control Drop		Total dP In. wc	Percent Control Open	
			90% Total	100% Total	90% Total	100% Total		90% Total	100% Total
			(3) in. wc		(4) in. wc			(5) % (w/3% leakage)	
10.0	100	15	0.338	0.375	0.162	0.125	0.50	86.3	Full open
10.0	100	10	0.309	0.343	0.191	0.157	0.50	75.9	83.8
9.0	90	10	0.250	0.278	0.250	0.222	0.50	59.4	63.1
8.0	80	10	0.198	0.220	0.302	0.280	0.50	47.7	49.6
7.0	70	10	0.151	0.168	0.349	0.332	0.50	38.6	39.6
6.0	60	10	0.111	0.124	0.389	0.376	0.50	31.0	31.6
5.0	50	10	0.077	0.086	0.423	0.414	0.50	24.5	24.8
4.0	40	20	0.059	0.065	0.441	0.435	0.50	20.7	20.9
3.0	30	40	0.045	0.050	0.455	0.450	0.50	17.6	17.7
2.0	20	80	0.033	0.037	0.467	0.463	0.50	14.7	14.8
0	0	3	0.00031	0.00034	0.49969	0.49966	0.50	Full closed	Full closed

Courtesy of John Zink Co., LLC.⁴

TABLE 16.6

Theoretical Air Control Opening, Based on No Change in Control Flow Coefficient and 6% Leakage at the Full Closed Position

(1) Heat Release MMBtu/hr	Percent Design %	Percent X-Air (2) %	Throat Drop		Control Drop		Total dP In. wc	% Control Open	
			90% Total	100% Total	90% Total	100% Total		90% Total	100% Total
			(3) in. wc		(4) in. wc			(5)% (w/6% leakage)	
10.0	100	15	0.338	0.375	0.162	0.125	0.50	84.8	Full open
10.0	100	10	0.309	0.343	0.191	0.157	0.50	74.4	82.3
9.0	90	10	0.250	0.278	0.250	0.222	0.50	57.9	61.6
8.0	80	10	0.198	0.220	0.302	0.280	0.50	46.2	48.1
7.0	70	10	0.151	0.168	0.349	0.332	0.50	37.1	38.1
6.0	60	10	0.111	0.124	0.389	0.376	0.50	29.5	30.1
5.0	50	10	0.077	0.086	0.423	0.414	0.50	23.0	23.3
4.0	40	10	0.059	0.065	0.441	0.435	0.50	19.2	19.4
3.0	30	40	0.045	0.050	0.455	0.450	0.50	16.1	16.2
2.0	20	80	0.033	0.037	0.467	0.463	0.50	13.2	13.3
0	0	6	0.0012	0.0014	0.4988	0.4986	0.50	Full closed	Full closed

Courtesy of John Zink Co., LLC.⁴

16.4.4 MAINTAINING IGNITION

The most important function that a burner performs is to provide for the continuous and reliable ignition of the fuel and air passing through the burner over a specified range of operating conditions. Failure to do so could potentially lead to an explosion. Each burner is designed to provide a specific location in which a portion of the fuel and air is continuously introduced in near-stoichiometric proportions at velocities at or below the mixture flame speed, allowing for a continuous ignition zone. The fuel orifices in the burner designed for this purpose are often referred to as ignition ports. In the ignition zone, a steady flame is maintained that continuously ignites the fresh fuel/air mixture as it is introduced. The ignition zone is designed to operate over the specified range of operation of the burner. The flame from this ignition zone is then used to ignite the remainder of the fuel and air mixture. In natural-draft burners, the ignition zone is often situated in the eddy formed downstream of a step or ledge in the burner tile (see Figure 16.26), or in the wake of a bluff body “flame stabilizer” or “flame holder” (see Figure 16.27) located in the center of the combustion airstream.

Safe ignition of the fuel/air mixture depends on the compositions of the fuel and oxidant, which affect the flammability limits, ignition temperatures, and stoichiometry of the mixture. The flame speed is controlled by the stoichiometry and composition of the mixture. The ability to sustain a single point of ignition for a fuel/air mixture is controlled by both the stoichiometry and the velocity of the mixed stream. Wide ranges in capacity, excess air requirements, and fuel compositions make strict dependence on the mixed stream for stability unreliable. The development of low-velocity zones and recirculating eddies ensures a single point for maintaining an ignition zone over a broad range of operating conditions. Each burner is designed for a limited range of fuel and oxidant compositions and flow rates, and the burner should not be operated outside this range.

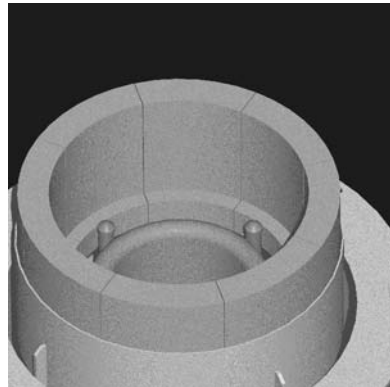


FIGURE 16.26 Ledge in the burner tile. (Courtesy of John Zink Co., LLC.⁴)

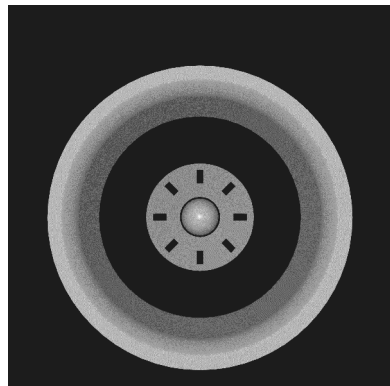


FIGURE 16.27 Flame stabilizer or flame holder. (Courtesy of John Zink Co., LLC.⁴)

“Stability” is a widely used term when describing combustion and burner performance. This term is applied to the range of conditions under which burners maintain their ignition. Outside those conditions, the burner may become unstable and therefore potentially dangerous. A condition may be created where the flame pulsates. There is no strict measurement of or unit for stability, and it is somewhat subjective unless the flame is obviously pulsing, for example.

16.4.5 MOLDING THE FLAME SHAPE

Many industrial applications have strict restrictions on the shape, size, and consistency of the flames in the combustor. The furnace chamber and burner flame in every process furnace are designed to provide for the efficient transfer of heat to the process load. Flame size and shape for the natural-draft burners used in the hydrocarbon processing industries is especially critical due to the sensitivity to overheating for the hydrocarbons being processed. The rate of heat transfer to the process tubes must be limited to prevent overheating of the process tubes leading to the formation of carbon or coke inside the process tubes. As a result, there are generally strict guidelines for the flame dimensions. Typical specifications for flames include maximum flame lengths and maximum flame widths. In some cases, there may even be some minimum flame dimensions specified. The number, heat release, and layout of the burners in the furnace are designed to provide the proper heat transfer pattern.

Controlling the air flow through the incoming ambient air approach distribution, tile throat sizing and shape, and the tile exit configuration provides the most reliable method for flame shape control. Introduction of the fuel into the established airflow streams provides the primary function in a raw-gas burner. The proper flame pattern is generated by the combination of fuel injection pattern provided by the fuel injectors and the burner tile and flame holder that controls the air flow. The fuel injectors are also often called *spuds* or *tips*. The injectors have fuel injection ports or orifices that introduce the main portion of the fuel into the air stream in a manner that generates the desired flame pattern or shape. The number, size, and orientation of the ports are critical for determining the overall flame shape. In conjunction with the fuel injectors, the air stream must be shaped in an appropriate manner by the airflow passages provided by the shape of the tile and flame holder.

In most cases, the flame cross section is round (see Figure 16.28). The fuel is normally injected symmetrically to maintain the round shape. In the hydrocarbon and petrochemical industries, round-flame burners are used in a wide variety of applications. They are typically fired vertically upward in the middle of the floor or hearth of the furnace between rows of tubes. The flames radiate their heat to the tubes containing hydrocarbon fluids.



FIGURE 16.28 Round-shaped flame. (Courtesy of John Zink Co., LLC.)



FIGURE 16.29 Flat-shaped flame. (Courtesy of John Zink Co., LLC.⁴)

Some applications require a fan-shaped or rectangular cross section (see [Figure 16.29](#)). This shape is often termed a “flat flame;” it typically has a fairly high aspect ratio (ratio of the longest side to the shortest side) and is rarely square in shape. In flat-flame burners, the burner tile (block or quarl) is generally rectangular and the fuel is injected in a manner to produce a flame that is essentially rectangular or “flat,” rather than round. In many cases, these flat-flame burners are fired along a refractory wall or floor (see [Figure 16.10](#)) to heat the wall so it can radiate to the load. These are commonly used in cracking-type applications, such as in the production of ethylene.

16.4.6 MINIMIZING POLLUTANT EMISSIONS

Because of increasing concern for the environment, pollutant emissions from most industrial combustion processes are highly regulated. A wide range of strategies has been used in natural-draft burners to minimize pollution emissions, particularly NO_x. The most popular techniques include air and fuel staging and internal furnace gas recirculation. A more recent technique is the use of ultra-lean premix, which has achieved very low levels of NO_x emissions.²⁹

16.5 BURNER TYPES

Natural-draft burners are typically classified based on the type of fuel being burned and how the fuel and air are mixed:

- Gas: premix and partial premix
- Gas: raw gas or nozzle mix
- Liquid
- Combination gas and liquid: raw gas and oil (typically)

The combining of any two or more burners is simply a matter of basing the design on the most difficult of the fuel types and adapting the other fuel distribution systems to the base design.

16.5.1 PREMIX AND PARTIAL PREMIX GAS

“Premix” is a term applied to burners where the fuel and the combustion air are completely mixed together prior to reaching the ignition zone. This type of burner usually provides for intimate mixing of the fuel and combustion O₂ prior to the ignition zone. However, it is also possible for the fuel

and air to be relatively unmixed before reaching the ignition zone, depending on the burner design. This may be deliberate or simply poor design, depending on the objectives of the combustion process. Partial premix burners mean that some but not all of the fuel and air are mixed prior to reaching the ignition zone.

In natural-draft burners, the motive energy to inspirate the combustion air is supplied by the low-mass, high-potential-energy-stream fuel. The fuel gas is metered through one or more orifices at the entrance to a venturi or mixer. The entrained air stream is made available at zero, or virtually zero, velocity at the same location. The conversion of the potential energy from the pressure of the fuel stream to kinetic energy in the form of velocity is completed within the air supply zone. The free fuel jet expands and decelerates. Conservation of momentum requires that the reduction in velocity be balanced by an increase in the mass of the moving stream. This additional mass is the entrained ambient air.

Burners designed with an inspirating arrangement typically require fewer adjustments to the air control. The utilization of the fuel momentum determines the amount of air inspirated, which is proportional to the gas flow. Therefore, reducing the fuel mass momentum reduces the amount of air entrained. The efficiency of the venturi and the restriction imposed by the fuel/air distribution nozzle are the limits to the capacity (volume) of air that can be inspirated.

Another benefit to this design is the flame volume created. If the air inspiration design is efficient, the resulting flame volume of this premixed burner will be much smaller than that of other low air pressure drop burners. Conversely, if this premixing is inefficient, the flame may actually be larger than a raw gas burner due to the reduction in the secondary air mixing energy. By utilizing the majority of the available energy of the fuel stream to achieve the primary premix, the remaining energy for any required secondary air mixing is reduced to only that available from the air due to the draft loss.

Fuel metering is a further benefit of this burner style. Because all of the fuel is typically metered through a single orifice for each venturi, the size of the orifice is maximized. Larger diameter orifices, as long as they do not jeopardize the function of the burner, are a benefit because they minimize the chances of plugging from dirty fuels.

One of the basic limitations to this type of burner is the burning characteristic of fuels. Each fuel composition has a different reaction rate, which is dependent on the concentrations of the fuel, the oxygen, and any inert components. This rate also depends on the temperature of the mixture. The reaction rate is often quantified in terms of flame speed, which is the velocity at which the flame will propagate. The design of the injection system into the ignition and combustion zones depends on this same burning characteristic of the design fuel. Changes in the firing rate or the fuel will result in a change in the flame volume, velocity, and burning characteristics at the distribution tip. If the fuel/air mixture is within combustible limits, and the velocity is not maintained above the flame propagation speed, the flame front moves back toward the incoming fuel/air flow streams. In the worst case, this flashback condition may result in flames being translated completely outside the designed ignition and flame zone causing mechanical and structural damage. If this mis-positioned flame actually establishes itself outside of confining equipment, major safety problems may occur.

16.5.2 RAW-GAS OR NOZZLE-MIX

Raw-gas (diffusion or nozzle-mix) burners are designed to introduce the fuel and air separately into the ignition zone. The mixing of the fuel and combustion air is done at or after the ignition point of the burner. Typically, these burners provide for the major, or metering, pressure drop for both the fuel and air immediately prior to the ignition zone.

By separating the fuel from the combustion air prior to the ignition zone, there is no possibility of flashback. Therefore, the raw-gas style of design can effectively handle a wide range of fuels without concern for equipment damage or personnel safety. Turndown on a raw-gas burner is limited only to the method of stabilization, the flammability limits of the fuel, and the controllable and safety lower pressure limits of the fuel system.

Because the combustion air is supplied through and metered by the throat of the burner, the air flow must be adjusted as the fuel flow rate changes, for efficient operation. The incoming air flow rate depends primarily on the furnace draft rather than on inspiration by the fuel. Unlike venturi operation, where the air flow rate is proportional to the fuel flow rate, in raw-gas burners the air flow rate is not proportional to the fuel rate. This can mean an excessive amount of combustion air when the firing rate is reduced, unless the air flow is adjusted. The ability to efficiently combust the fuel and transfer the heat is directly related to the amount of excess air. Therefore, it becomes necessary to control the air with every change in fuel flow or fuel composition or there will be a related change in efficiency. This is typically done with an individual burner damper or register. In a limited number of applications, a common inlet air header is used and the air flow rate to an entire furnace can be controlled with a single damper.

Another problem intrinsic to the raw-gas design condition comes from the fuel distribution system. Multiple fuel injection points are often required to shape the flame, distribute the fuel into the combustion air stream, and mix the fuel with the air. Breaking the fuel flow into multiple metering orifices while maintaining high potential energy (pressure) can lead to small fuel injection ports or orifices. These small orifices are highly subject to fouling problems due to dirty fuel quality and foreign material in the piping.

Natural-draft burners utilize quiescent zones for stabilization. These low-flow, low-pressure zones can be generated through the use of flow stream disruption. Cones or bluff bodies located in the throat of the burner are a common form of flow stream disruption. Flow disrupters or shields around fuel tips and ledges or sharp changes in the burner block (tile or quarl) profile are also common. In all cases, these mechanisms are basically designed to prevent a portion of the combustion air from leaving the designed ignition zone prior to the introduction of fuel. They provide pockets of a continuously renewing combustible mixture at a location where the velocity is lower than the flame propagation speed.

16.5.3 OIL OR LIQUID FIRING

Oil firing is more complicated than fuel gas firing because the oil must be atomized and vaporized before it can be properly burned. Atomization involves producing a relatively fine spray or mist of droplets that will vaporize quickly. Industrial natural-draft oil burners typically utilize twin fluid atomizers and employ steam as the atomizing medium. Compressed air or even high-pressure fuel gas, rather than steam, can be utilized in some applications.

Some internal mix, twin fluid atomizers form a gas/liquid emulsion, which then issues from the fuel tip. This type of atomizer is shown in Figure 16.30. The oil issues from a single port at the entry to the atomizer section. Steam is injected into the oil stream through multiple ports forming



FIGURE 16.30 Internal mix twin fluid atomizer. (Courtesy of John Zink Co., LLC.⁴)

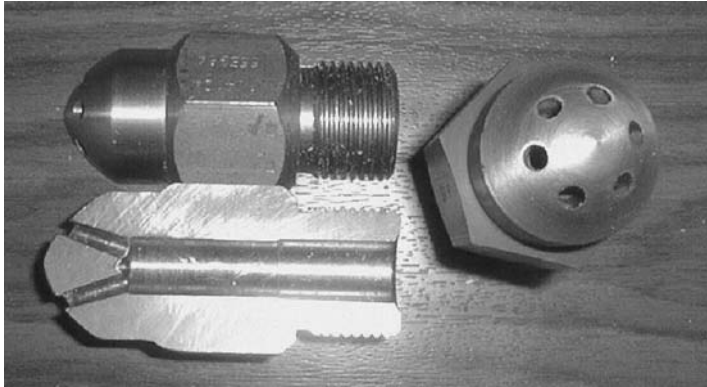


FIGURE 16.31 Port mix twin fluid atomizer. (Courtesy of John Zink Co., LLC.⁴)

the emulsion. This oil/steam emulsion then travels to the chamber between the atomizer section and the exit ports. Multiple exit ports are placed on the tip, which allows for enhanced mixing of the spray and the combustion air, flame shaping, and stabilization. Internal mix atomizers often utilize a steam pressure that is maintained at 10 to 30 psig (70 to 210 kPa) above the oil pressure over the operating range of the burner. The oil pressure may be 100 to 120 psig (700 to 800 kPa) at the maximum firing rate.

Port mix, twin fluid atomizers (see [Figure 16.31](#)) use the atomizing media to form a thin liquid annulus on the inner surface of the port. The high velocity of the atomizing media pushes the liquid along the length of the port shearing and stretching the liquid into a thin film. These atomizers generally operate with a constant steam pressure, typically 120 to 150 psig (800 to 1000 kPa) over the entire operating range of the burner. The oil pressure may be 100 to 150 psig (700 to 1000 kPa) at the maximum firing rate.

In each case, internal mix or port mix, droplets are formed as the liquid forms a sheet as it exits the port and this sheet then breaks up as it expands. The size of the droplets formed depends on the relative velocity of the liquid sheet and the surrounding media. It also depends on the viscosity, surface tension, and density of the liquid, size of the port, momentum of the fuel, and ratio of fuel to atomizing media.

16.5.3.1 High-Viscosity Liquid Fuels

Most of the industrial liquid fuels fired are high viscosity or heavy fuel oils, including no. 6 fuel oil, bunker C oil, residual fuel oil, pitch, tar, and vacuum tower bottoms. Most heavy fuel oils are the residue from the oil refining process and are considered low-value byproducts. Some of these high-viscosity fuels can be solid or nearly solid at room temperature. Nearly all high-viscosity liquid fuels must be heated in order to be efficiently atomized. Typically, for best atomization, the viscosity of the oil should be in the range of 100 to 250 SSU. This often requires the heavy oil to be heated to the range of 200 to 250°F (90 to 120°C). However, a heavy pitch may require a temperature of 600°F (320°C) to achieve the proper viscosity for atomization.

Heavy fuel oils have high boiling points and are therefore difficult to vaporize. Many heavy oil burners have special refractory tiles, sometimes called regenerative or *regen* tiles (see [Figure 16.32](#)), that redirect the intense flame radiation back to the root of the spray to enhance vaporization rates and help stabilize the oil flame. Some other heavy oil burners utilize swirlers to promote internal recirculation of the hot combustion products back into the flame root to enhance heating of the spray (see [Figure 16.33](#)).

FIGURE 16.32 Regen tile for enhancing oil flame stabilization. (Courtesy of John Zink Co., LLC.⁴)

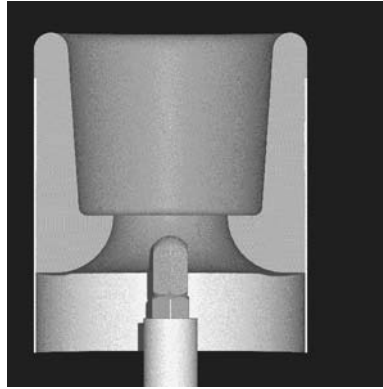
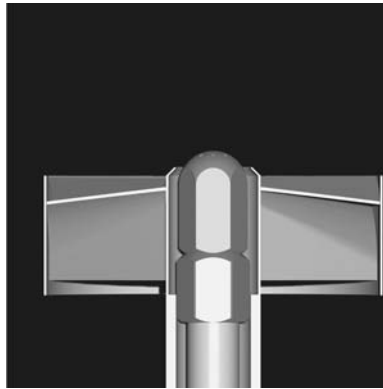


FIGURE 16.33 Swirler for enhancing oil flame stabilization. (Courtesy of John Zink Co., LLC.⁴)



16.5.3.2 Low-Viscosity Liquid Fuels

Low-viscosity liquid fuels include light oils such as no. 2 fuel oil, naphtha, and byproduct waste liquids containing a variety of hydrocarbon byproducts such as alcohols. These liquids are also typically fired using twin fluid atomizers. However, care must be taken to avoid overheating low-boiling-point fuels. Vaporization of the liquid within the oil gun can cause disruption in the flow within the atomizer, leading to unsteady operation. Many light liquid fuels require compressed air rather than steam atomization. The air serves not only as the atomizing medium, but also as a source of combustion air. Because light oils generally have lower boiling points compared to heavy oils, they are easier to vaporize. Their flames can often be stabilized using simple bluff body stabilizers instead of swirlers or special tiles that are typically needed for heavy oils.

16.6 BURNER CONFIGURATION

Burners can be mounted in the furnace or heater floor to fire vertically upward, in the heater wall to fire horizontally, or in the roof to fire vertically downward. The major consideration required for burner design is to ensure the proper support for the burner tile. Burner blocks for floor-mounted service can typically be simply placed on the furnace steel or burner mounting plate. Burner blocks for horizontal mounting must be supported by tile case assemblies and must be held in place so that they do not move if subjected to vibration. Roof-mounted tiles must have support surfaces cast into them so that they can hang from steel supports in the furnace roof.

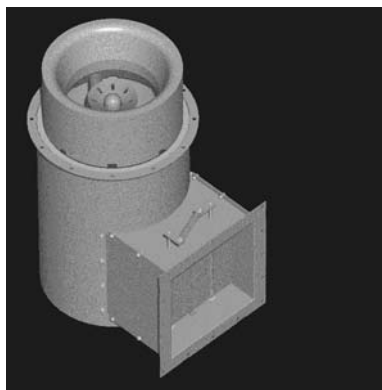


FIGURE 16.34 Typical conventional raw-gas burner.
(Courtesy of John Zink Co., LLC).⁴

16.6.1 ROUND-FLAME BURNER

The following figures illustrate the different types of burners that are typically used in refinery and petrochemical furnaces. The round-flame burner is the most universal design and used in many applications. [Figure 16.34](#) illustrates a typical raw gas conventional burner. This burner is used where NO_x emissions are not a primary concern and a short flame is desired.

[Figure 16.35](#) shows a typical premix gas burner. A premix round-flame burner is useful when a short heater does not have enough draft to supply the required combustion air. The premix burner uses the fuel jet as a motive force to allow the burner to pull in part or all of its combustion air. However, there may be other considerations such as flame shape that will influence the choice of burner style as premix flames are often shorter than raw gas (diffusion) flames.

[Figure 16.36](#) shows a typical round/conical flame combination oil and gas burner. This burner can be used to burn gas or liquid fuels. This versatility is desirable in applications with liquid fuels or where gas fuels may be in short supply at various times throughout the year and an alternative fuel must be fired to maintain a process. [Figure 16.37](#) shows a typical round/conical flame, high-intensity combination oil and gas burner. This burner is used in applications where a high heat release per burner is required, but also a short flame length is required.

16.6.2 FLAT-FLAME BURNER

Some applications require a flat- or fan-shaped (rectangular) flame due to the close proximity of process tubes or due to the fact that the burner is fired along a wall. [Figure 16.38](#) shows a typical staged-fuel flat-flame gas burner. This burner produces a free-standing flame and is used in applications where the process tubes are close to the centerline of the burner.

The advantage in using this particular burner is that the fuel staging can significantly reduce NO_x emissions. Based on fired capacity, they can utilize single or multiple primary and staged injectors to affect the proper fuel distribution to produce the desired flame pattern. A flat-flame burner can be fired in two basic configurations, wall-fired or free-standing.

16.6.2.1 Wall-Fired Flat-Flame Burners

A wall-fired, flat-flame burner is similar to a free-standing flat-flame burner except that it is installed and fired against a refractory wall (e.g., see [Figure 16.12](#)). By directing the fuel jets toward the wall, the flame heats the refractory wall, which, in turn, radiates heat to the process tubes facing the wall. Wall-fired burners are typically used in ethylene furnaces.

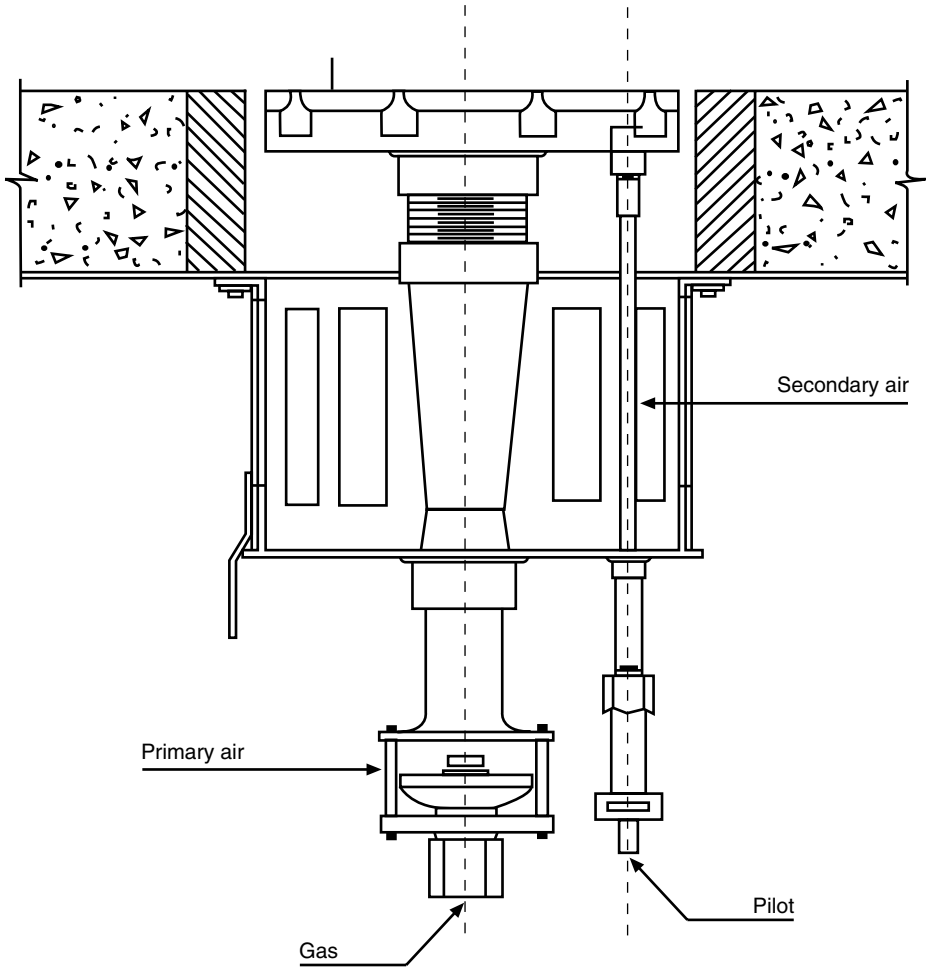


FIGURE 16.35 Typical premix gas burner. (Courtesy of John Zink Co., LLC.³)

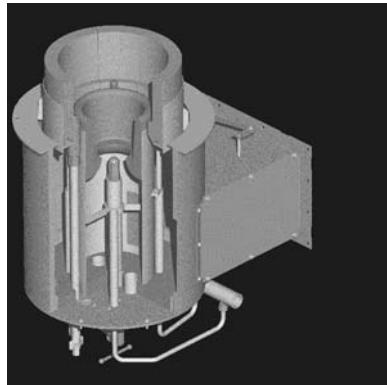


FIGURE 16.36 Typical round-flame combination burner. (Courtesy of John Zink Co., LLC.⁴)

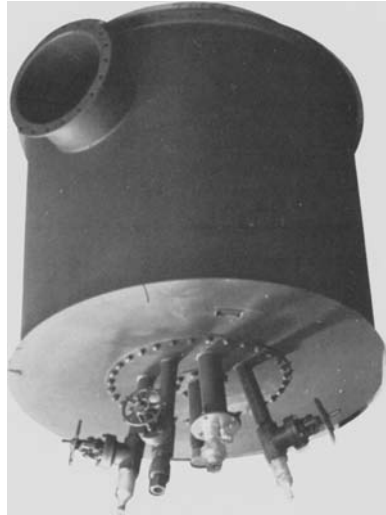


FIGURE 16.37 Typical round-flame, high-intensity combination burner. (Courtesy of John Zink Co., LLC.⁴)

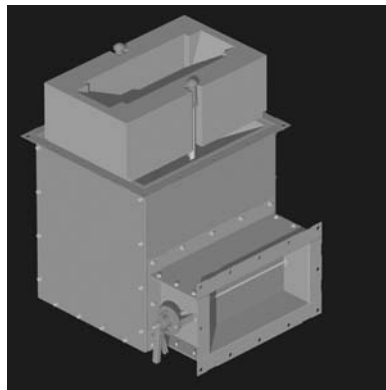


FIGURE 16.38 Typical staged-fuel, flat-flame burner. (Courtesy of John Zink Co., LLC.⁴)

16.6.2.2 Free-Standing Flat-Flame Burners

A free-standing flat-flame burner (see [Figure 16.29](#)) is used in applications where it is necessary to fire a burner in a narrow space between two sets of process tubes. The tube spacing often requires the use of a flat-flame burner, instead of round-flame burners that are normally used in these applications. A staged-fuel, flat flame is shaped by firing staged fuel jets opposite one another. This makes the flame shape into a fan. The flame thickness is typically less than or equal to the burner tile width. The fuel injectors are specifically designed to produce a relatively narrow flame width to avoid flame impingement on the nearby process tubes.

16.6.3 RADIANT WALL BURNERS

Radiant wall burners (see [Figure 16.11](#)) are used in cracking furnaces. These burners are mounted through the furnace wall and produce a thin, flat, circular disk of flame adjacent to the wall. There are typically multiple rows of burners equally spaced in a grid pattern on walls. The burners from row to row may be staggered or aligned (see [Figure 16.39](#)). The burners uniformly heat the walls, which radiate heat to the process tubes on the centerline of the furnace. [Figure 16.40](#) shows a drawing of a typical radiant wall burner.

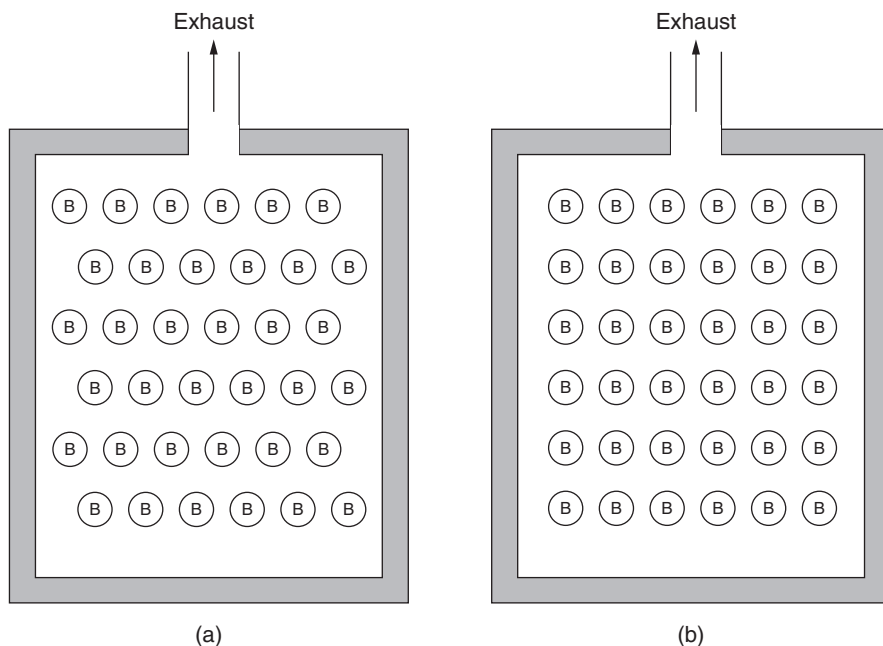


FIGURE 16.39 Elevation view of radiant wall burner arrangements: (a) staggered and (b) aligned.

Many applications, such as reformers and cracking furnaces, require high furnace temperatures in the radiant section of the heater to produce the required high process temperatures. In addition, very uniform heat transfer to the process tubes is needed. In such operations, a flat-flame burner that fires adjacent to a refractory wall, is utilized in conjunction with radiant wall burners.

16.6.4 DOWN-FIRED BURNERS

A down-fired burner is a burner that is fired vertically into a furnace from the ceiling (see Figure 16.4). Typically, these burners produce a flame that is round (conical) in shape. These burners are utilized in applications such as hydrogen reformers or ammonia reformers. Down-fired burners are often dual-fuel burners firing a make-up fuel and a waste gas. The make-up fuel can be gaseous, such as natural gas or a propane/butane blend. The make-up fuel may also be a liquid such as naphtha, no. 2 fuel oil, or diesel oil.

16.7 MATERIALS SELECTION

Burner materials are selected for strength, corrosion resistance, and, in many cases, temperature resistance. Carbon steel is used for most metal parts unless temperature or corrosion considerations require more resistant alloys. Cast iron or carbon steel can be utilized for fuel gas manifolds. The fuel gas riser material between the manifold and the fuel injector tip is generally carbon steel for ambient air service and 304 SS for parts in contact with air temperatures greater than 700°F (370°C). Fuel injector tips for premix burners may be cast iron. Cast steel or cast stainless steel may be required for fuel gases containing appreciable levels of hydrogen (typically >50 vol%) due to hydrogen embrittlement of carbon steel. Raw-gas burners typically use 300 series stainless steel gas tips. Tips for oil burners are normally 416 SS. For oils containing erosive particles, T-1 tool steel is generally used. Atomizers for oil service are normally brass for lower sulfur oils and 303 SS

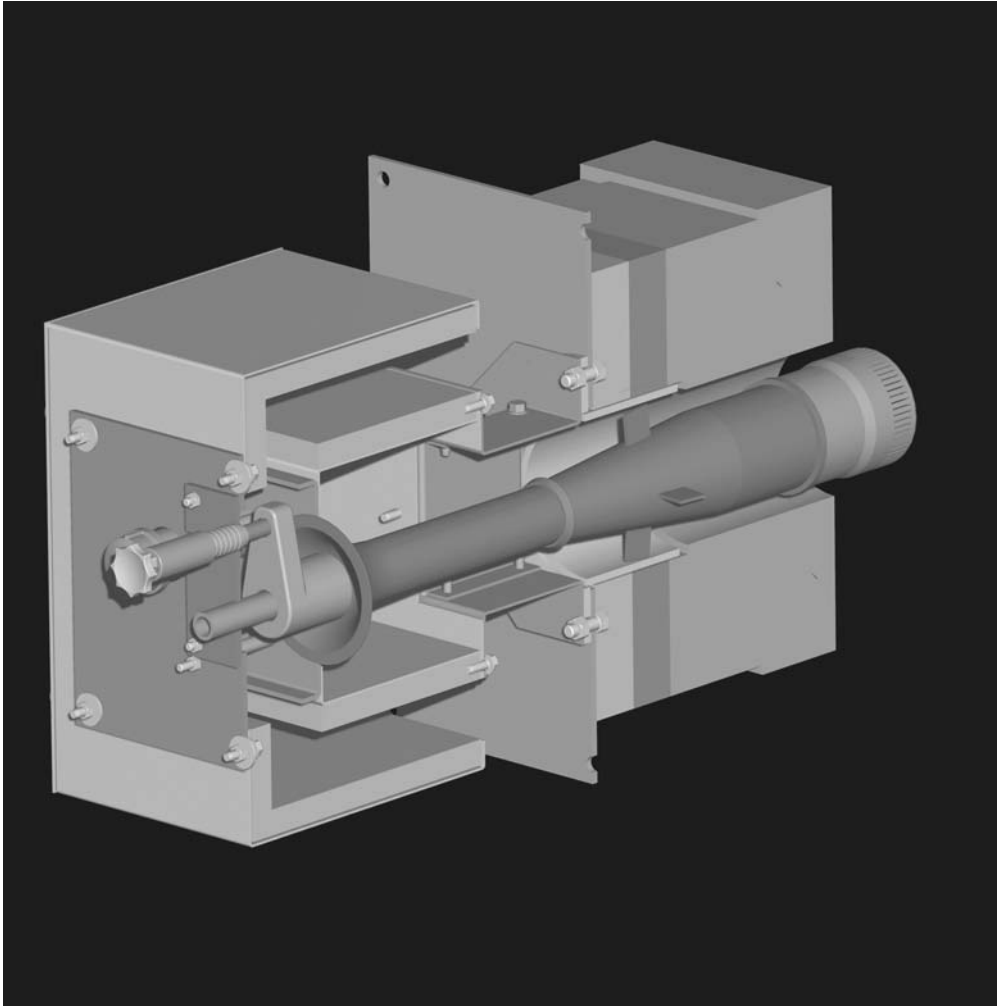


FIGURE 16.40 Typical radiant wall burner. (Courtesy of John Zink Co., LLC.⁴)

for oils containing higher sulfur contents. Other oil injector parts are carbon steel, although nitride-hardened parts may be used for erosive liquids. Flame stabilizer cones and swirlers are normally 300 series stainless steel.

Mineral wool is commonly used for noise reduction in the burner air inlet plenums. The burner block (tile) material is typically 55 to 60% alumina refractory with a 3000°F (1650°C) service temperature. Primary oil tiles may require 90% alumina refractory if the combined vanadium and sodium in the oil is greater than 50 ppm by weight.

16.8 CONCLUSIONS

Natural-draft burners are not commonly used in most industrial combustion applications, but are used extensively in the hydrocarbon and petrochemical industries. In this burner design, the combustion air is drawn into the burner rather than being supplied by a blower or fan, as is the case with forced-draft burners. One method for drawing in the air is by using the energy of a high-pressure fuel (>20 psig), which is usually widely available in refineries and petrochemical plants.

There, the fuel is typically a byproduct of the chemical production process of refining hydrocarbon fluids and is under some pressure by virtue of the transport through the plant piping. However, high fuel pressures are often not available in most other industries, which is one of the reasons natural-draft burners are not commonly used elsewhere. Another method for drawing in air is by the suction created by the draft in the furnace. Therefore, the conditions needed to practically use natural-draft burners for high heat release rates in furnaces and heaters are present in some industries but not others. While there are some cost savings associated with not having to buy a combustion air fan and the operating costs to run it, there are also some other factors to be considered. For example, natural-draft burners are typically larger than forced-draft burners for a given heat release rate, so the burner cost may be higher. Natural-draft burners are somewhat subject to weather conditions, particularly to the wind, which may adversely affect both the air flow into the burner and the furnace draft that may fluctuate as wind gusts flow over the exhaust stack outlet. This shows the importance of proper burner selection and design to ensure adequate performance for a given application.

REFERENCES

1. R.D. Reed, *Furnace Operations*, third edition, Gulf Publishing, Houston, 1981.
2. C.E. Baukal, Ed., *The John Zink Combustion Handbook*, CRC Press, Boca Raton, FL, 2001.
3. C.E. Baukal, Chapter 1: Introduction, in *The John Zink Combustion Handbook*, C.E. Baukal, Ed., CRC Press, Boca Raton, FL, 2001.
4. R.T. Waibel and M. Claxton, Chapter 11: Burner Design, in *The John Zink Combustion Handbook*, C.E. Baukal, Ed., CRC Press, Boca Raton, FL, 2001.
5. American Petroleum Institute, Burners for Fired Heaters in General Refinery Services, API 535, first edition, Washington, D.C., July 1995.
6. American Petroleum Institute, Fired Heaters for General Refinery Services, API 560, Washington, D.C., November 1996.
7. R. Hayes, C.E. Baukal, P. Singh, and D. Wright, Fuel Composition Effects on NO_x, *Proc. Air & Waste Management Association's 94th Annual Conf. & Exhibition*, Orlando, FL, June 24–28, 2001.
8. U.S. Dept. of Energy, Office of Industrial Technology, Petroleum — Industry of the Future: Energy and Environmental Profile of the U.S. Petroleum Refining Industry, U.S. DOE, Washington, D.C., December 1998.
9. U.S. Dept. of Energy, Office of Industrial Technology, Industrial Combustion Technology Roadmap, U.S. DOE, Washington, D.C., April 1999.
10. W.L. Nelson, *Petroleum Refinery Engineering*, second edition, McGraw-Hill, New York, 1941.
11. G.R. Martin, Heat-flux imbalances in fired heaters cause operating problems, *Hydrocarbon Processing*, 77(5), 103–109, 1998.
12. R. Nogay and A. Prasad, Better design method for fired heaters, *Hydrocarbon Processing*, 64(11), 91–95, 1985.
13. A. Garg and H. Ghosh, Good heater specifications pay off, *Chem. Eng.*, 95(10), 77–80, 1988.
14. H. Futami, R. Hashimoto, and H. Uchida, Development of new catalyst and heat-transfer design method for steam reformer, *J. Fuel Soc. Japan*, 68(743), 236–243, 1989.
15. H. Gunardson, *Industrial Gases in Petrochemical Processing*, Marcel Dekker, New York, 1998.
16. J.D. Fleshman, FW Hydrogen Production, in *Handbook of Petroleum Refining Processes*, 2nd edition, R.A. Myers, Ed., McGraw-Hill, New York, chap. 6.2, 1996.
17. J.S. Plotkin and A.B. Swanson, New technologies key to revamping petrochemicals, *Oil & Gas J.*, 97(50), 108–114, 1999.
18. D.Q. Kern, *Process Heat Transfer*, McGraw-Hill, New York, 1950.
19. N.P. Lieberman, *Troubleshooting Process Operations*, PennWell Books, Tulsa, OK, 1991.
20. H.S. Bell and L. Lowy, Equipment, in *Petroleum Processing Handbook*, W.F. Bland and R.L. Davidson, Eds., McGraw-Hill, New York, 1967, chap. 4.
21. E.B. Sanderford, Alternative Control Techniques Document — NO_x Emissions from Process Heaters, U.S. Environmental Protection Agency report EPA-453/R-93-015, February 1993.
22. L.A. Thrash, Annual Refining Survey, *Oil and Gas Journal*, 89(11), 86–105, 1991.

23. S.A. Shareef, C.L. Anderson, and L.E. Keller, Fired Heaters: Nitrogen Oxides Emissions and Controls, U.S. Environmental Protection Agency, Research Triangle Park, NC, EPA Contract No. 68-02-4286, June 1988.
24. H.L. Berman, Fired heaters. II. Construction materials, mechanical features, performance monitoring, in *Process Heat Exchange*, V. Cavaseno, Ed., Chem. Eng., McGraw-Hill, New York, 1979, 293–302.
25. A.J. Johnson and G.H. Auth, *Fuels and Combustion Handbook*, first edition, McGraw-Hill, New York, 1951.
26. G.L. Shires, Furnaces, in *The International Encyclopedia of Heat & Mass Transfer*, G.F. Hewitt, G.L. Shires, and Y.V. Polezhaev, Eds., CRC Press, Boca Raton, FL, 1997 493–497.
27. H.L. Berman, Fired heaters. I. Finding the basic design for your application, in *Process Heat Exchange*, V. Cavaseno, Ed., Chem. Eng., McGraw-Hill, New York, 1979, 287–292, .
28. V. Ganapathy, *Applied Heat Transfer*, PennWell Books, Tulsa, OK, 1982.
29. W. Bussman, R. Poe, B. Hayes, J. McAdams, and J. Karan, Low NO_x burner technology for ethylene cracking furnaces, *Proc. 13th Ethylene Producers' Conf.*, New York: American Institute of Chemical Engineers, Vol. 10, 714–740, 2001.

17 Burners for Industrial Boilers

Lev Tsirulnikov, Ph.D., John Guarco, and Timothy Webster

CONTENTS

- 17.1 Introduction
- 17.2 NO_x Formation
 - 17.2.1 Thermal NO_x Formation
 - 17.2.2 Prompt NO_x Formation
 - 17.2.3 Fuel NO_x Formation
- 17.3 Conventional Burners
- 17.4 Flue Gas Recirculation
- 17.5 Low-NO_x Burners
 - 17.5.1 Air-Staged, Low-NO_x Burners
 - 17.5.2 Fuel-Staged, Low-NO_x Burners
 - 17.5.3 Fuel-Induced Recirculation Burners
- 17.6 Low-NO_x Oil Firing
 - 17.6.1 Internal Mix Atomizers
 - 17.6.2 External Mix Atomizers
 - 17.6.3 Mechanical Atomizers
- 17.7 Additional NO_x Reduction Techniques
 - 17.7.1 Furnace Gas Recirculation
 - 17.7.2 Steam Injection
- 17.8 Ultra-Low-NO_x Burners
 - 17.8.1 Premix Burners
 - 17.8.2 Rapid Mix Burners
 - 17.8.3 Ultra-Low-NO_x Burner Operation

17.1 INTRODUCTION

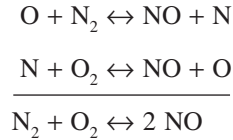
The purpose of a burner is to combine fuel and an oxidant (typically air) together and provide sufficient ignition energy to initiate and sustain the combustion process. This being the case, the main functions that a burner must address can be separated into the three categories: fuel injection, air introduction, and flame stabilization. Burners specifically designed for use in industrial boilers are most commonly of the circular register design, range in size from heat inputs of 20 to 400 million British thermal units (Btu) per hour, operate with forced-draft fans supplying the combustion air, and burn gas or liquid hydrocarbon fuels. These burners are generally classified by the amount of nitrogen oxide (NO_x) emissions they produce: conventional burners, low-NO_x burners, and ultra-low-NO_x burners.

17.2 NO_x FORMATION

To discuss NO_x reduction techniques, it is first necessary to briefly review the basic theory behind NO_x formation. Burning hydrocarbon fuels will form NO_x via three major processes: thermal NO_x formation, prompt NO_x formation, and fuel NO_x formation.

17.2.1 THERMAL NO_x FORMATION

Thermal NO_x formation is a route where high flame temperatures cause nitrogen molecules from the combustion air to break apart and combine with oxygen to form nitric oxide. The sequence is complicated, but the following two steps represent the essential features:



Combustion is a free-radical process whereby the reactions include intermediate species. In the above sequence, atomic oxygen attacks a nitrogen molecule to yield nitric oxide and a nitrogen radical. In the second step, the nitrogen radical attacks diatomic oxygen to produce another nitric oxide molecule and replenish the oxygen atom. The sequences sum to the overall reaction of one nitrogen and one oxygen molecule producing two nitric oxide molecules.

If we presume that the first step is rate limiting (disruption of the N–N triple bond) and that oxygen is in partial equilibrium ($\frac{1}{2} \text{O}_2 \leftrightarrow \text{O}$), then we generate the following integral kinetic rate equation:

$$[\text{NO}] = \int A e^{-\frac{b}{T}} [\text{N}_2] \sqrt{[\text{O}_2]} dt$$

where A and b are kinetic rate constants, T is the absolute temperature, square brackets denote the concentrations of the enclosed species, and t is the time.

From the rate equation, we deduce that “thermal NO_x” is primarily a function of temperature, but is also affected by oxygen concentration and the time at those conditions. [Figure 17.1](#) illustrates this relationship between thermal NO_x formation and flame temperature.

17.2.2 PROMPT NO_x FORMATION

Another way that NO_x is formed is called the prompt mechanism. As the fuel pyrolyzes, it generates fuel radicals, which combine with available nitrogen to produce carbon radicals. These carbon radicals oxidize promptly at the flame front to generate NO_x and other species. Under fuel-rich

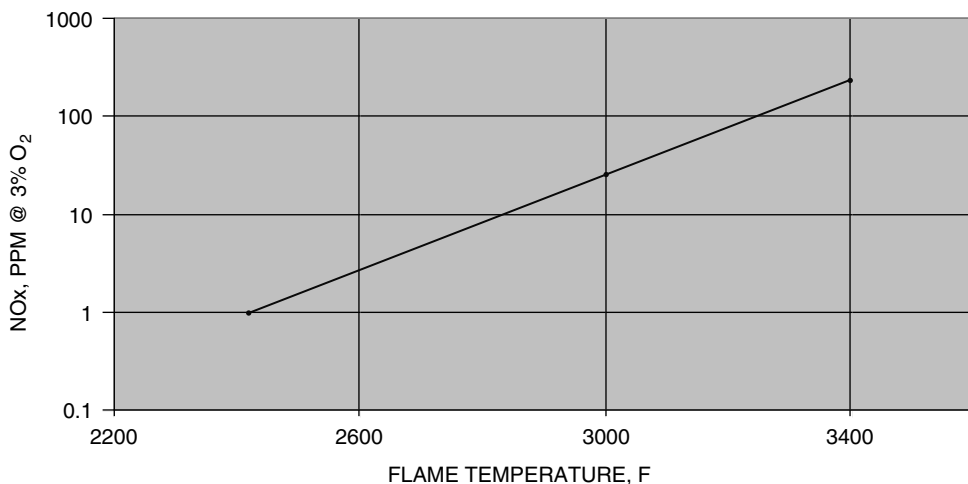
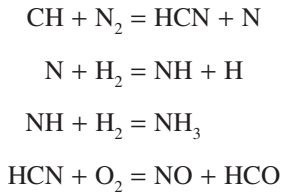
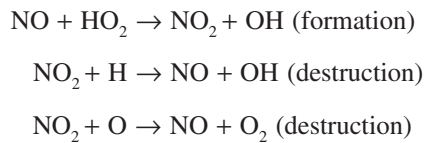


FIGURE 17.1 Thermal NO_x vs. flame temperature.

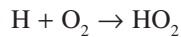
conditions, particularly when the stoichiometry is less than 0.6, both HCN and NH₃ can be formed through the rapid reaction of CH with N₂ to form HCN and N. As combustion continues, the HCN and NH₃ oxidize and result in the generation of NO_x. The following four reactions represent the basics of this process:



A part of the prompt NO formed is then converted into NO₂. A mechanism for this conversion is presented in the following reactions:



where the HO₂ radical is formed via:



Below a stoichiometry of 0.5, almost all NO_x formed is attributable to “prompt NO_x.” The rate of formation of prompt NO_x is very rapid, being complete in under 1 msec. Although prompt NO_x is temperature sensitive, the temperature sensitivity is not as great as with thermal NO_x. Unlike thermal NO_x, simply lowering the peak flame temperatures will not reduce prompt NO_x into the single digit range. Even if the reaction temperature is lowered to 2400°F, under fuel-rich conditions, significant amounts of prompt NO_x still remain, as seen in Figure 17.2. To control the formation of prompt NO_x, it is necessary to take steps in the burner design to minimize the formation of sub-stoichiometric regions within the flame.

17.2.3 FUEL NO_x FORMATION

The final NO_x formation mechanism is fuel specific and based on the level of nitrogen that is bound as part of the fuel molecule itself. If nitrogen is a part of the fuel molecule, once the molecular bonds are broken during the combustion process, this nitrogen is freed up as nitrogen radicals. These nitrogen radicals will now attack diatomic oxygen molecules, as described during the thermal NO_x formation process, to form NO_x. Natural gas and most other industrial gas fuels contain no

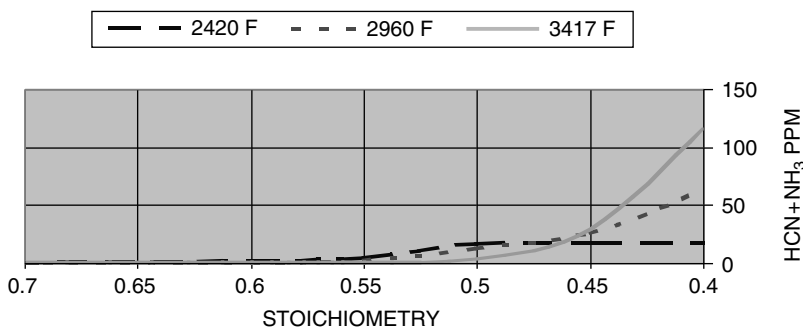


FIGURE 17.2 Prompt NO_x formation.

fuel-bound nitrogen and, therefore, form no “fuel NOx.” However, most commonly used liquid hydrocarbon fuels, such as grades no. 2 through no. 6 fuel oil, contain between 0.01% and 0.50% by weight of fuel-bound nitrogen, which can contribute to between 20 and 80% of the total NOx formed firing these fuels.

17.3 CONVENTIONAL BURNERS

Conventional burners, as seen in Figure 17.3, trace their lineage back to the days of ship-mounted boilers, where boilers had to be kept as small and light as possible thus making the requirement for short flames very important. The fact that without these boilers in operation, a ship could be left dead in the water, resulting in the need for the burners to reliably operate regardless of changes to the fuel or air supply. The maneuvering demands of the ship also required that these burners be able to operate across a wide range of firing rates and to be able to change firing rate quickly.

To accomplish all these goals, the design resulted in burners that typically mixed air and fuel as rapidly as possible to create a highly stable flame that was also as short as possible. Conventional burners commonly employ a series of vane-type louvers, called registers and shown in Figure 17.4, around the outer periphery of the burner to impart a swirling motion to the combustion air. The fuel was injected into this swirling vortex of air, as evenly as possible, right at the exit of the burner. The gas fuel injection was accomplished through a gas header that surrounded the burner exit, called a gas ring, which was drilled with a series of holes to inject the gas into the air stream as it exits the burner. The firing of liquid fuels was accomplished using a “gun-style” atomizer (see Figure 17.5) installed right down the center of the burners.

The absence of air in the center of the burner, caused by the swirling action of the burner, could result in fuel-rich pockets in the burner center when firing liquid fuels resulting in smoking. Therefore, in liquid fuel firing applications, a bluff body was commonly used at the end of the atomizer.

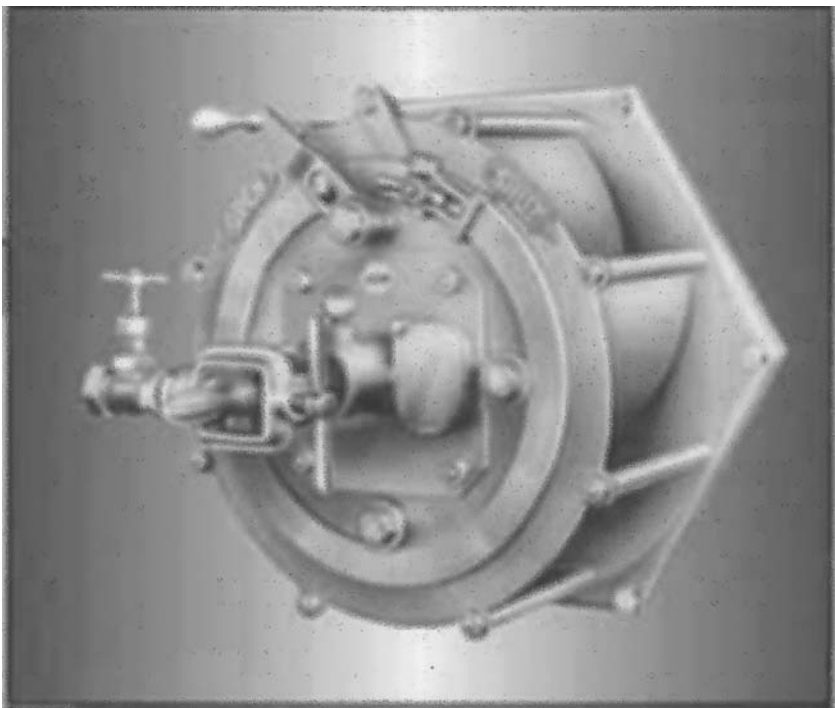


FIGURE 17.3 Conventional register-style burner.

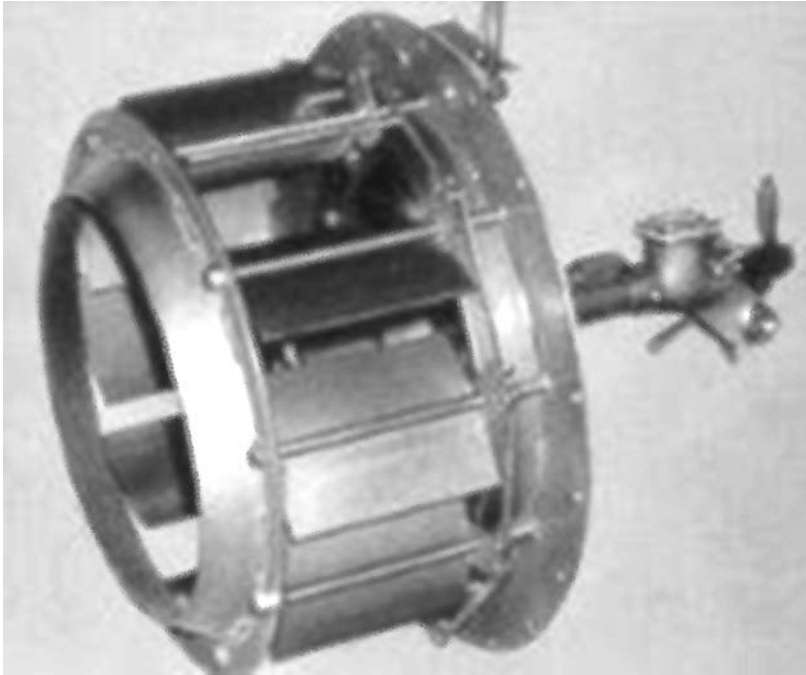


FIGURE 17.4 Register burner louver vanes.

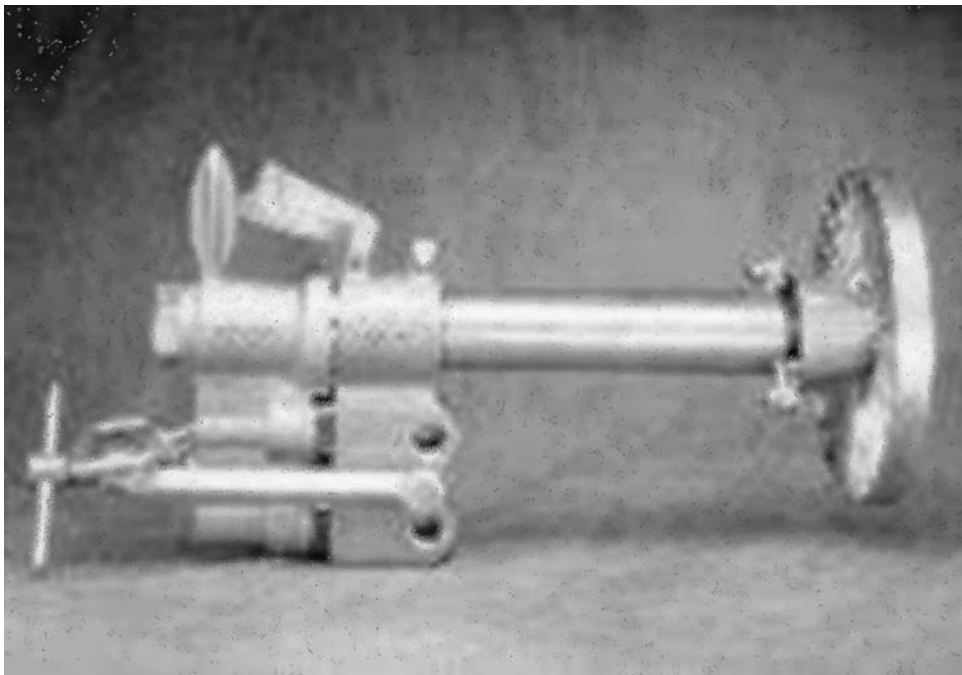


FIGURE 17.5 Oil atomizer gun assembly.

The purpose of the bluff body was to create a small recirculation zone in the center of the burner to help draw some of the combustion air back into the center of the burner to prevent the fuel-rich pockets. The positions of the air register louvers could also be adjusted to increase or decrease the amount of swirl added to the air, either speeding up or slowing down the mixing speed of the burner. The pressure drop on these burners was usually kept very low, with airside pressure drops of between 3 and 6 inches of water column (in. w.c.) and gas side pressures of 10 to 30 in. w.c.

The swirling fuel and air mixture exited the burner and entered the furnace through a refractory throat, conical in shape and ranging from 6 to 24 in. in depth. This throat helped stabilize the ignition process by providing a hot surface against which the rotational momentum of the burner “scrubbed” the fuel-air mixture. The result of this design was a burner that produced a short, hot, swirling flame that was extremely tolerant to rapid changes in firing rate and a wide range of excess air. The drawback to this design was that the intensity of the combustion produced extremely high thermal NO_x emissions, and the rapid fuel-air mixing also did nothing to retard fuel NO_x emissions while firing liquid fuels. However, these designs produced little or no prompt NO_x emissions.

17.4 FLUE GAS RECIRCULATION

One of the first methods of NO_x reduction was the use of flue gas recirculation (FGR), whereby a portion of the stack gases was returned and mixed with the combustion air to the burner. This added additional mass flow into the combustion zone across which the heat release was distributed, and thereby lowered the temperature and accompanying thermal NO_x formation. The introduction of FGR into the combustion air increases the overall mass of the reactants, and hence the products, in the combustion process. The increased mass, as well as the increased reactant diffusion time requirement, reduces the overall flame temperature. The fact that the flue gases being returned also have very low oxygen levels, typically 2 to 4%, resulted in a lowering of the volumetric oxygen concentration entering the combustion zone, which also helps to retard NO_x formation by limiting oxygen availability. FGR was added to many conventional burners, and could result in NO_x reduction ranging from 20 to 75%, depending on the amount added, the fuel being fired, and the initial NO_x level. The problems with FGR addition to conventional burners were three-fold: (1) additional fan capacity had to be used to transport the hot flue gases to the burner combustion air system, resulting in increased capital and operating costs; (2) very high levels of flue gases were often required to reduce NO_x emissions to acceptable levels; and (3) high rates of FGR, typically over 20%, decreased the flame temperature to the point where burner operation began to become unstable.

17.5 LOW-NO_x BURNERS

Low-NO_x burners were designed to eliminate or minimize the impact of these concerns by (1) reducing NO_x as much as possible without the use of FGR, (2) maximizing the NO_x reduction from FGR when required to minimize the amount needed, and (3) providing a burner design that was extremely stable with very high rates of FGR.

The first technique used in the design of low-NO_x burners was the concept of air staging. Instead of injecting all the combustion air at one point, burners began to separate the air into two or even three different streams that would be injected at various points.

17.5.1 AIR-STAGED, LOW-NO_x BURNERS

The basis of design is to develop a stratified flame structure with specific sections of the flame operating fuel-rich and other sections operating fuel-lean, as shown in [Figure 17.6](#). The burner design thus provides for the internal staging of the flame to achieve reductions in NO_x emissions while maintaining a stable flame. Controlling combustion stoichiometry to fuel-rich conditions

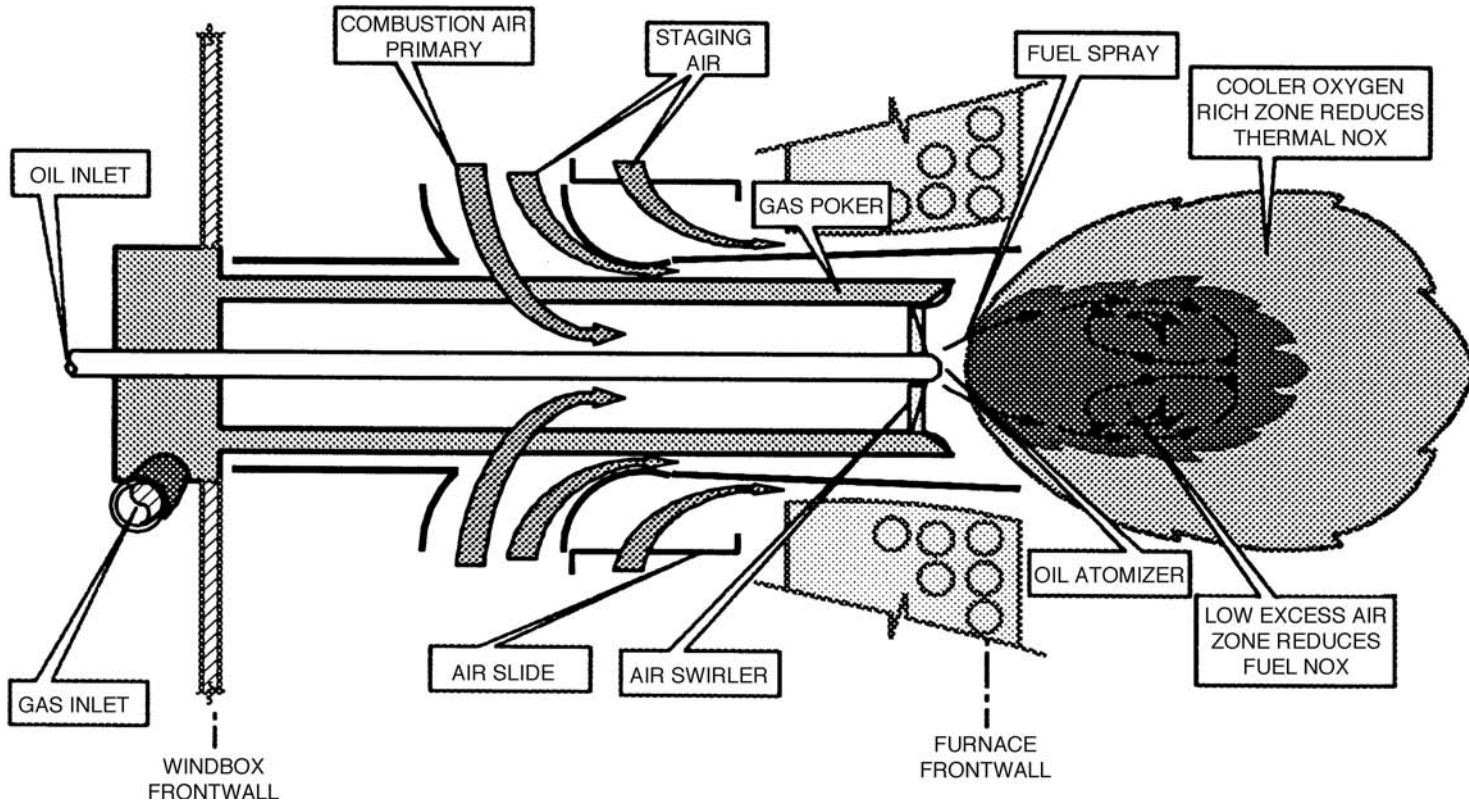


FIGURE 17.6 Staged-air, low combustion schematic.

inhibits NO_x production, especially in the burner's flame front. Operating the flame fuel-rich also reduces burner NO_x emissions dependence on the burner zone heat release (BZHR) characteristics of the boiler furnace. This is especially important in applications where very high BZHR near full load can result in an exponential increase in NO_x emissions.

Staging of the air into the combustion zone serves to slow down the combustion process and separate the flame into different zones, some that operate fuel-rich and some that operate fuel-lean. The fuel-rich and fuel-lean zones both combust at lower peak temperatures than a uniform fuel-air mixture, resulting in lower thermal NO_x formation. The combustion products from these two zones then combine to complete the combustion process and result in the completed oxidation of the fuel. By creating a fuel-rich zone in the front part of the flame, one can also reduce the conversion of fuel-bound nitrogen to NO_x and thereby lower fuel NO_x formation as well. However, the increase in sub-stoichiometric zones in the flame actually increases the prompt NO_x formation in these burners. The increase in prompt NO_x is more than offset by the large decreases in thermal and fuel NO_x, when applicable and, therefore, total NO_x production from these burners is still lower. The delayed mixing of fuel and air also leads to an increase in flame lengths, and staged burners can have flames that are 25 to 50% longer than conventional burners of the same heat input. This helps reduce NO_x by subjecting the flame to more of the furnace waterwall surface area, which also helps to draw heat from the combustion process and cool the flame. However, increasing the flame length must be carefully balanced with available furnace depth; otherwise, flame impingement can occur. Flame impingement will result in unburned fuel being emitted from the boilers in the form of both hydrocarbon emissions and carbon monoxide. This is an emissions problem, an efficiency problem, and can be detrimental to boiler tube life.

Staged air burners, such as the one shown in Figure 17.7, typically rely on little or no swirling of the combustion air in order to slow fuel-air mixing. A small amount of primary air, typically 10 to 20% of the total combustion air, is routed down the center of the burner. Most burner designs

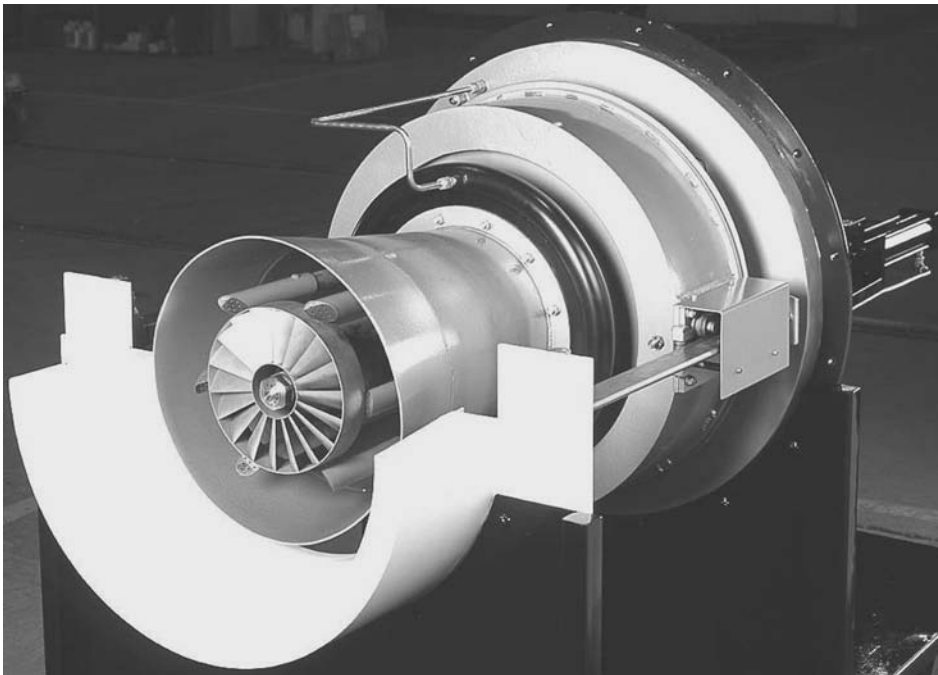


FIGURE 17.7 Staged-air low-NO_x burner.



FIGURE 17.8 Staged-air, low-NO_x burner swirler and gas injectors.

employ a curved bladed swirler, as depicted in Figure 17.8, to impart rotational momentum to this primary air. This swirled primary air creates a rotational vortex in the front of the burner, which serves several functions. It entrains a portion of fuel, creating a fuel-rich region immediately in front of the burner. This effect can be enhanced in some burners by designing fuel injectors that inject a portion of the fuel directly into this area. Because the burner flame front was established as a fuel-rich premixed flame, it results in increased flame speed and, in turn, flame stability. Combustion stoichiometry approaching a perfect premixed flame will broaden the flammability range of the fuel, ensure the maintenance of a flammable mixture over a broad range of burner throat velocities and fuel injection rates, and keep the burner operating reliably, even at extremely low flame temperatures.

This anchored base flame provides a location for the burner flame scanner to reliably sight the flame. The swirling primary air also generates a reverse flow in the form of a self-generating annular vortex that helps recirculate hot combustion gases from within the flame zone, thereby providing additional ignition energy to the fuel-air mixture and increasing the mass flow in this region to limit peak temperatures. In addition to controlling NO_x formation, operating under fuel-rich conditions results in the production of combustion intermediates that can result in the destruction of previously formed NO_x. In a reducing environment, NO can act as an oxidizer to react with these combustion intermediates, resulting in the reduction of NO to N₂. As such, NO,

necessarily formed to satisfy the requirements of establishing a strong flame front, can be scavenged by this mechanism.

To achieve complete fuel burnout at minimum excess air, the burner design must provide for fuel-lean zones to directly interact with the center fuel-rich sections. Creating a secondary air zone where the majority of the combustion air is introduced (65 to 90%) accomplishes this. The air injected into this zone is typically injected axially, with little or no swirl. Multiple gas fuel injectors are also located in this zone, and high-pressure fuel ranging from 5 to 15 psig is commonly used. The multiple high-pressure fuel jets allow for the free-jet entrainment of large amounts of air into the base of these flames. Separate air and fuel lanes are created, which eventually interact to provide the completely mixed fuel-lean combustion products from this zone. For liquid fuel firing applications, a center-mounted atomizer is used with specially drilled injection holes to direct the fuel into the secondary air flow. This secondary zone surrounds the fuel-rich primary zone, which ensures that the “rich” products of combustion from the center flame pass through the oxidizing zone for complete fuel burnout. The burner design typically allows control of the stoichiometry of the oxidizing zone from being pure air to having varying degrees of excess oxygen. This controls NO_x formation by causing the fuel burnout to occur in the form of a premixed flame rather than a diffusion flame.

To increase the flexibility of combustion staging and flame shaping capabilities, some low-NO_x burner designs are equipped with a tertiary air zone installed at the outer periphery of the burner throat. The tertiary air, which can be swirled or completely axial, is mixed in the furnace with the bulk furnace gas to achieve complete fuel burnout. This provides for the complete burnout of the fuel in the post-combustion zone where NO_x formation is inhibited by lower combustion temperature and reduced O₂ concentration. In cases when both the secondary and the tertiary air flows are straight, changes in the ratio between their flow rates actually do not visibly impact the combustion process, including NO_x generation. For such designs, the tertiary air flow is required, primarily to maintain flame dimensions.

The amount of air used in the tertiary zone can range from 10 to 15%; however, more tertiary air flow will increase the flame length because it adds an additional delay to the combustion process. The amount of tertiary air is commonly adjustable to allow maximum staging that can be tailored to the furnace geometry. Tertiary air flow also helps to cool the burner refractory throat by creating an air wall between the hot combustion gases and the refractory. This reduces the amount of heat that hot refractory will re-radiate back into the flame, lowering thermal NO_x formation, and helps to increase refractory life. However, because the burners no longer scrub the fuel-air mixture against the hot refractory, as was done on conventional burners, the refractory does little to aid in flame shaping or stability.

The register draft loss on low-NO_x burners is typically higher than that of conventional burners, with 6 to 8 in. w.c. of airside pressure drop being common. Air-staged, low-NO_x burners resulted in dramatic reductions in NO_x formation, and cut NO_x emissions from gas fuel firing by 50% or more. These burners can also be very effectively utilized in conjunction with FGR to achieve NO_x reductions as high as 85%, and have demonstrated operational stability with FGR rates greater than 40% in some cases.

Reductions from liquid fuel firing were also achieved; however, these reductions were not dramatic because much of the NO_x from those fuels was “fuel NO_x.” Reducing the amount of fuel NO_x formed can be achieved by taking further steps to create a fuel-rich primary combustion zone. In this case, the fuel-bound nitrogen, that is liberated as nitrogen radicals in the initial combustion process, cannot find sufficient oxygen to bond with and form NO_x. These nitrogen radicals will then recombine and form diatomic nitrogen. To accomplish this, staged-air, low-NO_x burners are often employed in conjunction with frontwall or sidewall NO_x ports for use during liquid firing. In this mode, the ports are opened during liquid firing and a portion of the combustion air, typically 15 to 35%, enters the furnace through the ports, bypassing the burner air register. This creates a fuel-rich flame across the entire burner front, and allows the port air to mix into the flame body

further down the furnace to complete combustion. As is the case with tertiary air, more staging of air to the ports does result in increased flame length.

17.5.2 FUEL-STAGED, LOW-NO_x BURNERS

In an effort to reduce the NO_x emissions firing gaseous fuels, without using FGR, several additional NO_x reduction techniques have been developed and applied to low-NO_x burners. The most common has been the use of fuel staging, whereby a portion of the fuel, anywhere from 50 to 90%, is injected directly into the furnace outside the air register. This process relies on the use of a highly stable center or core flame, which helps create and maintain a fuel-lean primary combustion zone at the burner front. Because all the combustion air is introduced through burner air register, but only a portion of the gas fuel is introduced here, the burner itself is operating at extremely high excess air levels. Without the use of the center-fired gas flame to provide a stable ignition source, the high excess air levels found in the primary combustion zone would not be able to reliably sustain stable combustion. By operating fuel-lean, both thermal NO_x and prompt NO_x formation is reduced in this zone.

The remainder of the gas fuel is introduced through gas injectors, inserted through the boiler furnace front wall, without any accompanying combustion air. Different designs for the gas injectors result in gas supply pressure requirements ranging from 6 to 22 psig for most applications. The center flame, containing a small amount of internally recirculated furnace gases, behaves like a regular high-temperature turbulent gas flame. The outer gas injectors supply the remaining fuel, which is a majority of the total gaseous fuel, into the secondary and tertiary air flows. The staged secondary flames are formed as the outside injector gas jets enter into the straight secondary and tertiary air flows and are ignited by the hot combustion products from the center flame. The injectors are located at a set distance from the center flame and divided from it by a layer of combustion products and air. This allows the gas jets to entrain additional amounts of inert, high-temperature furnace gases, prior to entering the combustion zone. The diluted fuel and furnace gas mixture limits the temperature rise resulting from the combustion process, dramatically reducing the formation of thermal NO_x. This outer gas injector fuel consumes the excess oxygen left over from the fuel-lean combustion zone, which has also generated its own combustion products. This method of internal furnace gas entrainment, combined with the fuel-lean primary zone combustion products, results in a secondary combustion zone that is equivalent to a burner operating with high levels of FGR. The NO_x reduction that can be achieved with this type of fuel staging can be equivalent to that of an air-staged, low-NO_x burner operating with FGR levels of 10 to 15%.

17.5.3 FUEL-INDUCED RECIRCULATION BURNERS

An alternate type of advanced low NO_x gas burner design utilizes flue gases mixed with the gas fuel, called fuel-induced recirculation (FIR), instead of with the combustion air to reduce NO_x. The burner uses the motive force of the fuel to inspirate flue gases from the boiler exhaust and mix them into the gas fuel prior to injection into the combustion zone. To provide sufficient motive force, fuel gas supply pressures ranging from 10 to 25 psig are usually required. The mixture of fuel and flue gas results in a diluted fuel, similar to a low Btu fuel gas, which generates lower NO_x emissions. The use of flue gases mixed with the fuel, instead of with the combustion air has proven to be 30 to 50% more effective at NO_x reduction. Substantial horsepower savings are also realized with this technology, through the use of available fuel pressure as the means of transporting the flue gases instead of fans. The burner design involves multiple gas nozzles supplied from a single fuel plenum to induce flue gases from an integral flue gas plenum. This requires only a single fuel gas and a single flue gas connection at the burner front. The design provides a large amount of burner nozzle area for maximum dilution, and stages the injection of both the fuel and air for added NO_x reduction. The high levels of dilution achieved by this burner design will reduce NO_x by 80 to 85% over the levels being achieved by a conventional burner.

17.6 LOW-NO_x OIL FIRING

Because the methods of fuel staging discussed previously are applied to gas firing only, they have no real effect on NO_x emissions while firing liquid fuels. When firing liquid fuels, these burners operate simply as air-staged, low-NO_x burners, with fuel staging provided only by advanced atomizer sprayer plate designs.

Boiler burners are designed to utilize many types of mechanical, dual fluid, and, occasionally, rotary cup oil atomizers. Most of these atomizers are fitted onto oil “guns” similar to the ones shown in Figure 17.9. For dual fluid atomizers, they are separated into “external mix” atomizers and “internal mix” atomizers, based on how the fuel and atomizing medium interact. The atomizing medium used is typically either steam or pressurized air; however, some tough-to-combust liquid fuels may utilize a gas fuel as the atomizing media.

17.6.1 INTERNAL MIX ATOMIZERS

Internal mix atomizers such as the “T-jet” typically require a relatively large amount of atomizing medium consumption, on the order of 0.1 to 0.3 pounds of medium per pound of fuel, but provide excellent atomization quality, with a typical Sauder mean diameter (SMD) of 75 μm at a fuel viscosity of 100 SSU. The supply pressure for the atomizing medium must be kept above the oil pressure to prevent oil from entering the atomizing medium supply lines. Operating pressures for internal mix atomizers range between 85 and 300 psig for the oil, with the atomizing medium pressure typically regulated to a differential pressure 15 to 30 psig higher than that of the oil. The turndown ratio for these atomizers, depending on the oil supply pressure, can be as high as 10:1.



FIGURE 17.9 Two oil atomizers.

17.6.2 EXTERNAL MIX ATOMIZERS

External mix atomizers such as the “Y-jet” require much less steam consumption than internal mix atomizers, on the order of 0.05 to 0.07 pounds of medium per pound of fuel; however, the atomization quality is slightly reduced, with a typical SMD of 125 μm at a fuel viscosity of 100 SSU. Due to the external mixing of these atomizers, there is very little chance for oil to enter the atomizing medium supply lines. Therefore, these atomizers do not require that the supply pressure for the atomizing medium be kept above the oil pressure. Operating pressures for Y-jet type atomizers range between 85 and 300 psig for the oil, with the atomizing medium pressure typically regulated to a constant pressure of 85 to 150 psig. The turndown ratio for these atomizers, depending on the oil supply pressure, can be as high as 10:1.

17.6.3 MECHANICAL ATOMIZERS

The two main types of mechanical atomizers are “simplex” and “spill-return” atomizers. Oil enters a mechanical atomizer through slots that expel the oil tangentially into a circular “whirling” chamber. The vortex created by the tangential entry into the whirling chamber is essential for good-quality atomization. For a spill-return flow atomizer, a portion of the supply flow will return back into the oil gun through a series of holes located at the back of the atomizer. The remaining oil exits the atomizer through either a single hole or a series of holes located at the front end (furnace side) of the atomizer. The “return” oil backpressure is controlled to adjust the firing rate, and the returned oil is recirculated back through the oil supply system. Simplex atomizers are simply a spill-return atomizer without the return flow, wherein the supply pressure to the atomizer is controlled to regulate the firing rate and no oil returns.

Burner performance has been improved using specially designed return-flow atomizers to maximize combustion efficiency and minimize NO_x. These atomizers produce good atomization quality at full load, with a typical SMD of 125 μm at a fuel viscosity of 100 SSU. However, atomization degrades rapidly with decreasing flow on these atomizer types, thereby limiting turndown. For this reason, to achieve satisfactory operating turndown, the oil pressures for simplex-type atomizers range between 300 and 600 psig. The turndown ratio for these atomizers, depending on the oil supply pressure, is very low (typically 2:1).

The delivered flow supplied by a spill-return atomizer depends on the return backpressure, which is essentially the same pressure as the atomizer would require if it were operating in simplex mode. The differential between the supply and return oil pressures, which can range between 100 and 350 psig, allows these atomizers a greater turndown range (up to 4:1). Operating pressures for spill-return atomizers typically range between 400 and 1000 psig.

17.7 ADDITIONAL NO_x REDUCTION TECHNIQUES

Some additional NO_x reduction techniques have been applied that affect both gas and liquid fuel NO_x emissions.

17.7.1 FURNACE GAS RECIRCULATION

One such technique is to use the burner air register, through the use of a venturi design, as a method of pulling furnace gases back into the burner and mixing them with the combustion air. In this design, ports in the boiler furnace front wall are ducted to the low pressure point in the air register venturi, as shown in [Figure 17.10](#), where the negative static pressure will create a suction that draws furnace gases back into the burner. The mixing of the combustion air with the high-temperature, incomplete combustion products, contained in the above internally recirculated flow, is highly effective in reducing thermal NO_x formation within the burner firing either gas or liquid fuel. It has also been established that introduction of the “hot” furnace gas flow, containing significant concentrations of

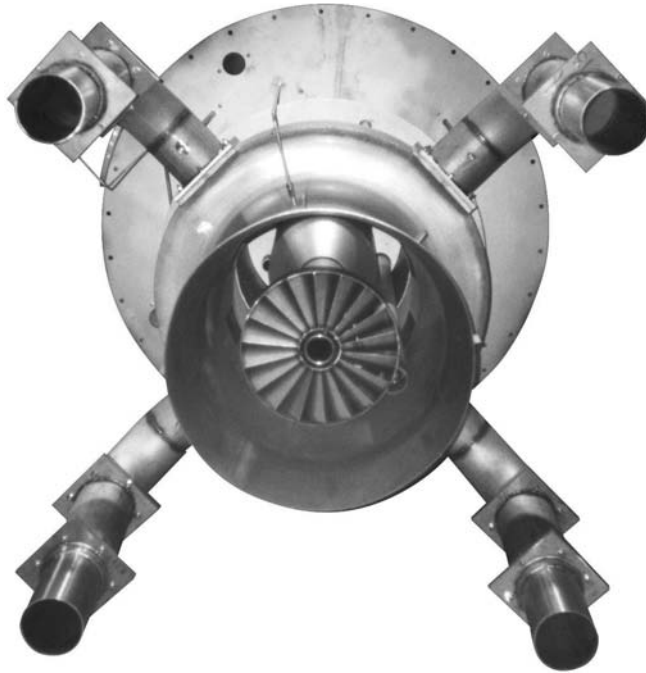


FIGURE 17.10 Burner equipped with furnace gas recirculation ducts.

incomplete combustion products into combustion air, reduces not only the thermal NO_x, but also the prompt NO_x concentrations. This effect distinguishes its impact from that of regular FGR, containing negligible concentrations of incomplete combustion products, which is capable of only reducing thermal NO_x emissions.

17.7.2 STEAM INJECTION

Another method that has been applied to reduce NO_x emissions from either gas or liquid fuel combustion has been the use of steam injection. Flue gas formed by the complete combustion of natural gas at low excess air levels contains at least 15% water vapor by weight. However, it is well known that introducing even a small additional amount of moisture into a burner flame usually brings a significant NO_x reduction, which depends not only on amount of moisture but also on the furnace and burner design, combustion air temperature, and excess air. In addition to these factors, the location where moisture is introduced into the furnace or flame is also very important. Steam acts to absorb heat from the combustion process and reduce thermal NO_x formation.

It has been established on a few industrial boilers that the NO_x reduction effectiveness of moisture injection is changed when FGR is used as well. Even in cases with the same combustion conditions, the same amount of the moisture introduced at the same point can provide different NO_x reductions, depending on whether the moisture is steam, water, or a mixture of both. However, because steam is also available at very high pressures, the energy of the steam jets can also be used as a method to increase fuel-air mixing within the burner and to entrain furnace gases into the flame front. However, the injection of steam always comes with the additional boiler operating costs associated with generating the steam for injection, unless a source of waste steam is available for use. Water treatment costs can also represent a significant impact in cases where high levels of chemical treatment of boiler feedwater is necessary. The use of water injection, in place of steam, also has operational costs associated with it, both with the power required for pumping and with the latent heat of vaporization that cannot be recovered by the boiler and, therefore, decreases the thermal efficiency of the unit.

17.8 ULTRA-LOW-NO_x BURNERS

Low-NO_x burners utilize staged combustion to delay the mixing of fuel and air, creating an initial fuel-rich combustion zone and adding air downstream to complete combustion. In this process, oxygen availability is limited, peak flame temperature is lowered, and thermal NO_x formation is reduced. Thermal NO_x can be further reduced through other techniques, such as the addition of flue gas recirculation (FGR) or steam injection. However, the prompt NO_x created in the initial fuel-rich zone remains, and it is this prompt NO_x formation that has prevented low-NO_x burners from achieving sub-10-ppm NO_x levels.

By “starting over” with NO_x formation fundamentals, it was determined that the most direct method of achieving ultra-low-NO_x emissions from a gas flame is to: (1) avoid fuel-rich regions with their corresponding potential for prompt NO_x, and (2) lower the flame temperature to reduce thermal NO_x to the desired level. To accomplish this, an ultra-low-NO_x burner design must first avoid fuel-rich regions, which can be accomplished in one of two ways.

17.8.1 PREMIX BURNERS

The first way to avoid fuel-rich regions is by premixing the fuel gas with some or all of the combustion air to ensure that the mixture contains at least 80% of the oxygen required for combustion. The drawback to this design is that a premixed volume of fuel and air can “flashback” to the point where the mixing occurs if the injection velocity is allowed to decrease below the flame speed. This becomes a concern as the burner firing rate is lowered, and commonly results in a limitation of only 3:1 or 4:1 turndown on premixed burner designs. One method to overcome this is through the use of a variable burner exit geometry, which decreases the size of the injection orifice as the firing rate is lowered, keeping the velocity above the flame speed and preventing flashback. Another method that has been successfully applied involves the introduction of the fuel-air mixture through a mesh-type surface combustor that also acts as a flame arrestor. Both methods have been shown to extend the operational turndown of these burners into the range required for typical industrial boiler applications; however, certain operational, reliability, and maintenance concerns still exist with both methods.

17.8.2 RAPID MIX BURNERS

The second method to accomplish the elimination of fuel-rich zones is by rapidly mixing gaseous fuel and air near the burner exit, as shown in [Figure 17.11](#). The rapid mixing results in a nearly uniform fuel/air mixture at the ignition point, which virtually eliminates prompt NO_x formation. In effect, the burner performs like a premix burner with one important distinction: because the fuel is added inside the burner, just upstream of the burner exit, the extremely small premixed volume eliminates the possibility of flashback inherent in premix burner designs. A couple of methods of initiating this rapid fuel/air mixing have been utilized. In the first method, swirler geometry, burner internal geometry, gas injector design, and quarl expansion are all matched to rapidly mix the fuel from a series of very fine gas injection orifices with the axially flowing combustion air. A portion of the combustion air/fuel mixture injected through the burner center is swirled to promote internal recirculation of a large amount of hot combustion gases. In an alternate method, high-pressure steam jets are used to provide rotational mixing momentum in the primary combustion zone for fuel/air mixing, as well as serving to reduce thermal NO_x.

17.8.3 ULTRA-LOW-NO_x BURNER OPERATION

Contrary to operation with staged combustion low-NO_x burners, where NO_x reductions are often accompanied by increases in other emissions, such as carbon monoxide (CO), unburned hydrocarbons (UBHCs), and volatile organic compounds (VOCs), ultra-low-NO_x burners, like the one shown

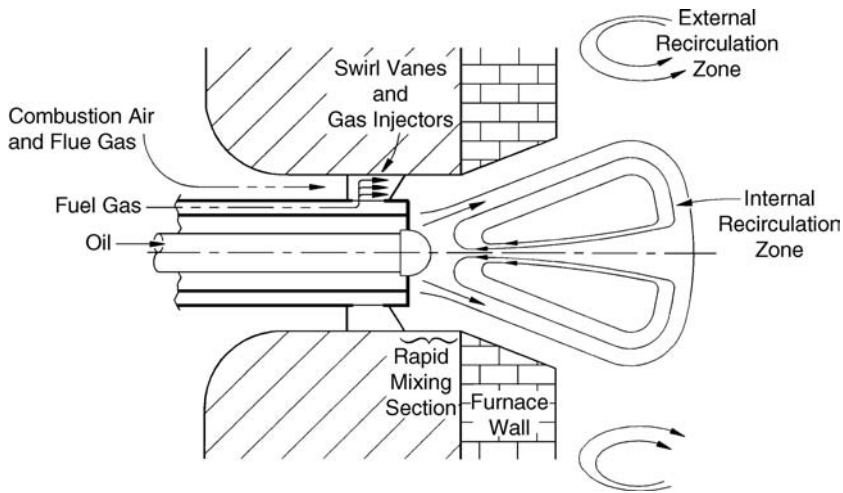


FIGURE 17.11 Rapid mix burner schematic.



FIGURE 17.12 Ultra-low-NOx burner.

in Figure 17.12, easily achieve reductions in all of these emissions simultaneously. The rapid and complete combustion that eliminates prompt NO_x also results in the virtual elimination of CO, UBHC, and VOC formation from ultra-low-NO_x burners.

Thermal NO_x is then minimized using FGR, which can also be combined with steam injection to lower the amount of FGR required to control flame temperature. A typical industrial boiler application will require the use of 25 to 30% FGR to reach sub-10 ppm NO_x operation. Some ultra-low-NO_x burners have shown that their flames remain stable at 60% FGR, which enables the burner to operate at lower flame temperatures and NO_x levels, with a “blowoff” point of about 3 ppm NO_x.

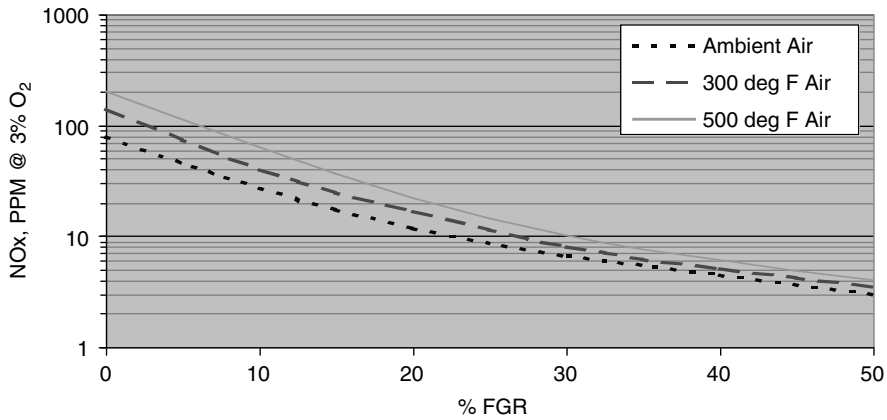


FIGURE 17.13 Effect of FGR vs. air preheat on ultra-low-NO_x burners.



FIGURE 17.14 Ultra-low-NO_x burner flame.

Contrary to conventional low-NO_x burner theory, increasing excess air reduces NO_x formation in ultra-low-NO_x burners. Because the burners employ premixing or near-perfect mixing, the fuel already has access to all of the oxygen required at the ignition point. Increasing excess air just serves to reduce the peak flame temperatures and, therefore, excess air has the same cooling effect as FGR. This provides major advantages in high excess-air combustion applications, such as dryers, where FGR is impractical or unavailable. In boiler applications, where FGR is available, it is preferred due to its lower impact on the boiler efficiency than high excess air, and its lower operating cost impact when compared to steam injection.

The ultra-low-NO_x design is also what allows the burner to operate with preheated combustion for increased efficiency, and still retain single-digit emissions performance by simply increasing

the FGR rate to compensate for the higher air temperature. For example, increasing the combustion air temperature from ambient (80°F) to an air preheat of 300°F would require an increase in FGR rate from 27 to 32% to maintain emissions at 9 ppm. Further increasing the air preheat to 500°F would require a respective increase in FGR rate to 43%, which can be seen in [Figure 17.13](#).

In addition to low emissions, another benefit of the ultra-low-NOx burner design is an extremely stable and very short flame, as shown in [Figure 17.14](#). It is approximately half that of a staged air burner, which eliminates the potential for flame impingement, a common problem experienced with low-NOx burner retrofits. The air-side pressure loss for most ultra-low-NOx burners is typically higher than that for low-NOx burners, at 8 to 12 in. w.c. The fuel pressure requirements, however, do not differ significantly from air-staged low-NOx burners.

For oil firing, the ultra-low-NOx burner utilizes a conventional center-mounted atomizer assembly. The burner operates as a staged-air low-NOx burner when firing oil, with fuel staging provided by advanced atomizer designs and air staging provided by the burners primary and secondary air flows. This allows emissions performance on oil firing equivalent to other low-NOx burners.

18 Multi-Burner Boiler Applications

Lev Tsirulnikov Ph.D., John Guarco, and Timothy Webster

CONTENTS

- 18.1 Boiler-Specific Burner Requirements
 - 18.1.1 Conventional Burner Technology for Boilers
 - 18.1.2 Low-NO_x Burner Technology for Boilers
 - 18.1.3 Staged Burner Design Philosophy
 - 18.1.4 Design Features of Low-NO_x Burners
 - 18.1.5 Effects of Burner Retrofits on Boiler Performance
- 18.2 Boiler Design Impacts on NO_x Emissions Correlations
 - 18.2.1 Boiler Design
 - 18.2.2 Excess Air
 - 18.2.2.1 Theoretical Effect of Excess Air on NO_x
 - 18.2.2.2 Empirical Evidence of the Effect of Excess Air on NO_x
 - 18.2.3 Boiler Load Influence on NO_x
 - 18.2.4 Boiler/System Condition Impacts on Combustion and NO_x Formation
 - 18.2.4.1 Boiler Cleanliness
 - 18.2.4.2 Furnace Air-In Leakage Influence
 - 18.2.4.3 Fuel Oil Temperature
- 18.3 Current State-of-the-Art Concepts for Multi-Burner Boilers
 - 18.3.1 Combustion Optimization
 - 18.3.1.1 Equalization of Windbox Air Flow
 - 18.3.1.2 Fuel Flow Balancing Techniques
 - 18.3.2 Methods to Reduce NO_x Emissions
 - 18.3.2.1 NO_x Reduction by FGR Implementation
 - 18.3.2.2 Multi-Stage Combustion on Utility Boilers
 - 18.3.2.3 Water and Steam Injection for NO_x Reduction on Utility Boilers
 - 18.3.2.4 Special Features of Low NO_x Gas/Oil Combustion on Utility Boilers

18.1 BOILER-SPECIFIC BURNER REQUIREMENTS

The requirements for furnaces and burners of gas/oil-fired utilities and industrial boilers are based on long-term operational experience and comprehensive testing of different new designs and retrofits of boiler equipment. These requirements are changing with the times. [Figure 18.1](#) shows typical utility boilers. A typical single-burner industrial boiler is shown in [Figure 18.2](#).



FIGURE 18.1 Typical utility boilers.

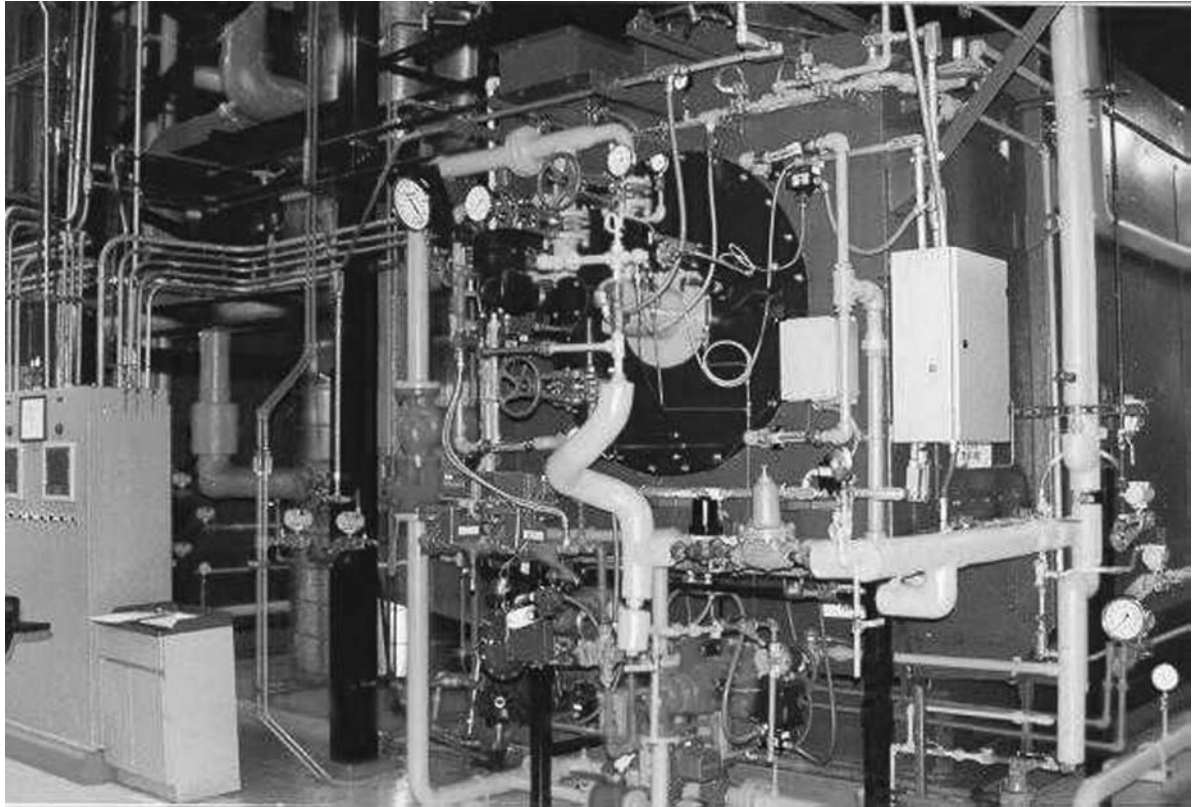


FIGURE 18.2 Typical single-burner industrial boiler.

Prior to the establishment of NO_x emission rate control requirements in the United States and other countries, performance data for furnace and burner design of utility and industrial boilers usually had to match the following common accepted requirements:

- High reliability during long-term operation
- Simplicity and reliability of gas and oil fuel ignition
- High flame stability while firing either gas or oil fuels, even at full turndown
- Provision for designed superheated and reheated steam temperatures while firing either gas or oil fuels at full turndown during long-term operation
- High thermal efficiency and low concentrations of incomplete combustion products (ICPs) while firing either gas or oil fuels using comparatively low excess air, even at full turndown
- Low combustion air system pressure drop, especially the burner register draft loss
- Simplicity of burner/windbox maintenance and adjustment
- Ease of automatic mode operation and fuel change-over between gas and oil
- Provision of restricted flame dimensions to match the dimensions of an existing or newly designed furnace
- Allowing operation with no flame impingement on either the target or side walls of the furnace that promoted reliability of all high-temperature heat exchange surfaces — especially water-wall, superheater, and reheater tubes.

To match these requirements for any boiler application, it was necessary to carefully review how a retrofit burner design should be implemented for each particular retrofit furnace. Prior to the establishment of NO_x emission rate control requirements, burner performance was typically evaluated as a function of ICP concentration levels at low excess air conditions. While firing either oil or gas fuels in preheated air, optimal low excess air burner designs provided carbon monoxide (CO), hydrogen (H₂), and unburned hydrocarbon concentrations of less than 200 ppm at excess oxygen (O₂) levels ranging between 0.2 and 0.6% at full load, as well as O₂ levels less than 1% over a 3:1 turndown range. In many European countries, such as Germany, France, Italy, and Belgium, the low excess air gas/oil burners acceptable condition was considered to be CO less than 1000 ppm and opacity less than 6%. The opacity numbers were measured using the Ringelman or Baharac method.

In some countries, the burner performance was evaluated specific to each boiler design. For example, in Russia, all industrial and relatively small utility boilers with steam flow capacities of up to 220,000 lb/hr (100,000 kg/hr) with preheated air were designed with up to six burners, each with rated heat inputs of up to 170×10^6 Btu/hr (50 MW_l). Larger utility boilers having capacities from 440,000 to 1,800,000 lb/hr (200,000 to 820,000 kg/hr) superheated steam flow were designed with up to eight burners, each with rated heat inputs of up to 400×10^6 Btu/hr (120 MW_l). All ICP concentrations in the flue gas, including both CO and H₂, were required to be less than 1000 ppm at O₂ levels less than 1%. To obtain lower ICP values, burner air velocities were increased to at least 160 ft/sec (50 m/sec), with 300 ft/sec (90 m/sec) preferred.

Until recently, there were two operational parameters used to regulate the combustion processes in boilers to achieve the required operational characteristics: (1) the variation of fuel and air input, and (2) the regulation of reheated/superheated steam temperature. The many years of operating this way resulted in significant difficulties such as:

- Reduction of reliability due to frequent failures of high temperature heat exchange surfaces
- Loss of reheated/superheated steam temperature during full turndown operation
- Overfiring of the unit

Experience has shown that controlling the combustion processes to allow maintenance of key operational parameters within a given range, including superheated and reheated steam temperatures, best solved these problems. Combustion control yielded the most efficient and reliable boiler operation, independent of load, fuel type, or other conditions.

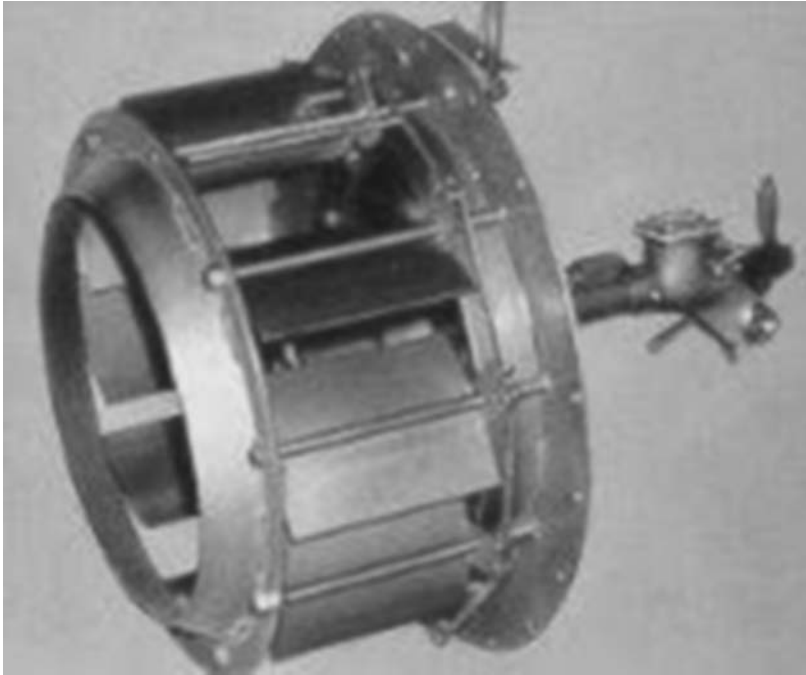


FIGURE 18.3 Swirl burner.

18.1.1 CONVENTIONAL BURNER TECHNOLOGY FOR BOILERS

Older generations of burners, such as the register, or swirl burner shown in [Figure 18.3](#), were considered very reliable and were the staple of the industry for many years. They consisted of several main parts, including a diffuser, air doors, a throat ring, and a fuel supply system. They operated on a principle of precisely controlling the swirl of the burner by adjusting the air doors, either open or closed. In an ideal situation, each burner in a multi-burner windbox should receive an equal amount of air mass flow. However, in the real world, the burner-to-burner mass flow distribution varied up to $\pm 30\%$ of the average mass flow. The typical compensation for deviations in mass flow was to close down on the air doors of the burners receiving too much air. This, in turn, affected the swirl of the burner, taking it away from the optimal single-burner performance setting.

Flame length, which depended largely on heat input, was the critical burner design parameter during this time period. Flame impingement on either the target or side walls was not allowed. [Figure 18.4](#) shows the average flame length for natural gas and #6 oil as a function of burner heat input in an experimental furnace. Other parameters included preheated air of $\sim 570^{\circ}\text{F}$ (300°C) and O_2 levels less than 1%. The oil was mechanically atomized at ~ 280 to 300 psig (19 to 20 barg) and at 248 to 266°F (120 to 130°C).

Conventional gas and gas/oil burners usually produce flames with fixed parameters. However, the combustion processes can be modified by varying the aerodynamic and chemical structure of flows fed into the furnace via burners. In this case, in addition to the typical requirements listed above, the burner design should provide the following possibilities:

- Changing the direction or reversing the fuel/air mixture swirl to cause interaction of the flame vortices, which simplifies the problem of increasing the furnace wall heat absorption rate when switching from oil to gas while retaining the same O_2 levels in the furnace
- Changing the swirl intensity, flame length, flow density, and static pressure across the furnace cross section, as well as along the length of the combustion zone

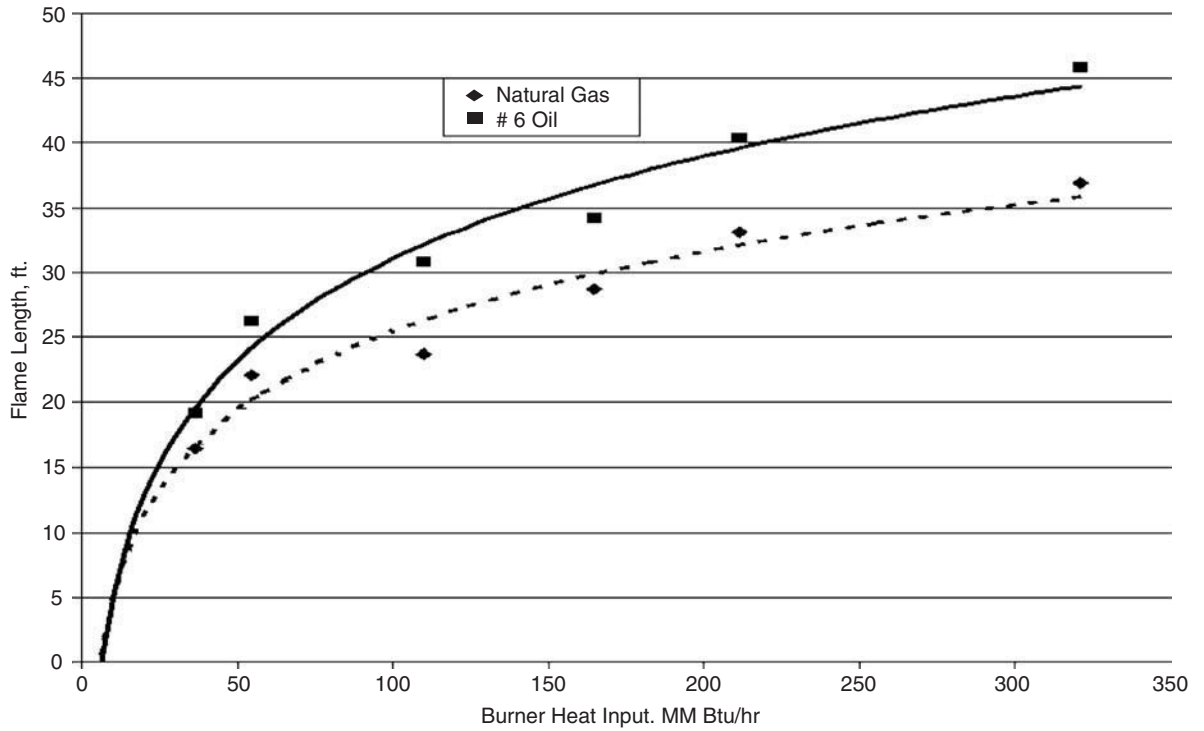


FIGURE 18.4 Average flame length as a function of burner heat input.

- Varying the flue gas recirculation (FGR) rates to control the primary firing zone to enable both stable combustion and low emission formation

Regulating not only the aerodynamic properties of the flame, but also the chemical structure and emission properties of the gas and oil combustion products, can further increase the effect of burners on combustion processes. The chemical structure and emission properties of a flame can be varied using controlled fuel input.

18.1.2 LOW-NO_x BURNER TECHNOLOGY FOR BOILERS

The objective of the modern typical boiler burner retrofit is to reduce NO_x. Two NO_x reduction techniques for boilers are combustion modification and back-end (post-treatment) clean-up. Combustion modifications include low-NO_x burners, low excess air, over-fired air, flue gas recirculation (FGR), fuel-induced recirculation, reburn, and water/steam tempering. Back-end clean-up techniques include selective catalytic reduction (SCR) and selective noncatalytic reduction (SNCR). This chapter focuses on the combustion modification techniques of low-NO_x burners, low excess air, over-fired air, flue gas recirculation, and fuel-induced recirculation.

When the U.S. and other countries mandated NO_x control, in addition to the requirements listed in the previous section, this new requirement became the dictating feature that determined the quality of burner/furnace performance. As a result, many low-NO_x burners, designed for a plethora of different boiler design and heat input capacities, firing gas and/or oil with preheated and ambient air, were developed in the U.S. and many other countries.

The situation is complicated by numerous contradictions between the operational baseline conditions for the existing boiler on the one hand, and the new NO_x requirements on the other hand. For example, all NO_x reduction combustion methods will increase flame length and redistribute the heat flux between radiant and convective heating surfaces. However, the flame length is restricted by the current furnace dimensions. Also, increasing heat flux in the superheater/reheater surfaces is not allowed because it will degrade the lifetime of these surfaces. Decreasing the total area of these surfaces increases their reliability, but reduces the boiler thermal efficiency.

Another contradiction is related to the desire to get simultaneous NO_x reduction and reduction of incomplete combustion products (ICPs). Lowering O₂ levels will decrease NO_x, but it will increase the ICPs. To reduce ICP concentrations, O₂ levels must be increased and fuel/air mixing must be improved. However, these actions will tend to increase NO_x. Solving these problems simultaneously is very difficult for both existing and new design furnaces, especially on utility boilers.

There are other complications on dual-fuel boilers. It is necessary to provide the designed reheated and superheated steam temperatures over long-term operation while firing fuels generating different flame properties over the full turndown load range. The luminescence of an oil flame is significantly higher than that of a gas flame (see Chapter 6). Assuming all other conditions are the same, furnace heat absorption is less and the furnace exit gas temperature is higher while firing gas. Higher exit gas temperatures create conditions for more intense thermal NO_x generation in all industrial boilers and most utility applications for 50 to 150 MW_e power units. On larger-capacity utility boilers, the NO_x is higher while firing gas than while firing oil. A more detailed explanation is given in Chapter 18.3.2.3. Typically, the NO_x while firing oil is higher due to fuel-bound nitrogen (N_f). Fuel-bound nitrogen usually ranges from 0.2 to 0.45% wt., but can be as high as 0.7 to 1% in #6 oil. Because the effectiveness of various NO_x reduction methods is different with gas and oil firing, it makes sense, in principle, to implement different NO_x reduction methods for each fuel. However, doing so will complicate boiler operations so much that such designs would not be acceptable to the customer. Attempts to implement NO_x reduction methods for both fuels create situations, where different methods are selected for the same boiler design installed at different power plants. The method chosen depends on many operational parameters, such as annual consumption and seasonal distribution of each fuel, local climate, annual average load, levels and frequency of load peaks, and stack height.

Today's low-NO_x burner relies on control of the combustion air in several component streams, as well as the controlled injection of fuel into the air streams at selected points for maintaining stable, attached flames with low NO_x generation. A typical venturi-style low-NO_x burner is shown in Figure 18.5 and Figure 18.6. Primary and secondary air enters the burner radially through the venturi and exits the burner axially with a primary air swirl defined by the fixed blade axial swirler. The swirler determines the size and strength of the recirculation zone. A tertiary air stream flows between the venturi base and the burner throat quarl. Tertiary air separates some of the combustion air from the main flame, effectively staging combustion and reducing NO_x. For natural gas firing, fuel can be introduced through internal or external poker or gas rings and can also be injected through a central gas pipe with multiple orifices at the furnace end. A single, conventional atomized burner (oil gun) located along the burner centerline typically supplies the oil. The oil gun may use dual fluid, mechanical, or rotary cup atomization.

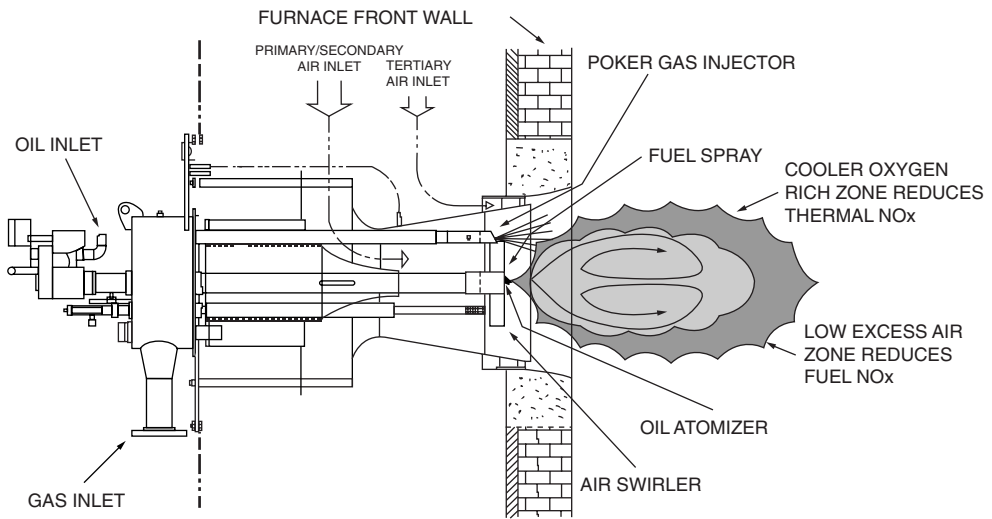


FIGURE 18.5 A typical low NO_x burner: venturi style.



FIGURE 18.6 A typical low-NO_x burner: a venturi style (second example).

18.1.3 STAGED BURNER DESIGN PHILOSOPHY

Most of today's low-NO_x burner designs implement staged combustion principles as an effective way to reduce NO_x. The staged burner should also be designed to provide the maximum degree of flexibility in achieving high burner turndown, low NO_x, and improved flame shaping capability. The design basis of a staged burner is to develop a stratified flame structure with specific sections of the flame operating fuel-rich and other sections operating fuel-lean. The burner design thus provides for the internal staging of the flame to achieve NO_x reductions while maintaining a stable flame.

Controlling combustion stoichiometry to fuel-rich conditions inhibits NO_x production, especially in the burner's flame front. Operating the flame fuel-rich also reduces the burner NO_x dependence on the burner zone heat release (BZHR) rate, which is discussed in Section 18.2.1. This is especially important in applications where a very high BZHR near full load can result in an exponential increase in NO_x.

In addition to controlling NO_x formation, operating under fuel-rich conditions will aid in the production of combustion intermediates that can result in the destruction of previously formed NO_x. In a reducing environment, NO can act as an oxidizer to react with these combustion intermediates, resulting in the reduction of NO to N₂. Therefore, NO, necessarily formed to satisfy the requirements of establishing a strong flame front, can be scavenged by the process and reduced to N₂.

To achieve complete fuel burnout at minimum O₂, the burner design must provide direct interaction of fuel-lean zones with the center fuel-rich sections. This ensures that the "rich" products of combustion from the center flame pass through the oxidizing zone for complete fuel burnout. The burner design allows control of the stoichiometry of the oxidizing zone to range from being pure air to having varying degrees of excess oxygen. This controls NO_x formation by causing the fuel burnout to occur in the form of a premixed flame rather than a diffusion flame. The operational flexibility is provided in the burner design to control stoichiometry to achieve minimum NO_x.

Flame stability should also be a design focus for a staged burner. The stability criterion is to maintain a minimum turndown capability on a gas firing ratio of 8:1 over a broad range of excess O₂. To achieve this objective, it is necessary to carefully select the burner throat velocity and the velocity profile.

The burner flame front should be a fuel-rich premixed flame designed to increase flame speed and, in turn, flame stability. Combustion stoichiometry, approaching a perfect premixed flame, is established at the burner flame front. This condition broadens the flammability range of the fuel and ensures the maintenance of a flammable mixture over a broad range of burner throat velocities and fuel injection rates.

Controlling air distribution within the burner throat improves flame-shaping capability. Provisions are made in the burner design to allow the burner to operate as a low excess air burner as well as a low-NO_x burner with an extended flame envelope.

18.1.4 DESIGN FEATURES OF LOW-NO_x BURNERS

Some of the standard design features of low NO_x burners include:

- Flame stability at low excess air rates for reliable, energy-efficient boiler operation.
- High turndown ratios for wide-range boiler operation.
- Well-distributed air flow to control the flame envelope and provide even heat flux.
- Known flame length and diameter to suit furnace firing lane without impinging on boiler tubes or furnace walls.
- Elimination of combustion-induced vibrations of the boiler, due to the aerodynamics of the register design and turbine blade diffuser.

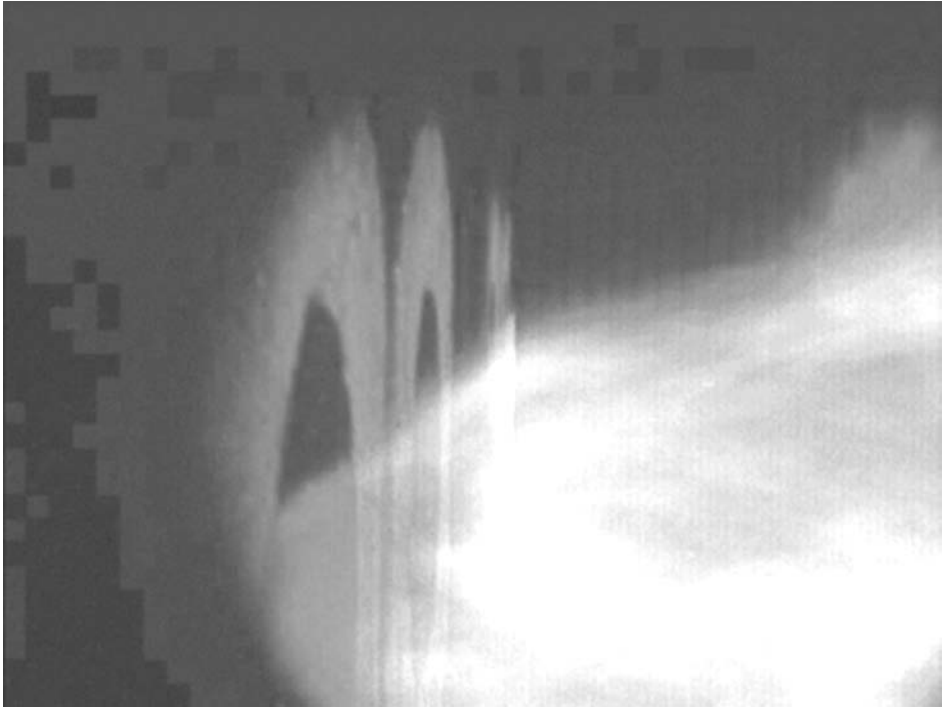


FIGURE 18.7 A strong flame front established within a maximum of 0.5 diffuser diameters off the face of the diffuser.

- A strong flame front established within a maximum of 0.5 diffuser diameters of the face of the diffuser, as depicted in [Figure 18.7](#). The flame front should not move during changes in the firing rate, thus providing a stable flame for scanning, resulting in reliable operation.
- For gaseous fuel firing, a multiple-poker gas burner assembly with “poker shoes” (gas nozzles) oriented to provide internal fuel staging.

18.1.5 EFFECTS OF BURNER RETROFITS ON BOILER PERFORMANCE

Low-NO_x burners have different flame characteristics from their predecessors, the low excess air burners. Therefore, the probability exists that the differences will affect boiler performance. Performance changes would only occur by an alteration of the heat absorption pattern in the furnace, thus affecting the amount of heat going to the boiler backpass. The overall furnace heat absorption could either increase or decrease due to factors such as flame distance to walls, flame temperatures, flame emissivity, and characteristics of ash deposits on furnace walls. The impact on boiler performance will vary by unit and by fuel. In some cases, there will be no impact; but, in most cases, there will be either a positive or negative impact experienced. Historically, however, there has been no net effect on boiler performance that would be considered extreme. Atomizer tip design can drastically impact boiler performance, but total boiler performance is always a balancing act between key variables such as NO_x and water wall temperatures.

To assess the impact on boiler performance, certain information is typically monitored during the testing of low-NO_x burners. Important data includes superheated and reheated steam temperatures, superheater and reheater tube surface temperatures, and any operational parameters that affect or control steam temperatures. The boiler performance variation resulting from a change in overall O₂ levels is not considered in this analysis. The actual impacts on boiler efficiencies are relatively small and there are many complicating factors, including furnace and heat recovery area cleanliness, fuel composition, sootblower availability, operational variability, and others.

18.2 BOILER DESIGN IMPACTS ON NO_x EMISSIONS CORRELATIONS

The two major mechanisms for the formation of NO_x are: (1) NO_x formed by the oxidation of N_f (fuel NO_x) and (2) the thermal fixation of atmospheric nitrogen (thermal NO_x). Separate NO_x correlations have been developed for each. These correlations can be combined to predict the total NO_x emissions for a selected burner design based on the fuel nitrogen content and boiler design.

The conversion of N_f to NO_x depends on oxygen availability and N_f content. Thus, for a given burner system at constant excess air, the key variable controlling fuel NO_x formation is N_f content. Previous studies have shown that the N_f conversion efficiency is inversely proportional to the nitrogen content of the fuel. High conversion efficiencies are observed with low N_f, and low efficiencies are seen with high N_f.

18.2.1 BOILER DESIGN

Based on the strong dependency of thermal NO_x on flame zone temperature, thermal NO_x formation for wall-fired boilers has been correlated with the ratio of heat input to furnace size and the number of firing walls. For this correlation, the ratio of heat input to the furnace burner zone area is defined as the burner zone heat release (BZHR) rate. The BZHR represents the boiler heat release rate divided by the water-cooled surface area in the burner zone (10^6 Btu/hr-ft²), and is a measure of the “bulk furnace temperature.” The NO_x created within this zone depends on this bulk temperature by an exponential relationship, as discussed in previous chapters. The burner zone is defined as the six-sided surface bounded by the furnace walls and imaginary horizontal planes located one burner row spacing above the top row and below the bottom row of burners. The area of any division walls within this volume is also included in the calculation of the BZHR. A correction is made for re-radiation from any refractory on the floor, walls, or the burner throats. An example of the effects of boiler design on NO_x is shown in [Figure 18.8](#), where the same heat input is placed in two drastically different-sized boilers.

The correlation between thermal NO_x and BZHR rate has been developed using an extensive database of gas- and oil-fired utility boilers. [Figure 18.9](#) shows the NO_x of various boilers included in the database on oil and gas, respectively. NO_x of industrial boilers with comparable degrees of NO_x control were found to be consistent with the BZHR rate correlations.

The correlations between N_f conversion and thermal NO_x can be used to extrapolate burner NO_x from one boiler to another. The increase in NO_x observed with fuel oil compared to natural gas, which contains no nitrogen, is used to estimate fuel NO_x for the selected burner. N_f conversion is then calculated based on the nitrogen content. The correlation of N_f conversion can subsequently be used to project fuel NO_x for fuels containing differing amounts of nitrogen. Thermal NO_x is determined from NO_x with natural gas. The correlation with BZHR is used to project the measured thermal NO_x for the selected burner from one boiler to another. Total projected NO_x emissions for the burner can then be determined by adding the fuel NO_x and thermal NO_x contributions for the fuel and boiler of interest. The amount of air preheat can also have a dramatic effect on NO_x, CO, and particulate emission rates, as well as on flame stability.

18.2.2 EXCESS AIR

18.2.2.1 Theoretical Effect of Excess Air on NO_x

It is well known that thermal NO_x formation primarily depends on the flame temperature, excess air in the flame, and residence time. However, the flame temperature also depends on excess air. Demonstrating the calculated data for natural gas combustion under regular boiler conditions, with

FURNACE SIZE EFFECTS ON NO_x EMISSION RATES

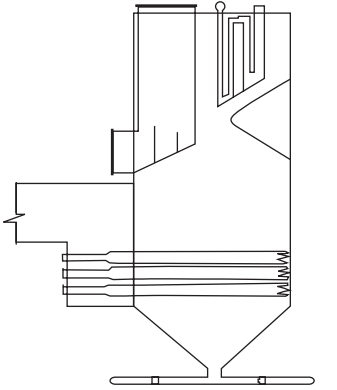
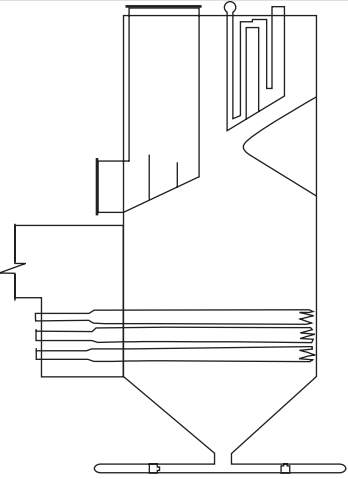
UNIT DESIGN PARAMETER	HIGH HEAT RELEASE RATE	LOW/MEDIUM HEAT RELEASE RATE
FURNACE ELEVATION (SAME AS SIZE UNIT)		
BURNER ZONE VOLUME	$(3 \times \text{BURNER SPACING}) \times \text{WIDTH} \times \text{DEPTH}$	$1.66 \times (\text{HIGH HRR VOLUME})$
BURNER ZONE HEAT RELEASE RATE	88,000 BTU/Hr/ft ³	53,000 BTU/Hr/ft ³
NO _x @ MCR GAS FIRING*		
LOW EXCESS AIR BURNER	0.66 Lb/Million BTU	0.22 Lb/Million BTU
LOW NO _x BURNER	0.39 Lb/Million BTU	0.16 Lb/Million BTU

FIGURE 18.8 The effects of boiler design on NO_x.

an excess air factor α value close to unity, increased excess air causes NO_x to rise considerably; then, as excess air is further increased, the increase in NO_x slows down, reaches a maximum, and then NO_x is reduced as excess air is further increased.

According to some experimental studies, no maximum is attained and the NO_x = f(α) dependence approaches the stabilized section of the exponential curve. A difference between the mentioned two contradicting results brings different approaches to optimized low-NO_x combustion evaluations.

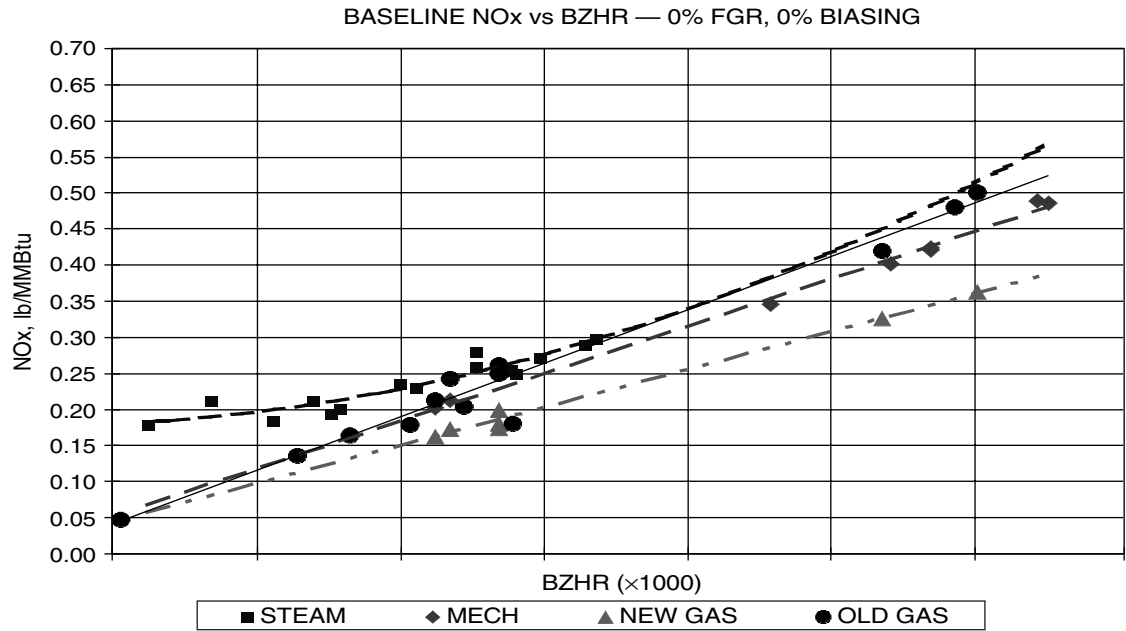


FIGURE 18.9 The NO_x of various boilers included in the database on oil and gas.

That is why it is important to discuss the existence of the NO_x maximum and to consider it in some details. For simplicity, we can consider a natural gas (containing no bound nitrogen) combustion process, as a result of which NO_x is formed only from nitrogen in the combustion air. A deficiency of oxidant, NO_x depends more on α than it does on temperature; and when $\alpha > 1$ (mostly when $\alpha > 1.2$), when the rate of combustion reactions increases, the effect of temperature proves to be the dominant one. Therefore, despite the fact that the theoretical combustion temperature in the region of $\alpha > 1$ systematically falls with increased α , the NO_x increases as long as the thermal NO_x formation is not made more difficult due to a considerable decrease in the temperature level. In this case, there is also a decrease in the NO_x in the flue gas volume due to dilution by the excess air. When firing a fuel oil that contains N_f, it is unlikely that the nature of the above-considered curve NO_x vs. O₂ will change, but in all probability the downward branch of the curve will be flatter.

When comparing the well-known empirical dependency of the ICP component concentrations on α with the empirical NO_x data as a function of α , confirmed with the theoretically calculated dependencies on α , it was found that the excess air factor α value at which a furnace's ICP losses virtually disappear, almost coincides with the values of α corresponding to the NO_x maximum. It follows that the NO_x dependence on excess air has the form of an extreme function with a maximum NO_x value corresponding to that α value at which virtually complete fuel combustion is attained under the given conditions. Hence, if NO_x and α are determined by reliable and adequately accurate methods, the absence of an experimentally established maximum on the test curve NO_x vs. O₂ (or α) leads to an assumption that the fuel is not completely burned, thus indicating the need not only to improve the combustion process, but also to check the validity of the methods used to measure ICP and NO_x in the given α range.

18.2.2.2 Empirical Evidence of the Effect of Excess Air on NO_x

Detailed empirical data sets were obtained under identical operational conditions at approximately full (~94%) load while firing natural gas and #6 oil (containing 0.22 to 0.32% N_f) with preheated air on the two neighboring 165 MW_e utility boilers of the TGM-94 model (~1,100,000 lb/hr or 500,000 kg/hr superheated steam flow), installed at the same power plant. The furnaces were balanced draft and had air-in leakage of 8 to 10%. The two boilers were almost identical except for one difference: the first boiler was equipped with 21 burners, rated at $\sim 100 \times 10^6$ Btu/hr (30 MW_t) heat input each, having a single swirled airflow channel, and the second boiler was equipped with 9 burners, rated at $\sim 230 \times 10^6$ Btu/hr (67 MW_t) heat input each, having two airflow channels, one of which is a swirled portion consisting of ~15% of the total air flow. On both boilers, the burners were installed in three rows on the front wall (3 × 7 and 3 × 3, respectively). The boilers were equipped with an FGR system designed to supply up to 14% FGR flow (isolated from the air flow), supplied directly to the furnace through slots located on the target wall, opposite the lower burner row. The test data while firing either or both fuels, both with and without FGR implementation, shown in [Figure 18.10](#) and [Figure 18.11](#), confirm well-known dependencies of NO_x concentrations on O₂.

Differences can be seen between the maximum NO_x numbers and, accordingly, between the shapes of the curves obtained from these two boilers. These discrepancies are associated with distinctions in the combustion processes related to the differences between the mentioned burner designs, heat inputs, and numbers of burners. The measured flame temperatures while firing gas under full load and all other conditions being equal show that, on the boiler equipped with nine burners, the maximum flame temperature is ~160°F (70°C) higher, resulting in a significant NO_x difference of 100 to 120 ppm (NO_x is ~20 to 24% higher than for the boiler equipped with nine burners). The increased temperature has resulted in a stronger dependency of NO_x on O₂ on the boiler equipped with nine burners, both with and without FGR, as demonstrated in [Figure 18.11](#).

The above data, as well as other test data obtained on 150- to 800-MW_e utility boilers, under similar operational conditions, illustrate a significantly lower NO_x level on #6 oil (even while containing N_f of up to ~0.7%) in comparison with NO_x numbers on gas. An explanation of this

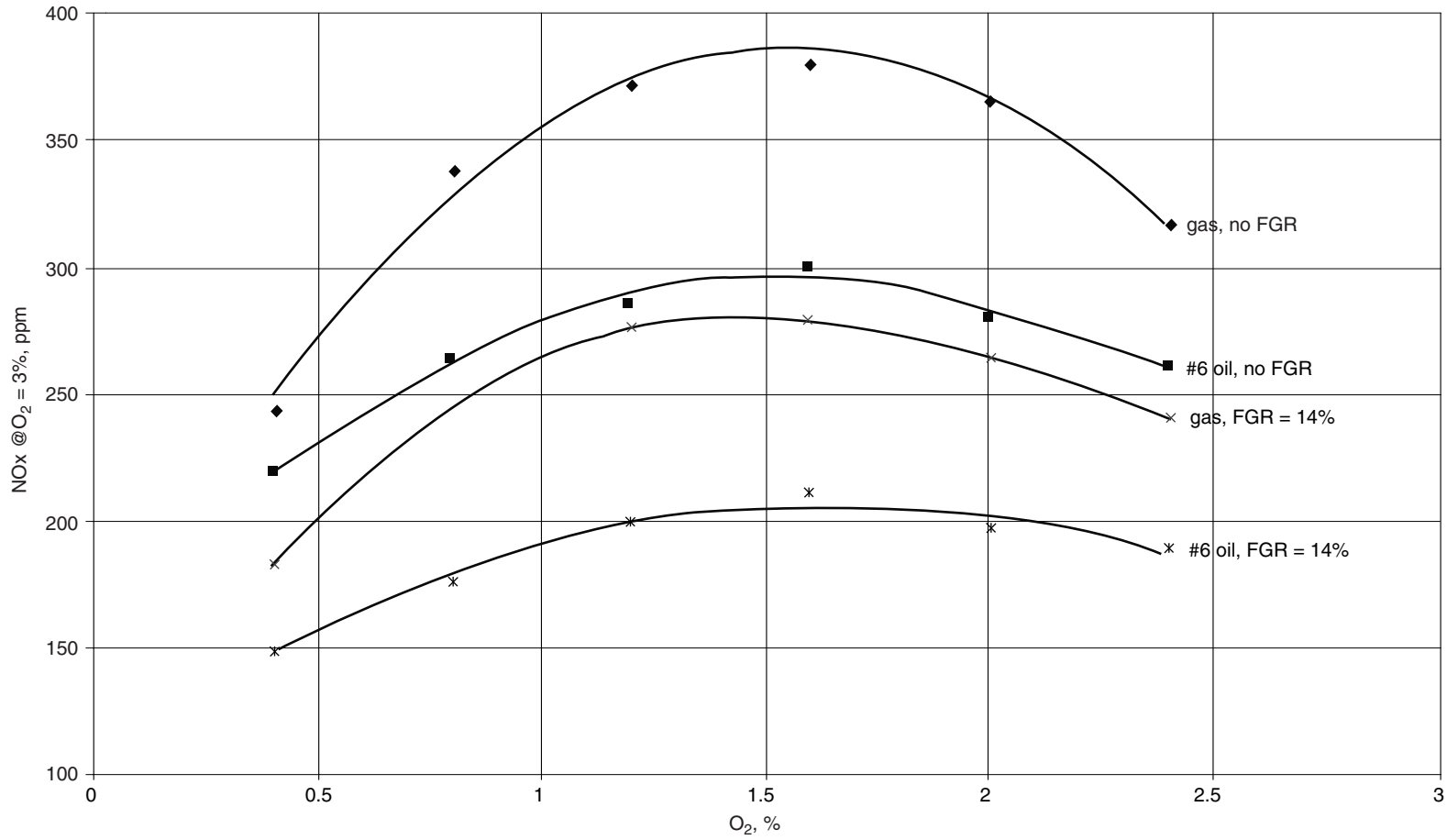


FIGURE 18.10 NOx dependence on excess O₂-21 burner boiler.

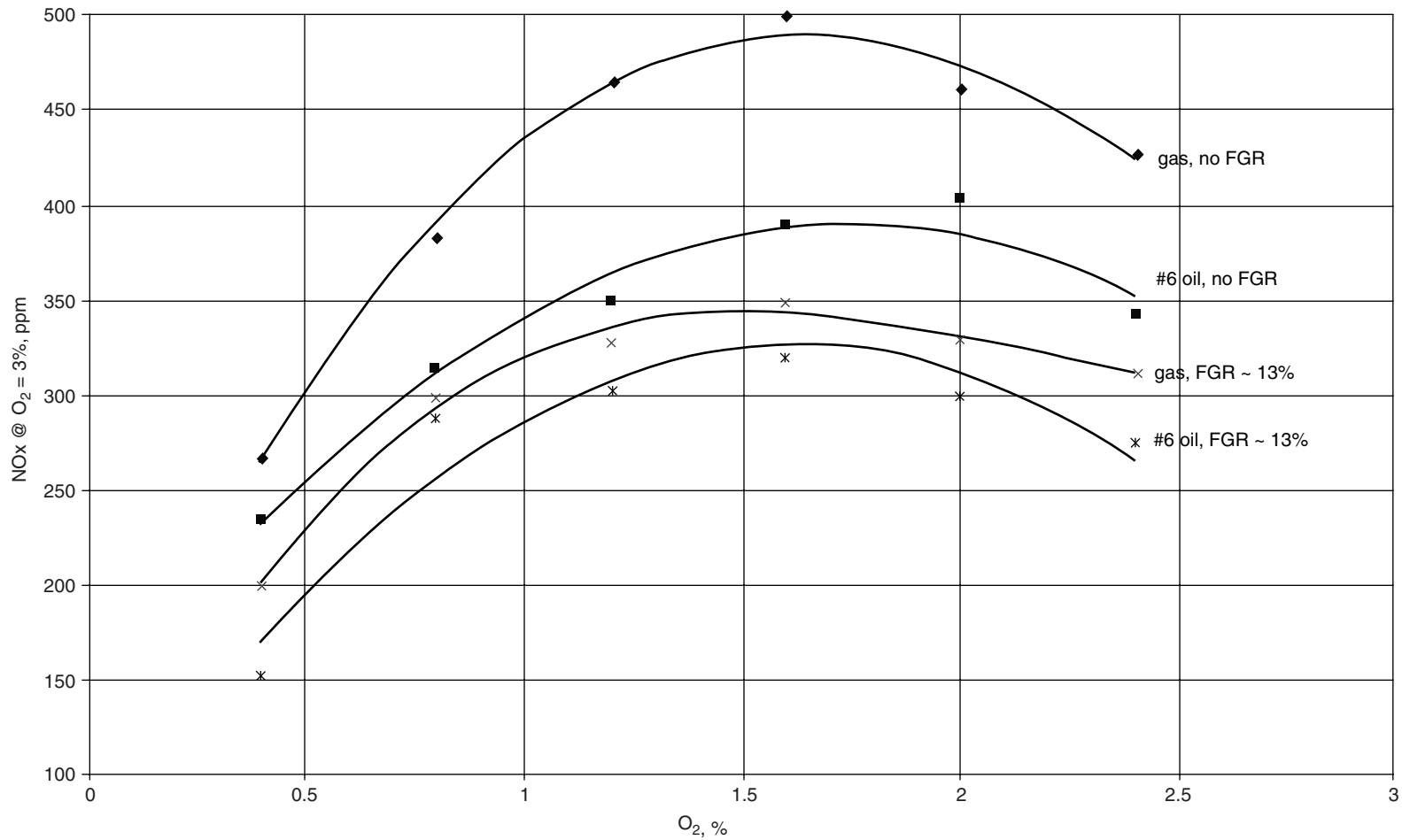


FIGURE 18.11 NOx dependence on excess O₂-9 burner boiler.

fact, contradicting the empirical data obtained on industrial and comparatively smaller utility boilers (where NO_x numbers are higher while firing oil), is presented in the Chapter 17.3.2.3.

18.2.3 BOILER LOAD INFLUENCE ON NO_x

The relationship between NO_x and load was investigated on many utility boilers over their full load ranges, while firing either or both fuels. A detailed investigation was performed on the two TGM-94 boilers described above (see Chapter 17.2.2). The test results obtained at ~94, 75, 50, and ~30% loads, with and without FGR, are shown in Figure 18.12 (gas) and Figure 18.13 (#6 oil). With O₂ levels between 1.2 and 1.6%, over the entire load range CO concentrations were in the 50- to 150-ppm range while firing gas. When firing #6 oil on both boilers, over the entire load range, under the same O₂, the CO and opacity did not exceed 100 ppm and 10%, respectively.

Figure 18.14 shows the data of the combined (load and FGR) influence on NO_x on a 200-MW_e boiler of the TGME-206 model, having no furnace air in-leakage, equipped with 12 low-NO_x venturi-style burners installed in two rows on the rear wall. The boiler was tested at loads ranging from 100 to 53% while firing natural gas at comparatively low O₂ levels (0.8 to 1%), and with 6 to 7% and 12 to 14% FGR flows. The FGR was mixed with the combustion air upstream of the windbox. Under all the above conditions, CO concentrations were less than 20 ppm.

Confirmation of these empirical dependencies on many utility boilers, equipped with various number, design, and arrangement of burners, while firing gas and oil with preheated air (500 to 700°F or 260 to 370°C), is shown in Figure 18.12 to Figure 18.14. All available data obtained on 150- to 800-MW_e boilers, firing natural gas in the load range of 100 to 30%, have been generalized in Figure 18.15 as a dependence of relative NO_x (defined as a ratio between NO_x numbers at current loads and the NO_x number at full load) on relative load. It is seen that relative NO_x is a power function of relative load in the ~1.25 degree. While firing natural gas, significant changes in the O₂ range, FGR flow level, preheated air and FGR temperatures, and other operational conditions provide comparatively small derivations from the mentioned average degree number.

With firing #6 oil under the same other operational conditions on utility boilers, in general, the power function degree number depends on N_f concentration in the oil. The higher the N_f, the lower the degree number. Corresponding test data, obtained at 17 boilers of 150 (three), 165 (eight), 210 (one), and 300 (five) MW_e utility boilers at full load with an O₂ range of 0.6 to 1.2%, are shown in Figure 18.16. With the exception of one 150-MW_e boiler, all boilers were equipped with FGR systems of various designs. Increasing FGR flow from 0 to 14% (on the 165- and 210-MW_e boilers) and to 18% (on the other boilers) influences deviations from the average test data curve but does not change the established dependence.

Similar dependencies have also been established on industrial single-burner and multi-burner boilers, while firing either gas and/or oil, with ambient and preheated air, and without staged combustion. With ambient air, the shapes of the experimental curves, established on the 22,000- to 385,000-lb/hr (10,000- to 175,000-kg/hr) steam flow boilers, with firing both gas and #6 oil (0.22 to 0.49% N_f) in the 100 to 25% load range, are similar to a linear dependence, as indicated in Figure 18.17. On preheated air (300 to 500°F or 150 to 260°C), all curves are power functions with the ~1.25 and (1.1 to 1.2) degree numbers on gas and #6 oil, respectively, as in Figure 18.18.

A clear conclusion was made based on the above empirical test data: as load decreases (as the flame temperature is reduced due to BZHR), the NO_x level also decreases. A reduction in the original NO_x level (full load) limits the potential opportunity to achieve a required NO_x reduction at lower loads, resulting in a reduction in the effectiveness of all NO_x reduction methods. This conclusion was made based on evaluations of data obtained on utility boilers, while using all known NO_x reduction methods. For example, on the TGME-206 boiler with 12 venturi burners, ~14% FGR implementation provides ~70% and ~56% NO_x reduction at 100% and 80% loads, respectively. For industrial boilers with ambient air, this effectiveness reduction is a little more pronounced due to the significantly lower flame temperature level in the industrial boiler furnaces.

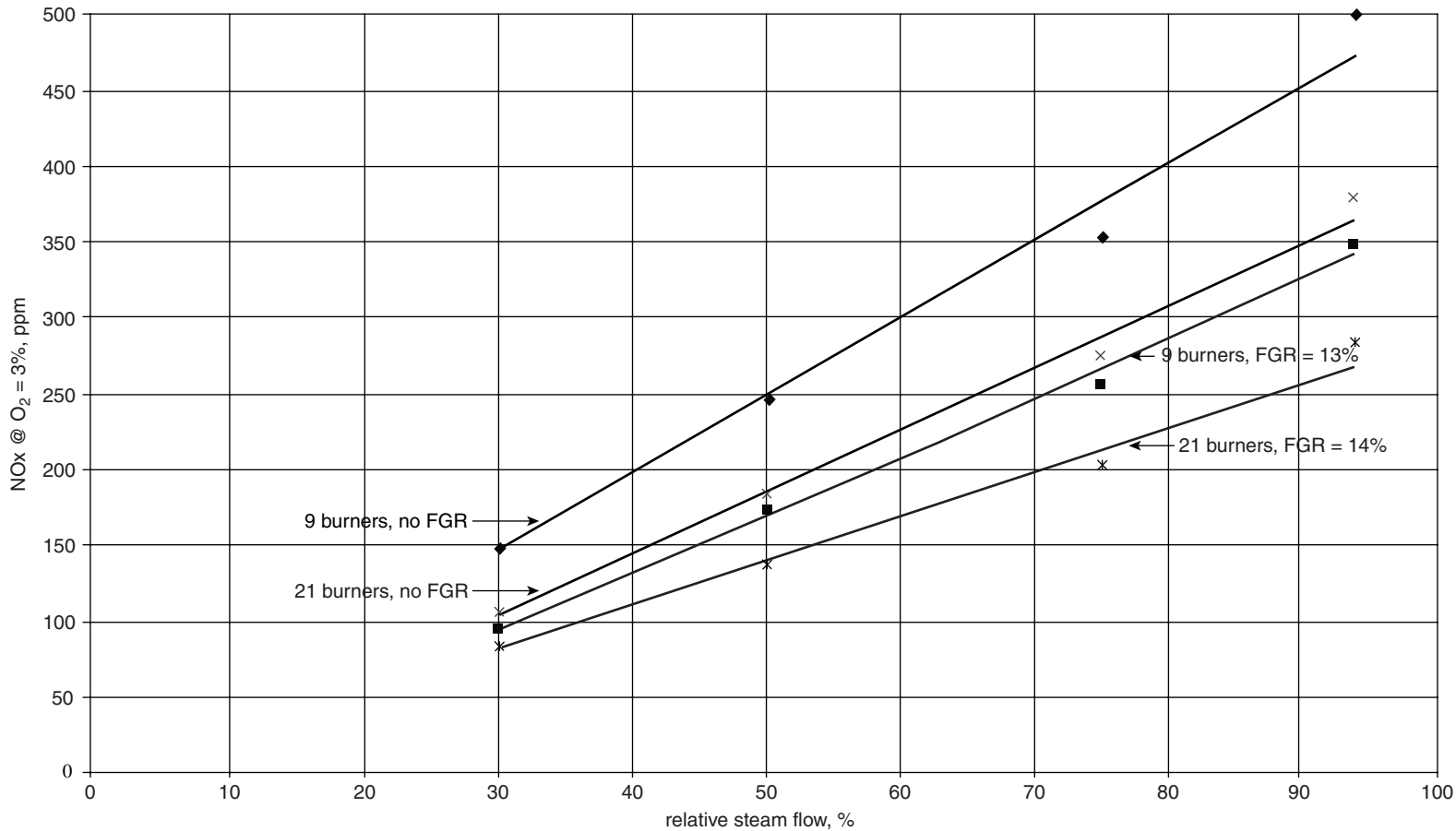


FIGURE 18.12 Test results obtained at ~94, 75, 50, and 30% loads, with and without FGR (gas).

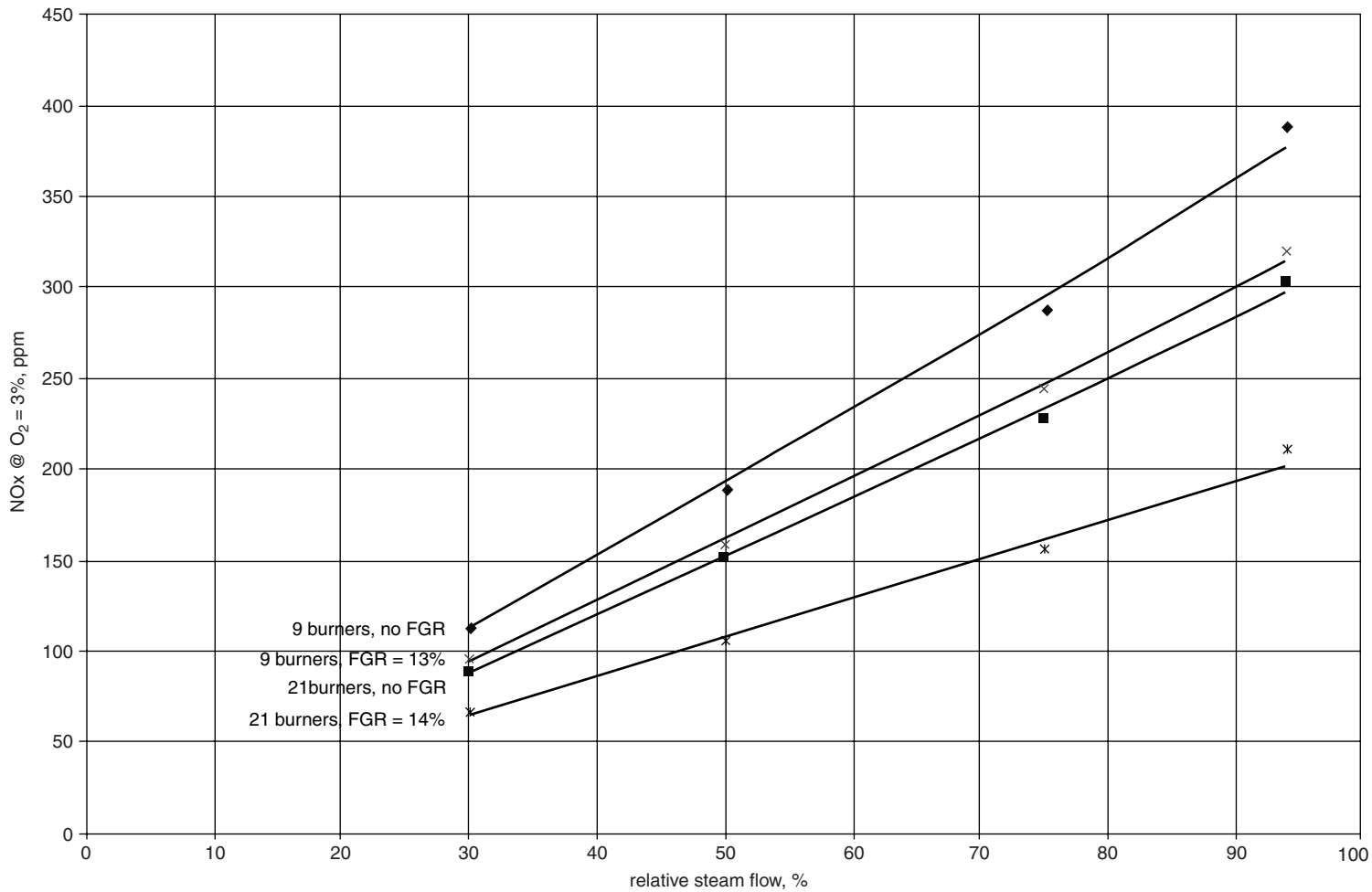


FIGURE 18.13 Test results obtained at ~94, 75, 50, and 30% loads, with and without FGR (#6 oil).

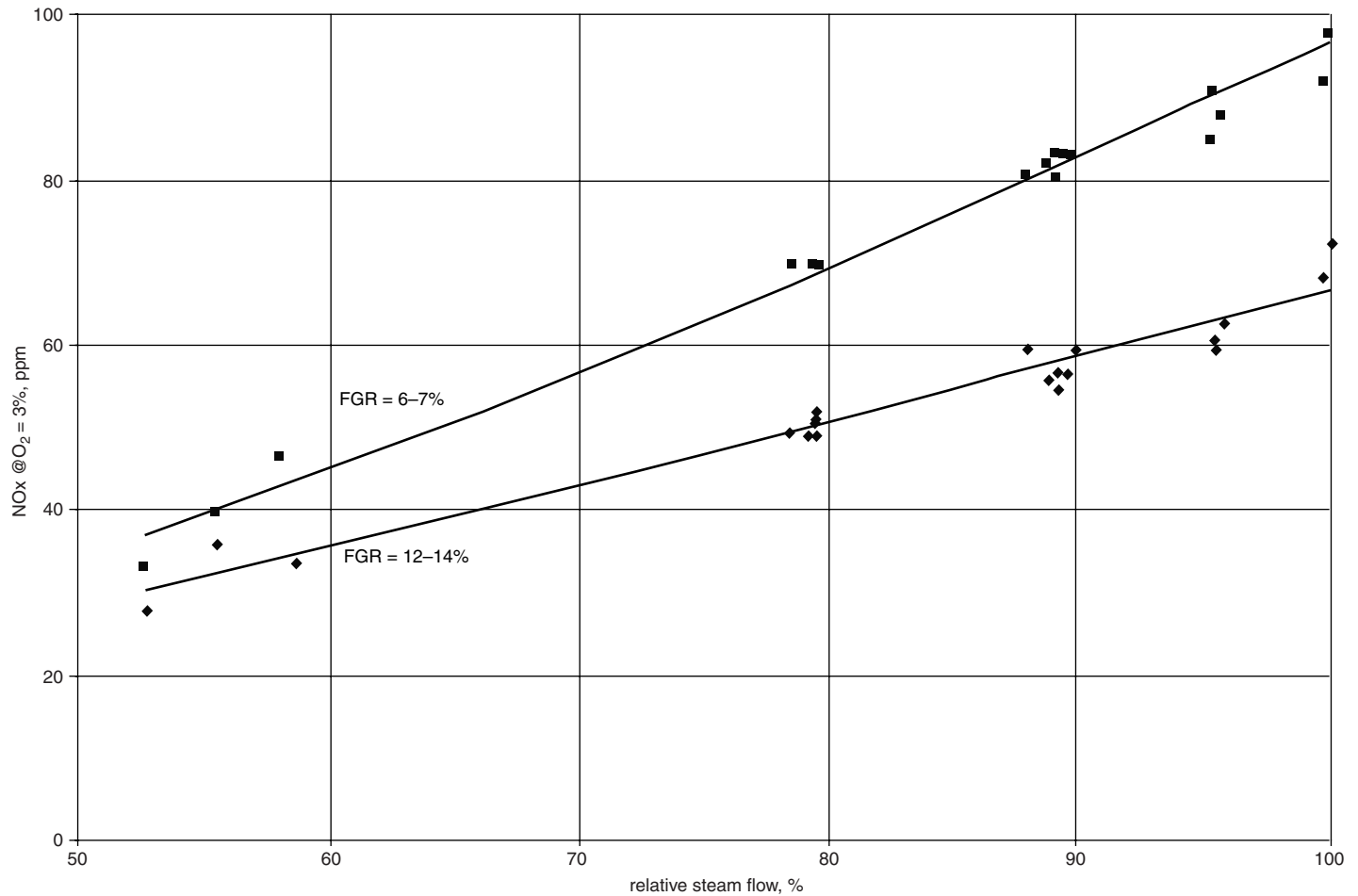


FIGURE 18.14 Combined (load and FGR) influence on NO_x on a 200-MW_e boiler of the TGME-206 model, having no furnace air-in leakage, equipped with 12 low-NO_x venturi-style burners installed in two rows on the rear wall.

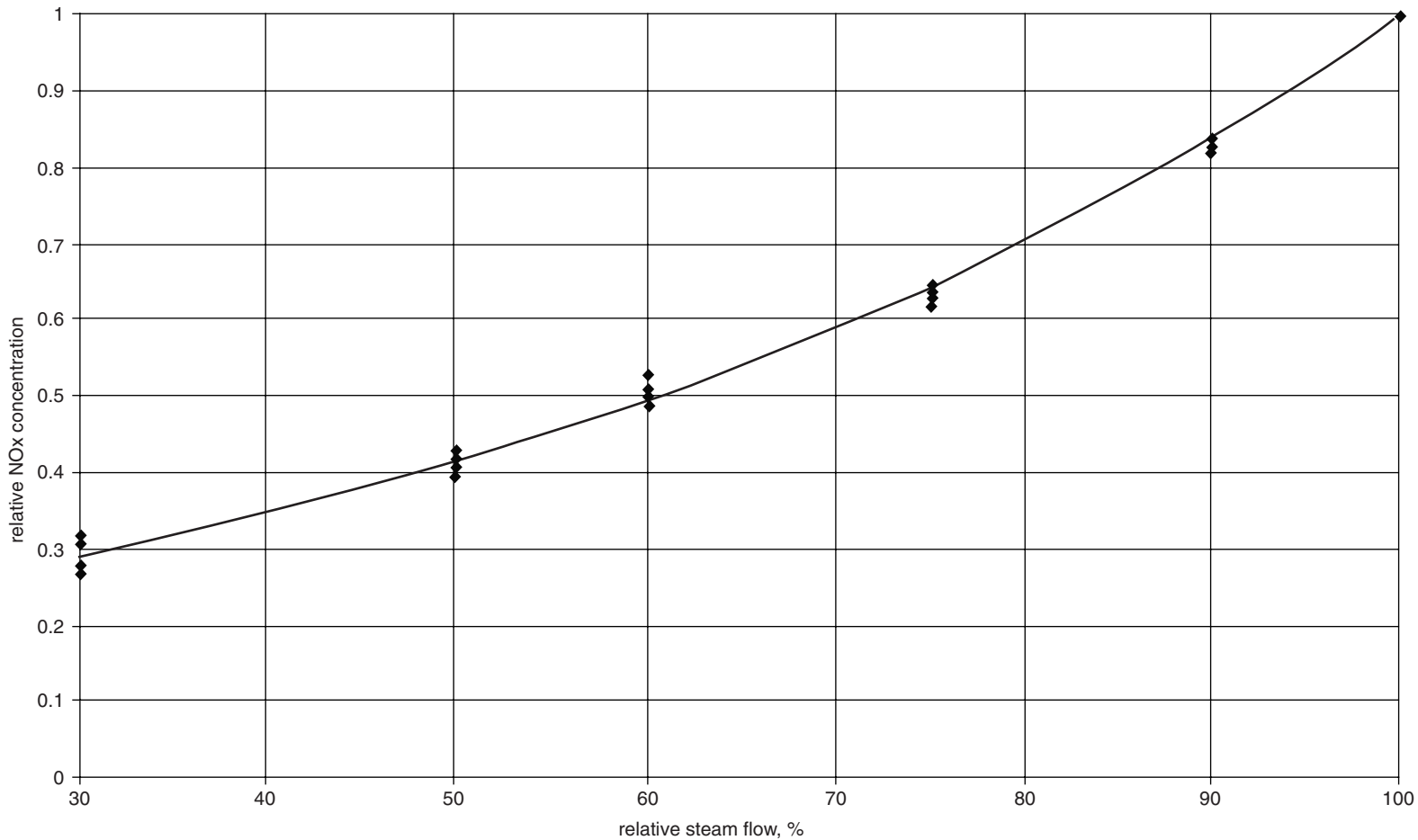


FIGURE 18.15 All available data obtained on 150- to 800-MW_e boilers, firing natural gas in the load range of 100 to 30%.

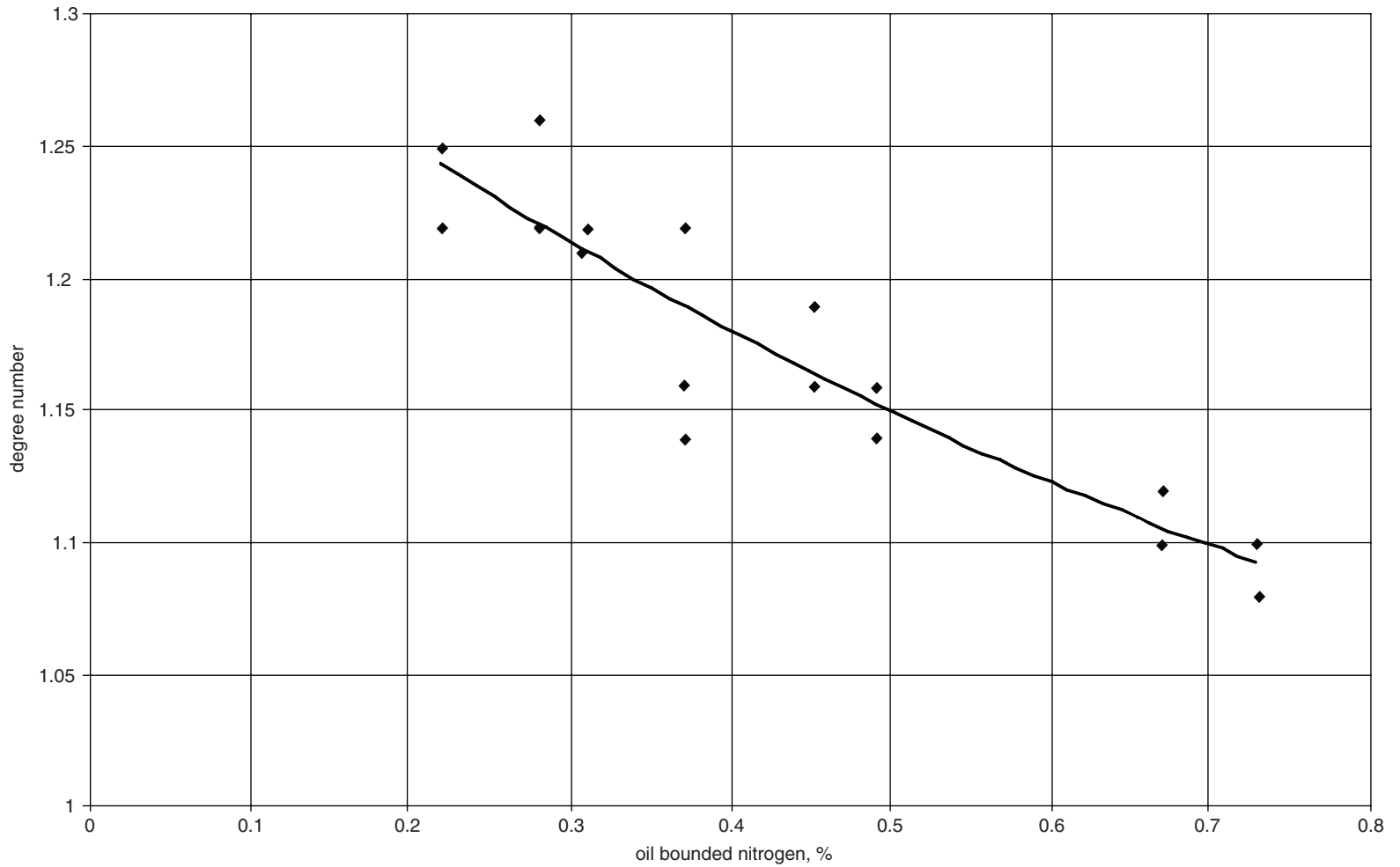


FIGURE 18.16 Seventeen boilers of 150- (three), 165- (eight), 210- (one), and 300- (five) MW_e utility boilers at full load with an O₂ range of 0.6 to 1.2%.

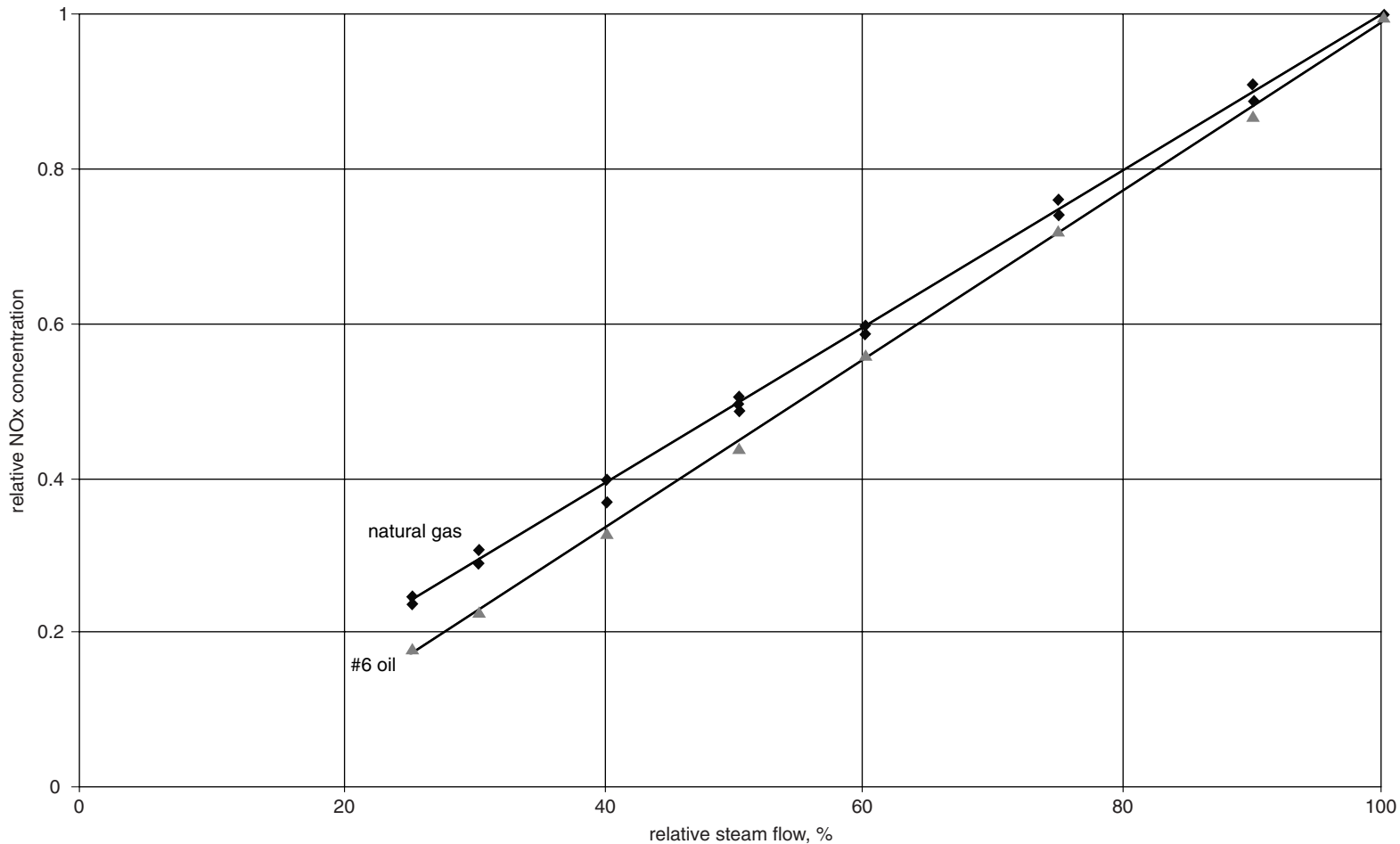


FIGURE 18.17 With ambient air, the shapes of the experimental curves, established on the 22–385,000 lb/hr (175,000 kg/hr) steam flow boilers firing both gas and #6 oil (0.22 to 0.49% N_p) in the 100 to 25% load range, are similar to a linear dependence.

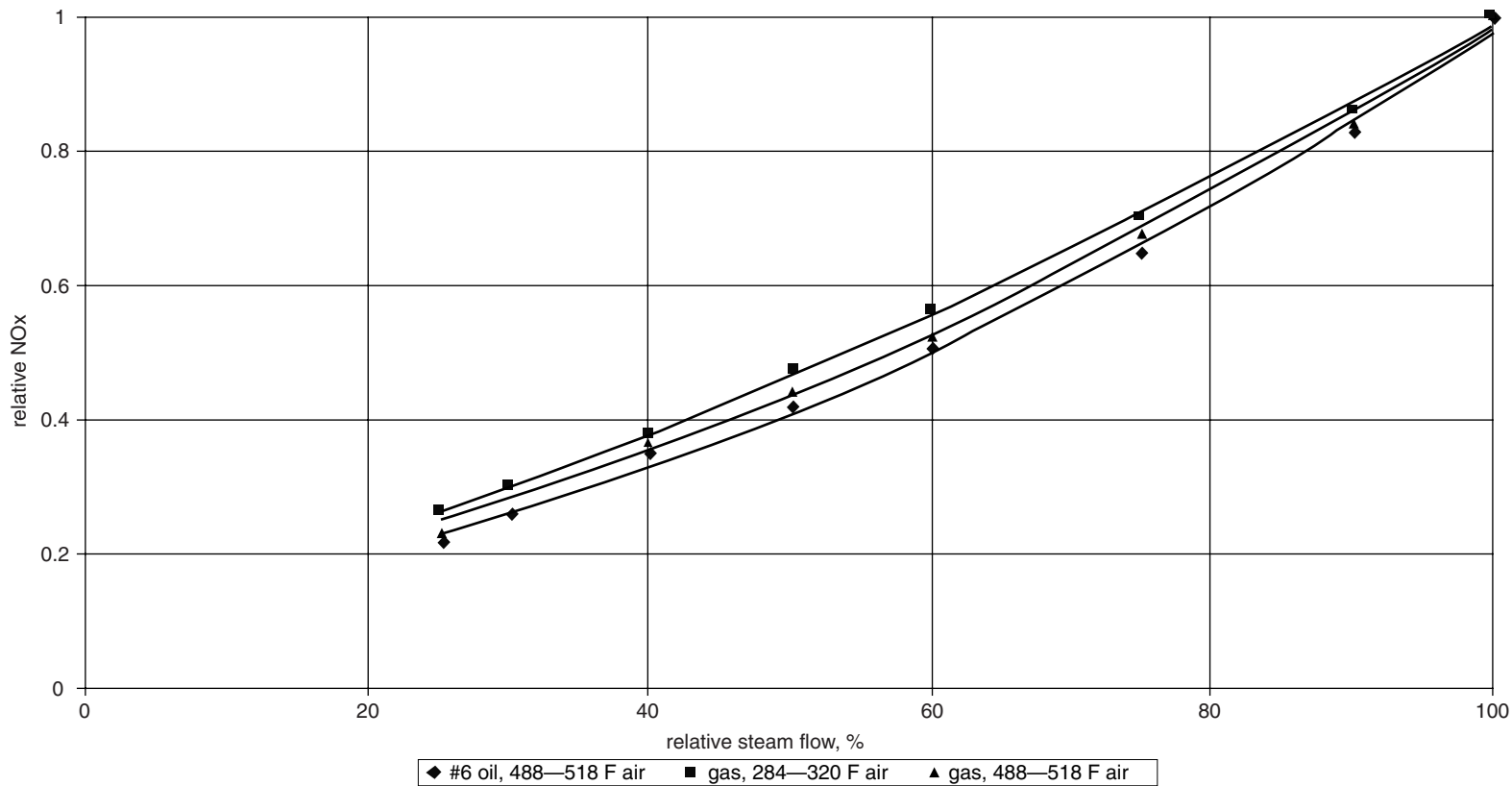


FIGURE 18.18 On preheated air (300 to 500°F), all curves are power functions with the ~ 1.25 and (1.1 to 1.2) degree numbers on gas and #6 oil, respectively.

18.2.4 BOILER/SYSTEM CONDITION IMPACTS ON COMBUSTION AND NO_x FORMATION

A new philosophy for NO_x reduction is emerging among multi-burner power boiler users. This philosophy sees the entire boiler as a combustion system where NO_x reduction can be accomplished and maintained in a three-step process:

1. Installation of new low-NO_x burners delivers the required NO_x reduction.
2. Improved maintenance protocols sustain the achieved NO_x reductions.
3. Optimized operational protocols achieve the best overall combustion and boiler performance.

Boiler design parameters such as air preheater (APH) design, superheater (SH) configuration, and the amount of refractory in the furnace also have major impacts on the amount of NO_x reduction achievable on a given boiler.

The cornerstone of this NO_x reduction philosophy is still, as it has been for years, the low-NO_x burner. Proven low-NO_x burners, along with a physical windbox model, provide the required NO_x reduction, but sustaining this NO_x reduction requires the improved maintenance and optimized operational protocols. With a balanced airflow distribution, balanced fuel flow distribution, and a set of proven low-NO_x burners, the combustion system's foundation is established for the desired NO_x reduction.

However, the NO_x reduction provided by the low-NO_x burner is only the first part of the process. The boiler must be properly maintained to sustain the NO_x reduction. Proper maintenance must address boiler cleanliness, the percentage of air in-leakage, and oil heater maintenance. The maintenance protocols affecting boiler cleanliness include proper soot-blowing practices on a daily basis and boiler washes during outages.

18.2.4.1 Boiler Cleanliness

The impact of boiler cleanliness on NO_x became very apparent when the results of NO_x testing, while firing residual fuel oil on the same unit, showed a dramatic 23% increase in NO_x as compared to results of NO_x testing performed just months earlier, with the same atomizer and at the same unit conditions. A visual inspection of the boiler indicated that it was well seasoned or dirty. A waterwall wash was performed during the next available outage, about a week later. After the outage, another NO_x test was performed; the results of this testing revealed a 25% decrease in NO_x as compared to the pre-outage results. The effect of furnace cleanliness on NO_x is shown in [Figure 18.19](#).

The second indication of the impact of boiler cleanliness on NO_x came when a sister unit started up after the low-NO_x burner retrofit. The start-up testing measured residual fuel oil (RFO) NO_x higher than any that had been previously measured with identical low-NO_x burners and atomizers at the first unit.

As the data sets from the units were analyzed, it became apparent that the relative level of furnace cleanliness could be correlated to the flue gas temperature entering the air preheater (APHGIT). It was also found that the second unit had extremely high APHGIT. The unit's soot-blowing practices were analyzed to determine the level of heat recovery area cleanliness, and it was found that many of the soot blowers were out of service. Upon minimizing the number of soot blowers out of service, the RFO NO_x on the sister unit fell to a level equal to those measured with identical low-NO_x burners and atomizers at the first unit. [Figure 18.20](#) exemplifies the impact of heat recovery area cleanliness on NO_x.

18.2.4.2 Furnace Air-In Leakage Influence

The impact of air-in leakage on burner performance is a phenomenon of balanced-draft boilers. There is a significant difference between NO_x generation conditions existing in forced-draft (pressurized)

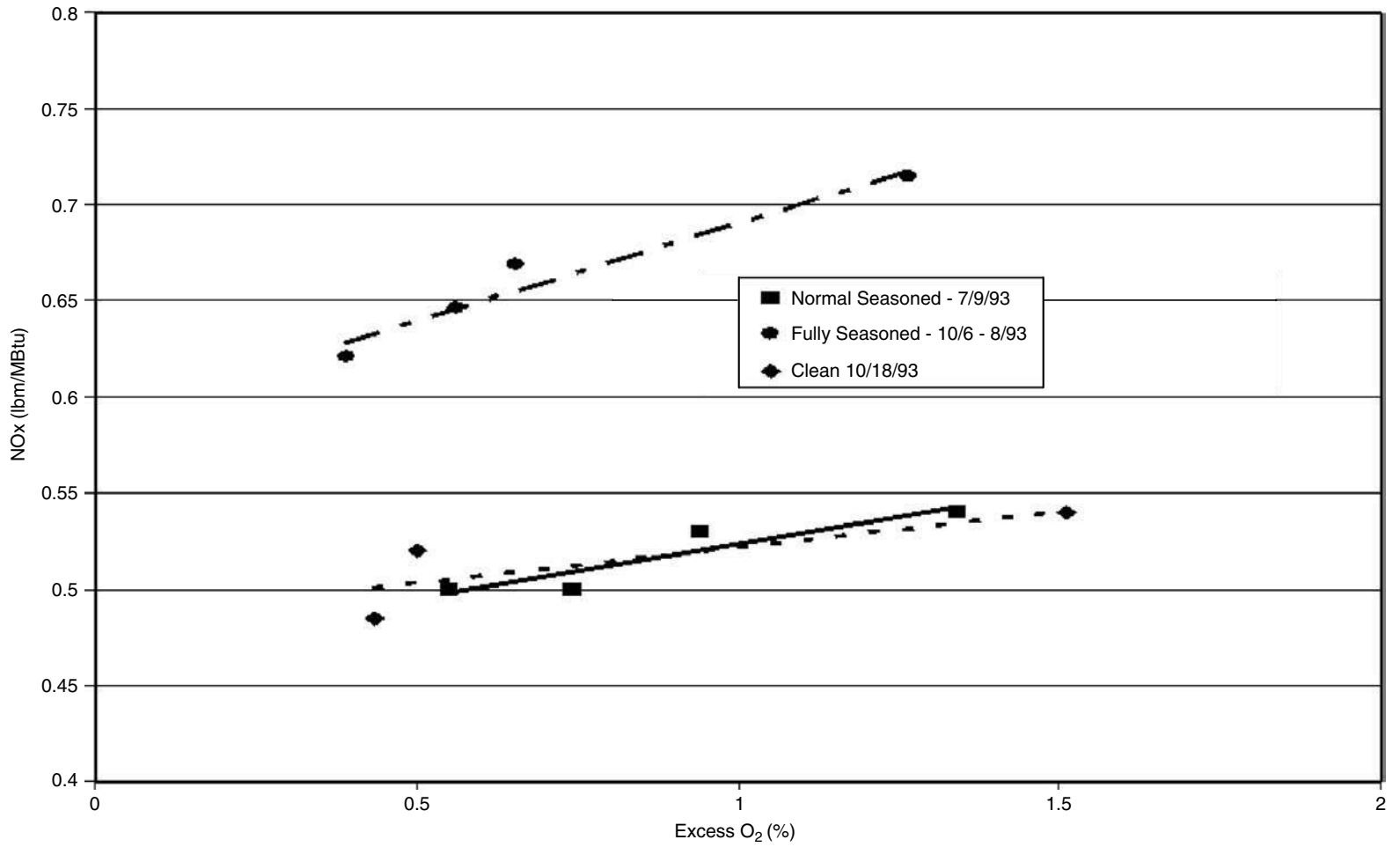


FIGURE 18.19 Effect of furnace cleanliness on NO_x.

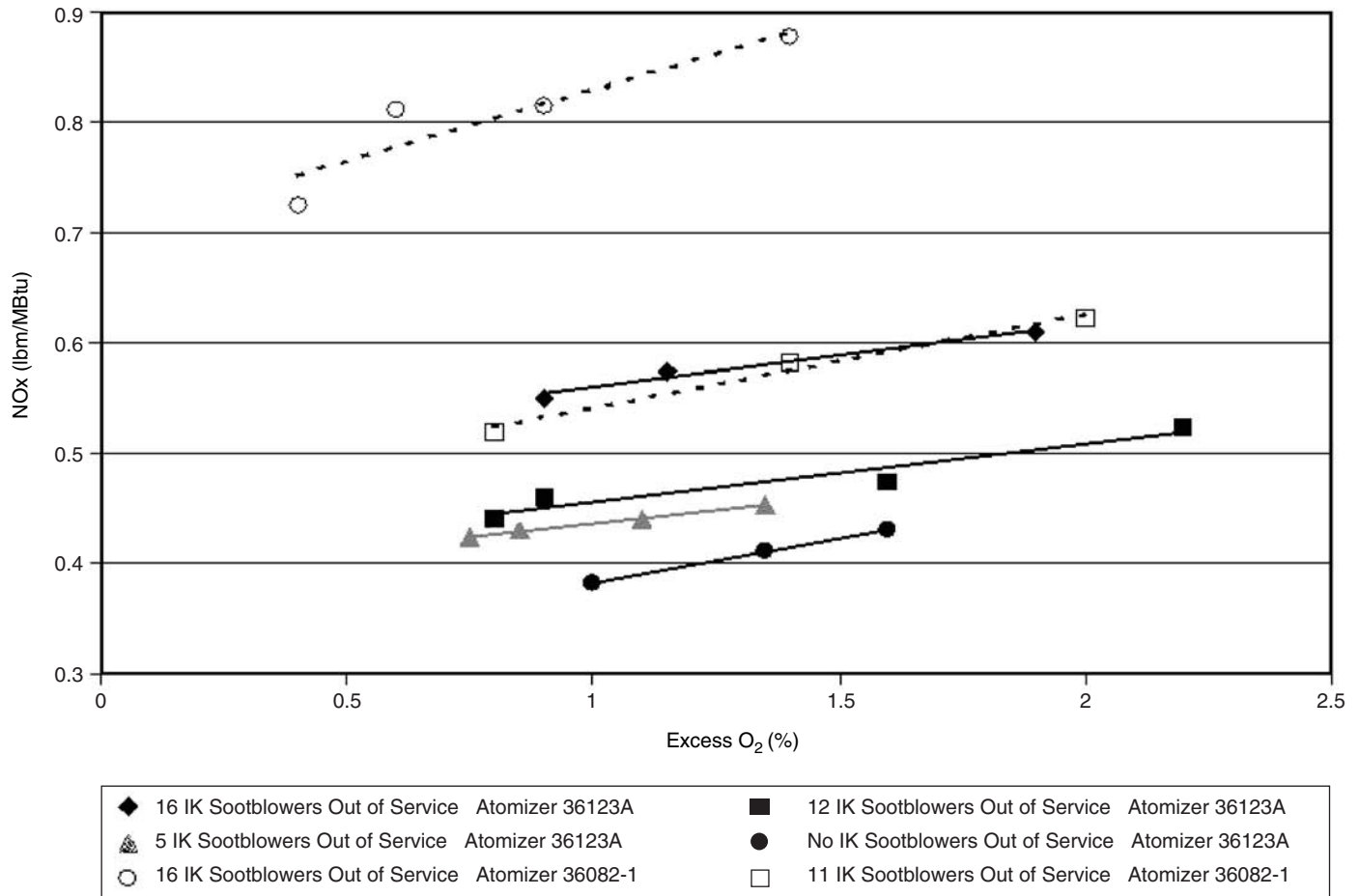


FIGURE 18.20 The impact of heat recovery area (HRA) cleanliness on NO_x.

and balanced furnaces. In pressurized furnaces under typical single-stage (unbiased) conditions, all the combustion air flow enters the furnace through the burners, and the O_2 required for complete combustion can be minimized. In balanced-draft furnaces, there is usually an air in-leakage of at least 3 to 5% (sometimes it exceeds 10%), sometimes leading to sub-stoichiometric combustion air flow coming through the burners. In-leakage air participates in the combustion process as well, providing complete combustion at slightly higher O_2 levels for many applications.

If the in-leakage location is within the furnace, the air deficit in the burners provides a self-stage combustion that complicates ICP burning out on the one hand, but can reduce NOx on the other (again depending on the in-leakage location). With other conditions remaining constant in pressurized and balanced furnaces, an NOx reduction of up to 15 to 18% is available. This was established by testing three sets of identical utility boilers: (1) 200-MW_e boiler with 12 burners on the rear wall, (2) 300-MW_e opposed fired boilers with 16 burners, (3) 150-MW_e opposed boilers with 6 burners. A comparison was made of NOx data measured in these similar utility boiler sets, one operating with a balanced draft and one operating with a forced draft, while firing gas at full load and with ~0% FGR flow.

However, if the in-leakage location is downstream of the furnace exit, in-leakage can have detrimental effects on the perceived performance of the burners. O_2 measurements taken at the top of the furnace can be approximately 0.8% lower than the control room O_2 measurements taken at the economizer outlet. In many cases, the mentioned difference between O_2 measurements is higher. This air in-leakage between the furnace exit and the economizer outlet can shift the NOx vs. O_2 and opacity vs. O_2 curves upward along the O_2 axis, as shown in [Figure 18.21](#).

18.2.4.3 Fuel Oil Temperature

Problems with the main fuel oil heaters can reduce the maximum fuel oil temperature, therefore raising the minimum viscosity attainable. The increased viscosity will increase the Sauter mean diameter of the atomized droplets, thus causing higher opacity. The increased droplet size will increase the excess O_2 required for complete combustion. NOx will increase due to the increased excess oxygen levels. The viscosity required by most burner vendors is 80 to 100 SSU.

18.3 CURRENT STATE-OF-THE-ART CONCEPTS FOR MULTI-BURNER BOILERS

18.3.1 COMBUSTION OPTIMIZATION

18.3.1.1 Equalization of Windbox Air Flow

Considering that air in the combustion process accounts for approximately 94% of the mass flow, numerous observations on boiler combustion systems have shown that correct air distribution and peripheral entry condition are key factors in the achievement of high performance (low NOx, low O_2 , and low CO). The concept of equal stoichiometry at each burner results in the minimal O_2 , NOx, and CO. The most direct way to achieve this is to ensure equal distribution of air and fuel to each burner. Airflow distribution is difficult because it requires a reliable and repeatable flow measuring system in each burner; as well as a means to correct the air flow without disrupting the peripheral inlet distribution or adding swirl to the air flow.

Mass flow deviations should be minimized to enable lower post-combustion O_2 , CO, and NOx concentrations. The lowest post-combustion O_2 concentration possible is constrained by the burner most starved for air. This starved burner will generate a high CO concentration and, consequently, the total O_2 must be raised to minimize the formation of CO in that burner. Minimizing burner-to-burner FGR deviations will even out the flame temperatures and, therefore, minimize the NOx formation from each burner. Equal inlet velocities and elimination of swirl through each burner are also crucial

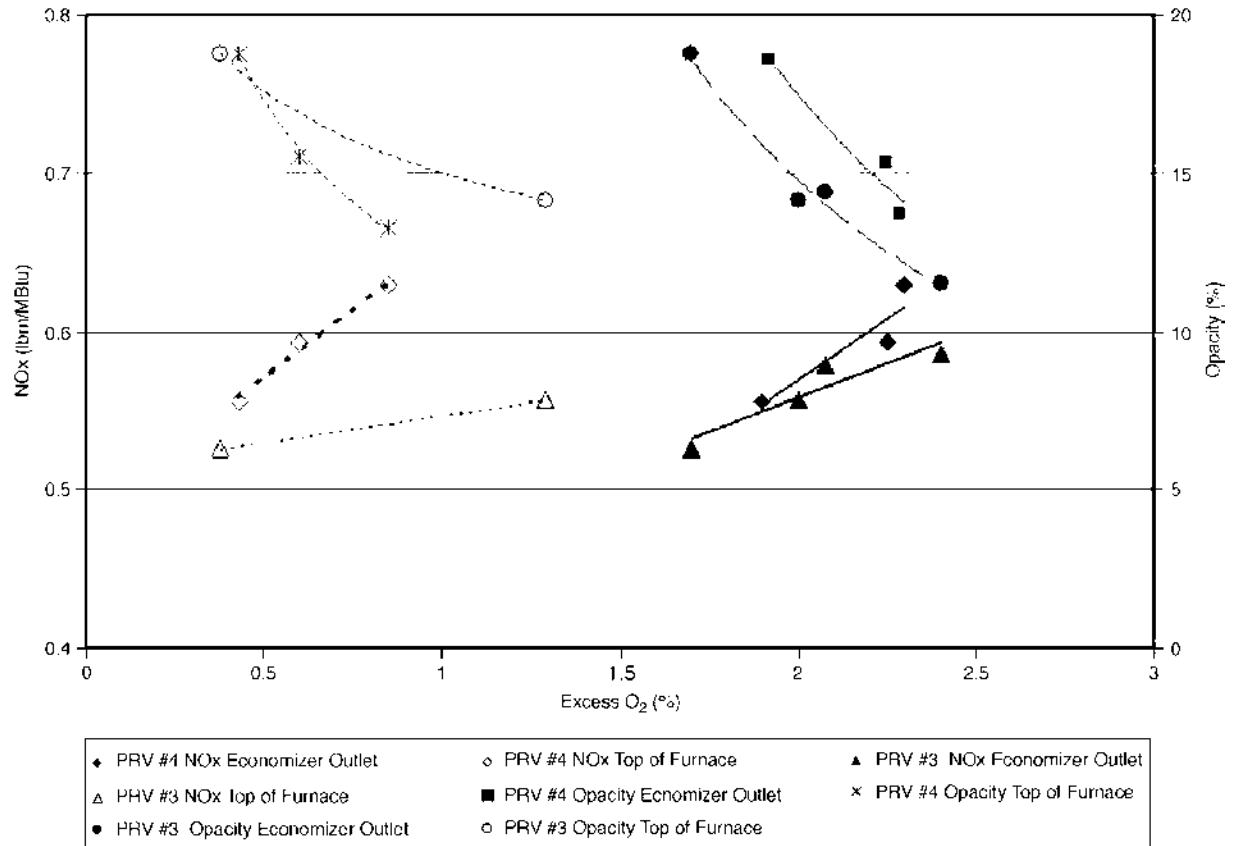


FIGURE 18.21 Air in-leakage between the furnace exit and the economizer outlet can shift the NO_x vs. O₂, and opacity vs. O₂ curves upward along the O₂ axis.

to burner performance. Because low-NO_x burners rely on the injection of fuel at precise locations within burner air flow, it is imperative that the proper air flow be present at these locations. Likewise, for optimum performance, the only swirl present must be that created by the burner itself.

No burner can be expected to simultaneously correct imbalances in the draft system *and* precisely control fuel/air mixing to minimize NO_x formation. Air flow modeling, as discussed in Chapter 11, prepares the air flow for the burner, allowing the burner to precisely control fuel/air mixing for maximum NO_x reduction. This approach has freed burner designers to focus solely on NO_x control, increasing the effectiveness of known control techniques to their maximum extent.

18.3.1.2 Fuel Flow Balancing Techniques

Fuel flow balance is just as important as air flow in reducing O₂ levels. A rough balance of fuel flow distribution is relatively easy to achieve by balancing pressure drops in the fuel header; that is, equalizing the fuel pressure at each burner, thus assuring that each burner is receiving the same amount of fuel.

Once the air flow has been balanced by a windbox model and the fuel pressures at each burner have been equalized, the unit is in the proper starting condition for the concept of fuel balancing to be taken a step further to reduce O₂ and maximize boiler efficiency. This goes back to the concept that there is probably one burner that is limiting the O₂ reduction. Even when the field data indicate that the air mass flow is within $\pm 5\%$ of average, and all the burners indicate equal fuel pressures (assuming that equal fuel pressures means equal fuel flow), the burner that is -5% in air flow will be running at an O₂ level that is approximately 1% lower than the average.

For further balancing, the unit should first be brought to MCR conditions and O₂ should be lowered to a point where the CO is in the 200- 400-ppm range on gaseous fuel, or opacity is in the 12 to 14% by EPA Method 9 for oil. The burner with the highest CO/opacity should be found and the fuel to that burner reduced slightly, resulting in a reduction in the overall CO/opacity level. This is an iterative process and should be repeated until any further fuel adjustments either show no effect, or increase the CO/opacity level.

The trick to this method of burner optimization is to find the burner with the highest CO/opacity. Ideally, on a multi-burner boiler, there should be a measurement grid at the economizer outlet that has been mapped out for burner stratification and measurement probes have been placed along the burner centerlines. CO measurements taken from this grid, at the conditions specified above, typically give a clear indication of the burner with the lowest amount of stoichiometric air. Lacking a mapped out grid, when the boiler is brought to the conditions outlined above, a visual inspection of the flames will typically indicate the “problem burner” as the one that has the “dirtiest” or “sootiest” flame.

18.3.2 METHODS TO REDUCE NO_x EMISSIONS

Combustion modification techniques developed to reduce NO_x emissions include low excess air operation, fuel- and air-staged burner design, staged combustion (off-stoichiometric or biased firing), reduced air preheat, flue gas recirculation, fuel-induced recirculation, reburn, and water tempering. As discussed in Section 18.2.2, low excess air operation limits the oxygen availability in the combustion zone and is highly effective in controlling fuel NO_x formation and, to a lesser extent, thermal NO_x.

The NO_x problem forced the development of various completely different furnace designs, usually implementing low-NO_x burners and FGR systems, sometimes containing over-fired air ports for supply of air and/or air/FGR mixtures to the furnace space located above the burners. There are single wall burner utility boilers where air ports are located on the target wall. Also, there are low-NO_x industrial and utility boilers containing special furnace devices for steam/water injection in the combustion zone and for fuel injection in the post-combustion zone (a kind of reburning).

Actually, any of the mentioned methods is capable of reducing NO_x by up to 35 to 40%, but it cannot satisfy the strictest of today's NO_x requirements. These applications require implementation of at least two NO_x reduction methods. It is important to note that, as with the example of boiler load and FGR in Section 18.2.3, the efficiency of the implemented methods depends on their sequence. The first NO_x reduction method is much more efficient than the second one. This conclusion has been confirmed on many utility boilers retrofits where up to four NO_x reduction methods were used. That is why a combination using more than three methods on the same boiler is typically inefficient.

18.3.2.1 NO_x Reduction by FGR Implementation

It is well known that thermal NO_x can be effectively controlled by reducing the flame temperature. The most effective technique is the use of FGR, which when mixed with the combustion air acts as a diluent to decrease the flame temperature, and sometimes (at high FGR rates) even increases the flame luminescence. FGR with lower temperatures will be more effective in flame temperature reduction.

Usually, FGR is taken after an economizer where temperatures range between 500 to 800°F (260 to 430°C), the O₂ range is typically between 1 to 3%, and actual ICP concentrations are negligible. A FGR fan is usually required to supply FGR flow to the combustion air flow or to the furnace.

There are also applications where a comparatively cold exit flue gas (240 to 320°F; 120 to 160°C) is taken from ID fan outlet and supplied, for example, to FD fan inlet or to windbox. This flue gas usually contains much more excess O₂, especially on the boilers equipped with air preheaters having comparatively large air leakage characteristics. Empirical data show that, if this air leakage can be minimized, this "cool" FGR gas can provide 25 to 30% higher relative NO_x reduction as compared to the "hot" FGR, but it has a more severe impact on boiler thermal efficiency reduction. FGR flow can also be induced into the combustion air forced draft fan inlet, allowing the use of FGR without requiring a separate FGR fan.

FGR can also be taken from the furnace zone adjacent to the burner exit, and can be induced back into the combustion air flow, also allowing the use of FGR without requiring a separate FGR fan. Unlike regular, comparatively cold FGR flows, this flue gas has temperatures of at least 2000°F and 2200°F (1100 and 1200°C) with gas and oil firing, respectively, it consists mostly of unreacted air (O₂ ~ 16 to 19%) and ICP. This method is completely different from all others above because its effectiveness cannot be associated with significant changes in the flame temperature conditions or lowering the O₂ concentration in the combustion air. The effectiveness of this method relies on interactions between reagents participating in NO formation and both radicals and ICP that are present in high concentrations, which slow the NO formation reactions rates, thereby reducing NO_x output.

Flue gas can be recirculated in a number of ways: directly to the furnace through slots located under, above, around, or between the burners; through over-fired air ports or ports located on the target wall; premixing the FGR flow with the combustion air upstream of the windbox (called premix FGR) (this is typically accomplished via a sparger section as depicted in [Figure 18.22](#), mixing the FGR at the burner exit (called plenum FGR), and premixing the FGR with the gaseous fuel (on oil, the flue gas would pass through the fuel gas piping). This technique of flue gas entrainment is called fuel dilution and uses no additional fan power because it is typically induced into the fuel stream by the fuel pressure itself, or by pressure energy supplied via an intermediate media such as steam if the available fuel pressure is not high enough. Also, FGR can be supplied to the boiler hopper; this method is typically used only for steam temperature control.

Various levels of NO_x reductions can be achieved at the same FGR rates using these different techniques. [Figure 18.23](#) (illustrating test data from 150-, 165-, 200-, and 300-MW_e boilers) and [Figure 18.24](#) (800-MW_e boiler) show full load gas firing test data received on utility boilers equipped with different burner designs, numbers, and arrangements, with O₂ levels of 0.8 to 1.4%.

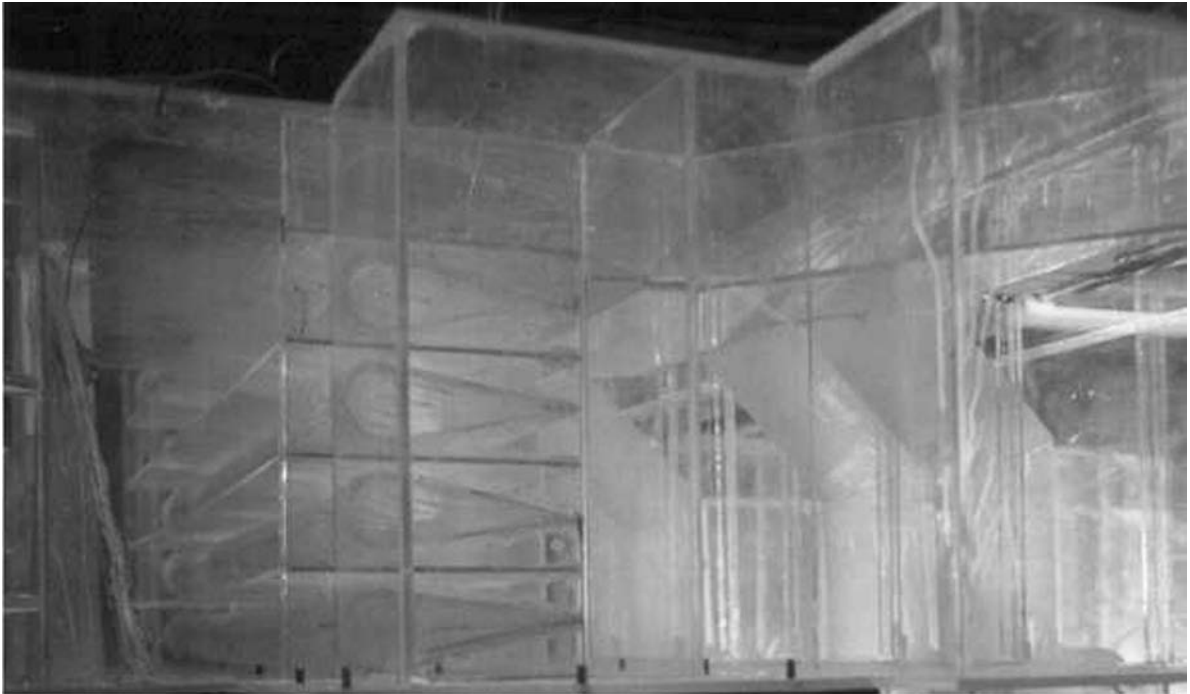


FIGURE 18.22 Premixing the FGR flow with the combustion air upstream of the windbox (called premix FGR, this is typically accomplished via a sparger).

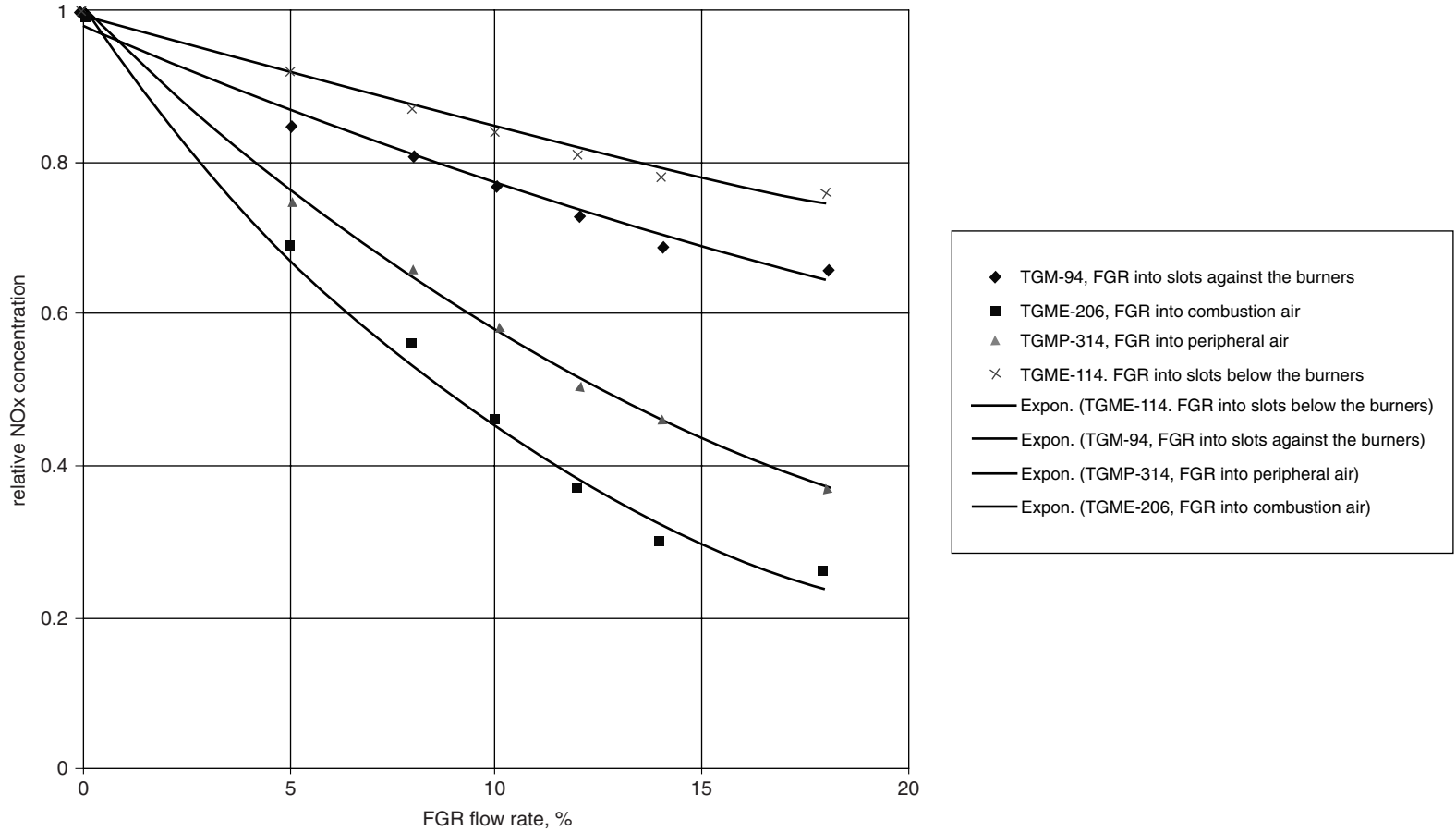


FIGURE 18.23 Test data from 150, 165, 200, and 300 MW_e boilers.

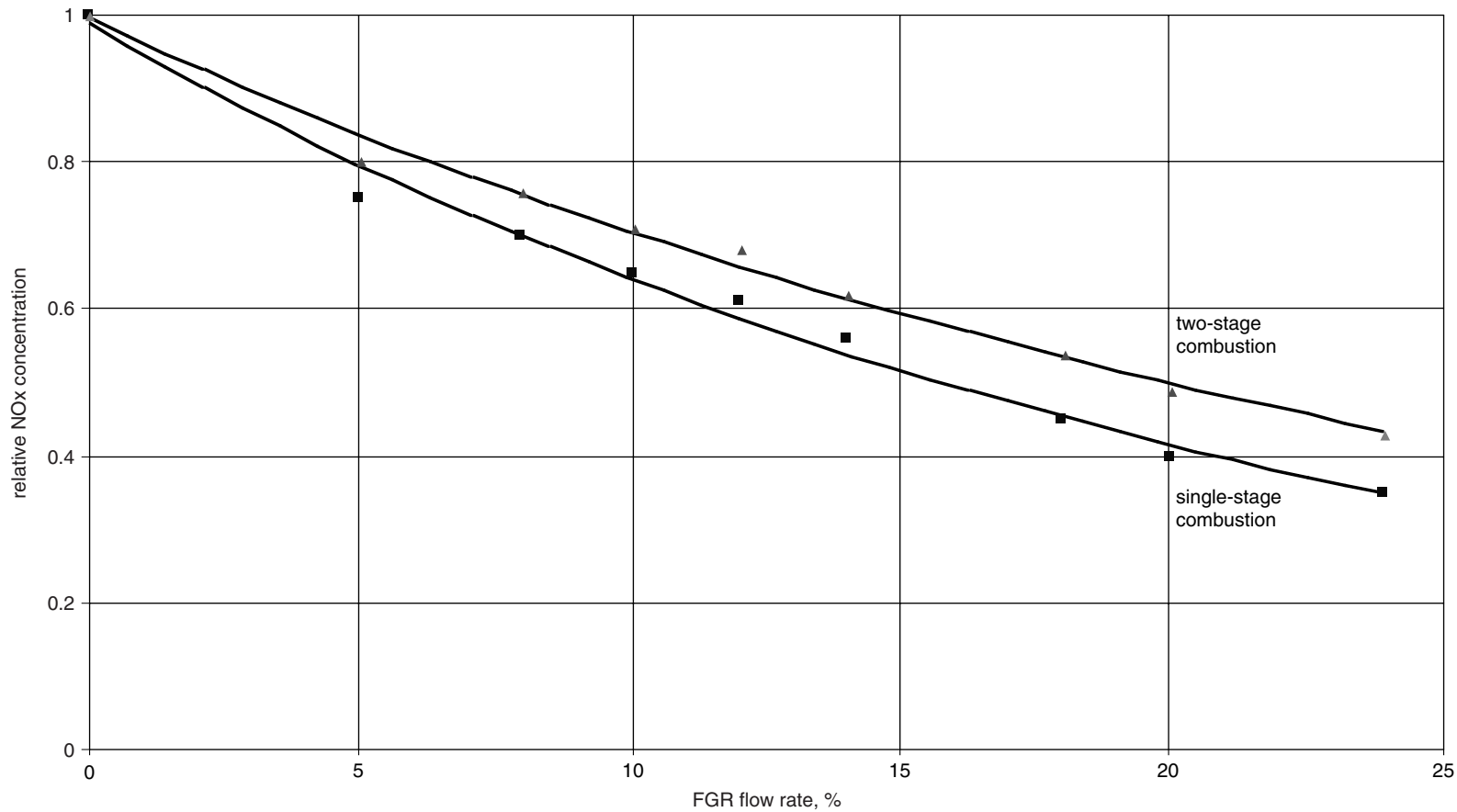


FIGURE 18.24 800-MW_e boiler.

It should be noted that all curves shown in these figures are exponential, meaning that it would make sense to determine an optimal operational FGR rate. This optimal limit will be different for each boiler application, because it depends on the boiler design (and accordingly on FGR impact on the boiler operational parameters). The data presented show that the typical optimal FGR rate range for NO_x reduction is 14 to 18%. The NO_x reductions experienced through FGR implementation, as described above, explain why it is the most frequently implemented NO_x reduction technique on newly designed and low-NO_x retrofit boilers.

Figure 18.23 shows that the most effective conventional FGR supply system for low NO_x is to provide a high-quality mixture of the FGR and combustion air, as with the venturi-style, low-NO_x burners installed at the 200-MW_e TGME-206 boiler (single wall burner installation), where 10, 12, and 18% FGR flows provided 54, 63, and 74% NO_x reduction, respectively. A comparatively high NO_x reduction efficiency is also achieved on the 300-MW_e boiler of TGME-314 model (16 burners installed in two rows on opposed firing walls), where straight FGR flow is mixed with the burner air flow. Methods used to supply FGR directly into the furnace, implemented on the TGM-114 (opposite wall burner installation, 150 MW_e) and the TGM-94 (single wall burner installation, 165 MW_e), are dramatically less effective.

Figure 18.24 demonstrates the test data obtained on the 800-MW_e boiler of model TGME-204 (36 low-NO_x burners installed in three rows on two opposed firing walls) with full load single- and two-stage gas combustion (with 33% air supplied through over-fired air ports located above the top burners) at O₂ levels of 0.8 to 1.2%. As previously discussed, it is only natural that the NO_x reduction provided by premixing FGR with combustion air flow is less effective with two-stage combustion, when the flame temperature level is significantly lower. However, the 46 and 57% NO_x reduction achieved with 18 and 24% FGR flow rates, respectively, during two-stage gas combustion, can still be considered a comparatively high efficiency because it is the second NO_x reduction method implemented (see Chapter 17.3.2). At full load on this boiler, the total NO_x reduction exceeds 80% (from 600 to 620, to 90 to 95 ppm), and CO levels less than 200 ppm at O₂ levels of 0.8 to 1.2%. This NO_x reduction was achieved utilizing a combination of: low-NO_x burner retrofit, two-stage gas combustion, premixed FGR, and water injection in the primary and secondary combustion air flows. The same scope of work was repeated on three neighboring 800-MW_e boilers of the same design installed at this power plant. On all four units, total NO_x reductions of 81 to 85% were achieved.

Similar full load NO_x reduction data have been obtained on packaged industrial boilers equipped with a single venturi-style low-NO_x burner, firing gas with ambient air. The data are presented in Figure 18.25.

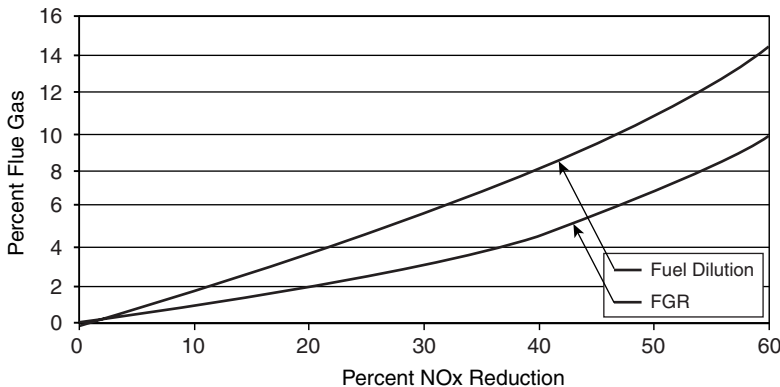


FIGURE 18.25 Full load NO_x reduction data obtained on packaged industrial boilers equipped with a single venturi-style low-NO_x burner, firing gas with ambient air.

Recent developments have shown that, when firing gaseous fuels, using fuel dilution (mentioned above) to induce flue gas into the gaseous fuel is truly the most effective method of FGR supply (~25% more effective, as shown in [Figure 18.25](#)). As per the test data, while natural gas firing at 2.5 to 4.5 O₂, NO_x can be reduced by 66% with 12 to 13% fuel dilution flow.

The reasoning why fuel dilution provides more efficient NO_x reduction as compared to conventional FGR supply methods is as follows. When natural gas (conditionally CH₄) is fired with combustion air, without the use of FGR or fuel dilution, every CH₄ molecule encounters a certain quantity of oxygen molecules, which it is dependent on; the excess O₂ level, the mixing quality of the fuel with the air, and the diffusion rates of the CH₄ and O₂ at the flame front region as shown in [Figure 18.26\(A\)](#). The combustion reaction rates (including reactions for incomplete combustion products burnout, prompt NO_x and thermal NO_x generation) are dependent on the actual excess O₂, the combustion air temperature, and the fuel/air mixture quality. These variables also determine, along with the given burner/furnace design, the heat release and heat distribution within the furnace, which in turn determines the shape of the temperature profile curve, as well as the maximum temperature value and its location within the given furnace. Concurrently, these specific features of the temperature conditions have a major impact on the determination of the above combustion reaction rates.

When CH₄ is fired with combustion air containing typical FGR, with all other combustion conditions being the same as in the previous example, every CH₄ molecule will encounter a lower quantity of oxygen molecules than it would without FGR. The FGR impedes the diffusion of O₂ toward the flame front, as depicted by the increased combustion product content on the air side (slight darkening on the air side) in [Figure 18.26\(B\)](#). The difference between the quantity of oxygen values in these two cases depends on both the FGR composition and the FGR flow rate. For example, for a boiler design operating under a positive furnace pressure (i.e., no air in-leakage in either the furnace or the convective path) and providing an equal distribution of the combustion products in both the furnace exit cross-section as well as in the convective path cross sections, the FGR composition will be similar to the combustion product composition leaving the furnace. Because the combustion air makes up ~94% of the mass flow within the combustion process, by supplying an FGR flow rate of ~11%, the oxygen concentration in the combustion air/FGR mixture is reduced by the same 11% (being only slightly diluted, this is why there is only a slight darkening on the air side in [Figure 18.26 \(B\)](#)). Also, the flame temperature level in the furnace is reduced primarily due to the addition of the FGR mass. The magnitude of the temperature reduction caused by this phenomenon depends on the FGR temperature; relatively high-temperature FGR flows will provide less flame temperature reduction than relatively low-temperature FGR flows. The combination of the decreased O₂ concentration and the lowered flame temperature level results in reduced reaction rates of all the combustion reactions mentioned above, including those reactions that are responsible for NO_x generation in the given furnace.

When CH₄ containing fuel dilution is fired with combustion air in the same furnace, combustion conditions change significantly from the examples previously discussed: because the CH₄ is only ~6% of the mass flow within the combustion process, the fuel dilution has a much greater dilution effect on CH₄. If the fuel dilution rate is the same as the FGR rate previously discussed (i.e., 11%), the dilution is equivalent to a 2 fuel dilution:1 fuel molecular ratio, as depicted with the heavy darkening on the fuel side in [Figure 18.26\(C\)](#). Due to this phenomenon, when a diluted fuel fires, the flame temperature becomes significantly lower in comparison with the second case, related to natural gas firing in the combustion air containing the same FGR flow. The reduced flame temperature influences all of the above combustion reaction rates, including reactions that are responsible for NO_x generation in the given furnace. This explains why the NO_x reduction efficiency of fuel dilution is so much greater than that of FGR. On the other hand, the mentioned flame temperature reduction (associated with the substitution of FGR with fuel dilution of the same percentage and temperature) reduces heat release in the furnace, increases the furnace exit flue gas temperature, and increases heat release in the boiler convective path, especially in the superheater

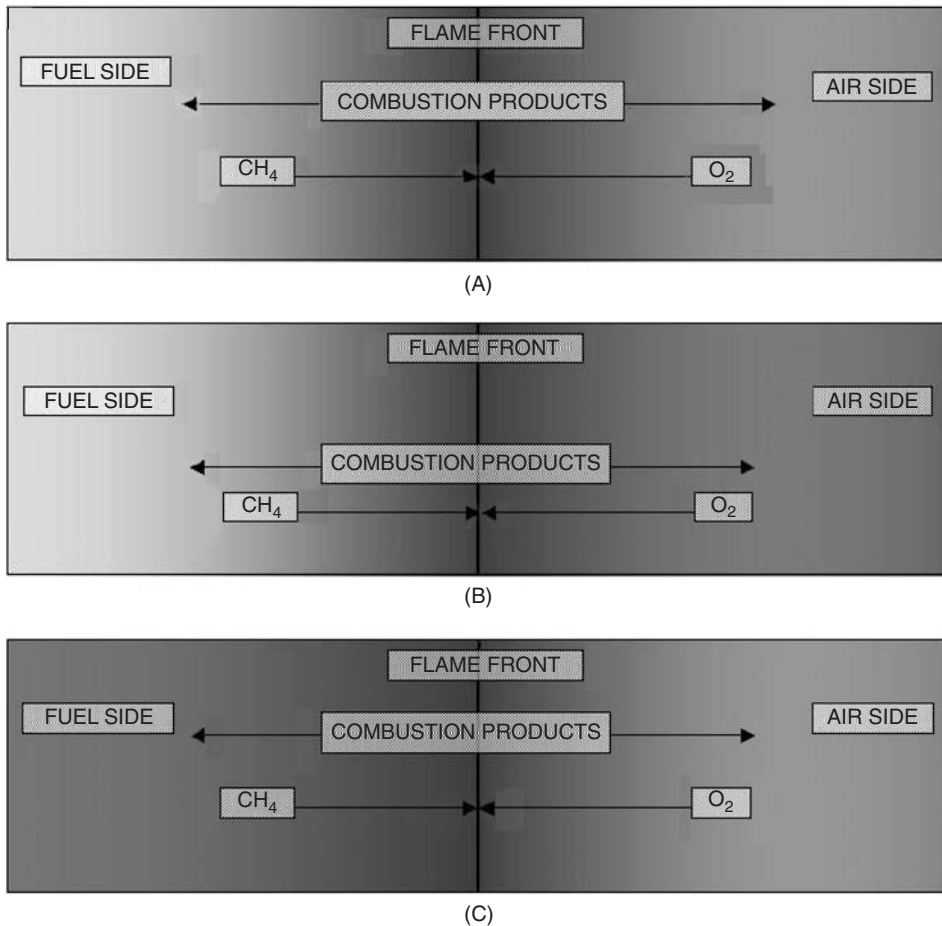


FIGURE 18.26 (A) When natural gas (conditionally CH_4) is fired with combustion air, without the use of FGR or fuel dilution; (B) when CH_4 is fired with combustion air containing typical FGR, with all other combustion conditions being the same as in the previous example; and (C) 1 fuel molecular ratio, as depicted with the heavy darkening on the fuel side.

and reheater sections. Also, the flue gas temperature will be increased throughout the convective path, including the stack flue gas temperature, which reduces the boiler thermal efficiency.

Fuel dilution can also be implemented in combination with FGR premixed in the combustion air and/or steam injection. A combination of fuel dilution and steam injection can provide a total NO_x reduction of up to ~82%.

Low flue gas recirculation rates (<20%) typically have a relatively minor impact on boiler performance (in many cases on utility boilers, it can be compensated for by increasing the turbine's efficiency; on industrial boilers, this loss is unrecoverable). However, high FGR rates (>20%) can significantly impact boiler performance, especially the redistribution of heat flux between radiant surfaces and high-temperature convective heat exchange surfaces of utility boilers and, accordingly, on superheated/reheated steam temperature. Excessive use of flue gas recirculation can result in significantly increased superheated and reheated steam temperatures, or significantly increased superheat and reheat attemperation spray flows, the later affecting boiler efficiency. In addition, power expenses recalculated for thermal efficiency losses are estimated at 0.03 to 0.05% per 1% FGR. These facts explain why FGR was (before NO_x requirements were established) typically only used to control and regulate reheated and superheated steam temperatures at minimum loads.

A typical older boiler would be designed to provide the required steam temperature and flows without FGR at full load, but at partial loads (usually $< \sim 70\%$), FGR was switched on to maintain steam temperatures. FGR flow rates were increased as load continued to decrease. Modern boiler designs incorporate FGR for both NO_x reduction and steam temperature control. At higher loads (100 to 80%) FGR is typically used for NO_x reduction; however, as above, at partial loads, FGR is typically used for steam temperature control.

Very large amounts of premixed FGR, above 45%, can affect flame stability with conventional burner designs, while plenum FGR has been tested on some burners up to 70% with no noticeable effect on flame stability. Depending on the FGR supply method, the FGR/air mixing quality will be different, and, accordingly, flame stability, vibration, and other negative issues of combustion (especially in the case of firing natural gas in ambient air) can be met even at low FGR amounts. However, these problems are not typically experienced when FGR flow rates are below 14 to 18%.

Alternative techniques to reduce flame temperature involve reduced air preheat, and water or steam injection. Water or steam injection will result in efficiency losses that are unrecoverable, while reduced air preheat can be achieved with no loss in efficiency if steam surface changes are made.

18.3.2.2 Multi-Stage Combustion on Utility Boilers

Staged combustion involves delaying the mixing of fuel and air, and is effective for both thermal and fuel NO_x control. Typically, staged combustion creates an initial fuel-rich combustion zone with air added downstream to complete combustion. Staged combustion can be achieved by the use of low-NO_x burners (internal staging), over-fired air ports, operating existing burners with biased fuel firing or with burners-out-of-service (BOOS). Biased fuel firing for a large, wall-fired unit is implemented by operating the lower burners with reduced combustion air and/or increased fuel to produce a fuel-rich zone in the lower portion of the furnace. The upper burners are operated with a corresponding increase in air or decrease in fuel to complete fuel burnout. An extreme form of staging involves operation with an upper row of burners out of service or its equivalent over-fired air ports. In this case, fuel is shut off to these burners and the burners are operated with air only.

The principal of stagewise fuel combustion involves the arbitrary division of the flame into two or more stages. In most cases, in the first, high-temperature stage, combustion takes place with an excess air factor of less than unity and, in the subsequent stages, which have a comparatively low temperature level, secondary combustion of the previously ICPs occurs with relatively high excess air. Thus, NO_x formation is retarded in the first stage, because there is insufficient oxygen in the reaction zone and, in the subsequent stages, due to the relatively low temperature of the flame. This has established the advantages of stagewise combustion as an NO_x reduction method over other methods.

There are various methods of performing staged combustion in furnaces. The most well-known and studied methods are based on the three following options:

1. Gas/oil combustion with a significant air deficit in all burners and supplying a certain part of the total air flow directly to the furnace through ports or slots located above the burners
2. Redistribution of air flows between the burners located at different rows
3. Redistribution of fuel flows between the burners located at different rows

All the mentioned options are directed to get a “vertical” fuel/air unbalance in the furnace: excess fuel and air deficit in the lower part and, on the contrary, excess air and fuel deficit in the top part of the combustion zone. However, when a boiler changes over to stagewise fuel combustion with a “vertical” unbalance in the fuel:air ratio, concentrations of all ICPs — including carcinogenic substances — increase. Much test data exists confirming the above conclusion. An example is shown in [Figure 18.27](#) where test data obtained on a model TGM-94 boiler are presented. It can be seen that a 50% NO_x reduction while firing gas is reached at $\sim 18\%$ over-fire air flow, but CO

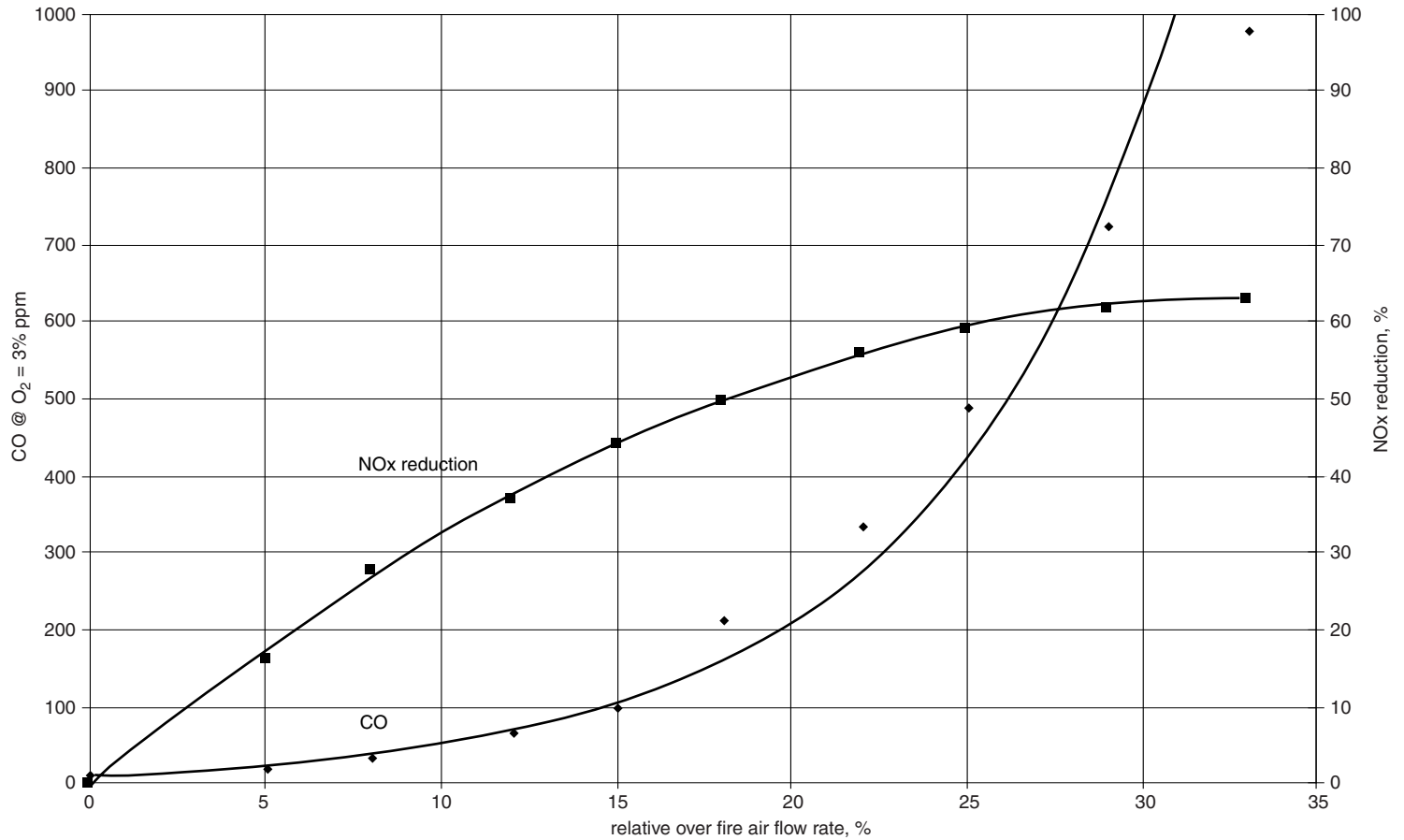


FIGURE 18.27 Test data obtained on a model TGM-94 boiler.

has increased to ~200 ppm. Further increasing the “vertical” unbalance to 25% results in ~60% NO_x reduction; however, CO has increased to ~400 ppm. Increases in CO concentrations and other ICPs are typical of “vertical” stage combustion. The data for this boiler also indicated that staged combustion operation while firing gas at ~18% over-fired air flow reduced the boiler efficiency by ~0.85%.

Another system of stagewise combustion, with a “horizontal” unbalance of the fuel:air ratio, gives rise to substantial reductions of ICP emissions; however, it results in increased NO_x. This method of staged combustion utilizes the interaction of fresh combustion air jets directed from ports or slots located opposite the burners, with fuel radicals and already formed ICP in flames generated by burners receiving sub-stoichiometric air. It intensifies the combustion process and especially burnout while firing oil, as illustrated with [Figure 18.28](#) where test data was obtained on a TGM-84 (~950,000 lb/hr or 430,000 kg/hr steam flow) co-generating boiler firing #6 oil. The data show that this method provides reductions of opacity, carcinogenic substances, and a small CO reduction from ~38 to ~24 ppm. However, NO_x increases very quickly: on average, 1% of the secondary air flow brings a relative NO_x increase of ~1.2%. The boiler data from this testing indicated that this method can be applied for applications requiring increased reheated/superheated steam temperatures. Moreover, this method increases the boiler thermal efficiency and reduces operational power expenses due to decreasing the air resistance of air path. On the above boiler, ~15% secondary air flow increased the total efficiency by 1.1%. These data indicate that optimally designed three-stage fuel combustion systems could be developed with simultaneous “vertical” and “horizontal” imbalances of the fuel:air ratio.

Using calculations explaining the above data as a basis for preliminary design work, a new furnace was developed. The furnace had three burner rows and slots above the upper row located on the furnace front wall. FGR could either be premixed with the combustion air going through the burners and slots, supplied directly into the furnace through slots located on the rear wall, opposite the lower burners, or in both locations. The primary air flow was supplied through the burners; secondary and tertiary air flows were redirected to the slots located on the rear and front walls, respectively.

Tests were performed over a boiler load range of 100 to 40%, α is 1.05 to 1.11 firing gas, and at full load, α is 1.03 to 1.1, firing #6 oil. To obtain reliable data on the NO_x reduction effectiveness of stagewise combustion, tests were carried out in alternate modes, with measurements being made during single-stage combustion under the same load, excess air factor, FGR, and other combustion conditions. Comparative tests when firing oil were carried out with oil supplied from the same tank. All results were compared with the baseline conditions of single-stage combustion, in which the secondary and the tertiary air flow dampers were fully throttled, it being conditionally assumed that their relative flows were ~0.

The test data comparing single- and three-stage gas combustion are shown in [Figure 18.29](#). It is seen that transferring from single- to three-stage combustion at ~10% secondary air flow yields NO_x reductions of ~40 and ~63%, with tertiary air flows of 15 and 25%, respectively. This NO_x reduction is accompanied by a corresponding CO increase from ~135 to 165 ppm during single-stage combustion of 260 to 290 and 350 to 400 ppm, accordingly. Under the above conditions, operation with FGR was not required at any point over the entire load range. The decrease in thermal efficiency was 0.3 to 0.4%, much less dramatic than either two-stage combustion (with a “vertical” imbalance) or FGR fan operation. The same retrofit was performed on six neighboring TGM-94 boilers installed at this power plant.

18.3.2.3 Water and Steam Injection for NO_x Reduction on Utility Boilers

Water and/or steam injection systems have been installed on many multi-burner boiler applications for NO_x reduction. However, due to the associated decrease in boiler thermal efficiency, these systems are only used when required to reach a high level of NO_x reduction, such as at full load conditions,

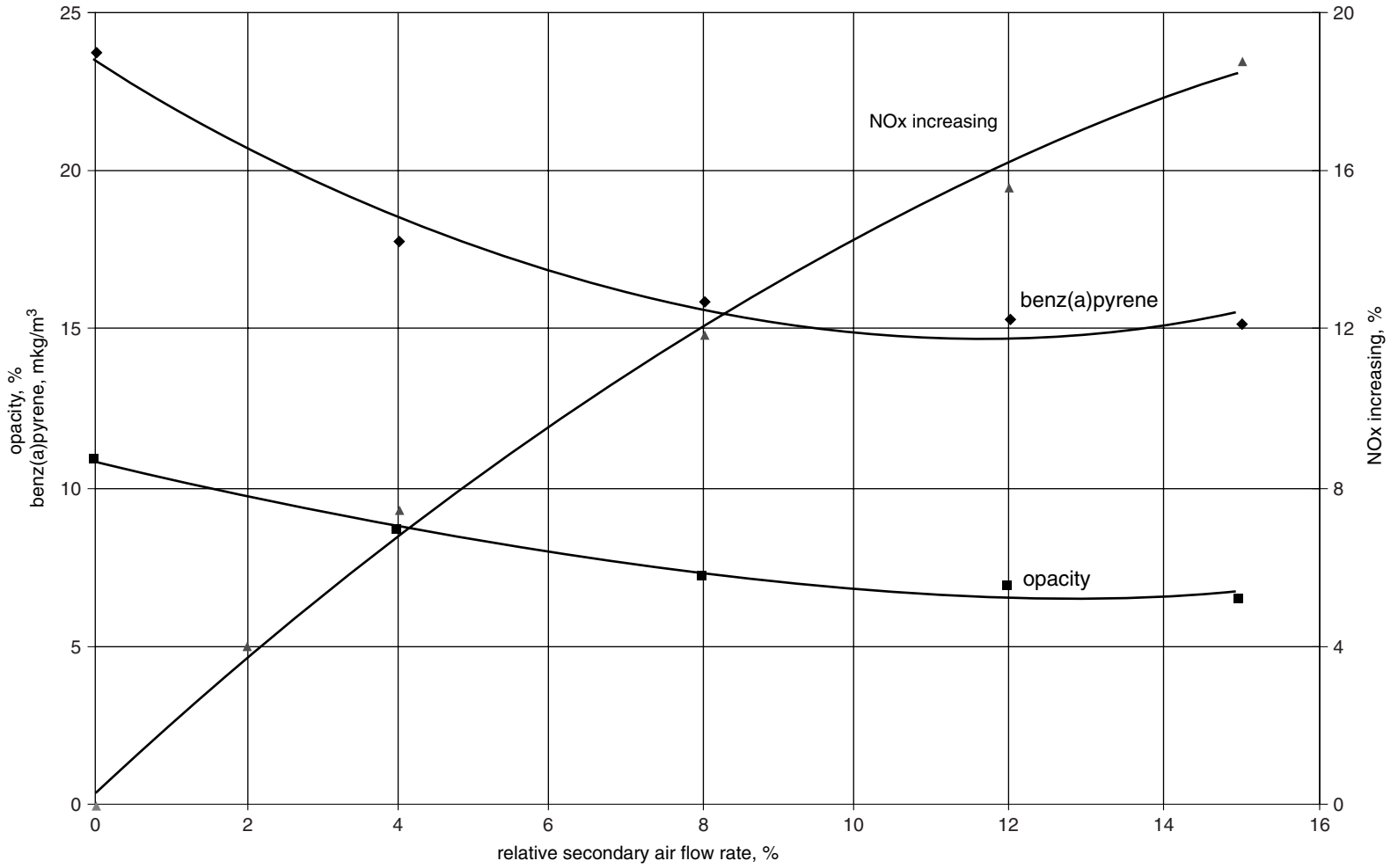


FIGURE 18.28 Stagewise method intensifies the combustion process and especially burnout while firing oil.

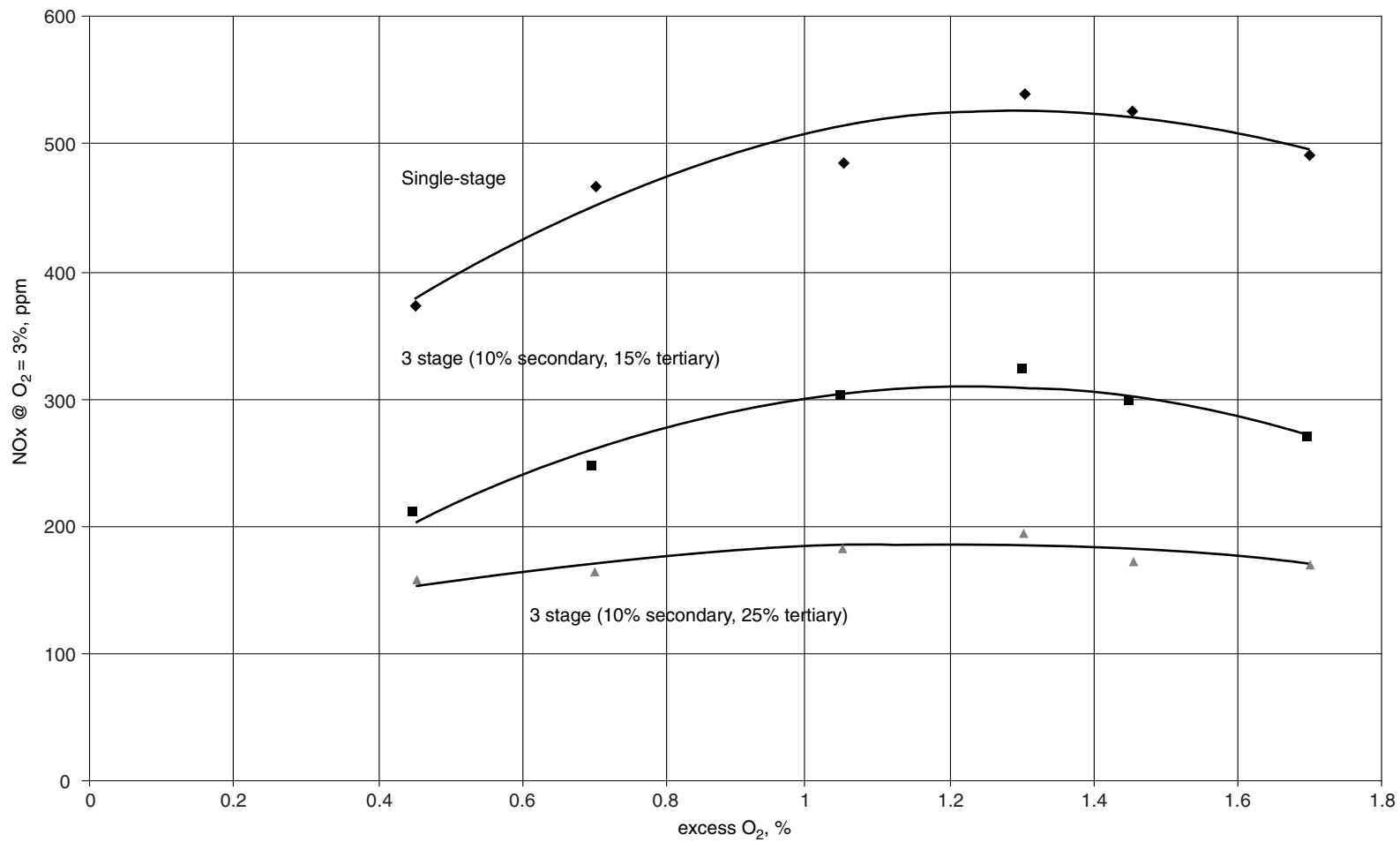


FIGURE 18.29 Data comparing single- and three-stage gas combustion.

and are generally turned off at lower loads when more conventional NO_x reduction methods can maintain the NO_x level requirements.

18.3.2.3.1 Water Injection Effectiveness

Water injection is most effective for high BZHR utility boilers firing natural gas, where a significant NO_x reduction can be achieved with a comparatively low water flow rate injected into the preheated combustion air flow (e.g., water injection reduced NO_x by 35% on a 816-MBtu/sf-hr BZHR boiler).

The impact of water injection on boiler thermal efficiency was studied in detail on two boilers: a 165-MW_e TGM-94 and a 300-MW_e TGMP-314 while firing natural gas at full load. Although initial thermal efficiency values were different for the two boilers (91.9% for TGM-94 and 94.7% for TGMP-314 — both at LHV), thermal efficiency reduction numbers were almost identical, i.e., (~62%).

18.3.2.3.2 Steam Injection Effectiveness

Injecting steam, instead of water, into the combustion air reduces the NO_x reduction effectiveness for a given mass of water injection. As an example, for a given application, NO_x reduction was ~28% with steam as compared to ~46% with water. When the water injection flow rate was increased, the associated NO_x reduction effectiveness was ~51% for water injection and ~41% for steam injection. However, the NO_x reduction efficiency decrease associated with steam injection was accompanied by a lower thermal efficiency reduction due to the added latent heat of the steam. The thermal efficiency decrease was ~0.27% with steam injection, as compared to ~0.62% with water injection (i.e., ~2.3 times lower).

18.3.2.3.3 General Evaluation of Water/Steam Injection Effectiveness

The above discussion demonstrates how high levels of NO_x reduction can be achieved with water/steam injection, and that these reductions are comparable to the NO_x reduction effectiveness reached with FGR described in Chapter 17.3.2.1.

Unlike FGR, however, a water/steam injection does not require significant capital investment, but does have a much larger negative impact on boiler thermal efficiency (as an order of magnitude, percents with water, tenths of percents with steam, as compared to hundredths of percents with FGR). Although water and steam injection are associated with a negative impact on boiler efficiency, the simplicity and high effectiveness of this NO_x reduction method implementation, combined with very low capital expenses, make it very attractive for many multi-burner boiler owners.

18.3.2.4 Special Features of Low NO_x Gas/Oil Combustion on Utility Boilers

Chapters 17.1.2 and 17.2.2.2 show that there are some utility boilers where NO_x is higher while firing natural gas than that experienced while firing #6 oil. For example, data obtained on the TGM-94 boilers presented in Figures 18.10 through Figure 18.13 demonstrate that the NO_x while gas firing is ~24 to 27% higher as compared with NO_x data obtained while firing #6 oil under the same load (~94%), O₂ (1.4 ± 0.2%), and other operational conditions.

This phenomena of the NO_x while firing gas being higher compared with the NO_x data obtained while firing #6 oil has been experienced during testing of many former-U.S.S.R. utility boilers in the size range of 165 to 800 MW_e. In some cases, NO_x while firing gas exceeded the NO_x while firing #6 oil (even containing 0.67 to 0.73% N_f) by ~50%. On the contrary, on utility boilers in the size range of 25 to 80 MW_e, the NO_x while firing #6 oil exceeded the NO_x while firing gas by about 25%; moreover, as N_f values increased (from 0.22 to 0.73%), the greater the margin between the NO_x while firing #6 oil and the NO_x while firing gas. Likewise, on industrial boilers, the NO_x was almost always higher while firing #6 oil, and differences of 24 to 36% and 12 to 18%, respectively, were typically experienced with ambient and preheated air. However, intermediate results were obtained while testing utility boilers in the size range of 100 to 150 MW_e where

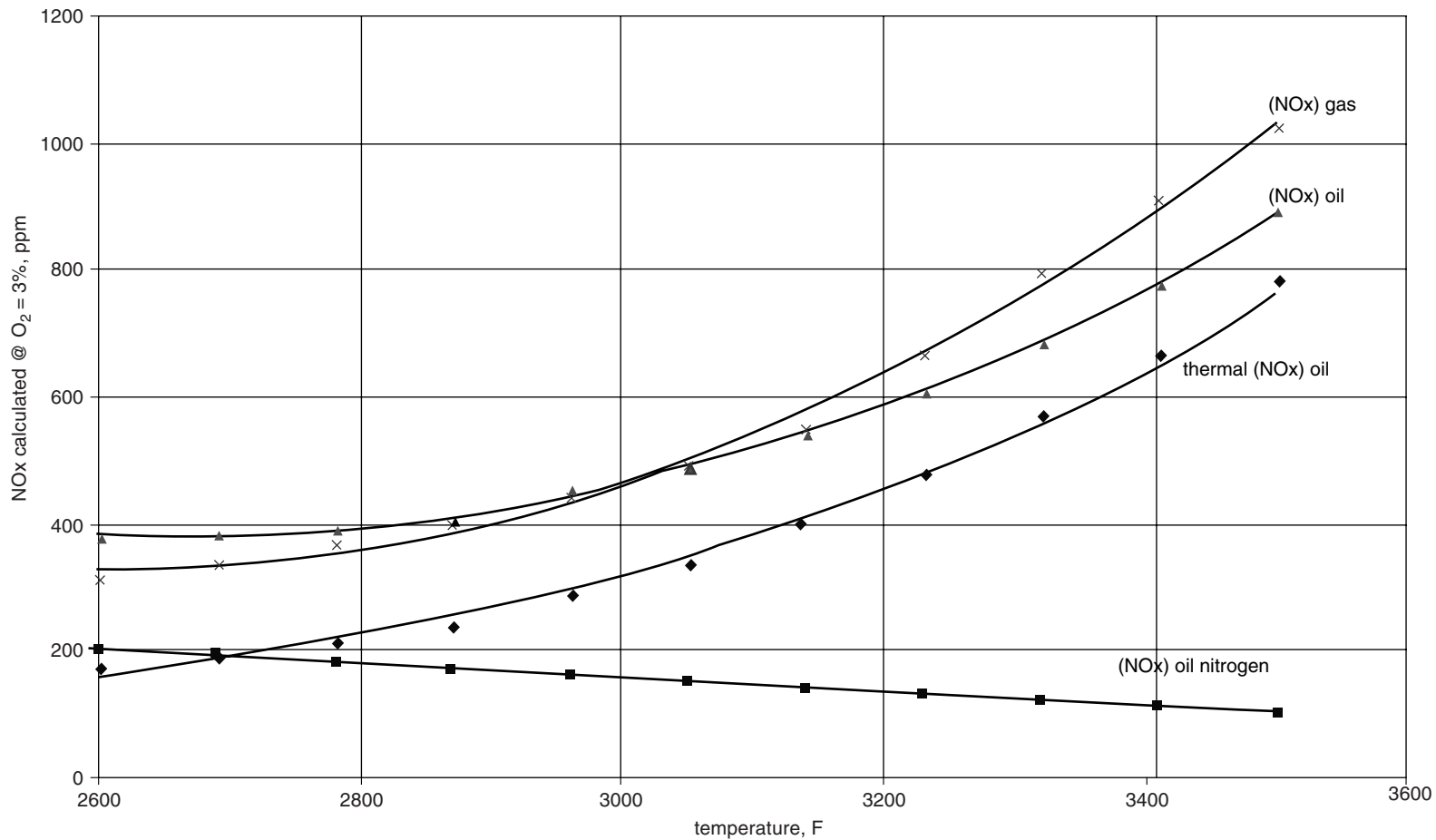


FIGURE 18.30 The corresponding NOx concentration curve, calculated for excess air factor $\alpha = 1$.

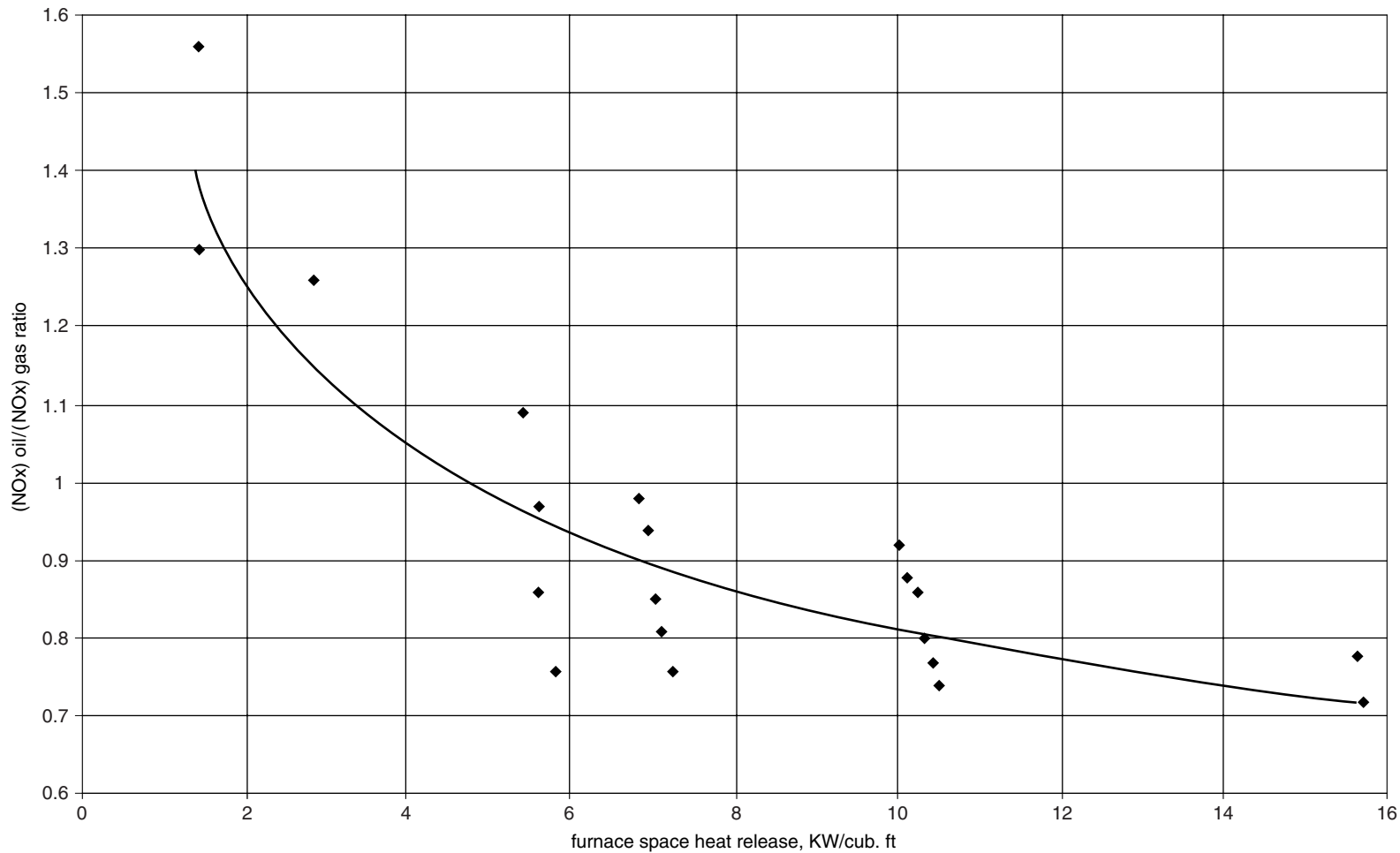


FIGURE 18.31 The ratio between NOx numbers obtained with gas and oil firing are considered as a function of the furnace space heat release.

differences between the NO_x numbers for the two fuels were less than $\pm 10\%$. The controversial data obtained on these boilers of different designs and capacities can be explained based on the well-known influence of the flame temperature on NO_x formation.

While firing natural gas containing no N_f, NO_x can only be generated by the oxidation of nitrogen contained in the combustion air. This NO_x generation can only occur by one of two mechanisms: thermal NO_x formation due to flame temperatures of above 2780°F (1527°C), mostly in the burner zone heat release (BZHR) space, its concentration rises with temperature in an exponential manner; prompt NO_x formation in the beginning of the flame where the temperature level is significantly lower. Under usual combustion conditions, its concentration is much less than the thermal NO_x concentration; prompt NO_x has a slight dependency on temperature. Under certain furnace conditions required for low-NO_x combustion, the thermal NO_x concentration can be reduced to the prompt NO_x concentration level, or even less. However, these conditions have little influence on prompt NO_x.

While firing natural gas (conditionally consisting of methane only), the maximum combustion temperature level depends solely on excess air and the combustion air temperature. The corresponding NO_x concentration curve, calculated for excess air factor $\alpha = 1$, is shown in [Figure 18.30](#).

When firing oil-containing N_f, there are two sources of NO_x formation: air nitrogen and fuel nitrogen. In addition to the two mechanisms available for gas firing, a third mechanism is available as well: oxidation of the partially destructed nitrogen-containing compositions that occur in the beginning of the flame, whose concentrations decrease slightly with increasing temperature.

[Figure 18.30](#) shows calculated NO_x curves for both nitrogen sources, and their summed values. It shows that oxidation of 0.5% N_f can generate NO_x of up to ~ 200 ppm. When we consider the processes in the comparatively cold furnaces designed for industrial and small utility boilers (50 to 100 MW_e), the above 200 ppm will far outweigh the thermal NO_x formation. Because these processes are occurring at relatively low temperatures, they indicate relatively low NO_x levels from these boilers, and an oil-firing NO_x level much higher than the gas-firing NO_x level. In the 120-150-MW_e boilers, temperatures can reach 2900 to 3100°F (1600 to 1700°C). [Figure 18.30](#) indicates that the curves calculated for gas and oil firing intersect within this temperature interval, indicating relatively equal NO_x levels while firing either gas or oil. For units greater than 165 MWe, the flame temperature can reach between 3200 and 3500°F (1800 and 1900°C). This temperature increase results in a gas-firing NO_x level much higher than the oil-firing NO_x level.

The above explanation can be confirmed with the data presented in [Figure 18.31](#), where the ratio between NO_x numbers obtained with gas and oil firing are considered as a function of the furnace space heat release. Furnace designs for increasingly higher-capacity utility boilers are usually (with very few exceptions) accompanied by a significant increase in heat release as related to the furnace volume. Thus, the design of these boilers allows the analysis of the ratio between NO_x numbers and this designed parameter. Despite experimental data deviations from the average empirically established curve, the strong character of this dependence cannot be doubted.

19 Duct Burners

Stephen L. Somers

CONTENTS

- 19.1 Introduction
- 19.2 Applications
 - 19.2.1 Co-generation
 - 19.2.1.1 Introduction
 - 19.2.1.2 Combined Cycle Systems
 - 19.2.2 Air Heating
 - 19.2.3 Fume Incineration
 - 19.2.4 Stack Gas Reheat
- 19.3 Burner Technology
 - 19.3.1 In-Duct or Inline Configuration
 - 19.3.2 Grid Configuration (Gas Firing)
 - 19.3.3 Grid Configuration (Liquid Firing)
 - 19.3.4 Design Considerations
 - 19.3.4.1 Fuels
 - 19.3.4.2 Combustion Air and Turbine Exhaust Gas
 - 19.3.4.3 Augmenting Air
 - 19.3.4.4 Equipment Configuration and TEG/Combustion Air Flow Straightening
 - 19.3.4.5 Wing Geometry Variations
 - 19.3.4.6 Emissions
 - 19.3.5 Maintenance
 - 19.3.5.1 Normal Wear and Tear
 - 19.3.5.2 Damage
 - 19.3.5.3 Fuel Quality/Composition
 - 19.3.6 Accessories
 - 19.3.6.1 Burner Management System
 - 19.3.6.2 Fuel Train
 - 19.3.7 Design Guidelines and Codes
 - 19.3.7.1 NFPA 85 (National Fire Protection Association)
 - 19.3.7.2 FM (Factory Mutual)
 - 19.3.7.3 UL (Underwriters Laboratories)
 - 19.3.7.4 ANSI B31.1 and B31.3 (American National Standards Institute)
 - 19.3.7.5 Others
- References

19.1 INTRODUCTION

Linear grid and in-duct burners were used for many years to heat air for drying operations before use in co-generation systems became widespread. Some of the earliest heating systems were merely a gas lance inserted into the air stream. Other systems mixed fuel and air in an often-complicated configuration to fire into a relatively low-temperature recirculating process air stream with oxygen depleted by combustion or water vapor. General use in high-temperature, depleted oxygen streams downstream of gas turbines began in the early 1960s and such systems were used to increase steam production in waste heat boilers for process use in industrial applications, or to drive steam turbine-generators for electrical peaking utility plants. Gas turbines have become larger and more efficient in the intervening years, and duct burner supplemental heat input has increased correspondingly.

Linear burners are applied where it is desired to spread heat uniformly across a duct, whether in ambient air or oxygen-depleted streams. In-duct designs are more commonly used in fluidized bed boilers and small co-generation systems.

19.2 APPLICATIONS

19.2.1 CO-GENERATION

19.2.1.1 Introduction

Co-generation implies simultaneous or consecutive production of two or more forms of energy, most commonly electrical (electric power), thermal (steam, heat transfer fluid, or hot water), and pressure (compressor). For the purposes of this discussion, the basic process involves combustion of fossil fuel in an engine (reciprocating or turbine) that drives an electric generator, coupled with a recovery device that converts the heat from the engine exhaust into a usable energy form.¹ Production of recovered energy can be increased independently of the engine through supplementary firing provided by a special burner type known as a *duct burner* (sometimes called a *grid burner*). Most modern industrial systems will also include flue gas emissions control devices. A typical plant schematic is shown in [Figure 19.1](#).

Reciprocating engines (typically diesel cycle) are often used in smaller systems (10 MW and lower) and offer the advantage of lower capital and maintenance costs but produce relatively high levels of pollutants. Turbine engines are used in both small and large systems (3 MW and above) and, although more expensive, generally emit lower levels of regulated air pollutants.

The fossil fuels used in co-generation systems may consist of almost any liquid or gaseous hydrocarbon, although natural gas and various commercial grades of fuel oil are most commonly used. Mixtures of hydrocarbon gases and hydrogen found in plant fuel systems are often used in “cogen” facilities near refining and petrochemical facilities. Duct burners are capable of firing all fuels suitable for the engine/turbine, as well as many that are not, including heavy oils and waste gases.

Heat recovery for large systems is accomplished in a convective waste heat boiler, commonly referred to as a “heat recovery steam generator” (HRSG). Smaller systems may utilize a steam or hot water boiler, a process heater, or some type of gas-to-gas heat exchanger.

Supplementary firing is often incorporated into the boiler of HRSG design as it can increase thermal input for production of steam as demanded by the process. The device that provides the supplementary firing is a duct burner, so called because it is installed in the duct connecting the engine/turbine exhaust to the heat recovery device, or just downstream of a section of the HRSG superheater (see [Figure 19.2](#) and [Figure 19.3](#)). These systems are often referred to as “duct fired.” The oxygen required for the duct burner combustion process is provided by the residual oxygen

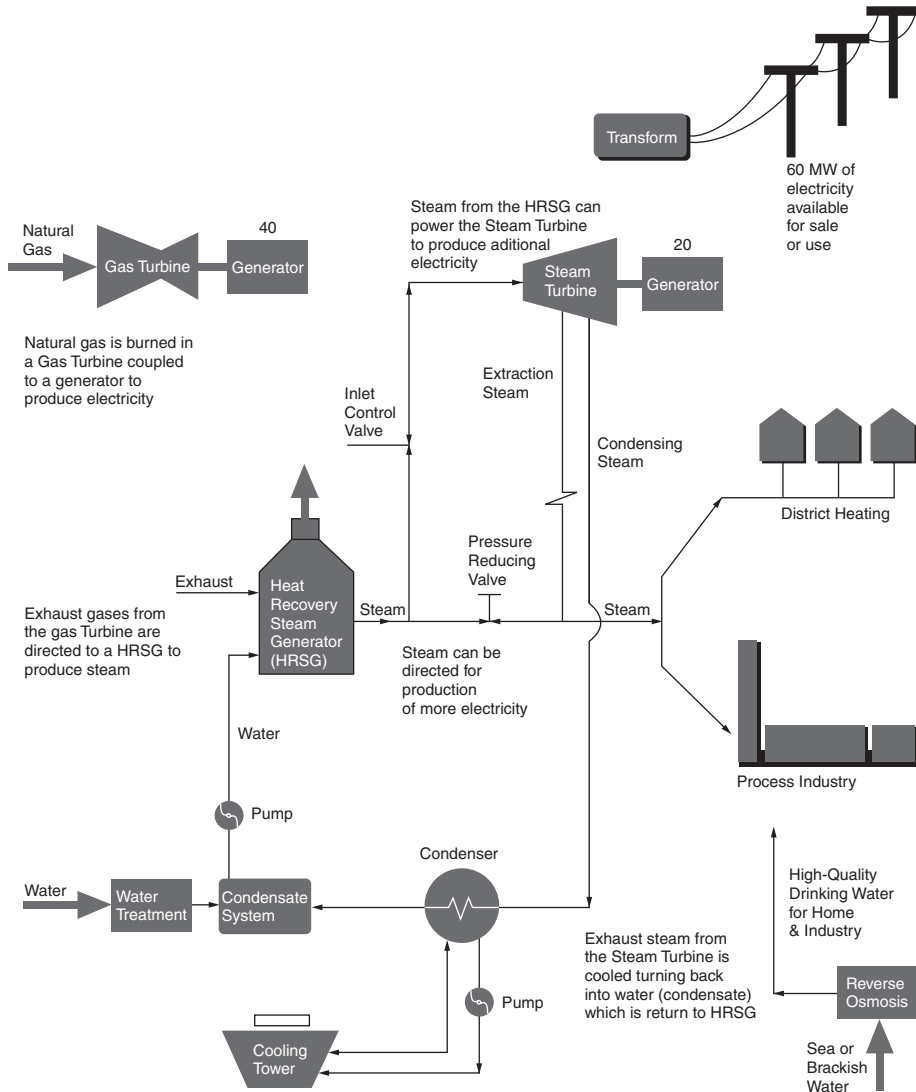


FIGURE 19.1 Typical plant schematic.

in the hot flue gas exhausted from the gas turbine. The flue gas is usually called turbine exhaust gas (TEG) or gas turbine exhaust (GTE).

19.2.1.2 Combined Cycle Systems

Combined cycle systems incorporate all components of the simple cycle configuration with the addition of a secondary electrical production device, usually a steam turbine or generator set powered by the high-pressure steam produced in the HRSG. This arrangement is attractive when the plant cannot be located near an economically viable steam user. Also, when used in conjunction with a duct burner, the steam turbine or generator can provide additional power during periods of high or “peak” demand. The arrangement whereby electricity is generated from the relatively high-grade waste heat before use in a process is called a “topping cycle.”

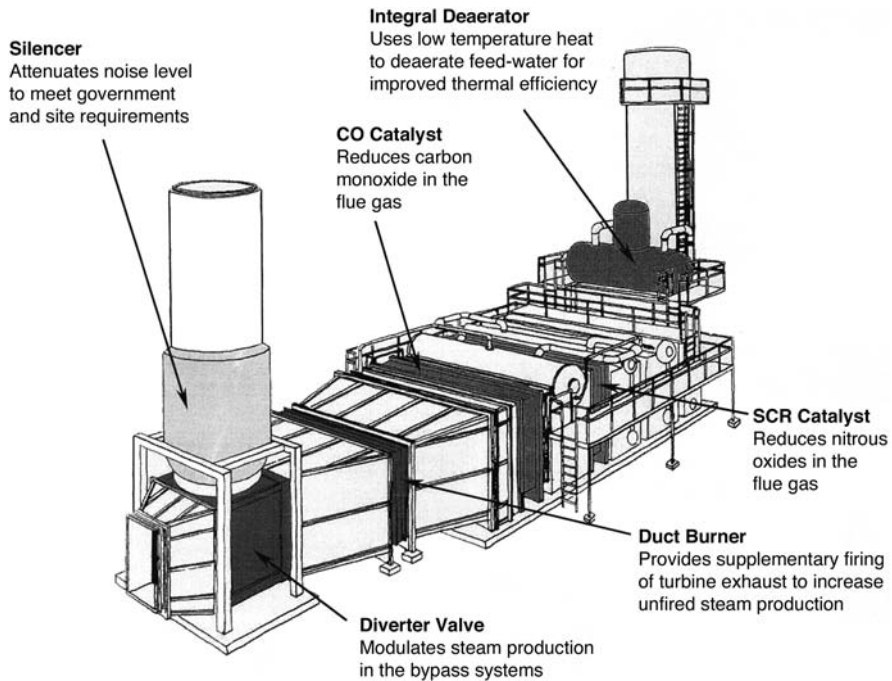


FIGURE 19.2 Typical location of duct burners.

19.2.2 AIR HEATING

Duct burners are suitable for a wide variety of direct-fired air heating applications where the physical arrangement requires mounting inside a duct, and particularly for processes where the combustion air is at an elevated temperature and/or contains less than 21% oxygen. Examples include:

- *Fluidized bed boilers.* Burners are installed in combustion air ducts and are only used to provide heat to the bed during start-up. At cold conditions, the burner is fired at maximum capacity with fresh ambient air, but as combustion develops in the bed, cross exchange with stack gas increases the air temperature and velocity. Burners are shut off when the desired air preheat is reached and the bed can sustain combustion unaided.
- *Combustion air blower inlet preheat.* Burners are mounted upstream of a blower inlet to protect against thermal shock caused by ambient air in extremely cold climates (-40°F ; $^{\circ}\text{C}$ and below). This arrangement is only suitable when the air will be used in a combustion process as it will contain combustion products from the duct burner.
- Drying applications in which isolation of combustion products from the work material is not required. For example, certain paper and wallboard manufacturing operations.

19.2.3 FUME INCINERATION

Burners are mounted inside ducts or stacks carrying exhaust streams primarily composed of air with varying concentrations of organic contaminants. Undesirable components are destroyed both by an increase in the gas stream bulk temperature and through contact with localized high temperatures created in the flame envelope. Particular advantages of the duct burner include higher thermal

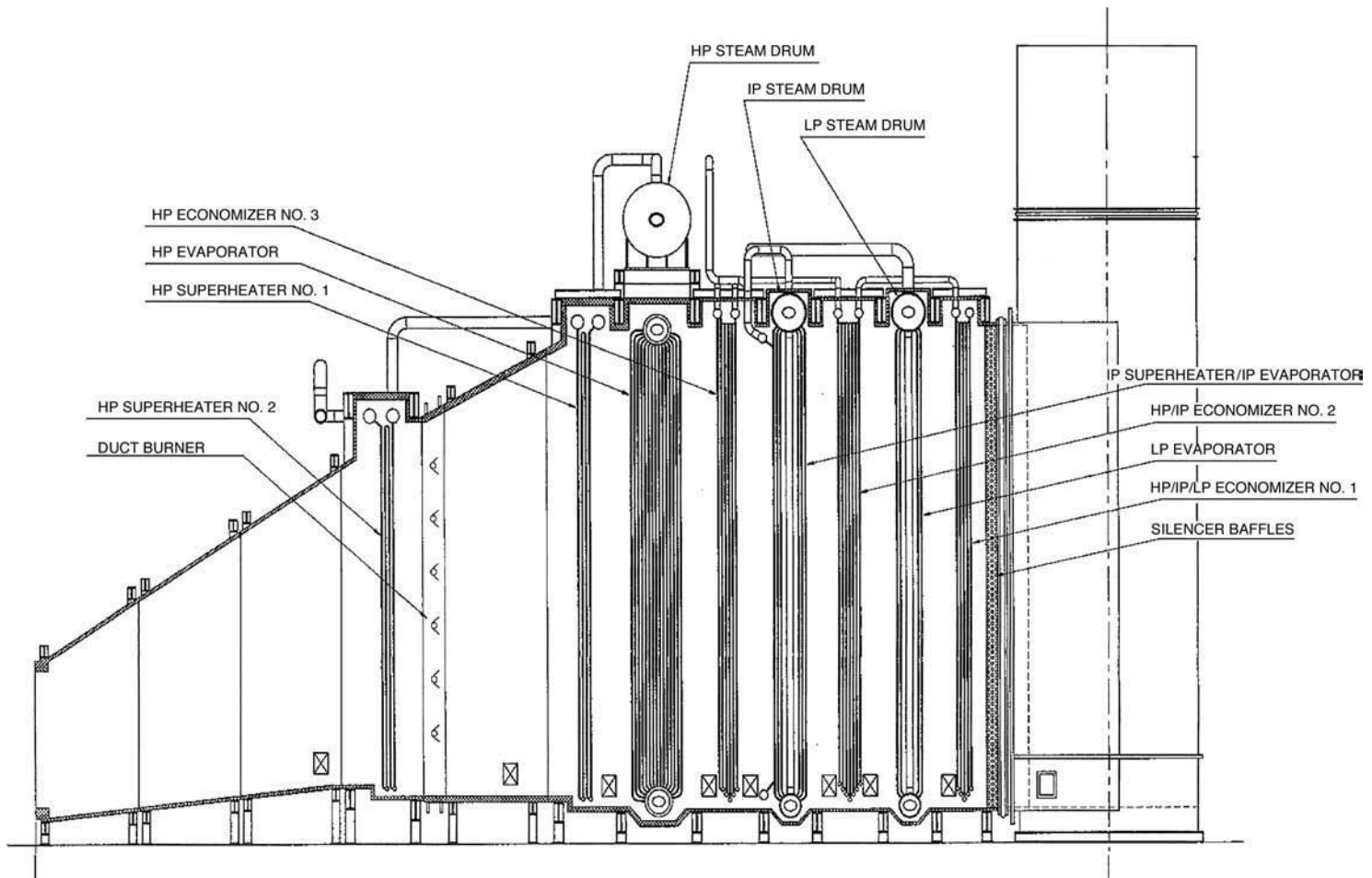


FIGURE 19.3 Schematic of HRSG.

efficiency as no outside air is used, lower operating cost as no blower is required, and improved destruction efficiency resulting from distribution of the flame across the duct section with a grid-type design.

19.2.4 STACK GAS REHEAT

Mounted at or near the base of a stack, the heat added by a duct burner will increase natural draft, possibly eliminating a need for induced-draft or eductor fans. In streams containing a large concentration of water vapor, the additional heat can also reduce or eliminate potentially corrosive condensation inside the stack. An additional source of augmenting combustion air is added if the stack gas oxygen concentration is too low to support combustion. This arrangement may also provide a corollary emissions reduction benefit (see Chapter 19.2.3).

19.3 BURNER TECHNOLOGY

19.3.1 IN-DUCT OR INLINE CONFIGURATION

Register or axial flow burner designs are adapted for installation inside a duct. The burner head is oriented such that flame will be parallel to and co-flow with the air or TEG stream, and the fuel supply piping is fed through the duct sidewall, turning 90° as it enters the burner. Depending on the total firing rate and duct size, only one burner may be sufficient, or several may be arrayed across the duct cross section. In-line burners typically require more air/TEG pressure drop, produce longer flames, and offer a less-uniform heat distribution than the grid type. On the other hand, they are more flexible in burning liquid fuels, can be more easily modified to incorporate augmenting air, and sometimes represent a less-expensive option for high firing rates in small ducts without sufficient room for grid elements.

19.3.2 GRID CONFIGURATION (GAS FIRING)

A series of linear burner elements that span the duct width are spaced at vertical intervals to form a grid. Each element is comprised of a fuel manifold pipe fitted with a series of flame holders (or wings) along its length. Fuel is fed into one end of the manifold pipe and discharged through discrete ports or through multi-port tips at intervals along its length, or through holes drilled directly into the pipe. Gas ports are positioned such that fuel is injected in co-flow with the TEG. The flame stabilizers meter turbine exhaust gas or air flow into the flame zone, thus developing low-pressure zones and eddy currents that anchor ignition. They also shield the flame to maintain suitably high flame temperatures for stability, while also preventing excessive flame cooling which might cause high emissions. Parts exposed to TEG and the flame zone are typically of high-temperature alloy construction.

19.3.3 GRID CONFIGURATION (LIQUID FIRING)

As with the gas-fired arrangement, a series of linear burner elements comprised of a pipe and flame holders (wings) spans the duct width. However, instead of multiple discharge points along the pipe length, liquid fuel is injected at one point per element through the duct sidewall, and directed parallel to the flame holders (cross-flow to the TEG). This configuration utilizes the duct cross section for containment of the flame length, thus allowing a shorter distance between the burner and downstream boiler tubes. The injection device, referred to as a “side-fired oil gun,” utilizes a mechanical nozzle supplemented by low-pressure air (2 to 8 psi) to break the liquid fuel into small droplets (atomization) that will vaporize and burn readily. Although most commonly used for light fuels, this arrangement is also suitable for some heavier fuels where the viscosity can be lowered by heating. In some cases, steam may be required instead of low-pressure air for adequate atomization of heavy fuels.

19.3.4 DESIGN CONSIDERATIONS

19.3.4.1 Fuels

19.3.4.1.1 *Natural Gas*

Natural gas is, by far, the most commonly used fuel as it is readily available in large volumes throughout much of the industrialized world. Because of its ubiquity, combustion characteristics are well understood and most burner designs are developed for this fuel.

19.3.4.1.2 *Refinery/Chemical Plant Fuels*

Refineries and chemical plants are large consumers of both electrical and steam power, which makes them ideal candidates for co-generation. In addition, these plants maintain extensive fuel systems to supply the various direct- and indirect-fired processes, as well as to make the most economical use of residual products. This latter requirement presents special challenges for duct burners, because the available fuels often contain high concentrations of higher molecular weight or unsaturated hydrocarbons with a tendency to condense and/or decompose inside burner piping. The location of burner elements inside the TEG duct, surrounded by high-temperature gases, exacerbates the problem. Plugging and failure of injection nozzles, or even the distribution pipe, may occur, with a corresponding decrease in online availability and increase in maintenance costs.

With appropriate modifications, however, duct burners can function reliably with most hydrocarbon-based gaseous fuels. Design techniques include full insulation of internal burner element manifolds, insulation and heat tracing of external headers and pipe trains, specially designed runners to reduce residence time, and blending of fuel and steam. Steam can also be used to periodically purge the burner elements of solid deposits before plugging occurs, and it may have some value in regasifying deposits via the “Water-Gas Shift” reaction.

19.3.4.1.3 *Low Heating Value*

By-product gases produced in various industrial processes such as blast furnaces, coke ovens, reformers, and flexicokers, or from mature landfills, contain combustible compounds along with significant concentrations of inert components, thus resulting in relatively low heating values (range 50 to 500 Btu/scf). These fuels burn more slowly and at lower peak temperatures than conventional fuels, and thus require special design considerations. Fuel pressure is reduced to match injection velocity to flame speed, and some form of shield or “canister” is employed to provide a protected flame zone with sufficient residence time to promote complete combustion before the flame is exposed to the quenching effects of TEG.

Other design considerations that must be considered include moisture content and particulate loading. High moisture concentration results in condensation within the fuel supply system, which in turn produces corrosion and plugging. Pilots and igniters are particularly susceptible to the effects of moisture because of small fuel port sizes, small igniter gap tolerance, and the insulation integrity required to prevent “shorting” of electrical components. A well-designed system may include a knock-out drum to remove liquids and solids, insulation and heat-tracing of piping to prevent or minimize condensation, and low-point drains to remove condensed liquids. Problems are usually most evident after a prolonged period of shutdown.

Solid particulate can cause plugging in gas injector ports and other fuel system components and should therefore be removed to the maximum practical. In general, particle size should be no greater than 25% of the smallest port, and overall loading should be no greater than 5 ppm by volume (weight).

19.3.4.1.4 *Liquid Fuels*

In co-generation applications, duct burners are commonly fired with the same fuel as the turbine, which is typically limited to light oils such as no. 2 diesel, kerosene, or naphtha. For other applications, specially modified side-fired guns or an in-line design can be employed to burn heavier oils such as no. 6 and some waste fuels.

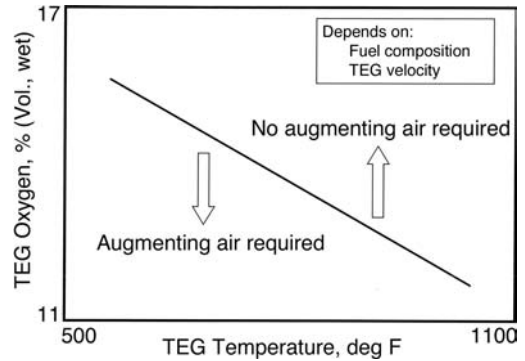


FIGURE 19.4 O₂ vs. temperature.

19.3.4.2 Combustion Air and Turbine Exhaust Gas

19.3.4.2.1 Temperature and Composition

Oxygen used for supplementary firing in HRSG co-generation applications is provided by the residual in the turbine exhaust gas instead of from an external source of air. Because this flue gas is already at an elevated temperature, duct burner thermal efficiency can approach 100%, as relatively little heat is required to raise the combustion product temperature to the final fired temperature entering the boiler. TEG, however, contains less oxygen than fresh air, typically between 11 and 16% by volume, which in conjunction with the TEG temperature significantly affects the combustion process. As the oxygen concentration and TEG temperature decrease, products of incomplete combustion (CO and unburned hydrocarbons) occur more readily, eventually progressing to combustion instability. The effect of low oxygen concentrations can be partially offset by higher temperature; and, conversely, higher oxygen concentrations will partially offset the detrimental effects of low TEG temperatures. This general relationship is depicted graphically by Figure 19.4. Duct burner emissions are discussed in more detail elsewhere in this chapter.

One measure used to predict potential combustion success is the calculated adiabatic flame temperature with a stoichiometric mixture. The burner can then be designed to create a local high-temperature condition for stable combustion, while not allowing premature quenching by the remaining excess TEG. Flame speed is another measure of combustibility and can be calculated for unusual fuel constituents.

The oxygen remaining from the turbine combustion is usually many times greater than required for supplemental firing. The final concentration of O₂ after supplemental firing is frequently still above 10%. In the extreme, a fully fired boiler is possible, with the residual O₂ as low as 2%. Fully fired HRSGs can produce large amounts of steam but are rare because the economics favor the power-to-heat ratio of unfired or supplemental fired HRSG.

19.3.4.2.2 Turbine Power Augmentation

During periods of high electrical demand, various techniques are employed by turbine suppliers to increase power output, and most methods increase the concentration of water vapor in the TEG. The corresponding effect is a reduction in TEG oxygen concentration and temperature with consequent effects on duct burner combustion. Depending on the amount of water vapor used, CO emissions may simply rise or, in extreme cases, the flame may become unstable. The former effect can be addressed with an allowance in the facility operating permit or by increasing the amount of CO catalyst in systems so equipped. The latter requires air augmentation for the duct burner, a process wherein fresh air is injected at a rate sufficient to raise the TEG oxygen concentration to a suitable level.

19.3.4.2.3 Velocity and Distribution

Regardless of whether TEG or fresh air is used, velocity across the flame stabilizers must be sufficient to promote mixing of the fuel and oxygen, but not so great as to prevent the flame from anchoring

to the burner. Grid-type configurations can generally operate with velocities ranging from 20 to 90 fps (feet per second) and pressure drops of less than 0.5 inches water column (in. w.c.). In-line or register burners typically require velocities of 100 to 150 fps with a pressure drop of 2 to 6 in. w.c.

Grid burners are designed to distribute heat uniformly across the HRSG or boiler tube bank, and thus require a reasonably uniform distribution of TEG or air to supply the fuel with oxygen. Nonuniform distribution creates localized areas of low velocity resulting in poor flame definition along with high emissions of CO and unburned hydrocarbons. In addition, the variable flows will affect the burner flame length and boiler inlet temperature profile. Gas turbine exhaust flow patterns combined with the rapidly diverging transition duct will almost always produce an unsatisfactory flow profile that must be corrected by means of a redistribution or straightening device. Likewise, the manner in which an alternate ambient air source is introduced into a duct may also result in flow maldistribution requiring some level of correction. Selection and design of flow straightening devices are discussed elsewhere in this chapter.

In instances where the bulk TEG or air velocity is lower than that required for proper burner operation, flow straightening alone is not sufficient. It becomes necessary to restrict a portion of the duct cross section at or near the plane of the burner elements, thereby increasing the “local” velocity across flame holders. This restriction, also referred to as “blockage,” commonly consists of unfired runners or similar shapes uniformly distributed between the firing runners. The extra blockage is almost always needed for duct burners embedded in the superheater section of the HRSG, and less often required for duct burners located in the inlet transition duct. The designer must also account for the exhaust gas flow conditions at various turbine load and ambient air temperature.

In-line or register burners inject fuel in only a few (or possibly only one) positions inside the duct, and can therefore be positioned in an area of favorable flow conditions, assuming the flow profile is known. On the other hand, downstream heat distribution is less uniform than with grid designs and flames may be longer. As with grid-type burners, in some cases it may be necessary to block portions of the duct at or just upstream of the burners to force a sufficient quantity of TEG or air through the burner.

19.3.4.2.4 Ambient Air Firing (air-only systems and HRSG backup)

Velocity and distribution requirements for air systems are similar to those for TEG, although inlet temperature is not a concern because of the relatively higher oxygen concentration. As with TEG applications, the burner elements are exposed to the products of combustion, so material selection must take into account the maximum expected fired temperature.

Ambient (or fresh) air backup for HRSGs presents special design challenges. Because of the temperature difference between ambient air and TEG, designing for the same mass flow and fired temperature will result in velocity across the burner being approximately one-third that of the TEG case. Reducing the air flow to save on fan horsepower may make the design unwieldy or impossible. If the cold-condition velocity is outside the acceptable range, it will be necessary to add blockage, as described elsewhere in this chapter. Fuel input capacity must be also be increased to provide the heat required to raise the air from ambient to the design firing temperature. By far, the most difficult challenge is related to flow distribution. Regardless of the manner in which backup air is fed into the duct, a flow profile different from that produced by the TEG is virtually certain. Flow straightening devices can therefore not be optimized for either case, but instead require a compromise design to provide acceptable flow distribution and pressure drop results for both operating modes. If the two flow patterns are radically different, it may ultimately be necessary to alter the air injection arrangement independent of the TEG duct straightening device.

19.3.4.3 Augmenting Air

As turbines have become more efficient and more work is extracted in the form of, for example, electricity, the oxygen level available in the TEG continues to decrease. To some extent, a correspondingly higher TEG temperature provides some relief for duct burner operation.

In some applications, however, an additional oxygen source may be required to augment that available in the turbine exhaust gas when the oxygen content in the TEG is not sufficient for combustion at the available temperature of the TEG. If the mixture adiabatic flame temperature is not high enough to sustain a robust flame in the highly turbulent stream, the flame may become unstable.

The problem can be exacerbated when the turbine manufacturer adds large quantities of steam or water for NO_x control and power augmentation. A corresponding drop in TEG temperature and oxygen concentration occurs because of dilution. The TEG temperature is also reduced in installations where the HRSG manufacturer splits the steam superheater and places tubes upstream of the duct burner.

By combining results from field measurements with data from their research and development facilities, manufacturers have defined the oxygen requirement with respect to TEG temperature and fuel composition and are able to quantify the amount of augmenting air required under most conditions likely to be encountered. In cases where augmenting air is required, the flow may be substantial — from 30 to 100% of the theoretical air required for the supplemental fuel. It is not normally feasible to raise the level of oxygen in the entire stream to an acceptable level, so it is raised only in the locality of the burner in specially designed systems.

The augmenting air runner of one manufacturer consists of a graduated air delivery tube designed to ensure constant velocity across the length of the tube. Equal distribution of augmenting air across the face of the tube is imperative. The augmenting air is discharged from the tube into a plenum and passes through a second distribution grid to further equalize the flow. The air passes through perforations in the flame holder where it is intimately mixed with the fuel in the primary combustion zone. This intimate mixing ensures corresponding low CO and UHC emissions under most conditions likely to be encountered. Once the decision has been made to supply augmenting air to a burner, it is an inevitable result of the design that the augmenting air will be part of the normal operating regime of the combustion runner.

19.3.4.4 Equipment Configuration and TEG/Combustion Air Flow Straightening

The turbine exhaust gas/combustion air velocity profile at the duct burner plane must be within certain limits to ensure good combustion efficiency and, in co-generation applications, this is rarely achieved without flow straightening devices. Even in nonfired configurations, it may be necessary to alter the velocity distribution to make efficient use of the boiler heat transfer surface. [Figure 19.6](#) shows a comparison of flow variation with and without flow straightening.

The modern HRSG has become a huge structure, often rising five stories in the air and up to four times as wide as their 1960-era ancestors. The duct burners are commonly positioned in the TEG inlet duct, either upstream of the first bank of heat transfer tubes or nested in the boiler superheater section between banks of tubes. In the former case, a straightening device would be mounted just upstream of the burner, while in the latter, it is mounted either upstream of the first tube bank or between the first tube bank and (upstream of) the burner. Although not very common, some HRSG design configurations utilize two stages of duct burners with heat transfer tube banks in between and a flow straightening device upstream of the first burner. Such an arrangement is, however, problematic, because the TEG downstream of the first stage burner may not have the required combination of oxygen and temperature properties required for proper operation of the second stage burner.

Perforated plates extending across the entire duct cross section are most commonly used for flow straightening, because experience has shown they are less prone to mechanical failure than vane-type devices, although they require a relatively high pressure drop. The pattern and size of perforations can be varied to achieve the desired distribution. Vanes can produce comparable results with significantly less pressure loss, but require adequate structural reinforcement to withstand the flow-induced vibration inherent in HRSG systems. Regardless of the method used, flow pattern complexity, particularly in TEG applications, usually dictates the use of either physical or computational fluid dynamics (CFD) modeling for distributor design optimization (see [Figure 19.5](#)).

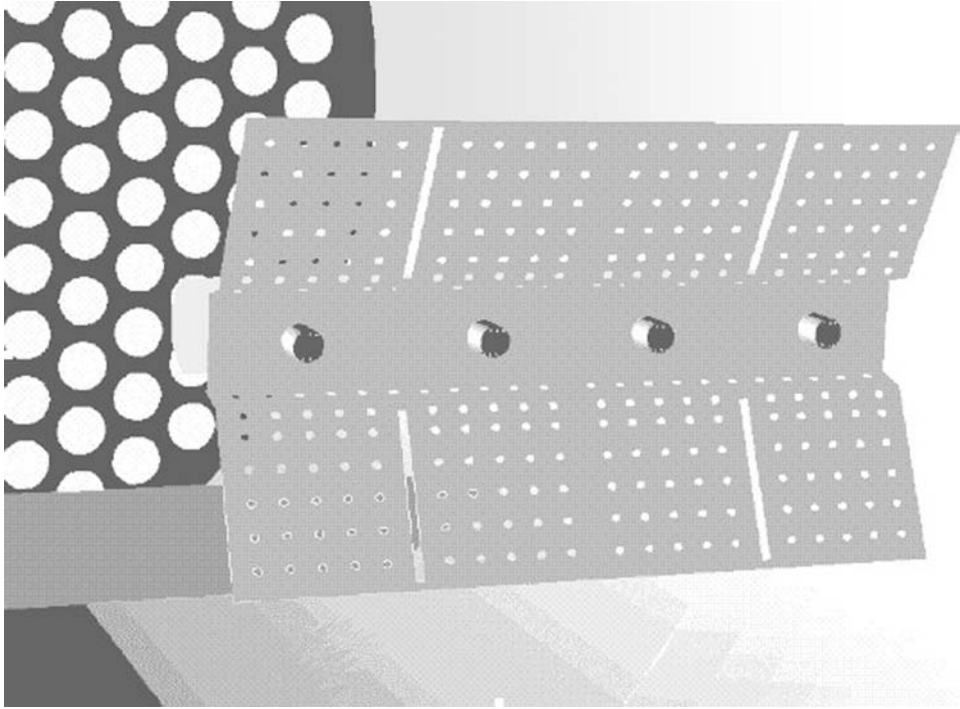


FIGURE 19.5 CFD model of duct burner element.

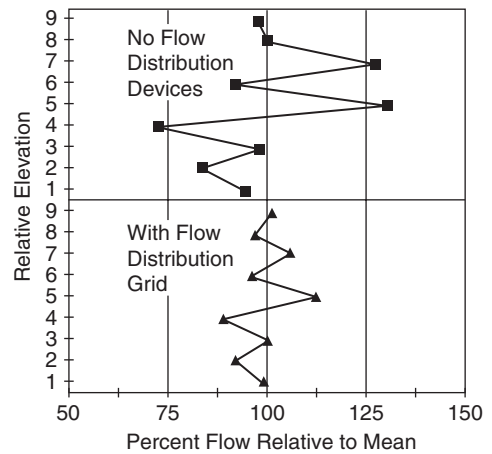


FIGURE 19.6 Comparison of flow variation with and without straightening device.

19.3.4.4.1 Physical Modeling

TEG/air flow patterns are determined by inlet flow characteristics and duct geometry, and are subject to both position and time variation. The design of an efficient (low pressure loss) flow-straightening device is therefore not a trivial exercise, and manual computational methods are impractical. Historically, physical models, commonly 1:6 to 1:12 scale, are constructed, and flow characteristics are analyzed by measuring pressure or velocity and by flowing air with smoke tracers or water with polymer beads through the model (see Figure 19.7). The simulation velocity is maintained in

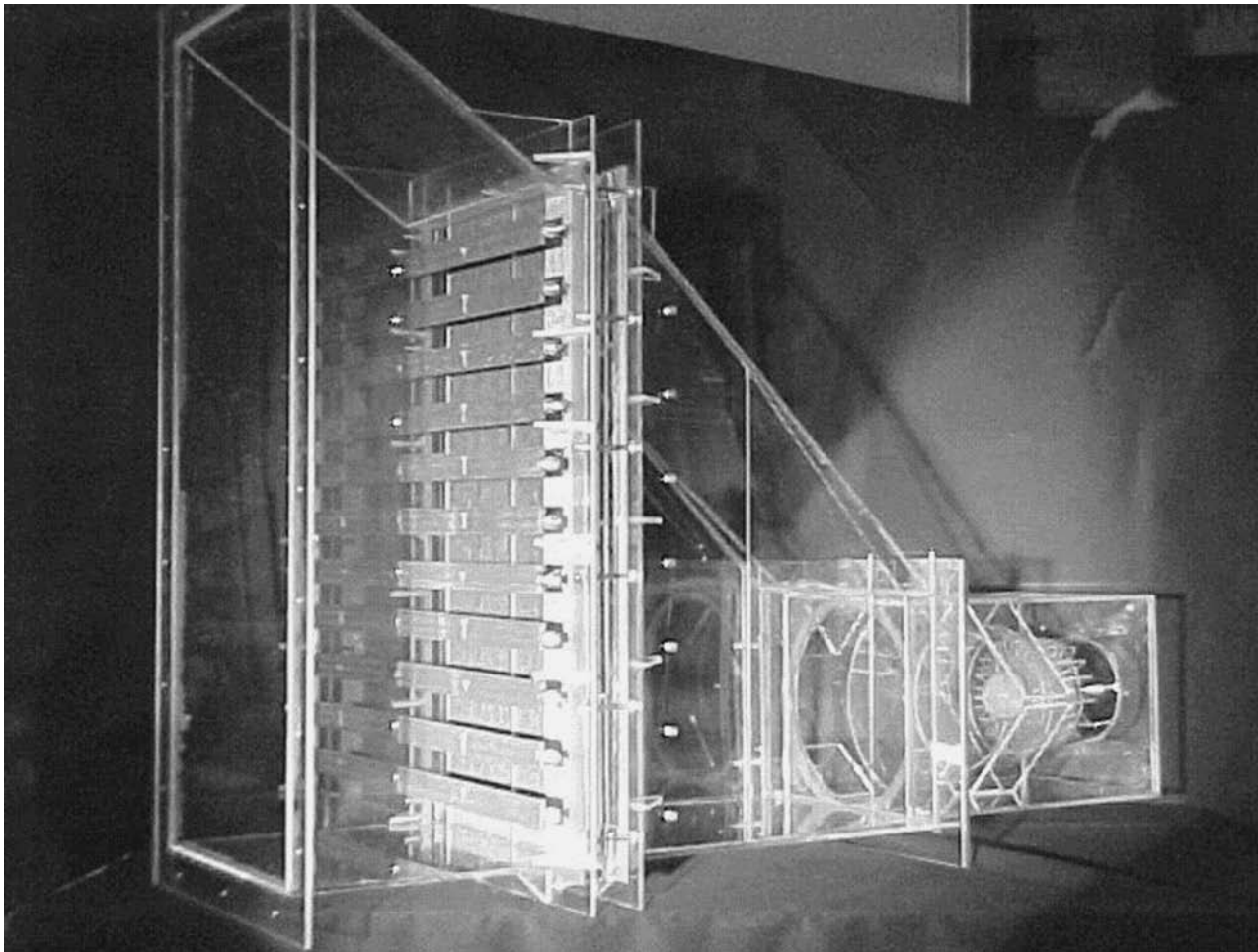


FIGURE 19.7 Physical model of burner.

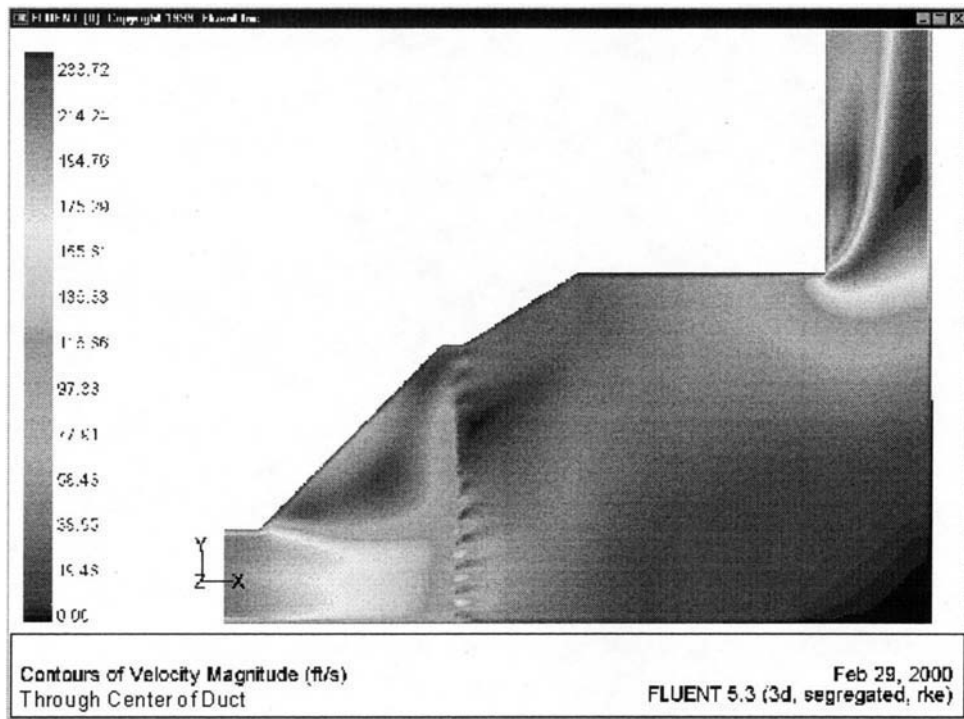


FIGURE 19.8 Sample result of CFD modeling performed on a burner.

the turbulent flow regime for scaling but may not be directly related to the actual condition. This method is generally accepted and produces reasonable results, although the tests conducted at ambient conditions (known as “cold flow”) are not capable of simulating buoyant effects that may occur at elevated temperatures.

19.3.4.4.2 Computational Fluid Dynamic (CFD) Modeling

Flow modeling with CFD, using a computer-generated drawing of the inlet duct geometry, is capable of predicting flow pattern and pressure drop in the turbine exhaust flow path. The model can account for swirl flow in three dimensions to accurately predict pressure drop and to subsequently design a suitable device to provide uniform flow. The CFD model must be quite detailed to calculate flow patterns incident and through a perforated grid or tube bank, while also keeping the overall model solution within reasonable computation time. Care must be taken to evaluate the model because shortcuts to reduce complexity by assuming symmetry may hide the adverse effect of turbine-induced swirl. Combustion effects can be included in the calculations at the cost of increased computation time. Emissions calculations are not yet reliable, however. [Figure 19.8](#) shows a sample result of CFD modeling performed on an HRSG inlet duct.

19.3.4.5 Wing Geometry Variations

19.3.4.5.1 Flame Holders

Design of the flame stabilizer, or flame holder, is critical to the success of supplementary firing. Effective emission control requires that the TEG be metered into the flame zone in the required ratio to create a combustible mixture and ensure that the combustion products do not escape before the reactions are complete. Each duct burner manufacturer has developed proprietary designs in response to new turbine and HRSG design requirements, to enable them to provide the desired results.

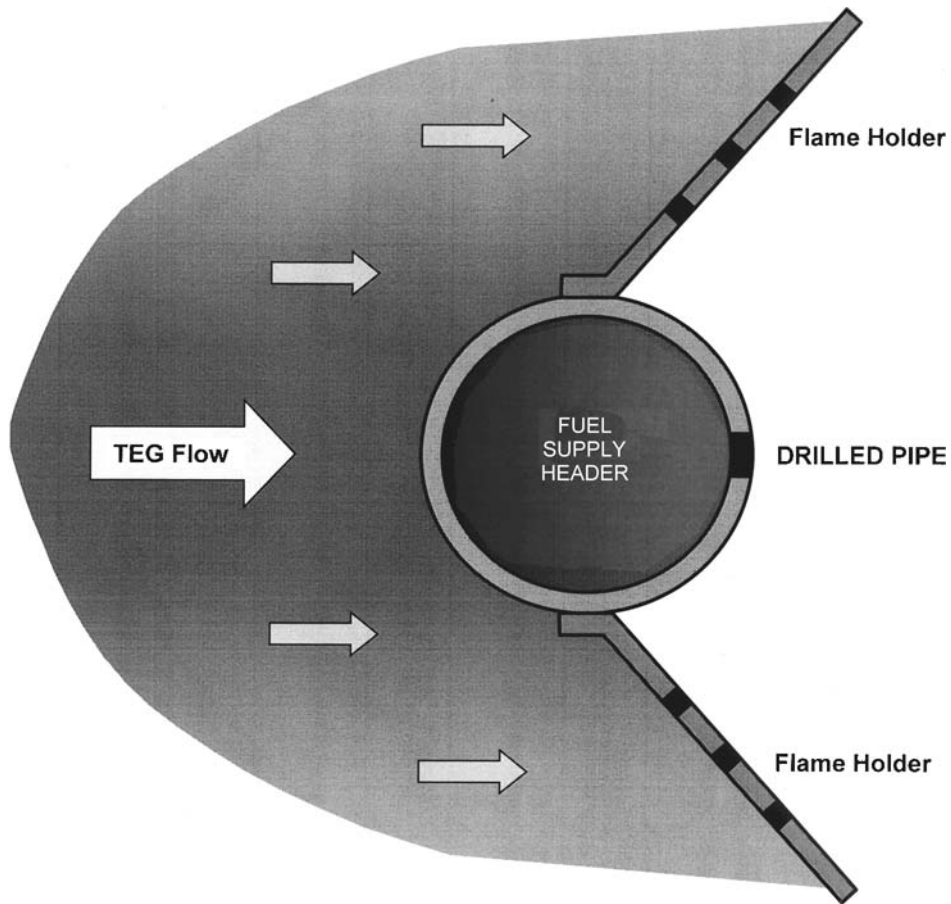


FIGURE 19.9 Drilled pipe duct burner.

19.3.4.5.2 Basic Flame Holder

In its basic form, a fuel injection system and a zone for mixing with oxidant are all that is required for combustion. For application to supplemental firing, the simple design shown in [Figure 19.9](#) consists of an internal manifold or “runner,” usually an alloy pipe with fuel injection orifices spaced along the length. A bluff body plate, with or without perforations, is attached to the pipe to protect the flame zone from the turbulence in the exhaust gas duct. The low-pressure zone pulls the flame back onto the manifold. This primitive runner may overheat the manifold and cause distortion of the metallic parts and internal coking. Emissions are unpredictable with changing geometry and CO is usually much higher than the current typically permitted levels of 0.04 to 0.1 lb/MMBtu (HHV basis).

19.3.4.5.3 Low Emissions Design

Modifications to the design for lower emission performance generally include a larger cross section in the plane normal to the exhaust flow. The increased blocked area protects the fuel injection zone and increases residence time. The NO_x is reduced by staging the oxygen-depleted TEG; the CO/UHC is reduced by the delayed quenching and back mixing. The correct flow rate of TEG is metered through orifices in the flame holder, and the fuel injection velocity and angle are designed to enhance combustion efficiency. The flame zone is pushed away from the internal manifold

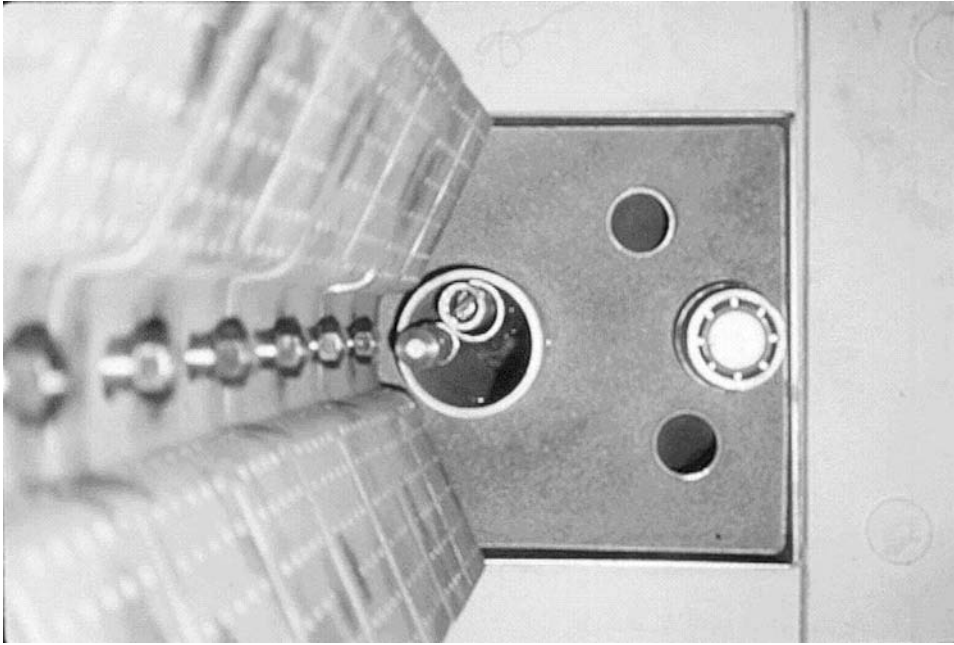


FIGURE 19.10 Low-emission duct burner.

(“runner” pipe), creating space for cooling TEG to bathe the runner and flame holder and enhance equipment life.

Each manufacturer approaches the geometry somewhat differently. Some manufacturers use cast alloy pieces welded together to provide the required blockage. These standard pieces are difficult to customize to specific applications and often add significant weight. Hot burning fuels, such as hydrogen, may not receive the cooling needed to protect the metal from oxidation. Alternately, fuels subject to cracking (e.g., propylene) may not have the oxygen needed to minimize coke build-up.

Another manufacturer supplies custom designs to accommodate velocity extremes, while maintaining low emissions. In the design shown in [Figure 19.10](#), the flame holder is optimized with CFD and research experimentation to enhance mixing and recirculation rate. Special temperature-resistant materials of construction are easily accommodated. This supplier also uses patented removable fuel tips with multiple orifices, which can be customized to counteract any unexpected TEG flow distribution discovered after commercial operation. [Figure 19.11](#) depicts the flow patterns of air/TEG and fuel in relation to the typical duct burner flame holder.

19.3.4.6 Emissions

19.3.4.6.1 *NO_x and NO vs. NO₂*

Formation of NO and NO₂ is the subject of ongoing research to understand the complex reactions (see Chapter 6). Potentially, several oxides of nitrogen (NO_x) can be formed during the combustion process, but only nitric oxide (NO) and nitrogen dioxide (NO₂) occur in significant quantities. NO is colorless and NO₂ has a reddish-brown color.

In the elevated temperatures found in the flame zone in a typical HRSG turbine exhaust duct, NO formation is favored almost exclusively over NO₂ formation. Turbine exhaust NO_x was historically 95% NO and 5% NO₂, although newer turbines have increased this ratio to 70/30. In the high temperature zone, NO₂ dissociates to NO via the following mechanism:



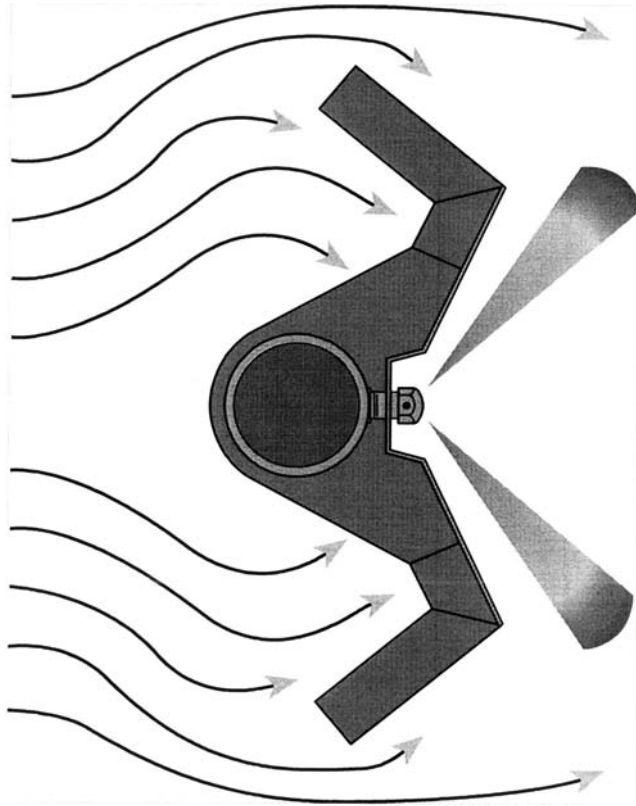
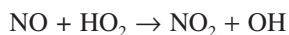


FIGURE 19.11 Flow patterns around flame stabilizer.

However, after the TEG exits the hot zone and enters the cooling zone at the boiler tubes, reaction slows and the NO_2 is essentially fixed. At the cooler stack outlet, the entrained NO is very slowly oxidized to NO_2 through a complex photochemical reaction with atmospheric oxygen. The plume will be colorless unless the NO_2 increases to about 15 ppm, at which time a yellowish tint is visible. Care must be taken in duct burner design because NO can also be oxidized to NO_2 in the immediate post-flame region by reactions with hydroperoxyl radicals:



if the flame is rapidly quenched. This quenching can occur because of the large quantity of excess TEG commonly present in duct burner applications. Conversion to NO_2 may be even higher at fuel turn-down conditions where the flame is smaller and colder. NO_2 formed in this manner can contribute to “brown plume” problems and may even convert some of the turbine exhaust NO to NO_2 . Co-generation units with catalyst to oxidize CO will have an increase in NO_2 and SO_3 content, which must be considered in the design of the NO_x removal system.

There are two principle mechanisms in which nitrogen oxides are formed:

1. *Thermal NO_x*. The primary method is thermal oxidation of atmospheric nitrogen in the TEG by combustion-generated oxygen free radicals by way of the Zeldovitz mechanism. NO_x formed in this way is called *thermal NO_x*. As the temperature increases in the combustion zone and surrounding environment, increased amounts of nitrogen (N_2) and

oxygen (O_2) from the TEG are ionized and converted to NO. Thermal NO_x formation is predominant in the peak temperature zones of the flame.

2. *Fuel-Bound Nitrogen NO_x*. The secondary method to form NO_x is the reaction of oxygen with nitrogen that is chemically bound in compounds contained in the fuel. NO_x formed in this manner is called *fuel* NO_x. Large amounts of NO_x can be formed by fuels that contain molecularly bound nitrogen, such as, for example, amines and cyanates. If a gaseous fuel such as natural gas contains diluent N_2 , it simply behaves as atmospheric nitrogen and will form NO_x only if it disassociates in the high-temperature areas. However, if the gaseous fuel contains, for example, ammonia (NH_3), this nitrogen is considered to be bound. In the low concentrations typically found in gaseous fuels, the conversion to NO_x is close to 100% and can have a major impact on NO_x emissions.

Bound nitrogen in liquid fuel is contained in the long carbon chain molecules. Distillate oil is the most common oil fired in duct burners as a liquid fuel. The fuel-bound nitrogen content is usually low, in the range of 0.05 weight percent. Conversion to NO_x is believed to be 80 to 90%. For no. 6 oil, containing 0.30 weight percent nitrogen, the conversion rate to NO_x would be about 50%. Other heavy waste oils or waste gases with high concentrations of various nitrogen compounds may add relatively high emissions. Consequently, fuel NO_x can be a major source of nitrogen oxides and, in liquid firing, may predominate over thermal NO_x.

The impact of temperature on NO_x production in duct burners is not as pronounced as in, for example, fired heaters or package boilers. One reason is that both the bulk fired temperature and the adiabatic flame temperature are lower than in fired process equipment.

When used to provide supplementary firing of turbine exhaust, duct burners are generally considered to be “low-NO_x” burners. Because the turbine exhaust contains reduced oxygen, the peak flame temperature is reduced and the reaction speed for O_2 and free radical N^+ to form NO_x is thus lowered. The burners also fire into much lower average bulk temperatures, usually less than 1600°F, than, for example, process burners or fired boilers. The high-temperature zones in the duct burner flames are smaller due to large amounts of flame quenching by the excess TEG. Finally, mixing is rapid and therefore retention time in the high-temperature zone is very brief.

The same duct burner, when used to heat atmospheric air, is no longer considered “Low NO_x” because the peak flame temperature approaches the adiabatic flame temperature in air.

Clearly, operating conditions have a major impact on NO formation during combustion. To properly assess NO_x production levels, the overall operating regime must be considered, including TEG composition, fuel composition, duct firing temperature, and TEG flow distribution.

19.3.4.6.2 *Visible Plumes*

Stack plumes are caused by moisture and by impurities in the exhaust. Emitted NO is colorless and odorless while NO₂ is brownish in color. If the NO₂ level in the flue gas exceeds about 15 to 20 ppm, the plume will take on a brownish haze. NO_x also reacts with water vapor to form nitrous and nitric acids. Sulfur in the fuel may oxidize to SO₃ and react with condensate or ammonia in the stack effluent, causing a more persistent white plume. Both nitric acid and sulfuric acid are components of “acid rain.”

19.3.4.6.3 *CO, VOC, Sox, and Particulate*

Carbon Monoxide. Carbon monoxide (CO), a product of incomplete combustion, has become a major permitting concern in gas turbine-based co-generation plants. Generally, CO emissions from modern industrial and aero-derivative gas turbines are very low at the design condition, in the range of a few parts per million (ppm). There are occasional situations in which CO emissions from the turbine increase because of a high rate of water injection for NO_x control or at operation at partial load. The primary concern in this section is the potentially large CO contribution from supplementary firing. The same low-temperature combustion environment that suppresses NO_x formation is

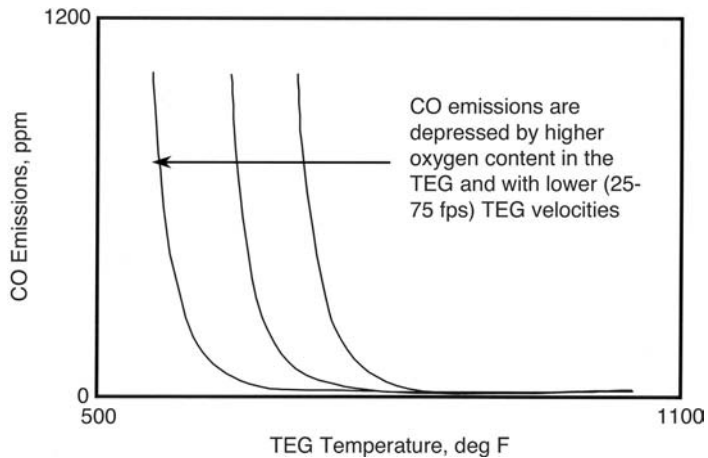


FIGURE 19.12 Effect of conditions on CO formation.

obviously unfavorable for complete oxidation of CO to CO₂. Increased CO production occurs when a fuel is combusted under fuel-rich conditions or when a flame is quenched before complete burnout. These conditions causing CO production (see Figure 19.12) can occur if there is poor distribution of TEG to the duct burner which, in the extreme, causes some burner elements to fire fuel-rich and others fuel-lean, depending on the efficiency of the TEG distribution device. The downstream residence time is seldom long enough to allow the extra CO to mix and completely react with the excess oxygen.

The factors affecting CO emissions include:³

- Turbine exhaust gas maldistribution
- Low TEG approach temperature
- Low TEG oxygen content
- Flame quench on “cold” screen tubes
- Improperly designed flame holders that allow flame quench by relatively cold TEG
- Steam or water injection
- Low firing rate promoting quenching
- Insufficient residence time or burnout distance

Unburned Hydrocarbons (UHCs). In a mechanism similar to CO generation, unburned hydrocarbons are formed in the exhaust gas when fuel is burned without sufficient oxygen, or if the flame is quenched before combustion is complete. UHCs can consist of hydrocarbons (defined as any carbon-hydrogen molecule) of one carbon or multiple carbon molecules. The multiple carbon molecules are often referred to as long-chain hydrocarbons. Unburned hydrocarbons are generally classified in two groups:

1. Unburned hydrocarbons reported as methane
2. Nonmethane hydrocarbons or volatile organic compounds (VOCs)

The reason for the distinction and greater concern for VOCs is that longer chain hydrocarbons play a greater role in the formation of photochemical smog. VOCs are usually defined as molecules of two carbons or greater, or sometimes three carbons or greater. These definitions are set by local air quality control boards and vary across the United States.

UHCs can be reduced by correct combustion of the fuel and by a CO oxidation catalyst. However, hydrocarbon compounds will always be present in trace quantities, regardless of how the HRSG system is operated. Both UHCs and VOCs are typically higher when firing with liquid fuels.

Sulfur Dioxide. Sulfur dioxide (SO₂) is a colorless gas that has a characteristic smell in concentrations as low as 1 ppm. Sulfur dioxide is formed when sulfur (S) in the fuel combines with oxygen (O₂) in the TEG. If oxygen is present (from excess of combustion) and the temperature is correct, the sulfur will further combine and be converted to sulfur trioxide (SO₃). SO₂ is also converted to SO₃ by the CO oxidation catalyst. These oxides of sulfur are collectively known as SOx.

Except for sulfur compounds present in the incoming particulate matter, all of the sulfur contained in the fuel is converted to SO₂ or SO₃. Sulfur dioxide will pass through the boiler system to eventually form the familiar “acid rain” unless a gas-side scrubbing plant is installed. Sulfur trioxide can, in the cooler stages of the gas path, combine with moisture in the exhaust gas to form sulfuric acid (H₂SO₄). This material is highly corrosive and will be deposited in ducts and the economizer, if the exhaust gas is below condensing temperatures. Natural gas fuels are, fortunately, very low in sulfur and do not usually cause a problem. However, some oil fuels and plant gases can be troublesome in this respect.

Particulate Matter (PM). Particulate emissions are formed from three main sources: ash contained in liquid fuels, unburned carbon in gas or oil, and SO₃. The total amount of particulate is often called TSP (total suspended particulate). There is a concern for the smaller sized portion of the TSP, as this stays suspended in air for a longer period of time. The PM-10 is the portion of the total particulate matter that is less than 10 microns (1 × 10⁻⁶ m) in size. Particles smaller than PM-10 are on the order of smoke.

Typical NOx and CO emissions for various fuels are shown in Table 19.1.

19.3.5 MAINTENANCE

19.3.5.1 Normal Wear and Tear

If nothing has been replaced in the past 5 years and the burner (or turbine/HRSG set) is operated fairly continuously, it is likely that some tips, pilot parts, or flame stabilizers may require replacement.

TABLE 19.1
Typical NOx and CO Emissions from Duct Burners

Gas	NOx (lb/10 ⁶ Btu Fired)	CO (lb/10 ⁶ Btu Fired)
Natural gas	0.10	0.04–0.08
Hydrogen gas	0.15	0.00
Refinery gas	0.1–0.15	0.03–0.08
Plant gas	0.11	0.04–0.01
Flexicoker gas	0.08	0.01
Blast furnace gas	0.03–0.05	0.12
Producer gas	0.05–0.1	0.08
Syn fuels	0.08–0.12	0.08
Propane	0.14	0.12
Butane	0.14	0.12

Note: NOx emissions from butane and propane can be modified by direct steam injection into gas or burner flame. CO emissions are highly dependent on residence time, TEG approach temperature, and HRSG fired temperature.

19.3.5.2 Damage

This refers to damage due to misuse, system upsets, or poor maintenance practices. Older systems designed without sufficient safety interlocks (TEG trip, high temperature) sometimes expose parts to excessively high temperatures, which results in equipment warpage and oxidation failure. Because of the severe conditions, it is not always possible to predict where failure might occur.

19.3.5.3 Fuel Quality/Composition

Some refinery fuels or waste fuels contain unsaturated components and/or liquid carryover. Eventually, these compounds will form solids in the runner pipes or directly in tips, which results in plugging and eventual failure. Products of corrosion may also accumulate in fuel piping, particularly when the burner is fired intermittently.

The following are some items to look for when operational problems are encountered:

- *Plugged gas ports, which are evidenced by gaps in the flame or high fuel pressure.* Gas ports may simply consist of holes drilled into the element manifold pipe, or they may be located in individual removable tips. Designs of the former type may be re-drilled or else the entire manifold pipe must be replaced. Discrete tips can be replaced individually, as required.
- *Warped flame holders (wings).* Some warping is normal and will not affect flame quality, but excessive deformation such as “curling” around the gas ports will degrade the combustion and emissions performance. Most grid-type burner designs permit replacement of individual flame holder segments.
- *Oxidation of flame holders (wings) or portions of flame holders.* If more than one quarter of the flame holder is missing, it is a good candidate for replacement. Fabricated and cast designs are equally prone to oxidation over time. If oxidation is caused by flame recirculation behind the runner, the TEG flow should be modified to remove the recirculation. Most grid-type burner designs permit replacement of individual flame holder segments. For hot burning fuels (hydrogen and unsaturated hydrocarbons), materials suitable for higher temperatures may be substituted.
- *Severe sagging of runner pipes (grid design only).* If the manifold pipe is no longer supported at both ends, it should be replaced. Beyond that relatively extreme condition, sagging at midspan in excess of approximately 1 to 2 inches (3 to 5 cm) per 10 ft of length should be corrected by runner replacement and/or installation of an auxiliary support.

19.3.6 ACCESSORIES

19.3.6.1 Burner Management System

All fuel burning systems should incorporate controls that provide for safe manual light-off and shutdown, as well as automatic emergency shutdown upon detection of critical failures. Control logic may reside in a packaged flame safeguard module, a series of electromechanical relays, a programmable logic controller (PLC), or a distributed control system (DCS). At a minimum, the duct burner management system should include following:

- Flame supervision for each burner element
- Proof of completed purge and TEG/combustion air flow before ignition can be initiated
- Proof of pilot flame before main fuel can be activated
- Automatic fuel cutoff upon detection of flame failure, loss of TEG/combustion air, and high or low fuel pressure

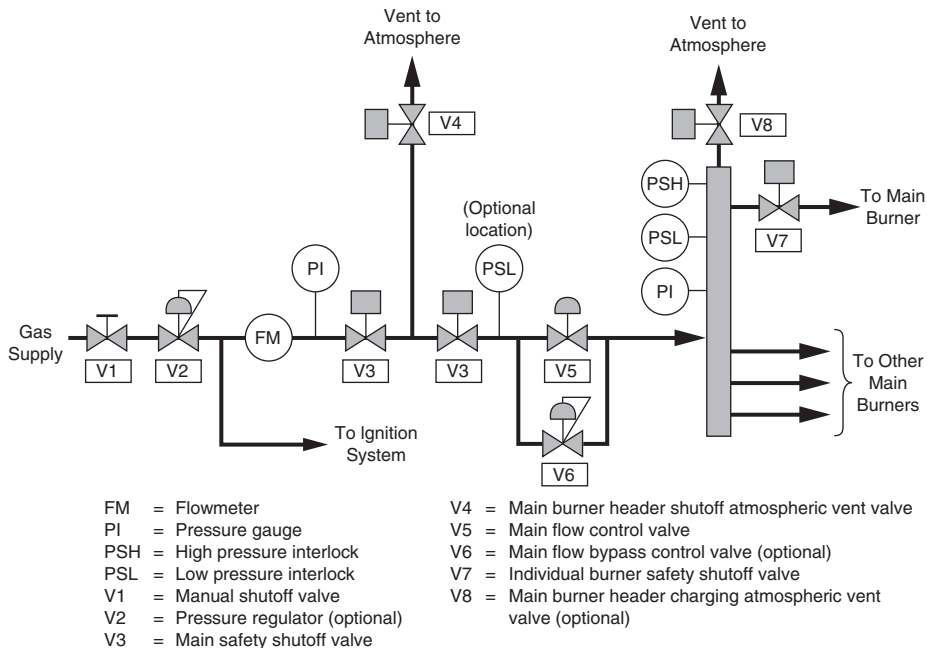


FIGURE 19.13 Typical main gas fuel train: multiple elements with individual firing capability.

Other interlocks designed to protect downstream equipment may also be included, such as high boiler tube temperature or loss of feed water.

19.3.6.2 Fuel Train

Fuel flow to the burners is controlled by a series of valves, safety devices, and interconnecting piping mounted to a structural steel rack or skid. A properly designed fuel train will include the following, at a minimum:

- At least one manual block valve
- Two automatic block valves in series
- One vent valve between the automatic block valves (gas firing only)
- Flow control valve
- High and low fuel pressure switches
- Two pressure gages, one each at the fuel inlet and outlet

Depending on the custom and operating requirements at a particular plant, pressure regulation, flow measurement devices, and pressure transmitters may also be incorporated. See [Figure 19.13](#) and [Figure 19.14](#) for typical duct burner main fuel system piping arrangements.

19.3.7 DESIGN GUIDELINES AND CODES

19.3.7.1 NFPA 85 (National Fire Protection Association)

First issued for HRSG systems in 1995 as NFPA 8506 and combined into NFPA 85 with other boiler applications in 2000, this standard has become the *de facto* guideline for heat recovery steam generators in the U.S. and in many other countries that have not developed their own national standards. Specific requirements for burner safety systems are included, but as stated in the foreword,

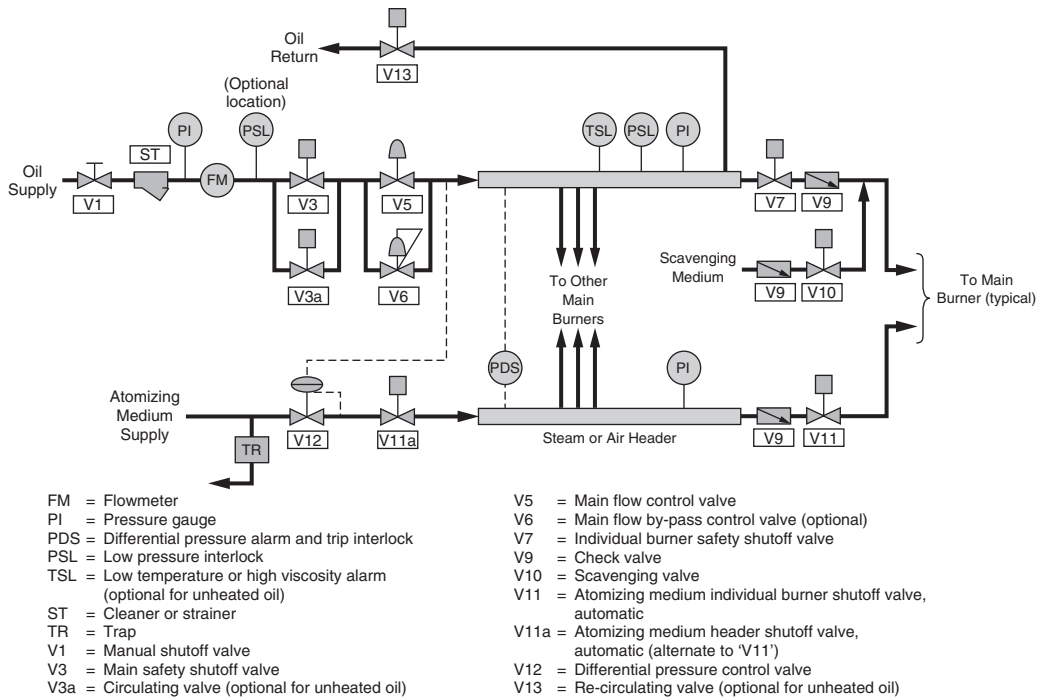


FIGURE 19.14 Typical main oil fuel train: multiple elements.

it does not encompass specific hardware applications, nor should it be considered a “cookbook” for the design of a safe system. Prior to the issuance of HRSG standards, designers often adapted NFPA standards for fired boilers to HRSG systems, which resulted in design inconsistencies.²

19.3.7.2 FM (Factory Mutual)

An insurance underwriter that publishes guidelines on combustion system design, Factory Mutual also “approves” specific components such as valves, pressure switches, and flame safeguard equipment that meet specific design and performance standards. Manufacturers are given permission to display the FM symbol on approved devices. Although FM approval may be required for an entire combustion control system, it is more common for designers to simply specify the use of FM-approved components.

19.3.7.3 UL (Underwriters Laboratories)

Well known in the U.S. for its certification of a broad range of consumer and industrial electrical devices, UL authorizes manufacturers to display their label on specific items that have demonstrated compliance with UL standards. Combustion system designers will frequently require the use of UL-approved components in burner management systems and fuel trains. Approval can also be obtained for custom-designed control systems, although this requirement generally applies only to a few large cities and a few regions in the U.S.

19.3.7.4 ANSI B31.1 and B31.3 (American National Standards Institute)

These codes address piping design and construction. B31.1 is incorporated in the NFPA 85 guideline, while B31.3 is generally used only for applications in refining/petrochemical plants.

19.3.7.5 Others

The following may also apply to duct burner system designs, depending on the country where equipment will be operated:

- National Electrical Code (NEC)
- Canadian Standards Association (CSA) and province requirements (i.e., TSSA)
- International Electrotechnical Commission (IEC)
- European Committee for Electrotechnical Standardization (CENELEC)

REFERENCES

1. Fisk, Robert W. and VanHousen, Robert L., *Cogeneration Application Considerations*, GE Power Systems, Schenectady, NY, 1996.
2. NFPA 85 *Boiler and Combustion Systems Hazards Code*, 2001 Edition, NFPA, Quincy, MA, 2001.
3. Waibel, Richard T. and Somers, Steve, "Retrofitting Duct Burners for CO Control," Paper presented at *American Flame Research Committee*, 1996 meeting.

20 Air-Oxy/Fuel Burners

Charles E. Baukal, Jr., Ph.D., P. E.

CONTENTS

- 20.1 Introduction
- 20.2 Typical Use Methods
 - 20.2.1 Air Enrichment
 - 20.2.2 O₂ Lancing
 - 20.2.3 Oxy/Fuel
 - 20.2.4 Air-Oxy/Fuel
 - 20.2.5 Low-Purity O₂
- 20.3 Basics
 - 20.3.1 Definitions
 - 20.3.2 Operating Regimes
 - 20.3.3 Combustion Products
 - 20.3.4 Properties
 - 20.3.4.1 Flame Temperature
 - 20.3.4.2 Available Heat
 - 20.3.4.3 Ignition Characteristics
 - 20.3.4.4 Flue Gas Modification
- 20.4 General Benefits
 - 20.4.1 Increased Productivity
 - 20.4.2 Higher Thermal Efficiencies
 - 20.4.3 Improved Flame Characteristics
 - 20.4.3.1 Higher Turndown Ratio
 - 20.4.3.2 Increased Flame Stability
 - 20.4.3.3 Better Ignition Characteristics
 - 20.4.3.4 Flame Shape Control
 - 20.4.4 Lower Exhaust Gas Volumes
 - 20.4.5 Higher Heat Transfer Efficiency
 - 20.4.6 Reduced Costs
 - 20.4.7 Increased Flexibility
 - 20.4.8 Improved Operations
- 20.5 Potential Problems
 - 20.5.1 Refractory Damage
 - 20.5.1.1 Overheating
 - 20.5.1.2 Corrosion
 - 20.5.2 Nonuniform Heating
 - 20.5.2.1 Hot Spots
 - 20.5.2.2 Reduction in Convection
 - 20.5.3 Flame Disturbance

- 20.5.4 Increased Pollutant Emissions
 - 20.5.4.1 NO_x
 - 20.5.4.2 Noise
- 20.5.5 Flashback
- 20.6 Industrial Heating Applications
 - 20.6.1 Metals
 - 20.6.2 Minerals
 - 20.6.3 Incineration
 - 20.6.4 Other
- 20.7 Conclusions
- References

20.1 INTRODUCTION

Most industrial heating processes require substantial amounts of energy, which is commonly generated by combusting hydrocarbon fuels such as natural gas or oil. Most combustion processes use air as the oxidant. In many cases, these processes can be enhanced using an oxidant that contains a higher proportion of O₂ than that in air. This is known as *oxygen-enhanced combustion* or OEC.¹ Air consists of approximately 21% O₂ and 79% N₂ (by volume). One example of OEC is using an oxidant consisting of air, blended with pure O₂. Another example is using high-purity O₂ as the oxidant, instead of air. This is usually referred to as *oxy/fuel* combustion (see Chapter 21).

New developments have made oxy/fuel combustion technology more amenable to a wide range of applications. In the past, the benefits of using oxygen could not always offset the added costs. New oxygen-generation technologies, such as pressure and vacuum swing adsorption,² have substantially reduced the cost of separating O₂ from air. This has increased the number of applications where using oxygen to enhance performance is cost justified. Another important development is the increased emphasis on the environment. In many cases, OEC can substantially reduce pollutant emissions.³ This has also increased the number of cost-effective applications. The Gas Research Institute in Chicago, IL⁴ and the U.S. Dept. of Energy⁵ sponsored independent studies which predict that OEC will be a critical combustion technology in the very near future.

Historically, air/fuel combustion has been the conventional technology used in nearly all industrial heating processes. Oxygen-enhanced combustion systems are becoming more common in a variety of industries. When traditional air/fuel combustion systems have been modified for OEC, many benefits have been demonstrated. Typical improvements include increased thermal efficiency, increased processing rates, reduced flue gas volumes, and reduced pollutant emissions.

Many industrial heating processes can be enhanced by replacing some or all of the air with high-purity oxygen.^{4,6} Typical applications include metal heating and melting, glass melting, and minerals calcining. In a report for the Gas Research Institute, the following applications were identified as possible candidates for OEC:⁷

- Processes that have high flue gas temperatures, typically in excess of 2000°F (1400K)
- Processes that have low thermal efficiencies, typically due to heat transfer limitations
- Processes that have throughput limitations which could benefit from additional heat transfer without adversely affecting product quality
- Processes that have dirty flue gases, high NO_x emissions, or flue gas volume limitations

When air is used as the oxidizer, only the O₂ is needed in the combustion process. By eliminating N₂ from the oxidizer, many benefits can be realized.

20.2 TYPICAL USE METHODS

Oxygen has been commonly used to enhance combustion processes in four primary ways: (1) adding O_2 into the incoming combustion air stream, (2) injecting O_2 into an air/fuel flame, (3) replacing the combustion air with high-purity O_2 , and (4) separately providing combustion air and O_2 to the burner. These methods are discussed next.

20.2.1 AIR ENRICHMENT

Figure 20.1 shows an air/fuel process where the air is enriched with O_2 . This can be referred to as low-level O_2 enrichment or premix enrichment. Many conventional air/fuel burners can be adapted for this technology.⁸ The O_2 is injected into the incoming combustion air supply, usually through a diffuser to ensure adequate mixing. This is usually an inexpensive retrofit that can provide substantial benefits. Typically, the added O_2 will shorten and intensify the flame. However, there may be some concern if too much O_2 is added to a burner designed for air/fuel. The flame shape may become unacceptably short. The higher flame temperatures may damage the burner or burner block. The air piping may need to be modified for safety reasons to handle higher levels of O_2 .

20.2.2 O_2 LANCING

Figure 20.2 shows another method for enriching an air/fuel process with O_2 . As in the first method, this is also generally used for lower levels of O_2 enrichment. However, oxygen lancing may have

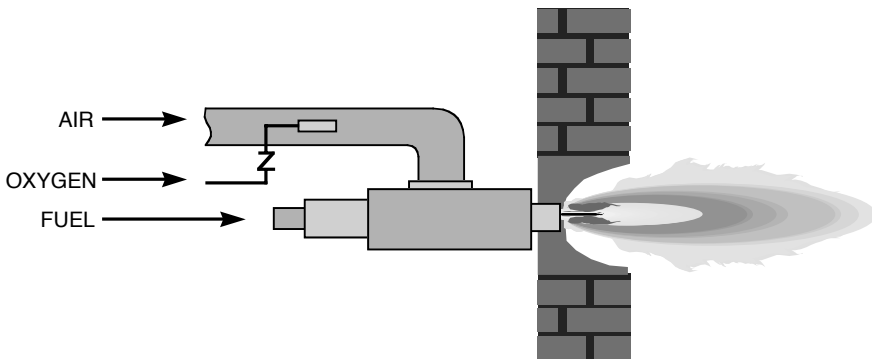


FIGURE 20.1 Schematic of an oxygen-enriched air/fuel burner.¹

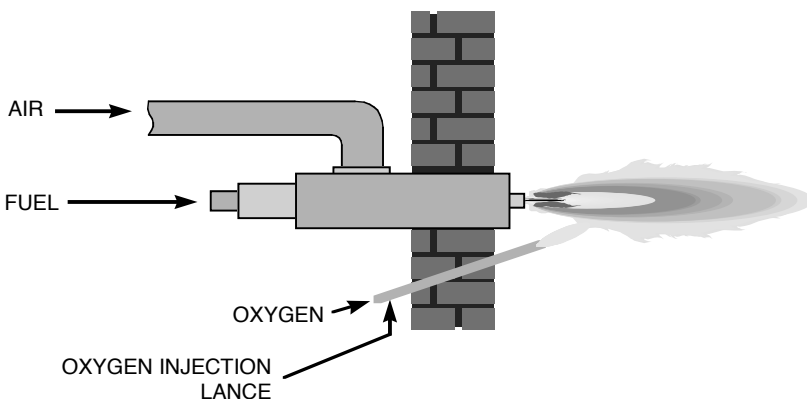


FIGURE 20.2 Schematic of oxygen lancing into an air/fuel burner.¹

several advantages over air enrichment. No modifications to the existing air/fuel burner need to be made. Typically, the NO_x emissions are lower using O₂ lancing compared to premixing because this is a form of staging, which is a well-accepted technique for reducing NO_x.⁹ Depending on the injection location, the flame shape can be lengthened by staging the combustion reactions. The flame heat release is generally more evenly distributed than with premix O₂ enrichment. Under certain conditions, O₂ lancing between the flame and the load causes the flame to be pulled toward the load. This improves the heat transfer efficiency. Therefore, there is less likelihood of overheating the air/fuel burner, the burner block, and the refractory in the combustion chamber. Another variant of this staging method involves lancing O₂, not into the flame, but somewhere else in the combustion chamber. One example of this technique is known as oxygen-enriched air staging or OEAS (see [Figure 20.47](#) and [Figure 20.49](#)). In that technology, O₂ lancing is an inexpensive retrofit for existing processes. One potential disadvantage is the cost to add another hole in the combustion chamber for the lance. This includes both the installation costs and the lost productivity. However, the hole is typically very small.

One specific embodiment of O₂ lancing is known as undershot enrichment, where O₂ is lanced into the flame from below. The lance is located between the burner and the material being heated. While air enrichment increases the flame temperature uniformly, the undershot technique selectively enriches the underside of the conventional flame, thereby concentrating extra heat downward toward the material being heated. While the mixing of oxygen and combustion air is not as complete with undershot oxygen as with premixing, this disadvantage is often outweighed by the more effective placement of the extra heat. Another benefit is that the refractory in the roof of the furnace generally receives less heat compared to air enrichment. This usually increases the life of the roof.

20.2.3 OXY/FUEL

Figure 20.3 shows a third method using OEC, commonly referred to as oxy/fuel combustion. In nearly all cases, the fuel and the oxygen remain separated inside the burner. They do not mix until reaching the outlet of the burner. This is commonly referred to as a nozzle-mix burner, which produces a diffusion flame. There is no premixing of the gases for safety reasons. Because of the extremely high reactivity of pure O₂, there is the potential for explosion if the gases are premixed. In this method, high-purity oxygen (>90% O₂ by volume) is used to combust the fuel. As will be discussed later, there are several ways of generating the O₂. In an oxy/fuel system, the actual purity of the oxidizer will depend on which method has been chosen to generate the O₂. Oxy/fuel combustion has the greatest potential for improving a process, but it also may have the highest operating cost. Oxy/fuel technology is discussed in more detail in Chapter 21.

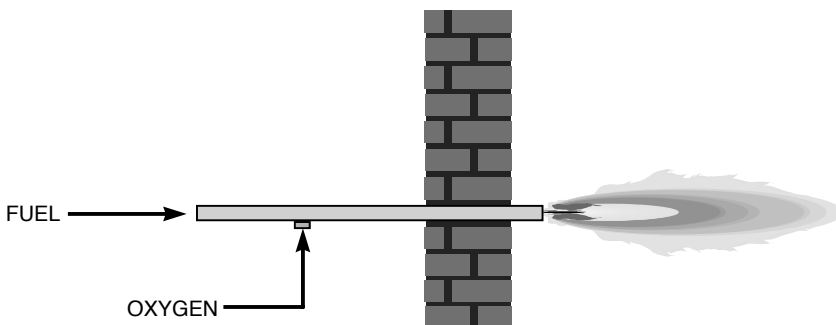


FIGURE 20.3 Schematic of an oxy/fuel burner.¹

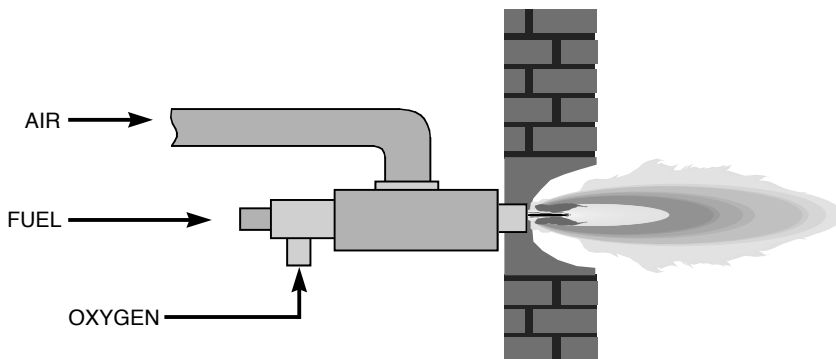


FIGURE 20.4 Schematic of an air-oxy/fuel burner.¹

20.2.4 AIR-OXY/FUEL

The fourth common method of using OEC involves separately injecting air and O₂ through a burner, as shown in [Figure 20.4](#). It is sometimes referred to as an air-oxy/fuel burner. This is a variation of the first three methods. In some cases, an existing air/fuel burner can be easily retrofitted by inserting an oxy/fuel burner through it.¹⁰ In other cases, a specially designed burner can be used.¹¹ This OEC method can have several advantages. It can typically use higher levels of O₂ than the air enrichment and O₂ lancing methods, which yields higher benefits. However, the operating costs are less than for oxy/fuel, which uses very high O₂ levels. The flame shape and heat release pattern can be adjusted by controlling the amount of O₂ used in the process. It is also a generally inexpensive retrofit. Many air/fuel burners are designed for dual fuels, usually a liquid fuel-like oil, and a gaseous fuel-like natural gas. The oil gun in the center of the dual fuel burner can usually be easily removed and replaced by either an O₂ lance or an oxy/fuel burner.

With this OEC method, the oxidizer composition can be specified in an alternate way. Instead of giving the overall O₂ concentration in the oxidizer, the oxidizer can be given as the fraction of the total oxidizer that is air and the fraction of the total oxidizer that is pure O₂. The equivalent overall O₂ in the oxidizer can be calculated as:

$$\Omega = \frac{20.9}{0.209(\text{vol.}\% \text{ O}_2) + (\text{vol.}\% \text{ air})} \quad (20.1)$$

This conversion in Equation 20.1 is graphically shown in [Figure 20.5](#). For example, the oxidizer can be specified as a blend of 60% O₂ and 40% air. That ratio of O₂ to air produces an equivalent of 39.8% overall O₂ in the oxidizer.

20.2.5 LOW-PURITY O₂

In some cases, it may be advantageous to use a technique such as vacuum or pressure swing adsorption (VSA/PSA) to produce oxygen because of significant cost reductions compared to cryogenic production methods. PSA/VSA methods use much less power-per-unit of oxygen produced. However, the oxygen purity is somewhat less than 100% in order to gain this power advantage. Typical purities are in the range of 90 to 95%, although they can be higher or lower depending on the design. Nearly all the benefits are achieved compared to using 100% purity, but at a much reduced cost. The main disadvantage is the potential to produce higher NO_x emissions.

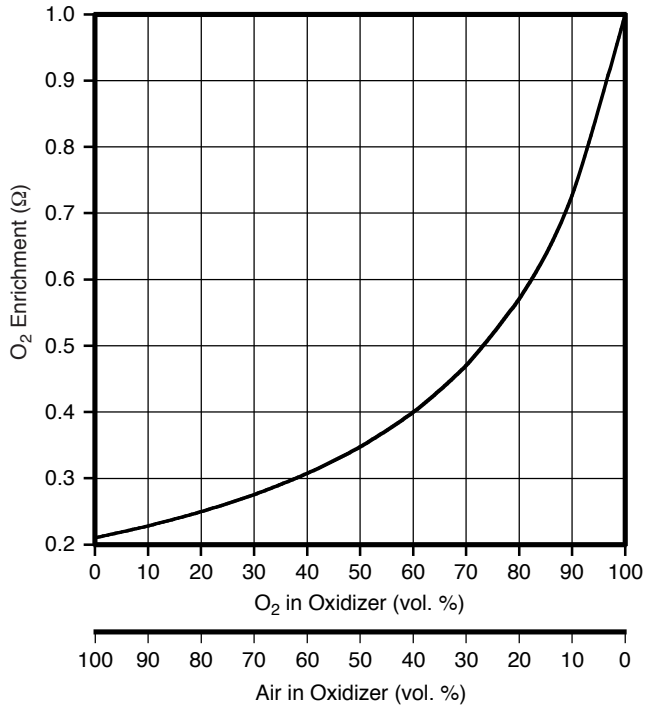


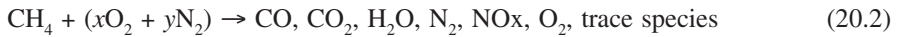
FIGURE 20.5 Oxidizer compositions for blends of air and pure O₂.¹

20.3 BASICS

In this section, methane (CH₄) is used to represent a typical fuel in a heating process. The analysis would be similar for other fuels.

20.3.1 DEFINITIONS

A generalized CH₄ combustion reaction can be written as:



The stoichiometry can be defined as:

$$S = \frac{\text{volume flow rate of O}_2 \text{ in the oxidizer}}{\text{volume flow rate of CH}_4} \quad (20.3)$$

Note that this definition differs slightly from the one commonly used in industry, where the stoichiometry is usually defined as the total oxidizer flow divided by the fuel flow. The problem with the definition commonly used in industry is that the stoichiometry must be recalculated whenever the oxidizer composition changes and stoichiometric conditions change for each oxidizer composition. This is not a concern if air is always used as the oxidizer, which is the case for the vast majority of combustion processes. The benefit of the definition used here is that stoichiometry is independent of the oxidizer composition, so stoichiometric conditions are the same for any oxidizer composition. In Equation 20.2, $S = x/1 = x$. Theoretically, for the complete combustion of CH₄, $S = 2.0$. Actual flames generally require some excess O₂ for complete combustion of the fuel. This is due

to incomplete mixing between the fuel and oxidant. For the fuel-rich combustion of CH₄, S < 2.0. For the fuel-lean combustion of CH₄, S > 2.0.

The O₂ mole fraction in the oxidizer can be defined as:

$$\Omega = \frac{\text{volume flow rate of O}_2 \text{ in the oxidizer}}{\text{Total volume flow rate of oxidizer}} \quad (20.4)$$

Using Equation 20.2, $\Omega = x/(x + y)$. If the oxidizer is air, $\Omega = 0.21$. If the oxidizer is pure O₂, $\Omega = 1.0$. The O₂ enrichment level is sometimes used. This refers to the incremental O₂ volume above that found in air. For example, if $\Omega = 0.35$, then the O₂ enrichment would be 14% (35% to 21%).

20.3.2 OPERATING REGIMES

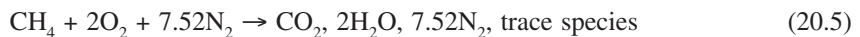
There have been two common operating regimes for oxygen-enhanced combustion. The first or lower regime is usually referred to as *low-level enrichment* ($\Omega < 0.30$). This is commonly used in retrofit applications where only a few modifications need to be made to the existing combustion equipment. It is used when only incremental benefits are required. For example, in many cases, the production rate in a heating process can be significantly increased even with only relatively small amounts of oxygen enrichment. In most cases, air/fuel burners can successfully operate up to about $\Omega = 0.28$ with no modifications.¹² For $\Omega > 0.28$, the flame may become unstable or the flame temperature may become too high for a burner designed to operate under air/fuel conditions. In some cases, it may be possible to make minor burner modifications to permit operation at slightly higher O₂ concentrations.

The other common operating regime is usually referred to as *high-level enrichment*, where high-purity oxygen ($\Omega > 0.90$) is used. This is used in higher temperature applications where the benefits of higher purity oxygen justify the added costs. The heating process is greatly intensified by the high-purity oxygen. In a retrofit situation, existing air/fuel burners are replaced by burners specifically designed to use the higher levels of O₂.

It has only been in the past decade that a significant number of combustion systems have been operated in the intermediate oxygen regime or *medium-level enrichment* ($0.30 < \Omega < 0.90$). Again, these usually require specially designed burners or retrofits of existing burners.

20.3.3 COMBUSTION PRODUCTS

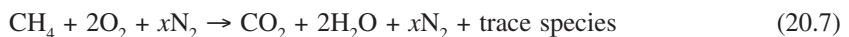
The stoichiometric combustion of CH₄ with air can be represented by the following global equation:



It can be seen that more than 70 vol% of the exhaust gases is N₂. Similarly, a stoichiometric O₂/CH₄ combustion process can be represented by:



The volume of exhaust gases is significantly reduced by the elimination of N₂. In general, a stoichiometric oxygen-enhanced methane combustion process can be represented by:



where $0 \leq x \leq 7.52$, depending on the oxidizer.

The actual composition of the exhaust products from the combustion reaction depends on several factors, including the oxidizer composition Ω , the temperature of the gases, and the stoichiometry S.

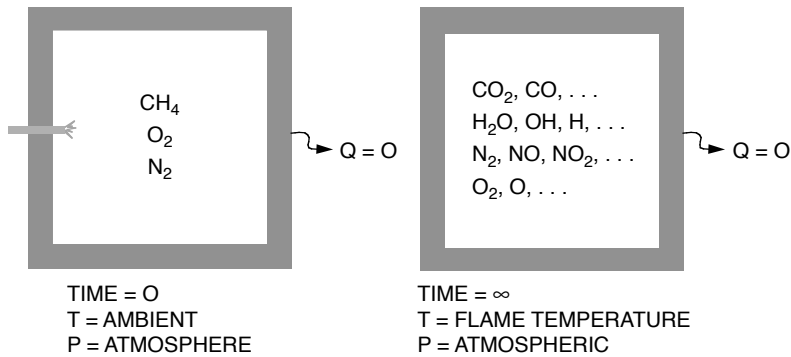


FIGURE 20.6 Adiabatic equilibrium reaction process.¹

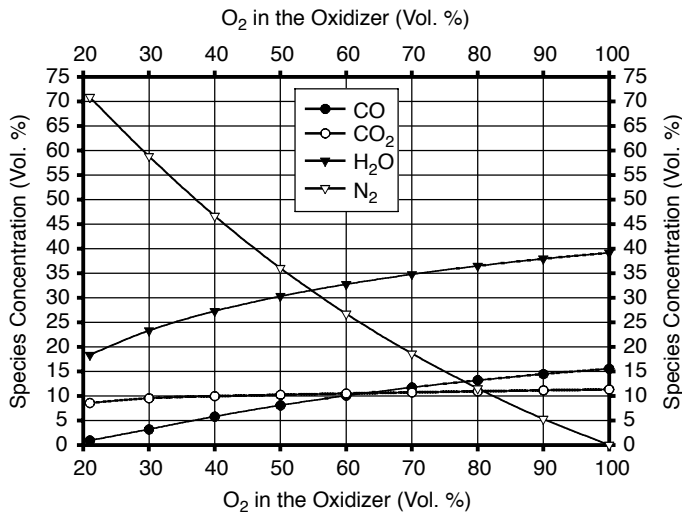


FIGURE 20.7 Predicted major species concentrations vs. oxidizer composition for an adiabatic equilibrium stoichiometric CH₄ flame.¹

A diagram showing an adiabatic equilibrium combustion reaction is shown in Figure 20.6. This is not the case in an actual combustion process where heat is lost from the flame by radiation. Figure 20.7 shows the predicted major species for the adiabatic equilibrium combustion of CH₄ as a function of the oxidizer composition. The calculations were made using a NASA computer program that minimizes the Gibbs free energy of a gaseous system.¹³ An equilibrium process means that there is an infinite amount of time for the chemical reactions to take place, or the reaction products are not limited by chemical kinetics. In actuality, the combustion reactions are completed in fractions of a second. An adiabatic process means that no heat is lost during the reaction, or that the reaction occurs in a perfectly insulated chamber. As expected, Figure 20.7 shows that as N₂ is removed from the oxidizer, the concentration of N₂ in the exhaust products decreases correspondingly. Likewise, there is an increase in the concentrations of CO₂ and H₂O. For this adiabatic process, there is a significant amount of CO at higher levels of O₂ in the oxidizer. Figure 20.8 shows the predicted minor species for the same conditions as Figure 20.7. Note that trace species have been excluded from this figure. The radical species H, O, and OH all increase with the O₂ in the oxidizer. Unburned fuel in the form of H₂ and unreacted oxidizer in the form of O₂ also increase

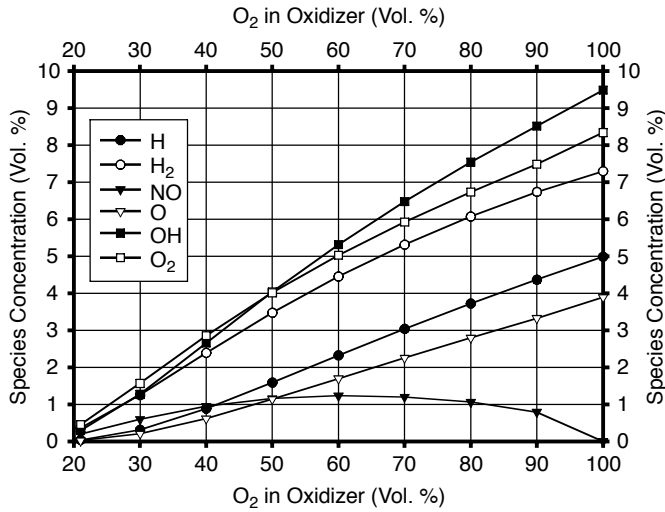


FIGURE 20.8 Predicted minor species concentrations vs. oxidizer composition for an adiabatic equilibrium stoichiometric CH₄ flame.¹

with the O₂ concentration in the oxidizer. This increase in radical concentrations, unburned fuel in the form of CO and H₂, and unreacted O₂ are all due to chemical dissociation, which occurs at high temperatures.

The actual flame temperature is lower than the adiabatic equilibrium flame temperature due to radiation from the flame. The actual flame temperature is determined by how well the flame radiates its heat and how well the combustion system, including the load and the refractory walls, absorbs that radiation. A highly luminous flame generally has a lower flame temperature than a highly nonluminous flame. The actual flame temperature will also be lower when the load and the walls are more radiatively absorptive. This occurs when the load and walls are at lower temperatures and have higher radiant absorptivities. These effects are discussed in more detail in Chapter 2. As the gaseous combustion products exit the flame, they typically lose more heat by convection and radiation as they travel through the combustion chamber. The objective of a combustion process is to transfer the chemical energy contained in the fuel to the load, or in some cases to the combustion chamber. The more thermally efficient the combustion process, the more heat that is transferred from the combustion products to the load and to the combustion chamber. Therefore, the gas temperature in the exhaust stack is desirably much lower than in the flame in a thermally efficient heating process. The composition of the combustion products then changes with gas temperature.

Figure 20.9 shows the predicted major species for the equilibrium combustion of CH₄ with “air” (21% O₂, 79% N₂) and with pure O₂ as a function of the gas temperature. The highest possible temperature for the air/CH₄ and the O₂/CH₄ reaction is the adiabatic equilibrium temperature of 3537°F (2220K) and 5038°F (3054K), respectively. For the air/CH₄ reaction, there is very little change in the predicted gas composition as a function of temperature. For the O₂/CH₄ reaction, there is a significant change in the composition as the gas temperature increases above about 3000°F (1900K). Figure 20.10 shows the predicted minor species for the same conditions as in Figure 20.9. Again, NO has been specifically excluded. For air/CH₄, none of the minor species exceeds 1% by volume. As the gas temperature increases, chemical dissociation increases. For the O₂/CH₄ flame, significant levels of unreacted fuel (CO and H₂), radical species (O, H, and OH), and unreacted O₂ are present at high gas temperatures.

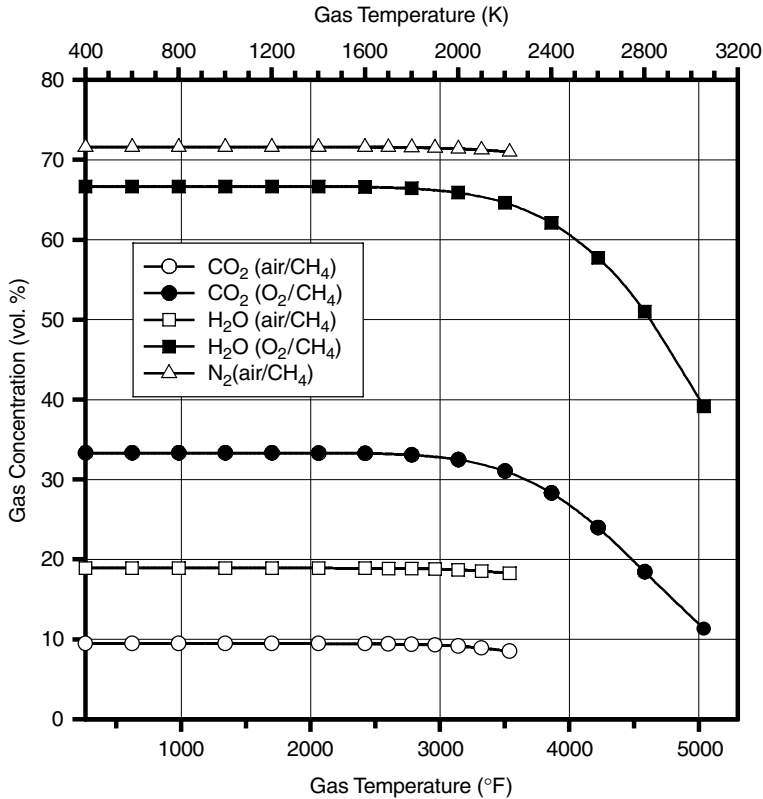


FIGURE 20.9 Equilibrium calculations for the predicted gas composition of the major species as a function of the gas temperature for air/CH₄ and O₂/CH₄ flames.¹

Figure 20.11 shows the predicted major species for the adiabatic equilibrium combustion of CH₄ with “air” (21% O₂, 79% N₂) and with pure O₂ as a function of the stoichiometry. For the air/CH₄ flames, the N₂ concentration in the exhaust gases strictly increases with the stoichiometry. The H₂O and the CO₂ concentrations peak at stoichiometric conditions (S = 2.0). For the O₂/CH₄ flames, the peak H₂O concentration occurs at slightly fuel-rich conditions (S < 2.0). The predicted CO₂ concentration strictly increases with stoichiometry for the range of stoichiometries shown. Similarly, Figure 20.12 shows the predicted minor species.

20.3.4 PROPERTIES

20.3.4.1 Flame Temperature

The flame temperature increases significantly when air is replaced with oxygen because N₂ acts as a diluent that reduces the flame temperature. Figure 20.13 is a plot of the adiabatic equilibrium flame temperature for H₂, CH₄, and C₃H₈ combustion, as a function of the oxidizer composition, for a stoichiometric combustion process.¹⁴ The flame temperature varies from about 3600 to 5000°F (2255 to 3033K) for air and pure oxygen, respectively. The graph shows a rapid rise in the flame temperature from air up to about 60% O₂ in the oxidizer. The flame temperature increases at a slower rate at higher O₂ concentrations. Table 20.1 shows the adiabatic flame temperature for some common gaseous fuels.

Figure 20.14 is a similar plot of the adiabatic equilibrium flame temperature for CH₄ flames as a function of the stoichiometry, for four different oxidizer compositions ranging from air to pure O₂.

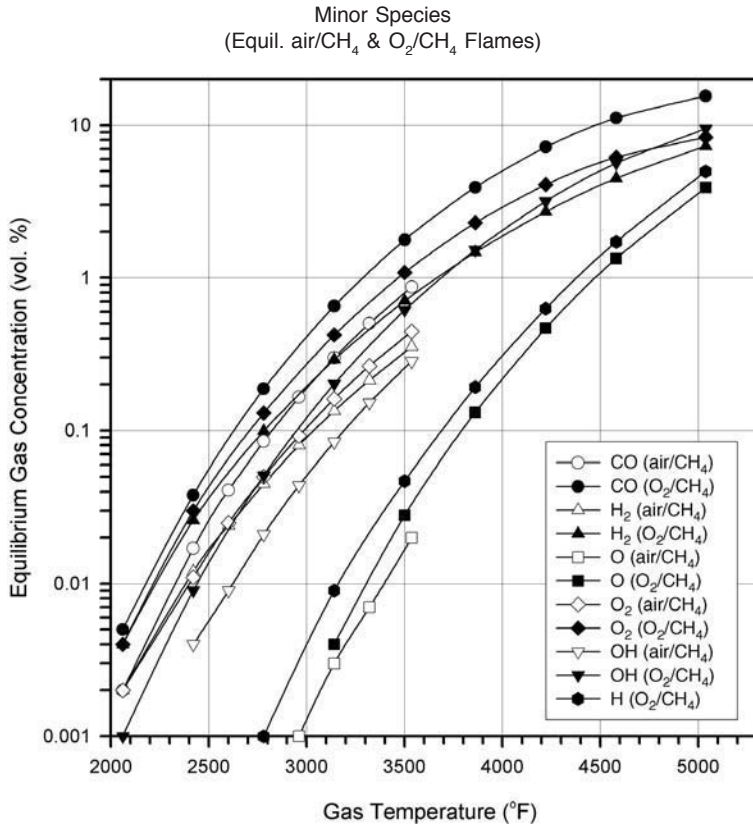


FIGURE 20.10 Equilibrium calculations for the predicted gas composition of the minor species as a function of the gas temperature for air/CH₄ and O₂/CH₄ flames.¹

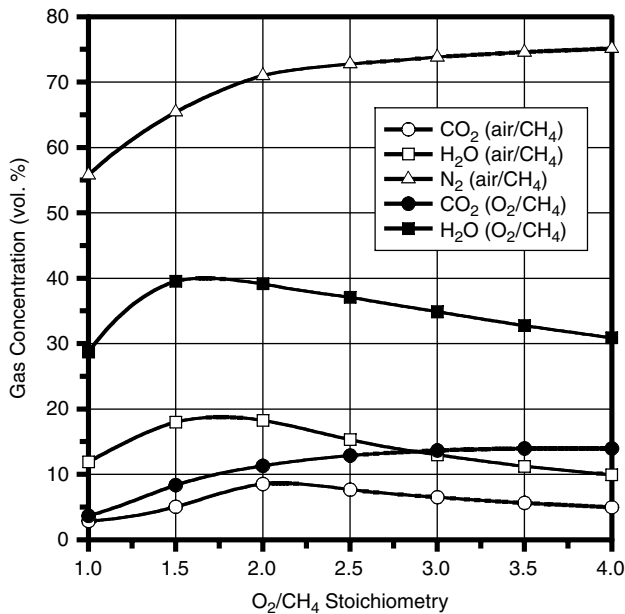


FIGURE 20.11 Adiabatic equilibrium calculations for the predicted gas composition of the major species as a function of the stoichiometry for air/CH₄ and O₂/CH₄ flames.¹

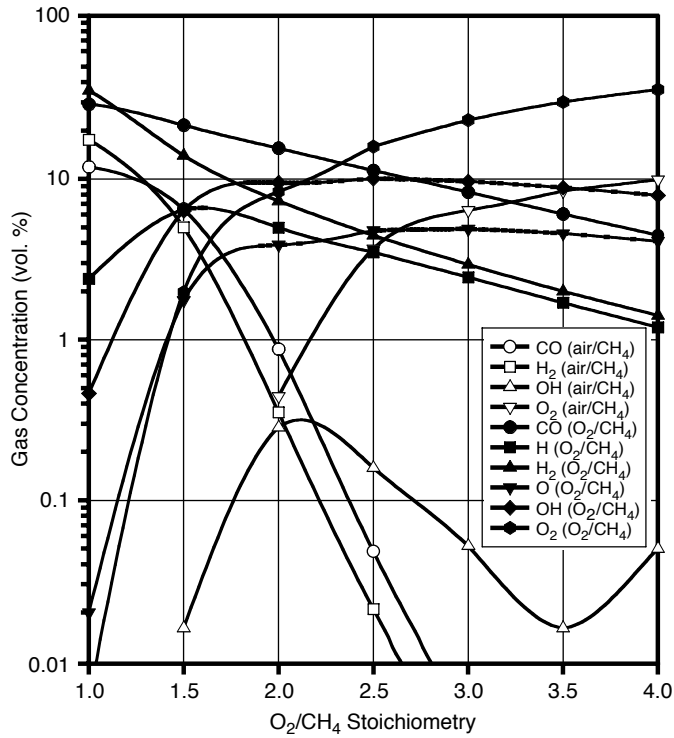


FIGURE 20.12 Adiabatic equilibrium calculations for the predicted gas composition of the minor species as a function of the stoichiometry for air/CH₄ and O₂/CH₄ flames.¹

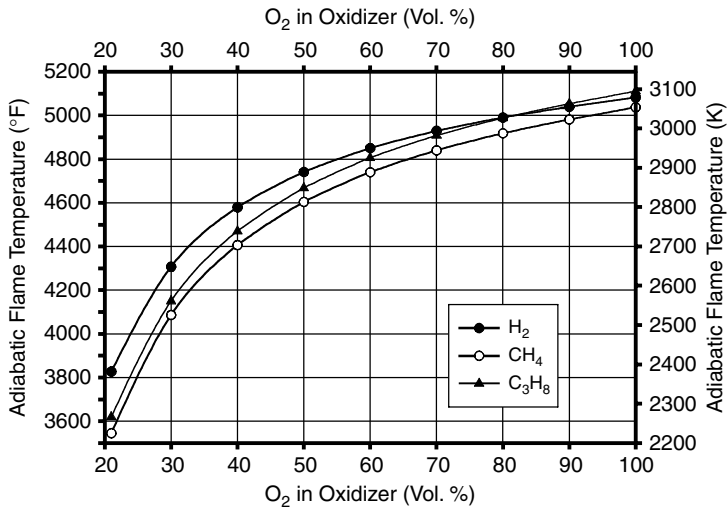


FIGURE 20.13 Adiabatic flame temperature vs. oxidizer composition for adiabatic equilibrium stoichiometric H₂, CH₄, and C₃H₈ flames.¹⁴

TABLE 20.1
Adiabatic Flame Temperatures¹

Fuel	Air		O ₂	
	(°F)	(K)	(°F)	(K)
H ₂	3807	2370	5082	3079
CH ₄	3542	2223	5036	3053
C ₂ H ₂	4104	2535	5556	3342
C ₂ H ₄	3790	2361	5256	3175
C ₂ H ₆	3607	2259	5095	3086
C ₃ H ₆	4725	2334	5203	3138
C ₃ H ₈	3610	2261	5112	3095
C ₄ H ₁₀	3583	2246	5121	3100
CO	3826	2381	4901	2978

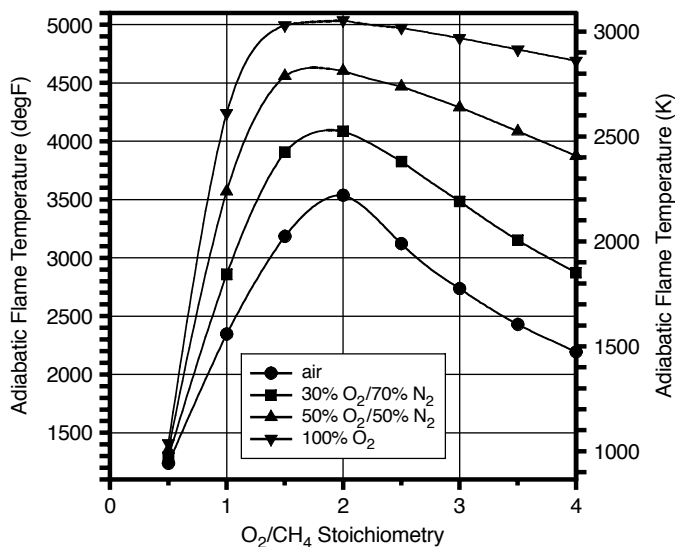


FIGURE 20.14 Adiabatic flame temperature vs. stoichiometry for a CH₄ flame and various oxidizers.¹

The peak flame temperatures occur at stoichiometric conditions. The lower the O₂ concentration in the oxidizer, the more the flame temperature is reduced by operating at nonstoichiometric conditions (either fuel-rich or fuel-lean). This is due to the higher concentration of N₂, which absorbs heat and lowers the overall temperature. Actual flame temperatures will be less than those given in Figure 20.13 and Figure 20.14 because of heat losses from the flame, which is not an adiabatic process.

Figure 20.15 shows how the adiabatic flame temperature varies as a function of the oxidizer preheat temperature. The increase in flame temperature is relatively small for the O₂/CH₄ flame because the increased sensible heat of the O₂ is only a fraction of the chemical energy contained in the fuel. For the air/CH₄ flames, preheating the air has a more dramatic impact because the increase in sensible heat is very significant due to the large mass of air in the combustion reaction.

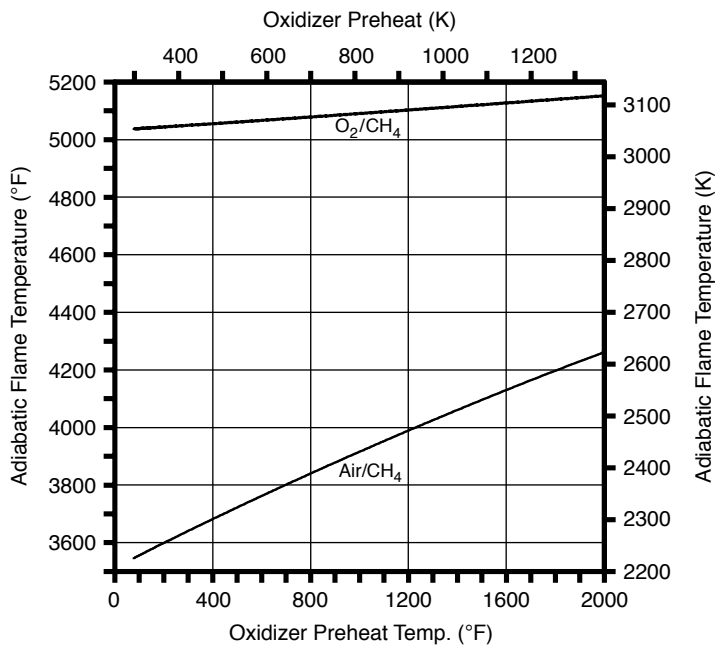


FIGURE 20.15 Adiabatic flame temperature vs. oxidizer preheat temperature for stoichiometric air/CH₄ and O₂/CH₄ flames.¹

20.3.4.2 Available Heat

Available heat is defined as the gross heating value of the fuel, less the energy carried out of the combustion process by the hot exhaust gases. N₂ in air acts as a ballast that carries energy out with the exhaust. Figure 20.16 is a graph of the available heat for the combustion of CH₄ as a function of the O₂ concentration in the oxidizer, for three different exhaust gas temperatures. As the exhaust gas temperature increases, the available heat decreases because more energy is carried out of the exhaust stack. There is an initial rapid increase in available heat as the O₂ concentration in the oxidizer increases from the 21% found in air. That is one reason why O₂ enrichment has been a popular technique for using OEC because the incremental increase in efficiency is very significant.

Figure 20.17 shows how the available heat, for stoichiometric air/CH₄ and O₂/CH₄ flames, varies as a function of the exhaust gas temperature. As the exhaust temperature increases, more energy is carried out of the combustion system and less remains in the system. The available heat decreases to zero at the adiabatic equilibrium flame temperature where no heat is lost from the gases. The figure shows that even at gas temperatures as high as 3500°F (2200K), the available heat of an O₂/CH₄ system is still as high as 60%. The figure also shows that it is usually not very economical to use air/CH₄ systems for high-temperature heating and melting processes. At an exhaust temperature of 2500°F (1600K), the available heat for the air/CH₄ system is only a little over 30%. Heat recovery in the form of preheated air is commonly used for higher temperature heating processes to increase the thermal efficiencies.

Figure 20.18 shows how the available heat increases with the oxidizer preheat temperature. The thermal efficiency of the air/CH₄ doubles by preheating the air to 2000°F (1400K). For the O₂/CH₄ flames, the increase in efficiency is much less dramatic by preheating the O₂. This is because the initial efficiency with no preheat is already 70% and because the mass of the O₂ is not nearly as significant in the combustion reaction as compared to the mass of air in an air/fuel flame. There are also safety concerns when flowing hot O₂ through piping, heat recuperation equipment, and a burner.

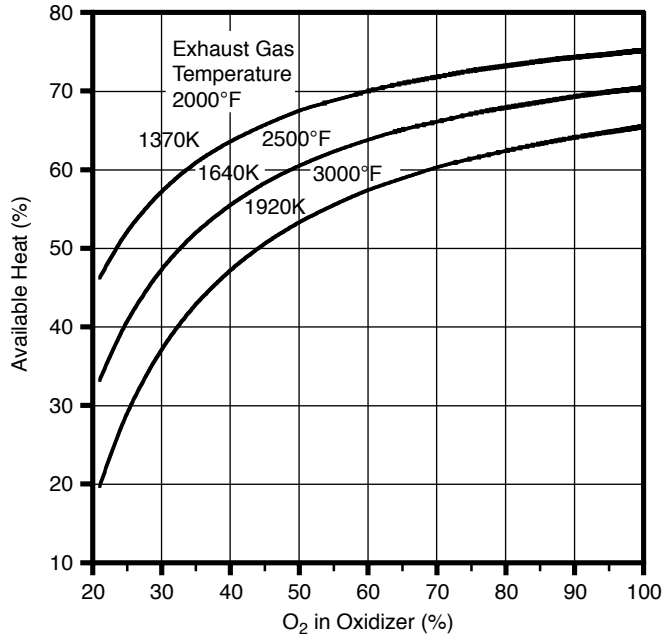


FIGURE 20.16 Available heat vs. oxidizer composition for a stoichiometric CH₄ flame at exhaust temperatures of 2000, 2500, and 3000°F (1370, 1640, 1920K).¹

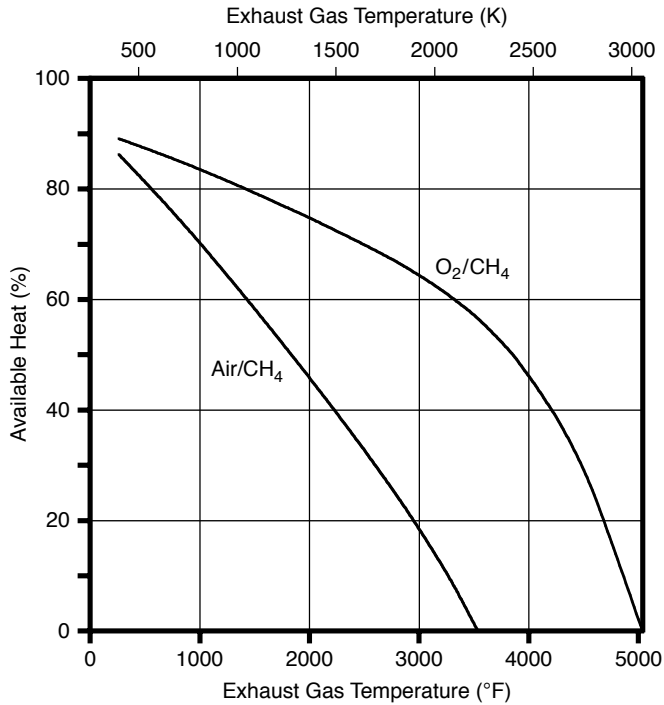


FIGURE 20.17 Available heat vs. exhaust gas temperature for stoichiometric air/CH₄ and O₂/CH₄ flames.¹

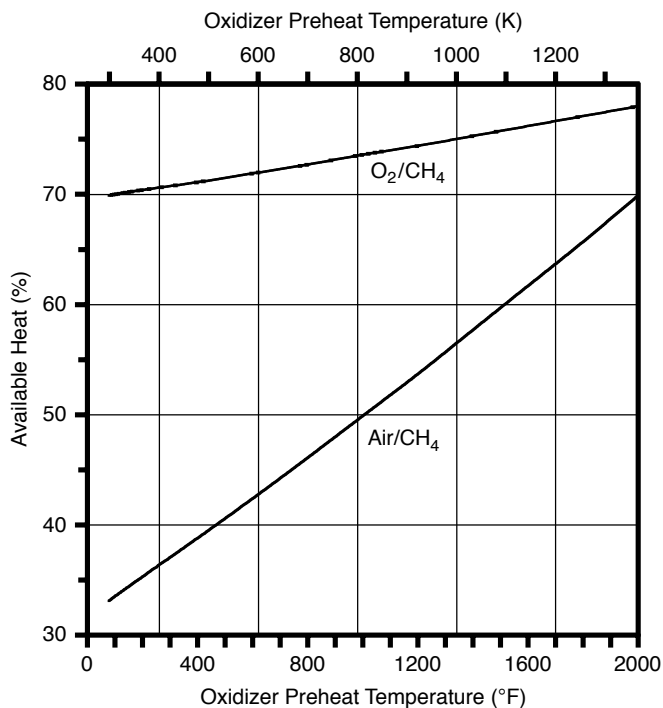


FIGURE 20.18 Available heat vs. oxidizer preheat temperature for stoichiometric, equilibrium air/CH₄, and O₂/CH₄ flames at an exhaust gas temperature of 2500°F (1644K).¹

The fuel savings for a given technology can be calculated using the available heat curves:

$$\text{Fuel Savings (\%)} = \left(1 - \frac{AH_2}{AH_1} \right) \times 100 \quad (20.8)$$

where AH_1 is the available heat of the base case process and AH_2 is the available heat using a new technology. For example, if the base case process has an available heat of 30% and the available heat using the new technology is 45%, then the fuel savings = $(1 - 45/30) \times 100 = -50\%$, which means that 50% less fuel is needed for process 2 compared to process 1.

20.3.4.3 Ignition Characteristics

20.3.4.3.1 Flammability Limits

As the oxygen concentration in the oxidizer increases, the flammability limits for the fuel increase. Figure 20.19 shows the increase for CH₄ combustion with oxidizers having a range of O₂ concentrations.¹⁵ The upper flammability limit increases linearly with the O₂ concentration in the oxidizer, while the lower flammability limit is nearly constant for oxidizers with more than about 35% O₂ in the oxidizer. Table 20.2 shows examples of how using O₂ instead of air widens the flammability range for a given fuel.

20.3.4.3.2 Flame Speeds

OEC increases the flames speed as shown in Figure 20.20. In a flame, the flame front is located where the gas velocity going away from the burner equals the flame velocity going toward the burner.

TABLE 20.2
Flammability Limits (Vol.% Fuel in Fuel/Oxidizer Mixture) of Common Fuels in Air and in O₂¹

Fuel	Limit in Air		Limit in O ₂	
	Lower	Upper	Lower	Upper
H ₂	4.1	74	4.0	94
CH ₄	5.3	14	5.4	59
C ₂ H ₆	3.2	12.5	4.1	50
C ₃ H ₈	2.4	9.5	—	—
C ₂ H ₄	3.0	29	3.1	80
C ₃ H ₆	2.0	11	2.1	53
CO	12.5	74	16	94

Adapted from Turin and Huebler.¹⁵

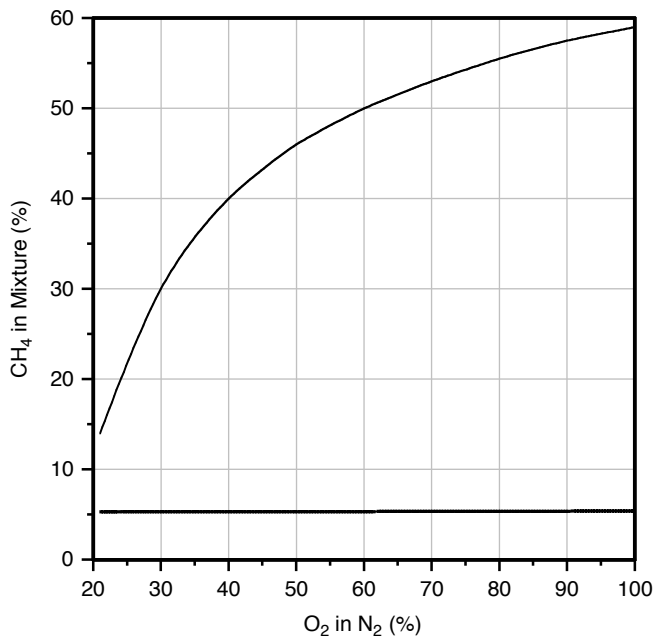


FIGURE 20.19 Upper and lower flammability limits vs. oxidizer composition for a CH₄ flame.¹

The gas velocity exiting the burner must be at least equal to the flame speed. If not, the flame will flashback inside the burner, leading to either flame extinguishment or to an explosion. Because flame speeds are higher using OEC, the burner exit velocities in an oxygen-enhanced combustion system are usually higher than in air/fuel systems.

20.3.4.3.3 Ignition Energy

Less energy is required for ignition using OEC, as shown in Figure 20.21.¹⁶ This means that it is easier to ignite flames with OEC compared to air/fuel flames where much of the ignition energy is absorbed by the diluent nitrogen. The disadvantage is that it is also easier to inadvertently ignite an OEC system, which is why the proper safety precautions must be followed.

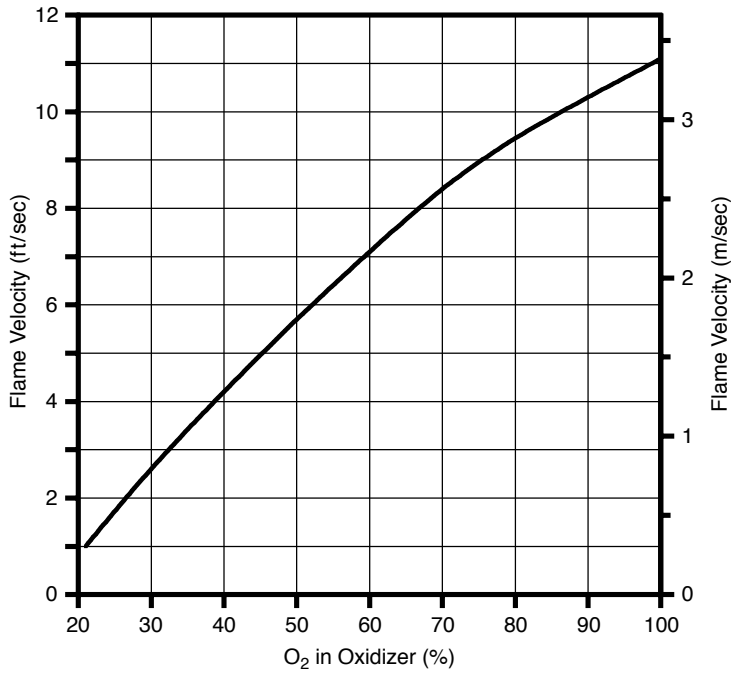


FIGURE 20.20 Normal flame propagation velocity vs. oxidizer composition for a stoichiometric CH₄ flame.¹

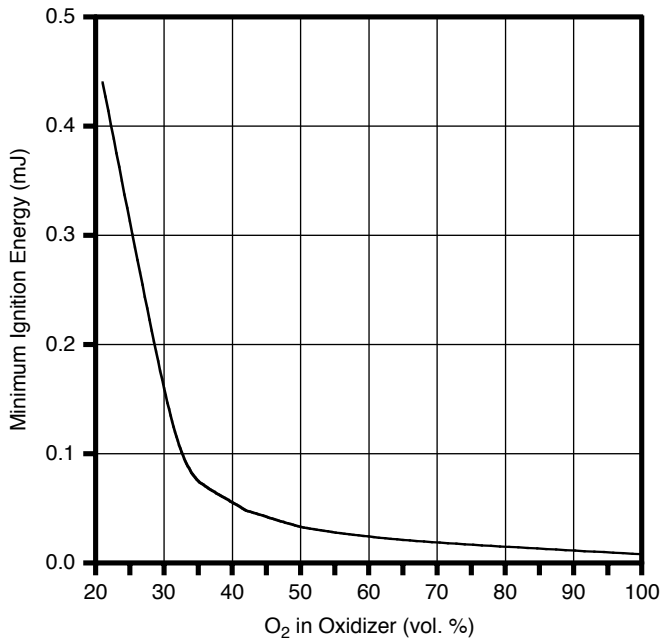


FIGURE 20.21 Minimum ignition energy vs. oxidizer composition for an atmospheric pressure, stoichiometric CH₄ flame.¹

20.3.4.3.4 Ignition Temperature

Using OEC also reduces the ignition temperature. Figure 20.22 shows the ignition temperature for CH_4 as a function of the O_2 concentration in the oxidizer ranging from 15 to 35% O_2 .¹⁷ Table 20.3 shows ignition temperatures for gaseous fuels combusted with air and with pure O_2 .¹⁸ The graph and the table both show that it is easier to ignite flames that are enhanced with oxygen.

20.3.4.4 Flue Gas Modification

20.3.4.4.1 Reduced Volume

Oxygen-enhanced combustion basically involves removing N_2 from the oxidizer. One obvious change compared to air/fuel combustion is the reduction in the flue gas volume. Figure 20.23 shows the exhaust gas flow rate, normalized to the fuel flow rate, for the stoichiometric combustion of CH_4 where it has been assumed that all the combustion products are CO_2 , H_2O , and N_2 (except when the oxidizer is pure O_2). This means that for each unit volume of fuel, 3 normalized volumes of gas are produced for oxy/fuel compared to 10.5 volumes for air/fuel. The reduction in flue gas volume is even larger when considering the increased fuel efficiency using OEC. Less fuel is required to process a given amount of material; therefore, fewer exhaust products are generated.

TABLE 20.3
Ignition Temperatures in Air and in Oxygen¹

Fuel	Air		O_2	
	(°F)	(K)	(°F)	(K)
H_2	1062	845	1040	833
CH_4	1170	905	1274	829
C_3H_8	919	766	874	741
C_4H_{10}	766	681	541	556
CO	1128	882	1090	861

Adapted from Reference 18.

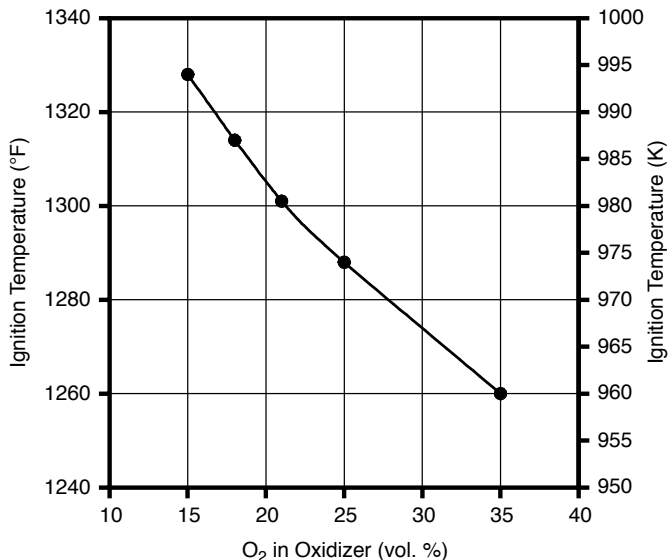


FIGURE 20.22 Ignition temperature vs. oxidizer composition for a stoichiometric CH_4 flame.¹

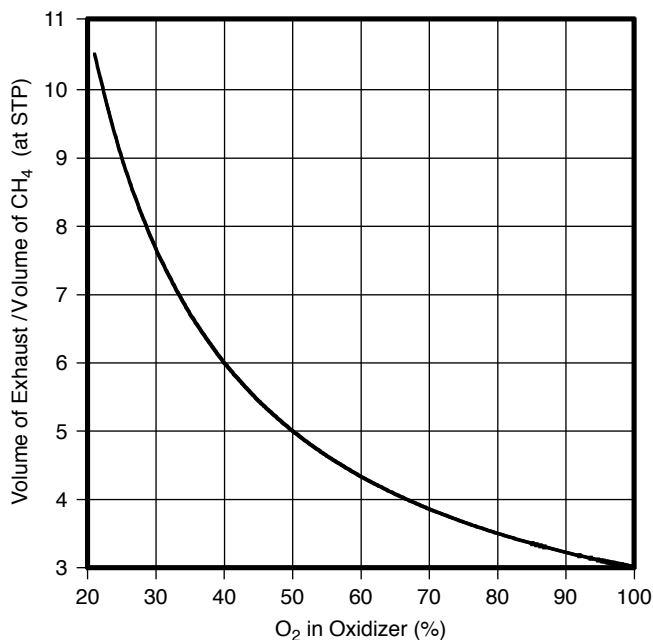


FIGURE 20.23 Normalized flue gas volume vs. oxidizer composition for a stoichiometric CH₄ flame.¹

20.3.4.4.2 Different Composition

Another potential benefit of OEC related to the flue gas is that the composition is significantly different than that produced by air/fuel combustion, as was shown in Figure 20.7. The products of combustion of a stoichiometric oxy/methane flame are approximately one-third CO₂ and two-thirds H₂O by volume compared to air/methane, which has about 71% N₂, 10% CO₂, and 19% H₂O. Any pollutants, such as NO_x or SO_x, are easier to remove in an oxy/fuel exhaust, because they are in much higher concentrations compared to the air/fuel exhaust stream, which is highly diluted by N₂. If the water is condensed from the exhaust products, the remaining gas is nearly all CO₂ for an oxy/fuel exhaust. Because CO₂ has been identified as a global warming gas, it can be more easily recovered from an oxy/fuel combustion system compared to an air/fuel system. The CO₂ can then either be used in another process, such as deep well injection for oil recovery, or it can be “disposed” of, such as by deep ocean injection.

20.4 GENERAL BENEFITS

Air consists of approximately 79% N₂ and 21% O₂, by volume. Only the O₂ is needed in the combustion reaction. By eliminating N₂, many benefits can be realized. These benefits include increased productivity, energy efficiency, turndown ratio, and flame stability, with reduced exhaust gas volume and pollutant emissions. These benefits are discussed next.

20.4.1 INCREASED PRODUCTIVITY

In most high-temperature heating processes, flame radiation is the dominant mode of heat transfer (see Chapter 6). Radiation is dependent on the fourth power of the absolute temperature. The higher temperatures associated with OEC increase the radiation from the flame to the load. This then increases the heat transfer to the load, which leads to increased material processing rates through

the combustion chamber. Therefore, more material can be processed in an existing system, or new systems can be made smaller for a given processing rate. This is particularly important where space in a plant is limited. The environment benefits because of the reduction in the size of the equipment since less material and energy are needed in fabricating the combustion system. To take advantage of increased processing rates, the rest of the production system must be capable of handling the increased throughput. For example, the material handling system may need to be modified to handle the increased material flow rates.

The incremental costs of adding OEC to an existing combustion system are usually small compared to the capital costs of either expanding an existing system or adding new equipment to increase production. This has historically been one of the most popular reasons for using OEC. The advantage of OEC is that it can also be used intermittently to meet periodic demands for increased production. For example, if the demand for aluminum cans increases during the summer because of increased beverage consumption, OEC can be used at that time to meet the increased demand for aluminum. If the demand decreases in the winter, then the OEC system could be throttled back or turned off until it is needed again. In most cases, using OEC would be much more economical than adding new equipment for increased capacity if the increased production demands are only temporary.

20.4.2 HIGHER THERMAL EFFICIENCIES

By using oxygen instead of air, more energy goes into the load, instead of being wasted in heating N_2 . The energy needed to make O_2 from air is only a small fraction of the energy used in the combustion process. Therefore, the overall process uses less energy for a given amount of production due to the higher available heat. In some instances, the cost of the oxygen can be offset by the reduction in fuel costs because of the increase in energy efficiency. This is often the case when OEC is used to supplement a process that uses electricity, which is generally more expensive than fossil fuel combustion. In some cases, it is possible to substitute a less expensive source of energy for an existing source of energy. For example, in the glass industry, the furnaces are fueled primarily by oil or natural gas and commonly “boosted” with electrical energy. It has been shown that some or all of the more expensive electrical energy can be eliminated by the proper use of OEC.

One common reason for using OEC is a reduction in the specific fuel consumption where less fuel is required for a given unit of production because of the improvement in available heat. A recent study projects that, for example, the cost of natural gas was expected to rise by about 10% from 1993 to the year 2000.⁷ At the same time, the cost of oxygen was expected to decrease by 10% due to lower electricity costs and improvements in oxygen production technology. The rising cost of fuel and the lowering cost of oxygen both make OEC a more attractive technology based solely on fuel savings.

Oxy/fuel combustion has been used in many applications in the steel industry, including both continuous and batch reheat furnaces, soaking pits, and ladle preheaters. Fuel savings of up to 60% have been reported.¹⁹ Typical fuel savings achieved by converting from air/fuel to oxy/fuel combustion are given in Table 20.4.²⁰ Another example, from the glass industry, is Spectrum Glass, which reported fuel savings of 50% when it converted from air/fuel to oxy/fuel in its glass melting furnaces.²¹

20.4.3 IMPROVED FLAME CHARACTERISTICS

20.4.3.1 Higher Turndown Ratio

As previously shown in Figure 20.19 and Table 20.2, as the oxygen concentration in the oxidizer increases, the flammability limits for the fuel increase. This leads to an increased turndown ratio for the combustion system. A flame can exist under a wider range of conditions. For example, an air/ CH_4

TABLE 20.4
Fuel Savings by Retrofitting Air/Fuel
Systems with Oxy/Fuel¹

Industry	Fuel Savings (%)
Steel	40–60
Aluminum, lead	40
Copper	40–60
Glass	30–40
Waste incineration	50
Sulfuric acid recovery	50

Adapted from Reference 20.

flame could exist at stoichiometries between about 1.3 and 3.8. An O₂/CH₄ flame could exist at stoichiometries between about 0.7 and almost 18. This is a consequence of removing the diluent N₂.

20.4.3.2 Increased Flame Stability

Oxygen-enhanced flames have higher flame speeds than air/fuel flames. This means that to prevent either flashback or flame extinguishment, the minimum gas exit velocities for an OEC flame must be higher than those for an air/fuel flame. The potential for flashback is discussed further in Section 20.5.5.

Lewis and von Elbe have defined the critical boundary velocity gradient for a cylindrical tube as follows:

$$g = \frac{4V}{\pi R^3} \quad (20.9)$$

where V is the volumetric flow of a premixed mixture of fuel and oxidizer and R is the radius of the tube.²² For flashback, V is the minimum flow rate before the flame is extinguished due to flashback. The critical boundary velocity gradients for flashback were experimentally determined for premixed methane flames using a round tube. At stoichiometric conditions, the gradient was approximately 2100 and 510,000 s⁻¹ for oxidizers of air and pure oxygen, respectively. This shows that much higher exit velocities can be used with OEC without blowing off the flame. These higher velocities generally produce more stable flames that are not as easily disturbed by flow patterns within a combustion chamber.

20.4.3.3 Better Ignition Characteristics

As shown in Figure 20.21 and Figure 20.22, another benefit of using OEC compared to air is that less energy is required for ignition which occurs at a lower temperature. This means that it is easier to ignite flames with OEC compared to air/fuel flames. The disadvantage is that it is also easier to inadvertently ignite an OEC system, which is why the proper safety precautions must be followed. This improvement in ignition characteristics can be especially important when using liquid or solid fuels, which are generally more difficult to ignite compared to gaseous fuels.

20.4.3.4 Flame Shape Control

OEC can be used to control the shape of a flame for an existing air/fuel system. For example, pre-mix enrichment of oxygen into a combustion air stream has been used to shorten the flame length. Undershot enrichment can be used to lengthen a flame. Retrofitting an air/fuel system with

oxygen in an air-oxy/fuel configuration has also been used to control the flame to produce a desired shape. Controlling the flame shape may be done to avoid overheating the refractory in a given location, or to change the heat flux and temperature profiles within the combustion chamber.

20.4.4 LOWER EXHAUST GAS VOLUMES

Eliminating ballast N_2 from air can reduce the exhaust gas flow rate by as much as 96%.²³ In glass manufacturing processes, flue gas reductions from 93 to 98% by mass have been measured.²³ This reduction in the flue gas volume has several advantages. The size of the exhaust gas ductwork can be reduced. Alternatively, OEC has been used effectively to increase production in combustion systems, which are at the limit of their exhaust gas capacity. Normally, increasing capacity would also require a larger flue gas treatment system. However, the flue gas volume actually decreases with OEC, so no new ductwork and treatment equipment are required. Another benefit of the reduction in the flue gas volume is that it can increase the efficiency of the existing flue gas treatment equipment.²⁴ This is because it is easier to treat the exhaust gases since the pollutant emissions are in higher concentrations and therefore easier to remove. The size of the post-treatment equipment can be proportionately reduced, due to the lower flow rates. This saves space, energy, materials, and money.

For a given combustion chamber, the flue gas volume reduction has the added benefit of reducing the average gas velocity by almost an order of magnitude. Lower gas velocities entrain fewer fine particles from the waste. This reduces particulate emissions. Another potential advantage of the reduced velocity in the combustor chamber is the increased residence time. In an incinerator, increased residence time usually increases the level of destruction of undesired organic species in the off gases.

20.4.5 HIGHER HEAT TRANSFER EFFICIENCY

It has been argued that the efficiency of transferring heat from the flame to the load can be increased using OEC.²⁵ In a nonluminous flame, the flame emissivity is higher for an oxygen-enhanced flame, compared to an air/fuel flame. This is due to the higher concentrations of CO_2 and H_2O , which are the gases that radiate in a flame.²⁶ There is no radiation from the N_2 in the flame. These effects are discussed in Chapters 2 and 6.

20.4.6 REDUCED COSTS

Because OEC intensifies the combustion process and reduces the volume of flue gases, many combustion chambers and the associated equipment can be significantly reduced in size. OEC can be used to reduce the cost of the off-gas treatment system.²⁴ Reducing the equipment size can reduce the construction costs and the space required for the heating system.

In some cases, OEC can be used to reduce the costs of raw materials used in a process. Processes that have raw materials containing fine particles generally require some type of baghouse or scrubbing system to remove any particulates that might be entrained in the flue gases so they are not emitted into the atmosphere. For a given size combustion system, replacing air/fuel combustion with OEC can dramatically reduce the amount of particles entrained in the exhaust gases because the gas velocities are much lower, as some or all of the nitrogen is removed from the system. Not only does this reduce the cost of cleaning up the exhaust gases, but it also reduces raw material costs because less is carried out of the system. Specific examples are given in the application sections of this book.

Another type of raw materials saving is an improvement in the process where less material is needed for a given product. One example is in the glass industry where colorants are used to color the glass. Spectrum Glass reported savings of \$20,000/year in colorants when it converted from air/fuel to oxy/fuel because of the improvement in color stabilization using OEC.²¹

20.4.7 INCREASED FLEXIBILITY

There are many other benefits specific to a given process that can be achieved. OEC can increase the flexibility of a heating system.²⁷ In some cases, a wider range of materials can be processed with OEC compared to air/fuel combustion. In other cases, OEC may be required if very high melting temperatures are required. For example, some ceramic and refractory products require firing temperatures of 2900°F (1900K) and higher.²⁸ Those temperatures are difficult if not impossible to achieve with standard air/fuel combustion with no air preheating. A heating system can also be brought up to operating conditions more quickly with OEC compared to air/fuel systems because of the higher heating intensity. For example, it has been shown that using OEC in metal reheat furnaces can substantially improve the ability to start up and shut down quickly.²⁹

A combustion process can react more quickly to changes because of the higher heating intensity. This reduces the time, for example, that it takes to change processing rates or to change the product mix. OEC can give tighter control of the heating profile because of the higher intensity.

20.4.8 IMPROVED OPERATIONS

OEC can improve product quality. For example, the proper use of OEC in a glass furnace can reduce the number of rejects. Quality improvements have been documented in nonferrous smelting, lamp-making, chemical incineration, enamel fritting, and in both ceramic and lime kiln operations.³⁰

By adding oxygen to an existing air/fuel combustion system, the flame length usually shortens. Some oxy/fuel burners are specifically designed to have a short flame length to either intensify the heat release or to better fit into a given furnace geometry to prevent flame impingement on the refractory wall opposite the burner. Shortening existing air/fuel flames or using short flame-length oxy/fuel burners can reduce wear on the refractory by reducing the effects of direct flame impingement on the walls.³¹ As discussed in the next section, however, the improper use of oxygen in a combustion system can lead to refractory damage due to the higher flame temperatures associated with OEC.

20.5 POTENTIAL PROBLEMS

There are potential problems associated with the use of oxygen-enhanced combustion if the system is not properly designed. Many of the potential problems can be generally attributed to the increased combustion intensity.

20.5.1 REFRACTORY DAMAGE

20.5.1.1 Overheating

As previously shown, oxygen-enhanced flames generally have significantly higher flame temperatures compared to conventional air/fuel flames. If the heat is not properly distributed, the intensified radiant output from the flame can cause refractory damage. Today's OEC burners are designed for uniform heat distribution to avoid overheating the refractory surrounding the burner. The burners are normally mounted in a refractory burner block, which is then mounted into the combustion chamber. The burner blocks are made of advanced refractory materials, such as zirconia or alumina, and are designed for long, maintenance-free operation.

If the burner position and firing rate in the furnace are improperly chosen, refractory damage can result. For example, if the flame from an OEC burner is allowed to impinge directly on the wall of a furnace, most typical refractory materials would be damaged. This can be prevented by the proper choice of the burner design and positioning. The flame length should not be so long

that it impinges on the opposite wall. The burner mounting position in the furnace should be chosen to avoid aiming the flame directly at furnace refractories.

20.5.1.2 Corrosion

Another potential refractory problem can result from the increased volatile concentration in the combustion chamber by using OEC. This is a particular problem in the glass industry, for example, where corrosive volatile species are emitted during the glassmaking process. By removing the large quantity of diluent N₂ normally present in air/fuel combustion, these volatile species are now at much higher concentrations in the gas space. This can cause damage to the refractories by corrosion.

20.5.2 NONUNIFORM HEATING

This is an important concern when retrofitting existing systems that were originally designed for air/fuel combustion. By intensifying the combustion process with OEC, there is the possibility of adversely affecting the heat and mass transfer characteristics within the combustion chamber. These issues are only briefly discussed here.

20.5.2.1 Hot Spots

OEC normally increases the flame temperature, which also increases the radiant heat flux from the flame to the load. If the increased radiant output is very localized, then there is the possibility of producing hot spots on the load. This could lead to overheating, which might damage or degrade the product quality. Today, burners for OEC have been specifically designed to avoid this problem.

20.5.2.2 Reduction in Convection

As shown in [Figure 20.23](#), the total volume flow rate of exhaust products is significantly reduced using OEC. However, the average gas temperature is usually higher, but not by enough to offset the reduced gas flow rate. The convective heat transfer from the exhaust gases to the load may be reduced as a result. Another important aspect of convection is mass transfer. In some heating processes, especially those related to drying or removing volatiles, the reduced gas flow rate in the combustion chamber could adversely affect the mass transfer process. This can be offset using a burner that incorporates furnace gas recirculation, which increases the bulk volume flow inside the combustion chamber to help in removing volatiles that evolve from the load during the heating process.

20.5.3 FLAME DISTURBANCE

In recent years, the trend in burner design for OEC has been toward lower momentum flames. One example is the Cleanfire[®] burner (see [Figure 20.24](#)³²), which has been used extensively in the glass industry.³³ These lower momentum flames tend to be longer and more luminous than the high-intensity burners that have traditionally been used in the past. One issue that needs to be considered is that these low momentum flames can be more easily disturbed than the high momentum flames. One example is when low momentum OEC flames are added or partially retrofitted into a furnace containing high momentum air/fuel burners. The high momentum flames can adversely affect the combustion characteristics of the low momentum flames if the geometry is not properly designed. This may be a problem especially if a high momentum burner is directly opposed to and firing at a low momentum burner. Another example of possible flame disturbance is where low momentum flames are located near the exhaust of the furnace. If there are many burners in the furnace, the large exhaust gas flow past a low momentum flame can again disturb those flames. The problem



FIGURE 20.24 Cleanfire burner.³²

of flame disturbance can be eliminated by the proper choice of burners, burner mounting positions, and burner operating conditions.

20.5.4 INCREASED POLLUTANT EMISSIONS

20.5.4.1 NO_x

When O₂ enrichment is used in an existing air/fuel combustion system, there may be an increase in NO_x emissions.³⁴ This is due to the increased flame temperature, which increases thermal NO_x formation.

20.5.4.2 Noise

As shown in [Figure 20.20](#), the flame velocity increases with OEC compared to air/fuel combustion. This means that the gas velocities exiting the burner must be increased to compensate for the higher flame speed. These higher gas velocities can increase the jet noise of the burner. The older-style, high-intensity oxy/fuel burners used in metal melting applications were generally very noisy in the open air. However, the noise was generally muffled by the refractory-lined combustion chamber. Also, although the gas velocities were high, the total volume flow rate was much lower by removing N₂ from the oxidizer, which also was a mitigating factor for the noise. Today, the low momentum oxy/fuel burners are actually quieter than many air/fuel burners. Noise is discussed in more detail in Chapter 7.

20.5.5 FLASHBACK

The use of OEC intensifies the combustion reactions. One consequence of this higher reactivity is the increased risk of flashback. Flashback occurs when the gas velocity exiting the burner is less than the flame velocity. This causes the flame front to move toward the burner. If the fuel and the

oxidizer are premixed, the flame can burn inside the burner housing, which creates the potential for an explosion. As shown in Figure 20.25, the gradient for flashback increases rapidly as the oxygen concentration in the oxidizer increases. This means that the minimum volumetric flow rate increases with OEC to prevent flashback. For blowoff, V is the maximum flow rate before the flame is extinguished due to blowoff.

In premixed systems, there is often a provision for arresting the flame if it should flash back. It may be a separate device known as a flame arrestor, or it may simply be incorporated into the burner design. The general idea in most flame arrestors is to remove enough heat from a flame that is flashing back to cool the flame down below its ignition point. In essence, the third leg of the combustion triangle (Figure 20.26) is removed to extinguish the flame because neither the fuel nor the oxidizer can be removed quickly enough to prevent the flame from flashing back.

In virtually all combustion systems using OEC, the fuel and the oxidizer are not mixed until they exit the burner. This is commonly known as a nozzle-mix burner. This essentially eliminates the potential for an explosion caused by flashback. If the flame were to flash back toward the burner, it would be extinguished at the burner nozzle. The flame would not continue to travel into the

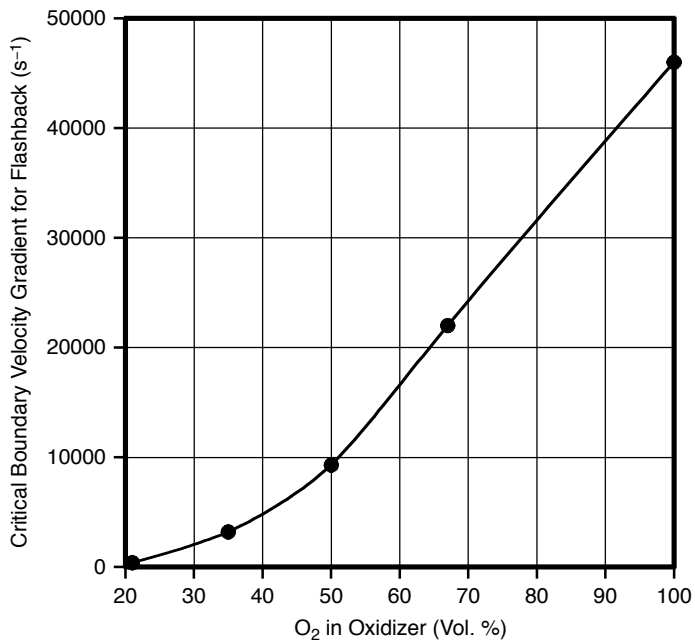


FIGURE 20.25 Critical boundary velocity gradient for flashback vs. oxidizer composition for a stoichiometric premixed methane flame through a cylindrical tube.¹

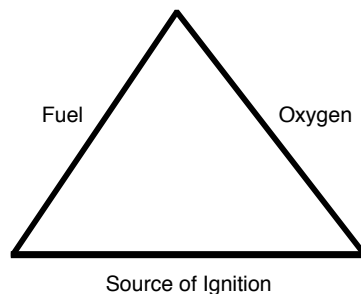


FIGURE 20.26 Combustion triangle.¹

TABLE 20.5
Industrial Applications of Oxygen-Enhanced Combustion

Industry	Furnaces/Kilns	Primary Benefits ^a
Aluminum	Remelting	1, 2
	Coke calcining	1
Cement	Calcining	1
Chemical	Incineration	1, 2, 3, 4
Clay	Brick firing	1, 2, 3
Copper	Smelting	1, 2, 3
	Anode	2
Glass	Regenerative melters	1, 2, 4
	Unit melters	1, 2, 4
	Day tanks	1, 2, 4
Iron and steel	Soaking pits	2, 1
	Reheat furnaces	2, 1
	Ladle preheat	1
	Electric arc melters	1, 2
	Forging furnaces	1, 2
Petroleum	FCC regenerator	1
	Claus sulfur	1
Pulp and paper	Lime kilns	1, 2, 3
	Black liquor	1, 2

^aBenefits of oxygen: 1 = productivity improvement, 2 = energy savings, 3 = quality improvement, 4 = emissions reduction.

With permission from North American Mfg. Co.³⁵

burner as there would no longer be a stoichiometric mixture because the fuel and the oxidizer are separated inside the burner. Therefore, the potential risk of flashback is eliminated by not premixing the fuel and the oxidizer inside the burner.

20.6 INDUSTRIAL HEATING APPLICATIONS

Oxygen-enhanced combustion is used in a wide range of industrial heating applications. In general, OEC has been used in high-temperature heating and melting processes that are either very inefficient or not possible with air/fuel combustion. Table 20.5 shows some of the common reasons why OEC has been used in a variety of industrial applications.³⁵ This section is only intended to give a brief introduction to those applications that are broadly categorized as metals, minerals, incineration, and other. Such applications are briefly discussed here.

20.6.1 METALS

Heating and melting metal was one of the first industrial uses of oxygen-enhanced combustion and continues to be an important application today. OEC has been widely used in both large, integrated steel mills as well as in smaller mini-mills.³⁶ It has also been used in the production of nonferrous metals such as aluminum, brass, copper, and lead.³⁷

The concept of using an oxygen/fuel burner within an air/fuel burner provides the aluminum melter with the flexibility of using either burner, or a combination of both burners (see Figure 20.27). This innovative approach, developed by Air Products and Chemicals, Inc. (Allentown, PA) under the trade name of EZ-Fire[™], has proved to be very successful in the aluminum industry.¹⁰

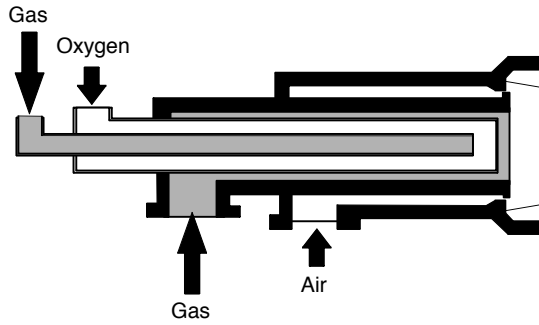


FIGURE 20.27 Air-oxy/fuel burner used in aluminum melting applications.¹

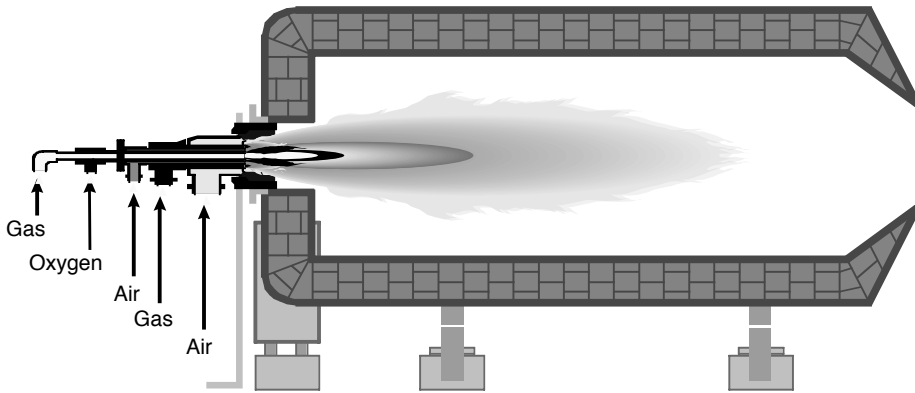


FIGURE 20.28 Air-oxy/fuel burner in a rotary aluminum processing furnace.¹

This differs considerably from both conventional oxygen-enriched techniques and the oxy/fuel burners typically used for melting in the metals industries. This technology is retrofittable on existing air/fuel combustion systems. As shown in Figure 20.28, an oxy/fuel burner is installed in the center of the conventional air/fuel burner. This approach marries the existing air/fuel burner with a retrofitted nonwater-cooled oxy/fuel burner, providing the more efficient heat transfer and available heat benefits of oxy/fuel while maintaining the external flame characteristics of air/fuel. The result is a low-capital-cost, air-oxygen/fuel combustion system that improves the furnace efficiency and lowers production costs.

During meltdown, the oxygen/fuel burner is used along with the air/fuel burner to provide maximum melt rates and minimum flue gas volumes, while during holding and casting, only the air/fuel burner is used. For the melting of aluminum, a combination of air-oxy/fuel combustion provides the best results. The outer air/fuel flame envelope provides a shielding effect for the hot oxygen/fuel inner flame. By firing the oxygen/fuel inner burner on a fuel-rich mixture, flame luminosity is increased as combustion radicals and gas particles are heated to incandescence by the hot oxy/fuel flame. This, in turn, improves the radiative heat transfer of the flame to the charge material and furnace wall while preventing excess oxygen from contacting the load and causing metal oxidation.

Some specific examples of the effects of burner design on NO_x emissions in air-oxy/fuel burners will be used to illustrate the importance of the burner itself, in addition to its operating

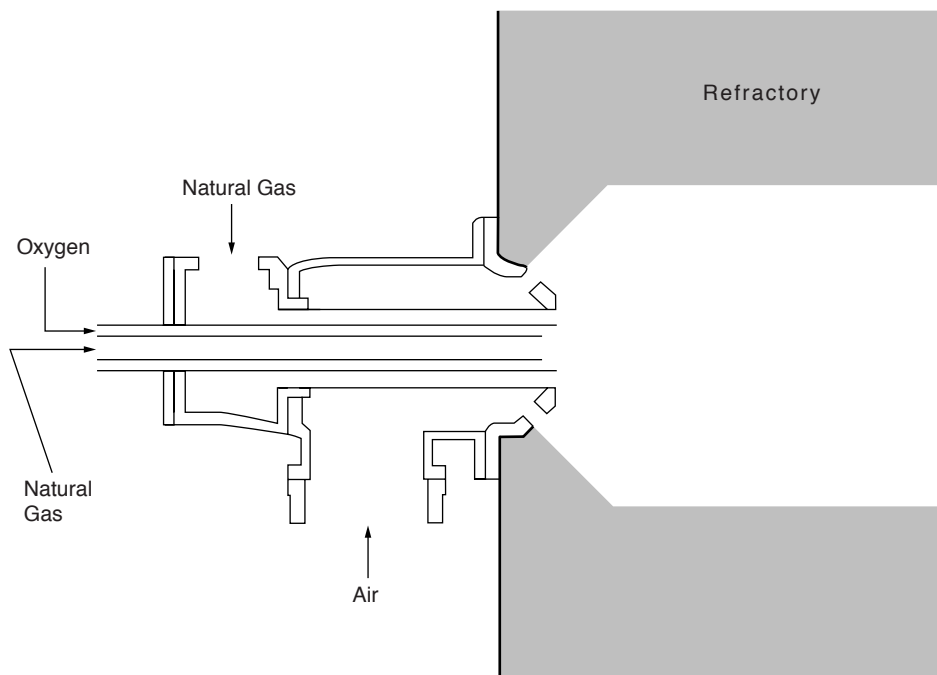


FIGURE 20.29 EZ-0 burner drawing. (Source: U.S. Patent and Trademark Office.³⁹)

conditions. A series of burner designs known as EZ-Fire™ were developed by Air Products and Chemicals, Inc. (Allentown, PA). Figure 20.29 shows a drawing of a first-generation model (referred to here as EZ-0) designed to use a gaseous fuel such as natural gas and a combined oxidant of air and pure oxygen.¹⁰ This design was designed for easy retrofitting of an existing air/fuel burner to increase the throughput of industrial combustion processes, particularly aluminum production. It was not designed for low-NOx emissions and, in fact, increased NOx compared to air/fuel-only combustion. The increased emissions were unacceptable, which led to the development of a second-generation model (referred to here as EZ-1) shown in Figure 20.30.⁴⁰ Two variants of this design are shown in Figure 20.31 and Figure 20.32, referred to here as EZ-1A and EZ-1B, respectively.

During the development of the EZ-1, another series of burner designs (referred to here as EZ-3) was developed and tested. As will be shown, these did not reduce NOx emissions as much as the EZ-1 configuration. Figure 20.33 is a drawing of the EZ-3A configuration consisting of an annular design with a full flare between the middle oxygen passage and the outer air passage. Figure 20.34 shows the effect of the length of the burner block on NOx emissions. For this design, the shorter the block, the lower the NOx. Figure 20.35 shows a similar burner design with only a half flare between the oxygen and air passages. Figure 20.36 shows that the larger internal burner block diameter and the shortest internal burner block length generally produced lower NOx emissions. Figure 20.37 is a drawing of the same burner shown in Figure 20.35, except with seventeen 0.5-in. holes in the half flare. Figure 20.38 again shows that the burner with no burner tile produced less NOx than the 7-in.-long tile. In Figure 20.39, the flare was completely removed. Figure 20.40 again shows that for a fixed internal burner block diameter of 8 in., the shorter the burner block, the lower the NOx emissions. Figure 20.41 shows that the EZ-1 design produced less NOx than any of the EZ-3 designs. This figure also shows that the addition of the flare increased NOx emissions.

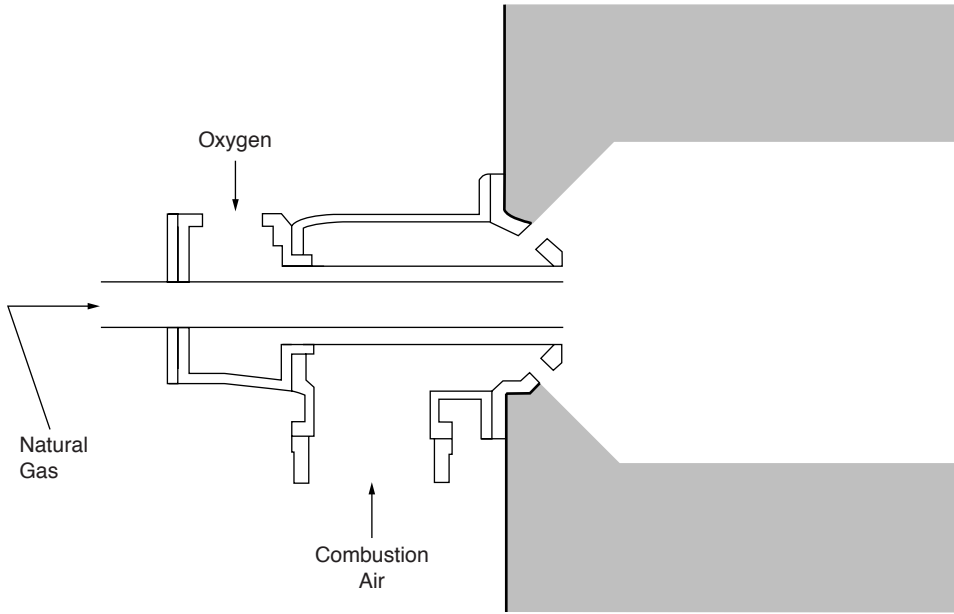


FIGURE 20.30 EZ-1 burner drawing. (Source: U.S. Patent and Trademark Office.³⁸)

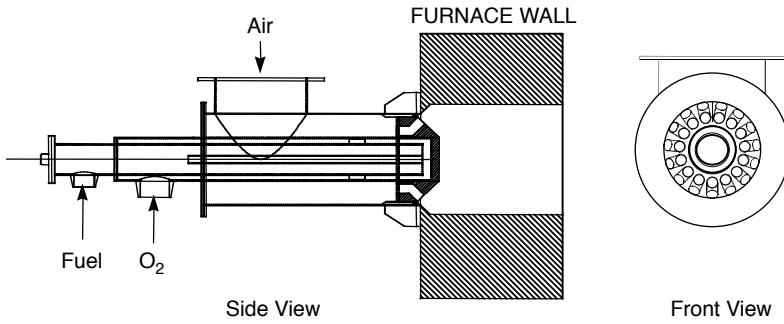


FIGURE 20.31 EZ-1A burner drawing. (Source: U.S. Patent and Trademark Office.³⁸)

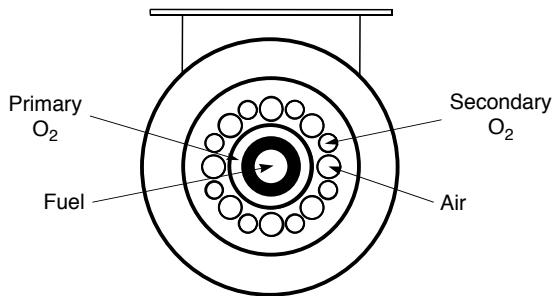


FIGURE 20.32 EZ-1B burner drawing. (Source: U.S. Patent and Trademark Office.³⁸)

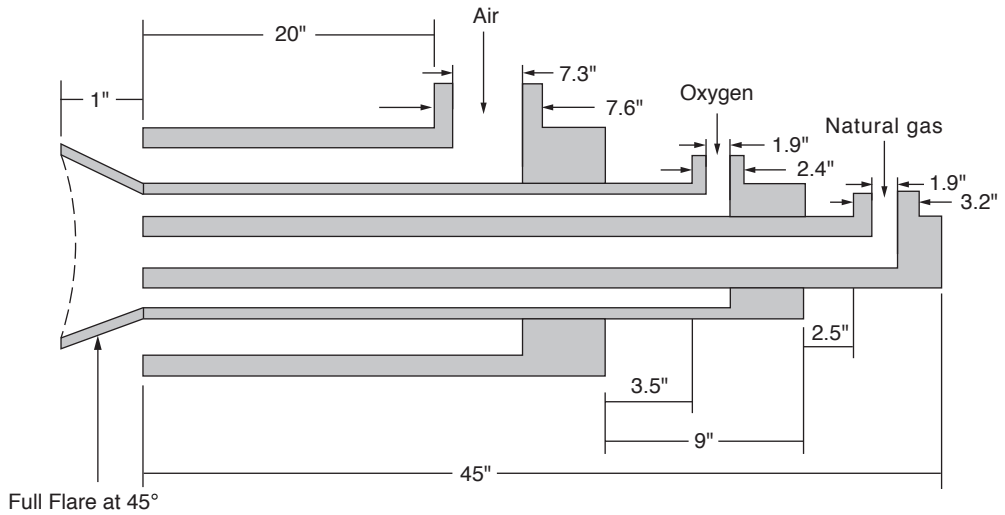


FIGURE 20.33 EZ-3A burner drawing. (Source: U.S. Patent and Trademark Office.³⁸)

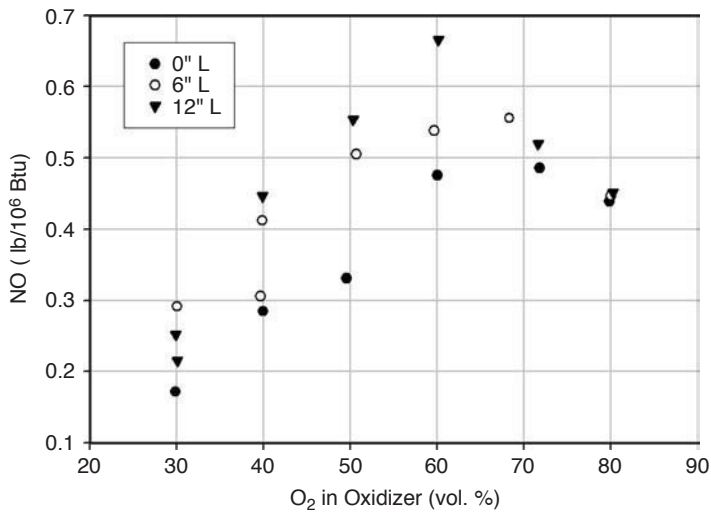


FIGURE 20.34 Measured NO vs. oxidant composition and burner block length for an EZ-3A with an 8-in. ID burner block. (Source: U.S. Patent and Trademark Office.³⁸)

A third-generation EZ-Fire design (referred to here as EZ-4) was developed and tested.³⁹ A drawing of this model is shown in Figure 20.42. As can be seen, the half-moon-shaped air passages are significantly different than the previous designs. In addition, oxygen lances were added in the middle of the air passages. This design was tested to vary the amount of oxygen injected through these lances compared to the amount injected through the central oxygen annulus. Figure 20.43 shows field measurements of the NO_x from the EZ-1A (Figure 20.31), EZ-1B (Figure 20.32), and EZ-4 (Figure 20.42) designs. The EZ-4 produced considerably less NO_x compared to the EZ-1 designs. Figure 20.44 shows that lancing some of the oxygen through the air passage can significantly reduce NO_x compared to no O₂ lancing.

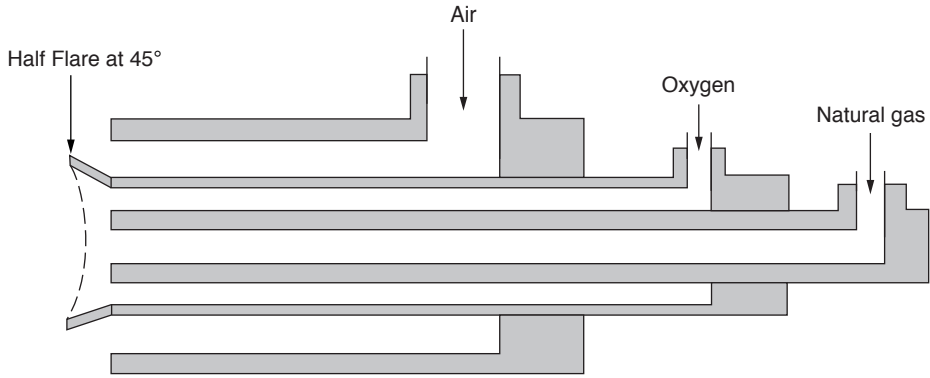


FIGURE 20.35 EZ-3B burner drawing. (Source: U.S. Patent and Trademark Office.³⁸)

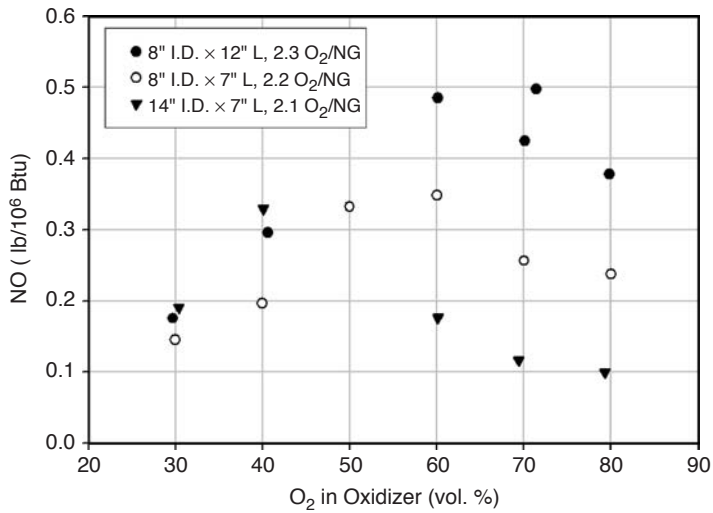


FIGURE 20.36 Measured NO vs. oxidant composition and burner block shape for an EZ-3B with no holes in the half flare. (Source: U.S. Patent and Trademark Office.³⁸)

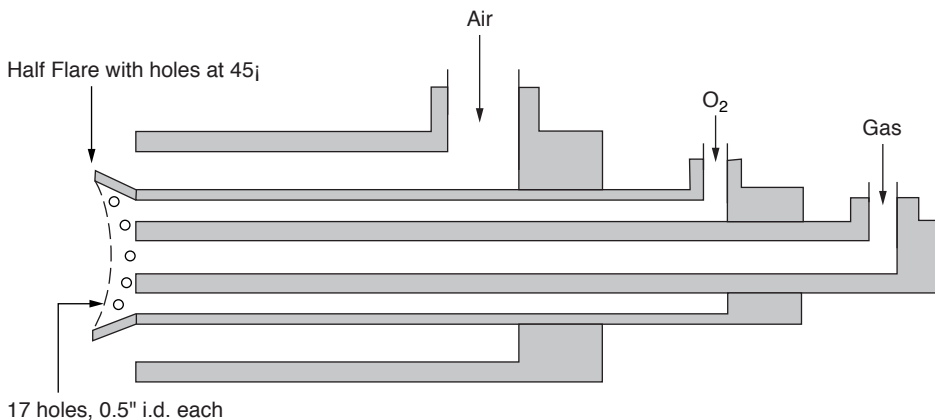


FIGURE 20.37 EZ-3B burner with holes in the flare. (Source: U.S. Patent and Trademark Office.³⁸)

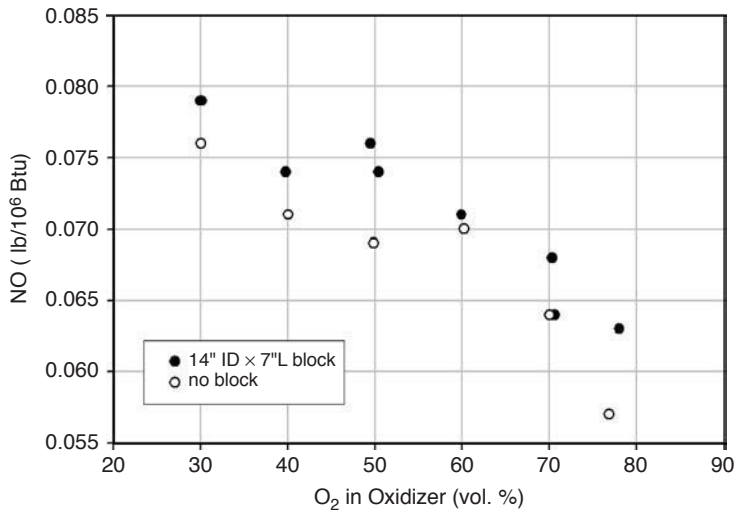


FIGURE 20.38 Measured NO vs. oxidant composition and burner block shape for an EZ-3B with holes in the half flare. (Source: U.S. Patent and Trademark Office.³⁸)

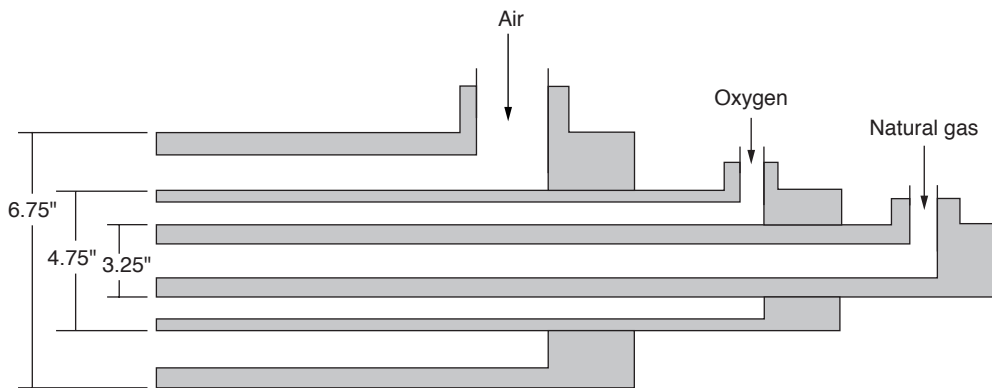


FIGURE 20.39 EZ-3C burner drawing. (Source: U.S. Patent and Trademark Office.³⁸)

20.6.2 MINERALS

Here, minerals refers to glass, cement, lime, bricks, and other related materials that require high-temperature heating and melting during their manufacture. OEC has been used in all of these applications.

Due to the very low energy efficiency and the use of individual burners, the air/fuel unit melters are very amenable to oxygen-enhanced combustion techniques, including supplemental oxy/fuel boosting (see Figure 20.45⁴⁰), premix oxygen enrichment, and full oxy/fuel combustion. Oxy/fuel unit melters have been built as large as 350 tons (320 metric tons) per day of glass to as small as 500 pounds (230 kg) of glass per day.

Abbasi et al. (1996) described a new process known as oxygen-enriched air staging (OEAS).⁴¹ A schematic of the process for an endpoint furnace (see Figure 20.46) is shown in Figure 20.47.⁴²

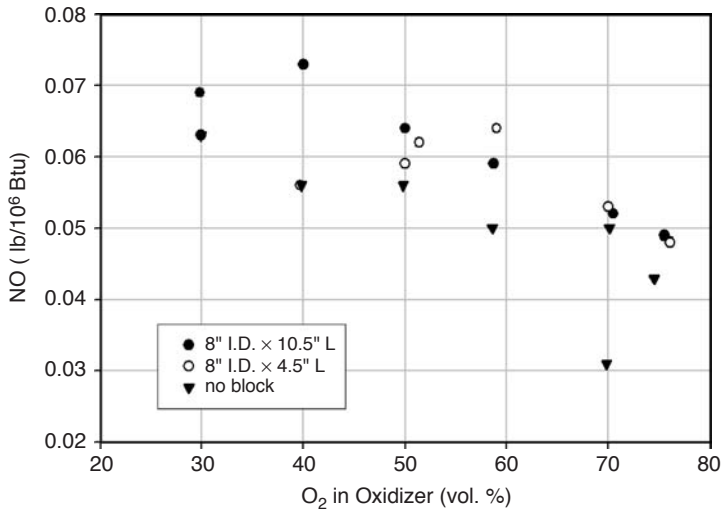


FIGURE 20.40 Measured NO vs. oxidant composition and burner block length for an EZ-3C with an 8-in. ID burner block. (Source: U.S. Patent and Trademark Office.³⁸)

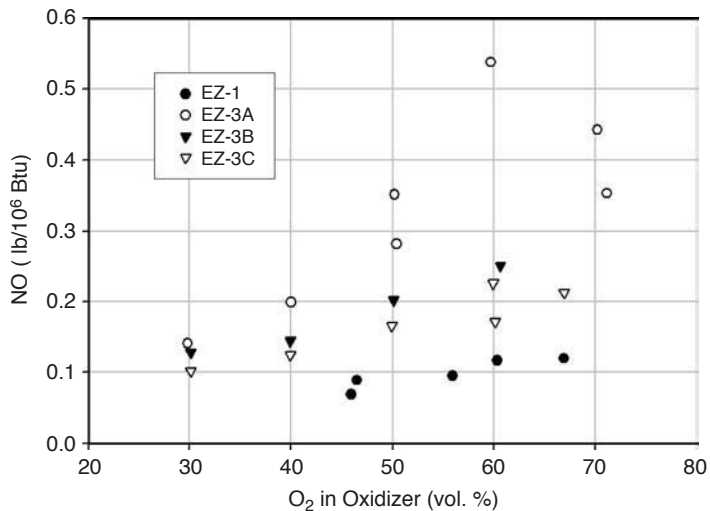


FIGURE 20.41 Measured NO vs. oxidant composition and burner design where the burners had no burner block, the O₂:NG stoichiometry was approximately 2.3, and the firing rate was 3 × 10⁶ Btu/hr. (Source: U.S. Patent and Trademark Office.³⁸)

A schematic for application of the process on a sideport furnace (see [Figure 20.48](#)) is shown in [Figure 20.49](#). While the primary objective of the technology is to reduce NO_x emissions (50 to 70% reduction was measured), there are also some effects on heat transfer. Because the preheated air flames are now initially fuel-rich, they are more luminous and, therefore, more radiative. The secondary oxygen added to the exhaust products completes the combustion before the gases exit the furnace. This secondary combustion zone helps to spread the heat transfer over a wider region in the furnace, which helps to make the heat flux more uniform.

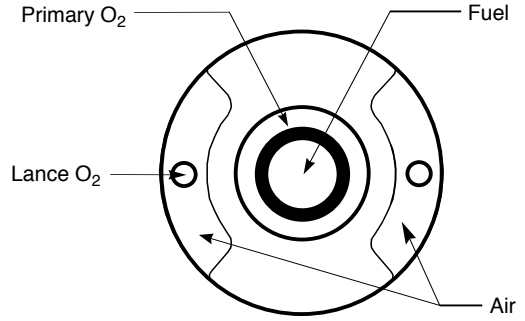


FIGURE 20.42 EZ-4 burner drawing. (Source: U.S. Patent and Trademark Office.³⁹)

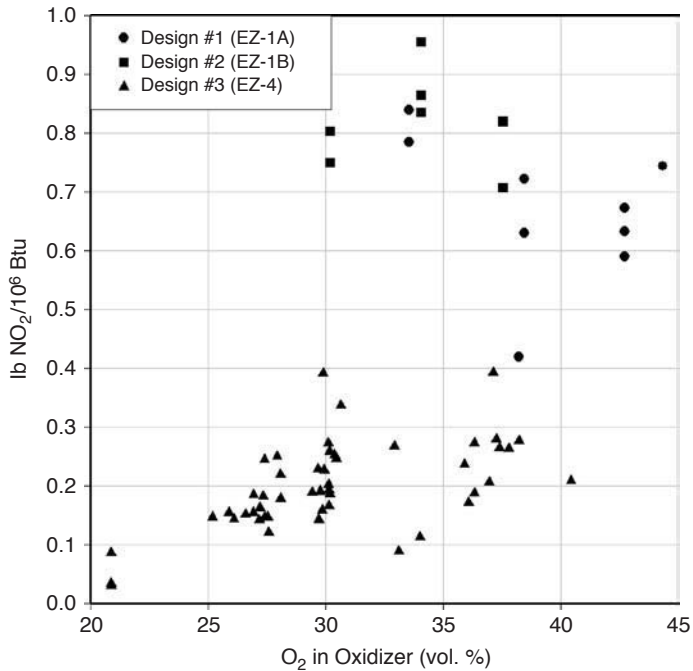


FIGURE 20.43 Measured NO₂ vs. oxidant composition and burner design (EZ-1A, EZ-1B, EZ-4) where the burners had no burner block and the O₂:NG stoichiometry was approximately 2.0; the firing rate and the O₂ flow through the lances of EZ-4 varied. (Source: U.S. Patent and Trademark Office.³⁹)

OEC has been used in a variety of ways in the glass industry. Figure 20.50 shows the use of oxygen-enhanced combustion in a glass furnace by lancing oxygen into the flames of the burners. Figure 20.51 shows oxygen-enhanced combustion in a glass furnace. Figure 20.52 shows the effect on the economics of using oxygen-enhanced combustion to control NO_x and particulate emissions.⁴³

Another technique for controlling dust emissions is through the use of oxygen-enhanced combustion. This is done by replacing a substantial amount of the air used for combustion with high-purity oxygen. Figure 20.53 shows oxygen-enhanced combustion applied to a rotary kiln. Essentially, this amounts to removing large quantities of inert nitrogen from the system. This has two positive effects on dust emissions. The first is that the overall system thermal efficiency is

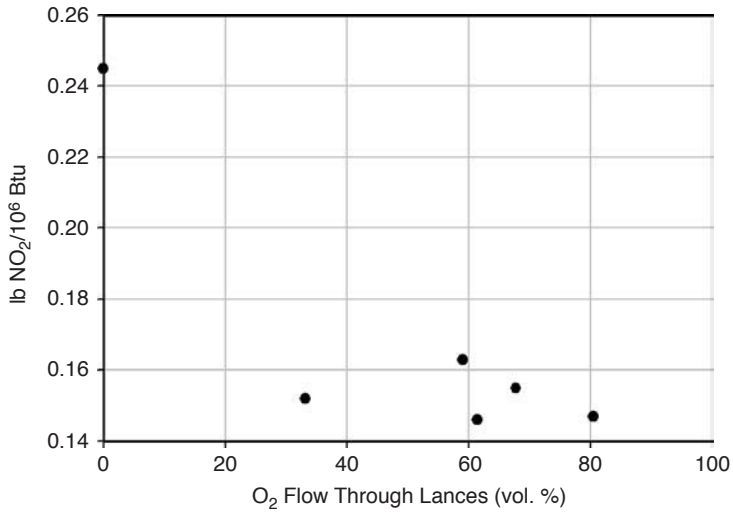


FIGURE 20.44 Measured NO₂ vs. the fraction of oxygen through the lances in the EZ-4 burner for an overall O₂:NG stoichiometry of approximately 2.0 and approximately 27% O₂ in the combined oxidizer. (Source: U.S. Patent and Trademark Office.³⁹)

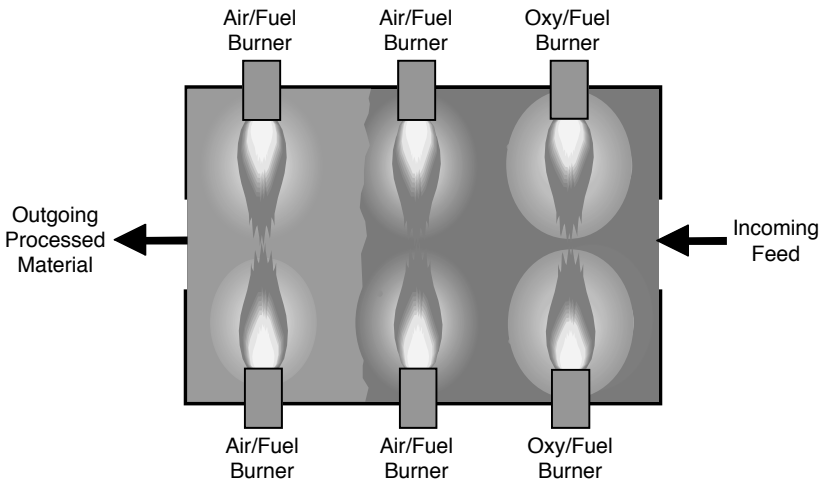


FIGURE 20.45 Plan view of oxy/fuel boosting in a glass furnace.⁴⁰

improved so that less fuel needs to be fired for a given production rate. Less fuel means less flue gas and therefore less particle entrainment. The second positive effect is also related to particle entrainment. By removing large quantities of nitrogen, the flue gas volume decreases, which reduces particle entrainment. Low levels of oxygen enrichment, however, can increase NO_x emissions so there may be a trade-off of one emission for another. Often, oxygen-enhanced combustion is used in this application to increase throughput for a given size kiln and auxiliary equipment. This means that the firing rate may not be decreased, but the material processing rate is increased. The overall

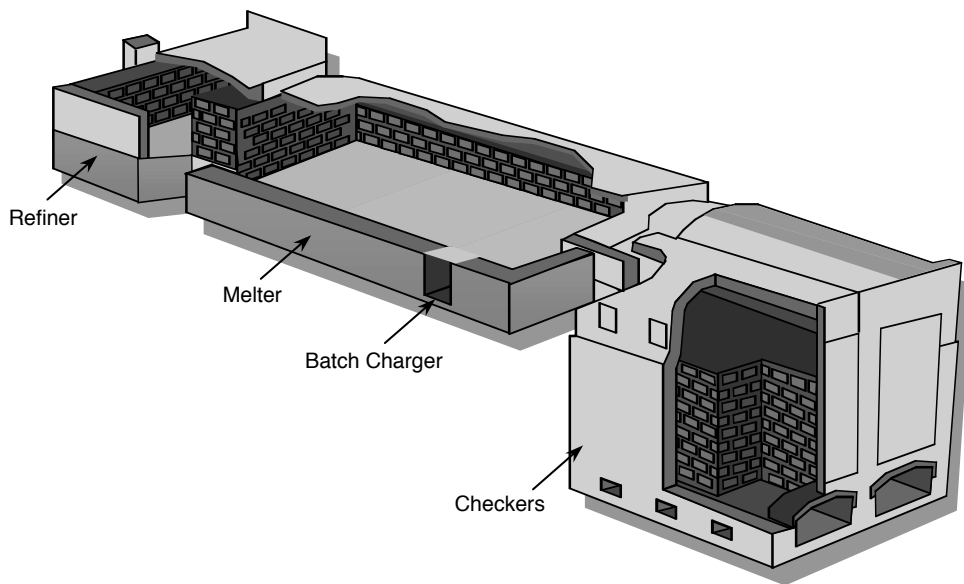


FIGURE 20.46 End-port regenerative melter.⁴³

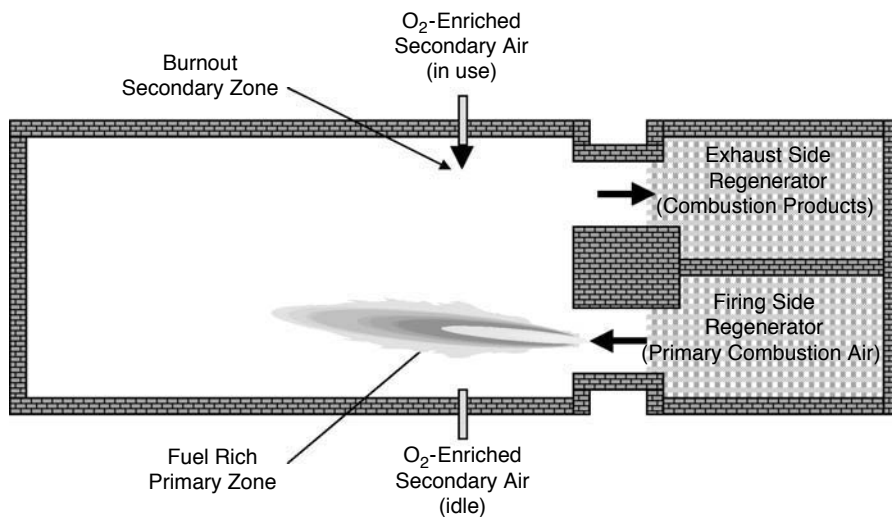


FIGURE 20.47 Oxygen-enriched air staging in an end-port regenerative furnace.

dust emissions may actually increase, although they may decrease on a unit production basis (e.g., tons of clinker).

20.6.3 INCINERATION

OEC has been used to enhance the performance of portable incinerators used to clean up contaminated soil.⁴⁴ It has also been used in municipal solid waste incinerators and in boilers burning waste fuels. Many of the benefits associated with oxygen-enhanced combustion (OEC) relate to

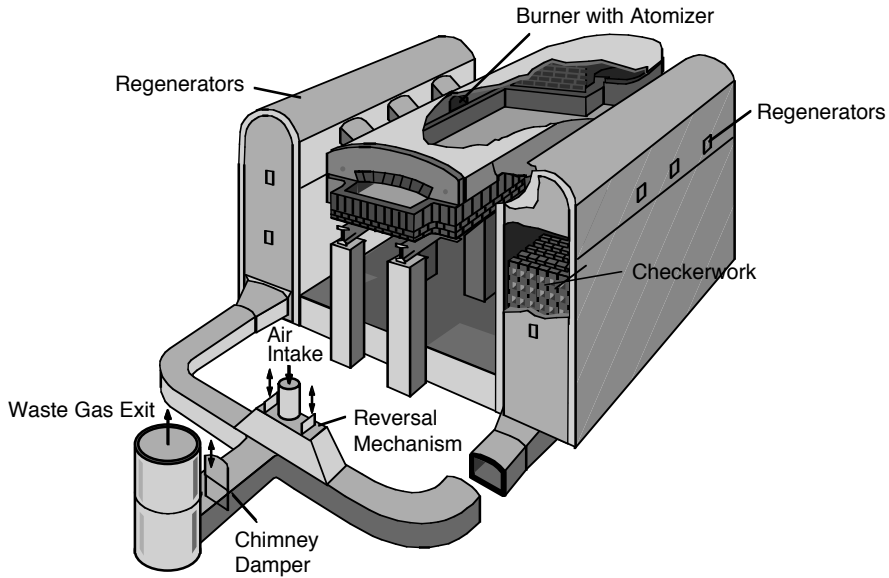


FIGURE 20.48 Side-port regenerative melter.⁴³

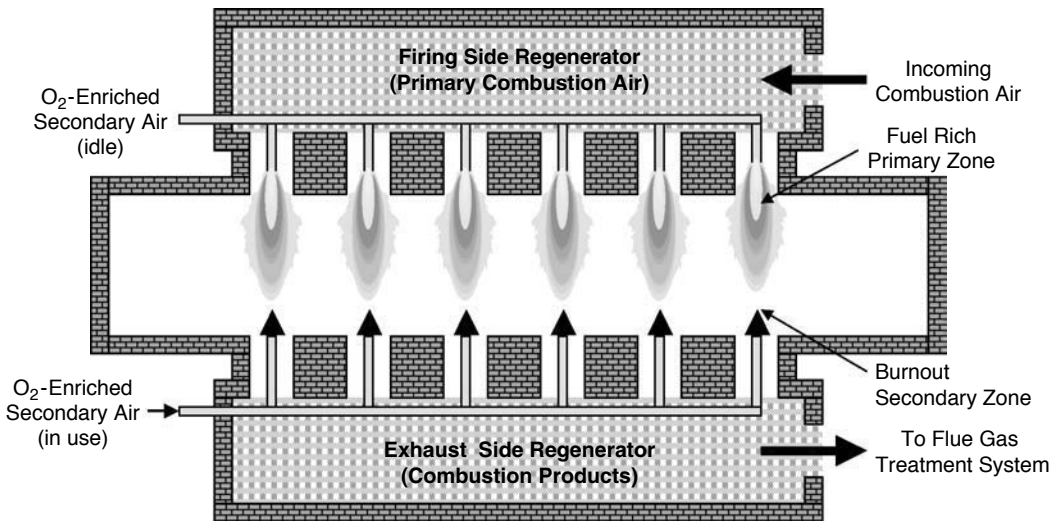


FIGURE 20.49 Oxygen-enriched air staging in a side-port regenerative furnace.

increasing the partial pressure of O_2 in the incinerator. The combustion process becomes more reactive, which tends to increase the destruction efficiency of any hydrocarbons in the system. This lowers the pollutant emissions. A schematic of some of the benefits of using OEC is shown in [Figure 20.54](#). Figure 20.55 shows a schematic of oxygen lancing used to enhance the performance of an incinerator. Figure 20.56 shows the use of oxygen enrichment to enhance the performance of a municipal solid waste incinerator. [Figure 20.57](#) shows the use of oxygen enrichment in a sludge incinerator.

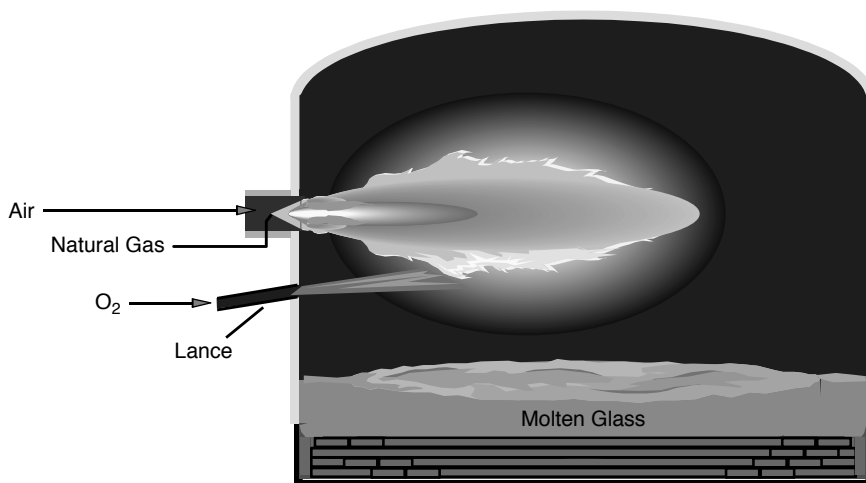


FIGURE 20.50 Oxygen lancing into the flames in a glass furnace.

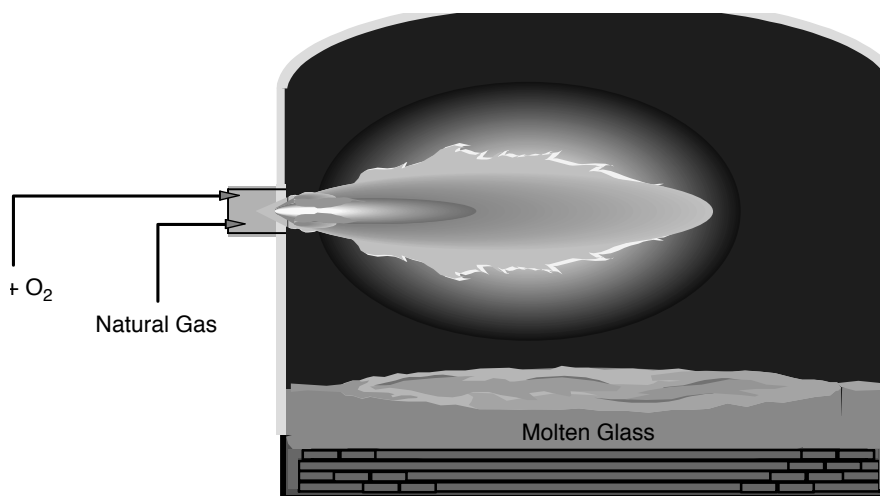


FIGURE 20.51 Oxygen-enhanced combustion in a glass furnace.

20.6.4 OTHER

OEC has been used in a wide variety of specialty applications that are not discussed in detail in this book. Some of these include gasifying organic materials and vitrifying residual ash,⁴⁵ removing unburned carbon from fly ash,⁴⁶ and oxygen enrichment of fluid catalytic crackers.⁴⁷

20.7 CONCLUSIONS

There are a number of factors that make the future look bright for OEC. Separate reports on the industrial uses of OEC sponsored by the U.S. Department of Energy in 1987²⁵ and the Gas Research Institute in 1989⁴ have been published. New advancements are continually being made in existing and new (e.g., Reference 48) oxygen generation technologies. This should

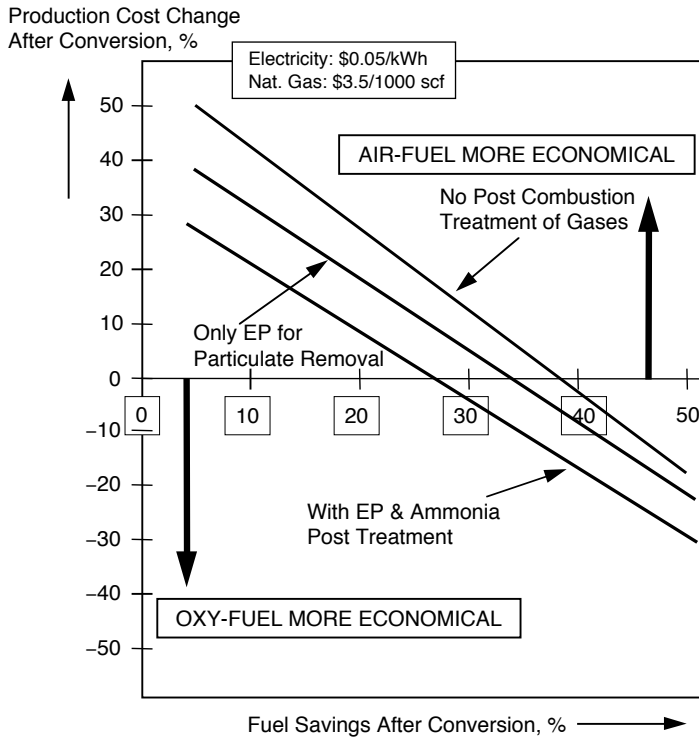


FIGURE 20.52 Effect of NO_x and particulate controls on process economics for air/fuel vs. oxy/fuel combustion.⁴³

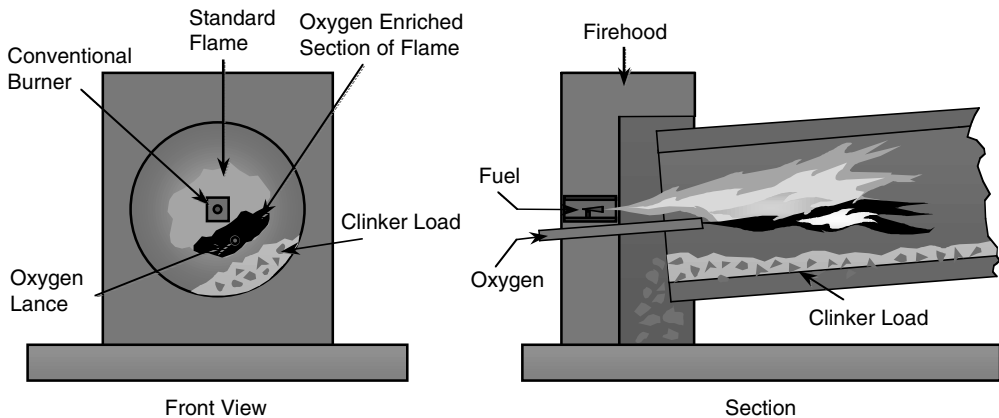


FIGURE 20.53 Oxygen-enhanced combustion in a rotary kiln.

reduce the cost to the end user, which should expand the number of amenable applications. Studies are being conducted to further improve the energy efficiency of OEC processes using novel methods of heat recovery⁴⁹ and integrating the air separation process with the combustion system.²⁰

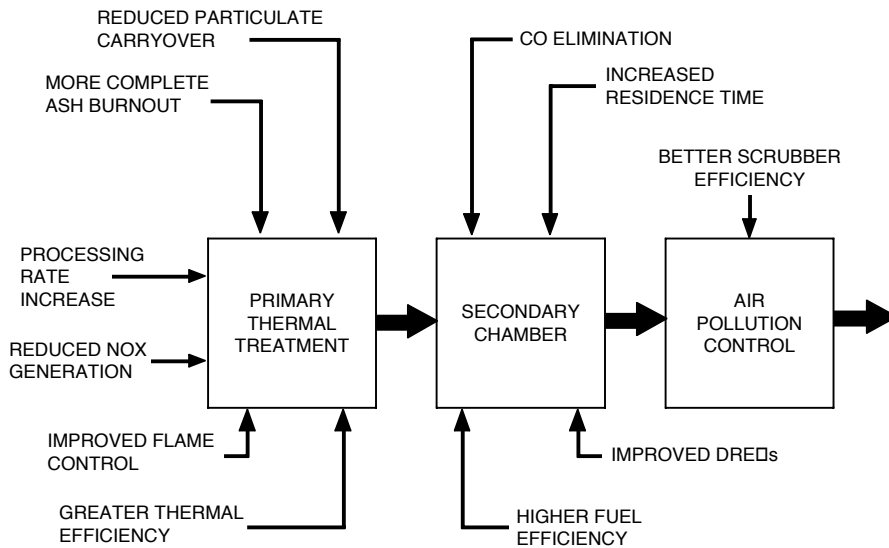


FIGURE 20.54 Benefits of using oxygen in waste incineration applications.¹

There are many areas related to the use of OEC that need further research. In a recent report for the U.S. Department of Energy, the following were recommended for further research:⁵⁰

- Use oxygen enrichment to increase furnace efficiency in the petroleum industry
- Investigate the benefits and disadvantages of varying the oxidizer composition ranging from air to pure O₂
- Measure the NO_x from oxygen-enriched burners in steel reheat furnaces
- Optimize the amount of O₂ injection into cupolas used in the foundry industry to recuperate energy from the CO produced in the process
- Optimize glass-melting processes that use oxygen/fuel combustion, including the development of computer models
- Quantify furnace efficiency and productivity improvements using OEC in aluminum melting
- Develop NO_x reduction technologies for OEC in aluminum processes

Another major area for further research in the use of OEC is the design of the combustion chambers. In nearly all cases, OEC has been adapted and retrofitted to existing furnace designs. In the future, the design of new furnaces that will use OEC should be investigated to optimize the increased radiant heat transfer, reduced convective heat transfer, and reduced gas volume flow rates.

There are numerous examples of using oxygen-enhanced combustion in a wide variety of industrial heating applications. In some cases, low level O₂ enrichment of an existing air/fuel combustion system can have dramatic results. In other cases, oxy/fuel burners may be used to provide needed solutions.

Lower cost O₂, coupled with the significant environmental and operating benefits of OEC, make OEC an attractive technology. Research continues to assess its effectiveness in a wide range of applications.

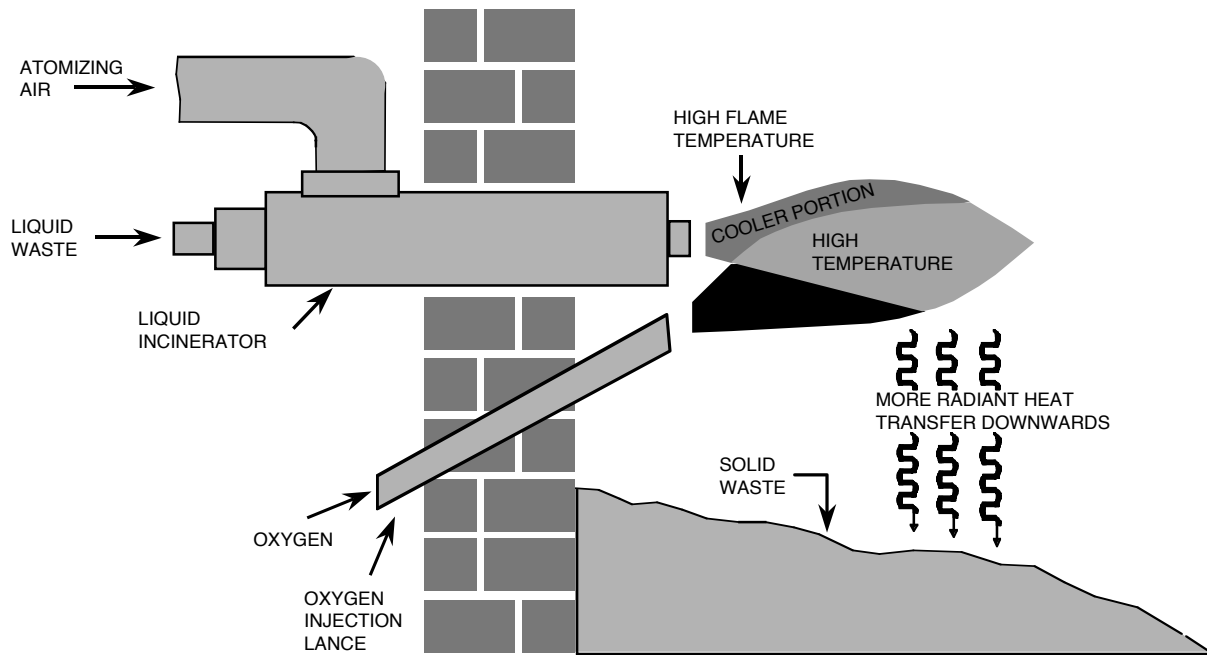


FIGURE 20.55 Oxygen lancing into an incinerator.¹

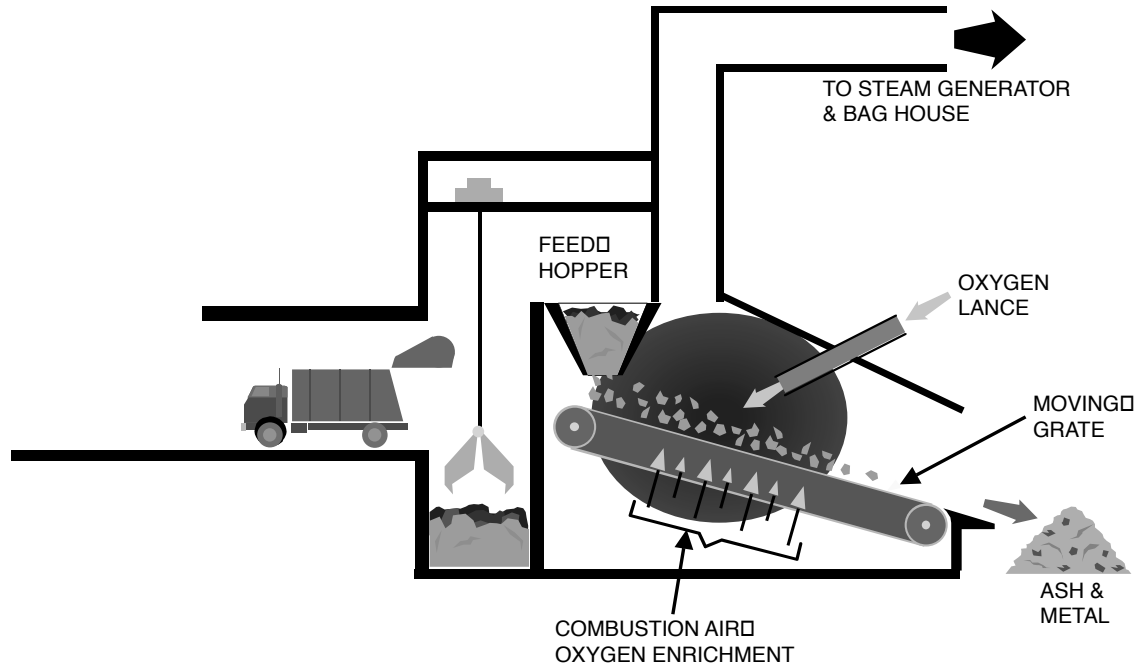


FIGURE 20.56 Oxygen enrichment of a municipal solid waste incinerator.¹

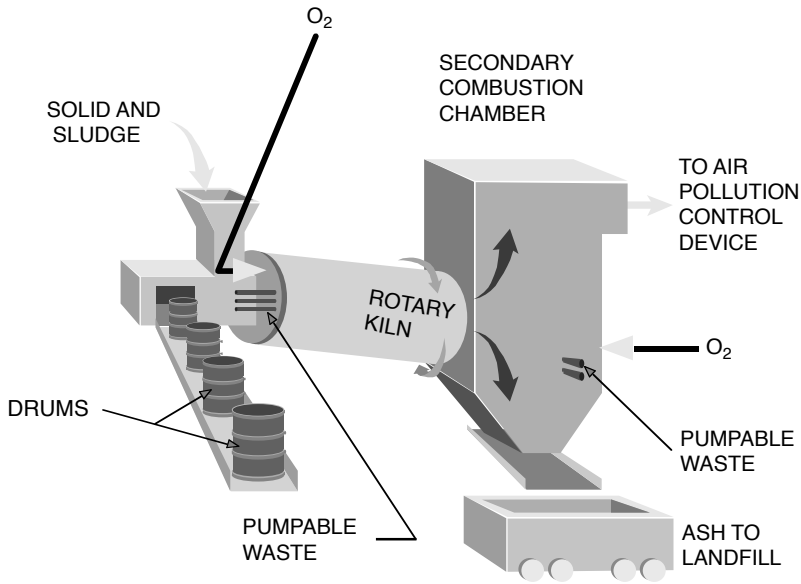


FIGURE 20.57 Oxygen enrichment of a sludge incinerator.¹

REFERENCES

1. Baukal, C.E., Ed., *Oxygen-Enhanced Combustion*, CRC Press, Boca Raton, FL, 1998.
2. McGuinness, R.M. and Kleinberg, W.T., Oxygen Production, Chapter 3 in *Oxygen-Enhanced Combustion*, Baukal, C.E., Ed., CRC Press, Boca Raton, FL, 1998.
3. Baukal, C.E., Pollutant Emissions, Chapter 2 in *Oxygen-Enhanced Combustion*, Baukal, C.E., Ed., CRC Press, Boca Raton, FL, 1998.
4. Williams, S.J., Cuervo, L.A., and Chapman, M.A., High-Temperature Industrial Process Heating: Oxygen-Gas Combustion and Plasma Heating Systems, Gas Research Institute Report GRI-89/0256, Chicago, IL, July 1989.
5. Chace, A.S., Hazard, H.R., Levy, A., Thekdi, A.C., and Ungar, E.W., Combustion Research Opportunities for Industrial Applications — Phase II, U.S. Dept. of Energy report DOE/ID-10204-2, Washington, D.C., 1989.
6. Baukal, C.E., Eleazer, P.B., and Farmer, L.K., Basis for Enhancing Combustion by Oxygen Enrichment, *Industrial Heating*, LIX (2), 22, 1992.
7. Benedek, K.R. and Wilson, R.P., The Competitive Position of Natural-Gas in Oxy-Fuel Burner Applications, Gas Research Institute Report GRI-96-0350, Chicago, IL, September 1996.
8. Joshi, S.V., Becker, J.S., and Lytle, G.C., Effects of Oxygen Enrichment on the Performance of Air-Fuel Burners, in *Industrial Combustion Technologies*, Lukasiewicz, Amer. Soc. Metals, 165, 1986.
9. U.S. Environmental Protection Agency, Alternative Control Techniques Document — NO_x Emissions from Utility Boilers, EPA Report EPA-453/R-94-023, Research Triangle Park, NC, 1994.
10. Bazarian, E.R., Heffron, J.F., and Baukal, C.E., Method for Reducing NO_x Production During Air-Fuel Combustion Processes, U.S. Patent 5,308,239, 1994.
11. Gitman, G.M., Method and Apparatus for Generating Highly Luminous Flame, U.S. Patent 4,797,087, 1989.
12. Dalton, A.I. and Tyndall, D.W., Oxygen Enriched Air/Natural Gas Burner System Development, NTIS Report PB91-167510, Springfield, VA, 1989.
13. Gordon, S. and McBride, B.J., Computer Program for Calculation of Complex Chemical Equilibrium Compositions, Rocket Performance, Incident and Reflected Shocks, and Chapman-Jouguet Detonations, NASA Report SP-273, 1971.
14. Baukal, C.E., Ed., *The John Zink Combustion Handbook*, CRC Press, Boca Raton, FL, 2001.

15. Turin, J.J. and Huebler, J., Gas-Air-Oxygen Combustion Studies, Report no. I.G.R.-61, American Gas Association, 1951.
16. Lewis, B. and von Elbe, G., *Combustion, Flames and Explosions of Gases*, third edition, Academic Press, New York, 1987.
17. American Gas Association, *Gas Engineers Handbook*, Industrial Press Inc., New York, 2/72, 1965.
18. Gibbs, B.M. and Williams, A., Fundamental Aspects on the Use of Oxygen in Combustion Processes—A Review, *J. Inst. Energy*, June, 74, 1983.
19. Farrell, L.M., Pavlack, T.T., and Rich, L., Operational and Environmental Benefits of Oxy-Fuel Combustion in the Steel Industry, *Iron & Steel Engineer*, March, 35, 1995.
20. Ding, M.G. and Du, Z., Energy & Environmental Benefits of Oxy-Fuel Combustion, *Proceedings of the 1995 International Conference on Energy & Environment*, Shanghai, China, May 1995, Begell House Inc., New York, 674.
21. Grisham, S., Oxy-Conversion for a Smaller Furnace Yields Big Results, *American Glass Review*, May–June, 12, 1997.
22. Harris, M.E., Grumer, J., Von Elbe, G., and Lewis, B., Burning Velocities, Quenching, and Stability Data on Nonturbulent Flames of Methane and Propane with Oxygen and Nitrogen, *Third Symposium on Combustion, Flame and Explosion Phenomena*, Williams & Wilkins Co., Baltimore, 1949, 80.
23. Brown, J.T., Glass Melting: The Elegance of Direct-Fired Oxy-Fuel, *Ceramic Industry*, March 1992, 47.
24. Gill, J.H. and Quiel, J.M., *Incineration of Hazardous, Toxic, and Mixed Wastes*, North American Mfg. Co., Cleveland, 1993.
25. Kobayashi, H., Oxygen Enriched Combustion System Performance Study, Phase I Interim/Final Report, Volume I: Technical and Economic Analysis, U.S. Dept. of Energy report DOE/ID/12597, Washington, D.C., March 1987.
26. Hottel, H.C. and Sarofim, A.F., *Radiative Transfer*, McGraw-Hill, New York, 1967.
27. DeLucia, M., Oxygen Enrichment in Combustion Processes: Comparative Experimental Results from Several Application Fields, *J. Energy Resources Tech.*, 113, 122, 1991.
28. Industrial Heating Equipment Association, *Combustion Technology Manual*, fifth edition, Arlington, VA, 1994.
29. Becker, J.S. and Farmer, L.K., Rapid Fire Heating System Uses Oxy-Gas Burners for Efficient Metal Heating, *Ind. Heating*, 62(3), 74–78, 1995.
30. Dafoe, B.M., *Report of Committee F: Industrial and Commercial Utilization of Gases*, International Gas Union, Switzerland, 1991.
31. Cornforth, J.R., *Combustion Engineering and Gas Utilisation*, third edition, E & FN Spon, London, 1992.
32. Gershtein, V.Y. and Baukal, C.E., CFD in Burner Development, Chapter 7 in *Oxygen-Enhanced Combustion*, Baukal, C.E., Ed., CRC Press, Boca Raton, FL, 1998.
33. Slavejkov, A.G., Baukal, C.E., Joshi, M.L., and Nabors, J.K., Oxy-Fuel Glass Melting with a High-Performance Burner, *Ceramic Bulletin*, 71(3), 340, 1992.
34. Guerrero, P.S., Rebello, W.J., Ally, M.R., and Jain, R., Combustion Characteristics of Fuels with Preheated Oxygen Enriched Air, in *Industrial Combustion Technologies*, Lukasiewicz, M.A., Ed., American Society of Metals, 1986, 187.
35. Reed, R.J., *North American Combustion Handbook*, third edition, Vol. II, Part 13, 1997.
36. Kistler, M.D. and Becker, J.S., Ferrous Metals, Chapter 5 in *Oxygen-Enhanced Combustion*, Baukal, C.E., Ed., CRC Press, Boca Raton, FL, 1998.
37. Saha, D. and Baukal, C.E., Nonferrous Metals, Chapter 5 in *Oxygen-Enhanced Combustion*, Baukal, C.E., Ed., CRC Press, Boca Raton, FL, 1998.
38. Baukal, C.E., Slavejkov, A.G., and Monroig, L.W., Method and Apparatus for Reducing NO_x Production During Air-Oxygen-Fuel Combustion, U.S. Patent 5,611,683 issued March 18, 1997.
39. Baukal, C.E., Gershtein, V.Y., Heffron, J.F., Best, R.C., and Eleazer, P.B., Method and Apparatus for Reducing NO_x Production during Air-Oxygen/Fuel Combustion, U.S. Patent 5,871,343, issued February 16, 1999.
40. Baukal, C.E., *Heat Transfer in Industrial Combustion*, CRC Press, Boca Raton, FL, 2000.

41. Abbasi, H.A., Grosman, R.E., Donaldson, L.W., Youssef, C.F., Joshi, M.L., and Hope, S.R., A Low-NO_x Retrofit Technology for Regenerative Glass Melters, *Proc. 1995 International Gas Research Conf.*, Vol. II, Dolenc, D.A., Ed., Government Institutes, Rockville, MD, 1996, 2322–2331.
42. Baukal, C.E., *Industrial Combustion Pollution and Control*, Marcel Dekker, New York, 2004.
43. Eleazer, P.B. and Hoke, B.C., Glass, in *Oxygen-Enhanced Combustion*, Baukal, C.E., Ed., CRC Press, Boca Raton, FL, 1998, 215–236.
44. Baukal, C.E., Waste Incineration, Chapter 8 in *Oxygen-Enhanced Combustion*, Baukal, C.E., Ed., CRC Press, Boca Raton, FL, 1998.
45. Bishop, N.G. and Taylor, G., Method and Apparatus for Gasifying Organic Materials and Vitrifying Residual Ash, U.S. Patent 5,584,255, issued Dec. 17, 1996.
46. Martinez, M.P., Apparatus and Process for Removing Unburned Carbon in Fly Ash, U.S. Patent 5,555,821, issued Sept. 17, 1996.
47. Tamhankar, S., Menon, R., Chou, T., Ramachandran, R., Hull, R., and Watson, R., Enrichment Can Decrease NO_x, SO_x Formation, *Oil & Gas J.*, 94(10), 60, 1996.
48. U.S. Dept. of Energy, Assessment of Thermal Swing Absorption Alternatives for Producing Oxygen Enriched Combustion Air, Report DOE/CE-040762T-H1, U.S. Dept. of Energy, Washington, D.C., April 1990.
49. Air Products and Chemicals, Inc., Development of an Advanced Glass Melting System: The Thermally Efficient Alternative Melter “Team,” U.S. Dept. of Energy Report DOE/CE/40917, February 1992.
50. Keller, J.G., Soelberg, N.R., and Kessinger, G.F., Industry-Identified Combustion Research Needs, U.S. Dept. of Energy Report INEL-95/0578 (DE96003785), 1995.

21 Oxy-Fuel Burners

Hisashi Kobayashi, Ph.D. and Rémi Tsiava, Ph.D.

CONTENTS

- 21.1 Introduction
 - 21.2 Motivations to Use Oxy-Fuel Burners and Applications
 - 21.2.1 Potential Benefits
 - 21.2.1.1 High Flame Temperature and Heat Transfer
 - 21.2.1.2 Fuel Savings
 - 21.2.1.3 Production Increase
 - 21.2.1.4 Reduction of Pollutants
 - 21.2.1.5 Capital Reduction
 - 21.2.1.6 Yield and Quality Improvements
 - 21.2.1.7 Other Considerations
 - 21.2.2 Applications of Oxy-Fuel Burners
 - 21.3 General Design Considerations for Oxy-Fuel Burners
 - 21.3.1 Oxygen Safety
 - 21.3.2 Fuel Input
 - 21.3.3 Flame Temperature
 - 21.3.4 Heat Transfer
 - 21.3.5 Flame Stability
 - 21.3.6 Burner Materials and Size
 - 21.3.7 Burner Design Tools and Method
 - 21.4 Oxy-Fuel Burners for High-Temperature Industrial Furnaces
 - 21.4.1 Concentric Pipe Oxy-Fuel Burner
 - 21.4.2 Oxy-Oil Burners
 - 21.4.3 Flat-Flame Burners
 - 21.4.4 Low-NO_x Oxy-Fuel Burners
 - 21.4.4.1 Burners Using In-Furnace Gas Recirculation
 - 21.4.4.2 Burners Using Oscillating Combustion
 - 21.4.4.3 Burners Using Staged Combustion
 - 21.5 Customized Oxy-Burners for Chemical Process Applications
 - 21.5.1 Oxy-Burners for Sulfuric Acid Recovery
 - 21.5.2 Oxy-Burners for Waste Incineration and Fly Ash Vitrification
 - 21.6 Small-Size Oxy-Fuel Burners for Specialized Functions
 - 21.6.1 Polishing Burners
 - 21.6.2 Forehearth Burners
 - 21.6.3 Mould Lubrification in Glass Process
 - 21.7 Oxygen and Combustion Safety
 - 21.8 Summary
 - Reference
-

21.1 INTRODUCTION

Burners using industrial-purity oxygen (typically 90 to 99.9+% O₂) are conventionally called “oxy-fuel” burners. Because of the high cost of oxygen in the early days of air separation technologies, oxy-fuel burners were originally developed only for special high-flame-temperature applications that air burners could not perform. Welding with an oxy-acetylene flame, flame polishing of glass surfaces, and oxygen cutting of steel plates are some examples. The development of oxy-fuel burners has historically been driven by the oxygen manufacturers, as a special burner is needed for each new oxygen combustion application developed. As the oxygen manufacturers improved the air separation technologies and reduced the cost of oxygen, large-volume oxygen applications requiring on-site oxygen production plants were introduced for high-temperature industrial processes such as steel refining and copper smelting to improve the productivity and the product quality. Oxygen pipelines have been built in certain industrial areas to supply large amounts of oxygen to multiple users, and the resulting availability of low-cost oxygen further encouraged oxy-fuel burner applications. Today, oxy-fuel burners are used in a wide range of industrial furnaces to improve productivity and fuel efficiency and to reduce pollutant emissions.

As with air burners, there are many different oxy-fuel burner designs available to end users. Each different design was developed to overcome a problem or achieve a certain goal, depending on the application. These could include various flame shapes, low NO_x production, or dual fuel capability. Understanding the attributes of an oxy-fuel burner and overlaying them with the requirements of the process and the needs of the end user are key to selecting the proper burner for a particular application. In many situations, seeking advice from the burner manufacturers, who have significant design and hands-on experience with each burner type, is the best way to ensure that the selected burner will perform satisfactorily in the application.

21.2 MOTIVATIONS TO USE OXY-FUEL BURNERS AND APPLICATIONS

Oxy-fuel combustion creates an obvious increase in operating costs as the end user now must purchase the oxidant in addition to the fuel. The benefits achieved with oxy-fuel burners must be greater than the cost of oxygen. The following points briefly review some of the major motivators for using oxy-fuel burners in an industrial heating or melting process. Some of the benefits are applicable in all cases, while others may be application specific. Chapter 20 discusses changes in combustion conditions with oxygen enrichment and generic benefits. More detailed discussions on the applications and benefits of oxy-fuel combustion can be found in References 1 through 5.

21.2.1 POTENTIAL BENEFITS

21.2.1.1 High Flame Temperature and Heat Transfer

High adiabatic flame temperature and high heat release rate and transfer are the main benefits for which traditional applications of oxy-fuel burners were developed. Welding with an oxy-acetylene flame, flame polishing of glass surfaces, and oxygen cutting of steel plates are some of examples of applications that take advantage of these oxy-fuel flame characteristics.

21.2.1.2 Fuel Savings

The use of oxygen in a heating process eliminates the nitrogen introduced with combustion air from the process and hence eliminates the energy required to heat the nitrogen from inlet temperature to outlet temperature. For high-temperature processes (>2200°F or 1200°C) with no heat recovery, fuel savings when using oxygen can exceed 50%. As heat recovery is employed with the air combustion system, the savings achievable when switching to oxy-fuel combustion are reduced. A simple heat and mass balance on the furnace under each operating condition can provide accurate

information as to the fuel consumption using oxygen. The key parameters to consider are the flue gas temperatures and air preheat temperatures for the process.

21.2.1.3 Production Increase

Oxy-fuel flames are more compact than air flames and more energy can be released in a given furnace space, which often permits greater productivity from an existing furnace. The value of production increase would normally justify the additional cost associated with the oxygen. The amounts of additional fuel and oxygen required and the increase in production achievable are the key parameters for evaluating this benefit of oxy-fuel burners. The fuel and oxygen requirement can be determined via furnace energy balance calculations. However, the amount of production increase achievable requires a much more detailed study of the furnace conditions and its current limitations. Fan capacity or flue gas handling limitations can easily be overcome using oxygen, but maximum furnace temperature or heat flux limits require careful selection and placement of oxy-fuel burners to yield productivity improvements.

21.2.1.4 Reduction of Pollutants

Reduction of pollutants such as particulates and NO_x has become an increasingly important objective for using oxy-fuel combustion in recent years. When applied properly, and with proper control of flame temperature and localized stoichiometric conditions through burner design, oxy-fuel burners can reduce NO_x emissions by 80 to 95% due to the elimination of nitrogen from the furnace atmosphere. Particulate emissions are often reduced due to reduced carryover or volatilization caused by the reduction in flue gas volume. With reduced flue gas volumes, existing flue gas cleanup equipment such as electrostatic precipitators and scrubbers can run more efficiently and the size of new equipment can be reduced.

21.2.1.5 Capital Reduction

When a furnace is converted to oxy-fuel combustion, many of the auxiliary systems for preheating or delivering air to the furnace are eliminated. The size of the flue gas handling system is reduced substantially. The capital costs of installing, replacing, and disposing of large gas handling systems is no longer required; this can favorably influence the economics, especially if these systems require replacement periodically. An example is the elimination of regenerators used for glass-melting furnaces.

21.2.1.6 Yield and Quality Improvements

The yield and quality of products may change in some heating or melting processes as a result of higher furnace temperatures and higher concentrations of combustion products such as H₂O and CO₂. For example, oxy-fuel fired glass-melting furnaces often result in a reduced number of gas bubbles (seeds) in the product. On the other hand, a higher concentration of H₂O and CO₂ in the furnace gas increases the oxidation potential and could potentially increase metal oxidation loss. The impacts of oxy-fuel burners on product yields and quality are very process specific and must be evaluated for each application.

21.2.1.7 Other Considerations

Other factors that need to be considered for oxy-fuel combustion include:

1. Reduced flue gas volume often results in reduced maintenance for oxy-fuel fired furnaces as it relates to furnace doors and dampers.
2. Higher productivity typically results in higher furnace wall temperature. The life of refractory wall may diminish as a result.

3. Air blower and burner noise is reduced significantly with oxy-fuel burners.
4. Elimination of air preheating systems results in more space around the furnace, which could be utilized to increase the size and capacity of the furnace without expanding the rest of the plant.
5. Better flame stability is achieved with oxy-fuel combustion, which provides wider operating ranges and faster response to load changes.
6. Degradation of furnace efficiency of an air-fired system caused by the deterioration of recuperators and regenerators is avoided.

21.2.2 APPLICATIONS OF OXY-FUEL BURNERS

Oxy-fuel burners are widely used in high-temperature industrial furnaces to improve productivity and fuel efficiency, to reduce emissions of pollutants, and to eliminate the capital and maintenance costs of an air preheater. Significant fractions of glass melting furnaces, steel scrap melting furnaces (electric arc furnaces), steel reheat furnaces, soaking pits, forging furnaces, ladles, aluminum melting furnaces, copper smelting and anode furnaces, hazardous waste incinerators, rotary enamel frit furnaces, and rotary lead melting furnaces are fired with oxy-fuel burners (see [Figure 21.1](#)).

Glass melting furnaces require a well-controlled temperature profile to produce a proper molten glass flow pattern for melting batch materials and fining gas bubbles. Wall and roof temperatures approach the upper limit of allowable refractory material temperatures, so a nearly uniform refractory temperature is critical to avoid refractory damage. Water-cooled burners often experience corrosion and fouling problems due to condensation of alkali vapors present in the furnace. Non-water-cooled oxy-fuel burners producing a long and wide flame are generally preferred. Relatively low momentum burners are used as high flame velocities tend to accelerate volatilization of alkali compounds. Multiple burners are placed in the side walls to provide good flame coverage over the molten glass surface and to avoid flame impingement and hot spots on refractory walls and crown. Both cylindrical and flat-flame burners are used.^{6,7}

Electric arc steel scrap melting furnaces require high intensity and high flame temperature burners to accelerate the melting of scrap steel by high-momentum impinging flames. Typically, three burners are mounted on the cylindrical side wall to fire between the three electrodes. These burners are used to supplement the main source of energy provided by electric arc and also provide extra oxygen with carbon injection for foamy slag operation and for post-combustion of CO. Because of extreme temperature conditions in these furnaces, the burners are usually water cooled and of rugged design. The burners are typically designed to provide an oxygen lancing mode of operation to reduce the carbon content of molten steel.^{8,9}

Steel reheating furnaces, soaking pits, and forging furnaces require uniform heating of steel ingots, slabs, blooms, or billets to the rolling temperature. Burners for this application need to be able to produce uniform furnace temperatures and adapt to the various geometry changes associated with differently shaped steel pieces. High-momentum, low flame temperature oxy-fuel burners are often used to provide uniform heating and low NO_x emissions.¹⁰

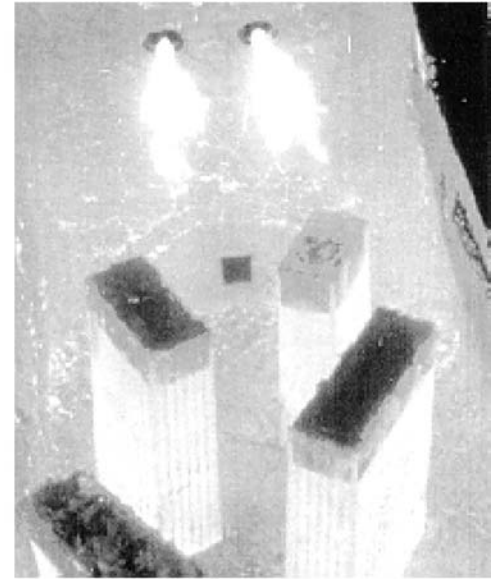
Aluminum melting furnaces require rapid melting of scrap with minimal formation of dross (mixture of metal and metal oxides). Oxy-fuel burners are used in reverberatory furnaces and rotary melters to improve productivity and to reduce fuel consumption.¹¹

High-intensity oxy-fuel burners are used in copper reverberatory furnaces for smelting operations. Most copper smelting, however, is done by flash smelting processes using specially designed oxy-fuel burners. Oxy-fuel burners are also used in copper converters and anode furnaces.

In hazardous waste incinerators, organic waste materials are oxidized to carbon dioxide and water vapor, and halogens, metallic, and other impurities are either scrubbed out or transformed into nonhazardous solids. The small flue gas volume of oxy-fuel combustion provides a longer residence time and substantially reduces the size of the flue gas cleaning system. High-momentum oxy-fuel burners are used to provide good mixing and rapid combustion in rotary kiln incinerators.



(a)



(b)

FIGURE 21.1 Examples of furnaces fired with Praxair oxy-fuel burners: (a) aluminum melting furnace and (b) steel soaking pit.

Specially designed oxygen waste burners are used for special incinerators for chemical waste streams.^{12,13}

Rotary enamel frit melting furnaces and rotary lead melting furnaces are small batch furnaces typically fired with a single oxy-fuel burner. The small furnace size and high productivity requirement are met by applying a burner designed to provide a compact flame of the length needed to impinge on the surface of the batch materials.

Some furnaces in the steel, glass, aluminum, copper, and cement industries are heated primarily with conventional air-fuel combustion systems and also equipped with supplementary oxy-fuel burners. Production rate increase is the most common objective and the improvement of product quality is also important. Reduction of pollutants such as particulates and NO_x has also become an important objective in recent years. Supplemental oxygen combustion has also been successfully applied to waste incinerators and chemical process furnaces such as the Claus sulfur reactor, sulfuric acid recovery furnaces, and the fluidized bed catalyst regenerator for the fluid catalytic cracking process of petroleum. The economics of these applications are dominated by the value of the increased production and generally can support the high cost of oxygen delivered as bulk liquid.

There are many small oxy-fuel burners used in welding metals and fire-polishing glass surfaces. These special burners are unique in design and described in Chapter 21.6.

21.3 GENERAL DESIGN CONSIDERATIONS FOR OXY-FUEL BURNERS

Combustion with oxygen is characterized by a higher adiabatic flame temperature, a higher flame speed, a lower ignition temperature, and a wider flammability range than is the case in combustion with air. Traditional rapid nozzle-mix oxy-fuel burners produce stable, short, very intense, high-temperature flames. Many of the original oxy-fuel burner applications, such as welding and melting of steel scrap, were designed specifically to take advantage of the high temperature and high heat transfer properties of oxy-fuel flames. For burners of this type, water cooling of burner components is often required to protect the burner face from intense radiation from the flame and furnace walls. In the applications of oxy-fuel burners for common industrial furnaces such as glass melting and steel reheating furnaces, the high intensity of the traditional oxy-fuel flame is considered undesirable to the process and to the furnace refractory, and also raises concerns related to high thermal NO_x formation. New types of oxy-fuel burner have been developed to provide more uniform heating of the entire furnace while retaining the main benefits of oxy-fuel combustion: high heat transfer, fuel savings, and reduced emissions. In this section, general combustion characteristics of air and oxygen combustion and general design considerations for oxy-fuel burners are discussed.

21.3.1 OXYGEN SAFETY

Many materials used for air burners are not compatible for oxygen service. Special safety considerations are required in selecting materials, designing, fabricating, and operating oxy-fuel burners. These considerations are discussed in Chapter 21.7.

21.3.2 FUEL INPUT

In combustion with air, about 70% of the volume of the flue gas is nitrogen. Thus, most of the sensible heat loss in the flue gas is due to heating the nitrogen contained in air. When oxygen is used in place of air for combustion, most nitrogen in the flue gas is eliminated and the flue gas heat loss is reduced substantially. As a result, the useful heat to the furnace or the available heat of combustion is increased substantially with oxy-fuel combustion and the required fuel input is reduced. To size oxy-fuel burners properly for a process, it is important to be able to predict the fuel savings that will be achieved with oxy-fuel combustion. The higher the flue gas temperature, the greater the

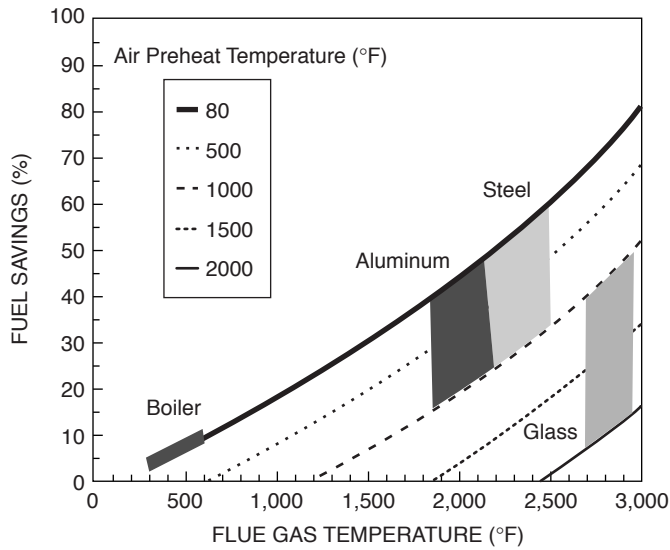


FIGURE 21.2 Fuel savings with oxy-fuel combustion (fuel = methane, 2% O₂ in flue gas).

fuel savings that will result from converting from air to oxygen combustion. As compared with the flue gas temperature, the type of fuel and the excess air level have a relatively small influence on fuel savings. Because most air combustion systems for high-temperature furnaces are equipped with heat recovery systems to preheat combustion air, the temperature of combustion air also has a large influence on fuel savings. Figure 21.2 shows percent fuel savings as a function of flue gas temperature in a natural gas-fired furnace when preheated combustion air is replaced by pure oxygen. Each curve represents a different air preheat temperature. The uppermost curve shows the case of replacing combustion air at ambient air temperature, that is, when no air preheating is employed.

Typical fuel savings achieved for glass melting furnaces, steel heating furnaces, aluminum melting furnaces, and boilers are indicated by the shaded areas. The glass melting furnaces operate at about 2700 to 3000°F and inherently represent high potential for fuel savings. However, most large glass melting furnaces for manufacture of containers and flat glass are equipped with efficient regenerators to preheat combustion air to 2000 to 2400°F. As a result, predicted fuel savings with oxygen combustion for these glass furnaces based only on exhaust sensible heat loss are typically 10 to 20%. (Actual fuel savings are significantly greater than indicated in this graph due to the reduction of radiative heat loss through regenerator ports.) Fiberglass furnaces equipped with recuperators and other smaller glass furnaces are less efficient and fuel savings of 30 to 50% are typically achieved with oxygen combustion. Steel reheat furnaces and soaking pits operate at flue gas temperatures of about 2100 to 2400°F. The air preheat temperature is typically less than 1000°F and fuel savings of 30 to 60% are achieved with oxygen combustion. Aluminum melting furnaces operate at lower flue gas temperatures of about 1800 to 2100°F, but often no heat recovery is used. Consequently, fuel savings of 30 to 50% are typically achieved. By comparison, boiler furnaces are very efficient with extensive convective heat transfer surfaces to heat feedwater and to raise steam temperature. Flue gas temperatures of 300 to 600°F are typical. As a result, fuel savings of only about 5 to 10% are achievable by reducing sensible heat with oxygen combustion.

21.3.3 FLAME TEMPERATURE

High flame temperature is one of the most prominent features of traditional oxy-fuel combustion. Oxy-combustion is significantly different from air combustion in dissociation phenomena, radiant heat transfer, and formation of NO_x in the flame. The extremely high temperatures of oxy-fuel

flames cause dissociation of part of the combustion products into CO, H₂, OH, and other radicals. These chemical species can be measured in large amounts in oxy-flames even if the burner operates at fuel-lean conditions. Table 21.1 provides the molar fraction of dissociated species in the combustion products of a stoichiometric methane/oxygen flame at different temperatures.

With methane and pure oxygen at ambient temperature, the adiabatic flame temperature is about 5000°F (2760°C), as compared about 3520°F (1940°C) for methane-air combustion. The theoretical flame temperature simply represents the practical upper limit of flame temperature when the fuel and oxidant are mixed rapidly and ignited. The actual flame temperature of oxy-fuel burners can be controlled to a desired level by burner design. As discussed further in Chapter 21.4.4, internal or external flue gas recirculation (FGR) is one of the most effective ways of reducing the flame temperature for reduction of thermal NO_x emissions.

Figure 21.3 shows the adiabatic flame temperature of methane burned with a mixture of pure oxygen and flue gas containing 2% oxygen concentration as a function of the oxygen concentration in the oxygen-flue gas mixture at different oxidant preheat temperatures. The bottom curve represents the case of oxygen mixed with flue gas cooled to ambient temperature. The other curves represent various degrees of mixing of hot flue gas with oxygen, especially by in-furnace FGR.

TABLE 21.1
Molar Fractions of Dissociated Species from Adiabatic Equilibrium
Stoichiometric Combustion of Methane with Oxygen

Temp. (°C)	1600	1800	2000	2200	2500	2780
CO ₂	0.328	0.322	0.304	0.271	0.194	0.114
H ₂ O	0.658	0.651	0.636	0.605	0.518	0.390
CO	0.001	0.006	0.020	0.046	0.102	0.152
H ₂	0.0	0.003	0.008	0.017	0.040	0.071
OH	0.001	0.004	0.01	0.021	0.054	0.096
O	0.0	0.0	0.0	0.002	0.012	0.040
H	0.0	0.0	0.0	0.003	0.015	0.049
O ₂	0.010	0.014	0.021	0.035	0.064	0.088

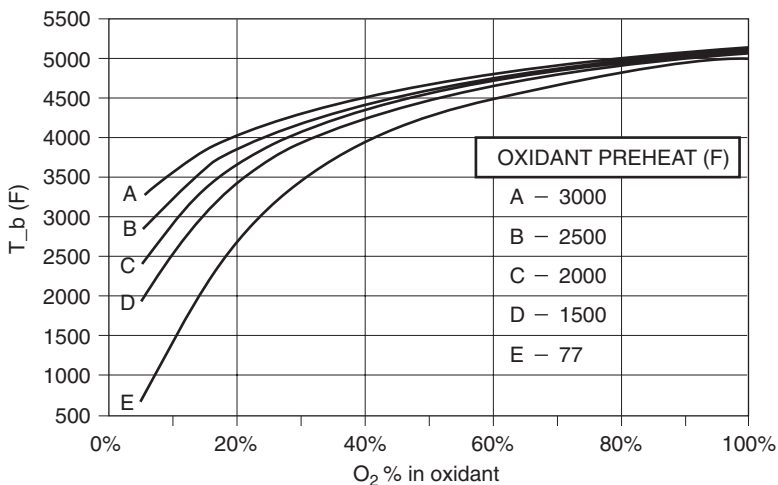


FIGURE 21.3 Adiabatic flame temperature vs. %O₂.

Separated high-velocity oxygen jets are often used to aerodynamically mix hot flue gas into the oxygen jets in a furnace. As more flue gas is mixed into the oxygen jets, the concentration of oxygen in the mixture decreases and the temperature increases. As seen from [Figure 21.3](#), the flame temperature is reduced substantially as the concentration of oxygen is reduced and can be controlled to a temperature even lower than that of a typical air flame. It is interesting to note that at about 25 to 30% O₂ in the oxygen-hot flue gas mixture, or by mixing about 4 volumes of hot flue gas with oxygen, the flame temperature about equals that of a methane-ambient air flame. The reason this occurs at a higher oxygen concentration than the oxygen concentration of air (20.9% O₂) is the higher specific heat of carbon dioxide and water vapor in flue gas compared with that of nitrogen.

21.3.4 HEAT TRANSFER

Heat transfer efficiency is an important consideration for burner and furnace designs. High flame temperature and high luminosity generally improve the heat transfer rate through higher flame radiation. Because of this, a common misunderstanding is that the higher efficiency achieved by oxy-fuel combustion is caused by high oxy-fuel flame temperatures and that reducing the flame temperature would result in lower furnace efficiency. In fact, studies and actual experience show that the overall thermal efficiency of an oxy-fuel fired furnace is very insensitive to the type and temperature of the oxy-fuel flames. The reason for this can be understood by considering the effects of heat transfer on the sensible heat loss to flue gas. A reduction in heat transfer to a furnace load results in an increase in flue gas temperature and increases the amount of sensible heat contained in the flue gas. Because the volume of the flue gas in an oxy-fuel fired furnace is reduced dramatically to 15 to 25% of that of an equivalent air fired furnace, an increase in flue gas temperature causes only a minor increase in the flue gas sensible heat loss under oxygen combustion. On the other hand, a relatively small increase in the bulk furnace gas temperature causes a sharp increase in the gas-to-load radiative heat transfer rate due to the strong temperature dependence of radiative heat transfer. Thus, any loss in heat transfer attributable to a reduction in oxy-fuel flame temperature is naturally compensated by an increase in gas-to-load radiative heat transfer caused by a small increase in the bulk furnace gas temperature. In fact, oxygen combustion is inherently efficient in heat transfer because higher concentrations of CO₂ and H₂O in the furnace atmosphere and the much longer gas residence time enhance radiative heat transfer.

In most industrial furnaces, uniform temperature and heat flux distributions over the furnace heat load are critical requirements. Flame temperature, shape, luminosity, momentum, and burner placement are all important parameters influencing the temperature and heat flux distributions. In converting a furnace fired with air burners to oxy-fuel firing, the number of burners required and their placement on furnace walls may be significantly different from those of the original air-fired configuration. Because the flame characteristics of oxy-fuel burners can vary widely, depending on burner design, detailed heat transfer analysis of the furnace using a CFD model is often performed to determine the optimum burner configuration.

21.3.5 FLAME STABILITY

Oxy-fuel flames are generally very stable due to the high flame velocity and wide flammability range of different fuels in oxygen. For example, the blow-off fuel velocity of a turbulent natural gas free jet in an oxygen atmosphere may exceed 1000 ft./s as compared with that in ambient air, which is in a range of 50 to 200 ft./s, depending on the nozzle configurations. Because of this stability, great flexibility is afforded in oxy-fuel burner design. Very high fuel and oxygen velocities, sometimes exceeding sonic velocities, are used in high momentum oxy-fuel burners. Unlike air burners, the refractory burner port is not required to provide flame stability, and water-cooled burners are often used without a burner port. With nonwater-cooled oxy-fuel burners, however, refractory burner ports are generally required to protect the metallic part of the oxy-fuel burner from furnace heat.

21.3.6 BURNER MATERIALS AND SIZE

The selection of materials for oxy-fuel burners and piping skirts requires special safety considerations for oxygen service, as further discussed in Chapter 21.7. High-temperature alloys are typically used for fuel and oxygen nozzles on the burner face, which is exposed to intense radiation from the oxy-fuel flame and hot furnace walls. In air burner design, combustion air provides sufficient cooling of burner components. By comparison, the volume flow rate of oxygen is small and may not provide proper cooling. To prevent burner overheating in some oxy-fuel burner designs, controlled mixing of fuel and oxygen near the burner face to prevent high heat release is combined with a narrow burner port to reduce the radiation heat flux from the flame and the hot furnace walls. Refractory burner materials are used in other burner designs for high-temperature furnace applications. Water-cooled copper and stainless steel are also used in some oxy-fuel burners to provide greater nozzle design flexibility.

The size of an oxy-fuel burner is typically very small compared to the equivalent air burner, due not only to the reduced volume flow rate of the oxidant, but also to the reduced fuel input and the high fuel and oxygen velocities. For example, a typical 10 MMBtu/hr (3 MW) cold air burner may have a diameter of about 15 in. and an equivalent oxy-fuel burner with 6 MMBtu/hr (2 MW) may have a diameter of only 4 in.

21.3.7 BURNER DESIGN TOOLS AND METHOD

Numerical simulation has become an essential tool for the development of new generations of industrial burners. To meet the continuous needs of increasing the energy efficiency and the flexibility of the new combustion systems while reducing their pollutant emissions, better control of the physical phenomena is required. The numerical simulation is not only a major asset to reduce development times and costs, but also to reduce the risks when the experimental developments using pilot-scale facilities are limited. Today, numerical simulation tools are widely used to estimate the flame heat release and the heat transfers to the walls or to the load in various industrial processes and furnaces. They are also used to estimate pollutant emissions such as NO_x emissions. Radiation represents the predominant mode of heat transfer in oxy-fuel combustion systems where the maximum temperature reaches more than 2000K (3140°F). Therefore, in combustion with oxygen, it is essential to use an accurate model to calculate radiative heat transfer in gases. For example, the weighted sum of gray gas (WSGG) model, generally used in industrial configurations (less time consuming than the CK model) could overpredict radiative fluxes in industrial glass melting furnace by more than 10%.¹⁴ In the same way, special models must be used to calculate the formation of NO in high-temperature flames. The classical models available in the commercial codes generally significantly overestimate nitrogen oxides formed in oxygen flames.¹⁵⁻¹⁶ In the future, numerical simulation tools will be used to predict the flame stability, and to develop the burner closed-loop control systems that will be driven by process information.

21.4 OXY-FUEL BURNERS FOR HIGH-TEMPERATURE INDUSTRIAL FURNACES

There are two types of burners, according to whether the reactants are mixed before (i.e., premixed combustion) or after (i.e., postmixed combustion) injection into the combustion chamber. Premixed combustion is seldom used for high firing rate burners for safety reasons, especially for oxy-fuel combustion. Only postmixed flame burners are described in this section.

The design of oxy-fuel burners depends on the nature of the fuel (gas, liquid, or solid) and the expected shape or characteristics of the flame. In the following sub-sections, the basic technologies

of oxy-gas burners are discussed first, followed by unique design considerations for liquid fuel burners. The two final sub-sections focus on flat-flame and low-NO_x oxy-fuel burners.

21.4.1 CONCENTRIC PIPE OXY-FUEL BURNER

Before providing a detailed description of industrial burners, it is useful to recall the main characteristics of oxy-fuel flames, which differ significantly from the traditional air flames. In addition to the increased flame temperature, the use of oxygen, by removing the ballast of nitrogen, allows a significant increase in the fluid injection velocities in the combustion chamber or in the furnace. Thus, a drastic increase of the mass flow rates of the reactants enables extremely high volumetric heat release rates (Btu/ft³ or W/m³) while keeping a good flame stability. With oxy-fuel combustion, flame stability problems arise in a quite different way from air combustion. Unlike air burners, it is not necessary for industrial oxygen burners to use stabilization devices (flame holders, swirling flows, etc.). Therefore, the first designs of oxygen burners simply consisted of concentric tubes inserted in a protective water-cooled sheath. A practical design is to use two concentric tubes to inject the reactants as two parallel concentric jets. The mixing of fuel and oxygen is carried out close to the burner tip by turbulent shear and diffusion of the two jets. [Figure 21.4](#) illustrates this burner concept.

The expected shapes and dimensions of the flame for a specific process can be obtained by some modifications to the burner tip geometry, such as the relative position of the fluid exits and the direction of the flows. For example, to ensure faster mixing, one of the two gases (oxygen, in general) can be injected at the burner tip from two different sections, as illustrated on [Figure 21.5](#). With this design of burner, a fast mixing leads to a transparent, long, and narrow flame.

A burner dedicated to the combustion of hydrocarbon gases and more specifically to the production of H₂/CO mixtures consists of a jet of oxygen in the center surrounded by an annular converging jet of natural gas (see [Figure 21.6](#)). This ensures a fast and more effective mixing and leads to short flames. The injection velocities of each fluid stand between 20 and 50 m/s and the exit velocity of the mixture in combustion between 60 and 100 m/s.

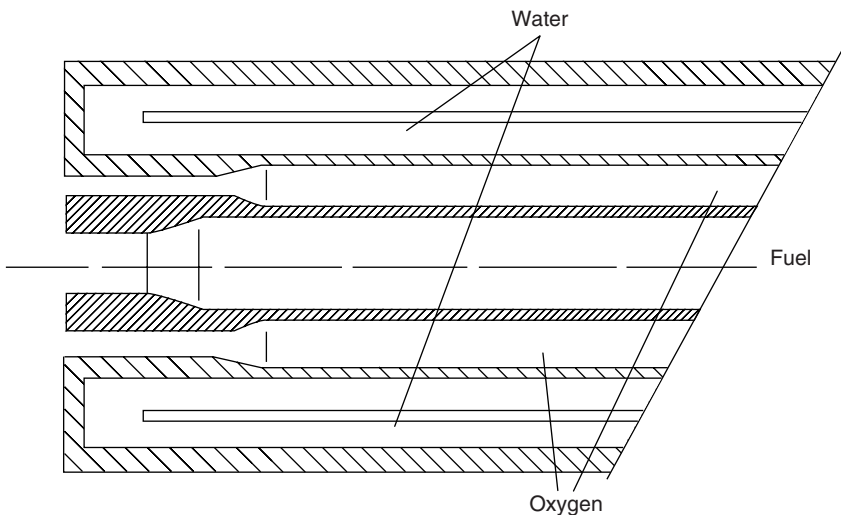


FIGURE 21.4 Oxygen pipe-in-pipe burner.

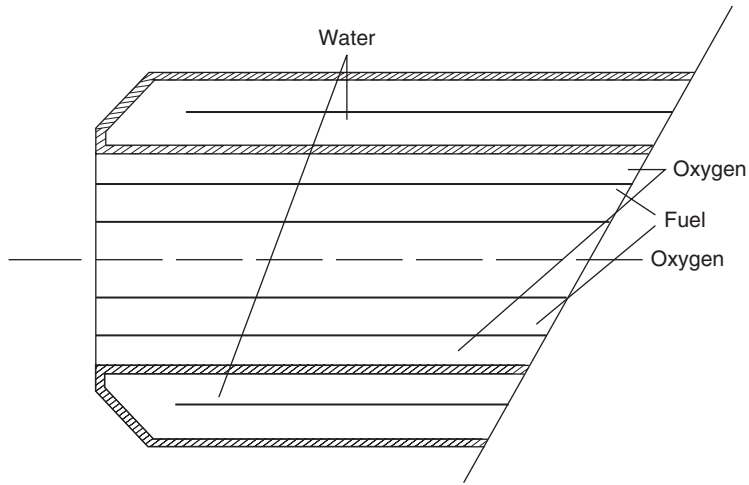


FIGURE 21.5 Oxygen twin impulsion pipe-in-pipe burner.

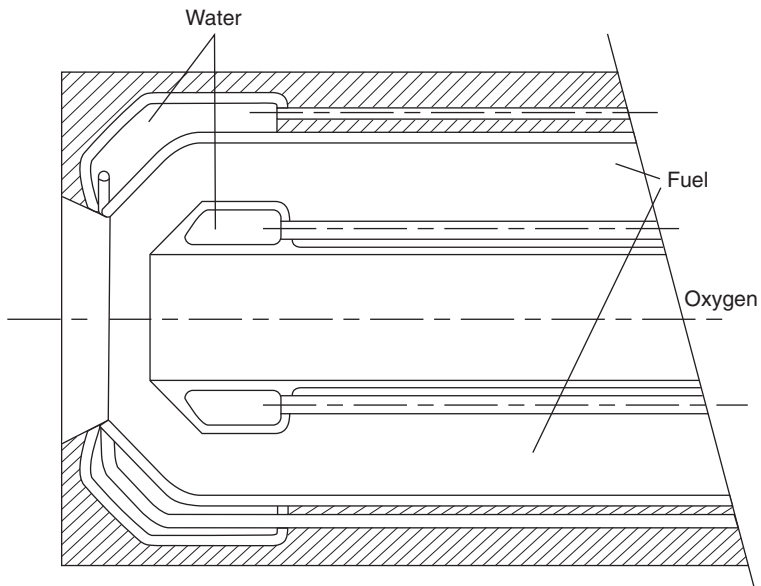


FIGURE 21.6 Texaco oxygen burner.

There is another category of burner design — multiple nozzle burners — in which at least one fluid injection line ends in a series of nozzles of varied forms and sizes. An example of this design of burner is shown in [Figure 21.7](#).

Improvements have been made to these first-generation burners, and the burner water cooling system has been eliminated. Similar to air burners, a ceramic part (burner block) isolates the metallic burner tip from the radiation of the flame and of the furnace walls. The metallic parts are cooled by convection of the fuel and oxygen flows. Examples of this generic burner design include the Praxair J Burner¹⁷ and the Air Liquid's ALGLASS burner,¹⁸ which is shown in [Figure 21.8](#). The ALGLASS concept is shown in [Figure 21.9](#).

Although industrial burners — and particularly oxy-fuel burners — are often based on generic concepts, it is not uncommon to adapt and tune a combustion design to a specific process

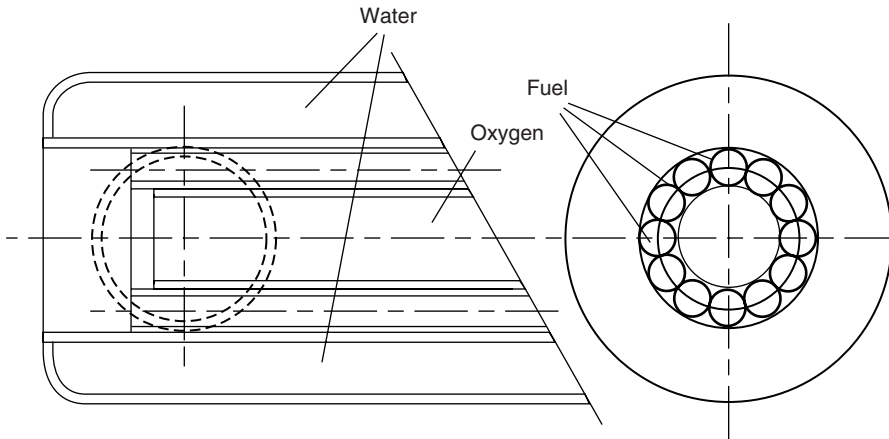


FIGURE 21.7 Chemetron oxygen burner.

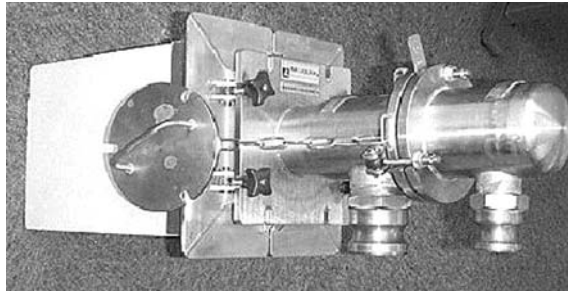


FIGURE 21.8 ALGLASS™ oxygen burner.

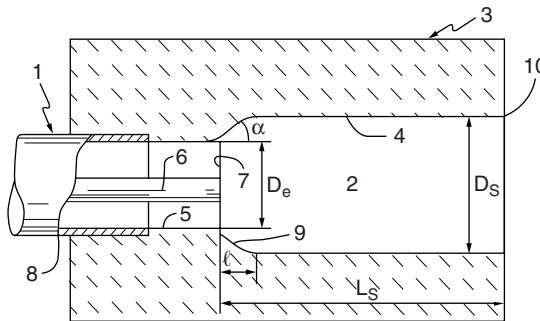


FIGURE 21.9 ALGLASS concept.

in order to optimize heating quality, combustion performances, and flame/process interaction. Such developments have been carried out for the purpose of implementing oxy-fuel combustion technologies within the steel reheating process, particularly in continuous billet or slab reheat furnaces, and also preheat zones of annealing/galvanizing lines or stainless pickling/annealing lines. The benefits of oxy-burners for these types of applications are various, but can be directly linked to the improvement of furnace efficiency, energy optimization, and, above all, capacity increase. In many cases, oxy-burners are used to boost furnace production and are

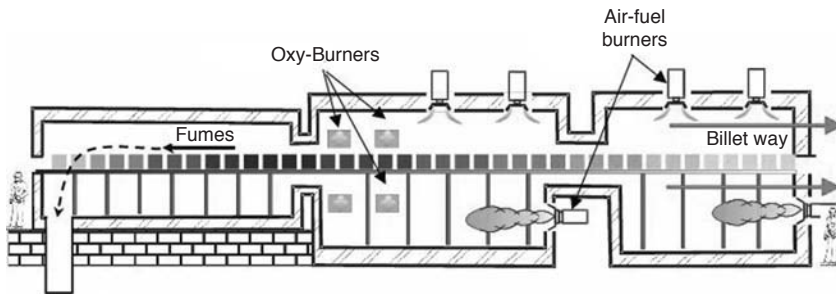


FIGURE 21.10 Walking-beam billet furnace with oxy-fuel burners.

added to complement existing air-fuel burners. New oxy-flame burners are usually installed near the charge end of a furnace (Figure 21.10) and allow the addition of very efficient heating power for furnace de-bottlenecking.

Because side-wall burner positioning is encouraged, oxy-fuel burner design must ensure sufficient development of the flame inside the furnace. Indeed, in such configurations, oxy-flames are influenced by the crosswind of the furnace flue gas, the velocity of which ranges from 2 to 5 m/s in reheat furnaces and 9 to 10 m/s in annealing lines. To avoid flame deflection, a high-momentum jet is recommended, which generates a stable flame, well stabilized at the burner tip. Finally, the oxy-fuel burner specifications for such an application must include the following characteristics:

- High-momentum jet to avoid flame deflection toward the wall
- High flexibility to allow fast ignition and shutdown (i.e., oxy-burners are only used when a production rate increase is needed)
- Large power turndown ratio to follow the setpoint prescribed by the furnace control system
- Compactness and high maintainability without water cooling
- Tunable flame length to adapt radiant heat transfer to the product and optimize temperature homogeneity

The pipe-in-pipe concept can be easily modified to fulfill these requirements and, consequently, is often used for steel reheating applications. Figure 21.11 provides an example of ALROLL™ burners installed in a billet reheat furnace.¹⁹

21.4.2 OXY-OIL BURNERS

Liquid fuel or oil burner development has acquired renewed interest due to the worldwide availability of fuel oil and to the high thermal efficiency and low NO_x emissions of oxygen fuel-oil combustion systems. For oxy-oil burners, scaling rules are based on the characteristic time scales of the physicochemical phenomena that control two-phase combustion;²⁰ that is:

- Droplet vaporization, function of droplets size, and atomization quality
- Reactant mixing, which depends on flow structure (i.e., on burner geometry and injection velocities)
- Chemical reaction time, which depends on the mass diffusivity of reactants and flame velocity

The evaluation of these characteristic time scales shows that for air combustion, the vaporization and chemical time scales are of the same order; and that for oxy-oil combustion, the vaporization time scale is two orders of magnitude larger than the chemical time scale.²¹

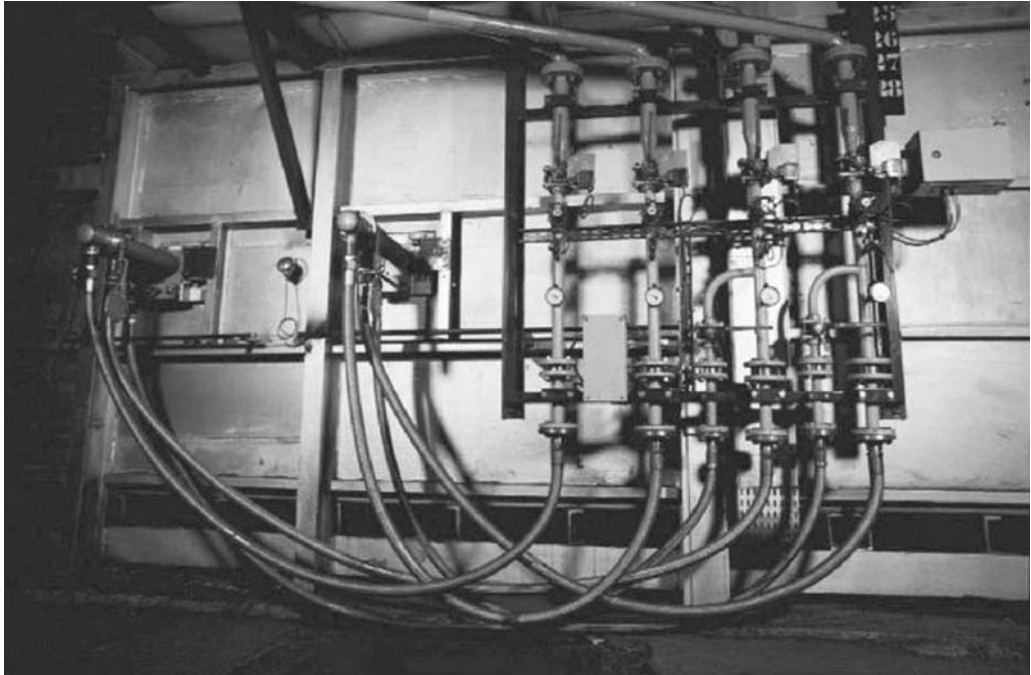


FIGURE 21.11 ALROLL™ oxygen burners installed on the side wall of a billet reheat furnace.

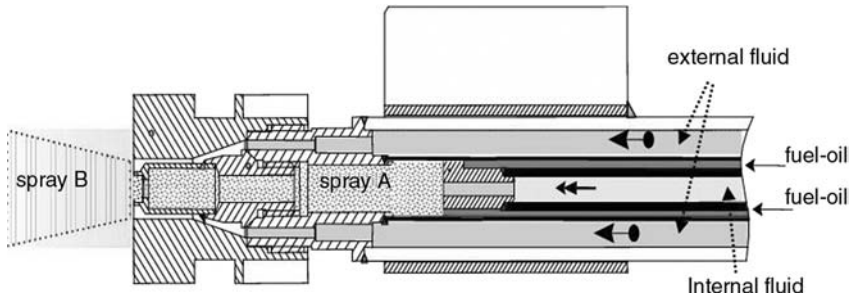


FIGURE 21.12 Air Liquide DUAL™ injector.

Therefore, the atomization technology will have a strong impact on flame structure, flame length or width, or flame stability in the case of oxy-oil combustion.

Two physical phenomena are used to atomize liquid fuels. The first is based on the impact between an atomizing fluid and the liquid flow (and/or liquid against the atomizer wall); the second one is based on the instability developing at the interface between the liquid and the gas when the two flows are parallel. There are two ways to practically make use of the above phenomena: internal and external atomization, whether the atomization takes place inside or outside the nozzle body prior to the injection plane.

In internally mixing twin-fluid atomizers, the atomization stage is achieved in a closed environment. For such configurations, the liquid is often spread on an adapted surface before coming in contact with the gaseous flow, often known as an "pre-filming atomizer." An internal atomizer is very efficient and flexible enough to handle high-viscosity oils, but the main drawback is the risk of flashback, especially when using oxygen as the atomizing fluid. The Air Liquide Dual²² atomizer uses this atomization principle (see Figure 21.12).

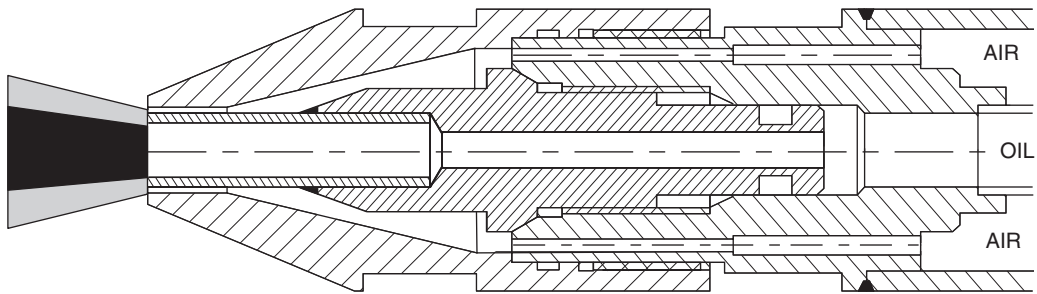


FIGURE 21.13 Air Liquide Robust™ injector.

In this design, the oil circular film is first broken up by the internal atomization gas flow. Then this first mixture is atomized externally by the second, high-velocity gas flow. This two-step atomization process allows a larger flame length range as a function of atomization pressure and to stabilize the flame.

In externally mixing twin-fluid atomizers, a low-velocity (3 ft./s or 1 m/s) liquid jet is broken up by a high-velocity (164 ft./s or 50 m/s) gas flow outside the atomization system. An example is the Air Liquide Robust atomizer shown in [Figure 21.13](#).

The external fluid is also useful for cooling the lance and the injector. This kind of atomizer is recommended to be used flush with the wall or with a small offset with various atomization gas types: air, natural gas, steam, or oxygen. External atomization is less efficient. However, because mixing occurs outside the nozzle, these devices are considered to offer lower risk from a safety perspective.

In mechanical atomization systems (pressure nozzles), a liquid jet submitted to a high pressure flows with high velocity toward a small-diameter nozzle. Mechanical atomization is widely used in fuel-oil burners. It is attractive due to the single fluid requirement for atomization, simplified piping, and simple atomizer construction. Its disadvantages include the low turndown ratio of that atomizer technology, a relatively short life span (due to tip erosion), and more frequent cleaning requirements (due to the small orifice).

Oxy-oil burners are primarily used in continuous melting furnaces (e.g., for glass-type applications). The main motivations of the oil burner users are often the following: reduced maintenance time of the burners, higher energy efficiency, and low pollutant emissions levels. To meet these requirements, oxy-fuel oil burners tend to adopt configurations in which the reactants are brought by separate injections and mixed outside the burner block. This is the case in the ALGLASS FC burner, which is particularly appropriate for most glass-type applications. In this geometry, the oil atomizer is installed at the bottom of refractory burner block, while oxygen is injected at a lower velocity from two injectors located at the top of the block. The oxygen flow is directed toward the fuel oil spray. A wide horizontal spray is achieved using the Trident²³ injector, as illustrated in [Figure 21.14](#), which shows three oil injection orifices with diverging horizontal directions.

21.4.3 FLAT-FLAME BURNERS

Industrial processes often use large-size furnaces and require a long and homogeneous energy transfer to the load. To fulfil this requirement, flat-flame burners have been developed by several manufacturers. The principal idea that guides the design of these burners is to maximize the flame coverage over the furnace heat load, by developing a long and wide flame close to the load. A design option to achieve this goal consists of distributing the fuel injections in a plane parallel to the load and also injecting oxygen in a separate parallel plane. The number of injections, the relative position, or the distance between the planes of injection of fuel and oxidant are the main parameters that control the shape of the flame and the heat release. [Figure 21.15](#) provides an example of this

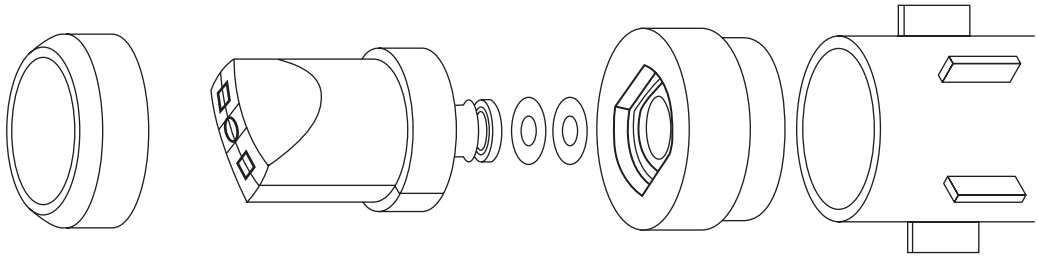
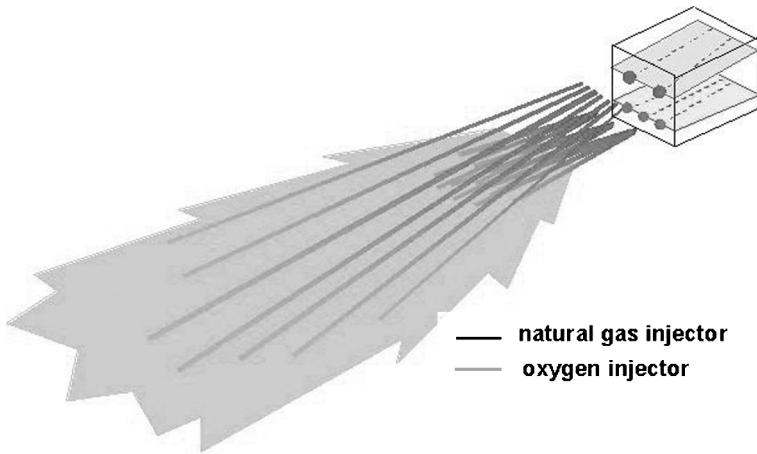


FIGURE 21.14 Trident injector for ALGLASS FC™ burner.



Burner operation principle

FIGURE 21.15 Schematic of ALGLASS FC™ oxygen burner.²⁴

concept of burner. The oxygen flow is placed above the fuel flow and slopes toward the load so as to bring the flame closer to the load.

The concepts of a flat-flame burner can be classified in two main categories according to whether the root of flame is confined in a pre-combustion chamber or established directly in the furnace. The principal reasons to confine the root of flame is to make the flame less sensitive to the aerodynamic conditions inside the furnace and to provide better control of flame characteristics and stability. A potential concern with this design concept is thermal stress and potential damage to the refractory material due to the heat release in the confined space of the pre-combustion chamber.

Flat-flame burners were originally developed several years ago for wide glass melting furnaces and then applied to many other industrial fields, such as melting of enamel frits and ferrous or nonferrous metals. Experience from these applications showed better transfer to the load and lower fuel consumption. Moreover, by maximizing the volume of flame and by increasing the transfer of energy to the load, the flat-flame burners showed low NO_x emissions.

21.4.4 LOW-NO_x OXY-FUEL BURNERS

The reduction of NO_x emissions has become an important requirement in many burner applications. Due to the high flame temperature of oxy-fuel combustion, it is often viewed as producing high NO_x emissions. Contrary to conventional wisdom, oxy-fuel combustion actually provides an inherent advantage in NO_x reduction, because nitrogen contained in combustion air is largely eliminated. In key NO-forming reactions, both the rate of formation of NO from nitrogen molecules (thermal

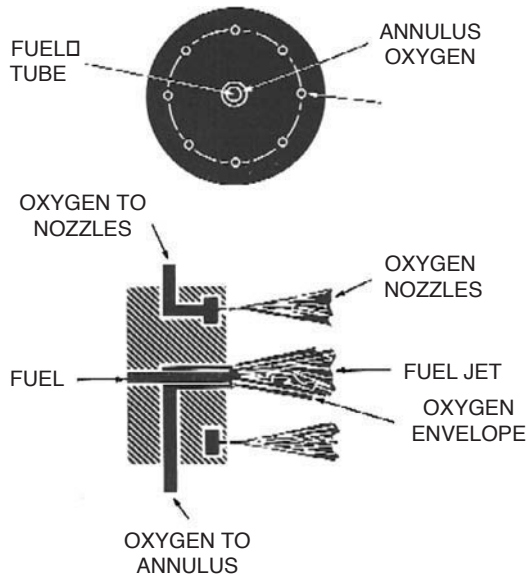


FIGURE 21.16 Praxair “A” Burner using in-furnace FGR.

NO_x) and that from fuel radicals (prompt NO_x) are proportional to the concentration of N₂. Advanced oxy-fuel burners described in this section are designed to control flame temperature and stoichiometric conditions to achieve very low NO_x emissions.

21.4.4.1 Burners Using In-Furnace Gas Recirculation

Oxy-fuel burners using in-furnace flue gas recirculation (FGR) were first developed in the late 1970s to provide a high-momentum, low-temperature flame mimicking the traditional air flame.²⁵ Figure 21.16 shows a schematic diagram of Praxair “A” Burner™. The key design principle of the “A” burner is the “aspiration” of furnace gases using high-velocity oxygen jets to produce “simulated hot air” prior to mixing with fuel. The main oxygen nozzles are separated from the central fuel nozzle to prevent direct mixing of fuel and oxygen near the burner face. The concentration of oxygen in the oxygen jet decreases along the jet length due to the entrainment of furnace flue gas according to the turbulent jet theory. By adjusting the diameter of the oxygen nozzle and the separation distance between the fuel nozzle and the oxygen nozzles, the amount of flue gas entrained into the oxygen jets prior to mixing with the fuel jet is controlled. As discussed in Figure 21.3, the flame temperature of this oxy-fuel burner is much lower than that of a direct mix type oxy-fuel burner. In low-NO_x air burners using FGR, flame stability becomes a limiting factor in operating the burner with very high FGR ratios. In the Praxair “A” burner design, a small amount of oxygen, typically less than 5% of the total oxygen flow, is used around the central fuel jet to anchor the fuel jet and provide excellent flame stability. As a result, the burner can operate at very high FGR ratios and at a lower flame temperature than a typical low-NO_x air burner using FGR.

Figure 21.17 shows the effects of oxygen-enriched combustion on NO_x emissions for two commercial air burners (Bloom and Kinemax) and two commercial oxy-fuel burners (Oxytherm and Praxair “A”) in a test furnace.²⁶ Oxygen enrichment of combustion air in the air burners increased the flame temperature and resulted in sharp increases of NO_x emissions. As the oxygen enrichment level was increased, NO_x emissions peaked and started to decrease. At high concentrations of oxygen, NO_x emissions decreased linearly with oxygen concentration. A comparison of the two oxy-fuel burners showed that the Praxair “A” Burner produced NO_x emissions about an order of magnitude less than those from the Oxytherm burner. There are two competing factors in NO_x formation under

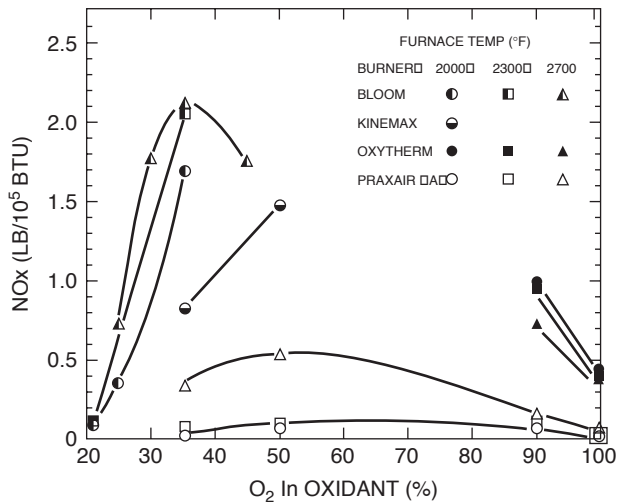


FIGURE 21.17 NO_x emissions under oxygen-enriched conditions.

oxygen-enriched combustion conditions: flame temperature and nitrogen concentration. In air combustion, the nitrogen concentration in the furnace atmosphere is about 70%. When air is enriched with oxygen, the effect of the higher flame temperature dominates and results in a sharp increase in NO_x emissions. As the enrichment level increases and approaches pure oxygen, the effect of the decreasing nitrogen concentration starts to dominate. A peak in NO_x emissions is formed at mid range. In the Zeldovich mechanism of thermal NO_x formation, the rate of NO_x formation is proportional to the nitrogen concentration. For example, if the nitrogen concentration is reduced to 7% with oxygen-enriched combustion and the flame temperature is kept constant, it would result in a tenfold reduction in NO_x formation. This is the reason why the “A” Burner produced very low NO_x emissions for a wide range of oxygen concentrations. By contrast, the Oxytherm oxy-fuel burner produced significant NO_x emissions even when pure oxygen was used, because the natural gas used in the test contained about 2% nitrogen and the flame temperature of the Oxytherm burner was very high. Most industrial furnaces operate at close to atmospheric pressure and normally experience significant ambient air infiltration. It is important to control the flame temperature of oxy-fuel burners to achieve low NO_x emissions even when pure oxygen is used for combustion.

The concept of in-furnace FGR was further advanced in the late 1980s to the conditions approaching those of a “homogeneous reactor” in which the furnace temperature and species concentrations are uniform throughout the furnace. The concept of this unique combustion process, known as “dilute oxygen combustion” (DOC), is shown in Figure 21.18.²⁷ The basic concept is to react fuel with a hot, dilute oxidant containing only 2 to 10% oxygen to produce a low flame temperature “reaction zone.” As shown in Figure 21.3, the flame temperature of DOC can become as low as 500°F (260°C) above the temperature of hot oxidant. An oxygen or air jet is injected into the furnace, separated by some distance from the fuel jet, to produce “hot dilute oxidant” by jet entrainment of furnace gas in a “mixing zone.” The reaction zone and the mixing zone are segregated within the furnace to prevent direct mixing and combustion of the undiluted oxidant and fuel. One or more pairs of oxidant and fuel jets are placed on the furnace walls to create furnace gas recirculation patterns that promote dilution of oxidant and good mixing of fuel. The stability of combustion requires hot furnace gases in this process. A minimum furnace temperature of 1400°F is typically required.

A hybrid technology²⁸ (Figure 21.19) combining a separated jet combustion device with a secondary oxygen injection system has been developed recently. In this design, the secondary oxygen jets

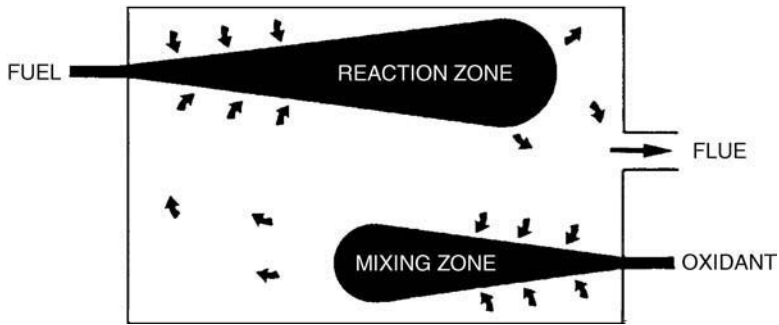


FIGURE 21.18 Dilute oxygen combustion (DOC) process.

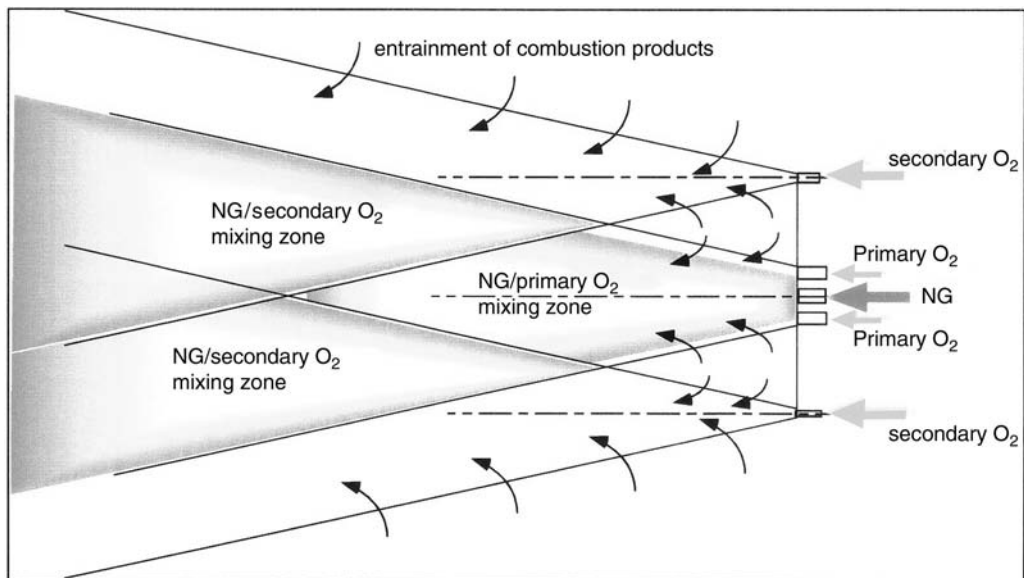


FIGURE 21.19 Diluted jet burner concept.

are positioned far from the primary ones, to produce hot oxidizing mixtures with low oxygen content, before they mix and react with the primary oxygen-fuel mixture. The distribution of oxygen between the two oxygen injection systems allows the combination of the principal advantages of the two preceding technologies; that is, a good flame stability and a very homogeneous temperature in the furnace. [Figure 21.20](#) compares the performance of a 2-MW diluted jet burner with those of other oxy-fuel burners in a pilot-scale furnace at high temperatures ($1420^{\circ}\text{C} = 2588^{\circ}\text{F}$ and $1500^{\circ}\text{C} = 2732^{\circ}\text{F}$). NO_x emissions from the diluted jet combustion technology²⁸ are very low and also show a very weak dependence on the nitrogen concentration in the furnace atmosphere.

21.4.4.2 Burners Using Oscillating Combustion

Oscillating combustion²⁸ for an oxy-fuel burner was developed in the 1990s to improve the energy efficiency and environmental performance of industrial combustion technologies. The basic idea of this low- NO_x primary technique is to create successive fuel-rich and fuel-lean zones within the flame, while operating the burner globally at stoichiometric conditions. The concept is schematically shown in [Figure 21.21](#).

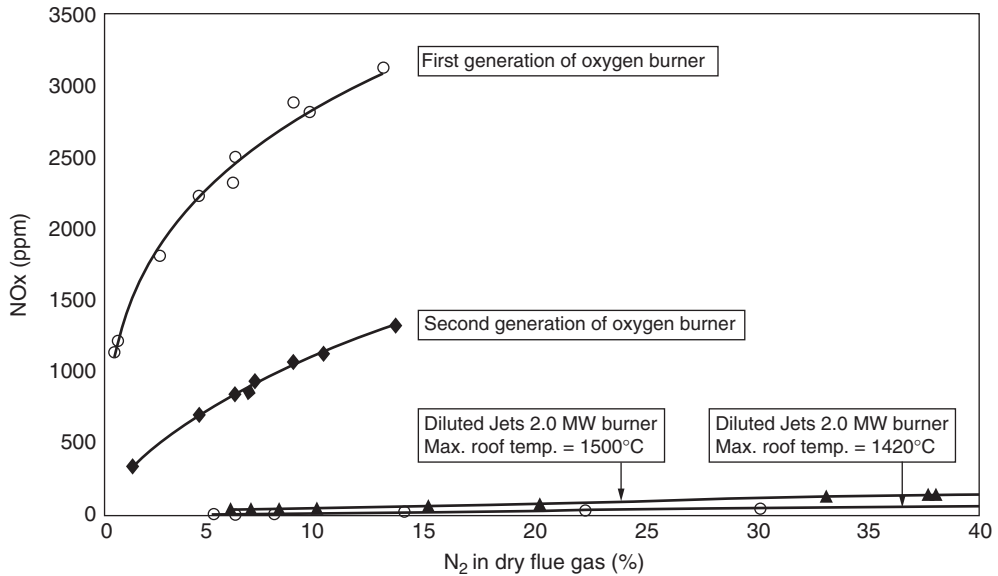


FIGURE 21.20 NO_x emissions in pilot-scale furnace of 1-MW oxygen combustion technologies.

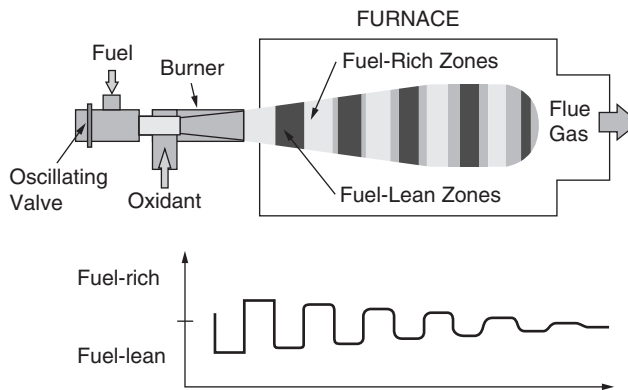


FIGURE 21.21 Oscillating combustion burner.

The pulsated flame is achieved by forced oscillation of the fuel flow rate, using a special valve. It is a solid-state proportioning (SSP) valve. A schematic drawing is shown in [Figure 21.22](#).

An elastomer disk is sandwiched between the fixed and movable pistons. The actuator is energized and oscillated at the required oscillating frequency. The force exerted by the moving piston on the elastomer disk causes it to plug and restrict the flow passage, which provides required flow oscillations. It is well known that NO_x formation is sensitive to temperature, especially in high-temperature flames such as pure oxygen flames

As shown in [Figure 21.23](#), an excess of either fuel or oxygen reduces the flame temperature and thus the NO_x formation rate. Early experiments on pilot furnaces have shown that up to 90% NO_x reduction can be achieved without lowering heat transfer, when pulsating both gases in opposite phases. This technology is designed to easily retrofit existing combustion systems, by the installation of oscillating valves and associated electronics to control the frequency and amplitude of the flow oscillations. The pulsating frequency and amplitude should be adjusted for each combustion system, and the phases of the oscillating flames in multi-burner systems

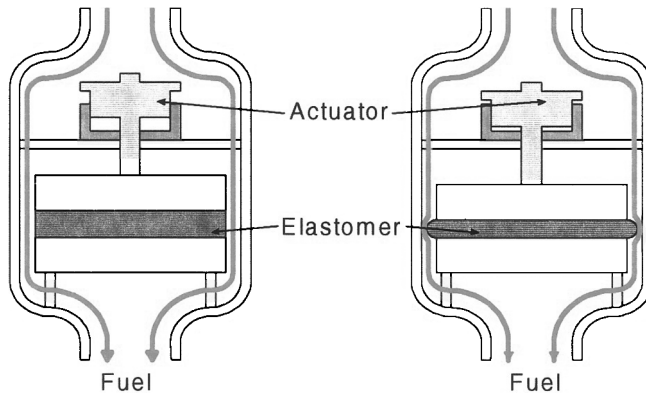


FIGURE 21.22 SSP valve operation schematic.

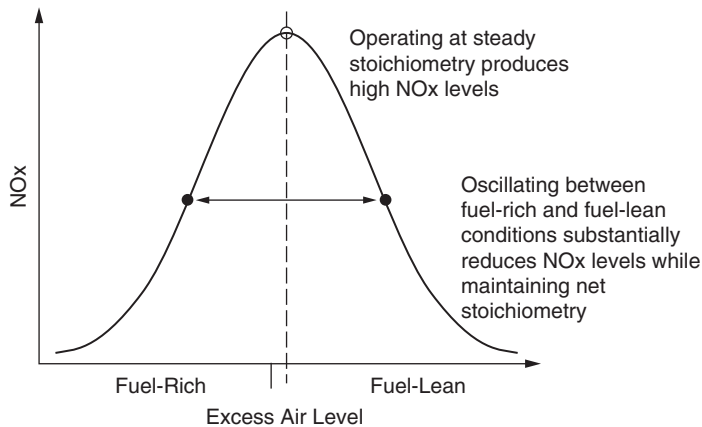


FIGURE 21.23 NO_x vs. stoichiometry.

should be staggered in sequence to avoid pulsating the whole flow in the furnace. Several years of field tests and application to different industrial processes showed that oscillating combustion is a competitive technology to reduce NO_x emissions, which allows 20 to 40% NO_x reduction for existing combustion systems. It has wide applicability and provides a cost-effective NO_x reduction option for steel, glass, aluminum, and other applications.

21.4.4.3 Burners Using Staged Combustion

Staged combustion is one of the primary reduction techniques of the emissions of nitrogen oxides for the industrial combustion systems. This technique consists of staging in the flame injection of one of the reactants (usually the oxidant) so as to create a primary combustion zone in fuel excess, and then a secondary zone in which additional oxygen is provided to complete combustion. In general, the primary combustion zone is the site of maximal heat release in the flame. The fuel excess in this zone limits the flame temperature at a level significantly lower than that of the stoichiometric flame. A lower temperature generally contributes to the reduction of thermal NO_x emissions, but the lack of sufficient oxygen in this primary zone is the principal element leading to a significant NO_x reduction, regardless of origin (i.e., either thermal NO or prompt NO). The simplest way to implement this technique on industrial furnaces, when the furnace wall space is available, is to add secondary oxygen lances to a traditional burner, in such a way that the flows

from the lances meet the primary zone flame only at a sufficient distance inside the furnace. Burner operation must be regulated in a fuel-rich condition and the supplemental oxygen is injected from the lances to complete the combustion. A good knowledge of the flow pattern inside the furnace, as well as good control of the injection conditions of the fluids, are essential to maximize the reduction of NO_x emissions. For a good performance evaluation of any combustion system, it is recommended that one simultaneously measure NO_x and CO emissions. The optimum for the operating condition of the combustion system is normally obtained for the intersection point of the two emission curves vs. the level of staging of the oxidant (i.e., the primary zone stoichiometric ratio). An example of a staged combustion oxy-fuel system consists of placing an oxygen lance under an oxygen burner and diverting part of oxygen feeding the burner to the lance. A valve arrangement to enable variable oxygen flows to the main burner and the lance is preferred. There are many other design options, but they all follow the same concept of two combustion zones with different stoichiometric conditions.

21.5 CUSTOMIZED OXY-BURNERS FOR CHEMICAL PROCESS APPLICATIONS

Combustion with pure oxygen is not only used for the traditional industrial processes such as glass or metal melting or the reheating of steel products, but is also used for chemical processes such as fly ash vitrification, reprocessing of chlorinated or sulfurized products, or the incineration of aqueous residues. Three of these specific applications of oxy-combustion are described in the following sub-sections.

21.5.1 OXY-BURNERS FOR SULFURIC ACID RECOVERY

Sulfuric acid recycling in a methyl methacrylate monomer (MMA) plant is an example of an industrial process for which a special oxygen combustion technology was developed. Stringent anti-pollution regulations and high production capacity requirement for a monomer production plant led to the development of an oxygen combustion system that was combined with other advanced technologies (two-staged, steam-heated vacuum evaporator; waste heat boiler; gas cleaning system; etc.) to double the sulfuric acid regeneration capacity of the plant.

The MMA product boils off in the esterifier vessels, leaving an aqueous solution known as by-products acid (BPA). Approximately 3 tons of BPA are generated for every ton of MMA produced, so the quantity of spent acid generated is substantial. Initially, the spent acid is preconcentrated in a two-stage, steam-heated vacuum evaporator. Then the concentrated acid is burned, using oxygen burners. Finally, the resulting SO₂ gas is cleaned and recovered as acid and oleum in a gas cleaning system. Burning the BPA in a pure oxygen atmosphere reduces the equipment size by a factor of about 2 compared to operation in air only. This saves cost, permits a large degree of vessel shop fabrication, avoids gas distribution problems in very large equipment, and avoids structural limitations on furnace brickwork. Pure oxygen combustion also allows energy savings — about 30% of the energy required for air-based operation, taking into account the energy consumed in producing oxygen itself.

The preconcentrated BPA containing ammonium sulfate and heavy organics is decomposed in the furnace at over 1832°F (1000°C). The chamber is lined with refractory brick. Natural gas is fired with oxygen to provide the energy required to decompose the acid. Operating conditions in the furnace must be controlled within narrow limits. If the oxygen excess in the flue gases is too high, sulfur trioxide will form, resulting in yield loss. If reducing conditions are approached, the organics will not be completely oxidized and elemental sulfur will form, which will sublime and block downstream equipment as the gases are cooled. Application of oxygen combustion burners to a SAR furnace with its highly corrosive atmosphere posed particular problems. In particular, it was

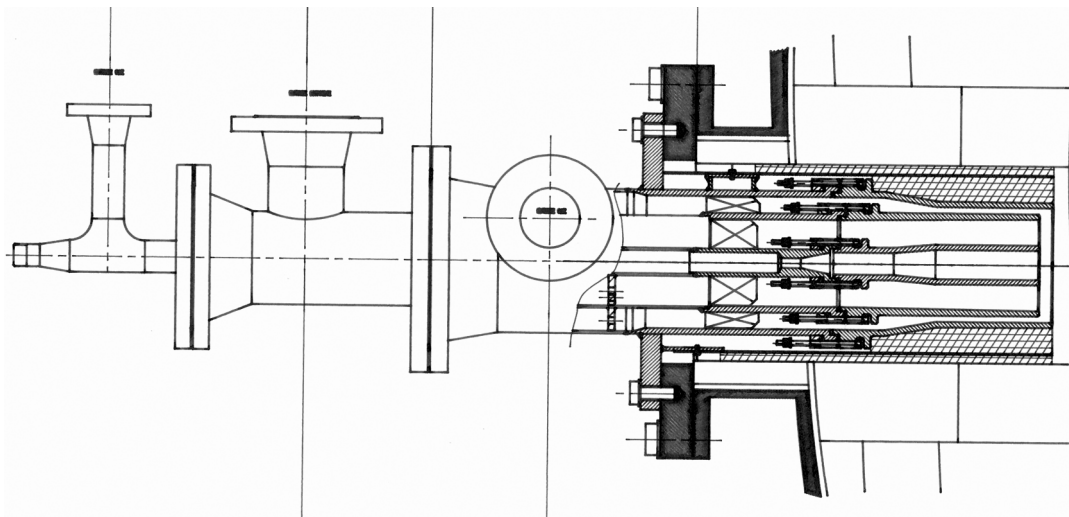


FIGURE 21.24 Oxygen burner scheme.

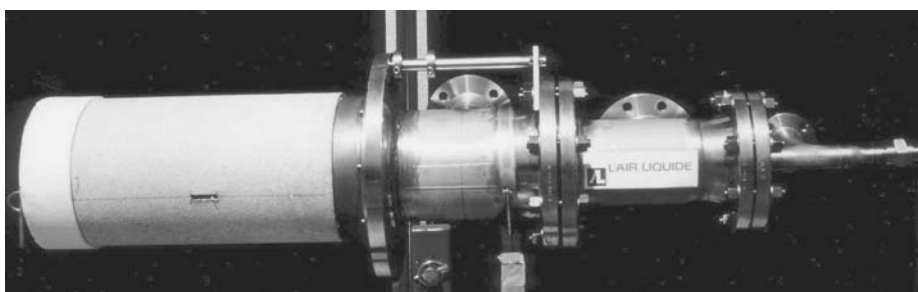


FIGURE 21.25 25-MW oxygen burner.

necessary to ensure that sufficient mixing occurs and that the kinetics of the various decomposition reactions are not adversely affected by the use of pure oxygen.

At the start of the development program, it was not known whether the oxygen/fuel burners could provide the required mixing and residence time necessary to achieve the desired conversions. In addition, there was a concern that radiation from the high-temperature flame would result in damage to the furnace refractories, and to the burner itself, in a highly acidic environment. It was therefore necessary to optimize and test the detailed mechanical configuration of the burner.

An 85-MMBtu/hr (25-MW) burner was developed (see [Figure 21.24](#)). This combustion technology (see [Figure 21.25](#)) enabled the required conversion of sulfur to SO_2 without producing undesirable by-products. Its performance primarily depends on burner design, BPA feed positions and droplet sizes, and flame stoichiometry.

21.5.2 OXY-BURNERS FOR WASTE INCINERATION AND FLY ASH VITRIFICATION

The use of oxygen in waste incineration is mostly driven by the incineration of low calorific value liquid waste, the possibility to design mobile incineration units or by vitrification applications, as well as new oxygen production technologies. The removal of the ballast of nitrogen in oxy-combustion improves the kinetics of combustion (i.e., increases the oxygen partial pressure and combustion temperature), increases the flammability range, and lowers the self-ignition temperature. For example, methylene chloride is nonflammable with air under atmospheric conditions; whereas

with oxygen, the lower and upper flammability limits are 16 and 66%, respectively. Combustion with oxygen allows increases in the performance of incineration processes. For example, combustion with oxygen allows one to minimize common problems of the incineration processes, such as flame instabilities or pyrolytic pockets. The most important benefit, however, is to enable incineration of aqueous wastes with low calorific values (LHV < 1800 Btu/lb or 1000 kcal/kg). In incineration with air, the lowest LHV values allowing for flame stabilization are close to 3600 Btu/lb (2000 kcal/kg). The removal of the ballast of nitrogen allows the stabilization of flames for LHV above 1530 Btu/lb (850 kcal/kg); this leads to auxiliary fuel savings and the elimination of waste evaporation or concentration stages preliminary to the incineration.

Another example is the possibility offered by oxy-combustion to treat waste with a low volatile content, such as irradiated graphite. Tests showed the feasibility to incinerate with pure oxygen in a cyclone furnace or with enriched air in a fluidized bed reactor. A final example of chemical process applications of oxygen burner technology concerns vitrification applications. Vitrification (homogenization by melting) is a form of chemical stabilization while reducing the volume. It is a process that requires large quantities of concentrated energy. Plasma, electric arc melting, and oxy-fuel combustion have been successfully applied. Recent progress in fume filtration has generated new and more residual wastes of different kinds, such as fly ash, bottom ash, and sludge. All of these materials have a common characteristic of containing a rather hazardous part, basically heavy metals, chlorides, and sulfurous compounds, with the major part of mineral oxides (e.g., SiO₂, CaO, Al₂O₃). Vitrification technology takes advantage of the similarity between the chemical composition of ash and that of common glass, and transforms the incoming ash into a glass product. When ash is transformed into vitrified state, the treated ash performs very well in a leaching test under the recently passed laws concerning maximum leaching values for landfill waste disposal. An effective vitrification demands a strong thermal gradient, while keeping a smooth flame; the oxygen burner shows excellent performance in these two aspects.

An advantage of an oxy-fuel flame as an energy source in vitrification is lower NO_x emissions compared with high-temperature air flames. Ash often contains some organic residues (carbon, hydrocarbons, dioxins, etc.) and the use of an oxy-fuel flame enables full combustion of most residual organic components in ash. It is also possible to separate heavy metals from the mineral matrix by the action of oxy-fuel flames.

21.6 SMALL-SIZE OXY-FUEL BURNERS FOR SPECIALIZED FUNCTIONS

For many years, the glass industry has been using combustion with pure oxygen for the finishing process of glass products (polishing, forming, etc.) or for lubricating moulds. The burners used for these applications are small firing rate burners (typically several thousand Btu/hr or few kilowatts), and their design characteristics and operating conditions are specific to the dedicated process. More recently, another technology of small-size oxygen burners was developed for temperature control on glass distribution systems in forehearth. Small-size burner technologies developed for some of these specific applications are described below.

21.6.1 POLISHING BURNERS

Burners used for flame polishing rough edges on glass bottles usually require hot, intense flames that burn in a small area. They utilize gaseous fuels and may employ other unconventional fuels such as hydrogen if ordinary fuels do not produce the proper flame temperature. The approaches in burner design focus on flame shape and usually try to match the hot point of the flame to the passing object's geometry to perform the polishing. Burners typically consist of long, slot-type geometries or multiple conical burners whose positioning can be adjusted. An example of this burner technology is shown in [Figure 21.26](#) and [Figure 21.27](#), which provide examples of flame polishing production lines.

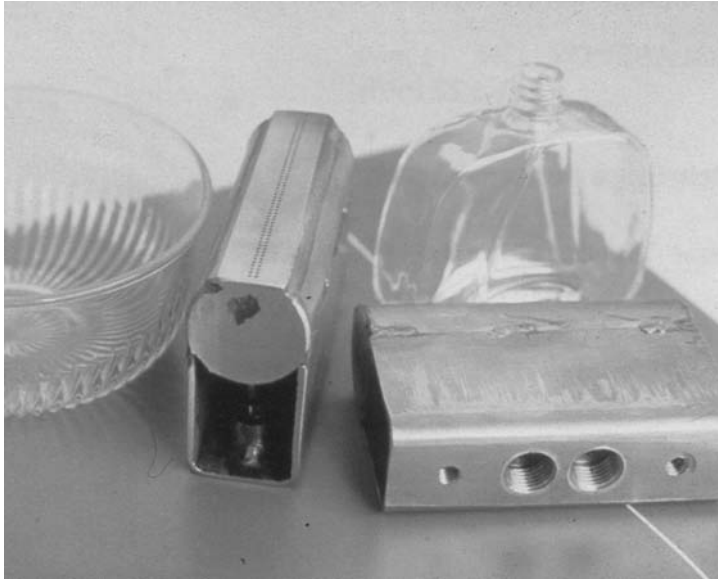


FIGURE 21.26 Glass flame polishing burner.



FIGURE 21.27 Glass flame polishing production line.

21.6.2 FOREHEARTH BURNERS

In the production of glass objects, molten glass is produced in a glass melting furnace from raw materials (batch) and recycled glass (cullet). The molten glass is transferred from the glass melting furnace through a glass distribution system, to the processing section, to a forming machine in which molten glass is processed into the desired glass shape or article. The glass distribution system may include distribution channels, feeders, and forehearths. Typical forehearths are designed to receive molten glass from the furnace and condition the glass to make it suitable for processing, and then convey it to the glass processing section or machine. Forehearths generally include a refractory trough along which the molten glass flows and which is covered with an insulating roof.

Traditional systems for heating glass in a forehearth system use combustion burners of premixed design in which the fuel (e.g., natural gas) and combustion air are premixed together in the correct stoichiometric ratio before they enter the burners. However, the use of premixed air-fuel burners for glass distribution systems such as channels and forehearths is not totally satisfactory. Such burners provide very poor fuel efficiency and, due to the high volume of combustion gases, the associated emissions are quite high. Moreover, most forehearth systems require precise temperature control of the glass, as small as 1°C, which is difficult to attain with air-fuel burners. Another disadvantage of the premixed air-fuel firing system is the very limited turndown ratio, which, in turn, limits the level of control on the forehearth when responding to a temperature control signal to either increase or decrease fuel input. The turndown ratio (i.e., the high firing rate of the burner divided by the low firing rate of the burner) for typical premixed air-fuel burners is only 4:1, due to flashback or blow-off phenomena.

To overcome these problems, some of premixed air-fuel burners have been replaced with post-mixed oxy-fuel burners. There are various arrangements of tube-in-tube design oxy-fuel burners for forehearth applications.

21.6.3 MOULD LUBRICATION IN GLASS PROCESS

Lubricating technologies are used in the glass industry and more specifically for the manufacturing of hollowware, such as bottles and containers. One of the more important steps in the manufacturing of hollowware is the forming of hot glass gob. This happens in individual section (IS) or rotary machines, in which a red-hot glass gob is filled in a mould, where it gets shaped by blowing air and is then taken out. This gob then becomes a so-called “parison,” which is a pre-form of the final hollowware. During this operation, strongly nonreversible thermal transfers take place between the hot glass (~920°F or 1200K) and the relatively cold mould (~670°F or 750K). To prevent any sticking of the glass to the mould, to obtain a good skin quality of the glass article (i.e., to prevent surface defects), and to avoid a quick damaging of the mould, the inside surfaces of the mould must be lubricated before the glass gob comes in contact. The conventional technology commonly used is manual swabbing, consisting of an oil-based soot graphite solution being deposited on the mould surface by an operator using a saturated swab. An alternative method for mould lubrication is to deposit a carbon black layer on the internal mould surface that is in contact with the glass, using a specific technique. Different techniques using fuel-rich flames are available; for example, the LINDE, OWENSBROCKWAY, or T.A. Seeman’s process. Air Liquide has developed a specific technology (ALBLACK™) that uses a natural gas/oxygen pilot flame to initiate cracking of an acetylene pulse, as shown in [Figure 21.28](#) and [Figure 21.29](#).

This technology deposits a thin carbon film on the metallic casting mould surface by acetylene gas decomposition at high temperature, providing mould lubrication for automated manufacturing operations. Some of the advantages of this process include:

- Improved skin quality of the glassware
- Easy automation of the forming machine
- Complete elimination of pollution caused by oil lubricants

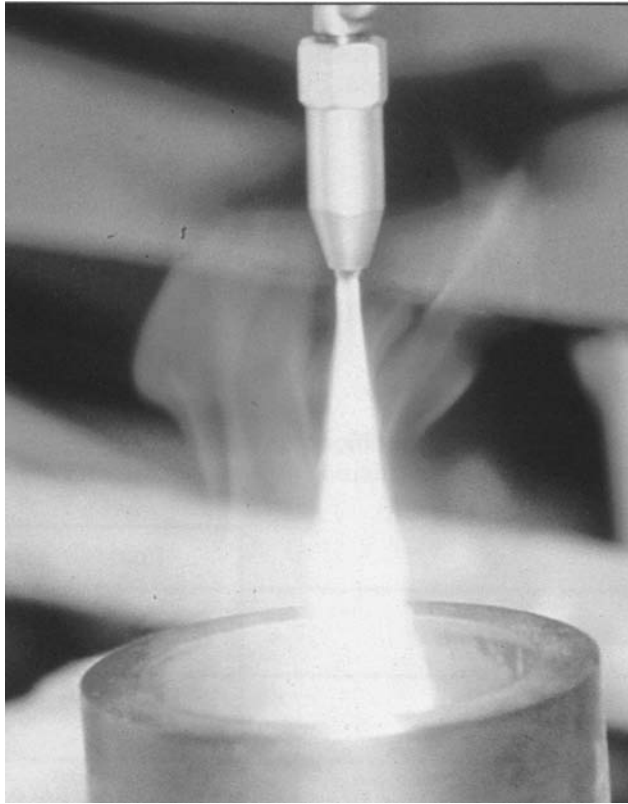


FIGURE 21.28 ALBLACK™ oxygen burner.



FIGURE 21.29 ALBLACK™ process.

- Improvement in working conditions by eliminating oil fumes
- Improvement in product quality
- Mould loading (glazing) reduction
- Regular and reproducible carbon film deposit

21.7 OXYGEN AND COMBUSTION SAFETY

Safety and reliability are very important requirements for any combustion system. The use of oxygen enrichment or high-purity oxygen for combustion requires special design considerations due to the high reactivities of oxygen and oxygen-enriched air with various materials. Two different aspects of safety need to be addressed: (1) the safety of the oxygen supply and flow control system, and (2) the safety of oxygen-enriched combustion and burner management.

Many materials that do not burn with air can be ignited and burn vigorously in an oxygen atmosphere. For example, carbon steel pipes, especially when not properly cleaned for oxygen service, can ignite and cause an “oxygen pipe fire.” For safe storage and distribution of oxygen, proper selection, sizing, and cleaning of all materials for oxygen service, including storage tanks, pipes, piping components, valves, flanges, gauges, gaskets, and sealing compounds, are required. The design and manufacturing guidelines for oxygen storage and distribution systems are, for the most part, well established and available from the publications of the Compressed Gas Association.³⁰⁻³⁵ However, the design and engineering of oxygen systems should always be performed by qualified engineers with proper safety training, education, and experience. Industrial gas oxygen suppliers, who have excellent safety records in the operation of numerous bulk oxygen storage and distribution systems, provide turnkey installations for various industrial applications.

For combustion safety and burner management, the basic design principles of the safety interlock systems are the same for both air and oxygen enriched systems. Prevention of combustibles or explosive mixtures in the furnace, monitoring of flame, and detection and correction of off-stoichiometric conditions, are among the most important design features. It is recommended that all safety standards for air burner systems also be incorporated into the design of oxygen enriched combustion systems. In addition, special design considerations should be given to prevent accidental accumulation of oxygen enriched air in or near the furnace. With oxygen enrichment, the minimum ignition temperature of a fuel-oxidant mixture is reduced and the higher flammability limit is significantly widened compared to those of the equivalent fuel-air mixture. Thus, the likelihood of potential formation and ignition of flammable mixtures tends to increase in the event of accidental accumulation of both fuel and oxygen enriched air in the furnace.

Proper purging of a furnace prior to initiating the ignition sequence is an important safety step. In air-fired furnaces, combustion air is available for use as the purge gas. In an oxy-fuel-fired furnace, a separate purge gas stream, typically blower air or nitrogen, is required to ensure proper purging. Further details on oxygen combustion safety can be found in National Fire and Protection Agency’s (NFPA) Standard 86, “Ovens and Furnaces,” which is generally considered the accepted standard for regulating the safe design of combustion equipment.³⁶ With proper design, construction, and a good in-plant safety program, the operation of the oxygen combustion system is as safe and reliable as a well-designed air combustion system.

21.8 SUMMARY

Oxy-fuel burners have been adopted in a wide range of industrial furnaces to improve productivity and fuel efficiency, to reduce emissions of pollutants, and, in some applications, to improve product quality and yield or to eliminate the capital and maintenance costs of air preheaters. Significant fractions of glass melting furnaces, steel scrap melting furnaces, electric arc furnaces, steel reheat furnaces, soaking pits, forging furnaces, ladles, aluminum melting furnaces, copper smelting and

anode furnaces, hazardous waste incinerators, rotary enamel frit furnaces, and rotary lead melting furnaces are fired with oxy-fuel burners.

As with air burners, many different oxy-fuel burner designs have been developed and are available to end users. Each different design was developed to overcome a problem or achieve a certain goal, depending on the application. Traditional oxy-fuel burners produce a high flame temperature and intense heat transfer, and are typically used in high-temperature melting processes. Low-NO_x oxy-fuel burners are designed to produce low flame temperatures comparable to those of low-NO_x air burners, while retaining the other benefits of oxy-fuel combustion. These burners use one of three design features: (1) in-furnace recirculation of flue gas, (2) off-stoichiometric oscillating combustion, or (3) staged combustion. As the concentration of nitrogen molecules in the combustion space is reduced with full oxy-fuel combustion to less than one tenth that of air combustion, NO_x emissions as low as one tenth of those from low-NO_x air burners have been demonstrated.

Customized oxy-fuel burners are available for specific applications such as the Claus sulfur recovery process, the sulfuric acid recovery process, waste incineration processes, and ash vitrification processes. Also, small oxy-fuel burners are available for special applications such as glass surface polishing and uniform heating in glass forehearth. New sensor and control technologies have been adapted for some oxy-fuel burner systems to enhance and to optimize burner performance.

Understanding the attributes of an oxy-fuel burner and overlaying them with the requirements of the process and the needs of the end user are key to selecting the proper burner for a particular application. In many situations, seeking advice from the burner manufacturers, who have significant design and hands-on experience with each burner type, is the best way to ensure that the selected burner will perform satisfactorily in the application. In addition, the use of oxygen enrichment for combustion requires special design considerations due to the high reactivities of oxygen and oxygen-enriched air with various materials. The design and engineering of oxygen systems should always be performed by qualified engineers with the proper safety training, education, and experience. Industrial gas oxygen suppliers, who have excellent safety records of numerous bulk oxygen storage and distribution systems, provide turnkey installations for various industrial applications.

REFERENCES

1. H. Kobayashi, Oxygen Enriched Combustion System Performance Study, Vol. I: Technical and Economic Analysis, Prepared for the U.S. Dept. of Energy, Idaho Operations Office, Idaho Falls, ID, Report No. DOE/ID/12597, March 1987.
2. Kobayashi, H., Oxygen Enriched Combustion System Performance Study, Phase I Final Report Volume II: Market Assessment, U.S. Dept. of Energy, Report No. DOE/ID/12597-1, September 1988.
3. Duboudin T. et al., The advantages of pure oxygen in high temperature processes, *Proceeding IFRF ToTeM8 loughborough*, November 1993.
4. Dugué J. et al., Comparison between high air preheat and pure oxygen combustion in pilot scale and industrial furnaces, IFRF ToTeM13, April 1999, Akersloot.
5. Baukal, C.E., Ed., *Oxygen-Enhanced Combustion*, CRC Press, Boca Raton, FL, 1998.
6. Snyder, W.J., Burner Fulfills Performance Promise in Service, *Glass Industry*, July 1999, pp. 23–24.
7. Van des Hout, J.J. and Duboudin T., Oxy-fuel furnace L4 after 2.5 years of operation, *Proceeding: Glastec*, Dusseldorf, October 1998.
8. Mathur, P.C., Fundamentals and operating results of Praxair CoJet technology, *Iron and Steelmaker*, March 1999, 59–64.
9. Grant, M.G., Principles and strategy of EAF post-combustion, *58th Electric Furnace Conference*, November 2000, Orlando, FL.
10. Farrell, L.M., Pavlack, T.T., and Rich, L., Operational and Environmental Benefits of Oxy-Fuel Combustion in the Steel Industry, *12th Process Technology Conference Proceedings, Iron and Steel Society*, 1993.

11. Stewart, Jr., D.L., Aluminum Melting Technology — Current Trends and Future Opportunities, *The 131st TMS Annual Meeting*, Seattle, WA, February 18–20, 2002.
12. Ho, M. and Ding, M.G., The Use of Oxygen in Hazardous Waste Incineration — A State of the Art Review, *HMCRI's 9th National Conference and Exhibition SUPERFUND '88*, Washington, D.C., November 28–30, 1988.
13. Baudoin, P. et al., The use of pure oxygen in incineration processes, laboratory and pilot scale experiments, modeling and industrial applications, *Proceeding Incineration Conference*, 1994, Houston.
14. Ammouri, F. et al., A comparison between weighted sum of gray gases and spectral CK radiation models for heat transfer calculations in furnaces, Société Française des Thermiciens, Journée d'études du 14 février 1996.
15. Samaniego, J.-M. et al., Mechanism of nitric oxide formation in oxygen-natural gas combustion, *27th Symp. (Int.) on Combustion*, 1998.
16. Labégorre, B. et al., NO_x formation modelling in oxygen-natural gas industrial flames, *AFRC/JFRC Int. Symp.*, 1998, Hawaï.
17. U.S. Patent 5,267, 850, Fuel Jet Burner, December 7, 1993.
18. U.S. Patent 5,620,316, Working Hole for Oxyburner, April 15, 1997.
19. Delabroy, O., Performance enhancement of reheating furnaces with oxygen combustion, *Mettallurgy Int. Meeting*, Luxembourg, October 1998.
20. Delabroy O. et al., Experimental characterization of industrial spray injectors in oxy-combustion, *ILASS Europe*, 1998.
21. Leroux B., Ph.D. thesis, Etude Expérimentale des Flamme Oxygène. Fuel Liquide, Laboratoire d'Énergétique Moléculaire et Macroscopique, Ecole Centrale Paris, France, 2002.
22. U.S. Patent 6,135,366, Injector of Fuel in the Form of a Mist for an Oil Burner, October 24, 2000.
23. U.S. Patent 5,833,447, Combustion Process and Apparatus Containing Separated Injections of Fuel, November 10, 1998.
24. Legiret, T., Advanced oxygen burner for glass industry, *Glass Sci. Tech.*, 1997.
25. U.S. Patent 4,378,205, Oxygen Aspirator Burner and Process for Firing a Furnace, March 29, 1983.
26. Kwan, Y. et al., Oxygen Enriched Combustion System Performance Study, Phase I: Final Report Volume III: Burner Tests and Combustion Modeling, prepared for the U.S. Dept. of Energy, September 1988.
27. U.S. Patent 5,076,779, Segregated Zoning Combustion, December 31, 1991.
28. U.S. Patent 6,196,831, Combustion Process for Burning Fuel, March 6, 2001.
29. Charon, O. et al., Pulsated O₂/fuel flame as a new technique for low NO_x emission, *Comb. Sci. Tech.*, 1993, Vol. 93.
30. CGA pamphlet P-14, Accidental Prevention in Oxygen-Rich and Oxygen-Deficient Atmospheres, Compressed Gas Association, Arlington, VA, 1992.
31. CGA G-4, Oxygen, Compressed Gas Association, Arlington, VA, 1996.
32. CGA G-4.1, Cleaning Equipment for Oxygen Services, Compressed Gas Association, Arlington, VA, 1996.
33. CGA G-4.3, Commodity Specification for Oxygen, Compressed Gas Association, Arlington, VA, 1994.
34. CGA G-4.4, Industrial Practices for Gaseous Oxygen Transmission and Distribution Piping System, Compressed Gas Association, Arlington, VA, 1993.
35. CGA O2-DIR, Directory of Cleaning Agents for Oxygen Service, Compressed Gas Association, Arlington, VA, 1997.
36. NFPA 86, Ovens and Furnaces, National Fire Protection Agency, Quincy, MA, 1995.

Section IV

Appendices

Appendix A

Common Conversions

1 Btu =	252.0 cal 1055 J	1 in. =	2.540 cm 25.40 mm
1 Btu/ft ³ =	0.00890 cal/cm ³ 0.0373 MJ/m ³	1 J =	0.000948 Btu 0.239 cal 1 W/sec
1 Btu/hr =	0.0003931 hp 0.2520 kcal/hr 0.2931 W	1 kcal =	3.968 Btu 1000 cal 4187 J
1,000,000 Btu/hr =	0.293 MW	1 kcal/hr =	3.968 Btu/hr 1.162 J/sec
1 Btu/hr-ft ² =	0.003153 kW/m ²	1 kcal/m ³ =	0.1124 Btu/ft ³ 4187 J/m ³
1 Btu/hr-ft-°F =	1.730 W/m-K	1 kg =	2.205 lb
1 Btu/hr-ft ² -°F =	5.67 W/m ² -K	1 kg/hr-m =	0.00278 g/sec-cm 0.672 lb/hr-ft
1 Btu/lb =	0.5556 cal/g 2326 J/kg	1 kg/m ³ =	0.06243 lb/ft ³
1 Btu/lb-°F =	1 cal/g-°C 4187 J/kg-K	1 kW =	3413 Btu/hr 1.341 hp 660.6 kcal/hr
1 cal =	0.003968 Btu 4.187 J	1 kW/m ² =	317.2 Btu/hr-ft ²
1 cal/cm ² -sec =	3.687 Btu/ft ² -sec 41.87 kW/m ²	1 kW/m ² -°C =	176.2 Btu/hr-ft ² -°F
1 cal/cm-sec-°C =	241.9 Btu/ft-hr-°F 418.7 W/m-K	1 lb =	0.4536 kg
1 cal/g =	1.80 Btu/lb 4187 J/kg	1 lb/ft ³ =	0.0160 g/cm ³ 16.02 kg/m ³
1 cal/g-°C =	1 Btu/lb-°F 4187 J/kg-K	1 lbm/hr-ft =	0.413 centipoise
1 centipoise =	2.421 lbm/hr-ft	1 m =	3.281 ft
1 cm ² /sec =	100 centistokes 3.874 ft ² /hr	1 mm =	0.03937 in.
1 ft =	0.3048 m	1 m ² /sec =	10.76 ft ² /sec
1 ft ² /sec =	0.0929 m ² /sec	1 mton =	1000 kg 2205 lb
1 g/cm ³ =	1000 kg/m ³ 62.43 lb/ft ³ 0.03613 lb/in. ³	1 MW =	3,413,000 Btu/hr 1000 kW
1 hp =	33,000 ft-lb/min 550 ft-lb/sec 641.4 kcal/hr 745.7 W	1 therm =	100,000 Btu
		1 W =	1 J/sec
		1 W/m-K =	0.5778 Btu/ft-hr-°F

TEMPERATURE CONVERSIONS

$$\begin{aligned}
 ^\circ\text{C} &= 5/9 (^{\circ}\text{F} - 32) & ^{\circ}\text{F} &= 9/5 (^{\circ}\text{C} + 32) \\
 \text{K} &= ^\circ\text{C} + 273.15 & ^{\circ}\text{R} &= ^{\circ}\text{F} + 459.67
 \end{aligned}$$

From: Baukal, C.E., *Heat Transfer in Industrial Combustion*, CRC Press, Boca Raton, FL, 2000.

Appendix B

Design Data

TABLE B.1
Areas and Circumferences of Circles and Drill Sizes

Drill Size	Diameter (in.)	Circumference (in.)	Area (in.)	Area (ft)
80	0.0135	0.042 41	0.000 143	0.000 000 9
79	0.0145	0.045 55	0.000 165	0.000 001 1
1/64"	0.0156	0.049 09	0.000 191	0.000 001 3
78	0.0160	0.050 27	0.000 201	0.000 001 4
77	0.0180	0.056 55	0.000 254	0.000 001 8
76	0.0200	0.062 83	0.000 314	0.000 002 2
75	0.0210	0.065 97	0.000 346	0.000 002 4
74	0.0225	0.070 69	0.000 398	0.000 002 8
73	0.0240	0.075 40	0.000 452	0.000 003 1
72	0.0250	0.078 54	0.000 491	0.000 003 4
71	0.0260	0.081 68	0.000 531	0.000 003 7
70	0.0280	0.087 96	0.000 616	0.000 004 3
69	0.0292	0.091 73	0.000 670	0.000 004 7
68	0.0310	0.097 39	0.000 755	0.000 005 2
1/12"	0.0313	0.098 18	0.000 765	0.000 005 3
67	0.0320	0.100 53	0.000 804	0.000 005 6
66	0.0330	0.103 67	0.000 855	0.000 005 9
65	0.0350	0.109 96	0.000 962	0.000 006 7
64	0.0360	0.113 10	0.001 018	0.000 007 1
63	0.0370	0.116 24	0.001 075	0.000 007 5
62	0.0380	0.119 38	0.001 134	0.000 007 9
61	0.0390	0.122 52	0.001 195	0.000 008 3
60	0.0400	0.125 66	0.001 257	0.000 008 7
59	0.0410	0.128 81	0.001 320	0.000 009 2
58	0.0420	0.131 95	0.001 385	0.000 009 6
57	0.0430	0.135 09	0.001 452	0.000 010 1
56	0.0465	0.146 08	0.001 698	0.000 011 8
3/64"	0.0469	0.147 26	0.001 73	0.000 012 0
55	0.0520	0.163 36	0.002 12	0.000 014 7
54	0.0550	0.172 79	0.002 38	0.000 016 5
53	0.0595	0.186 93	0.002 78	0.000 019 3
1/16"	0.0625	0.196 35	0.003 07	0.000 021 3

TABLE B.1 (Continued)
Areas and Circumferences of Circles and Drill Sizes

Drill Size	Diameter (in.)	Circumference (in.)	Area (in.)	Area (ft)
52	0.0635	0.199 49	0.003 17	0.000 022 0
51	0.0670	0.210 49	0.003 53	0.000 024 5
50	0.0700	0.219 91	0.003 85	0.000 026 7
49	0.0730	0.229 34	0.004 19	0.000 029 1
48	0.0760	0.238 76	0.004 54	0.000 031 5
5/64"	0.0781	0.245 44	0.004 79	0.000 033 3
47	0.0785	0.246 62	0.004 84	0.000 033 6
46	0.0810	0.254 47	0.005 15	0.000 035 8
45	0.0820	0.257 61	0.005 28	0.000 036 7
44	0.0860	0.270 18	0.005 81	0.000 040 3
43	0.0890	0.279 60	0.006 22	0.000 043 2
42	0.0935	0.293 74	0.006 87	0.000 047 7
3/32"	0.0937	0.294 52	0.006 90	0.000 047 9
41	0.0960	0.301 59	0.007 24	0.000 050 3
40	0.0980	0.307 88	0.007 54	0.000 052 4
39	0.0995	0.312 59	0.007 78	0.000 054 0
38	0.1015	0.318 87	0.008 09	0.000 056 2
37	0.1040	0.326 73	0.008 49	0.000 059 0
36	0.1065	0.334 58	0.008 91	0.000 061 9
7/64"	0.1094	0.343 61	0.009 40	0.000 065 2
35	0.1100	0.345 58	0.009 50	0.000 066 0
34	0.1110	0.348 72	0.009 68	0.000 067 2
33	0.1130	0.355 00	0.010 03	0.000 069 6
32	0.1160	0.364 43	0.010 57	0.000 073 4
31	0.1200	0.376 99	0.011 31	0.000 078 5
1/8"	0.1250	0.392 70	0.012 27	0.000 085 2
30	0.1285	0.403 70	0.012 96	0.000 090 1
29	0.1360	0.427 26	0.014 53	0.000 100 9
28	0.1405	0.441 39	0.015 49	0.000 107 7
9/64"	0.1406	0.441 79	0.015 53	0.000 107 9
27	0.1440	0.442 39	0.016 29	0.000 113 1
26	0.1470	0.461 82	0.016 97	0.000 117 9
25	0.1495	0.469 67	0.017 55	0.000 121 9
24	0.1520	0.477 52	0.018 15	0.000 126 0
23	0.1540	0.483 81	0.018 63	0.000 129 4
5/32"	0.1562	0.490 87	0.019 17	0.000 133 1
22	0.1570	0.493 23	0.019 36	0.000 134 4
21	0.1590	0.499 51	0.019 86	0.000 137 9
20	0.1610	0.505 80	0.020 36	0.000 141 4
19	0.1660	0.521 51	0.021 64	0.000 150 3
18	0.1695	0.532 50	0.022 56	0.000 156 7
11/64"	0.1719	0.539 96	0.023 20	0.000 161 1
17	0.1730	0.543 50	0.023 51	0.000 163 2
16	0.1770	0.556 06	0.024 61	0.000 170 9

TABLE B.1 (Continued)
Areas and Circumferences of Circles and Drill Sizes

Drill Size	Diameter (in.)	Circumference (in.)	Area (in.)	Area (ft)
15	0.1800	0.565 49	0.025 45	0.000 176 7
14	0.1820	0.571 77	0.026 02	0.000 180 7
13	0.1850	0.581 20	0.026 88	0.000 186 7
3/16"	0.1875	0.589 05	0.027 61	0.000 191 7
12	0.1890	0.593 76	0.028 06	0.000 194 8
11	0.1910	0.600 05	0.028 65	0.000 199 0
10	0.1930	0.606 33	0.029 40	0.000 203 2
9	0.1960	0.615 75	0.030 17	0.000 209 5
8	0.1990	0.625 18	0.031 10	0.000 216 0
7	0.2010	0.631 46	0.031 73	0.000 220 4
13/64"	0.2031	0.638 14	0.032 41	0.000 224 8
6	0.2040	0.640 89	0.032 69	0.000 227 0
5	0.2055	0.645 60	0.033 17	0.000 230 3
4	0.2090	0.656 59	0.034 31	0.000 238 2
3	0.2130	0.669 16	0.035 63	0.000 247 5
7/32"	0.2187	0.687 22	0.037 58	0.000 261 0
2	0.2210	0.694 29	0.038 36	0.000 266 4
1	0.2280	0.716 28	0.040 83	0.000 283 5
A	0.2340	0.735 13	0.043 01	0.000 298 7
15/64"	0.2344	0.736 31	0.043 14	0.000 299 6
B	0.2380	0.747 70	0.044 49	0.000 308 9
C	0.2420	0.760 27	0.046 00	0.000 319 4
D	0.2460	0.772 83	0.047 53	0.000 330 1
E = 1/4"	0.2500	0.785 40	0.049 09	0.000 340 9
F	0.2570	0.807 39	0.051 87	0.000 360 2
G	0.2610	0.819 96	0.053 50	0.000 371 5
17/64"	0.2656	0.834 41	0.055 42	0.000 384 9
H	0.2660	0.835 67	0.055 57	0.000 385 9
I	0.2720	0.854 52	0.058 11	0.000 403 5
J	0.2770	0.870 22	0.060 26	0.000 418 5
K	0.2810	0.882 79	0.062 02	0.000 430 7
9/32"	0.2812	0.883 57	0.062 13	0.000 431 5
L	0.2900	0.911 06	0.066 05	0.000 458 7
M	0.2950	0.926 77	0.068 35	0.000 474 7
19/64"	0.2969	0.932 66	0.069 22	0.000 480 7
N	0.3030	0.951 90	0.071 63	0.000 500 7
5/16"	0.3125	0.981 75	0.076 70	0.000 532 6
O	0.3160	0.992 75	0.078 43	0.000 544 6
P	0.3230	1.014 74	0.081 94	0.000 569 0
21/64"	0.3281	1.030 8	0.084 56	0.000 587 2
Q	0.3320	1.043 0	0.086 57	0.000 601 2
R	0.3390	1.065 0	0.090 26	0.000 626 8
11/32"	0.3437	1.079 8	0.092 81	0.000 644 5
S	0.3480	1.093 3	0.095 11	0.000 660 5

TABLE B.1 (Continued)
Areas and Circumferences of Circles and Drill Sizes

Drill Size	Diameter (in.)	Circumference (in.)	Area (in.)	Area (ft)
T	0.3580	1.124 7	0.100 6	0.000 699 0
23/64"	0.3594	1.129 0	0.101 4	0.000 704 4
U	0.3680	1.156 1	0.106 4	0.000 738 6
3/8"	0.3750	1.178 1	0.110 5	0.000 767 0
V	0.3770	1.184 4	0.111 6	0.000 775 2
W	0.3860	1.212 7	0.117 0	0.000 812 7
25/64"	0.3906	1.227 2	0.119 8	0.000 832 2
X	0.3970	1.247 2	0.123 8	0.000 859 6
Y	0.4040	1.269 2	0.128 2	0.000 890 2
13/32"	0.4062	1.276 3	0.129 6	0.000 900 1
Z	0.4130	1.297 5	0.134 0	0.000 930 3
27/64"	0.4219	1.325 4	0.139 8	0.000 970 8
7/16"	0.4375	1.3745	0.1503	0.001 044
29/64"	0.4531	1.4235	0.1613	0.001 120
15/32"	0.4687	1.4726	0.1726	0.001 198
31/64"	0.4844	1.5217	0.1843	0.001 280
1/2"	0.5000	1.5708	0.1964	0.001 364
33/64"	0.5156	1.6199	0.2088	0.001 450
17/32"	0.5313	1.6690	0.2217	0.001 539
35/64"	0.5469	1.7181	0.2349	0.001 631
9/16"	0.5625	1.7672	0.2485	0.001 726
37/64"	0.5781	1.8162	0.2625	0.001 823
19/32"	0.5938	1.8653	0.2769	0.001 923
39/64"	0.6094	1.9144	0.2917	0.002 025
5/8"	0.6250	1.9635	0.3068	0.002 131
41/64"	0.6406	2.0126	0.3223	0.002 238
21/32"	0.6562	2.0617	0.3382	0.002 350
43/64"	0.6719	2.1108	0.3545	0.002 462
11/16"	0.6875	2.1598	0.3712	0.002 578
23/32"	0.7188	2.2580	0.4057	0.002 818
3/4"	0.7500	2.3562	0.4418	0.003 068
25/32"	0.7812	2.4544	0.4794	0.003 329
13/16"	0.8125	2.5525	0.5185	0.003 601
27/32"	0.8438	2.6507	0.5591	0.003 883
7/8"	0.8750	2.7489	0.6013	0.004 176
29/32"	0.9062	2.8471	0.6450	0.004 479
15/16"	0.9375	2.9452	0.6903	0.004 794
31/32"	0.9688	3.0434	0.7371	0.005 119
1"	1.0000	3.1416	0.7854	0.005 454
1 1/16"	1.0625	3.3379	0.8866	0.006 157
1 1/8"	1.1250	3.5343	0.9940	0.006 903
1 3/16"	1.1875	3.7306	1.1075	0.007 691
1 1/4"	1.2500	3.9270	1.2272	0.008 522
1 5/16"	1.3125	4.1233	1.3530	0.009 396

TABLE B.1 (Continued)
Areas and Circumferences of Circles and Drill Sizes

Drill Size	Diameter (in.)	Circumference (in.)	Area (in.)	Area (ft)
1 3/8"	1.3750	4.3170	1.4849	0.010 31
1 7/16"	1.4375	4.5160	1.6230	0.011 27
1 1/2"	1.5000	4.7124	1.7671	0.012 27
1 9/16"	1.5625	4.9087	1.9175	0.013 32
1 5/8"	1.6250	5.1051	2.0739	0.014 40
1 11/16"	1.6875	5.3014	2.2365	0.015 53
1 3/4"	1.7500	5.4978	2.4053	0.016 70
1 13/16"	1.8125	5.6941	2.5802	0.017 92
1 7/8"	1.8750	5.8905	2.7612	0.019 18
1 15/16"	1.9375	6.0868	2.9483	0.020 47
2"	2.0000	6.2832	3.1416	0.021 82
2 1/16"	2.0625	6.4795	3.3410	0.023 20
2 1/8"	2.1250	6.6759	3.5466	0.024 63
2 3/16"	2.1875	6.8722	3.7583	0.026 10
2 1/4"	2.2500	7.0686	3.9761	0.027 61
2 5/16"	2.3125	7.2649	4.2000	0.029 17
2 3/8"	2.3750	7.4613	4.4301	0.030 76
2 7/16"	2.4375	7.6576	4.6664	0.032 41
2 1/2"	2.5000	7.8540	4.9087	0.034 09
2 9/16"	2.5625	8.0503	5.1572	0.035 81
2 5/8"	2.6250	8.2467	5.4119	0.037 58
2 11/16"	2.6875	8.4430	5.6727	0.039 39
2 3/4"	2.7500	8.6394	5.9396	0.041 25
2 13/16"	2.8125	8.8357	6.2126	0.043 14
2 7/8"	2.8750	9.0323	6.4918	0.045 08
2 15/16"	2.9375	9.2284	6.7771	0.047 06
3"	3.0000	9.4248	7.0686	0.049 09
3 1/16"	3.0625	9.6211	7.3662	0.051 15
3 1/8"	3.1250	9.8175	7.6699	0.053 26
3 3/16"	3.1875	10.014	7.9798	0.055 42
3 1/4"	3.2500	10.210	8.2958	0.057 36
3 5/16"	3.3125	10.407	8.6179	0.059 85
3 3/8"	3.3750	10.603	8.9462	0.062 13
3 7/16"	3.4375	10.799	9.2806	0.064 45
3 1/2"	3.5000	10.996	9.6211	0.066 81
3 9/16"	3.5625	11.192	9.9678	0.069 22
3 5/8"	3.6250	11.388	10.321	0.071 67
3 11/16"	3.6875	11.585	10.680	0.074 17
3 3/4"	3.7500	11.781	11.045	0.076 70
3 13/16"	3.8125	11.977	11.416	0.079 28
3 7/8"	3.8750	12.174	11.793	0.081 90
3 15/16"	3.9375	12.370	12.177	0.084 56
4"	4.0000	12.566	12.566	0.087 26
4 1/16"	4.0625	12.763	12.962	0.090 02

TABLE B.1 (Continued)
Areas and Circumferences of Circles and Drill Sizes

Drill Size	Diameter (in.)	Circumference (in.)	Area (in.)	Area (ft)
4 1/8"	4.1250	12.959	13.364	0.092 81
4 3/16"	4.1875	13.155	13.772	0.095 64
4 1/4"	4.2500	13.352	14.186	0.098 52
4 5/16"	4.3125	13.548	14.607	0.101 4
4 3/8"	4.3750	13.745	15.033	0.104 3
4 7/16"	4.4375	13.941	15.466	0.107 4
4 1/2"	4.5000	14.137	15.904	0.110 4
4 9/16"	4.5625	14.334	16.349	0.113 5
4 5/8"	4.6250	14.530	16.800	0.1167
4 11/16"	4.6875	14.726	17.257	0.1198
4 3/4"	4.7500	14.923	17.721	0.1231
4 13/16"	4.8125	15.119	18.190	0.1263
4 7/8"	4.8750	15.315	18.665	0.1296
4 15/16"	4.9375	15.512	19.147	0.1330
5"	5.0000	15.708	19.635	0.1364
5 1/16"	5.0625	15.904	20.129	0.1398
5 1/8"	5.1250	16.101	20.629	0.1433
5 3/16"	5.1875	16.297	21.135	0.1468
5 1/4"	5.2500	16.493	21.648	0.1503
5 5/16"	5.3125	16.690	22.166	0.1539
5 3/8"	5.3750	16.886	22.691	0.1576
5 7/16"	5.4375	17.082	23.221	0.1613
5 1/2"	5.5000	17.279	23.758	0.1650
5 9/16"	5.5625	17.475	24.301	0.1688
5 5/8"	5.6250	17.671	24.851	0.1726
5 11/16"	5.6875	17.868	25.406	0.1764
5 3/4"	5.7500	18.064	25.967	0.1803
5 13/16"	5.8125	18.261	26.535	0.1843
5 7/8"	5.8750	18.457	27.109	0.1883
5 15/16"	5.9375	18.653	27.688	0.1923
6"	6.0000	18.850	28.274	0.1963
6 1/8"	6.1250	19.242	29.465	0.2046
6 1/4"	6.2500	19.649	30.680	0.2131
6 3/8"	6.3750	20.028	31.919	0.2217
6 1/2"	6.5000	20.420	33.183	0.2304
6 5/8"	6.6250	20.813	34.472	0.2394
6 3/4"	6.7500	21.206	35.785	0.2485
6 7/8"	6.8750	21.598	37.122	0.2578
7"	7.0000	21.991	38.485	0.2673
7 1/8"	7.1250	22.384	39.871	0.2769
7 1/4"	7.2500	22.777	41.283	0.2867
7 3/8"	7.3750	23.169	42.718	0.2967
7 1/2"	7.5000	23.562	44.179	0.3068
7 5/8"	7.6250	23.955	45.664	0.3171

TABLE B.1 (Continued)
Areas and Circumferences of Circles and Drill Sizes

Drill Size	Diameter (in.)	Circumference (in.)	Area (in.)	Area (ft)
7 3/4"	7.7500	24.347	47.173	0.3276
7 7/8"	7.8750	24.740	48.707	0.3382
8"	8.0000	25.133	50.266	0.3491
8 1/8"	8.1250	25.525	51.849	0.3601
8 1/4"	8.2500	25.918	53.456	0.3712
8 3/8"	8.3750	26.301	55.088	0.3826
8 1/2"	8.5000	26.704	56.745	0.3941
8 5/8"	8.6250	27.096	58.426	0.4057
8 3/4"	8.7500	27.489	60.132	0.4176
8 7/8"	8.8750	27.882	61.862	0.4296
9"	9.0000	28.274	63.617	0.4418
9 1/8"	9.1250	28.667	65.397	0.4541
9 1/4"	9.2500	29.060	67.201	0.4667
9 3/8"	9.3750	29.452	69.029	0.4794
9 1/2"	9.5000	29.845	70.882	0.4922
9 5/8"	9.6250	30.238	72.760	0.5053
9 3/4"	9.7500	30.631	74.662	0.5185
9 7/8"	9.8750	31.023	76.589	0.5319
10"	10.0000	31.416	78.540	0.5454
10 1/8"	10.1250	31.809	80.516	0.5591
10 1/4"	10.2500	32.201	82.516	0.5730
10 3/8"	10.3750	32.594	84.541	0.5871
10 1/2"	10.5000	32.987	86.590	0.6013
10 5/8"	10.6250	33.379	88.664	0.6157
10 3/4"	10.7500	33.772	90.763	0.6303
10 7/8"	10.8750	34.165	92.886	0.6450
11"	11.0000	34.558	95.033	0.6600
11 1/8"	11.1250	34.950	97.205	0.6750
11 1/4"	11.2500	35.343	99.402	0.6903
11 3/8"	11.3750	35.736	101.6	0.7056
11 1/2"	11.5000	36.128	103.9	0.7213
11 5/8"	11.6250	36.521	106.1	0.7371
11 3/4"	11.7500	36.914	108.4	0.7530
11 7/8"	11.8750	37.306	110.8	0.7691
12"	12.0000	37.699	113.1	0.7854
12 1/4"	12.2500	38.485	117.9	0.819
12 1/2"	12.5000	39.269	122.7	0.851
12 3/4"	12.7500	40.055	127.7	0.886
13"	13.0000	40.841	132.7	0.921
13 1/4"	13.2500	41.626	137.9	0.957
13 1/2"	13.5000	42.412	143.1	0.995
13 3/4"	13.7500	43.197	148.5	1.031
14"	14.0000	43.982	153.9	1.069
14 1/4"	14.2500	44.768	159.5	1.109

TABLE B.1 (Continued)
Areas and Circumferences of Circles and Drill Sizes

Drill Size	Diameter (in.)	Circumference (in.)	Area (in.)	Area (ft)
14 1/2"	14.5000	45.553	165.1	1.149
14 3/4"	14.7500	46.339	170.9	1.185
15"	15.0000	47.124	176.7	1.228
15 1/4"	15.2500	47.909	182.7	1.269
15 1/2"	15.5000	48.695	188.7	1.309
15 3/4"	15.7500	49.480	194.8	1.352
16"	16.0000	50.266	201.1	1.398
16 1/4"	16.2500	51.051	207.4	1.440
16 1/2"	16.5000	51.836	213.8	1.485
16 3/4"	16.7500	52.622	220.4	1.531
17"	17.0000	53.407	227.0	1.578
17 1/4"	17.2500	54.193	233.7	1.619
17 1/2"	17.5000	54.978	240.5	1.673
17 3/4"	17.7500	55.763	247.5	1.719
18"	18.0000	56.548	254.5	1.769
18 1/4"	18.2500	57.334	261.6	1.816
18 1/2"	18.5000	58.120	268.8	1.869
18 3/4"	18.7500	58.905	276.1	1.920
19"	19.0000	59.690	283.5	1.969
19 1/4"	19.2500	60.476	291.0	2.022
19 1/2"	19.5000	61.261	298.7	2.075
19 3/4"	19.7500	62.047	306.4	2.125
20"	20.0000	62.832	314.2	2.182
20 1/4"	20.2500	63.617	322.1	2.237
20 1/2"	20.5000	64.403	330.1	2.292
20 3/4"	20.7500	65.188	338.2	2.348
21"	21.0000	65.974	346.4	2.405
21 1/4"	21.2500	66.759	354.7	2.463
21 1/2"	21.5000	67.544	363.1	2.521
21 3/4"	21.7500	68.330	371.5	2.580
22"	22.0000	69.115	380.1	2.640
22 1/4"	22.2500	69.901	388.8	2.700
22 1/2"	22.5000	70.686	397.6	2.761
22 3/4"	22.7500	71.471	406.5	2.823
23"	23.0000	72.257	415.5	2.885
23 1/4"	23.2500	73.042	424.6	2.948
23 1/2"	23.5000	73.828	433.7	3.012
23 3/4"	23.7500	74.613	443.0	3.076
24"	24.0000	75.398	452.4	3.142
24 1/4"	24.2500	76.184	461.9	3.207
24 1/2"	24.5000	76.969	471.4	3.274
24 3/4"	24.7500	77.755	481.1	3.341
25"	25.0000	78.540	490.9	3.409
25 1/4"	25.2500	79.325	500.7	3.477

TABLE B.1 (Continued)
Areas and Circumferences of Circles and Drill Sizes

Drill Size	Diameter (in.)	Circumference (in.)	Area (in.)	Area (ft)
25 1/2"	25.5000	80.111	510.7	3.547
25 3/4"	25.7500	80.896	520.8	3.616
26"	26.0000	81.682	530.9	3.687
26 1/4"	26.2500	82.467	541.2	3.758
26 1/2"	26.5000	83.252	551.6	3.830
26 3/4"	26.7500	84.038	562.0	3.903
27"	27.0000	84.823	572.6	3.976
27 1/4"	27.2500	85.609	583.2	4.050
27 1/2"	27.5000	86.394	594.0	4.125
27 3/4"	27.7500	87.179	604.8	4.200
28"	28.0000	87.965	615.8	4.276
28 1/4"	28.2500	88.750	626.8	4.353
28 1/2"	28.5000	89.536	637.9	4.430
28 3/4"	28.7500	90.321	649.2	4.508
29"	29.0000	91.106	660.5	4.587
29 1/4"	29.2500	91.892	672.0	4.666
29 1/2"	29.5000	92.677	683.5	4.746
29 3/4"	29.7500	93.463	695.1	4.827
30"	30.0000	94.248	706.9	4.909
31"	31.0000	97.390	754.8	5.241
32"	32.0000	100.53	804.3	5.585
33"	33.0000	103.67	855.3	5.940
34"	34.0000	106.81	907.9	6.305
35"	35.0000	109.96	962.1	6.681
36"	36.0000	113.10	1017.9	7.069
37"	37.0000	116.24	1075.2	7.467
38"	38.0000	119.38	1134.1	7.876
39"	39.0000	122.52	1194.6	8.296
40"	40.0000	125.66	1256.6	8.727
41"	41.0000	128.81	1320.3	9.168
42"	42.0000	131.95	1385.4	9.621
43"	43.0000	135.09	1452.2	10.08
44"	44.0000	138.23	1520.5	10.56
45"	45.0000	141.37	1590.4	11.04
46"	46.0000	144.51	1661.9	11.54
47"	47.0000	147.66	1734.9	12.04
48"	48.0000	150.80	1809.6	12.57
49"	49.0000	153.94	1885.7	13.10
50"	50.0000	157.08	1963.5	13.64

TABLE B.2
Physical Properties of Pipe

Nominal Pipe Size, OD, in.	Schedule Number			Wall Thick- ness, in.	I.D., in.	Inside Area, sq. in.	Metal Area, sq. in.	Sq. Ft. Outside Surface, per ft	Sq. Ft. Inside Surface, per ft	Weight per ft, lb	Weight of Water per ft, lb	Moment of Inertia, in. ⁴	Section Modulus, in. ³	Radius Gyration, in.
	a	b	c											
1/8 0.405	10S	0.049	0.307	0.0740	0.0548	0.106	0.0804	0.186	0.0321	0.00088	0.00437	0.1271
	40	Std	40S	0.068	0.269	0.0568	0.0720	0.106	0.0705	0.245	0.0246	0.00106	0.00525	0.1215
	80	XS	80S	0.095	0.215	0.0364	0.0925	0.106	0.0563	0.315	0.0157	0.00122	0.00600	0.1146
1/4 0.540	10S	0.065	0.410	0.1320	0.0970	0.141	0.1073	0.330	0.0572	0.00279	0.01032	0.1694
	40	Std	40S	0.088	0.364	0.1041	0.1250	0.141	0.0955	0.425	0.0451	0.00331	0.01230	0.1628
	80	XS	80S	0.119	0.302	0.0716	0.1574	0.141	0.0794	0.535	0.0310	0.00378	0.01395	0.1547
3/8 0.675	10S	0.065	0.545	0.2333	0.1246	0.177	0.1427	0.423	0.1011	0.00586	0.01737	0.2169
	40	Std	40S	0.091	0.493	0.1910	0.1670	0.177	0.1295	0.568	0.0827	0.00730	0.02160	0.2090
	80	XS	80S	0.126	0.423	0.1405	0.2173	0.177	0.1106	0.739	0.0609	0.00862	0.02554	0.1991
1/2 0.840	10S	0.083	0.674	0.3570	0.1974	0.220	0.1765	0.671	0.1547	0.01431	0.0341	0.2692
	40	Std	40S	0.109	0.622	0.3040	0.2503	0.220	0.1628	0.851	0.1316	0.01710	0.0407	0.2613
	80	XS	80S	0.147	0.546	0.2340	0.3200	0.220	0.1433	1.088	0.1013	0.02010	0.0478	0.2505
	160	0.187	0.466	0.1706	0.3830	0.220	0.1220	1.304	0.0740	0.02213	0.0527	0.2402
	...	XXS	...	0.294	0.252	0.0499	0.5040	0.220	0.0660	1.714	0.0216	0.02425	0.0577	0.2192
3/4 1.050	5S	0.065	0.920	0.6650	0.2011	0.275	0.2409	0.684	0.2882	0.02451	0.0467	0.349
	10S	0.083	0.884	0.6140	0.2521	0.275	0.2314	0.857	0.2661	0.02970	0.0566	0.343
	40	Std	40S	0.113	0.824	0.5330	0.3330	0.275	0.2157	1.131	0.2301	0.0370	0.0706	0.334
	80	XS	80S	0.154	0.742	0.4320	0.4350	0.275	0.1943	1.474	0.1875	0.0448	0.0853	0.321
	160	0.218	0.614	0.2961	0.5700	0.275	0.1607	1.937	0.1284	0.0527	0.1004	0.304
	...	XXS	...	0.308	0.434	0.1479	0.7180	0.275	0.1137	2.441	0.0641	0.0579	0.1104	0.284

	5S	0.065	1.185	1.1030	0.2553	0.344	0.3100	0.868	0.478	0.0500	0.0760	0.443
	10S	0.109	1.097	0.9450	0.4130	0.344	0.2872	1.404	0.409	0.0757	0.1151	0.428
1	40	Std	40S	0.133	1.049	0.8640	0.4940	0.344	0.2746	1.679	0.374	0.0874	0.1329	0.421
1.315	80	XS	80S	0.179	0.957	0.7190	0.6390	0.344	0.2520	2.172	0.311	0.1056	0.1606	0.407
	160	0.250	0.815	0.5220	0.8360	0.344	0.2134	2.844	0.2261	0.1252	0.1903	0.387
	...	XXS	...	0.358	0.599	0.2818	1.0760	0.344	0.1570	3.659	0.1221	0.1405	0.2137	0.361
	5S	0.065	1.530	1.839	0.326	0.434	0.401	1.107	0.797	0.1038	0.1250	0.564
	10S	0.109	1.442	1.633	0.531	0.434	0.378	1.805	0.707	0.1605	0.1934	0.550
1-1/4	40	Std	40S	0.140	1.380	1.496	0.669	0.434	0.361	2.273	0.648	0.1948	0.2346	0.540
1.660	80	XS	80S	0.191	1.278	1.283	0.881	0.434	0.335	2.997	0.555	0.2418	0.2913	0.524
	160	0.250	1.160	1.057	1.107	0.434	0.304	3.765	0.458	0.2839	0.342	0.506
	...	XXS	...	0.382	0.896	0.631	1.534	0.434	0.2346	5.214	0.2732	0.341	0.411	0.472
	5S	0.065	1.770	2.461	0.375	0.497	0.463	1.274	1.067	0.1580	0.1663	0.649
	10S	0.109	1.682	2.222	0.613	0.497	0.440	2.085	0.962	0.2469	0.2599	0.634
1-1/2	40	Std	40S	0.145	1.610	2.036	0.799	0.497	0.421	2.718	0.882	0.310	0.326	0.623
1.900	80	XS	80S	0.200	1.500	1.767	1.068	0.497	0.393	3.631	0.765	0.391	0.412	0.605
	160	0.281	1.338	1.406	1.429	0.497	0.350	4.859	0.608	0.483	0.508	0.581
	...	XXS	...	0.400	1.100	0.950	1.885	0.497	0.288	6.408	0.412	0.568	0.598	0.549
	5S	0.065	2.245	3.960	0.472	0.622	0.588	1.604	1.716	0.315	0.2652	0.817
	10S	0.109	2.157	3.650	0.776	0.622	0.565	2.638	1.582	0.499	0.420	0.802
2	40	Std	40S	0.154	2.067	3.360	1.075	0.622	0.541	3.653	1.455	0.666	0.561	0.787
2.375	80	XS	80S	0.218	1.939	2.953	1.477	0.622	0.508	5.022	1.280	0.868	0.731	0.766
	160	0.343	1.689	2.240	2.190	0.622	0.442	7.444	0.971	1.163	0.979	0.729
	...	XXS	...	0.436	1.503	1.774	2.656	0.622	0.393	9.029	0.769	1.312	1.104	0.703
	5S	0.083	2.709	5.76	0.728	0.753	0.709	2.475	2.499	0.710	0.494	0.988
	10S	0.120	2.635	5.45	1.039	0.753	0.690	3.531	2.361	0.988	0.687	0.975
2-1/2	40	Std	40S	0.203	2.469	4.79	1.704	0.753	0.646	5.793	2.076	1.530	1.064	0.947
2.875	80	XS	80S	0.276	2.323	4.24	2.254	0.753	0.608	7.661	1.837	0.193	1.339	0.924
	160	0.375	2.125	3.55	2.945	0.753	0.556	10.01	1.535	2.353	1.637	0.894
	...	XXS	...	0.552	1.771	2.46	4.030	0.753	0.464	13.70	1.067	2.872	1.998	0.844

TABLE B.2 (Continued)
Physical Properties of Pipe

Nominal Pipe Size, OD, in.	Schedule Number			Wall Thick- ness, in.	I.D., in.	Inside Area, sq. in.	Metal Area, sq. in.	Sq. Ft. Outside Surface, per ft	Sq. Ft. Inside Surface, per ft	Weight per ft, lb	Weight of Water per ft, lb	Moment of Inertia, in. ⁴	Section Modulus, in. ³	Radius Gyration, in.
	a	b	c											
3 3.500	5S	0.083	3.334	8.73	0.891	0.916	0.873	3.03	3.78	1.301	0.744	1.208
	10S	0.120	3.260	8.35	1.274	0.916	0.853	4.33	3.61	1.822	1.041	1.196
	40	Std	40S	0.216	3.068	7.39	2.228	0.916	0.803	7.58	3.20	3.02	1.724	1.164
	80	XS	80S	0.300	2.900	6.61	3.020	0.916	0.759	10.25	2.864	3.90	2.226	1.136
	160	0.437	2.626	5.42	4.210	0.916	0.687	14.32	2.348	5.03	2.876	1.094
...	XXS	...	0.600	2.300	4.15	5.470	0.916	0.602	18.58	1.801	5.99	3.43	1.047	
3-1/2 4.000	5S	0.083	3.834	11.55	1.021	1.047	1.004	3.47	5.01	1.960	0.980	1.385
	10S	0.120	3.760	11.10	1.463	1.047	0.984	4.97	4.81	2.756	1.378	1.372
	40	Std	40S	0.226	3.548	9.89	2.68	1.047	0.929	9.11	4.28	4.79	2.394	1.337
	80	XS	80S	0.318	3.364	8.89	3.68	1.047	0.881	12.51	3.85	6.28	3.14	1.307
4 4.500	5S	0.083	4.334	14.75	1.152	1.178	1.135	3.92	6.40	2.811	1.249	1.562
	10S	0.120	4.260	14.25	1.651	1.178	1.115	5.61	6.17	3.96	1.762	1.549
	40	Std	40S	0.237	4.026	12.73	3.17	1.178	1.054	10.79	5.51	7.23	3.21	1.510
	80	XS	80S	0.337	3.826	11.50	4.41	1.178	1.002	14.98	4.98	9.61	4.27	1.477
	120	0.437	3.626	10.33	5.58	1.178	0.949	18.96	4.48	11.65	5.18	1.445
	160	0.531	3.438	9.28	6.62	1.178	0.900	22.51	4.02	13.27	5.90	1.416
...	XXS	...	0.674	3.152	7.80	8.10	1.178	0.825	27.54	3.38	15.29	6.79	1.374	
5 5.563	5S	0.109	5.345	22.44	1.868	1.456	1.399	6.35	9.73	6.95	2.498	1.929
	10S	0.134	5.295	22.02	2.285	1.456	1.386	7.77	9.53	8.43	3.03	1.920
	40	Std	40S	0.258	5.047	20.01	4.30	1.456	1.321	14.62	8.66	15.17	5.45	1.878
	80	XS	80S	0.375	4.813	18.19	6.11	1.456	1.260	20.78	7.89	20.68	7.43	1.839
	120	0.500	4.563	16.35	7.95	1.456	1.195	27.04	7.09	25.74	9.25	1.799
	160	0.625	4.313	14.61	9.70	1.456	1.129	32.96	6.33	30	10.8	1.760
...	XXS	...	0.750	4.063	12.97	11.34	1.456	1.064	38.55	5.62	33.6	12.1	1.722	

	5S	0.109	6.407	32.20	2.231	1.734	1.677	5.37	13.98	11.85	3.58	2.304
	10S	0.134	6.357	31.70	2.733	1.734	1.664	9.29	13.74	14.4	4.35	2.295
6	40	Std	40S	0.280	6.065	28.89	5.58	1.734	1.588	18.97	12.51	28.14	8.5	2.245
6.625	80	XS	80S	0.432	5.761	26.07	8.40	1.734	1.508	28.57	11.29	40.5	12.23	2.195
	120	0.562	5.501	23.77	10.70	1.734	1.440	36.39	10.30	49.6	14.98	2.153
	160	0.718	5.189	21.15	13.33	1.734	1.358	45.30	9.16	59	17.81	2.104
	...	XXS	...	0.864	4.897	18.83	15.64	1.734	1.282	53.16	8.17	66.3	20.03	2.060
	5S	0.109	8.407	55.5	2.916	2.258	2.201	9.91	24.07	26.45	6.13	3.01
	10S	0.148	8.329	54.5	3.94	2.258	2.180	13.40	23.59	35.4	8.21	3.00
	20	0.250	8.125	51.8	6.58	2.258	2.127	22.36	22.48	57.7	13.39	2.962
	30	0.277	8.071	51.2	7.26	2.258	2.113	24.70	22.18	63.4	14.69	2.953
8	40	Std	40S	0.322	7.981	50.0	8.40	2.258	2.089	28.55	21.69	72.5	16.81	2.938
8.625	60	0.406	7.813	47.9	10.48	2.258	2.045	35.64	20.79	88.8	20.58	2.909
	80	XS	80S	0.500	7.625	45.7	12.76	2.258	1.996	43.39	19.80	105.7	24.52	2.878
	100	0.593	7.439	43.5	14.96	2.258	1.948	50.87	18.84	121.4	28.14	2.847
	120	0.718	7.189	40.6	17.84	2.258	1.882	60.63	17.60	140.6	32.6	2.807
	140	0.812	7.001	38.5	19.93	2.258	1.833	67.76	16.69	153.8	35.7	2.777
	...	XXS	...	0.875	6.875	37.1	21.30	2.258	1.800	72.42	16.09	162	37.6	2.757
	160	0.906	6.813	36.5	21.97	2.258	1.784	74.69	15.80	165.9	38.5	2.748
	5S	0.134	10.482	86.3	4.52	2.815	2.744	15.15	37.4	63.7	11.85	3.75
	10S	0.165	10.420	85.3	5.49	2.815	2.728	18.70	36.9	76.9	14.3	3.74
	20	0.250	10.250	82.5	8.26	2.815	2.683	28.04	35.8	113.7	21.16	3.71
	0.279	10.192	81.6	9.18	2.815	2.668	31.20	35.3	125.9	23.42	3.70
	30	0.307	10.136	80.7	10.07	2.815	2.654	34.24	35.0	137.5	25.57	3.69
10	40	Std	40S	0.365	10.020	78.9	11.91	2.815	2.623	40.48	34.1	160.8	29.9	3.67
10.750	60	XS	80S	0.500	9.750	74.7	16.10	2.815	2.553	54.74	32.3	212	39.4	3.63
	80	0.593	9.564	71.8	18.92	2.815	2.504	64.33	31.1	244.9	45.6	3.60
	100	0.718	9.314	68.1	22.63	2.815	2.438	76.93	29.5	286.2	53.2	3.56
	120	0.843	9.064	64.5	26.24	2.815	2.373	89.20	28.0	324	60.3	3.52
	140	1.000	8.750	60.1	30.6	2.815	2.291	104.13	26.1	368	68.4	3.47
	160	1.125	8.500	56.7	34.0	2.815	2.225	115.65	24.6	399	74.3	3.43

TABLE B.2 (Continued)
Physical Properties of Pipe

Nominal Pipe Size, OD, in.	Schedule Number			Wall Thick- ness, in.	I.D., in.	Inside Area, sq. in.	Metal Area, sq. in.	Sq. Ft. Outside Surface, per ft	Sq. Ft. Inside Surface, per ft	Weight per ft, lb	Weight of Water per ft, lb	Moment of Inertia, in. ⁴	Section Modulus, in. ³	Radius Gyration, in.	
	a	b	c												
12 12.750	5S	0.165	12.420	121.2	6.52	3.34	3.25	19.56	52.5	129.2	20.27	4.45	
	10S	0.180	12.390	120.6	7.11	3.34	3.24	24.20	52.2	140.5	22.03	4.44	
	20	0.250	12.250	117.9	9.84	3.34	3.21	33.38	51.1	191.9	30.1	4.42	
	30	0.330	12.090	114.8	12.88	3.34	3.17	43.77	49.7	248.5	39.0	4.39	
	...	Std	40S	0.375	12.000	113.1	14.58	3.34	3.14	49.56	49.0	279.3	43.8	4.38	
	40	0.406	11.938	111.9	15.74	3.34	3.13	53.53	48.5	300	47.1	4.37	
	...	XS	80S	0.500	11.750	108.4	19.24	3.34	3.08	65.42	47.0	362	56.7	4.33	
	60	0.562	11.626	106.2	21.52	3.34	3.04	73.16	46.0	401	62.8	4.31	
	80	0.687	11.376	101.6	26.04	3.34	2.978	88.51	44.0	475	74.5	4.27	
	100	0.843	11.064	96.1	31.5	3.34	2.897	107.20	41.6	562	88.1	4.22	
	120	1.000	10.750	90.8	36.9	3.34	2.814	125.49	39.3	642	100.7	4.17	
	140	1.125	10.500	86.6	41.1	3.34	2.749	139.68	37.5	701	109.9	4.13	
	160	1.312	10.126	80.5	47.1	3.34	2.651	160.27	34.9	781	122.6	4.07	
	14 14.000	10	0.250	13.500	143.1	10.80	3.67	3.53	36.71	62.1	255.4	36.5	4.86
		20	0.312	13.376	140.5	13.42	3.67	3.5	45.68	60.9	314	44.9	4.84
		30	Std	...	0.375	13.250	137.9	16.05	3.67	3.47	54.57	59.7	373	53.3	4.82
40		0.437	13.126	135.3	18.62	3.67	3.44	63.37	58.7	429	61.2	4.80	
...		XS	...	0.500	13.000	132.7	21.21	3.67	3.4	72.09	57.5	484	69.1	4.78	
...		0.562	12.876	130.2	23.73	3.67	3.37	80.66	56.5	537	76.7	4.76	
60		0.593	12.814	129.0	24.98	3.67	3.35	84.91	55.9	562	80.3	4.74	
...		0.625	12.750	127.7	26.26	3.67	3.34	89.28	55.3	589	84.1	4.73	
...		0.687	12.626	125.2	28.73	3.67	3.31	97.68	54.3	638	91.2	4.71	
80		0.750	12.500	122.7	31.2	3.67	3.27	106.13	53.2	687	98.2	4.69	
...		0.875	12.250	117.9	36.1	3.67	3.21	122.66	51.1	781	111.5	4.65	
100		0.937	12.126	115.5	38.5	3.67	3.17	130.73	50.0	825	117.8	4.63	
120		1.093	11.814	109.6	44.3	3.67	3.09	150.67	47.5	930	132.8	4.58	
140		1.250	11.500	103.9	50.1	3.67	3.01	170.22	45.0	1127	146.8	4.53	
160		1.406	11.188	98.3	55.6	3.67	2.929	189.12	42.6	1017	159.6	4.48	

	10	0.250	15.500	188.7	12.37	4.19	4.06	42.05	81.8	384	48	5.57
	20	0.312	15.376	185.7	15.38	4.19	4.03	52.36	80.5	473	59.2	5.55
	30	Std	...	0.375	15.250	182.6	18.41	4.19	3.99	62.58	79.1	562	70.3	5.53
	0.437	15.126	179.7	21.37	4.19	3.96	72.64	77.9	648	80.9	5.50
	40	XS	...	0.500	15.000	176.7	24.35	4.19	3.93	82.77	76.5	732	91.5	5.48
	0.562	14.876	173.8	27.26	4.19	3.89	92.66	75.4	813	106.6	5.46
	0.625	14.750	170.9	30.2	4.19	3.86	102.63	74.1	894	112.2	5.44
16	60	0.656	14.688	169.4	31.6	4.19	3.85	107.50	73.4	933	116.6	5.43
16.000	0.687	14.626	168.0	33.0	4.19	3.83	112.36	72.7	971	121.4	5.42
	0.750	14.500	165.1	35.9	4.19	3.8	122.15	71.5	1047	130.9	5.40
	80	0.842	14.314	160.9	40.1	4.19	3.75	136.46	69.7	1157	144.6	5.37
	0.875	14.250	159.5	41.6	4.19	3.73	141.35	69.1	1193	154.1	5.36
	100	1.031	13.938	152.6	48.5	4.19	3.65	164.83	66.1	1365	170.6	5.30
	120	1.218	13.564	144.5	56.6	4.19	3.55	192.29	62.6	1556	194.5	5.24
	140	1.437	13.126	135.3	65.7	4.19	3.44	223.50	58.6	1760	220.0	5.17
	160	1.593	12.814	129.0	72.1	4.19	3.35	245.11	55.9	1894	236.7	5.12
	10	0.250	17.500	240.5	13.94	4.71	4.58	47.39	104.3	549	61.0	6.28
	20	0.312	17.376	237.1	17.34	4.71	4.55	59.03	102.8	678	75.5	6.25
	...	Std	...	0.375	17.250	233.7	20.76	4.71	4.52	70.59	101.2	807	89.6	6.23
	30	0.437	17.126	230.4	24.11	4.71	4.48	82.06	99.9	931	103.4	6.21
	...	XS	...	0.500	17.000	227.0	27.49	4.71	4.45	93.45	98.4	1053	117.0	6.19
	40	0.562	16.876	223.7	30.8	4.71	4.42	104.75	97.0	1172	130.2	6.17
	0.625	16.750	220.5	34.1	4.71	4.39	115.98	95.5	1289	143.3	6.15
18	0.687	16.626	217.1	37.4	4.71	4.35	127.03	94.1	1403	156.3	6.13
18.000	60	0.750	16.500	213.8	40.6	4.71	4.32	138.17	92.7	1515	168.3	6.10
	0.875	16.250	207.4	47.1	4.71	4.25	160.04	89.9	1731	192.8	6.06
	80	0.937	16.126	204.2	50.2	4.71	4.22	170.75	88.5	1834	203.8	6.04
	100	1.156	15.688	193.3	61.2	4.71	4.11	207.96	83.7	2180	242.2	5.97
	120	1.375	15.250	182.6	71.8	4.71	3.99	244.14	79.2	2499	277.6	5.90
	140	1.562	14.876	173.8	80.7	4.71	3.89	274.23	75.3	2750	306	5.84
	160	1.781	14.438	163.7	90.7	4.71	3.78	308.51	71.0	3020	336	5.77

TABLE B.2 (Continued)
Physical Properties of Pipe

Nominal Pipe Size, OD, in.	Schedule Number			Wall Thick- ness, in.	I.D., in.	Inside Area, sq. in.	Metal Area, sq. in.	Sq. Ft. Outside Surface, per ft	Sq. Ft. Inside Surface, per ft	Weight per ft, lb	Weight of Water per ft, lb	Moment of Inertia, in. ⁴	Section Modulus, in. ³	Radius Gyration, in.
	a	b	c											
20 20.000	10	0.250	19.500	298.6	15.51	5.24	5.11	52.73	129.5	757	75.7	6.98
	0.312	19.376	294.9	19.30	5.24	5.07	65.40	128.1	935	93.5	6.96
	20	Std	...	0.375	19.250	291.0	23.12	5.24	5.04	78.60	126.0	1114	111.4	6.94
	0.437	19.126	287.3	26.86	5.24	5.01	91.31	124.6	1286	128.6	6.92
	30	XS	...	0.500	19.000	283.5	30.6	5.24	4.97	104.13	122.8	1457	145.7	6.90
	0.562	18.876	279.8	34.3	5.24	4.94	116.67	121.3	1624	162.4	6.88
	40	0.593	18.814	278.0	36.2	5.24	4.93	122.91	120.4	1704	170.4	6.86
	0.625	18.750	276.1	38.0	5.24	4.91	129.33	119.7	1787	178.7	6.85
	0.687	18.626	272.5	41.7	5.24	4.88	141.71	118.1	1946	194.6	6.83
	0.750	18.500	268.8	45.4	5.24	4.84	154.20	116.5	2105	210.5	6.81
	60	0.812	18.376	265.2	48.9	5.24	4.81	166.40	115.0	2257	225.7	6.79
	0.875	18.250	261.6	52.6	5.24	4.78	178.73	113.4	2409	240.9	6.77
	80	1.031	17.938	252.7	61.4	5.24	4.70	208.87	109.4	2772	277.2	6.72
	100	1.281	17.438	238.8	75.3	5.24	4.57	256.10	103.4	3320	332	6.63
	120	1.500	17.000	227.0	87.2	5.24	4.45	296.37	98.3	3760	376	6.56
	140	1.750	16.500	213.8	100.3	5.24	4.32	341.10	92.6	4220	422	6.48
160	1.968	16.064	202.7	111.5	5.24	4.21	379.01	87.9	4590	459	6.41	

	10	0.250	23.500	434	18.65	6.28	6.15	63.41	188.0	1316	109.6	8.40
	0.312	23.376	430	23.20	6.28	6.12	78.93	186.1	1629	135.8	8.38
	20	Std	...	0.375	23.250	425	27.83	6.28	6.09	94.62	183.8	1943	161.9	8.35
	0.437	23.126	420	32.4	6.28	6.05	109.97	182.1	2246	187.4	8.33
	...	XS	...	0.500	23.000	415	36.9	6.28	6.02	125.49	180.1	2550	212.5	8.31
24	30	0.562	22.876	411	41.4	6.28	5.99	140.80	178.1	2840	237.0	8.29
24.000	0.625	22.750	406	45.9	6.28	5.96	156.03	176.2	3140	261.4	8.27
	40	0.687	22.626	402	50.3	6.28	5.92	171.17	174.3	3420	285.2	8.25
	0.750	22.500	398	54.8	6.28	5.89	186.24	172.4	3710	309	8.22
	60	0.968	22.064	382	70.0	6.28	5.78	238.11	165.8	4650	388	8.15
	80	1.218	21.564	365	87.2	6.28	5.65	296.36	158.3	5670	473	8.07
	100	1.531	20.938	344	108.1	6.28	5.48	367.40	149.3	6850	571	7.96
	120	1.812	20.376	326	126.3	6.28	5.33	429.39	141.4	7830	652	7.87
	140	2.062	19.876	310	142.1	6.28	5.20	483.13	134.5	8630	719	7.79
	160	2.343	19.314	293	159.4	6.28	5.06	541.94	127.0	9460	788	7.70
	10	0.312	29.376	678	29.1	7.85	7.69	98.93	293.8	3210	214	10.50
30	20	0.500	29.000	661	46.3	7.85	7.59	157.53	286.3	5040	336	10.43
30.000	30	0.625	28.750	649	57.6	7.85	7.53	196.08	281.5	6220	415	10.39

a = ASA B36.10 Steel-pipe schedule numbers

b = ASA B36.10 Steel-pipe nominal wall-thickness designations

c = ASA B36.19 Stainless-steel-pipe schedule numbers

TABLE B.3
Physical Properties of Tubing*

The following table gives dimensional data and weights of copper tubing used for automotive, plumbing, refrigeration, and heat exchanger services. For additional data see the standards handbooks of the Copper Development Association, Inc., the ASTM standards, and the "SAE Handbook."

Dimensions in this table are actual specified measurements, subject to accepted tolerances. Trade size designations are usually by actual OD, except for water and drainage tube (plumbing), which measures 1/8-in. larger OD. A 1/2-in. plumbing tube, for example, measures 5/8-in. OD, and a 2-in. plumbing tube measures 2 1/8-in. OD.

KEY TO GAGE SIZES

Standard-gage wall thicknesses are listed by numerical designation (14 to 21), BWG or Stubs gage. These gage sizes are standard for tubular heat exchangers. The letter *A* designates SAE tubing sizes for automotive service. Letter designations *K* and *L* are the common sizes for plumbing services, soft or hard temper.

OTHER MATERIALS

These same dimensional sizes are also common for much of the commercial tubing available in aluminum, mild steel, brass, bronze, and other alloys. Tube weights in this table are based on copper at 0.323 lb/in³. For other materials the weights should be multiplied by the following approximate factors:

aluminum	0.30	monel	0.96
mild steel	0.87	stainless steel	0.89
brass	0.95		

Size, OD		Wall Thickness			Flow Area		Metal Area, in. ²	Surface Area		Weight, lb/ft
in.	mm	in.	mm	gage	in. ²	mm ²		Inside, ft ² /ft	Outside, ft ² /ft	
1/8	3.2	.030	0.76	A	0.003	1.9	0.012	0.017	0.033	0.035
3/16	4.76	.030	0.76	A	0.013	8.4	0.017	0.034	0.049	0.058
1/4	6.4	.030	0.76	A	0.028	18.1	0.021	0.050	0.066	0.080
1/4	6.4	.049	1.24	18	0.018	11.6	0.031	0.038	0.066	0.120
5/16	7.94	.032	0.81	21A	0.048	31.0	0.028	0.065	0.082	0.109
3/8	9.53	.032	0.81	21A	0.076	49.0	0.033	0.081	0.098	0.134
3/8	9.53	.049	1.24	18	0.060	38.7	0.050	0.072	0.098	0.195
1/2	12.7	.032	0.81	21A	0.149	96.1	0.047	0.114	0.131	0.182
1/2	12.7	.035	0.89	20L	0.145	93.6	0.051	0.113	0.131	0.198
1/2	12.7	.049	1.24	18K	0.127	81.9	0.069	0.105	0.131	0.269
1/2	12.7	.065	1.65	16	0.108	69.7	0.089	0.97	0.131	0.344
5/8	15.9	.035	0.89	20A	0.242	156	0.065	0.145	0.164	0.251
5/8	15.9	.040	1.02	L	0.233	150	0.074	0.143	0.164	0.285
5/8	15.9	.049	1.24	18K	0.215	139	0.089	0.138	0.164	0.344
3/4	19.1	.035	0.89	20A	0.363	234	0.079	0.178	0.196	0.305
3/4	19.1	.042	1.07	L	0.348	224	0.103	0.174	0.196	0.362
3/4	19.1	.049	1.24	18K	0.334	215	0.108	0.171	0.196	0.418
3/4	19.1	.065	1.65	16	0.302	195	0.140	0.162	0.196	0.542
3/4	19.1	.083	2.11	14	0.268	173	0.174	0.151	0.196	0.674
7/8	22.2	.045	1.14	L	0.484	312	0.117	0.206	0.229	0.455
7/8	22.2	.065	1.65	16K	0.436	281	0.165	0.195	0.229	0.641
7/8	22.2	.083	2.11	14	0.395	255	0.206	0.186	0.229	0.800
1	25.4	.065	1.65	16	0.594	383	0.181	0.228	0.262	0.740
1	25.4	.083	2.11	14	0.546	352	0.239	0.218	0.262	0.927
1 1/8	28.6	.050	1.27	L	0.825	532	0.176	0.268	0.294	0.655

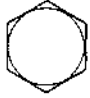
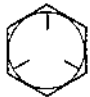
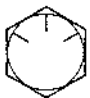

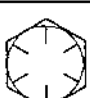
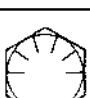
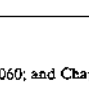
TABLE B.3 (Continued)
Physical Properties of Tubing*

Size, OD		Wall Thickness			Flow Area		Metal Area, in. ²	Surface Area		Weight, lb/ft
in.	mm	in.	mm	gage	in. ²	mm ²		Inside, ft ² /ft	Outside, ft ² /ft	
1 1/8	28.6	.065	1.65	16K	0.778	502	0.216	0.261	0.294	0.839
1 1/4	31.8	.065	1.65	16	0.985	636	0.242	0.293	0.327	0.938
1 1/4	31.8	.083	2.11	14	0.923	596	0.304	0.284	0.327	1.18
1 3/8	34.9	.055	1.40	L	1.257	811	0.228	0.331	0.360	0.884
1 3/8	34.9	.065	1.65	16K	1.217	785	0.267	0.326	0.360	1.04
1 1/2	38.1	.065	1.65	16	1.474	951	0.294	0.359	0.393	1.14
1 1/2	38.7	.083	2.11	14	1.398	902	0.370	0.349	0.393	1.43
1 5/8	41.3	.060	1.52	L	1.779	1148	0.295	0.394	0.425	1.14
1 5/8	41.3	.072	1.83	K	1.722	1111	0.351	0.388	0.425	1.36
2	50.8	.083	2.11	14	2.642	1705	0.500	0.480	0.628	1.94
2	50.8	.109	2.76	12	2.494	1609	0.620	0.466	0.628	2.51
2 1/8	54.0	.070	1.78	L	3.095	1997	0.449	0.520	0.556	1.75
2 1/8	54.0	.083	2.11	14K	3.016	1946	0.529	0.513	0.556	2.06
2 5/8	66.7	.080	2.03	L	4.77	3078	0.645	0.645	0.687	2.48
2 5/8	66.7	.095	2.41	13K	4.66	3007	0.760	0.637	0.687	2.93
3 1/8	79.4	.090	2.29	L	6.81	4394	0.950	0.771	0.818	3.33
3 1/8	79.4	.109	2.77	12K	6.64	4284	1.034	0.761	0.818	4.00
3 5/8	92.1	.100	2.54	L	9.21	5942	1.154	0.897	0.949	4.29
3 5/8	92.1	.120	3.05	11K	9.00	5807	1.341	0.886	0.949	5.12
4 1/8	104.8	.110	2.79	L	11.92	7691	1.387	1.022	1.080	5.38
4 1/8	104.8	.134	3.40	10K	11.61	7491	1.682	1.009	1.080	6.51

* Compiled and computed.

From: *The CRC Handbook of Mechanical Engineering*, CRC Press, Boca Raton, FL, 1998.

TABLE B.4
SAE Grades for Steel Bolts

SAE grade no.	Size range incl.	Proof strength, † kpsi	Tensile strength, † kpsi	Material	Head marking
1	$\frac{1}{4}$ - $1\frac{1}{2}$			Low- or medium-carbon steel	
2	$\frac{1}{2}$ - $1\frac{1}{2}$ $\frac{3}{4}$ - $1\frac{1}{2}$	55 33	74 60		
5	$\frac{1}{4}$ -1 $1\frac{1}{2}$ - $1\frac{1}{2}$	85 74	120 105	Medium-carbon steel, Q & T	
5.2	$\frac{1}{4}$ -1	85	120	Low-carbon martensite steel, Q & T	
7	$\frac{1}{4}$ - $1\frac{1}{2}$	105	133	Medium-carbon alloy steel, Q & T ‡	
8	$\frac{1}{4}$ - $1\frac{1}{2}$	120	150	Medium-carbon alloy steel, Q & T	
8.2	$\frac{1}{4}$ -1	120	150	Low-carbon martensite steel, Q & T	





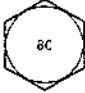




†Minimum values.

‡Roll threaded after heat treatment.

sources: See "Helpful Hints," by Russell, Burdsall & Ward Corp., Mentor, Ohio 44060; and Chap. 23.

From: The CRC Press Handbook of Mechanical Engineering, CRC Press, Boca Raton, FL, 1998.

TABLE B.5
ASTM Grades for Steel Bolts




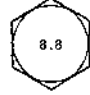



ASTM designation	Size range incl.	Proof strength, † kpsi	Tensile strength, † kpsi	Material	Head marking
A307	$\frac{1}{2}$ to 4			Low-carbon steel	
A325 type 1	$\frac{1}{2}$ to 1	85	120	Medium-carbon steel, Q & T	
	$1\frac{1}{8}$ to $1\frac{1}{2}$	74	105		
A325 type 2	$\frac{1}{2}$ to 1	85	120	Low-carbon martensite steel, Q & T	
	$1\frac{1}{8}$ to $1\frac{1}{2}$	74	105		
A325 type 3	$\frac{1}{2}$ to 1	85	120	Weathering steel, Q & T	
	$1\frac{1}{8}$ to $1\frac{1}{2}$	74	105		
A354 grade BC				Alloy steel, Q & T	
A354 grade BD	$\frac{1}{2}$ to 4	120	150	Alloy steel, Q & T	
A449	$\frac{1}{2}$ to 1	85	120	Medium-carbon steel, Q & T	
	$1\frac{1}{8}$ to $1\frac{1}{2}$	74	105		
	$1\frac{1}{2}$ to 3	55	90		
A490 type 1	$\frac{1}{2}$ to $1\frac{1}{2}$	120	150	Alloy steel, Q & T	
A490 type 3				Weathering steel, Q & T	

† Minimum value.

Sources: See "Helpful Hints," by Russell, Burdiss & Ward Corp., Mentor, Ohio 44060; and Chapter 23

From: *The CRC Press Handbook of Mechanical Engineering*, CRC Press, Boca Raton, FL, 1998.

TABLE B.6
Properties for Metric Steel Bolts, Screws, and Studs

Property class	Size range incl.	Proof strength, MPa	Tensile strength, MPa	Material	Head marking
4.6	M5–M36	225	400	Low- or medium-carbon steel	
4.8	M1.6–M16	310	420	Low- or medium-carbon steel	
5.8	M5–M24	380	520	Low- or medium-carbon steel	
8.8	M1.6–M36	600	830	Medium-carbon steel, Q & T	
9.8	M1.6–M16	650	900	Medium-carbon steel, Q & T	
10.9	M5–M36	830	1040	Low-carbon martensite steel, Q & T	
12.9	M1.6–M36	970	1220	Alloy steel, Q & T	

sources: "Helpful Hints," by Russell, Burdsall & Waard Corp., Mentor, Ohio 44060; see also Chapter 23 and SAE standard J1199, and ASTM standard F568.

From: The CRC Press Handbook of Mechanical Engineering, CRC Press, Boca Raton, FL, 1998.

Appendix C

Material Properties

TABLE C.1
Alphabetical List of Atomic Weights for Common Elements¹

Name	Symbol	At. No.	Atomic Weight	Footnotes
Actinium	Ac	89	[227]	
Aluminum	Al	13	26.981538(2)	
Americium	Am	95	[243]	
Antimony	Sb	51	121.760(1)	g
Argon	Ar	18	39.948(1)	g r
Arsenic	As	33	74.92160(2)	
Astatine	At	85	[210]	
Barium	Ba	56	137.32(7)	
Berkelium	Bk	97	[247]	
Beryllium	Be	4	9.012182(3)	
Bismuth	Bi	83	208.98038(2)	
Bohrium	Bh	107	[264]	
Boron	B	5	10.811(7)	g m r
Bromine	Br	35	79.904(1)	
Cadmium	Cd	48	112.411(8)	g
Calcium	Ca	20	40.078(4)	g
Californium	Cf	98	[251]	
Carbon	C	6	12.0107(8)	g r
Cerium	Ce	58	140.116(1)	g
Cesium	Cs	55	132.90545(2)	
Chlorine	Cl	17	35.4527(9)	m
Chromium	Cr	24	51.9961(6)	
Cobalt	Co	27	58.933200(9)	
Copper	Cu	29	63.546(3)	r
Curium	Cm	96	[247]	
Dubnium	Db	105	[262]	
Dysprosium	Dy	66	162.59(3)	g
Einsteinium	Es	99	[252]	
Erbium	Er	68	167.26(3)	g
Europium	Eu	63	151.964(1)	g
Fermium	Fm	100	[257]	
Fluorine	F	9	18.9984032(5)	
Francium	Fr	87	[223]	
Gadolinium	Gd	64	157.25(3)	g
Gallium	Ga	31	69.723(1)	
Germanium	Ge	32	72.61(2)	
Gold	Au	79	196.96655(2)	
Hafnium	Hf	72	178.49(2)	
Hassium	Hs	108	[269]	
Helium	He	2	4.002602(2)	g r

TABLE C.1 (Continued)
Alphabetical List of Atomic Weights for Common Elements¹

Name	Symbol	At. No.	Atomic Weight	Footnotes
Holmium	Ho	67	164.93032(2)	
Hydrogen	H	1	1.00794(7)	g m r
Indium	In	49	114.818(3)	
Iodine	I	53	126.90447(3)	
Iridium	Ir	77	192.217(3)	
Iron	Fe	26	55.845(2)	
Krypton	Kr	36	83.80(1)	g m
Lanthanum	La	57	138.9055(2)	g
Lawrencium	Lr	103	[262]	
Lead	Pb	82	207.2(1)	g r
Lithium	Li	3	6.941(2)	g m r
Lutetium	Lu	71	174.967(1)	g
Magnesium	Mg	12	24.3050(6)	
Manganese	Mn	25	54.938049(9)	
Meitnerium	Mt	109	[268]	
Mendelevium	Md	101	[258]	
Mercury	Hg	80	200.59(2)	
Molybdenum	Mo	42	95.94(1)	g
Neodymium	Nd	60	144.24(3)	g
Neon	Ne	10	20.1797(6)	g m
Neptunium	Np	93	[237]	
Nickel	Ni	28	58.6934(2)	
Niobium	Nb	41	92.90638(2)	
Nitrogen	N	7	14.00674(7)	g r
Nobelium	No	102	[259]	
Osmium	Os	76	190.23(3)	g
Oxygen	O	8	15.9994(3)	g r
Palladium	Pd	46	106.42(1)	g
Phosphorus	P	15	30.973761(2)	
Platinum	Pt	78	195.078(2)	
Plutonium	Pu	94	[244]	
Polonium	Po	84	[209]	
Potassium	K	19	39.0983(1)	g
Praseodymium	Pr	59	140.90765(2)	
Promethium	Pm	61	[145]	
Protactinium	Pa	91	231.03588(2)	
Radium	Ra	88	[226]	
Radon	Rn	86	[222]	
Rhenium	Re	75	186.207(1)	
Rhodium	Rh	45	102.90550(2)	
Rubidium	Rb	37	85.4678(3)	g
Ruthenium	Ru	44	101.07(2)	g
Rutherfordium	Rf	104	[261]	
Samarium	Sm	62	150.36(3)	g
Scandium	Sc	21	44.955910(8)	
Seaborgium	Sg	106	[266]	
Selenium	Se	34	78.96(3)	
Silicon	Si	14	28.0855(3)	r

TABLE C.1 (Continued)
Alphabetical List of Atomic Weights for Common Elements¹

Name	Symbol	At. No.	Atomic Weight	Footnotes
Silver	Ag	47	107.8682(2)	g
Sodium	Na	11	22.989770(2)	
Strontium	Sr	38	87.62(1)	g r
Sulfur	S	16	32.066(6)	g r
Tantalum	Ta	73	180.9479(1)	
Technetium	Tc	43	[98]	
Tellurium	Te	52	127.60(3)	g
Terbium	Tb	65	158.92534(2)	
Thallium	Tl	81	204.3833(2)	
Thorium	Th	90	232.0381(1)	g
Thulium	Tm	69	168.93421(2)	
Tin	Sn	50	118.710(7)	g
Titanium	Ti	22	47.867(1)	
Tungsten	W	74	183.84(1)	
Uranium	U	92	238.0289(1)	g m
Vanadium	V	23	50.9415(1)	
Xenon	Xe	54	131.29(2)	g m
Ytterbium	Yb	70	173.04(3)	g
Yttrium	Y	39	88.90585(2)	
Zinc	Zn	30	65.39(2)	
Zirconium	Zr	40	92.224(2)	g

g – geological specimens are known in which the element has an isotopic composition outside the limits for normal material. The difference between the atomic weight of the element in such specimens and that given in the table may exceed the stated uncertainty.

m – modified isotopic compositions may be found in commercially available material because it has been subjected to an undisclosed or inadvertent isotopic fractionation. Substantial deviations in atomic weight of the element from that given the table can occur.

r – range in isotopic composition of normal terrestrial material prevents a more precise atomic weight being given; the tabulated atomic weight value should be applicable to any normal material.

This table of atomic weights is reprinted from the 1995 report of the IUPAC Commission on Atomic Weights and Isotopic Abundances. The Standard Atomic Weights apply to the elements as they exist naturally on Earth, and the uncertainties take into account the isotopic variation found in most laboratory samples. Further comments on the variability are given in the footnotes.

The number in parentheses following the atomic weight value gives the uncertainty in the last digit. An entry in brackets indicates that mass number of the longest-lived isotope of an element that has no stable isotopes and for which a Standard Atomic Weight cannot be defined because of wide variability in isotopic composition (or complete absence) in nature.

REFERENCE

IUPAC Commission on Atomic Weights and Isotopic Abundances, Atomic Weights of the Elements, 1995, *Pure Appl. Chem.*, 68, 2339, 1996.

Source: Courtesy of CRC Press.¹

TABLE C.2
Volumetric Analysis of Typical Gaseous Fuel Mixtures

Fuel Gas Component	Natural Gas				LPG		Refinery Gases (Dry)						Waste Gases	
	Tulsa	Alaska	Netherlands	Algeria	Propane	Butane	Cracked Gas	Coking Gas	Reforming Gas	FCC Gas	Refinery Gas Sample 1	Refinery Gas Sample 2	PSA Gas	Flexicoking Gas
CH ₄	93.4%	99%	81%	87%	—	—	65%	40%	28%	32%	36%	53%	17%	1%
C ₂ H ₄	—	—	—	—	—	—	3%	3%	7%	7%	5%	2%	—	—
C ₂ H ₆	2.7%	—	3%	9%	—	—	16%	21%	28%	9%	18%	19%	—	—
C ₃ H ₆	—	—	—	—	—	—	2%	1%	3%	15%	8%	6%	—	—
C ₃ H ₈	0.6%	—	0.4%	2.7%	100%	—	7%	24%	22%	25%	20%	14%	—	—
C ₄ H ₈	—	—	—	—	—	100%	1%	—	—	—	—	—	—	—
C ₄ H ₁₀	0.2%	—	0.1%	1.1%	—	—	3%	7%	7%	0%	2%	1%	—	—
C ₅ & Higher	—	—	—	—	—	—	1%	—	—	—	—	—	—	—
H ₂	—	—	—	—	—	—	3%	4%	5%	6%	3%	3%	28%	21%
CO	—	—	—	—	—	—	—	—	—	—	—	—	10%	20%
CO ₂	0.7%	—	0.9%	—	—	—	—	—	—	—	—	—	44%	10%
N ₂	2.4%	1%	14%	0%	—	—	—	—	—	7%	8%	3%	<1%	45%
H ₂ O	—	—	—	—	—	—	—	—	—	—	—	—	<1%	3%
O ₂	—	—	—	—	—	—	—	—	—	—	—	—	—	—
H ₂ S	—	—	—	—	—	—	—	—	—	—	—	—	—	—
Total	100%	100%	100%	100%	100%	100%	100%	100%	100%	100%	100%	100%	100%	100%

Data compiled from a variety of sources.

TABLE C.3
Physical Constants of Typical Gaseous Fuel Mixtures

Fuel Gas Component	Natural Gas				LPG		Refinery Gases (Dry)						Waste Gases	
	Tulsa	Alaska	Netherlands	Algeria	Propane	Butane	Cracked Gas	Coking Gas	Reforming Gas	FCC Gas	Refinery Gas Sample 1	Refinery Gas Sample 2	PSA Gas	Flexicoking Gas
Molecular weight	17.16	16.1	18.51	18.49	44.1	58.12	22.76	28.62	30.21	29.18	28.02	24.61	25.68	23.73
Lower heating value (LHV), Btu/SCF	913	905	799	1025	2316	3010	1247	1542	1622	1459	1389	1297	263	131
Higher heating value (HHV), Btu/SCF	1012	1005	886	1133	2517	3262	1369	1686	1769	1587	1515	1421	294	142
Specific gravity (14.696 psia/60°F, Air = 1.0)	0.59	0.56	0.64	0.64	1.53	1.1	0.79	0.99	1.05	1.01	0.97	0.85	0.89	0.82
Wobbe number, HHV/(SG ^{1/2})	1318	1343	1108	1416	2035	3110	1540	1694	1726	1579	1538	1541	312	157
Isentropic coefficient (C _p /C _v)	1.30	1.31	1.31	1.28	1.13	1.10	1.24	1.19	1.19	1.20	1.21	1.23	1.33	1.38
Stoichiometric air required, SCF/MMBtu	10554	10567	10554	10525	10369	10371	10402	10379	10322	10234	10311	10375	9667	8265
Stoichiometric air required, lb _m /MMBtu	805	806	805	803	791	791	794	792	787	781	787	792	738	630
Air required for 15% excess air, SCF/MMBtu	12138	12152	12138	12104	11925	11926	11962	11936	11870	11769	11858	11931	11117	9505
Air required for 15% excess air, lb _m /MMBtu	923	924	923	920	907	907	910	908	903	895	902	907	845	723
Volume of dry combustion products, SCF/MMBtu	10983	10956	11141	10953	10962	10996	10890	10909	10871	10847	10911	10904	11722	13517
Weight of dry combustion products, lb _m /MMBtu	865	862	876	863	870	874	861	864	862	860	864	862	985	1103
Volume of wet combustion products, SCF/MMBtu	13257	13258	13415	13163	12788	12757	12935	12862	12771	12689	12821	12902	14198	15585
Weight of wet combustion products, lb _m /MMBtu	973	971	984	968	957	958	958	957	952	948	864	957	1102	1201
Adiabatic flame temperature, °F	3306	3308	3284	3317	3351	3351	3342	3348	3359	3371	3353	3345	3001	2856

Note: All values calculated using 60°F fuel gas and 60°F, 50% relative humidity combustion air.

TABLE C.4
Physical Constants of Typical Gaseous Fuel Mixture Components

Fuel Gas No.	Component	Chemical Formula	Molecular Weight	Boiling Point 14.696 psia (°F)	Vapor Pressure 100°F (psia)	Specific Heat Capacity, C_p 60°F & 14.696 psia (Btu/lb _m /°F)	Latent Heat of Vaporization 14.696 psia & Boiling Point (Btu/lb _m)	Gas Density, 14.696 psia, 60°F																Theoretical Air Required (lb _m /10,000 Btu)	Flammability Limits (vol% in air mixture)							
								Ideal Gas, 14.696 psia, 60°F								Heating Value																
								Specific Gravity (Air = 1)	Gas Density (lb _m /ft ₃)	Specific Volume (ft ³ /lb _m)	Btu/scf				Btu/lb _m				Unit Volume per Unit Volume of Combustible				Unit Mass per Unit Mass of Combustible									
											LHV (Net)	HHV (Gross)	LHV (Net)	HHV (Gross)	O ₂	N ₂	Air	CO ₂	H ₂ O	N ₂	SO ₂	O ₂	N ₂				Air	CO ₂	H ₂ O	N ₂	SO ₂	
Paraffin (alkane) Series (C_nH_{2n+2})																																
1	Methane	CH ₄	16.04	-258.69	—	0.5266	219.22	0.554	0.042	23.651	912	1,013	21.495	23.845	2.0	7.547	9.547	1.0	2.0	7.547	—	3.989	13.246	17.235	2.743	2.246	13.246	—	7.219	5.0	15.0	1
2	Ethane	C ₂ H ₆	30.07	-127.48	—	0.4097	210.41	1.038	0.079	12.618	1,639	1,792	20.418	22.323	3.5	13.206	16.706	2.0	3.0	13.206	—	3.724	12.367	16.092	2.927	1.797	12.367	—	7.209	2.9	13.0	2
3	Propane	C ₃ H ₈	44.10	-43.67	190	0.3881	183.05	1.522	0.116	8.604	2,385	2,592	19.937	21.669	5.0	18.866	23.866	3.0	4.0	18.866	—	3.628	12.047	15.676	2.994	1.624	12.047	—	7.234	2.1	9.5	3
4	<i>n</i> -Butane	C ₄ H ₁₀	58.12	31.10	51.6	0.3867	165.65	2.007	0.153	6.528	3,113	3,373	19.679	21.321	6.5	24.526	31.026	4.0	5.0	24.526	—	3.578	11.882	15.460	3.029	1.550	11.882	—	7.251	1.8	8.4	4
5	Isobutane	C ₄ H ₁₀	58.12	10.90	72.2	0.3872	157.53	2.007	0.153	6.528	3,105	3,365	19.629	21.271	6.5	24.526	31.026	4.0	5.0	24.526	—	3.578	11.882	15.460	3.029	1.550	11.882	—	7.268	1.8	8.4	5
6	<i>n</i> -Pentane	C ₅ H ₁₂	72.15	96.92	15.57	0.3883	153.59	2.491	0.190	5.259	3,714	4,017	19.507	21.095	8.0	30.186	38.186	5.0	6.0	30.186	—	3.548	11.781	15.329	3.050	1.498	11.781	—	7.267	1.4	8.3	6
7	Isopentane	C ₅ H ₁₂	72.15	82.12	20.44	0.3827	147.13	2.491	0.190	5.259	3,705	4,017	19.459	21.047	8.0	30.186	38.186	5.0	6.0	30.186	—	3.548	11.781	15.329	3.050	1.498	11.781	—	7.283	1.4	8.3	7
8	Neopentane	C ₅ H ₁₂	72.15	49.10	35.9	0.3666	135.58	2.491	0.190	5.259	3,692	3,994	19.390	20.978	8.0	30.186	38.183	5.0	6.0	30.186	—	3.548	11.781	15.329	3.050	1.498	11.781	—	7.307	1.4	8.3	8
9	<i>n</i> -Hexane	C ₆ H ₁₄	86.18	155.72	4.956	0.3664	143.95	2.975	0.227	4.403	4,415	4,767	19.415	20.966	9.5	35.846	45.346	6.0	7.0	35.846	—	3.527	11.713	15.240	3.064	1.463	11.713	—	7.269	1.2	7.7	9
Napthene (cycloalkane) Series (C_nH_{2n})																																
10	Cyclopentane	C ₅ H ₁₀	70.13	120.60	9.917	0.2712	137.35	2.420	0.180	5.556	3,512	3,764	19.005	20.368	7.5	27.939	35.180	5.0	5.0	28.939	—	3.850	11.155	14.793	3.146	1.283	11.155	—	7.262	—	—	10
11	Cyclohexane	C ₆ H ₁₂	84.16	177.40	3.267	0.2901	153.25	2.910	0.220	5.545	4,180	4,482	18.849	20.211	9.0	33.528	42.970	6.0	6.0	33.528	—	4.620	13.386	17.750	3.146	1.283	11.155	—	7.848	1.3	8.4	11
Olefin Series (C_nH_{2n})																																
12	Ethene (Ethylene)	C ₂ H ₄	28.05	-154.62	—	0.3622	207.57	0.969	0.074	13.525	1,512	1,613	20.275	21.636	3.0	11.320	14.320	2.0	2.0	11.320	—	3.422	11.362	14.784	3.138	1.284	11.362	—	6.833	2.7	34.0	12
13	Propene (Propylene)	C ₃ H ₆	42.08	-53.90	226.4	0.3541	188.18	1.453	0.111	9.017	2,185	2,336	19.687	21.048	4.5	16.980	21.480	3.0	3.0	16.980	—	3.422	11.362	14.784	3.138	1.284	11.362	—	7.024	2.0	10.0	13
14	1-Butene (Butylene)	C ₄ H ₈	56.11	20.75	63.05	0.3548	167.94	1.937	0.148	6.762	2,885	3,086	19.493	20.854	6.0	22.640	28.640	4.0	4.0	22.640	—	3.422	11.362	14.784	3.138	1.284	11.362	—	7.089	1.6	9.3	14
15	Isobutene	C ₄ H ₈	56.11	19.59	63.4	0.3701	169.48	1.937	0.148	6.762	2,868	3,069	19.376	20.737	6.0	22.640	28.640	4.0	4.0	22.640	—	3.422	11.362	14.784	3.138	1.284	11.362	—	7.129	1.6	—	15
16	1-Pentene	C ₅ H ₁₀	70.13	85.93	19.115	0.3635	154.46	2.421	0.185	5.410	3,585	3,837	19.359	20.720	7.5	28.300	35.800	5.0	5.0	28.300	—	3.422	11.362	14.784	3.138	1.284	11.362	—	7.135	1.4	8.7	16
Aromatic Series (C_nH_{2n-6})																																
17	Benzene	C ₆ H ₆	78.11	176.17	3.224	0.2429	169.31	2.697	0.206	4.857	3,595	3,746	17.421	18.184	7.5	28.300	35.800	6.0	3.0	28.300	—	3.072	10.201	13.274	3.380	0.692	10.201	—	7.300	1.38	7.98	17
18	Toluene	C ₇ H ₈	92.14	231.13	1.032	0.2598	154.84	3.181	0.243	4.118	4,296	4,497	17.672	18.501	9.0	33.959	42.959	7.0	4.0	33.959	—	3.125	10.378	13.504	3.343	0.782	10.378	—	7.299	1.28	7.18	18
19	<i>o</i> -Xylene	C ₈ H ₁₀	106.17	291.97	0.264	0.2914	149.1	3.665	0.280	3.574	4,970	5,222	17.734	18.633	10.5	39.619	50.119	8.0	5.0	39.619	—	3.164	10.508	13.673	3.316	0.848	10.508	—	7.338	1.18	6.48	19
20	<i>m</i> -Xylene	C ₈ H ₁₀	106.17	282.41	0.326	0.2782	147.2	3.665	0.280	3.574	4,970	5,222	17.734	18.633	10.5	39.619	50.119	8.0	5.0	39.619	—	3.164	10.508	13.673	3.316	0.848	10.508	—	7.338	1.18	6.48	20
21	<i>p</i> -Xylene	C ₈ H ₁₀	106.17	281.05	0.342	0.2769	144.52	3.665	0.280	3.574	4,970	5,222	17.734	18.633	10.5	39.619	50.119	8.0	5.0	39.619	—	3.164	10.508	13.673	3.316	0.848	10.508	—	7.338	1.18	6.48	21

Additional Fuel Gas Components

22 Acetylene	C ₂ H ₂	26.04	-119	—	0.3966	—	0.899	0.069	14.572	1.448	1,499	20,769	21,502	2.5	9.433	11.933	2.0	1.0	9.433	—	3.072	10.201	13.274	3.380	0.692	10.201	—	7.300	2.5	80	22
23 Methyl alcohol	CH ₃ OH	32.04	148.1	4.63	0.3231	473	1.106	0.084	11.841	767	868	9,066	10,258	1.5	5.660	7.160	1.0	2.0	5.660	—	4.498	4.974	6.482	1.373	1.124	4.974	—	6.309	6.72	36.5	23
24 Ethyl alcohol	C ₂ H ₅ OH	46.07	172.92	2.3	0.3323	367	1.590	0.121	8.236	1,449	1,600	11,918	13,161	3.0	11.320	14.320	2.0	3.0	11.320	—	2.084	6.919	9.003	1.911	1.173	6.919	—	6.841	3.28	18.95	24
25 Ammonia	NH ₃	17.03	-28.2	212	0.5002	587.2	0.588	0.045	22.279	364	441	7,966	9,567	0.75	2.830	3.582	—	1.5	3.330	—	1.409	4.679	6.008	—	1.587	5.502	—	6.298	15.50	27.00	25
26 Hydrogen	H ₂	2.02	-423.0	—	3.4080	193.9	0.070	0.005	188.217	274.6	325.0	51,625	61,095	0.5	1.887	2.387	—	1.0	1.887	—	7.936	26.323	34.290	—	8.937	26.353	—	5.613	4.00	74.20	26
27 Oxygen	O ₂	32.00	-297.4	—	0.2186	91.6	1.105	0.084	11.858	—	—	—	—	—	—	—	—	—	—	—	—	—	—	—	—	—	—	—	—	—	27
28 Nitrogen	N ₂	29.16	-320.4	—	0.2482	87.8	0.972	0.074	13.472	—	—	—	—	—	—	—	—	—	—	—	—	—	—	—	—	—	—	—	—	—	28
29 Carbon monoxide	CO	28.01	-313.6	—	0.2484	92.7	0.967	0.074	13.546	321.9	321.9	4,347	4,347	0.5	1.877	2.387	1.0	—	1.887	—	—	1.897	2.468	1.571	—	1.870	—	5.677	12.50	74.20	29
30 Carbon dioxide	CO ₂	44.01	-109.3	—	0.1991	238.2	1.519	0.116	8.621	—	—	—	—	—	—	—	—	—	—	—	—	—	—	—	—	—	—	—	—	—	30
31 Hydrogen sulfide	H ₂ S	34.08	-76.6	394.0	0.2380	235.6	1.177	0.090	11.133	595	646	6,537	7,097	1.5	5.660	7.160	—	1.0	5.660	1.0	1.410	4.682	6.093	—	0.529	4.682	1.880	8.585	4.30	45.50	31
32 Sulfur dioxide	SO ₂	64.06	14.0	88	0.1450	166.7	2.212	0.169	5.923	—	—	—	—	—	—	—	—	—	—	—	—	—	—	—	—	—	—	—	—	—	32
33 Water vapor	H ₂ O	18.02	212.0	0.9492	0.4446	970.3	0.622	0.047	21.061	—	—	—	—	—	—	—	—	—	—	—	—	—	—	—	—	—	—	—	—	—	33
34 Air	—	29.97	-317.6	—	0.2400	92	1.000	0.076	13.099	—	—	—	—	—	—	—	—	—	—	—	—	—	—	—	—	—	—	—	—	—	34

TABLE C.5
Combustion Data for Hydrocarbons*

Hydrocarbon	Formula	Higher heating value (vapor), Btu/lb _m	Theor. air/fuel ratio, by mass	Max flame speed, ft/sec	Adiabatic flame temp (in air), °F	Ignition temp (in air), °F	Flash point, °F	Flammability limits (in air), % by volume	
PARAFFINS OR ALKANES									
Methane	CH ₄	23875	17.195	1.1	3484	1301	gas	5.0	15.0
Ethane	C ₂ H ₆	22323	15.899	1.3	3540	968–1166	gas	3.0	12.5
Propane	C ₃ H ₈	21669	15.246	1.3	3573	871	gas	2.1	10.1
<i>n</i> -Butane	C ₄ H ₁₀	21321	14.984	1.2	3583	761	–76	1.86	8.41
<i>iso</i> -Butane	C ₄ H ₁₀	21271	14.984	1.2	3583	864	–117	1.80	8.44
<i>n</i> -Pentane	C ₅ H ₁₂	21095	15.323	1.3	4050	588	< –40	1.40	7.80
<i>iso</i> -Pentane	C ₅ H ₁₂	21047	15.323	1.2	4055	788	< –60	1.32	9.16
Neopentane	C ₅ H ₁₂	20978	15.323	1.1	4060	842	gas	1.38	7.22
<i>n</i> -Hexane	C ₆ H ₁₄	20966	15.238	1.3	4030	478	–7	1.25	7.0
Neohexane	C ₆ H ₁₄	20931	15.238	1.2	4055	797	–54	1.19	7.58
<i>n</i> -Heptane	C ₇ H ₁₆	20854	15.141	1.3	3985	433	25	1.00	6.00
Triptane	C ₇ H ₁₆	20824	15.141	1.2	4035	849	—	1.08	6.69
<i>n</i> -Octane	C ₈ H ₁₈	20796	15.093	—	—	428	56	0.95	3.20
<i>iso</i> -Octane	C ₈ H ₁₈	20770	15.093	1.1	—	837	10	0.79	5.94
OLEFINS OR ALKENES									
Ethylene	C ₂ H ₄	21636	14.807	2.2	4250	914	gas	2.75	28.6
Propylene	C ₃ H ₆	21048	14.807	1.4	4090	856	gas	2.00	11.1
Butylene	C ₄ H ₈	20854	14.807	1.4	4030	829	gas	1.98	9.65
<i>iso</i> -Butene	C ₄ H ₈	20737	14.807	1.2	—	869	gas	1.8	9.0
<i>n</i> -Pentene	C ₅ H ₁₀	20720	14.807	1.4	4165	569	—	1.65	7.70
AROMATICS									
Benzene	C ₆ H ₆	18184	13.297	1.3	4110	1044	12	1.35	6.65
Toluene	C ₇ H ₈	18501	13.503	1.2	4050	997	40	1.27	6.75
<i>p</i> -Xylene	C ₈ H ₁₀	18663	13.663	—	4010	867	63	1.00	6.00
OTHER HYDROCARBONS									
Acetylene	C ₂ H ₂	21502	13.297	4.6	4770	763–824	gas	2.50	81.0
Naphthalene	C ₁₀ H ₈	17303	12.932	—	4100	959	174	0.90	5.9

* Based largely on: *Gas Engineers' Handbook*, American Gas Association, Inc., Industrial Park, 1967.

REFERENCES

- American Institute of Physics Handbook*, 2nd ed., D.E. Gray, Ed., McGraw-Hill Book Company, NY, 1963.
Chemical Engineer's Handbook, 4th ed., R.H. Perry, C.H. Chilton, and S.D. Kirkpatrick, Eds., McGraw-Hill Book Company, NY, 1963.
Handbook of Chemistry and Physics, 53rd ed., R.C. Weast, Ed., The Chemical Rubber Company, Cleveland, OH, 1972; gives the heat of combustion of 500 organic compounds.
Handbook of Laboratory Safety, 2nd ed., N.V. Steere, Ed., The Chemical Rubber Company, Cleveland, OH, 1971.
Physical Measurements in Gas Dynamics and Combustion, Princeton University Press, 1954.

Note: For heating value in J/kg, multiply the value in Btu/lb_m by 2324. For flame speed in m/s, multiply the value in ft/s by 0.3048.

From: *The CRC Press Handbook of Mechanical Engineering*, CRC Press, Boca Raton, FL, 1998.

TABLE C.6
Thermodynamic Data for Common Substances

\bar{h}_f° and \bar{g}_f° (kJ/kmol), \bar{s}° (kJ/kmol•K)

Substance	Formula	\bar{h}_f°	\bar{g}_f°	\bar{s}°
Carbon	C(s)	0	0	5.74
Hydrogen	H ₂ (g)	0	0	130.57
Nitrogen	N ₂ (g)	0	0	191.50
Oxygen	O ₂ (g)	0	0	205.03
Carbon monoxide	CO(g)	-110,530	-137,150	197.54
Carbon dioxide	CO ₂ (g)	-393,520	-394,380	213.69
Water	H ₂ O(g)	-241,820	-228,590	188.72
	H ₂ O(l)	-285,830	-237,180	69.95
Hydrogen peroxide	H ₂ O ₂ (g)	-136,310	-105,600	232.63
Ammonia	NH ₃ (g)	-46,190	-16,590	192.33
Oxygen	O(g)	249,170	231,770	160.95
Hydrogen	H(g)	218,000	203,290	114.61
Nitrogen	N(g)	472,680	455,510	153.19
Hydroxyl	OH(g)	39,460	34,280	183.75
Methane	CH ₄ (g)	-74,850	-50,790	186.16
Acetylene	C ₂ H ₂ (g)	226,730	209,170	200.85
Ethylene	C ₂ H ₄ (g)	52,280	68,120	219.83
Ethane	C ₂ H ₆ (g)	-84,680	-32,890	229.49
Propylene	C ₃ H ₆ (g)	20,410	62,720	266.94
Propane	C ₃ H ₈ (g)	-103,850	-23,490	269.91
Butane	C ₄ H ₁₀ (g)	-126,150	-15,710	310.03
Pentane	C ₅ H ₁₂ (g)	-146,440	-8200	348.40
Octane	C ₈ H ₁₈ (g)	-208,450	17,320	463.67
	C ₈ H ₁₈ (l)	-249,910	6610	360.79
Benzene	C ₆ H ₆ (g)	82,930	129,660	269.20
Methyl alcohol	CH ₃ OH(g)	-200,890	-162,140	239.70
	CH ₃ OH(l)	-238,810	-166,290	126.80
Ethyl alcohol	C ₂ H ₅ OH(g)	-235,310	-168,570	282.59
	C ₂ H ₅ OH(l)	-277,690	174,890	160.70

Source: Adapted from Wark, K. 1983. *Thermodynamics*, 4th ed. McGraw-Hill, New York, as based on JANAF Thermochemical Tables, NSRDS-NBS-37, 1971; *Selected Values of Chemical Thermodynamic Properties*, NBS Tech. Note 270-3, 1968; and *API Research Project 44*, Carnegie Press, 1953.

From: *The CRC Handbook of Thermal Engineering* CRC Press, Boca Raton, FL, 2000.

TABLE C.7
Properties of Dry Air at Atmospheric Pressure

Symbols and Units:

- K = absolute temperature, degrees Kelvin
- deg C = temperature, degrees Celsius
- deg F = temperature, degrees Fahrenheit
- ρ = density, kg/m³
- c_p = specific heat capacity, kJ/kg·K
- c_p/c_v = specific heat capacity ratio, dimensionless
- μ = viscosity, N·s/m² × 10⁶ (For N·s/m² (= kg/m·s) multiply tabulated values by 10⁻⁶)
- k = thermal conductivity, W/m·k × 10³ (For W/m·K multiply tabulated values by 10⁻³)
- Pr = Prandtl number, dimensionless
- h = enthalpy, kJ/kg
- V_s = sound velocity, m/s

Temperature			Properties							
K	deg C	deg F	ρ	c_p	c_p/c_v	μ	k	Pr	h	V_s
100	-173.15	-280	3.598	1.028		6.929	9.248	.770	98.42	198.4
110	-163.15	-262	3.256	1.022	1.420 2	7.633	10.15	.768	108.7	208.7
120	-153.15	-244	2.975	1.017	1.416 6	8.319	11.05	.766	118.8	218.4
130	-143.15	-226	2.740	1.014	1.413 9	8.990	11.94	.763	129.0	227.6
140	-133.15	-208	2.540	1.012	1.411 9	9.646	12.84	.761	139.1	236.4
150	-123.15	-190	2.367	1.010	1.410 2	10.28	13.73	.758	149.2	245.0
160	-113.15	-172	2.217	1.009	1.408 9	10.91	14.61	.754	159.4	253.2
170	-103.15	-154	2.085	1.008	1.407 9	11.52	15.49	.750	169.4	261.0
180	-93.15	-136	1.968	1.007	1.407 1	12.12	16.37	.746	179.5	268.7
190	-83.15	-118	1.863	1.007	1.406 4	12.71	17.23	.743	189.6	276.2
200	-73.15	-100	1.769	1.006	1.405 7	13.28	18.09	.739	199.7	283.4
205	-68.15	-91	1.726	1.006	1.405 5	13.56	18.52	.738	204.7	286.9
210	-63.15	-82	1.684	1.006	1.405 3	13.85	18.94	.736	209.7	290.5
215	-58.15	-73	1.646	1.006	1.405 0	14.12	19.36	.734	214.8	293.9
220	-53.15	-64	1.607	1.006	1.404 8	14.40	19.78	.732	219.8	297.4
225	-48.15	-55	1.572	1.006	1.404 6	14.67	20.20	.731	224.8	300.8
230	-43.15	-46	1.537	1.006	1.404 4	14.94	20.62	.729	229.8	304.1
235	-38.15	-37	1.505	1.006	1.404 2	15.20	21.04	.727	234.9	307.4
240	-33.15	-28	1.473	1.005	1.404 0	15.47	21.45	.725	239.9	310.6
245	-28.15	-19	1.443	1.005	1.403 8	15.73	21.86	.724	244.9	313.8
250	-23.15	-10	1.413	1.005	1.403 6	15.99	22.27	.722	250.0	317.1
255	-18.15	-1	1.386	1.005	1.403 4	16.25	22.68	.721	255.0	320.2
260	-13.15	8	1.359	1.005	1.403 2	16.50	23.08	.719	260.0	323.4
265	-8.15	17	1.333	1.005	1.403 0	16.75	23.48	.717	265.0	326.5
270	-3.15	26	1.308	1.006	1.402 9	17.00	23.88	.716	270.1	329.6
275	+1.85	35	1.285	1.006	1.402 6	17.26	24.28	.715	275.1	332.6
280	6.85	44	1.261	1.006	1.402 4	17.50	24.67	.713	280.1	335.6
285	11.85	53	1.240	1.006	1.402 2	17.74	25.06	.711	285.1	338.5
290	16.85	62	1.218	1.006	1.402 0	17.98	25.47	.710	290.2	341.5
295	21.85	71	1.197	1.006	1.401 8	18.22	25.85	.709	295.2	344.4
300	26.85	80	1.177	1.006	1.401 7	18.46	26.24	.708	300.2	347.3
305	31.85	89	1.158	1.006	1.401 5	18.70	26.63	.707	305.3	350.2
310	36.85	98	1.139	1.007	1.401 3	18.93	27.01	.705	310.3	353.1
315	41.85	107	1.121	1.007	1.401 0	19.15	27.40	.704	315.3	355.8
320	46.85	116	1.103	1.007	1.400 8	19.39	27.78	.703	320.4	358.7

* Condensed and computed from: Tables of Thermal Properties of Gases, National Bureau of Standards Circular 564, U.S. Government Printing Office, November 1955.

From: *The CRC Press Handbook of Thermal Engineering*, CRC Press, Boca Raton, FL, 2000.

TABLE C.7 (Continued)
Properties of Dry Air at Atmospheric Pressure

Temperature			Properties							
<i>K</i>	<i>deg C</i>	<i>deg F</i>	ρ	c_p	c_p/c_v	μ	k	Pr	h	V_s
325	51.85	125	1.086	1.008	1.400 6	19.63	28.15	.702	325.4	361.4
330	56.85	134	1.070	1.008	1.400 4	19.85	28.53	.701	330.4	364.2
335	61.85	143	1.054	1.008	1.400 1	20.08	28.90	.700	335.5	366.9
340	66.85	152	1.038	1.008	1.399 9	20.30	29.28	.699	340.5	369.6
345	71.85	161	1.023	1.009	1.399 6	20.52	29.64	.698	345.6	372.3
350	76.85	170	1.008	1.009	1.399 3	20.75	30.03	.697	350.6	375.0
355	81.85	179	0.994 5	1.010	1.399 0	20.97	30.39	.696	355.7	377.6
360	86.85	188	0.980 5	1.010	1.398 7	21.18	30.78	.695	360.7	380.2
365	91.85	197	0.967 2	1.010	1.398 4	21.38	31.14	.694	365.8	382.8
370	96.85	206	0.953 9	1.011	1.398 1	21.60	31.50	.693	370.8	385.4
375	101.85	215	0.941 3	1.011	1.397 8	21.81	31.86	.692	375.9	388.0
380	106.85	224	0.928 8	1.012	1.397 5	22.02	32.23	.691	380.9	390.5
385	111.85	233	0.916 9	1.012	1.397 1	22.24	32.59	.690	386.0	393.0
390	116.85	242	0.905 0	1.013	1.396 8	22.44	32.95	.690	391.0	395.5
395	121.85	251	0.893 6	1.014	1.396 4	22.65	33.31	.689	396.1	398.0
400	126.85	260	0.882 2	1.014	1.396 1	22.86	33.65	.689	401.2	400.4
410	136.85	278	0.860 8	1.015	1.395 3	23.27	34.35	.688	411.3	405.3
420	146.85	296	0.840 2	1.017	1.394 6	23.66	35.05	.687	421.5	410.2
430	156.85	314	0.820 7	1.018	1.393 8	24.06	35.75	.686	431.7	414.9
440	166.85	332	0.802 1	1.020	1.392 9	24.45	36.43	.684	441.9	419.6
450	176.85	350	0.784 2	1.021	1.392 0	24.85	37.10	.684	452.1	424.2
460	186.85	368	0.767 7	1.023	1.391 1	25.22	37.78	.683	462.3	428.7
470	196.85	386	0.750 9	1.024	1.390 1	25.58	38.46	.682	472.5	433.2
480	206.85	404	0.735 1	1.026	1.389 2	25.96	39.11	.681	482.8	437.6
490	216.85	422	0.720 1	1.028	1.388 1	26.32	39.76	.680	493.0	442.0
500	226.85	440	0.705 7	1.030	1.387 1	26.70	40.41	.680	503.3	446.4
510	236.85	458	0.691 9	1.032	1.386 1	27.06	41.06	.680	513.6	450.6
520	246.85	476	0.678 6	1.034	1.385 1	27.42	41.69	.680	524.0	454.9
530	256.85	494	0.665 8	1.036	1.384 0	27.78	42.32	.680	534.3	459.0
540	266.85	512	0.653 5	1.038	1.382 9	28.14	42.94	.680	544.7	463.2
550	276.85	530	0.641 6	1.040	1.381 8	28.48	43.57	.680	555.1	467.3
560	286.85	548	0.630 1	1.042	1.380 6	28.83	44.20	.680	565.5	471.3
570	296.85	566	0.619 0	1.044	1.379 5	29.17	44.80	.680	575.9	475.3
580	306.85	584	0.608 4	1.047	1.378 3	29.52	45.41	.680	586.4	479.2
590	316.85	602	0.598 0	1.049	1.377 2	29.84	46.01	.680	596.9	483.2
600	326.85	620	0.588 1	1.051	1.376 0	30.17	46.61	.680	607.4	486.9
620	346.85	656	0.569 1	1.056	1.373 7	30.82	47.80	.681	628.4	494.5
640	366.85	692	0.551 4	1.061	1.371 4	31.47	48.96	.682	649.6	502.1
660	386.85	728	0.534 7	1.065	1.369 1	32.09	50.12	.682	670.9	509.4
680	406.85	764	0.518 9	1.070	1.366 8	32.71	51.25	.683	692.2	516.7
700	426.85	800	0.504 0	1.075	1.364 6	33.32	52.36	.684	713.7	523.7
720	446.85	836	0.490 1	1.080	1.362 3	33.92	53.45	.685	735.2	531.0
740	466.85	872	0.476 9	1.085	1.360 1	34.52	54.53	.686	756.9	537.6
760	486.85	908	0.464 3	1.089	1.358 0	35.11	55.62	.687	778.6	544.6
780	506.85	944	0.452 4	1.094	1.355 9	35.69	56.68	.688	800.5	551.2
800	526.85	980	0.441 0	1.099	1.354	36.24	57.74	.689	822.4	557.8
850	576.85	1 070	0.415 2	1.110	1.349	37.63	60.30	.693	877.5	574.1
900	626.85	1 160	0.392 0	1.121	1.345	38.97	62.76	.696	933.4	589.6
950	676.85	1 250	0.371 4	1.132	1.340	40.26	65.20	.699	989.7	604.9
1 000	726.85	1 340	0.352 9	1.142	1.336	41.53	67.54	.702	1 046	619.5
1 100	826.85	1 520	0.320 8	1.161	1.329	43.96			1 162	648.0
1 200	926.85	1 700	0.294 1	1.179	1.322	46.26			1 279	675.2
1 300	1 026.85	1 880	0.271 4	1.197	1.316	48.46			1 398	701.0
1 400	1 126.85	2 060	0.252 1	1.214	1.310	50.57			1 518	725.9
1 500	1 220.85	2 240	0.235 3	1.231	1.304	52.61			1 640	749.4
1 600	1 326.85	2 420	0.220 6	1.249	1.299	54.57			1 764	772.6
1 800	1 526.85	2 780	0.196 0	1.288	1.288	58.29			2 018	815.7
2 000	1 726.85	3 140	0.176 4	1.338	1.274				2 280	855.5
2 400	2 126.85	3 860	0.146 7	1.574	1.238				2 853	924.4
2 800	2 526.85	4 580	0.124 5	2.259	1.196				3 599	983.1

TABLE C.8
Properties of Gases and Vapors in English and Metric Units

<i>Common name(s)</i>	<i>Acetylene (Ethyne)</i>	<i>Butadiene</i>	<i>n-Butane</i>	<i>Isobutane (2-Methyl propane)</i>
<i>Chemical formula</i>	C_2H_2	C_4H_6	C_4H_{10}	C_4H_{10}
<i>Refrigerant number</i>	—	—	600	600a
CHEMICAL AND PHYSICAL PROPERTIES				
Molecular weight	26.04	54.09	58.12	58.12
Specific gravity, air = 1	0.90	1.87	2.07	2.07
Specific volume, ft ³ /lb	14.9	7.1	6.5	6.5
Specific volume, m ³ /kg	0.93	0.44	0.405	0.418
Density of liquid (at atm bp), lb/ft ³	43.0		37.5	37.2
Density of liquid (at atm bp), kg/m ³	693.		604.	599.
Vapor pressure at 25 deg C, psia			35.4	50.4
Vapor pressure at 25 deg C, MN/m ²			0.024 4	0.347
Viscosity (abs), lbm/ft-sec	6.72×10^{-6}		4.8×10^{-6}	
Viscosity (abs), centipoises ^a	0.01		0.007	
Sound velocity in gas, m/sec	343	226	216	216
THERMAL AND THERMODYNAMIC PROPERTIES				
Specific heat, c_p , Btu/lb-deg F or cal/g-deg C	0.40	0.341	0.39	0.39
Specific heat, c_p , J/kg-K	1 674.	1 427.	1 675.	1 630.
Specific heat ratio, c_p/c_v	1.25	1.12	1.096	1.10
Gas constant R , ft-lb/lb-deg R	59.3	28.55	26.56	26.56
Gas constant R , J/kg-deg C	319	154.	143.	143.
Thermal conductivity, Btu/hr-ft-deg F	0.014		0.01	0.01
Thermal conductivity, W/m-deg C	0.024		0.017	0.017
Boiling point (sat 14.7 psia), deg F	-103	24.1	31.2	10.8
Boiling point (sat 760 mm), deg C	-75	-4.5	-0.4	-11.8
Latent heat of evap (at bp), Btu/lb	264		165.6	157.5
Latent heat of evap (at bp), J/kg	614 000		386 000	366 000
Freezing (melting) point, deg F (1 atm)	-116	-164.	-217.	-229
Freezing (melting) point, deg C (1 atm)	-82.2	-109.	-138	-145
Latent heat of fusion, Btu/lb	23.		19.2	
Latent heat of fusion, J/kg	53 500		44 700	
Critical temperature, deg F	97.1		306	273.
Critical temperature, deg C	36.2	171.	152.	134.
Critical pressure, psia	907.	652.	550.	537.
Critical pressure, MN/m ²	6.25		3.8	3.7
Critical volume, ft ³ /lb			0.070	
Critical volume, m ³ /kg			0.004 3	
Flammable (yes or no)	Yes	Yes	Yes	Yes
Heat of combustion, Btu/ft ³	1 450	2 950	3 300	3 300
Heat of combustion, Btu/lb	21 600	20 900	21 400	21 400
Heat of combustion, kJ/kg	50 200	48 600	49 700	49 700

^aFor N·sec/m² divide by 1 000.

Note: The properties of pure gases are given at 25°C (77°F, 298 K) and atmospheric pressure (except as stated).
From: *The CRC Press Handbook of Thermal Engineering*, CRC Press, Boca Raton, FL, 2000.

TABLE C.8 (Continued)
Properties of Gases and Vapors in English and Metric Units

<i>Common name(s)</i>	<i>1-Butene (Butylene)</i>	<i>cis-2-Butene</i>	<i>trans-2-Butene</i>	<i>Isobutene</i>
<i>Chemical formula</i>	C_4H_8	C_4H_8	C_4H_8	C_4H_8
<i>Refrigerant number</i>	—	—	—	—
CHEMICAL AND PHYSICAL PROPERTIES				
Molecular weight	56.108	56.108	56.108	56.108
Specific gravity, air = 1	1.94	1.94	1.94	1.94
Specific volume, ft ³ /lb	6.7	6.7	6.7	6.7
Specific volume, m ³ /kg	0.42	0.42	0.42	0.42
Density of liquid (at atm bp), lb/ft ³				
Density of liquid (at atm bp), kg/m ³				
Vapor pressure at 25 deg C, psia				
Vapor pressure at 25 deg C, MN/m ²				
Viscosity (abs), lbm/ft-sec				
Viscosity (abs), centipoises ^a				
Sound velocity in gas, m/sec	222	223.	221.	221.
THERMAL AND THERMODYNAMIC PROPERTIES				
Specific heat, c_p , Btu/lb-deg F or cal/g-deg C	0.36	0.327	0.365	0.37
Specific heat, c_p , J/kg·K	1 505.	1 368.	1 527.	1 548.
Specific heat ratio, c_p/c_v	1.112	1.121	1.107	1.10
Gas constant R , ft-lb/lb-deg F	27.52			
Gas constant R , J/kg-deg C	148.			
Thermal conductivity, Btu/hr-ft-deg F				
Thermal conductivity, W/m-deg C				
Boiling point (sat 14.7 psia), deg F	20.6	38.6	33.6	19.2
Boiling point (sat 760 mm), deg C	-6.3	3.7	0.9	-7.1
Latent heat of evap (at bp), Btu/lb	167.9	178.9	174.4	169.
Latent heat of evap (at bp), J/kg	391 000	416 000.	406 000.	393 000.
Freezing (melting) point, deg F (1 atm)	-301.6	-218.	-158.	
Freezing (melting) point, deg C (1 atm)	-185.3	-138.9	-105.5	
Latent heat of fusion, Btu/lb	16.4	31.2	41.6	25.3
Latent heat of fusion, J/kg	38 100	72 600.	96 800.	58 800.
Critical temperature, deg F	291.			
Critical temperature, deg C	144.	160.	155.	
Critical pressure, psia	621.	595.	610.	
Critical pressure, MN/m ²	4.28	4.10	4.20	
Critical volume, ft ³ /lb	0.068			
Critical volume, m ³ /kg	0.004 2			
Flammable (yes or no)	Yes	Yes	Yes	Yes
Heat of combustion, Btu/ft ³	3 150	3 150.	3 150.	3 150.
Heat of combustion, Btu/lb	21 000	21 000.	21 000.	21 000.
Heat of combustion, kJ/kg	48 800	48 800.	48 800.	48 800.

^aFor N-sec/m² divide by 1 000.

TABLE C.8 (Continued)
Properties of Gases and Vapors in English and Metric Units

<i>Common name(s)</i>	<i>Carbon dioxide</i>	<i>Carbon monoxide</i>	<i>Ethane</i>	<i>Ethylene (Ethene)</i>
<i>Chemical formula</i>	<i>CO₂</i>	<i>CO</i>	<i>C₂H₆</i>	<i>C₂H₄</i>
<i>Refrigerant number</i>	<i>744</i>	<i>—</i>	<i>170</i>	<i>1150</i>
CHEMICAL AND PHYSICAL PROPERTIES				
Molecular weight	44.01	28.011	30.070	28.054
Specific gravity, air = 1	1.52	0.967	1.04	0.969
Specific volume, ft ³ /lb	8.8	14.0	13.025	13.9
Specific volume, m ³ /kg	0.55	0.874	0.815	0.87
Density of liquid (at atm bp), lb/ft ³	—	—	28.	35.5
Density of liquid (at atm bp), kg/m ³	—	—	449.	569.
Vapor pressure at 25 deg C, psia	931.	—	—	—
Vapor pressure at 25 deg C, MN/m ²	6.42	—	—	—
Viscosity (abs), lbm/ft-sec	9.4 × 10 ⁻⁶	12.1 × 10 ⁻⁶	64. × 10 ⁻⁶	6.72 × 10 ⁻⁶
Viscosity (abs), centipoises ^a	0.014	0.018	0.095	0.010
Sound velocity in gas, m/sec	270.	352.	316.	331.
THERMAL AND THERMO-DYNAMIC PROPERTIES				
Specific heat, <i>c_p</i> , Btu/lb-deg F or cal/g-deg C	0.205	0.25	0.41	0.37
Specific heat, <i>c_p</i> , J/kg-K	876.	1 046.	1 715.	1 548.
Specific heat ratio, <i>c_p/c_v</i>	1.30	1.40	1.20	1.24
Gas constant <i>R</i> , ft-lb/lb-deg F	35.1	55.2	51.4	55.1
Gas constant <i>R</i> , J/kg-deg C	189.	297.	276.	296.
Thermal conductivity, Btu/hr-ft-deg F	0.01	0.014	0.010	0.010
Thermal conductivity, W/m-deg C	0.017	0.024	0.017	0.017
Boiling point (sat 14.7 psia), deg F	-109.4 ^b	-312.7	-127.	-155.
Boiling point (sat 760 mm), deg C	-78.5	-191.5	-88.3	-103.8
Latent heat of evap (at bp), Btu/lb	246.	92.8	210.	208.
Latent heat of evap (at bp), J/kg	572 000.	216 000.	488 000.	484 000.
Freezing (melting) point, deg F (1 atm)	—	-337.	-272.	-272.
Freezing (melting) point, deg C (1 atm)	—	-205.	-172.2	-169.
Latent heat of fusion, Btu/lb	—	12.8	41.	51.5
Latent heat of fusion, J/kg	—	—	95 300.	120 000.
Critical temperature, deg F	88.	-220.	90.1	49.
Critical temperature, deg C	31.	-140.	32.2	9.5
Critical pressure, psia	1 072.	507.	709.	741.
Critical pressure, MN/m ²	7.4	3.49	4.89	5.11
Critical volume, ft ³ /lb	—	0.053	0.076	0.073
Critical volume, m ³ /kg	—	0.003 3	0.004 7	0.004 6
Flammable (yes or no)	No	Yes	Yes	Yes
Heat of combustion, Btu/ft ³	—	310.	—	1 480.
Heat of combustion, Btu/lb	—	4 340.	22 300.	20 600.
Heat of combustion, kJ/kg	—	10 100.	51 800.	47 800.

^aFor N-sec/m² divide by 1 000.

TABLE C.8 (Continued)
Properties of Gases and Vapors in English and Metric Units

<i>Common name(s)</i>	<i>Hydrogen</i>	<i>Methane</i>	<i>Nitric oxide</i>	<i>Nitrogen</i>
<i>Chemical formula</i>	H_2	CH_4	NO	N_2
<i>Refrigerant number</i>	702	50	—	728
CHEMICAL AND PHYSICAL PROPERTIES				
Molecular weight	2.016	16.044	30.006	28.013 4
Specific gravity, air = 1	0.070	0.554	1.04	0.967
Specific volume, ft ³ /lb	194.	24.2	13.05	13.98
Specific volume, m ³ /kg	12.1	1.51	0.814	0.872
Density of liquid (at atm bp), lb/ft ³	4.43	26.3	—	50.46
Density of liquid (at atm bp), kg/m ³	71.0	421.	—	808.4
Vapor pressure at 25 deg C, psia	—	—	—	—
Vapor pressure at 25 deg C, MN/m ²	—	—	—	—
Viscosity (abs), lbm/ft·sec	6.05×10^{-6}	7.39×10^{-6}	12.8×10^{-6}	12.1×10^{-6}
Viscosity (abs), centipoises ^a	0.009	0.011	0.019	0.018
Sound velocity in gas, m/sec	1 315.	446.	341.	353.
THERMAL AND THERMODYNAMIC PROPERTIES				
Specific heat, c_p , Btu/lb·deg F or cal/g·deg C	3.42	0.54	0.235	0.249
Specific heat, c_p , J/kg·K	14 310.	2 260.	983.	1 040.
Specific heat ratio, c_p/c_v	1.405	1.31	1.40	1.40
Gas constant R , ft·lb/lb·deg F	767.	96.	51.5	55.2
Gas constant R , J/kg·deg C	4 126.	518.	277.	297.
Thermal conductivity, Btu/hr·ft·deg F	0.105	0.02	0.015	0.015
Thermal conductivity, W/m·deg C	0.018 2	0.035	0.026	0.026
Boiling point (sat 14.7 psia), deg F	−423.	−259.	−240.	−320.4
Boiling point (sat 760 mm), deg C	20.4 K	−434.2	−151.5	−195.8
Latent heat of evap (at bp), Btu/lb	192.	219.2	—	85.5
Latent heat of evap (at bp), J/kg	447 000.	510 000.	—	199 000.
Freezing (melting) point, deg F (1 atm)	−434.6	−296.6	−258.	−346.
Freezing (melting) point, deg C (1 atm)	−259.1	−182.6	−161.	−210.
Latent heat of fusion, Btu/lb	25.0	14.	32.9	11.1
Latent heat of fusion, J/kg	58 000.	32 600.	76 500.	25 800.
Critical temperature, deg F	−399.8	−116.	−136.	−232.6
Critical temperature, deg C	−240.0	−82.3	−93.3	−147.
Critical pressure, psia	189.	673.	945.	493.
Critical pressure, MN/m ²	1.30	4.64	6.52	3.40
Critical volume, ft ³ /lb	0.53	0.099	0.033 2	0.051
Critical volume, m ³ /kg	0.033	0.006 2	0.002 07	0.003 18
Flammable (yes or no)	Yes	Yes	No	No
Heat of combustion, Btu/ft ³	320.	985.	—	—
Heat of combustion, Btu/lb	62 050.	2 2900.	—	—
Heat of combustion, kJ/kg	144 000.	—	—	—

^aFor N·sec/m² divide by 1 000.

TABLE C.8 (Continued)
Properties of Gases and Vapors in English and Metric Units

<i>Common name(s)</i>	<i>Nitrous oxide</i>	<i>Oxygen</i>	<i>Propane</i>	<i>Propylene (Propene)</i>
<i>Chemical formula</i>	<i>N₂O</i>	<i>O₂</i>	<i>C₃H₈</i>	<i>C₃H₆</i>
<i>Refrigerant number</i>	<i>744A</i>	<i>732</i>	<i>290</i>	<i>1 270</i>
CHEMICAL AND PHYSICAL PROPERTIES				
Molecular weight	44.012	31.998 8	44.097	42.08
Specific gravity, air = 1	1.52	1.105	1.52	1.45
Specific volume, ft ³ /lb	8.90	12.24	8.84	9.3
Specific volume, m ³ /kg	0.555	0.764	0.552	0.58
Density of liquid (at atm bp), lb/ft ³	76.6	71.27	36.2	37.5
Density of liquid (at atm bp), kg/m ³	1 227.	1 142.	580.	601.
Vapor pressure at 25 deg C, psia			135.7	166.4
Vapor pressure at 25 deg C, MN/m ²			0.936	1.147
Viscosity (abs), lbm/ft-sec	10.1 × 10 ⁻⁶	13.4 × 10 ⁻⁶	53.8 × 10 ⁻⁶	57.1 × 10 ⁻⁶
Viscosity (abs), centipoises ^a	0.015	0.020	0.080	0.085
Sound velocity in gas, m/sec	268.	329.	253.	261.
THERMAL AND THERMO-DYNAMIC PROPERTIES				
Specific heat, <i>c_p</i> , Btu/lb-deg F or cal/g-deg C	0.21	0.220	0.39	0.36
Specific heat, <i>c_p</i> , J/kg-K	879.	920.	1 630.	1 506.
Specific heat ratio, <i>c_p/c_v</i>	1.31	1.40	1.2	1.16
Gas constant <i>R</i> , ft-lb/lb-deg F	35.1	48.3	35.0	36.7
Gas constant <i>R</i> , J/kg-deg C	189.	260.	188.	197.
Thermal conductivity, Btu/hr-ft-deg F	0.010	0.015	0.010	0.010
Thermal conductivity, W/m-deg C	0.017	0.026	0.017	0.017
Boiling point (sat 14.7 psia), deg F	-127.3	-297.3	-44.	-54.
Boiling point (sat 760 mm), deg C	-88.5	-182.97	-42.2	-48.3
Latent heat of evap (at bp), Btu/lb	161.8	91.7	184.	188.2
Latent heat of evap (at bp), J/kg	376 000.	213 000.	428 000.	438 000.
Freezing (melting) point, deg F (1 atm)	-131.5	-361.1	-309.8	-301.
Freezing (melting) point, deg C (1 atm)	-90.8	-218.4	-189.9	-185.
Latent heat of fusion, Btu/lb	63.9	5.9	19.1	
Latent heat of fusion, J/kg	149 000.	13 700.	44 400.	
Critical temperature, deg F	97.7	-181.5	205.	197.
Critical temperature, deg C	36.5	-118.6	96.	91.7
Critical pressure, psia	1 052.	726.	618.	668.
Critical pressure, MN/m ²	7.25	5.01	4.26	4.61
Critical volume, ft ³ /lb	0.036	0.040	0.073	0.069
Critical volume, m ³ /kg	0.002 2	0.002 5	0.004 5	0.004 3
Flammable (yes or no)	No	No	Yes	Yes
Heat of combustion, Btu/ft ³	—	—	2 450.	2 310.
Heat of combustion, Btu/lb	—	—	21 660.	21 500.
Heat of combustion, kJ/kg	—	—	50 340.	50 000.

^aFor N-sec/m² divide by 1 000.

TABLE C.8 (Continued)
Properties of Gases and Vapors in English and Metric Units

<i>Common name(s)</i>	<i>Sulfur dioxide</i>
<i>Chemical formula</i>	<i>SO₂</i>
<i>Refrigerant number</i>	<i>764</i>
CHEMICAL AND PHYSICAL PROPERTIES	
Molecular weight	64.06
Specific gravity, air = 1	2.21
Specific volume, ft ³ /lb	6.11
Specific volume, m ³ /kg	
Density of liquid (at atm bp), lb/ft ³	42.8
Density of liquid (at atm bp), kg/m ³	585.
Vapor pressure at 25 deg C, psia	56.6
Vapor pressure at 25 deg C, MN/m ²	0.390
Viscosity (abs), lbm/ft-sec	8.74×10^{-6}
Viscosity (abs), centipoises ^a	0.013
Sound velocity in gas, m/sec	220.
THERMAL AND THERMO-DYNAMIC PROPERTIES	
Specific heat, <i>c_p</i> , Btu/lb-deg F or cal/g-deg C	0.11
Specific heat, <i>c_p</i> , J/kg·K	460.
Specific heat ratio, <i>c_p/c_v</i>	1.29
Gas constant <i>R</i> , ft-lb/lb-deg F	24.1
Gas constant <i>R</i> , J/kg-deg C	130.
Thermal conductivity, Btu/hr-ft-deg F	0.006
Thermal conductivity, W/m-deg C	0.010
Boiling point (sat 14.7 psia), deg F	14.0
Boiling point (sat 760 mm), deg C	-10.
Latent heat of evap (at bp), Btu/lb	155.5
Latent heat of evap (at bp), J/kg	362 000.
Freezing (melting) point, deg F (1 atm)	-104.
Freezing (melting) point, deg C (1 atm)	-75.5
Latent heat of fusion, Btu/lb	58.0
Latent heat of fusion, J/kg	135 000.
Critical temperature, deg F	315.5
Critical temperature, deg C	157.6
Critical pressure, psia	1 141.
Critical pressure, MN/m ²	7.87
Critical volume, ft ³ /lb	0.03
Critical volume, m ³ /kg	0.001 9
Flammable (yes or no)	No
Heat of combustion, Btu/ft ³	—
Heat of combustion, Btu/lb	—
Heat of combustion, kJ/kg	—

^aFor N·sec/m² divide by 1 000.

Cartridge brass (70% Cu, 30% Zn)	1188	8530	380	110	33.9	75	95	137	149				
							360	395	425				
Constantan (55% Cu, 45% Ni)	1493	8920	384	23	6.71	17	19						
						237	362						
Germanium	1211	5360	322	59.9	34.7	232	96.8	43.2	27.3	19.8	17.4	17.4	
						190	290	337	348	357	375	395	
Gold	1336	19,300	129	317	127	327	323	311	298	284	270	255	
						109	124	131	135	140	145	155	
Iridium	2720	22,500	130	147	50.3	172	153	144	138	132	126	120	111
						90	122	133	138	144	153	161	172
Iron													
Pure	1810	7870	447	80.2	23.1	134	94.0	69.5	54.7	43.3	32.8	28.3	32.1
						216	384	490	574	680	975	609	654
Armco		7870	447	72.7	20.7	95.6	80.6	65.7	53.1	42.2	32.3	28.7	31.4
						215	384	490	574	680	975	609	654
Carbon steels													
Plain carbon (Mn ≤ 1%, Si ≤ 0.1%)		7854	434	60.5	17.7			56.7	48.0	39.2	30.0		
								487	559	685	1169		
AISI 1010		7832	434	63.9	18.8			58.7	48.8	39.2	31.3		
								487	559	685	1168		
Carbon-silicon (Mn ≤ 1%, 0.1% < Si ≤ 0.6%)		7817	446	51.9	14.9			49.8	44.0	37.4	29.3		
								501	582	699	971		
Carbon-manganese-silicon (1% < Mn ≤ 1.6%, 0.1% < Si ≤ 0.6%)		8131	434	41.0	11.6			42.2	39.7	35.0	27.6		
								487	559	685	1090		
Chromium (low) steels													
½Cr-¼Mo-Si (0.18% C, 0.65% Cr, 0.23% Mo, 0.6% Si)		7822	444	37.7	10.9			38.2	36.7	33.3	26.9		
								492	575	688	969		
1 Cr-½ Mo (0.16% C, 1% Cr, 0.54% Mo, 0.39% Si)		7858	442	42.3	12.2			42.0	39.1	34.5	27.4		
								492	575	688	969		
1Cr-V (0.2% C, 1.02% Cr, 0.15% V)		7836	443	48.9	14.1			46.8	42.1	36.3	28.2		
								492	575	688	969		

TABLE C.9 (Continued)
Properties of Metals

Composition	Melting Point (K)	Properties at 300 K				Properties at Various Temperatures (K)									
		ρ (kg/m ³)	c_p [J/(kg · K)]	λ [W/(m · K)]	$\kappa \times 10^6$ (m ² /sec)	λ [W/(m · K)]/ c_p [J/(kg · K)]									
						100	200	400	600	800	1000	1200	1500	2000	2500
Stainless steels															
AISI 302		8055	480	15.1	3.91			17.3	20.0	22.8	25.4				
								512	559	585	606				
AISI 304	1670	7900	477	14.9	3.95	9.2	12.6	16.6	19.8	22.6	25.4	28.0	31.7		
						272	402	515	557	582	611	640	682		
AISI 316		8238	468	13.4	3.48			15.2	18.3	21.3	24.2				
								15.2	18.3	21.3	24.2				
AISI 347		7978	480	14.2	3.71			15.8	18.9	21.9	24.7				
								513	559	585	606				
Lead	601	11,340	129	35.3	24.1	39.7	36.7	34.0	31.4						
						118	125	132	142						
Magnesium	923	1740	1024	156	87.6	169	159	153	149	146					
						649	934	1074	1170	1267					
Molybdenum	2894	10,240	251	138	53.7	179	143	134	126	118	112	105	98	90	86
						141	224	261	275	285	295	308	330	380	459
Nickel															
Pure	1728	8900	444	90.7	23.0	164	107	80.2	65.6	67.6	71.8	76.2	82.6		
						232	383	485	592	530	562	594	616		
Nichrome (80% Ni, 20% Cr)	1672	8400	420	12	3.4			14	16	21					
								480	525	545					
Inconel X-750 (73% Ni, 15% Cr, 6.7% Fe)	1665	8510	439	11.7	3.1	8.7	10.3	13.5	17.0	20.5	24.0	27.6	33.0		
								372	473	510	546	626	—	—	
Niobium	2741	8570	265	53.7	23.6	55.2	52.6	55.2	58.2	61.3	64.4	67.5	72.1	79.1	
						188	249	274	283	292	301	310	324	347	
Palladium	1827	12,020	244	71.8	24.5	76.5	71.6	73.6	79.7	86.9	94.2	102	110		
						168	227	251	261	271	281	291	307		

Platinum																
Pure	2045	21,450	133	71.6	25.1	77.5	72.6	71.8	73.2	75.6	78.7	82.6	89.5	99.4		
						100	125	136	141	146	152	157	165	179		
Alloy 60Pt-40Rh (60% Pt, 40% Rh)	1800	16,630	162	47	17.4			52	59	65	69	73	76			
Rhenium	3453	21,100	136	47.9	16.7	58.9	51.0	46.1	44.2	44.1	44.6	45.7	47.8	51.9		
						97	127	139	145	151	156	162	171	186		
Rhodium	2236	12,450	243	150	49.6	186	154	146	136	127	121	116	110	112		
						147	220	253	274	293	311	327	349	376		
Silicon	1685	2330	712	148	89.2	884	264	98.9	61.9	42.2	31.2	25.7	22.7			
						259	556	790	867	913	946	967	992			
Silver	1235	10,500	235	429	174	444	430	425	412	396	379	361				
						187	225	239	250	262	277	292				
Tantalum	3269	16,600	140	57.5	24.7	59.2	57.5	57.8	58.6	59.4	60.2	61.0	62.2	64.1	65.6	
						110	133	144	146	149	152	155	160	172	189	
Thorium	2023	11,700	118	54.0	39.1	59.8	54.6	54.5	55.8	56.9	56.9	58.7				
						99	112	124	134	145	156	167				
Tin	505	7310	227	66.6	40.1	85.2	73.3	62.2								
						188	215	243								
Titanium	1953	4500	522	21.9	9.32	30.5	24.5	20.4	19.4	19.7	20.7	22.0	24.5			
						300	465	551	591	633	675	620	686			
Tungsten	3660	19,300	132	174	68.3	208	186	159	137	125	118	113	107	100	95	
						87	122	137	142	145	148	152	157	167	176	
Uranium	1406	19,070	116	27.6	12.5	21.7	25.1	29.6	34.0	38.8	43.9	49.0				
						94	108	125	146	176	180	161				
Vanadium	2192	6100	489	30.7	10.3	35.8	31.3	31.3	33.3	35.7	38.2	40.8	44.6	50.9		
						258	430	515	540	563	597	645	714	867		
Zinc	693	7140	389	116	41.8	117	118	111	103							
						297	367	402	436							
Zirconium	2125	6570	278	22.7	12.4	33.2	25.2	21.6	20.7	21.6	23.7	26.0	28.8	33.0		
						205	264	300	322	342	362	344	344	344		

Source: From G.F. Hewitt, G.L. Shires, and T.R. Bott, Eds., *Process Heat Transfer*, CRC Press, Boca Raton, FL, 1994, 1022-1025.